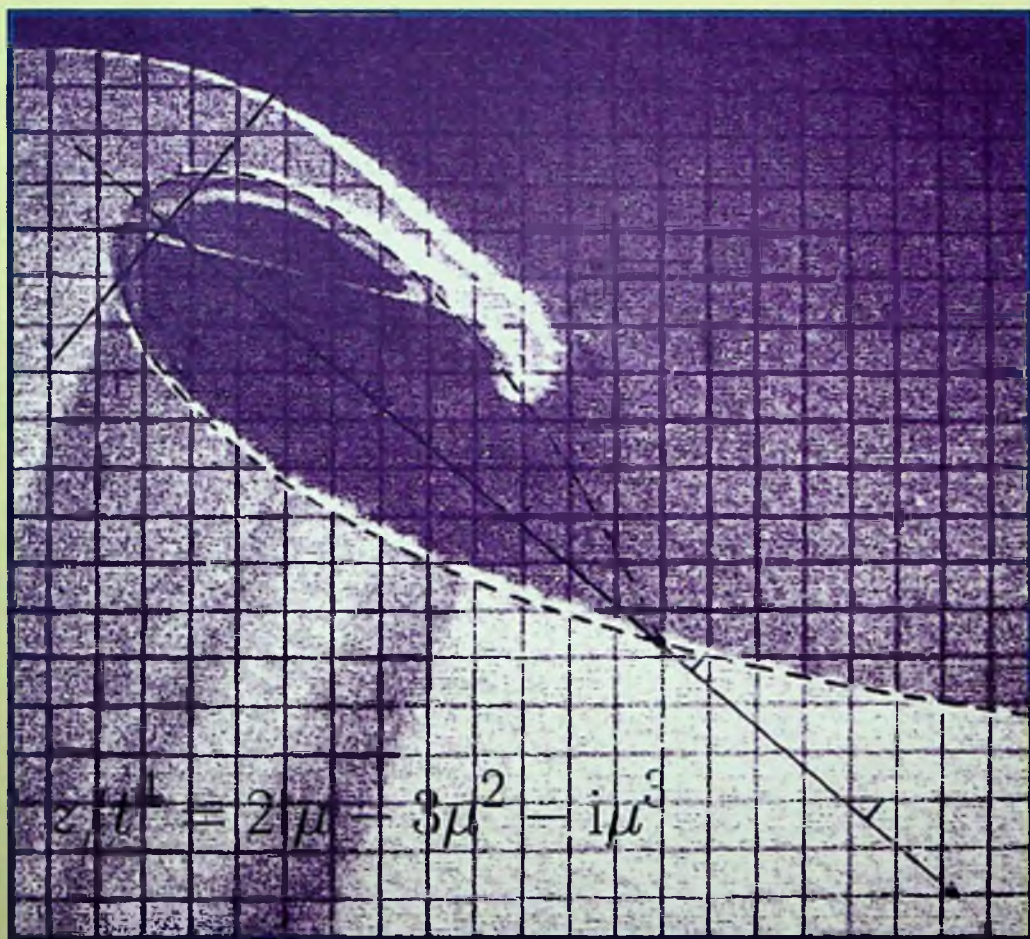


Advanced Series on Ocean Engineering — Volume 35


DYNAMICS OF WATER WAVES

Selected Papers of
Michael Longuet-Higgins

Volume 1



S G Sajjadi
editor

 World Scientific

DYNAMICS OF WATER WAVES

Selected Papers of
Michael Longuet-Higgins

Volume 1

ADVANCED SERIES ON OCEAN ENGINEERING

Series Editor-in-Chief

Philip L-F Liu (*Cornell University*)

Published

- Vol. 24 Introduction to Nearshore Hydrodynamics
by Ib A. Svendsen (Univ. of Delaware, USA)
- Vol. 25 Dynamics of Coastal Systems
by Job Dronkers (Rijkswaterstaat, The Netherlands)
- Vol. 26 Hydrodynamics Around Cylindrical Structures (Revised Edition)
by B. Mutlu Sumer and Jørgen Fredsøe (Technical Univ. of Denmark, Denmark)
- Vol. 27 Nonlinear Waves and Offshore Structures
by Cheung Hun Kim (Texas A&M Univ., USA)
- Vol. 28 Coastal Processes: Concepts in Coastal Engineering and Their Applications to Multifarious Environments
by Tomoya Shibayama (Yokohama National Univ., Japan)
- Vol. 29 Coastal and Estuarine Processes
by Peter Nielsen (The Univ. of Queensland, Australia)
- Vol. 30 Introduction to Coastal Engineering and Management (2nd Edition)
by J. William Kamphuis (Queen's Univ., Canada)
- Vol. 31 Japan's Beach Erosion: Reality and Future Measures
by Takaaki Uda (Public Works Research Center, Japan)
- Vol. 32 Tsunami: To Survive from Tsunami
by Susumu Murata (Coastal Development Inst. of Technology, Japan),
Fumihiko Imamura (Tohoku Univ., Japan),
Kazumasa Katoh (Musashi Inst. of Technology, Japan),
Yoshiaki Kawata (Kyoto Univ., Japan),
Shigeo Takahashi (Port and Airport Research Inst., Japan) and
Tomotsuka Takayama (Kyoto Univ., Japan)
- Vol. 33 Random Seas and Design of Maritime Structures, 3rd Edition
by Yoshimi Goda (Yokohama National University, Japan)
- Vol. 34 Coastal Dynamics
by Willem T. Bakker (Delft Hydraulics, Netherlands)
- Vol. 35 Dynamics of Water Waves: Selected Papers of Michael Longuet-Higgins
Volumes 1-3
edited by S. G. Sajjadi (Embry-Riddle Aeronautical University, USA)
- Vol. 36 Ocean Surface Waves: Their Physics and Prediction
(Second Edition)
by Stanisław R. Massel (Institute of Oceanology of the Polish Academy of Sciences, Sopot, Poland)

*For the complete list of titles in this series, please write to the Publisher.

Advanced Series on Ocean Engineering — Volume 35

DYNAMICS OF WATER WAVES

Selected Papers of
Michael Longuet-Higgins

Volume 1

editor

S G Sajjadi

Embry-Riddle Aeronautical University, USA



World Scientific

NEW JERSEY • LONDON • SINGAPORE • BEIJING • SHANGHAI • HONG KONG • TAIPEI • CHENNAI

Published by

World Scientific Publishing Co. Pte. Ltd.

5 Toh Tuck Link, Singapore 596224

USA office: 27 Warren Street, Suite 401-402, Hackensack, NJ 07601

UK office: 57 Shelton Street, Covent Garden, London WC2H 9HE

British Library Cataloguing-in-Publication Data

A catalogue record for this book is available from the British Library.

Advanced Series on Ocean Engineering — Vol. 35

DYNAMICS OF WATER WAVES

Selected Papers of Michael Longuet-Higgins

Volumes 1-3

Copyright © 2013 by World Scientific Publishing Co. Pte. Ltd.

All rights reserved. This book, or parts thereof, may not be reproduced in any form or by any means, electronic or mechanical, including photocopying, recording or any information storage and retrieval system now known or to be invented, without written permission from the Publisher.

For photocopying of material in this volume, please pay a copying fee through the Copyright Clearance Center, Inc., 222 Rosewood Drive, Danvers, MA 01923, USA. In this case permission to photocopy is not required from the publisher.

ISBN 978-981-4322-51-5 (Set)

ISBN 978-981-4322-52-2 (Vol. 1)

ISBN 978-981-4322-53-9 (Vol. 2)

ISBN 978-981-4322-54-6 (Vol. 3)



Printed in Singapore by B & Jo Enterprise Pte Ltd

Preface by S G Sajjadi

It is a pleasure and honour to write this brief preface to introduce this three-volume selection of papers by a close colleague, Professor Michael Longuet-Higgins, FRS.

As a biographical sketch written by him follows this preface I will limit myself to some thoughts of mine having to do with his influence on our community. From the recognition which Professor Longuet-Higgins has received in appreciation of his work I would like to mention his work on microseisms.

Scientists have long known about microseisms, but, until recently, no one could determine where they came from. Microseisms were first recorded as a strange, continuous buzz on the earliest seismometers, devices that measure earthquakes. Every year, the cumulative energy released by these small vibrations equals the amount of energy released globally from earthquakes. Records of microseismic activity give scientists a history of wave interaction in Earth's oceans since the early 20th century. They are also used to examine the history of storms over the ocean. Scientists are interested in learning where these microseisms originate because the information can help them monitor stress in Earth's crust.

The theory of the origin of microseisms was first introduced in 1950 by Michael Longuet-Higgins whilst at the University of Cambridge in England. Longuet-Higgins suggested that the vibrations originated in places where ocean waves were traveling in opposite directions toward each other at the same frequency and at a certain ocean depth. According to his theory, when these waves collide, they combine to form stationary waves that remain in a constant position over large areas of the ocean. These waves create tall, pulsing columns of pressure that repeatedly beat down on the ocean floor, causing it to vibrate. The vibrations generate seismic surface waves, which spread out thousands of miles and are detected by seismometers as noise. This new study on microseisms, which appeared in the March 2007 issue of the Proceedings of the Royal Society, Series A was part of interdisciplinary collaboration, which included Longuet-Higgins and researchers from the California Institute of Technology, Pasadena and the Hydrologic Research Center in San Diego.

This three volume set presents selected original research papers of Professor Longuet-Higgins in the various areas of water waves, ocean dynamics, and fluid mechanics. I believe they will serve as a milestone and beacon for future generations.

Apart from the subject area covered in these three volumes, Longuet-Higgins has published papers in other fields such as electromagnetic measurement of

tidal streams and ocean currents, time-varying currents depending on the Earth's rotation, projective geometry, etc. These papers have not been included in the present selection, but it is hoped that they will be published in a separate volume in the near future.

Finally, my thanks are due to a number of publishers for their permissions for photographic reproduction of the original papers. In particular I wish to thank the Royal Society of London, the Oxford University Press, the Cambridge University Press, MacMillan Publishing Co., the Journal of Physical Oceanography, the Journal of Marine Research, the American Physical Society, the American Geophysical Union, Prentice-Hall, Pergamon Press and Elsevier Publishing Co.

S G Sajjadi
ERAU, Florida
December 2008

Preface by Michael Longuet-Higgins

The practical consequences of wave motion for both the coastal engineer and the geophysicist are many and varied, and new applications constantly arise to keep the subject alive. At the same time, surface waves challenge the fluid dynamist to find an explanation for such spectacular phenomena as wave breaking, when the upper surface overturns on itself.

The present collection of original papers is not intended to cover the whole subject. It is simply a selection of basic contributions by a single author and his collaborators. On reflection, the papers can be seen to have been guided by certain points of view: (1) a preference for simple or “physical” explanations where possible, and particularly for geometrical interpretations. (2) a desire to solve problems by accurate analysis initially, but then to find simpler approximate models, easier to apply in practice. (3) an acknowledgement of the need to compare theoretical results with field observations or laboratory experiments. Like many other subjects, fluid mechanics advances by putting one foot forward and then the other.

For convenience, this collection is arranged according to subjects. Included in this first Volume are the author’s principal papers on microseisms; on mass transport by water waves; on stochastic processes, especially applied to wind-waves; on various mechanisms of wave generation by wind; and on the theory and consequences of radiation stresses (momentum flux due to waves). Conference papers are generally omitted, since usually they consists of reviews of the original papers, doubtless in a more readable form. Preceding each group of papers, there is a brief introduction giving the circumstances under which the papers were written, and providing further background information.

As an appendix to Volume III, a list is given of the author’s papers on other subjects. Some, as for instance time-varying ocean currents, are closely related to papers in this Collection, while other subjects are widely different.

My thanks are due to Professor SG Sajjadi for offering to undertake the editing of this selection of my papers. I would also like to express my indebtedness to some of my mentors, colleagues and collaborators, aside from those named explicitly in the subsequent text. In particular I wish to mention CV Durrell, the senior mathematics don at Winchester College, for his thorough mathematical grounding, and for his encouragement of my first forays into mathematical research; to Dr George Deacon, leader of Group W at the Admiralty Research Laboratory at Teddington, England, from 1944 to 1949 and subsequently the first Director of the UK National Institute of Oceanography at Witley, for his consistent support; to Norman Barber, a senior physicist in

group W; he was my first research supervisor who introduced me to “physical” ways of looking at mathematical problems; to Sir Harold Jeffreys, for his inspiring lectures on probability and statistics at Cambridge University; and to Sir Geoffrey Taylor, for his inimitable style of research. Walter Munk has been a long-time friend and advocate. It is be appropriate to mention those many anonymous referees who have helped me on my scientific journey.

Perhaps the greatest credit of all should go to the subject of water waves for affording the student such great pleasure and interest, and to the waves themselves, for following so obediently the laws of mathematical physics.

A Brief Biography

In 1943, at the age of seventeen, the author entered Trinity College, Cambridge, with a scholarship in mathematics from Winchester College, the school where he had spent the first four years of World War II. Already he had acquired a taste for research in geometry. By the summer of 1945, he had qualified for a Cambridge BA in mathematics. He was then required to do three years "work of national importance." Fortunately for him, he was assigned to "Group W" (for waves) at the Admiralty Research Laboratory, Teddington. This Group had been formed in June 1944 to study the long-distance propagation of ocean waves in preparation for projected military operations in the Pacific Ocean. The Group had been spectacularly successful, and its lease of life had been extended, with wider terms of reference. During three years at Teddington (1945–8), he worked not only on the theory of wind waves but also on the geomagnetic induction of voltages by tidal streams, and on the generation of oceanic microseisms. In September 1945, he returned to Cambridge to read for a PhD. There was, however, no break in his research; he continued to develop the same subjects of interest, reporting at the end of each term to Sir Harold Jeffreys, and later to Dr Robert Stoneley. In 1951, he was awarded a 4-year research Fellowship (Title A) at Trinity College. The first year (1951–2) he spent in the USA as a Commonwealth Fund Fellow, staying first at the Woods Hole Oceanographic Institute on Cape Code, Massachusetts, and then at the Scripps Institution of Oceanography at La Jolla, California, with Walter Munk. At Scripps he became interested in wave generation by wind, in the statistical properties of sea states, and in several other topics.

On his return to England in 1952, he spent two years of his Research Fellowship in Cambridge after which he accepted Dr George Deacon's invitation to join the newly formed NIO, the UK's National Institute of Oceanography, at Witley in Surrey. There he was to spend thirteen happy and fruitful years, working (mainly) on ocean waves. After 1963, he concentrated more on time-varying ocean currents, especially those which depend essentially on the rotation of the Earth. This period also included visiting appointments in the Mathematics Department at MIT (1957–8), the University of Adelaide, Australia (1964) and at the University of California, San Diego (1961–2 and 1966–7). In 1963, he was elected to the Royal Society of London. From 1967 to 1969, he spent two years assisting in the expansion of the Department of Oceanography at Oregon State University, in Corvallis, Oregon, but in 1969, he was appointed to a Royal Society Research Professorship, to be held jointly at Cambridge University, in the Department of Applied Mathematics and Theoretical Physics, and at The

National Institute of Oceanography at Witley. Once there, he decided on a multi-faceted attack on the problem of wave breaking, involving both theory and innovative experiments in the field and laboratory. He was also free to pursue research in other subjects.

In 1989, on reaching the age of formal retirement, he wished to continue doing research and for two years joined the La Jolla Institute in San Diego, California. In 1991, he was appointed to a position as a Senior Research Physicist at the Institute for Nonlinear Science in the University of California, San Diego, with an Adjunct Professorship at the Scripps Institution of Oceanography. There he turned attention to the natural sources of underwater sound, particularly the sound produced by the creation of bubbles in breaking waves (previously this sound was call “wind noise”). Financial support came mainly from the US Office of Naval Research and from the National Science Foundation. Since his second “retirement” in 2001, he has used his freedom as a Research Physicist Emeritus to indulge his interest in a variety of problems without the necessity of applying for outside grants. These interests have included the damping of incoming swells by sand ripples, and the construction of very simple but accurate approximations to gravity waves of limiting steepness.

Contents

Preface by <i>S G Sajjadi</i>	v
Preface by <i>Michael Longuet-Higgins</i>	vii
A Brief Biography	ix

Volume I

Introductory Notes for Part B	1
B. Oceanic Microseisms	3
B1. Sea Waves and Microseisms, <i>Nature, Lond.</i> 162 (1948) 700 (with F. Ursell).	5
B2. A Theory of the Origin of Microseisms, <i>Phil. Trans. R. Soc. Lond. A</i> 243 (1950) 1–35.	7
B3. An Experimental Study of the Pressure Variations in Standing Water Waves, <i>Proc. R. Soc. Lond. A</i> 206 (1951) 424–435 (with R.I.B. Cooper).	43
B4. Can Sea Waves Cause Microseisms? <i>Proc. Symposium on Microseisms</i> , U.S. Nat. Acad. Sci. Publ. 306 (1952) 74–93.	55
Introductory Notes for Part C	75
C. Mass Transport in Water Waves	77
C1. Mass Transport in Water Waves, <i>Phil. Trans. R. Soc. Lond. A</i> 245 (1953) 535–581.	79
C2. On the Decrease of Velocity with Depth in an Irrotational Water Wave, <i>Proc. Cam. Phil. Soc.</i> 49 (1953) 552–560.	126
C3. The Mechanics of the Boundary-Layer Near the Bottom in a Progressive Wave (Appendix to a paper by R.C.H. Russell and J.D.C. Osorio), <i>Proc. 6th Conf. on Coastal Eng.</i> (Miami, 1957), pp. 183–193.	135

[†]Conference papers (not included).

C4.	Mass Transport in the Boundary Layer at a Free Oscillating Surface, <i>J. Fluid Mech.</i> 8 (1960) 293–306.	146
C5.	Steady Currents Induced by Oscillations Round Islands, <i>J. Fluid Mech.</i> 42 (1970) 701–720.	160
C6.	Peristaltic Pumping in Water Waves, <i>J. Fluid Mech.</i> 137 (1983) 393–407.	181
Introductory Notes for Part D		197
D. Stochastic Processes		199
D1.	On the Statistical Distribution of the Heights of Sea Waves, <i>J. Mar. Res.</i> 11 (1952) 245–266.	201
D2.	The Statistical Distribution of the Maxima of a Random Function, <i>Proc. R. Soc. Lond. A</i> 237 (1956) 212–232 (with D.E. Cartwright).	223
D3.	Statistical Properties of a Moving Wave-Form, <i>Proc. Cam. Phil. Soc.</i> 52 (1956) 234–245.	244
D4.	On the Velocities of the Maxima in a Moving Wave-Form, <i>Proc. Cam. Phil. Soc.</i> 53 (1957) 230–233.	256
D5.	The Statistical Analysis of a Random, Moving Surface, <i>Phil. Trans. R. Soc. Lond. A</i> 249 (1957) 321–387.	260
D6.	Statistical Properties of an Isotropic Random Surface, <i>Phil. Trans. R. Soc. Lond. A</i> 250 (1957) 157–174.	327
D7.	A Statistical Distribution Arising in the Study of the Ionosphere, <i>Proc. Phys. Soc. B</i> 70 (1957) 559–565.	345
D8.	On the Intervals Between Successive Zeros of a Random Function, <i>Proc. R. Soc. Lond. A</i> 246 (1958) 99–118.	352
D9.	The Statistical Distribution of the Curvature of a Random Gaussian Surface, <i>Proc. Cam. Phil. Soc.</i> 54 (1958) 439–453.	372
D10.	The Distribution of the Sizes of Images Reflected in a Random Surface, <i>Proc. Cam. Phil. Soc.</i> 55 (1959) 91–100.	387

-
- D11. The Focusing of Radiation by a Random Surface When the Source is at a Finite Distance, 397
Proc. Cam. Phil. Soc. **56** (1960) 27–40.
- D12. Reflection and Refraction at a Random Moving Surface. 411
I. Pattern and Paths of Specular Points,
J. Opt. Soc. Amer. **50** (1960) 838–844.
- D13. Reflection and Refraction at a Random Moving Surface, 418
II. Number of Specular Points in a Gaussian Surface,
J. Opt. Soc. Amer. **50** (1960) 845–850.
- D14. Reflection and Refraction at a Random Moving Surface, 424
III. Frequency of Twinkling in a Gaussian Surface,
J. Opt. Soc. Amer. **50** (1960) 851–856.
- D15.[†] The Statistical Geometry of Random Surfaces, pp. 105–144 —
in *Hydrodynamic Instability*, ed. C.C. Lin, Amer. Math. Soc.,
Providence (1960).
- D16. The Distribution of Intervals Between Zeros of a Stationary 430
Random Function,
Phil. Trans. R. Soc. Lond. A **254** (1962) 557–599.
- D17. Bounding Approximations to the Distribution of Intervals 473
Between Zeros of a Stationary Gaussian Process pp. 63–88
in *Time Series Analysis*, ed. M. Rosenblatt, John Wiley and Sons,
New York, (1962).
- D18. The Effect of Non-Linearities on Statistical Distributions in the 499
Theory of Sea Waves,
J. Fluid Mech. **17** (1963) 459–480.
- D19. Modified Gaussian Distributions for Slightly Nonlinear Variables, 521
Radio Sci. **68D** (1964) 1049–1062.
- D20. On the Joint Distribution of the Periods and Amplitudes of 535
Sea Waves,
J. Geophys. Res. **80** (1975) 2688–2694.
- D21. On the Distribution of the Heights of Sea Waves: 542
Some Effects on Nonlinearity and Finite Band Width,
J. Geophys. Res. **85** (1980) 1519–1523.
- D22. On the Skewness of Sea-Surface Slopes, 547
J. Phys. Oceanog. **12** (1982) 1283–1291.

D23.	On the Joint Distribution of Wave Periods and Amplitudes in a Random Wave Field, <i>Proc. R. Soc. Lond. A</i> 389 (1983) 241–258.	556
D24.†	Can Optical Measurements Help in the Interpretation of Radar Backscatter?, pp. 121–127 in <i>Satellite Microwave Remote Sensing</i> , ed. T.D. Allan, Ellis Horwood, Chichester (1983).	–
D25.	Statistical Properties of Wave Groups in a Random Sea State, <i>Phil. Trans. R. Soc. Lond. A</i> 312 (1984) 219–250.	574
D26.†	Wave Group Statistics, pp. 15–35 in <i>Oceanic Whitecaps</i> , eds. E.C. Monahan and G. MacNiocaill, (D. Reidel Publ. Co., Dordrecht, 1985).	–
D27.	On the Skewness of Sea-Surface Elevation, <i>J. Fluid Mech.</i> 164 (1986) 487–498 (with M.A. Srokosz).	606
D28.	An Effect of Sidewalls on Waves in a Wind Wave Channel, <i>J. Geophys. Res.</i> 95 (1990) 1765.	618
Introductory Notes for Part F		619
F. Wave Analysis and Wave Generation		621
F1.	Bounds for the Integral of a Non-Negative Function in Terms of its Fourier Coefficients, <i>Proc. Cam. Phil. Soc.</i> 51 (1955) 590–603.	623
F2.	Observations of the Directional Spectrum of Sea Waves Using the Motions of a Floating Buoy, pp. 111–136 in <i>Ocean Wave Spectra</i> , Prentice Hall, New York, 1963 (with D.E. Cartwright and N.D. Smith).	637
F3.†	The Directional Spectrum of Ocean Waves, and Processes of Wave Generation, <i>Proc. R. Soc. Lond. A</i> 265 (1962) 286–315.	–
F4.	A Nonlinear Mechanism for the Generation of Sea Waves, <i>Proc. R. Soc. Lond. A</i> 311 (1969) 371–389.	663
F5.	Action of a Variable Stress at the Surface of Water Waves, <i>Phys. Fluids</i> 12 (1969) 737–740.	682

F6.	Some Effects of Finite Steepness on the Generation of Waves by Wind pp. 393–403, in <i>A Voyage of Discovery (George Deacon 70th Anniversary Vol.)</i> , Pergamon Press, Oxford (1977).	686
F7.	Theory of Weakly Damped Stokes Waves: A New Formulation and its Physical Interpretation, <i>J. Fluid Mech.</i> 235 (1992) 319–324.	697
Introductory Notes for Part G		703
G. Radiation Stresses		705
G1.	Changes in the Form of Short Gravity Waves on Long Waves and Tidal Currents, <i>J. Fluid Mech.</i> 8 (1960) 565–583 (with R.W. Stewart).	707
G2.	The Changes in Amplitude of Short Gravity Waves on Steady Non-Uniform Currents, <i>J. Fluid Mech.</i> 10 (1961) 529–549 (with R.W. Stewart).	726
G3.	Radiation Stress and Mass Transport in Gravity Waves, with Application to ‘Surf Beats’, <i>J. Fluid Mech.</i> 13 (1962) 481–504 (with R.W. Stewart).	747
G4.	A Note on Wave Set-Up, <i>J. Mar. Res.</i> 21 (1963) 4–10 (with R.W. Stewart).	771
G5.	Radiation Stresses in Water Waves; a Physical Discussion, with Applications, <i>Deep-Sea Res.</i> 11 (1964) 529–562 (with R.W. Stewart).	778
G6.	On the Wave-Induced Difference in Mean Sea Level Between the Two Sides of a Submerged Breakwater, <i>J. Mar. Res.</i> 25 (1967) 148–153.	812
G7.	Longshore Currents Generated by Obliquely Incident Sea Waves, 1, <i>J. Geophys. Res.</i> 75 (1970) 6778–6789.	818
G8.	Longshore Currents Generated by Obliquely Incident Sea Waves, 2, <i>J. Geophys. Res.</i> 75 (1970) 6790–6801.	830
G9. [†]	The Average Wave Forces Acting on Wave Power Machines, <i>J. Soc. Underwater Tech.</i> 2 (1976) 4–8.	—

- | | | |
|------|---|-----|
| G10. | The Mean Forces Exerted by Waves on Floating or Submerged Bodies with Applications to Sand Bars and Wave Power Machines,
<i>Proc. R. Soc. Lond. A</i> 352 (1977) 463–480. | 842 |
| G11. | The Propagation of Short Surface Waves on Longer Gravity Waves,
<i>J. Fluid Mech.</i> 177 (1987) 293–306. | 864 |
| G12. | The Orbiting Double Pendulum: An Analogue to Interacting Gravity Waves,
<i>Proc. R. Soc. Lond. A</i> 418 (1988) 281–299
(with K. Dysthe, F.S. Henyey and R.L. Schult). | 878 |
| G13. | Laboratory Measurements of Modulation of Short-Wave Slopes by Long Surface Waves,
<i>J. Fluid Mech.</i> 233 (1991) 389–404
(with S.J. Miller and O.H. Shemdin). | 897 |

Volume II

- | | | |
|---|--|------------|
| Introductory Notes for Part H | | 913 |
| H. Waves in Shallow Water; Beach Processes | | 915 |
| H1. | The Refraction of Sea Waves in Shallow Water,
<i>J. Fluid Mech.</i> 1 (1956) 163–176. | 917 |
| H2. | On the Transformation of a Continuous Spectrum by Refraction,
<i>Proc. Cam. Phil. Soc.</i> 53 (1957) 226–229. | 932 |
| H3. | Sea Waves and Beach Cusps,
<i>Geogr. J.</i> 128 (1962) 194–201 (with D.W. Parkin). | 936 |
| H4. | On the Trapping of Wave Energy Round Islands,
<i>J. Fluid Mech.</i> 29 (1967) 781–821. | 944 |
| H5.† | Recent Progress in the Study of Longshore Currents, pp. 203–248
in <i>Waves on Beaches, and Resulting Sediment Transport</i> ,
ed. R.E. Meyer, Academic Press, 1971. | — |
| H6.† | The Mechanics of the Surf Zone,
<i>Proc. 13th Int. Cong. on Theoretical and Applied Mechanics</i> ,
Moscow, Springer-Verlag (1972) pp. 213–228. | — |
| H7. | On the Nonlinear Transformation of Wave Trains in Shallow Water,
<i>Archiw. Hydrotech.</i> 24 (1977) 445–457. | 985 |

H8.	Oscillating Flow Over Steep Sand Ripples, <i>J. Fluid Mech.</i> 107 (1981) 1–35.	998
H9.	Wave Set-Up, Percolation and Undertow in the Surf Zone, <i>Proc. R. Soc. Lond. A</i> , 390 (1983) 283–291.	1033
H10.	On Wave Set-Up in Shoaling Water with a Rough Sea Bed, <i>J. Fluid Mech.</i> 527 (2005) 217–234.	1046
Introductory Notes for Part I		1065
I. Nonlinear Interactions in Surface Waves		1067
I1.	Resonant Interactions Between Two Trains of Gravity Waves, <i>J. Fluid Mech.</i> 12 (1962) 321–332.	1069
I2.	Phase Velocity Effects in Tertiary Wave Interactions, <i>J. Fluid Mech.</i> 12 (1962) 333–336 (with O.M. Phillips).	1081
I3.	An Experiment on Third-Order Resonant Wave Interactions, <i>J. Fluid Mech.</i> 25 (1966) 417–435 (with N.D. Smith).	1085
I4.	On the Nonlinear Transfer of Energy in the Peak of a Gravity-Wave Spectrum: A Simplified Model, <i>Proc. R. Soc. Lond. A</i> 347 (1975) 311–328.	1104
Introductory Notes for Part K		1123
K. Steep, Steady Gravity Waves		1125
K1.	On the Form of the Highest Progressive and Standing Waves in Deep Water, <i>Proc. R. Soc. Lond. A</i> 331 (1973) 445–456.	1127
K2.	On the Mass, Momentum, Energy and Circulation of a Solitary Wave, <i>Proc. R. Soc. Lond. A</i> 337 (1974), 1–13.	1139
K3.	On the Mass, Momentum, Energy and Circulation of a Solitary Wave II, <i>Proc. R. Soc. Lond. A</i> 340 (1974), 471–493 (with J.D. Fenton).	1152
K4.	Integral Properties of Periodic Gravity Waves of Finite Amplitude, <i>Proc. R. Soc. Lond. A</i> 342 (1975) 157–174.	1175

-
- K5. On the Speed and Profile of Steep Solitary Waves, 1193
Proc. R. Soc. Lond. A **350** (1976) 175–189
(with J.G.B. Byatt-Smith).
- K6. Theory of the Almost-Highest Wave: The Inner Solution, 1208
J. Fluid Mech. **80** (1977) 721–741 (with M.J.H. Fox).
- K7. Theory of the Almost-Highest Wave. Part 2. Matching and 1229
Analytic Extension,
J. Fluid Mech. **85** (1978) 769–786 (with M.J.H. Fox).
- K8. Some New Relations Between Stokes's Coefficients in the 1247
Theory of Gravity Waves,
J. Inst. Math. Appl. **22** (1978) 261–283.
- K9. The Almost-Highest Wave: A Simple Approximation, 1260
J. Fluid Mech. **94** (1979) 269–273.
- K10.[†] The Orbital Motion in Steep Water Waves —
(Appendix to a paper by J.H. Nath),
Proc. 16th Int. Conf. on Coastal Eng. Hamburg, 1979,
pp. 874–877.
- K11. Why is a Water Wave like a Grandfather Clock?, 1265
Phys. Fluids **22** (1979) 1828–1829.
- K12. The Trajectories of Particles in Steep, Symmetric Gravity Waves, 1267
J. Fluid Mech. **94** (1979) 497–517.
- K13. Spin and Angular Momentum in Gravity Waves, 1288
J. Fluid Mech. **97** (1980) 1–25.
- K14. Trajectories of Particles at the Surface of Steep Solitary Waves, 1313
J. Fluid Mech. **110** (1981) 239–247.
- K15. On Integrals and Invariants for Inviscid, Irrotational Flow 1322
Under Gravity,
J. Fluid Mech. **134** (1983) 155–159.
- K16. New Integral Relations for Gravity Waves of Finite Amplitude, 1327
J. Fluid Mech. **149** (1984) 205–215.
- K17. Bifurcation in Gravity Waves, 1338
J. Fluid Mech. **151** (1985) 457–475.

- K18.† A New Way to Calculate Steep Gravity Waves, pp. 1–15 in
The Ocean Surface,
eds. Y. Toba and H. Mitsuyasu, D. Reidel Publishing Co.,
Dordrecht, 1985. —
- K19. The Asymptotic Behaviour of the Coefficients in Stokes's Series 1357
for Surface Gravity Waves,
I.M.A. J. Appl. Math. **34** (1985) 269–277.
- K20. Accelerations in Steep Gravity Waves, 1366
J. Phys. Oceanogr. **15** (1985) 1570–1579.
- K21. Accelerations in Steep Gravity Waves: 1376
II. Subsurface Accelerations,
J. Phys. Oceanogr. **16** (1986) 1332–1337.
- K22. Eulerian and Lagrangian Aspects of Surface Waves, 1382
J. Fluid Mech. **173** (G.I. Taylor Symposium Vol., 1986)
683–706.
- K23.† Eulerian and Lagrangian Wave Measurements, —
Proc. Ocean Struc. Dyn. Symp. (Corvallis, Oregon, 1986)
1–32.
- K24. Lagrangian Moments and Mass Transport in Stokes Waves, 1407
J. Fluid Mech. **179** (1987) 547–555.
- K25. Measurements of the Vertical Acceleration in Wind Waves, 1416
J. Phys. Oceanogr. **17** (1987) 3–11
(with J.A. Ewing and M.A. Srokosz).
- K26. Lagrangian Moments and Mass Transport in Stokes Waves. 1425
Part 2. Water of Finite Depth,
J. Fluid Mech. **186** (1988) 321–336.
- K27. Asymptotic Theory for the Almost-Highest Solitary Wave, 1441
J. Fluid Mech. **317** (1996) 1–19 (with M.J.H. Fox).
- K28. A Close One-Term Approximation to the Highest Stokes 1460
Wave on Deep Water.
Ocean Engrg. **33** (2006) 2012–2024 (with R.C.T. Rainey).

Introductory Notes for Part M	1473
M. Capillary-Gravity Waves	1475
M1. The Generation of Capillary Waves by Steep Gravity Waves, <i>J. Fluid Mech.</i> 16 (1963) 138–159.	1477
M2. Limiting Forms for Capillary-Gravity Waves, <i>J. Fluid Mech.</i> 194 (1988) 351–375.	1499
M3. Capillary-Gravity Waves of Solitary Type on Deep Water, <i>J. Fluid Mech.</i> 200 (1989) 451–470.	1524
M4. Capillary Rollers and Bores, <i>J. Fluid Mech.</i> 240 (1992) 659–679.	1544
M5. Capillary-Gravity Waves of Solitary Type and Envelope Solitons on Deep Water, <i>J. Fluid Mech.</i> 252 (1993) 703–711.	1565
M6. Parasitic Capillary Waves: A Direct Calculation, <i>J. Fluid Mech.</i> 301 (1995) 79–107.	1574
M7. Surface Manifestations of Turbulent Flow, <i>J. Fluid Mech.</i> 308 (1996) 15–29.	1603
M8. Capillary Jumps on Deep Water, <i>J. Phys. Oceanogr.</i> 26 (1996) 1957–1965.	1618
M9. Experiments on Capillary-Gravity Waves of Solitary Type on Deep Water, <i>Phys. Fluids</i> 9 (1997) 1963–1968 (with X. Zhang).	1627
M10. Viscous Dissipation in Steep Capillary-Gravity Waves, <i>J. Fluid Mech.</i> 344 (1997) 271–289.	1633
M11.† Solitary Waves on Deep Water, pp. 149–167 in <i>Wind-Over-Wave Couplings. Perspectives and Prospects</i> , eds. S.G. Sajjadi, N.H. Thomas and J.C.R. Hunt, Oxford, Clarendon Press, 356 pp. (1999).	—

Volume III

Introductory Notes for Part L	1653
L. Unsteady Free-Surface Flows; Wave Breaking	1657
L1. On Wave Breaking and the Equilibrium Spectrum of Wind-Generated Waves, <i>Proc. R. Soc. Lond. A</i> 310 (1969) 151–159.	1659
L2. A Class of Exact, Time-Dependent, Free-Surface Flows, <i>J. Fluid Mech.</i> 55 (1972) 529–543.	1668
L3. Periodicity in Whitecaps, <i>Nature, Lond.</i> 239 (1972) 449–451 (with M. Donelan and J.S. Turner).	1685
L4. A Model of Flow Separation at a Free Surface, <i>J. Fluid Mech.</i> 57 (1973) 129–148.	1690
L5. Review of: ‘Breaking Waves’, (film) by G.B. Olsen and S.P. Kjeldsen, <i>J. Fluid Mech</i> 57 (1973) 624.	1710
L6. An ‘Entraining Plume’ Model of a Spilling Breaker, <i>J. Fluid Mech.</i> 63 (1974) 1–20 (with J.S. Turner).	1711
L7. Breaking Waves — In Deep and Shallow Water, <i>Proc. 10th Symp. on Naval Hydrodynamics</i> , (Cambridge, Mass. 1974), pp. 597–605.	1731
L8.† Recent Developments in the Study of Breaking Waves, <i>Proc. 15th Conf. on Coastal Eng.</i> (Honolulu, 1976) pp. 441–460.	—
L9. Self-Similar, Time-Dependent Flows with a Free Surface, <i>J. Fluid Mech.</i> 73 (1976) 603–620.	1740
L10. The Deformation of Steep Surface Waves on Water. I. A Numerical Method of Computation, <i>Proc. R. Soc. Lond. A</i> 350 (1976) 1–26 (with E.D. Cokelet).	1758
L11.† A Calculation of Unsteady Surface Waves, <i>Proc. 14th IUTAM Cong.</i> (Delft, Holland, 1976), pp. 423–424 (with E.D. Cokelet).	—

- L12.† Advances in the Calculation of Steep Surface Waves and Plunging Breakers, *Proc. 2nd Int. Conf. on Numerical Ship Hydrodynamics*, Berkeley, 1976 pp. 332–346. —
- L13.† The Calculation of Steep Gravity Waves, *Proc. 2nd Conf. on Behaviour of Offshore Structures*, Trondheim, Norway (1976) 2, pp. 27–39 (with E.D. Cokelet and M.J. Fox). —
- L14. The Instabilities of Gravity Waves of Finite Amplitude in Deep Water. I. Superharmonics, *Proc. R. Soc. Lond. A* 360 (1978) 471–488. 1784
- L15. The Instabilities of Gravity Waves of Finite Amplitude in deep water. II. Subharmonics *Proc. R. Soc. Lond. A* 360 (1978) 489–505. 1802
- L16. The Deformation of Steep Surface Waves on Water. II. Growth of Normal-Mode Instabilities, *Proc. R. Soc. Lond. A* 364 (1978) 1–28 (with E.D. Cokelet). 1819
- L17.† On the Dynamics of Steep Gravity Waves in Deep Water, pp. 199–220 in *Turbulent Fluxes Through the Sea Surface, Wave Dynamics, and Prediction*, eds. A. Favre and K. Hasselman, Plenum Publ., 1978. —
- L18. A Technique for Time-Dependent Free-Surface Flows, *Proc. R. Soc. Lond. A* 371 (1980) 441–451. 1847
- L19. On the Forming of Sharp Corners at a Free Surface, *Proc. R. Soc. Lond. A* 371 (1980) 453–478. 1858
- L20. Modulation of the Amplitude of Steep Wind Waves, *J. Fluid Mech.* 99 (1980) 705–713. 1884
- L21.† The Unsolved Problem of Breaking Waves, (Keynote Address), *Proc. 17th Int. Conf. on Coastal Engineering* (Sydney, Australia, 1980) pp. 1–28. —
- L22. On the Overturning of Gravity Waves, *Proc. R. Soc. Lond. A* 376 (1981) 377–400. 1893

-
- L23.† A Parametric Flow for Breaking Waves, —
Proc. Int. Symp. on Hydrodynamics in Ocean Engineering
(Trondheim, 1981), pp. 121–135.
- L24. Parametric Solutions for Breaking Waves, 1917
J. Fluid Mech. 121 (1981) 403–424.
- L25. Bubbles, Breaking Waves and Hyperbolic Jets at a Free Surface, 1939
J. Fluid Mech. 127 (1983) 103–121.
- L26. Rotating Hyperbolic Flow: Particle Trajectories and 1958
Parametric Representation,
J. Mech. Appl. Math. 36 (1983) 247–270.
- L27. Measurements of Breaking Waves by a Surface Jump Meter, 1982
J. Geophys. Res. 88 (1983) 9823–9831 (with N.D. Smith).
- L28.† Towards the Analytic Description of Overturning Waves, pp. 1–24 —
in *Nonlinear Waves*, ed. L. Debnath, Cambridge Univ. Press, 1983.
- L29.† Surface Wave Interactions, Keynote Address, pp. 29–34 —
in *Proc. 9th Australasian Fluid Mech. Conf*
(Auckland, New Zealand), 1986, 29–34.
- L30. On the Stability of Steep Gravity Waves, 1991
Proc. R. Soc. Lond. A 396 (1984) 269–280.
- L31. Bifurcation and Instability in Gravity Waves, 2003
Proc. R. Soc. Lond. A 403 (1986) 167–187.
- L32. A Stochastic Model for Sea Surface Roughness I. Wave Crests, 2024
Proc. R. Soc. Lond. A 410 (1987) 19–33.
- L33.† Advances in Breaking-Wave Dynamics, pp. 209–230 —
in *Wave Dynamics and Radio Probing of the Ocean Surface*,
eds. O.M. Phillips and K. Hasselmann, Plenum Publ.,
New York, 1987.
- L34.† Measurements of Breaking Waves, —
in *Wave Dynamics and Radio Probing of the Ocean Surface*,
eds. O.M. Phillips and K. Hasselmann, Plenum Publ.,
New York, 1987, 257–264 (with N.D. Smith).

- L35.[†] Mechanisms of Wave Breaking in Deep Water, pp. 1–30
in *Sea Surface Sound*, ed. B. R. Kerman, D. Reidel Publ. Co.,
Dordrecht, 1988.
- L36.[†] The Dynamics of Bragg-Scattering Waves on the Sea Surface,
pp. 57–83 in *Mathematics in Remote Sensing*,
ed. S.R. Brooks, Oxford, Clarendon Press (1989)
- L37. Flow Separation Near the Crests of Short Gravity Waves, 2039
J. Phys. Oceanogr. **20** (1990) 595–599.
- L38. A Stochastic Model of Sea-Surface Roughness. II, 2044
Proc. R. Soc. Lond. A **435** (1991) 405–422.
- L39. Highly-Accelerated, Free-Surface Flows, 2062
J. Fluid Mech. **248** (1993) 449–475.
- L40. Crest Instabilities of Gravity Waves. 2089
Part 1. The Almost-Highest Wave,
J. Fluid Mech. **258** (1994) 115–129 (with R.P. Cleaver).
- L41. Crest Instabilities of Gravity Waves. 2104
Part 2. Matching and Asymptotic Analysis,
J. Fluid Mech. **259** (1994) 333–344
(with R.P. Cleaver and M.J.H. Fox).
- L42. A Fractal Approach to Breaking Waves, 2116
J. Phys. Oceanogr. **24** (1994) 1834–1838.
- L43.[†] The Initiation of Spilling Breakers, Keynote Address, —
Proc. Int. Symp. on Waves — Physical and Numerical Modelling,
University of British Columbia, Vancouver, B.C.,
21–24 August 1994, pp. 24–48.
- L44. On the Disintegration of the Jet in a Plunging Breaker, 2121
J. Phys. Oceanogr. **25** (1995) 2458–2462.
- L45. The Crest Instability of Steep Gravity Waves or How Do Short 2126
Waves Break?, pp. 237–246 in *The Air Sea Interface*,
eds. M.A. Donelan, W.H. Hui and W.J. Plant, Toronto, Canada,
Univ. of Toronto Press (1996) 789 pp.

L46.	Crest Instabilities of Gravity Waves. Part 3. Nonlinear Development and Breaking, <i>J. Fluid Mech.</i> 336 (1997) 33–50 (with D.G. Dommermuth).	2136
L47.	On the Crest Instabilities of Steep Surface Waves, <i>J. Fluid Mech.</i> 336 (1997) 51–68 (with M. Tanaka).	2154
L48.†	Progress Toward Understanding How Waves Break, <i>Proc. 21st Symp. on Naval Hydrodynamics, Trondheim, Norway, 24–28 June 1996, Washington, D.C.,</i> Nat. Acad. Sci. Press (1997), pp. 7–28.	—
L49.	Shear Instability in Spilling Breakers, <i>Proc. R. Soc. Lond. A</i> 446 (1994) 399–409.	2172
L50.	Instabilities of a Horizontal Shear Flow with a Free Surface, <i>J. Fluid Mech.</i> 364 (1998) 147–162.	2183
Introductory Notes for Part N		2199
N. Standing Waves		2201
N1.	Theory of Water Waves Derived from a Lagrangian. Part 1. Standing Waves, <i>J. Fluid Mech.</i> 423 (2000) 275–291.	2203
N2.	Vertical Jets from Standing Waves, <i>Proc. R. Soc. Lond. A</i> 457 (2001) 495–510.	2220
N3.	On the Breaking of Standing Waves by Falling Jets, <i>Phys. Fluids</i> 13 (2001) 1652–1659 (with D.G. Dommermuth).	2236
N4.	Vertical Jets from Standing Waves: The Bazooka Effect, pp. 195–204 in <i>IUTAM Symp. on Free Surface Flows</i> , ed. Y.D. Shikhmurzaev, Kluwer Acad. Publ. (2001).	2244
N5.	Vertical Jets from Standing Waves. II, <i>Proc. R. Soc. Lond. A</i> 457 (2001) 2137–2149 (with D.G. Dommermuth).	2253
N6.	Asymptotic Forms for Jets from Standing Waves, <i>J. Fluid Mech.</i> 447 (2001) 287–297.	2266

- N7. On Steep Gravity Waves Meeting a Vertical Wall:
A Triple Instability,
J. Fluid Mech. **466** (2002) 305–318 (with D.A. Drazen).
- N8.† Standing Waves in the Ocean, pp. 201–218 in *Wind over Waves II: Forecasting and Fundamentals of Applications*, eds. S.G. Sajjadi and J.C.R. Hunt, Horwood Publ., Chichester, U.K., (2003) 232 pp.

Introductory Notes for Part B

B. Oceanic Microseisms

Papers B1 to B4

Oceanic microseisms are small movements of the ground recorded by sensitive seismographs. They are quite independent of any seismic signals due to distant earthquakes. The author's interest in microseisms originated in 1946 when Dr George Deacon, then leader of Group W, noticed that the microseisms recorded at Kew Observatory near London followed closely the amplitude of the ocean waves recorded at Group W's station in North Cornwall. Remarkably, the dominant wave period of the microseisms, which varied in time, was consistently half that of the corresponding ocean waves. The papers recorded in Section B tell the story of how an explanation of this phenomenon, now generally accepted, was first formulated.

Paper B1 is a preliminary note announcing the basic idea behind the theory. A first version of the complete theory appeared as an internal Admiralty Report in July 1948, but the final version, Paper B3, was not submitted for publication until after the author returned to Cambridge and had performed experiments confirming the soundness of the hydrodynamical theory. These experiments are described in Paper B4. The complete theory takes into consideration as well the compressibility of sea water. Paper B3, however, is most advantageously read in conjunction with the simplified account given in Paper B6. In addition, B6 provides further historical information; see p. 85. Both B3 and B6 emphasize the important role of sea-water compressibility in amplifying the energy of the microseisms by "organ-pipe resonance" in certain depths of water (typically 3 km for ocean waves of period 12 s). This largely ignored effect has only recently been confirmed quantitatively by field observations, see Kedar et al. (2008): "The origin of deep ocean microseisms in the North Atlantic Ocean," *Proc. R. Soc. Lond., A*, **464**, pp. 777–793.

Two papers, B6 and B7, not reproduced here, were concerned with the correction or rebuttal of statements made by other authors.

It may be noted that the statistical treatment of a random sea state, as given in Papers B3 is a precursor of the modern representation of sea surface elevation by a stochastic integral (Phillips 1966). In 1950, this mathematical tool was not yet available.

The same mechanism as is responsible for oceanic microseisms, namely the interaction of oppositely travelling sea waves, has also been found to give rise

to microbaroms, which are similar oscillations occurring in the atmosphere. For detailed references, see Paper N8 titled "Standing waves in the ocean," in Volume III of this collection.

B. Oceanic Microseisms

(Reprinted from *Nature*, vol. 162, p. 700, October 30, 1948)

Sea Waves and Microseisms

It is well known¹ that the pressure variations beneath a progressive gravity wave of Stokes's type are insufficient, in deep water, to generate microseisms of the observed magnitude. This is because the pressure variations on the sea-bed decrease exponentially with the depth. The following argument, however, shows the existence, in a general class of wave motions, of 'second-order' pressure variations which are not attenuated with the depth.

The surface elevation in a simple stationary wave, for example, is given, in Lamb's notation², by

$$(A) \quad \eta = a \cos kx \cos \sigma t + O(a^2),$$

where

$$\sigma^2 = gk \tanh kh.$$

Consider the mass of water contained between the bottom $z = -h$, the surface $z = \eta$ and the two vertical planes $x = 0, \lambda$ where $\lambda = 2\pi/k$. There is no flow across the vertical planes and therefore this mass of water consists always of the same particles. Therefore, if F is the vertical component of the total external force acting on the mass, we have, summing the equations of motion for each particle of mass m and cancelling internal forces,

$$F = \Sigma m \frac{d^2z}{dt^2} = \frac{1}{g} \frac{d^2}{dt^2} (\text{potential energy}).$$

Now the forces across the vertical boundaries contribute nothing to F ; the pressure p_0 at the free surface contributes a downwards force λp_0 and gravity a constant force $\lambda \rho gh$. Hence

$$F = \lambda(p - p_0 - \rho gh),$$

where p is the mean pressure on the bottom. Now for the stationary wave (A) we have, neglecting compressibility,

$$\begin{aligned} \text{potential energy} &= \int_0^\lambda \frac{1}{2} \rho g \eta^2 dx \\ &= \frac{1}{2} \lambda \rho g a^2 \cos^2 \sigma t + O(a^3). \end{aligned}$$

Hence

$$(B) \quad \frac{p - p_0}{\rho} = gh - \frac{1}{2} a^2 \sigma^2 \cos 2\sigma t + O(a^3).$$

The second term is of order (wave-height)², which explains why it is not revealed in the ordinary first-order theory. It is also of double the fundamental frequency and, for a given frequency and amplitude, is independent of the depth h . Equation (B) has been derived by Miche³ in the course of a complete evaluation of the second approximation to the stationary wave-motion. By a slight extension of the present argument one can evaluate the mean pressure below the series of long-crested waves given by

$$(C) \quad \eta = \sum_{m,n} a_{m,n} \cos (mkx + nky + \sigma_{m,n}t + \epsilon_{m,n}),$$

where m and n are integers and

$$\sigma_{m,n}^2 = (m^2 + n^2)^{1/2} gk \tanh (m^2 + n^2)^{1/2} kh, \quad (\sigma_{mn} \geq 0).$$

If p is the mean pressure on the bottom, we find

$$(D) \quad \frac{p - p_0}{\rho} = gh -$$

$$\sum_{m,n} a_{m,n} a_{-m,-n} \sigma_{m,n}^2 \cos (2\sigma_{m,n}t + \epsilon_{m,n} + \epsilon_{-m,-n}).$$

Hence this type of pressure fluctuation occurs whenever wave-trains cross which are of the same frequency and travel in opposite directions (corresponding to integers (m,n) , $(-m,-n)$). A single wave train gives zero fluctuation in the mean pressure.

These results provide the basis for a new theory of microseism generation. They explain how microseisms come to be generated in deep water^{4,5}, and why the frequency of the microseisms is sensibly double that of the waves associated with them⁶. The theoretical orders of magnitude are in agreement with those observed. A fuller account of the theory is in preparation.

M. S. LONGUET-HIGGINS
F. URSELL

Admiralty Research Laboratory,
Teddington, Middlesex.

May 20.

¹ Gutenberg, B., *Bull. Seis. Soc. Amer.*, **21**, 1 (1931).

² Lamb, H., "Hydrodynamics" (6th edit., Camb., 1932).

³ Miche, M., *Ann. des Ponts et Chaussées*, Nos. 1-4 (1944).

⁴ Banerji, S. K., *Phil. Trans. Roy. Soc., A*, **229**, 287 (1930).

⁵ Gilmore, M. H., *Bull. Seis. Soc. Amer.*, **36**, 89 (1946).

⁶ Deacon, G. E. R., *Nature*, **160**, 419 (1947).

Reproduced with permission from *Phil. Trans. R. Soc. Lond. A* 243 (1950) 1–35.

[1]

A THEORY OF THE ORIGIN OF MICROSEISMS

By M. S. LONGUET-HIGGINS

Department of Geodesy and Geophysics, University of Cambridge

(Communicated by H. Jeffreys, F.R.S.—Received 19 September 1949—

Revised 18 March 1950—Read 30 March 1950)

CONTENTS

	PAGE		PAGE
1. INTRODUCTION	2	4. WAVE MOTION IN A HEAVY COMPRESSIBLE FLUID	17
2. PRESSURE VARIATIONS IN A PERIODIC WAVE TRAIN	4	5. THE DISPLACEMENT OF THE GROUND DUE TO SURFACE WAVES	26
3. GENERAL TYPES OF WAVE MOTION	10	6. CONCLUSIONS	34
		REFERENCES	35

In the past it has been considered unlikely that ocean waves are capable of generating micro-seismic oscillations of the sea bed over areas of deep water, since the decrease of the pressure variations with depth is exponential, according to the first-order theory generally used. However, it was recently shown by Miche that in the second approximation to the standing wave there is a second-order pressure variation which is not attenuated with depth and which must therefore ultimately predominate over the first-order pressure variations. In §§ 2 and 3 of the present paper the general conditions under which second-order pressure variations of this latter type will occur are considered. It is shown that in an infinite wave train there is in general a second-order pressure variation at infinite depth which is applied equally over the whole fluid and is associated with no particle motion. In the case of two progressive waves of the same wave-length travelling in opposite directions this pressure variation is proportional to the product of the (first-order) amplitudes of the two waves and is of twice their frequency. The pressure variation at infinite depth is found to be closely related to changes in the potential energy of the wave train as a whole. By introducing the two-dimensional frequency spectrum of the motion it is shown that in the general case variations in the mean pressure over a wide area only occur when the spectrum contains wave groups of the same wave-length travelling in opposite directions. (These are called opposite wave groups.)

In § 4 the effect of the compressibility of the water is considered by evaluating the motion of an opposite pair of waves in a heavy compressible fluid to the second order of approximation. In place of the pressure variation at infinite depth, waves of compression are set up, and there is resonance between the bottom and the free surface when the depth of water is about $(\frac{1}{2}n + \frac{1}{4})$ times the length of a compression wave (n being an integer). The motion in a surface layer whose thickness is of the order of the length of a Stokes wave is otherwise unaffected by the compressibility.

Section 5 is devoted to the question whether the second-order pressure variations in surface waves are capable of generating microseisms of the observed order of magnitude. By considering the displacement of the sea bed due to a concentrated force at the upper surface of the water it is shown that the effect of resonance will be to increase the disturbance by a factor of the order of 5 over its value in shallow water. The results of §§ 3 and 4 are used to derive an expression for the vertical displacement of the ground in terms of the frequency characteristics of the waves. The displacement from a storm area of 1000 sq. km. is estimated to be of the order of 6.5 μ , at a distance of 2000 km.

Ocean waves may therefore be the cause of microseisms, provided that there is interference between groups of waves of the same frequency travelling in opposite directions. Suitable conditions of wave interference may occur at the centre of a cyclonic depression or possibly if there is wave reflexion from a coast. In the latter case the microseisms are likely to be smaller, except perhaps locally. Confirmation of the present theory is provided by the observations of Bernard and Deacon, who discovered independently that the period of the microseisms is in many cases about half that of the ocean waves associated with them.

1. INTRODUCTION

The word 'microseisms' is commonly used to denote the continuous oscillations of the ground of periods between 3 and 10 sec. which are recorded by all sensitive seismographs, and which are not due to earthquakes or to local causes such as rain, traffic or gusts of wind. Since the original researches of Bertelli in the latter half of the nineteenth century, many investigations have confirmed the close connexion of microseisms with disturbed weather conditions, especially with those centred over the sea. Increased microseismic activity tends to occur simultaneously over large areas of Europe or of North America (Gutenberg 1931, 1932; Lee 1934), and the greatest disturbance is found to be in a coastal region bordering on a well-developed depression. It is not true conversely (Whipple & Lee 1935) that depressions of the same intensity necessarily give rise to the same amplitude of microseisms. However, Ramirez (1940), by using a triangular arrangement of seismographs, has shown beyond doubt that microseisms at St Louis, Missouri, are received from the direction of depressions off the Atlantic coast. His methods of direction-finding have also formed the basis of a successful project for tracking hurricanes in the Caribbean area (Gilmore 1946).

Several suggestions as to the cause of microseisms have been put forward, none of which, however, is entirely satisfactory. Gherzi (1932) has considered microseisms to be due to 'pumping' of the atmosphere such as is sometimes shown on barographs near the centre of intense tropical cyclones. This cause cannot be excluded for storms of tropical intensity, where observations taken in the path of the storm show that the amplitude may be as much as 0.2 mm. of mercury (Bradford 1935). Ramirez, however, has pointed out (1940) that there is practically no connexion between the microseisms at St Louis and the barograph oscillations at St Louis or Florissant, even during the close passage of a tornado during March 1938. Also the periods of the oscillations quoted by Gherzi for the Shanghai typhoon are of several minutes, which would appear to be too long. It is considerably more doubtful whether microseisms could be caused by the much milder atmospheric oscillations found in temperate latitudes. The observations of Baird & Banwell in New Zealand (1940) have indicated amplitudes of only a few inches of air.

Scholte (1943) has sought to demonstrate that microseisms may be generated by atmospheric pressure on the surface of the sea, by showing that the amplitude of the compression waves generated by an oscillatory pressure spread sufficiently widely over the sea surface is as great as 10^{-4} times the amplitude of the gravity waves (ocean waves) so generated. The weakness of this argument is apparent. Ocean waves are not generated by oscillating pressure distributions of the type described by Scholte, but more probably by a systematic difference of pressure between the front and rear slopes of the crests of a wave train (Jeffreys 1925). The effect of a pressure distribution of this latter type, while tending continually to increase the energy of the gravity waves, would tend to cancel out for the much longer waves of compression.

An earlier theory, due originally to Wiechert and until recently strongly supported by Gutenberg, was that microseisms are caused by the impact of waves breaking against a steep coast. It is argued in favour of this theory that there is a statistical correlation between, for example, the amplitude of the microseisms at Hamburg and the height of the waves off the coast of Norway (Tams 1933). This theory will account for some of the facts, although it

THEORY OF THE ORIGIN OF MICROSEISMS

involves a coefficient for the proportion of the wave energy imparted to the ground which some may consider too high (Bradford 1935). Observations also seem to show that microseisms associated with storms at sea may be recorded several hours before the waves reach the coast (Banerji 1930; Ramirez 1940; Deacon 1949), so that a further explanation, at any rate of these latter observations, is required.

Possibly the most natural explanation of microseisms, and one that might have been previously considered more seriously but for theoretical objections, is that they are generated by pressure variations on the sea bed due to ocean waves raised by the wind. It is unfortunate that in the past use has had to be made of Stokes's well-known theory of progressive waves, with the result that the pressure variations on the bottom, at any rate in deep water, appeared far too small (Gutenberg 1931; Whipple & Lee 1935). The physical reasons for this are twofold. In the first place the pressure variations in a progressive wave decrease exponentially with depth, and secondly the wave-length of gravity waves is extremely small compared to that of seismic waves, so that the contributions from different part of the sea bed effectively cancel one another. Banerji (1930) sought a way out by supposing that the water motion is not strictly irrotational, but his analysis cannot be defended. It was also shown (Whipple & Lee 1935) that the compressibility of the water makes little difference to the general result. † A further difficulty was that investigation of the wave periods usually showed them to be considerably greater than the corresponding periods of the microseisms. Bernard's careful studies of the periods of swell off the coast of Morocco (1937, 1941 *a, b*) indicated that they were in fact about twice the microseism periods. In a comparison of the Kew seismograms with records of waves taken at Perranporth in Cornwall, Deacon (1947) independently arrived at the same conclusion.

It has been pointed out (Longuet-Higgins & Ursell 1948) that Miche, in a theoretical study of wave motion (1944), discovered that the mean pressure on the bottom beneath a train of standing waves is not constant, as in a progressive wave, but fluctuates with an amplitude independent of the depth and proportional to the square of the wave height. This oscillation is of precisely the type required for the generation of ground movement, for not only is it unattenuated with depth (and is therefore the most important term at depths greater than about half a wave-length) but also, being in phase at all points of the bottom, it is suitable for producing long seismic waves. A further remarkable fact is that the frequency of this pressure variation is twice the fundamental frequency of the waves. Owing to the customary neglect of terms of higher order than the first, this term had been overlooked, the standing wave being in the first approximation the sum of two progressive waves of equal amplitudes travelling in opposite directions. A shorter proof of Miche's result, bringing to

† An attempt was made by Banerji (1935) to show that the compressibility of the water would allow pressure variations of the same period as the surface waves to be transmitted to depths great compared with the wave-length. However, an error in his analysis was pointed out by Whipple & Lee (1935, p. 295). In the same paper (1935) Banerji describes experiments in which he set up waves of length 2 to 6 cm. in tanks of depth 84 to 108 cm. and observed the oscillations in a tube of diameter 4 cm. sunk to varying depths and open at the lower end. Appreciable oscillations were observed at all depths. Banerji's results are difficult to interpret, but it seems unlikely that the compressibility of the water can have affected experiments on this scale. J. Darbyshire has also pointed out that the period of the oscillations shown in plates XXVII and XXVIII of Banerji's paper lies between 0.6 and 0.75 sec.; these cannot have been of the same period as the surface waves unless the latter were of length 56 to 88 cm., or comparable with the depth and width of the tank.

light the physical reasons for the existence of this pressure oscillation, was given by Longuet-Higgins & Ursell (1948). A generalization of this proof led the present author to the conclusion (see §3) that variations in the mean pressure over a wide area arise as a result of the interference of groups of waves of the same wave-length, but not necessarily of equal amplitude, travelling in opposite directions.

For a few years previously Bernard (1941 *a, b*) had held the view, unsupported at that time by hydrodynamical theory, that standing waves (Fr. *clapotis*) were the cause of microseisms. He had suggested that favourable conditions for standing waves would arise at the centre of a cyclonic depression or possibly off a steep coast where there was reflexion from the shore (this idea is to be distinguished from Wiechert's surf theory, although similar conditions would favour the generation of microseisms on either hypothesis). Bernard does not appear to have foreseen the doubling of the frequency of the unattenuated pressure variations in a standing wave, for he is inclined to suggest other causes for the difference between the frequencies of the microseisms and those of the waves (Bernard 1941 *a*, p. 10).

In the present paper we shall first investigate, in §§2 and 3, the physical reasons for the existence of unattenuated pressure variations of the type occurring in the standing wave and the general conditions under which they will occur; in §4 the effect of the compressibility of the water on the wave motion will be considered; and in §5, using the results of §§3 and 4, it will be shown that the second-order pressure variations due to surface waves are of the right order of magnitude for producing microseismic oscillations of the sea bed. We shall also consider briefly under what meteorological circumstances waves suitable for generating microseisms may be expected to be produced.

2. PRESSURE VARIATIONS IN A PERIODIC WAVE TRAIN

2.1. *The attenuation of pressure variations and particle velocities with depth*

Although the second-order pressure variations in a standing wave in deep water are not attenuated exponentially with the depth, the unattenuated terms are not associated with any motion of the particles. That this is possible may be seen as follows. Let rectangular co-ordinates (x, y, z) be taken with the origin in the undisturbed level of the free surface and the z -axis vertically downwards. For simplicity we shall consider motion in two dimensions (x, z) only; similar arguments are, however, applicable to motion in three dimensions. We assume that the motion is irrotational, and that it is periodic in the x -direction with wave-length λ . The components of velocity (u, w) are given by

$$u = -\frac{\partial\phi}{\partial x}, \quad w = -\frac{\partial\phi}{\partial z}, \quad (1)$$

where, since the fluid is incompressible, we have

$$\nabla^2\phi = -\left(\frac{\partial u}{\partial x} + \frac{\partial w}{\partial z}\right) = 0. \quad (2)$$

The equations of motion may be integrated (see Lamb 1932, §20) to give the Bernoulli equation

$$\frac{p-p_2}{\rho} - gz = \frac{\partial\phi}{\partial t} - \frac{1}{2}(u^2 + w^2) + \theta(t), \quad (3)$$

THEORY OF THE ORIGIN OF MICROSEISMS

5

where p denotes the pressure, ρ the density, g the acceleration of gravity, p_s the pressure at the free surface (supposed constant) and $\theta(t)$ is a function of the time t only. ϕ itself contains an arbitrary function of t ; but this may be made definite by specifying that the mean value of ϕ with respect to x , taken over one wave-length, is zero. Similarly, by a suitable choice of axes the mean value of u may be made zero (both conditions may be satisfied for all values of z and t). Then, since ϕ is a harmonic function periodic in x and bounded when $z > 0$, it may be shown that in water of infinite depth ϕ , u and w all diminish with z at least as rapidly as $\exp(-2\pi z/\lambda)$ (to all orders of approximation). Therefore when z exceeds about half a wave-length we have from equation (3)

$$\frac{\bar{p}-p_s}{\rho}-gz = \theta(t). \quad (4)$$

Thus, although the particle velocities in any irrotational periodic motion must decrease exponentially with the depth, the pressure may still be a function of the time t . The pressure variation (4), being simultaneous over the whole fluid, is the same as if a uniform pressure $\theta(t)$ were applied to the free surface, the fluid being at rest. $\theta(t)$, being the limit of (3) when z tends to infinity, may be called the pressure variation at infinite depth. $\theta(t)$ does not in general vanish, though in one case, namely, that of the progressive wave, we may show that it is a constant; for in equation (3) every term except $\theta(t)$ is then a function of $(x-ct)$ and z , where c is the wave velocity. Therefore θ also is a function of $(x-ct)$. Hence θ , being independent of x , is independent of t also.

In general, since $\theta(t)$ is in phase at all points, there is a fluctuation in the mean pressure with respect to x on any plane $z = \text{constant}$. Thus if \bar{p} denote the mean pressure with respect to x in the interval $0 \leq x \leq \lambda$ we have from (3)

$$\frac{\bar{p}-p_s}{\rho}-gz = -\frac{1}{\lambda} \int_0^\lambda \frac{1}{2}(u^2+w^2) dx + \theta(t) \quad (5)$$

(since the mean value of ϕ vanishes by hypothesis); and for large values of z we have

$$\frac{\bar{p}-p_s}{\rho}-gz = \theta(t). \quad (6)$$

The occurrence of an unattenuated pressure variation at infinite depth is therefore closely associated with a variation in the mean pressure on the plane $z = \text{constant}$. As we saw in § 1, it is the variation in the mean pressure which is likely to be of physical importance in producing seismic oscillations of the sea bed.

2.2. Evaluation of the mean pressure

We shall now obtain a general expression for the mean pressure over a given area of the plane $z = \text{constant}$, from which the special cases of the standing and the progressive wave may be very simply derived. It will not be assumed, in the first place, either that the motion is irrotational or periodic. Some of the equations will therefore be applicable to the more general types of motion to be discussed in § 3.

A very general relation between the vertical motion of a mass M of fluid consisting always of the same particles and the vertical forces acting upon it may be obtained as follows.

M. S. LONGUET-HIGGINS ON A

Suppose that (x, z) are rectangular co-ordinates referring always to the same particle of the fluid in the Lagrangian manner, so that x and z are functions of the time t and of the co-ordinates (x_0, z_0) at some fixed instant, say $t = 0$. The equation of motion in the vertical direction is

$$\frac{\partial p}{\partial z} - g\rho = -\frac{1}{\rho} \frac{\partial^2 z}{\partial t^2}, \quad (7)$$

and the equation of continuity may be expressed in the form

$$\rho dx dz = \rho_0 dx_0 dz_0, \quad (8)$$

where ρ_0 is the density when $t = 0$. Now we have

$$\int_M \rho \frac{\partial^2 z}{\partial t^2} dx dz = \int_M \rho_0 \frac{\partial^2 z}{\partial t^2} dx_0 dz_0 = \frac{\partial^2}{\partial t^2} \int_M \rho_0 z dx_0 dz_0 = \frac{\partial^2}{\partial t^2} \int_M \rho z dx dz. \quad (9)$$

Therefore on integrating equation (7) over the fluid M we find

$$\int_M \frac{\partial p}{\partial z} dx dz - \int_M g\rho dx dz = -\frac{\partial^2}{\partial t^2} \int_M \rho z dx dz. \quad (10)$$

In evaluating the integrals in equation (10) we may treat x, z and t as the independent variables, though the boundaries of M are now functions of t . The right-hand side of (10) may clearly be written $-\frac{1}{g} \frac{\partial^2 V}{\partial t^2}$, where V is the potential energy of the fluid M .

Suppose now that, in any wave motion at the free surface of an incompressible fluid, M denotes the body of fluid which at time $t = 0$ is contained between the free surface $z = \zeta$, the horizontal plane $z = z'$ and the two vertical planes $x = x_1$ and $x = x_2$. If p' denotes the pressure in the plane $z = z'$, and p_s the constant pressure at the free surface, we have, at the initial instant,

$$\int_M \frac{\partial p}{\partial z} dx dz = \int_{x_1}^{x_2} (p' - p_s) dx = (p' - p_s) (x_2 - x_1), \quad (11)$$

where \bar{p}' denotes the mean value of p' with respect to x . Similarly we have, since ρ is assumed to be constant,

$$\int_M g\rho dx dz = g\rho \int_{x_1}^{x_2} (z' - \zeta) dx = g\rho z' (x_2 - x_1) - g\rho \int_{x_1}^{x_2} \zeta dx. \quad (12)$$

To evaluate the third term in equation (10) we need an expression for the integral at times other than the initial instant. Suppose then that at time t the fluid M is bounded by the surfaces

$$z = \zeta(x, t), \quad z = z' + \zeta'(x, t), \quad x = \xi_1(z, t) \quad \text{and} \quad x = \xi_2(z, t),$$

where

$$\zeta'(x, 0) = 0, \quad \xi_1(z, 0) = x_1, \quad \xi_2(z, 0) = x_2. \quad (13)$$

The (x, z) co-ordinates of the intersections of the surfaces $z = \zeta'$, $(z' + \zeta')$ with the surfaces $x = \xi_1, \xi_2$ may be denoted by (α_1, γ_1) , (α'_1, γ'_1) ; (α_2, γ_2) , (α'_2, γ'_2) respectively, these being functions of t . Then we have

$$\int_M z dx dz = \int_{\alpha_1}^{\alpha_2} \frac{1}{2} (z' + \zeta')^2 dx - \int_{\alpha_1}^{\alpha_2} \frac{1}{2} \zeta'^2 dx + \int_{\gamma_2}^{\gamma'_1} \zeta_2 z dz - \int_{\gamma_1}^{\gamma'_1} \zeta_1 z dz - \frac{1}{2} [\alpha_2 \gamma_2'^2 - \alpha_1 \gamma_1'^2 - \alpha_2 \gamma_2^2 + \alpha_1 \gamma_1^2]. \quad (14)$$

On differentiating twice with respect to t we find

$$\begin{aligned} \frac{\partial^2}{\partial t^2} \int_M z dx dz = & \int_{\alpha_1}^{\alpha_2} \frac{\partial^2}{\partial t^2} \frac{1}{2} (z' + \zeta')^2 dx - \int_{\alpha_1}^{\alpha_2} \frac{\partial^2}{\partial t^2} \frac{1}{2} \zeta'^2 dx + \int_{\gamma_2}^{\gamma'_1} \frac{\partial^2}{\partial t^2} \zeta_2 z dz - \int_{\gamma_1}^{\gamma'_1} \frac{\partial^2}{\partial t^2} \zeta_1 z dz \\ & + 2[\dot{\alpha}_2 \dot{\gamma}_2' \gamma_2' - \dot{\alpha}_1 \dot{\gamma}_1' \gamma_1' - \dot{\alpha}_2 \dot{\gamma}_2 \gamma_2 + \dot{\alpha}_1 \dot{\gamma}_1 \gamma_1], \quad (15) \end{aligned}$$

THEORY OF THE ORIGIN OF MICROSEISMS

7

where a dot denotes partial differentiation with respect to t . At the initial instant we have

$$\alpha_1 = \alpha'_1 = x_1, \quad \alpha_2 = \alpha'_2 = x_2, \quad \gamma'_1 = \gamma'_2 = z'. \quad (16)$$

Therefore, if ζ_1 and ζ_2 denote the values of ζ when $x = x_1$ and x_2 , equation (10) becomes

$$\frac{\bar{p} - \bar{p}_s - gz'}{\rho} = \frac{1}{x_2 - x_1} \int_{x_1}^{x_2} \left[\frac{\partial^2}{\partial t^2} (\frac{1}{2}\zeta'^2 - \frac{1}{2}\zeta'^2) - z'\xi - g\zeta \right] dx - \frac{1}{x_2 - x_1} \left[\int_{\zeta_1}^{x'} \xi_2 z dz - \int_{\zeta_1}^{x'} \xi_1 z dz \right] - \frac{2}{x_2 - x_1} [\dot{\alpha}'_2 \dot{\gamma}'_2 \gamma'_2 - \dot{\alpha}'_1 \dot{\gamma}'_1 \gamma'_1 - \dot{\alpha}_2 \dot{\gamma}_2 \gamma_2 + \dot{\alpha}_1 \dot{\gamma}_1 \gamma_1]. \quad (17)$$

The above equation may be put into a form which is independent of the initial instant chosen. For if (u', w') denote the components of velocity in the plane $z = z'$ we have, at the initial instant,

$$\frac{\partial^2}{\partial t^2} (\frac{1}{2}\zeta'^2) = \zeta' \xi' + \xi'^2 = w'^2. \quad (18)$$

Also by considering $D^2(\zeta' - z)/Dt^2$, where D/Dt denotes differentiation following the motion, we find

$$\zeta' = \dot{w}' - \frac{\partial}{\partial x} (u' w'). \quad (19)$$

Similarly

$$\xi'_i = \dot{u}_i - \frac{\partial}{\partial z} (u_i w_i) \quad (i = 1, 2), \quad (20)$$

where (u_i, w_i) are the velocity components in the plane $x = x_i$. Since $(u_i, \dot{\gamma}_i)$ and $(\dot{\alpha}'_i, \dot{\gamma}'_i)$ are equal to the components of velocity at (x_i, ζ) and (x_i, z') , we have finally, after integrating by parts and dropping the dashes,

$$\frac{\bar{p} - \bar{p}_s - gz}{\rho} = \frac{1}{x_2 - x_1} \int_{x_1}^{x_2} \left[\frac{\partial^2}{\partial t^2} (\frac{1}{2}\zeta^2) - w^2 - z\dot{w} - g\zeta \right] dx - \frac{1}{x_2 - x_1} \left[\int_{\zeta}^{z'} (\dot{u}z + uw) dz - (uwz)_{z=\zeta} \right]_{x=x_1}^{x=x_2}. \quad (21)$$

The above equation is now valid for all values of z and t . In equation (21) the first group of terms would give the mean pressure on the plane $z = \text{constant}$ if the planes $x = x_1, x_2$ were assumed to be vertical barriers. The second group of terms gives the correction due to the motion across these planes.

By allowing x_2 to tend to x_1 in equation (21) an expression for the pressure at any given point can be obtained. Thus

$$\frac{\bar{p} - \bar{p}_s - gz}{\rho} = \frac{\partial^2}{\partial t^2} (\frac{1}{2}\zeta^2) - w^2 - z\dot{w} - g\zeta - \frac{\partial}{\partial x} \left[\int_{\zeta}^{z'} (\dot{u}z + uw) dz - (uwz)_{z=\zeta} \right]. \quad (22)$$

It may easily be verified that in a periodic wave motion in deep water the first-order terms on the right-hand side of (22) decrease exponentially with the depth.

Suppose now that the motion is periodic in x with wave-length λ . If we write $x_1 = 0$, $x_2 = \lambda$ in equation (21) the second group of terms then vanishes identically. Further, if the origin is assumed to be in the mean surface level we have

$$\int_0^\lambda g\zeta dx = 0; \quad (23)$$

and since the net flow of water across the plane $z = \text{constant}$ is zero we have also

$$\int_0^\lambda z \bar{w} dx = z \frac{\partial}{\partial t} \int_0^\lambda w dx = 0. \quad (24)$$

Therefore the mean pressure over one wave-length is given by

$$\frac{\bar{p} - \bar{p}_s}{\rho} - gz = \frac{1}{\lambda} \frac{\partial^2}{\partial t^2} \int_0^\lambda \frac{1}{2} \zeta^2 dx - \frac{1}{\lambda} \int_0^\lambda w^2 dx. \quad (25)$$

If, in addition, the motion is irrotational we find by comparison with (5) that the function $\theta(t)$ is given by

$$\theta(t) = \frac{1}{\lambda} \frac{\partial^2}{\partial t^2} \int_0^\lambda \frac{1}{2} \zeta^2 dx + \frac{1}{\lambda} \int_0^\lambda \frac{1}{2} (u^2 - w^2) dx. \quad (26)$$

It may be verified that the second term is independent of z , for

$$\frac{\partial}{\partial z} \int_0^\lambda (u^2 - w^2) dx = \int_0^\lambda \left(u \frac{\partial u}{\partial x} + w \frac{\partial w}{\partial x} \right) dx = [uw]_0^\lambda, \quad (27)$$

which vanishes by the periodicity of the motion. In deep water, since u and w decrease exponentially with depth, the pressure variation at infinite depth is given by

$$\theta(t) = \frac{1}{\lambda} \frac{\partial^2}{\partial t^2} \int_0^\lambda \frac{1}{2} \zeta^2 dx. \quad (28)$$

In water of constant finite depth h the vertical velocity w vanishes when $z = h$. From (25) we see that the mean pressure variation on the bottom is also given by the right-hand side of (28). Thus both the pressure variation at infinite depth and the mean pressure on the bottom in the case of constant finite depth, depend on a second-order function of the wave amplitude, closely associated with changes in the potential energy of the wave train.

It will be noticed that the equations so far obtained are exact, and that no assumptions depending on the smallness of the wave amplitude have been made.

2.3. *The standing wave and progressive wave*

We shall now use the formulae of the previous section to evaluate the mean pressure on the bottom in some special cases of wave motion. This may be done, as we shall see, by consideration of the first approximation only.

Let the water be of constant depth h . Consider a motion which in the first approximation consists of two progressive waves of equal wave-length λ and period T travelling in opposite directions. The equation of the free surface is given by

$$\zeta = a_1 \cos(kx - \sigma t) + a_2 \cos(kx + \sigma t) + O(a^2 k), \quad (29)$$

$$\text{where } k = 2\pi/\lambda, \sigma = 2\pi/T \text{ and } \sigma^2 = gk \tanh kh \quad (30)$$

(Lamb 1932, p. 364). The last term in equation (29) represents a remainder of second or higher order in the wave amplitudes a_1 and a_2 which it will not be necessary to evaluate. When $z = h$, w vanishes, and so from equation (25) the mean pressure \bar{p}_h on the bottom is given by

$$\begin{aligned} \frac{\bar{p}_h - \bar{p}_s}{\rho} - gh &= \frac{1}{\lambda} \frac{\partial^2}{\partial t^2} \int_0^\lambda \frac{1}{2} [a_1 \cos(kx - \sigma t) + a_2 \cos(kx + \sigma t)]^2 dx + O(a^3 \sigma^2 k^2) \\ &= \frac{\partial^2}{\partial t^2} \frac{1}{2} (a_1^2 + a_2^2 + 2a_1 a_2 \cos 2\sigma t) + O(a^3 \sigma^2 k^2) \\ &= -2a_1 a_2 \sigma^2 \cos 2\sigma t, \end{aligned} \quad (31)$$

THEORY OF THE ORIGIN OF MICROSEISMS

9

to the second order of approximation. Thus the mean pressure fluctuation on the bottom is of twice the frequency of the waves and proportional to the product of the wave amplitudes. For a given period T it is also independent of the depth h .

Two special cases are of interest. First, when the amplitude of one of the opposing waves is zero, that is, in the case of a single progressive wave, the right-hand side of equation (31) vanishes. The mean pressure on the bottom is therefore constant. Secondly, when the amplitudes of the two waves are equal and

$$a_1 = a_2 = \frac{1}{2}a, \quad (32)$$

say, we have a standing wave given by

$$\zeta = a \cos kx \cos \sigma t + O(a^2k). \quad (33)$$

From equation (31) we have then

$$\frac{\bar{p}_h - \bar{p}_z}{\rho} - gh = -\frac{1}{2}a^2\sigma^2 \cos 2\sigma t. \quad (34)$$

Therefore in a standing wave the mean pressure on the bottom varies with twice the frequency of the original wave and with an amplitude proportional to the square of the wave amplitude.

Equation (34) was obtained by Miche (1944, p. 73, equation (85)) after evaluating the second approximation to the wave motion in full.

A physical explanation of these two results, and of the difference between them, may be given as follows. Consider first the standing wave given by equation (33). When $t = (n + \frac{1}{2})T$, n being an integer, the wave surface is approximately flat. The centre of gravity of the whole wave train is therefore at its lowest point. On the other hand, when $t = nT$ the wave crests are fully formed and the centre of gravity has risen, since water has been transferred from below to above the mean level (this is equivalent to saying that the potential energy is increased). This raising and lowering of the centre of gravity occurs twice in a complete cycle. But the vertical motion of the centre of gravity of any mass of fluid is determined solely by the vertical external forces acting upon it. Of these, the force due to gravity is constant, and the pressure on the free surface supplies a constant additional downwards force. There remains the pressure on the bottom, which must therefore fluctuate in a similar manner, with twice the frequency of the waves.

In a progressive wave, on the other hand, similar considerations show that the mean pressure on the bottom is constant. For the potential energy, and hence also the centre of mass, of the whole wave train remains at a constant level throughout. There can be therefore no fluctuation in the mean pressure on the bottom.

It should be possible to verify formulae (31) and (34) quite simply by experiment, since these terms represent the only pressure variations measurable at a depth of more than half a wave-length. The water should be almost still at this depth, so that the formation of eddies round the measuring apparatus would be avoided. A standing wave could be produced in a long wave tank by the reflexion of a wave train from a vertical barrier at one end of the tank. If the inclination of the barrier to the horizontal were varied, reflected waves of different amplitude would be obtained, since for small inclinations some energy would almost certainly be absorbed at the barrier itself. In the first-order theory of surface waves the absorption of energy at the barrier cannot be taken into account without assuming a

singularity at the origin, and the amount of energy absorbed is indeterminate. However, by the present method the coefficient of reflexion could be determined experimentally, since the pressure variation on the bottom (at a few wave-lengths from the barrier) is directly proportional to the amplitude of the reflected wave. Hence also some indication could probably be obtained as to the amount of wave reflexion taking place at a steep coast and from beaches of different gradients.

3. GENERAL TYPES OF WAVE MOTION

Perfectly periodic wave trains of standing or progressive type rarely occur in practice, and in the present section we shall consider the pressure variation in wave motions of more general type. When the motion is not perfectly periodic in space the pressure variation at infinite depth, in the sense of § 2.1, no longer exists, but expressions may still be found for the mean pressure or the total force over a given area of the plane $z = \text{constant}$. These assume a simple form provided that the area is large enough for the motion across the boundaries to become negligible.

3.1. *The force on a given area of the plane $z = \text{constant}$*

Still considering motion in two dimensions only, let \mathbf{F} denote the variable part of the total force, per unit distance in the y -direction, acting on the plane $z = z'$ in the interval $-R < x < R$, i.e.

$$\frac{\mathbf{F}}{\rho} = 2R \left(\frac{\bar{p} - p_t}{\rho} - gz \right), \quad (35)$$

where \bar{p} is the mean pressure on the plane $z = z'$ in this interval. Then from equation (21) we have

$$\frac{\mathbf{F}}{\rho} = \int_{-R}^R \left[\frac{\partial^2}{\partial t^2} \left(\frac{1}{2} \zeta^2 \right) - w^2 - z\dot{w} - g\zeta \right] dx - \left[\int_{\zeta}^{z'} (\dot{u}z + uw) dz - (uwz)_{z=\zeta} \right]_{-R}^R. \quad (36)$$

Now since the flow of water across the horizontal plane $z = z'$ ($-R < x < R$) is equal to the net flow across the vertical planes $x = \pm R$ ($z > z'$), we have

$$\int_{-R}^R z\dot{w} dx = \left[z \int_x^h \dot{u} dz \right]_{-R}^R, \quad (37)$$

where h denotes the depth of water (not necessarily constant); if the depth is supposed infinite, the upper limit of the integral must be replaced by ∞ . Similarly, if the mean level of the free surface $z = \zeta$ is zero at time $t = 0$ we have

$$\int_{-R}^R g\zeta dx = \left[\int_0^t dt \int_{\zeta}^h gu dz \right]_{-R}^R. \quad (38)$$

Hence from equation (36), after integrating by parts,

$$\begin{aligned} \frac{\mathbf{F}}{\rho} = \int_{-R}^R \left[\frac{\partial^2}{\partial t^2} \left(\frac{1}{2} \zeta^2 \right) - w^2 \right] dx - \left[z \int_{\zeta}^h \dot{u} dz - g \int_0^t dt \int_{\zeta}^h u dz \right]_{-R}^R \\ - \left[\int_{\zeta}^h \left\{ \int_{\zeta}^h \dot{u} dz + uw \right\} dz - (uwz)_{z=\zeta} \right]_{-R}^R. \end{aligned} \quad (39)$$

THEORY OF THE ORIGIN OF MICROSEISMS

Let us consider the relative magnitudes of the terms in equation (39). We suppose that the motion is wave-like, in the sense that the energy is nearly all confined to a narrow range of frequencies in the frequency spectrum (as defined in § 3.2); and that the mean frequency $\sigma/2\pi$ corresponds to a wave-length λ which is small compared with R . In general, the relative phase of the motion at two widely separated points of the x -axis will be random. We may, however, suppose that the motion is regular and periodic over any interval of the x -axis less than or equal to $2R_1$, say. We suppose also that the motion is initially confined to an interval $-R_2 < x < R_2$ (where R_2 may be very great compared with R_1), that is, that the elevation and vertical velocity of the free surface at points outside this interval are initially zero. There will be three distinct cases:

Case 1. $R \leq R_1$, i.e. the motion is regular over the whole interval $-R < x < R$. Then

$$\int_{-R}^R \left[\frac{\partial^2}{\partial t^2} \left(\frac{1}{2} \zeta^2 \right) - w^2 \right] dx \quad (40)$$

is of order $a^2 \sigma^2 R$, where a is the maximum wave elevation. If we assume for the moment that u and w are of order $a\sigma$ and that

$$\left[\int_{\zeta}^z u dz \right]_{-R}^R \quad (41)$$

is of order $a\sigma\lambda$ for all z , the remaining terms in (39) are of order $a\sigma^2\lambda z$ or $a\sigma^2\lambda^2$ at the most (if g is of order $\lambda\sigma^2$). Hence if R/k and R/z were sufficiently large we should have

$$\frac{F}{\rho} = \int_{-R}^R \left[\frac{\partial^2}{\partial t^2} \left(\frac{1}{2} \zeta^2 \right) - w^2 \right] dx \quad (42)$$

approximately. It must, however, be verified that these second-order pressure variations, which are in phase over the whole interval, do not produce any significant motion across the planes $x = \pm R$. Now if we consider the displacement produced by the pressure distribution

$$\frac{p}{\rho} = \begin{cases} 2a^2\sigma^2 \cos 2\sigma t & (|x| < R), \\ 0 & (|x| > R), \end{cases} \quad (43)$$

acting on the upper surface of deep water we find that the velocities in the planes $x = \pm R$ are of order $a^2\sigma/\lambda$ (we ignore a logarithmic singularity at $z = 0$, which is due to the local discontinuity in pressure), and that the total flow (41) is of order $a^2\sigma \log(R/\lambda)$. The assumption that (41) is of order independent of R therefore needs slight modification in this case, but since $\log(R/\lambda)$ is small compared with R/λ the validity of equation (42) is not affected.

When z is small compared with λ the approximation (42) is valid under the condition $Ra/\lambda^2 \ll 1$. However, the first-order terms in (39), taken together, may be expected to decrease rapidly with the depth, and when z is greater than about $\frac{1}{2}\lambda$ the largest terms in the remainder will arise from the unattenuated pressure variations of second order. Hence (42) will be valid under the less restrictive conditions $R/\lambda \gg 1$ and $R/z \gg 1$. Since the second term in (42) will be small compared with the first we shall then have

$$\frac{F}{\rho} = \frac{\partial^2}{\partial t^2} \int_{-R}^R \frac{1}{2} \zeta^2 dx. \quad (44)$$

In particular (44) will be valid if z is of order λ and $R/\lambda \gg 1$.

Case 2. $R_1 < R \leq R_2$. In this case suppose the interval $-R < x < R$ to be divided into smaller intervals of length less than or equal to $2R_1$. We assume that the motion in each of the smaller



M. S. LONGUET-HIGGINS ON A

12

intervals is regular but that the phase differences between successive intervals are random. Since the sum of n vectors of comparable magnitude in random-phase relationship with one another increases like $n^{1/2}$ the integral (40) will be of order $a^2\sigma^2R_1(R/R_1)^{1/2}$. If we assume that the velocities are bounded and that the total flow across any plane $x = \text{constant}$ is of order $a\sigma\lambda$ or $a^2\sigma \log(R_1/\lambda)$ at most, equations (42) and (44) will be valid under conditions similar to case 1; in particular, (44) will hold if z is of order λ and $(RR_1)^{1/2}/\lambda \gg 1$.

Case 3. $R > R_2$. By allowing R to tend to infinity an exact expression for the total force \mathbf{F} over the whole plane $z = \text{constant}$ may be obtained. The velocity potential of the motion due to an initial elevation of the free surface concentrated in the line $x = z = 0$ is proportional to $gtz(x^2 + z^2)^{-1}$, when $gt^2(x^2 + z^2)^{-1}$ is small (see Lamb 1932, § 238). A similar result will hold when the initial disturbance is distributed over a finite interval of the x -axis. Hence for very large R the velocities across the planes $x = \pm R$ will initially be proportional to R^{-2} , and the total flow (41) will be proportional to R^{-1} . The terms in (39) to be evaluated at the planes $x = \pm R$ therefore tend to zero. But since the total potential energy is finite, we may assume that the first integral in (39) converges. Hence the total force \mathbf{F} over the whole plane is given by

$$\frac{\mathbf{F}}{\rho} = \int_{-\infty}^{\infty} \left[\frac{\partial^2}{\partial t^2} \left(\frac{1}{2} \zeta^2 \right) - w^2 \right] dx. \quad (45)$$

When z is greater than about $\frac{1}{2}\lambda$ the second term in the integrand will be small compared with the first, so that

$$\frac{\mathbf{F}}{\rho} = \frac{\partial^2}{\partial t^2} \int_{-\infty}^{\infty} \frac{1}{2} \zeta^2 dx \quad (46)$$

approximately.

The previous results may be extended without difficulty to motion in three dimensions. Let \bar{p} denote the mean pressure on the plane $z = \text{constant}$ inside the square S given by $-R < x < R$, $-R < y < R$, and let \mathbf{F} denote the variable part of the total force acting on the plane inside S , i.e.

$$\frac{\mathbf{F}}{\rho} = 4R^2 \left(\frac{\bar{p} - \bar{p}_z}{\rho} - gz \right). \quad (47)$$

If the motion inside S is assumed to be wave-like with mean wave-length λ then we may establish that

$$\frac{\mathbf{F}}{\rho} = \int_{-R}^R \int_{-R}^R \left[\frac{\partial^2}{\partial t^2} \left(\frac{1}{2} \zeta^2 \right) - w^2 \right] dx dy \quad (48)$$

under similar conditions; in particular, if z is comparable with λ , and R/λ and $(RR_1)^{1/2}/\lambda$ are both large compared with unity, where $2R_1$ is the side of the largest square over which the second-order pressure variations are effectively in phase. Since the motion diminishes rapidly with depth, we shall have in this case also

$$\frac{\mathbf{F}}{\rho} = \frac{\partial^2}{\partial t^2} \int_{-R}^R \int_{-R}^R \frac{1}{2} \zeta^2 dx dy. \quad (49)$$

If it is supposed that the motion is initially confined to a finite region of the (x, y) plane we may show that the motion produces a force \mathbf{F} over the whole plane given by

$$\frac{\mathbf{F}}{\rho} = \int_{-\infty}^{\infty} \int_{-\infty}^{\infty} \left[\frac{\partial^2}{\partial t^2} \left(\frac{1}{2} \zeta^2 \right) - w^2 \right] dx dy. \quad (50)$$

Again, when z is greater than about $\frac{1}{2}\lambda$ we have approximately

$$\frac{\mathbf{F}}{\rho} = \frac{\partial^2}{\partial t^2} \int_{-\infty}^{\infty} \int_{-\infty}^{\infty} \frac{1}{2} \zeta^2 dx dy. \quad (51)$$

THEORY OF THE ORIGIN OF MICROSEISMS

3.2. *The two-dimensional frequency spectrum*

In order to be able to describe the motion of the sea surface in terms of its frequency characteristics, we shall now introduce the two-dimensional frequency spectrum. The mean pressure, or total force, over a large area may be derived immediately from the frequency spectrum owing to the connexion of the mean pressure with the potential energy of the waves.

Any continuous and absolutely integrable function $f(x, y)$ of two variables may be expressed in the form

$$f(x, y) = \Re \int_{-\infty}^{\infty} \int_{-\infty}^{\infty} F(u, v) e^{i(ukx+vk y)} du dv \quad (52)$$

$$\text{or} \quad f(x, y) = \int_{-\infty}^{\infty} \int_{-\infty}^{\infty} \frac{1}{2} [F(u, v) + F^*(-u, -v)] e^{i(ukx+vk y)} du dv, \quad (53)$$

$$\text{where} \quad \frac{1}{2} [F(u, v) + F^*(-u, -v)] = (k/2\pi)^2 \int_{-\infty}^{\infty} \int_{-\infty}^{\infty} f(x, y) e^{-i(ukx+vk y)} dx dy, \quad (54)$$

provided that the right-hand side of (54) is also absolutely integrable (Bochner 1932, § 44). In the above equations \Re denotes the real part and F^* denotes the conjugate complex function of F . The value of

$$\frac{1}{2} [F(u, v) - F^*(-u, -v)] \quad (55)$$

is still indeterminate.

Let $z = \zeta$ be the equation of the free surface in any wave motion in two horizontal dimensions. We shall assume the general conditions necessary for the validity of the following work, and in particular the possibility of differentiating under the integral sign. Suppose then that the values of ζ and $\partial\zeta/\partial t$ at the initial instant $t = 0$ are expanded in the forms

$$(\zeta)_{t=0} = \Re \int_{-\infty}^{\infty} \int_{-\infty}^{\infty} A e^{i(ukx+vk y)} du dv, \quad (56)$$

$$\left(\frac{\partial\zeta}{\partial t}\right)_{t=0} = \Re \int_{-\infty}^{\infty} \int_{-\infty}^{\infty} B e^{i(ukx+vk y)} du dv, \quad (57)$$

A and B being functions of (u, v) . We may impose the further condition

$$B = i\sigma A \quad (58)$$

where σ is the positive function of u and v given by

$$\sigma^2 = (u^2 + v^2)^{\frac{1}{2}} gk \tanh(u^2 + v^2)^{\frac{1}{2}} kh. \quad (59)$$

By equation (54) we have then, using equation (58),

$$\frac{1}{2}(A + A^*) = (k/2\pi)^2 \int_{-\infty}^{\infty} \int_{-\infty}^{\infty} (\zeta)_{t=0} e^{-i(ukx+vk y)} dx dy, \quad (60)$$

$$\frac{1}{2}(i\sigma A - i\sigma A^*) = (k/2\pi)^2 \int_{-\infty}^{\infty} \int_{-\infty}^{\infty} \left(\frac{\partial\zeta}{\partial t}\right)_{t=0} e^{-i(ukx+vk y)} dx dy, \quad (61)$$

where A_{-} denotes $A(-u, -v)$. These last equations are equivalent to the single equation

$$A = (k/2\pi)^2 \int_{-\infty}^{\infty} \int_{-\infty}^{\infty} \left(\zeta + \frac{1}{i\sigma} \frac{\partial\zeta}{\partial t}\right)_{t=0} e^{-i(ukx+vk y)} dx dy. \quad (62)$$

Consider now the expression

$$\eta = \Re \int_{-\infty}^{\infty} \int_{-\infty}^{\infty} A e^{i(ukx+vk y + \sigma t)} du dv, \quad (63)$$

where A is determined by (62). The expression under the integral sign represents a wave whose crests are parallel to the line

$$ux + vy = 0, \quad (64)$$

and whose wave-length λ is given by

$$\lambda = \frac{2\pi}{(u^2 + v^2)^{1/2} k}. \quad (65)$$

By equation (59) this wave satisfies the period equation for waves in water of constant depth h , and hence η is also a solution, to the first order of approximation. But from (5) and (57) we have

$$(\zeta)_{t=0} = (\eta)_{t=0}, \quad \left(\frac{\partial \zeta}{\partial t}\right)_{t=0} = \left(\frac{\partial \eta}{\partial t}\right)_{t=0}. \quad (66)$$

Now an irrotational motion is uniquely determined by the initial values of the surface elevation and its rate of change with time (for the difference between two motions with the same initial conditions has initially no kinetic or potential energy). It follows that $\zeta = \eta$, i.e.

$$\zeta = \Re \int_{-\infty}^{\infty} \int_{-\infty}^{\infty} A e^{i(ukx + vky + \sigma t)} du dv \quad (67)$$

for all times t .

Any given free motion of the sea surface may therefore be analyzed (in the first approximation) into the sum of a number of wave components of all possible wave-lengths and travelling in all possible directions. This analysis, by equation (62), is unique. Each wave component corresponds to a vector \overline{OP} in the (x, y) plane drawn from the origin to the point $P(-uk, -vk)$. The direction of \overline{OP} gives the direction of propagation of the wave, and the length of \overline{OP} is, from equation (65), equal to 2π divided by the wave-length. Wave components of the same length will correspond to points P lying on the same circle centre O , and diametrically opposite points will correspond to wave components of the same wave-length but travelling in opposite directions. Such pairs of wave components play an important part in the following theory and will be called opposite wave components.

Equation (67) may also be written in the form

$$\zeta = \int_{-\infty}^{\infty} \int_{-\infty}^{\infty} \frac{1}{2} (A e^{i\sigma t} + A^* e^{-i\sigma t}) e^{i(ukx + vky)} du dv. \quad (68)$$

Hence by an extension of the Parseval-Plancherel theorem (Bochner 1932, §§ 41.5 and 44.8) we have

$$\int_{-\infty}^{\infty} \int_{-\infty}^{\infty} \zeta^2 dx dy = (2\pi/k)^2 \int_{-\infty}^{\infty} \int_{-\infty}^{\infty} \left| \frac{1}{2} (A e^{i\sigma t} + A^* e^{-i\sigma t}) \right|^2 du dv, \quad (69)$$

since the integral on the left-hand side is convergent. After simplifying the right-hand side, we have

$$\int_{-\infty}^{\infty} \int_{-\infty}^{\infty} \frac{1}{2} \zeta^2 dx dy = \Re(\pi/k)^2 \int_{-\infty}^{\infty} \int_{-\infty}^{\infty} (AA^* + AA_- e^{2i\sigma t}) du dv. \quad (70)$$

Thus the potential energy of the motion is given by

$$\Re \rho g (\pi/k)^2 \int_{-\infty}^{\infty} \int_{-\infty}^{\infty} (AA^* + AA_- e^{2i\sigma t}) du dv. \quad (71)$$

Similarly, we find for the kinetic energy

$$\Re \rho g (\pi/k)^2 \int_{-\infty}^{\infty} \int_{-\infty}^{\infty} (AA^* - AA_- e^{2i\sigma t}) du dv, \quad (72)$$

THEORY OF THE ORIGIN OF MICROSEISMS

and so the total energy is given by

$$2\rho g(\pi/k)^2 \int_{-\infty}^{\infty} \int_{-\infty}^{\infty} AA^* du dv \quad (73)$$

(the above integral being real). The total energy therefore depends only upon the square of the modulus of the wave amplitude $A(u, v)$. On the other hand, both the potential and the kinetic energies separately vary with the time and depend on the product AA_- .

3.3. Pressure variations in terms of the frequency spectrum

We are now in a position to determine the general conditions for a variation in the mean pressure or total force acting on a large area of the plane $z = \text{constant}$. We consider first the simpler case when the area includes the whole (x, y) plane.

From equations (68) and (69) we have

$$\begin{aligned} \frac{\mathbf{F}}{\rho} &= \Re(\pi/k)^2 \frac{\partial^2}{\partial t^2} \int_{-\infty}^{\infty} \int_{-\infty}^{\infty} (AA^* + AA_- e^{2i\sigma t}) du dv \\ &= -\Re 4(\pi/k)^2 \int_{-\infty}^{\infty} \int_{-\infty}^{\infty} AA_- \sigma^2 e^{2i\sigma t}. \end{aligned} \quad (74)$$

Now A and A_- are the complex amplitudes of opposite wave-components in the frequency-spectrum. It follows from (74) that

(1) Variations in \mathbf{F} arise only from opposite pairs of wave components in the frequency spectrum.

(2) The contribution to \mathbf{F} from any opposite pair of wave components is of twice their frequency and proportional to the product of their amplitudes.

(3) The total force \mathbf{F} is the integrated sum of the contributions from all opposite pairs of wave components separately.

A wave group may be defined as a motion in which most of the energy is confined to a small region of the (u, v) plane, excluding the origin. Thus a single group of waves will not cause variations in the total force \mathbf{F} . In order that \mathbf{F} should be appreciable the motion must contain at least two wave groups which are opposite, in the sense that some wave components of the first group are opposite to some wave components of the second.

In practice we must consider the force \mathbf{F} over only a finite region of the (x, y) plane. Let this be the square S ($-R < x < R$, $-R < y < R$). We define a hypothetical motion ζ' such that at any time ζ' and $\partial\zeta'/\partial t$ are equal to the corresponding values of ζ and $\partial\zeta/\partial t$ inside S and zero outside. This motion will not satisfy the equations of motion, especially near the boundaries of S , but we shall now have

$$\frac{\mathbf{F}}{\rho} = \frac{\partial^2}{\partial t^2} \int_{-R}^R \int_{-R}^R \frac{1}{2} \zeta'^2 dx dy = \frac{\partial^2}{\partial t^2} \int_{-\infty}^{\infty} \int_{-\infty}^{\infty} \frac{1}{2} \zeta'^2 dx dy. \quad (75)$$

We also define $A'(u, v; t)$ by the equations

$$\left. \begin{aligned} \zeta' &= \Re \int_{-\infty}^{\infty} \int_{-\infty}^{\infty} A' e^{i(ukx + vky + \sigma t)} du dv, \\ \frac{\partial \zeta'}{\partial t} &= \Re \int_{-\infty}^{\infty} \int_{-\infty}^{\infty} i\sigma A' e^{i(ukx + vky + \sigma t)} du dv. \end{aligned} \right\} \quad (76)$$

Then we have, as before,

$$A' e^{i\sigma t} = (k/2\pi)^2 \int_{-\infty}^{\infty} \int_{-\infty}^{\infty} \left(\zeta' + \frac{1}{i\sigma} \frac{\partial \zeta'}{\partial t} \right) e^{-i(ukx + vky)} dx dy. \quad (77)$$

If the actual motion is given by equation (67) we have on substitution in (77)

$$\begin{aligned}
 A'(u, v; t) &= (k/2\pi)^2 \int_{-R}^R \int_{-R}^R dx dy \int_{-\infty}^{\infty} \int_{-\infty}^{\infty} du_1 dv_1 \\
 &\quad \times \frac{1}{2} \left[A(u_1, v_1) \left(1 + \frac{\sigma_1}{\sigma} \right) e^{-i[(u-u_1)kx + (v-v_1)ky + (\sigma-\sigma_1)t]} \right. \\
 &\quad \left. + A^*(u_1, v_1) \left(1 - \frac{\sigma_1}{\sigma} \right) e^{-i[(u+v_1)kx + (v+v_1)ky + (\sigma+\sigma_1)t]} \right], \quad (78)
 \end{aligned}$$

where σ is written for $\sigma(u_1, v_1)$. Since k is still at our disposal we may put

$$2\pi/k = 2R. \quad (79)$$

Then, after integration with respect to x and y , we find

$$\begin{aligned}
 A'(u, v; t) &= \frac{1}{2} \int_{-\infty}^{\infty} \int_{-\infty}^{\infty} A(u_1, v_1) \left(1 + \frac{\sigma_1}{\sigma} \right) \frac{\sin(u-u_1)\pi}{(u-u_1)\pi} \frac{\sin(v-v_1)\pi}{(v-v_1)\pi} e^{-i(\sigma-\sigma_1)t} du_1 dv_1 \\
 &\quad + \frac{1}{2} \int_{-\infty}^{\infty} \int_{-\infty}^{\infty} A^*(u_1, v_1) \left(1 - \frac{\sigma_1}{\sigma} \right) \frac{\sin(u+u_1)\pi}{(u+u_1)\pi} \frac{\sin(v+v_1)\pi}{(v+v_1)\pi} e^{-i(\sigma+\sigma_1)t} du_1 dv_1 \\
 &= I_1 + I_2, \quad (80)
 \end{aligned}$$

say. Now by hypothesis the frequency spectrum of ζ consists chiefly of waves whose wave-length, given by (65), is small compared with $2R$. From (79) it follows that $A(u_1, v_1)$ is appreciably large only when $(u_1^2 + v_1^2)^{\frac{1}{2}}$ is large. But the factors in the denominators of I_1 and I_2 make the integrands small except when $(u_1, v_1) \doteq (u, v)$ in the first case and $(u_1, v_1) \doteq (-u_1, -v_1)$ in the second. In either case $\sigma_1 \doteq \sigma$, so that the contribution from I_2 is small, while that from I_1 gives

$$A'(u, v; t) \doteq \int_{-\infty}^{\infty} \int_{-\infty}^{\infty} A(u_1, v_1) \frac{\sin(u-u_1)\pi}{(u-u_1)\pi} \frac{\sin(v-v_1)\pi}{(v-v_1)\pi} e^{-i(\sigma-\sigma_1)t} du_1 dv_1. \quad (81)$$

Although A' is dependent upon t , the integrals for $\partial A'/\partial t$, $\partial^2 A'/\partial t^2$, ... contain factors $(\sigma - \sigma_1)$, $(\sigma - \sigma_1)^2$, ... which are small over the critical range of integration near (u, v) . These expressions are therefore small, and A' is only a slowly varying quantity.

From equations (75) we have then

$$\begin{aligned}
 \frac{\mathbf{F}}{\rho} &= \Re(\pi/k)^2 \frac{\partial^2}{\partial t^2} \int_{-\infty}^{\infty} \int_{-\infty}^{\infty} (A' A'^* + A' A'_- e^{2i\sigma t}) du dv \\
 &= -\Re \mathcal{A}(\pi/k)^2 \int_{-\infty}^{\infty} \int_{-\infty}^{\infty} A' A'_- \sigma^2 e^{2i\sigma t} du dv. \quad (82)
 \end{aligned}$$

The expression for the force \mathbf{F} over a finite area is therefore similar to that over the whole plane, except that the original spectrum A is replaced by the new spectrum A' . Equation (81) shows that A' is the weighted mean of 'neighbouring' wave components in the original spectrum. Conversely each wave component in the original spectrum contributes to 'neighbouring' components of the new spectrum. From equations (65) and (79), the number of wave-lengths of any wave component intercepted on the x -axis inside S is u , and the corresponding number on the y -axis is v . The width of the spread pattern in (81) is of order unity. Hence, for this purpose, 'neighbouring' wave components are those such that the number of

THEORY OF THE ORIGIN OF MICROSEISMS

wave-lengths intercepted on any diameter of S does not differ by more than 2 or 3 from the corresponding number for the original wave component.

The replacement of the 'sharp' spectrum A by the 'blurred' spectrum A' may be considered as the result of our inability to define the spectrum exactly from a knowledge of the conditions over only a limited region. For practical purposes, however, the amount of blurring will not usually affect the frequency characteristics of F to a very great extent.

4. WAVE MOTION IN A HEAVY COMPRESSIBLE FLUID

In the present investigation the water has so far been treated as incompressible. This assumption is only valid so long as the time taken for a disturbance to be propagated to the bottom is small compared with the period of the waves, that is,

$$h/c \ll T \quad \text{or} \quad h \ll cT, \quad (83)$$

where c is the velocity of sound in water. For ocean waves h may be of the order of several kilometres, c is about 1.4 km./sec. and T lies between about 5 and 20 sec. The condition (83) is therefore no longer satisfied. It follows that in practice the compressibility of the water must be taken into account.

Surface waves in a heavy compressible fluid were first considered by Pidduck (1910, 1912) in connexion with the propagation of an impulse applied to the surface of the water. His method involves the neglect of squares and products of the displacements and is thus only a first-order theory. The relation obtained by him between the period and wave-length of the waves was discussed by Whipple & Lee (1935), who showed that for waves of a few seconds' period two possible types exist. On the one hand there is a motion approximating very nearly to an ordinary surface wave in incompressible fluid, in which the particle displacement decreases exponentially downwards (to the first order). This may be called a gravity-type wave. On the other hand, there are long waves controlled chiefly by the compressibility of the medium, and hardly attenuated at all with depth. These may be called compression-type waves. Stoncley (1926) and Scholte (1943) have in addition taken into account the elasticity of the sea bed. Here again the two types of wave may be distinguished.

The pressure variations of particular interest to us are, however, of the second order, and to investigate these it will be necessary to work to the second approximation. In the following we shall consider a case of special interest, namely, the motion which in the first approximation is a standing wave of gravity type. We shall find that in the second approximation long compression-type waves appear. One consequence of this is that in the second-order theory pure gravity-type or pure compression-type waves do not in general exist; the one type of wave cannot exist without the other. As a compensating advantage, however, our work leads us to the distinction of two definite regions of the fluid in one of which gravity, and in the other compressibility, is the controlling factor.

4.1. *General equations*

Take Cartesian axes (x, y, z) with the origin in the undisturbed free surface, the y -axis parallel to the wave crests, and the z -axis vertically downwards. It is assumed that the motion is periodic in the x -direction with wave-length λ . Let $z = h$ be the equation of the rigid bottom and $z = \zeta$ the equation of the free surface. Also let \mathbf{u} = velocity, p = pressure,

M. S. LONGUET-HIGGINS ON A

ρ = density, and let p_s and ρ_s denote the (constant) values of p and ρ at the free surface. We shall assume that viscosity is negligible and that the velocity is irrotational, so that

$$\mathbf{u} = -\text{grad } \phi. \quad (84)$$

We assume also that ρ is a function of p only. Then the equations of motion may be integrated (Lamb 1932, § 20) to give

$$\frac{\partial \phi}{\partial t} - \frac{1}{2} \mathbf{u}^2 + gz - P = 0, \quad (85)$$

where ϕ contains an arbitrary function of the time t and where

$$P = \int_{\rho_s, p}^{\rho, p} \rho \frac{dp}{\rho}. \quad (86)$$

We assume, lastly, as the relation connecting p and ρ ,

$$\frac{dp}{d\rho} = c^2 = \text{constant}, \quad (87)$$

that is, the velocity of sound c in the medium is constant. Then from equation (86)

$$P = c^2 \int_{\rho_s, p}^{\rho, p} \rho \frac{dp}{\rho} = c^2 \log(\rho/\rho_s). \quad (88)$$

Now the equation of continuity may be written

$$\frac{D\rho}{Dt} - \rho \nabla^2 \phi = 0, \quad (89)$$

where D/Dt denotes differentiation following the motion. Hence

$$\nabla^2 \phi = \frac{1}{\rho} \frac{D\rho}{Dt} = \frac{D}{Dt} (\log \rho), \quad (90)$$

and so from (88)

$$\nabla^2 \phi = \frac{1}{c^2} \frac{DP}{Dt}. \quad (91)$$

On eliminating P between equations (85) and (91) we have

$$\begin{aligned} c^2 \nabla^2 \phi &= \frac{D}{Dt} \left(\frac{\partial \phi}{\partial t} - \frac{1}{2} \mathbf{u}^2 + gz \right) \\ &= \frac{\partial^2 \phi}{\partial t^2} - \frac{\partial}{\partial t} \left(\frac{1}{2} \mathbf{u}^2 \right) + \mathbf{u} \cdot \text{grad } \frac{\partial \phi}{\partial t} - \mathbf{u} \cdot \text{grad } \left(\frac{1}{2} \mathbf{u}^2 \right) - g \frac{\partial \phi}{\partial z}. \end{aligned} \quad (92)$$

But
$$\mathbf{u} \cdot \text{grad } \frac{\partial \phi}{\partial t} = \mathbf{u} \cdot \frac{\partial}{\partial t} (\text{grad } \phi) = -\frac{\partial}{\partial t} \left(\frac{1}{2} \mathbf{u}^2 \right) \quad (93)$$

Hence
$$\frac{\partial^2 \phi}{\partial t^2} - c^2 \nabla^2 \phi - g \frac{\partial \phi}{\partial z} - \frac{\partial}{\partial t} \left(\frac{1}{2} \mathbf{u}^2 \right) - \mathbf{u} \cdot \text{grad } \left(\frac{1}{2} \mathbf{u}^2 \right) = 0. \quad (94)$$

This is our differential equation for ϕ . We consider now the conditions to be satisfied at the boundaries.

The boundary condition in the plane $z = h$ is simply

$$\left(\frac{\partial \phi}{\partial z} \right)_{z=h} = 0. \quad (95)$$

THEORY OF THE ORIGIN OF MICROSEISMS

At the free surface $z = \zeta$ we have $p = p_s$, and therefore

$$P_{z=\zeta} = 0. \quad (96)$$

Thus from equation (85)
$$\left(\frac{\partial\phi}{\partial t} - \frac{1}{2}u^2 + gz\right)_{z=\zeta} = 0. \quad (97)$$

Since a particle in the free surface always remains in the free surface we have also

$$\left(\frac{DP}{Dt}\right)_{-z} = 0, \quad (98)$$

and so from (91)

$$(\nabla^2\phi)_{z=\zeta} = 0. \quad (99)$$

Equations (97) and (99) are to be satisfied at the surface $z = \zeta$. It is more convenient, however, to replace these by conditions to be satisfied in the plane $z = 0$. This may be done by expanding the equations in a Taylor series as follows:

$$\left(\frac{\partial\phi}{\partial t} - \frac{1}{2}u^2\right)_{z=0} + \zeta\left(\frac{\partial^2\phi}{\partial t\partial z} - u \cdot \frac{\partial u}{\partial z} + g\right)_{z=0} + \dots = 0 \quad (100)$$

and

$$(\nabla^2\phi)_{z=0} + \zeta\left(\frac{\partial}{\partial z} \nabla^2\phi\right)_{z=0} + \dots = 0. \quad (101)$$

In order to define the solution completely it is necessary to add a further condition derived from the assumption that the origin is in the undisturbed free surface. Since the mass contained below the free surface is the same as in the undisturbed state we have

$$\int_0^\lambda dx \int_\zeta^h \rho dz = \int_0^\lambda dx \int_0^h \rho_0 dz, \quad (102)$$

where a suffix 0 denotes the value in the undisturbed state. Equation (102) may be written

$$\int_0^\lambda dx \int_0^h (\rho - \rho_0) dz - \int_0^\lambda dx \int_0^\zeta \rho dz = 0. \quad (103)$$

In the second term let ρ be expanded in a Taylor series from $z = 0$. After integrating with respect to z we have

$$\int_0^\lambda dx \int_0^h (\rho - \rho_0) dz - \int_0^\lambda dx \left[\zeta\rho_{z=0} + \frac{1}{2}\zeta^2\left(\frac{\partial\rho}{\partial z}\right)_{z=0} + \dots \right] = 0. \quad (104)$$

From equations (85) and (88), ρ is given in terms of ϕ by

$$\rho/\rho_s = e^{p/c^2} = e^{(\partial\phi/\partial t - \frac{1}{2}u^2 + gz)/c^2} \quad (105)$$

so that

$$\rho_0/\rho_s = e^{gz/c^2}. \quad (106)$$

We also have, from (87),

$$p - p_s = c^2(\rho - \rho_s), \quad (107)$$

$$p_0 - p_s = c^2\rho_s e^{gz/c^2 - 1}. \quad (108)$$

We seek solutions for ϕ by a method of successive approximations. Let

$$\left. \begin{aligned} \phi &= \epsilon\phi_1 + \epsilon^2\phi_2 + \dots, \\ \mathbf{u} &= \epsilon\mathbf{u}_1 + \epsilon^2\mathbf{u}_2 + \dots, \\ \zeta &= \epsilon\zeta_1 + \epsilon^2\zeta_2 + \dots, \\ p - p_0 &= \epsilon p_1 + \epsilon^2 p_2 + \dots, \\ \rho - \rho_0 &= \epsilon\rho_1 + \epsilon^2\rho_2 + \dots, \end{aligned} \right\} \quad (109)$$

M. S. LONGUET-HIGGINS ON A

where ϵ is a small parameter. On substituting in equations (94), (95) and (101) and equating coefficients of the first power of ϵ we have

$$\left. \begin{aligned} \frac{\partial^2 \phi_1}{\partial t^2} - c^2 \nabla^2 \phi_1 - g \frac{\partial \phi_1}{\partial z} &= 0, \\ \left(\frac{\partial \phi_1}{\partial z} \right)_{z=h} &= 0, \\ (\nabla^2 \phi_1)_{z=0} &= 0, \end{aligned} \right\} \quad (110)$$

and from equations (84), (100), (105) and (107)

$$\left. \begin{aligned} \mathbf{u}_1 &= -\text{grad } \phi_1, \\ g \zeta_1 &= - \left(\frac{\partial \phi_1}{\partial t} \right)_{z=0}, \\ \rho_1 / \rho_s &= c^2 \rho_1 / \rho_s = \frac{\partial \phi_1}{\partial t} e^{2\gamma z}, \end{aligned} \right\} \quad (111)$$

where $\gamma = g/2c^2$. Similarly for the second approximation we find

$$\left. \begin{aligned} \frac{\partial^2 \phi_2}{\partial t^2} - c^2 \nabla^2 \phi_2 - g \frac{\partial \phi_2}{\partial z} &= \frac{\partial}{\partial t} (\mathbf{u}_1^2), \\ \left(\frac{\partial \phi_2}{\partial z} \right)_{z=h} &= 0, \\ (\nabla^2 \phi_2)_{z=0} &= -\zeta_1 \left(\frac{\partial}{\partial z} \nabla^2 \phi_1 \right)_{z=0}, \end{aligned} \right\} \quad (112)$$

and

$$\left. \begin{aligned} \mathbf{u}_2 &= -\text{grad } \phi_2, \\ g \zeta_2 &= - \left(\frac{\partial \phi_2}{\partial t} - \frac{1}{2} \mathbf{u}_1^2 \right)_{z=0} - \zeta_1 \left(\frac{\partial^2 \phi_1}{\partial z \partial t} \right)_{z=0}, \\ \rho_2 / \rho_s &= c^2 \rho_2 / \rho_s = \left[\frac{\partial \phi_2}{\partial t} - \frac{1}{2} \mathbf{u}_1^2 + \frac{1}{2c^2} \left(\frac{\partial \phi_1}{\partial t} \right)^2 \right] e^{2\gamma z}. \end{aligned} \right\} \quad (113)$$

On substituting for ρ and ζ in equation (104) and equating coefficients of ϵ and ϵ^2 we obtain the further conditions on ϕ_1 and ϕ_2

$$2\gamma \int_0^\lambda dx \int_0^h dz \frac{\partial \phi_1}{\partial t} e^{2\gamma z} + \int_0^\lambda dx \left(\frac{\partial \phi_1}{\partial t} \right)_{z=0} = 0 \quad (114)$$

and

$$\begin{aligned} &2\gamma \int_0^\lambda dx \int_0^h dz \frac{\partial \phi_2}{\partial t} e^{2\gamma z} + \int_0^\lambda dx \left(\frac{\partial \phi_2}{\partial t} \right)_{z=0} \\ &= 2\gamma \int_0^\lambda dx \int_0^h dz \left[\frac{1}{2} \mathbf{u}_1^2 - \frac{1}{2c^2} \left(\frac{\partial \phi_1}{\partial t} \right)^2 \right] e^{2\gamma z} + \int_0^\lambda dx \left[\frac{1}{2} \mathbf{u}_1^2 + \frac{1}{g} \frac{\partial \phi_1}{\partial t} \frac{\partial^2 \phi_1}{\partial z \partial t} - \frac{1}{2c^2} \left(\frac{\partial \phi_1}{\partial t} \right)^2 \right]_{z=0}. \end{aligned} \quad (115)$$

Suppose that ϕ and ζ are any periodic functions satisfying equations (94), (95), (100) and (101). If P and ρ are defined by (105) then these equations imply also (89), (96) and (98). Provided $\text{grad } P$ is not identically zero, (96) and (98) show that $z = \zeta$ is a surface moving with the fluid. But since the equation of continuity (89) is satisfied, it follows that the left-hand side of (102), (103) or (104) is at most a constant. Hence any periodic solution $\phi_1 = \phi_1^*$ of equations (110) must make the left-hand side of equation (114) a constant, say C_1^* . Then a solution of (114) is given by

$$\phi_1 = \phi_1^* - C_1^* e^{-2\gamma h t}. \quad (116)$$

THEORY OF THE ORIGIN OF MICROSEISMS

But this also satisfies equations (110). Hence if ϕ_1^* is any periodic solution of (110) a solution of all four equations (110) and (114) may be found by adding to ϕ_1^* a constant multiple of t (that is, by increasing the pressure uniformly). Similarly if ϕ_2^* is any periodic solution of (112) a solution of all four equations (112) and (115) may be found by adding to ϕ_2^* a constant multiple of t . These results may be verified directly by differentiating equations (114) and (115) with respect to t and using equations (110) and (112).

4.2. First approximation and period equation

Let us assume for ϕ_1 a simple progressive wave of the form

$$\phi_1 = Z(z) e^{i(kx + \sigma t)}, \quad (117)$$

where $k = 2\pi/\lambda$, $\sigma = 2\pi/T$ and Z is a function of z only. Writing

$$Z = e^{-\gamma z} Z_1(z), \quad (118)$$

and substituting in the first of equations (110) we find

$$\frac{d^2 Z_1}{dz^2} - \alpha^2 Z_1 = 0, \quad (119)$$

where

$$\alpha^2 = k^2 - \sigma^2/c^2 + \gamma^2. \quad (120)$$

Assuming $\alpha \neq 0$ we have

$$Z_1 = A e^{\alpha z} + B e^{-\alpha z}, \quad (121)$$

where A and B are constants, and hence

$$\phi_1 = [A e^{-(\gamma-\alpha)z} + B e^{-(\gamma+\alpha)z}] e^{i(kx + \sigma t)}. \quad (122)$$

From the last two of equations (110) we have two simultaneous equations for A and B :

$$\begin{aligned} &-(\gamma-\alpha) e^{-(\gamma-\alpha)h} A - (\gamma+\alpha) e^{-(\gamma+\alpha)h} B = 0, \\ &\{(\gamma-\alpha)^2 - k^2\} A + \{(\gamma+\alpha)^2 - k^2\} B = 0. \end{aligned} \quad (123)$$

Let $\Delta(\sigma, k)$ denote the determinant of these equations, so that

$$\begin{aligned} \Delta(\sigma, k) &= -(\gamma-\alpha) \{(\gamma+\alpha)^2 - k^2\} e^{-(\gamma-\alpha)h} + (\gamma+\alpha) \{(\gamma-\alpha)^2 - k^2\} e^{-(\gamma+\alpha)h} \\ &= -2 e^{-\gamma h} [\gamma(\gamma^2 - \alpha^2 - k^2) \sinh \alpha h + \alpha(\gamma^2 - \alpha^2 + k^2) \cosh \alpha h]. \end{aligned} \quad (124)$$

In order that non-zero solutions of (123) may exist, $\Delta(\sigma, k)$ must vanish, giving

$$f(\alpha h) = \alpha h \coth \alpha h - P(\alpha h)^2 - Q = 0, \quad (125)$$

where

$$P = \frac{g}{h\sigma^2}, \quad Q = \gamma h(1 - P\gamma h). \quad (126)$$

If σ and h are given, (125) is an equation for determining α and hence k and λ . When αh tends to zero, f tends to the finite value $(1-Q)$, which will be assumed to be positive. When αh is large and positive $f(\alpha h)$ is negative. But, writing $\eta = \alpha^2 h^2$, we may easily show that $d^2 f/d\eta^2$ is always negative when α is real, so that f has only one positive zero, which corresponds to a wave of gravity type. There are an infinity of imaginary zeros, each corresponding to a wave of compression type (Whipple & Lee 1935). It may also be shown that $f(\alpha h)$ has no complex zeroes.

We shall now assume that α is the positive real root of equation (125). Since $f(\gamma h)$ is positive it follows that

$$\gamma^2 < \alpha^2, \quad k^2 > \sigma^2/c^2 > 0, \quad (127)$$

M. S. LONGUET-HIGGINS ON A

22

so that the corresponding value of k is real. Then from equations (123) we have

$$\phi_1 = [(\gamma + \alpha) e^{-\alpha h - (\gamma - \alpha)z} - (\gamma - \alpha) e^{\alpha h - (\gamma + \alpha)z}] e^{i(kx + \sigma t)}. \quad (128)$$

This solution also satisfies equation (114). Since the equations for the first approximation are all linear the sum of any number of solutions is also a solution. We may therefore take as our first approximation

$$\phi_1 = [(\gamma + \alpha) e^{-\alpha h - (\gamma - \alpha)z} - (\gamma - \alpha) e^{\alpha h - (\gamma + \alpha)z}] [b_1 \sin(kx - \sigma t) + b_2 \sin(kx + \sigma t)], \quad (129)$$

representing two waves of the same wave-length travelling in opposite directions.

4.3. Second approximation

After substituting in equations (112) and (115) and simplifying we find the following equations for ϕ_2 :

$$\begin{aligned} \frac{\partial^2 \phi_2}{\partial t^2} - c^2 \nabla^2 \phi_2 - g \frac{\partial \phi_2}{\partial z} \\ = [C^{(2)} e^{-2(\gamma - \alpha)z} + C^{(2)} e^{-2(\gamma + \alpha)z} - 2C^{(3)} e^{-2\gamma z}] [b_1^2 \sin 2(kx - \sigma t) - b_2^2 \sin 2(kx + \sigma t)] \\ + [C^{(4)} e^{-2(\gamma - \alpha)z} + C^{(5)} e^{-2(\gamma + \alpha)z} - 2C^{(6)} e^{-2\gamma z}] 2b_1 b_2 \sin 2\sigma t, \end{aligned} \quad (130)$$

$$\left(\frac{\partial \phi_2}{\partial z} \right)_{z=h} = 0, \quad (131)$$

$$(\nabla^2 \phi_2)_{z=0} = D [b_1^2 \sin 2(kx - \sigma t) - b_2^2 \sin 2(kx + \sigma t) + 2b_1 b_2 \sin 2\sigma t], \quad (132)$$

$$2\gamma \int_0^h dx \int_0^h dz \frac{\partial \phi_2}{\partial t^2} e^{2\gamma z} + \int_0^h dx \left(\frac{\partial \phi_2}{\partial t} \right)_{z=0} = E^{(1)} (b_1^2 + b_2^2) + E^{(2)} 2b_1 b_2 \cos 2\sigma t, \quad (133)$$

where $C^{(1)}$, $C^{(2)}$, ..., $C^{(6)}$, D and $E^{(1)}$ are constants given by

$$\left. \begin{aligned} C^{(1)} &= -\sigma \{(\gamma - \alpha)^2 - k^2\} (\gamma + \alpha)^2 e^{-2\alpha h}, & C^{(4)} &= -\sigma \{(\gamma - \alpha)^2 + k^2\} (\gamma + \alpha)^2 e^{-2\alpha h}, \\ C^{(2)} &= -\sigma \{(\gamma + \alpha)^2 - k^2\} (\gamma - \alpha)^2 e^{2\alpha h}, & C^{(5)} &= -\sigma \{(\gamma + \alpha)^2 + k^2\} (\gamma - \alpha)^2 e^{2\alpha h}, \\ C^{(3)} &= -\sigma \{\gamma^2 - \alpha^2 - k^2\} (\gamma^2 - \alpha^2), & C^{(6)} &= -\sigma \{\gamma^2 - \alpha^2 + k^2\} (\gamma^2 - \alpha^2), \end{aligned} \right\} \quad (134)$$

$$\text{and} \quad D = -\frac{4g}{g} \gamma \alpha^2 (\gamma^2 - \alpha^2), \quad E^{(1)} = -\lambda \alpha^2 (\gamma^2 - \alpha^2) \quad (135)$$

(the value of $E^{(2)}$ will not be required). We first eliminate the right-hand side of equation (130) by the substitution

$$\phi_2 = [F^{(1)} e^{-2(\gamma - \alpha)z} + F^{(2)} e^{-2(\gamma + \alpha)z} - 2F^{(3)} e^{-2\gamma z}] [b_1^2 \sin 2(kx - \sigma t) - b_2^2 \sin 2(kx + \sigma t)] \\ + [F^{(4)} e^{-2(\gamma - \alpha)z} + F^{(5)} e^{-2(\gamma + \alpha)z} - 2F^{(6)} e^{-2\gamma z}] 2b_1 b_2 \sin 2\sigma t + \phi_2', \quad (136)$$

where

$$\left. \begin{aligned} F^{(1)} &= \frac{C^{(1)}}{-4\sigma^2 - 4c^2\{(\gamma - \alpha)^2 - k^2\} + 2g(\gamma - \alpha)}, \\ F^{(2)} &= \frac{C^{(2)}}{-4\sigma^2 - 4c^2\{(\gamma + \alpha)^2 - k^2\} + 2g(\gamma + \alpha)}, \\ F^{(3)} &= \frac{C^{(3)}}{-4\sigma^2 - 4c^2(\gamma^2 - k^2) + 2g\gamma} \end{aligned} \right\} \quad (137)$$

THEORY OF THE ORIGIN OF MICROSEISMS

and

$$\left. \begin{aligned} F^{(4)} &= \frac{C^{(4)}}{-4\sigma^2 - 4c^2(\gamma - \alpha)^2 + 2g(\gamma - \alpha)}, \\ F^{(5)} &= \frac{C^{(5)}}{-4\sigma^2 - 4c^2(\gamma + \alpha)^2 + 2g(\gamma + \alpha)}, \\ F^{(6)} &= \frac{C^{(6)}}{-4\sigma^2 - 4c^2\gamma^2 + 2g\gamma}. \end{aligned} \right\} \quad (138)$$

This gives

$$\frac{\partial^2 \phi'_2}{\partial t^2} - c^2 \nabla^2 \phi'_2 - g \frac{\partial \phi'_2}{\partial z} = 0, \quad (139)$$

$$\left(\frac{\partial \phi'_2}{\partial z} \right)_{z=h} = G^{(1)} [b_1^2 \sin 2(kx - \sigma t) - b_2^2 \sin 2(kx + \sigma t)] + G^{(2)} 2b_1 b_2 \sin 2\sigma t, \quad (140)$$

$$(\nabla^2 \phi'_2)_{z=0} = (D + H^{(1)}) [b_1^2 \sin 2(kx - \sigma t) - b_2^2 \sin 2(kx + \sigma t)] + (D + H^{(2)}) 2b_1 b_2 \sin 2\sigma t, \quad (141)$$

$$2\gamma \int_0^h dx \int_0^h dz \frac{\partial \phi'_2}{\partial t} e^{2\gamma z} + \int_0^h dx \left(\frac{\partial \phi'_2}{\partial t} \right)_{z=0} = E^{(1)} (b_1^2 + b_2^2) + (E^{(2)} + I) 2b_1 b_2 \cos 2\sigma t, \quad (142)$$

$$\text{where } \left. \begin{aligned} G^{(1)} &= 2(\gamma - \alpha) e^{-2(\gamma - \alpha)h} F^{(1)} + 2(\gamma + \alpha) e^{-2(\gamma + \alpha)h} F^{(2)} - 4\gamma e^{-2\gamma h} F^{(3)}, \\ G^{(2)} &= 2(\gamma - \alpha) e^{-2(\gamma - \alpha)h} F^{(4)} + 2(\gamma + \alpha) e^{-2(\gamma + \alpha)h} F^{(5)} - 4\gamma e^{-2\gamma h} F^{(6)}. \end{aligned} \right\} \quad (143)$$

$$\text{and } \left. \begin{aligned} H^{(1)} &= -4\{(\gamma - \alpha)^2 - k^2\} F^{(1)} - 4\{(\gamma + \alpha)^2 - k^2\} F^{(2)} + 8(\gamma^2 - k^2) F^{(3)}, \\ H^{(2)} &= -4(\gamma - \alpha)^2 F^{(4)} - 4(\gamma + \alpha)^2 F^{(5)} + 8\gamma^2 F^{(6)}. \end{aligned} \right\} \quad (144)$$

We now write

$$\phi'_2 = [J^{(1)} e^{-(\gamma - \alpha)z} + J^{(2)} e^{-(\gamma + \alpha)z}] [b_1^2 \sin 2(kx - \sigma t) - b_2^2 \sin 2(kx + \sigma t)] + [J^{(3)} e^{-(\gamma - \alpha)z} + J^{(4)} e^{-(\gamma + \alpha)z}] 2b_1 b_2 \sin 2\sigma t + \phi''_2, \quad (145)$$

$$\text{where } \alpha'^2 = 4k^2 - 4\sigma^2/c^2 + \gamma^2, \quad \alpha''^2 = -4\sigma^2/c^2 + \gamma^2, \quad (146)$$

and $J^{(1)}$, $J^{(2)}$, $J^{(3)}$ and $J^{(4)}$ are to be chosen so as to reduce the right-hand sides of equations (140) and (141) to zero. We must have

$$\left. \begin{aligned} -(\gamma - \alpha') e^{-(\gamma - \alpha')h} J^{(1)} - (\gamma + \alpha') e^{-(\gamma + \alpha')h} J^{(2)} &= G^{(1)}, \\ \{(\gamma - \alpha')^2 - 4k^2\} J^{(1)} + \{(\gamma + \alpha')^2 - 4k^2\} J^{(2)} &= D + H^{(1)}, \end{aligned} \right\} \quad (147)$$

$$\text{and } \left. \begin{aligned} -(\gamma - \alpha'') e^{-(\gamma - \alpha'')h} J^{(3)} - (\gamma + \alpha'') e^{-(\gamma + \alpha'')h} J^{(4)} &= G^{(2)}, \\ (\gamma - \alpha'')^2 J^{(3)} + (\gamma + \alpha'')^2 J^{(4)} &= D + H^{(2)}, \end{aligned} \right\} \quad (148)$$

giving

$$\left. \begin{aligned} J^{(1)} &= \frac{\{(\gamma + \alpha')^2 - 4k^2\} G^{(1)} + (\gamma + \alpha') e^{-(\gamma + \alpha')h} (D + H^{(1)})}{\Delta(2\sigma, 2k)}, \\ J^{(2)} &= -\frac{\{(\gamma - \alpha')^2 - 4k^2\} G^{(1)} + (\gamma - \alpha') e^{-(\gamma - \alpha')h} (D + H^{(1)})}{\Delta(2\sigma, 2k)}, \end{aligned} \right\} \quad (149)$$

and

$$\left. \begin{aligned} J^{(3)} &= \frac{(\gamma + \alpha'')^2 G^{(2)} + (\gamma + \alpha'') e^{-(\gamma + \alpha'')h} (D + H^{(2)})}{\Delta(2\sigma, 0)}, \\ J^{(4)} &= -\frac{(\gamma - \alpha'')^2 G^{(2)} + (\gamma - \alpha'') e^{-(\gamma - \alpha'')h} (D + H^{(2)})}{\Delta(2\sigma, 0)}, \end{aligned} \right\} \quad (150)$$

M. S. LONGUET-HIGGINS ON A

$$\text{where } \left. \begin{aligned} \Delta(2\sigma, 2k) &= -2e^{-\gamma h} [\gamma(\gamma^2 - \alpha'^2 - 4k^2) \sinh \alpha' h + \alpha'(\gamma^2 - \alpha'^2) \cosh \alpha' h], \\ \Delta(2\sigma, 0) &= -2e^{-\gamma h} [\gamma(\gamma^2 - \alpha''^2) \sinh \alpha'' h + \alpha''(\gamma^2 - \alpha''^2) \cosh \alpha'' h], \end{aligned} \right\} \quad (151)$$

provided neither $\Delta(2\sigma, 2k)$ nor $\Delta(2\sigma, 0)$ vanishes. Now if θ is any real number we have

$$\Delta(\theta\sigma, \theta k) = -2e^{-\gamma h} \sinh \beta h [\gamma(1 - 2k^2c^2/\sigma^2) + \beta \coth \beta h] \theta^2 \sigma^2 / c^2, \quad (152)$$

$$\text{where } \beta^2 = \theta^2(k^2 - \sigma^2/c^2) + \gamma^2. \quad (153)$$

Since $(k^2 - \sigma^2/c^2)$ is positive (equation (127)), β^2 is a positive, increasing function of θ^2 . But $\beta \coth \beta h$ is an increasing function of β^2 when $\beta^2 > 0$ and hence is an increasing function of θ^2 . Equation (152) then shows that $\Delta(\theta\sigma, \theta k)$ cannot vanish for more than one positive value of θ . But $\Delta(\sigma, k)$ vanishes and therefore $\Delta(2\sigma, 2k)$ cannot vanish.

It is quite possible, on the other hand, that $\Delta(2\sigma, 0)$ may be zero. The physical significance of this case will be discussed later. For the present it will be assumed that $\Delta(2\sigma, 0)$ is different from zero.

As a result of our choice of $J^{(1)}$, etc., we have for ϕ_2'' the following equations:

$$\left. \begin{aligned} \partial^2 \phi_2'' - c^2 \nabla^2 \phi_2'' - g \frac{\partial \phi_2''}{\partial z} &= 0, \\ \left(\frac{\partial \phi_2''}{\partial z} \right)_{z=h} &= 0, \\ (\nabla^2 \phi_2'')_{z=0} &= 0, \\ 2\gamma \int_0^\lambda dx \int_0^h dz \frac{\partial \phi_2''}{\partial t} e^{2\gamma z} + \int_0^\lambda dx \left(\frac{\partial \phi_2''}{\partial t} \right)_{z=0} &= E^{(1)}(b_1^2 + b_2^2) + (E^{(2)} + I + K) 2b_1 b_2 \cos 2\sigma t, \end{aligned} \right\} \quad (154)$$

where K is a constant. Now it was shown earlier that a solution of all four equations (112) and (114) could be obtained by adding a constant multiple of t to any given solution of (112). It follows, by subtraction, that a solution of all four equations (154) and (155) may be obtained by adding a constant multiple of t to any solution of (154). But (154) are satisfied by $\phi_2'' = 0$. Hence we have

$$\phi_2'' = C'' t, \quad (156)$$

where on substitution in (155) we find

$$\lambda e^{2\gamma h} C'' = E^{(1)}(b_1^2 + b_2^2). \quad (157)$$

$$\text{We have incidentally shown that } E^{(2)} + I + K = 0. \quad (158)$$

We therefore have finally

$$\begin{aligned} \phi_2 &= [F^{(1)} e^{2\alpha x} + F^{(2)} e^{-2\alpha x} - 2F^{(3)}] e^{-2\gamma z} [b_1^2 \sin 2(kx - \sigma t) - b_2^2 \sin 2(kx + \sigma t)] \\ &+ [F^{(4)} e^{2\alpha x} + F^{(5)} e^{-2\alpha x} - 2F^{(6)}] e^{-2\gamma z} 2b_1 b_2 \sin 2\sigma t \\ &+ [J^{(1)} e^{\alpha' z} + J^{(2)} e^{-\alpha' z}] e^{-\gamma z} [b_1^2 \sin 2(kx - \sigma t) - b_2^2 \sin 2(kx + \sigma t)] \\ &+ [J^{(3)} e^{\alpha'' z} + J^{(4)} e^{-\alpha'' z}] e^{-\gamma z} 2b_1 b_2 \sin 2\sigma t \\ &+ E^{(1)} k^{-1} e^{-2\gamma h} (b_1^2 + b_2^2) t. \end{aligned} \quad (159)$$

4.4. Discussion

For ocean waves we may take

$$g = 0.98 \times 10^3 \text{ cm./sec.}, \quad c = 1.4 \times 10^5 \text{ cm./sec.} \quad (160)$$

$$\sigma = 0.5 \text{ sec.}^{-1}, \quad h < 10^6 \text{ cm.}$$

$$\text{This gives } P\gamma h = 1.0 \times 10^{-4}, \quad \gamma h < 2.5 \times 10^{-2}, \quad (161)$$

$$\text{and so } Q = \gamma h(1 - P\gamma h) < 2.5 \times 10^{-2}. \quad (162)$$

THEORY OF THE ORIGIN OF MICROSEISMS

Since $ah \coth ah \geq 1$ for all real values of a , equation (126) shows that Pa_h is of the same order as $\coth ah$. Hence

$$\gamma/\alpha = P\gamma h/Pa_h \approx 10^{-4}. \quad (163)$$

Our method will be to evaluate the constants in equation (159) by expanding in powers of γ/α . From (126) we have

$$\coth ah = Pa_h[1 + O(\gamma/\alpha)], \quad (164)$$

so that

$$\sigma^2/c^2 = 2\gamma\alpha/Pa_h = 2\gamma\alpha \tanh ah[1 + O(\gamma/\alpha)] \quad (165)$$

and

$$k^2 = \alpha^2[1 + 2(\gamma/\alpha) \tanh ah + O(\gamma/\alpha)^2]. \quad (166)$$

Hence, retaining only the terms of highest order in γ/α , we find

$$\left. \begin{aligned} F^{(1)} &= \frac{\gamma\alpha^3}{\sigma} \frac{e^{-ah} \sinh ah}{\cosh^2 ah}, & F^{(4)} &= \frac{\gamma\alpha^3}{\sigma} e^{-2ah} \tanh ah, \\ F^{(2)} &= \frac{\gamma\alpha^3 e^{ah} \sinh ah}{\sigma \cosh^2 ah}, & F^{(5)} &= \frac{\gamma\alpha^3}{\sigma} e^{2ah} \tanh ah, \\ F^{(3)} &= -\frac{\gamma\alpha^3}{\sigma} \tanh ah, & F^{(6)} &= -\frac{\gamma\alpha^3}{2\sigma} \tanh ah, \end{aligned} \right\} \quad (167)$$

$$\left. \begin{aligned} J^{(1)} &= -\frac{3\alpha^4}{4\sigma} \frac{e^{-\alpha^2 h}}{\sinh^2 ah}, & J^{(3)} &= \frac{\alpha^4}{\sigma} \frac{e^{-\alpha^2 h} \cosh 3ah}{\cosh^2 ah \cosh ah}, \\ J^{(2)} &= -\frac{3\alpha^4}{4\sigma} \frac{e^{\alpha^2 h}}{\sinh^2 ah}, & J^{(4)} &= \frac{\alpha^4}{\sigma} \frac{e^{\alpha^2 h} \cosh 3ah}{\cosh^2 ah \cosh ah}, \end{aligned} \right\} \quad (168)$$

$$E^{(1)} = \lambda\alpha^4, \quad \alpha'^2 = 4\alpha^2, \quad \alpha''^2 = -4\sigma^2/c^2. \quad (169)$$

When $b_1 b_2 \neq 0$ the first two terms in equation (159) are negligible compared with the fourth. If we also neglect quantities of order γh (though not those of order $(\gamma\alpha)^{\frac{1}{2}} h$), ah , $\alpha'h$, $\alpha''h$ and $e^{\gamma h}$ may be replaced by kh , $2kh$, $2i\sigma h/c$ and 1 respectively, and we have

$$\sigma^2 = gk \tanh kh, \quad (170)$$

$$\phi_1 = \frac{\sigma \cosh k(z-h)}{k \sinh kh} [a_1 \sin(kx - \sigma t) - a_2 \sin(kx + \sigma t)], \quad (171)$$

$$\begin{aligned} \phi_2 &= -\frac{3\sigma \cosh 2k(z-h)}{8 \sinh^4 kh} [a_1^2 \sin 2(kx - \sigma t) - a_2^2 \sin 2(kx + \sigma t)] \\ &\quad - \frac{\sigma \cosh 3kh}{8 \sinh^2 kh} \frac{\cos 2\sigma(z-h)/c}{\cos 2\sigma h/c} 2a_1 a_2 \sin 2\sigma t \\ &\quad + \frac{\sigma}{4 \sinh^2 kh} (a_1^2 + a_2^2) \sigma t, \end{aligned} \quad (172)$$

where

$$a_1 = \frac{\sigma}{2k^2 \sinh kh} b_1, \quad a_2 = -\frac{\sigma}{2k^2 \sinh kh} b_2. \quad (173)$$

Let λ_g and λ_c denote the wave-lengths of a gravity wave and a compression wave respectively. Thus

$$\lambda_g = 2\pi/k, \quad \lambda_c = 2\pi c/\sigma, \quad \lambda_g/\lambda_c = (\gamma/\alpha)^{\frac{1}{2}} \tanh^{\frac{1}{2}} ah. \quad (174)$$

When z is less than say $\frac{1}{2}\lambda_g$, equations (170), (171) and (172) show that the motion is independent of c and therefore unaffected by the compressibility of the water. When z is comparable with λ_g , both e^{-kz} and e^{-kh} are small, and so from equation (172) the pressure ϕ_2 is given by

$$\frac{\partial \phi_2}{\partial z} = -2a_1 a_2 \sigma^2 \cos 2\sigma t. \quad (175)$$

Finally, when z is of the same order as λ_c , the motion reduces to the compression wave

$$\phi_2 = \frac{\sigma \cos 2\sigma(z-h)/c}{\cos 2\sigma h/c} \sin 2\sigma t. \quad (176)$$

This wave may be regarded as being generated by the unattenuated pressure variation (175). When $\cos 2\sigma h/c$ (or more exactly $\Delta(2\sigma, 0)$) is zero, ϕ_2 becomes infinite, a situation corresponding to resonance. The necessary condition for resonance is that

$$2\sigma h/c \doteq (n + \frac{1}{2})\pi \quad (n = 0, 1, 2, \dots), \quad (177)$$

that is, that the depth should be about $(\frac{1}{2}n + \frac{1}{4})$ times the length of the compression wave (176).

The ocean may therefore be divided into two regions, namely, (1) a surface layer where thickness is of order λ_g , where the motion is controlled by gravity alone and is the same as if the water as a whole were incompressible, and (2) the main part of the ocean where the motion is small and controlled only by compressibility. The distinction of two such regions is probably valid in more general types of wave motion. In equation (94) the gravity term $g\partial\phi/\partial z$ is in general small compared with the compressibility term $c^2\nabla^2\phi$. It is only near the free surface, where $\nabla^2\phi$ vanishes (equation (99)), that gravity predominates. The pressure variations at a depth λ_g , that is, in the lower part of the surface layer, are of order $\rho\sigma^2 a^2$, where a is the mean amplitude at the free surface. These will produce compression waves in which the displacements are of order a^2/λ_c . But the latter will be small compared with the vertical displacement of the centre of gravity of the surface layer, which is of order a^2/λ_g , and hence will not affect the motion in the surface layer.

5. THE DISPLACEMENT OF THE GROUND DUE TO SURFACE WAVES

In the present section we shall estimate the displacement of the ground due to a given storm at sea. Since observations are not made in the storm area itself, it is not appropriate to consider the displacement of the sea bed due to an infinite train of waves passing overhead. The storm is more correctly considered as a disturbance of finite area from which energy is propagated outwards in all directions.

The velocities of seismic waves in the sea bed being comparable with the velocity of sound in water, the general results suggested in §4.4 are likely to remain true when the elasticity of the sea bed is also taken into account. Thus the mean pressure at a depth of say $\frac{1}{2}\lambda_g$ over any given area of the sea surface may be derived as in §3, and the amplitude of the elastic waves may be calculated as though this pressure distribution were applied to the upper surface of the ocean. Since λ_g/λ_c is of the order of 10^{-2} , the storm area may be divided into a number of squares S whose side $2R$ is large compared with λ_g but only a fraction, say less than one-half, of the length of an elastic wave in the sea bed. Thus the amplitude of the compression waves from any given square S will be of the same order of magnitude as if the whole force were concentrated to a point at the centre of the square. The displacement from the whole storm may then be found by summing the energies from all the different squares.

5.1. *The displacement due to a concentrated force*

We take as our model an ocean of constant depth h overlying a sea bed of uniform density and elasticity. For the reasons given above, we shall be able to make use of the first-order theory of elastic waves in such a model, which was first investigated by Stoneley (1926).

THEORY OF THE ORIGIN OF MICROSEISMS

27

The motion due to a concentrated force applied to the upper surface of the water was stated by Scholte (1943). We shall evaluate the solution rather more completely, using the method of contour integration due to Sommerfeld (1909) and Jeffreys (1926).

Let ρ_1 and ρ_2 be the densities of the water and of the sea bed, let $c = \alpha_1$ be the velocity of sound in water and α_2 and β_2 the velocities of compressional and distortional waves in the sea bed. Then if an oscillatory force $e^{i\sigma t}$ is applied to the surface of the water at the origin, the vertical displacement of the sea bed measured downwards is given by (Scholte 1943)

$$W(\sigma, r) e^{i\sigma t} = -\frac{1}{2\pi} \int_0^\infty \frac{J_0(\xi r) \xi d\xi}{\rho_2 \sigma^2 G(\xi)} e^{i\sigma t}, \quad (178)$$

where r is the horizontal distance from the origin, J_0 is Bessel's function of the first kind of zero order and $G(\xi)$ is given by

$$G(\xi) = (\beta_2/\sigma)^4 [(2\xi^2 - \sigma^2/\beta_2^2)^2 (\xi^2 - \sigma^2/\alpha_2^2)^{-1} - 4\xi^2 (\xi^2 - \sigma^2/\beta_2^2)^2] \cosh (\xi^2 - \sigma^2/\alpha_1^2)^{\frac{1}{2}} h \\ + (\rho_1/\rho_2) (\xi^2 - \sigma^2/\alpha_1^2)^{-1} \sinh (\xi^2 - \sigma^2/\alpha_1^2)^{\frac{1}{2}} h. \quad (179)$$

In order to ensure that the displacements at infinite depth are bounded, the signs of the radicals in equation (179) must be chosen so that the real parts of $(\xi^2 - \sigma^2/\alpha_1^2)^{\frac{1}{2}}$ and $(\xi^2 - \sigma^2/\beta_2^2)^{\frac{1}{2}}$ are positive or zero. ξ being considered as a complex variable, this restricts us initially to one sheet of the Riemann surface bounded by the cuts

$$\Re(\xi^2 - \sigma^2/\alpha_1^2)^{\frac{1}{2}} = 0, \quad \Re(\xi^2 - \sigma^2/\beta_2^2)^{\frac{1}{2}} = 0. \quad (180)$$

It will be seen that the choice of sign for $(\xi^2 - \sigma^2/\alpha_1^2)^{\frac{1}{2}}$ is immaterial, since $\cosh (\xi^2 - \sigma^2/\alpha_1^2)^{\frac{1}{2}} h$ and $(\xi^2 - \sigma^2/\alpha_1^2)^{-1} \sinh (\xi^2 - \sigma^2/\alpha_1^2)^{\frac{1}{2}} h$ are both single-valued functions of ξ , analytic at all points.

When σ is real the integral in equation (178) is indeterminate owing to the vanishing of $G(\xi)$ at certain points of the real axis. To obtain a correct interpretation we suppose σ to be complex, and take the limit as $\arg \sigma$ tends to zero. The final solution then contains converging or diverging waves according as $\arg \sigma$ tends to zero through positive or negative values. Since we require the waves to diverge we choose the latter case. Now it can be shown that, when $-\frac{1}{2}\pi < \arg \sigma < 0$, $G(\xi)$ has no zeroes in the sector $0 \leq \arg \xi \leq \frac{1}{2}\pi - \sigma$. There are therefore no zeroes on the real axis, and, in the limit when $\arg \sigma$ tends to 0, the zeroes of G approach the real axis from below. Hence the path of integration in equation (178) should be indented above the real axis near the zeroes of G (see figure 1*b*). Further, the cuts in the ξ -plane given by (180) are arcs of rectangular hyperbolas which, as $\arg \sigma$ tends to zero, approach the positive axis from below (see figure 1*a*). Hence the path of integration should be taken along the upper side of the cuts.

To evaluate the right-hand side of equation (178) we write

$$J_0(\xi r) = \frac{1}{2} [Hs_0(\xi r) + Hi_0(\xi r)] \quad (181)$$

(for the notation see Jeffreys & Jeffreys 1946, p. 544) and consider the integral in two parts. When σ is real it may be shown that G has no complex zeroes. Hence for the part involving Hs_0 the contour of integration may be deformed into the imaginary axis from 0 to ico together with an arc of infinite radius in the first quadrant. For the part involving Hi_0 the path of integration may be deformed into (a) the imaginary axis from 0 to $-ico$, (b) a

M. S. LONGUET-HIGGINS ON A

contour Γ enclosing the cuts in the ξ -plane (see figure 1c), (c) small circles enclosing the zeroes of $G(\xi)$ in the clockwise sense and (d) an arc of infinite radius in the fourth quadrant. The contribution from the integrals along the imaginary axis are equal and opposite, while, since (Jeffreys & Jeffreys 1946)

$$\text{Hs}_0(z) \sim \left(\frac{2}{\pi z}\right)^{1/2} e^{i(z-i\pi)}, \quad \text{Hi}_0(z) \sim \left(\frac{2}{\pi z}\right)^{1/2} e^{-i(z-i\pi)}, \quad (182)$$

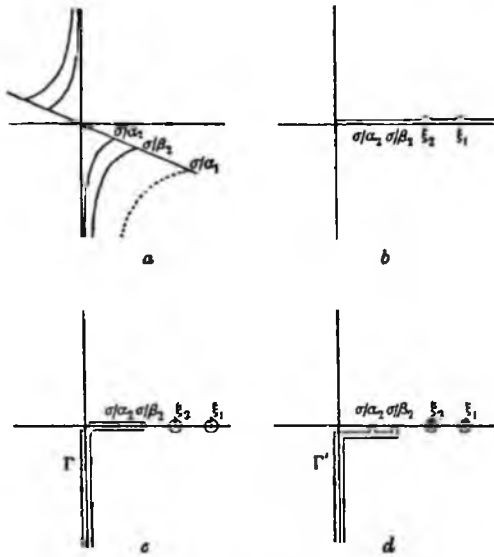


FIGURE 1. Contours of integration in the ξ -plane.

for large $|z|$ and $-\pi + \epsilon \leq \arg z \leq \pi - \epsilon$, the integrals along the two infinite arcs tend to zero. By slightly deforming the contour Γ as in figure 1d, it is easily shown that the contribution from this part of the integral diminishes at least as rapidly as r^{-1} when r is large. Hence the main contribution comes from the neighbourhood of the zeroes, being $-2\pi i$ times the sum of the residues of the integrand there. On replacing Hi_0 by its asymptotic formula (182) we find

$$W(\sigma, r) e^{i\sigma t} \sim \frac{\sigma^t}{\rho_2 \beta_2^{5/2} (2\pi r)^{1/2}} \sum_{m=1}^N c_m e^{i(\sigma t - \xi_m r + (m+1)\pi)}, \quad (183)$$

where

$$c_m = (-)^m \frac{(\beta_2/\sigma)^{5/2} \xi_m^{1/2}}{dG(\xi_m)/d\xi_m}, \quad (184)$$

and $\xi_1, \xi_2, \dots, \xi_N$ denote the positive zeroes of $G(\xi)$ in descending order of magnitude. It can be shown that when $\alpha_1 < \beta_2$ all the zeroes are greater than σ/β_2 . The zeroes of $G(\xi)$ separate alternately the zeroes of $\cosh(\xi^2 - \sigma^2/\alpha_1^2)^{1/2} h$, and if the latter function has n zeroes in the interval $\sigma/\beta_2 < \xi < \infty$, then N equals either n or $(n+1)$. When $\sigma h/\beta_2$ is small there is just one zero ξ_1 .

THEORY OF THE ORIGIN OF MICROSEISMS

Each term in equation (183) represents a diverging wave of length $2\pi/\xi_m$ and of amplitude proportional to c_m . In figure 2 c_1, c_2, c_3 and c_4 are plotted against $\sigma h/\beta_2$ for the following constants:

$$\left. \begin{aligned} \rho_1 &= 1.0 \text{ g./cm.}^3, & \alpha_1 &= 1.4 \text{ km./sec.}, \\ \rho_2 &= 2.5 \text{ g./cm.}^3, & \beta_2 &= 2.8 \text{ km./sec.} \end{aligned} \right\} \quad (185)$$

and with Poisson's hypothesis $\alpha_2 = \sqrt{3}\beta_2$. The corresponding values of ξ_1, ξ_2, ξ_3 and ξ_4 are given in table 1. It will be seen that c_1 increases rapidly to a maximum at about $\sigma h/\beta_2 = 0.85$ before falling away finally to zero. This maximum value occurs when the depth is about 0.27 times the wave-length of a compression wave in water, and may be interpreted as the

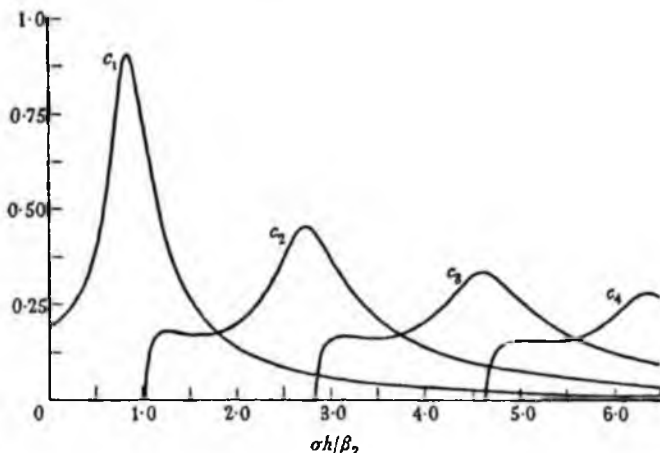


FIGURE 2. The amplitude of the vertical displacement of the sea bed as a function of the depth h . effect of resonance. The amplitude does not, however, become infinite owing to the propagation of energy away from the source of the disturbance. c_2, c_3 and c_4 show similar resonance peaks when $\sigma h/\beta_2 = 2.7, 4.1$ and 6.3 respectively. There are also maxima in the earlier parts of each curve. This might be expected from the fact that the group-velocity curve has two stationary values (Press & Ewing 1948). These do not, however, coincide exactly with the maxima in figure 2.

We define \bar{W}^2 to be the sum of the squared moduli of the terms in equation (183). Thus

$$\bar{W} = \frac{\sigma^4}{\rho_2 \beta_2^{5/2} (2\pi r)^4} \left[\sum_{m=1}^N c_m^2 \right]^{1/2}. \quad (186)$$

5.2. The displacement of the ground in terms of the frequency spectrum of the waves

From equation (82) we see that the wave motion in any given square S will cause a vertical displacement δ' of the ground given by

$$\delta' = -\Re 4\rho(\pi/k)^2 \int_{-\infty}^{\infty} \int_{-\infty}^{\infty} A' A'_- \sigma^2 W(2\sigma, r) e^{2i\sigma t} du dv, \quad (187)$$

where r is the distance from the centre of the square and $W(\sigma, r)$ is given by (183). We shall now find an expression for the order of magnitude of the right-hand side of equation (187).

M. S. LONGUET-HIGGINS ON A

TABLE I

(a)								
$\xi_1 \beta_2 / \sigma$	$\sigma h / \beta_2$	ϵ_1	$\xi_1 \beta_2 / \sigma$	$\sigma h / \beta_2$	ϵ_1	$\xi_1 \beta_2 / \sigma$	$\sigma h / \beta_2$	ϵ_1
1.0877	0.00	0.191	1.3784	0.89	0.890	1.8439	1.68	0.205
1.0954	0.10	0.206	1.4142	0.92	0.857	1.8974	1.99	0.139
1.1402	0.48	0.368	1.4832	0.99	0.769	1.9494	2.59	0.078
1.1832	0.63	0.565	1.5492	1.06	0.649	1.9748	3.23	0.049
1.2247	0.72	0.728	1.6126	1.13	0.542	1.9875	3.87	0.034
1.2649	0.77	0.837	1.6733	1.22	0.444	1.9975	4.87	0.021
1.3038	0.82	0.894	1.7321	1.33	0.355	2.0000	5.31	0.017
1.3416	0.85	0.908	1.7889	1.48	0.276	2.0025	5.92	0.014
(b)								
$\xi_2 \beta_2 / \sigma$	$\sigma h / \beta_2$	ϵ_2	$\xi_2 \beta_2 / \sigma$	$\sigma h / \beta_2$	ϵ_2	$\xi_2 \beta_2 / \sigma$	$\sigma h / \beta_2$	ϵ_2
1.0000	1.01	0.000	1.0677	1.58	0.170	1.3784	3.06	0.351
1.0005	1.03	0.038	1.0770	1.72	0.172	1.4142	3.14	0.316
1.0025	1.04	0.076	1.0863	1.86	0.180	1.4832	3.33	0.256
1.0050	1.06	0.108	1.0954	1.98	0.194	1.5492	3.54	0.206
1.0100	1.09	0.141	1.1402	2.39	0.318	1.6125	3.79	0.165
1.0198	1.14	0.168	1.1832	2.58	0.418	1.6733	4.00	0.131
1.0296	1.20	0.178	1.2247	2.70	0.454	1.7321	4.47	0.101
1.0392	1.28	0.180	1.2649	2.80	0.448	1.7889	4.99	0.076
1.0488	1.36	0.177	1.3038	2.89	0.421	1.8439	5.73	0.054
1.0583	1.46	0.173	1.3416	2.97	0.386	1.8974	6.96	0.034
(c)								
$\xi_3 \beta_2 / \sigma$	$\sigma h / \beta_2$	ϵ_3	$\xi_3 \beta_2 / \sigma$	$\sigma h / \beta_2$	ϵ_3	$\xi_3 \beta_2 / \sigma$	$\sigma h / \beta_2$	ϵ_3
1.0000	2.83	0.000	1.0488	3.21	0.165	1.2247	4.60	0.330
1.0005	2.84	0.036	1.0583	3.32	0.163	1.2649	4.83	0.305
1.0025	2.86	0.070	1.0677	3.44	0.162	1.3038	4.96	0.275
1.0050	2.88	0.098	1.0770	3.58	0.164	1.3416	5.09	0.245
1.0100	2.91	0.126	1.0863	3.73	0.171	1.3784	5.22	0.218
1.0198	2.97	0.151	1.0954	3.86	0.184	1.4142	5.36	0.194
1.0296	3.04	0.163	1.1402	4.30	0.280	1.4832	5.67	0.154
1.0392	3.11	0.166	1.1832	4.53	0.331	1.5492	6.02	0.123
(d)								
$\xi_4 \beta_2 / \sigma$	$\sigma h / \beta_2$	ϵ_4	$\xi_4 \beta_2 / \sigma$	$\sigma h / \beta_2$	ϵ_4	$\xi_4 \beta_2 / \sigma$	$\sigma h / \beta_2$	ϵ_4
1.0000	4.64	0.000	1.0198	4.80	0.138	1.0677	5.30	0.154
1.0005	4.65	0.031	1.0296	4.87	0.150	1.0770	5.44	0.157
1.0025	4.67	0.065	1.0392	4.95	0.155	1.0863	5.60	0.164
1.0050	4.69	0.090	1.0488	5.05	0.156	1.0954	5.73	0.175
1.0100	4.73	0.115	1.0583	5.17	0.155	1.1402	6.21	0.250

From the definition given in § 3.3, $A'(a, v; t_1)$ is the frequency spectrum of the hypothetical free motion in which, at time $t = t_1$, ζ and $\partial\zeta/\partial t$ take their actual values within S but are zero outside. When $t = t_1$ all the potential energy and nearly all the kinetic energy are contained inside S . Hence the total energy in the square is given by

$$2\rho g(\pi/k)^2 \int_{-\infty}^{\infty} \int_{-\infty}^{\infty} A' A'^* du dv = (2\pi/k)^2 E, \quad (188)$$

where E denotes the mean energy per unit area of S . We define the mean amplitude a of the motion within S as half the height, from peak to trough, of the simple progressive wave

THEORY OF THE ORIGIN OF MICROSEISMS

31

train having the same mean energy per unit area. The mean energy of a wave train of amplitude a being $\frac{1}{2}\rho g a^2$, we have from (188)

$$a^2 = \int_{-\infty}^{\infty} \int_{-\infty}^{\infty} A' A'^* du dv, \quad (189)$$

When considering a group of waves (see § 3.3) we suppose that all the energy is confined to a certain range of frequencies and directions characteristic of the group. This range will be very nearly the same for the 'blurred' spectrum A' as for the original spectrum A . Let Ω be the region in which the point $P(-uk, -vk)$, defining the length and direction of the wave components of the group, must lie. We also use Ω to denote the area of this region. Then the area of the corresponding region in the (u, v) -plane is Ω/k^2 . Hence the root-mean-square value \bar{A} of the modulus of A' is given by

$$\bar{A}^2 \Omega / k^2 = \int_{-\infty}^{\infty} \int_{-\infty}^{\infty} A' A'^* du dv, \quad (190)$$

or from equation (188)

$$\bar{A} = ak/\Omega^{\frac{1}{2}}. \quad (191)$$

The case of most practical importance is when the motion consists of two distinct wave groups, say A'_1 and A'_2 . We denote the mean amplitudes of these groups by a_1 and a_2 respectively and the corresponding areas in their frequency spectra by Ω_1 and Ω_2 . The root-mean-square values of A'_1 and A'_2 are given by

$$\bar{A}_1 = a_1 k / \Omega_1^{\frac{1}{2}}, \quad \bar{A}_2 = a_2 k / \Omega_2^{\frac{1}{2}}. \quad (192)$$

On writing $A' = A'_1 + A'_2$ in equation (187) we have

$$\delta' = -\Re 4\rho(\pi/k)^2 \iint_{\Omega_1 + \Omega_2} (A'_1 + A'_2) (A'_{1-} + A'_{2-}) \sigma^2 W(2\sigma, \tau) e^{2i\sigma t} du dv, \quad (193)$$

where A'_{1-} , etc., is written briefly for $A'_1(-u, -v)$. Since Ω_1 defines a progressive wave group, it will contain no opposite pair of wave components, nor, similarly, will Ω_2 . Thus equation (193) reduces to

$$\delta' e^{-2i\sigma t} = -\Re 8\rho(\pi/k)^2 \iint_{\Omega_{12}} A'_1 A'_{2-} \sigma^2 W(2\sigma, \tau) e^{2i(\sigma - \sigma_{12})t} du dv, \quad (194)$$

where Ω_{12} denotes the region common to Ω_1 and $-\Omega_2$, and we have introduced σ_{12} , the mean value of σ over Ω_{12} .

Now it may be assumed that there is no correlation between the phases of wave components at different points in the original spectrum A . The same will in general be true for the modified spectrum A' , but because of the 'blurring' function (equation (81)) there may be some correlation for points that are close together in the (u, v) -plane. The degree of correlation will depend on the separation of the points concerned relative to the width of the blurring function, which we have seen is of order unity. Values of $A(u, v)$ much closer than this will be highly correlated, while those much more widely separated will be hardly correlated at all. Suppose then that the range of integration in (194) is divided into unit squares and the integration carried out over each square separately. The final result will be the sum of Ω_{12}/k^2 vectors of random phase and each of the order of magnitude of

$$8\rho(\pi/k)^2 \bar{A}_1 \bar{A}_2 \sigma_{12}^2 W(2\sigma_{12}, \tau). \quad (195)$$

Hence the order of magnitude of δ' is given by

$$\delta' \approx 8\rho(\pi/k)^2 \bar{A}_1 \bar{A}_2 \sigma_{12}^2 (\Omega_{12}/k) W(2\sigma_{12}, r) e^{2i\sigma_{12}t}. \quad (196)$$

Similarly, if the total storm area is Λ there will be $\Lambda k^2/4\pi^2$ separate squares S into which the storm area is divided. Hence the amplitude δ of the displacement from the whole storm is of the order

$$\delta \approx 8\rho(\pi/k)^2 \bar{A}_1 \bar{A}_2 \sigma_{12}^2 (\Lambda^{\frac{1}{2}} \Omega_{12}/2\pi) W(2\sigma_{12}, r) e^{2i\sigma_{12}t}. \quad (197)$$

To the same order of approximation W , which may be the sum of two or more terms, may be replaced by \bar{W} (equation (186)). On substituting from equations (192) we have finally

$$\delta \approx 4\pi\rho a_1 a_2 \sigma_{12}^2 (\Lambda \Omega_{12}/\Omega_1 \Omega_2)^{\frac{1}{2}} \bar{W}(2\sigma_{12}, r) e^{2i\sigma_{12}t}. \quad (198)$$

As we should expect, this formula for δ is independent of the size of the squares chosen for the subdivision of the generating area Λ . It depends only on the total generating area, on the mean wave height of each group and on the areas of the corresponding two-dimensional frequency spectra, defined by Ω_1 and Ω_2 . All these are quantities of which rough estimates can in practice be made. It is interesting to remark that although δ increases as the square root of the area common to Ω_1 and $-\Omega_2$, it also diminishes with the square root of Ω_1 and Ω_2 . Hence, in general, the more widely the energy is distributed in the spectrum the smaller is the resulting disturbance.

5.3. Discussion

We proceed now to consider the application of equation (198) in some practical cases. As was first intuitively suggested by Bernard (1941*a*), the necessary condition for the generation of microseisms on the present hypothesis is the interference of groups of waves of the same wave-length travelling in opposite directions. Although not much is at present known about the generation of waves by surface winds, observation certainly suggests that a wind blowing steadily in one direction will in the course of time generate waves or swell travelling mainly in that direction, or in a direction not differing by more than 45° from it. We must therefore either look for cases in which two wind systems are in some way opposed, or else assume the possible reflexion of wave energy from a steep coast.

Bernard suggested that favourable conditions for wave interference would be found at the centre of a cyclonic depression, where waves originating on all sides of the depression might be received. It is known that in a circular depression the winds, though mainly along the isobars, have also a component inwards towards the centre, and in fact observation of sea conditions in the 'eye' of a cyclone tend to confirm this expectation. It is well known that in such regions relatively low wind velocities may be combined with high and chaotic seas such as would be characteristic of wave interference.

Suppose then that in the centre of a circular depression in the Atlantic wave energy is being received equally from all directions with a range of periods between 10 and 16 sec. The wave-length λ in deep water being given approximately by $\lambda = gT^2/2\pi$, where T is the period, we have $\lambda_1 < \lambda < \lambda_2$, where

$$\lambda_1 = 1.54 \times 10^4 \text{ cm.}, \quad \lambda_2 = 4.00 \times 10^4 \text{ cm.}$$

THEORY OF THE ORIGIN OF MICROSEISMS

The energy in the frequency spectrum is contained in an annular region lying between the two circles having their centres at the origin and radii $2\pi/\lambda_1$ and $2\pi/\lambda_2$ respectively. This region may be divided by any diameter of the circles into two equal regions Ω_1 and Ω_2 , where

$$\Omega_1 = \Omega_2 = \Omega_{12} = 2 \cdot 15 \times 10^{-7} \text{ cm.}^{-2}.$$

Assuming $\Lambda = 1000 \text{ km.}^2$, $\sigma_{12} = 2\pi/13 \text{ sec.}^{-1}$, $a_1 = a_2 = 3 \text{ m.}$,

we find that the coefficient of $\bar{W} e^{2i\sigma_{12}t}$ in equation (198) is $1 \cdot 8 \times 10^{15}$ dynes. If also

$$h = 3 \text{ km.}, \quad r = 2000 \text{ km.},$$

we find $\bar{W}(2\sigma_{12}, r) = 1 \cdot 8 \times 10^{-19} \text{ cm./dynes}$, giving as the amplitude of the displacement, from peak to trough,

$$2|\delta| = 6 \cdot 5 \times 10^{-4} \text{ cm.} = 6 \cdot 5 \mu.$$

The above estimate shows that the theory is in agreement with observation as regards the order of magnitude of the expected ground movement. It has been assumed that the energy is uniformly distributed within the given range of frequencies. Any concentration of energy within a narrower band in the frequency range would tend in general to increase the amplitude of the microseisms. It has also been assumed that \bar{W} is constant over the whole frequency range. From the chosen value of σ_{12} we have $2\sigma_{12}h/\beta_2 = 1 \cdot 03$, so that, from figure 1, $[\Sigma c_m]^{\dagger}$ is 0.69 or about three-quarters of its maximum value. However, since $[\Sigma c_m]^{\dagger}$ is never less than its value of 0.191 for shallow water, and increases to 0.91 within the frequency range, the mean value chosen is certainly not a serious over-estimate.

Most cyclonic depressions are themselves in movement over the ocean with a speed comparable to that of the waves. This movement may considerably increase the effective area of wave interference. For, if the velocity of the depression as a whole exceeds the group velocity of the waves, the waves generated by winds on one side of the depression and travelling in the same general direction will interfere with those generated at a later time on the other side of the depression and travelling in the opposite direction. Thus, even if the winds blew directly along the isobars and only generated waves running strictly in that direction, there would still be a 'trail' of wave interference in the wake of the depression. In general, therefore, the motion of a depression may be expected to increase the amplitude of the microseisms generated.

The amplitude of the microseisms due to coastal wave reflexion is more difficult to estimate, since less is known about the amount of energy reflected from a sloping beach. The reflected wave is usually hidden from observation by the much larger amplitude of the incoming wave, although if the crests of the reflected wave are not parallel to those of the incoming wave the former can sometimes be clearly seen. Effective interference will take place only at those parts of the coast where the shore-line is perpendicular to the direction of propagation of some components of the wave group, and the narrower the range of directions of the incoming waves, the more critically will the amount of reflexion depend upon the direction of the shore-line. The refraction of the wave crests parallel to the shore-line in shallowing water will operate in favour of effective wave interference, although the amount of refraction is small until the depth is less than about half a wave-length.

As an example consider a swell of mean amplitude $a_1 = 2 \text{ m.}$ and period 12 to 16 sec., whose direction of propagation lies within an angle of 30° . This gives $\Omega_1 = 1 \cdot 4 \times 10^{-8} \text{ cm.}^{-2}$.

The direction of the reflected wave energy is then also spread over an angle of 30° . Supposing, however, the shore-line to make a mean angle of 10° with the mean direction of the incoming waves, only one-third of the angle of the reflected waves overlaps that of the incoming waves. Thus $\Omega_2 = 1.4 \times 10^{-8} \text{ cm.}^{-2}$, $\Omega_{12} = 0.47 \times 10^{-8} \text{ cm.}^{-2}$. If we assume that the reflected wave extends a distance of 10 km. from the shore with a mean amplitude equal to 5% of that of the incoming wave, and if the effective shore-line is 600 km. in length, we have $\Lambda = 6000 \text{ sq. km.}$, $a_2 = 0.1 \text{ m.}$ Taking $h = 0$, $\tau = 1000 \text{ km.}$, we find from (198) that $2|\delta| = 0.3\mu$. This amplitude is rather smaller than that in the case considered previously. We conclude that the largest microseisms are probably due to wave interference in mid-ocean, although coastal reflexion may be a more common cause of microseisms of smaller amplitude. Exceptions may occur for stations near to the coast.

It has been seen that the microseism amplitudes may be increased by a factor of the order of 5 owing to the greater response of the physical system for certain depths of water. In practice, with an ocean of non-uniform depth, the amplitude will be affected by the depth of water at all points between the generating area and the observing station. Since, however, the energy density is greatest near the source of the disturbance, the depth of water in the generating area itself may be expected to be of most importance.

In so far as the sea waves must be considered to possess not a single frequency but a spectrum of finite width, we may expect that the unequal response of the ocean will cause an apparent shift of the spectrum towards those frequencies for which the response is a maximum. In the case of disturbances due to coastal reflexion, which in most instances would take place in shallow water, less frequency shift is to be expected. On the other hand, the coefficient of reflexion will very probably depend both upon the height and wave-length of the waves. There will probably also be a lengthening of the average wave period with increasing distance from the storm area, owing to the more rapid viscous damping of the higher frequencies in the spectrum. Evidence of this effect has been given by Gutenberg (1932).

6. CONCLUSIONS

Unattenuated pressure variations of the type discovered by Miche in the standing wave are a phenomenon of more general occurrence. They are due essentially to changes in the potential energy of the whole wave train. The general condition for fluctuations in the mean pressure over a wide area of the sea surface is that the frequency spectrum should contain groups of waves of the same wave-length travelling in opposite directions. The pressure fluctuations are then of twice the frequency of the corresponding waves and are proportional to the product of the wave amplitudes. Waves of compression in the ocean and sea bed should be set up, which may be of sufficient amplitude to be recorded as microseisms. For certain depths of the ocean the displacements will be increased by a factor of the order of 5 owing to resonance.

On the present theory suitable conditions of wave interference would arise near the centre of a cyclonic depression, as suggested by Bernard, but more particularly if the depression is moving rapidly. The effect of wave interference over deep water would be probably greater, under favourable conditions, than the effect of coastal wave reflexion, though the latter may be the determining factor for stations near to the coast. The periods of the microseisms

THEORY OF THE ORIGIN OF MICROSEISMS

35

should be half those of the corresponding waves, though an apparent shift in the frequency spectrum may be expected owing to the variation of the frequency response with the depth of the ocean and to the more rapid damping of the higher frequencies.

I should like to express my thanks to Dr G. E. R. Deacon of the Admiralty Research Laboratory for suggesting the subject of the present investigation and for his encouragement during the early stages. I am much indebted to Professor H. Jeffreys for many valuable suggestions, and to him and to Dr R. Stoneley for advice in the preparation of this paper. Publication is by kind permission of the Admiralty.

REFERENCES

- Baird, H. F. & Banwell, C. J. 1940 *N.Z. J. Sci. Tech.* 21B, 314.
 Banerji, S. K. 1930 *Phil. Trans. A*, 229, 287.
 Banerji, S. K. 1935 *Proc. Indian Acad. Sci.* 1, 727.
 Bernard, P. 1937 *C.R. Acad. Sci., Paris*, 205, 163.
 Bernard, P. 1941a *Bull. Inst. océanogr. Monaco*, 38, no. 800.
 Bernard, P. 1941b *Étude sur l'Agitation Microsismique*. Presses Universitaires de France.
 Bochner, S. 1932 *Vorlesungen über Fouriersche Integrale*. Leipzig: Akademische Verlagsgesellschaft.
 Bradford, D. C. 1935 *Bull. Seism. Soc. Amer.* 25, 323.
 Deacon, G. E. R. 1947 *Nature*, 160, 419.
 Deacon, G. E. R. 1949 *Ann. N.Y. Acad. Sci.* 51, 3, 475.
 Gherzi, E. 1932 *Beitr. Geophys.* 36, 20.
 Gilmore, M. H. 1946 *Bull. Seism. Soc. Amer.* 36, 89.
 Gutenberg, B. 1931 *Bull. Seism. Soc. Amer.* 21, 1.
 Gutenberg, B. 1932 *Handb. Geophys. Berl.* 4, 263.
 Jeffreys, H. 1925 *Proc. Roy. Soc. A*, 107, 189.
 Jeffreys, H. 1926 *Proc. Camb. Phil. Soc.* 23, 472.
 Jeffreys, H. & Jeffreys, B. S. 1946 *Methods of mathematical physics*. Cambridge University Press.
 Lamb, H. 1904 *Phil. Trans. A*, 203, 1.
 Lamb, H. 1932 *Hydrodynamics*, 6th ed. Cambridge University Press.
 Lee, A. W. 1934 *Geophys. Mem.* no. 62.
 Levi-Civita, T. 1925 *Math. Ann.* 93, 264.
 Longuet-Higgins, M. S. & Ursell, F. 1948 *Nature*, 162, 700.
 Miche, M. 1944 *Ann. Ponts Chauss.* 2, 42.
 Pidduck, F. B. 1910 *Proc. Roy. Soc. A*, 83, 347.
 Pidduck, F. B. 1912 *Proc. Roy. Soc. A*, 86, 396.
 Press, F. & Ewing, M. 1948 *Trans. Amer. Geophys. Un.* 29, 163.
 Ramirez, J. E. 1940 *Bull. Seism. Soc. Amer.* 30, 35-84 and 139-178.
 Scholte, J. G. 1943 *Versl. gewone Vergad. Akad. Amst.* 52, 669.
 Sommerfeld, A. 1909 *Ann. Phys., Lpz.*, 28, 665.
 Stoneley, R. 1926 *Mon. Not. R. Astr. Soc. Geophys. Suppl.* 1, 349.
 Tams, E. 1933 *Z. Geophys.* 9, 23-30 and 295-300.
 Whipple, F. J. W. & Lee, A. W. 1935 *Mon. Not. R. Astr. Soc. Geophys. Suppl.* 3, 287.

Errata

- p.6. equation (7); right-hand side should be $-\rho \frac{\partial^2 z}{\partial t^2}$.
 line below equation (13): for $z = \zeta'$ read $z = \zeta$.
- p.7. equation (17): for $z'\bar{\xi}$ read $z'\bar{\zeta}$.
 equation (18): for $\zeta'\bar{\xi}$ read $\zeta'\bar{\zeta}$.
- p.10. equation (39): for $-g$ read $+g$.
 integral in last bracket should be $\int_{\zeta}^z \left\{ -\int_{\zeta}^z \dot{u} dz + uw \right\} dz$.
- p.16. in text between (80) and (81): for $(-u_1, -v_1)$ read $(-u, -v)$.
- p.19. equation (108): right-hand side should be $c^2 \rho_s e^{gz/c^2} - 1$.
- p.23. equation (144): in second equation for $F^{(1)}$ read $F^{(4)}$.
- p.24. equations (157): last term in first equation is $\alpha'(y^2 - \alpha'^2 + 4k^2) \cosh \alpha'h$.
 equation (154): for $\partial^2 \phi_2''$ read $\frac{\partial^2 \phi''}{\partial t^2}$.
 equation (159): in last term, for k^{-1} read λ^{-1} .
- p.25. equation (168): in expressions for $J^{(3)}$, $J^{(4)}$ insert a factor $\frac{1}{4}$.

*Reprinted without change of pagination from the
Proceedings of the Royal Society, A, volume 206, 1951*

An experimental study of the pressure variations in standing water waves

BY R. I. B. COOPER AND M. S. LONGUET-HIGGINS

Department of Geodesy and Geophysics, University of Cambridge

(Communicated by R. Stoneley, F.R.S.—Received 9 December 1950)

Although the first-order pressure variations in surface waves on water are known to decrease exponentially downwards, it has recently been shown theoretically that in a standing wave there should be some second-order terms which are unattenuated with depth. The present paper describes experiments which verify the existence of pressure variations of this type in waves of period 0.45 to 0.50 sec. When the motion consists of two progressive waves of equal wave-length travelling in opposite directions, the amplitude of the unattenuated pressure variations is found to be proportional to the product of the wave amplitudes. This property is used to determine the coefficient of reflexion from a sloping plane barrier.

1. INTRODUCTION

In the well-known first-order theory of surface waves in deep water (Lamb 1932, chap. 9) the pressure fluctuations at a given point in any periodic wave motion decrease exponentially with the depth. Thus in a progressive wave of length λ , $= 2\pi/k$, of period T , $= 2\pi/\sigma$, and height $2a$ from crest to trough, the pressure fluctuations p_1 are given by

$$p_1 = \rho g a e^{-kz} \cos(kx - \sigma t), \quad (1)$$

where ρ is the density and g is the acceleration of gravity, t denotes the time and x and z are horizontal and vertical co-ordinates, z being measured downwards from the mean surface level. The wave-length and period are connected by the relation

$$\sigma^2 = gk \quad \text{or} \quad \lambda = gT^2/2\pi. \quad (2)$$

Therefore, at depths greater than about half a wave-length, the first-order pressure variations are very small. The work of Levi-Civita (1925) also shows that in a progressive wave the pressure variations are attenuated exponentially to all orders of approximation. Now, in the first approximation two progressive waves of equal wave-length and amplitude travelling in opposite directions combine to form a standing wave. The first-order pressure terms are of the form

$$p_1 = 2\rho ga e^{-kz} \cos kx \cos \sigma t, \quad (3)$$

and are therefore attenuated exponentially as in a progressive wave. However, Miche (1944) recently showed that the second-order pressure variations in a standing wave do not tend to zero but to the value

$$(p_2)_\infty = 2\rho a^2 \sigma^2 \cos 2\sigma t. \quad (4)$$

Although this term is of second order it will become predominant over the first-order term at depths greater than about half a wave-length. Since it is independent of both x and z it represents a pressure variation applied uniformly over the whole fluid; it is of twice the fundamental frequency. A physical explanation of the existence of this term has been given (Longuet-Higgins 1950), and it has been shown that in the general case when two waves of equal length but of different amplitudes a_1 and a_2 encounter one another travelling in opposite directions the unattenuated pressure variation is given by

$$(p_2)_\infty = 2\rho a_1 a_2 \sigma^2 \cos 2\sigma t. \quad (5)$$

The standing wave is the special case where the two wave amplitudes are equal, the progressive wave the special case where one of them is zero.

The existence of second-order pressure variations of this type is not only of theoretical interest but may also be of importance in practice. Under suitable conditions the pressure variations in ocean waves may extend to considerable depths, and it has been suggested (Longuet-Higgins 1950) that these may be one cause of the small oscillations of the earth's crust which are generally known as microseisms. The present experiments were undertaken with the purpose of verifying the existence of these pressure variations on a model scale, and of showing how they may be used to determine the amount of wave reflexion from different types of obstacle.

2. APPARATUS

The experiments were carried out in a wooden tank of length 970 cm., depth 50 cm. and width 24 cm. (see figure 1). At one end of the tank waves were generated by a paddle *A* consisting of a rectangular metal plate of width 23.5 cm. hinged at its lower edge and made to oscillate about a mean vertical position by a crank-shaft

driven by a $\frac{1}{4}$ h.p. electric motor. By an adjustment to the arm of the crank the amplitude of the waves could be varied at will; the wave period, and hence the wave-length, was controlled through the speed of the motor. It was found convenient to use waves of period about 0.5 sec., the corresponding wave-length (about 40 cm.) being less than the depth of the tank but sufficiently large compared with the measuring apparatus.

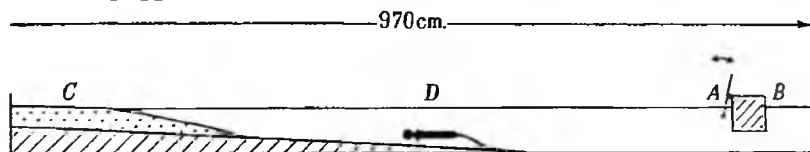


FIGURE 1. Vertical section of the wave tank, showing the relative positions of the paddle (*A*), wave-absorber (*B*), sand beach (*C*) and hydrophone (*D*).

Between the paddle and the near end of the tank was a honeycomb arrangement of metal sheets (*B* in figure 1) designed to destroy the wave energy on that side of the paddle. Waves travelled down the tank towards the far end, where they were either absorbed by a shallow sand beach (*C*), or reflected from a suitable reflector inserted in the tank. The regularity of the waves depended slightly on the depth at which the paddle was hinged. In the present experiments the hinge was at 10 cm., or about a quarter of a wave-length, below the surface, this giving a steady, sinusoidal wave profile. It was found that the wave surface could be made smoother by previously wetting the sides of the tank to a level higher than the wave crests.

Measurements of wave height were made with a hook-and-point gauge consisting of a thin wire (the point) extending vertically downwards into the water and fixed relatively to a similar inverted wire (the hook) extending upwards from below. Both wires were rigidly attached to a sliding vertical scale. The apparatus was initially adjusted so that the point, when lowered from above, first made contact with the still-water surface at the same scale reading as that at which the hook broke the surface when raised from below. To measure the wave height, the gauge was first raised until each crest just touched the point and then lowered until each trough just missed the hook; the difference between the two readings was taken to be the wave height $2a$.

The wave period was measured by timing, with a stop-watch, the passage of 20 successive crests past a fixed point.

The motor quickly accelerated from rest and reached an almost steady speed in about 2.5 sec. The speed was unaffected by the presence of the water, the energy imparted to the waves being in fact negligible.

The pressure was measured with a quartz-crystal hydrophone of a type constructed at the Admiralty Mining Establishment.* This consisted of a circular brass head, 9 cm. in diameter and 2 cm. thick, attached to a brass cylindrical body 6 cm. in diameter and 50 cm. long. The hydrophone head contained two circular quartz crystals cemented, back-to-back, to a central brass plate, the outer faces of the crystals being cemented also to two outer brass plates which were electrically

* The authors are indebted to the Admiralty for permission to describe this apparatus.

common but insulated from the body. Rubber sheet $\frac{1}{16}$ in. thick was cemented to the outer plates and clamped to the hydrophone head by a brass ring, making a water-tight seal. When pressure was applied, an electrical signal was developed between the inner and the two outer brass plates. The outer plates were connected to earth via a small resistance used for the purpose of calibration; the inner plate was connected to the grid of the first valve of a pre-amplifier contained in the body of the hydrophone. A cable, carrying power supplies and leads for the output signal and for calibration, entered the end of the body through a water-tight rubber gland. The electrical signal from the hydrophone was passed through an adjustable attenuator to a second amplifier, whose output operated an Esterline-Angus recording millimeter. To reduce 'noise', series resistors and shunt capacities were incorporated between the stages, making the gain appreciable only between 1 and 10 c./sec. (Such an arrangement, however, necessarily introduces some phase distortion.)

Let K denote the piezo-electric constant of quartz, R the resistance of the crystals, A the area of the outer brass plates and C the capacity of the plates and their leads. Then it may be shown that an oscillatory pressure $p_0 \cos \sigma t$ applied to the plates of the hydrophone produces a voltage $V \cos \sigma t$ given by

$$V/p = KA/C,$$

provided that $\sigma^2 R^2 C^2 \gg 1$, a condition satisfied in the present case. The theoretical sensitivity of the hydrophone head, based on the above formula, was

$$1.5 \times 10^{-5} \text{ V/dyne-cm.}^{-2}.$$

To calibrate the apparatus a voltage equivalent to, say, 100 dynes-cm.⁻² and of the appropriate frequency was injected across the small calibrating resistor in the hydrophone head, and the deflexion of the millimeter was then compared with that produced by the waves.

When the pressure was not uniform, it was assumed that the deflexion was the same as would be produced by a uniform pressure equal to the mean pressure over the plates of the hydrophone. Since the plates were circular, and the pressure p theoretically obeyed Laplace's equation $\nabla^2 p = 0$, this mean pressure was equal to the value of p at the centre of the plates.

The hydrophone was suspended in a horizontal position from two iron bars laid across the top of the tank, the head being away from the paddle (see figure 1). The plates of the hydrophone head were set in a vertical plane, in order to cause the least possible disturbance to the motion. Though the support was not rigid, the motion of the hydrophone itself was very small, and no difference in the measured pressure could be detected when the body was attached rigidly to the walls of the tank.

The estimated limits of accuracy of the different measurements are as follows; each figure represents the maximum error:

wave height $2a$:	± 0.02 cm.
wave period T :	± 0.01 sec.
depth z to centre of hydrophone:	± 0.05 cm.

Thus for waves of height 1.0 cm. and period 0.5 sec. the maximum error in the theoretical first-order pressure variation $\rho g a e^{-\sigma^2 z/g}$ at a depth of 15 cm. is 13 %. The maximum error in the second-order pressure variation $2\rho a^2 \sigma^2$ is 8 %.

The theoretical sensitivity of the hydrophone was known to within 5 %, and the voltage and frequency of the calibration signal could each be set to within 3 % of their desired values. The deflexion of the recorder was read to the nearest tenth of a division (the attenuator was adjusted so that the deflexion was normally about 1.5 divisions). A change of 3 % in the frequency of the calibration signal involved a change of not more than 6 % in the amplitude of the response. Hence the actual pressure could be measured with certainty to within about 20 %.

In each of the above estimates of the maximum error, allowance has been made for both a random and a systematic part. Though the rough analysis just given is sufficient for our purpose, we may notice that, since the systematic errors from independent sources do not necessarily tend in the same direction, the combined systematic errors are probably less than those given above. Also, because of the random errors, the accuracy of the measurements will be improved by taking the mean of several observations.

3. THE PROGRESSIVE WAVE

When the motor was switched on, a train of waves advanced down the tank, the wave front travelling with approximately the theoretical group velocity $gT/4\pi$. The arrival of the wave front was preceded by several rather longer waves due perhaps partly to dispersion and partly to the initial acceleration of the paddle. In the steady state the wave height was found to diminish with distance from the paddle. The decrease was of the order of a few units per cent per metre, and was attributed mainly to friction at the sides of the tank. No significant variation in the wave height across the tank was observed, and, with the wave amplitudes used, the motion appeared to be entirely two-dimensional.

It will be convenient to denote by x and z respectively the horizontal distance of the centre of the hydrophone head from the paddle and its vertical distance below the mean surface level. A typical record of the pressure, taken at $x = 400$ cm. and $z = 8.8$ cm., is shown in figure 2*a*. $X_1 Y_1$ is a calibration signal equivalent to 100 dyne-cm.⁻² at the frequency of the waves, and TT' is a time trace operated by a clock which made and broke an electrical circuit once every half-second. The paddle motor was first switched on at O . Until the point A , the deflexion of the pen is negligible, indicating there is no signal due to vibration of the motor or paddle. On the arrival of the wave front the pressure variations increase quickly to a maximum and remain at a nearly constant amplitude. The theoretical time of arrival, supposing the front to travel with the group velocity, is denoted by G . In the steady state the pressure variations were of the same period as the waves.

A similar record, but taken at $z = 17.3$ cm., is shown in figure 2*b*. The calibration signal $X_1 Y_1$ represents 25 dynes-cm.⁻². It will be seen that the pressure variations are reduced to about one-quarter of their previous value.

To measure the amplitude of the pressure variations, the mean value was taken of twenty successive oscillations of the recorder pen in the steady state (for

Pressure variations in standing water waves

example, PQ in figure 2*a*). The period was deduced by timing the waves in the tank simultaneously, and a calibration signal of the appropriate frequency was afterwards injected. Three successive sets of observations were made for eight different values of z . The mean values of the three measured pressures at each depth are

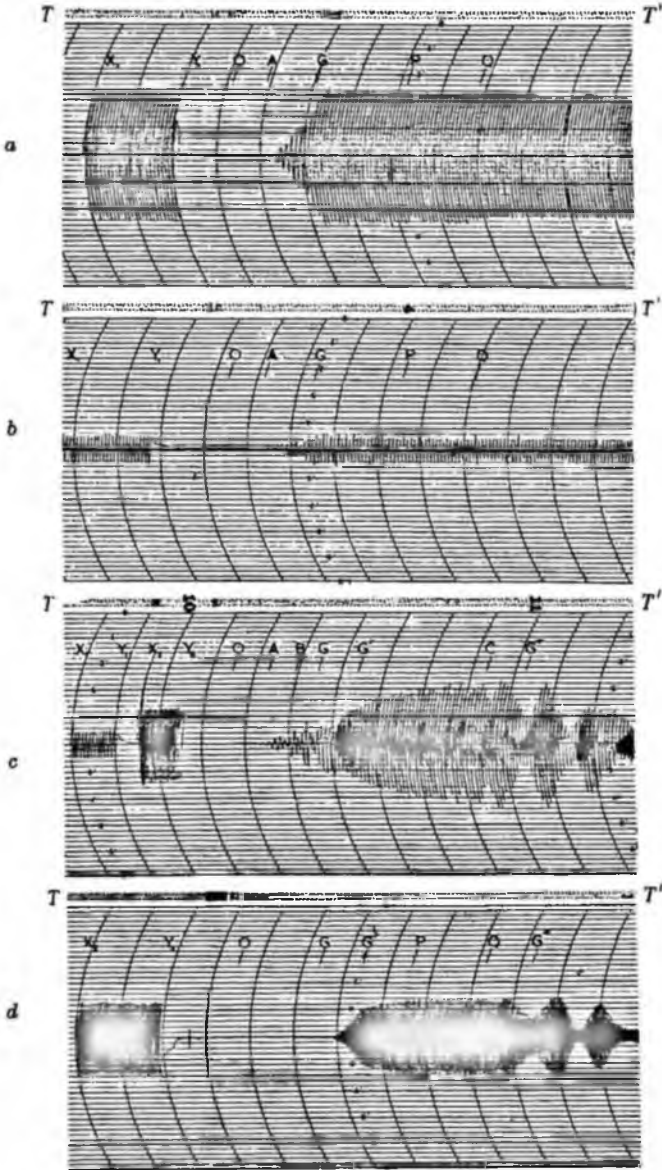


FIGURE 2. Typical records of pressure variations in progressive and reflected trains of waves. *a*, progressive wave, $z = 8.8$ cm.; *b*, progressive wave, $z = 17.3$ cm.; *c*, reflected wave, $z = 17.3$ cm.; *d*, reflected wave, $z = 37.0$ cm.

given in the second column of table 1. For each observation of the pressure a separate observation of the wave height $2a$ was made at a point immediately over the hydrophone head. The theoretical pressure, given in the third column of table 1, was calculated from the formula

$$p_{th.} = \rho g u e^{-\sigma^2 z/g},$$

using the mean values of the twenty-four observations of $2a$ and T , which were 1.11 cm. and 0.453 sec. respectively. Pressure variations of less than 10 dyne-cm.⁻² could not be measured accurately; but it was verified that at depths between 29.0 and 38.8 cm. (the greatest value of z possible) the pressure variations were less than 5 dyne-cm.⁻².

TABLE 1. COMPARISON OF THE MEASURED AND THEORETICAL VALUES OF THE PRESSURE VARIATIONS AT DIFFERENT DEPTHS IN A PROGRESSIVE WAVE

$x = 400$ cm. $h = 41.6$ cm. $2a = 1.11$ cm. $T = 0.453$ sec.			
z (cm.)	$P_{meas.}$ (dyne-cm. ⁻²)	$P_{th.}$ (dyne-cm. ⁻²)	$P_{meas.}/P_{th.}$
6.5	152	151	1.01
8.5	97	102	0.95
10.5	65	69	0.94
12.5	46.6	47.3	0.98
14.5	30.4	31.4	0.97
16.5	19.6	21.2	0.92
18.5	14.0	15.4	0.91
20.5	9.7	9.5	1.02

In view of the limits of accuracy of the experiments given in §2, the agreement between the second and third columns of table 1 is satisfactory. The measured pressure closely obeys the exponential law of decrease down to a depth equal to half the wave-length, and probably deeper. The mean value of the ratios in the last column is 0.96.

4. THE STANDING WAVE

To produce a standing wave, a smooth aluminium sheet, of the same width as the tank, was inserted into the water to act as a reflector. Figure 2c shows the pressure at the same point as in figure 2b when the distance l of the reflector from the paddle was 800 cm. $X_1 Y_1$ is a calibration signal representing 25 dynes-cm.⁻² at the fundamental frequency of the waves, and $X_2 Y_2$ represents 100 dynes-cm.⁻² at twice this frequency. On the first arrival of the waves (point A) the pressure variations are similar to those in the progressive wave. However, as soon as the reflected waves arrive (point B) the record begins to differ, and at G' , the theoretical time of arrival of the reflected wave front, a second-order component of twice the original frequency has appeared. Later an almost steady state is reached in which components of both frequencies are present. At C , however, the record begins to degenerate owing to the arrival of the waves reflected a second time from the paddle. (G'' denotes the theoretical time of arrival of the twice-reflected wave front.)

In figure 2*d* the depth has been increased to 37.0 cm. The first-order pressure variations become very small, and the arrival of the first wave train can hardly be detected on the record. The only pressure variations are now of twice the fundamental frequency, which appear, as before, on the arrival of the reflected wave front. When the reflector was removed the pressure variations quickly became negligible.

To determine the amplitude of the second-order pressure variations, the reflector was placed at $l = 500$ cm. and the hydrophone at such a depth that the first-order pressure variations were small. It can easily be shown that the apparent effect of a small first-order term is to increase and decrease alternately the amplitude of the (second-order) oscillations by very nearly the same amount, leaving the mean amplitude practically unchanged. The amplitude was determined from forty successive oscillations (PQ in figure 2*d*) in the steady state, before the record degenerated owing to the twice-reflected waves. Three sets of measurements were taken, at four different depths z . The mean values of the pressure at each depth are given in the second column of table 2. It was difficult to measure the height of the standing waves accurately during the short time that they remained regular. Accordingly, the height of the progressive wave in the absence of the reflector was first determined. Owing to the attenuation of the waves with distance along the tank the reflected wave was expected to be slightly smaller than the incident wave. To allow for this effect the wave height was measured at $x = 500$ cm.; for, on the assumption that the attenuation of the waves along the tank was exponential, the wave height at $x = 500$ cm. should be the geometric mean of the height of the incident and reflected waves at $x = 400$ cm. The mean values of the sixteen observations of wave height and period were 0.99 cm. and 0.461 sec. respectively. The theoretical pressure was calculated from the formula

$$p_{th.} = 2\rho a^2 \sigma^2.$$

TABLE 2. COMPARISON OF MEASURED AND THEORETICAL PRESSURE VARIATIONS AT DIFFERENT DEPTHS IN A STANDING WAVE

$z = 400$ cm. $l = 500$ cm. $h = 41.2$ cm. $2a = 0.99$ cm. $T = 0.461$ sec.

z (cm.)	$p_{meas.}$ (dyne-cm. ⁻²)	$p_{th.}$ (dyne-cm. ⁻²)	$p_{meas.}/p_{th.}$
21.5	88	91	0.97
26.5	87	91	0.96
31.5	90	91	0.99
36.5	94	91	1.03

Table 2 shows that the difference between the measured and theoretical values is again very slight, and the measured values show no significant dependence on z . The mean value of the ratios in the last column is 0.99.

By carrying out similar observations at a constant depth but at distances from the reflector varying over a range of a quarter of a wave-length, it was verified that the unattenuated pressure variations were also independent of x . Because of the phase shift in the amplifier no attempt was made to determine the relative

phases of first- and second-order pressure variations, but it was found that near a nodal plane the first-order variations were relatively small.

To determine the dependence of the unattenuated pressure variations on the wave height, similar observations were made with wave heights $2a$ lying between 0.65 and 1.75 cm. The results are given in table 3. Each figure represents the mean of three observations. It will be seen that the pressure variations increase very nearly as the square of the wave height. With waves of greater amplitude than about 2.0 cm., the wave crests in the standing wave became unstable, and a sideways oscillation was set up across the tank, destroying the two-dimensional motion.

TABLE 3. MEASURED AND THEORETICAL PRESSURE VARIATIONS IN THE STANDING WAVE, FOR DIFFERENT VALUES OF THE WAVE AMPLITUDE

$x = 400$ cm. $l = 500$ cm. $z = 35.4$ cm. $h = 41.3$ cm. $T = 0.473$ sec.

$2a$ (cm.)	$P_{\text{meas.}}$ (dyne-cm. ⁻²)	$P_{\text{th.}}$ (dyne-cm. ⁻²)	$P_{\text{meas.}}/P_{\text{th.}}$
0.65	37	37	1.00
0.82	58	59	0.98
1.06	90	99	0.91
1.21	126	129	0.98
1.58	207	219	0.95
1.75	250	270	0.93

5. PARTIAL REFLEXION

To obtain interference between two opposite wave trains of known but unequal amplitude, the reflector used in §4 was replaced by another designed to reflect only part of the wave energy. This consisted of a rectangular metal sheet, of the same width as the tank, extending to a variable depth h' below the mean surface level. The reflexion coefficient from a vertical barrier of this kind has been obtained theoretically, for low waves, by Ursell (1947). Since the unattenuated pressure variations are in theory proportional to the height of the reflected wave, their amplitude should be given by $2\rho\beta a^2\sigma^2$, where a is the amplitude of the corresponding progressive wave at the point where the reflector is inserted, and β is the reflexion coefficient.

Three successive series of observations were carried out as for the standing wave, with values of h' lying between 2.0 and 10.0 cm. (Over this range β increases from 0.26 to nearly unity.) The measured and theoretical values of the pressure are compared in table 4. There is fair agreement, although for the smaller values of h' the measured pressure is rather lower than might be expected.

Let us consider whether the distance of the hydrophone from the reflector (100 cm.) is great enough for the reflected wave train to be regarded as infinite in length. If we suppose a uniform pressure variation p' , given by

$$p' = \begin{cases} 2\rho\beta a^2\sigma^2 \cos 2\sigma t & (x < l), \\ 0 & (x > l), \end{cases}$$

433 *Pressure variations in standing water waves*

to be applied to the upper surface of the water, then it may be shown that the pressure variation within the fluid is given by

$$p' = \left[1 - \frac{1}{\pi} \tan^{-1} \frac{z}{x-l} - \frac{1}{\pi} \sum_{n=1}^{\infty} \tan^{-1} \frac{(-)^n 2(x-l)z}{4n^2h^2 + (x-l)^2 - z^2} \right] 2\rho\beta a^2 \sigma^2 \cos 2\sigma t,$$

(neglecting surface displacements). Taking $(l-x) = 100$ cm., $z = 36.6$ cm. and $h = 41.5$ cm. we find that the expression in square brackets equals 0.98. Thus, the pressure variations should be reduced only by about 2 % owing to this cause.

TABLE 4. MEASURED AND THEORETICAL PRESSURE VARIATIONS IN A PARTIALLY REFLECTED TRAIN OF WAVES

$x = 400$ cm.	$l = 500$ cm.	$z = 36.6$ cm.	$h = 41.5$ cm.	$T = 0.458$ sec.	$2a = 0.847$ cm.
h' (cm.)	β^*	$p_{th.}$ (dyne-cm. ⁻²)	$p_{meas.}$ (dyne-cm. ⁻²)	$p_{meas.}/p_{th.}$	
2.0	0.26	18	13	0.72	
3.0	0.58	39	33	0.84	
4.0	0.81	55	44	0.80	
5.0	0.94	64	54	0.84	
6.0	0.97	66	59	0.89	
7.0	0.99	67	69	0.95	
10.0	1.00	68	65	0.91	

* From Ursell (1947).

From the last column of table 4 we see that the difference between the measured and the theoretical pressures is on the whole greater for the smaller values of h' , that is, when the lower edge of the reflector is nearer the surface of the water. Hence it is reasonable to attribute the discrepancy to a loss of energy at the lower edge of the reflector, where the velocity theoretically becomes infinite. In practice we may expect that a thin boundary layer will be formed and that eddies will be thrown off alternately in either direction.

6. REFLEXION FROM A SLOPING BEACH

The measurement of second-order pressure variations provides a convenient method of determining by experiment the reflexion coefficient from a reflector of any given form; for since the theoretical amplitude is $2\rho\beta a^2 \sigma^2$, β may be deduced if both a , σ and the actual amplitude are known. Alternatively, it may be assumed, consistently with the results of §4, that the reflexion coefficient from the smooth vertical reflector extending to the bottom equals unity. The reflexion coefficient in the given case may then be obtained simply as the ratio of the second-order pressure variations to those in the case of the vertical reflector. The latter method has the advantage that it is independent of the absolute sensitivity of the hydrophone and that it does not necessarily involve measurement of the wave height and period.

As an illustration of the second method a brief study was made of the reflexion coefficient from a plane barrier inclined at a varying angle α to the horizontal. Three measurements were taken at each position of the reflector, and between each

observation a separate measurement was made with the reflector vertical. The mean values of the three corresponding ratios are given in table 5. It will be seen that between 90° and 45° the reflexion coefficient does not differ much from unity. After 45° there is a sharp decline, and at 15° the reflexion coefficient is less than 10%. Thus at the lower angles nearly all the wave energy is absorbed at the barrier. There was no genuine 'breaking' of the waves; but at 15° the foremost edge of the wave began to be visibly turbulent.

TABLE 5. COEFFICIENT OF REFLEXION β FROM A SMOOTH PLANE BARRIER INCLINED AT AN ANGLE α TO THE HORIZONTAL

$x = 400$ cm. $z = 35.6$ cm. $h = 41.5$ cm. $l = 500$ to 630 cm. $2a = 1.01$ cm.
 $T = 0.45$ sec. Temperature = 13.5° C.

α	β	α	β
90°	1.00	30°	0.72
75°	0.92	25°	0.56
60°	0.99	20°	0.31
45°	0.87	15°	0.08

CONCLUSIONS

The foregoing experiments have shown very clearly, for waves of half-second period, the difference in character between the pressure variations in progressive and in reflected trains of waves. In a purely progressive wave the pressure variations obey the exponential law of decrease down to a depth of at least half a wave-length, and below this depth are very small. However, if any of the wave energy is reflected, appreciable second-order pressure variations, proportional to the amplitude of the reflected wave, appear at all depths. Equations (1), (4) and (5) of §1 have been verified as accurate well within the limits of error of the experiments.

Since the second-order pressure variations increase as the square of the wave height they are relatively more important for waves of large amplitude; and they exert a considerable total force on the sides and bottom of the tank and on the reflector. For standing waves of height 1.8 cm. the second-order pressure variations were of the order of 320 dyne-cm.⁻², giving a total force on the reflector of 3.07×10^5 dynes or about 0.31 kg. The force corresponding to the first-order pressure variations was only 0.13 kg.

The formulae of §1, which are independent of the viscosity, should hold equally well for waves on the same scale as ocean waves. The chief difference between the waves used in the present experiments and the ocean waves occurring in practice is that the latter are usually much less regular; a generalization of the simple formulae to the case of waves having a general type of frequency spectrum has been given elsewhere (Longuet-Higgins 1950).

The reflexion coefficient for a sloping plane reflector is nearly unity when the reflector is vertical, and decreases steadily with the inclination to the horizontal, as might be expected. Since, however, the reflexion coefficient in this case depends on the viscosity, the same values will not necessarily apply to waves of different

435 *Pressure variations in standing water waves*

period and wave-length. For ocean waves, some energy will be dissipated in breaking, which will also increase the turbulence present in the water. It would be useful to investigate in the laboratory the effect of wave height and period on the reflexion coefficient, on both sides of the breaking-point. It may also be possible to obtain information as to the amount of reflexion of ocean waves by comparing the frequency spectra of the pressure at points off a sloping beach and off a headland or harbour wall.

The authors are much indebted to Professor J. A. Steers and Mr W. V. Lewis for permission to use the wave tank in the laboratory of the Department of Geography, Cambridge.

REFERENCES

- Lamb, H. 1932 *Hydrodynamics*, 6th ed. Cambridge University Press.
Levi-Civita, T. 1925 *Math. Ann.* 93, 264.
Longuet-Higgins, M. S. 1950 *Phil. Trans. A*, 243, 1.
Miche, M. 1944 *Ann. Ponts Chauss.* 2, 42.
Ursell, F. 1947 *Proc. Camb. Phil. Soc.* 43, 374.

From: Proc. Symposium on Microseisms, Harriman, N.Y., Sept. 1952, pp. 74-93.
Washington D. C., N.A.S. - N.R.C. Publ. No. 306 (1953).

CAN SEA WAVES CAUSE MICROSEISMS?

By M. S. Languet-Higgins
Trinity College at Cambridge

Abstract—This paper is an exposition of the "wave interference" theory of microseisms. Simple proofs are given of the existence, in water waves, of second-order pressure fluctuations which are not attenuated with depth. Such pressure fluctuations in sea waves may be sufficiently large to cause microseisms. The necessary conditions are the interference of opposite groups of waves, such as may occur in cyclones or by the reflection of waves from a coast.

Introduction—It has long been known that there is some connection between certain types of microseisms and deep atmospheric depressions over the ocean; and the similarity between microseisms and sea waves — their periodic character and the increase of their amplitude during a "storm" — naturally suggests some causal relation between them. But until recently there have seemed to be many difficulties, both theoretical and observational, to supposing that sea waves could, by direct action on the sea bed, be the cause of all these microseisms; for the latter have been recorded while the corresponding sea waves were still in deep water, whereas theory seemed to show that the pressure fluctuations associated with water waves were quite insufficient, at such depths, to produce any appreciable movement of the ground.

However, recent theoretical work in hydrodynamics has altered this situation: Miche (1944), in quite another connection, discovered the existence, in a standing wave, of second order pressure variations which are not attenuated with the depth; a much shorter demonstration of this result was given by Languet-Higgins and Ursell (1948), and the result was extended by the present author (1950) to more general systems of waves. In the latter paper it was shown that such pressure variations may be quite sufficient, under certain circumstances, to produce the observed ground movement, the chief conditions required being the interference of waves of the same wavelength, but not necessarily of the same amplitude, travelling in opposite directions. This, then, may be called the "wave interference theory."

In the latter paper (which will be referred to as I) the results on which the theory depends

were derived in a general and concise form, with detailed proofs. In view of the interest of the subject it seems desirable to clarify the main ideas behind the theory and to discuss further some of the more unexpected results. This will be attempted in the present paper, in which we shall rely as far as possible on physical reasoning, and refer where necessary to the former paper for rigorous proofs of the results quoted. We shall conclude with a brief historical review of the theory.

1. **The importance of the mean pressure**—Let us suppose that seismic waves are to be generated by some kind of oscillating pressure distribution acting on the surface of the earth or of the sea bed. If the period of the oscillation is T , and the corresponding wavelength of seismic waves is L , then the pressure distribution over an area whose diameter is small compared with L may be regarded as being applied at the same point, so far as the resulting disturbance is concerned; for the time-difference involved in applying any pressure at another point of the area would be small compared with T . Hence the resulting disturbance is of the same order of magnitude as if the mean pressure over the area were applied at the point. Now the wavelength of a seismic wave is many times that of a gravity-wave (sea wave) of the same period. It is therefore appropriate to consider the properties of the mean pressure, over a large number of wavelengths, in different kinds of gravity-wave. We shall first consider some very special but physically interesting cases, when the waves are perfectly periodic and the wave-train is infinite in length. It will be assumed for the moment that the water is incompressible.

2. **The progressive wave**—Consider any periodic, progressive disturbance which moves, unchanged in form, with velocity c (see figure 1). Let $\bar{p}(t)$ denote the mean pressure on a fixed horizontal plane (say the bottom) between two fixed points, A, B, separated by a wave length

We may show that $\bar{p}(t)$ is a constant. Let A and B denote the points, separated from A and B respectively by a distance ct . Then since the motion progresses with velocity c the mean pressure over 'A'B' at time t equals the mean pressure over A B at time 0, i.e. $\bar{p}(0)$;

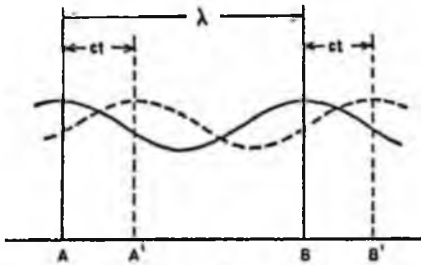


Figure 1. Positions of the profile of a progressive wave at two different times.

the total force on $A'B'$ is $\lambda \bar{p}$ (0). But since the motion is periodic the force on $A A'$ equals the force on $B B'$. Hence, by subtraction, the force on $A B$ equals $\lambda \bar{p}$ (0); and the mean pressure on $A B$ equals \bar{p} (0) which is independent of the time. Thus there is no fluctuation in the mean pressure on the bottom over one wave-length, or over a whole number of wavelengths; in any interval containing more than N wavelengths the fluctuation in the mean pressure is less than $N^{-1} p_{\max}$ where p_{\max} is the maximum pressure in the interval. In other words, in a progressive wave the contributions to the disturbance from different parts of the sea bed tend to cancel one another out.

There is a second reason why progressive water waves may be expected to be relatively ineffective in producing seismic oscillations of the sea bed: not only the mean pressure fluctuation \bar{p} , but also the pressure fluctuation p at each point decreases very rapidly with depth and is very small below about one wavelength from the surface. This fact is closely connected with the vanishing of the mean pressure fluctuation; the motion below a certain horizontal plane can be regarded as being generated by the pressure fluctuations in that plane; and hence we should expect that the contributions to the motion from the pressure in different parts of the plane would tend to cancel one another out.

3. The standing wave—Consider now a standing wave, and let A and B be the points where two antinodal lines, a wavelength apart, meet the bottom (see figure 2). To a first approximation, a standing wave can be regarded as the sum of two progressive waves of equal wavelength and amplitude travelling in opposite directions. Therefore the mean pressure on the bottom between $A B$ vanishes to a first approximation. However, the summation of the waves is not exact; if two progressive motions, each satisfying the boundary condition of constant pressure at the free surface, are added, (i.e. if the velocities at each point in space are added) there is no "free surface" in

the resulting motion along which the pressure is always exactly constant; although if the elevations of the free surface are added in the usual way, the pressure is constant along this surface, to a first approximation. We should not expect the motions to be exactly superposable, on account of the non-linearity of the equations of motion.

It can be seen from the following simple argument that the mean pressure on the bottom, in a standing wave, must fluctuate. Consider the mass of water contained between the bottom, the free surface, and the two nodal planes shown in figure 2. Since there is no flow across the nodal planes, this mass consists always of the same particles; therefore the motion of the center of gravity of this mass is that due to the external forces alone which act upon it. Figure 2 shows the mass of water in four phases of the motion, separated by intervals of one quarter of a complete period. In the first and third phases the wave crests are fully formed, and in the second and fourth phases the surface is relatively flat (though never exactly flat; see Martin et al., 1952). When the crests are formed the centre of gravity of the mass is higher than when the surface is flat, since fluid has, on the whole, been transferred from below the mean surface level to above it. Thus the centre of gravity is raised and lowered twice in a complete cycle. But

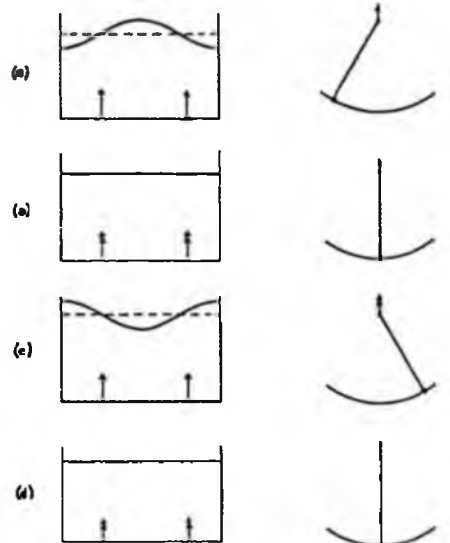


Figure 2. Comparison of a standing wave with a swinging pendulum, at four different phases of the motion separated by a quarter of a period.

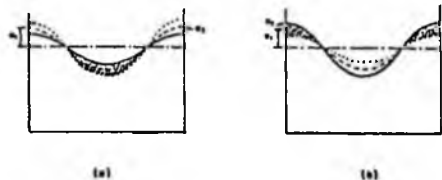


Figure 3. Two phases of the interference between two waves of equal length but different amplitudes a_1 and a_2 travelling in opposite directions. The profile of the first wave (dashed line) is reduced to rest by superposing on the system a velocity $-c$; the second wave appears to travel over the first with velocity $-2c$. The full line shows the final wave form.

the external forces acting on the mass are, first, that due to gravity, which is constant, (the total mass being constant); secondly the force from the atmosphere, which is also constant, since the pressure p_0 at the free surface, if constant, will produce a constant downwards force λp_0 ; thirdly the forces across the vertical planes, which must have zero vertical component, the motion being symmetrical about these planes; and, lastly, the force on the bottom, which equals $\lambda \bar{p}$. Since all the other external forces besides $\lambda \bar{p}$ are constant it follows that \bar{p} must fluctuate with the time. In figures 2(a) and 2(c) the mass of water above the mean level is proportional to the wave amplitude a ; since it is raised through a distance of the order of a , the displacement of the centre of gravity, and hence the mean pressure fluctuation, is proportional to a^2 .

An explicit expression for p can easily be derived. Let z denote the vertical coordinate of a particular element of fluid of mass m , so that z is a function of the time t and of, say, the position of the fluid element when $t = 0$. If F denotes the vertical component of the external forces acting on the mass of water, we have, on summing the equations of mo-

tion for each element of fluid, and cancelling the internal forces:

$$F = \sum (m \frac{\partial^2 z}{\partial t^2}) = \frac{\partial^2}{\partial t^2} (\sum m z) \quad (1)$$

the summation being over all the particles. The expression in brackets on the right-hand side will be recognized as g^{-1} times the potential energy of the waves; in an incompressible fluid

$$\sum m z = \rho \int_0^\lambda \frac{1}{2} \zeta^2 dx + \text{constant} \quad (2)$$

where x is a horizontal coordinate, ρ is the density, λ is the wavelength, and $\zeta(x, t)$ is the vertical displacement of the free surface. But by our previous remarks

$$F = \lambda (\bar{p} - p_0 - \rho g h), \quad (3)$$

where h is the mean depth of water. On equating (1) and (3) we find

$$\frac{\bar{p} - p_0}{\rho} - g h = \frac{\partial^2}{\partial t^2} \frac{1}{\lambda} \int_0^\lambda \frac{1}{2} \zeta^2 dx. \quad (4)$$

Now for a standing wave

$$\zeta = a \cos kx \cos \sigma t \quad (5)$$

where $k = 2\pi/\lambda$ and $\sigma = 2\pi/\tau$ (τ being the wave period), and higher-order terms have been omitted. On substituting in (4) we find, after simplification,

$$\frac{\bar{p} - p_0}{\rho} - g h = -\frac{1}{2} a^2 \sigma^2 \cos 2\sigma t \quad (6)$$

This shows that to the second order, the mean pressure \bar{p} fluctuates sinusoidally, with twice the frequency of the original wave, and with an amplitude proportional to the square of the wave amplitude. The pressure fluctuation is independent of the depth, for a given wave period, though of course the depth enters into the relation of the wave period to the wavelength, given by

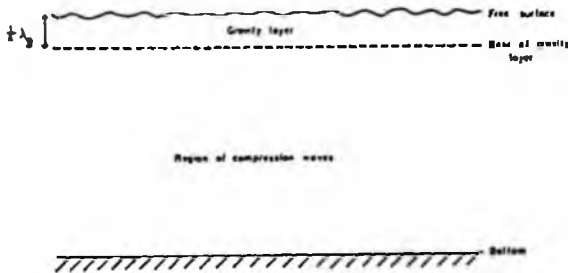


Figure 4. Waves in a heavy, compressible fluid.

$$\sigma^2 = g k \tanh kh \quad (7)$$

There is a close analogy with the motion of a pendulum (see figure 2). In a complete cycle the bob of the pendulum is raised and lowered twice, through a distance proportional to the square of the amplitude of swing, when this is small. The only forces acting on the pendulum are gravity, which is constant, and the reaction at the support. Hence there must be a second-order fluctuation in the vertical component of the reaction at the support. Furthermore the reaction will be least when the pendulum is at the top of the swing (the potential energy is greatest) and will be greatest when the pendulum is at the bottom of its swing (the potential energy is least).

It will be noticed that the above analytical proof does not necessarily involve the idea of the centre of gravity, whose vertical coordinate \bar{z} is defined by

$$(\Sigma m) \bar{z} = \Sigma (m z) \quad (8)$$

The theorem on the centre of gravity that was used previously is in fact usually derived from equation (1); but in the present proof we have appealed directly to the original equations of motion for the individual particles, without introducing \bar{z} .

4. Two progressive waves.—The above proof can easily be extended to the more general case of two waves of equal period but unequal amplitude travelling in opposite directions. For, such a disturbance is exactly periodic in space. Thus we may consider a region one wavelength in extent, as for the standing wave. This will not always contain the same mass of

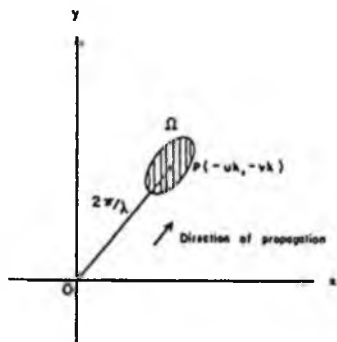


Figure 5. The spectrum representation of a wave group.

water; but, owing to the periodicity, the vertical reaction on the bottom due to the flow of water across one vertical boundary will be exactly cancelled by that due to the flow across the opposite boundary (see I Section 2.2); thus equation (4) is still exactly valid. The wave profile in this case is represented by

$$\zeta = a_1 \cos(kx - \sigma t) + a_2 \cos(kx + \sigma t) \quad (9)$$

and so

$$\frac{1}{\lambda} \int_0^\lambda \kappa \zeta^2 dx = \kappa (a_1^2 + a_2^2 + 2a_1 a_2 \cos 2\sigma t) \quad (10)$$

giving

$$\frac{\bar{p} - \bar{p}_0}{\rho} - g h = -2a_1 a_2 \sigma^2 \cos 2\sigma t \quad (11)$$

The mean pressure fluctuation on the bottom is therefore proportional to the product of the two wave amplitudes a_1 and a_2 . When these two are equal ($a_1 = a_2 = \frac{1}{2} a$) we have the case of the standing wave, and when one is zero ($a_1 = a$; $a_2 = 0$) we have the case of the single progressive wave.

A physical explanation of this result may be given as follows. Suppose that one of the waves, say the wave of amplitude a_1 , is reduced to rest by superposing on the whole system a velocity $-c$ in the direction of x decreasing (this will not affect the pressure distribution on the bottom). The second wave will now travel over the first with a velocity $-2c$. The crests of the second wave will pass alternately the troughs and the crests of the first wave—each twice in a complete period. Figure 3 shows the two phases. One may pass from figure 3(a) to figure 3(b) by transferring a mass of fluid, proportional to a_2 , from a trough to a crest of the original wave, i.e. through a vertical distance proportional to a_1 (the transferred mass does not of course consist of identically the same particles of water). The vertical displacement of the centre of gravity of the whole mass is therefore shifted by an amount proportional to $a_1 a_2$; and hence the fluctuation in \bar{p} is also proportional to $a_1 a_2$.

5. Attenuation of the particle motion.—The fact that there is a pressure fluctuation on the bottom even in deep water does not, however, mean that there is movement at those depths. In fact it may be shown (Longuet-Higgins 1953) that in exactly space-periodic motion, whether in a simple progressive wave or a combination of such waves, the particle motion decreases exponentially with the depth, apart from a possible steady current. Now if the velocities at great depths are zero, or steady, it follows from the equations of motion that the pressure-gradient must be independent of the time. Thus if there is a pres-

sure fluctuation it must be uniform in space, i.e. it must be applied equally at all points of the fluid. This indicates that below a certain depth, in a strictly space-periodic motion, the pressure fluctuations are uniform and equal to the fluctuation $\bar{p}(t)$ in the mean pressure on the bottom, which has been evaluated. The effect of the waves, at great depths, is then the same as would be produced by an oscillating pressure applied uniformly at the upper surface of the fluid—for example an oscillation of the atmospheric pressure. Alternately one may imagine a rigid plane or raft to be floating on the surface of the water and completely covering it, and the pressure to be applied to this plane by means of a weight attached to a spring and oscillating in a vertical direction.

6. An experimental verification—The above results were verified experimentally (Cooper and Longuet-Higgins 1951) in the following way. Waves were generated at one end of a wave tank and allowed to travel towards the far end, where they were dissipated on a sloping beach. The pressure beneath the waves was detected by means of a hydrophone and was recorded continuously. On starting the motion from rest, no appreciable pressure fluctuations were recorded until the wave-front, travelling with approximately the group-velocity of the waves, passed over the hydrophone. The pressure fluctuations then built up quickly to a constant amplitude, and had a period equal to that of the waves. The amplitude agreed well with the first-order theory; it diminished exponentially with depth, and was negligible below about half a wavelength.

A vertical barrier was then placed in the wave tank, between the hydrophone and the beach, which reflected the waves back over the hydrophone. As soon as the reflected wave

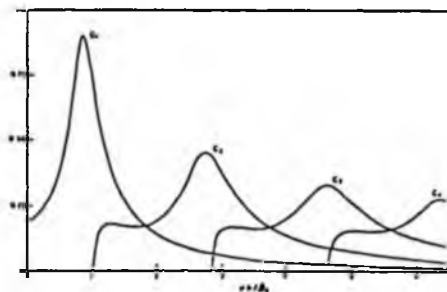


Figure 7. Graph of C_1 , C_2 , C_3 and C_4 as function of gh/β_2 , showing the relative amplitude of the vertical displacement of the "sea bed" in the first four modes.

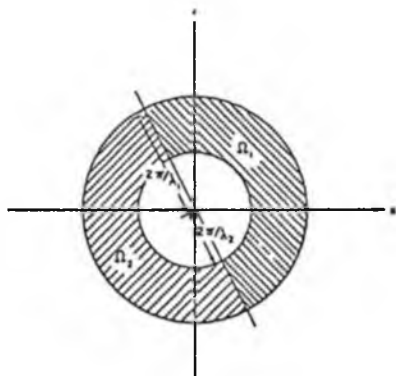


Figure 8. The form of the wave spectrum in a circular atom.

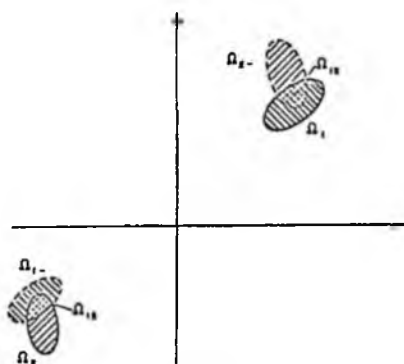


Figure 6. The regions of interference of two groups of waves in the spectrum.

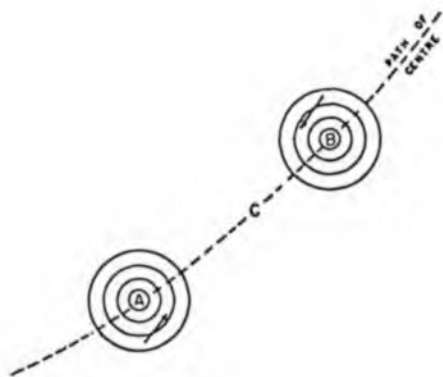


Figure 9. Wave interference caused by moving cyclonic depression.

front arrived over the hydrophone the appearance of the pressure record was changed. At moderate depths there were not only first-order pressure fluctuations from the incident and the reflected wave, but also considerable second-order pressure fluctuations, of twice the fundamental frequency. At greater depths the first-order pressure fluctuations become negligible and only the pressure fluctuations of double the frequency remained. The amplitude of these was in good agreement with equation (6). When the barrier was removed, and the rear end of the reflected wave train had passed the hydrophone, the second-order pressure fluctuations rapidly died out.

Interference between waves of unequal amplitude was obtained by placing in the tank a vertical barrier extending only to a certain depth below the free surface, which allowed the waves to be partly reflected and partly transmitted. The coefficient of reflection from such a barrier is known theoretically for different ratios of the depth of the barrier to the wavelength of the waves, and it was verified that the amplitude of the second-order pressure fluctuations was proportional to the amplitude of the reflected wave. Indeed this property seems to provide a convenient method of actually measuring the coefficient of reflection from different types of obstacles or from plane beaches.

Since standing waves produce only second-order pressure fluctuations below moderate depths one would expect that, if pressure fluctuations were induced deep in the water, standing waves of half the frequency would be produced at the surface. An experiment of this

kind was in fact performed by Faraday (1831); (see Section 13 of the present paper) who produced standing waves, of half the fundamental frequency, by means of a vibrating lath inserted in a basin of water. Faraday remarked that the general result was little influenced by the depth of water: "I have seen the water in a barrow, and that on the head of an upright cask in a brewer's van passing over stones, exhibit these elevations." (1831, footnote to p. 334). The present author has observed a similar phenomenon on board ship: a pool of water on deck, when excited by the vibration of the ship's engines, sometimes shows a standing-wave pattern whose amplitude gradually builds up to a maximum, and then collapses; the process is repeated indefinitely.

7. Standing waves in a compressible fluid—The water has so far been assumed to be incompressible, and we have seen that in this case the pressure fluctuations below about half a wavelength from the surface occur simultaneously at all points of the fluid. But this can only be true if the least time taken for a disturbance to be propagated to the bottom and back is small compared with the period of the waves. In the deep oceans, where the speed of sound is about 1.4 km/sec and the depth may be of the order of several kilometers, this time may be several seconds. Thus the compressibility of the water must be considered.

The first-order theory of waves in a heavy, compressible fluid (in which all squares and products of the displacements are neglected) indicates that water waves of a few seconds' period fall into two classes (Whipple and Lee 1935). On the one hand there are waves approximating very nearly to ordinary surface waves in an incompressible fluid, in which the particle displacement decreases exponentially downwards, to first order; these may be called gravity-waves. On the other hand there are long waves controlled chiefly by the compressibility of the medium and hardly attenuated at all with depth; these may be called compression-waves; their velocity is nearly the velocity of sound in water. The wavelengths of a gravity-wave and a compression wave will be denoted by λ_g and λ_c respectively. For waves of period 10 sec. λ_g/λ_c is of the order of 10^{-2} .

However, the pressure variations which are of interest to us at present are of second order. To investigate the effect of the compressibility, therefore, a complete example, namely a motion which in the first approximation is a standing gravity-wave, has been worked out in full to a second approximation (I Section 4). The result is as follows.

Near the free surface, that is within a distance small compared with λ_c , the waves are unaffected by the compressibility of the water

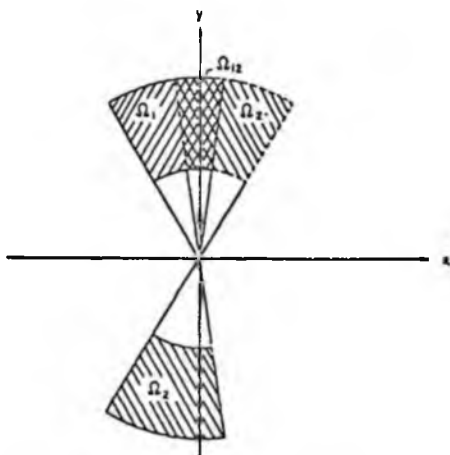


Figure 10. The spectrum representation of incident and reflected wave-groups.

—as one might expect, since a disturbance could be propagated almost instantaneously through this layer. At a distance of about $\frac{1}{2} \lambda_g$ from the free surface the first-order pressure variations are much attenuated, and the second-order pressure variations are practically those given by the incompressible theory (equation [6]). Below this level the displacements are comparatively small, but, instead of the uniform, unattenuated pressure fluctuations in the incompressible fluid, there is now a compression wave, whose planes of equal phase are horizontal: the pressure field in this wave is given by

$$\frac{P - P_0}{\rho} - g z = -\frac{1}{2} a^2 \sigma^2 \frac{\cos 2\sigma(z-h)/c'}{\cos 2\sigma h/c'} \cos 2\sigma t \quad (12)$$

very nearly, where z is the vertical coordinate measured downwards from the mean surface level, and c' is the velocity of sound in water. This wave can be regarded as being generated by the unattenuated pressure variation (6). There is a resonance, or "organ-pipe," effect: when $\cos 2\sigma h/c'$ vanishes, the pressure on the bottom ($z \approx h$) becomes infinite. This happens when

$$2\sigma h/c' = (n + \frac{1}{2})\pi \quad (13)$$

that is, when the depth is $(\frac{1}{2}n + \frac{1}{4})$ times the length of the compression wave. In general, however, the displacements in the compression wave are small, being only of the order of a^2/λ_c ; the displacement of the centre of gravity of the layer at the surface of thickness $\frac{1}{2} \lambda_g$ is of the order of a^2/λ_g . This explains why the compressibility of the fluid below has little effect on the pressure fluctuations at the base of the surface layer.

We have then the following picture (see figure 4): there is a surface-layer, of depth about $\frac{1}{2} \lambda_g$, in which the compressibility of the water is, in general, unimportant: this may be called the "gravity-layer." Below this layer there exist only second-order compression waves, generated by the gravity-waves in the surface layer, and of twice their frequency.

8. Application to sea waves—So far we have considered only the very special cases of perfectly periodic and two-dimensional waves. Such waves cannot be expected to occur in the ocean, although the sea surface usually shows a certain degree of periodicity. We shall now consider how the sea surface is to be described in this more general case.

It can be shown (See I Section 3.2) that any free motion of the sea surface can be expressed as a Fourier integral:

$$\zeta(x, y, t) = R \int_{-\infty}^{\infty} \int_{-\infty}^{\infty} A(u, v) e^{i(ukx + vky + \sigma t)} du dv \quad (14)$$

where (x, y) are horizontal coordinates, k is a constant and σ is a function of (u, v) :

$$\sigma^2 = gk(u^2 + v^2)^{1/2} \tanh(u^2 + v^2)^{1/2} kh \quad (15)$$

$A(u, v)$ is in general complex, and R denotes the real part. The expression under the integral sign represents a long-crested wave with crests parallel to the line

$$u x + v y = 0 \quad (16)$$

and of wavelength λ given by

$$\lambda = \frac{2\pi}{(u^2 + v^2)^{1/2} k} \quad (17)$$

If the point $P, = (-uk, -vk)$ is plotted in the (x, y) plane (see figure 5) the direction of the vector OP is the direction of propagation of the wave-component and the length of OP equals 2π divided by the wavelength. Points on a circle centre O correspond to wave-components of the same wavelength; diametrically opposite points correspond to waves of the same length but travelling in opposite directions. When the energy is mainly grouped about one wavelength and direction, the complex amplitude $A(u, v)$ will be appreciably large only in a certain range of values of (u, v) , say Ω , as in figure 5. The narrower this region, the more regular will be the appearance of the waves.

The spectrum $A(u, v)$ of the waves is determined uniquely by the motion of the free surface, at a particular instant, over the whole plane (see I, Section 3.2). Since we shall want to consider the wave motion in only a certain part of the plane, say a square S of side $2R$, it is convenient to define a motion ζ' which, at any time, has the same value as ζ inside S but is zero outside. Let A' be the spectrum function of ζ' , so that

$$\zeta' = R \int_{-\infty}^{\infty} \int_{-\infty}^{\infty} A'(u, v) e^{i(ukx + vky + \sigma t)} du dv \quad (18)$$

A' is very closely related to A ; if k is chosen so that

$$k = \pi / R \quad (19)$$

$$A'(u, v) = \int_{-\infty}^{\infty} \int_{-\infty}^{\infty} A(u_1, v_1) \frac{\sin(u-u_1)\pi}{(u-u_1)\pi} \frac{\sin(v-v_1)\pi}{(v-v_1)\pi} e^{-i(\sigma-\sigma_1)t} du_1 dv_1 \quad (20)$$

where $\sigma_1 = \sigma(u_1, v_1)$. In other words A' is the weighted average of values of A over neighboring wavelengths and directions. Since u and v are proportional to the number of wavelengths intercepted by the x - and y -axis in S , a "neighboring" wave component is one which has nearly the same number of wavelengths, in each direction, in S . A' gives a "blurred" picture of A ; but the larger the side of the square, the less is the blurring. The region Ω' in the (u, v) -plane which corresponds to the blurred spectrum will be almost the same as the region Ω corresponding to the original spectrum. A' also varies slowly with the time—the waves in S change gradually—but this rate of change is slow compared with the rate of change of the wave profile, or compared with $\sigma A'$.

The energy of the waves is given very simply in terms of the spectrum function A' ; in fact, if a denotes the amplitude of the single long-crested wave which has the same mean energy inside S ,

$$a^2 = \int_{-\infty}^{\infty} \int_{-\infty}^{\infty} A'A'^* du dv \quad (21)$$

where a star denotes the conjugate complex function (I equation [189]). a may be called the equivalent wave amplitude of the motion.

9. General conditions for fluctuations in the mean pressure—We shall evaluate the mean pressure \bar{p} at the base of the gravity-layer, i.e. at a distance of about $\frac{1}{2} \lambda_g$ below the free surface, over a square of side $2R$. (Here λ_g refers to the mean wavelength of the predominant components in the spectrum.) Consider first the two-dimensional case. The mass of water contained between the surfaces $z = \zeta$ and $z = \frac{1}{2} \lambda_g$ and the planes $x = \pm R$ no longer consists of the same particles of water; but it is possible to extend the analysis of Section 3 so as to take account of the motion across the boundaries (see I Section 2.2). Provided that the horizontal extent $2R$ of the interval is large compared with λ_g the effect of the flow across the vertical boundaries can be neglected (I Section 3.1). Further, since the motion decreases rapidly with depth the effect of flow

and if R is large compared with the wavelengths associated with most energy in the spectrum then (see I Section 3.3)

across the horizontal plane $z = \frac{1}{2} \lambda_g$ is small. The expression for the mean pressure variation is therefore the same as if the free surface were the only moving boundary:

$$\frac{\bar{p} - \bar{p}_0}{\rho} - \frac{1}{2} g \lambda_g = \frac{\delta^2}{\delta t^2} \frac{1}{2R} \int_{-R}^R \frac{1}{2} \zeta^2 dx \quad (22)$$

Similarly in the three-dimensional case

$$\frac{\bar{p} - \bar{p}_0}{\rho} - \frac{1}{2} g \lambda_g = \frac{\delta^2}{\delta t^2} \frac{1}{4R^2} \int_{-R}^R \int_{-R}^R \frac{1}{2} \zeta^2 dx dy \quad (23)$$

that is

$$\frac{\bar{p} - \bar{p}_0}{\rho} - \frac{1}{2} g \lambda_g = \frac{\delta^2}{\delta t^2} \frac{1}{4R^2} \int_{-\infty}^{\infty} \int_{-\infty}^{\infty} \frac{1}{2} \zeta'^2 dx dy \quad (24)$$

since ζ' vanishes outside the square S . Now the expression on the right-hand side is closely related to the potential energy of the motion ζ' , and can be simply expressed in terms of the Fourier spectrum-function A' . In fact (I Section 3.2)

$$\int_{-\infty}^{\infty} \int_{-\infty}^{\infty} \frac{1}{2} \zeta'^2 dx dy = \quad (25)$$

$$R(\pi/k)^2 \int_{-\infty}^{\infty} \int_{-\infty}^{\infty} (A'A'^* + A'A'_1 e^{2i\sigma t}) du dv$$

where $A^!$ stands for $A^1(-u, -v)$, and is the amplitude of the wave component opposite to $A(u, v)$. On substituting in (24) we have

$$\frac{\bar{p} - P_0}{\rho} - \frac{1}{2} g \lambda_g = -R \int_{-\infty}^{\infty} \int_{-\infty}^{\infty} \sigma^2 A^! A^1 e^{2i\sigma t} du dv \quad (26)$$

This shows that fluctuations in the mean pressure p arise only from opposite pairs of wave components in the spectrum; that the contribution to p from any opposite pair of wave components is of twice their frequency and proportional to the product of their amplitudes; and that the total pressure fluctuation is the integrated sum of the contributions from all opposite pairs of wave components separately.

The necessary condition for the occurrence

$$\frac{\bar{p} - P_0}{\rho} - \frac{1}{2} g \lambda_g \sim 2a_1 a_2 \sigma_{12}^2 (\Omega_{12}/\Omega_1 \Omega_2)^{1/2} k e^{2i\sigma_{12} t} \quad (27)$$

where σ_{12} is the mean value of σ in Ω_{12} . Thus the mean pressure on S increases proportionately to the square root of the region Ω_{12} of overlap of the wave groups, and inversely as the square root of Ω_1 and Ω_2 separately, for fixed values of a_1 and a_2 .

10. Calculation of the ground movement—In order to estimate the movement of the ground, at great distances, due to waves in a storm area A , we suppose the storm area to be divided up into a number of squares S of side $2R$ such that

$$\delta' \sim 4R^2 \cdot 2a_1 a_2 \sigma_{12}^2 (\Omega_{12}/\Omega_1 \Omega_2)^{1/2} k \bar{W} (2\sigma_{12}, r) e^{2i\sigma_{12} t} \quad (28)$$

where r is the distance from the center of the storm and $\bar{W}(\sigma, r)e^{i\sigma t}$ is the movement of the ground at distance r due to a unit pressure oscillation $e^{i\sigma t}$ applied at a point in the mean free surface. The pressure can be considered to be applied in the mean free surface rather than at the base of the gravity-layer, since the latter is relatively thin compared with the length of the seismic waves. To find the total

$$\delta \sim 4\pi \cdot a_1 a_2 \sigma_{12}^2 (\Lambda \Omega_{12}/\Omega_1 \Omega_2)^{1/2} \bar{W} (2\sigma_{12}, r) e^{2i\sigma_{12} t} \quad (29)$$

To calculate $\bar{W}(\sigma, r)$ we may consider the disturbance due to a force applied at the surface of a compressible fluid of depth h (representing the ocean) overlying a semi-infinite elastic medium (representing the sea bed). Although this model takes no account of varia-

of second-order pressure fluctuations of this type is, therefore, that the sea disturbance should contain some wave-groups of appreciable amplitude which are "opposite," i.e. such that part at least of the corresponding region in the Fourier spectrum is opposite to some other part. For example, if Ω lies entirely on one side of a diameter of the (u, v) -plane, the mean pressure fluctuation, to the present order, vanishes.

An important case is when the disturbance consists of just two wave groups, corresponding to regions Ω_1 and Ω_2 , and of equivalent amplitudes a_1 and a_2 (see figure 6). Ω_{12} and Ω_2 denote the regions opposite to Ω_1 and Ω_2 and Ω_{12} and Ω_{12} denote the regions common to Ω_1 and Ω_2 and to Ω_{12} and Ω_{12} respectively. Effectively, then, the integration in (26) is carried out over the two regions Ω_{12} and Ω_{12} . When the spectrum is narrow an order of magnitude for the integral on the right-hand side of (26) can be obtained. It may be shown (see I Section 5.2) that

S contains many wavelengths λ_g of the sea waves, but is only a fraction, say less than half, of the length of a seismic wave λ_s in the ocean and sea bed. This we may do, since the wavelengths of seismic waves are of the same order as the wavelengths of compression waves in water; therefore λ_g/λ_s is of the order of 10^{-2} . The mean pressure or total force on the base the gravity-layer can be calculated as in Section 8; the vertical movement of the ground δ' due to the waves in this square is of the same order as if the force were concentrated to a point at the center of the square, i.e.

displacement δ from the storm we may add the energies from the different squares S , on the assumption that the contributions from the different squares are independent. Since there are $\Lambda/4R^2$ such squares in the whole storm area, this means that the disturbance δ' from each individual square is to be multiplied by $\Lambda^{1/2}/2R$. Hence we have

tions in the depth of water, or of the propagation of the waves from the sea bed to the land or across geological discontinuities, it can nevertheless be expected to give a reasonable estimate of the order of magnitude of the ground movement.

The disturbance $W(\sigma, r) e^{i\sigma t}$ at great distances from the oscillating point source $e^{i\sigma t}$ consists of one or more waves of surface type,

$$W(\sigma, r) e^{i\sigma t} = \frac{\sigma h}{\rho_2 \beta_2 (2\pi r)^{1/2}} \sum_m C_m e^{i[\sigma t - \beta_2 r + (m + \frac{1}{4})\pi]} \quad (30)$$

where ρ_2 is the density of the elastic medium, β_2 the velocity of secondary waves in the medium, $2\pi/\lambda_m$ is the wavelength of the m th wave and C_m is a constant amplitude depending on the depth of water and on the elastic properties of the fluid and the underlying medium. The first wave has no nodal plane between the free surface and the "sea bed," the second has one nodal plane, the third two, and so on. When the depth h of the water is small, only the first type of wave can exist; the others appear successively as the depth is increased. Graphs of C_1, C_2, \dots have been computed for some typical values of the constants: ρ_1 (the density of the fluid) = 1.0 g./cm³; c^1 (velocity of compression waves in water) = 1.4 km./sec.; β_1 = 2.8 km./sec., and with Poisson's hypothesis, that the ratio of the velocities of compressional and distortional waves in the medium is $\sqrt{3}$. The results are shown in figure 7, where C_1, C_2, C_3 and C_4 are plotted against oh/β_2 . C_1 , for example, increases to a maximum when $oh/\beta_2 = 0.85$, i.e. when $h = 0.27 \times 2\pi c^1/\sigma$, or h is about one-quarter of the wavelength of a compression wave in water. This maximum may therefore be interpreted as a resonance peak. The amplitude, however, does not become infinite as in the case of the infinite wave-train discussed in Section 7, since now energy is being propagated outwards from the generating area. C_2, C_3 , and C_4 have similar resonance peaks when $oh/\beta_2 = 2.7, 4.1$ and 5.3 , respectively, i.e. when the depth is 0.86, 1.31 and 2.0 times the length of a compression wave in water. A measure W of the total disturbance can be obtained by summing the energies from each wave. Thus

$$\bar{W} = \frac{\sigma h}{\rho_2 \beta_2^{5/2} (2\pi r)^{1/2}} \left(\sum_m C_m^2 \right)^{1/2} \quad (31)$$

11. Practical examples.—We have seen that a necessary condition for the occurrence of the type of pressure fluctuations studied in this paper is that the motion of the sea surface should contain at least some wave groups of the same wavelength traveling in opposite directions. We shall briefly consider some situations in which this may occur.

(a) A circular depression. The "eye" or center of a circular depression is a region of comparatively low winds; yet there are often observed to be high and chaotic seas in this region (which indicates the interference of more than one group of swell). Thus, the

i.e. waves spreading out radially in two dimensions (see I Section 5.1). Thus

waves in the "eye" must have originated in other parts of the storm. Now the winds in a circular depression are mainly along the isobars, but in some parts of the storm they usually possess a radial component inwards. In addition, some wave energy may well be propagated inwards at an angle to the wind. This then may account for the high waves at the center of the storm.

If wave energy is being received equally from all directions, the energy in the spectrum will be in an annular region between two circles of radii $2\pi/\lambda_1$ and $2\pi/\lambda_2$, where λ_1 and λ_2 are the least and greatest wavelengths in the spectrum (see figure 8). This region may be divided into two regions Ω_1 and Ω_2 by any diameter through the origin. Let us take numerical values appropriate to a depression in the Atlantic Ocean. Suppose that the wave-periods lie between 10 and 16 seconds, so that $\lambda_1 = 1.54 \times 10^4$ cm., $\lambda_2 = 4.00 \times 10^4$ cm. and hence $\Omega_1 = \Omega_2 = \Omega_{12} = 2.16 \times 10^{17}$ cm.². Assuming $\Lambda = 1000$ km² (corresponding to a circular storm area of diameter 17 km.), $\sigma_{12} = 2\pi/13$ sec.⁻¹, $a_1 = a_2 = 3\pi$, $h = 3$ km. and $r = 2,000$ km. we find from (29) that $|\delta| = 3.2 \times 10^{-4}$ cm., or 3.2μ . The peak-to-trough amplitude of the displacement is 6.5μ . This is of the same order of magnitude as the observed ground movement.

(b) A moving cyclone. Consider a cyclone which is in motion with a speed comparable to that of the waves. Figure 9 represents the position of the cyclone at two different times. When the center of the storm is at A, say, winds on one side of the storm (marked with an arrow) will generate waves travelling in the direction of motion of the storm; these will be propagated with the appropriate group velocity. When the storm has reached B, winds on the opposite side will generate waves travelling in the opposite direction; and if the storm is moving faster than the group-velocity of the waves, there will be a region C where the two groups of waves will meet. Thus, in the trail of a fast-moving cyclone we may expect a considerable region of wave interference.

(c) Reflection from a coast. The extent of wave reflection from a coast is hard to judge, since the reflected waves are usually hidden by the incoming waves; but when the waves strike a coast or headland obliquely the reflected waves can sometimes be clearly seen. Effective wave interference will take place only on the parts of the coast where the shoreline is

parallel to the crests of some wave components of the incoming waves, but refraction of the waves by the shoaling water will tend to bring the crests parallel to the shore.

If the incoming waves are represented by a region Ω_1 in the spectrum, then we may assume that the reflected waves are represented by a region Ω_2 which is the reflection of Ω_1 in the line through O parallel to the shoreline (see figure 10, in which the x -axis is taken parallel to the shoreline). Ω_2 is then the reflection of Ω_1 in the line through O perpendicular to the shoreline (the y -axis).

Suppose that the period of the incoming swell lies between 12 and 16 seconds, that its direction is spread over an angle of 30° , and that its mean direction makes an angle of 10° with the perpendicular to the shoreline. Then we find $\Omega_1 = \Omega_2 = 1.4 \times 10^{-8} \text{ cm.}^{-2}$, $\Omega_1 = 1/3 \Omega_2 = 0.47 \times 10^{-8} \text{ cm.}^{-2}$. If the effective shoreline is 600 km. in length and the region of interference extends, on the average, 10 km. from the shore, then $\Lambda = 6,000 \text{ km.}^2$. If also $a_1 = 2m$, $a_2 = 0.1m$ (a reflection coefficient of 5%) and if $r = 2,000 \text{ km.}$, then we find from (26) (assuming $h = 0$) that $2|\delta| = 0.3\mu$. Since this amplitude is somewhat smaller than in case (a), we may conclude that coastal reflection does not give rise to the largest disturbances at inland stations, though it may be a more common cause of microseisms near to the coast.

Besides the examples given above there is another possible class of cases, namely when a swell meets an opposing wind. For example, coastal swell may be subject to an offshore wind, or there may be a sudden reversal of the direction of the wind at the passage of a cold front.* The wind will doubtless tend to diminish the amplitude of the original swell, but it may also tend to generate waves travelling in the opposite direction, the amplitude of which may increase rapidly on account of the roughness of the sea surface. However, in none of the first three cases discussed above is it necessary to assume that such action takes place.

12. Observational tests.—The present theory suggests several possible kinds of experimental investigation. The first is a comparison of the periods of microseisms and of the sea waves possibly associated with them, (which should be about twice the microseism periods). There is a general agreement between the periods, in that the range of microseism periods is from about 3 to 10 seconds while the periods of high sea waves vary from about 6 to 20 seconds. Further, the periods of both microseisms and sea waves both increase, in general, during a time of increased disturbance. The close two-to-one ratio between the periods of sea waves and of the corresponding microseisms which was found by Bernard (1937 and 1941) and re-

lated by Deacon (1947) and Darbyshire (1948) is highly suggestive, though not conclusive. A similar, though less detailed study by Kishinouye (1951) during the passage of a tropical cyclone, has not confirmed the relationship. Comparisons of this kind are, however, inconclusive, unless it can be shown that the microseisms can be associated uniquely with the recorded sea waves. The meteorological conditions are rarely so simple, and the recording stations so well placed, that it is possible to be certain of the connection; the examples selected by Darbyshire (1950) were, however, chosen with this requirement in mind.

Figure 7 shows that the displacement of the "sea bed" may vary by a factor of the order of 5, depending on the depth of the "ocean." Although the model chosen is extremely simplified, we can nevertheless infer that the amplitude of microseisms should, on the present theory, depend considerably on the depth of water in the path of the microseisms; the depth in the generating area itself, where the energy-density is greatest, should be of the most critical importance. Comparisons between the microseisms due to storms in different localities would therefore be of considerable interest. It should be noticed that the unequal response of the ocean to different frequencies may result in a displacement of the spectrum towards those frequencies for which the response is a maximum.

The nature of the frequency spectrum of sea waves under various conditions is of fundamental importance, and further studies should be undertaken. The wavelengths and directions of the components of the spectrum, both for swell and for waves in the generating area, could be studied by means of aerial photographs or altimeter records taken from an airplane. An estimate of the amount of wave reflection from a coast might be obtained by techniques similar to those which were used in the model experiments described in Section 7, that is, by comparing the frequency spectra of pressure records taken at different depths in the water, or off different parts of the same coast where the bottom gradient varied. The effect of an opposing wind on a swell might be investigated on a model scale, by generating progressive waves in the usual manner and then exposing them to an artificial wind; the growth of the opposing waves would be measured by means of the second-order pressure fluctuations deep in the water.

It would be of great interest to record the pressure fluctuations on the ocean floor directly, if the practical difficulties of making measurements at such depths can be overcome. A pressure recorder has been designed for this purpose by F. E. Pierce, of the National Institute of Oceanography.

* See also the author's comment on the paper by Frank Press.

13. Historical notes.—It was known to FARADAY (1831), who refers to earlier work by Oersted, Wheatstone and Weber, that fluid resting on a vibrating elastic plate will form itself into short-crested standing waves. Faraday was the first to show, by an ingenious optical method, that the period of the standing waves is twice that of the vibrations of the plate. The waves that he used were mostly "ripples," controlled predominantly by surface tension, since their wavelength lay between $\frac{1}{4}$ and $\frac{3}{8}$ inch. In the same paper (1831) Faraday describes many other interesting experimental studies of waves in water, mercury and air.

About fifty years later Rayleigh (1883 b) repeated Faraday's experiments and verified, by a slightly different method, the doubling of the period. In a theoretical paper (1883 a) Rayleigh gives general consideration to the problem of how a system can be maintained in vibration with a period which is a multiple of the period of the driving force. He refers in particular to Melde's experiment, in which a stretched string is made to vibrate by the longitudinal oscillation of a tuning fork attached to one end; such a phenomenon is sometimes called "subharmonic resonance."

Neither Faraday (1831) nor Rayleigh (1883) evaluated the second-order pressure fluctuations associated with standing waves. This, however, was done by MICHE (1944) in a different connection, using a Lagrangian system of coordinates. Miche noticed the unattenuated terms, and, though he does not mention microseisms, he remarks, "on peut aussi se demander si ces pulsations de pression, malgré leur faible intensité relative, n'exercent pas une action non négligeable sur la tenue des fonds soumis au clapotis." (1944, p. 74.)

The wave interference theory seems to have arisen as follows. In 1946 Deacon, following similar studies by Bernard (1937, 1941 a) compared the period and amplitude of swell off the coast of Cornwall, England, with the corresponding microseisms at Kew, and found a two-to-one ratio between the periods (Deacon 1947). F. Biesel, then visiting England, pointed out to Deacon Miche's theoretical work on standing waves. Miche's results, however, cannot be applied directly to sea waves, since exact standing waves do not occur in the ocean. Moreover, his method is not easily generalized, since it involves a complete evaluation of the second approximation to the wave motion. A very simple proof of Miche's result, however, which depended essentially on the idea of the vertical motion of the center of gravity of the whole wave train, was found by Longuet-Higgins and Ursell (1948); the advantage of this method was that the second-order pressure fluctuations on the bottom could then be obtained immediately from the first approximation to the surface ele-

vation. It then became possible to extend the results to much more general and realistic types of wave motion. A complete theory, giving the necessary conditions for the occurrence of this type of pressure fluctuation, taking into account the compressibility of the ocean, and determining the order of magnitude of the ground movement, was given by Longuet-Higgins (1950).

It is interesting that Bernard (1941 a, b) had suggested, with intuitive reasoning, that microseisms might be caused by the standing-type waves observed to occur at the center of cyclonic depressions:

"J'ai cru qu'on pourrait trouver la raison de cette particularité dans le caractère que présentent les mouvements de la mer au centre des dépressions cycloniques: la houle s'y dresse aux vagues pyramidales constituant un clapotis gigantesque dont les points de plus ample oscillation peuvent être autant des sources de pression périodique sur le fond de la mer, pression qui donnera naissance à un mouvement oscillatoire de même période du sol . . ."

"Un clapotis analogue, avec oscillations sur place du niveau de l'eau, se produit lorsque la houle, se réfléchissant sur un obstacle, vient interférer avec les ondes incidentes . . ."

"Au contraire, dans le cas d'un train d'ondes de front continu et de déplacement constant, les points ou les mouvements sont de phase opposée donneront sur le fond de la mer des pressions de sens contraire, et la longueur d'onde des oscillations microseismiques étant beaucoup plus grande que celle de la houle, les mouvements transmis par le sol à une certaine distance seront pratiquement simultanés, mais opposés, et ils interféreront, de sorte que l'effet total du train de vagues à l'extérieur sera nul." (BERNARD, 1941 a, p. 7.)

However, Bernard did not apparently see that the corresponding pressure fluctuations must have a frequency twice that of the waves; for he suggests other causes for the observed doubling of the frequencies in the case of coastal waves." (Bernard, 1941a, p. 10.)

REFERENCES

- BERNARD, P., *Relations entre la houle sur la côte du Maroc et l'agitation microseismique en Europe occidentale*, C. R. Acad. Sci., Paris, v. 205, pp. 163-165, 1937.
- BERNARD, P., *Sur certaines propriétés de la houle étudiées à l'aide des surcristallisations séismographiques*, Bull. Inst. Océanogr. Monaco, v. 38, No. 800, pp. 1-18, 1941.
- BERNARD, P., *Etude sur l'agitation microseismique et ses variations*, Ann. Inst. Phys. Globe, v. 10, pp. 1-77, 1941.

- COOPER, R. I. B., and LONGUET-HIGGINS, M. S., *An experimental study of the pressure variations in standing water waves*. *Proc. Roy. Soc. A*, v. 206, pp. 424-435, 1951.
- DARBYSHIRE, J., *Identification of microseismic activity with sea waves*. *Proc. Roy. Soc. A*, v. 160, pp. 439-448, 1930.
- DEACON, G. E. R., *Relations between sea waves and microseisms*. *Nature*, v. 160, pp. 411-421, 1947.
- FARADAY, M., *On a periodic class of acoustical figures, and on certain forms assumed by groups of particles upon vibrating elastic surfaces. Appendix: On the forms and states assumed by fluids in contact with vibrating elastic surfaces*. *Phil. Trans. Roy. Soc.*, pp. 319-340, 1831.
- KISHINOUE, F., *Microseisms and sea waves*. *Bull. Earthqu. Res. Inst.*, v. 29, pp. 677-682, 1961.
- LONGUET-HIGGINS, M. S., and URSELL, F., *Sea waves and microseisms*. *Nature*, v. 162, p. 700, 1948.
- LONGUET-HIGGINS, M. S., *A theory of the origin of microseisms*. *Phil. Trans. Roy. Soc. A*, v. 243, pp. 1-35, 1950.
- LONGUET-HIGGINS, M. S., *On the decrease of velocity with depth in an irrotational surface wave*. (In press) 1952.
- MARTIN, J. C., MOYCE, W. J., PENNEY, W. G., PRICE, A. T., and THORNHILL, C. K., *Some gravity-wave problems in the motion of perfect liquids*. *Phil. Trans. Roy. Soc. A*, v. 244, pp. 231-281, 1952.
- MICHE, M., *Mouvements ondulatoires de la mer en profondeur constants ou décroissants*. *Ann. Ponts et Chaussées*, v. 114, pp. 25-37, 131-164, 270-292, 896-905, 1944.
- RAYLEIGH, LORD, *On maintained vibrations*. *Phil. Mag.*, vol. 15, pp. 229-235, 1883.
- RAYLEIGH, LORD, *On the crispations of fluid resting upon a vibrating support*. *Phil. Mag.*, v. 16, pp. 50-58, 1883.
- WHIFFLE, F. J. W., and LEE, A. W., *Notes on the theory of microseisms*. *Mon. Not. Roy. Astr. Soc., Geophys. Suppl.*, v. 2, pp. 287-297, 1935.

Discussion

G. E. R. Deacon (*National Institute of Oceanography at Teddington*)

The wave-interference theory explains, for the first time, how energy sufficient to generate long, regular, microseisms is communicated to the ground. It has been clear for a long time that the occurrence of microseisms is associated with the presence of sea waves, but it could not be proved that the waves played an essential part in the energy transfer.

Although each breaker, as it crashes on the coast, must cause a local disturbance, and has been shown to do so, the variations in the moment of impact along a stretch of coast, and

the shortness of the wavelength compared with that of 3 to 10 second microseisms, make it most unlikely that the actual heating of surf on a coast could produce the long microseismic waves that can be detected far from the coast.

The exponential decrease in wave movement with depth was sufficient reason why a train of progressive waves should not disturb the sea bottom at great depths, and at lesser depths the contributions from different parts of the sea bed would tend to cancel each other out. Taking account of the compressibility of the water made no significant difference to this conclusion.

If the conviction held by many who had studied microseisms, that sea waves are directly concerned in the generation of microseisms were to be confirmed, we had to find a theory which showed that sea waves were modified in such a way that they were able to cause regular changes in pressure, acting simultaneously over large areas of the sea bed. During the past few years it has, in addition, become necessary to explain why the periods of the microseismic waves are half those of the sea waves, and how the effect of wind and wave-height could vary with the depth of water, being sometimes greater in deep water than in shallow.

The new wave-interference theory seems to fill these requirements, and to be capable of withstanding the test of more precise and well-directed observations.

It is not easy for the non-mathematician to understand the precise demonstration that two trains of waves of the same wavelengths, meeting each other in opposite directions, will cause variations in pressure on the sea bed with twice the frequency of the surface waves, but Dr. Longuet-Higgins has done his best to explain it in non-technical terms. The deduction is simplified by considering the vertical movements of the centre of gravity of a water mass bounded by two vertical nodal planes, and by a comparison with the changing tension in the string of a pendulum. It is perhaps not very difficult to accept the result intuitively, as Bernard (1941) did, particularly if we remember the convincing agreement between theory and observation obtained by measurements in a tank.

There is also confirmation of the mean pressure changes and their ability to produce microseisms that can be detected far from the coast, in the work of Darbyshire (1950). As Dr. Longuet-Higgins says in his paper, confirmation of the two to one relationship between wave and microseism periods does not completely verify the theory, but when, as Darbyshire showed, the trend of a band of swell from long to short periods was exactly paralleled by proportionate changes in the microseism periods there is little room to doubt that the waves caused the microseisms.

If the previous literature is re-examined, bearing the wave-interference theory, and what we already know about waves, in mind, some of the apparent contradictions to which emphasis has been given appear explainable. The example given by Whipple and Lee (1935) of almost identical isobaric charts of two depressions south-east of Greenland, one associated with intense microseismic activity and the other with practically none, is not such an obstacle when the previous histories of the two depressions are studied. One had moved rapidly northwards over the ocean, with plenty of opportunity for wave interference, whereas the other had developed over the land. Similar attempts to estimate wave interference might explain why less microseismic activity was found with a depression over the mouth of the St. Lawrence river and an anticyclone over the Great Lakes than when the positions of the depression and anticyclone were reversed; or why, with a shallow depression off the east coast of Japan, the microseisms were larger on the coast of China while the wind was stronger off the coast of Japan.

There is, however, not much to be gained by studying cases which are not fully documented. We must, as Dr. Longuet-Higgins emphasizes, learn more about the conditions which give rise to wave interference; we must select examples in which the meteorological conditions are sufficiently simple for us to be certain of the connection between the storm and the microseisms, and we must measure the waves and the microseisms as precisely as modern techniques will allow. It is possible that some of the present misunderstanding is due to faulty interpretation of records from seismometers that are highly tuned to the short-period end of the microseism range, and faulty estimation of the sea surface or wave and microseism recordings, in which the size of a long period oscillation can be underestimated owing to the interruption of its swing by minor, shorter, waves.

The wave-interference theory is, to say the least, an excellent working hypothesis, and if it is subjected to further question and experiment, of the standard set by Dr. Longuet-Higgins and his co-workers, we must move rapidly towards a full solution.

It seems to me that the subject has now been put on a systematic basis, and that its progress must be more rapid. In spite of some setbacks we shall soon be in a better position to take full advantage of the practical possibilities.

I think that Dr. Longuet-Higgins's historical note gives a proper account of the development of the new theory.

REFERENCES

- BERNARD, P., *Etude sur l'agitation microseismique et ses variations*. Ann. Inst. Phys. Globa, v. 19, pp. 1-77, 1941.
- DARBYSHIRE, J., *Identification of microseism activity with sea waves*. Proc. Roy. Soc. A., v. 160, pp. 439-448, 1956.
- WHIPPLE, F. J. W., and LEE, A. W., *Notes on the theory of microseisms*. Mon. Not. Roy. Ast. Soc. Geophys. Suppl., v. 2 pp. 287-297, 1936.

Discussion

JACOB E. DINGER

Naval Research Laboratory

As a discussion of the theoretical paper "Can Sea Waves Cause Microseisms," I should like to present some of the data and interpretations obtained by the Naval Research Laboratory on various field trips during the hurricane seasons of the past several years.

The data considered here is concerned with hurricanes which have followed paths in the Western Atlantic and Caribbean. It has been a primary objective of this work to obtain evidence which might help to determine where the area of microseism generation is with respect to the hurricane center and to determine under what condition a hurricane can generate microseisms. In furthering this objective it has become of interest to study the data in the light of various theories to see if the data lends support to any of these theories.

During the hurricane seasons of 1948-1951 records of microseisms have been obtained at points in the Bahamas, Florida, North Carolina and Washington D. C. as various hurricanes have followed varying paths in the Western Atlantic. The following observations have in general been true for all these hurricanes:

- (1) Storms which generate in the Middle Atlantic and approach the seismograph locations do not produce appreciable microseismic activity until the storm moves over the continental shelf or, over the shallower waters surrounding the Islands of the Caribbean Sea. This same observation is pointed out by Donn (1952).
- (2) As the storm recedes, the microseisms continue at a much higher level of amplitude as compared to the same distance from the seismograph location during the approach of the storm.
- (3) The point of nearest approach is not necessarily the time of maximum amplitude.

The above observations can be interpreted as giving evidence that the storm must move

over the shallower waters of the continental shelf before microseisms are recorded and that the wake of the storm continues to be important in the generation of microseisms. This and similar observations in the light of the Longuet - Higgins (1950) theory, together with the work of Deacon (1947) and Darbyshire (1950), prompted the Naval Research Laboratory group to conduct field experiments during the 1951 hurricane season designed to obtain data which could assist in determining whether any correlation appears to exist between microseisms and hurricane-generated ocean waves.

The installations of the field experiments included the following:

- (1) A tripartite station on the West End of Grand Bahama.
- (2) The installation of two wave gages at Cocoa Beach, Florida, through the cooperation of the Beach Erosion Board and the University of California. These gages were of the pressure-sensitive type; the one was similar to the type developed by Woods Hole, and used quite extensively by the Beach Erosion Board, and the other was developed by the University of California. These gages were in water depths of about 29 and 46 feet respectively.



Figure 1. Map Showing Paths of Hurricanes "Easy" and "How"

- (3) A single horizontal-component seismograph was placed on the grounds of the U. S. Navy Underwater Sound Reference Laboratory at Orlando, Florida. This location is approximately 50 miles inland from Cocoa Beach, and therefore can be considered isolated from local surf vibrations, which can cause high seismic noise near the shore.

The simultaneous data of microseisms and water waves obtained by these installations during the two hurricanes of the 1951 season is of special interest in that the paths of the storms were radically different. Figure 1 shows the paths of the two storms "Easy" and "How." "Easy" followed a path which was well out over deep water during its entire course (except near its end when it moved over the Banks of Newfoundland). Its nearest approach to Florida was about 650 miles.

Hurricane "How" generated in the Gulf of Mexico, rapidly moved across Florida, and entered the Atlantic with the center passing slightly to the south of the wave-recorded location. Both of these storms produced high waves on Florida but the character of the waves was considerably different and the microseismic activity was greatly different. The two storms therefore provide an interesting comparison.

Figure 2 gives results of the simultaneous recordings of microseisms and water waves throughout the period hurricane "Easy" was in existence. The wave-gage data was analyzed by the Beach Erosion Board to give the significant wave height and period plotted as curves C and D respectively. A measure of the amplitude of the microseisms was obtained by measuring the area enclosed by the envelope of the microseisms during a 15 minute interval, an interval being used every two hours and in

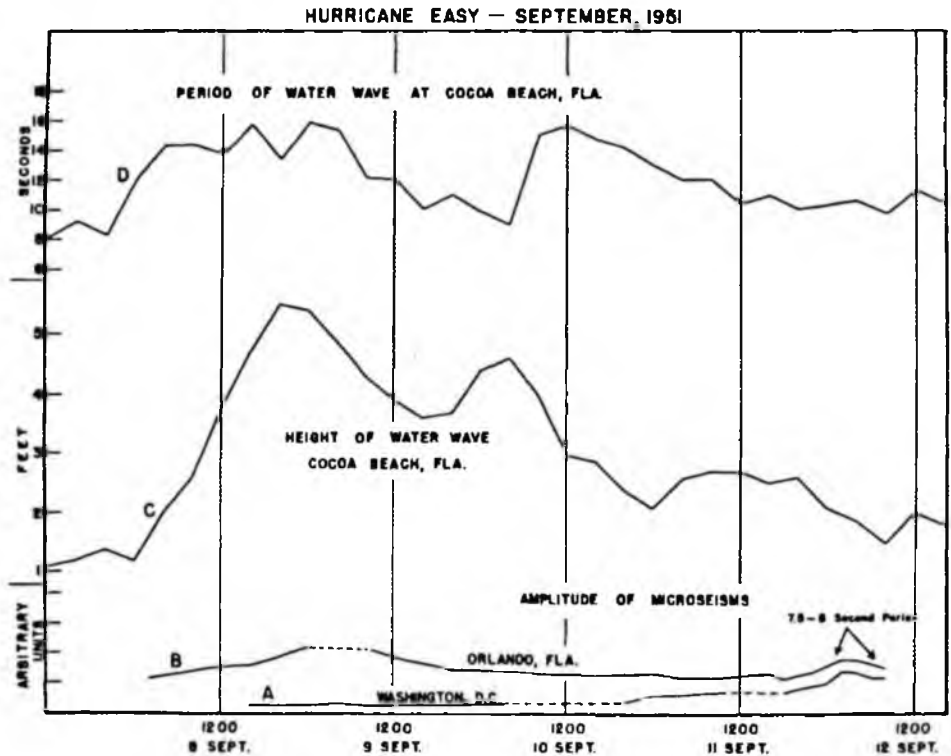


Figure 2. Microseismic and Water Wave Activity During Hurricane "Easy".

some parts of the record every hour. The relative position of curves A and B has no significance since the two curves have been shifted with respect to each other. However, the value of the arbitrary units for A and B is the same.

The sharp increase in both wave height and period as shown in curves C and D on the morning of September 8 accompanied the arrival of the swell from "Easy." Data from a Beach Erosion Board gage at Cape Henry and a report from Weather Ship H, several hundred

miles east of Charleston, N. C., also gives added evidence that the wave activity shown by curves C and D on Sept. 8 is associated with the arrival of swell from "Easy." The microseisms as recorded at Orlando on 8 Sept. show some increase in amplitude at approximately the same time as the maximum wave activity at Cocoa Beach. This increase in amplitude was not at all pronounced; in fact this particular period of microseisms normally would not have received any attention as being an indication of anything unusual. The record was too erratic to permit an analysis of the most pro-

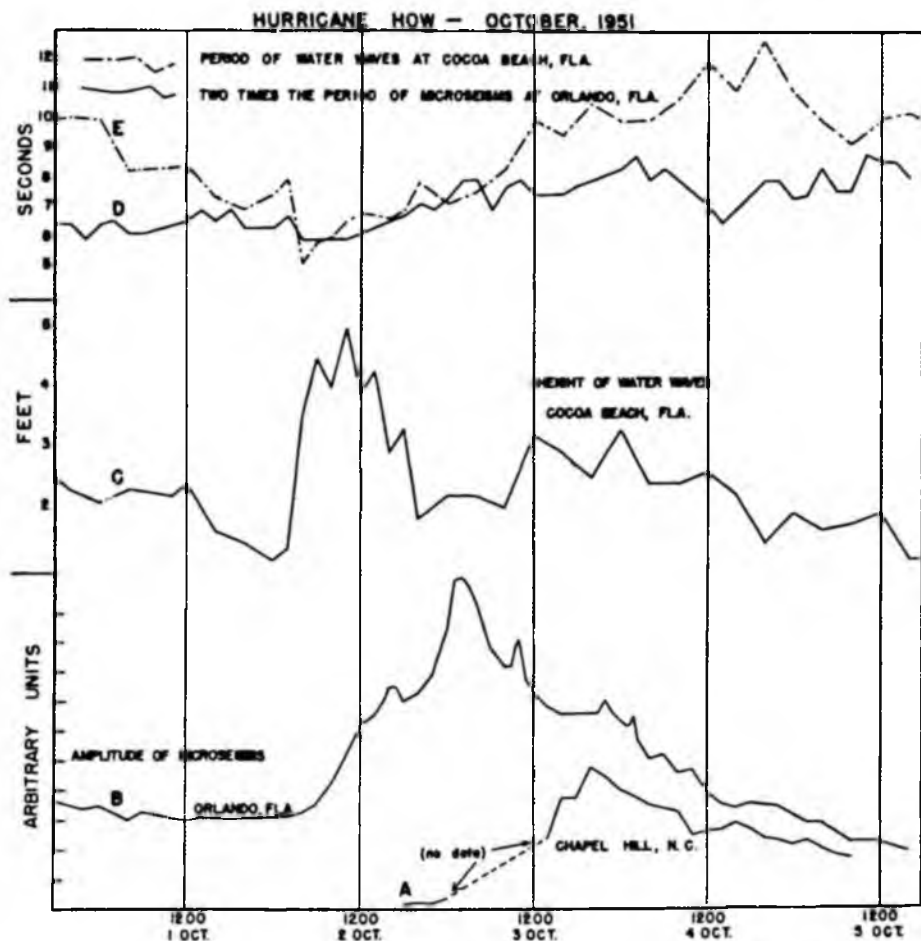


Figure 3. Microseismic and Water Wave Activity During Hurricane "How".

nounced period. The slight increase in microseisms during the wave activity can be interpreted as being associated with the swell rather than being generated directly under the storm for these reasons:

- (1) No simultaneous increase in microseisms occurred in Washington.
- (2) Microseisms generated under the storm should also have shown increased activity before the arrival of swell.

According to the Longuet-Higgins theory, a standing-wave pattern is required to transfer the water wave energy to microseisms. A standing wave pattern can conceivably be established upon reflection of the incoming swell by a sufficiently steep coast. The low level of microseismic activity during the swell from "Easy" would indicate, if the Longuet-Higgins theory is of importance, that the reflected wave energy along the Florida coast is very small. Because of the very gradual slope of the shore along Florida one would indeed expect low reflections.

The fact that no microseisms of any consequence were recorded during the period this intense storm remained over deep water indicates either one of two things: (1) microseisms were not generated by any method or (2) the generated microseisms were almost completely attenuated before reaching the continent. The data obtained by NRL is unable to resolve which of these two factors is the important one. Carder (1951) has presented evidence to indicate that the attenuation of microseisms propagated through the floor of the Western Atlantic is much greater than the attenuation over continental land masses. If attenuation is the important factor, then the attenuation may vary with the nature of the ocean floor and thus the results could be different in various parts of the world. Darbyshire (1950), Hanerji (1935) and others have presented evidence that microseisms are generated in deep water and have been recorded at distant points in the case of storms over the Eastern Atlantic, the mid-Bay of Bengal, and the Pacific. In view of these observations which contrasts with the observations in the Western Atlantic it may be inferred that attenuation is a much greater factor in the Western Atlantic than in certain other parts of the world.

It is of interest to point out the fact that longer period (7.5 to 8.0 second) microseisms are evident on curves A and B, Figure 4, as occurring at Washington and Orlando on the morning of 12 September. The records of these microseisms were nicely formed and of a regular nature. The simultaneity in time and period of these microseisms at Washington and Orlando would indicate a common area of generation. The fact that the storm at this

particular time was dissipating itself over the shallow areas off the coast of Newfoundland is further evidence that a storm moving from deep water to shallow water begins to generate microseisms. Intense winter microseisms are frequently observed when low-pressure areas move over this portion of the North Atlantic.

Let us consider Figure 3 which shows simultaneous data on wave and microseismic activity obtained during hurricane "How." The wave gage was fortuitously placed in a strategic location slightly to the north of the area where the storm entered the Atlantic. We may therefore assume that, if waves are responsible for the generation of microseisms, the waves as measured at this time should yield the best possible correlation inasmuch as the waves were confined to the water areas near the gages. Let us therefore compare the water wave amplitude and the position of the storm. We note an abrupt increase in wave amplitude during the early morning of 2 October, reaching a maximum about 1200 and dropping off abruptly about 2000. Referring again to Figure 1 we see that the forward part of the storm entered the Atlantic in the morning of 2 October with strong winds blowing from south-southeast and bringing waves toward Cocoa Beach. At about 1200 the center of the storm moved into the Atlantic and by 2000 the winds in the trailing part of the hurricane were from the north, thus effecting a reversal of wind as it existed 20 hours previously over this area. This reversal of wind is evident on the wave records by a rather abrupt decrease in wave amplitude. On Figure 3 we see from curve C that the maximum microseisms occurred just after the wind reversal. From curves D and E we observe that during the period when the water wave activity was confined to an area near the wave recorder the period of the water waves was closely two times the period of the microseisms. It should also be pointed out that the magnitude of the arbitrary units used as a measure of microseismic amplitude on the Orlando records during "Easy" and "How" are the same. It is apparent that, although the height of water waves recorded during the two storms is about the same, the amplitude of the microseisms during "How" was five or six times as large as the amplitude during "Easy" and in the case of "How" the amplitude was very outstanding above the normal background.

From the above facts one may make the following interpretations:

- (1) The correlation between one half the period of the waterwave and the period of the microseisms during "How" lends support to the Longuet-Higgins theory.
- (2) The reversal of wind and the setting up of waves in a direction more or

less in opposition to the waves generated a few hours previously may be a very effective method of producing the necessary standing wave system.

One may also refer here to the association of microseisms with cold fronts to support the thought that a relatively sudden reversal of wind over shallow water areas provides a condition for microseism generation. Typical weather conditions off the eastern North American coast, prior to the arrival of a cold front, include moderately strong southerly winds. These winds would develop waves travelling in a northerly direction of relatively small amplitude and short period. Following the passage of the cold front the wind direction normally changes abruptly to the northwest. It is reasonable that at some time, shortly after the passage of the front, waves developed by the northwest winds will have periods and wavelengths nearly equal to that of the dying swell from the south. Thus, a standing wave component could exist which would have the potential for excitation of microseisms in accordance with the Longuet-Higgins theory.

REFERENCES

BANERJI, S. K., *Theory of Microseisms. Proc. Indian Acad. Sci., A 1; 727-763, 1935.*
 CARDER, D. C., *Earthquake Notes*, Vol. 22, Sept. 1951.
 DARRYSHIRE, J., *Identification of Microseismic Activity with Sea Waves. Proc. Roy. Soc., 202A; 439-448, Aug. 7, 1950.*
 DEACON, G. E. R., *Relations between Sea Waves and Microseisms. Nature 160; 419-421, 1947.*
 DONN, W. L., *Cyclonic Microseisms Generated in the Western North Atlantic Ocean, J. of Meteor. 9; 81-71, Feb. 1952.*
 LONGUET-HIGGINS, M. S., *A Theory of the Origin of Microseisms. Phil. Tran. Roy. Soc. A., 243; 1-35, 1950.*

Discussion

J. G. SCHOLTE

Royal Netherlands Meteorological Institute

The existence of an unattenuated pressure variation in the ocean was already suspected by Whipple and Lee (1935) and some years later Bernard (1941) also suggested that a standing wave-system produced in some way microseisms, but the well-known exponential decrease of gravity waves precluded any understanding of the process. However, in 1942 Miche proved that in the case of standing gravity waves in an incompressible

ocean a second order pressure variation exists which is not essentially influenced by the depth. Moreover, as the frequency of this variation is twice that of the ocean waves and as Bernard had observed that the period of microseisms is roughly half that of sea waves, Longuet-Higgins and Ursell (1948) supposed that this second order effect is the primary cause of some microseisms.

The formula obtained by Miche can be derived by a small extension of the theory of gravity waves. Consider the irrotational motion in an incompressible ocean of infinite depth; for simplicity's sake we suppose the movement to be two-dimensional.

The horizontal (u) and vertical (w) components of the velocity are determined by a velocity-potential:

$$u = - \partial \phi / \partial x \text{ and } w = - \partial \phi / \partial z.$$

From the equations of motion

$$D u / D t = - \frac{\partial p}{\partial x} \text{ and } \frac{D w}{D t} = - \frac{\partial p}{\partial z} + g \rho$$

where D/Dt = a differentiation following the motion of the fluid, and p = the pressure, we obtain

$$\frac{\partial \phi}{\partial t} - \frac{1}{2} q^2 + g z = \frac{p - p_0}{\rho}$$

with $q^2 = u^2 + w^2$ and p_0 = the constant pressure at the free surface.

Placing the origin in the undisturbed surface the equation of this surface is

$$z = \zeta, \quad g \zeta = \left(- \frac{\partial \phi}{\partial t} + \frac{1}{2} q^2 \right) \quad z = \zeta$$

The potential ϕ has to satisfy the equation of continuity $\Delta \phi = 0$ and the boundary condition

$$D/Dt \left(\frac{\partial \phi}{\partial t} - \frac{1}{2} q^2 + g z \right) = 0 \text{ for } z = \zeta, \text{ or}$$

$$\frac{\partial^2 \phi}{\partial t^2} = g \frac{\partial \phi}{\partial z} + \frac{\partial q^2}{\partial t} + \frac{1}{2} q \Delta q^2 \text{ for } z = \zeta \dots \dots \dots (1)$$

A wave system consisting of two plane progressive waves travelling in opposite directions:

$$\phi_1 = \frac{g}{\nu} \left\{ a_1 \sin(kx - \nu t) - a_2 \sin(kx + \nu t) \right\} e^{-kz} \text{ with } a_1 \approx a_2$$

fulfils $\Delta \phi = 0$ and satisfies the boundary condition equation 1, to a first approximation if $ka \gg 1$ and $\nu^2 = gk$. For a second approximation we put $\phi = \phi_1 + \nu a^2$ where $d \approx d_1$; neglecting terms of third and higher order in

$$\zeta = a_1 \cos (kx - \nu t) + a_2 \cos (kx + \nu t)$$

$$\zeta_2 = -\frac{1}{2} k \left\{ \frac{a_1^2 \cos 2(kx - \nu t) + a_2^2 \cos 2(kx + \nu t) + 2a_1 a_2 \cos 2kx}{2} \right\}$$

$$\text{and the pressure} = p_0 + \rho \nu^2 z - \rho g \zeta, e^{-kz} - \frac{1}{2} \rho \nu^2 (a_1^2 + a_2^2 - 2a_1 a_2 \cos 2t) e^{-2kz} - 2\rho a_1 a_2 \nu^2 \cos 2\nu t.$$

Obviously at large depths ($kz \gg 1$) the varying part of the pressure is

$$p = 2\rho a_1 a_2 \nu^2 \cos 2\nu t \dots \dots \dots (2)$$

which is the result obtained by Miche for a standing wave system ($a_1 = a_2$).

Considering a rather general irrotational movement LONGUET-HIGGINS (1950) was able to generalize equation (2) and to calculate the amplitude of microseisms caused by an arbitrary wave-like motion of the ocean. His final formula (his equation 198) may be interpreted in the following (inexact) way.

The Miche force of the square λ^2 , where λ = the mean wavelength of the interfering progressive waves, is according to (2) equal to

$$2\rho a_1 a_2 \nu^2 \lambda^2$$

If the microseismic amplitude caused by a concentrated unit force with frequency 2ν at a distance r is denoted by $w(2\nu, z)$ the total amplitude will be

$$2\rho a_1 a_2 \nu^2 \lambda^2 w(2\nu, z)$$

Supposing the phases of ocean waves at points separated by a distance of a wavelength to be uncorrelated the amplitude generated by a storm with an area A will be of the order

$$\left(\frac{A}{\lambda^2}\right)^{\frac{1}{2}} 2\rho a_1 a_2 \nu^2 \lambda^2 w(2\nu, z)$$

With $A = 10^3 \text{ km}^2$ and $\lambda = 0.25 \text{ km}$ ($\nu = \frac{1}{2}$) the vertical amplitude at a distance of 3000 km. appears to be 9.4μ , which is of the order of the observed amplitudes. The detailed investigation of Longuet-Higgins shows that this has to be multiplied by a factor which depends on the frequency spectrum of the wave system. For instance, if the energy of the movement is uniformly divided in every direction within a range of wave lengths between λ_1 and λ_2 this factor is

$$\left\{ \frac{\pi}{2} \left(\frac{\lambda_1}{\lambda_2} - \frac{\lambda_2}{\lambda_1} \right) \right\}^{\frac{1}{2}}$$

if we obtain $a^2 f = a_1 a_2 \sin 2\nu t$.

The corresponding surface elevation $\zeta = \zeta_1 + \zeta_2$, with

the numerical value of this quantity is about 0.54 if $\lambda_1 = 400$ meters and $\lambda_2 = 154$ meters. The vertical amplitude is then 5μ , and the horizontal 3μ .

This theory undoubtedly explains the phenomenon of microseisms in a straightforward way. The only difficulty which it encounters is the fact that microseisms occur very often, while it is a matter of considerable doubt whether standing waves of rather large amplitudes are as common.

REFERENCES

- LONGUET-HIGGINS, M. S., and URSELL, F., *Sea waves and microseisms*. *Nature*, v. 162, p. 700, 1948.
- MICHE, M., *Mouvements ondulatoires de la mer en profondeur constante ou décroissants*. *Ann. Ponts et Chaussées*, v. 114, pp. 26-87, 131-164, 270-292, 398-408, 1944.
- WHIFFLE, F. J. W., and LEE, A. W., *Notes on the theory of microseisms*. *Mon. Not. Roy. Astr. Soc., Geophys. Suppl.*, v. 3, pp. 287-297, 1935.

Discussion from the Floor

Haskell. (Questioning Longuet-Higgins.) Ocean waves are coherent over more than just one wave length, so shouldn't the area of generation be subdivided into areas that are larger than one wave length on a side—perhaps the wave lengths? (Longuet-Higgins answered, perhaps so.)

Longuet-Higgins. (In answer to Press's question, "what if the wave periods on the surface occur off the peak of your resonance curve?") The sea waves must be considered as possessing not a single period, say 12 seconds, but a frequency spectrum of a certain width, say 8-16 seconds (the pressure fluctuations would then be from 4 to 8 seconds period.) The spectrum of the microseisms should be a combination of the spectrum of the pressure variations and that of a response curve. If the most prominent period of the pressure variations occurs off the peak of the resonance curve, the most prominent period of the microseisms would be expected to be displaced towards the peak.

Introductory Notes for Part C

C. Mass Transport in Water Waves

Papers C1 to C6

The papers in this section were stimulated originally by some remarkable experiments due to RA Bagnold (1947) conducted at Imperial College, London, during World War II. These showed that in water waves advancing towards a shoreline there was, near the bottom, a strong forward jet, contradicting the classical expression given by Stokes (1881) for waves in water of finite depth. Paper C1 below gives an explanation of this phenomenon. The mathematical theory, in fact, is similar to that used by Rayleigh in 1881 to explain the circulation of air in a Kundt's tube, with the difference that it is here applied to progressive, not standing, waves.

The existence of a boundary-layer at the bottom implies that the waves are not irrotational, as was assumed by Stokes. The motion is initially irrotational when started from rest, but vorticity is propagated inwards from the boundaries, either by convection or diffusion. This paper (C1) was the first to give general equations for this effect, under certain assumptions, among which are smallness of the wave amplitude compared to wavelength, and uniform density of the fluid. Later authors have generalized these equations, showing the important effects of non-uniform density of the fluid, especially near a surface of discontinuity.

Paper C2 shows formally that in any regular, irrotational wave, even if the amplitude is finite, the mass-transport velocity must decrease monotonically with the mean depth of a particle below the surface. Hence the bottom jets observed by Bagnold (see above) can be explained only by the presence of vortical flows.

The equations of viscous motion (the full Navier-Stokes equations) are of higher order than the Euler-Lagrange equations often used for water waves. So paper C3 provides a simple "physical" explanation for the forward bottom-jet observed by Bagnold (and subsequently confirmed by others), in the special case of a progressive wave. It also shows that the analytic expression for the maximum velocity in the jet is not only independent of the viscosity (or the eddy viscosity) but is also robust; it remains valid even when the viscosity is non-uniform, provided that the viscosity is a function only of the mean height of a particle above the bottom.

Paper C4 turns attention to the upper surface of the water, where the normal and tangential velocities are unconstrained but the pressure is assumed constant. Here a different type of boundary-layer is found. Instead of the mass-transport velocity just beyond the boundary-layer being determined theoretically, it is the

normal gradient of the mass-transport velocity which is determined. The latter is measured by a simple experiment, and the theoretical value is confirmed.

In paper C5, the general theory of paper C1 is applied to the ideal case of a circular island which finds itself subject to a broad ocean current such as a periodic tidal or inertial oscillation. The current induces a local wave close to the island, and the corresponding mass-transport velocity or steady streaming is calculated. A simple experiment, corresponding to an island with vertical sides, confirms the theory (see Figure 3 of paper C5).

A much later paper (C6) suggests an explanation of how a shallow-water wave passing over a thin flexible bag filled with water can pump the water down-wave, circulating it back via an external pipe — a possible means of extracting energy from the waves.

C. Mass Transport in Water Waves

Reproduced with permission from *Phil. Trans. R. Soc. Lond. A* 245 (1953) 535-581.

[535]

MASS TRANSPORT IN WATER WAVES

By M. S. LONGUET-HIGGINS

Trinity College, University of Cambridge

(Communicated by R. Stoneley, F.R.S.—Received 14 October 1952—Read 19 February 1953)

CONTENTS

	PAGE		PAGE
PART I. THE INTERIOR OF THE FLUID	536	PART III. WAVES IN WATER OF UNIFORM DEPTH	566
1. Introduction	536	10. Introduction	566
2. Definition of the mass-transport velocity \bar{U}	540	11. The boundary layer at the bottom	567
3. The stream function for \bar{U}	542	12. The boundary layer at the free surface	569
4. The equations of motion	543	13. Motion in the interior: the conduction solution	570
PART II. THE BOUNDARY LAYERS	548	14. Motion in the interior: the convection solution	573
5. Introduction	548	15. Discussion	576
6. Co-ordinates and general equations	548	16. Comparison with observation	577
7. The velocities are prescribed at the boundary	555	REFERENCES	581
8. The stresses are prescribed at the boundary	560		
9. Determination of Ψ in the interior	563		

It was shown by Stokes that in a water wave the particles of fluid possess, apart from their orbital motion, a steady second-order drift velocity (usually called the mass-transport velocity). Recent experiments, however, have indicated that the mass-transport velocity can be very different from that predicted by Stokes on the assumption of a perfect, non-viscous fluid. In this paper a general theory of mass transport is developed, which takes account of the viscosity, and leads to results in agreement with observation.

Part I deals especially with the interior of the fluid. It is shown that the nature of the motion in the interior depends upon the ratio of the wave amplitude a to the thickness δ of the boundary layer: when a^2/δ^2 is small the diffusion of vorticity takes place by viscous 'conduction'; when a^2/δ^2 is large, by convection with the mass-transport velocity. Appropriate field equations for the stream function of the mass transport are derived. The boundary layers, however, require separate consideration.

In part II special attention is given to the boundary layers, and a general theory is developed for two types of oscillating boundary: when the velocities are prescribed at the boundary, and when the stresses are prescribed. Whenever the motion is simple-harmonic the equations of motion can be integrated exactly. A general method is described for determining the mass transport throughout the fluid in the presence of an oscillating body, or with an oscillating stress at the boundary.

In part III, the general method of solution described in parts I and II is applied to the cases of a progressive and a standing wave in water of uniform depth. The solutions are markedly different from the perfect-fluid solutions with irrotational motion. The chief characteristic of the progressive-wave solution is a strong forward velocity near the bottom. The predicted maximum velocity near the bottom agrees well with that observed by Bagnold.

PART I. THE INTERIOR OF THE FLUID

I. INTRODUCTION

As was pointed out by Stokes in a classical memoir (1847), the individual particles in a progressive, irrotational wave do not describe exactly closed paths; besides their orbital motion they possess also a second-order mean velocity (called the mass-transport velocity) in the direction of wave propagation. If the equation of the free surface is

$$z = a e^{i(kx - \sigma t)} + O(a^2 k), \quad (1)$$

where x and z are horizontal and vertical co-ordinates (z measured downwards), t is the time, a is the wave amplitude, $k = 2\pi \div$ wave-length, and $\sigma = 2\pi \div$ wave period, then Stokes's expression for the mass-transport velocity \bar{U} is equivalent to

$$\bar{U} = \frac{a^2 \sigma k \cosh 2k(z-h)}{2 \sinh^2 kh} + C, \quad (2)$$

where h is the depth and C is an arbitrary constant. If it is assumed that the total horizontal transport is zero, we must have

$$C = -\frac{a^2 \sigma \sinh 2kh}{4h \sinh^2 kh} = -\frac{a^2 \sigma}{2h} \coth kh. \quad (3)$$

In deep water ($kh \gg 1$) equation (2) becomes simply

$$\bar{U} = a^2 \sigma k e^{-2kz} \quad (4)$$

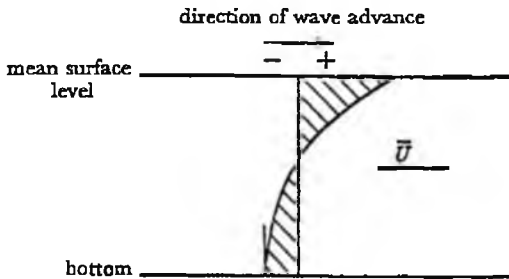


FIGURE 1. A typical profile of the mass-transport velocity in a progressive, irrotational wave ($kh = 1.0$).

The velocity profile for a typical ratio of depth to wave-length ($kh = 1$) is shown in figure 1. It will be seen that the velocity increases steadily with height above the bottom and that on the bottom itself the velocity gradient is zero. Both these features can be shown to be necessary consequences of the irrotational character of the motion, and not to depend on the smallness of the wave amplitude as assumed by Stokes (an elegant geometrical proof for waves in deep water was given by Rayleigh (1876); proofs for finite depths have been given by Ursell (1953) and Longuet-Higgins (1953)).

The irrotational wave is not the only type of wave theoretically possible in a perfect fluid: in the exact solution of Gerstner (1809) and Rankine (1863) the particles describe exactly

MASS TRANSPORT IN WATER WAVES

537

circular orbits, and the mass-transport velocity vanishes identically; indeed, Dubreil-Jacotin (1934) has shown that a wave motion may be superposed upon a steady stream having an arbitrary velocity distribution, so that the mass-transport velocity could take any desired value. The hypothesis of irrotational motion was assumed by Stokes on the ground that, under conservative forces, no vorticity can be generated in the interior of a uniform fluid, even with viscosity; if, therefore, the motion is started from rest it must initially be irrotational. The mass transport is then uniquely determined.

However, the mass-transport velocities observed in laboratory experiments may differ markedly from those predicted by the irrotational theory, especially in water of moderate depth. Thus Bagnold (1947) has found a strong forward velocity near the bottom and a weaker backward velocity at higher levels—the exact opposite of the Stokes velocity distribution. Other observers (Caligny 1878; King 1948) have found a forward drift both near the bottom and near the free surface, with a backward drift between.

It appears, therefore, that some assumption on which Stokes's theory is based is not valid. Now, in the theory of perfect fluids it is supposed that at a solid boundary the fluid may 'slip', i.e. that it may have a tangential velocity relative to the boundary. In fact, however, the particles of fluid in contact with the boundary must have the same velocity as the boundary itself; on the bottom, for example, they must be at rest. But quite near the bottom the fluid is observed to be in motion with velocities comparable to that in the interior of the fluid, so that in general there must be a strong velocity gradient near the bottom. This implies that there is in fact strong vorticity in the neighbourhood of the bottom; and it will be seen that, even if the vorticity is confined to a layer of infinitesimal thickness, the total amount of vorticity must still be finite. In an oscillating motion this vorticity will be of alternating sign; and the question then presents itself: will any of the vorticity spread into the interior of the fluid, or will it remain in the neighbourhood of the boundary?

In considering the diffusion of vorticity, the viscosity of the fluid must be taken into consideration; for, although the viscous terms in the equations of motion vanish when the motion is irrotational, they do not do so when there is vorticity. Although the viscosity may be small it cannot be neglected near the boundaries; for it is found that, as the viscosity tends to zero, so the thickness of the boundary layer decreases; the viscous terms in the equation of horizontal motion, which depend upon the second normal derivative of the velocity, remain of finite magnitude.

A straightforward method of taking into account the viscosity would be to proceed by successive approximations as in Stokes's solution for a perfect fluid; that is, in the first approximation to neglect all terms proportional to the square of the displacement; in the second approximation to neglect all terms proportional to the cube, and so on—all the viscous terms being retained. For surface waves in water of uniform depth there are now four boundary conditions: both components of velocity must vanish on the bottom, and both components of stress must vanish at the free surface. This was the method by which the present author originally approached the problem. The first approximation, which had been calculated by Hough (1896) and Bassett (1888), is practically identical with the perfect-fluid solution except that there are now transitional boundary layers at the bottom and at the free surface, and that the motion has a small attenuation, either with the horizontal co-ordinate x or with the time t (Hough and Basset considered only the latter case).

M. S. LONGUET-HIGGINS ON

To obtain the mass transport, the present author took the solution to a second approximation; and when this was done some new and unexpected features appeared. These will be briefly described here, although another method, as will be explained below, was later found to be more satisfactory.

Two cases were considered: the progressive wave and the standing wave. On the assumption that the total mass transport in a horizontal direction was zero, a unique solution for the mass-transport distribution was found. But, when the viscosity was made to tend to zero, the limiting velocity distribution was different from the irrotational, perfect-fluid solution. The thickness of the boundary layers at the bottom and at the free surface tended to zero; but the mass-transport velocity just outside these layers tended to a value different from zero and from that in the Stokes solution. In the progressive wave, the forward velocity near the bottom (i.e. just beyond the boundary layer) was given by

$$\bar{U} = \frac{5}{4} \frac{a^2 \sigma k}{\sinh^2 kh}, \quad (5)$$

and the velocity gradient near the surface was given by

$$\frac{\partial \bar{U}}{\partial z} = -4a^2 \sigma k \coth kh; \quad (6)$$

this is twice the corresponding value for the irrotational wave (cf. equation (2)). In the interior of the fluid the velocity distribution was given by the sum of the distribution (2) and a parabolic distribution, which was adjusted so that equations (5) and (6) and the condition that the total horizontal flow should be zero were all satisfied. Some theoretical velocity profiles, for different ratios of depth to wave-length, will be illustrated in figure 6, part III.

The case of a standing wave, in which the surface elevation is given by

$$z = 2a \cos kx \cos \sigma t, \quad (7)$$

had already been partly evaluated by Rayleigh (1883), who showed that there must be a circulation in cells of width one-quarter of a wave-length, very similar to that occurring in a Kundt's tube. The magnitude of the circulation is independent of the viscosity, when this is small. Rayleigh considered only the case of deep water, and he did not take into account the boundary conditions at the free surface. In the general case when the depth is finite the present author found that the mass-transport velocity near the bottom (just outside the boundary layer) is given by

$$\bar{U} = -\frac{3}{2} \frac{a^2 \sigma k}{\sinh^2 kh} \sin 2kx; \quad (8)$$

the velocity gradient near the free surface is zero,

$$\frac{\partial \bar{U}}{\partial z} = 0. \quad (9)$$

(The distribution of the mass transport in a typical standing wave will be illustrated in figure 7, part III.) The solution again differs from the corresponding solution when the motion is irrotational; in an irrotational standing wave the mass-transport velocity vanishes everywhere.

MASS TRANSPORT IN WATER WAVES

539

An interpretation of these results may be given as follows. Suppose the motion is generated from rest by conservative forces, or by propagation of the waves from outside into the region considered. Then at first the motion in the interior will be irrotational, and the mass transport will be given by Stokes's expression. But this state is not permanent; vorticity will diffuse inwards from the boundary layers at the bottom and at the free surface until a quasi-steady state, given by the viscous solution, is obtained. Thus the Stokes solution describes the initial motion (except very near the bottom); the viscous solution describes the final motion.

However, the method by which these results were derived is open to criticism: the process of approximation involves, in general, the neglect of the inertia terms in the equations of motion compared with the viscous terms; and this implies, as is shown in this part of the present paper, that the amplitude a of the motion should be small compared with the thickness δ of the boundary layer (δ is defined as $(2\nu/\sigma)^{1/2}$, where ν is the kinematic viscosity). It can also be shown that, unless $a \ll \delta$, it is not permissible to use Stokes's classical method of obtaining the boundary conditions at the free surface, for this involves expansion in a Taylor series, which is only valid if the displacement of the free surface is small compared with all other distances involved. Since the thickness of the boundary layer may be of the order of a few millimetres only, this condition seems to restrict the validity of the solution to very small waves indeed.

In this paper a different, and more general, approach is adopted. We start from the two fundamental assumptions that the velocity is periodic in time, and that the motion can be expressed as a perturbation of a state of rest. A general definition of the mass-transport velocity \bar{U} can then be given (see § 2), and equations of motion for \bar{U} can be derived. On examining these equations it is found that the expression for the diffusion of the vorticity consists of two parts. The first represents viscous diffusion, similar to the diffusion of heat in a solid, and the second represents diffusion by convection with the mass-transport velocity itself. These two sets of terms may be called 'conduction' and 'convection' terms respectively. The equations used by Stokes and Rayleigh are only valid, in the interior of the fluid, when the convection terms are small compared with the conduction terms, which restricts the solution to waves of very small amplitude ($a \ll \delta$). If, on the other hand, $a \gg \delta$, the motion is governed by convection; there is then a quite different field equation for the motion in the interior of the fluid (see § 4).

The boundaries, however, require special consideration, on account of the large velocity gradients encountered there. These are treated in part II, again in a general manner, so that the results could be applied to motions other than those of a standing or progressive wave in uniform depth. A general, oscillatory motion of the boundary is assumed, and moving co-ordinates relative to the boundary are taken. A boundary-layer approximation is made, similar to that used by Schlichting (1932) for a cylinder oscillating in an infinite fluid. Two different types of boundary layer are considered: first when the normal and tangential components of velocity at the boundary are prescribed (a special case being a fixed boundary or bottom); secondly, when the normal and tangential stresses are prescribed (a special case being a free surface, when both components of stress must vanish). In both cases the equations of motion can be integrated through the boundary layer, although the order of magnitude of the velocity gradients is different. In the first case the

M. S. LONGUET-HIGGINS ON

540

mass-transport velocity beyond the boundary layer (i.e. just in the interior of the fluid) is determined in terms of the boundary conditions and the known first-order motion; it differs in general from the mass-transport velocity at the boundary itself. In the second case it is the normal gradient of the mass-transport velocity which is determined just beyond the boundary layer, and this also differs from the velocity gradient at the surface itself.

The boundary-layer method just described has the advantage of not depending for its validity on the smallness of the ratio a/δ . By combining the new 'boundary conditions' with one or other of the field equations for the interior of the fluid which are derived in part I, the mass-transport velocity throughout the field can be completely evaluated. In part III the method is applied to the special cases of the progressive and standing waves in water of uniform depth. The 'conduction solution', i.e. the solution for small values of a/δ , is identical with that obtained by the method of successive approximations described above, as one would expect. The 'convection solution', however, is indeterminate for the progressive wave, and for the standing wave there are infinitely many solutions. Indeed, it seems very probable that for such large wave amplitudes the mass-transport velocity in the interior of the fluid is unstable; the assumption of periodicity then breaks down.

However, the solution in the boundary layers is still well determined, and is suitable for comparison with observation. In the last section of part III the experiments of Bagnold (1947) and others are discussed, and rather good agreement with the theory is found.

2. DEFINITION OF THE MASS-TRANSPORT VELOCITY

When the motion is not progressive, an exact definition of the mass-transport velocity for waves of finite amplitude, such as was given by Rayleigh (1876), is no longer possible; but for small motions a definition may be given as follows.

Let $\mathbf{u}(\mathbf{x}, t)$ denote the velocity at the point \mathbf{x} , = (x, y, z) , at time t . We assume, first, that the motion is periodic in time with period τ :

$$\mathbf{u}(\mathbf{x}, t+\tau) = \mathbf{u}(\mathbf{x}, t); \quad (10)$$

secondly, that \mathbf{u} is expressible asymptotically as a power series:

$$\mathbf{u} = \epsilon \mathbf{u}_1 + \epsilon^2 \mathbf{u}_2 + \dots, \quad (11)$$

where ϵ is a small quantity and $\mathbf{u}_1, \mathbf{u}_2$, etc., are of order l/τ . Here l denotes a typical length in the geometry of the system, for example, the wave-length if the motion is periodic in space. Equation (11) implies that we are considering the motion as a perturbation of a state of rest. The order of magnitude of the displacements is ϵl , or a , where a denotes the wave amplitude, so that ϵ is of order a/l . Thirdly, if a bar denotes the mean value with respect to time over a complete period, we assume

$$\overline{\mathbf{u}_1} = 0, \quad (12)$$

that is, there are no steady first-order currents. It may not, however, be assumed that $\overline{\mathbf{u}_2}$ is zero.

Let $\mathbf{U}(\mathbf{x}_0, t)$ denote the velocity of the particle whose co-ordinates at time $t = 0$ are \mathbf{x}_0 . Then the displacement of the particle from its original position is

$$\int_0^t \mathbf{U} dt. \quad (13)$$

MASS TRANSPORT IN WATER WAVES

541

We have therefore

$$\mathbf{U} = \mathbf{u}\left(\mathbf{x}_0 + \int_0^t \mathbf{U} dt, t\right), \quad (14)$$

$$= \mathbf{u}(\mathbf{x}_0, t) + \int_0^t \mathbf{U} dt \cdot \text{grad } \mathbf{u}(\mathbf{x}_0, t) + \dots, \quad (15)$$

by Taylor's theorem. Since \mathbf{U} is of a same order as \mathbf{u} we assume that

$$\mathbf{U} = \epsilon \mathbf{U}_1 + \epsilon^2 \mathbf{U}_2 + \dots, \quad (16)$$

whence, on substituting in (15) and equating coefficients of ϵ and ϵ^2 , we have

$$\mathbf{U}_1 = \mathbf{u}_1, \quad (17)$$

$$\mathbf{U}_2 = \mathbf{u}_2 + \int_0^t \mathbf{u}_1 dt \cdot \text{grad } \mathbf{u}_1, \quad (18)$$

and therefore

$$\overline{\mathbf{U}}_1 = \overline{\mathbf{u}}_1 = 0, \quad (19)$$

$$\overline{\mathbf{U}}_2 = \overline{\mathbf{u}}_2 + \overline{\int_0^t \mathbf{u}_1 dt \cdot \text{grad } \mathbf{u}_1}. \quad (20)$$

The lower limit of integration in (20) has been omitted, since it contributes nothing to the mean value. Thus, besides the first-order oscillatory velocity $\epsilon \mathbf{U}_1$, each particle possesses a steady drift velocity given by

$$\overline{\mathbf{U}} = \epsilon^2 \overline{\mathbf{U}}_2 = \epsilon^2 \left(\overline{\mathbf{u}}_2 + \overline{\int_0^t \mathbf{u}_1 dt \cdot \text{grad } \mathbf{u}_1} \right) \quad (21)$$

to the second order of approximation. If \mathbf{U}_3 , \mathbf{U}_4 , etc., are calculated, they are found to be aperiodic in general, so that no mean value independent of the initial value of t can be assigned to them. Indeed, \mathbf{U} cannot in general be expected to be a periodic function of t , since in the course of time a particle may drift into a region where the motion is quite different from that at its initial position. The progressive wave is an exception, since each particle remains at a nearly constant level; but the period of the motion for a fixed particle then depends upon the vertical co-ordinate z_0 . Thus the mass transport can only be defined, in general, if terms of higher order than the second are neglected, that is, for small motions. We shall therefore define the mass-transport velocity as being that given by equation (21).

The mass-transport velocity may be measured as the ratio of the displacement \mathbf{d} of a particle to the length t of the corresponding time interval provided that $|\mathbf{d}| \ll t$ and that the contribution to \mathbf{d} from the second-order terms is large compared with that from the first-order terms; this implies $|\epsilon^2 \overline{\mathbf{U}}_2 t| \gg |\epsilon \mathbf{U}_1 t|$ and so $t \gg \epsilon^{-1} \tau$. Both conditions are satisfied if ϵ is sufficiently small and if t is of order, say, $\epsilon^{-1/2}$.

Let \mathbf{f} be any periodic quantity associated with the motion and let

$$\mathbf{f} = \epsilon \mathbf{f}_1 + \epsilon^2 \mathbf{f}_2 + \dots, \quad (22)$$

where $\overline{\mathbf{f}}_1$ is zero. Then we may show similarly that the mean value of \mathbf{f} following a particle is given by

$$\epsilon^2 \left(\overline{\mathbf{f}}_2 + \overline{\int_0^t \mathbf{u}_1 dt \cdot \text{grad } \mathbf{f}_1} \right) \quad (23)$$

M. S. LONGUET-HIGGINS ON

to the second order of approximation. Suppose \mathbf{f} is the acceleration,

$$\mathbf{f} = \frac{\partial \mathbf{u}}{\partial t} + \mathbf{u} \cdot \text{grad } \mathbf{u}; \quad (24)$$

then
$$\mathbf{f}_1 = \frac{\partial \mathbf{u}_1}{\partial t}, \quad \mathbf{f}_2 = \frac{\partial \mathbf{u}_2}{\partial t} + \mathbf{u}_1 \cdot \text{grad } \mathbf{u}_1, \quad (25)$$

and the mean value of \mathbf{f} following a particle is therefore given by

$$\begin{aligned} & \epsilon^2 \left(\overline{\frac{\partial \mathbf{u}_2}{\partial t}} + \overline{\mathbf{u}_1 \cdot \text{grad } \mathbf{u}_1} + \overline{\int \mathbf{u}_1 dt \cdot \text{grad } \frac{\partial \mathbf{u}_1}{\partial t}} \right), \\ & = \epsilon^2 \left(\overline{\frac{\partial \mathbf{u}_2}{\partial t}} + \frac{\partial}{\partial t} \left\{ \overline{\int \mathbf{u}_1 dt \cdot \text{grad } \mathbf{u}_1} \right\} \right), \\ & = \frac{\epsilon^2}{\tau} \left[\mathbf{u}_2 + \int \mathbf{u}_1 dt \cdot \text{grad } \mathbf{u}_1 \right]_{t=0}^{\tau}, \end{aligned} \quad (26)$$

which vanishes by the periodicity of the motion.

The mean acceleration of a particle is therefore of a higher order than the second. This, indeed, is what we should expect. For the mean acceleration over one complete period is the difference between the initial and final velocities, divided by τ . But since in this time the particle has advanced through a distance of second order, the difference between the velocities at the initial and final positions of the particle is of third order at most.

3. THE STREAM FUNCTION FOR $\bar{\mathbf{U}}$

In the following we shall restrict ourselves to the consideration of two-dimensional motion only; thus if u , v and w are the components of the velocity, v is zero, and u and w are independent of the horizontal co-ordinate y . Assuming the fluid to be incompressible we have

$$\frac{\partial u}{\partial x} + \frac{\partial w}{\partial z} = 0, \quad (27)$$

whence
$$(u, w) = \left(\frac{\partial \psi}{\partial z}, -\frac{\partial \psi}{\partial x} \right), \quad (28)$$

where ψ is a stream function. The vorticity is given by

$$\frac{\partial u}{\partial z} - \frac{\partial w}{\partial x} = \nabla^2 \psi. \quad (29)$$

We may write

$$\left. \begin{aligned} (u, w) &= \epsilon(u_1, w_1) + \epsilon^2(u_2, w_2) + \dots, \\ \psi &= \epsilon\psi_1 + \epsilon^2\psi_2 + \dots, \end{aligned} \right\} \quad (30)$$

so that

$$\left. \begin{aligned} \frac{\partial u_i}{\partial x} + \frac{\partial w_i}{\partial z} &= 0, \\ (u_i, w_i) &= \left(\frac{\partial \psi_i}{\partial z}, -\frac{\partial \psi_i}{\partial x} \right), \quad (i = 1, 2, \dots), \\ \frac{\partial u_i}{\partial z} - \frac{\partial w_i}{\partial x} &= \nabla^2 \psi_i \end{aligned} \right\} \quad (31)$$

MASS TRANSPORT IN WATER WAVES

543

From (12), the arbitrary function of the time contained in ψ_1 may be chosen so that

$$\overline{\psi_1} = 0. \quad (32)$$

The components ($\epsilon^2 \overline{U_2}, \epsilon^2 \overline{W_2}$) of the mass-transport velocity are given by

$$\left. \begin{aligned} \overline{U_2} &= \overline{u_2} + \overline{\int u_1 dt \frac{\partial u_1}{\partial x} + \int w_1 dt \frac{\partial u_1}{\partial z}}, \\ \overline{W_2} &= \overline{w_2} + \overline{\int u_1 dt \frac{\partial w_1}{\partial x} + \int w_1 dt \frac{\partial w_1}{\partial z}}. \end{aligned} \right\} \quad (33)$$

Now if A and B denote any periodic quantities we have identically

$$\overline{\frac{\partial A}{\partial t} B + A \frac{\partial B}{\partial t}} = \overline{\frac{\partial}{\partial t} (AB)} = \frac{1}{T} [AB]_{t=0}^{t=T} = 0. \quad (34)$$

Hence

$$\left. \begin{aligned} \overline{U_2} &= \overline{u_2} + \overline{\int \frac{\partial \psi_1}{\partial z} dt \frac{\partial^2 \psi_1}{\partial x \partial z}} - \overline{\int \frac{\partial \psi_1}{\partial x} dt \frac{\partial^2 \psi_1}{\partial z^2}} = \frac{\partial \Psi}{\partial z}, \\ \overline{W_2} &= \overline{w_2} - \overline{\int \frac{\partial \psi_1}{\partial z} dt \frac{\partial^2 \psi_1}{\partial z^2}} + \overline{\int \frac{\partial \psi_1}{\partial x} dt \frac{\partial^2 \psi_1}{\partial x \partial z}} = -\frac{\partial \Psi}{\partial x}, \end{aligned} \right\} \quad (35)$$

where

$$\Psi = \overline{\psi_2} + \overline{\int \frac{\partial \psi_1}{\partial z} dt \frac{\partial \psi_1}{\partial x}}. \quad (36)$$

Thus $\epsilon^2 \Psi$ is a stream function for the mass-transport velocity $\overline{\mathbf{U}}$.

4. THE EQUATIONS OF MOTION

The equations of motions for a viscous, incompressible fluid may be written

$$\left(\frac{\partial}{\partial t} + u \frac{\partial}{\partial x} + w \frac{\partial}{\partial z} - \nu \nabla^2 \right) (u, w) = - \left(\frac{\partial}{\partial x}, \frac{\partial}{\partial z} \right) \left(\frac{p}{\rho} - gz \right) \quad (37)$$

in the usual notation. On differentiating the first component of (37) with respect to z and the second with respect to x , and subtracting, we find

$$\left(\frac{\partial}{\partial t} + u \frac{\partial}{\partial x} + w \frac{\partial}{\partial z} - \nu \nabla^2 \right) \nabla^2 \psi = 0, \quad (38)$$

and hence

$$\left(u \frac{\partial}{\partial x} + w \frac{\partial}{\partial z} - \nu \nabla^2 \right) \nabla^2 \psi = 0. \quad (39)$$

The second and third terms in equation (38) represent minus the rate of change of the vorticity at a fixed point due to convection; the last term, which is similar to a term in the equation of heat conduction, represents minus the rate of change of the vorticity due to viscous diffusion. On substituting from equations (30) and formally equating the coefficient of the highest power of ϵ to zero we have, from (38),

$$\left(\frac{\partial}{\partial t} - \nu \nabla^2 \right) \nabla^2 \psi_1 = 0, \quad (40)$$

and from (39)

$$\left(u_1 \frac{\partial}{\partial x} + w_1 \frac{\partial}{\partial z} \right) \nabla^2 \psi_1 - \nu \nabla^4 \psi_2 = 0. \quad (41)$$

Equation (40) gives $\nabla^2\psi_1 = \nu \int \nabla^4\psi_1 dt$, (42)

so that on substitution in (41) we have

$$\nabla^4\bar{\psi}_2 = \left(u_1 \frac{\partial}{\partial x} + w_1 \frac{\partial}{\partial z} \right) \int \nabla^4\psi_1 dt. \quad (43)$$

Hence the field equation for Ψ in terms of ψ_1 is

$$\nabla^4\Psi = \left(u_1 \frac{\partial}{\partial x} + w_1 \frac{\partial}{\partial z} \right) \int \nabla^4\psi_1 dt + \nabla^4 \int \frac{\partial\psi_1}{\partial z} dt \frac{\partial\psi_1}{\partial x}. \quad (44)$$

The introduction of viscous terms into the equations of motion involves a new fundamental length δ , $\equiv (2\nu/\sigma)^{1/2}$, and a new dimensionless ratio a/δ . In the case of water waves, if $\nu = 0.01 \text{ cm}^2/\text{s}$ and $\tau = 1.0 \text{ s}$, we see that δ is of the order of 0.02 cm . We may therefore assume that

$$\delta/l \ll 1 \quad (45)$$

(but not necessarily that $a/\delta \ll 1$). Now, a typical periodic solution of the equations

$$\left(\frac{\partial}{\partial t} - \nu \nabla^2 \right) f = 0, \quad \mathcal{J} = 0 \quad (46)$$

is given by

$$f_0 = e^{i(k_1x + k_2z + n\sigma t)}, \quad (47)$$

where n is a positive integer and

$$k_1^2 + k_2^2 = -in\sigma/\nu = -in/\delta^2. \quad (48)$$

Hence, in a direction perpendicular to the plane

$$\mathcal{R}(ik_1x + ik_2z) = 0 \quad (49)$$

f_0 must increase or decrease by a factor e in a distance of the order of δ . If f_0 is to remain bounded in the interior of the fluid, it can be appreciably large only in the neighbourhood of the boundaries, and must decrease inwards exponentially.

It is useful to distinguish between the 'boundary layer' or the region near the boundaries whose thickness is of the order of δ , and the 'interior' of the fluid, or the region 'beyond', i.e. inside, the boundary layer. For the remainder of the present section we shall be concerned only with the motion in the interior.

From equations (32) and (40) we see that $\nabla^2\psi_1$ satisfies equations (46). Therefore, assuming that $\nabla^2\psi_1$ is expressible as the sum of functions of the type (47) over any region of the interior, we may expect that

$$\nabla^2\psi_1 \rightarrow 0 \quad (50)$$

exponentially inwards. The second-order terms in equation (38) now give

$$\left(\frac{\partial}{\partial t} - \nu \nabla^2 \right) \nabla^2\psi_2 \rightarrow 0 \quad (51)$$

in the interior, so that by a similar argument we may expect that

$$\nabla^2(\psi_2 - \bar{\psi}_2) \rightarrow 0 \quad (52)$$

exponentially inwards. Equation (50) states that in the interior the first-order vorticity is exponentially small, while equation (52) states that the second-order vorticity becomes

MASS TRANSPORT IN WATER WAVES

545

independent of the time, though it is not necessarily zero. From the third-order terms in (38) we now have

$$\left(\frac{\partial}{\partial t} - \nu \nabla^2\right) \nabla^2 \psi_3 + \left(u_1 \frac{\partial}{\partial x} + w_1 \frac{\partial}{\partial z}\right) \nabla^2 \bar{\psi}_2 \rightarrow 0, \quad (53)$$

so that

$$\nabla^2 \psi_3 = - \left(\int u_1 dt \frac{\partial}{\partial x} + \int w_1 dt \frac{\partial}{\partial z} \right) \nabla^2 \bar{\psi}_2 + \nabla^2 \psi'_3, \quad (54)$$

where

$$\nabla^2 (\psi'_3 - \bar{\psi}'_3) \rightarrow 0. \quad (55)$$

Let us now return to equation (39) and retain temporarily all the terms up to the fourth order. Assuming (50) and (52) we have, in the interior,

$$\epsilon^4 \left[\left(u_1 \frac{\partial}{\partial x} + w_1 \frac{\partial}{\partial z} \right) \nabla^2 \psi_3 + \left(u_2 \frac{\partial}{\partial x} + w_2 \frac{\partial}{\partial z} \right) \nabla^2 \bar{\psi}_2 \right] - \nu \nabla^4 (\epsilon^2 \bar{\psi}_2 + \epsilon^3 \bar{\psi}_3 + \epsilon^4 \bar{\psi}_4) = 0. \quad (56)$$

We may substitute for $\nabla^2 \psi_3$ from equation (54). Then since

$$\left(u_1 \frac{\partial}{\partial x} + w_1 \frac{\partial}{\partial z} \right) \nabla^2 \psi_3 \rightarrow \left(u_1 \frac{\partial}{\partial x} + w_1 \frac{\partial}{\partial z} \right) \nabla^2 \bar{\psi}_3 = 0, \quad (57)$$

in the interior of the fluid we have

$$\epsilon^4 \left[- \left(u_1 \frac{\partial}{\partial x} + w_1 \frac{\partial}{\partial z} \right) \left\{ \left(\int u_1 dt \frac{\partial}{\partial x} + \int w_1 dt \frac{\partial}{\partial z} \right) \nabla^2 \bar{\psi}_2 \right\} + \left(u_2 \frac{\partial}{\partial x} + w_2 \frac{\partial}{\partial z} \right) \nabla^2 \bar{\psi}_2 \right] - \nu \nabla^4 (\epsilon^2 \bar{\psi}_2 + \epsilon^3 \bar{\psi}_3 + \epsilon^4 \bar{\psi}_4) = 0. \quad (58)$$

Now if A , B and C are any three periodic quantities we have identically

$$A \frac{\partial}{\partial x} \left(B \frac{\partial C}{\partial x} \right) = A \frac{\partial B}{\partial x} \frac{\partial C}{\partial x} + AB \frac{\partial^2 C}{\partial x^2}. \quad (59)$$

But, if $A = \partial B / \partial t$, and C is independent of the time,

$$AB \frac{\partial^2 C}{\partial x^2} = B \frac{\partial B}{\partial t} \frac{\partial^2 C}{\partial x^2} = \frac{1}{2\tau} [B^2]_0 \frac{\partial^2 C}{\partial x^2} = 0. \quad (60)$$

Thus writing

$$A = u_1, \quad B = \int u_1 dt, \quad C = \nabla^2 \psi_2 = \nabla^2 \bar{\psi}_2, \quad (61)$$

we have

$$u_1 \frac{\partial}{\partial x} \left(\int u_1 dt \frac{\partial}{\partial x} \nabla^2 \psi_2 \right) = \left(u_1 \frac{\partial}{\partial x} \int u_1 dt \right) \frac{\partial}{\partial x} \nabla^2 \bar{\psi}_2, \quad (62)$$

and therefore (using equation (34))

$$u_1 \frac{\partial}{\partial x} \left(\int u_1 dt \frac{\partial}{\partial x} \nabla^2 \psi_2 \right) = - \left(\int u_1 dt \frac{\partial u_1}{\partial x} \right) \frac{\partial}{\partial x} \nabla^2 \bar{\psi}_2. \quad (63)$$

Similarly

$$w_1 \frac{\partial}{\partial z} \left(\int w_1 dt \frac{\partial}{\partial z} \nabla^2 \psi_2 \right) = - \left(\int w_1 dt \frac{\partial w_1}{\partial z} \right) \frac{\partial}{\partial z} \nabla^2 \bar{\psi}_2 \quad (64)$$

and

$$\begin{aligned} u_1 \frac{\partial}{\partial x} \left(\int w_1 dt \frac{\partial}{\partial z} \nabla^2 \psi_2 \right) + w_1 \frac{\partial}{\partial z} \left(\int u_1 dt \frac{\partial}{\partial x} \nabla^2 \psi_2 \right) \\ = - \left(\int u_1 dt \frac{\partial w_1}{\partial x} \right) \frac{\partial}{\partial z} \nabla^2 \bar{\psi}_2 - \left(\int w_1 dt \frac{\partial u_1}{\partial z} \right) \frac{\partial}{\partial x} \nabla^2 \bar{\psi}_2. \end{aligned} \quad (65)$$

M. S. LONGUET-HIGGINS ON

Therefore on substitution in equation (58) we find

$$\epsilon^4 \left(\overline{U}_2 \frac{\partial}{\partial x} + \overline{W}_2 \frac{\partial}{\partial z} \right) \nabla^2 \overline{\psi}_2 - \nu \nabla^4 (\epsilon^2 \overline{\psi}_2 + \epsilon^3 \overline{\psi}_3 + \epsilon^4 \overline{\psi}_4) = 0, \quad (66)$$

where \overline{U}_2 and \overline{W}_2 are given by (35). The first group of terms on the left-hand side represents minus the rate of change of the vorticity due to convection by the mass-transport velocity. The second group of terms represents minus the rate of change of the vorticity due to viscous 'conduction'. These groups of terms may be called the convection terms and the conduction terms respectively.

Suppose that all terms in (66) of higher order than the second are neglected. We then have

$$\nabla^4 \overline{\psi}_2 = 0, \quad (67)$$

or

$$\nabla^4 \Psi = \nabla^4 \left[\frac{\partial \psi_1}{\partial z} \frac{dt}{dx} \frac{\partial \psi_1}{\partial x} \right], \quad (68)$$

which are the equations that would be obtained by setting $\nabla^2 \psi_1 = 0$ in the right-hand side of equations (43) and (44). But, if the velocity gradients in the interior of the fluid are not large, then the ratio of the convection terms to the conduction terms in equation (66) is of order $\epsilon^2 \sigma / \nu$, that is, of order a^2 / δ^2 . Therefore a *necessary* condition for the validity of equations (67) and (68) in the interior of the fluid is that $a^2 / \delta^2 \ll 1$.

In most practical cases, however, we shall have $a \gg \delta$; so that the 'conduction equation' (67) will not apply. We should expect in this case that the appropriate field equation would be that obtained by equating to zero the convection terms on the left-hand side of (66). This cannot be deduced from the preceding analysis, which rests on the assumption that $a^2 / \delta^2 \ll 1$; but the same equation can be derived by another method. Let us assume that the viscous terms in the original equation of motion (38) are entirely negligible; thus

$$\left(\frac{\partial}{\partial t} + u \frac{\partial}{\partial x} + w \frac{\partial}{\partial z} \right) \nabla^2 \psi = 0 \quad (69)$$

and

$$\left(u \frac{\partial}{\partial x} + w \frac{\partial}{\partial z} \right) \nabla^2 \psi = 0. \quad (70)$$

On substituting from (30) and equating coefficients of ϵ successively to zero we have from (69), in the first approximation,

$$\frac{\partial}{\partial t} (\nabla^2 \psi_1) = 0, \quad (71)$$

so that $\nabla^2 \psi_1$ is independent of t . Thus, by (32),

$$\nabla^2 \psi_1 = \nabla^2 \overline{\psi}_1 = 0. \quad (72)$$

From the second-order terms in (69)

$$\frac{\partial}{\partial t} (\nabla^2 \psi_2) + \left(u_1 \frac{\partial}{\partial x} + w_1 \frac{\partial}{\partial z} \right) \nabla^2 \psi_1 = 0. \quad (73)$$

Since the second group of terms vanishes,

$$\frac{\partial}{\partial t} (\nabla^2 \psi_2) = 0, \quad (74)$$

and so

$$\nabla^2 \psi_2 = \nabla^2 \overline{\psi}_2. \quad (75)$$

MASS TRANSPORT IN WATER WAVES

547

Similarly in the third approximation

$$\frac{\partial}{\partial t}(\nabla^2\psi_3) + \left(u_1 \frac{\partial}{\partial x} + w_1 \frac{\partial}{\partial z}\right) \nabla^2\bar{\psi}_2 = 0, \quad (76)$$

so that

$$\nabla^2\psi_3 = - \left\{ \int u_1 dt \frac{\partial}{\partial x} + \int w_1 dt \frac{\partial}{\partial z} \right\} \nabla^2\bar{\psi}_2. \quad (77)$$

The terms of highest order in (70) give

$$\left(\bar{u}_1 \frac{\partial}{\partial x} + \bar{w}_1 \frac{\partial}{\partial z}\right) \nabla^2\bar{\psi}_3 + \left(\bar{u}_2 \frac{\partial}{\partial x} + \bar{w}_2 \frac{\partial}{\partial z}\right) \nabla^2\bar{\psi}_2 = 0. \quad (78)$$

On substituting from (78) into (77) and using the relations (63), (64) and (65) we obtain

$$\left(\bar{U}_2 \frac{\partial}{\partial x} + \bar{W}_2 \frac{\partial}{\partial z}\right) \nabla^2\bar{\psi}_2 = 0, \quad (79)$$

or, from (35) and (36),

$$\left(\frac{\partial\Psi}{\partial z} \frac{\partial}{\partial x} - \frac{\partial\Psi}{\partial x} \frac{\partial}{\partial z}\right) \nabla^2\left(\Psi - \int \frac{\partial\psi_1}{\partial z} dt \frac{\partial\psi_1}{\partial x}\right) = 0. \quad (80)$$

In deriving (79) the first non-zero term omitted owing to the neglect of the viscosity is $\epsilon^2\nu\nabla^4\bar{\psi}_2$ (since $\nabla^4\psi_1$ is zero); the largest terms retained are the fourth-order terms in equation (79). Hence a *necessary* condition for the validity of these equations is that

$$\epsilon^2\nu\nabla^4\bar{\psi}_2 \ll \epsilon^4\left(\bar{U}_2 \frac{\partial}{\partial x} + \bar{W}_2 \frac{\partial}{\partial z}\right) \nabla^2\bar{\psi}_2, \quad (81)$$

and hence that $a^2 \gg \delta^2$.

Equations (68) and (80) may be called the 'conduction equation' and the 'convection equation' respectively.

Let us consider equation (79) more closely. It may be written in the form

$$\frac{\partial(\Psi, \nabla^2\bar{\psi}_2)}{\partial(x, z)} = 0, \quad (82)$$

where the left-hand side is the Jacobian of Ψ and $\nabla^2\bar{\psi}_2$. Thus $\nabla^2\bar{\psi}_2$ is functionally related to Ψ :

$$\nabla^2\bar{\psi}_2 = F(\Psi), \quad (83)$$

or by (36)

$$\nabla^2\left(\Psi - \int \frac{\partial\psi_1}{\partial z} dt \frac{\partial\psi_1}{\partial x}\right) = F(\Psi). \quad (84)$$

Hence the vorticity is constant along a stream-line. Also, since ψ_1 satisfies Laplace's equation we have, on differentiation,

$$\begin{aligned} \nabla^2 \int \frac{\partial\psi_1}{\partial z} dt \frac{\partial\psi_1}{\partial x} &= 2 \int \frac{\partial^2\psi_1}{\partial x \partial z} dt \frac{\partial^2\psi_1}{\partial x^2} + 2 \int \frac{\partial^2\psi_1}{\partial z^2} dt \frac{\partial^2\psi_1}{\partial x \partial z} \\ &= 2 \int \frac{\partial^2\psi_1}{\partial x \partial z} dt \frac{\partial^2\psi_1}{\partial z^2} - 2 \int \frac{\partial^2\psi_1}{\partial z^2} dt \frac{\partial^2\psi_1}{\partial x \partial z} \\ &= -4 \int \frac{\partial^2\psi_1}{\partial x^2} dt \frac{\partial^2\psi_1}{\partial x \partial z}, \end{aligned} \quad (85)$$

using equation (34). From (84) and (85) we obtain

$$\nabla^2\Psi = F(\Psi) - 4 \int \frac{\partial^2\psi_1}{\partial x^2} dt \frac{\partial^2\psi_1}{\partial x \partial z}, \quad (86)$$

an alternative form of the conduction equation.

PART II. THE BOUNDARY LAYERS

5. INTRODUCTION

In part I the mass-transport velocity in any oscillatory motion was defined, and field equations were obtained for the mass-transport stream function Ψ in the interior. It was shown, however, that the neighbourhood of the boundaries requires special consideration, on account of the large velocity gradients encountered there; it can no longer be assumed, for example, that the first-order vorticity is zero, as in the interior of the fluid.

An exact solution of the problem of an oscillating plane boundary, in a fluid at rest at infinity, was given by Stokes (1851). Lamb (1932, p. 662) gave the solution to the closely related problem of a semi-infinite fluid, with a fixed plane boundary, moving under the action of a harmonically oscillating body force. In these exact solutions the vorticity remains always in the neighbourhood of the boundaries, and the motion beyond a layer of thickness of the order of δ , $= (2\nu/\sigma)^{1/2}$, is zero. Also the mass-transport velocity vanishes identically. Approximate solutions for wave motion in water of finite or infinite depth have been given by Basset (1888), Hough (1896) and Lamb (1932). In these approximate solutions the vorticity is also confined to the boundaries, to the first approximation; but to obtain the mass transport it is necessary to study the second-order terms.

The objections to a direct extension of the solutions of Basset and Hough to a second approximation have been discussed in part I. Briefly, the method would only be valid for very small values of the ratio a/δ , where a is the wave amplitude. A different method, for the case of a circular cylinder oscillating in an infinite fluid, was used by Schlichting (1932). This involved initial neglect of δ/l , where l was the radius of the cylinder—essentially a boundary-layer approximation. It will be found that in Schlichting's analysis there is no implied restriction on the ratio a/δ for the motion near the boundaries.* In the following we shall use a similar approximation to Schlichting's, but treat a much more general problem, assuming an arbitrary oscillating motion of the boundaries, and taking into consideration more than one type of boundary condition.

6. CO-ORDINATES AND GENERAL EQUATIONS

Since the normal displacement of the boundary may be large compared with δ , a co-ordinate system must be chosen which is attached to the moving boundary. As in part I, assume the motion to be two-dimensional and independent of y and let

s = arc length measured along the boundary,

n = distance measured inwards along a normal.

$\kappa(s, t)$ = curvature of the boundary (positive when concave inwards),

(see figure 2*a*). The co-ordinates (s, n) are to be chosen so as to be in the same sense, right-handed or left-handed, as the cartesian co-ordinates (x, z) of part I. (s, n) are orthogonal,

* However, for the interior of the fluid Schlichting uses the 'conduction equation' (see §4), which may not be justifiable.

MASS TRANSPORT IN WATER WAVES

549

the lines $n = \text{constant}$, being parallel curves. The square of the displacement corresponding to small increments ds, dn is

$$\eta^2 ds^2 + dn^2, \quad (87)$$

where

$$\eta = 1 - \eta\kappa. \quad (88)$$

If q_s and q_n denote the components of velocity, resolved parallel to the directions of s and n increasing, the equation of continuity

$$\frac{\partial q_s}{\partial s} + \frac{\partial}{\partial n}(\eta q_n) = 0 \quad (89)$$

implies the existence of a stream function ψ such that

$$(q_s, q_n) = \left(\frac{\partial \psi}{\partial n}, -\frac{1}{\eta} \frac{\partial \psi}{\partial s} \right). \quad (90)$$

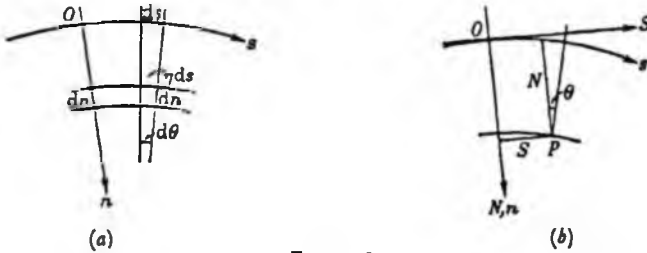


FIGURE 2

To find the normal and tangential stresses we temporarily introduce rectangular coordinates (S, N) tangential to (s, n) at the origin. The corresponding velocity components q_S and q_N are given by

$$\left. \begin{aligned} q_S &= q_s \cos \theta - q_n \sin \theta, \\ q_N &= q_s \sin \theta + q_n \cos \theta, \end{aligned} \right\} \quad (91)$$

where θ is the angle between the normals $s = 0$ and $s = \text{constant}$ (see figure 2b). Thus

$$\theta = \int_0^s \kappa ds, \quad \frac{\partial \theta}{\partial s} = \kappa, \quad \frac{\partial \theta}{\partial n} = 0. \quad (92)$$

When $s = 0 = \theta$ we have

$$\left. \begin{aligned} q_S &= q_s, & \frac{\partial q_S}{\partial s} &= \frac{\partial q_s}{\partial s} - \kappa q_n, & \frac{\partial q_S}{\partial n} &= \frac{\partial q_s}{\partial n} \\ q_N &= q_n, & \frac{\partial q_N}{\partial s} &= \frac{\partial q_n}{\partial s} + \kappa q_s, & \frac{\partial q_N}{\partial n} &= \frac{\partial q_n}{\partial n} \end{aligned} \right\} \quad (93)$$

The normal stress p_{nn} and the tangential stress p_{ss} are given, when $s = 0$, by

$$\left. \begin{aligned} \frac{1}{\rho v} (p_{nn} + p) &= 2 \frac{\partial q_N}{\partial N} = 2 \frac{\partial q_n}{\partial n}, \\ \frac{1}{\rho v} p_{ss} &= \frac{\partial q_S}{\partial N} + \frac{\partial q_N}{\partial S} = \frac{\partial q_s}{\partial n} + \frac{1}{\eta} \frac{\partial q_n}{\partial s}, \end{aligned} \right\} \quad (94)$$

M. S. LONGUET-HIGGINS ON

where p is the mean pressure. Thus from (93)

$$\left. \begin{aligned} \frac{1}{\rho v} (p_{nn} + p) &= -2 \frac{\partial}{\partial n} \left(\frac{1}{\eta} \frac{\partial \psi}{\partial s} \right), \\ \frac{1}{\rho v} p_{ns} &= \frac{\partial^2 \psi}{\partial n^2} + \frac{1}{\eta} \left[\kappa \frac{\partial \psi}{\partial n} - \frac{\partial}{\partial s} \left(\frac{1}{\eta} \frac{\partial \psi}{\partial s} \right) \right]. \end{aligned} \right\} \quad (95)$$

Since the form of these equations is independent of the position of the origin, they are valid for all values of (s, n) .

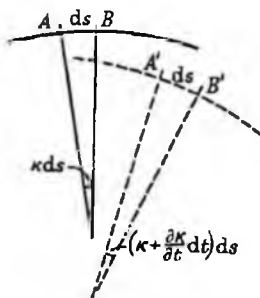


FIGURE 3

To describe the motion of the co-ordinate system, let

$V_s(s, t)$ = velocity of the point $(s, 0)$ parallel to the boundary,

$V_n(s, t)$ = velocity of the point $(s, 0)$ normal to the boundary,

$\Omega(s, t)$ = angular velocity of the normal $s = \text{constant}$ (positive in the sense of θ increasing).

Then the velocity components of the point having co-ordinates (s, n) are

$$(V_s - n\Omega, V_n), \quad (96)$$

and if (\dot{s}, \dot{n}) denotes the rate at which the co-ordinates of a particular element of fluid are increasing, and (q_s, q_n) denotes its actual velocity in space, we have

$$\dot{s} = \frac{1}{\eta} (q_s - V_s + n\Omega), \quad \dot{n} = q_n - V_n. \quad (97)$$

The following relations between V_n , V_s and Ω will be of use:

$$\left. \begin{aligned} \frac{\partial V_s}{\partial s} - \kappa V_n &= 0, \\ \frac{\partial V_n}{\partial s} + \kappa V_s &= \Omega, \end{aligned} \right\} \quad (98)$$

$$\frac{\partial \kappa}{\partial t} = \frac{\partial \Omega}{\partial s}. \quad (99)$$

These may be proved as follows. Consider the normals to the surface at two neighbouring points A and B , separated by an arc-length ds (see figure 3). Suppose that, in a short time dt , A and B are displaced to A' and B' respectively. The displacements of A perpendicular

MASS TRANSPORT IN WATER WAVES

551

and parallel to the normal at A are $V_s dt$ and $V_n dt$; thus, if the tangent and normal at A are taken as co-ordinate axes, the vector $\overline{AA'}$ is given by

$$\overline{AA'} = (V_s, V_n) dt. \quad (100)$$

Similarly, the displacements of B perpendicular and parallel to the normal at B are

$$\left(V_s + \frac{\partial V_s}{\partial s} ds\right) dt \quad \text{and} \quad \left(V_n + \frac{\partial V_n}{\partial s} ds\right) dt.$$

But the normal at B makes an angle κds with the normal at A . Hence, referred to the tangent and normal at A , we have

$$\overline{BB'} = \left(V_s + \frac{\partial V_s}{\partial s} ds - \kappa ds V_n, V_n + \frac{\partial V_n}{\partial s} ds + \kappa ds V_s\right) dt \quad (101)$$

to the present order of approximation. From (100) and (101)

$$\overline{BB'} - \overline{AA'} = \left(\frac{\partial V_s}{\partial s} - \kappa V_n, \frac{\partial V_n}{\partial s} + \kappa V_s\right) ds dt. \quad (102)$$

Now in time dt the vector \overline{AB} remains of constant length ds (neglecting ds^3) and turns through a small angle Ωdt . The displacement of the vector AB is therefore given by

$$\overline{A'B'} - \overline{AB} = (0, \Omega dt ds). \quad (103)$$

But since

$$\overline{AA'} + \overline{A'B'} = \overline{AB'} = \overline{AB} + \overline{BB'}, \quad (104)$$

the left-hand sides of (102) and (103) are equal. This proves equations (98). Equation (99) may be proved similarly: if \widehat{AB} , $\widehat{A'B'}$, etc., denote the angles between the normals at A and B , A' and B' , etc., we have

$$\widehat{AB} = \kappa ds, \quad \widehat{A'B'} = \left(\kappa + \frac{\partial \kappa}{\partial t} dt\right) ds. \quad (105)$$

Also

$$\widehat{AA'} = \Omega dt, \quad \widehat{BB'} = \left(\Omega + \frac{\partial \Omega}{\partial s} ds\right) dt. \quad (106)$$

But

$$\widehat{AA'} + \widehat{A'B'} = \widehat{AB'} = \widehat{AB} + \widehat{BB'}, \quad (107)$$

from which (99) follows.

As a result of the first of equations (98) we may write

$$V_s = \frac{\partial \psi^{(b)}}{\partial t}, \quad V_n = -\frac{1}{\eta} \frac{\partial \psi^{(b)}}{\partial s}, \quad (108)$$

where

$$\psi^{(b)} = -\int \eta V_n ds, \quad (109)$$

and therefore

$$q_s - V_s = \frac{\partial \psi'}{\partial n}, \quad q_n - V_n = -\frac{1}{\eta} \frac{\partial \psi'}{\partial s}, \quad (110)$$

where

$$\psi' = \psi - \psi^{(b)} = \psi + \int \eta V_n ds. \quad (111)$$

Clearly $\psi^{(b)}$ is a stream function for the motion of the boundary itself; ψ' is a stream function for the motion 'relative to the boundary'. There is in general no stream function for the

M. S. LONGUET-HIGGINS ON

motion of the co-ordinate system at points other than on the boundary, since the term $(-n\Omega, 0)$ in (96) represents a divergent velocity field. From (97) and (110) we have

$$s = \frac{1}{\eta} \left(\frac{\partial \psi'}{\partial n} + n\Omega \right), \quad \dot{n} = -\frac{1}{\eta} \frac{\partial \psi'}{\partial s}. \quad (112)$$

Consider now the equations of motion. Equation (38), which is obtained after elimination of the mean pressure p , may be expressed in the invariant form

$$\left(\frac{D}{Dt} - \nu \nabla^2 \right) \omega = 0, \quad (113)$$

where D/Dt denotes differentiation following the motion, ∇^2 is Laplace's operator and ω is the vorticity of the fluid:

$$\omega = \nabla^2 \psi. \quad (114)$$

With the present co-ordinates

$$\frac{D}{Dt} \equiv \frac{\partial}{\partial t} + s \frac{\partial}{\partial s} + \dot{n} \frac{\partial}{\partial n} \quad (115)$$

and

$$\nabla^2 \equiv \frac{1}{\eta} \left[\frac{\partial}{\partial s} \left(\frac{1}{\eta} \frac{\partial}{\partial s} \right) + \frac{\partial}{\partial n} \eta \left(\frac{\partial}{\partial n} \right) \right]. \quad (116)$$

Thus (113) can be written

$$\left[\frac{\partial}{\partial t} + \frac{1}{\eta} \left(\frac{\partial \psi'}{\partial n} + n\Omega \right) \frac{\partial}{\partial s} - \frac{1}{\eta} \frac{\partial \psi'}{\partial s} \frac{\partial}{\partial n} - \nu \nabla^2 \right] \nabla^2 \psi = 0, \quad (117)$$

∇^2 being given by (116).

For future reference it will be convenient to state also the equation of motion for each component of the velocity separately. If the co-ordinates (S, N) are taken to refer to a definite instant of time, say $t = 0$, then we have

$$\left. \begin{aligned} \left(\frac{D}{Dt} - \nu \nabla^2 \right) q_s &= -\frac{\partial}{\partial S} \left(\frac{p}{\rho} - gz \right), \\ \left(\frac{D}{Dt} - \nu \nabla^2 \right) q_n &= -\frac{\partial}{\partial N} \left(\frac{p}{\rho} - gz \right). \end{aligned} \right\} \quad (118)$$

Now when $t = 0$,

$$\left. \begin{aligned} \frac{\partial q_s}{\partial t} &= \frac{\partial q_s}{\partial t} - \Omega q_n, \\ \frac{\partial q_n}{\partial t} &= \frac{\partial q_n}{\partial t} + \Omega q_s. \end{aligned} \right\} \quad (119)$$

Also, from equations (91) we find

$$\left. \begin{aligned} \frac{\partial^2 q_s}{\partial s^2} &= \frac{\partial^2 q_s}{\partial s^2} - \kappa^2 q_s - 2\kappa \frac{\partial q_n}{\partial s} - \frac{d\kappa}{ds} q_n, & \frac{\partial^2 q_s}{\partial n^2} &= \frac{\partial^2 q_s}{\partial n^2}, \\ \frac{\partial^2 q_n}{\partial s^2} &= \frac{\partial^2 q_n}{\partial s^2} - \kappa^2 q_n + 2\kappa \frac{\partial q_s}{\partial s} + \frac{d\kappa}{ds} q_s, & \frac{\partial^2 q_n}{\partial n^2} &= \frac{\partial^2 q_n}{\partial n^2}, \end{aligned} \right\} \quad (120)$$

whence, after some simplification, we have

$$\left. \begin{aligned} \nabla^2 q_s &= \frac{\partial^2 q_s}{\partial n^2} - \frac{1}{\eta} \frac{\partial^2 q_n}{\partial s \partial n} - \frac{1}{\rho \nu} \kappa p_{ns}, \\ \nabla^2 q_n &= \frac{\partial^2 q_n}{\partial n^2} + \frac{1}{\eta} \frac{\partial^2 q_s}{\partial s \partial n} - \frac{1}{\rho \nu \eta} \frac{\partial p_{ns}}{\partial s}. \end{aligned} \right\} \quad (121)$$

MASS TRANSPORT IN WATER WAVES

553

The equations of motion are therefore

$$\left(\frac{\partial q_s}{\partial t} - \Omega q_n\right) + s\left(\frac{\partial q_t}{\partial s} - \kappa q_n\right) + \bar{n}\frac{\partial q_t}{\partial n} - \nu\left(\frac{\partial^2 q_t}{\partial n^2} - \frac{1}{\eta}\frac{\partial^2 q_n}{\partial s \partial n}\right) + \frac{1}{\rho}\kappa p_{ns} = -\frac{1}{\eta}\frac{\partial}{\partial s}\left(\frac{p}{\rho} - gz\right) \quad (122)$$

and
$$\left(\frac{\partial q_n}{\partial t} + \Omega q_s\right) + s\left(\frac{\partial q_n}{\partial s} + \kappa q_s\right) + \bar{n}\frac{\partial q_n}{\partial n} - \nu\left(\frac{\partial^2 q_n}{\partial n^2} + \frac{1}{\eta}\frac{\partial^2 q_s}{\partial s \partial n}\right) + \frac{1}{\rho\eta}\frac{\partial p_{ns}}{\partial s} = -\frac{\partial}{\partial n}\left(\frac{p}{\rho} - gz\right). \quad (123)$$

Up to the present point no approximations of any kind have been made.

In order to define the mass-transport velocity we assume, first, that the motion at each point of space is time-periodic, and that the co-ordinate system is also chosen in a periodic way; all functions of the velocities, for given co-ordinates (s, n) , are then periodic in t . Secondly, we assume that the motion is expressible in the form of an asymptotic series

$$\psi = \varepsilon\psi_1 + \varepsilon^2\psi_2 + \dots, \quad (124)$$

and we write

$$q_s = \varepsilon q_{s1} + \varepsilon^2 q_{s2} + \dots, \quad (125)$$

with similar expressions for $q_n, V_s, V_n, \Omega, \bar{s}, \bar{n}, \psi^{(b)}$ and ψ' . Thus the motion of the co-ordinate system, defined by V_s, V_n and Ω , is of first order at most. On the other hand, we write

$$\left. \begin{aligned} \kappa &= \kappa_0 + \varepsilon\kappa_1 + \varepsilon^2\kappa_2 + \dots, \\ \eta &= \eta_0 + \varepsilon\eta_1 + \varepsilon^2\eta_2 + \dots, \end{aligned} \right\} \quad (126)$$

allowing for a curvature κ_0 of the boundary in the undisturbed state. As in § 2 the mean values of the first-order velocities at each point in space are supposed to be zero. Thus, if the co-ordinates (S, N) are chosen as above, we have with an obvious notation

$$\overline{q_{s1}} = \overline{q_{n1}} = 0, \quad (127)$$

where a bar denotes mean values with respect to time. It follows from (91) that

$$\overline{q_{s1}} = \overline{q_{n1}} = 0, \quad (128)$$

since θ is constant with respect to time except possibly for a first-order variation. It may be shown also that

$$\overline{V_{s1}} = \overline{V_{n1}} = 0, \quad (129)$$

and, since

$$\overline{\Omega} = \frac{\partial \theta}{\partial t} = [\theta]_{t=0}^{t=\infty} = 0, \quad (130)$$

we have

$$\overline{\Omega_1} = \overline{\Omega_2} = \dots = 0. \quad (131)$$

From (98) and (99) we have also the useful relations

$$\left. \begin{aligned} \frac{\partial V_{s1}}{\partial s} - \kappa_0 V_{n1} &= 0, \\ \frac{\partial V_{n1}}{\partial s} + \kappa_0 V_{s1} &= \Omega_{s1}, \\ \frac{\partial \kappa_1}{\partial t} &= \frac{\partial \Omega_1}{\partial s}. \end{aligned} \right\} \quad (132)$$

Since, from (88),

$$\eta_0 = 1 - \kappa_0 n, \quad \eta_1 = -\kappa_1 n, \quad (133)$$

it follows, by the third of equations (132), that

$$\eta_1 = -\int \frac{\partial}{\partial s} (n\Omega_1) dt. \quad (134)$$

M. S. LONGUET-HIGGINS ON

The choice of the normal $s = 0$ is still at our disposal. If the boundary is rigid, the origin $(0, 0)$ may be chosen to be a point on the boundary and fixed relative to it, so that, at all points on the boundary,

$$V_s = q_s, \quad V_n = q_n. \quad (135)$$

On the other hand, it may be more convenient to take the origin at the point of intersection of the boundary with a line fixed in space, say a line normal to the position of the undisturbed surface. Since the angle between this line and the normal to the moving surface is of first order in ϵ , it follows that $V_s(0, t)$ is of order ϵ^2 at most, i.e.

$$V_{s1} = 0 \quad (136)$$

when $s = 0$. But from (132) we have

$$\frac{\partial V_{s1}}{\partial s} = \kappa_0 V_{n1}, \quad (137)$$

so that when κ_0 vanishes V_{s1} is constant along the boundary and (136) holds for all values of s . In other words, if the undisturbed surface has no curvature, the co-ordinates may be chosen so that V_{s1} vanishes at all points of the surface.

In precisely the same way as in § 2, it may be shown that the mean rate of increase of the co-ordinates (s, n) of a particle is given, to order ϵ^2 , by

$$\epsilon^2 \left[(\bar{s}_2, \bar{n}_2) + \left(\int \dot{s}_1 dt \frac{\partial}{\partial s} + \int \dot{n}_1 dt \frac{\partial}{\partial n} \right) (\dot{s}_1, \dot{n}_1) \right], \quad (138)$$

where, from (112),

$$\left. \begin{aligned} \dot{s}_1 &= \frac{1}{\eta_0} \left(\frac{\partial \psi'_1}{\partial n} + n \Omega_1 \right), & \dot{n}_1 &= -\frac{1}{\eta_0} \frac{\partial \psi'_1}{\partial s}, \\ \bar{s}_2 &= \frac{1}{\eta_0} \left(\frac{\partial \bar{\psi}'_2}{\partial n} - \frac{\eta_1}{\eta_0} \frac{\partial \bar{\psi}'_1}{\partial n} - \frac{\eta_1}{\eta_0} n \Omega_1 \right), & \bar{n}_2 &= -\frac{1}{\eta_0} \left(\frac{\partial \bar{\psi}'_2}{\partial s} - \frac{\eta_1}{\eta_0} \frac{\partial \bar{\psi}'_1}{\partial s} \right). \end{aligned} \right\} \quad (139)$$

But the position of the co-ordinate axes remains on the average unchanged. We therefore define the components of the mass-transport velocity $\epsilon^2(\bar{Q}_{s2}, \bar{Q}_{n2})$ by the equations

$$\left. \begin{aligned} \frac{1}{\eta_0} \bar{Q}_{s2} &= \bar{s}_2 + \int \dot{s}_1 dt \frac{\partial \dot{s}_1}{\partial s} + \int \dot{n}_1 dt \frac{\partial \dot{s}_1}{\partial n}, \\ \bar{Q}_{n2} &= \bar{n}_2 + \int \dot{s}_1 dt \frac{\partial \dot{n}_1}{\partial s} + \int \dot{n}_1 dt \frac{\partial \dot{n}_1}{\partial n}. \end{aligned} \right\} \quad (140)$$

It can be shown by direct differentiation, using equation (134) and the periodic property of the motion (equation (34)), that

$$\bar{Q}_{s2} = \frac{\partial \Psi}{\partial n}, \quad \bar{Q}_{n2} = -\frac{1}{\eta_0} \frac{\partial \Psi}{\partial s}, \quad (141)$$

where Ψ , which is a stream function for the mass-transport velocity, is given by

$$\Psi = \bar{\psi}'_2 + \frac{1}{\eta_0} \int \left(\frac{\partial \bar{\psi}'_1}{\partial n} + n \Omega_1 \right) dt \frac{\partial \bar{\psi}'_1}{\partial s}, \quad (142)$$

$$= \bar{\psi}'_2 - \eta_0 \int \dot{s}_1 dt \dot{n}_1. \quad (143)$$

MASS TRANSPORT IN WATER WAVES

555

In order to simplify the above equations we shall now make a boundary-layer approximation. The procedure we shall adopt will be, first, to neglect all quantities of order δ/l (where $\delta = (2\nu/\sigma)^{1/2}$ and l is a typical length associated with the geometry of the system), then to find a first-order solution in powers of ϵ , and finally to derive the mass transport. The initial neglect of δ/l involves relative errors of the order of δ/l in the first approximation. But it will be found that, although the normal velocity gradients may be of order $a\sigma/\delta$, the corresponding components of the normal velocity \bar{n} relative to the boundaries are in that case of order $a\sigma\delta/l$; by equation (140), the mass transport remains a homogeneous second-order function of the velocities. Hence the relative errors involved in the mass-transport velocity are only of order δ/l ; no restrictions on the ratio a/δ are implied.

The orders of magnitude of the different terms will depend, however, on the type of condition to be satisfied at the boundary. The two cases where the tangential velocity and the tangential stress, respectively, are prescribed will therefore be considered separately (§§ 7 and 8).

The velocity gradients in the interior of the fluid are assumed to be of ordinary magnitude, i.e. of order $a\sigma/l$. Thus, over distances which are small compared with l the velocity may be assumed to be uniform. The velocities or velocity gradients in the boundary layer, which may vary rapidly in the boundary layer itself, will tend to their relatively constant values 'just beyond the boundary layer', that is, in a region whose distance from the boundary is greater than a few multiples of δ but is still small compared with l . For points in this region we shall write $n = \infty$, with the understanding that this implies only $\delta \ll n \ll l$. Thus the components of the velocity just beyond the boundary layer will be denoted by $q_s^{(\infty)}$ and $q_n^{(\infty)}$; those at the surface itself by $q_s^{(0)}$ and $q_n^{(0)}$.

7. THE VELOCITIES ARE PRESCRIBED AT THE BOUNDARY

When $n = 0$ we have

$$\frac{\partial\psi}{\partial s} = -V_n = -q_n^{(0)}, \quad \frac{\partial\psi'}{\partial s} = 0, \quad (144)$$

and
$$\frac{\partial\psi}{\partial n} = q_s^{(0)}, \quad \frac{\partial\psi'}{\partial n} = q_s^{(0)} - V_s. \quad (145)$$

Assuming the tangential velocity $\partial\psi/\partial n$ to be of order unity (in powers of δ/l) throughout the boundary layer, we have

$$\frac{\partial^2\psi}{\partial s\partial n} = O(1), \quad (146)$$

and therefore, on integrating from $n = 0$,

$$\frac{\partial\psi}{\partial s} = -V_n + O(\delta/l), \quad \frac{\partial\psi'}{\partial s} = O(\delta/l). \quad (147)$$

But, since the tangential velocity $q_s^{(\infty)}$ just beyond the boundary layer in general differs from $q_s^{(0)}$, we must have

$$\frac{\partial^2\psi}{\partial n^2} = O(\delta/l)^{-1}, \quad \frac{\partial^2\psi'}{\partial n^2} = O(\delta/l)^{-2}, \quad (148)$$

and so on. $\psi^{(k)}$ and its derivatives being of order unity at most, we have also (since $\psi' = \psi - \psi^{(k)}$)

$$\frac{\partial \psi'}{\partial n} = O(1), \quad \frac{\partial^2 \psi'}{\partial n^2} = O(\delta/l)^{-1}, \quad \frac{\partial^3 \psi'}{\partial n^3} = O(\delta/l)^{-2}, \quad (149)$$

etc. Each differentiation of ψ' with respect to n raises the order of magnitude by a factor $(\delta/l)^{-1}$, whereas differentiation with respect to s leaves the order of magnitude unchanged. Retaining only the terms of highest order, we have from (88) and (112)

$$\eta = 1 \quad (150)$$

and

$$\dot{s} = \frac{\partial \psi'}{\partial n}, \quad \dot{n} = -\frac{\partial \psi'}{\partial s}. \quad (151)$$

The equation of motion (117) becomes

$$\left(\frac{\partial}{\partial t} + \frac{\partial \psi'}{\partial n} \frac{\partial}{\partial s} - \frac{\partial \psi'}{\partial s} \frac{\partial}{\partial n} - \nu \frac{\partial^2}{\partial n^2} \right) \frac{\partial^2 \psi'}{\partial n^2} = 0, \quad (152)$$

and on taking mean values with respect to time we have

$$\overline{\left(\frac{\partial \psi'}{\partial n} \frac{\partial}{\partial s} - \frac{\partial \psi'}{\partial s} \frac{\partial}{\partial n} - \nu \frac{\partial^2}{\partial n^2} \right) \frac{\partial^2 \psi'}{\partial n^2}} = 0. \quad (153)$$

In the first approximation (in powers of ϵ) we have from (152)

$$\left(\frac{\partial}{\partial t} - \nu \frac{\partial^2}{\partial n^2} \right) \frac{\partial^2 \psi'_1}{\partial n^2} = 0, \quad (154)$$

and so

$$\left(\frac{\partial}{\partial t} - \nu \frac{\partial^2}{\partial n^2} \right) \frac{\partial \psi'_1}{\partial n} = \frac{\partial}{\partial t} (q_{s1}^{(0)} - V_{s1}), \quad (155)$$

for the expression on the left-hand side, being independent of n , equals its value just beyond the boundary layer. From (154)

$$\frac{\partial^2 \psi'_1}{\partial n^2} = \nu \int \frac{\partial^4 \psi'_1}{\partial n^4} dt, \quad (156)$$

and from (155)

$$\frac{\partial \psi'_1}{\partial n} = \nu \int \frac{\partial^3 \psi'_1}{\partial n^3} dt + (q_{s1}^{(0)} - V_{s1}). \quad (157)$$

The terms of lowest order in ϵ in equation (153) give

$$\overline{\left(\frac{\partial \psi'_1}{\partial n} \frac{\partial}{\partial s} - \frac{\partial \psi'_1}{\partial s} \frac{\partial}{\partial n} \right) \frac{\partial^2 \psi'_1}{\partial n^2}} - \nu \frac{\partial^4 \overline{\psi'_2}}{\partial n^4} = 0, \quad (158)$$

and so from (156)

$$\frac{\partial \psi'_1}{\partial n} \int \frac{\partial^3 \psi'_1}{\partial s \partial n^3} dt - \frac{\partial \psi'_1}{\partial s} \int \frac{\partial^3 \psi'_1}{\partial n^3} dt - \frac{\partial^4 \overline{\psi'_2}}{\partial n^4} = 0. \quad (159)$$

Now from (142), to the present approximation,

$$\Psi = \overline{\psi_2} + \int \frac{\partial \psi'_1}{\partial n} dt \frac{\partial \psi'_1}{\partial s}. \quad (160)$$

MASS TRANSPORT IN WATER WAVES

If (142) is differentiated four times with respect to n it will be seen that the terms of highest order in δ/l are simply those that would be obtained by differentiating (160) four times. Thus, by Leibniz's theorem

$$\frac{\partial^4 \Psi'}{\partial n^4} = \frac{\partial^4 \psi_2'}{\partial n^4} + \int \frac{\partial^2 \psi_1'}{\partial n^2} dt \frac{\partial^2 \psi_1'}{\partial s} + 4 \int \frac{\partial^4 \psi_1'}{\partial n^4} dt \frac{\partial^2 \psi_1'}{\partial s \partial n} + 6 \int \frac{\partial^3 \psi_1'}{\partial n^3} dt \frac{\partial^3 \psi_1'}{\partial s \partial n^2} + 4 \int \frac{\partial^2 \psi_1'}{\partial n^2} dt \frac{\partial^4 \psi_1'}{\partial s \partial n^3} + \int \frac{\partial \psi_1'}{\partial n} dt \frac{\partial^5 \psi_1'}{\partial s \partial n^4}. \quad (161)$$

On substituting for $\partial^4 \psi_2'/\partial n^4$ from (159) and using a property of the periodicity (equation (34)), we find

$$\frac{\partial^4 \Psi'}{\partial n^4} = 4 \int \frac{\partial^4 \psi_1'}{\partial n^4} dt \frac{\partial^2 \psi_1'}{\partial s \partial n} + 6 \int \frac{\partial^3 \psi_1'}{\partial n^3} dt \frac{\partial^3 \psi_1'}{\partial s \partial n^2} + 4 \int \frac{\partial^2 \psi_1'}{\partial n^2} dt \frac{\partial^4 \psi_1'}{\partial s \partial n^3}. \quad (162)$$

This is our differential equation for Ψ' in terms of ψ_1' . It may be integrated as follows: from (156) and (157) (and (34))

$$\int \frac{\partial^4 \psi_1'}{\partial n^4} dt \frac{\partial^2 \psi_1'}{\partial s \partial n} + \int \frac{\partial^2 \psi_1'}{\partial n^2} dt \frac{\partial^4 \psi_1'}{\partial s \partial n^3} = \int \frac{\partial^4 \psi_1'}{\partial n^4} dt \frac{\partial}{\partial s} \left[\nu \int \frac{\partial^3 \psi_1'}{\partial n^3} dt + (q_{s1}^{(\infty)} - V_{s1}) \right] - \nu \int \frac{\partial^4 \psi_1'}{\partial n^4} dt \int \frac{\partial^3 \psi_1'}{\partial s \partial n^3} dt = \int \frac{\partial^4 \psi_1'}{\partial n^4} dt \frac{\partial}{\partial s} (q_{s1}^{(\infty)} - V_{s1}). \quad (163)$$

Thus (162) may be written

$$\frac{\partial^4 \Psi'}{\partial n^4} = \int \frac{\partial^4 \psi_1'}{\partial n^4} dt \frac{\partial}{\partial s} (q_{s1}^{(\infty)} - V_{s1}) + 3 \frac{\partial^2}{\partial n^2} \int \frac{\partial^2 \psi_1'}{\partial n^2} dt \frac{\partial^2 \psi_1'}{\partial s \partial n}. \quad (164)$$

On integrating twice from $n = \infty$, where $\frac{\partial^3 \psi_1'}{\partial n^3}$, $\frac{\partial^2 \psi_1'}{\partial n^2}$, $\frac{\partial \psi_1'}{\partial n}$ and $\frac{\partial^2 \Psi'}{\partial n^2}$ vanish to the present order, we have

$$\frac{\partial^2 \Psi'}{\partial n^2} = \int \frac{\partial^2 \psi_1'}{\partial n^2} dt \frac{\partial}{\partial s} (q_{s1}^{(\infty)} - V_{s1}) + 3 \int \frac{\partial^2 \psi_1'}{\partial n^2} dt \frac{\partial^2 \psi_1'}{\partial s \partial n}, \quad (165)$$

which can also be written

$$\frac{\partial^2 \Psi'}{\partial n^2} = 4 \int \frac{\partial^2 \psi_1'}{\partial n^2} dt \frac{\partial}{\partial s} (q_{s1}^{(\infty)} - V_{s1}) + 3 \int \frac{\partial^2 \psi_1'}{\partial n^2} dt \left(\frac{\partial^2 \psi_1'}{\partial s \partial n} \right)_{\infty}. \quad (166)$$

On integrating once more, from $n = 0$, we have

$$\left(\frac{\partial \Psi'}{\partial n} \right)_0^n = 4 \int \left(\frac{\partial \psi_1'}{\partial n} \right)_0^n dt \frac{\partial}{\partial s} (q_{s1}^{(\infty)} - V_{s1}) + 3 \int_0^n \left[\int \frac{\partial^2 \psi_1'}{\partial n^2} dt \left(\frac{\partial^2 \psi_1'}{\partial s \partial n} \right)_{\infty} \right] dn. \quad (167)$$

Now when $n = 0$ we have from (144), (145) and (160)

$$\left(\frac{\partial \Psi'}{\partial n} \right)_{n=0} = (q_{s2}^{(0)} - V_{s2}) + \int (q_{s1}^{(0)} - V_{s1}) dt \frac{\partial}{\partial s} (q_{s1}^{(0)} - V_{s1}), \quad (168)$$

so that altogether

$$\begin{aligned} \frac{\partial \Psi'}{\partial n} &= 4 \int \left(\frac{\partial \psi_1'}{\partial n} \right)_0^n dt \frac{\partial}{\partial s} (q_{s1}^{(\infty)} - V_{s1}) + 3 \int_0^n \left[\int \frac{\partial^2 \psi_1'}{\partial n^2} dt \left(\frac{\partial^2 \psi_1'}{\partial s \partial n} \right)_{\infty} \right] dn \\ &\quad + (q_{s2}^{(0)} - V_{s2}) + \int (q_{s1}^{(0)} - V_{s1}) dt \frac{\partial}{\partial s} (q_{s1}^{(0)} - V_{s1}). \end{aligned} \quad (169)$$

Suppose that the first-order motion is simple harmonic, that is, that ψ_1 , $q_{s1}^{(0)}$, etc., are given by the real parts of complex quantities proportional to $e^{i\sigma t}$. Then equation (155) becomes

$$\left(i\sigma - \nu \frac{\partial^2}{\partial n^2}\right) \frac{\partial \psi_1'}{\partial n} = i\sigma(q_{s1}^{(0)} - V_{s1}), \quad (170)$$

the general solution of which is given by

$$\frac{\partial \psi_1'}{\partial n} = (q_{s1}^{(0)} - V_{s1}) + A e^{\alpha n} + B e^{-\alpha n}, \quad (171)$$

where A and B are arbitrary constants and

$$\alpha = (i\sigma/\nu)^{1/2} = \frac{1+i}{\delta}. \quad (172)$$

Since the solution is to remain finite in the interior of the fluid, A must vanish. The second constant B must be chosen so as to satisfy the boundary condition

$$\left(\frac{\partial \psi_1'}{\partial n}\right)_{n=0} = q_{s1}^{(0)} - V_{s1}. \quad (173)$$

Hence we have

$$\frac{\partial \psi_1'}{\partial n} = (q_{s1}^{(0)} - V_{s1}) + (q_{s1}^{(0)} - q_{s1}^{(0)}) e^{-\alpha n}. \quad (174)$$

Thus the first-order velocity tends to its value in the interior of the fluid exponentially, but with a phase depending on n , since α is complex. A graph of the function $(e^{-\alpha n} - 1) e^{i\sigma t}$ for different values of t is given by Lamb (1932, p. 623) to illustrate the motion in the neighbourhood of a plane boundary when the fluid at infinity is oscillating harmonically. Equation (174) shows that in the first approximation the boundary may be regarded as plane and $q_{s1}^{(0)}$, $q_{s1}^{(0)}$ and V_{s1} as independent of s as well as n . However, the fact that these velocities are not completely independent of s produces a small normal velocity relative to the boundary, given by

$$-\frac{\partial \psi_1'}{\partial s} = -n \frac{\partial}{\partial s} (q_{s1}^{(0)} - V_{s1}) + \frac{\partial}{\partial s} (q_{s1}^{(0)} - q_{s1}^{(0)}) \frac{1}{\alpha} (e^{-\alpha n} - 1). \quad (175)$$

Just beyond the boundary layer this velocity is given by

$$-\left(\frac{\partial \psi_1'}{\partial s}\right)_{n=\infty} = -\frac{1}{\alpha} \frac{\partial}{\partial s} (q_{s1}^{(0)} - q_{s1}^{(0)}). \quad (176)$$

In considering the second-order terms a development of the notation will be useful. If F_1 and F_2 are any two periodic quantities of the form

$$F_1 = \mathcal{R}f_1 e^{i\sigma t}, \quad F_2 = \mathcal{R}f_2 e^{i\sigma t}, \quad (177)$$

where f_1 and f_2 are complex and independent of t , and \mathcal{R} denotes the real part, we have

$$\begin{aligned} F_1 F_2 &= \frac{1}{2}(f_1 e^{i\sigma t} + f_1^* e^{-i\sigma t}) \times \frac{1}{2}(f_2 e^{i\sigma t} + f_2^* e^{-i\sigma t}) \\ &= \frac{1}{4}(f_1 f_2 e^{2i\sigma t} + f_1^* f_2^* e^{-2i\sigma t} + f_1 f_2^* + f_1^* f_2), \end{aligned} \quad (178)$$

a star (*) being used to denote the conjugate complex quantity. Thus

$$\overline{F_1 F_2} = \frac{1}{4}(f_1 f_2^* + f_1^* f_2) = \mathcal{R} \frac{1}{2} f_1 f_2^* = \mathcal{R} \frac{1}{2} f_1^* f_2. \quad (179)$$

MASS TRANSPORT IN WATER WAVES

559

If the symbol \mathcal{R} is omitted in (177) and (179) we may write

$$\overline{F_1 F_2} = \frac{1}{2} F_1 F_2^* = \frac{1}{2} F_1^* F_2, \quad (180)$$

it being understood that the real part only is to be taken. Any group of terms in a product may therefore be replaced as a whole by the conjugate complex group of terms.

From equation (174) we have

$$\left. \begin{aligned} \left(\frac{\partial \psi'_1}{\partial n}\right)_0 &= (q_{s1}^{(0)} - q_{s1}^{(\infty)}) (e^{-\alpha n} - 1), \\ \frac{\partial^2 \psi'_1}{\partial n^2} &= -(q_{s1}^{(0)} - q_{s1}^{(\infty)}) \alpha e^{-\alpha n}, \\ \left(\frac{\partial^2 \psi'_1}{\partial s \partial n}\right)_\infty &= \frac{\partial}{\partial s} (q_{s1}^{(0)} - q_{s1}^{(\infty)}) e^{-\alpha n}. \end{aligned} \right\} \quad (181)$$

On substituting these results in (169) and integrating the second term using (172) we find

$$\begin{aligned} \frac{\partial \Psi}{\partial n} &= \frac{2}{i\sigma} (q_{s1}^{(0)} - q_{s1}^{(\infty)}) \frac{\partial}{\partial s} (q_{s1}^{(\infty)*} - V_{s1}^*) (e^{-\alpha n} - 1) + \frac{3(1+i)}{4i\sigma} (q_{s1}^{(0)} - q_{s1}^{(\infty)}) \frac{\partial}{\partial s} (q_{s1}^{(0)*} - q_{s1}^{(\infty)*}) (e^{-(\alpha+\alpha^*)n} - 1) \\ &\quad + \overline{(q_{s2}^{(0)} - V_{s2})} + \frac{1}{2i\sigma} (q_{s1}^{(0)} - V_{s1}) \frac{\partial}{\partial s} (q_{s1}^{(0)*} - V_{s1}^*). \end{aligned} \quad (182)$$

Just beyond the boundary layer we have

$$\begin{aligned} \left(\frac{\partial \Psi}{\partial n}\right)_{n=\infty} &= -\frac{2}{i\sigma} (q_{s1}^{(0)} - q_{s1}^{(\infty)}) \frac{\partial}{\partial s} (q_{s1}^{(\infty)*} - V_{s1}^*) - \frac{3(1+i)}{4i\sigma} (q_{s1}^{(0)} - q_{s1}^{(\infty)}) \frac{\partial}{\partial s} (q_{s1}^{(0)*} - q_{s1}^{(\infty)*}) \\ &\quad + \overline{(q_{s2}^{(0)} - V_{s2})} + \frac{1}{2i\sigma} (q_{s1}^{(0)} - V_{s1}) \frac{\partial}{\partial s} (q_{s1}^* - V_{s1}^*). \end{aligned} \quad (183)$$

Thus the tangential component of the mass-transport velocity is determined by the tangential velocity $q_s^{(0)}$ at the boundary, the tangential velocity $q_s^{(\infty)}$ just beyond the boundary layer, and the velocity V_s , which depends partly on the movement of the boundary and partly on the choice of origin. When there is no stretching of the boundary we may take

$$V_s = q_s^{(0)}. \quad (184)$$

Equations (182) and (183) then become

$$\frac{\partial \Psi}{\partial n} = \frac{1}{4i\sigma} (q_{s1}^{(0)} - q_{s1}^{(\infty)}) \frac{\partial}{\partial s} (q_{s1}^{(0)*} - q_{s1}^{(\infty)*}) [8(1 - e^{-\alpha n}) + 3(1+i)(e^{-(\alpha+\alpha^*)n} - 1)] \quad (185)$$

$$\text{and} \quad \left(\frac{\partial \Psi}{\partial n}\right)_{n=\infty} = \frac{5-3i}{4i\sigma} (q_{s1}^{(0)} - q_{s1}^{(\infty)}) \frac{\partial}{\partial s} (q_{s1}^{(0)*} - q_{s1}^{(\infty)*}), \quad (186)$$

respectively. In particular when the boundary is stationary we have

$$q_s^{(0)} = 0, \quad (187)$$

and so

$$\frac{\partial \Psi}{\partial n} = \frac{1}{4i\sigma} q_{s1}^{(\infty)} \frac{\partial q_{s1}^{(\infty)*}}{\partial s} [8(1 - e^{-\alpha n}) + 3(1+i)(e^{-(\alpha+\alpha^*)n} - 1)] \quad (188)$$

and

$$\left(\frac{\partial \Psi}{\partial n}\right)_{n=\infty} = \frac{5-3i}{4i\sigma} q_{s1}^{(\infty)} \frac{\partial q_{s1}^{(\infty)*}}{\partial s}. \quad (189)$$

M. S. LONGUET-HIGGINS ON

At the boundary itself the normal component of mass-transport velocity vanishes and so Ψ must be constant. In general the normal component of the mass-transport velocity can be found from the equation

$$\frac{\partial \Psi}{\partial s} = \frac{\partial}{\partial s} \int_0^n \frac{\partial \Psi}{\partial n} dn. \quad (190)$$

For example, when the boundary is stationary we have from (188)

$$\frac{\partial \Psi}{\partial s} = -\frac{1}{4i\sigma} \left(\frac{\partial q_{s1}^{(\infty)}}{\partial s} \frac{\partial q_{s1}^{(\infty)*}}{\partial s} + q_{s1}^{(\infty)} \frac{\partial^2 q_{s1}^{(\infty)*}}{\partial s^2} \right) \frac{1}{\alpha} [8(1 - \alpha n - e^{-\alpha n}) + 3i(e^{-(\alpha + \alpha^*)n} + (\alpha + \alpha^*)n - 1)], \quad (191)$$

and so

$$\left(\frac{\partial \Psi}{\partial s} \right)_{n=0} = -\frac{1}{4i\sigma} \left(\frac{\partial q_{s1}^{(\infty)}}{\partial s} \frac{\partial q_{s1}^{(\infty)*}}{\partial s} + q_{s1}^{(\infty)} \frac{\partial^2 q_{s1}^{(\infty)*}}{\partial s^2} \right) \frac{1}{\alpha} [(8 - 3i) - (8 - 3i)\alpha n + 3i\alpha^* n]. \quad (192)$$

8. THE STRESSES ARE PRESCRIBED AT THE BOUNDARY

Let $\rho_{ns}^{(0)}$ denote the tangential stress at the boundary, which is assumed to be of order $\rho\nu\alpha\sigma/l$. We have then

$$\left(\frac{\partial \psi}{\partial s} \right)_{n=0} = -V_n, \quad \left[\left(\frac{\partial^2}{\partial n^2} - \frac{\partial^2}{\partial s^2} + \kappa \frac{\partial}{\partial n} \right) \psi \right]_{n=0} = \frac{1}{\rho\nu} \rho_{ns}^{(0)}. \quad (193)$$

If we assume

$$\frac{\partial^2 \psi}{\partial n^2} = O(1) \quad (194)$$

(in powers of δ/l), it follows that $\partial\psi/\partial s$ and $\partial\psi/\partial n$ are constant, to this order, throughout the boundary layer. Thus

$$\frac{\partial \psi}{\partial n} = -V_n = -q_n^{(0)}, \quad \frac{\partial \psi'}{\partial n} = O(\delta/l), \quad (195)$$

$$\frac{\partial \psi}{\partial s} = q_s^{(0)}, \quad \frac{\partial \psi'}{\partial n} = q_s^{(0)} - V_s. \quad (196)$$

The second of the two boundary conditions (193) may therefore be written

$$\left(\frac{\partial^2 \psi}{\partial n^2} \right)_{n=0} = \frac{1}{\rho\nu} \rho_{ns}^{(0)} - \left(\frac{\partial V_n}{\partial s} + \kappa q_s^{(0)} \right), \quad (197)$$

or alternatively, since, when $n = 0$,

$$\nabla^2 \psi = \left(\frac{\partial^2}{\partial s^2} + \frac{\partial^2}{\partial n^2} - \kappa \frac{\partial}{\partial n} \right) \psi, \quad (198)$$

we have

$$(\nabla^2 \psi)_{n=0} = \frac{1}{\rho\nu} \rho_{ns}^{(0)} - 2 \left(\frac{\partial V_n}{\partial s} + \kappa q_s^{(0)} \right). \quad (199)$$

But the value of $\partial^2 \psi / \partial n^2$ just beyond the boundary layer in general differs from that given by (197). Therefore we must have

$$\frac{\partial^3 \psi}{\partial n^3} = O(\delta/l)^{-1}, \quad \frac{\partial^4 \psi}{\partial n^4} = O(\delta/l)^{-2}, \quad (200)$$

and hence also

$$\frac{\partial^2 \psi'}{\partial n^2} = O(1), \quad \frac{\partial^3 \psi'}{\partial n^3} = O(\delta/l)^{-1}, \quad \frac{\partial^4 \psi'}{\partial n^4} = O(\delta/l)^{-2}, \quad (201)$$

MASS TRANSPORT IN WATER WAVES

561

each further differentiation with respect to n raising the order of magnitude by $(\delta/l)^{-1}$. It should be noticed, however, that there is a break in the sequence, since both $\partial\psi'/\partial n$ and $\partial^2\psi'/\partial n^2$ are $O(1)$. This introduces a significant difference between the present case and that considered in § 7.

The equation of motion (117) now becomes

$$\left(\frac{\partial}{\partial t} + \frac{\partial\psi'}{\partial n} \frac{\partial}{\partial s} - \frac{\partial\psi'}{\partial s} \frac{\partial}{\partial n} - \nu \frac{\partial^2}{\partial n^2}\right) \nabla^2\psi = 0. \quad (202)$$

This may be compared with equation (152), where the corresponding terms are of a higher order of magnitude. It is not possible in the present case to replace $\nabla^2\psi$ by $\partial^2\psi/\partial n^2$ or by $\partial^2\psi'/\partial n^2$. In the first approximation we now have

$$\left(\frac{\partial}{\partial t} - \nu \frac{\partial^2}{\partial n^2}\right) \nabla^2\psi_1 = 0, \quad (203)$$

and so
$$\nabla^2\psi_1 = \nu \int \frac{\partial^2}{\partial n^2} \nabla^2\psi_1 dt = \nu \int \frac{\partial^4\psi_1}{\partial n^4} dt. \quad (204)$$

On taking mean values in equation (202) we find

$$\overline{\left(\frac{\partial\psi_1}{\partial n} \frac{\partial}{\partial s} - \frac{\partial\psi_1}{\partial s} \frac{\partial}{\partial n}\right) \nabla^2\psi_1} = \nu \frac{\partial^2}{\partial n^2} \nabla^2\bar{\psi}_2 = \nu \frac{\partial^4\bar{\psi}_2}{\partial n^4}, \quad (205)$$

so that, by (204),
$$\overline{\left(\frac{\partial\psi_1}{\partial n} \frac{\partial}{\partial s} - \frac{\partial\psi_1}{\partial s} \frac{\partial}{\partial n}\right) \int \frac{\partial^4\psi_1}{\partial n^4} dt} - \frac{\partial^4\bar{\psi}_2}{\partial n^4} = 0, \quad (206)$$

as in equation (159). The mass-transport velocity is constant throughout the boundary layer; for from (139)

$$\left. \begin{aligned} s &= \frac{\partial\psi'}{\partial n} = q_s^{(0)} - V_s = O(1), & \dot{n} &= -\frac{\partial\psi'}{\partial s} = O(\delta/l), \\ \frac{\partial s}{\partial n} &= \frac{\partial^2\psi'}{\partial n^2} + \kappa \frac{\partial\psi'}{\partial n} + \Omega = O(1), & \frac{\partial \dot{n}}{\partial s} &= -\frac{\partial^2\psi'}{\partial s \partial n} = O(1), \end{aligned} \right\} \quad (207)$$

and so from (140)
$$\frac{\partial^4\bar{\Psi}}{\partial n^4} = \overline{(q_s^{(0)} - V_s)} + \int \overline{(q_s^{(0)} - V_s)} dt. \quad (208)$$

However the velocity gradient $\partial^2\psi'/\partial n^2$ is not constant. We have from (142), after differentiating four times, using Leibniz's theorem, and retaining only the terms of highest order,

$$\frac{\partial^4\bar{\Psi}}{\partial n^4} = \frac{\partial^4\bar{\psi}_2}{\partial n^4} + \int \frac{\partial^4\psi_1}{\partial n^4} dt \frac{\partial\psi_1}{\partial s} + 4 \int \frac{\partial^4\psi_1}{\partial n^4} dt \frac{\partial^2\psi_1}{\partial s \partial n} + \int \frac{\partial^4\psi_1}{\partial n^4} dt \frac{\partial^3\psi_1}{\partial s \partial n^2}, \quad (209)$$

which may be compared with equation (161). Thus, from (206),

$$\frac{\partial^4\bar{\Psi}}{\partial n^4} = 4 \int \frac{\partial^4\psi_1}{\partial n^4} dt \frac{\partial^2\psi_1}{\partial s \partial n} \quad (210)$$

$$= 4 \int \frac{\partial^2}{\partial n^2} \nabla^2\psi_1 dt \frac{\partial}{\partial s} (q_s^{(0)} - V_s). \quad (211)$$

On integrating from $n = \infty$ we have

$$\frac{\partial^4\bar{\Psi}}{\partial n^4} = 4 \int \frac{\partial}{\partial n} \nabla^2\psi_1 dt \frac{\partial}{\partial s} (q_s^{(0)} - V_s), \quad (212)$$

M. S. LONGUET-HIGGINS ON

562

and on integrating from $n = 0$

$$\left(\frac{\partial^2 \Psi}{\partial n^2}\right)_0^n = 4 \int \overline{(\nabla^2 \psi_1) \frac{\partial}{\partial s} (q_{n1}^{(0)} - V_{s1})}. \quad (213)$$

To obtain a boundary condition for Ψ when $n = 0$ we have from (140) and (141), after differentiating with respect to n ,

$$\frac{\partial}{\partial n} \left(\frac{1}{\eta_0} \frac{\partial \Psi}{\partial n} \right) = \frac{\partial \bar{s}_2}{\partial n} + \int \frac{\partial \bar{s}_1}{\partial n} dt \frac{\partial \bar{s}_1}{\partial s} + \int \bar{s}_1 dt \frac{\partial^2 \bar{s}_1}{\partial s \partial n} + \int \frac{\partial \bar{n}_1}{\partial n} dt \frac{\partial \bar{s}_1}{\partial n} + \int \bar{n}_1 dt \frac{\partial^2 \bar{s}_1}{\partial n^2}, \quad (214)$$

or, since \bar{n}_1 vanishes and $\partial \bar{n}_1 / \partial n$ equals $-\partial \bar{s}_1 / \partial s$,

$$\left(\frac{\partial^2 \Psi}{\partial n^2} + \kappa_0 \frac{\partial \Psi}{\partial n} \right)_{n=0} = \frac{\partial \bar{s}_2}{\partial n} + 2 \int \frac{\partial \bar{s}_1}{\partial n} dt \frac{\partial \bar{s}_1}{\partial s} + \int \bar{s}_1 dt \frac{\partial^2 \bar{s}_1}{\partial s \partial n}. \quad (215)$$

But from (207)
$$\frac{\partial \bar{s}}{\partial n} = \frac{\partial^2 \psi}{\partial n^2} + \kappa (q_{n1}^{(0)} - V_s) + \Omega, \quad (216)$$

so that from (197) and (132)

$$\left(\frac{\partial \bar{s}}{\partial n} \right)_{n=0} = \frac{1}{\rho \nu} p_{ns}^{(0)}. \quad (217)$$

Hence

$$\left(\frac{\partial^2 \Psi}{\partial n^2} \right)_{n=0} + \kappa_0 \frac{\partial \Psi}{\partial n} = \frac{1}{\rho \nu} \left[\overline{p_{ns2}^{(0)}} + 2 \int \overline{p_{ns1}^{(0)} dt \frac{\partial}{\partial s} (q_{n1}^{(0)} - V_{s1})} + \int \overline{(q_{n1}^{(0)} - V_{s1}) dt \frac{\partial p_{ns1}^{(0)}}{\partial s}} \right]. \quad (218)$$

Thus altogether

$$\begin{aligned} \frac{\partial^2 \Psi}{\partial n^2} + \kappa_0 \frac{\partial \Psi}{\partial n} &= 4 \int \overline{(\nabla^2 \psi_1) \frac{\partial}{\partial s} (q_{n1}^{(0)} - V_{s1})} \\ &+ \frac{1}{\rho \nu} \left[\overline{p_{ns2}^{(0)}} + 2 \int \overline{p_{ns1}^{(0)} dt \frac{\partial}{\partial s} (q_{n1}^{(0)} - V_{s1})} + \int \overline{(q_{n1}^{(0)} - V_{s1}) dt \frac{\partial p_{ns1}^{(0)}}{\partial s}} \right]. \end{aligned} \quad (219)$$

From (219) we have, on replacing V_{n1} by $q_{n1}^{(0)}$,

$$(\nabla^2 \psi_1)_{n=0} = \frac{1}{\rho \nu} p_{ns1}^{(0)} - 2 \left(\frac{\partial q_{n1}^{(0)}}{\partial s} + \kappa_0 q_{n1}^{(0)} \right), \quad (220)$$

so that (219) can be written

$$\begin{aligned} \frac{\partial^2 \Psi}{\partial n^2} + \kappa_0 \frac{\partial \Psi}{\partial n} &= 4 \int \overline{\nabla^2 \psi_1 dt \frac{\partial}{\partial s} (q_{n1}^{(0)} - V_{s1})} + 8 \int \left(\frac{\partial q_{n1}^{(0)}}{\partial s} + \kappa_0 q_{n1}^{(0)} \right) dt \frac{\partial}{\partial s} (q_{n1}^{(0)} - V_{s1}) \\ &+ \frac{1}{\rho \nu} \left[\overline{p_{ns2}^{(0)}} - 2 \int \overline{p_{ns1}^{(0)} dt \frac{\partial}{\partial s} (q_{n1}^{(0)} - V_{s1})} + \int \overline{(q_{n1}^{(0)} - V_{s1}) dt \frac{\partial p_{ns1}^{(0)}}{\partial s}} \right]. \end{aligned} \quad (221)$$

Also Ψ is to be constant along the boundary.

When the first-order motion is simple harmonic, equation (203) becomes

$$\left(i\sigma - \nu \frac{\partial^2}{\partial n^2} \right) \nabla^2 \psi_1 = 0. \quad (222)$$

The only solution of this equation which is finite for large n and which satisfies the boundary condition (220) is

$$\nabla^2 \psi_1 = \left[\frac{1}{\rho \nu} p_{ns1}^{(0)} - 2 \left(\frac{\partial q_{n1}^{(0)}}{\partial s} + \kappa_0 q_{n1}^{(0)} \right) \right] e^{-an}. \quad (223)$$

MASS TRANSPORT IN WATER WAVES

563

Thus from (219)

$$\frac{\partial^2 \Psi}{\partial n^2} + \kappa_0 \frac{\partial \Psi}{\partial n} = \frac{2}{i\sigma} \left[\frac{1}{\rho\nu} - 2 \left(\frac{\partial q_{n1}^{(0)}}{\partial s} + \kappa_0 q_{s1}^{(0)} \right) \right] \frac{\partial}{\partial s} (q_{s1}^{(0)*} - V_{s1}^*) (e^{-an} - 1) \\ + \frac{1}{\rho\nu} \left[\overline{\rho_{ns2}^{(0)}} + \frac{1}{i\sigma} \rho_{ns1} \frac{\partial}{\partial s} (q_{s1}^{(0)*} - V_{s1}^*) + \frac{1}{2i\sigma} (q_{s1}^{(0)} - V_{s1}) \frac{\partial \rho_{ns1}^{(0)*}}{\partial s} \right], \quad (224)$$

and just beyond the boundary layer we have from (221)

$$\left(\frac{\partial^2 \Psi}{\partial n^2} + \kappa_0 \frac{\partial \Psi}{\partial n} \right)_{n=\infty} = \frac{4}{i\sigma} \left(\frac{\partial q_{n1}^{(0)}}{\partial s} + \kappa_0 q_{s1}^{(0)} \right) \frac{\partial}{\partial s} (q_{s1}^{(0)*} - V_{s1}^*) \\ + \frac{1}{\rho\nu} \left[\overline{\rho_{ns2}^{(0)}} - \frac{1}{i\sigma} \rho_{ns1} \frac{\partial}{\partial s} (q_{s1}^{(0)*} - V_{s1}^*) + \frac{1}{2i\sigma} (q_{s1}^{(0)} - V_{s1}) \frac{\partial \rho_{ns1}^{(0)*}}{\partial s} \right]. \quad (225)$$

At a free surface $\rho_{ns}^{(0)}$ vanishes, making the last group of terms in (224) and (225) zero. If also $\kappa_0 = 0$, then the co-ordinates may be chosen so that V_{s1} vanishes (see § 6). We have then

$$\frac{\partial^2 \Psi}{\partial n^2} = \frac{4}{i\sigma} \frac{\partial q_{n1}^{(0)}}{\partial s} \frac{\partial q_{s1}^{(0)*}}{\partial s} (1 - e^{-an}), \quad (226)$$

and just beyond the boundary layer

$$\left(\frac{\partial^2 \Psi}{\partial n^2} \right)_{n=\infty} = \frac{4}{i\sigma} \frac{\partial q_{n1}^{(0)}}{\partial s} \frac{\partial q_{s1}^*}{\partial s}. \quad (227)$$

Thus, in the present case, it is the normal gradient of the mass transport which is determined throughout the boundary layer.

9. DETERMINATION OF Ψ IN THE INTERIOR

Suppose that it is desired to find a periodic motion satisfying, at the boundaries, one of two types of condition: either the normal and the tangential velocities are prescribed to be equal to $q_n^{(0)}$ and $q_s^{(0)}$ respectively or else the normal and tangential stresses are to be equal to $\rho_{nn}^{(0)}$ and $\rho_{ns}^{(0)}$ respectively. Suppose also that a perfect-fluid solution ψ_a exists, satisfying Laplace's equation in the interior of the fluid, having the normal velocity $q_n^{(0)}$ at the first type of boundary, and having a value of p equal to $-\rho_{nn}^{(0)}$ at the second type of boundary. (ψ_a will not of course satisfy the other two boundary conditions, in general.) Let $\epsilon\psi_{a1}$ be the first approximation to ψ_a in powers of ϵ ; ψ_{a1} is to be considered as being referred to co-ordinates normal and tangential to the boundaries. Since ψ_{a1} satisfies Laplace's equation, it satisfies also the equations of viscous motion in the interior of the fluid. Also, since p , apart from the hydrostatic pressure, is a function of the velocities of the order of $\rho a \sigma^2 l$ (see equation (122)) and since, from equation (94),

$$p_{nn} = -p + O(\rho\nu a \sigma/l) \quad (228)$$

it follows that $\epsilon\psi_{a1}$ gives the prescribed value of the normal stress p_{nn} , with relative errors of the order of $(\delta/l)^2$. Further, from §§ 7 and 8 we see that by adding to ψ_{a1} functions, say ψ_{b1} , which vanish exponentially inwards from the boundaries, the conditions of prescribed tangential stress or velocity may be satisfied (to order ϵ). The functions $\epsilon\psi_{b1}$ produce also

M. S. LONGUET-HIGGINS ON

additional stresses and velocities normal to the boundaries. But, considered as functions of the velocities, these are at most of order δ/l relative to the corresponding functions for $\epsilon\psi_{a1}$. Hence $\epsilon(\psi_{a1} + \psi_{b1})$ satisfies all the prescribed boundary conditions for $\epsilon\psi_1$, with neglect only of δ/l . In the interior of the fluid $\epsilon\psi_1$ tends exponentially to $\epsilon\psi_{a1}$. Hence the velocities $q_{s1}^{(\omega)}$, $q_{s1}^{(0)}$, V_{s1} and V_{n1} may be calculated by the ordinary theory of perfect fluids, and will be correct to order δ/l in the interior. The effect of surface tension, which enters only into the normal stress, may be taken into account by calculating its effect on ψ_{a1} in the usual way.

Thus the theory of perfect fluids can be expected to describe the motion in the interior of the fluid successfully to order ϵ . But to order ϵ^2 this is not so. From §7 we see that when the normal and tangential velocities at the boundary are given, the mass-transport velocity $\partial\Psi/\partial n$ just beyond the boundary layer is well determined, and not arbitrary as in the theory of a perfect fluid. To the present order of approximation the velocity is independent of the viscosity, and, as ν tends to zero, it tends to a value different from that at the boundaries. This phenomenon was noticed by Schlichting (1932) and Rayleigh (1883) in special cases. Similarly, from §8, when the tangential stress is prescribed at the boundary the normal gradient of the mass-transport velocity, or rather $\left(\frac{\partial^2\Psi}{\partial n^2} + \kappa_0 \frac{\partial\Psi}{\partial n}\right)$, is determined just beyond the boundary layer.

To determine Ψ in the interior of the fluid, suppose that the first-order solution ψ_{a1} is found by the classical theory; $q_{s1}^{(0)}$, $q_{n1}^{(0)}$, $q_{s1}^{(\omega)}$, etc., are then known. At the first type of boundary we have

$$\frac{\partial\Psi}{\partial s} = 0, \quad (229)$$

and just beyond the boundary layer (if the velocities are expressed as the real parts of complex quantities)

$$\begin{aligned} \frac{\partial\Psi}{\partial n} = 4 \int \overline{(q_{s1}^{(\omega)} - q_{s1}^{(0)}) dt} \frac{\partial}{\partial s} (q_{s1}^{(\omega)} - V_{s1}) - \frac{3(1+i)}{2} \int \overline{(q_{s1}^{(\omega)} - q_{s1}^{(0)}) dt} \frac{\partial}{\partial s} (q_{s1}^{(\omega)} - q_{s1}^{(0)}) \\ + \overline{(q_{s2}^{(0)} - V_{s2})} + \int \overline{(q_{s1}^{(0)} - V_{s1}) dt} \frac{\partial}{\partial s} (q_{s1}^{(0)} - V_{s1}) \end{aligned} \quad (230)$$

by (183). Since the boundary layer is only of thickness δ , the second condition may be supposed to be satisfied at the boundary itself, or at the mean boundary, for this will not affect the value of Ψ in the interior to the present approximation. Similarly, at the second type of boundary we have

$$\frac{\partial\Psi}{\partial s} = 0, \quad (231)$$

and from (221)

$$\begin{aligned} \frac{\partial^2\Psi}{\partial n^2} + \kappa_0 \frac{\partial\Psi}{\partial n} = 8 \int \overline{\left(\frac{\partial q_{n1}^{(0)}}{\partial s} + \kappa_0 q_{n1}^{(0)}\right) dt} \frac{\partial}{\partial s} (q_{s1}^{(0)} - V_{s1}) \\ + \frac{1}{\rho\nu} \left[\overline{\beta_{11s2}^{(0)}} - 2 \int \overline{\beta_{s1s1}^{(0)} dt} \frac{\partial}{\partial s} (q_{s1}^{(0)} - V_{s1}) + \int \overline{(q_{s1}^{(0)} - V_{s1}) dt} \frac{\partial^2 \beta_{n11}^{(0)}}{\partial s} \right]. \end{aligned} \quad (232)$$

In the interior of the fluid the field equation may be taken to be either (68) or (86), according as $a^2 \ll \delta^2$ or $a^2 \gg \delta^2$. Solutions of these equations may be called conduction solutions and convection solutions respectively, corresponding to the names for the equations suggested in §4.

MASS TRANSPORT IN WATER WAVES

565

Since the conduction equation is of the fourth order we may expect that a conduction solution satisfying all the boundary conditions exists in general. But since the convection equation is only of the second order, a convection solution can be expected to exist only in special cases.

Let us consider more closely the conditions to be satisfied by the convection solution near a free surface, say $z = 0$. Setting $p_{n1}^{(0)} = \kappa_0 = V_{x1} = 0$ in equation (232), we have

$$\frac{\partial^2 \Psi}{\partial n^2} = 8 \int \frac{\partial q_{n1}^{(0)}}{\partial s} dt \frac{\partial q_{s1}^{(0)}}{\partial s}, \quad (233)$$

or, on replacing (s, n) by (x, z) ,

$$\left(\frac{\partial^2 \Psi}{\partial z^2} \right)_{z=0} = -8 \int \frac{\partial^2 \psi_{a1}}{\partial x^2} dt \frac{\partial^2 \psi_{a1}}{\partial x \partial z}. \quad (234)$$

Now since Ψ is constant when $z = 0$ we have from the convection equation (86)

$$\left(\frac{\partial^2 \Psi}{\partial z^2} \right)_{z=0} = \text{constant} - 4 \int \frac{\partial^2 \psi_{a1}}{\partial x^2} dt \frac{\partial^2 \psi_{a1}}{\partial x \partial z}. \quad (235)$$

From (234) and (235) it follows that a necessary condition is

$$\int \frac{\partial^2 \psi_{a1}}{\partial x^2} dt \frac{\partial^2 \psi_{a1}}{\partial x \partial z} = \text{constant}, \quad (236)$$

or

$$\int \frac{\partial^2 \psi_{a1}}{\partial z^2} dt \frac{\partial^2 \psi_{a1}}{\partial x \partial z} = \text{constant}, \quad (237)$$

since ψ_{a1} satisfies Laplace's equation. This is equivalent to

$$\int \frac{\partial^2 \psi_{a1}}{\partial x \partial z^2} dt \frac{\partial^2 \psi_{a1}}{\partial x \partial z} + \frac{\partial^2 \psi_{a1}}{\partial z^2} \int \frac{\partial^2 \psi_{a1}}{\partial z^2} dt = 0 \quad (238)$$

(on differentiating with respect to x and using the property of the periodicity, equation (34)). Now the condition of constant normal pressure at the free surface gives, for the perfect-fluid solution,

$$\frac{\partial^2 \phi_{a1}}{\partial t^2} - g \frac{\partial \phi_{a1}}{\partial z} = 0, \quad (239)$$

where ϕ_{a1} is the velocity potential corresponding to ψ_{a1} (Stokes 1847). On differentiating with respect to x and replacing $\partial \phi_{a1} / \partial x$ by $-\partial \psi_{a1} / \partial z$ we have

$$\frac{\partial^2 \psi_{a1}}{\partial z \partial t^2} - g \frac{\partial \psi_{a1}}{\partial z^2} = 0. \quad (240)$$

Thus the left-hand side of (238) may be written

$$\frac{1}{g} \left[\frac{\partial^2 \psi_{a1}}{\partial x \partial z \partial t} \frac{\partial^2 \psi_{a1}}{\partial x \partial z} + \frac{\partial^2 \psi_{a1}}{\partial z^2} \frac{\partial^2 \psi_{a1}}{\partial z^2 \partial t} \right]. \quad (241)$$

Each term vanishes, by the periodicity; thus the necessary condition is satisfied. The proof can be extended to the case when the surface tension is taken into account. Hence, if both normal and tangential stresses at the surface vanish, it may be possible to satisfy the condition (232); but if the stresses do not vanish a convection solution cannot in general be found.

PART III. WAVES IN WATER OF UNIFORM DEPTH

10. INTRODUCTION

In parts I and II a general method was described for finding the mass-transport velocity in any oscillatory motion of small amplitude, given the first-order motion for a perfect fluid. In this part the method will be applied to the case of waves in water of uniform depth.

As shown in part I, the motion in the interior of the fluid has a different character when the ratio a^2/δ^2 is small, and when it is large, compared with unity (a denotes the amplitude of the first-order oscillation, and $\delta = (2\nu/\sigma)^{1/2}$, where ν is the viscosity and $2\pi/\sigma$ is the period). In the first case the vorticity is diffused throughout the fluid by viscous conduction, and in the second case by convection with the mass-transport velocity. There are two different field equations for the two cases (equations (68) and (84)). The mass transport near the boundaries, however, does not depend critically on the ratio a/δ , but is determined by the first-order motion and the local boundary conditions. The thickness of the boundary layer is of order δ . Just beyond this layer either the mass-transport velocity $\partial\Psi/\partial n$ itself or its normal gradient $\partial^2\Psi/\partial n^2$ takes a certain definite value, depending on whether the boundary is fixed or 'free'; and, by combining the known values of $\partial\Psi/\partial n$ or $\partial^2\Psi/\partial n^2$ just beyond the boundaries with the approximate field equations for the stream function Ψ in the interior of the fluid, a 'conduction solution' or a 'convection solution' may be obtained.

In order to treat the progressive and the standing wave together we shall consider a motion which, in the first approximation, consists of two waves of the same period and wave-length travelling in opposite directions; that is, we suppose that the equation of the free surface is

$$z = a_1 \cos(kx - \sigma t) + a_2 \cos(kx + \sigma t) \quad (242)$$

in the usual notation; or, if the real part only is taken,

$$z = (a_1 e^{-ikx} + a_2 e^{ikx}) e^{i\sigma t}. \quad (243)$$

The corresponding stream function is given by

$$e^{i\psi_{01}} = -\frac{\sigma \sinh k(z-h)}{k \sinh kh} (a_1 e^{-ikx} - a_2 e^{ikx}) e^{i\sigma t} \quad (244)$$

(Stokes 1847). The condition of constant pressure at the free surface gives

$$\sigma^2 = gk \tanh kh. \quad (245)$$

To obtain a single progressive wave of amplitude a travelling in the direction of x increasing we shall write

$$a_1 = a, \quad a_2 = 0. \quad (246)$$

To obtain a standing wave of amplitude $2a$ we shall write

$$a_1 = a_2 = a. \quad (247)$$

We shall first evaluate the motion in the boundary layers, and then proceed to consider the motion in the interior of the fluid. Finally, the results will be compared with some observations of mass-transport velocities.

MASS TRANSPORT IN WATER WAVES

11. THE BOUNDARY LAYER AT THE BOTTOM

In equation (188) we write

$$s = -x, \quad n = h - z, \quad (248)$$

and

$$\epsilon q_{11}^{(m)} = \frac{\sigma}{\sinh kh} (a_1 e^{-kx} - a_2 e^{kx}) e^{i\sigma t}. \quad (249)$$

This gives

$$\epsilon^2 \frac{\partial \Psi}{\partial z} = \frac{\sigma k}{4 \sinh^2 kh} (a_1^2 - a_2^2 - 2a_1 a_2 \sin 2kx) [8(1 - e^{-\alpha(h-z)}) - 3(1+i)(1 - e^{-(\alpha+\alpha^*)(h-z)})]. \quad (250)$$

Now

$$\alpha(h-z) = (1+i) \frac{h-z}{\delta}. \quad (251)$$

Thus, retaining only the real part, we have

$$\epsilon^2 \frac{\partial \Psi}{\partial z} = \frac{\sigma k}{4 \sinh^2 kh} \left[(a_1^2 - a_2^2) f^{(p)} \left(\frac{h-z}{\delta} \right) + 2a_1 a_2 \sin 2kx f^{(s)} \left(\frac{h-z}{\delta} \right) \right], \quad (252)$$

where

$$\left. \begin{aligned} f^{(p)}(\mu) &= 5 - 8 e^{-\mu} \cos \mu + 3 e^{-2\mu}, \\ f^{(s)}(\mu) &= -3 + 8 e^{-\mu} \sin \mu + 3 e^{-2\mu}. \end{aligned} \right\} \quad (253)$$

(a) *The progressive wave*

Assuming (246) we have

$$\epsilon^2 \frac{\partial \Psi}{\partial z} = \frac{a^2 \sigma k}{4 \sinh^2 kh} f^{(p)} \left(\frac{h-z}{\delta} \right). \quad (254)$$

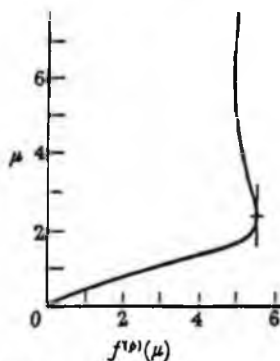


FIGURE 4. Graph of $f^{(p)}(\mu)$, representing the profile of the mass-transport velocity in the boundary layer at the bottom, in a progressive wave.

$f^{(p)}(\mu)$, which represents the typical velocity profile near the bottom for the progressive wave, is plotted against μ in figure 4. It will be seen that $f^{(p)}(\mu)$ is always positive and, when μ tends to infinity, tends to the value 5. Thus, just beyond the boundary layer,

$$\epsilon^2 \frac{\partial \Psi}{\partial z} = \frac{5a^2 \sigma k}{4 \sinh^2 kh}. \quad (255)$$

Also
$$\frac{df^{(s)}}{d\mu} = 8\sqrt{2} e^{-\mu} \sin\left(\mu + \frac{1}{2}\pi\right) - 6 e^{-2\mu}, \quad (256)$$

so that stationary values of the velocity occur when

$$\sin\left(\mu + \frac{1}{2}\pi\right) = \frac{3}{4\sqrt{2}} e^{-\mu}. \quad (257)$$

The lowest root is given by

$$\mu = 2.306, \quad f^{(s)} = 5.505, \quad (258)$$

so that the maximum value of the velocity is given by

$$e^2 \left(\frac{\partial \Psi}{\partial z}\right)_{\text{max.}} = 1.376 \frac{a^2 \sigma k}{\sinh^2 kh}. \quad (259)$$

Subsequent maxima or minima occur when

$$\mu + (m - \frac{1}{2})\pi \quad (m = 2, 3, \dots). \quad (260)$$

(b) *The standing wave*

Assuming (247) we have

$$e^2 \frac{\partial \Psi}{\partial z} = \frac{1}{2} \frac{a^2 \sigma k}{\sinh^2 kh} \sin 2kx f^{(s)} \left(\frac{h-z}{\delta}\right). \quad (261)$$

$f^{(s)}(\mu)$ is plotted against μ in figure 5. As μ tends to infinity $f^{(s)}$ tends to -3 . Thus just beyond the boundary layer we have

$$e^2 \frac{\partial \Psi}{\partial z} = -\frac{3}{2} \frac{a^2 \sigma k}{\sinh^2 kh} \sin 2kx. \quad (262)$$

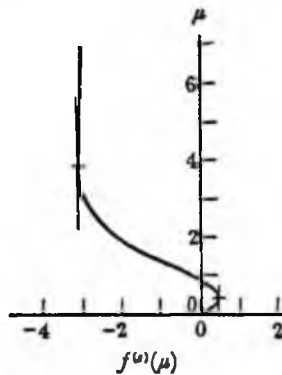


FIGURE 5. Graph of $f^{(s)}(\mu)$, representing the profile of the mass-transport velocity in the boundary layer at the bottom, in a standing wave.

However, for small values of μ , $f^{(s)}$ takes positive values. There is one zero, namely, when $\mu = 0.93$. Since

$$\frac{df^{(s)}}{d\mu} = 8\sqrt{2} e^{-\mu} \sin\left(\mu + \frac{1}{2}\pi\right) - 6 e^{-2\mu}, \quad (263)$$

maxima and minima occur when

$$\sin\left(\mu + \frac{1}{2}\pi\right) = \frac{3}{4\sqrt{2}} e^{-\mu}. \quad (264)$$

MASS TRANSPORT IN WATER WAVES

569

The first two stationary values occur when

$$\mu = 0.49, \quad f^{(1)} = -0.41 \quad (265)$$

and

$$\mu = 3.94, \quad f^{(2)} = 3.11. \quad (266)$$

Subsequent maxima or minima occur when

$$\mu \doteq (m - \frac{1}{2})\pi \quad (m = 3, 4, \dots). \quad (267)$$

We see from (261) that the horizontal mass-transport velocity varies as $\sin 2kx$; in the planes $x = 0, \pm \frac{1}{2}\lambda, \pm \frac{3}{2}\lambda, \dots$, it is zero, and in the planes $x = \pm \frac{1}{4}\lambda, \pm \frac{3}{4}\lambda, \dots$, it is a maximum. The particles very close to the bottom tend to move towards the planes of greatest horizontal first-order motion and away from the planes where the motion is purely vertical, but for larger values of $(h-z)/\delta$ the particles drift in the reverse sense. Hence there is a circulation in the boundary layer itself, in cells whose length is $\frac{1}{2}\lambda$. The vertical velocity is given by

$$e^2 \frac{\partial \Psi'}{\partial z} = \frac{a^2 \delta k^2 \sigma}{\sinh^2 kh} \cos 2kx \int_0^{(h-z)/\delta} f^{(1)}(\mu) d\mu. \quad (268)$$

This vanishes when $(h-z)/\delta = 0$ and 1.47.

12. THE BOUNDARY LAYER AT THE FREE SURFACE

Since the boundary is moving we retain at first the co-ordinates (s, n) . In equation (226) we write

$$e g_{n1}^{(0)} = i\sigma(a_1 e^{-iks} + a_2 e^{iks}) e^{i\sigma t} \quad (269)$$

and

$$e g_{n2}^{(0)} = -\sigma \coth kh (a_1 e^{-iks} - a_2 e^{iks}) e^{i\sigma t}, \quad (270)$$

giving

$$e^2 \frac{\partial^2 \Psi'}{\partial n^2} = -4\sigma k^2 \coth kh (a_1^2 - a_2^2 - 2ia_1 a_2 \sin 2ks) (1 - e^{-an}). \quad (271)$$

Thus, retaining only the real part of (271) we have

$$e^2 \frac{\partial^2 \Psi'}{\partial n^2} = 4\sigma k^2 \coth kh \left[(a_1^2 - a_2^2) g^{(1)}\left(\frac{n}{\delta}\right) + 2a_1 a_2 \sin 2ks g^{(2)}\left(\frac{n}{\delta}\right) \right], \quad (272)$$

where

$$g^{(1)}(\mu) = -1 + e^{-\mu} \cos \mu, \quad (273)$$

$$g^{(2)}(\mu) = -e^{-\mu} \sin \mu. \quad (274)$$

(a) *The progressive wave*

In this case

$$e^2 \frac{\partial^2 \Psi'}{\partial n^2} = 4a^2 \sigma k \coth kh g^{(1)}\left(\frac{n}{\delta}\right). \quad (275)$$

As μ tends to infinity $g^{(1)}$ tends to -1 . Thus, just beyond the boundary layer the velocity gradient is given by

$$e^2 \frac{\partial^2 \Psi'}{\partial n^2} = -4a^2 \sigma k \coth kh, \quad (276)$$

which is twice the corresponding value for the irrotational wave (see Stokes 1847). Hence there is a vorticity given by

$$e^2 \nabla^2 \overline{\Psi'} = -2a^2 \sigma k^2 \coth kh. \quad (277)$$

From (273) we see that $g^{(1)}$ is always negative except at the free surface, where it vanishes. The stationary values of $g^{(1)}$ are given by

$$\mu = (m - \frac{1}{2})\pi \quad (m = 1, 2, \dots). \quad (278)$$

M. S. LONGUET-HIGGINS ON

570

The greatest value of the velocity gradient is given by

$$m = 1, \quad \mu = \frac{3}{4}\pi, \quad g^{(b)} = -1.67. \quad (279)$$

(b) *The standing wave*

In this case we have from (274)

$$\epsilon^2 \frac{\partial^2 \Psi}{\partial n^2} = 8a^2 \sigma k \coth kh \sin 2ks g^{(s)} \left(\frac{n}{\delta} \right). \quad (280)$$

As μ tends to infinity $g^{(s)}$ tends to zero. Thus, just beyond the boundary layer

$$\epsilon^2 \frac{\partial^2 \Psi}{\partial n^2} = 0, \quad (281)$$

as in the irrotational wave. In the boundary layer itself the velocity gradient may take both positive and negative values. The stationary values of $g^{(s)}$ are given by

$$\mu = (m - \frac{3}{4})\pi \quad (m = 1, 2, \dots). \quad (282)$$

The greatest and least values of the velocity gradient occur when

$$\mu = \frac{1}{4}\pi, \quad g^{(s)} = -0.67, \quad (283)$$

and

$$\mu = \frac{3}{4}\pi, \quad g^{(s)} = 0.14, \quad (284)$$

respectively. The velocity gradient vanishes when

$$\mu = m\pi \quad (m = 0, 1, 2, \dots). \quad (285)$$

13. MOTION IN THE INTERIOR: THE CONDUCTION SOLUTION

As boundary conditions for the motion in the interior we find the values of $\partial\Psi/\partial n$ (or $\partial^2\Psi/\partial n^2$) just beyond the boundary layers ($n \gg \delta$), and suppose that these are to be taken at the mean boundary itself. Thus from (252) and (273) we have, so far as the motion in the interior is concerned,

$$\epsilon^2 \left(\frac{\partial \Psi}{\partial z} \right)_{z=h} = \frac{\sigma k}{4 \sinh^2 kh} [5(a_1^2 - a_2^2) - 6a_1 a_2 \sin 2kx] \quad (286)$$

and

$$\epsilon^2 \left(\frac{\partial^2 \Psi}{\partial z^2} \right)_{z=0} = -\frac{2\sigma k^2 \sinh 2kh}{\sinh^2 kh} (a_1^2 - a_2^2). \quad (287)$$

On each of the mean boundaries Ψ is to be constant. The arbitrary constant in Ψ may be chosen so as to make Ψ vanish at the upper boundary. Thus

$$(\Psi)_{z=0} = 0 \quad (288)$$

and

$$(\Psi)_{z=h} = \text{constant}. \quad (289)$$

Also from equation (244) we have

$$\epsilon^2 \int \frac{\partial \psi_{a1}}{\partial z} dz + \frac{\partial \psi_{a1}}{\partial x} = \frac{\sigma \sinh 2k(z-h)}{4 \sinh^2 kh} (a_1^2 - a_2^2), \quad (290)$$

so that the conduction equation for Ψ in the interior of the fluid is, by equation (68),

$$\nabla^4 \Psi = \nabla^2 \frac{\sigma \sinh 2k(z-h)}{4 \sinh^2 kh} (a_1^2 - a_2^2), \quad (291)$$

MASS TRANSPORT IN WATER WAVES

571

However, the equations (286) to (289) and (291) are not quite sufficient to determine Ψ uniquely; one further condition is required. We may suppose that

$$(\Psi)_{z=h} = 0, \quad (292)$$

i.e. that the total horizontal flow due to the mass transport is zero. Assume a solution of the form

$$\epsilon^2 \Psi = \frac{\sigma}{4 \sinh^2 kh} [(a_1^2 - a_2^2) \{ \sinh 2k(z-h) + Z^{(0)}(z) \} + 2a_1 a_2 \sin 2kx Z^{(1)}(z)]. \quad (293)$$

Then $Z^{(0)}$ and $Z^{(1)}$ must satisfy

$$\left. \begin{aligned} \frac{d^4 Z^{(0)}}{dz^4} &= 0, \\ \left(\frac{dZ^{(0)}}{dz} \right)_{z=h} &= 3k, & (Z^{(0)})_{z=h} &= 0, \\ \left(\frac{d^2 Z^{(0)}}{dz^2} \right)_{z=0} &= -4k^2 \sinh 2kh, & (Z^{(0)})_{z=0} &= \sinh 2kh \end{aligned} \right\} \quad (294)$$

and

$$\left. \begin{aligned} \left(\frac{d^2}{dz^2} - 4k^2 \right)^2 Z^{(1)} &= 0, \\ \left(\frac{dZ^{(1)}}{dz} \right)_{z=h} &= -3k, & (Z^{(1)})_{z=h} &= 0, \\ \left(\frac{d^2 Z^{(1)}}{dz^2} \right)_{z=0} &= 0, & (Z^{(1)})_{z=0} &= 0. \end{aligned} \right\} \quad (295)$$

The solutions of these equations are given by

$$Z^{(0)} = \sinh 2kh + 3kz + k^2 h^2 \sinh 2kh (z^2/h^2 - 2z^2/h^2 + z/h) + \frac{1}{2} (\sinh 2kh + 3kh) (z^2/h^3 - 3z/h) \quad (296)$$

and

$$Z^{(1)} = \frac{2kh \cosh 2kh \sinh 2kz - 2kz \cosh 2kz \sinh 2kh}{\sinh 4kh - 4kh}. \quad (297)$$

This gives the solution (293) uniquely. But if the condition (294) is relaxed an arbitrary multiple of

$$a^2 \sigma (z^3/h^3 - 3z/h) \quad (298)$$

may be added to Ψ . The expression (298) represents a parabolic velocity distribution which vanishes on the bottom and has zero velocity gradient at the free surface.

(a) *The progressive wave*

When $a_1 = a$, $a_2 = 0$, we have from (293) and (296)

$$\epsilon^2 \frac{\partial \Psi}{\partial z} = a^2 \sigma k F^{(0)}(z/h), \quad (299)$$

where $F^{(0)}(\mu) = \frac{1}{4 \sinh^2 kh} \left[2 \cosh 2kh(\mu-1) + 3 + kh \sinh 2kh(3\mu^2 - 4\mu + 1) + 3 \left(\frac{\sinh 2kh}{2kh} + \frac{3}{2} \right) (\mu^2 - 1) \right]. \quad (300)$

In figure 6, $F^{(v)}$ is plotted against μ for $kh = 0.5, 1.0$ and 1.5 . It will be seen that the curve is always concave towards the right. For small values of kh the velocity is greatest near the bottom. When kh is negligible we have

$$F^{(v)}(\mu) = \frac{5}{8k^2h^2}(3\mu^2 - 1), \quad (301)$$

and so

$$\epsilon^2 \frac{\partial^2 \Psi}{\partial z^2} = \frac{5b^2 \sigma k}{8}(3z^2/h^2 - 1), \quad (302)$$

where b is the amplitude of the horizontal motion:

$$b = a \coth kh = a/kh. \quad (303)$$

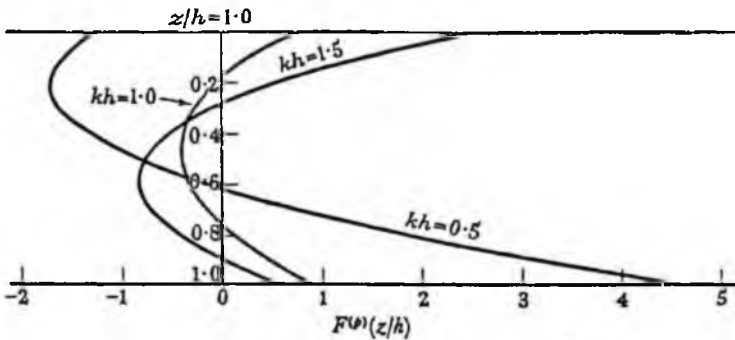


FIGURE 6. Graphs of $F^{(v)}(z/h)$ when $kh = 0.5, 1.0$ and 1.5 , representing the profile of the mass-transport velocity in the interior of the fluid in a progressive wave (conduction solution).

Equation (302) gives a parabolic velocity distribution, which is zero when $z/h = \sqrt{3}$ and has a vertical tangent at the mean free surface. However, for small values of kh the present approximation may not be good unless the wave amplitude a is very small; for the method can only be expected to remain valid if the mass-transport velocity is small compared with the orbital velocity of the particles; it will be seen that this requires $a/h \ll 1$.

For large values of kh the velocity is greatest near the free surface. When $(kh)^{-1}$ and e^{-kh} are negligible we have

$$F^{(v)}(\mu) = \frac{1}{2}kh(3\mu^2 - 4\mu + 1), \quad (304)$$

and hence

$$\epsilon^2 \frac{\partial^2 \Psi}{\partial z^2} = \frac{1}{2}a^2 \sigma k^2 h (3z^2/h^2 - 4z/h + 1). \quad (305)$$

This represents a parabolic velocity distribution which is zero when $z/h = 1$ and $z/h = \frac{1}{3}$, and has a vertical tangent when $z/h = \frac{2}{3}$.

(b) *The standing wave*

When $a_1 = a_2 = a$ we have from (293)

$$\epsilon^2 \Psi = \frac{a^2 \sigma}{2 \sinh^2 kh} \sin 2kx Z^{(v)}(z), \quad (306)$$

$Z^{(v)}$ being given by (297). Contours of the function $\sin 2kx Z^{(v)}(z)$ when $kh = 1.0$ are shown in figure 7. The circulation is in cells bounded by the vertical planes $x = \frac{1}{2}m\lambda$ (where m is any

MASS TRANSPORT IN WATER WAVES

573

integer) and by the horizontal planes $z = 0$ and $z = h$. It may be shown that $Z^{(6)}(z)$ has only one stationary value, given by

$$2kz \tanh 2kz = 2kh \coth 2kh - 1. \quad (307)$$

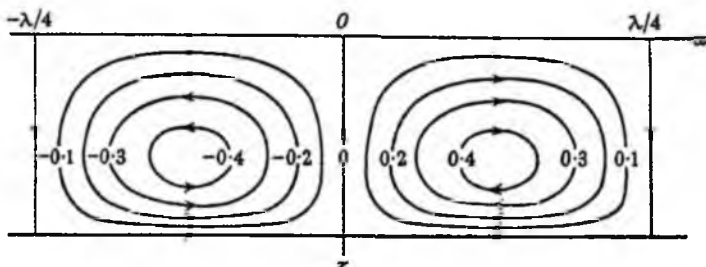


FIGURE 7. Contours of $\sin 2kx Z^{(6)}(z)$ when $kh=1.0$, representing the circulation of mass transport in a standing wave (conduction solution).

Hence there is only one cell in each vertical line. When kh is small we have

$$e^{2z}\Psi = -\frac{3}{2}b^2\sigma kh \sin 2kx (z^3/h^3 - z/h), \quad (308)$$

where b is given by (303), so that there is a point of zero velocity where

$$x = (\frac{1}{2}m + \frac{1}{4})\lambda, \quad z/h = \sqrt{3}. \quad (309)$$

When kh is large we find

$$e^{2z}\Psi = \frac{3}{2}a^2\sigma \sin 2kx e^{-2kz} 2k(h-z) e^{-2k(h-z)}. \quad (310)$$

This is the special case found by Rayleigh (1883).^{*} The velocities are very small, owing to the factor e^{-2kz} . The circulation is driven by the tangential velocity near the bottom, and takes place almost entirely within a quarter of a wave-length from the bottom. There is a point of zero velocity where

$$x = (\frac{1}{2}m + \frac{1}{4})\lambda, \quad 2k(h-z) = 1, \quad h-z = \lambda/4\pi. \quad (311)$$

14. MOTION IN THE INTERIOR: THE CONVECTION SOLUTION

The boundary conditions for Ψ are given, as before, by equations (286) to (289), but the field equation, from equation (84), is now

$$\nabla^2 \left[\Psi - \frac{\sigma \sinh 2k(z-h)}{4 \sinh^2 kh} (a_1^2 - a_2^2) \right] = F(\Psi). \quad (312)$$

(a) *The progressive wave*

In this case a solution is simply

$$e^{2z}\Psi = \frac{a^2\sigma}{4 \sinh^2 kh} H(z), \quad (313)$$

^{*} Rayleigh did not examine the motion near the free surface, or show that the mass-transport velocity gradient vanishes there. His solution is therefore incomplete, even for waves in deep water; for, a non-zero velocity gradient near the free surface would produce additional velocities near the bottom of order $a^2\sigma k e^{-2kz}$, which are comparable with those produced by the tangential velocity near the bottom.

where $H(z)$ is an arbitrary function satisfying only the conditions

$$\left. \begin{aligned} \left(\frac{\partial H}{\partial z}\right)_{z=h} &= 5k, \\ \left(\frac{\partial^2 H}{\partial z^2}\right)_{z=0} &= -2k^2 \sinh 2kh, \\ (H)_{z=0} &= 0, \end{aligned} \right\} \quad (314)$$

and, if the total horizontal flow is assumed to be zero,

$$(H)_{z=h} = 0; \quad (315)$$

for, equation (313) defines z as a function of Ψ , and then F can be defined by equation (312). The motion represented is a horizontal flow depending only on z . It can only be defined further if the conditions at $x = \pm\infty$ are specified.

(b) *The general case*

When neither a_1 nor a_2 vanishes, we assume, as the simplest hypothesis, that F is a linear function of Ψ :

$$F(\Psi) = \frac{C\sigma k^2}{4 \sinh^2 kh} (a_1^2 - a_2^2) - r^2 \Psi \quad (316)$$

where C and r are constants to be determined. The differential equation for Ψ is then

$$(\nabla^2 + r^2) \Psi = \frac{\sigma(a_1^2 - a_2^2)}{4 \sinh^2 kh} [Ck^2 + 4k^2 \sinh 2k(z-h)]. \quad (317)$$

Let

$$\epsilon^2 \Psi = \frac{\sigma}{4 \sinh^2 kh} \left[(a_1^2 - a_2^2) \left\{ \frac{Ck^2}{r^2} + \frac{4k^2}{4k^2 + r^2} \sinh 2k(z-h) + Z^{(p)}(z) \right\} + 2a_1 a_2 \sin 2kz Z^{(q)}(z) \right]. \quad (318)$$

Then $Z^{(p)}$ and $Z^{(q)}$ must satisfy

$$\left. \begin{aligned} \left(\frac{d^2}{dz^2} + r^2\right) Z^{(p)} &= 0, \\ \left(\frac{dZ^{(p)}}{dz}\right)_{z=h} &= \frac{(12k^2 + 5r^2)k}{4k^2 + r^2}, \\ \left(\frac{d^2 Z^{(p)}}{dz^2}\right)_{z=0} &= -\frac{(2k^2 + r^2)8k^2}{4k^2 + r^2} \sinh 2kh, \\ (Z^{(p)})_{z=0} &= -\frac{Ck^2}{r^2} + \frac{4k^2}{4k^2 + r^2} \sinh 2kh, \end{aligned} \right\} \quad (319)$$

and

$$\left. \begin{aligned} \left(\frac{d^2}{dz^2} + r^2 - 4k^2\right) Z^{(q)} &= 0, \\ \left(\frac{dZ^{(q)}}{dz}\right)_{z=h} &= -3k, & (Z^{(q)})_{z=h} &= 0, \\ \left(\frac{d^2 Z^{(q)}}{dz^2}\right)_{z=0} &= 0, & (Z^{(q)})_{z=0} &= 0. \end{aligned} \right\} \quad (320)$$

MASS TRANSPORT IN WATER WAVES

575

From the first and the last two of equations (319) it follows that

$$C = -4 \sinh 2kh. \quad (321)$$

The first three equations give

$$Z^{(y')} = \frac{(12k^2 + 5r^2)k \sin rz}{(4k^2 + r^2)r \cos rh} + \frac{(2k^2 + r^2)8k^2 \sinh 2kh \cos r(z-h)}{(4k^2 + r^2)r^2 \cos rh}. \quad (322)$$

Equations (320) possess a solution

$$Z^{(y')} = -3k \frac{\sin(r^2 - 4k^2)^{1/2} z}{(r^2 - 4k^2)^{1/2} \cos(r^2 - 4k^2)^{1/2} h}, \quad (323)$$

provided that

$$r^2 = 4k^2 + m^2\pi^2/h^2, \quad (324)$$

where m is a positive integer. In this case (323) may also be written

$$Z^{(y')} = (-1)^{m+1} \frac{3kh}{m\pi} \sin(m\pi z/h). \quad (325)$$

Once m is chosen, both $Z^{(y')}$ and $Z^{(y)}$ are completely defined. There is an infinite number of solutions, each corresponding to a different integer m , but solutions corresponding to different values of m are not of course superposable. Now when $z = h$ we have

$$\epsilon^{2\psi} = \frac{\sigma(a_1^2 - a_2^2)}{4 \sinh^2 kh} \left[-\frac{4k^2}{r^2} \sinh 2kh + \frac{(12k^2 + 5r^2)k}{(4k^2 + r^2)r} \tan rh + \frac{(2k^2 + r^2)8k^2}{(4k^2 + r^2)r} \sinh 2kh \sec rh \right]. \quad (326)$$

It may be shown that the expression in square brackets cannot vanish when $kh > 0$. Hence the present solution does not represent a motion having zero total horizontal flow, except when $a_1^2 = a_2^2$ (the case of the standing wave).

(c) *The standing wave*

When $a_1 = a_2 = a$ we have from (318) and (315)

$$\epsilon^{2\psi} = (-1)^{m+1} \frac{3}{2mn} \frac{\sigma k h a^2}{\sinh^2 kh} \sin 2kx \sin(m\pi z/h). \quad (327)$$

This represents a circulation in cells similar to those in the conduction solution (§ 13), except that in each vertical line there are now m cells instead of only one as formerly. The vertical boundaries of the cells are the planes $x = \frac{1}{2}m'\lambda$ (where m' is any integer), and the horizontal boundaries are the planes $z = m''h/m$ ($0 \leq m'' \leq m$). The circulations in adjacent cells are in opposite senses; those in the lowest cells are in the same sense as the circulations in the corresponding cells in the conduction solution.

The results of the present section may be summarized by saying that for the progressive wave the convection solution is arbitrary, for the standing wave there is an infinity of possible solutions, and in the general case of two opposite waves of unequal amplitude there exists an infinity of homogeneous solutions of the present type; these, however, represent motions with non-zero total horizontal flow.

15. DISCUSSION

The conduction and convection solutions for the first-order motion which is represented by (244) are exact, to the present degree of approximation. However, owing to the dissipation of energy by viscosity, equation (244) itself is only approximate; for the motion cannot be exactly periodic in both space and time. The assumption usually made (see Basset 1888; Hough 1896) is that the motion is periodic in space and has a small decrement in time. But since one of our fundamental assumptions is that the motion is periodic in time, we must here suppose that the motion is attenuated in a horizontal direction. For a progressive wave in which the energy is propagated in the direction of x increasing, there will be an exponential decrease with x ; instead of a 'standing wave' we may consider the sum of two progressive waves attenuated in opposite directions.

Now the energy dissipation E per unit volume is proportional to $\rho\nu$ times (velocity gradient)². Thus in the interior of the fluid, and in the boundary layer at the free surface, E is only of order $\rho\nu a^2\sigma^2k^2$, or $\rho g a^2\sigma k(\delta/l)^2$, where l is the wave-length. But in the boundary layer at the bottom the velocity gradients are of order $a\sigma/\delta$, and hence the energy dissipation is of order $\rho g a^2\sigma k$ per unit volume, or $\rho g a^2\sigma(\delta/l)$ per unit area of the bottom. Thus most of the energy dissipation takes place in the boundary layer at the bottom, provided the depth is not too great. But the transfer of energy horizontally can be shown to be almost independent of the viscosity, so that the proportional rate of attenuation horizontally is of order δ/l per unit wave-length at most. This is of the same order as quantities already neglected.

The conduction solution for the progressive wave given in § 13, which is independent of the horizontal co-ordinate x , satisfies also the convection equations; for the stream-lines are parallel, and the vorticity along each is constant. It might therefore be supposed that the solution is valid for all values of a^2/δ^2 . However, if the horizontal attenuation of the waves is taken into account there must be a small vertical component of velocity, and the conduction terms no longer vanish identically. It then becomes difficult to find a convection solution. The conduction solution, on the other hand, can easily be modified to take account of the attenuation. Since the vertical velocities are small it is possible that, for the progressive wave, the range of validity of the conduction solution (for which it was specified that $a^2/\delta^2 \ll 1$) is slightly greater than that assumed. However, in the case of the standing wave, where the convection terms do not vanish identically, the condition $a^2/\delta^2 \ll 1$ cannot be relaxed.

Let us now consider the possible sequence of events, supposing that the motion is started from a state of rest. For definiteness suppose that waves are generated in a rectangular tank of length L , width D , and depth h (where L is large compared with a wave-length) by an oscillating plunger or paddle at one end of the tank. If a progressive wave is considered, the waves may be supposed to be dissipated by a 'beach' or wave absorber at the far end of the tank, or they may be partially or wholly reflected by a suitable obstacle placed in the tank; if they are wholly reflected a standing wave is formed.

Observation has shown (see Cooper & Longuet-Higgins 1950) that the wave energy travels down the tank with approximately the theoretical group velocity $g/2\sigma$, and that soon after the passage of the 'wave front' the first-order motion is well established. The mass-

MASS TRANSPORT IN WATER WAVES

577

transport distribution in the boundary layers can be expected to be set up almost immediately, for it depends, as was shown in part II, only on the first-order motion and on the local boundary conditions. There may be some departures from the theoretical velocity distribution owing to the presence of large velocity gradients just beyond the boundary layer, for these might not at first be small compared with the velocity gradients in the boundary layer itself, as was assumed. But after a few cycles the velocity gradients just beyond the boundary layer can be expected to be smoothed out by the viscosity.

In the interior of the fluid the motion will at first be irrotational, since no vorticity can be generated there. The mass-transport distribution should therefore be as described by Stokes (1847). Subsequently the nature of the motion will depend upon the ratio a^2/δ^2 . If $a^2/\delta^2 \ll 1$, that is, for very small waves indeed, the motion would be as described by the conduction solutions of § 13 (except possibly near the vertical sides of the tank, where the motion has not yet been considered). In order that the solution should be valid it must be supposed that the width D of the tank is great compared with the depth h of water. By analogy with the diffusion of heat, the time taken for the vorticity to diffuse into the interior and for a steady state to be reached will be of the order of h^2/ν .

In nearly all practical cases, however, we shall have $a^2/\delta^2 \gg 1$, so that, if a steady state exists, it is given by the convection solution of § 14. For the progressive wave, this solution is arbitrary, or rather it depends on the boundary conditions imposed at $x = \pm\infty$. In practice, therefore, we may expect that the motion will depend upon the special conditions at the wave maker and the wave absorber respectively; vorticity will be generated at these points and will be diffused horizontally along the stream-lines. The time taken for the whole interior of the tank to be affected in this way is of the order of $L/(a^2\sigma k)$. In the meantime, some vorticity will be diffused inwards from the bottom, from the free surface and from the vertical sides by viscous conduction. The width affected in this manner is of the order of $(L\nu/a^2\sigma k)^{1/2}$ (this quantity is assumed to be small compared with h or D). However, it is by no means certain that a steady state will exist which is compatible with the boundary conditions at both the wave maker and at the wave absorber, or that, if it exists, it is stable. The situation is even less predictable when one considers a partially reflected wave, for which no convection solution satisfying the condition of zero total transport has been found, or the standing wave, for which there is an infinity of such solutions.

16. COMPARISON WITH OBSERVATION

It appears from the preceding discussion that the theory can best be compared with observation, first, in the boundary layers, where the motion is well-determined irrespective of the ratio a^2/δ^2 , and, secondly, in the interior of the fluid before vorticity has had time to be diffused inwards; the motion should then be described by Stokes's irrotational theory. Not many quantitative determinations of mass-transport velocity have been made under controlled conditions, but the chief observations will now be discussed.

Caligny (1878)

The earliest quantitative observations seem to be due to Bertin & Caligny (Caligny 1878). These authors used a tank of length 29.7 m, depth 47 cm and width 50 cm; the depth

of water was 36 cm. Waves were generated at one end by a steam-driven plunger, travelled down to the far end and were dissipated on a sloping plane 'beach'. The movement of particles of resin suspended in the fluid was observed through glass windows in a side wall of the tank. Caligny gives the following values of the mean horizontal velocity for waves of period 1 s, wave-length 130 cm and height 6 cm:

distance above bottom (cm)	0	5	9	15	23	27	36
mean velocity (cm/s)	0.4	0.0	-0.3	-0.5	0.0	0.3	0.5

This shows a forward velocity both near the bottom and near the free surface, with a negative velocity between. Assuming $\sigma = 2\pi \text{ s}^{-1}$, $k = 2\pi/130 \text{ cm}^{-1}$, $h = 36 \text{ cm}$ and $a = 3 \text{ cm}$ we find that the theoretical velocity just in the interior of the fluid, according to equation (255), is 0.45 cm/s, in good agreement with the observation at the lowest level. The velocity gradient near the free surface was not recorded; the theoretical value given by equation (276) is -0.56 s^{-1} , compared with a mean value of -0.02 s^{-1} between the two observations nearest the upper surface. Caligny, however, mentions that the observations at the uppermost levels were rather scattered. This might either be because the motion was not steady, or because the velocity gradient was so large that the velocity depended critically on the depth of the particle of resin below the free surface.

In some previous but less precise experiments (1861) Caligny had observed a backward movement of grains of sand and resin on the bottom. But this movement diminished rapidly with distance from the wave maker and seems to have been due to the fact that locally the waves were not progressive.

Mitchim (1939)

A systematic experimental study of deep-water waves was made by Mitchim (1939) using a tank 60 ft. long, 1 ft. wide and 3 ft. deep. The depth of water was 2.5 ft., and the wave-lengths investigated were from 2 to 5 ft., or less than twice the depth of water; thus the waves were, effectively, in deep water. The motion was generated at one end of the tank by a wooden flap hinged on the bottom, and was dissipated at the far end on a sloping plane beach. The mass-transport velocities below the free surface were measured by photographing the tracks of white liquid particles suspended in the fluid; the velocities at the surface were measured by observing the progress of a small wooden cylinder $\frac{1}{4}$ in. in diameter.

The surface velocities agreed fairly well with the irrotational theory, being mostly within 20%. The velocities in the interior were in qualitative agreement with the irrotational theory, being forward near the surface and backward at the lower levels; but the scatter of the observations, even on the same run, was such that it seems unlikely that a steady state had been reached. No observations very near the bottom are reported.

The United States Beach Erosion Board (1941)

Some mass-transport observations are included in an experimental study of surface waves by the United States Beach Erosion Board (1941). The wave-lengths λ used were between 3.5 and 12.2 ft., and the depth of water was between 1 and 3 ft. There were no observations near the bottom, nor is it stated for how long the waves had been running at the time of the observation. In deep water ($h > \frac{1}{2}\lambda$) there was reasonable agreement with

MASS TRANSPORT IN WATER WAVES

579

Stokes's theory in the upper half of the fluid (though no observations within 2 in. of the surface are given); in shallow water ($h < \frac{1}{2}\lambda$) the agreement with Stokes's theory was poor and the observations show considerable scatter; it seems unlikely that a steady state had been reached.

Bagnold (1947)

In the course of a study of the movement of sand by water waves, Bagnold (1947) also made observations of the motion of the water particles themselves. His apparatus consisted of a glass-sided channel 11 m long, 30 cm wide and 30 cm deep, opening at one end into a slightly deeper channel 3 m long. A paddle hinged at the bottom of the deeper channel generated waves which travelled down the channel and were dissipated on a beach of pebbles or sand. To observe the mass transport, grains of dye impregnated with fluorescein were inserted into the water; these fell to the bottom, leaving a vertical streak which then gradually deformed, giving a direct picture of the velocity profile.

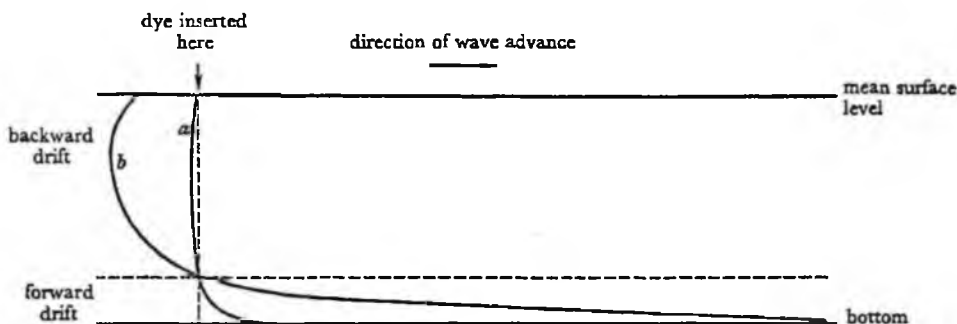


FIGURE 8 (after Bagnold 1947). Successive positions of the dye streak, indicating the profile of the mass-transport velocity (*a*) after one wave (*b*) after 10 waves.

Bagnold's first observations were made with a sandless bed, the bottom being of painted wood. His sketch of a typical velocity profile is reproduced in figure 8. It shows a strong forward drift near the bottom, and a weaker backward drift at higher levels. The uppermost part of the profile was unsteady; but in all cases there was a forward bend at the top of the curve.

The velocity of the foremost tip of the dye was observed; Bagnold's two series of observations are tabulated in the final column of table 1 (*a*) and (*b*). The parameters used by him to define the motion were the period $2\pi/\sigma$, the wave height $2a$ and the height of the wave troughs above the bottom ($h-a$ in the present notation). For each observation the non-dimensional parameter $\sigma^2 h/g$ has been calculated, and kh found from equation (245). In the fourth column of table 1 is given the theoretical maximum velocity in the boundary layer, calculated from equation (259).

The agreement between the last two columns of table 1 (*a*) is within 15%, which is satisfactory considering the errors probably involved in the observations. In table 1 (*b*) there is good agreement at the two ends of the range of observation, but some discrepancy

M. S. LONGUET-HIGGINS ON

for intermediate values. No explanation of the 'kink' in the experimental curve has been found.

On reaching the point at which the waves broke, the dye was observed to rise vertically from the bottom and to become dispersed in the upper layers, which drifted slowly away from the shore. From the velocities in table 1 we should expect that the motion, if controlled by convection, would be established in a few minutes. After starting the paddle, a few minutes were always allowed for the motion to settle down; afterwards the velocity profile remained the same shape indefinitely. However, the initial drift profile could not be observed very well owing to a 'seiche' which was set up in the tank when the motion was started.

TABLE 1. COMPARISON OF THE OBSERVED AND THEORETICAL MASS-TRANSPORT VELOCITIES NEAR THE BOTTOM IN A PROGRESSIVE WAVE

τ (s)	$\sigma^2 h/g$	kh	$U_{\max.}$ (cm/s)	$U_{\text{obs.}}$ (cm/s)
(a) $a = 3.0$ cm, $h = 18.0$ cm				
0.78	1.05	1.24	3.1	3.0
0.88	0.83	1.06	3.6	3.2
0.95	0.71	0.86	3.8	3.6
1.08	0.55	0.82	4.4	3.8
1.32	0.37	0.65	4.9	4.1
1.58	0.26	0.53	5.3	4.6
(b) $a = 1.55$ cm, $h = 14.5$ cm				
0.59	1.67	1.77	0.5	0.5
0.78	0.96	1.17	1.0	1.4
0.98	0.61	0.87	1.3	2.2
1.09	0.49	0.76	1.4	2.0
1.30	0.35	0.63	1.5	1.8
1.57	0.24	0.51	1.6	1.6

Similar observations to those of Bagnold, but on an inclined wooden ramp, were made by King (1948). In this case the forward movement was found both near the bottom and near the free surface, with backward movement between.

Conclusions

The strong forward velocities near the bottom, which were observed by Bagnold and by Bertin & Caligny, are accounted for quantitatively by the present theory. In a progressive wave we may expect a forward bending of the velocity profile near the free surface—twice that predicted by the irrotational theory—but no careful observations are yet available. In the standing wave there should be a circulation in the bottom boundary layer in cells of width one-quarter of a wave-length. Although there are some indications from the motion of sand particles that this may be so, there is as yet no direct experimental verification.

The observations of mass transport in the interior of the fluid may be divided into two classes: those in deep water and those in shallow water. In deep water the observations seem to be not greatly different from those predicted by the irrotational theory—as one would expect if the waves had not been running for long. In shallow water the observations appear to be very scattered; it is uncertain whether, in any of the observations quoted, a steady state had been reached.

MASS TRANSPORT IN WATER WAVES

581

Further experiments are desirable to determine the range of validity of the boundary-layer theory for progressive waves, to verify the results predicted for standing waves and to determine whether the motion in the interior is stable.

REFERENCES

- Bagnold, R. A. 1947 *J. Instn Civ. Engrs*, 27, 467.
 Basset, A. B. 1888 *Hydrodynamics*, vol. 2. Cambridge: Deighton and Bell.
 Caligny, A. F. H. de 1861 *C.R. Acad. Sci., Paris*, 52, 1309.
 Caligny, A. F. H. de 1878 *C.R. Acad. Sci., Paris*, 87, 10.
 Cooper, R. I. B. & Longuet-Higgins, M. S. 1950 *Proc. Roy. Soc. A*, 206, 424.
 Dubreil-Jacotin, M. L. 1934 *J. Math.* 13, 217.
 Gerstner, F. J. von 1809 *Ann. Phys., Lpz.*, 32, 412.
 Hough, S. S. 1896 *Proc. Lond. Math. Soc.* 28, 284.
 King, C. A. M. 1948 Ph.D. Dissertation. Cambridge (unpublished).
 Lamb, H. 1932 *Hydrodynamics*, 6th ed. Cambridge University Press.
 Longuet-Higgins, M. S. 1953 *Proc. Camb. Phil. Soc.* (in the press).
 Mitchim, C. F. 1939 M.Sc. Dissertation, University of California (unpublished).
 Rankine, W. J. M. 1863 *Phil. Trans.* 153, 127.
 Rayleigh, Lord 1876 *Phil. Mag.* (5), 1, 267.
 Rayleigh, Lord 1883 *Phil. Trans. A*, 175, 1.
 Schlichting, H. 1932 *Phys. Z.* 33, 327.
 Stokes, G. G. 1847 *Trans. Camb. Phil. Soc.* 8, 441.
 Stokes, G. G. 1851 *Trans. Camb. Phil. Soc.* 9, 20.
 United States Beach Erosion Board 1941 *Technical Report*, no. 1. Washington: U.S. Government Printing Office.
 Ursell, F. 1953 *Proc. Camb. Phil. Soc.* 49, 145.

Reprinted from the *Proceedings of the Cambridge Philosophical Society*,
Volume 49, Part 3, pp. 552-560, 1953.

PRINTED IN GREAT BRITAIN

ON THE DECREASE OF VELOCITY WITH DEPTH IN AN IRROTATIONAL WATER WAVE

By M. S. LONGUET-HIGGINS

Communicated by H. JEFFREYS

Received 15 December 1952

ABSTRACT. The following theorems are proved for irrotational surface waves of finite amplitude in a uniform, incompressible fluid:

(a) In any space-periodic motion (progressive or otherwise) in uniform depth, the mean square of the velocity is a decreasing function of the mean depth z below the surface. Hence the fluctuations in the mean pressure \bar{p} increase with z .

(b) In any space-periodic motion in infinite depth, the particle motion tends to zero exponentially as z tends to infinity. The pressure fluctuations at great depths are therefore simultaneous, but they do not in general tend to zero.

(c) In a progressive periodic wave in uniform depth the mass-transport velocity is a decreasing function of the mean depth of a particle below the free surface, and the tangent to the velocity profile is vertical at the bottom. This result conflicts with observations in wave tanks, and shows that the waves cannot be wholly irrotational.

(d) Analogous results are proved for the solitary wave.

The present paper discusses the vertical attenuation of certain physical quantities associated with irrotational wave motion. The interest of these quantities arises in different connexions, but because of a similarity in the analytical methods employed it is convenient to consider them together.

In the well-known approximate theory of surface waves (see Lamb (2) chap. 9), in which squares or products of the displacements are neglected, both the pressure fluctuations and the particle motion decrease rapidly downward from the surface; in deep water this decrease is exponential. It was therefore surprising when Miche (6) discovered that in a standing wave there are second-order fluctuations in the pressure even at infinite depths. Similar pressure variations have been shown to occur in a more general case, when the motion consists, in the first approximation, of two waves of the same wave-length, though not necessarily the same amplitude, travelling in opposite directions (Longuet-Higgins (3)). It is of some interest, therefore, to consider whether, in higher approximations than the first, the particle motion possesses a property similar to the pressure fluctuations or whether it decays rapidly with depth in all cases.

The results proved in §§ 1 and 2 of the present paper are for any irrotational motion which is periodic in space—for example, a progressive or a standing wave, or a motion which in the first approximation is a combination of two progressive waves of equal length. Periodicity in time, however, is not required. In § 1 it is shown by a simple argument that the *mean* square of the velocity at a given depth z is a decreasing function of z , and hence also that the *mean* value of the dynamical part of the pressure increases with z . In § 2 upper bounds are found for the velocity; when the depth is infinite the velocity diminishes exponentially. These results are independent of the

553 *Decrease of velocity with depth in an irrotational water wave*

pressure condition at the free surface, and follow from purely kinematical considerations, assuming the fluid to be incompressible and the motion irrotational. No approximations depending on the smallness of the wave amplitude are made. In deep water, therefore, the decay of the particle motion must be exponential to all orders of approximation.

One consequence of this result is that the pressure fluctuations at great depths, though depending in general on the time t , must be uniform in space.

In § 3 the mass-transport velocity of the waves is considered. It was Stokes (8) who first showed that in a progressive irrotational wave the particle orbits are not closed, but that each particle has in general an average, non-zero forward motion (called the mass-transport velocity). Stokes's method was approximate only. An exact and very elegant geometrical demonstration of this property was given by Rayleigh (7). The existence of a forward mass-transport velocity relative to the fluid at great depths was shown by him to be a consequence of the irrotational character of the motion. However, Rayleigh's proof is valid only for water of infinite depth; his argument does not apply when the depth is uniform and finite. Recently Ursell (10) presented an analytical proof, found by him some years previously, which extends Rayleigh's result to water of finite depth; he showed that the mass-transport velocity must be an increasing, or at any rate a non-decreasing, function of the depth, and that the tangent to the (mass-transport) velocity profile is vertical at the bottom itself. These results are of considerable interest, since wave-tank experiments have shown that for real fluids there is, on the contrary, a strong forward velocity near the bottom, in water of moderate depth (see, for example, Bagnold (1)); hence there must be a strong vorticity near the bottom, and the assumption of irrotational motion is invalid for real waves. Bagnold's observations have been accounted for quantitatively by the present writer (4) by introducing the viscous terms into the equations of motion. The original discrepancy between theory and observation has in fact led, in the paper just quoted, to a fundamental re-examination of the theory of mass transport and of the diffusion of vorticity in an oscillatory motion.

The method of proof used by Ursell (10) was to translate the first part of Rayleigh's geometrical proof into analytical terms; that is, he supposed that the progressive wave was reduced to a steady state by superposing a constant velocity $-c$ on the system (c being the wave velocity) and then found the time T taken by a particle to travel along a stream-line over a complete wave-length in the form

$$T(\psi) = \int_0^{\phi(\lambda)} \left[\left(\frac{\partial x}{\partial \phi} \right)^2 + \left(\frac{\partial z}{\partial \phi} \right)^2 \right] d\phi,$$

where λ is the wave-length, x and z are horizontal and vertical coordinates, and ϕ and ψ are the potential and stream function respectively. Then, by expanding x and z in Fourier series he showed that T was an increasing function of ψ , and hence that the mass-transport velocity increased with height above the bottom. In § 3 of the present paper we shall give a slightly simpler proof which avoids the use of a Fourier series expansion; $T(\psi)$ is shown to be an increasing function of ψ by direct differentiation; the analysis is precisely similar to that used in § 1.

Analogous results for an irrotational solitary wave are proved in §4. Here the advantage of the present method compared with that of Ursell (10) is also apparent; for the present method avoids altogether the use of Fourier integrals.

The usual notation will be used: x and z are rectangular coordinates, z being measured vertically downwards from the mean surface level. u and w denote the components of the velocity, which is two-dimensional and takes place in the (x, z) -plane. λ is the wave-length, h the mean depth of the fluid, p the pressure and ρ the density. The velocity potential and the stream function are denoted by ϕ and ψ . The fluid is assumed to be uniform and incompressible. A bar will be used to denote mean values with respect to x over a complete wave-length.

1. *In any space-periodic motion the mean square velocity at a given depth is a decreasing function of z .*

Since the motion is irrotational the components of velocity are given by

$$u = \frac{\partial \phi}{\partial x}, \quad w = \frac{\partial \phi}{\partial z}, \quad (1)$$

where, by the equation of continuity,

$$\nabla^2 \phi = \frac{\partial u}{\partial x} + \frac{\partial w}{\partial z} = 0. \quad (2)$$

The mean square of the velocity at a fixed depth is given by

$$\bar{q}^2 = \frac{1}{\lambda} \int_0^\lambda (u^2 + w^2) dx = \frac{1}{\lambda} \int_0^\lambda \left[\left(\frac{\partial \phi}{\partial x} \right)^2 + \left(\frac{\partial \phi}{\partial z} \right)^2 \right] dx. \quad (3)$$

Differentiating with respect to z , we have

$$\begin{aligned} \frac{\partial}{\partial z} (\bar{q}^2) &= \frac{2}{\lambda} \int_0^\lambda \left[\frac{\partial \phi}{\partial x} \frac{\partial^2 \phi}{\partial x \partial z} + \frac{\partial \phi}{\partial z} \frac{\partial^2 \phi}{\partial z^2} \right] dx \\ &= \frac{2}{\lambda} \int_0^\lambda \left[\frac{\partial \phi}{\partial x} \frac{\partial^2 \phi}{\partial x \partial z} - \frac{\partial \phi}{\partial z} \frac{\partial^2 \phi}{\partial x^2} \right] dx, \end{aligned} \quad (4)$$

by equation (2). But

$$\int_0^\lambda \left[\frac{\partial \phi}{\partial x} \frac{\partial^2 \phi}{\partial x \partial z} + \frac{\partial \phi}{\partial z} \frac{\partial^2 \phi}{\partial x^2} \right] dx = \left[\frac{\partial \phi \partial \phi}{\partial x \partial z} \right]_0^\lambda = 0, \quad (5)$$

by the periodicity of the motion. Thus

$$\frac{\partial}{\partial z} (\bar{q}^2) = \frac{4}{\lambda} \int_0^\lambda \frac{\partial \phi}{\partial x} \frac{\partial^2 \phi}{\partial x \partial z} dx. \quad (6)$$

On differentiating a second time we have similarly

$$\begin{aligned} \frac{\partial^2}{\partial z^2} (\bar{q}^2) &= \frac{4}{\lambda} \int_0^\lambda \left[\left(\frac{\partial^2 \phi}{\partial x \partial z} \right)^2 + \frac{\partial \phi}{\partial x} \frac{\partial^3 \phi}{\partial x \partial z^2} \right] dx \\ &= \frac{4}{\lambda} \int_0^\lambda \left[\left(\frac{\partial^2 \phi}{\partial x \partial z} \right)^2 - \frac{\partial \phi}{\partial x} \frac{\partial^3 \phi}{\partial x^3} \right] dx \\ &= \frac{4}{\lambda} \int_0^\lambda \left[\left(\frac{\partial^2 \phi}{\partial x \partial z} \right)^2 + \left(\frac{\partial^2 \phi}{\partial x^2} \right)^2 \right] dx. \end{aligned} \quad (7)$$

555 *Decrease of velocity with depth in an irrotational water wave*

The right-hand side of (7) can never be negative; so that $\partial(\bar{q}^2)/\partial z$ is an increasing function of z . But, on the bottom $z = h$, $\partial\phi/\partial z$ vanishes, and hence also do $\partial^2\phi/\partial x\partial z$ and $\partial(\bar{q}^2)/\partial z$. Therefore $\partial(\bar{q}^2)/\partial z$ is never positive when $z \leq h$ and so \bar{q}^2 is a decreasing function of z . This proves the result.

(We may note that, since $\partial\phi/\partial z$ also satisfies Laplace's equation and is periodic in x ,

$$\frac{\partial^3}{\partial z^3}(\bar{q}^2) = \frac{16}{\lambda} \int_0^\lambda \frac{\partial^2\phi}{\partial x\partial z} \frac{\partial^3\phi}{\partial x\partial z^2} dx \quad (8)$$

and

$$\frac{\partial^4}{\partial z^4}(\bar{q}^2) = \frac{16}{\lambda} \int_0^\lambda \left[\left(\frac{\partial^3\phi}{\partial x\partial z^3} \right)^2 + \left(\frac{\partial^3\phi}{\partial x^2\partial z} \right)^2 \right] dx. \quad (9)$$

Hence, by exactly similar arguments,

$$\frac{\partial^3(\bar{q}^2)}{\partial z^3} \leq 0, \quad \frac{\partial^4(\bar{q}^2)}{\partial z^4} \geq 0, \quad (10)$$

and in general

$$\frac{\partial^{2n-1}(\bar{q}^2)}{\partial z^{2n-1}} \leq 0, \quad \frac{\partial^{2n}(\bar{q}^2)}{\partial z^{2n}} \geq 0, \quad (11)$$

for every positive integer n .)

Since the density of the kinetic energy is proportional to q^2 the result may be stated in the form: *the mean density of kinetic energy is a decreasing function of the depth.*

Some corollaries may also be deduced. We have

$$\begin{aligned} \frac{\partial}{\partial z}(\overline{u^2 - w^2}) &= \frac{\partial}{\partial z} \frac{1}{\lambda} \int_0^\lambda \left[\left(\frac{\partial\phi}{\partial x} \right)^2 - \left(\frac{\partial\phi}{\partial z} \right)^2 \right] dx \\ &= \frac{2}{\lambda} \int_0^\lambda \left[\frac{\partial\phi}{\partial x} \frac{\partial^2\phi}{\partial x\partial z} - \frac{\partial\phi}{\partial z} \frac{\partial^2\phi}{\partial z^2} \right] dx \\ &= \frac{2}{\lambda} \int_0^\lambda \left[\frac{\partial\phi}{\partial x} \frac{\partial^2\phi}{\partial x\partial z} + \frac{\partial\phi}{\partial z} \frac{\partial^2\phi}{\partial x^2} \right] dx = 0 \end{aligned} \quad (12)$$

by equation (5). Therefore

$$\overline{u^2} - \overline{w^2} = C, \quad (13)$$

where C is a function of the time only. Since, at any instant, $\overline{u^2}$ and $\overline{w^2}$ differ by a constant, and their sum \bar{q}^2 is a decreasing function of z , each separately must be a decreasing function of z . Thus *the mean square of each component of velocity is a decreasing function of the depth.*

The total pressure p is given by the Bernoulli equation

$$\frac{p}{\rho} = -\frac{\partial\phi}{\partial t} - \frac{1}{2}q^2 + gz + F(t) \quad (14)$$

(see Lamb (2), § 20), where g denotes gravity and $F(t)$ is a function of the time t only. The dynamical part of the pressure, that is, the difference between the actual pressure and the pressure in the fluid at rest, is given by

$$\frac{p'}{\rho} = \frac{p}{\rho} - gz = -\frac{\partial\phi}{\partial t} - \frac{1}{2}q^2 + F(t). \quad (15)$$

ϕ is not yet completely determined, since the addition of an arbitrary function of t would not affect the velocities. Suppose then that ϕ and $F(t)$ are chosen so that the mean value of ϕ over a wave-length, at a certain depth z , is zero:

$$\bar{\phi} = \frac{1}{\lambda} \int_0^\lambda \phi dx = 0. \quad (16)$$

Now
$$\frac{\partial \bar{\phi}}{\partial z} = \frac{1}{\lambda} \int_0^\lambda \frac{\partial \phi}{\partial z} dx = 0, \quad (17)$$

since the total flow across any horizontal plane is zero. Therefore (12) holds for all values of z . On taking mean values in equation (15) we have

$$\frac{\bar{p}'}{\rho} = -\frac{1}{2} \bar{q}^2 + F(t). \quad (18)$$

It follows that \bar{p}' is an increasing function of z : *the mean value of the dynamical part of the pressure increases with the depth.*

The function $F(t)$ may be evaluated explicitly in terms of the displacement ζ of the free surface. It has been shown (see Longuet-Higgins (3), equation (28)) that

$$\frac{\bar{p}'}{\rho} = \frac{\partial^2}{\partial t^2} \left(\frac{1}{2} \bar{\zeta}^2 \right) - \bar{w}^2, \quad (19)$$

and so, on comparison with (18),

$$F(t) = \frac{\partial^2}{\partial t^2} \left(\frac{1}{2} \bar{\zeta}^2 \right) + \frac{1}{2} (\bar{u}^2 - \bar{w}^2). \quad (20)$$

2. *In any space-periodic motion in infinite depth, the motion tends to zero exponentially with depth (the frame of reference being suitably chosen).*

To prove this result a stronger method is required. From equations (1) and (2) above we have

$$u - iw = f(Z), \quad (21)$$

where $f(Z)$ is an analytic function of the complex variable

$$Z = x + iz. \quad (22)$$

$f(Z)$ is only defined when $0 \leq z \leq h^*$; but since w vanishes when $z = h$, $f(Z)$ may be continued analytically to the region $h \leq z \leq 2h$ by simple reflexion in the line $z = h$.

Consider a large rectangle $ABCD$ with vertices at the points $(R, 0)$, $(-R, 0)$, $(-R, 2h)$ and $(R, 2h)$ respectively. If $Z_0 = x_0 + iz_0$, is any point inside $ABCD$, we have by Cauchy's theorem

$$f(Z_0) = \frac{1}{2\pi i} \int_{ABCD} \frac{f(Z)}{Z - Z_0} dZ. \quad (23)$$

Now $f(Z)$ is periodic in x and therefore bounded as x tends to infinity. Thus on the sides BC and DA the integrand is of order R^{-1} . As R tends to infinity the contributions from these sides of the rectangle therefore tend to zero. Hence we have

$$f(Z_0) = \frac{1}{2\pi i} \lim_{R \rightarrow \infty} \left[- \int_{-R}^R \frac{f(x)}{x - Z_0} dx + \int_{-R}^R \frac{f(x)}{x + 2ih - Z_0} dx \right] \quad (24)$$

$$= \frac{1}{2\pi i} [-I_1 + I_2], \quad (25)$$

say. Now since the integrand tends to zero for large x we have

$$I_1 = \lim_{N \rightarrow \infty} \sum_{n=-N}^N \int_0^\lambda \frac{f(x+n\lambda)}{x+n\lambda-Z_0} dx \quad (26)$$

$$= \lim_{N \rightarrow \infty} \sum_{n=-N}^N \int_0^\lambda \frac{f(x)}{x+n\lambda-Z_0} dx \quad (27)$$

* Strictly $f(Z)$ is only defined when $\zeta \leq z \leq h$; but we assume that f can be continued analytically up to the mean surface level $z = 0$.

557 *Decrease of velocity with depth in an irrotational water wave*

by the periodicity of f . When $z_0 > \epsilon > 0$ the above series is uniformly convergent, so that the order of summation and integration may be reversed, giving

$$I_1 = \int_0^\lambda f(x) \left[\lim_{N \rightarrow \infty} \sum_{n=-N}^N \frac{1}{x + n\lambda - Z_0} \right] dx \quad (28)$$

$$= \int_0^\lambda f(x) \frac{\pi}{\lambda} \cot \frac{\pi(x - Z_0)}{\lambda} dx \quad (29)$$

by a known result (see, for example, Titchmarsh (9)).

Now since the total flow of water across any horizontal plane is zero we have

$$\int_0^\lambda w dx = 0 \quad (30)$$

for all z and t . By imposing on the axes a suitable horizontal velocity we may also make

$$\int_0^\lambda u dx = 0 \quad (31)$$

for particular values of z and t . But

$$\frac{\partial}{\partial z} \int_0^\lambda u dx = \frac{\partial}{\partial z} [\phi]_0^\lambda = \left[\frac{\partial \phi}{\partial z} \right]_0^\lambda, \quad (32)$$

which vanishes by the periodicity, and from the Bernoulli equation (10) we have

$$\frac{\partial}{\partial t} \int_0^\lambda u dx = \left[\frac{\partial \phi}{\partial t} \right]_0^\lambda = \left[\frac{p}{\rho} - \frac{1}{2} q^2 + gz + F(t) \right]_0^\lambda, \quad (33)$$

which again vanishes by the periodicity. Hence (31) is valid for all values of z and t . From (30) and (31) we have then

$$\int_0^\lambda f(Z) dx = 0, \quad (34)$$

so that (29) may be written

$$I_1 = \int_0^\lambda f(x) \frac{\pi}{\lambda} \left[\cot \frac{\pi(x - Z_0)}{\lambda} - 1 \right] dx \quad (35)$$

$$= \int_0^\lambda f(x) \frac{ik \exp \{ ik(x - Z_0) \}}{1 - \exp \{ ik(x - Z_0) \}} dx, \quad (36)$$

where $k = 2\pi/\lambda$. Hence when $e^{-kz_0} < \frac{1}{2}$ (that is, when z_0 is greater than about $\frac{1}{2}\lambda$) we have

$$|I_1| < 4\pi e^{-kz_0} \max |f(x)|. \quad (37)$$

Similarly we may show that

$$I_2 = \int_0^\lambda f(x) \frac{ik \exp \{ ik(x + 2ih - Z_0) \}}{1 - \exp \{ ik(x + 2ih - Z_0) \}} dx, \quad (38)$$

so that when $\exp \{-k(2h - z_0)\} < \frac{1}{2}$ (which is certainly satisfied if $e^{-kz_0} < \frac{1}{2}$ and $0 \leq z_0 \leq h$), we have

$$|I_2| < 4\pi \exp \{-k(2h - z_0)\} \max |f(x)|. \quad (39)$$

Therefore from equation (25)

$$|f(Z_0)| \leq \frac{1}{2\pi} (|I_1| + |I_2|) < 4e^{-kh} \cosh k(z_0 - h) \max |f(x)|. \quad (40)$$

On dropping the suffix 0 we have

$$(u^2 + w^2)^{\frac{1}{2}} < 4e^{-kh} \cosh k(z - h) \max [(u^2 + w^2)^{\frac{1}{2}}]_{z=0}, \quad (41)$$

and on letting kh tend to infinity we find that in infinitely deep water

$$(u^2 + w^2)^{\frac{1}{2}} \leq 2e^{-kz} \max [(u^2 + w^2)^{\frac{1}{2}}]_{z=0}. \tag{42}$$

This proves the result.

u and w are each less than or equal to $(u^2 + w^2)^{\frac{1}{2}}$ in absolute value. Thus (42) implies that both components of velocity diminish exponentially.

If ϕ is chosen as in § 2, so that $\bar{\phi}$ vanishes, then we may show that ϕ also decreases exponentially. For since ϕ is continuous and its mean value when $0 < x < \lambda$ is zero, it follows that ϕ itself must be zero somewhere in this interval, say when $x = x'$. We have then

$$|\phi| = \left| \int_x^{x'} \frac{\partial \phi}{\partial x} dx \right| \leq |x - x'| m, \tag{43}$$

where m is the maximum value of $|\partial\phi/\partial x|$ in the interval. But $|x - x'| < \lambda$, and m is exponentially small; hence ϕ also is exponentially small.

From equation (11) we have then, at great depths,

$$\frac{p'}{\rho} = F(t), \tag{44}$$

so that the pressure fluctuation is a function of the time t only, and therefore occurs uniformly and simultaneously at all points; and from equation (16) we see that in this case $F(t)$ is given by

$$F(t) = \frac{\rho^2}{\rho l^2} \left(\frac{1}{2} \bar{v}^2 \right). \tag{45}$$

The above expression has been evaluated in some particular cases (see Longuet-Higgins and Ursell (5), and Longuet-Higgins (3), § 2.3). In general, $F(t)$ represents a pressure fluctuation of double the fundamental frequency of the waves.

3. *In a progressive wave in water of uniform depth the mass-transport velocity diminishes with the mean depth of the particle.*

Following Ursell (10) we first express Rayleigh's geometrical argument (Rayleigh (7)) in analytical terms. Let the motion be reduced to a steady state by referring it to axes moving in the direction of the waves with the wave velocity c . In the present section x, z, ϕ and ψ will denote the coordinates, velocity potential and stream function in the *steady-state* motion. If the orbital motion of the particles does not exceed c it follows that the horizontal component of the steady-state velocity is negative:

$$\frac{\partial \phi}{\partial x} = \frac{\partial \psi}{\partial z} < 0. \tag{46}$$

Now let ϕ and ψ be taken as fundamental coordinates, and x and z be expressed as functions of them. Let $s(\phi, \psi)$ denote the arc-length measured along a stream-line, $\psi = \text{constant}$, from the equipotential line $\phi = 0$. The motion being space-periodic, there will be another equipotential line $\phi = \phi_\lambda$ at a wave-length's distance from $\phi = 0$, where the motion is identical with that on $\phi = 0$. If the time taken for a particle to travel from $\phi = 0$ to $\phi = \phi_\lambda$ is denoted by $T(\psi)$, then the forward mass-transport velocity $U(\psi)$ may be defined by the equations

$$T = \frac{\lambda}{c - U}, \quad U = c - \frac{\lambda}{T}. \tag{47}$$

559 *Decrease of velocity with depth in an irrotational water wave*

Now the velocity q along a stream-line is given by the ratio of an increment $d\phi$ to the corresponding increment ds , ψ being kept constant; that is

$$q = \left(\frac{d\phi}{ds} \right)_{\psi \text{ constant}} = \left(\frac{\partial s}{\partial \phi} \right)^{-1}. \quad (48)$$

We have therefore
$$T = \int_0^{\phi_\lambda} q^{-1} ds = \int_0^{\phi_\lambda} \frac{\partial s}{\partial \phi} ds = \int_0^{\phi_\lambda} \left(\frac{\partial s}{\partial \phi} \right)^2 d\phi, \quad (49)$$

that is,
$$T = \int_0^{\phi_\lambda} \left[\left(\frac{\partial x}{\partial \phi} \right)^2 + \left(\frac{\partial z}{\partial \phi} \right)^2 \right] d\phi.$$

At this point Ursell (10) introduces a Fourier series expansion. However, since x, z are conjugate functions, $\partial z/\partial \phi$ can be replaced by $-\partial x/\partial \psi$, so that

$$T = \int_0^{\phi_\lambda} \left[\left(\frac{\partial x}{\partial \phi} \right)^2 + \left(\frac{\partial x}{\partial \psi} \right)^2 \right] d\phi.$$

x satisfies Laplace's equation in the coordinates ϕ and ψ , and all its derivatives are periodic in ϕ with period ϕ_λ . Therefore, precisely as in § 1, we have

$$\frac{\partial T}{\partial \psi} = 4 \int_0^{\phi_\lambda} \frac{\partial x}{\partial \phi} \frac{\partial x}{\partial \phi} \frac{\partial^2 x}{\partial \phi \partial \psi} d\phi \quad (50)$$

and
$$\frac{\partial^2 T}{\partial \psi^2} = 4 \int_0^{\phi_\lambda} \left[\left(\frac{\partial^2 x}{\partial \phi \partial \psi} \right)^2 + \left(\frac{\partial^2 x}{\partial \phi^2} \right)^2 \right] d\phi. \quad (51)$$

$\partial T/\partial \psi$ vanishes on the bottom $\psi = \psi_h$, since $\partial x/\partial \psi$, which equals $-\partial z/\partial \phi$, is zero. Since by (46) $\psi > \psi_h$ in general, it follows by an exactly similar argument that $\partial T/\partial \psi$ is in general positive. Thus U by (47) is an increasing function of ψ and so a decreasing function of the mean depth of the stream line. This proves the result.

It may be asked whether the analytical proof given above could not be translated back into geometrical terms. This is probably so; but the geometrical version would almost certainly be more complicated; for it will be seen that the proof essentially involves the curvature of the velocity-profile, that is, the second derivative of the velocity. In a geometrical proof, therefore, small quantities of the second or higher orders would have to be taken into account.

4. *The solitary wave.* Similar results may be proved for the solitary wave. In this case it is assumed that when $x \rightarrow \pm \infty$ the motion tends to zero, or that, when a uniform velocity is superimposed, the motion tends to a uniform stream. Thus the velocity at $+\infty$ equals that at $-\infty$. Instead of the mean velocity \bar{q}^2 , which over an infinite interval would be zero, we may consider the quantity

$$Q^2 = \int_{x_1}^{x_2} (u^2 + w^2) dx = \int_{x_1}^{x_2} \left[\left(\frac{\partial \phi}{\partial x} \right)^2 + \left(\frac{\partial \phi}{\partial z} \right)^2 \right] dx, \quad (52)$$

where x_1 and x_2 are made to tend to $+\infty$ and $-\infty$ respectively. In other words Q^2 , in the limit, is the square of the velocity at a given depth z integrated with respect to x from $-\infty$ to $+\infty$. Since the values of $\partial \phi/\partial x$, $\partial \phi/\partial z$ and their derivatives at the two ends of the interval are equal in the limit it follows, as before, that

$$\frac{\partial Q^2}{\partial z} \leq 0, \quad \frac{\partial^2 Q^2}{\partial z^2} \geq 0, \quad (53)$$

and hence (1) the total density of kinetic energy, integrated from $-\infty$ to $+\infty$, is a decreasing function of the depth z ; (2) the square of each component of velocity, integrated from $-\infty$ to $+\infty$ is a decreasing function of z ; (3) the dynamical part of the total force on a horizontal plane $z = \text{constant}$ increases with z .

To consider the mass transport we suppose, as in § 3, that the motion is reduced to a steady state by superposing on it a uniform horizontal velocity $-c$. The time T taken by a particle to travel along a stream-line $\psi = \text{constant}$ between the two equipotential lines $\phi = \phi_1$ and $\phi = \phi_2$ is given by

$$T(\psi) = \int_{\phi_1}^{\phi_2} \left[\left(\frac{\partial x}{\partial \phi} \right)^2 + \left(\frac{\partial x}{\partial \psi} \right)^2 \right] d\phi \quad (54)$$

(where x , ϕ and ψ now refer to the steady motion). The displacement of the particle with respect to the moving axes is $[x]_{\phi_1}^{\phi_2}$. Hence the displacement D with respect to stationary axes is given by

$$D = [x]_{\phi_1}^{\phi_2} + cT, \quad (55)$$

and so

$$\frac{\partial D}{\partial \psi} = \left[\frac{\partial x}{\partial \psi} \right]_{\phi_1}^{\phi_2} + c \frac{\partial T}{\partial \psi}. \quad (56)$$

Now as ϕ_1 and ϕ_2 tend to $-\infty$ and $+\infty$ respectively the flow, in the steady state, tends to a uniform stream, and so $\partial x / \partial \psi$ tends to zero. Thus, in the limit,

$$\frac{\partial D}{\partial \psi} = c \frac{\partial T}{\partial \psi}. \quad (57)$$

But since $\partial x / \partial \phi$, $\partial x / \partial \psi$, etc., tend, in the limit, to the same values at the two ends of the interval, we have from (54)

$$\frac{\partial T}{\partial \psi} \geq 0, \quad \frac{\partial^2 T}{\partial \psi^2} \geq 0. \quad (58)$$

Hence in the original motion: (4) the total horizontal displacement of a particle during the passage of a solitary wave is a decreasing function of the mean depth of the particle.

REFERENCES

- (1) BAGNOLD, R. A. *J. Instn. civ. Engrs.* 27 (1947), 447-69.
- (2) LAMB, H. *Hydrodynamics*, 6th ed. (Cambridge, 1932).
- (3) LONGUET-HIGGINS, M. S. *Phil. Trans. A*, 243 (1950), 1-35.
- (4) LONGUET-HIGGINS, M. S. *Phil. Trans. A* (in the Press).
- (5) LONGUET-HIGGINS, M. S. and URSELL, F. *Nature, Lond.*, 162 (1948), 700.
- (6) MICHE, M. *Ann. Ponts Chauss.* 114 (1944), 25-78.
- (7) RAYLEIGH, LORD. *Phil. Mag.* (5), 1 (1876), 257-79.
- (8) STOKES, G. G. *Trans. Camb. phil. Soc.* 8 (1847), 441-60.
- (9) TITCHMARSH, E. C. *Theory of functions*, 2nd ed. (Oxford, 1939), p. 113.
- (10) URSELL, F. *Proc. Camb. phil. Soc.* 49 (1953), 145-50.

Reproduced with permission from The American Society of Civil Engineers

Source: Proceedings of the International Conference on Coastal Engineering, No 6 (1957)

AN EXPERIMENTAL INVESTIGATION OF DRIFT PROFILES IN A CLOSED CHANNEL

It was found possible to obtain drift velocities set up by progressive waves in a closed channel, which were independent of position and time. It is probable however that the velocities would be disordered by circulations in a horizontal plane, if the waves were not confined to a narrow channel.

Stable drift profiles were not obtained with the very longest waves, those amounting to a succession of solitary waves, except when the waves were very low. Possibly the channel, which was only long enough to contain four of these waves at a time, was too short.

Near the bottom the drift velocities are as predicted by Longuet-Higgins for all values of kd that were investigated. Fig. 15 shows this agreement. This is in spite of the fact that the theory applies in the first place to laminar conditions, whereas the flow was nearly always turbulent. However in an appendix Longuet-Higgins has given reasons why the formula may be generally applicable in the turbulent case also.

For the surface and interior of the fluid there is no strictly applicable theory. However in deep water the surface drifts are found to be as in Stokes' irrotational theory. Further, when $0.7 < kd < 1.1$ the profiles in the interior are fairly well fitted by Longuet-Higgins' conduction solution. There is only one departure from this curve which is systematic. It is that for a given value of kd the lower waves produce bigger non-dimensional drift velocities.

The drift profiles are disrupted in the neighbourhood of breaking waves. This provides a mechanism capable of sustaining an offshore sand bar, because opposed bed drifts are set up which meet at the top of the bar.

When the waves do not break, the slope of the bed does not alter the drift curves a great deal and the theoretical values of the drift at the bed are almost equally applicable to waves over a horizontal or a gently sloping bed.

REFERENCES

- (1) Stokes, G. G. On the theory of Oscillatory Waves. Trans. Cambridge Phil. Soc., Vol VIII, p.441, read 1st March 1847 & Vol. IX, p.20, 1851.
- (2) Longuet-Higgins, M.S. Mass Transport in Water Waves. Phil. Trans. Roy. Soc. London, Series A, No. 903, Vol. 245, pp.535-581, 31st March 1953.
- (3) Caligny, A. F. H. de C. R. Acad. Sci., Paris Vol. 87, 10, 1878.
- (4) U.S. Beach Erosion Board. A Study of Progressive Oscillatory Waves in Water. Tech. Report No. 1, U.S. Govt. Printing Office, 1941.
- (5) Bagnold, R. A. Sand Movement by Waves: Some Small Scale Experiments with Sand of very Low Density. Jour. I.C.E., No. 4, 1946-47, p.447.
- (6) Lamb, H. Hydrodynamics. 6th Revised Edition. Chap. XI, para 347.

COASTAL ENGINEERING

APPENDIX

THE MECHANICS OF THE BOUNDARY-LAYER NEAR THE BOTTOM IN A PROGRESSIVE WAVE

M. S. Longuet-Higgins
National Institute of Oceanography,
Wormley, England

Mr. Russell has asked me to give a brief theoretical account of the somewhat paradoxical forwards drift in the boundary-layer near the bottom, which he and Mr. Osorio have measured. A general treatment of such boundary-layer effects is to be found in a previous paper⁽²⁾; but in the following I shall try to give a simple physical picture of one particular case, namely where the wave motion is purely progressive, and the bottom is rigid and level.

It is assumed at first that the viscosity is constant and that the motion is laminar - a condition not always satisfied in Mr. Russell's experiments. Under these circumstances it is shown that the mass-transport velocity near the bottom and just outside the boundary-layer is given by

$$U = \frac{5A^2}{4c}$$

where A is the amplitude of the horizontal oscillatory motion at the bottom and c is the wave velocity. Since, however, the observations are in agreement with this result even when the flow is turbulent, I also consider the case where the (constant) coefficient of viscosity is replaced by a coefficient of eddy viscosity depending on the distance from the bottom. I find then that the above formula is valid independently of the functional form of the viscous coefficient. This appears to be a step towards the explanation of the phenomenon in the turbulent case.

(1) The boundary layer at the bottom According to the first-order theory of surface waves, and from observation, a wave in water of finite depth produces near the bottom a horizontal oscillatory velocity given by

$$u_{oo} = A \cos(\sigma t - kx) \quad (1)$$

approximately, where

$$A = \frac{a\sigma}{\sinh kd}$$

However, on the bottom itself the velocity must be zero. It appears, then, that there is a region of strong shear very close to the bottom, where viscous stresses are important, and outside which they are relatively small. This region may be called the "boundary-layer".

To determine the horizontal motion within this layer, compare an element of fluid within the layer with an element just outside. (Fig. A1). The forces accelerating each element horizontally are the pressure

AN EXPERIMENTAL INVESTIGATION OF DRIFT PROFILES
IN A CLOSED CHANNEL

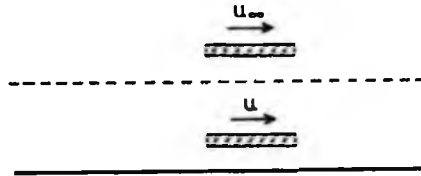


Fig. A1. Comparison of the motion of two fluid elements in and outside the boundary-layer.

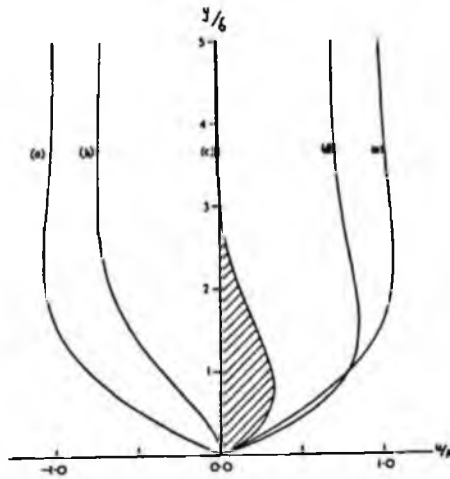


Fig. A2. The velocity-profiles (correct to first order) in the boundary-layer for five successive phases of the motion at intervals of $T/8$. (Vertical scale greatly exaggerated).

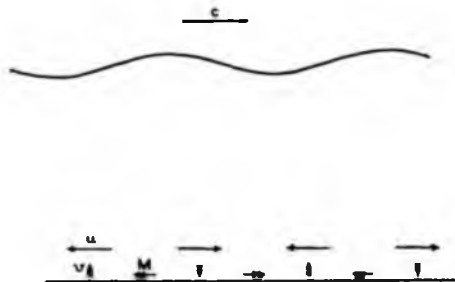


Fig. A3. Diagram showing the origin of the vertical motion in the boundary-layer.

COASTAL ENGINEERING

gradient $\partial \beta / \partial x$ and the viscous stress $\partial / \partial y (\rho \nu \partial u / \partial y)$. Now since the layer is very thin and the vertical acceleration is not large, the pressure gradient is practically the same for the two elements, while the viscous stress is appreciable only for the element within the layer. So the difference in their horizontal acceleration is due to the viscous stress only. Hence (neglecting second-order terms)

$$\frac{\partial u}{\partial t} = \frac{\partial u_{\infty}}{\partial t} + \frac{\partial}{\partial y} (\nu \frac{\partial u}{\partial y}). \quad (2)$$

When the viscosity is constant, the solution of this equation is

$$u = A \left[\cos(\sigma t - kx) - e^{-y/\delta} \cos(\sigma t - kx - y/\delta) \right] \quad (3)$$

where

$$\delta = \left(\frac{2\nu}{\sigma} \right)^{1/2}.$$

(Here y is measured vertically upwards from the bottom).

The motion is illustrated in Fig. A2, where the velocity profile is shown for various phases, at a fixed point. Effectively the velocity is the same as for a uniform fluid oscillating in the neighbourhood of a plane wall (see Lamb(5) § 347). The velocity tends very rapidly to its value u_{∞} just outside the layer, and the total thickness of the layer is of the same order as δ .

An important feature of the motion is that the phase of the velocity inside the layer tends in general to be in advance of the velocity just outside. The integrated flow in the layer increases indefinitely, of course, as y tends to infinity. But the component of the integrated flow which is in quadrature with u_{∞} is finite, and is given by the shaded area of the velocity-profile curve (c) in Fig. A3. Denoting this by M we have

$$M = \int_0^{\infty} u \, dy = \frac{1}{2} A \delta \sin(\sigma t - kx). \quad (4)$$

Now if the flow were uniform horizontally, as in Lamb's solution just mentioned, there would be no vertical component of motion. But since u varies sinusoidally with x , so also does the total flow M ; this produces a piling-up of mass within the layer which gives rise to a small but important vertical component of velocity. From Fig. A3 we see that just behind a crest the flow M is negative, and just in front of a crest it is positive. Hence beneath the crest itself there is "stretching" of the layer, giving a downwards velocity. Similarly beneath a trough there is a piling-up in the layer, giving an upwards velocity. Analytically, we have

$$v = \int_0^y \frac{\partial v}{\partial y} \, dy = \int_0^y \left(-\frac{\partial u}{\partial x} \right) \, dy = -\frac{\partial}{\partial x} \int_0^y u \, dy.$$

Paying attention only to the part of v that is in phase with u_{∞} , that is, the part arising from M we have

AN EXPERIMENTAL INVESTIGATION OF DRIFT PROFILES
IN A CLOSED CHANNEL

$$v_{\infty} = -\frac{\partial M}{\partial x} = -\frac{1}{2} A k \delta \cos(\omega t - kx). \quad (5)$$

This shows that the mean value of the product $u_{\infty} v_{\infty}$ is negative:

$$(\overline{uv})_{\infty} = -\frac{1}{4} A^2 k \delta < 0. \quad (6)$$

the significance of which will soon become apparent.

(2) The mean stress on the bottom If first-order terms only are considered, the mean stress on the bottom is identically zero. But we shall show, by a straightforward consideration of momentum, that to second order, the mean stress must in fact be positive.

Imagine a rectangle, one wavelength long, drawn in the fluid with its upper side CD just outside the boundary-layer and its lower side $C'D'$ on the bottom. When fluid having a horizontal velocity u crosses the upper side CD with velocity v there is a transfer of momentum across the boundary at the rate ρuv per unit horizontal distance. The mean rate of transfer of momentum across CD in this way is given by $\rho \overline{uv}$, the familiar Reynolds stress. Consider then the momentum balance inside the rectangle $CDD'C'$. Along the upper side viscous stresses are negligible and there is a transfer of momentum due to the Reynolds stress $\rho \overline{uv}$. On the lower side $C'D'$ the Reynolds stress vanishes (since $v=0$), but there is a mean viscous stress $\rho (\nu \partial u / \partial y)$. On the two vertical sides the conditions are identical by the periodicity of the motion, and so the transfer of momentum across one side just cancels the transfer across the other side. But the total momentum within the rectangle remains unchanged; therefore the viscous stress on the bottom must just balance the Reynolds stress at the top. In other words

$$\left(\nu \frac{\partial u}{\partial y} \right)_0 = -(\overline{uv})_{\infty}. \quad (7)$$

We have seen from eqn. (6) that the mean product $(\overline{uv})_{\infty}$ is negative. In other words there is a downwards transfer of momentum into the boundary-layer. To balance this, there must be a backwards stress on the layer at the bottom, that is to say a forwards gradient of mean velocity. In the case when the viscosity is constant we have

$$\frac{\partial \bar{u}}{\partial y} = -\frac{1}{\nu} (\overline{uv})_{\infty} = \frac{A^2}{2c\delta} > 0. \quad (8)$$

The velocity gradient at other levels within the layer may be obtained by considering a rectangle $CDD'C''$ (see Fig. 44) which has its lower side $C'D''$ at an arbitrary level within the boundary layer. The same considerations of momentum apply, but now account must be taken of both the viscous stress and the Reynolds stress at the level $C'D''$. This leads us at once to the relation

$$\nu \frac{\partial \bar{u}}{\partial y} = \overline{uv} - (\overline{uv})_{\infty}. \quad (9)$$

COASTAL ENGINEERING

If the viscosity is given, the profile of the mean velocity \bar{u} may be deduced by direct integration. This is done in §5, and we find

$$\bar{u} = \frac{1}{c} \overline{u_{\infty} u} + \frac{1}{2c} \overline{u^2} - \frac{\partial u}{\partial y} \int v dt \quad (10)$$

a result which does not depend upon the distribution of viscosity within the layer. For constant viscosity we obtain the left-hand curve shown in Fig. A5.

(3) The mass-transport velocity It is essential to distinguish between the mean velocity \bar{u} measured at a fixed point and the mass-transport velocity U , which may be defined as the mean velocity of the same particle of fluid averaged over a complete period (both \bar{u} and U being assumed small compared with the orbital velocity u). For example in the Stokes irrotational wave the mass transport velocity is always positive relative to the mean velocity. This is for two reasons: first because as a wave crest passes overhead the orbital velocity is positive, and so the particle "stays with the wave", spending slightly longer on the forwards part of its orbit than on the backwards part; secondly, the velocity of a particle is slightly greater at the top of its orbit, where it is travelling forwards, than at the bottom, where it is travelling backwards (see Fig. A6).

The same considerations apply, in general, in the boundary-layer; although the vertical displacements are very small, the vertical gradient of velocity is correspondingly large, so that both the effects just mentioned become appreciable. However, the phase difference between horizontal and vertical components of velocity is a function of the mean position of a particle within the layer.

Analytically, if P is the point on the orbit of a particle whose mean position is Q , the instantaneous velocity at P will differ from that at Q by an amount

$$\Delta u = \frac{\partial u}{\partial x} \Delta x + \frac{\partial u}{\partial y} \Delta y$$

where $\Delta x, \Delta y$ are the horizontal displacements of P from Q . These displacements are given by

$$\Delta x = \int u dt, \quad \Delta y = \int v dt \quad (11)$$

approximately, (apart from a constant term). Hence the difference between the mean velocity of the particle and the velocity at Q is given, to the second approximation, by

$$U = \bar{u} + \frac{\partial u}{\partial x} \int u dt + \frac{\partial u}{\partial y} \int v dt. \quad (12)$$

On the bottom itself, $u, v, \partial u/\partial x$ and $\partial v/\partial y$ all vanish, and so on differentiation we find

$$\frac{\partial U}{\partial y} = \frac{\partial \bar{u}}{\partial y} > 0. \quad (13)$$

AN EXPERIMENTAL INVESTIGATION OF DRIFT PROFILES
IN A CLOSED CHANNEL

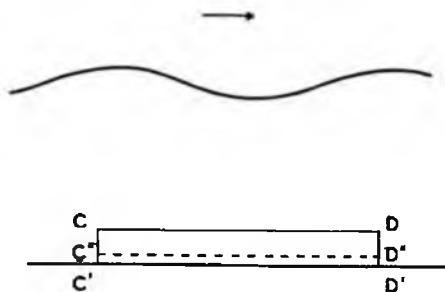


Fig. A4. Diagram for deriving the stress on the bottom.

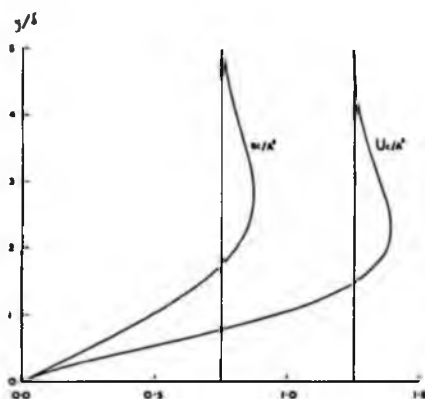


Fig. A5. The mean velocity \bar{u} and the mass-transport velocity U in the boundary-layer.

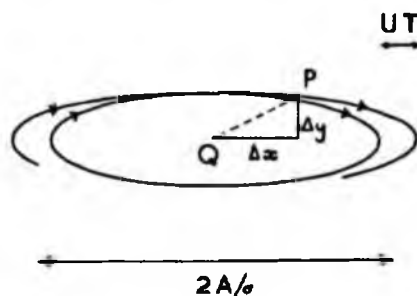


Fig. A6. How the mass-transport velocity arises, when $\bar{u} = 0$.

COASTAL ENGINEERING

Since U vanishes on the bottom itself, this shows that U must be positive very close to the bottom; here at least there is a forwards mass-transport velocity.

At other levels within the boundary-layer, however, the last two terms in eqn. (12) are not negligible. For a progressive wave we have

$$\frac{\partial u}{\partial x} \int u dt = -\frac{1}{c} \frac{\partial u}{\partial t} \int u dt = \frac{1}{c} \overline{u^2}$$

by eqn. (21) below, and so from (10)

$$U = \frac{1}{c} \left(\overline{u_{\infty} u} + \frac{3}{2} \overline{u^2} \right). \quad (14)$$

When $u \rightarrow u_{\infty}$ we have

$$U \rightarrow \frac{5}{2c} \overline{u_{\infty}^2}. \quad (15)$$

These remarkably simple formulae are independent of the absolute value of the viscosity and even (as will be shown) independent of the form of the distribution of viscosity within the layer. However, in the special case when the viscosity is constant and the motion sinusoidal we have on substitution from (3)

$$U = \frac{A^2}{4c} \left(5 - 8e^{-y/6} \cos y/6 + 3e^{-2y/6} \right). \quad (16)$$

This distribution is shown by the second curve in Fig. A5. U is always positive and has a maximum value

$$U = 1.376 \dots A^2/c \quad (17)$$

As $y/6$ tends to infinity

$$U \rightarrow 1.25 A^2/c \quad (18)$$

compared with the limiting value

$$\overline{u} \rightarrow 0.75 A^2/c \quad (19)$$

for the mean velocity.

(4) Discussion We have remarked that the formulae (14) and (15) are independent of the distribution of viscosity within the layer, provided that the flow is laminar. Now for turbulent but steady boundary-layers it has been shown that the flow may be quite well approximated by the laminar velocity profile, provided that in the outer part of the layer the ordinary viscosity is replaced by a uniform coefficient of eddy viscosity⁽⁶⁾. Now if the eddy viscosity fluctuates according to the instantaneous velocity gradient, then an oscillatory boundary-layer will not be strictly comparable with a steady boundary-layer. If on the other hand we assume that the eddy-viscosity of a small element of fluid does not fluctuate appreciably throughout a wave period it is possible to replace the ordinary kinematic viscosity ν by a coefficient which is constant for a particle, though varying with the mean distance of the

AN EXPERIMENTAL INVESTIGATION OF DRIFT PROFILES IN A CLOSED CHANNEL

particle from the bottom. Our result then indicates that the equation

$$U_{\infty} = \frac{S}{2c} \bar{u}_{\infty}^2$$

for the velocity just outside the boundary-layer is valid also when the flow is turbulent.

Moreover this expression is valid even when the motion, though periodic is not strictly harmonic, as will happen with long waves in shallow water when the form of a solitary wave is approached. Suppose that the velocity near the bottom, instead of being simply harmonic is given by an expression of the form

$$u_{\infty} = A_1 \cos(\sigma t - kx) + A_2 \cos 2(\sigma t - kx) + \dots \\ + B_2 \sin 2(\sigma t - kx) + \dots$$

in which the coefficients may be deduced theoretically or found from observation by Fourier analysis. Then the above expression gives

$$U_{\infty} = \frac{S}{4c} (A_1^2 + A_2^2 + \dots + B_2^2 + B_3^2 + \dots). \quad (20)$$

Although the mass-transport velocity just outside the layer has been shown to be independent of y , eqn. (2) shows that the distribution of the velocity within the layer is certainly dependent on the form of the viscosity. For this reason the expression (17) for the maximum velocity within the layer may not be valid for a turbulent layer.

However, what is observed in practical experiments is less likely to be the maximum velocity than the velocity just outside the layer, where the velocity gradients are less steep - especially if the boundary layer is thus and observations are made with streaks of dye. For, a slender tongue of dye is less easy to observe than a diffused cloud moving forwards with a relatively uniform velocity. It is fortunate that the latter velocity appears to be more easily predictable.

(5) Proof of eqn. (10) Finally shall prove our statement that eqn. (10) is true independently of the viscosity. Although the argument can at some length be translated into physical terms, it is simpler at this stage to give an analytical proof.

We start from eqn. (2) and (9), which are both valid even when the viscosity is a function of time and position. From (2) we have by integration with respect to t ,

$$u = u_{\infty} + \int \frac{\partial}{\partial y} \left(\nu \frac{\partial u}{\partial y} \right) dt$$

and therefore

$$\overline{uv} - (\overline{uv})_{\infty} = \overline{u_{\infty}v} + \overline{\int \frac{\partial}{\partial y} \left(\nu \frac{\partial u}{\partial y} \right) dt \cdot v} - (\overline{uv})_{\infty}.$$

COASTAL ENGINEERING

Since U vanishes on the bottom itself, this shows that U must be positive very close to the bottom; here at least there is a forwards mass-transport velocity.

At other levels within the boundary-layer, however, the last two terms in eqn. (12) are not negligible. For a progressive wave we have

$$\frac{\partial u}{\partial x} \int u dt = -\frac{1}{c} \frac{\partial u}{\partial t} \int u dt = \frac{1}{c} \overline{u^2}$$

by eqn. (21) below, and so from (10)

$$U = \frac{1}{c} \left(\overline{u_{\infty} u} + \frac{3}{2} \overline{u^2} \right). \quad (14)$$

When $u \rightarrow u_{\infty}$ we have

$$U \rightarrow \frac{5}{2c} \overline{u_{\infty}^2}. \quad (15)$$

These remarkably simple formulae are independent of the absolute value of the viscosity and even (as will be shown) independent of the form of the distribution of viscosity within the layer. However, in the special case when the viscosity is constant and the motion sinusoidal we have on substitution from (3)

$$U = \frac{A^2}{4c} \left(5 - 8 e^{-y/6} \cos y/6 + 3 e^{-2y/6} \right). \quad (16)$$

This distribution is shown by the second curve in Fig. A5. U is always positive and has a maximum value

$$U = 1.376 \dots A^2/c \quad (17)$$

As $y/6$ tends to infinity

$$U \rightarrow 1.25 A^2/c \quad (18)$$

compared with the limiting value

$$\bar{u} \rightarrow 0.75 A^2/c \quad (19)$$

for the mean velocity.

(4.) Discussion We have remarked that the formulae (14) and (15) are independent of the distribution of viscosity within the layer, provided that the flow is laminar. Now for turbulent but steady boundary-layers it has been shown that the flow may be quite well approximated by the laminar velocity profile, provided that in the outer part of the layer the ordinary viscosity is replaced by a uniform coefficient of eddy viscosity⁽⁶⁾. Now if the eddy viscosity fluctuates according to the instantaneous velocity gradient, then an oscillatory boundary-layer will not be strictly comparable with a steady boundary-layer. If on the other hand we assume that the eddy-viscosity of a small element of fluid does not fluctuate appreciably throughout a wave period it is possible to replace the ordinary kinematic viscosity ν by a coefficient which is constant for a particle, though varying with the mean distance of the

AN EXPERIMENTAL INVESTIGATION OF DRIFT PROFILES IN A CLOSED CHANNEL

particle from the bottom. Our result then indicates that the equation

$$U_{\infty} = \frac{\int}{2c} \overline{u^2}$$

for the velocity just outside the boundary-layer is valid also when the flow is turbulent.

Moreover this expression is valid even when the motion, though periodic is not strictly harmonic, as will happen with long waves in shallow water when the form of a solitary wave is approached. Suppose that the velocity near the bottom, instead of being simply harmonic is given by an expression of the form

$$u_{\infty} = A_1 \cos(\sigma t - kx) + A_2 \cos 2(\sigma t - kx) + \dots \\ + B_2 \sin 2(\sigma t - kx) + \dots$$

in which the coefficients may be deduced theoretically or found from observation by Fourier analysis. Then the above expression gives

$$U_{\infty} = \frac{\int}{4c} (A_1^2 + A_2^2 + \dots + B_2^2 + B_3^2 + \dots). \quad (20)$$

Although the mass-transport velocity just outside the layer has been shown to be independent of y , eqn. (2) shows that the distribution of the velocity within the layer is certainly dependent on the form of the viscosity. For this reason the expression (17) for the maximum velocity within the layer may not be valid for a turbulent layer.

However, what is observed in practical experiments is less likely to be the maximum velocity than the velocity just outside the layer, where the velocity gradients are less steep - especially if the boundary layer is thus and observations are made with streaks of dye. For, a slender tongue of dye is less easy to observe than a diffused cloud moving forwards with a relatively uniform velocity. It is fortunate that the latter velocity appears to be more easily predictable.

(5) Proof of eqn. (10) Finally shall prove our statement that eqn. (10) is true independently of the viscosity. Although the argument can at some length be translated into physical terms, it is simpler at this stage to give an analytical proof.

We start from eqn. (2) and (9), which are both valid even when the viscosity is a function of time and position. From (2) we have by integration with respect to t ,

$$u = u_{\infty} + \int \frac{\partial}{\partial y} \left(\nu \frac{\partial u}{\partial y} \right) dt$$

and therefore

$$\overline{uv} - (\overline{uv})_{\infty} = \overline{u_{\infty}v} + \overline{\int \frac{\partial}{\partial y} \left(\nu \frac{\partial u}{\partial y} \right) dt \cdot v} - (\overline{uv})_{\infty}.$$

COASTAL ENGINEERING

Now from the equation of continuity

$$\frac{\partial v}{\partial y} = - \frac{\partial u}{\partial x} = \frac{1}{c} \frac{\partial u}{\partial t}$$

and so

$$\overline{u_{\infty} v} - (\overline{u v})_{\infty} = \int_{\infty}^y \overline{u_{\infty} \frac{\partial v}{\partial y}} dy = \frac{1}{c} \int_{\infty}^y \overline{u_{\infty} \frac{\partial u}{\partial t}} dy$$

where the limit ∞ denotes a value of y large compared with δ but small compared with the wavelength or total depth. On substituting for $\partial u / \partial t$ from eqn. (2) we have

$$\overline{u_{\infty} v} - (\overline{u v})_{\infty} = \frac{1}{c} \int_{\infty}^y \overline{u_{\infty} \left[\frac{\partial u}{\partial t} + \frac{\partial}{\partial y} \left(v \frac{\partial u}{\partial y} \right) \right]} dy = \frac{1}{c} \overline{u_{\infty} v \frac{\partial u}{\partial y}}$$

since $\overline{u_{\infty} \partial u_{\infty} / \partial t}$ is identically zero. Further, if f and g denote any two periodic quantities then

$$\overline{f \frac{\partial g}{\partial t}} + \frac{\partial \overline{f g}}{\partial t} = \frac{\partial}{\partial t} (\overline{f g}) = \frac{1}{T} (\overline{f g})_{t_0}^{t_0+T} = 0 \quad (21)$$

and so in any averaged product of this type the operator $\partial / \partial t$ may be transferred from one member to the other, provided the sign is reversed at the same time. Thus for example

$$\overline{\frac{\partial}{\partial y} \left(v \frac{\partial u}{\partial y} \right) dt} \cdot v = - \frac{\partial}{\partial y} \left(v \frac{\partial u}{\partial y} \right) \int v dt.$$

On substituting these results in eqn. (9) we obtain

$$\overline{v \frac{\partial u}{\partial y}} = \frac{1}{c} \overline{u_{\infty} v \frac{\partial u}{\partial y}} - \frac{\partial}{\partial y} \left(v \frac{\partial u}{\partial y} \right) \int v dt. \quad (22)$$

We assume that the viscosity is constant following a particle but is a function $N(Y)$ of the mean height Y of the particle above the bottom, then at any fixed point (x, y) the viscosity will be a slightly varying function of the time. To the first approximation

$$v(x, y, t) = N(Y) - \frac{dN}{dY} \Delta y = N - \frac{dN}{dY} \int v dt.$$

Substituting in (22) and neglecting third-order terms we have

$$\left(N - \frac{dN}{dY} \int v dt \right) \frac{\partial u}{\partial y} = \frac{1}{c} N u_{\infty} \frac{\partial u}{\partial y} - \left(N \frac{\partial^2 u}{\partial y^2} + \frac{dN}{dY} \frac{\partial u}{\partial y} \right) \int v dt.$$

The terms involving dN/dY cancel, and on dividing through by N , which is a function of Y only, we obtain

$$\frac{\partial \bar{u}}{\partial y} = \frac{1}{c} \overline{u_{\infty} \frac{\partial u}{\partial y}} - \frac{\partial^2 \bar{u}}{\partial y^2} \int v dt.$$

This relation is entirely free from N . The last term can be written as

$$- \frac{\partial}{\partial y} \left(\frac{\partial u}{\partial y} \int v dt \right) + \frac{\partial u}{\partial y} \int \frac{\partial v}{\partial y} dt,$$

AN EXPERIMENTAL INVESTIGATION OF DRIFT PROFILES
IN A CLOSED CHANNEL

and since

$$\overline{\frac{\partial u}{\partial y} \int \frac{\partial v}{\partial y} dt} = \overline{\frac{\partial u}{\partial y} \int \frac{1}{c} \frac{\partial u}{\partial t} dt} = \frac{1}{c} \overline{\frac{\partial u}{\partial y} u} = \frac{1}{2c} \frac{\partial}{\partial y} \overline{u^2}$$

we have

$$\frac{\partial \bar{u}}{\partial y} = \frac{1}{c} \overline{u_{as} \frac{\partial u}{\partial y}} + \frac{1}{2c} \frac{\partial}{\partial y} \overline{u^2} - \frac{\partial}{\partial y} \left(\overline{\frac{\partial u}{\partial y} \int v dt} \right).$$

On integrating from $y=0$, where u and v vanish, we find eqn. (10)

Since the relation (12) between U and \bar{u} is purely kinematical, it follows that eqn. (14) and (15) also are independent of N .

ADDITIONAL REFERENCES

- (5) Lamb, H. *Hydrodynamics*, 6th ed. Cambridge U. Press, 1932.
- (6) Clauser, F. H. The turbulent boundary layer. *Advances in Applied Mechanics*, Vol. 4, pp.1-51, New York, Academic Press, 1956.

Reprinted without change of pagination from the
Journal of Fluid Mechanics, volume 8, part 2, pp. 293-306, 1960

Mass transport in the boundary layer at a free oscillating surface

By M. S. LONGUET-HIGGINS

National Institute of Oceanography, Wormley, Surrey

(Received 24 November 1959)

In a previous paper (1953*b*) it was shown theoretically that just below the boundary layer at the surface of a free wave the mass-transport gradient should be exactly twice that given by Stokes's irrotational theory. The present paper describes careful experiments which confirm the higher value of the gradient.

The results have an implication for any oscillatory boundary layer at the free surface of a fluid; such a boundary layer must generate a second-order mean vorticity which diffuses inwards into the interior of the fluid.

1. Introduction

Although it was Stokes (1847) who first theoretically predicted the existence of a mean forwards velocity of the particles (mass transport) in a water wave, only since the experimental work of Bagnold (1947) has it been realized that the mass-transport velocities may be very different quantitatively from those given by Stokes's irrotational theory. For example, Bagnold observed a strong forwards 'jet' close to the bottom, a phenomenon unaccountable on the hypothesis of irrotational motion. The whole distribution of the mass transport is in fact strongly influenced by viscous boundary layers both at the bottom and at the free surface, as was shown by the present author (1953*b*; this paper will be referred to as (I)).

The boundary-layer theory of (I) yielded two surprising results; first, that just above the boundary layer at the bottom the forward mass-transport velocity is independent of the viscosity and has the value

$$U_1 = \frac{5}{4} \frac{a^2 \sigma k}{\sinh^2 kh}, \quad (1.1)$$

where a denotes the amplitude of the waves at the surface, $2\pi/\sigma$ the wave period, $2\pi/k$ the wavelength and h the mean depth. This value is quite different from that obtained on the non-viscous theory of Stokes (1847).*

Secondly, just below the boundary layer at the *free surface* the vertical gradient of the mass-transport velocity is given by

$$\frac{\partial U}{\partial z} = -4a^2 \sigma k^2 \coth kh, \quad (1.2)$$

* Stokes's theory is given partially in Lamb's *Hydrodynamics* (1932, Ch. 9); the mass-transport velocity is there derived only in the case of deep water ($kh \gg 1$).

z being measured vertically downwards. This is also independent of the viscosity and moreover is exactly twice the value given by Stokes.

The value (1.1) has been well verified by the recent experimental studies of Vincent & Ruellan (1957), Russell & Osorio (1958) and Allen & Gibson (1959), though with a considerable scatter of observations in the last case.*

On the other hand no careful verification has yet been attempted of the gradient (1.2), which may be no less important in determining the distribution of mass transport throughout the fluid. Partly, no doubt, this is due to the greater experimental difficulty in making measurements close to a moving surface, and partly also to the weak stability of the motion near the surface, which can be easily disturbed by external influences, as will be explained in § 4.

Our purpose is to describe some experiments designed to measure the velocity gradient near the free surface. These do in fact confirm equation (1.2) as against Stokes's prediction.

The opportunity is taken to correct a theoretical calculation of Harrison (1908) on the same subject. Harrison's corrected calculation leads also to equation (1.2) but over a more restricted range of the amplitude a .

The validity of (1.2) implies that a second-order vorticity is generated by the oscillatory boundary layer and is diffused inwards into the fluid, as described in § 5 below. Moreover, a similar phenomenon must occur in any fluid motion where there is a free oscillating boundary, even though the mean velocity is zero to the first order. The value of the vorticity ω generated by any free surface in this way is given by equation (6.12).

2. Theory of the boundary layer

A general theory for an oscillating free boundary has been given in § 8 of (I). Here we shall present a simplified version, relying however on (I) for some of the results quoted.

On account of the thinness of the boundary layer in relation to the usual amplitude of the waves it is desirable to take co-ordinates (s, n) measured along and normal to the free surface itself (and therefore moving with the fluid). The co-ordinate n is supposed to be directed normally inwards into the fluid. In the notation of (I) the components of velocity tangential and normal to the surface are written q_s, q_n and these are related to the stream function ψ by

$$(q_s, q_n) = \left(\frac{\partial \psi}{\partial n}, -\frac{1}{\eta} \frac{\partial \psi}{\partial s} \right), \quad (2.1)$$

where $\eta = 1 - n\kappa$ and κ denotes the curvature of the surface. The vorticity is equal to $\nabla^2 \psi$ where

$$\nabla^2 \equiv \frac{1}{\eta} \left[\frac{\partial}{\partial s} \left(\frac{1}{\eta} \frac{\partial}{\partial s} \right) + \frac{\partial}{\partial n} \left(\eta \frac{\partial}{\partial n} \right) \right]. \quad (2.2)$$

* Vincent & Ruellan, as well as Allen & Gibson, actually compared their observations with the predicted *maximum* velocity in the boundary layer, which is about 10% greater than (1.1).

An extension of the result (1.1) to the case of turbulent flow is given by the author in an appendix to the paper of Russell & Osorio (1958).

It is supposed that q_s , q_n and ψ can be expanded asymptotically in the series

$$\left. \begin{aligned} q_s &= \epsilon q_{s1} + \epsilon^2 q_{s2} + \dots, \\ q_n &= \epsilon q_{n1} + \epsilon^2 q_{n2} + \dots, \\ \psi &= \epsilon \psi_1 + \epsilon^2 \psi_2 + \dots, \end{aligned} \right\} \quad (2.3)$$

where ϵ is a small parameter which may tend to zero and where the mean values of q_{s1} , q_{n1} are identically zero. The mass-transport velocity is then shown in (I) § 6 to be of order ϵ^2 ; its stream function is denoted by $\epsilon^2 \Psi$.

The case when the stresses vanish at the surface $n = 0$ is included in the discussion in (I) § 8. By applying a 'boundary-layer' approximation it is shown that ψ_1 satisfies the differential equation

$$\left(\frac{\partial}{\partial t} - \nu \frac{\partial^2}{\partial n^2} \right) \nabla^2 \psi_1 = 0. \quad (2.4)$$

Assuming that the tangential stress at the surface vanishes we have the boundary condition

$$\nabla^2 \psi_1 = -2 \frac{\partial q_{n1}}{\partial s} \quad (n = 0) \quad (2.5)$$

(derived from (220) of (I) by setting $p_{ns}^{(0)} = 0$ and $\kappa_0 = 0$). When the motion is simple-harmonic with angular frequency σ the appropriate solution of (2.4) and (2.5) is

$$\nabla^2 \psi_1 = -2 \frac{\partial q_{n1}^{(0)}}{\partial s} e^{-\alpha n}, \quad (2.6)$$

where $q_{n1}^{(0)}$ denotes the value of q_{n1} at $n = 0$ and

$$\alpha = \frac{1+i}{\delta}, \quad \delta = (2\nu/\sigma)^{\frac{1}{2}}. \quad (2.7)$$

It is understood that in (2.6) the real part of the right-hand side is to be taken. So the first-order vorticity $\nabla^2 \psi_1$ vanishes exponentially inwards, in a distance of order δ .

The differential equation satisfied by Ψ is given by (211) of (I) (in which V_{s1} is to be set equal to zero). We have

$$\frac{\partial^4 \Psi}{\partial n^4} = 4 \int \overline{\frac{\partial^2}{\partial n^2} \nabla^2 \psi_1 dt} \frac{\partial q_{s1}^{(0)}}{\partial s}, \quad (2.8)$$

where a bar denotes mean values with respect to the time. On integrating from outside the boundary layer, where $\partial^3 \Psi / \partial n^3$ is assumed to be relatively small, we have

$$\frac{\partial^3 \Psi}{\partial n^3} = 4 \int \overline{\frac{\partial}{\partial n} \nabla^2 \psi_1 dt} \frac{\partial q_{s1}^{(0)}}{\partial s}. \quad (2.9)$$

At the free surface $n = 0$, the boundary condition for Ψ is that

$$\frac{\partial^2 \Psi}{\partial n^2} = 0 \quad (n = 0) \quad (2.10)$$

(see equation (218) of (I)), and so from (2.9) and (2.10)

$$\frac{\partial^2 \Psi}{\partial n^2} = 4 \int \overline{(\nabla^2 \psi_1)^2 dt} \frac{\partial q_{s1}^{(0)}}{\partial s}. \quad (2.11)$$

In the case of simple-harmonic motion, when $\nabla^2\psi_1$ is given by (2.6) we have

$$\frac{\partial^2\Psi}{\partial n^2} = \frac{4}{i\sigma} \frac{\partial q_{n1}^{(0)}}{\partial s} \frac{\partial q_{s1}^{(0)*}}{\partial s} (1 - e^{-2n}), \quad (2.12)$$

where a star denotes the complex conjugate quantity and the real part of the product is to be taken. Hence, just beyond the boundary layer ($n \gg \delta$) we have

$$\frac{\partial^2\Psi}{\partial n^2} = \frac{4}{i\sigma} \frac{\partial q_{n1}^{(0)}}{\partial s} \frac{\partial q_{s1}^{(0)*}}{\partial s} \quad (n \gg \delta), \quad (2.13)$$

a value independent of the viscosity.

Now in the case of progressive gravity waves in water of uniform depth the orbital velocities at the surface are given by

$$\left. \begin{aligned} \epsilon q_{s1}^{(0)} &= a\sigma \coth kh e^{i(\sigma t - ks)}, \\ \epsilon q_{n1}^{(0)} &= ia\sigma e^{i(\sigma t - ks)}, \end{aligned} \right\} \quad (2.14)$$

approximately, so that (2.12) and (2.13) become

$$\epsilon^2 \frac{\partial^2\Psi}{\partial n^2} = 4a^2\sigma k^2 \coth kh (1 - e^{-2n/\delta}) \cos n/\delta \quad (2.15)$$

and

$$\epsilon^2 \frac{\partial^2\Psi}{\partial n^2} = -4a^2\sigma k^2 \coth kh \quad (u \gg \delta). \quad (2.16)$$

Since $\epsilon^2 \partial^2\Psi/\partial n^2$ is equal to the mean tangential component of mass transport ((I), § 6) and since n is approximately vertical, equation (2.16) is equivalent to (1.2).

As already remarked, this result represents exactly twice the gradient given by the irrotational theory of Stokes (1847).

3. Digression on a result of Harrison

It was pointed out to me by Professor P. S. Eagleson that a conclusion apparently different from the above was obtained by Harrison (1908). Harrison's method consisted of a direct expansion of the equations of motion and boundary conditions in terms of rectangular co-ordinates (x, z). This method has the disadvantage of being valid only for waves whose amplitude a is small compared with the thickness δ of the boundary layer. Nevertheless, since the range of validity of equation (2.16) certainly includes such small amplitudes, one would expect Harrison's result to agree with equation (2.16) over the restricted range.

Another formal difference between Harrison's solution and ours is that we have assumed the motion to be periodic in time, whereas Harrison allows for a slight exponential decrement proportional to $\nu k^2 t$. It can, however, be shown that such a slight decrement, or one proportional to $(\nu/\sigma)^{\frac{1}{2}} k^2 x$, does not affect the boundary-layer theory outlined in § 2.

Translated into our notation, Harrison's expression for the elevation of the free surface in waves on deep water is

$$\begin{aligned} -z &= a e^{-2\nu k^2 t} \cos(kx - \sigma t) \\ &+ a^2 k e^{-4\nu k^2 t} \left[\frac{1}{2} \cos 2(kx - \sigma t) - k(\nu^2/4gk)^{\frac{1}{2}} \sin 2(kx - \sigma t) \right] \end{aligned} \quad (3.1)$$

and for the mass-transport velocity (p. 115)

$$\begin{aligned}
 U = & a^2 \sigma k e^{-4\nu k^2 z} \\
 & \times \{e^{-2kz} + \frac{1}{2} k \delta \{4(\cos z/\delta - \sin z/\delta) e^{-(k+\delta^{-1})z} - \sin 2kz\} \\
 & + \nu k^2 / \sigma \{4 \sin z/\delta e^{-(k+\delta^{-1})z} - 3e^{-2z/\delta}\}] \quad (3.2)
 \end{aligned}$$

terms of higher order in ν being neglected. (Harrison's $\beta, \lambda, \mu, p, y$ are equivalent to our $a, \delta^{-1}, \delta^{-1}, -\sigma, -z$.) On differentiation with respect to z this gives us for the terms of highest order

$$\frac{\partial U}{\partial z} = -2a^2 \sigma k^2 (1 - 2e^{-z/\delta} \cos z/\delta) \quad (3.3)$$

which is not in agreement with (2.15). (The slight exponential decrement $e^{-4\nu k^2 z}$ is ignored.)

An examination of Harrison's analysis reveals the source of the discrepancy. For his second boundary condition on p. 111 he has assumed that the stress component p_{xy} vanishes at the free surface. This is incorrect, for in fact it is not p_{xy} but p_{ns} which must vanish, and the two differ by the second-order quantity

$$4\mu \frac{\partial \eta}{\partial x} \frac{\partial^2 \psi}{\partial x \partial y} \quad (3.4)$$

where $z = -\eta$ denotes the equation of the free surface. Hence to the left-hand side of his equation (12) should be added a term

$$2pk^2 \beta^2 e^{2a t} \quad (3.5)$$

This would add to his expression for U on p. 115 a term

$$-pk\beta^2 \sin 2ky e^{2a t}, \quad \sim -a^2 \sigma k e^{-4\nu k^2 z} \sin 2kz, \quad (3.6)$$

whence the gradient of U , for values of z comparable with δ , would be

$$\frac{\partial U}{\partial z} = -2a^2 \sigma k^2 (2 - 2e^{-z/\delta} \cos z/\delta) \quad (3.7)$$

in agreement with (2.15).

Doubtless the reason why Harrison overlooked his algebraical slip was that it happens by chance to bring the value for $(\partial U/\partial z)_{z \gg \delta}$ into exact agreement with the irrotational theory of Stokes, as might at first sight have been expected.

4. Observations

The actual measurement of velocity gradients near the free surface is a somewhat delicate matter owing not only to the movement of the surface itself but to the external influences by which it is easily affected. The presence of grease or other impurity in the form of a thin surface film may completely alter the gradient by restricting the free tangential motion of the particles and producing a forwards jet, as in the boundary layer at the bottom. Turbulent currents in the air may have a disturbing influence; and very slight temperature changes can produce strong velocity gradients associated with density currents; for if the length of the tank or wave system is restricted, the forwards mass transport at

one level must be compensated by a backwards flow at other levels; hence any temperature stratification will tend to intensify the horizontal shearing.

Further, the presence of obstacles in the water, even the vertical walls of a measuring tank, will alter the distribution of mass transport in the neighbourhood. The observations must therefore be made far enough from such obstacles for their effect to be negligible.

Lastly, it is extremely important to ensure that the wave motion is purely sinusoidal. In relatively deep water, for example ($\coth kh \neq 1$) equation (1.2) shows that $\partial U/\partial z$ is proportional to $a^2\sigma k^2$, that is to σ^5 since $\sigma^2 \doteq gk$. If any second harmonic, of amplitude a' , is present in the wave motion its effect on the velocity gradient will be in the ratio

$$32a'^2/a^2. \quad (4.1)$$

Even if a'/a is as little as 1/10 this will be sufficient to increase the observed velocity gradient by 32%. In shallow water waves, however, the relative effect is correspondingly less.

For the purpose of the experiments the wind-wave tank at the Hydraulics Research Station, Wallingford, was kindly made available. A full description of the apparatus is given in the paper by Russell & Osorio (1958). The tank is 185 ft. long, 4 ft. wide and has a maximum depth of 22 in. The wave generator is of a paddle type with a fixed or movable hinge at the bottom. The wave absorber consists of a shingle beach, at a slope of about 1 in 10. All the present observations were made from the centre window of the tank, which is about 90 ft. from the wave generator. The tank is covered, and is fitted with a fan capable of drawing air over the surface in the direction of the beach, at a mean speed of about 25 ft./s.

In preliminary trials of the wavemaker it was found that on switching off the motor, and after the main group of waves had passed the point of observation half-way down the tank, there persisted a train of waves of twice the frequency but of smaller amplitude, until their group-velocity in turn has carried them past the point of observation. The existence of this second harmonic was attributed to the form of linkage used in the wave generator which had in fact been designed so as to increase the velocity of the forward stroke compared with that of the backward stroke. The linkage was therefore modified with the result that the amplitude of the second harmonic at the point of observation was reduced to about 4% of that of the first harmonic. The error corresponding to (4.1) was thus reduced to about 5%.

Method of observation

A grid of lines was drawn (see figure 1) at an angle $\tan^{-1} 2$ to the vertical, and was attached to a metal sheet on the far side of the tank, in the plane of motion. A drop of black ink (Waterman's ink, diluted 3:1) was let fall from a syringe at a height of about 18 in. above the surface, between the viewer and the grid of lines. The drop penetrated about 1 cm below the surface, leaving a nearly vertical streak. Owing to the velocity gradient the streak gradually became inclined (figure 1), and the time τ taken for its mean inclination to become parallel to

the grid of lines was measured with a stop-watch. The velocity gradient was then taken to be

$$\frac{\partial U}{\partial z} = \frac{2}{\tau}. \quad (4.2)$$

The height $2a$ of the waves was measured against a grid on the near window of the tank, and the wave period was measured over 20 cycles with a stop-watch.

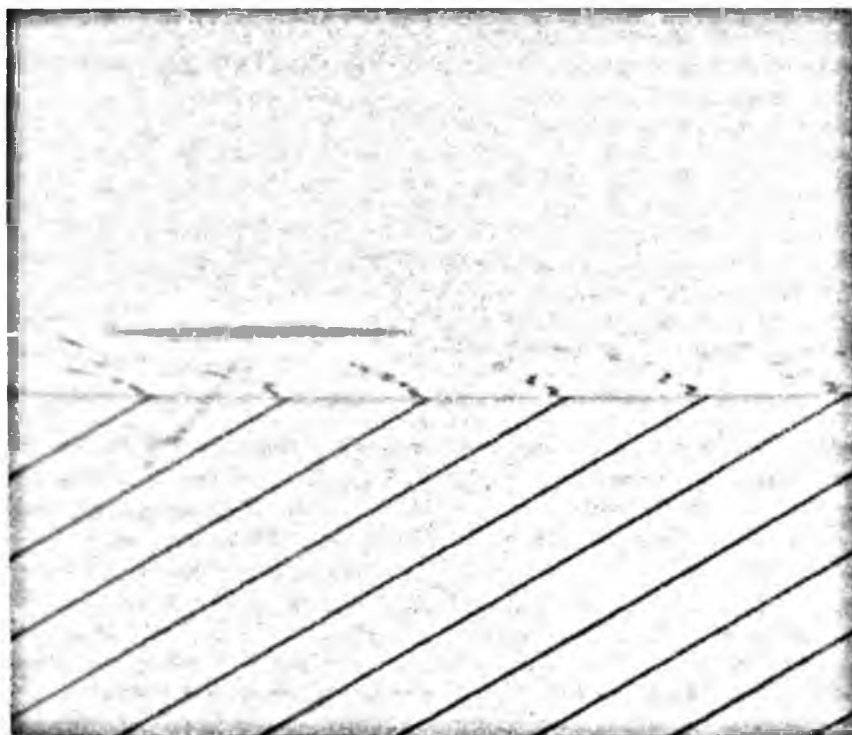


FIGURE 1. A photograph taken through the window of the tank from a point just below the surface of the wave. This shows the streak left by a drop of dilute ink, inclined after the passage of a few waves. (Some ink is left on the surface.) The lines in the background were drawn at an angle $\tan^{-1} 2$ to the vertical. The vertical separation of the lines was $\frac{1}{2}$ in.

Precautions

It was found that a thin film of oil or grease was nearly always present on the surface. In order to remove this, the fan was switched on for about 15 min, so that the surface film was driven up to the far end of the tank. Without further precautions the film would quickly have returned and covered the surface of the tank (at a rate of several cm/s). Accordingly, when the wind ceased a plastic curtain was immediately inserted in the tank at about 15 ft. from the beach. This prevented the return of the surface film, while allowing the transmission of waves from the generator to the beach.

The vigorous action of the wind also had the effect of thoroughly stirring the water, so that suspended particles were observed to be carried quickly from near

the bottom to the surface and back again. In this way any temperature gradient present in the tank was temporarily destroyed.

After switching off the wind, a period of 30–45 min was allowed for the tank to become quiet again, until a drop of ink or dye inserted in the water showed that the velocity gradients were negligible. The wave generator was then started and allowed to run for 5 min before observations were begun. This period gave time for the vorticity generated in the boundary layer to penetrate at least the upper 5 mm below the free surface (see § 5 below). Only those observations were

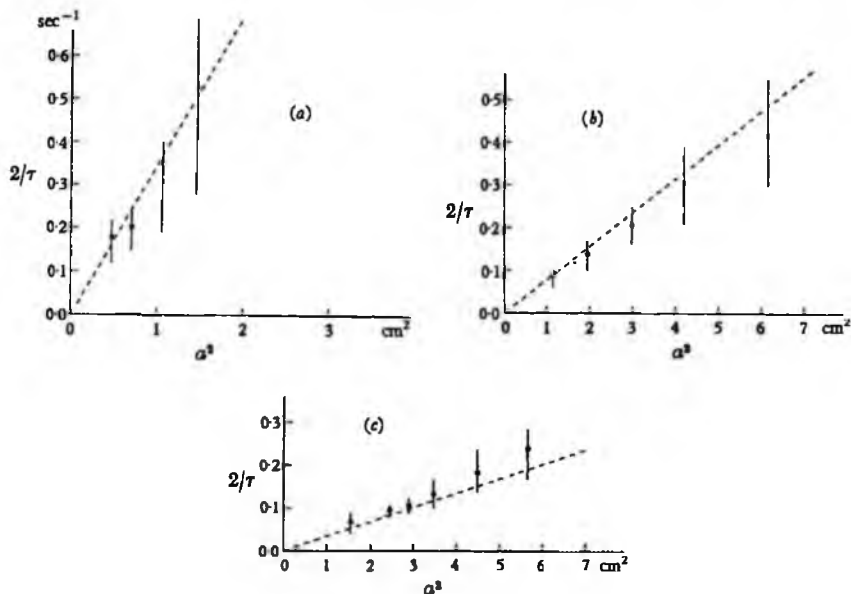


FIGURE 2. Results of observations at three different wave periods:
(a) $kh = 2.81$, (b) $kh = 1.54$, (c) $kh = 1.06$.

accepted in which the ink trace was initially vertical and remained in a practically straight line from 2 to 10 mm below the surface. At each run, ten acceptable observations were recorded: these were completed between 5 and 15 min after switching on the wave generator.

The choice of parameters for the experiments was limited: first, by the design of the wavemaker, which could not run safely at periods much less than 0.7 sec; secondly, by the method of observation, which is satisfactory only if the time of observation τ contains a sufficient number of wave cycles (about 10), for otherwise it is hard for the observer to judge accurately the moment when the mean inclination of the ink trace becomes parallel with the grid of lines; thirdly, by the presence of very weak gradients due to turbulent air movements and to residual effects of the stirring process described above: these last set the lower limit to the observed gradients.

Finally, three periods were chosen: $T = 0.65, 0.925$ and 1.20 sec corresponding to $kh = 2.81, 1.54$ and 1.06 , respectively, and a number of runs were made at

different amplitudes a , while the wave period was kept constant. The mean depth h was kept at 29.7 cm throughout the experiments.

The observed results are shown in figure 2, plotted in each case against the square of the wave amplitude a^2 . At each wave period, according to equation (1.2) the plotted points would be expected to lie on a straight line through the origin, as has been indicated in the figure. Each plotted point represents the mean of just ten consecutive observations, and the vertical lines through the points represent the total range of the same ten observations.

The most obvious feature of the results is the very wide scatter of observations, but this is in fact not much greater than would be expected considering the method of observation. It is perhaps puzzling that in figures 2(a) and (b) the mean values tend to lie slightly below the theoretical value while in figure 2(c) they lie somewhat above it; but this could be brought about by quite a small error in the measurement of wave period.

Two fairly definite conclusions may be drawn: (1) over the ranges of T , a and kh covered by the experiments the velocity gradient does tend to increase proportionally to a^2 approximately; and (2) the constant of proportionality is not far from that given by equation (1.2), and is certainly closer to (1.2) than to half this value.

5. Consequences for the interior of the fluid

Some implications of these results for the motion in the main body of the fluid may be briefly mentioned here.

Before the waves are started the vorticity is everywhere zero, and since vorticity cannot be generated within the fluid it follows that immediately after starting the waves the motion *beyond* the boundary layer is irrotational and will be given by Stokes's theory approximately. The difference between (1.2) and Stoke's value corresponds to a vorticity

$$\omega = -2a^2\sigma k^2 \coth kh, \quad (5.1)$$

which can be regarded as having been generated in the boundary layer itself, that is, within a distance of order $(\nu/\sigma)^{\frac{1}{2}}$ from the free surface. This vorticity will then begin to diffuse into the interior of the fluid.

Now it was shown in (I) that in a quasi-steady (that is, perfectly periodic) state of motion the vorticity ω in the interior of the fluid ($n \gg (\nu/\sigma)^{\frac{1}{2}}$) satisfies the equation

$$\mathbf{U} \cdot \nabla \omega - \nu \nabla^2 \omega = 0, \quad (5.2)$$

where \mathbf{U} denotes the mass-transport velocity.* The first term in (5.2) represents the transport of vorticity by convection with the mass-transport velocity, and the second term represents the transport of vorticity by viscous conduction. This result might also be expected on physical grounds (cf. Lamb 1932, §328); the motion being two-dimensional, there is no stretching of the vortex lines.

Before the vorticity in the interior is fully established the motion is not

* ω is of second order; the first-order vorticity vanishes in the interior; see (I), equation (50).

exactly periodic beyond the first order; but similar arguments suggest that the differential equation governing the distribution of vorticity in the interior is

$$\frac{\partial \omega}{\partial t} + \mathbf{U} \cdot \nabla \omega - \nu \nabla^2 \omega = 0. \quad (5.3)$$

In a regular progressive wave the mass-transport velocity is almost horizontal, apart from effects at the ends of tank. Any decrease in amplitude with distance also produces small vertical mass transports, but since the third term in (5.3) initially predominates near the surface it can be seen that most of the transport of vorticity in the layers nearest the free surface will take place by viscous 'conduction'.

Thus the equation governing the initial distribution of the vorticity just beyond the boundary layer is

$$\frac{\partial \omega}{\partial t} = \nu \nabla^2 \omega = \nu \frac{\partial^2 \omega}{\partial z^2}. \quad (5.4)$$

The solution of this equation with initial conditions

$$\omega = \begin{cases} 0, & z = 0, \quad t < 0, \\ \omega_0, & z = 0, \quad t > 0, \end{cases} \quad (5.5)$$

is well known:

$$\omega(z, t) = \frac{2\omega_0}{\sqrt{\pi}} \int_{z/2(\nu t)^{1/2}}^{\infty} e^{-\theta^2} d\theta, \quad (5.6)$$

which may also be written

$$1 - \frac{\omega}{\omega_0} = \frac{2}{\sqrt{\pi}} \int_0^Z e^{-\theta^2} d\theta \equiv f(Z), \quad (5.7)$$

where

$$Z = \frac{z}{2(\nu t)^{1/2}}. \quad (5.8)$$

For a fixed value of z , as $t \rightarrow \infty$ so $Z \rightarrow 0$ and $f(Z) \rightarrow 0$; hence $\omega \rightarrow \omega_0$. The following table gives some typical values of $f(Z)$

$2Z$	$f(Z)$
0.0018	0.001
0.0035	0.002
0.0089	0.005
0.0177	0.01
0.0355	0.02
0.095	0.05
0.178	0.01

Thus to ensure that the vorticity is within 10% of its value ω_0 at $z = 0$ we must have

$$\frac{z}{(\nu t)^{1/2}} \leq 0.178. \quad (5.9)$$

Taking $\nu = 0.013 \text{ cm}^2/\text{s}$ and $t = 5 \text{ min}$ we find $z \leq 0.47 \text{ cm}$.

However, the *mean* value of ω between 0 and z , defined by

$$\frac{\omega_{\text{mean}}}{\omega_0} = \frac{1}{Z} \int_0^Z f(Z) dZ, \quad (5.10)$$

is much closer to unity, as may be seen from the series expansion

$$\frac{\omega_{\text{mean}}}{\omega_0} = 1 - \frac{1}{\sqrt{\pi}} \left(Z - \frac{Z^3}{6} + \frac{Z^5}{30} - \frac{Z^7}{180} + \dots \right). \quad (5.11)$$

With the same values: $t = 5$ min, $z = 0.47$ cm, we find

$$\frac{\omega_{\text{mean}}}{\omega_0} = 0.950, \quad (5.12)$$

so that the mean velocity gradient in the upper 5 mm is within 5% of its ultimate value. It was this mean value which was measured in the experiments of § 4.

Generally, the width of the upper region influenced by the diffusion of vorticity from the oscillatory boundary layer will be of order $(\nu t)^{\frac{1}{2}}$, within the first few minutes. This region constitutes an outer 'boundary layer' of a different type from the oscillatory layer, the thickness of the latter being of order $(\nu T)^{\frac{1}{2}}$ only.*

At later times the fluid may be influenced by vorticity diffused in a similar way from the boundary layers at the bottom and sides of the tank. However, in most wave tanks it seems likely that the transport of vorticity by convection from the ends of the tank will intervene and ultimately predominate, so that conditions beyond the first few cm of fluid at the surface and bottom may depend somewhat on the type of wave generator or wave absorber which is used. The time required for vorticity to be convected from the ends of the tank through a distance x is clearly of order x/U . In the experiments described above this time was considerably greater than the time taken for the observations.

All the above predictions rely upon the assumption that the motion is laminar and the mass-transport current is predominantly horizontal and parallel to the wave velocity. Even slight winds may completely alter the character of the circulation (except near the bottom, where the motion is controlled by the bottom boundary layer). The possibility of the shearing motion becoming unstable of its own accord when the waves are sufficiently short and steep has also to be borne in mind. Indeed, this mechanism may contribute to the very marked turbulence that is present in all waves under the action of wind.

6. General implications

The analysis of § 2 shows that the effects just described are by no means peculiar to water waves, but will occur whenever there is an oscillatory fluid motion with a free boundary.

Thus from equation (2.11) we have just beyond the boundary, where $\nabla^2 \psi_1 \rightarrow 0$,

$$\frac{\partial^2 \Psi}{\partial n^2} = -4 \int \overline{(\nabla^2 \psi_1)_0} dt \frac{\partial q_{21}^{(0)}}{\partial s} \quad (n \gg \delta), \quad (6.1)$$

which combined with (2.5) becomes

$$\frac{\partial^2 \Psi}{\partial n^2} = 8 \int \overline{\frac{\partial q_{n1}^{(0)}}{\partial s} dt \frac{\partial q_{21}^{(0)}}{\partial s}} \quad (n \gg \delta). \quad (6.2)$$

* Harrison's solution for the interior (equation (3.2)) contains a term in $\sin kz$. It is hard to see how such a motion, not tending to zero as $z \rightarrow \infty$, could be realized in practice.

Since we are now dealing with the part of the fluid beyond the inner boundary layer, we may, to the present order in ϵ , replace the velocity q_{s1} , q_{n1} by $\partial\psi_1/\partial z$, $-\partial\psi_1/\partial x$, where (x, z) are rectangular co-ordinates tangential and normal to the mean boundary. Thus

$$\frac{\partial^2\Psi}{\partial z^2} = -8 \int \overline{\frac{\partial^2\psi_1}{\partial x^2} dt} \frac{\partial^2\psi_1}{\partial x \partial t}. \quad (6.3)$$

Since the mean boundary forms a streamline for the mass transport we must have also

$$\frac{\partial\Psi}{\partial x} = 0, \quad \frac{\partial^2\Psi}{\partial x^2} = 0, \quad (6.4)$$

so that the left-hand side of (6.3) can be replaced by $\nabla^2\Psi$. Now the mass-transport velocity is given in terms of ψ_1 and ψ_2 by

$$\Psi = \overline{\psi_2} + \int \overline{\frac{\partial\psi_1}{\partial z} dt} \frac{\partial\psi_1}{\partial x} \quad (6.5)$$

(see (I) § 3), and since by equation (85) of (I)

$$\nabla^2 \int \overline{\frac{\partial\psi_1}{\partial z} dt} \frac{\partial\psi_1}{\partial x} = -4 \int \overline{\frac{\partial^2\psi_1}{\partial x^2} dt} \frac{\partial^2\psi_1}{\partial x \partial z}, \quad (6.6)$$

it follows, on operating on both sides of (6.5) with ∇^2 , that

$$-8 \int \overline{\frac{\partial^2\psi_1}{\partial x^2} dt} \frac{\partial^2\psi_1}{\partial x \partial z} = \nabla^2 \overline{\psi_2} - 4 \int \overline{\frac{\partial^2\psi_1}{\partial x^2} dt} \frac{\partial^2\psi_1}{\partial x \partial z}. \quad (6.7)$$

Hence

$$\nabla^2 \overline{\psi_2} = -4 \int \overline{\frac{\partial^2\psi_1}{\partial x^2} dt} \frac{\partial^2\psi_1}{\partial x \partial z}. \quad (6.8)$$

This last expression, multiplied by ϵ^2 , represents the vorticity just in the interior of the fluid, for, beyond the boundary layer,

$$\nabla^2\psi_1 \rightarrow 0, \quad \nabla^2\psi_2 \rightarrow \nabla^2\overline{\psi_2} \quad (6.9)$$

(see (I) § 4) and therefore

$$\omega = \nabla^2\psi_2 \rightarrow \epsilon^2 \nabla^2 \overline{\psi_2} + \dots \quad (6.10)$$

Now write

$$\epsilon \frac{\partial\psi_1}{\partial z} = u, \quad -\epsilon \frac{\partial\psi_1}{\partial x} = w, \quad (6.11)$$

for the components of velocity tangential and normal to the mean position of the boundary (these differ from their corresponding values at the boundary by quantities of order ϵ^2). Our result can thus be written

$$\omega = 4 \overline{\frac{\partial u}{\partial x} \int \frac{\partial w}{\partial x} dt}. \quad (6.12)$$

In other words, the presence of the free boundary produces a mean vorticity in the interior given by (6.12). The modifications of this result needed to take account of any arbitrary tangential stresses applied at the surface may be deduced from the general formulae of (I) § 8.

It is interesting to note that so far as the distributon of mass transport in the interior is concerned the presence of the boundary is equivalent to a virtual stress

$$4\mu \frac{\partial u}{\partial x} \int \frac{\partial w}{\partial x} dt. \quad (6.13)$$

Since $\int w dt$ is equal to the surface elevation η , this last expression may be written

$$4\mu \frac{\partial u}{\partial x} \frac{\partial \eta}{\partial x} \quad (6.14)$$

which, as we saw in § 3, is equal to the difference between the stress components p_{xx} and p_{ns} . It is p_{ns} that vanishes and p_{xx} generally differs from zero on account of the tilting of the surface through an angle $\partial\eta/\partial x$. Thus we might say that the virtual stress (6.13) was due simply to the corrugation of the free surface; but this would be to neglect the structure of the boundary layer itself, throughout which the tangential stress, like the vorticity, is not uniform.

7. Conclusions

Our concluding picture is as follows. The periodic motion of the fluid produces in the first place boundary layers at both bottom and free surface whose thickness is of the order of $(\nu T)^{\frac{1}{2}}$, where ν denotes kinematic viscosity and T the period of the waves. In practical cases these oscillatory boundary layers have a thickness of only a few millimetres. But within the surface layer there is produced a second-order mean vorticity which, from the moment of starting the waves, begins to diffuse downwards into the fluid. After a time t the region affected by the vorticity is of order $(\nu t)^{\frac{1}{2}}$, provided t is not too great. This latter region may be thought of as a kind of outer boundary layer which finally may fill the whole fluid. Some vorticity may, however, be transported by convection as well as by viscous diffusion. Finally, the motion is no longer irrotational, but contains everywhere a second-order vorticity determined by the oscillatory layers at the boundaries.

I am indebted to the Director of the Hydraulics Research Station for permission to make use of the 185 ft. wind-wave tank there, and to Mr R. C. H. Russell and Mr F. A. Kilner for their interest and co-operation. The experiments described above were carried out with the assistance of Mr A. J. Bunting.

REFERENCES

- ALLEN, J. & GIBSON, D. H. 1959 Experiments on the displacement of water by waves of various heights and frequencies. *Min. Proc. Instn. Civ. Engrs*, **13**, 363-86.
- BAGNOLD, R. A. 1947 Sand movement by waves: some small-scale experiments with sand of very low density. *J. Inst. Civ. Engrs*, **27**, 447-69.
- HARRISON, W. J. 1908 The influence of viscosity and capillarity on waves of finite amplitude. *Proc. Lond. Math. Soc.* (2), **7**, 107-21.
- LAMB, H. 1932 *Hydrodynamics*, 6th ed. Cambridge University Press.
- LONGUET-HIGGINS, M. S. 1953a On the decrease of velocity with depth in an irrotational water wave. *Proc. Camb. Phil. Soc.* **49**, 552-60.
- LONGUET-HIGGINS, M. S. 1953b Mass transport in water waves. *Phil. Trans. A*, **245**, 535-81.

- RUSSELL, R. C. H. & OSORIO, J. D. C. 1958 An experimental investigation of drift profiles in a closed channel. *Proc. 6th Conf. on Coastal Engng, Miami*, 1957, pp. 171-93. Council on Wave Res., University of California, Berkeley.
- STOKES, G. G. 1847 On the theory of oscillatory waves. *Trans. Camb. Phil. Soc.* 8, 441-55; reprinted in *Math. Phys. Pap.* 1, 314-26.
- VINCENT, G. & RUELLAN, F. 1957 Contribution à l'étude des mouvements solides provoqués par la houle sur un fond horizontal. *Houille blanche*, B, 12, 605-722.
- VINCENT, G. 1958 Contribution to the study of sediment transport on a horizontal bed due to wave action. *Proc. 6th Conf. Coastal Engng, Miami*, 1957, pp. 326-55. Council on Wave Res., University of California, Berkeley.

Steady currents induced by oscillations round islands

By M. S. LONGUET-HIGGINS

Department of Applied Mathematics and Theoretical Physics, Silver Street, Cambridge,
and National Institute of Oceanography, Wormley, Surrey.

(Received 29 November 1969)

An oscillating current such as a tidal stream or an inertial oscillation may have a horizontal scale of the order of many times the local depth of water. Thus an island projecting from an otherwise uniform sea bed will give rise to a local, periodic disturbance near the island. It is shown that this disturbance may be resolved into two waves travelling in opposite senses round the island. If the particle orbits at large distances are circular, then only one of these waves has non-zero amplitude.

In addition to the oscillatory motion, however, there is a steady d.c. streaming, or mass-transport velocity, whose magnitude is of order $u^2/\sigma a$ where u denotes the magnitude of the oscillatory velocity at large distances, σ denotes the radian frequency, and a is the radius of the island. In this paper the profile of the streaming velocity is calculated for circular islands, with or without shoaling regions offshore. It is shown that resonance with the free modes trapped by the shoaling regions may greatly increase the streaming velocity. Viscosity (or horizontal mixing) also tends to increase the streaming velocity close to the shoreline.

The conclusions are supported by some simple model experiments. It is suggested that such streaming may partly account for the observed pattern of currents near Bermuda.

1. Introduction

The best-known example of a steady, rectified flow associated with an oscillatory motion is the mass-transport velocity in a progressive water wave, first discovered by Stokes (1847); (see also Longuet-Higgins 1953, 1960). It has been pointed out by Longuet-Higgins (1969*b*) that significant rectified flows are also to be expected in many types of long-period, oscillatory ocean currents, particularly in tides, internal waves and motions depending on bottom topography, such as double Kelvin waves.†

The aim of the present paper is to consider another topographic effect, the effect of an island which projects from the sea bed in an otherwise uniform, oscillating current.

Assuming the displacement in the initial oscillation to be small compared to

† Mass-transport in tidal flows was first considered by Hunt & Johns (1963). Pedlosky (1965), Robinson (1965, ch. 17, pp. 504-533) and Munk & Moore (1968) have suggested mass-transport effects in other types of current, but for a criticism of their analysis see Moore (1969).

the radius of the island, the first problem to be considered is the linear response of the fluid near the island to a forced oscillation in the ocean at large distances. This problem is solved in §2 below, for islands with vertical sides. For a circular island it is possible to evaluate the local disturbance caused by the island in very simple terms. Particularly, when the currents at large distances are inertial, it turns out that the disturbance is seen locally as a wave progressing anticlockwise round the island, in the northern hemisphere; the tangential velocity at the boundary is just double what it would be in the absence of the island.

The second-order currents associated with this flow are considered in §3. It is shown that the rectified flow outside a thin viscous boundary layer consists of a current circulating *anticlockwise* round the island and falling off rapidly with radial distance, like the inverse fifth power of the radius at first. But inside a thin viscous boundary layer, the mass-transport current is reinforced by viscosity. In fact the effect of viscosity is to multiply the non-viscous streaming velocity just beyond the boundary layer by a factor $\frac{5}{2}$ independent of ν . This effect is analogous to the effect of the viscous layer on the bottom in a progressive water wave (Longuet-Higgins 1953), experimentally verified by Allen & Gibson (1959) and others. After some time, the vorticity introduced by the viscous boundary layer diffuses outwards throughout the interior of the fluid, augmenting the initial circulation.

Some simple experiments to test this theoretical prediction are described in §4 of the present paper.

So far the discussion has referred to islands with vertical sides. On the other hand, when the island is surrounded by a shallow region or 'skirt', the possibility arises of free waves becoming trapped near the island, as was shown by Rhines (1969) in a particular case. Moreover, the amplitude of the forced oscillations may increase greatly near the resonant frequencies. In §5 we calculate both the amplitude of the forced oscillations and the magnitude of the steady mass-transport associated with them. Figure 6 is a typical plot of the relative magnification near the resonant frequencies. A simple model experiment is described in §6, in which oscillations were set up in a rotating basin containing islands of various shapes. Strong currents were observed to be circulating round the islands, consistent with the above predictions.

The possible connection of this phenomenon with the observed pattern of currents near Bermuda is discussed in §7.

2. Forced oscillations round a cylindrical island

We imagine an island with vertical sides, in an ocean of locally uniform depth h , in which there exists a large-scale system of oscillating currents. The latter may be inertial oscillations, tidal waves, planetary waves or other types of large-scale oscillation, and may be generated, for example, by tidal or atmospheric forces. The purpose of this section is to calculate the local effect of the island on this large-scale system of currents and in particular to find the form of the surface elevation at the edge of the island itself.

We shall suppose that the differential equation governing the surface elevation

ζ is the classical equation for long waves of small amplitude oscillating harmonically with radian frequency σ , in an ocean of uniform depth h and constant Coriolis parameter f , that is to say

$$\left(\nabla^2 + \frac{\sigma^2 - f^2}{gh}\right)\zeta = 0 \quad (2.1)$$

(see Lamb 1932). The associated current-vector \mathbf{u} is given by

$$\mathbf{u} = \frac{-g}{\sigma^2 - f^2} (i\sigma \nabla \zeta - \mathbf{f} \wedge \nabla \zeta), \quad (2.2)$$

where \mathbf{f} denotes the vertical vector of magnitude f . We assume that $\sigma^2 \neq f^2$, in general, but when it is appropriate we shall take the solutions to the limit as $\sigma \rightarrow \pm f$, bearing in mind that the limit may be singular.

Now for most applications, and certainly with islands of the dimensions of order 100 km the scale of the local disturbance will be exceedingly small compared to $\sqrt{(gh)}/f$. Since σ is assumed to be of the same order as f , it follows that in (2.1) the second term is negligible for practical purposes, and that ζ satisfies simply Laplace's equation,

$$\nabla^2 \zeta = 0. \quad (2.3)$$

In the present context (2.1) may be called the exact differential equation for ζ and (2.3) the approximate equation. A solution of the exact equation does exist representing waves trapped round a circular island (Longuet-Higgins 1969*a*). We shall find solutions to the approximate equation, and show that they do tend, in one case of special interest, to the corresponding exact solution.

Suppose first that we have a circular island of radius a . Let the rectangular components (u, v) of the current at large distances r from the centre of the island be given by

$$u = A e^{-i\sigma t}, \quad v = B e^{-i\sigma t}, \quad (2.4)$$

where A and B are complex constants. It is understood that the real part of the expressions on the right is to be taken. The radial and tangential components of velocity are then given by

$$\left. \begin{aligned} u_r &= u \cos \theta + v \sin \theta = C e^{i(\theta - \sigma t)} + D e^{-i(\theta + \sigma t)}, \\ u_\theta &= -u \sin \theta + v \cos \theta = iC e^{i(\theta - \sigma t)} - iD e^{-i(\theta + \sigma t)}, \end{aligned} \right\} \quad (2.5)$$

where $C = \frac{1}{2}(A - iB)$ and $D = \frac{1}{2}(A + iB)$. In other words, the motion can be formally separated into two component waves, one with complex amplitude C , rotating clockwise round the island (when $\sigma < 0$), the other with complex amplitude D , rotating anticlockwise.

To find the corresponding surface elevation we take (2.2) in the form,

$$\left. \begin{aligned} (\partial/\partial r)(g\zeta) &= i\sigma u_r + f u_\theta, \\ \frac{1}{r}(\partial/\partial \theta)(g\zeta) &= i\sigma u_\theta - f u_r, \end{aligned} \right\} \quad (2.6)$$

and assume that ζ vanishes at the origin. It follows that the surface elevation ζ_0 in the absence of the island is given uniquely by

$$g\zeta_0 = i(\sigma + f) C r e^{i(\theta - \sigma t)} + i(\sigma - f) D r e^{-i(\theta + \sigma t)}. \quad (2.7)$$

In inertial oscillations, ζ_0 vanishes. Such motion can be represented either by $C = 0$ and $\sigma = f$ or alternatively by $D = 0$ and $\sigma = -f$.

Now to take account of the presence of the island we add to (2.7) a surface elevation ζ_1 of the form,

$$g\zeta_1 = P(a^2/r) e^{i(\theta - \sigma t)} + Q(a^2/r) e^{-i(\theta + \sigma t)} \quad (2.8)$$

in which the constants P and Q are to be chosen so as to make the normal component of velocity vanish at the circumference $r = a$. Thus $\zeta = \zeta_0 + \zeta_1$ must satisfy

$$\left(i\sigma \frac{\partial \zeta}{\partial r} - \frac{f}{r} \frac{\partial \zeta}{\partial \theta} \right)_{r=a} = 0. \quad (2.9)$$

Hence
$$-(\sigma^2 - f^2)C - i(\sigma + f)P = 0, \quad (2.10)$$

with a similar equation for Q . Solutions of these equations are

$$P = -i(\sigma - f)C, \quad Q = -i(\sigma + f)D. \quad (2.11)$$

Therefore altogether we have

$$g\zeta = i[(\sigma + f)r - (\sigma - f)(a^2/r)] C e^{i(\theta - \sigma t)} + i[(\sigma - f)r + (\sigma + f)(a^2/r)] D e^{-i(\theta + \sigma t)}. \quad (2.12)$$

At the perimeter of the island this reduces to

$$g\zeta = 2ifa[C e^{i(\theta - \sigma t)} - D e^{-i(\theta + \sigma t)}]. \quad (2.13)$$

Thus if u_∞ denotes the transverse component of the velocity at infinity, the surface elevation at the edge of the island is simply given by

$$g\zeta = 2afu_\infty. \quad (2.14)$$

In the important case of inertial oscillations we take $D = 0$ and $\sigma \rightarrow -f$ in (2.12), giving

$$g\zeta = 2ifC(a^2/r) e^{i(\theta - \sigma t)}. \quad (2.15)$$

Thus, for inertial motions, the surface elevation progresses round the island in the clockwise sense, in the northern hemisphere. Since in this case ζ_0 vanishes, the surface elevation is given by ζ_1 , alone.

To find the components of velocity (u_r, u_θ) near the island, some care must be taken. The exact expressions

$$\left. \begin{aligned} u_r &= \frac{-1}{\sigma^2 - f^2} \left(i\sigma \frac{\partial}{\partial r} - \frac{f}{r} \frac{\partial}{\partial \theta} \right) g\zeta, \\ u_\theta &= \frac{-1}{\sigma^2 - f^2} \left(\frac{i\sigma}{r} \frac{\partial}{\partial \theta} + f \frac{\partial}{\partial r} \right) g\zeta \end{aligned} \right\} \quad (2.16)$$

may be used only when $\sigma^2 \neq f^2$. However, if we substitute in (2.16) from (2.12), we obtain in the general case,

$$\left. \begin{aligned} u_r &= \left(1 - \frac{a^2}{r^2} \right) [C e^{i(\theta - \sigma t)} + D e^{-i(\theta + \sigma t)}], \\ u_\theta &= i \left(1 + \frac{a^2}{r} \right) [C e^{i(\theta - \sigma t)} - D e^{-i(\theta + \sigma t)}]. \end{aligned} \right\} \quad (2.17)$$

It is remarkable that this solution is formally independent of the Coriolis parameter f and of the frequency σ . To find a solution for inertial motions we again let $D = 0$ and $\sigma = -f$ giving

$$\left. \begin{aligned} u_r &= \left(1 - \frac{a^2}{r^2}\right) C e^{i(\theta - \sigma t)}, \\ u_\theta &= i \left(1 + \frac{a^2}{r^2}\right) C e^{i(\theta - \sigma t)}. \end{aligned} \right\} \quad (2.18)$$

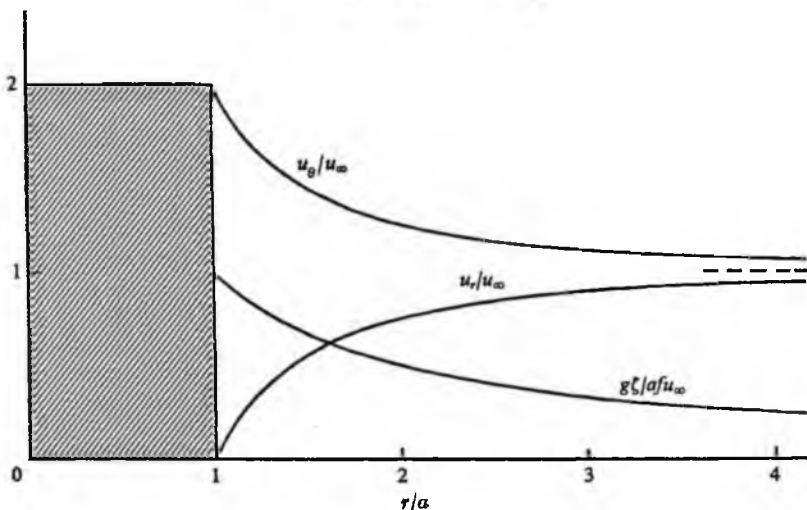


FIGURE 1. Graphs of the radial and tangential components u_r , u_θ of the orbital velocity in an oscillation in the neighbourhood of an island of radius a . The associated surface elevation is also shown.

These expressions for u_r , u_θ and ζ are illustrated in figure 1. At the circumference of the island equations (2.18) become simply

$$u_r = 0; \quad u_\theta = 2iC e^{i(\theta - \sigma t)}. \quad (2.19)$$

Comparing this with (2.5) we see that the presence of the island exactly doubles the transverse component of velocity at the perimeter.

It may be noted that (2.15) is also the first term in the asymptotic expansion of the *exact* solution of (2.1), namely,

$$g\zeta = 2ifC ka^2 K_1(k_r) e^{i(\theta - \sigma t)}, \quad (2.20)$$

where

$$k = \left(\frac{f^2 - \sigma^2}{gh}\right)^{\frac{1}{2}} \quad (\sigma^2 < f^2). \quad (2.21)$$

This represents a mode trapped exponentially at large distances from the island (Longuet-Higgins 1969*a*). Equation (2.15) is the limit of (2.20) when $af/\sqrt{gh} \rightarrow 0$. The expressions for the currents, (2.18), also correspond to (2.7) of the paper just referred to, if the constants in the factors $(1 \pm a^2/r^2)$ are replaced by terms varying only logarithmically with r .

Because in the present approximation the surface elevation ζ satisfies Laplace's equation (2.3) it is simple to extend these results to islands of other shape, by a conformal transformation. The boundary condition $\mathbf{u} \cdot \mathbf{n} = 0$ is transformed into the same condition at all non-singular points of the boundary, by (2.2). For example, the exterior of the elliptic island,

$$\frac{x^2}{a^2} + \frac{y^2}{b^2} = 1 \quad (a > b > 0), \quad (2.22)$$

having principal axes a and b , is transformed by the substitutor

$$\left. \begin{aligned} z &\equiv x + iy = \frac{1}{2}c \left(\lambda + \frac{1}{\lambda} \right), \\ \lambda &= \mu + i\nu, \\ c &= (a^2 - b^2)^{\frac{1}{2}}, \end{aligned} \right\} \quad (2.23)$$

into the exterior of the circle,

$$\mu^2 + \nu^2 = \frac{a+b}{a-b}. \quad (2.24)$$

Moreover, at infinite distance from the island, $z \sim \frac{1}{2}c\lambda$. So the corresponding expression for ζ is of the same form as for the circular island, but in terms of λ , not z . To obtain the corresponding expressions in terms of x and y we replace λ by that solution of the quadratic equation,

$$\lambda^2 + (2/c)z\lambda + 1 = 0, \quad (2.25)$$

which tends to infinity as $z \rightarrow \infty$. The expressions for the currents follow from the formula,

$$(u - iv) = \mathcal{R} \left\{ \frac{-g}{\sigma^2 - f^2} (i\sigma + f) \frac{d\zeta}{d\lambda} \frac{d\lambda}{dz} \right\}. \quad (2.26)$$

From this solution it can be shown that u , v and ζ are in antiphase at diametrically opposite points on the island, and that currents of near-inertial frequency are associated with a surface elevation which travels anticlockwise round the ellipse, as for the circle.

Similar transformations may be devised to cope with islands of more complicated shape. For *more* than one island (the 'archipelago problem'), extended techniques are available from potential theory. But in such a case variations of depth between the islands are likely to prove important also.

As suggested earlier (1969*a*), it is possible to understand the energy in the frequency-band centred on 0.73 c.p.d. at Oahu as the local manifestation of near-inertial currents on a wider scale surrounding the island. The observed phase difference of about 130° between Mokuoloe and Honolulu (Mokuoloe leading) can be interpreted as due to the tendency of the surface elevation to progress round the island in the clockwise direction. Although the angle subtended at the centre of the island by Mokuoloe and Honolulu is only about 40° , the difference may be explained by the tendency of some energy to be guided round the elongated ridge on which Oahu stands.

It should be stressed that motions of near-inertial frequency are not necessarily uniform currents, as is often supposed. The inertial frequency is the limiting frequency for many other types of motion, including internal waves and motions trapped by topography and β -effect. The possibility that they are internal waves cannot yet be dismissed. An interesting experimental program awaits those who wish to investigate the matter further.

3. Mass-transport currents

Let \mathbf{u} denote any time-periodic velocity field such that to the first order in the amplitude the mean velocity $\bar{\mathbf{u}}$ vanishes. If the (second-order) mean velocity of a marked particle (the Lagrangian mean velocity) be denoted by $\bar{\mathbf{u}}_L$, and the (second-order) mean velocity at a fixed position (the Eulerian mean velocity) be denoted by $\bar{\mathbf{u}}_E$, then it can be shown (see Longuet-Higgins 1953) that

$$\bar{\mathbf{u}}_L = \bar{\mathbf{u}}_E + \mathbf{U}, \quad (3.1)$$

where

$$\mathbf{U} = \overline{\int \mathbf{u} dt} \cdot \nabla \mathbf{u}. \quad (3.2)$$

The quantity \mathbf{U} has been called the Stokes velocity (Longuet-Higgins 1969*b*) after G. G. Stokes, who first evaluated this term for surface waves on water.

When the motion is practically two-dimensional, as in the present application, the two components U , V of the Stokes velocity may be expressed in terms of a stream-function ψ_s (cf. Longuet-Higgins 1953) as follows:

$$U = \frac{\partial \psi_s}{\partial y}, \quad V = -\frac{\partial \psi_s}{\partial x}, \quad (3.3)$$

where

$$\psi_s = \overline{u \int v dt} = -\overline{\int u dt v}. \quad (3.4)$$

In the radial co-ordinates suited to the present problem, the corresponding expressions are

$$U_r = \frac{1}{r} \frac{\partial \psi_s}{\partial \theta}, \quad U_\theta = -\frac{1}{r} \frac{\partial \psi_s}{\partial r}, \quad (3.5)$$

where

$$\psi_s = \overline{u_r \int u_\theta dt} = -\overline{\int u_r dt u_\theta}. \quad (3.6)$$

For the simple progressive motion given by (2.18) we have

$$\Psi = \frac{1}{2\sigma} \left(1 - \frac{a^2}{r^2}\right) CC^*, \quad (3.7)$$

where a star denotes the complex conjugate quantity. From (3.5) it follows that $U_r = 0$, as we should expect from symmetry, while

$$U_\theta = \frac{2a^5}{r^5} \frac{CC^*}{a\sigma}. \quad (3.8)$$

Thus the Stokes velocity is altogether tangential and falls off like the inverse fifth power of the radial distance r . At the circumference of the island ($r = a$) we have

$$U_\theta = 2CC^*/a\sigma. \quad (3.9)$$

To find either u_L or u_E we must employ the full dynamical equations for the mean motion. The motion is in effect two-dimensional and hence by analogy with surface waves on water (Longuet-Higgins 1953, §4), or otherwise, the differential equation for the stream function ψ_E of the Eulerian mean flow is

$$\left(\frac{\partial}{\partial t} - \nu \nabla^2\right) \nabla^2 \psi_E = 0. \quad (3.10)$$

Initially, if the motion is irrotational, we expect that $\psi_E \equiv 0$ everywhere, that is to say

$$\psi_L = \psi_s = \overline{u \int v dt}, \quad (3.11)$$

except near the boundary of the fluid. The subsequent development of the motion represents the diffusion of velocity outwards from the circumference of the island.

Near the boundary $r = a$, we expect a boundary layer of the type described in Longuet-Higgins (1953, §7). It is shown there that if the first-order normal and tangential velocities are given by q_n and q_s respectively then just beyond the boundary layer there is a tangential velocity given by

$$u_L = \frac{5i+3}{4\sigma} q_s \frac{\partial q_s^*}{\partial s} \quad (3.12)$$

(*loc. cit.* equation (189)), the co-ordinate s being measured tangentially to the boundary. In the present problem, we replace q_s by u_θ and s by $a\theta$. Thus

$$u_L = \frac{5i+3}{4a\sigma} u_\theta \frac{\partial u_\theta^*}{\partial \theta}. \quad (3.13)$$

For the progressive wave described by (2.19) we find then

$$u_L = 5CC^*/a\sigma, \quad (3.14)$$

which is to be compared to the non-viscous value given by (3.9). In other words, the presence of a viscous boundary layer increases the velocity near the boundary † in the ratio 5/2.

Is a final steady state possible? Writing $\partial/\partial t = 0$ in (3.10) we find that ψ_E has to satisfy the biharmonic equation in two dimensions, and therefore

$$\psi = Pr^2 \log r + Qr^2 + R \log r + S, \quad (3.15)$$

where P , Q , R , S are arbitrary constants. If u_E is to vanish at infinity, P and Q must both be zero. The value of S is immaterial, and if the boundary condition at $r = a$ is to be satisfied we must have

$$R = 3CC^*/\sigma, \quad (3.16)$$

† These paradoxical effects have been well verified by experiments in the case of water waves; see Russell & Osorio (1958); Allen & Gibson (1959). In the case of progressive waves it has been found experimentally that equation (3.12) is valid also for turbulent flows. A theoretical justification, (based on the assumption that the eddy viscosity is some function of the distance from the boundary) is given in an appendix to the paper by Russell & Osorio (1958).

so that the transverse component u_L of the Lagrangian mean velocity is given ultimately by

$$u_L = \left(\frac{2a^5}{r^5} + \frac{3a}{r} \right) \frac{CC^*}{a\sigma}. \tag{3.17}$$

More generally, when the motion consists of two progressive waves travelling in opposite directions (see (2.17)) then substitution in (3.6) gives for the Stokes velocity

$$\psi_s = \frac{a^4}{2\sigma r^4} (CC^* - DD^*) + \frac{1}{2\sigma} \left(\frac{a^4}{r^4} - 1 \right) (CD^* e^{2i\theta} - C^*D e^{-2i\theta}). \tag{3.18}$$

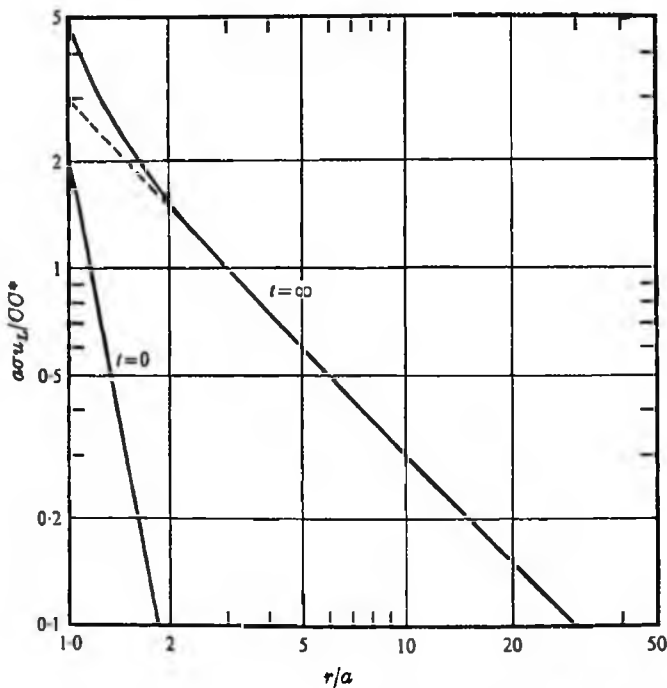


FIGURE 2. Graphs of the initial and final Lagrangian mean velocities u_L round an island of radius a , as a function of r/a .

When the amplitudes of the two waves are equal ($CC^* = DD^*$), the first term vanishes, and taking the origin of θ and t , so that C and D are real and equal, we have

$$\psi_s = \frac{i}{\sigma} \left(\frac{a^4}{r^4} - 1 \right) C^2 \sin 2\theta. \tag{3.19}$$

This represents a kind of dipole motion.

Similarly, (3.13) gives in general for the velocity just outside the boundary layer:

$$u_L = \frac{5}{a\sigma} (CC^* - DD^*) + \frac{3}{a\sigma} (CD^* e^{2i\theta} - C^*D e^{-2i\theta}). \tag{3.20}$$

When, as before, C and D are real and equal,

$$u_L = \frac{3C^2}{a\sigma} \sin 2\theta. \quad (3.21)$$

The result is similar to the streaming first found by Schlichting (1932) to occur in the presence of an oscillating cylinder. See also Batchelor (1967, ch. 5). The fluid enters the boundary layer at $\theta = 0^\circ$ and 180° in the plane of oscillation and leaves it at the intermediate points $\theta = \pm 90^\circ$.

It will be noticed that we have neglected friction on the bottom and taken into account only the friction at the vertical sides of the island. This may be justified if the vertical mixing is small compared to the horizontal mixing.

4. Experimental verification (i)

So long as the flow is practically two-dimensional and non-divergent, the mass transport currents depend only on the relative motion between the axis of the cylinder and the fluid at infinite distance. Hence these currents should be the same as if the fluid at infinity were stationary and the island were made to oscillate in a horizontal plane.

The latter arrangement is the more convenient experimentally. Accordingly, the author constructed a mechanism (shown in figure 3(a), plate 1), whereby a cylindrical can of radius $a = 3$ in. and length 9 in. could be made to oscillate so that its axis described a smaller vertical cylinder of radius $b = \frac{1}{2}$ in. Throughout the oscillation the orientation of the can remained fixed. This was achieved by fixing the can † to a rectangular frame pivoted on four joints, each of which was made to oscillate in parallel by four gear wheels driven from a central vertical shaft. This vertical shaft was driven by a bevel gear attached to a horizontal shaft, which in turn could be operated either by hand or by attachment to an electric motor.

The whole apparatus was then supported on two angle pieces laid across the top of a circular tank of diameter 30 in., as in figure 3(b), plate 1. The tank was filled with water to within 1 in. of the top of the can. With a syringe, some dilute ink was injected into the water close to the surface of the can and near its centre. The can was then made to oscillate by turning the handle as shown, or with an electric motor. The time t required for the ink to make a complete circuit was measured with a stop-watch, and also the mean period T of the first ten oscillations.

According to §3 above, the magnitude $|C|$ of the relative velocity between the fluid at infinity and the axis of the cylinder is equal to σb . Hence the streaming velocity just outside the oscillatory boundary layer is equal to $5\sigma b^2/a$ by (3.14). It follows that the time taken for a marked particle of fluid to complete a circuit of the cylinder, just outside the oscillatory boundary layer, is just equal to $a^2/5b^2$ periods of the oscillation. This result is independent not only of the viscosity but also of the period of oscillation, within the range of the present approximations.

† Kindly supplied by my wife.

Corresponding to the apparatus described above we have $a/b = 6$; hence the time required for a circuit is $6^2 \div 5$, that is 7.2, periods.

This simple result in practice is slightly complicated by the following considerations:

(i) The radius of the outer cylinder is finite. This introduces errors of order a^2/A^2 where A is the radius of the outer cylinder.

(ii) The surface is free. This introduces errors of order $\sigma^2 a/g$, where g denotes the acceleration of gravity.

(iii) The amplitude of the motion is finite. This introduces relative errors of order b/a .

(iv) The thickness of the oscillatory boundary layer, though small, is finite. This introduces errors of order δ/a , where $\delta = (\nu/\sigma)^{1/2}$.

(v) Outside the boundary layer the motion is not steady until a time of order $(\sigma - \alpha)^2/\nu$ after starting.

The presence of these errors, especially (iii), leads us to expect discrepancies of the order of 10% between the observations and the simple theory of §3.

Nevertheless, the experiment was tried. On starting the motion from rest by running the motor so that the mean period T of the first ten oscillations lay between 1.37 and 6.91 sec, it was found that the time taken for the first trace of dye to orbit the can lay always between 5.4 and 8.8 periods of oscillation with a mean of 7.3 periods (see table 1). The agreement was thus at least as good as expected.

T (sec)	t (sec)	N (= t/T)	Serial number of observation
1.37	7.4	5.4	3
1.81	12.3	6.8	2
2.58	20.5	7.9	1
3.52	24.2	6.9	4
4.65	37.8	8.1	5
	28.9	6.2	6
5.30	43.5	8.2	8
	38.5	7.3	9
6.91	60.4	8.8	7

TABLE 1. The observed number N of cycles taken by a particle to make a complete circuit of the cylinder in figure 3

5. Islands with sloping sides: free oscillations

So long as the sides of the island are vertical it is impossible for free waves to be trapped near the island unless the horizontal dimensions of the ocean are at least of order $\sqrt{(gh)}/f$ (see Longuet-Higgins 1969*a*). This restricts the practical possibility of wave trapping with vertical sides to baroclinic motions.

The situation is quite different if the island is surrounded by a sloping shelf or 'skirt'. Then trapping becomes reasonably possible, and a double infinity of free trapped motions appears. An example restricted to the case $\sigma \ll f$ has

been studied by Mysak (1967). Rhines (1967, 1969) has considered a more general case when the depth $h(r)$ is assumed to be given by

$$\bar{h} = \begin{cases} 0 & (0 < r < a), \\ \bar{h}_1(r/a)^\alpha & (a < r \leq b), \\ \bar{h}_2 & (b \leq r < \infty), \end{cases} \quad (5.1)$$

(see figure 4), α being any positive constant. † When $\alpha < 1$ the sloping 'skirt' is concave upwards; when $\alpha = 1$ the skirt is conical; and when $\alpha > 1$ it is convex. Continuity of \bar{h} at $r = b$ requires that $h_2 = \bar{h}_1(b/a)^\alpha$.

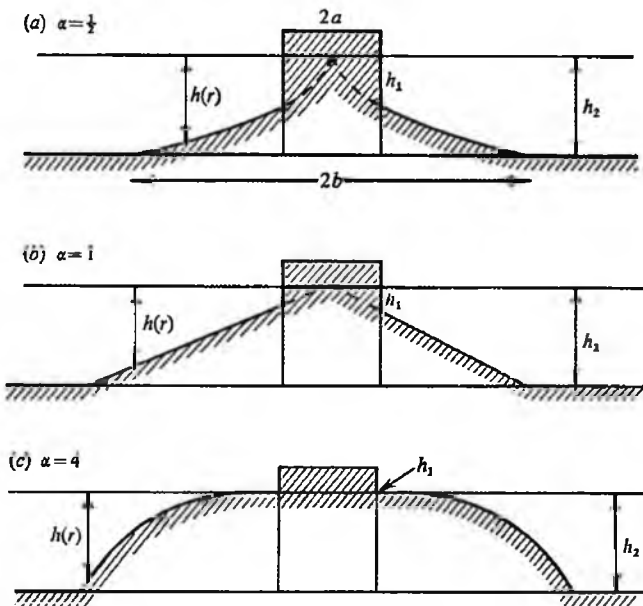


FIGURE 4. Cross-section of the model island with a 'skirt' given by (5.1) in three typical cases: (a) $\alpha = \frac{1}{2}$, (b) $\alpha = 1$, (c) $\alpha = 4$.

Rhines (1969, pp. 196–198) has considered the scattering of a Rossby wave by an island of the above form. Here we shall assume a simple model in which f is constant, and we shall consider simply the response to an oscillation whose form at infinity is given by (2.4) or (2.5). We shall then proceed as in §3 to calculate the corresponding mass transport velocities. Owing to the possibility of resonant excitation of the free modes, the mass-transport can be very greatly amplified.

Neglecting the dynamical effect of the horizontal convergence (which serves only to increase the hydrostatic pressure), we may assume the existence of a stream function ψ such that

$$\bar{h}u_r = \frac{1}{r} \frac{\partial \psi}{\partial \theta}, \quad \bar{h}u_\theta = -\frac{\partial \psi}{\partial r}. \quad (5.2)$$

† Rhines treated especially the case $\alpha = \frac{1}{2}$. Phillips (1966) considered the motion in an annular region between two concentric cylinders, when $\alpha = 2$.

From the conservation of potential vorticity it follows that ψ has to satisfy the differential equation,

$$\frac{\partial}{\partial t} \nabla \cdot \left(\frac{1}{h} \nabla \psi \right) - \mathbf{f} \cdot \nabla \left(\frac{1}{h} \right) \wedge \nabla \psi = 0, \tag{5.3}$$

where \mathbf{f} denotes the vector of magnitude f directed vertically. We now seek solutions to this equation in the form,

$$\psi = \hat{\psi}(r) e^{i(n\theta - \sigma t)}, \tag{5.4}$$

where n is a positive integer. We are particularly interested in the case $n = 1$. It follows that in the sloping region $a < r < b$, $\hat{\psi}$ must satisfy the ordinary differential equation,

$$\frac{d^2 \hat{\psi}}{dr^2} + \frac{1 - \alpha}{r} \frac{d\hat{\psi}}{dr} - \frac{n(n + \alpha f / \sigma)}{r^2} \hat{\psi} = 0. \tag{5.5}$$

In the constant-depth region $r > b$ we use the same equation but with α set equal to 0. We have further to satisfy the boundary conditions that

$$\left. \begin{aligned} \hat{\psi} &\rightarrow 0 && (r \rightarrow a), \\ \hat{\psi}, \frac{d\hat{\psi}}{dr} &\text{continuous} && (r \rightarrow b), \\ \hat{\psi} &\sim Cr^n && (r \rightarrow \infty). \end{aligned} \right\} \tag{5.6}$$

The differential equation (5.5) is satisfied by taking

$$\hat{\psi} = P_1(r/a)^{p_1} + P_2(r/a)^{p_2}, \tag{5.7}$$

where P_1, P_2 are arbitrary constants and p_1, p_2 are the roots (assumed different) of the quadratic equation,

$$p^2 - \alpha p + n(n + \alpha f / \sigma) = 0. \tag{5.8}$$

Thus

$$p_1, p_2 = \frac{1}{2} \alpha \pm \beta, \tag{5.9}$$

where

$$\beta = (n^2 + n\alpha f / \sigma + \alpha^2 / 4)^{\frac{1}{2}} \tag{5.10}$$

provided $\beta \neq 0$. The boundary condition at $r = a$ is satisfied by taking

$$P_1 = -P_2 = P,$$

say. Then we have

$$\hat{\psi} = 2P(r/a)^{\alpha/2} \sinh[\beta \ln(r/a)] \quad (a < r \leq b). \tag{5.11}$$

When $r > b$, the differential equation and the boundary condition at infinity are satisfied by

$$\hat{\psi} = Cr^n + Qr^{-n}, \tag{5.12}$$

where Q is a constant to be determined. Now to satisfy the boundary conditions at $r = b$ we must have

$$\left. \begin{aligned} 2P(b/a)^{\frac{1}{2}\alpha} \sinh \xi &= Cb^n + Qb^{-n}, \\ 2P(b/a)^{\frac{1}{2}\alpha} (\beta \cosh \xi + \frac{1}{2}\alpha \sinh \xi) &= nCb^n - nQb^{-n}, \end{aligned} \right\} \tag{5.13}$$

where

$$\xi = \beta \ln(b/a). \tag{5.14}$$

Thus the ratios of P , Q and C are given by the two equations

$$\left. \begin{aligned} P(b/a)^{\frac{1}{2}\alpha} [(n + \frac{1}{2}\alpha) \sinh \xi + \beta \cosh \xi] &= nCb^n, \\ P(b/a)^{\frac{1}{2}\alpha} [(n - \frac{1}{2}\alpha) \sinh \xi - \beta \cosh \xi] &= nQb^{-n}. \end{aligned} \right\} \quad (5.15)$$

The free modes are given by $C = 0$, $P \neq 0$, and so

$$(n + \frac{1}{2}\alpha) \sinh \xi + \xi \cosh \xi / \ln(b/a) = 0. \quad (5.16)$$

Since $\ln(b/a) > 0$, there are no real roots ξ ; but when β and ξ are imaginary, say $\beta = i\beta'$ and $\xi = i\xi'$, (5.16) becomes

$$\xi' \cot \xi' = -(n + \frac{1}{2}\alpha) \ln(b/a). \quad (5.17)$$

We see that for each value of n there is an infinite sequence of possible roots ξ'_1, ξ'_2, \dots such that $(m - \frac{1}{2})\pi < \xi'_m < (m + \frac{1}{2})\pi$. Each root ξ'_m corresponds to a possible free mode, and so to a resonant condition. Moreover, from (5.10) we have

$$n^2 + n\alpha f / \sigma + \frac{1}{4}\alpha^2 = -\beta'^2, \quad (5.18)$$

so that necessarily

$$\sigma / f < 0, \quad (5.19)$$

that is to say the free waves must progress clockwise round the island in the northern hemisphere ($f > 0$) and anticlockwise in the southern hemisphere. From (5.18) we have also

$$-\frac{\sigma}{f} = \frac{\alpha n}{n^2 + \frac{1}{2}\alpha^2 + \beta'^2} < \frac{\alpha n}{n^2 + \frac{1}{2}\alpha^2}. \quad (5.20)$$

The term on the right attains its maximum value 1 when $n = \frac{1}{2}\alpha$. Hence in all cases $|\sigma/f| < 1$, that is to say the frequency of the free modes is always less than the inertial frequency. It may be shown that the corresponding stream function $\hat{\psi}$, given by

$$\hat{\psi} = \begin{cases} 2iP(r/a)^{\frac{1}{2}\alpha} \sin[\beta' \ln(r/a)] & (a < r < b), \\ Cr^n, & (b < r < \infty), \end{cases} \quad (5.21)$$

has exactly m zeros in the interval $a < r < \infty$, as well as the zero at $r = a$. Outside $r = a$, $|\hat{\psi}|$ decreases monotonically and tends to 0 as $r \rightarrow \infty$. The corresponding circulation is in m cells in the radial direction, $2n$ cells in the transverse direction.

The relative frequencies σ/f of the free modes are shown in figure 5 as functions of b/a , for some typical values of the constant α .

We are now in a position to calculate the mass transport velocities in both forced and free oscillations. From (3.6) it follows that the stream function ψ_s for the Stokes velocity is given by

$$\psi_s = -\frac{1}{r} \frac{\partial \hat{\psi}}{\partial \theta} \int \frac{\partial \hat{\psi}}{\partial r} dt. \quad (5.22)$$

From (5.4) this is

$$\psi_s = \frac{n}{2\sigma r} \hat{\psi} \frac{d\hat{\psi}^*}{dr} = \frac{n}{4\sigma r} \frac{d|\hat{\psi}|^2}{dr}. \quad (5.23)$$

In the free oscillations, $\hat{\psi}$ has in general $(m - 1)$ maxima and $(m - 1)$ zeros in $a < r < \infty$, so that $|\hat{\psi}|^2$ has $(2m - 2)$ maxima. Hence the Stokes velocity $\partial\psi_s/\partial r$ changes sign $(2m - 2)$ times in $a < r < \infty$.

In the forced oscillations, we can calculate the Stokes velocity from (5.23). In particular, at the perimeter of the island, where ψ vanishes we have from (5.23)

$$U_s = \frac{n}{2\sigma a} \left| \frac{d\psi}{dr} \right|^2 = \frac{2n\beta^2 P^2}{\sigma a^3}, \tag{5.24}$$

β and P being given by (5.10) and (5.14).

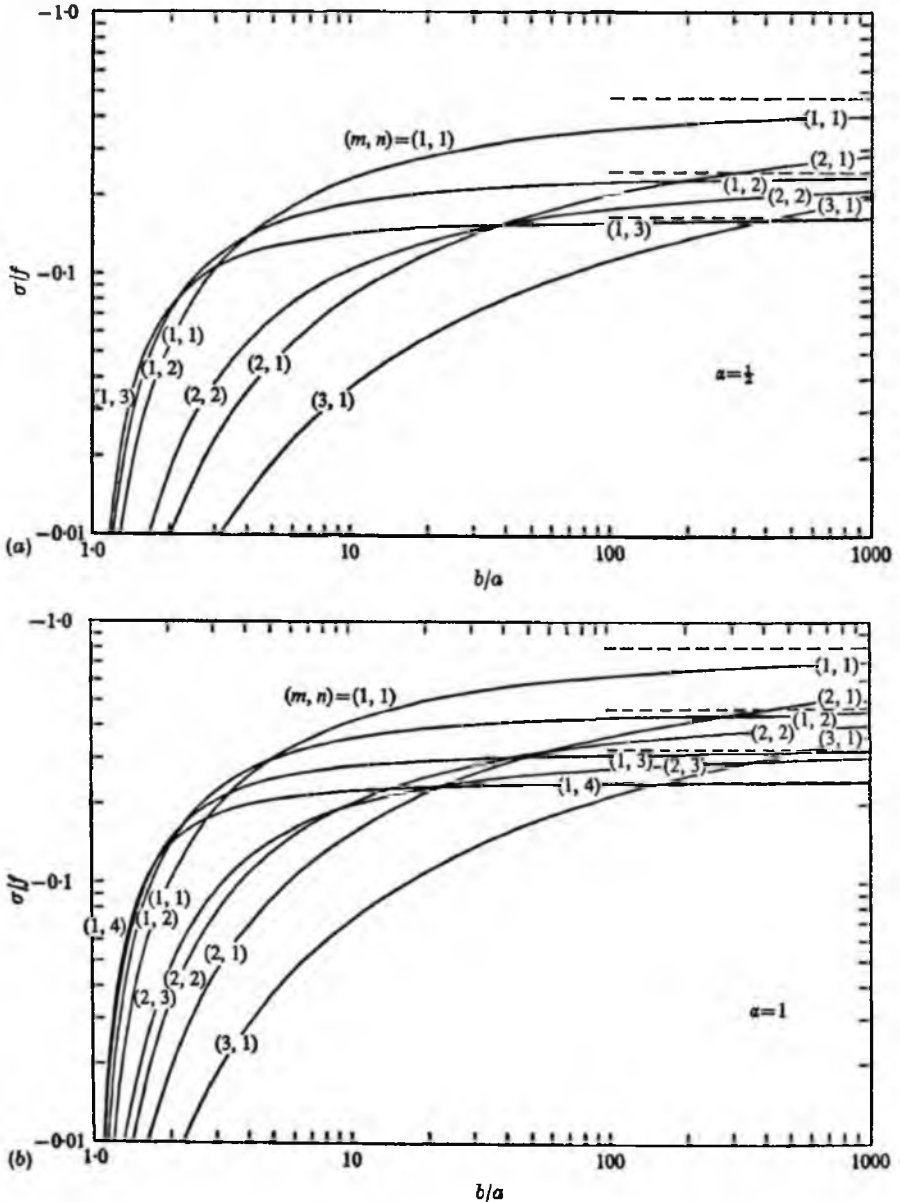


FIGURE 5 (a, b). For legend see p. 716.

716

M. S. Longuet-Higgins

In the important case $n = 1$, the total Stokes transport is given by the difference between $\rho\psi_s$ at infinity and ψ_s at $r = a$. Since ψ_s vanishes at $r = a$, and when $r > b$,

$$\hat{\psi}\hat{\psi}^* = CC^*r^2 + (CQ^* + C^*Q) + QQ^*r^{-2}, \quad (5.25)$$

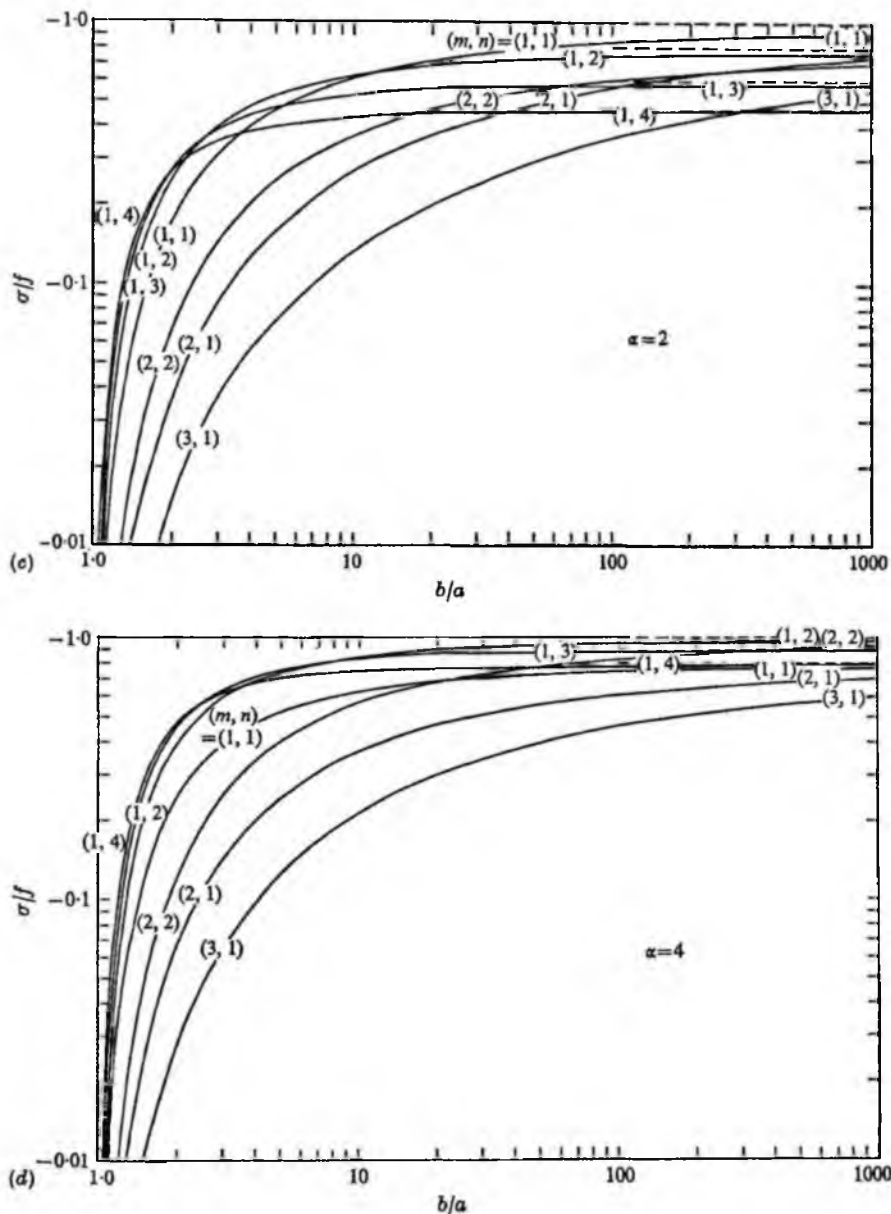


FIGURE 5. Graphs of the non-dimensional frequency (σ/f) for some of the lower modes, plotted as a function of b/a . The symbol (m, n) denotes the m th mode with azimuthal wave-number n . (a) $\alpha = \frac{1}{2}$, (b) $\alpha = 1$, (c) $\alpha = 2$, (d) $\alpha = 4$.

it follows from (5.22) that, as $r \rightarrow \infty$,

$$\psi_s \rightarrow CC^*/2\sigma. \tag{5.26}$$

This quantity has always the same sign as σ .

The angular momentum of the Stokes flow, on the other hand, is given by

$$\text{a.m.} = 2\pi\rho \int_a^\infty \frac{\partial\psi_s}{\partial r} r^2 dr. \tag{5.27}$$

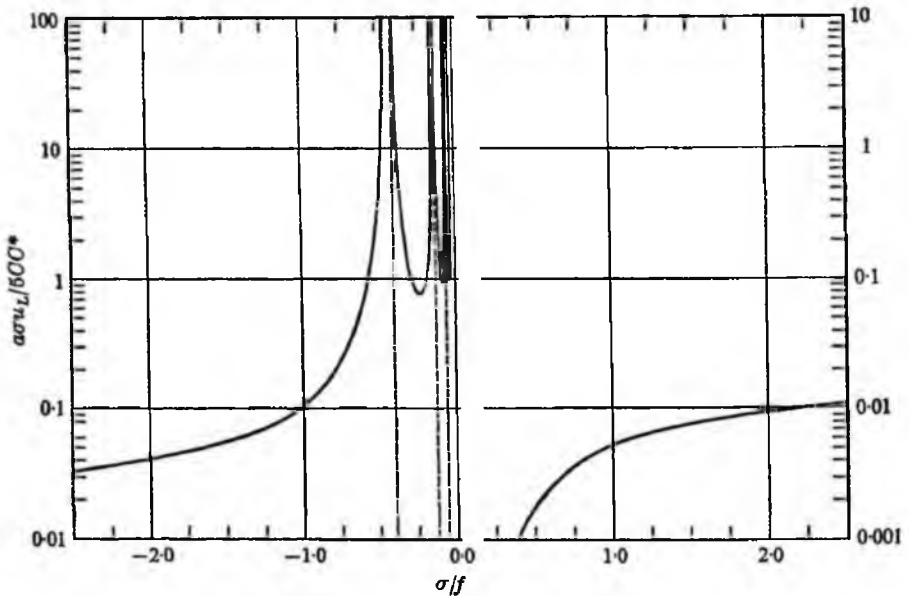


FIGURE 6. Relative magnitude of the mass-transport velocity near the perimeter of the island in a typical case: $\alpha = 2$, $b/a = 4$, showing the peaks at the resonant frequencies. The vertical scale on the right ($\sigma/f > 0$) is ten times that on the left.

In this expression ψ_s may be replaced by $(\psi_s - \psi_{s\infty})$, where $\psi_{s\infty}$ denotes the limit in (5.26). On integrating by parts, and using (5.22) and (5.24), we find

$$\text{a.m.} = -\frac{\pi\rho}{\sigma} (CQ^* + C^*Q). \tag{5.28}$$

This quantity may be either positive or negative, depending on the sign of Q . When the sides are vertical, we find from §3 that $Q = -Ca^2$ and so

$$\text{a.m.} = \frac{2\pi\rho a^2 CC^*}{\sigma}, \tag{5.29}$$

which has always the same sign as σ .

Consider now the Lagrangian mass-transport velocity u_L . This will depend on the viscous boundary conditions on the bottom and the vertical wall, and in general also on the time since the motion was started. But, on the vertical wall of the island, the velocity just outside the oscillatory boundary layer is given simply

by (3.12), provided we now substitute $q_s = (-\partial\psi/\partial r)_{r=\alpha}$. Since ψ is given by (5.4), we have then

$$u_L = \frac{5n}{4\sigma\alpha} \left| \frac{d\psi}{dr} \right|^2 = \frac{5n\beta^2 P^2}{\sigma\alpha^3}. \quad (5.30)$$

As before, the effect of viscosity is to multiply the mass-transport velocity near the perimeter of the island by the factor $5/2$.

As an example let us take $\alpha = 2$, $b/a = 4$ and $n = 1$. Then figure 5(c) indicates that we must expect resonance when $\sigma/f = -0.396$, -0.125 and -0.056 , corresponding to the three lowest modes, $m = 1, 2$ and 3 respectively. In figure 6 we show a graph of the non-dimensional quantity,

$$\frac{n\alpha\sigma u_L}{5CC^*} = |\beta P|^2. \quad (5.31)$$

This represents the relative magnification of the mass-transport velocity near the perimeter $r = \alpha$, compared to the mass transport in the absence of a surrounding 'skirt'. The amplification of the mass-transport near resonance can be clearly seen. By contrast, the response of the island to waves progressing in the clockwise direction ($\sigma/f > 0$) is remarkably small.

In calculating the amplitude of the forced oscillations, we have of course neglected the dissipation of energy by viscosity and also the detuning of the oscillations due to the slight dependence of the frequency on the amplitude. Both these effects will act to limit the amplitude near resonance.

6. Experimental verification (ii)

The following experiment provided a qualitative verification of the effects described in §5.

A circular tank of diameter 18 in. and depth about 6 in. was fitted with a false wax bottom in the form of a parabola, curved so as to be parallel to the free surface when rotating in equilibrium at a speed of 0.25 c/s. Projecting from the bottom of the tank were three islands. Two of these were circular cylinders with vertical sides and diameters 1 in. and $1\frac{1}{2}$ in. respectively (see figure 7). The third island was fitted with a 'skirt' corresponding to the parameters $\alpha = 2$, $b/a = 2$. The tank was placed on a rotating turntable and filled to a depth of about 3 in. (so as to cover the curved part of the skirted island). Aluminium powder was scattered on the surface to facilitate viewing the surface velocities.

The tank was then set in rotation at a speed of 0.25 c/s, and the relative motions were viewed through a rotascope.

On reaching the spin-up velocity one might have expected at first to see no relative motion between the fluid and the rotating tank. On the contrary, small oscillations, having the same period as the rotation, were observed in the main body of the fluid, due to the fact that the axis of rotation was not perfectly aligned with the vertical. The rotation of the tank being in the positive (eastwards) sense, the effect was to produce a component of gravity rotating in the

negative (westwards) sense relative to the rotating tank. The frequency σ of the oscillation was thus given by

$$\sigma/f = -\frac{1}{2}, \quad (6.1)$$

since f is equal to twice the angular rate of rotation.

Close to the islands, however, the most obvious feature of the motion was not the oscillatory motion so much as an intense d.c. component of flow directed anticlockwise round each island. The motion was more intense round the smaller of the two cylindrical islands. This is to be expected from (3.14), in which the mass transport velocity is inversely proportional to the radius a of the island.

The most intense current, however, was observed near the third island, the one with the skirt. A computation of the relative velocity (5.31) in the case $\alpha = 2$, $b/a = 2$ and $\sigma/f = -\frac{1}{2}$ shows that, for these values, the relative magnification is given by

$$\frac{a\sigma u_L}{5CC^*} = 4.432. \quad (6.2)$$

It was not possible to measure the drift currents accurately in this experiment but the observations appeared to be consistent with the above ratio. Further experiments are at present in progress.

7. Discussion

Equation (3.14) indicates that the order of magnitude of the streaming velocity is inversely proportional to the radius a of the island. It follows that the smaller the island, the greater the streaming velocity, within the present approximations. Hence a quite small island may be, as it were, a useful probe for detecting oscillatory motions in the surrounding ocean.

It does not seem altogether fanciful to suggest that the drift velocities observed in the neighbourhood of Bermuda by Stommel (1954) may be partly attributed to mass-transport streaming associated with oscillations nearby. From figure 1 of Stommel's paper it appears that the particle tracks nearly all circulate that island in the clockwise sense, and with times comparable to 15 days, or about 30 tidal cycles. If this is to be comparable with $a^2/5b^2$, where a is the mean radius of the island of Bermuda we must have $b/a \sim 0.08$, or, since $a \sim 5$ km, the half tidal displacement b must be of order 0.4 km. This is not inconsistent with what is known of the tidal currents in that area.

This investigation was begun at Oregon State University, Corvallis, under NSF Grant No. GA-1452 and completed at the National Institute of Oceanography, England. The experiments described in §6 were carried out with the assistance of Steve Wilcox at Oregon State University, using a rotating turntable and rotascope constructed at N.I.O. The experiments in §4 were first performed at my home in Cambridge, and subsequently at Wormley. John Simpson held the stopwatch.

REFERENCES

- ALLEN, J. & GIBSON, D. H. 1959 Experiments on the displacement of water by waves of various heights and frequencies. *Min. Proc. Instn Civ. Engrs.* **13**, 363-386.
- BATCHELOR, G. K. 1967 *An Introduction to Fluid Dynamics*. Cambridge University Press.
- HUNT, J. N. & JOHNS, B. 1963 Currents induced by tides and gravity waves. *Tellus*, **15**, 343-351.
- LAMB, H. 1932 *Hydrodynamics* (6th ed.). Cambridge University Press.
- LONGUET-HIGGINS, M. S. 1953 Mass transport in water waves. *Phil. Trans. A* **245**, 535-581.
- LONGUET-HIGGINS, M. S. 1960 Mass transport in the boundary layer at a free oscillating surface. *J. Fluid Mech.* **8**, 293-306.
- LONGUET-HIGGINS, M. S. 1969*a* On the trapping of long-period waves round islands. *J. Fluid Mech.* **37**, 773-784.
- LONGUET-HIGGINS, M. S. 1969*b* On the transport of mass by time-varying ocean currents. *Deep-Sea Res.* **16**, 431-477.
- MOORE, D. 1969 The mass transport velocity induced by free oscillations at a single frequency. *Geophys. Fluid Dynam.* (To be published.)
- MUNK, W. H. & MOORE, D. 1968 Is the Cromwell Current driven by equatorial Rossby waves? *J. Fluid Mech.* **33**, 241-259.
- MYSAK, L. A. 1967 On the theory of continental shelf waves. *J. Mar. Res.* **25**, 205-227.
- PEDLOSKY, J. 1965 A study of the time dependent ocean circulation. *J. Atmos. Sci.* **22**, 267-272.
- PHILLIPS, N. A. 1965 Elementary Rossby waves. *Tellus*, **17**, 295-301.
- REHNES, P. B. 1967 The influence of bottom topography on long-period waves in the ocean. Ph.D. Thesis, Cambridge University.
- REHNES, P. B. 1969 Slow oscillations in an ocean of varying depth. Part 2. Islands and seamounts. *J. Fluid Mech.* **37**, 191-205.
- ROBINSON, A. R. 1965 *Research Frontiers in Fluid Dynamics*. New York: Interscience.
- RUSSELL, R. C. H. & OSORIO, J. D. C. 1958 An experimental investigation of drift profiles in a closed channel. *Proc. 6th Conf. on Coastal Engng Miami 1957*, pp. 171-193.
- SCHLICHTING, H. 1932 Berechnung ebener periodischer Grenzschichtströmungen. *Phys. Z.* **33**, 327-335.
- STOKES, G. G. 1847 On the theory of oscillatory waves. *Trans. Camb. Phil. Soc.* **8**, 441-455.
- STOMMEL, H. 1954 Serial observations of drift currents in the central North Atlantic Ocean. *Tellus*, **6**, 203-214.



(a)



(b)

FIGURE 3. (a) A mechanism for oscillating a cylinder of radius 3 in. so that its axis describes a smaller cylinder of radius $\frac{1}{2}$ in. The orientation of the cylinder remains fixed.

(b) An experiment to measure the Lagrangian drift velocity near to the boundary of an oscillating cylinder, using the mechanism of figure 3(a).

Peristaltic pumping in water waves

By M. S. LONGUET-HIGGINS

Department of Applied Mathematics and Theoretical Physics, Silver Street, Cambridge,
 and Institute of Oceanographic Sciences, Wormley, Surrey

(Received 21 January 1983)

In this paper we calculate the streaming induced by gravity waves passing over a thin fluid layer, one side of which is rigid while the other is a flexible, inextensible membrane. The problem is relevant to some recent laboratory experiments by Allison (1983) on the pumping action of water waves.

On the assumption that the flow is laminar and that the lateral displacement b of the membrane is small compared with the thickness A of the fluid layer, we calculate the velocity profile of the streaming U within the layer. This depends on the ratio A/δ , where δ is the thickness of the Stokes layers at the upper and lower boundaries. When $0 < A/\delta < 6$ the boundary layers interact strongly and the velocity profile is unimodal. At large values of A/δ the profile of U exhibits thin 'jets' near the boundaries.

The calculated drift velocities agree as regards order of magnitude with those observed. However, the pressure gradients observed were larger than those calculated, due possibly to turbulence, but probably also to finite-amplitude and end-effects.

The theory given here can be considered as an extension of the theory of peristaltic pumping to flows at higher Reynolds number.

1. Introduction

In a recent experiment to extract power from the mass transport in water waves, Allison (1983) laid a flexible bag, 6 m long and 0.5 m wide, on the floor of a wave basin, with the longer side in the direction of wave propagation. The two ends of the bag were connected externally by a rigid pipe. In the presence of gravity waves of 0.8–2.5 s period it was found that mean circulation of fluid took place down-wave through the bag, returning via the pipe. If the pipe was constricted, a mean head of 1–2 cm of water was built up.

The aim of the present note is to analyse the fluid mechanics of this effect. We shall show that the pumping action is due very largely to viscosity, being similar to that occurring in organic tubes (Jaffrin & Shapiro 1971).

In any oscillating flow, the importance of viscosity in inducing a steady streaming close to a rigid or flexible boundary has been known ever since Rayleigh (1884) analysed the currents induced by standing oscillations in air or water. On the other hand for progressive motions, the streaming tangential to a membrane or solid boundary was first evaluated by Longuet-Higgins (1953). His analysis showed that just outside the Stokes layer, of thickness $\delta = (2\nu/\sigma)^{1/2}$, where ν is the kinematic viscosity and σ the radian frequency of oscillation, the tangential streaming velocity tended to the finite value

$$U = \frac{5q^2}{4c} \quad (1.1)$$

Here q denotes the amplitude of the first-order oscillatory velocity relative to the boundary, and c is the phase speed. Particularly interesting is the fact that the limiting value (1.1) is independent of ν and so remains non-negligible even when the Stokes layer itself is quite thin. This forwards streaming or jet near the bottom had been first noticed in water waves by Bagnold (1947), and was later confirmed by Russell & Osorio (1956) and many others.

It is a forwards streaming of this type which we suggest controls the flow within the flexible bag in Allison's experiment. A preliminary analysis is given below in §2, assuming the flow to be laminar and the separation Δ between upper and lower surfaces of the bag to be large compared with the thickness δ of the Stokes layers. In §§3 and 4 we extend the analysis to the situation of turbulent flow, and to when Δ/δ is not necessarily large. The theory gives a reasonable agreement with Allison's experiment. Further discussion follows in §§6 and 7.

2. A laminar model: $\delta \ll \Delta$

The situation is idealized as in figure 1(a). Homogeneous, incompressible fluid is contained between a rigid plane $z = 0$ and a flexible membrane at a mean distance Δ above the bottom. The vertical oscillations in the membrane are of amplitude b and travel to the right with speed c , so that the equation of the membrane is

$$z = \Delta + b \cos(kx - \sigma t), \quad (2.1)$$

where x and z are horizontal and vertical coordinates, k is the wavenumber, and $\sigma/k = c$. We shall assume at first that

$$k\Delta \ll 1, \quad (2.2)$$

that is, the wavelength is long compared with the thickness of the fluid layer, and

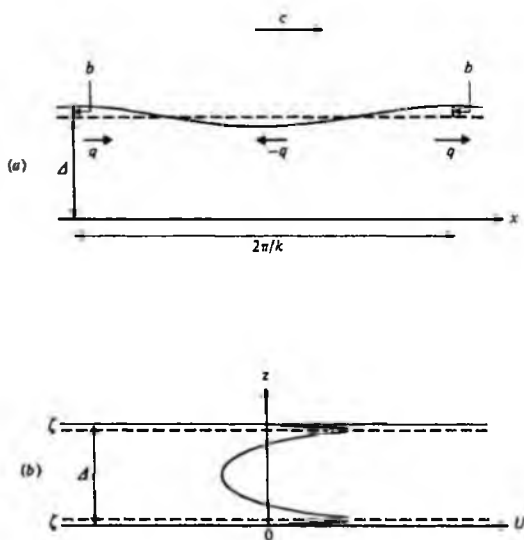


FIGURE 1. (a) A two-dimensional model of the flexible bag. (b) A typical profile of the streaming velocity U .

Peristaltic pumping in water waves

395

also

$$b/\Delta \ll 1, \quad (2.3)$$

that is, the vertical displacements are only a small fraction of the layer thickness; this latter restriction will be modified later. The motion will be treated at first as two-dimensional and independent of the y -coordinate.

The vertical velocity w vanishes on the bottom and, when $z = \Delta$, w is given by $b\sigma \sin(kx - \sigma t)$ to first order in bk . Hence in general

$$w = \frac{z}{\Delta} b\sigma \sin(kx - \sigma t) \quad (2.4)$$

everywhere outside the boundary-layers.

To begin with we shall assume

$$\delta = (2\nu/\sigma)^{\frac{1}{2}} \ll \frac{1}{2}\Delta, \quad (2.5)$$

so that outside the boundary-layer the horizontal velocity is given by

$$u = \frac{b\sigma}{k\Delta} \cos(kx - \sigma t) \quad (2.6)$$

to first order in bk . To this order the tangential velocity of the membrane is negligible, so that in (1.1) the amplitude q of the oscillatory velocity relative to the boundary is

$$q = \frac{b\sigma}{k\Delta} = \frac{bc}{\Delta} \quad (2.7)$$

at both upper and lower boundaries.

To evaluate the mean flow we note that, if there were no mean horizontal gradient in the pressure, the streaming velocity would be uniform and equal to (1.1) everywhere in the interior. In the presence of a mean pressure gradient ϖ we have to solve the equation

$$\nu \frac{\partial^2 \bar{u}}{\partial z^2} = \frac{\varpi}{\rho} + u \overline{\frac{\partial u}{\partial x}} + w \overline{\frac{\partial u}{\partial z}} \quad (2.8)$$

(see Longuet-Higgins 1953), where \bar{u} is the time-mean velocity at a fixed point. This is related to the streaming velocity U by

$$U = \bar{u} + \int u dt \frac{\partial u}{\partial x} + \int w dt \frac{\partial u}{\partial z}, \quad (2.9)$$

the last two terms representing the Stokes drift. In view of (2.4) and (2.6), this reduces to

$$U = \bar{u} + \frac{1}{2}q^2/c. \quad (2.10)$$

Since the second term on the right of (2.10) is independent of z , we have for U in the interior the same equation as for \bar{u} , namely

$$\frac{\partial^2 U}{\partial z^2} = \frac{\varpi}{\rho\nu} \quad (2.11)$$

with boundary conditions

$$U = \frac{5q^2}{4c} \quad \text{when } z \doteq 0, \Delta \quad (2.12)$$

(see figure 1b). The use of \doteq signifies that the condition has actually to be satisfied just outside each boundary-layer, but since $\delta \ll \Delta$ the difference is negligible. In

addition, to second order in bk the boundary condition can be taken as satisfied at the mean vertical position of the membrane, that is at $z = A$ and not on (2.1).

The solution to the problem (2.11), (2.12) is clearly

$$U = \frac{5q^2}{4c} + \frac{1}{2\rho\nu} \varpi z(z-A). \quad (2.13)$$

In other words, we add to the uniform velocity (1.1) a parabolic flow, symmetric about the central line, as in figure 1(b).

Corresponding to (2.13), the total volume flux M is given by

$$M = \frac{5q^2 A}{4c} - \frac{1}{12} \frac{\varpi A^3}{\rho\nu}. \quad (2.14)$$

If ϖ vanishes, the mean velocity is simply

$$\bar{U} = \frac{5q^2}{4c}, \quad (2.15)$$

while, if the flow is blocked so that M vanishes, we induce a pressure head

$$[p] = \varpi L = 15 \frac{\rho\nu L q^2}{A^2 c}, \quad (2.16)$$

where L is the total length of the flexible tube. In general the power P available per unit width of the tube is

$$P = \varpi L M. \quad (2.17)$$

From (2.14) this is a maximum when

$$\varpi = \frac{15\rho\nu q^2}{2A^2 c}, \quad (2.18)$$

so the maximum available power is given by

$$P_{\max} = \frac{75\rho\nu L q^4}{16A c^2}. \quad (2.19)$$

In all these expressions q^2/c may be replaced by $(b/A)^2 c$, where $2b$ is the overall vertical displacement of the membrane.

3. Comparison with observation

In Allison's experiment (1983, figure 6) the wave period $T = 2\pi/\sigma$ ranged from 0.8 to 2.5 s, in water of constant depth $h = 30$ cm. The wave height $2a$ was greatest at about 5.5 cm for waves of period about 1.2 s.

The amplitude b of the vertical displacement of the membrane was however measured as 1.0 cm for waves of 1.1 s period. This compares with a notional amplitude

$$b' = a \frac{\sinh kA}{\sinh kh} = 0.27 \text{ cm} \quad (3.1)$$

of vertical fluid motion at a height A above the bottom, in the absence of the flexible bag. From Allison's figure 2 we take $A = 4.0$ cm. Since $b > b'$ it appears that the presence of the membrane does affect the waves above the bag, increasing their amplitude, possibly by wave refraction.

For the waves of period 1.1 s we have from the linear dispersion relation

$$kh \tanh kh = \sigma^2 h / g = 1.00, \quad (3.2)$$

80

$$kh = 1.20 \quad (3.3)$$

and the wavelength $2\pi/k$ is about 1 m or three times the depth h . The phase speed c is 143 cm/s, and if we assume the ratio b/Δ in (2.7) to be constant despite variations in Δ across the width of the bag, then q is constant at $0.25c$ or about 36 cm/s. The mean-flow velocity (2.15) in the absence of an external pressure gradient would be 11.2 cm/s, in apparently good agreement with the measured velocity 13 cm/s at this wave period; see Allison's figure 8.

However two adjustments must be made. The cross-section Ω of the external pipe, diameter $d = 9.0$ cm, at the point of measured velocity, was

$$\Omega = \frac{1}{4}\pi d^2 = 64 \text{ cm}^2 \quad (3.4)$$

compared with the cross-section of the flexible bag, of width $W = 50$ cm. Assuming the upper surface of the bag to be parabolic, the cross-sectional area Ω' would be

$$\Omega' = \frac{2}{3}W\Delta = 133 \text{ cm}^2, \quad (3.5)$$

so that the theoretical flow velocity should be multiplied by a factor $\Omega'/\Omega = 2.1$. On the other hand, the external resistance to the flow, both from the turbine and from a pipe of non-uniform cross-section, would tend to reduce the flow, so that the observed flow is not necessarily in disagreement with the simple theory.

Consider the dependence of the flow velocity upon the wave period T . The effects of refraction, etc. being difficult to assess, we shall assume roughly that the amplitude b of the vertical displacement of the bag varied simply in proportion to the theoretical displacement b' . Carrying through the same calculation as above for $T = 1.1$ s, we arrive at the numbers shown in table 1. The velocity

$$V_{\max} = \frac{\Omega' 5 q^2}{\Omega 4 c} \quad (3.6)$$

shown on the right of table 1 will be seen to behave qualitatively in a similar way to the measured velocity, with a maximum at around $T = 1.2$ s instead of 1.1 s.

Consider now the maximum pressure head $[p]$ as given by (2.16). Clearly this depends critically on the thickness Δ of the fluid layer. Since in the experiment Δ was non-uniform over the width of the bag, being smaller near the two sides, (2.16) suggests there may have been some lateral circulation within the bag, in contrast with

T (s)	$\frac{\sigma^2 h}{g}$	kh	c (cm/s)	$2a$ (cm)	q (cm/s)	$\frac{q^2}{c}$ (cm/s)	V_{\max} (cm/s)	$[p]$ (dyn/cm ²)
0.8	1.886	1.962	120	3.0	13	1.3	3.4	21
0.9	1.490	1.613	160	4.5	24	3.2	8.3	53
1.0	1.207	1.373	137	5.0	31	6.9	17.9	113
1.1	0.998	1.198	143	5.0	35	8.9	23.5	143
1.2	0.838	1.064	148	5.5	42	11.8	30.6	194
1.3	0.714	0.960	151	5.0	40	10.6	27.5	174
1.4	0.616	0.875	154	4.2	35	8.0	20.8	132
1.5	0.537	0.805	156	4.2	36	8.4	17.7	138
2.0	0.362	0.579	163	3.5	33	6.8	20.8	112
2.5	0.193	0.454	166	2.5	25	3.7	9.6	61

TABLE 1. Wave parameters in figure 6 of Allison (1983)

our two-dimensional model. To estimate the actual mean pressure gradient it is perhaps reasonable to replace Δ by its mean value $\frac{2}{3}\Delta_0$, where $\Delta_0 = 4.0$ cm, the value at the centre of the cross-section. Then on taking $\nu = 0.013$ cm²/s we find for $[p]$ the numerical values given in the right-hand column of table 1. Clearly these are less than the observed mean pressures in Allison's figure 8 by an order of magnitude.

Inspection of table 1 suggests one possible reason for the discrepancy, for the Reynolds numbers

$$R = q\Delta/\nu \quad (3.7)$$

are of order 10^3 , implying that the flow within the flexible bag is possibly turbulent.

Now a formal extension of the theory of oscillatory boundary-layers to turbulent flow was given by Longuet-Higgins (1956), who showed that if the molecular viscosity ν were replaced by a coefficient of kinematic viscosity N which was a function only of the mean distance z of a particle from the boundary (N being constant following a particle), then in a progressive wave motion, though the details of the boundary layer depended on the form of $N(z)$, the limiting drift velocity U outside the layer was unaffected. That is to say (1.1) remained valid. Indeed, some such result was necessary to explain the observations by Russell & Osorio (1956).

In a turbulent flow the complete velocity profile (corresponding to (2.13) in the laminar conditions) must depend on the function $N(z)$. The observational evidence, combined with equation (2.16), suggests that in order of magnitude N should be about 10ν . The result of increasing the effective viscosity by this amount would be to multiply the thickness δ of the boundary layer by a factor $(N/\nu)^{\frac{1}{2}}$, or about 3. For waves of 1 s period, for instance, δ would be increased from 0.064 cm to about 0.2 cm. As this is beginning to be comparable to the half-thickness of the layer within the bag, there may in fact be some interaction between the upper and lower boundary layers, leading to a reduction in the net mean flow. We investigate this effect in §4.

4. Boundary-layer interactions: $\delta/\Delta = O(1)$

We now extend and generalize the analysis of §2 to a situation when the thickness of the boundary-layer is no longer small compared with the thickness of the fluid layer in the flexible bag. Thus we assume $\delta/\Delta = O(1)$, where $\delta = (2\nu/\sigma)^{\frac{1}{2}}$. However, the restrictions

$$k\Delta \ll 1, \quad b/\Delta \ll 1 \quad (4.1)$$

will be retained. The first of these implies that the wavelength is long compared with the thickness Δ of the layer, so that $\partial/\partial x \ll \partial/\partial z$ in general. The second implies that the stream function may be expanded in the form

$$\psi = \epsilon\psi_1 + \epsilon^2\psi_2 + \dots, \quad (4.2)$$

where ϵ is a small parameter of order b/Δ , and we may use the equations for the mass transport and mean flow developed by Longuet-Higgins (1953).

Thus for the first-order flow ψ_1 we have the differential equation

$$\left(\frac{\partial}{\partial t} - \nu\nabla^2\right)\nabla^2\psi_1 = 0, \quad (4.3)$$

in which ∇^2 may be approximated by $\partial^2/\partial z^2$. The boundary conditions are that

$$\psi_{1z} = 0, \quad \psi_{1z} = 0 \quad \text{when } z = 0, \quad (4.4)$$

$$\epsilon\psi_{1z} = -w, \quad \psi_{1z} = 0 \quad \text{when } z = \Delta, \quad (4.5)$$

Peristaltic pumping in water waves

399

where w denotes the vertical velocity imposed at the upper membrane. For a progressive wave this is given by (2.4). Using complex notation, so $\psi_1 \propto e^{i(kx-\sigma t)}$, we have

$$\psi_{1zzt} - \nu\psi_{1zzzz} = 0 \quad (4.6)$$

with

$$\psi_1 = 0, \quad \psi_{1z} = 0 \quad \text{when } z = 0, \quad (4.7)$$

$$\psi_1 = c\Delta e^{i(kx-\sigma t)}, \quad \psi_{1z} = 0 \quad \text{when } z = \Delta. \quad (4.8)$$

The solution of these equations is

$$\psi_1 = [A(\cosh \alpha z - 1) + B(\sinh \alpha z - \alpha z)] e^{i(kx-\sigma t)}, \quad (4.9)$$

where

$$\alpha = \left(\frac{\sigma}{i\nu}\right)^{1/2} = \frac{1-i}{\delta}, \quad (4.10)$$

and A and B are constants, satisfying

$$\begin{aligned} A(\cosh \alpha \Delta - 1) + B(\sinh \alpha \Delta - \alpha \Delta) &= c\Delta, \\ A \sinh \alpha \Delta + B(\cosh \alpha \Delta - 1) &= 0. \end{aligned} \quad (4.11)$$

For the stream function $\epsilon^2 \bar{\psi}_2$ of the mean motion at a fixed point in the fluid, we have from the momentum equations

$$\overline{\psi_{1z} \psi_{1xz}} - \overline{\psi_{1x} \psi_{1zz}} = -\frac{\bar{w}}{\rho \epsilon^2} + \nu \overline{\psi_{2zzz}}. \quad (4.12)$$

\bar{w} is the mean horizontal pressure gradient, ρ is the density, and an overbar denotes the mean value with respect to time. The terms on the left represent the convected momentum.

Since the motion is periodic in the x -direction, the first term $\overline{\psi_{1z} \psi_{1xz}}$ vanishes identically. In the second term, since the motion is progressive, we may replace $\partial/\partial x$ by $-c^{-1}\partial/\partial t$, and then use the property that if F and G are any two periodic quantities

$$\overline{F_t G + F G_t} = 0. \quad (4.13)$$

Hence

$$\overline{\psi_{1z} \psi_{1zz}} = -\frac{1}{c} \overline{\psi_{1t} \psi_{1zz}} = \frac{1}{c} \overline{\psi_1 \psi_{1zzt}}. \quad (4.14)$$

On substituting for ψ_{1zzt} from (4.6) we obtain for $\bar{\psi}_2$ the equation

$$\bar{\psi}_{2zzz} = -\frac{1}{c} \overline{\psi_1 \psi_{1zzzz}} + \frac{\bar{w}}{\rho \nu \epsilon^2}. \quad (4.15)$$

To obtain the mass-transport velocity we note that the stream function $\epsilon^2 \bar{\Psi}$ for the mass transport is related to $\bar{\psi}_2$ by

$$\bar{\Psi} = \bar{\psi}_2 + \int \bar{\psi}_{1z} dt \bar{\psi}_{1x} \quad (4.16)$$

in general (see Longuet-Higgins 1953, equation (36)). The second group of terms on the right corresponds to the Stokes drift. For progressive motion, on replacing ψ_{1z} by $-c^{-1}\psi_{1t}$ and using (4.13) we have

$$\int \bar{\psi}_{1z} dt \bar{\psi}_{1x} = -\frac{1}{c} \int \bar{\psi}_{1t} dt \bar{\psi}_{1x} = \frac{1}{c} \overline{\psi_{1z} \psi_1}, \quad (4.17)$$

so that (4.14) can be written

$$\bar{\Psi} = \bar{\psi}_2 + \frac{1}{2c} \overline{(\psi_1^2)}_z. \quad (4.18)$$

M. S. Longuet-Higgins

400

From (4.15) and (4.18) we obtain for Ψ the equation

$$\Psi_{zzz} = \frac{1}{2c} (\overline{\psi_1^2})_{zzzz} - \frac{1}{c} \overline{\psi_1 \psi_{1zzzz}} + \frac{w}{\rho v \epsilon^2}. \quad (4.19)$$

This can be further simplified. For by Leibnitz's theorem the first two terms on the right can be written

$$\frac{1}{c} (\overline{\psi_1 \psi_{1zzzz}} + 4\overline{\psi_{1z} \psi_{1zzz}} + 3\overline{\psi_{1zz}^2}) - \frac{1}{c} \overline{\psi_1 \psi_{1zzzz}} = \frac{1}{c} (\overline{\psi_{1z} \psi_{1zzz}} + \frac{3}{2} \frac{\partial^2}{\partial z^2} \overline{\psi_{1z}^2}). \quad (4.20)$$

But from (4.6) we have

$$\psi_{1zz} = \nu \int \psi_{1zzzz} dt, \quad (4.21)$$

and so on integration with respect to z

$$\psi_{1z} = \nu \int \psi_{1zzz} dt + Q, \quad (4.22)$$

where Q is independent of z . In fact

$$Q = \frac{\nu}{i\sigma} (\psi_{1zzz})_{z=0} = -\alpha B e^{i(kz - \sigma t)}. \quad (4.23)$$

Multiplying (4.22) by ψ_{1zzz} and averaging, we have

$$\overline{\psi_{1z} \psi_{1zzz}} = \overline{Q \psi_{1zzz}}. \quad (4.24)$$

From (4.19), (4.20) and (4.24) we have altogether

$$\Psi_{zzz} = \frac{1}{c} \overline{Q \psi_{1zzz}} + \frac{3}{2c} (\overline{\psi_{1z}^2})_{zz} + \frac{w}{\rho v \epsilon^2}. \quad (4.25)$$

To obtain the mass-transport velocity

$$U = \epsilon^2 \Psi_z \quad (4.26)$$

we now need only integrate (4.25) twice with respect to z , subject to the two boundary conditions

$$U = 0 \quad \text{when } z = 0 \quad \text{and } z = \Delta. \quad (4.27)$$

Since ψ_{1z} vanishes on both boundaries, we have immediately

$$U = \frac{\epsilon^2}{c} (\overline{Q \psi_{1z}} + \frac{3}{2} \overline{\psi_{1z}^2}) + \frac{w}{2\rho\nu} z(z - \Delta). \quad (4.28)$$

The total volume flux M is equal to $\epsilon^2 [\Psi]_0^\Delta$, and so

$$M = \frac{\epsilon^2}{c} \left\{ \overline{Q(\psi_1)_{z=\Delta}} + \frac{3}{2} \int_0^\Delta \overline{\psi_{1z}^2} dz \right\} - \frac{w \Delta^3}{12\rho\nu}. \quad (4.29)$$

In evaluating the time-averaged terms in (4.28) and (4.29) we may use the complex expressions (4.9) and (4.23) for ψ_1 and Q together with the rule

$$\overline{FG} = \frac{1}{2}(FG^* + F^*G) = \frac{1}{2} \text{Re } FG^*. \quad (4.30)$$

5. Discussion

Consider first the case when $\Delta \gg \delta$. Then from (4.10) we have $|\alpha\Delta| \gg 1$. Neglecting quantities of order $e^{-\alpha\Delta}$, we see from (4.11) that

$$A \doteq -B \doteq \frac{c\Delta}{\alpha\Delta - 2} \doteq \frac{c}{\alpha}. \quad (5.1)$$

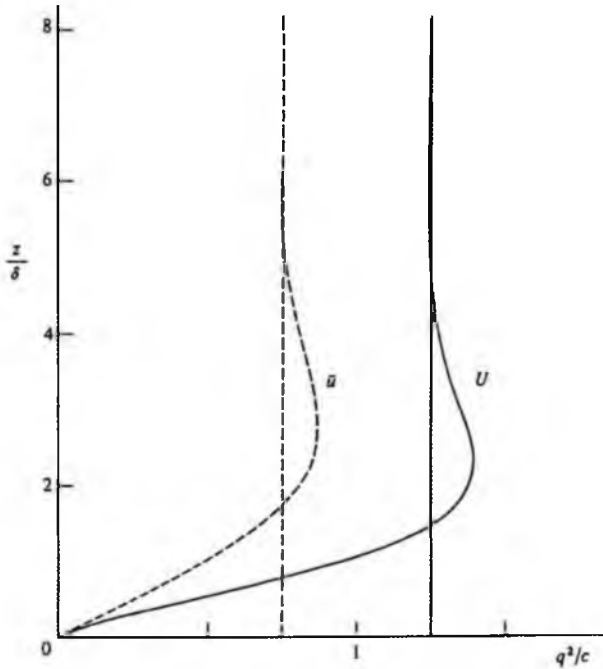


FIGURE 2. The streaming velocity U and the Eulerian-mean velocity \bar{u} in the boundary-layer at the bottom when $\varpi = 0$ and $\Delta/\delta \gg 1$.

Hence near the bottom, when $\alpha z = O(1)$, we find

$$\psi_1 = A(e^{-\alpha z} + \alpha z - 1)e^{i(kx - \sigma t)}. \quad (5.2)$$

This is the stream function for a Stokes layer (see Lamb 1932, §347) in which as $\alpha z \rightarrow \infty$ the horizontal velocity $\epsilon\psi_{1z}$ tends to $(bc/\Delta)e^{i(kx - \sigma t)}$, as in §2 above. Similarly near the upper surface, setting $z = \Delta + z'$, with $\alpha z' = O(1)$, we find, after approximating A and B more closely, that

$$\psi_1 = A(\alpha\Delta - 1 + \alpha z' - e^{\alpha z'})e^{i(kx - \sigma t)}, \quad (5.3)$$

which represents a similar Stokes layer on the underside of the membrane ($z' < 0$), but with an imposed vertical velocity $i\sigma b e^{i(kx - \sigma t)}$ as in §2.

It will be noticed that the two Stokes layers are nearly but not quite symmetrical with respect to the mean level, the strength of the bottom layer being greater than that at the upper membrane by a factor $|1 - 2/\alpha\Delta|^{-1}$, with a slight phase difference of order δ/Δ .

The mass-transport velocity U in the lower layer is easily calculated from (4.28) together with (5.2). When $\varpi = 0$ we obtain

$$U = \frac{q^2}{4c} \left(5 - 8e^{-2/\delta} \cos \frac{z}{\delta} + 3e^{-2z/\delta} \right), \quad (5.4)$$

where $q = bc/\Delta$, the amplitude of the first-order horizontal oscillatory velocity just outside the boundary layer. At this point the streaming velocity is $U = 5q^2/4c$ just as in (1.1). The velocity profile within the layer is shown in figure 2, plotted against z/Δ . We show also the profile of $\bar{u} = \epsilon^2 \bar{\psi}_{2z}$, the mean velocity at a fixed point. As will be seen, this tends to a different value, namely $3q^2/4c$, and is quite distinct from U .

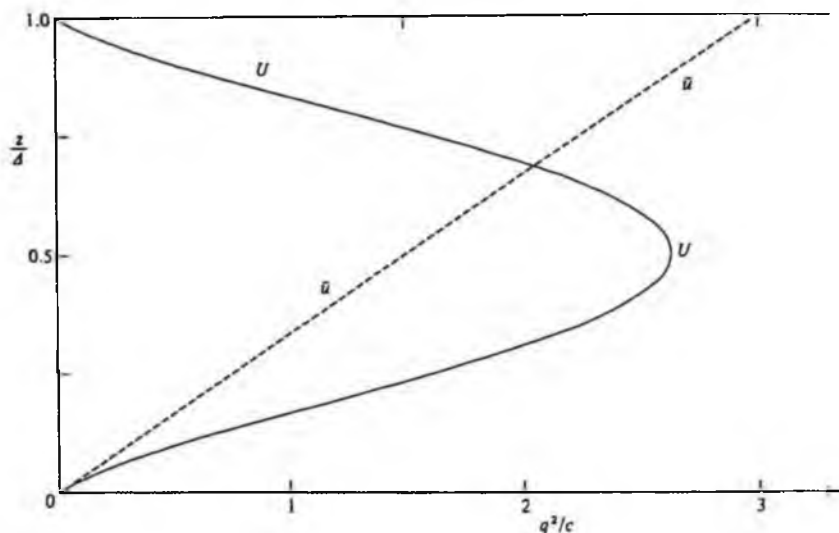


FIGURE 3. The streaming velocity U and the Eulerian-mean velocity u as functions of z/Δ , when $\omega = 0$ and $\Delta/\delta \ll 1$.

The streaming in the upper boundary-layer, which we get from (4.26) and (5.3), is entirely similar to (5.4), being given by reflecting (5.4) in the mean level $z = \frac{1}{2}\Delta$.

Thus we have shown that, in the case when $\Delta \gg \delta$, there is no significant interaction between the boundary-layers, and the mean flow is as described in §2.

In the opposite case when $\Delta \ll \delta$, the first-order solution (4.9) reduces to

$$\psi_1 = c\Delta \left(\frac{3z^2}{\Delta^2} - \frac{2z}{\Delta} \right) e^{i(kx - \sigma t)}, \quad (5.5)$$

so

$$\varepsilon\psi_{1z} = 6q\zeta(1-\zeta) e^{i(kx - \sigma t)}, \quad (5.6)$$

where $\zeta = z/\Delta$ and from (4.28)

$$U = \frac{3q^2}{c} [\zeta(1-\zeta) + 10\zeta^2(1-\zeta)^2] - \frac{1}{2} \frac{\omega\Delta^2}{\rho\nu} \zeta(1-\zeta). \quad (5.7)$$

This represents a quartic velocity profile (see figure 3) with a total transport

$$M = \frac{3q^2\Delta}{2c} - \frac{1}{12} \frac{\omega\Delta^3}{\rho\nu}. \quad (5.8)$$

If the flow is blocked so that $M = 0$, the resulting pressure-gradient w_{\max} is given by

$$w_{\max} = 18 \frac{\rho\nu q^2}{c\Delta^2}. \quad (5.9)$$

For general values of the ratio Δ/δ it is clear that the profile of the mass-transport velocity has the form

$$U = \frac{q^2}{c} \Phi\left(\zeta, \frac{\Delta}{\delta}\right) - \frac{\omega\Delta^2}{2\rho\nu} \zeta(1-\zeta), \quad (5.10)$$

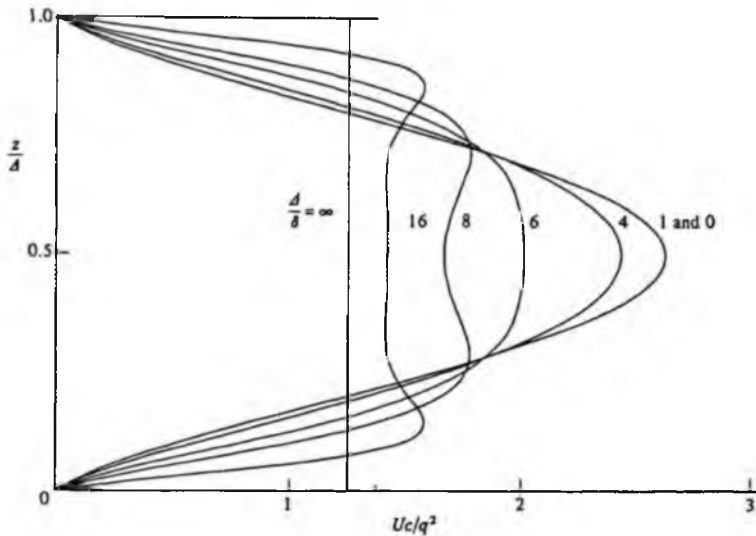


FIGURE 4. Profiles of the streaming velocity U when $\varpi = 0$ and $\Delta/\delta = 1, 4, 6, 8, 16$ and ∞ .

where q is the typical horizontal velocity bc/Δ (cf. (2.7)). If we define a Reynolds number R by

$$R = \frac{q\Delta}{\nu} = \frac{bc}{\nu} \quad (5.11)$$

then Δ/δ is related to R by

$$\frac{\Delta}{\delta} = \frac{k\Delta R^{\frac{1}{2}}}{(2bk)^{\frac{1}{2}}} \quad (5.12)$$

In figure 4 we have plotted the function Φ for a number of different values of Δ/δ . The transition from the profile (5.7) at low values of Δ/δ to the double boundary-layer profile (5.4) at high values of Δ/δ can be clearly seen. Between $\Delta/\delta = 1$ and 6 the velocity profile is unimodal. Between $\Delta/\delta = 6$ and 8 the curvature at the central level $z/\Delta = 0.5$ changes sign and the profile becomes bimodal. As Δ/δ increases further, the velocity maxima move apart towards the boundaries and new, less pronounced, oscillations develop near the centre. Finally as $\Delta/\delta \rightarrow \infty$ the profile tends to the limiting form indicated by the straight lines. This is the limiting form used in §2.

It can be seen that even when Δ/δ is as low as 4 there is a strong interaction between the two boundary layers. Remarkably, however, little change in the profile takes place when $\Delta/\delta < 4$. Indeed the profile for $\Delta/\delta = 1$ is practically indistinguishable from the limiting form (5.8) corresponding to $\Delta/\delta = 0$.

In figure 4 we have plotted only the profiles corresponding to zero pressure gradient, $\varpi = 0$. For general values of ϖ one has only to add a parabolic velocity profile, as in (4.28).

The profiles for U are all symmetric about the mean level, in spite of the asymmetry in the first-order velocity ψ_{1z} . The boundary conditions (4.7) and (4.8) for ψ_1 are indeed asymmetric, but could be made symmetric by the addition of a small transverse (vertical) velocity $-\frac{1}{2}b\sigma e^{i(kx-\sigma t)}$, independent of z . This would not affect the mechanics of the drift velocity U at lowest order in ϵ and $k\Delta$. Hence, provided that the amplitude b of the vertical displacement is small compared with the thickness

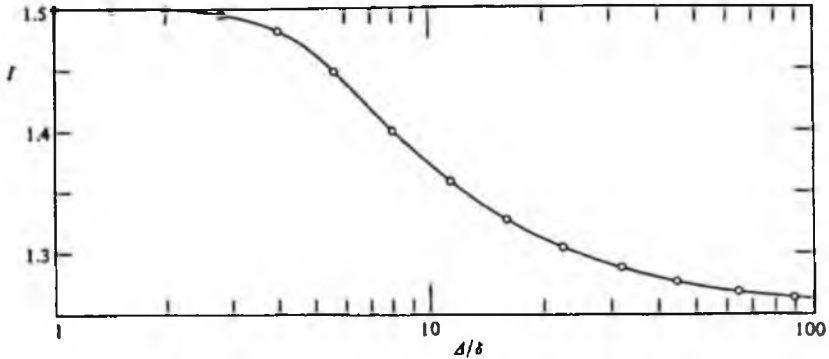


FIGURE 5. The integral I , giving the total mass flux in the fluid layer at zero pressure-gradient (see (5.13)).

Δ , and also that Δ is small compared with the wavelength, the mass transport velocity must be symmetric.

From equation (5.10) the total volume flux M can be expressed in the form

$$M = \frac{q^2 \Delta}{c} I\left(\frac{\Delta}{\delta}\right) - \frac{1}{12} \frac{\omega \Delta^3}{\rho \nu}, \quad (5.13)$$

where

$$I = \int_0^1 \Phi \, d\xi. \quad (5.14)$$

In figure 5 we have plotted I as a function of Δ/δ . Evidently I is almost a constant, lying always between the two limiting values 1.5 and 1.25.

From (5.13) the maximum pressure gradient w_{\max} is given by

$$w_{\max} = 12 \frac{\nu q^2}{\Delta^2 c} I, \quad (5.15)$$

or, if we express q in terms of the vertical displacement b at the upper boundary ($q = bc/\Delta$), then

$$w_{\max} = 12 \frac{\nu b^2 c}{\Delta^4} I. \quad (5.16)$$

This shows that, given the measured parameters b , c and Δ , the pressure gradient depends primarily upon ν , at least for small values of b/Δ . Thus the replacement of the laminar coefficient ν by an effective eddy coefficient ν_e might account for the observed pressure difference [p].

6. Effects of finite amplitude

When b/Δ is no longer small, the formulae of §5 must be modified. A general solution will not be attempted here, but we note that in the extreme case $b = \Delta$, when the whole layer is occluded by the perturbation, then $q = bc/\Delta = c$. Since the fluid is carried along with mean velocity c and the mean thickness of the layer is still equal to Δ , the transport M is

$$M = c\Delta = \frac{q^2 \Delta}{c}. \quad (6.1)$$

In other words (5.13), with $w = 0$, remains valid if we substitute $I = 1.00$. This represents a change of less than 50% from the value for $b/\Delta \ll 1$.

On the other hand the pressure gradient w must be more drastically affected by the finite amplitude. For in the constricted portions of the channel, where the fluid flow tends to be reversed, not only is the strength of the oscillating component of the current greater (at zero mean flux) owing to conservation of mass, but also the pressure gradient is more than proportionately increased. In the limiting case $b = A$ it is clear that w_{\max} must tend to infinity. Hence (5.15) and (5.16) must be serious underestimates, even at some values of b/A less than 1.

7. End-effects

We have so far neglected any effects due to the two ends of the bag. But if, for example, the flow in the pipe is blocked, the condition of zero net flow at the down-wave end may result in a reflected, damped elastic wave, which will tend to increase the amplitude p_1 of the pressure fluctuation there; in fact p_1 may be about double the corresponding amplitude far from the ends, i.e.

$$p_1 \sim 2\rho g a \operatorname{sech} kh, \quad (7.1)$$

and similarly for the fluctuation p_2 at the other end. The pressure difference between the two ends will be at most

$$p_1 + p_2 \sim 4\rho g a \operatorname{sech} kh \quad (7.2)$$

when the phases are opposite. This estimate agrees quite well with the relation between the peak-to-peak pressure P and the wave height H in figure 6 of Allison (1982). At the same time, the observed irregularities in the curve for P may be accounted for by phase differences between the two ends of the bag. The effect of the two ends on the *second-order* mean-pressure difference is, however, more difficult to estimate.

8. Conclusions

We have calculated the mean-drift velocities induced by water waves progressing over a thin flexible bag laid on the bed of a wave tank. The induced velocities are similar to those measured by Allison, but the calculated pressure gradients are smaller than those observed.

Among the assumptions in our calculation are that the flow was laminar, and that the amplitude of the vertical displacement b of the bag was small compared with the thickness A of the contained layer of fluid. Part of the discrepancy may be due to turbulence in the fluid. Although turbulence can be partly represented by an eddy viscosity $N(z)$, it is no longer true, in the presence of interaction between the boundary layers, that the streaming is independent of N .

A more probable cause for the discrepancies is the finite value of b/A . This ratio was assumed constant over the surface of the bag. But any values much greater than the assumed value of 0.27 would certainly have the effect of increasing the pressure gradient, without drastically altering the total mean flow.

For small displacements, the general method of calculation given in §4 above (which was developed previously for water waves) provides a very convenient framework for problems of this kind. In interpreting the theoretical solutions it is essential to distinguish between the Eulerian- and Lagrangian-mean velocities, a distinction not always observed in previous studies of peristaltic flow. An example is given in the Appendix.

Appendix. On the time-average velocity \bar{u}

As pointed out in §§2 and 4, the time-average \bar{u} of the velocity at a fixed point differs essentially from the particle drift velocity U . In fact from (4.16) we have in general

$$\bar{u} = U - \frac{1}{2c} (\overline{\psi_1^2})_{,zz} \quad (\text{A } 1)$$

$$= U - \frac{1}{c} (\overline{\psi_1 \psi_{1zz}} + \overline{\psi_{1z}^2}). \quad (\text{A } 2)$$

In figure 6 we have plotted \bar{u} for comparison with U in dimensionless form when $\Delta/\delta = \sqrt{14}$. As will be seen, not only is \bar{u} quite different from U , but it is also asymmetrical. Whereas U must vanish on both upper and lower boundary, \bar{u} need vanish only on the lower boundary $z = 0$.

The point is relevant to some previous discussions of peristaltic flow, for example Fung & Yih (1968) and Jaffrin & Shapiro (1971). Thus Fung & Yih studied the two-dimensional flow induced by small oscillations of the two boundaries of a thin fluid layer. Their analysis is directly comparable with ours, with a Reynolds number R' equivalent to our $(\Delta/\delta)^2/k\Delta$. In numerical examples they took $\frac{1}{2}k\Delta R'$ equal to 0.1, 0.4 and 7.0. However, their discussion is solely in terms of the second-order mean velocity \bar{u} , not the drift velocity U . The appropriate condition for a reflux, or reverse flow, is surely not $\bar{u} < 0$ but rather $U < 0$. Moreover, with a moving boundary the total flux M cannot be obtained by integrating \bar{u} up to the mean boundary; additional second-order terms are involved. Lastly, in Fung & Yih's paper it is not clear that the correct boundary condition $U = 0$ has been employed.

The correct solution to Fung & Yih's problem can in fact be written down immediately from the analysis of §4 above. Moving the origin O to the central level

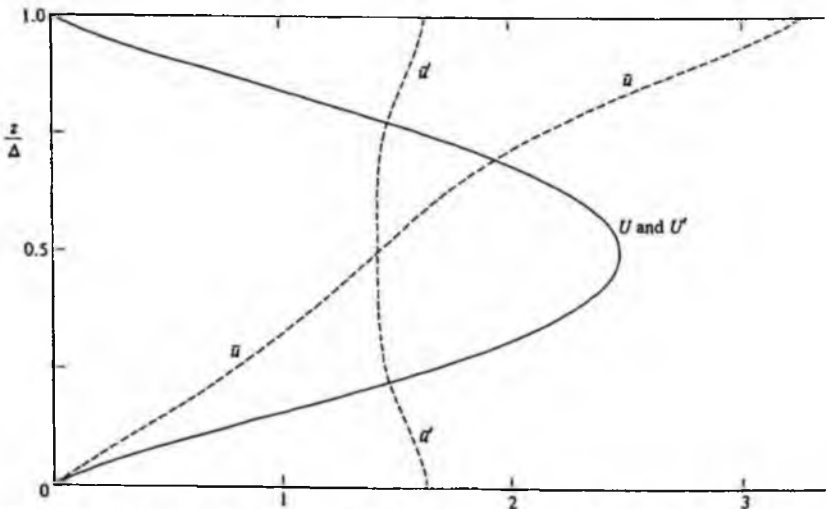


FIGURE 6. Comparison of the Eulerian- and Lagrangian-mean velocities (\bar{u} and U) when $\Delta/\delta = \sqrt{14} = 3.742$. Also shown is the Eulerian-mean velocity \bar{u}' in the problem of Fung & Yih (1968).

$z = \frac{1}{2}\Delta$ by writing $z' = z - \frac{1}{2}\Delta$ we have for the first-order motion ψ'_1 the boundary conditions

$$\begin{aligned}\psi'_1 &= \frac{1}{2}c\Delta e^{i(kz-\sigma t)}, & \psi_{1z} &= 0 & \text{when } z' &= \frac{1}{2}\Delta, \\ \psi'_1 &= -\frac{1}{2}c\Delta e^{i(kz-\sigma t)}, & \psi_{1z} &= 0 & \text{when } z' &= -\frac{1}{2}\Delta,\end{aligned}\quad (\text{A } 3)$$

where $\epsilon = b/\Delta$ and the amplitude of the vertical displacement at each membrane equals $\frac{1}{2}b$. The required solution is

$$\psi'_1 = \frac{\alpha z' \cosh(\frac{1}{2}\alpha\Delta) - \sinh \alpha z'}{\frac{1}{2}\alpha\Delta \cosh(\frac{1}{2}\alpha\Delta) - \sinh(\frac{1}{2}\alpha\Delta)} \frac{c\Delta}{2} e^{i(kz-\sigma t)}.\quad (\text{A } 4)$$

This compares with the first-order solution ψ_1 of (4.9), which can be expressed simply as

$$\psi_1 = \psi'_1 + \frac{1}{2}c\Delta e^{i(kz-\sigma t)}.\quad (\text{A } 5)$$

Clearly $\psi'_{1z} = \psi_{1z}$ and in (4.21) $Q' = Q$. Therefore by (4.26) the mass-transport velocity U' is given by

$$U' = U,\quad (\text{A } 6)$$

and so is described by the curves in figures 4-6.

The corresponding Eulerian-mean velocity \bar{u}' can be found from the relation

$$\bar{u}' = U' - \frac{\epsilon^2}{c} (\overline{\psi'_1 \psi_{1zz}} + \overline{\psi_{1z}^2}),\quad (\text{A } 7)$$

which in view of (A 5) reduces to

$$\bar{u}' = \bar{u} + \frac{1}{2}\epsilon^2\Delta e^{i(kz-\sigma t)} \overline{\psi_{1zz}}.\quad (\text{A } 8)$$

Numerical evaluation of this expression yields the curve for \bar{u}' in figure 6, which agrees closely with figure 3(c) of Fung & Yih (1968).

The fact that the Eulerian-mean velocities \bar{u} and \bar{u}' in the two problems are quite different, while the Lagrangian-mean velocities U and U' are equal confirms that the latter have a greater physical significance.

The author is indebted to Dr H. Allison for stimulating correspondence and to Drs T. J. Pedley and S. J. Hogan for comments.

REFERENCES

- ALLISON, H. 1983 Streaming of fluid under a near-bottom membrane for utilization of sea-wave energy. *J. Fluid Mech.* **137**, 385-392.
- BAGNOLD, R. A. 1947 Sand movement by waves: some small-scale experiments with sand of very low density. *J. Inst. Civ. Engrs Lond.* **27**, 447-469.
- BARTON, C. & RAYNOR, S. 1968 Peristaltic flow in tubes. *Bull. Math. Biophys.* **30**, 663-683.
- FUNG, Y. C. & YIH, C. S. 1968 Peristaltic transport. *Trans. ASME E: J. Appl. Mech.* **35**, 669-675.
- JAFFRIN, M. Y. & SHAPIRO, A. H. 1971 Peristaltic pumping. *Ann. Rev. Fluid Mech.* **3**, 13-36.
- LAMB, H. 1932 *Hydrodynamics*, 6th edn. Cambridge University Press.
- LONGUET-HIGGINS, M. S. 1953 Mass transport in water waves. *Phil. Trans. R. Soc. Lond.* **A 245**, 535-581.
- LONGUET-HIGGINS, M. S. 1956 The mechanics of the boundary-layer near the bottom in a progressive wave. In *Proc. 6th Intl Conf. on Coastal Engng.* **C. 10**, pp. 184-193.
- RAYLEIGH, LORD 1884 On the circulation of air observed in Kundt's tubes, and on some allied acoustical problems. *Phil. Trans. R. Soc. Lond.* **175**, 1-21.
- RUSSELL, R. C. H. & OSORIO, J. D. C. 1956 An experimental investigation of drift profiles in a closed channel. In *Proc. 6th Intl Conf. on Coastal Engng.* **C. 10**, pp. 171-183.

Introductory Notes for Part D

D. Stochastic Processes

Papers D1 to D28

The first paper D1 of this series was written at the Scripps Institution of Oceanography in La Jolla, in 1952. Subsequent papers are more abstract and therefore more generally applicable, but all are written with the analysis of the sea surface in mind.

Papers D2 to D4 are about the statistical properties of a function of a single random variable. Papers D5 to D7 extend these ideas to a function of three variables — two of space and one of time. Most of the quantities analyzed are essentially local, involving a function or its derivatives at one point, but D8 is the start of a series of studies of the intervals between zeros of a gaussian function, an easily measured property much used by oceanographers and others. This series of studies is continued in papers D16 and D17.

Papers D9 to D14 are about optical properties of gaussian surfaces, particularly the reflection of light from the sea surface; they were motivated by observations of the twinkling of sunlight, made while the author was vacationing on Beach Island off the coast of Maine.

Papers D18 and D19 were written in response to a colleague (H Charnock) who remarked that the sea surface “looked different when viewed upside-down”. Thus in wind-waves, the wave crests are generally sharper and more pointed than the wave troughs. These two papers extend the statistics of a gaussian (linear) model of the sea surface so as to include “weak” nonlinearities (but not strong nonlinearities such as wave breaking). A further paper D21 concentrates on the effects of weak nonlinearity on the distribution of wave heights in a sea state having a narrow frequency spectrum (c.f paper C1) and also some effects of a finite band-width. Paper D22, which discusses effects of capillarity and viscosity, is included in this series.

Paper D27, with MA Srokosz, applies the basic nonlinear theory of D18 to a practical problem which is of special importance for the accurate measurement of sea-surface elevation by orbiting satellites. (Such measurements are used for the calculation of ocean currents).

For many engineering purposes it is useful to know not merely the distribution of heights and the “periods” (defined as the time intervals between successive crests or crossings for the mean level) but also their joint distribution. This problem is solved approximately in paper D20, and to a higher approximation in D23.

Papers D25 and D26 (but especially D25) contain a thorough discussion of the meaning of a wave "group" and its statistical properties. The dynamics of wave groups are discussed in a later paper (Paper L19).

Lastly, paper D28 discusses the statistical effect of side-walls on the waves in a wind-wave channel, an effect often overlooked in laboratory experiments.

D. Stochastic Processes

Reprinted with permission from
SEARS FOUNDATION: JOURNAL OF MARINE RESEARCH
Vol. XI, No. 3, December 31, 1952. Pp. 254-266.

ON THE STATISTICAL DISTRIBUTION OF THE HEIGHTS OF SEA WAVES

BY

M. S. LONGUET-HIGGINS

Trinity College, Cambridge¹

ABSTRACT

The statistical distribution of wave-heights is derived theoretically on the assumptions (a) that the wave spectrum contains a single narrow band of frequencies, and (b) that the wave energy is being received from a large number of different sources whose phases are random. Theoretical relations are found between the root-mean-square wave-height, the mean height of the highest one-third (or highest one-tenth) waves and the most probable height of the largest wave in a given interval of time. There is close agreement with observation.

1. INTRODUCTION

At present several different quantities are in use for describing the state of the sea: for example, the mean height of the waves, the root-mean-square height, the height of the "significant" waves (defined by Sverdrup and Munk [1947] as the mean height of the highest one-third of all the waves), the maximum height over a given interval of time, and so on. The purpose of the following is to investigate the relationship of these quantities to one another in some special cases, and especially in the case when the spectrum of the waves consists of a single narrow frequency-band.

¹ The author is indebted to the Commonwealth Fund, New York, for a Fellowship to enable him to study at the Scripps Institution of Oceanography, where this paper was prepared.

For definiteness let us consider the elevation ζ of the sea surface at a fixed point, given as a function of the time t only. Much of the following, however, will apply to any oscillatory function of a single variable: for example, to the pressure at a point on the bottom, or to the rolling motion of a ship as measured by its angular deflection from the vertical. In general we shall denote by a the amplitude of ζ , which may be defined as half the distance in level between a wave crest and the preceding trough; thus $2a$ equals the wave-height. The period, or interval between successive crests, will be denoted by τ , or $2\pi/\sigma$, where $\sigma/2\pi$ is the frequency. I denotes any interval of the t -axis, of length T , in which the variable ζ is under consideration; it is supposed that $T \gg \tau$, i. e., the interval contains a large number of complete periods. The successive values of a in the interval I may

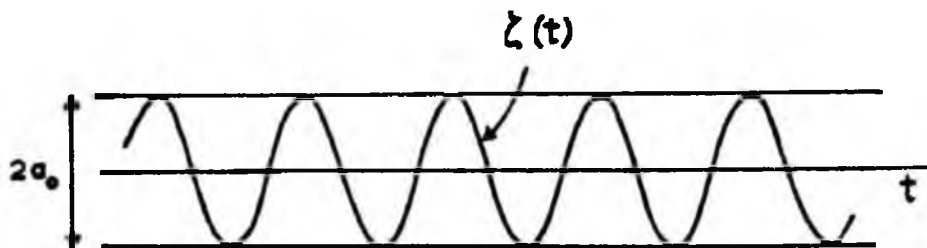


Figure 1. A simple sine-wave: definition of the wave amplitude.

be denoted by $a_1, a_2 \dots a_N$. If these are arranged in descending order of magnitude, the mean value of the first pN of these, where p is a fraction between 0 and 1, will be denoted by $a^{(p)}$. Thus the amplitude of Sverdrup and Munk's "significant waves" is $a^{(1/3)}$. The mean amplitude of all of the waves is $a^{(1)}$. It is clear that $a^{(p)}$ is a decreasing, or at any rate a nonincreasing, function of p ; and if a_{\max} is the maximum value of a in the interval, we have

$$a_{\max} > a^{(p)} > a^{(1)}. \quad (1)$$

The root-mean-square amplitude \bar{a} is defined by

$$\bar{a}^2 = \frac{1}{N} (a_1^2 + a_2^2 + \dots + a_N^2). \quad (2)$$

It may easily be shown that

$$\bar{a} > a^{(1)}. \quad (3)$$

Since \bar{a} is of physical significance in a wide class of cases, $a^{(p)}$ will normally be expressed in terms of \bar{a} . The mode is defined as the most frequently occurring wave amplitude and will be denoted by $\mu(a)$.

Example 1. Simple sine-wave. Suppose

$$\zeta = a_0 \cos \sigma t ; \quad (4)$$

then we have a simple sine-wave of period $2\pi/\sigma$ and amplitude a_0 (see Fig. 1). All the waves are of amplitude a_0 , and therefore

$$a_{max} = a^{(p)} = \bar{a} = \mu(a) = a_0 . \quad (5)$$

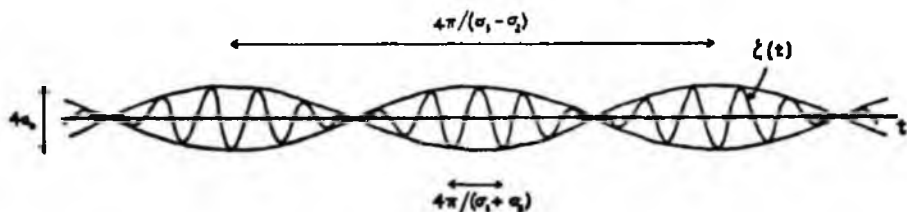


Figure 2. Combination of two sine-waves of slightly different frequency.

Example 2. Two sine-waves. Consider the sum of two sine-waves of equal amplitude but of very slightly differing period:

$$\zeta = a_0 \cos \sigma_1 t + a_0 \cos \sigma_2 t , \quad (6)$$

say, where $|\sigma_1 - \sigma_2| \ll |\sigma_1 + \sigma_2|$. We may write

$$\zeta = 2a_0 \cos \frac{\sigma_1 + \sigma_2}{2} t \cos \frac{\sigma_1 - \sigma_2}{2} t , \quad (7)$$

showing that the resultant consists of a carrier wave $\cos \frac{\sigma_1 + \sigma_2}{2} t$, whose period is nearly the same as that of the two component waves, modulated by an envelope function $2a_0 \cos \frac{\sigma_1 - \sigma_2}{2} t$, whose period, by hypothesis, is comparatively long (see Fig. 2). The maxima and minima of ζ occur nearly on the envelope and so are nearly equal in magnitude to the magnitude of the envelope function. In the limit they are distributed at even intervals along the t -axis. Taking the interval $0 < t < \pi/(\sigma_1 - \sigma_2)$ as typical, and supposing it contains N waves, we see that the highest pN waves will be contained in the interval $0 < t < p\pi/(\sigma_1 - \sigma_2)$. The mean amplitude $a^{(p)}$ of these is given by

$$\frac{p\pi}{\sigma_1 - \sigma_2} a^{(p)} = \int_0^{p\pi/(\sigma_1 - \sigma_2)} 2a_0 \cos \frac{\sigma_1 - \sigma_2}{2} t dt , \quad (8)$$

and hence

$$a^{(p)} = 2a_0 \cdot \frac{2}{p\pi} \sin \frac{p\pi}{2} . \quad (9)$$

The root-mean-square wave-height is given by

$$\frac{\pi}{\sigma_1 - \sigma_2} \bar{a}^2 = \int_0^{\pi/(\sigma_1 - \sigma_2)} 4a_0^2 \cos^2 \frac{\sigma_1 - \sigma_2}{2} t dt, \quad (10)$$

and hence

$$\bar{a}^2 = 2a_0, \quad \bar{a} = \sqrt{2} a_0. \quad (11)$$

Thus

$$a^{(p)}/\bar{a} = \sqrt{2} \cdot \frac{2}{p\pi} \sin \frac{p\pi}{2}. \quad (12)$$

In particular

$$\left. \begin{aligned} a^{(1/10)}/\bar{a} &= \frac{20\sqrt{2}}{\pi} \sin \frac{\pi}{20} = 1.408 \\ a^{(1/6)}/\bar{a} &= \frac{6\sqrt{2}}{\pi} \sin \frac{\pi}{6} = 1.350 \\ a^{(1/2)}/\bar{a} &= \frac{2\sqrt{2}}{\pi} \sin \frac{\pi}{2} = 0.901 \end{aligned} \right\} \quad (13)$$

$a^{(p)}/\bar{a}$ is plotted against p in Fig. 3. We have also

$$a_{\max} = 2a_0; \quad a_{\max}/\bar{a} = \sqrt{2}. \quad (14)$$

The statistical distribution of the wave amplitudes is evidently the same as that of the envelope function, which is that of the simple cosine curve

$$r = 2a_0 \cos \theta. \quad (15)$$

See Fig. 4. The probability that a point in the interval $0 < \theta < \pi/2$ lies in any given region of width $d\theta$ is $2|d\theta|/\pi$. Hence the probability $P(r)|dr|$ that the function (15) lies between r and $r + dr$ is given by

$$P(r) |dr| = \frac{2}{\pi} |d\theta|. \quad (16)$$

Thus, when $0 < r < 2a_0$,

$$P(r) = \frac{2}{\pi} \left| \frac{d\theta}{dr} \right| = \frac{2}{\pi} \frac{1}{2a_0 \sin \theta} = \frac{2}{\pi} \frac{1}{(4a_0^2 - r^2)^{1/2}}. \quad (17)$$

Clearly a can never exceed $2a_0$ or $\sqrt{2}\bar{a}$. Hence the probability-distribution $P(r)$ of the wave-height a is given by

$$P(r) = \begin{cases} \frac{2}{\pi} \frac{1}{(2\bar{a}^2 - r^2)^{1/2}}, & (r < \sqrt{2}\bar{a}) \\ 0, & (r > \sqrt{2}\bar{a}) \end{cases} \quad (18)$$

1952]

Longuet-Higgins: The Heights of Sea Waves

249

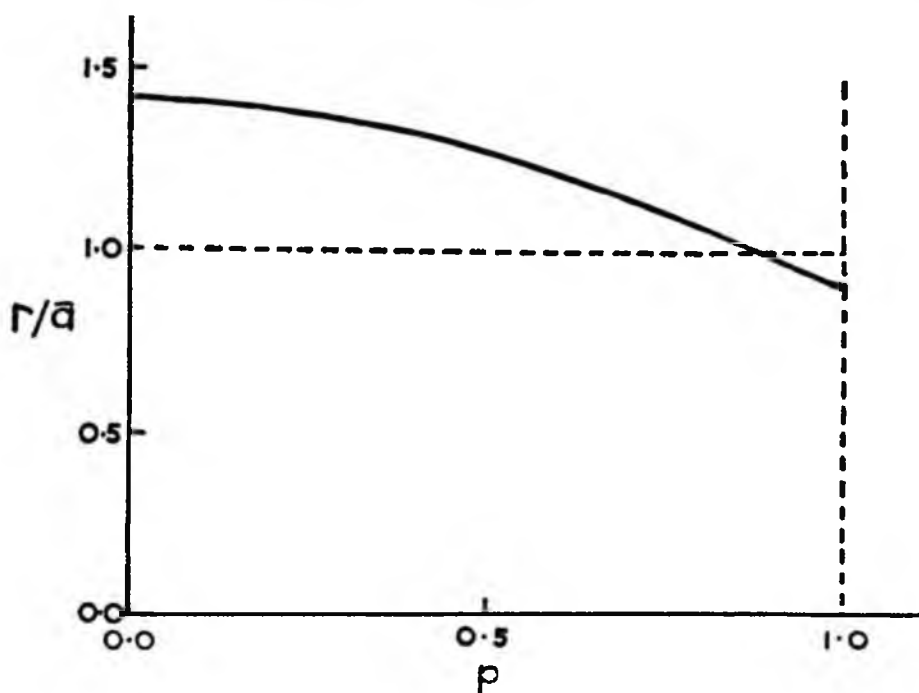


Figure 3. Graph of $a^{(p)}/a$ as a function of p , for two sine-waves of slightly different frequency.

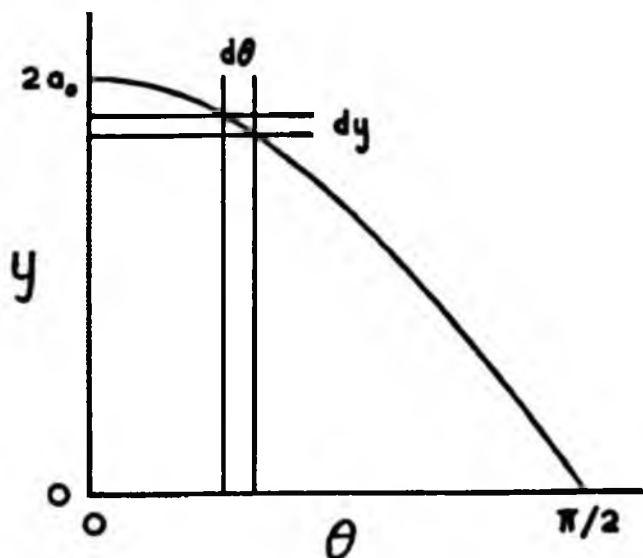


Figure 4. The curve $y = 2a_1 \cos \theta$.

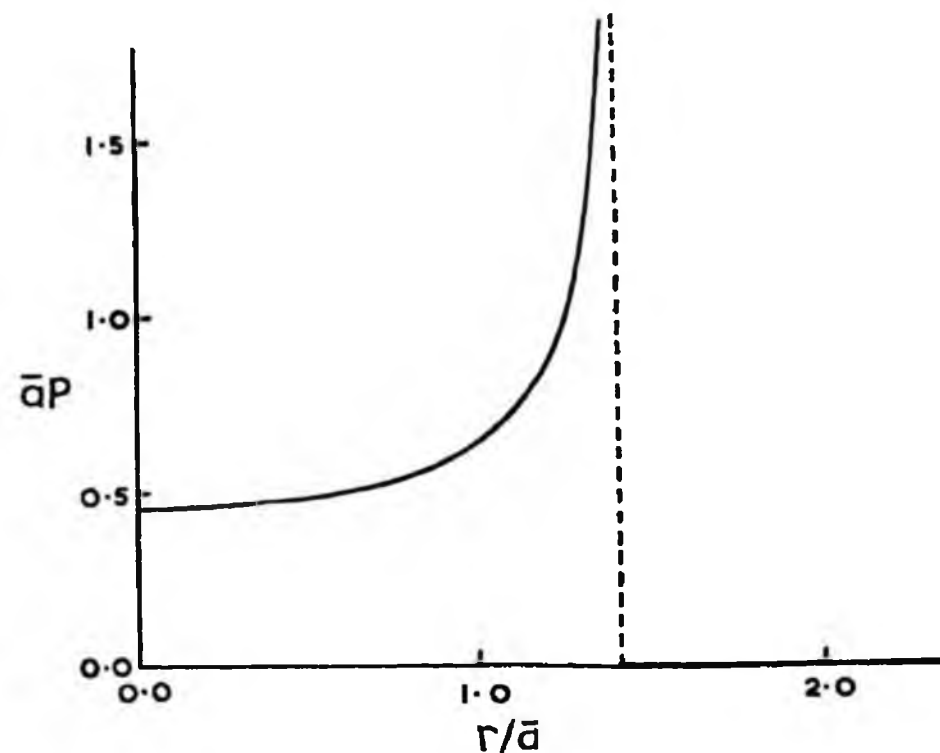


Figure 5. Frequency distribution of the wave amplitude for two sine-waves of slightly different frequency.

The function $\bar{a}P$ is plotted against r/\bar{a} in Fig. 5. It will be seen that P increases steadily with r and tends to infinity as r tends to $\sqrt{2\bar{a}}$. We have therefore

$$\mu(a) = \sqrt{2\bar{a}} = a_{\max}. \quad (19)$$

The foregoing examples, however, are very special cases which are unlikely to occur in practice. In the following we shall be concerned with a more realistic case, namely when the spectrum of the waves is narrow and the disturbance is made up of a number of random contributions. Such a case was considered by Rayleigh (1880) in connection with the amplitude of sound derived from many independent sources, and the theoretical distribution of maxima has been used in acoustics and in the theory of filters (for example, see Rice, 1944-5; Eckart, 1950). Indeed, Barber (1950) has already presented evidence that for waves there is rough agreement with this distribution. We shall consider rather carefully the application of this distribution to sea waves, find the theoretical values of $a^{(p)}/\bar{a}$ and the distribution of a_{\max}/\bar{a} , and compare the results with observation.

2. A NARROW WAVE-BAND

Let the wave elevation ζ in any interval I be expressed as a Fourier integral:

$$\zeta = \int_{-\infty}^{\infty} A(\sigma) e^{i\sigma t} d\sigma, \quad (20)$$

where the spectrum function $A(\sigma)$ may be complex and where it is understood that only the real part of the right-hand side is to be taken. Suppose that the spectrum consists of a single narrow frequency-band of wavelength $2\pi/\sigma_0$, say, so that $A(\sigma)$ is appreciable only for values of σ near σ_0 . We may write

$$\zeta = e^{i\sigma_0 t} \int_{-\infty}^{\infty} A(\sigma) e^{i(\sigma-\sigma_0)t} d\sigma. \quad (21)$$

In this expression $e^{i\sigma_0 t}$ represents a carrier wave of wavelength $2\pi/\sigma_0$, and the integral

$$B(t) = \int_{-\infty}^{\infty} A(\sigma) e^{i(\sigma-\sigma_0)t} d\sigma \quad (22)$$

is a slowly varying function which represents the envelope of the waves (see Fig. 6). As in Example 2 above, the maxima and minima

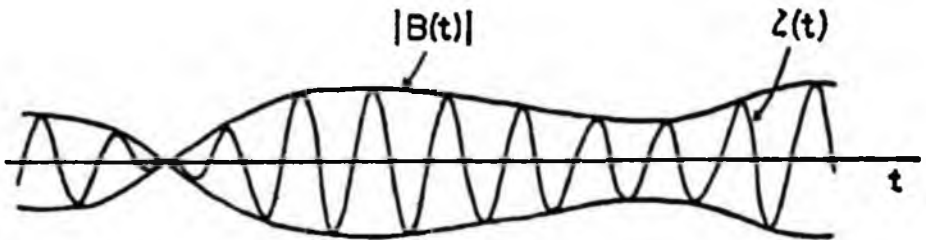


Figure 6. A disturbance $\zeta(t)$ having a narrow frequency band, and its envelope $|B(t)|$.

of ζ are spaced nearly evenly along the t -axis and are approximately equal to the value of $|B|$ at these points. It follows that the probability-distribution of the wave amplitudes is the same as the probability-distribution of $|B|$, which we shall therefore consider.

Now the wave-energy received at any point on the coast will have originated in many different places over a wide area. We may imagine that the generating area of the waves is divided into a large number of different regions, each of which will contribute to the wave-height ζ and to the envelope function B . If each region of the generating area is sufficiently large compared with a wavelength, it may be assumed that the phases of the contributions from different regions are inde-

pendent of one another. Then it is reasonable to assume that B is the sum of a very large number of small components of random phase. The probability-distribution of such a sum, which is known as the "random walk," was found by Rayleigh (1880) and has since been studied by many workers (for references, see Bartels, 1935). If the component vectors are b_1, b_2, \dots, b_M , i. e., if

$$B = b_1 + b_2 + \dots + b_M, \quad (23)$$

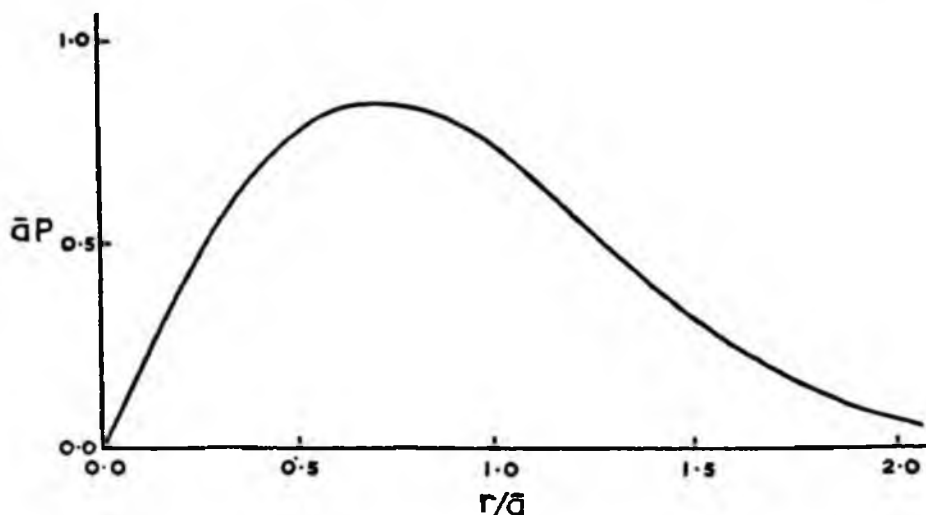


Figure 7. The "random walk" frequency distribution.

then the mean square value of $|B|$, taken over all relative phases of the component vectors, is given by

$$\bar{B}^2 = |b_1|^2 + |b_2|^2 + \dots + |b_M|^2, \quad (24)$$

and, under certain general restrictions on the size of the component vectors (see Khintchine, 1933) the probability that $|B|$ lie between r and $r + dr$ is given by

$$P(r)dr = e^{-r^2/\bar{B}^2} \cdot 2r/\bar{B}^2 dr. \quad (25)$$

Since the probability-distribution of $|B|$ equals that of the a 's, we have

$$\bar{B} = \bar{a}, \quad (26)$$

a quantity that can be estimated from observation; no detailed knowledge of the component vectors is required. Thus the probability-distribution of the a 's is given by

$$P(r) dr = e^{-r^2/\bar{a}^2} \cdot 2r/\bar{a}^2 dr = -de^{-r^2/\bar{a}^2}. \quad (27)$$

The function

$$\bar{a}P(r) = e^{-r/\bar{a}}. \quad 2r/\bar{a} \quad (28)$$

is shown in Fig. 7 (cf. Fig. 5). It will be seen that $P(r)$ is zero when $r = 0$, that it increases to a maximum, and then falls away rapidly for large values of r/\bar{a} . The total area under the curve is, of course, unity. The maximum value occurs when $r/\bar{a} = 1/\sqrt{2}$, so that the mode $\mu(a)$ is given by

$$\mu(a)/\bar{a} = \frac{1}{\sqrt{2}} = 0.717. \quad (29)$$

The chance $\varphi(r)$ that a should exceed a certain value r is given by

$$\varphi(r) = \int_r^{\infty} P(r) dr = e^{-r/\bar{a}}. \quad (30)$$

To find $a^{(p)}$, we note, first, that the proportion p of a 's which exceed a certain value r is equal to $\varphi(r)$, so that from (30)

$$p = e^{-r/\bar{a}}; \quad r = \left(\log \frac{1}{p} \right) \bar{a}. \quad (31)$$

The mean value $a^{(p)}$ of those a 's that are greater than r is given by

$$\varphi(r) a^{(p)} = \int_r^{\infty} r P(r) dr \quad (32)$$

or

$$e^{-r/\bar{a}} a^{(p)} = - \int_r^{\infty} r d e^{-r/\bar{a}} \quad (33)$$

from (27) and (30). After integrating the right-hand side by parts, we have

$$e^{-r/\bar{a}} a^{(p)} = r e^{-r/\bar{a}} + \int_r^{\infty} e^{-r/\bar{a}} dr, \quad (34)$$

and hence

$$\begin{aligned} a^{(p)}/\bar{a} &= r/\bar{a} + e^{r/\bar{a}} \int_r^{\infty} e^{-r/\bar{a}} dr/\bar{a} \\ &= \left(\log \frac{1}{p} \right) \bar{a} + \frac{1}{p} \int_{\left(\log \frac{1}{p} \right) \bar{a}}^{\infty} e^{-\theta} d\theta \end{aligned} \quad (35)$$

$$= \left(\log \frac{1}{p} \right) \bar{a} + \frac{1}{p} \frac{\sqrt{\pi}}{2} \left[1 - H \left\{ \left(\log \frac{1}{p} \right) \bar{a} \right\} \right], \quad (36)$$

where $H(\theta)$ is the probability function:

$$H(\theta) = \frac{2}{\sqrt{\pi}} \int_0^\theta e^{-\theta^2} d\theta. \tag{37}$$

Numerical values of $a^{(p)}/\bar{a}$ are given in Table I for some representative values of p . In particular, the mean $a^{(1)}$ is given by

$$a^{(1)}/\bar{a} = \frac{\sqrt{\pi}}{2} = 0.886. \tag{38}$$

TABLE I. REPRESENTATIVE VALUES OF $a^{(p)}/\bar{a}$ IN THE CASE OF A NARROW WAVE SPECTRUM

p	$a^{(p)}/\bar{a}$	p	$a^{(p)}/\bar{a}$
0.01	2.359	0.4	1.347
0.05	1.986	0.5	1.256
0.1	1.800	0.6	1.176
0.2	1.591	0.7	1.102
0.25	1.517	0.8	1.031
0.3	1.454	0.9	0.961
0.3333	1.416	1.0	0.886

The second moment of the distribution about the origin being \bar{a}^2 , by definition, we have for the second moment about the mean:

$$[\sigma(a)]^2 = \bar{a}^2 - a^{(1)2} = \bar{a}^2 \left(1 - \frac{\pi}{4}\right). \tag{39}$$

Thus the standard deviation $\sigma(a)$ is given by

$$\sigma(a)/\bar{a} = \left(1 - \frac{\pi}{4}\right)^{\frac{1}{2}} = 0.453. \tag{40}$$

$a^{(p)}/\bar{a}$ is shown as a function of p in Fig. 8, which may be compared with Fig. 3. An asymptotic formula for $a^{(p)}/\bar{a}$ when p approaches zero is found by further integration by parts in equation (35):

$$a^{(p)}/\bar{a} = \left(\log \frac{1}{p}\right)^{\frac{1}{2}} + \frac{1}{2} \left(\log \frac{1}{p}\right)^{-\frac{1}{2}} - \frac{1}{2} \cdot \frac{3}{2} \left(\log \frac{1}{p}\right)^{-\frac{3}{2}} + \frac{1}{2} \cdot \frac{3}{2} \cdot \frac{5}{2} \left(\log \frac{1}{p}\right)^{-\frac{5}{2}} \dots \tag{41}$$

Thus, in Fig. 8, as p tends to 0, $a^{(p)}/\bar{a}$ tends to infinity logarithmically. However, for the validity of this result it is essential that the fraction of the sample containing the highest pN wave amplitudes a shall not be too small; otherwise the present approximation will not hold.

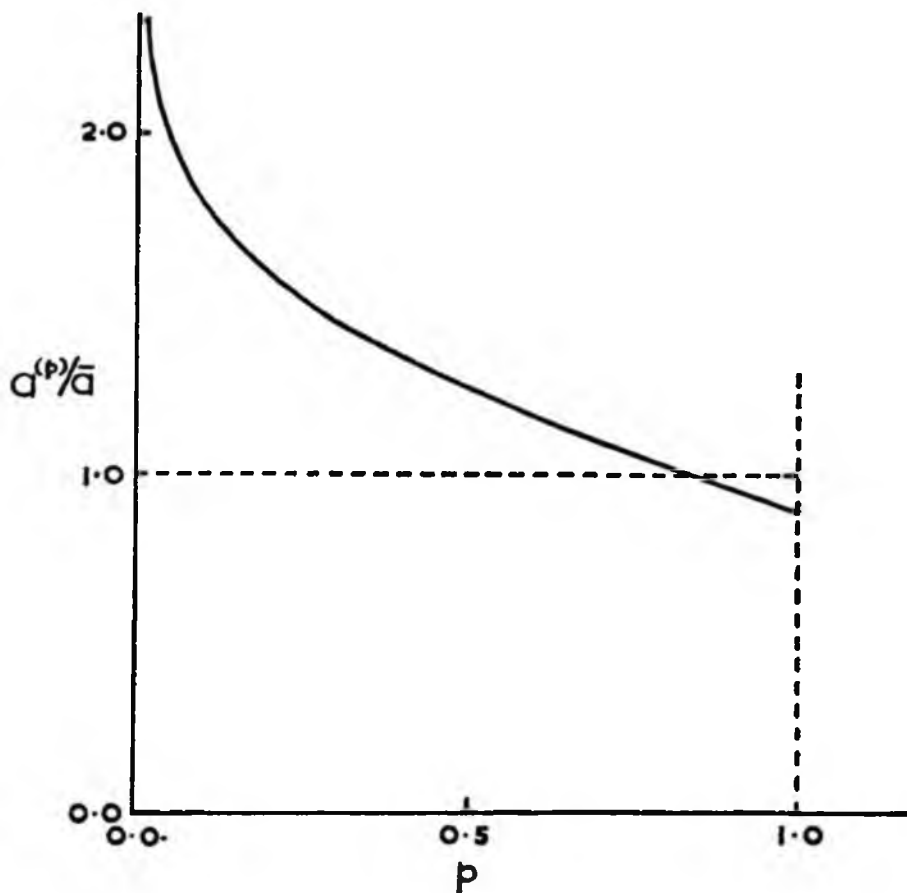


Figure 8. Graph of $a^{(p)}/\bar{a}$ as a function of p , for the narrow frequency band.

Suppose, for example, that we wish to find the expectancy $E(a_{\max})$ of the highest wave in an interval containing N waves. An approximate answer might be obtained by setting $p = 1/N$ and finding $a^{(1/N)}$. But this answer will not be exactly correct; for $a^{(1/N)}$ in fact represents the mean height of the $1/N$ th highest waves in a large sample, say a sample of size mN obtained by collecting together m samples, each containing N wave amplitudes. The m highest waves may not be distributed evenly, one in each of the samples; and if not, the mean of the highest waves, one from each group, will clearly be less than the mean of the m highest from all mN wave amplitudes together. Hence we see that the expected value of a_{\max} must be somewhat less than $a^{(1/N)}$.

Of course the ratios $a^{(p)}/\bar{a}$ found above refer to the total statistical "population" of wave amplitudes, or at least to a sample of theoretic-

cally infinite size selected at random from this population. In practice we have to consider samples of finite size N . For each ratio such as $a^{(p)}/\bar{a}$, theoretically there will be a corresponding probability-distribution depending on N . The expectancy value and the most probable value of $a^{(p)}/\bar{a}$ and of $a^{(p_1)}/a^{(p_2)}$ (where p_1 and p_2 are two different values of p) will differ slightly from the corresponding (exactly defined) values for the whole population. But when N and pN are large, these differences can be expected to be very small, and in the present discussion they will be neglected.

On the other hand, the expectancy of a_{max} , the maximum wave amplitude in a sample, depends fundamentally on the size of the sample.

One further point may be mentioned here. Strictly the analysis is valid only if the sampling of the wave amplitudes is random. In fact the sample consists of N consecutive wave amplitudes; since the envelope function varies slowly, there must be some correlation between members of the sample, especially when the spectrum is narrow. This may affect slightly the probability-distribution of, say, $a^{(p)}/\bar{a}$; but provided the record contains more than one or two wave groups, the effect of the "grouping" can be expected to be very small. Fluctuation of the envelope function may even act as a "randomising" process and may lead to observed ratios in closer agreement with the theoretical ratios than expected. At all events, the effect of "grouping" will be ignored in the present paper.

3. THE MAXIMUM WAVE AMPLITUDE

The probability-distribution of a_{max} may be derived as follows: The chance that any particular one of the a 's in the sample should be less than r , say, is

$$\int_0^r P(\tau) d\tau = 1 - \varphi(r), \quad (42)$$

where φ is given by equation (30). The chance that every a in the sample shall be less than r is therefore $(1 - \varphi)^N$; and the chance that at least one a shall exceed r is $1 - (1 - \varphi)^N$. The chance that the maximum a shall lie in the interval $(r, r + dr)$ is the chance that at least one a shall exceed r , minus the chance that at least one a shall exceed $r + dr$, that is,

$$-d[1 - (1 - \varphi)^N], = d(1 - \varphi)^N, \quad (43)$$

or

$$N(1 - \varphi)^{N-1} P dr, \quad (44)$$

since

$$\frac{d\varphi}{dr} = -P. \quad (45)$$

Thus the probability-distribution of a_{\max} is

$$N(1 - \varphi)^{N-1} P. \quad (46)$$

The expectation $E(a_{\max})$ of the maximum is given by

$$E(a_{\max}) = - \int_0^{\infty} r d [1 - (1 - \varphi)^N]. \quad (47)$$

On integrating by parts and assuming

$$r [1 - (1 - \varphi)^N] \rightarrow 0 \quad (48)$$

when $r \rightarrow \infty$, we have

$$E(a_{\max}) = \int_0^{\infty} [1 - (1 - \varphi)^N] dr. \quad (49)$$

On substitution from (30) we have

$$\begin{aligned} E(a_{\max})/\bar{a} &= \int_0^{\infty} [1 - (1 - e^{-r^2/a^2})^N] d\tau/\bar{a} \quad (50) \\ &= \frac{1}{2} \int_0^{\infty} [1 - (1 - e^{-\theta})^N] \theta^{-1/2} d\theta. \quad (50a) \end{aligned}$$

For small or moderately large values of N , the above integral can be evaluated by a direct expansion, using the binomial theorem; thus

$$\begin{aligned} E(a_{\max})/\bar{a} &= \\ \frac{1}{2} \int_0^{\infty} &\left[N e^{-\theta} - \frac{N(N-1)}{1.2} e^{-2\theta} + \dots (-)^{N\theta} e^{-N\theta} \right] \theta^{-1/2} d\theta, \quad (51) \end{aligned}$$

and since

$$\int_0^{\infty} e^{-n\theta} \theta^{-1/2} d\theta = n^{-1} \left(-\frac{1}{2} \right)! = \left(\frac{\pi}{n} \right)^{1/2}, \quad (52)$$

we have

$$E(a_{\max})/\bar{a} = \frac{\sqrt{\pi}}{2} \left[\frac{N}{\sqrt{1}} - \frac{N(N-1)}{1.2} \frac{1}{\sqrt{2}} + \dots (-)^{N+1} \frac{1}{\sqrt{N}} \right]. \quad (53)$$

Table II gives the exact values of the integral for $N = 1, 2, 5, 10$ and 20 . However, we are chiefly interested in values of N of the order of 50 or more, for which the binomial coefficients in (53) become so large that computation by means of that expression becomes impracticable.

An asymptotic expression for large values of N may be found as follows: write

$$\theta_0 = \log N; \quad e^{-\theta_0} = \frac{1}{N}; \quad \theta = \theta_0 + \theta', \quad (54)$$

say, then

$$(1 - e^{-\theta})^N = \left(1 - \frac{e^{-\theta'}}{N}\right)^N \doteq e^{-e^{-\theta'}}, \quad (55)$$

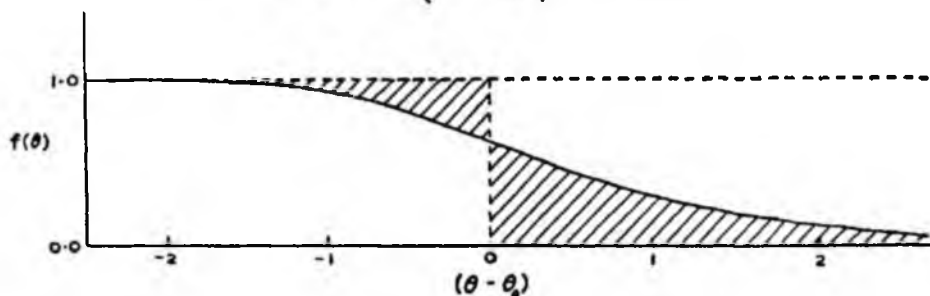


Figure 9. Graph of the function $f(\theta) = (1 - e^{-\theta})^N$ when N is large.

with errors of order $1/N$. Thus we see that the first function in the integrand of (43), i. e.,

$$f(\theta) = 1 - (1 - e^{-\theta})^N, \quad (56)$$

has a rather sudden drop from 1 to 0 in the neighborhood of θ_0 (see Fig. 9). We have, therefore,

$$\begin{aligned} I &= \frac{1}{2} \int_0^{\theta_0} \theta^{-1} d\theta + R \\ &= \theta_0^{-1} + R, \end{aligned} \quad (57)$$

where R is a remainder of order θ_0^{-1} at most; in fact

$$\begin{aligned} R &= \frac{1}{2} \theta_0^{-1} \left[- \int_{-\infty}^0 e^{-e^{-\theta'}} d\theta' + \int_0^{\infty} (1 - e^{-e^{-\theta'}}) d\theta' \right] + R' \\ &= \frac{1}{2} \theta_0^{-1} \left[- \int_1^{\infty} e^{-\frac{d\alpha}{\alpha}} + \int_0^1 (1 - e^{-\alpha}) \frac{d\alpha}{\alpha} \right] + R' \\ &= \frac{1}{2} \gamma \theta_0^{-1} + R', \end{aligned} \quad (58)$$

where R' is of order θ_0^{-1} at most and γ is Euler's constant ($= 0.5772, 2$; see Whittaker and Watson, 1950: 236). Thus

$$E(a_{\max}) / \bar{a} = (\log N)^{\frac{1}{2}} + \frac{1}{2} \gamma (\log N)^{-\frac{1}{2}} + 0 (\log N)^{-1}. \quad (59)$$

TABLE II. VALUES OF $E(a_{\max})/\bar{a}$ AND $\mu(a_{\max})/\bar{a}$ FOR DIFFERENT VALUES OF N , FOR A NARROW SPECTRUM

N	$(\log N)^{\dagger}$	$E(a_{\max})/\bar{a}$		$\mu(a_{\max})/\bar{a}$
		exact expression	asymptotic expression	
1	0.000	0.886	—	0.707
2	0.833	1.146	—	1.030
5	1.269	1.462	—	1.366
10	1.517	1.676	1.708	1.583
20	1.731	1.870	1.898	1.778
50	1.978	—	2.124	2.010
100	2.146	—	2.280	2.172
200	2.302	—	2.426	2.323
500	2.493	—	2.609	2.509
1,000	2.628	—	2.738	2.642
2,000	2.757	—	2.862	2.769
5,000	2.918	—	3.017	2.929
10,000	3.035	—	3.130	3.044
20,000	3.147	—	3.239	3.155
50,000	3.289	—	3.377	3.296
100,000	3.393	—	3.478	3.400

The above equation may be compared with equation (41) for $a^{(p)}/\bar{a}$ when $p = 1/N$. We see that $E(a_{\max})$ differs from $a^{(1/N)}$ in the second term of the asymptotic expansion. Since $\frac{1}{2}\sqrt{\gamma} = 0.28861$, we have $E(a_{\max}) < a^{(1/N)}$ as expected. For large N , however, $E(a_{\max})$ still increases like $(\log N)^{\dagger}$ and therefore tends to infinity with the length of the interval, though very slowly. Values of the asymptotic expression for $E(a_{\max})/\bar{a}$ are given in Table II for values of N ranging from 10 to 100,000. It will be seen that in this range $E(a_{\max})/\bar{a}$ increases only from about 1.7 to about 3.5. The asymptotic expression may be compared with the exact expression for $N = 10$ and 20. The differences in the two cases are 0.032 and 0.028 respectively, or about 2%. For $N \geq 50$ the error in the asymptotic expression is almost certainly less than 0.03; for large values of N the error may be expected to diminish proportionally to $(\log N)^{-1}$.

The "most probable" value of a_{\max} , which we shall denote by $\mu(a_{\max})$, is given simply by the maximum value of the probability-distribution (46), i. e., the maximum of

$$N(1 - e^{-r^2/\bar{a}^2})^{N-1} e^{-r^2/\bar{a}^2} \cdot 2r/\bar{a}. \quad (60)$$

Writing

$$\theta = r^2/\bar{a}^2, \quad (61)$$

we see that we must have

$$\frac{d}{d\theta} \left[\theta^{\frac{1}{2}} e^{-\theta} (1 - e^{-\theta})^{N-1} \right] = 0, \quad (62)$$

260

and hence

$$\frac{1}{2\theta} - 1 + \frac{(N-1)e^{-\theta}}{1-e^{-\theta}} = 0 \quad (63)$$

or

$$Ne^{-\theta} = 1 - \frac{1}{2\theta} (1 - e^{-\theta}) \quad (64)$$

or

$$\theta = \log N - \log \left[1 - \frac{1}{2\theta} (1 - e^{-\theta}) \right] \quad (65)$$

$$= \log N + O\left(\frac{1}{\theta}\right) \quad (66)$$

when N is large. Thus

$$\theta = \log N + O(\log N)^{-1}, \quad (67)$$

and the most probable value of a_{\max} is given by

$$\mu(a_{\max})/\bar{a} = \theta^{\frac{1}{2}} = (\log N)^{\frac{1}{2}} + O(\log N)^{-\frac{1}{2}}. \quad (68)$$

Thus there is no term in $(\log N)^{-\frac{1}{2}}$. Starting with the approximate value $(\log N)^{\frac{1}{2}}$, one may find closer approximations to $\mu(a_{\max})/\bar{a}$ by applying Newton's method of successive approximation (see, for example, Whittaker and Robinson, 1932: 84) in equation (65). Values of $\mu(a_{\max})/\bar{a}$ so found are given in the last column of Table II.

The chance that a_{\max} shall not exceed $(\log N)^{\frac{1}{2}}$ by more than a given amount may be found similarly. We have seen that the probability-distribution of a_{\max} is given by

$$\frac{d}{dr} (1 - \theta)^N = \frac{d}{dr} (1 - e^{-r^2/\bar{a}^2})^N. \quad (69)$$

If we define r_0 by the equations

$$r_0^2/\bar{a}^2 = \theta_0 = \log N; \quad e^{-r_0^2/\bar{a}^2} = \frac{1}{N}, \quad (70)$$

we have

$$\frac{d}{dr} \left(1 - \frac{e^{-(r^2-r_0^2)/\bar{a}^2}}{N} \right)^N = \frac{d}{dr} e^{-e^{-(r^2-r_0^2)/\bar{a}^2}} \quad (71)$$

approximately. The probability that a will be less than r is therefore

$$e^{-e^{-(r^2-r_0^2)/\bar{a}^2}}, \quad (72)$$

and the probability that a will be greater than r is

$$1 - e^{-e^{-(r^2-r_0^2)/\bar{a}^2}}. \quad (73)$$

4. DISCUSSION

The chief assumptions used in the derivation of the theoretical distribution $P(r)$ in sections 2 and 3 are: (a) that the frequency spectrum consist of a single narrow frequency band; and (b) that the waves be considered as the sum of a large number of contributions, all of about the same frequency, and of random phase. Let us consider under what conditions these assumptions should be satisfied.

In the first place, the analysis will not apply to regular trains of waves produced by a simple organized mechanism: for example, the waves generated by a paddle in a model wave tank, or the transverse waves produced by a ship; or the wave-height distribution resulting from the interference of two wave trains of the same amplitude but of slightly differing wavelength, as in Example 2 (p. 247). In the open sea such examples constitute very special and most unlikely cases.

The present analysis is meant to apply to wind-generated waves. Since the dimensions of a storm area are large compared with the wavelengths we are considering, it is fairly safe to suppose that the phases of contributions from different parts of the storm area are random. However, the range of frequencies may not be narrow; if there are two distinct sources of wave-energy, for example a distant storm and local winds, there may well be two distinct frequency-bands in the spectrum. The most satisfactory conditions would be represented by a single storm at a great distance (compared with the dimensions of the storm); for, in the course of propagation, different frequencies in the spectrum, being propagated with different velocities, will become spread out in space, and over a short interval of time only a narrow range will be present. It must be assumed that the time of recording is not too long, so that in this time the frequency and amplitude of the waves do not change significantly. On the other hand the time must be long enough to ensure that the sample of wave-heights is sufficiently representative; this requires that at least several "groups" of waves be included in the record.

The method of recording may affect the apparent frequency spectrum of the waves. For example, if the waves are recorded by measurement of pressure on the bottom, as is now usual, the high frequencies, which are attenuated rapidly with depth, will be damped out relative to the lower frequencies, and the corresponding frequency spectrum will therefore be narrower. Hence the present analysis may apply more closely to a record of pressure on the bottom than to the actual surface elevation. In fact, the free surface, if viewed very closely, will usually show a large number of short steep waves, which may constitute maxima and minima of the wave elevation but which

are not normally of interest to us; for example, they would not affect the rolling or heaving motion of a ship. Strictly speaking, we should consider only that modification of the spectrum which is relevant to the purpose in hand. A ship itself acts as a resonant filter, which will amplify those components in the spectrum which are close to its natural period. The present analysis, therefore, might very well be applied to the angular deflection of a ship's mast from the vertical; from an analysis of the rolling motion over a few minutes, one could easily compute the maximum roll that is likely to be encountered during, say, the next hour, assuming that the sea conditions remained constant; for, in the notation in Sections 2 and 3, one could estimate \bar{a} with fair accuracy from observation over the shorter interval and hence find $E(a_{\max})$ or $\mu(a_{\max})$ over the proposed longer interval.

However, an important restriction should be mentioned here. One of the conditions implied in assumption (b) above is that the contributions from different parts of the generating area should be superposable; that is, the mechanical system we are dealing with should be linear. This assumption can be shown to be valid for low waves in deep water; but clearly it will not hold for waves approaching the maximum height. For this reason the analysis could not be applied to surf or to waves in the open sea which are nearly at their maximum height. Nor could it be applied to the rolling motion of a ship when this is large enough for nonlinear terms to become important or when the rolling is so great that the ship may capsize.

With these restrictions in mind let us compare some previous observations with the theoretical results of Sections 2 and 3.

5. COMPARISON WITH OBSERVATION

Munk (1944),² in an analysis of wave records taken at the Scripps Institution, California, compared the mean height $H^{(3/10)}$ of the highest 30% of the waves with the mean height $H^{(1)}$ of all of the waves. He found

$$\frac{H^{(3/10)}}{H^{(1)}} = \frac{0.49}{0.32} = 1.53.$$

The theoretical value from Table I is given by

$$\frac{a^{(3/10)}}{a^{(1)}} = \frac{a^{(3/10)}/\bar{a}}{a^{(1)}/\bar{a}} = \frac{1.454}{0.886} = 1.64.$$

Seiwell (1948) found that in two different localities in the Atlantic (off Cuttyhunk Island and off Bermuda) the ratio of $a^{(4)}$ to $a^{(1)}$ was

² See also Snodgrass (1951) where these and other unpublished observations are summarized.

1.57. Putz (1950) studied 25 wave records from five different localities; the mean values of the ratios $a^{(1)}/a^{(1)}$ can be found from table 1 of his paper. They are respectively 1.59 (Oceanside, 4 records); 1.66 (Point Sur, 15 records); 1.66 (Hecata Head, 2 records); 1.55 (Guam, 3 records) and 1.54 (Point Arguello, 1 record). The mean of Putz's observations, weighted according to the number of records considered, is 1.63. The theoretical value, from Table I of this paper, is given by

$$\frac{a^{(1)}}{a^{(1)}} = \frac{1.416}{0.886} = 1.60,$$

which is in fairly close agreement.

Wiegel (1949) has studied wave records from three different localities off the Pacific Coast of the United States. He found, in the three cases, that

$$\frac{a^{(1/10)}}{a^{(1)}} = 1.27, 1.30, 1.30 \text{ (mean value 1.29).}$$

The individual estimates showed little scatter. Wiegel remarks, "Even more surprising was the fact that almost every point was within plus or minus ten per cent of this value (1.29)." The theoretical value, from Table I, is given by

$$\frac{a^{(1)}}{a^{(1)}} = \frac{1.800}{1.416} = 1.27,$$

which again is in quite close agreement.

Wiegel also compared the maximum wave from three 20-minute records each day with the mean height of the highest one-third waves. His observed values were equivalent to

$$\frac{E(a_{\max})}{a^{(1)}} = 1.85, 1.91, 1.85 \text{ (mean value 1.87).}$$

Assuming a mean wave period of 12 seconds, we have

$$N = \frac{60 \text{ minutes}}{12 \text{ seconds}} = 300,$$

for which we find from the asymptotic formula (59):

$$\frac{E(a_{\max})}{a} = 2.504.$$

Thus, theoretically,

$$\frac{E(a_{\max})}{a^{(1)}} = \frac{2.504}{1.416} = 1.77.$$

A possible explanation of the observed value of $E(a_{\max})/a^{(4)}$ being greater than the theoretical value is as follows. Suppose that during the day the state of the sea, as represented by the r. m. s. wave amplitude \bar{a} , underwent a change. If, during one of the three 20-minute records, the r. m. s. wave amplitude is much larger than, say twice, that in the other two, then the maximum wave amplitude will almost certainly be found in that record, and the expected value of the maximum will not be much less than twice the expected value if the wave characteristics had not changed; for $E(a_{\max})/\bar{a}$ is not much different for a 20-minute interval than for a 60-minute interval. On the other hand, $a^{(4)}$ will be multiplied by approximately 4/3. Therefore $E(a_{\max})/\bar{a}$ will be increased by about $2 \div 4/3$ or by 3/2. The same tendency is true in general.

Darbyshire (1953) has shown that in a 20-minute wave record the maximum wave-height is about twice the "equivalent wave-height," which is defined by him as the height of the uniform train of waves which would have the same total energy as the actual waves. On our present assumption that the spectrum of the waves contains only a single narrow band, the equivalent wave-height equals the root-mean-square wave height \bar{a} ; for, each wave in the record is approximately a sine-wave of the same length, and the energy per wavelength is proportional to a^2 . It may be more appropriate, in this case, to consider the most probable value $\mu(a_{\max})$ of the highest wave rather than the expectancy $E(a_{\max})$. For a mean wave period of 12 seconds we should have

$$N = \frac{20 \text{ minutes}}{12 \text{ seconds}} = 100,$$

and so from Table II

$$\mu(a_{\max})/\bar{a} = 2.17.$$

However, we see from Table II that $E(a_{\max})$ is only slightly greater. For longer wave periods, N , and therefore $\mu(a_{\max})/\bar{a}$, would be slightly less; the rather slow change in $\mu(a_{\max})$ with N would account for the success of the empirical rule irrespective of the period of the waves.

In examples quoted above, the discrepancy between theory and observation is in all cases less than 8%, and in some cases it is smaller still. In view of the somewhat strict assumptions made in deriving the theoretical probability-distribution, this agreement is surprisingly close; and it may indicate that the probability-distribution does not depend very critically upon the narrowness of the wave spectrum. For most practical purposes the theoretical values of $a^{(5)}/\bar{a}$ and $E(a_{\max})/\bar{a}$ can be used with confidence; thus, if one of the quantities \bar{a} , $a^{(1)}$, $a^{(4)}$, $a^{(1/10)}$ or $E(a_{\max})$ is known, the others may be estimated immediately.

The present discussion suggests that waves much higher than the average are likely to be extremely rare, for a given state of the sea. Table II shows that even in a time interval containing 100,000 waves, which for 10-second waves would be about $11\frac{1}{2}$ days, the most probable value of the highest wave is less than $3\frac{1}{2}$ times the root-mean-square value; of course it is unlikely that the waves would remain statistically constant throughout this interval. Equation (73) also shows that there is an extremely small chance that the most probable value of a_{\max} will be greatly exceeded. The general conclusion then appears that changes in the strength of the wind or other generating forces are more important in producing variability in the wave amplitude than is the statistical variation of the waves at any one time.

REFERENCES

- BARBER, N. F.
1950. Ocean waves and swell. Lecture published by Institution of Electrical Engineers, London. 22 pp.
- BARTELS, J.
1935. Random fluctuations, persistence and quasi-persistence in geophysical and cosmical periodicities. *Terr. Magn. atmos. Elect.*, 40: 1-60.
- DARBYSHIRE, J.
1953. The generation of waves by wind. *Philos. Trans., A.* (in press).
- ECKART, C. H. (ed.)
1950. Principles of underwater sound. National Defense Research Council, Summary Technical Reports, Division 6, vol. 7.
- KHINTCHINE, A.
1933. Asymptotische Gesetze der Wahrscheinlichkeitsrechnung. *Ergebn. Math.*, 2 (4): 1-77; Berlin, Julius Springer.
- MUNK, W. H.
1944. Proposed uniform procedure for observing waves and interpreting instrument records. Scripps Institution of Oceanography, Wave Report 26 (unpublished).
- PUTZ, R. R.
1950. Wave height variability; prediction of distribution function. Institute of Engineering Research, Berkeley, Technical Report HE-116-318 (unpublished).
- RAYLEIGH, LORD
1880. On the resultant of a large number of vibrations of the same pitch and of arbitrary phase. *Phil. Mag.*, 10: 73-78.
- RICE, S. O.
1944-45. The mathematical analysis of random noise. *Bell Syst. tech. J.*, 23: 282-332; 24: 46-156.
- SEIWELL, H. R.
1948. Results of research on surface waves of the western North Atlantic. *Pap. phys. Oceanogr. Met.*, 10 (4).

SNODGRASS, F. E.

1951. Wave recorders. Proc., 1st Conference on Coastal Engineering, pp. 69-81, published by Council on Wave Research, University of California, 1951 (ed., J. W. Johnson).

SVERDRUP, H. U. AND W. H. MUNK

1947. Wind, sea and swell: theory of relations for forecasting. Report N. 601, U. S. Navy Hydrographic Office.

WHITTAKER, E. T. AND G. ROBINSON

1932. Calculus of Observations. 2nd ed., Blackie, London. 395 pp.

WHITTAKER, E. T. AND G. N. WATSON

1950. Modern Analysis. 4th ed., Cambridge University Press. 608 pp.

WIEGEL, R. L.

1949. An analysis of data from wave recorders on the Pacific Coast of the United States. Trans. Amer. geophys. Un., 30: 700-704.

*Reprinted without change of pagination from the
Proceedings of the Royal Society, A, volume 237, pp. 212-232, 1956*

The statistical distribution of the maxima of a random function

By D. E. CARTWRIGHT AND M. S. LONGUET-HIGGINS

National Institute of Oceanography, Wormley

(Communicated by G. E. R. Deacon, F.R.S.—Received 14 April 1956)

This paper studies the statistical distribution of the maximum values of a random function which is the sum of an infinite number of sine waves in random phase. The results are applied to sea waves and to the pitching and rolling motion of a ship.

INTRODUCTION

Let $f(t)$ denote a continuous, random function of the time t , representing, for example, the height of the sea surface above a fixed point. It is interesting to inquire into the statistical distribution of the heights of the *maxima* of $f(t)$.

There are two distinct problems. On the one hand we may consider the total wave height $2a$, being defined as the difference in level between a crest (maximum) and the preceding trough (minimum). The statistical distribution of a is difficult to determine in the general case, but when $f(t)$ has a narrow frequency spectrum it may be shown that a is distributed according to a Rayleigh distribution

$$p(a) = \frac{2a}{m_0} e^{-a^2/m_0},$$

where m_0 is the root-mean-square value of $f(t)$ (see Rayleigh 1880). This distribution has been compared with the observed distribution of the heights of sea waves and it has been shown that many theoretical relations, for example the ratios of the mean wave height to the mean of the highest one-third waves or to the mean of the highest of N consecutive waves, are in close agreement with observation (Longuet-Higgins 1952). Application of the χ^2 -test to some histograms of wave heights has also indicated, apparently, no significant departure from the Rayleigh distribution (Watters 1953). It is certain, however, that for functions $f(t)$ having a broad frequency spectrum, the theoretical distribution of a must be different from the Rayleigh distribution.

Alternatively, we may consider the difference in height ξ between a crest and the mean level of the function $f(t)$. Although in practice ξ may be less convenient to measure than a (since the appropriate mean value is sometimes difficult to determine) the theoretical distribution of ξ is easier to obtain, and has been found for a wide class of random functions by Rice (1944, 1945) in connexion with the analysis of electrical noise signals. Rice's solution, which is only one out of many results in a long paper, has not been fully discussed, and it is the purpose of the present paper to examine the solution and to calculate some of the statistical parameters associated with it. We shall also apply the results to ocean waves and to the motion of ships at sea.

213 *Statistical distribution of the maxima of a random function*

In §1 we outline briefly Rice's derivation of the statistical distribution of the maxima ξ . The discussion shows that the distribution depends, surprisingly, on only two parameters: the root-mean-square value of $f(t)$, which we denote by $m_0^{\frac{1}{2}}$, and a parameter ϵ which, as we show in §2, represents the relative width of the frequency spectrum of $f(t)$. When ϵ is small, the distribution of ξ tends to a Rayleigh distribution, as we should expect, and when ϵ approaches its maximum value 1 the distribution of ξ tends to a Gaussian distribution.

One of the main differences between the two variables ξ and a is that ξ may take negative values (since some maxima may lie below the mean level) whereas a is always positive. The proportion r of maxima that are negative can be readily determined in practice, and in §3 we show that this proportion depends only upon ϵ . Hence if r is measured, ϵ can be estimated.

In §§4-6 we calculate the moments of the distribution, the mean values of the highest $1/n$ th of all the crest heights and the expectation of the highest in a sample of N crest heights, and we show how these quantities depend upon ϵ .

The distribution of crest heights, as measured from records of ocean wave phenomena, is compared with the theoretical distribution in §7. No significant difference is found. On the other hand, the crest-to-trough heights, examined in §8, are found to depart significantly from the Rayleigh distribution.

1. THE DISTRIBUTION OF MAXIMA

The random function $f(t)$ is represented as the sum of an infinite number of sine-waves

$$f(t) = \sum_n c_n \cos(\sigma_n t + \epsilon_n), \quad (1.1)$$

where the frequencies σ_n are distributed densely in the interval $(0, \infty)$, the phases ϵ_n are random and distributed uniformly between 0 and 2π , and the amplitudes c_n are such that in any small interval of frequency $d\sigma$

$$\sum_{\sigma_n=\sigma}^{\sigma+d\sigma} \frac{1}{2} c_n^2 = E(\sigma) d\sigma, \quad (1.2)$$

where $E(\sigma)$ is a continuous function of σ which will be called the energy spectrum of $f(t)$. The total energy per unit length of record is

$$m_0 = \int_0^{\infty} E(\sigma) d\sigma. \quad (1.3)$$

More generally we shall find it convenient to write

$$m_n = \int_0^{\infty} E(\sigma) \sigma^n d\sigma \quad (1.4)$$

for the n th moment of $E(\sigma)$ about the origin.

To find the distribution of maxima of $f(t)$ we note that, if $f(t)$ has a maximum in the interval $(t, t + dt)$, then in this interval $f'(t)$ must take values in a range of width $|f''(t)| dt$ very nearly; and the probability of this occurrence, and of f simultaneously lying in the range $(\xi_1, \xi_1 + d\xi_1)$, is

$$\int_{-\infty}^0 [p(\xi_1, 0, \xi_2) d\xi_1 | \xi_2 | dt] d\xi_2, \quad (1.5)$$

D. E. Cartwright and M. S. Longuet-Higgins 214

where $p(\xi_1, \xi_2, \xi_3)$ is the joint probability distribution of

$$(\xi_1, \xi_2, \xi_3) = (f, f', f''). \quad (1.6)$$

The mean frequency of maxima in the range $\xi_1 < f < \xi_1 + d\xi_1$ is therefore

$$F(\xi_1) d\xi_1 = \int_{-\infty}^0 [p(\xi_1, 0, \xi_3) | \xi_3 | d\xi_1] d\xi_3, \quad (1.7)$$

and the probability distribution of maxima is found by dividing this distribution by the total mean frequency of maxima, which is

$$N_1 = \int_{-\infty}^{\infty} \int_{-\infty}^0 p(\xi_1, 0, \xi_3) | \xi_3 | d\xi_1 d\xi_3. \quad (1.8)$$

Now from (1.6) we have

$$\left. \begin{aligned} \xi_1 &= f(t) = \sum_n c_n \cos(\sigma_n t + \epsilon_n), \\ \xi_2 &= f'(t) = -\sum_n c_n \sigma_n \sin(\sigma_n t + \epsilon_n), \\ \xi_3 &= f''(t) = -\sum_n c_n \sigma_n^2 \cos(\sigma_n t + \epsilon_n). \end{aligned} \right\} \quad (1.9)$$

ξ_1, ξ_2, ξ_3 are therefore each the sum of an infinite number of variables of zero expectation and random phase. Therefore, by the central limit theorem in three dimensions, the joint probability distribution of (ξ_1, ξ_2, ξ_3) is normal (under general conditions assumed to be satisfied by the amplitudes c_n ; see Rice 1944, 1945). The matrix of correlations or statistical averages $\Xi_{ij} = \overline{\xi_i \xi_j}$ is seen to be

$$(\Xi_{ij}) = \begin{pmatrix} m_0 & 0 & -m_2 \\ 0 & m_2 & 0 \\ -m_2 & 0 & m_4 \end{pmatrix}. \quad (1.10)$$

Hence

$$p(\xi_1, \xi_2, \xi_3) = \frac{1}{(2\pi)^{\frac{3}{2}} (\Delta m_2)^{\frac{1}{2}}} \exp \left\{ -\frac{1}{2} [\xi_1^2/m_2 + (m_4 \xi_1^2 + 2m_2 \xi_1 \xi_3 + m_0 \xi_3^2)/\Delta] \right\}, \quad (1.11)$$

where $\Delta = m_0 m_4 - m_2^2$. (1.12)

Substituting in (1.7) we have

$$F(\xi_1) = \frac{1}{(2\pi)^{\frac{3}{2}} (\Delta m_2)^{\frac{1}{2}}} \int_{-\infty}^0 \exp \left\{ -\frac{1}{2} (m_4 \xi_1^2 + 2m_2 \xi_1 \xi_3 + m_0 \xi_3^2)/\Delta \right\} | \xi_3 | d\xi_3. \quad (1.13)$$

On evaluating the integral and writing

$$\xi_1/m_0^{\frac{1}{2}} = \eta, \quad \Delta^{\frac{1}{2}}/m_2 = \delta \quad (1.14)$$

we obtain

$$F(\xi_1) = \frac{1}{(2\pi)^{\frac{3}{2}} m_0 m_4^{\frac{1}{2}}} e^{-\frac{1}{2}\eta^2} \left[e^{-\frac{1}{2}\eta^2/\delta^2} + (\eta/\delta) \int_{-\eta/\delta}^{\infty} e^{-\frac{1}{2}x^2} dx \right]. \quad (1.15)$$

The last integral can be expressed in terms of the known function

$$\operatorname{erf} x = \left(\frac{2}{\pi} \right)^{\frac{1}{2}} \int_0^x e^{-\frac{1}{2}x^2} dx. \quad (1.16)$$

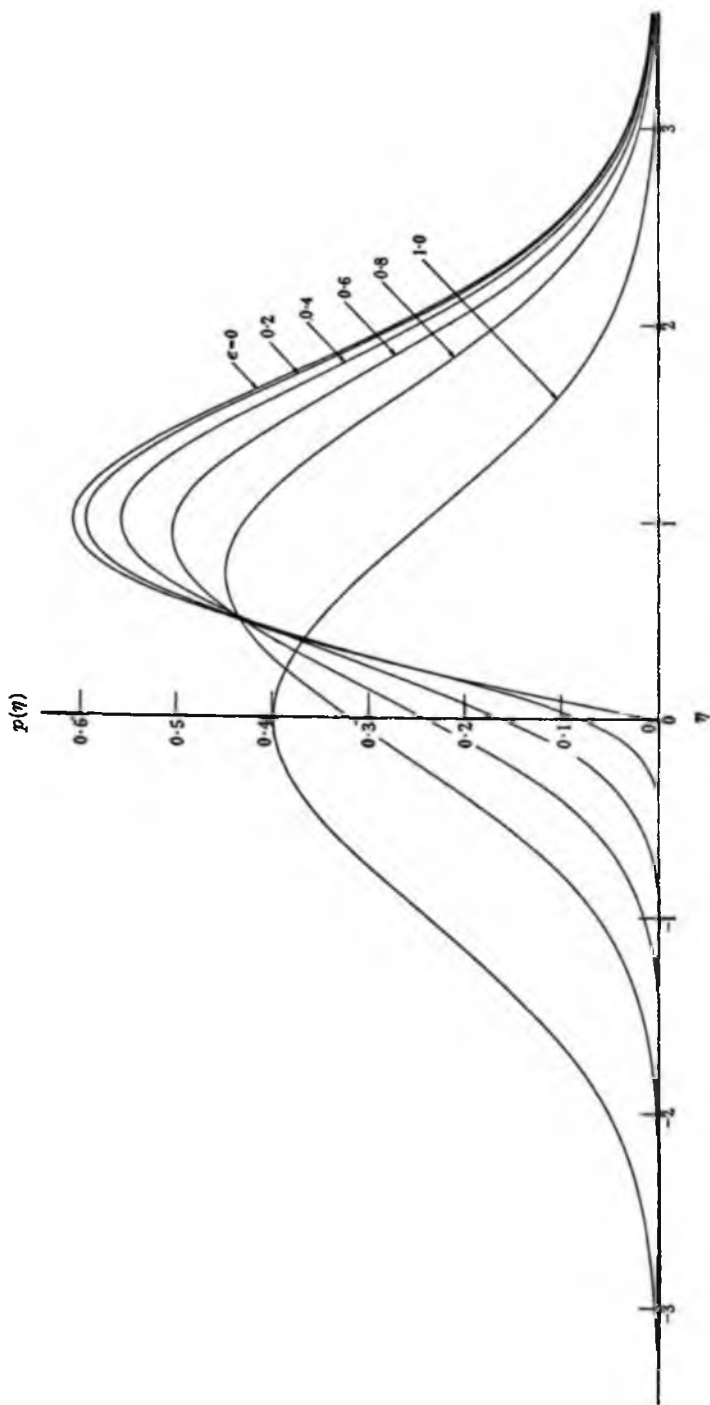
215 *Statistical distribution of the maxima of a random function*

FIGURE 1. Graphs of $p(\eta)$, the probability distribution of the heights of maxima ($\eta = \xi_i/m_0^{\frac{1}{2}}$) for different values of the width ϵ of the energy spectrum.

D. E. Cartwright and M. S. Longuet-Higgins 216

The probability distribution of η is $m_0^{\frac{1}{2}}$ times the distribution of ξ_1 :

$$p(\eta) = m_0^{\frac{1}{2}} p(\xi_1) = m_0^{\frac{1}{2}} F(\xi_1) / N_1. \quad (1.17)$$

From (1.8) we find
$$N_1 = \frac{1}{2\pi} \left(\frac{m_4}{m_2} \right)^{\frac{1}{2}}, \quad (1.18)$$

and so finally

$$p(\eta) = \frac{1}{(2\pi)^{\frac{1}{2}}} \left[\epsilon e^{-\frac{1}{2}\eta^2/\epsilon^2} + (1-\epsilon^2)^{\frac{1}{2}} \eta e^{-\frac{1}{2}\eta^2} \int_{-\infty}^{\eta(1-\epsilon^2)^{1/2}/\epsilon} e^{-\frac{1}{2}x^2} dx \right], \quad (1.19)$$

where
$$\epsilon^2 = \frac{\delta^2}{1+\delta^2} = \frac{\Delta}{m_0 m_4} = \frac{m_0 m_4 - m_2^2}{m_0 m_4}. \quad (1.20)$$

The function $f(t)$ is statistically symmetrical about the mean level $t = 0$. For, in equation (1.1) each phase angle ϵ_n might be increased or diminished by π without affecting the random character of the phases; and this would merely reverse the sign of $f(t)$. It follows that the statistical distribution of the minima is simply the reflexion of (1.20) in the mean level $\eta = 0$.

2. DISCUSSION

In equation (1.19) η denotes the ratio of the surface height to the r.m.s. height $m_0^{\frac{1}{2}}$. We see that the distribution of η depends only on the single parameter ϵ . A simple interpretation of ϵ is as follows. From (1.12) we have

$$\Delta = m_0 m_4 - m_2^2 = \int_0^\infty \int_0^\infty E(\sigma_1) E(\sigma_2) (\sigma_1^4 - \sigma_1^2 \sigma_2^2) d\sigma_1 d\sigma_2. \quad (2.1)$$

On interchanging σ_1 and σ_2 , and adding, we have

$$2\Delta = \int_0^\infty \int_0^\infty E(\sigma_1) E(\sigma_2) (\sigma_1^2 - \sigma_2^2)^2 d\sigma_1 d\sigma_2. \quad (2.2)$$

Since $E(\sigma)$ is essentially positive, it follows that $\Delta \geq 0$ and so

$$0 < \epsilon < 1. \quad (2.3)$$

For a very narrow spectrum, with the energy grouped around $\sigma = \sigma_0$, say, $E(\sigma_1)$ and $E(\sigma_2)$ are small except when σ_1 and σ_2 are both near to σ_0 ; but then the factor $(\sigma_1^2 - \sigma_2^2)^2$ in (2.2) is small and so

$$\epsilon \ll 1. \quad (2.4)$$

In general ϵ is a measure of the r.m.s. width of the energy spectrum E .

Clearly ϵ may take values indefinitely near 0. For a low-pass filter ($E = E_0$ when $\sigma < \sigma_0$, and $E = 0$ when $\sigma > \sigma_0$) we find

$$\epsilon = \frac{2}{3}. \quad (2.5)$$

ϵ may also take values indefinitely near 1. For suppose a proportion w of the energy is at frequency $\sigma = \sigma_1$, and $(1-w)$ at $\sigma = \sigma_2$; we have

$$\begin{aligned} m_2 &= m_0 \{ w \sigma_1^2 + (1-w) \sigma_2^2 \}, \\ m_4 &= m_0 \{ w \sigma_1^4 + (1-w) \sigma_2^4 \}. \end{aligned} \quad (2.6)$$

217 *Statistical distribution of the maxima of a random function*

When $\sigma_2/\sigma_1 \rightarrow \infty$ we see that $m_2^2/m_0 m_4 \rightarrow 1 - \omega$ and so

$$\epsilon^2 \rightarrow \omega, \quad (2.7)$$

which can be as near to unity as we please.

The first limiting case ($\epsilon \rightarrow 0$) gives the distribution for an infinitely narrow spectrum. From equation (1.19) we have then

$$p(\eta) = \begin{cases} \eta e^{-\frac{1}{2}\eta^2} & (\eta \geq 0), \\ 0 & (\eta \leq 0), \end{cases} \quad (2.8)$$

which is the Rayleigh distribution, or the distribution of the envelope of the waves (see Rice 1944, 1945; Barber 1950; Longuet-Higgins 1952).

The second limiting case ($\epsilon \rightarrow 1$) can occur, as we have shown, when one wave of high frequency and small amplitude is superposed on another disturbance of lower frequency. The high-frequency wave forms a 'ripple' on the remaining waves, and the distribution of maxima tends to the distribution of the surface elevation ($\xi_1/m_0^{\frac{1}{2}}$) itself. On letting ϵ tend to 1 in (1.19) we obtain

$$p(\eta) = \frac{1}{(2\pi)^{\frac{1}{2}}} e^{-\frac{1}{2}\eta^2}, \quad (2.9)$$

which, as we should expect, is a Gaussian distribution.

The distribution $p(\eta)$ has been plotted in figure 1 for $\epsilon = 0.0, 0.2, \dots, 1.0$. The transition from the Rayleigh distribution to the Gaussian distribution can be clearly seen.

3. THE PROPORTION OF NEGATIVE MAXIMA

This may be found by a simple geometrical argument as follows. Suppose that in a certain interval of time, say $(0, t)$, there are n_0^+ zero up-crossings, at which f passes from negative to positive values, and similarly suppose that there are n_0^- zero down-crossings. Also let there be n_1^+ positive maxima, n_1^- negative maxima, n_2^+ positive minima and n_2^- negative minima. Between a zero up-crossing and the next zero down-crossing the function is always positive, and so the number of maxima exceeds the number of minima by one. In other words, when n_0^- increases by 1, so also does $(n_1^+ - n_2^+)$. Similarly, when n_0^+ increases by 1, so does $(n_2^- - n_1^-)$. Therefore, if N_0^+ , N_0^- , N_1^+ , N_1^- , N_2^+ , N_2^- denote the average densities of zero up-crossings, etc., over a long interval we have

$$\left. \begin{aligned} N_0^+ &= N_1^+ - N_2^+, \\ N_0^- &= N_2^- - N_1^-. \end{aligned} \right\} \quad (3.1)$$

Now since $f(t)$ is statistically symmetrical about the mean level it follows that

$$\left. \begin{aligned} N_2^+ &= N_1^- = rN_1, \\ N_2^- &= N_1^+ = (1-r)N_1, \end{aligned} \right\} \quad (3.2)$$

where N_1 denotes the total density of maxima, and r denotes the proportion of negative maxima. So from (3.1)

$$N_0^+ = N_1(1 - 2r), \quad (3.3)$$

or

$$r = \frac{1}{2}(1 - N_0^+/N_1). \quad (3.4)$$

D. E. Cartwright and M. S. Longuet-Higgins 218

But from Rice (1944, 1945) and equation (1.18) we have

$$N_0^+ = \frac{1}{2\pi} \left(\frac{m_2}{m_0} \right)^{\frac{1}{2}}, \quad N_1 = \frac{1}{2\pi} \left(\frac{m_4}{m_0} \right)^{\frac{1}{2}}. \quad (3.5)$$

So equation (3.4) can be written

$$r = \frac{1}{2} \left[1 - \frac{m_2}{(m_0 m_4)^{\frac{1}{2}}} \right] = \frac{1}{2} [1 - (1 - \epsilon^2)^{\frac{1}{2}}]. \quad (3.6)$$

Hence the proportion of negative maxima increases steadily with the relative width of the spectrum. Conversely, we have

$$\epsilon^2 = 1 - (1 - 2r)^2. \quad (3.7)$$

This relation provides us with a ready means of estimating ϵ by simply counting the numbers of positive and negative maxima in a length of record.

4. THE MOMENTS OF $p(\eta)$

The n th moment μ'_n of the probability distribution $p(\eta)$ taken about the origin, is defined by

$$\mu'_n = \int_{-\infty}^{\infty} p(\eta) \eta^n d\eta. \quad (4.1)$$

The even moments ($n = 2r$) may be calculated by means of the moment-generating function

$$\int_{-\infty}^{\infty} e^{-\frac{1}{2}t\eta^2} p(\eta) d\eta \equiv \mu'_0 - \frac{t^2}{2 \cdot 1!} \mu'_2 + \frac{t^4}{2^2 \cdot 2!} \mu'_4 \dots \quad (4.2)$$

On substituting from (1.19) and evaluating the integral we find

$$\int_{-\infty}^{\infty} e^{-\frac{1}{2}t\eta^2} p(\eta) d\eta = (1 + \epsilon^2 t^2)^{\frac{1}{2}} (1 + t^2)^{-1}, \quad (4.3)$$

and so on, comparing coefficients of t^{2r} in these two equations, we have

$$\mu'_{2r} = 2^r r! \left[1 - \frac{1}{2} \epsilon^2 - \frac{1 \cdot 1}{2^2 \cdot 2!} \epsilon^4 - \dots - \frac{1 \cdot 1 \cdot 3 \dots (2r - 3)}{2^r \cdot r!} \epsilon^{2r} \right]. \quad (4.4)$$

The odd moments ($n = 2r + 1$) may be found in a similar way by means of the moment-generating function

$$\int_{-\infty}^{\infty} \eta t e^{-\frac{1}{2}t\eta^2} p(\eta) d\eta \equiv t \mu'_1 - \frac{t^3}{2 \cdot 1!} \mu'_3 + \frac{t^5}{2^2 \cdot 2!} \mu'_5 \dots \quad (4.5)$$

From (1.18) we have

$$\int_{-\infty}^{\infty} \eta t e^{-\frac{1}{2}t\eta^2} p(\eta) d\eta = \left(\frac{1}{2} \pi \right)^{\frac{1}{2}} (1 - \epsilon^2)^{\frac{1}{2}} t (1 + t^2)^{-\frac{3}{2}}, \quad (4.6)$$

and hence
$$\mu'_{2r+1} = \left(\frac{1}{2} \pi \right)^{\frac{1}{2}} (1 - \epsilon^2)^{\frac{1}{2}} \frac{1 \cdot 3 \cdot 5 \dots (2r + 1)}{(r!)^2}. \quad (4.7)$$

219 *Statistical distribution of the maxima of a random function*

In particular we have

$$\left. \begin{aligned} \mu'_0 &= 1, \\ \mu'_1 &= (\frac{1}{2}\pi)^{\frac{1}{2}}(1-\epsilon^2)^{\frac{1}{2}}, \\ \mu'_2 &= 2-\epsilon^2, \\ \mu'_3 &= (\frac{1}{2}\pi)^{\frac{1}{2}}(1-\epsilon^2)^{\frac{1}{2}} \cdot 3. \end{aligned} \right\} \quad (4.8)$$

We see that the mean μ'_1 is a steadily decreasing function of ϵ , the width of the spectrum. A non-dimensional quantity depending on ϵ is the ratio

$$\rho = \frac{\mu_1'^2}{\mu_0\mu_2'} = (\frac{1}{2}\pi) \frac{1-\epsilon^2}{2-\epsilon^2}. \quad (4.9)$$

The width of the spectrum is given in terms of ρ by the relation

$$\epsilon^2 = \frac{\pi-4\rho}{\pi-2\rho}. \quad (4.10)$$

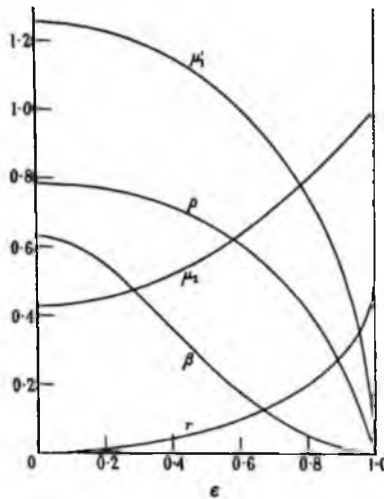


FIGURE 2. Graphs of the mean μ'_1 , variance μ_1 , skewness β , proportion τ of negative maxima, and $\rho (= \mu_1'^2/\mu_0\mu_2')$ as functions of ϵ .

On the other hand, we have the following two quantities which are independent of ϵ :

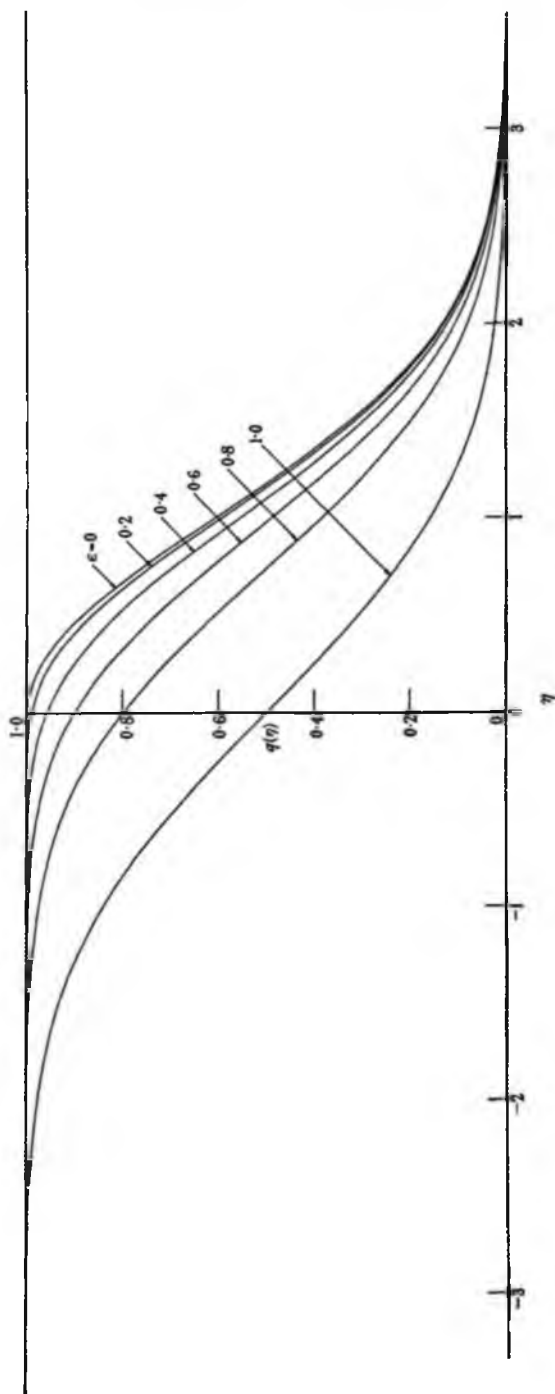
$$\mu_2'\mu_0' - \frac{1}{2}\pi\mu_1'^2 = 1, \quad \mu_3'/\mu_1' = 3. \quad (4.11)$$

The moments μ_n about the mean, which are defined by

$$\mu_n = \int_{-\infty}^{\infty} p(\eta) (\eta - \mu'_1)^n d\eta, \quad (4.12)$$

may be deduced immediately from the moments about the origin. In particular we have from (4.8)

$$\left. \begin{aligned} \mu_0 &= 1, \\ \mu_1 &= 0, \\ \mu_2 &= 1 - (\frac{1}{2}\pi - 1)(1 - \epsilon^2), \\ \mu_3 &= (\frac{1}{2}\pi)^{\frac{1}{2}}(\pi - 3)(1 - \epsilon^2)^{\frac{1}{2}}. \end{aligned} \right\} \quad (4.13)$$

FIGURE 3. Graphs of the cumulative probability $q(\eta)$, for different values of ϵ .

221 *Statistical distribution of the maxima of a random function*

The coefficient of skewness is given by

$$\beta = \frac{\mu_3}{\mu_2^{3/2}} = (\frac{1}{2}\pi)^{1/2}(\pi - 3) \left[\frac{1 - \epsilon^2}{1 - (\frac{1}{2}\pi - 1)(1 - \epsilon^2)} \right]^{1/2}. \quad (4.14)$$

We see that the standard deviation $\mu_2^{1/2}$ steadily increases as ϵ increases. β , on the other hand, steadily decreases.

The mean μ_1' , the variance μ_2 , the skewness β and the ratios r and ρ are shown graphically as functions of ϵ in figure 2.

In some practical cases we may know the distribution of the maxima $\xi_1 (= m_0^{1/2}\eta)$ experimentally and wish to make an estimate of the mean energy $m_0^{1/2}$. Let ν_n' and ν_n denote the n th moments, about the origin and about the mean, of the variate ξ_1 .

Then
$$\nu_n' = m_0^{1/2(n+1)}\mu_n', \quad \nu_n = m_0^{1/2(n+1)}\mu_n, \quad (4.15)$$

and so from (4.11)

$$\nu_2'\nu_0' - \frac{1}{2}\pi\nu_1'^2 = m_0^3, \quad \nu_3'/\nu_1' = 3m_0. \quad (4.16)$$

By forming either of these quantities, therefore, we may estimate m_0 .

5. THE CUMULATIVE PROBABILITY

The cumulative probability $q(\eta)$ may be defined as the probability of η exceeding a given value:

$$q(\eta) = \int_{\eta}^{\infty} p(\eta) d\eta. \quad (5.1)$$

Substituting from (1.19) we find

$$q(\eta) = \frac{1}{(2\pi)^{1/2}} \left[\int_{\eta/\epsilon}^{\infty} e^{-\frac{1}{2}x^2} dx + (1 - \epsilon^2)^{1/2} e^{-\frac{1}{2}\eta^2} \int_{-\infty}^{\eta(1-\epsilon^2)^{1/2}/\epsilon} e^{-\frac{1}{2}x^2} dx \right]. \quad (5.2)$$

When $\epsilon \rightarrow 0$,

$$q(\eta) \rightarrow \begin{cases} 1 & (\eta \leq 0), \\ e^{-\frac{1}{2}\eta^2} & (\eta \geq 0), \end{cases} \quad (5.3)$$

and when $\epsilon \rightarrow 1$,

$$q(\eta) \rightarrow \frac{1}{(2\pi)^{1/2}} \int_{\eta}^{\infty} e^{-\frac{1}{2}x^2} dx. \quad (5.4)$$

Graphs of $q(\eta)$ for these and intermediate values of ϵ are shown in figure 3. The proportion r of negative maxima is given by

$$r = \int_{-\infty}^0 p(\eta) d\eta = 1 - q(0), \quad (5.5)$$

which from (5.2) is

$$r = \frac{1}{2} [1 - (1 - \epsilon^2)^{1/2}], \quad (5.6)$$

in agreement with (3.6).

In some geophysical applications it is found convenient to consider only the higher waves, say the highest $1/n$ th of the total number in a sample. The $1/n$ th highest maxima correspond to those values of η greater than η' , say, where

$$q(\eta') = \int_{\eta'}^{\infty} p(\eta) d\eta = 1/n. \quad (5.7)$$

The average value of η for these maxima will be denoted by $\eta^{(1/n)}$, so that

$$\eta^{(1/n)} = n \int_{\eta'}^{\infty} p(\eta) \eta d\eta. \quad (5.8)$$

Clearly $\eta^{(1)}$ is the same as the mean μ'_1 . $\eta^{(1/n)}$ has been computed numerically for $n = 1, 2, 3, 5$ and 10 , and for different values of ϵ . The results are shown in figure 4. $\eta^{(1/n)}$ is apparently a decreasing function of ϵ . For small values of ϵ , say $\epsilon < 0.5$, the dependence of $\eta^{(1/n)}$ on ϵ is slight, but each curve gradually steepens, and it can be shown that as ϵ approaches 1 the gradient $\partial\eta^{(1/n)}/\partial\epsilon$ tends to $-\infty$. Near $\epsilon = 1$ the curves are all exactly similar in shape, being independent of n .

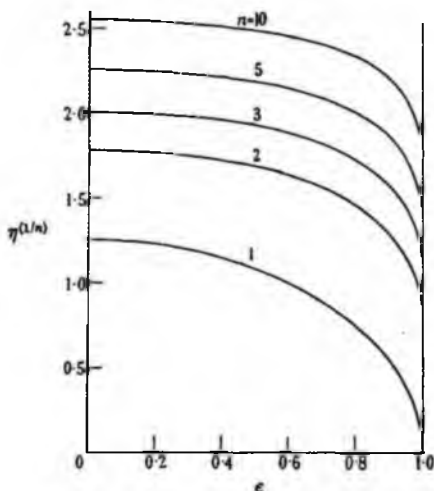


FIGURE 4. Graphs of $\eta^{(1/n)}$, the mean height of the $1/n$ th highest maxima, as a function of ϵ , for $n = 1, 2, 3, 5$ and 10 .

6. THE HIGHEST MAXIMUM IN A SAMPLE OF N

Suppose that a sample of N maxima is chosen at random; we wish to know the average value of the highest of these, η_{\max} . The problem has been considered in the case $\epsilon = 0$ (Longuet-Higgins 1952) and the expectation $\overline{\eta_{\max}}$ has been computed for values of N up to 20. For values of N greater than 50 (in which we are usually interested) it has been shown that the asymptotic formula

$$\eta_{\max}/(\mu'_2)^{\frac{1}{2}} \doteq (\ln N)^{\frac{1}{2}} + \frac{1}{2}\gamma(\ln N)^{-\frac{1}{2}} \quad (6.1)$$

is accurate to within 3%. (Here γ denotes Euler's constant, 0.5772....)

The formula (6.1) may be generalized to values of ϵ between 0 and 1 as follows. The probability distribution of η_{\max} is given by*

$$p(\eta_{\max}) = \frac{d}{d\eta_{\max}} [1 - q(\eta_{\max})]^N, \quad (6.2)$$

* We follow here the same method as in the paper just quoted. But a general study of the limiting form of the distribution of the largest member of a sample has been made by Fisher & Tippett (1928). For a more recent discussion see Gumbel (1954).

223 *Statistical distribution of the maxima of a random function*

where $q(\eta)$ is given by (5.1). Therefore we have

$$\overline{\eta_{\max.}} = \int_{-\infty}^{\infty} \eta \frac{d}{d\eta} [1 - q(\eta)]^N d\eta. \quad (6.3)$$

On separating the integral into two parts, from $-\infty$ to 0 and from 0 to ∞ , and integrating by parts we find

$$\overline{\eta_{\max.}} = \int_{-\infty}^0 [1 - q(\eta)]^N d\eta + \int_0^{\infty} \{1 - [1 - q(\eta)]^N\} d\eta. \quad (6.4)$$

When N is large $[1 - q(\eta)]^N$ is very small unless q is of order $1/N$. Now as x tends to infinity we have

$$\int_x^{\infty} e^{-\frac{1}{2}x^2} dx = e^{-\frac{1}{2}x^2} \left[\frac{1}{x} + O\left(\frac{1}{x^3}\right) \right], \quad (6.5)$$

and so from (5.2)

$$q(\eta) = (1 - \epsilon^2)^{\frac{1}{2}} e^{-\frac{1}{2}\eta^2} + O\left(\frac{1}{\eta^3} e^{-\frac{1}{2}\eta^2}\right) \quad (6.6)$$

for large values of η and when $0 \leq \epsilon < 1$. If q is of order $1/N$, η is of order $(\ln N)^{\frac{1}{2}}$. Therefore neglecting terms of order $(\ln N)^{-\frac{1}{2}}$ we have

$$q(\eta) = (1 - \epsilon^2)^{\frac{1}{2}} e^{-\frac{1}{2}\eta^2} = (1 - \epsilon^2)^{\frac{1}{2}} e^{-\theta}, \quad (6.7)$$

where $\theta = \frac{1}{2}\eta^2$. The first integral in (6.4) is negligible, and on substituting in the second we have

$$\overline{\eta_{\max.}} = \frac{1}{2^{\frac{1}{2}}} \int_0^{\infty} \{1 - [1 - (1 - \epsilon^2)^{\frac{1}{2}} e^{-\theta}]^N\} \theta^{-\frac{1}{2}} d\theta. \quad (6.8)$$

Writing $\theta_0 = \log [(1 - \epsilon^2)^{\frac{1}{2}} N]$, $\theta' = \theta - \theta_0$, (6.9)

and so
$$e^{-\theta} = \frac{e^{-\theta'}}{(1 - \epsilon^2)^{\frac{1}{2}} N}, \quad (6.10)$$

we have
$$\overline{\eta_{\max.}} = \frac{1}{2^{\frac{1}{2}}} \int_{-\theta_0}^{\infty} \left\{ 1 - \left[1 - \frac{e^{-\theta'}}{N} \right]^N \right\} (\theta_0 + \theta')^{-\frac{1}{2}} d\theta' \quad (6.11)$$

$$\doteq \frac{1}{2^{\frac{1}{2}}} \int_{-\theta_0}^{\infty} (1 - \exp[-e^{-\theta'}]) (\theta_0 + \theta')^{-\frac{1}{2}} d\theta', \quad (6.12)$$

with relative errors of order $1/N$ only. It may be shown (Longuet-Higgins 1952) that when θ_0 is large the above integral equals

$$2^{\frac{1}{2}} \left[\theta_0^{\frac{1}{2}} + \frac{1}{2} \gamma \theta_0^{-\frac{1}{2}} + O(\theta_0^{-\frac{3}{2}}) \right]. \quad (6.13)$$

Hence we have

$$\overline{\eta_{\max.}} \doteq 2^{\frac{1}{2}} \left\{ [\ln(1 - \epsilon^2)^{\frac{1}{2}} N]^{\frac{1}{2}} + \frac{1}{2} \gamma [\ln(1 - \epsilon^2)^{\frac{1}{2}} N]^{-\frac{1}{2}} \right\}, \quad (6.14)$$

which can also be written

$$\overline{\eta_{\max.}} / (\mu_2')^{\frac{1}{2}} \doteq \frac{[\ln(1 - \epsilon^2)^{\frac{1}{2}} N]^{\frac{1}{2}} + \frac{1}{2} \gamma [\ln(1 - \epsilon^2)^{\frac{1}{2}} N]^{-\frac{1}{2}}}{(1 - \frac{1}{2}\epsilon^2)^{\frac{1}{2}}}. \quad (6.15)$$

When $\epsilon \rightarrow 0$ this equation reduces to (6.1). The expression on the right-hand side of (6.15) is an increasing function of ϵ , when N is large. It follows that as the spectrum broadens, the ratio of the greatest in a sample to the root-mean-square will tend to increase.

When ϵ approaches 1 (so that $\ln(1 - \epsilon^2)^{\frac{1}{2}} N$ is not large compared with 1) the above formula is no longer valid. The corresponding expression for the general case is complicated and probably not of practical importance. We shall simply give the limiting form when $\epsilon \rightarrow 1$, and $p(\eta)$ is normal (equation (2.9)). Fisher & Tippett (1928) have shown that the average value of η_{\max} , in this case is given by

$$\overline{\eta_{\max}} = m + \frac{\gamma m}{1 + m^2} \quad (6.16)$$

approximately, where m is the mode of the distribution of η_{\max} , given by

$$(2\pi)^{\frac{1}{2}} m e^{\frac{1}{2}m^2} = N. \quad (6.17)$$

From (6.17) we have
$$m^2 = \ln\left(\frac{N^2}{2\pi}\right) - \ln m^2, \quad (6.18)$$

and so
$$m \doteq \left[\ln\left(\frac{N^2}{2\pi}\right) - \ln \ln\left(\frac{N^2}{2\pi}\right) \right]^{\frac{1}{2}}. \quad (6.19)$$

The leading term in (6.16) is thus

$$\overline{\eta_{\max}} \doteq 2^{\frac{1}{2}} \left[\ln \frac{N}{(2\pi)^{\frac{1}{2}}} \right]^{\frac{1}{2}}. \quad (6.20)$$

However, Fisher & Tippett have shown (1928) that for the normal distribution the limiting forms are approached exceptionally slowly. A table of the exact values of $\overline{\eta_{\max}}$ computed for values of N up to 1000 is given by Tippett (1925).

7. APPLICATIONS

It is interesting to verify that the distribution just discussed is applicable to records of sea waves and of associated phenomena. In this section we shall consider five such examples: a record of wave pressure at a fixed point on the sea bed; two continuous records of wave height made at sea by a shipborne instrument; one record of the angle of pitch of the ship, and one of the angle of roll. The widths of the corresponding Fourier spectra are fairly representative of the possible range $0 < \epsilon < 1$.

Typical sections of the records are shown in figure 5 (a) to (e). Each complete record lasted from 12 to 20 min and contained about 100 maxima and 100 minima. In order to increase the amount of data both maxima and minima were included in the sample. The analysis was carried out as follows. The ordinates A_n of all the stationary points in the record, measured from some common baseline, were numbered consecutively from 1 to N so that the maxima, say, corresponded to even values of n and the minima to odd values of n . The zero of the record was taken to be the mean of A_n :

$$\bar{A} = \frac{1}{N} \sum_{n=1}^N A_n. \quad (7.1)$$

The distribution of the variate

$$X_n = (-1)^n (A_n - \bar{A}) \quad (7.2)$$

was then studied. The histograms corresponding to the distribution of X_n are shown in figure 5 (a) to (e).

225 *Statistical distribution of the maxima of a random function*

To obtain the parameters for the theoretical distribution a harmonic analysis of the original record was made by means of the N.I.O. Fourier analyser (see Darbyshire & Tucker 1953). The range of frequency was divided into a number of equal

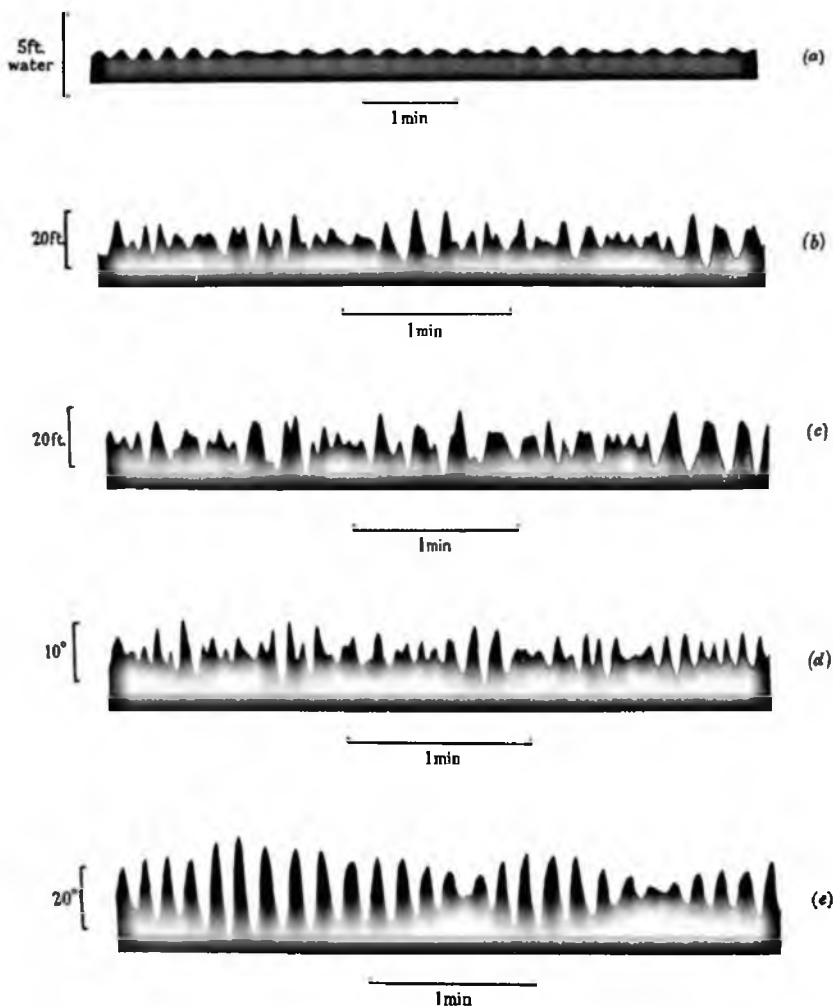


FIGURE 5. Typical short sections of the five records chosen for analysis. (a) pressure on the sea bed off Pendeen, Cornwall, 08.00 to 08.20, 15 March 1945; (b) wave height in the Bay of Biscay, 19.00 to 19.12, 11 November 1954; (c) wave height in the Bay of Biscay, 02.00 to 02.12, 12 November 1954; (d) angle of pitch of R.R.S. *Discovery II*, in North Atlantic, 13.21 to 13.33, 25 May 1954; (e) angle of roll of R.R.S. *Discovery II*, in North Atlantic, 14.05 to 14.17, 21 May 1954

narrow ranges each containing about 10 harmonics of the length of the record, and the energy $\sum \frac{1}{2} c_n^2$ was summed for each interval. The energy spectra are shown in figure 7 (a) to (e). The moments m_0 , m_2 and m_4 of the distribution were then calculated by multiplying the energy in each small range of frequency by 1, σ^2 and σ^4

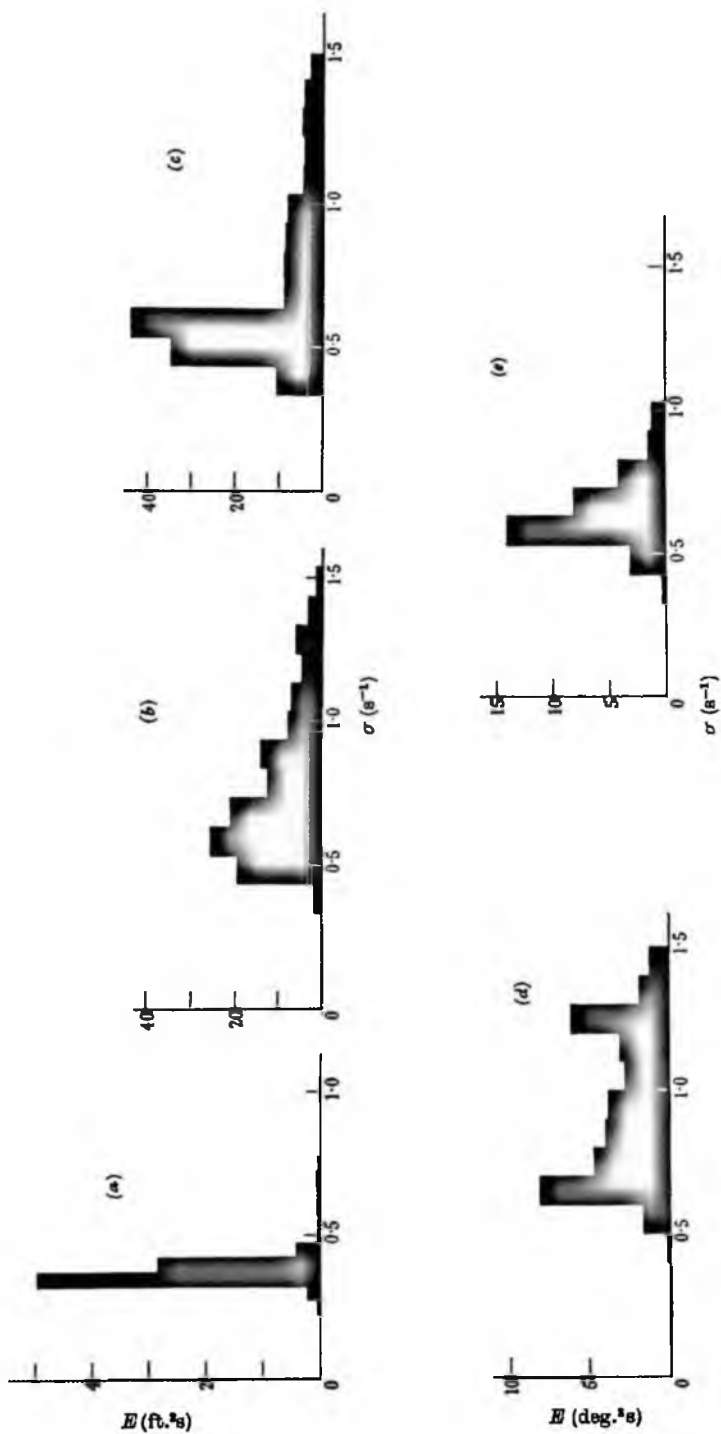


FIGURE 6. Energy spectra of the five records shown in figure 5.

227 Statistical distribution of the maxima of a random function

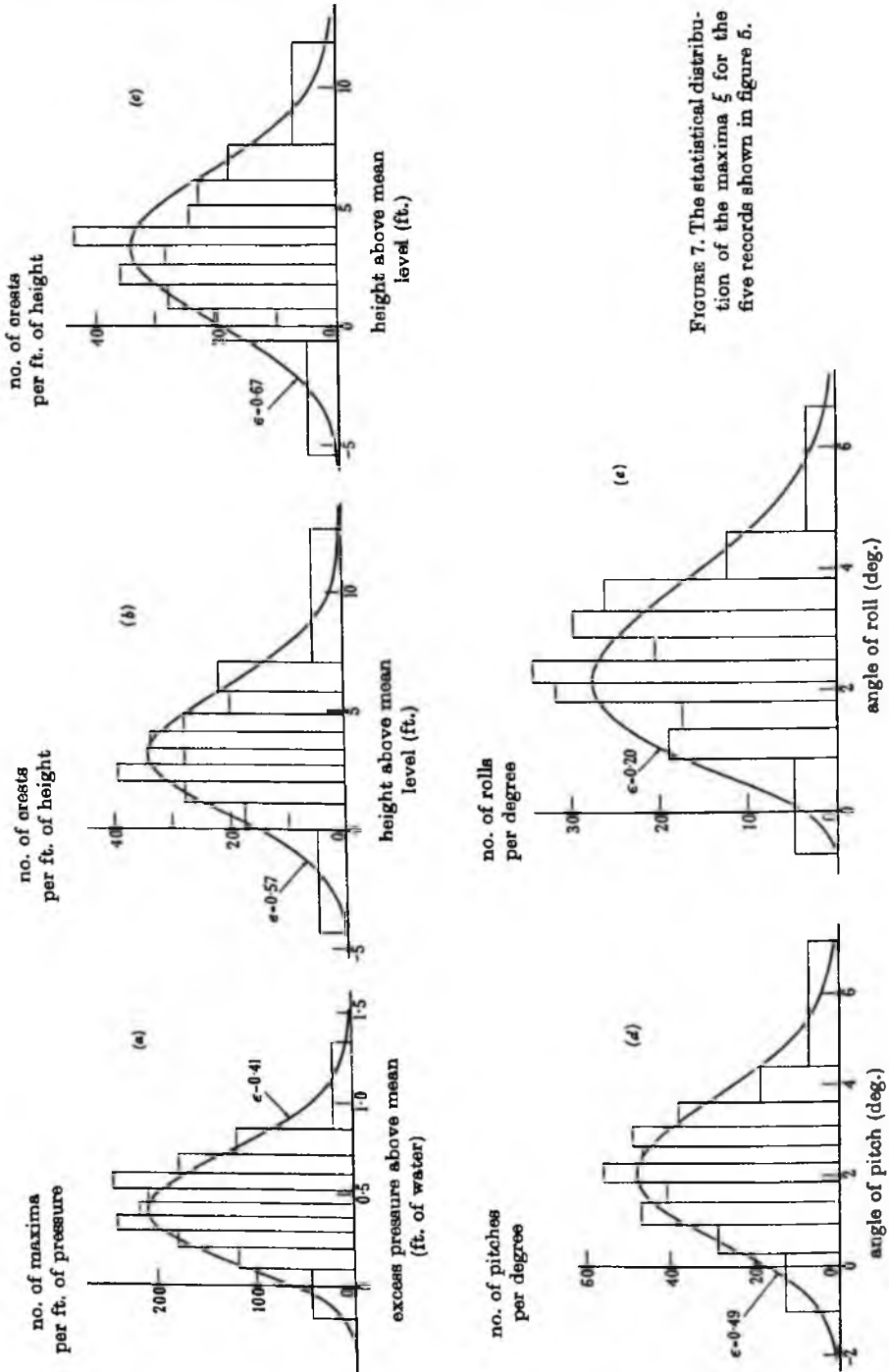


FIGURE 7. The statistical distribution of the maxima ξ for the five records shown in figure 5.

respectively. From these three moments the parameter ϵ defined by equation (1.20) was calculated. The corresponding curves of probability $p(\eta)$, multiplied by the total number N in each sample, are shown in figure 6 (a) to (e).

In constructing the histograms the horizontal scale has been divided, not into equal intervals, but into intervals such that the expected numbers of maxima in each interval (according to the theoretical distribution) are equal. The purpose is to avoid the small classes that must otherwise occur at the two ends of the distribution, and which make the application of the χ^2 significance test unsatisfactory unless the classes are amalgamated in some arbitrary way. The vertical scale is so chosen that, for each separate subclass, a rectangle whose height indicated the expected frequency of maxima would enclose the same area as is enclosed by the curve of theoretical frequency. The width of the two outermost rectangles is chosen quite arbitrarily, but this does not affect in any way the application of the χ^2 test. Some relevant data concerning the five records are given in table 1. The first record is of wave pressure measured on the sea bed in a depth of 110 ft. of water by a power-phone pressure recorder, in March 1945 (described by Barber & Ursell, 1948). The section of record in figure 5 (a) indicates a long, regular swell with a fairly narrow spectrum ($\epsilon = 0.41$). However, it contains a certain amount of energy outside the main frequency band.

TABLE 1. DATA FOR THE RECORDS IN FIGURES 5 TO 7

example	N	ϵ (from energy spectrum)	$P(\chi^2)$	ϵ (from τ)	ϵ (from ρ)
(a)	164	0.41	0.60	0.31	0.37
(b)	220	0.57	0.62	0.58	0.66
(c)	270	0.67	0.55	0.68	0.69
(d)	180	0.48	0.67	0.44	0.45
(e)	250	0.20	0.12	0.26	—

The second and third records are of waves in deep water (Bay of Biscay) measured by the shipborne wave recorder installed in R.R.S. *Discovery II*. The instrument has been described by Tucker (1952). The two records are somewhat more irregular than the pressure record and have correspondingly broader spectra ($\epsilon = 0.57$ and $\epsilon = 0.67$ respectively). This is due partly to the fact that the records of wave height contain more energy of higher frequency than the record of pressure.

The last two records are of the pitching and rolling motion of R.R.S. *Discovery II* in a seaway in the North Atlantic. The angles of pitch and roll were measured in the conventional manner by gyroscopes. The roll, in particular, has a very narrow spectrum ($\epsilon = 0.20$) and the record is correspondingly regular. This is as we should expect, since the rolling motion of a ship is only lightly damped, and is tuned sharply to oscillations having a period close to its period of free motion.

For each of the above records the quantity χ^2 was calculated, and also the probability of χ^2 exceeding this value. Since two parameters have been estimated from the sample (the mean height and the total frequency) χ^2 has in each case 8 degrees of freedom. From table 1 it will be seen that for none of the records is the probability of χ^2 significantly small.

229 *Statistical distribution of the maxima of a random function*

For each measured sample of X_n the quantities r (the proportion of negative maxima) and $\rho (= \mu_1^2 / \mu_0 \mu_2)$ have been found, and from the relations (3.7) and (4.10) two independent estimates of ϵ have been made. These are also given in table 1. It will be seen that in examples (b), (c) and (d) the values of ϵ are in good agreement with that derived from the moments of the energy function $E(\sigma)$. In examples (a) and (e) the estimate derived from r is not in such good agreement, but this is hardly surprising, since the number of negative maxima on which the estimate is based is rather small. In example 5, the estimate derived from ρ gives a small negative value for ϵ^2 , which is of course impossible. In all the other cases the alternative estimates of ϵ are so close to the original estimate as to make no significant difference to the probability of χ^2 .

8. CREST-TO-TROUGH WAVE HEIGHTS

In view of the agreement of the observed distributions of the heights of crests with the theoretical distribution it is interesting to study also the distribution of the crest-to-trough wave heights in the same records.

The local crest-to-trough wave amplitude a_n may be defined as half the absolute difference in height between a crest and the preceding trough, or between a trough and the preceding crest. Thus

$$a_n = \frac{1}{2}(X_n + X_{n-1}). \quad (8.1)$$

The statistical distribution of a_n is more difficult to obtain theoretically than that of X_n for general values of ϵ . However, when $\epsilon \ll 1$ the function $f(t)$ is a regular sine-wave with slowly varying phase and amplitude, so that $a_n = X_n$ very nearly. So we may expect a_n to be distributed according to the Rayleigh distribution (2.8). By considering a disturbance consisting of a small ripple superposed on a long wave ($\epsilon \sim 1$) it can be seen that the distribution of a_n must in general be different from the Rayleigh distribution, though not necessarily by very much. The general distribution no doubt depends on other parameters besides ϵ . Yet it is reasonable to expect that for small values of ϵ the observed distribution of a_n will be in better agreement with the Rayleigh distribution than for larger values of ϵ .

In figure 8 are shown the observed distributions of a_n in the five examples discussed in §7, together with the corresponding Rayleigh distributions

$$p(a) = \frac{a}{\bar{a}^2} e^{-a^2/\bar{a}^2},$$

where \bar{a} is the root-mean-square wave amplitude. The values of χ^2 and $P(\chi^2)$ are given in table 2. (χ^2 again has 8 degrees of freedom, since two parameters—in this case the total number in the sample and the root-mean-square amplitude—have been estimated.)

The table shows that the records with the smallest value of ϵ (examples (a), (d) and (e)) do not give significantly small values of $P(\chi^2)$. On the other hand, those with the two largest values of ϵ give very significant values of $P(\chi^2)$. This verifies our expectation that the observed distribution departs more from the Rayleigh distribution as the width of the energy spectrum increases.

From figure 8 it will be seen that the records with the two broad spectra deviate especially from the Rayleigh distribution for low values of the wave amplitude, having relatively more waves in that range. It appears that the mode of the distribution has a tendency to move to the left in the broader spectra.

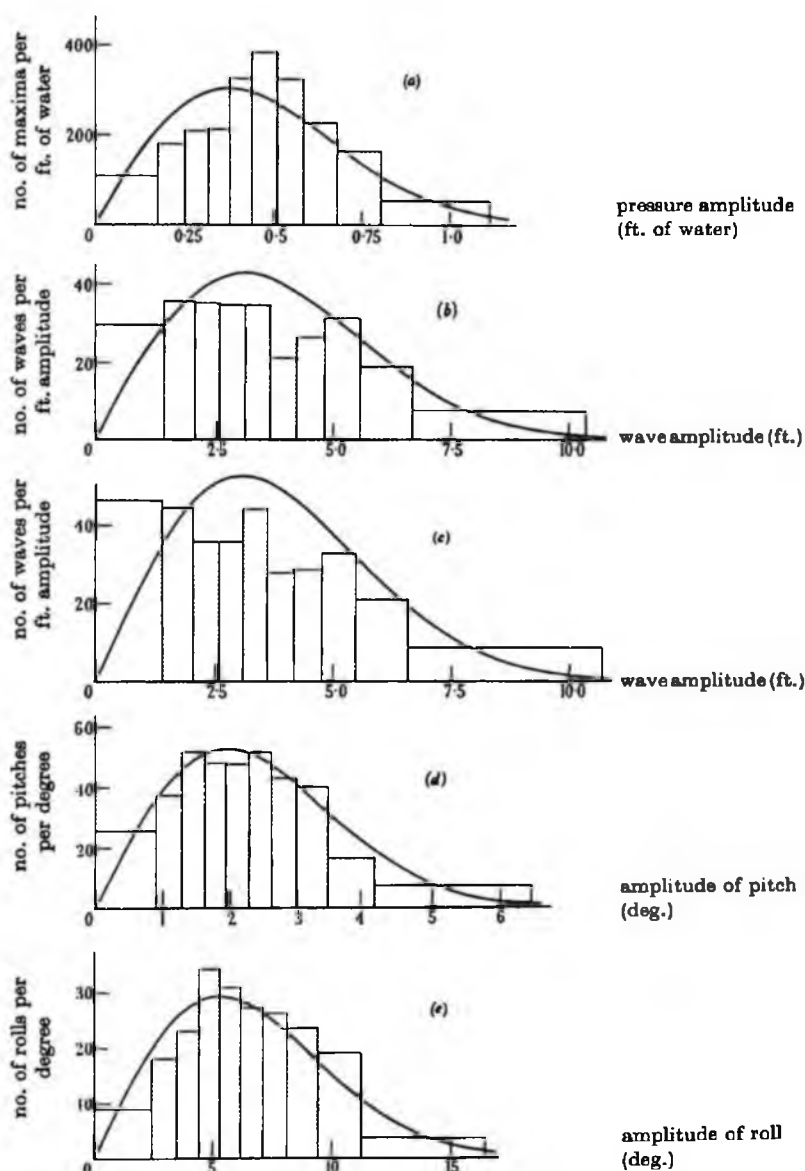


FIGURE 8. The statistical distribution of the crest-to-trough amplitudes for the five records shown in figure 5.

231 *Statistical distribution of the maxima of a random function*

Our conclusions may be compared with those of Watters (1953) who studied histograms of wave heights of 109 records, and compared 38 of these with the corresponding Rayleigh distributions (with variance chosen so as to give the best fit). Although some of the values of $P(\chi^2)$ were low (as small as 0.05) the values taken as a whole did not show a significant departure from the Rayleigh distributions. There are two possible explanations for this. First, the intervals of wave height were equal, and so there were many classes containing only very few heights. In applying the test these classes were arbitrarily pooled, and it can be shown that in several cases pooling the classes in a different way would have resulted in much lower values of χ^2 . (The difficulty is avoided by our present method of making the theoretical classes of uniform size.) Secondly, the widths of the energy spectra of the records studied by Watters were probably less than in examples (b) and (c) of the present paper, which were in fact chosen on account of their exceptional breadth.

TABLE 2. DATA FOR THE DISTRIBUTIONS OF FIGURE 8

example	ϵ	$P(\chi^2)$
(a)	0.41	0.33
(b)	0.57	0.001
(c)	0.67	0.000
(d)	0.48	0.55
(e)	0.20	0.51

9. CONCLUSIONS

If ξ denotes the height of a maximum of the random function $f(t)$ above the mean level, and if $m_{\frac{1}{2}}$ is the r.m.s. value of $f(t)$, then the statistical distribution of $\eta (= \xi/m_{\frac{1}{2}})$ is a function only of η and one other parameter ϵ , which defines the relative width of the energy spectrum of $f(t)$. ϵ lies between 0 and 1. When $\epsilon \rightarrow 0$, $p(\eta)$ tends to a Rayleigh distribution; when $\epsilon \rightarrow 1$, $p(\eta)$ tends to a Gaussian distribution. As ϵ increases from 0 to 1, the mean of $p(\eta)$ gradually decreases, the variance increases and the shewness decreases. The proportion of maxima that are negative steadily increases. The mean height of the highest $1/\eta$ th of the waves varies little for small values of ϵ , but tends always to decrease. The highest maximum in a sample of N maxima tends to decrease relative to m_0 but to increase relative to the r.m.s. height of the maxima.

The records of ocean waves and of ship motion which are discussed in the present paper show good agreement with the theoretical distributions, for various values of ϵ ranging from 0.20 to 0.68.

The theoretical distribution of crest-to-trough heights is known only for a narrow spectrum ($\epsilon = 0$), when it is a Rayleigh distribution. In three of the examples in this paper, for which $\epsilon < 0.5$ and the total number in the sample was less than 300, there was no significant departure from the Rayleigh distribution. On the other hand, the examples with the broadest spectra ($\epsilon = 0.57$ and $\epsilon = 0.67$) did show significant departures.

This indicates the need for a theoretical derivation of the crest-to-trough height distribution when $\epsilon > 0$. Meanwhile, for the purpose of practical prediction, it would

be better to deal with crest-heights rather than with crest-to-trough heights as is customary at present.

REFERENCES

- Barber, N. F. 1950 *Ocean waves and swell*. Lecture, Instn Elect. Engrs, Lond.
 Barber, N. F. & Ursell, F. 1948 *Phil. Trans. A*, **240**, 527.
 Darbyshire, J. & Tucker, M. J. 1953 *J. Sci. Instrum.* **30**, 212.
 Fisher, R. A. & Tippett, L. H. C. 1928 *Proc. Camb. Phil. Soc.* **24**, 180.
 Gumbel, E. J. 1954 *Appl. Math. ser. U.S. Bur. stand.* no. 33.
 Longuet-Higgins, M. S. 1952 *J. Mar. Res.* **11**, 245.
 Rayleigh, Lord 1880 *Phil. Mag.* **10**, 73.
 Rice, S. O. 1944 *Bell Syst. Tech. J.* **23**, 282.
 Rice, S. O. 1945 *Bell Syst. Tech. J.* **24**, 46.
 Tippett, L. H. C. 1925 *Biometrika*, **17**, 364.
 Tucker, M. J. 1952 *Nature, Lond.*, **170**, 657.
 Watters, J. K. 1953 *N.Z. J. Sci. Tech.* **B**, **34**, 409.

Reprinted from the *Proceedings of the Cambridge Philosophical Society*,
Volume 52, Part 2, pp. 234-245, 1956.

PRINTED IN GREAT BRITAIN

STATISTICAL PROPERTIES OF A MOVING WAVE-FORM

By M. S. LONGUET-HIGGINS

Received 27 June 1955

Many of the statistical properties of a random noise function $f(t)$ have been derived by Rice (4); for example, the mean frequency of zero crossings and the statistical distribution of maxima and minima. These distributions have been shown to apply quite accurately to physical phenomena; in particular, when $f(t)$ represents the height of sea waves at a certain point or the pressure at a fixed point on the sea bed (1, 3, 5).

In some applications, however, we wish to deal with moving wave-forms, and to distinguish between positive and negative directions. Thus we may be interested in finding the coefficient of reflexion of waves from a fixed obstacle. We have then to consider a random function depending on both a space variable x and a time variable t , and to consider statistical properties involving the motion of the surface as well as its configuration at any one time.

In the present paper a beginning is made with the consideration of essentially two such statistical distributions: the velocities of zeros and the frequency of 'twinkles'.

Imagine a line drawn through a given level of the function, say the mean, which we take to be zero. At a particular instant the function will cross this line at a number of points, the 'zeros' of $f(x, t)$. A moment later the zeros will have shifted to new positions. The ratio of displacement of each zero to the small increment of time may be called the velocity of the zero, say c ; clearly

$$c = -\frac{\partial f/\partial t}{\partial f/\partial x}.$$

It is the statistical distribution of c that is investigated in § 2. For purely progressive waves the velocities are of course mainly of the same sign; if some energy travels in the opposite sense the velocities will more often be negative. In general, the distribution of c is found to be symmetrical about a mean velocity which depends on the first moment of the energy distribution about the origin.

Certain associated distributions may be derived immediately. For example, the velocity of the surface at a given level, not necessarily the mean, has a similar statistical distribution; also the velocities of points having zero gradient, i.e. the maxima and minima of the wave-form.

Points on the surface having a constant gradient may appropriately be called specular points, being those points at which a distant observer would see his own image, or the image of another distant object, reflected in the surface. The movement of specular points, then, is very similar to the movement of the zeros, and may sometimes be more conveniently observed. Now it happens occasionally that a specular point, instead of moving to an adjacent position, vanishes completely, or alternatively one appears where there was previously none before. This will occur, in general, when the specular point coincides with a point of inflexion, and it is not difficult to see that

Statistical properties of a moving wave-form

specular points are created or annihilated in pairs. The creation or annihilation of a pair of specular points will be called a 'twinkle'.

In § 4 we investigate the frequency of twinkles, as a function of the energy spectrum of f . The frequency is given by equation (58). For a narrow group of waves travelling entirely in one direction, the frequency of twinkles is least; for standing waves it is a maximum, as one can observe by watching water waves reflected from a barrier. The frequency of twinkles depends also on the width of the energy spectrum and the angle from which the surface is viewed. The maximum frequency is found to be at an angle near the r.m.s. inclination of the surface. Thus by simple visual observations one can determine the r.m.s. surface slope of the wave, the width of the spectrum and the proportion of energy travelling in either direction.

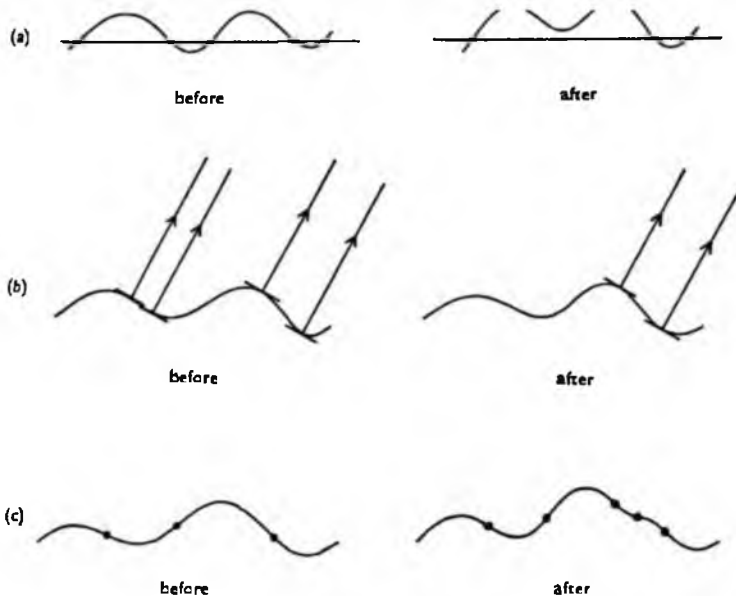


Fig. 1. Illustrating (a) twinkles, (b) twinkles, (c) crinkles. Any of the three events may be reversed in time.

We consider also two events analogous to a twinkle, namely, when a pair of zeros of f coincide and are annihilated (which we call a 'winkle') and when two points of inflexion are created (which we call a 'crinkle'). The frequencies of twinkles and crinkles are calculated in terms of the energy spectrum of f .

1. *Definitions.* Generalizing Rice (4) we consider a random function of two variables given by

$$f(x, t) = \sum_n c_n \cos(k_n x + \sigma_n t + \epsilon_n). \quad (1)$$

Thus f is represented as the sum of an infinite number of travelling sine-waves. The wave numbers k_n are densely distributed between $-\infty$ and ∞ , and $\sigma_n = \sigma(k_n)$ is an even function of k_n :

$$\sigma(-k) = \sigma(k), \quad (2)$$

so that each wave travels with the appropriate velocity $-\sigma_n/k_n$; positive and negative values of k_n correspond to waves travelling in opposite senses. The amplitudes c_n and phases ϵ_n are random variables, ϵ_n being distributed with uniform probability in the range $(0, 2\pi)$ and c_n being such that any small interval of wave number dk

$$\sum_{dk} \frac{1}{2} c_n^2 = E(k) dk. \quad (3)$$

$E(k)$ is a positive, continuous function of k which will be called the energy spectrum of f .

We shall write m_0 for the total energy per unit distance, defined by

$$m_0 = \int_{-\infty}^{\infty} E(k) dk, \quad (4)$$

and in general m_n for the n th moment

$$m_n = \int_{-\infty}^{\infty} k^n E dk. \quad (5)$$

Similarly, for the moments of the functions σE and $\sigma^2 E$ we write

$$\left. \begin{aligned} m'_n &= \int_{-\infty}^{\infty} k^n \sigma E dk, \\ m''_n &= \int_{-\infty}^{\infty} k^n \sigma^2 E dk. \end{aligned} \right\} \quad (6)$$

It is assumed that the moments exist up to all orders required.

We shall make use of the central limit theorem in n dimensions, which may be stated as follows.

Let ξ_1, \dots, ξ_n be n quantities, each the sum of a large number of independent variables whose expectation is zero. Then under certain general conditions (see Cramér (2)) the joint-probability distribution of ξ_1, \dots, ξ_n is normal:

$$p(\xi_1, \dots, \xi_n) = \frac{1}{(2\pi)^{n/2} \Delta^{1/2}} e^{-\frac{1}{2} M_{ij} \xi_i \xi_j}, \quad (7)$$

where M_{ij} is the inverse matrix to

$$\Xi_{ij} = \begin{pmatrix} \overline{\xi_1^2} & \overline{\xi_1 \xi_2} & \dots & \overline{\xi_1 \xi_n} \\ \overline{\xi_2 \xi_1} & \overline{\xi_2^2} & \dots & \overline{\xi_2 \xi_n} \\ \vdots & \vdots & \ddots & \vdots \\ \overline{\xi_n \xi_1} & \overline{\xi_n \xi_2} & \dots & \overline{\xi_n^2} \end{pmatrix}, \quad (8)$$

and

$$\Delta = |\Xi_{ij}|. \quad (9)$$

Here $\overline{\xi_i \xi_j}$ denotes the mean value of $\xi_i \xi_j$ over the probability space of the random variables.

Now f and its derivatives are, by definition, functions of this type and we have, for example,

$$f^2 = \sum_n \frac{1}{2} c_n^2 = m_0, \quad (10)$$

237 *Statistical properties of a moving wave-form*

so that the probability distribution of $\xi_1 = f$ is

$$p(\xi_1) = \frac{1}{(2\pi m_0)^{\frac{1}{2}}} e^{-\xi^2/2m_0}. \quad (11)$$

Similarly we have

$$\left. \begin{aligned} \left(\frac{\partial f}{\partial x}\right)^2 &= \sum_n \frac{1}{2} k_n^2 c_n^2 = m_2, \\ \left(\frac{\partial f}{\partial t}\right)^2 &= \sum_n \frac{1}{2} \sigma_n^2 c_n^2 = m_0'', \\ \frac{\partial f}{\partial x} \frac{\partial f}{\partial t} &= \sum_n \frac{1}{2} k_n \sigma_n c_n^2 = m_1'. \end{aligned} \right\} \quad (12)$$

so that the matrix of correlations for $\xi_2, \xi_3, = \partial f/\partial x, \partial f/\partial t$, is

$$\Xi_{ij} = \begin{pmatrix} m_2 & m_1' \\ m_1' & m_0'' \end{pmatrix}, \quad (13)$$

and the joint-probability distribution of ξ_2, ξ_3 is

$$p(\xi_2, \xi_3) = \frac{1}{2\pi \Delta_0^{\frac{1}{2}}} \exp[-(m_0'' \xi_2^2 - 2m_1' \xi_2 \xi_3 + m_2 \xi_3^2)/2\Delta_0], \quad (14)$$

where

$$\Delta_0 = m_2 m_0'' - m_1'^2. \quad (15)$$

The correlations of f with $\partial f/\partial x$ and $\partial f/\partial t$ are both zero, so that the probability distribution of $\xi_1, \xi_2, \xi_3, = f, \partial f/\partial x, \partial f/\partial t$, is given by

$$p(\xi_1, \xi_2, \xi_3) = p(\xi_1) p(\xi_2, \xi_3), \quad (16)$$

where $p(\xi_1)$ is given by (11) and $p(\xi_2, \xi_3)$ by (14).

2. *The velocities of zeros.* Consider the intersection of the curve $y = f(x, t)$ with a fixed line parallel to the x -axis, say $y = \xi_1$. In a short interval of time dt the intersection will have moved through a horizontal distance dx , where

$$\frac{\partial f}{\partial x} dx + \frac{\partial f}{\partial t} dt = 0. \quad (17)$$

Accordingly the velocity of the intersection is

$$c = \frac{dx}{dt} = -\frac{\partial f/\partial t}{\partial f/\partial x}. \quad (18)$$

The probability distribution of c is therefore the probability distribution of $-\xi_3/\xi_2$, where the distribution of ξ_2, ξ_3 is given by (14). To find the distribution of c let us write

$$-\xi_3/\xi_2 = \eta_1, \quad \xi_3 = \eta_2, \quad (19)$$

so that

$$J = \frac{\partial(\xi_2, \xi_3)}{\partial(\eta_1, \eta_2)} = \frac{\eta_2}{\eta_1^2}. \quad (20)$$

The probability of (η_1, η_2) lying in a small region of the (η_1, η_2) -plane is equal to the probability of (ξ_2, ξ_3) lying in the corresponding region of the (ξ_2, ξ_3) -plane—which has an area $|J|$ times as great. Hence the probability distribution of η_1, η_2 is given by

$$p(\eta_1, \eta_2) = \frac{1}{2\pi \Delta_0^{\frac{1}{2}}} \left| \eta_2 / \eta_1^2 \right| \exp \left[-\eta_2^2 (m_0'' / \eta_1^2 + 2m_1' / \eta_1 + m_2) / 2\Delta_0 \right]. \quad (21)$$

To find the distribution of $c = \eta_1$ we integrate the above expression with respect to η_2 from $-\infty$ to ∞ , obtaining

$$p(c) = \frac{\Delta_0^{\frac{1}{2}}}{\pi} \frac{1}{m_2 c^2 + 2m_1' c + m_0''}. \quad (22)$$

Let us consider this distribution. It has a maximum or mode when

$$c = -\frac{m_1'}{m_2} = \bar{c}, \quad (23)$$

say, and is symmetrical about its mean value, as may be seen by writing it in the form

$$p(c) = \frac{1}{\pi} \frac{\Delta_0^{\frac{1}{2}} / m_2}{(c - \bar{c})^2 + \Delta_0 / m_2^2}. \quad (24)$$

The even moments of the distribution, apart from the moment of zero order, are infinite, and so therefore is the standard deviation. However, a convenient measure of the spread of velocities is the interquartile range (i.e. the central range containing half the probability distribution), which is of width

$$w = 2\Delta_0^{\frac{1}{2}} / m_2. \quad (25)$$

As an example let us suppose that the spectrum of the function consists of two narrow bands, of equal wave-length but opposite direction. Let a proportion q of the energy be travelling in the positive direction, and a proportion $(1 - q)$ in the negative direction. Then if \bar{k} is the mean (absolute) wave number and $\bar{\sigma}$ the corresponding value of σ we have

$$m_2 = \bar{k}^2 m_0, \quad m_0'' = \bar{\sigma}^2 m_0, \quad m_1' = (1 - 2q) \bar{\sigma} \bar{k} m_0. \quad (26)$$

The mean velocity \bar{c} is therefore

$$\bar{c} = -\frac{m_1'}{m_2} = (2q - 1) \bar{\sigma} / \bar{k}, \quad (27)$$

and the interquartile range is

$$w = \frac{2\Delta_0^{\frac{1}{2}}}{m_2} = 4q^{\frac{1}{2}}(1 - q)^{\frac{1}{2}} \bar{\sigma} / \bar{k}. \quad (28)$$

For purely progressive waves $q = 1$ and so

$$\bar{c} = \bar{\sigma} / \bar{k}, \quad w = 0; \quad (29)$$

the velocities are all concentrated at the phase velocity $\bar{\sigma} / \bar{k}$. For standing waves $q = \frac{1}{2}$ and so

$$\bar{c} = 0, \quad w = 2\bar{\sigma} / \bar{k}; \quad (30)$$

the velocities are symmetrical about zero, and the half-width of the distribution is $2\bar{\sigma} / \bar{k}$, the greatest possible. Just half the velocities are greater in absolute magnitude than $\bar{\sigma} / \bar{k}$, half are less.

Statistical properties of a moving wave-form

We have seen that the relative distribution of c is independent of the level ξ_1 at which the velocity is measured, though there will necessarily be fewer crossings of any given level other than the zero level. From (16) the number of crossings per unit distance is proportional to $p(\xi_1)$ and so to $e^{-\xi_1^2/2m_0}$. The actual number of zero crossings per unit length of the x -axis has been determined by Rice (4); it is

$$N_0 = \frac{1}{\pi} \left(\frac{m_2}{m_0} \right)^{\frac{1}{2}}, \quad (31)$$

and in general, therefore, the number of crossings is

$$N_0 = \frac{1}{\pi} \left(\frac{m_2}{m_0} \right)^{\frac{1}{2}} e^{-\xi_1^2/2m_0}. \quad (32)$$

3. *Velocities of specular points.* In a precisely similar way we may determine the distribution of velocities of 'specular' points on the surface having a given gradient. By a similar argument to § 2 the velocity of a specular point is

$$c_1 = - \frac{\partial^2 f / \partial x \partial t}{\partial^2 f / \partial x^2}. \quad (33)$$

To find the distribution of c_1 we have only to raise the indices of the moments m_n in the previous distribution by two. Thus

$$p(c_1) = \frac{1}{\pi} \frac{\Delta_1^{\frac{1}{2}} / m_4}{(c_1 - \bar{c}_1)^2 + \Delta_1 / m_4^2}, \quad (34)$$

where the mean velocity \bar{c}_1 is given by

$$\bar{c}_1 = - \frac{m_3'}{m_4}, \quad (35)$$

and where

$$\Delta_1 = m_4 m_2'' - m_3'^2. \quad (36)$$

This distribution will include as a special case the velocities of maxima and minima (crests and troughs) of the surface.

By comparison with (32) we see that the number of specular points per unit length of the x -axis is

$$N_1 = \frac{1}{\pi} \left(\frac{m_4}{m_2} \right)^{\frac{1}{2}} e^{-\xi_1^2/2m_2}. \quad (37)$$

Similarly, the distribution of the velocities c_2 of points of inflexion is

$$p(c_2) = \frac{1}{\pi} \frac{\Delta_2^{\frac{1}{2}} / m_6}{(c_2 - \bar{c}_2)^2 + \Delta_2 / m_6^2}, \quad (38)$$

where

$$\bar{c}_2 = - \frac{m_5'}{m_6}, \quad \Delta_2 = m_6 m_4'' - m_5'^2; \quad (39)$$

the average number of points of inflexion per unit distance is

$$N_2 = \frac{1}{\pi} \left(\frac{m_6}{m_4} \right)^{\frac{1}{2}}. \quad (40)$$

4. *Frequency of twinkles.* If the specular points on a surface are observed continuously it will occasionally happen that one will disappear altogether, or, on the other hand, one will appear 'from nowhere'. A disappearance is caused by the specular point having no adjacent part of the surface to move to; its velocity becomes momentarily infinite. Such an event will occur, in general, when the specular point coincides with a maximum or a minimum of surface gradient (see Fig. 1). We shall call it a 'twinkle', including in this term also a reappearance of a specular point. From Fig. 1 it will be seen that the specular points are created or annihilated in pairs, a pair at each twinkle.

If the velocities of specular points were observed at one instant only, a twinkle would of course be an infinitely rare event. But supposing observation is continuous, one may inquire into the mean frequency of twinkles per unit distance per unit time. If this is denoted by F_1 then N_1/F_1 gives the average lifetime of a specular point, between appearance and disappearance.

We wish to find the probability of the event

$$\left(\frac{\partial f}{\partial x} = \text{constant}, \frac{\partial^2 f}{\partial x^2} = 0 \right) \quad (41)$$

in a time interval $(t, t + dt)$ and space interval $(x, x + dx)$. Let

$$\left. \begin{aligned} \frac{\partial f}{\partial x} &= \xi_2, & \frac{\partial^2 f}{\partial x^2} &= \xi_4, \\ \frac{\partial^2 f}{\partial x \partial t} &= \xi_5, & \frac{\partial^3 f}{\partial x^2 \partial t} &= \xi_6, & \frac{\partial^3 f}{\partial x^3} &= \xi_7. \end{aligned} \right\} \quad (42)$$

Now the pair of variables ξ_2, ξ_4 are functions of the pair of variables x, t . If therefore (x, t) is confined to a certain region of the (x, t) -plane having area $dxdt$, (ξ_2, ξ_4) is confined to the corresponding region of the (ξ_2, ξ_4) -plane, which is $|J|$ times as great, where

$$J = \frac{\partial(\xi_2, \xi_4)}{\partial(x, t)} = \xi_4 \xi_6 - \xi_5 \xi_7. \quad (43)$$

Therefore the probability of ξ_2, ξ_4 taking prescribed values ξ'_2, ξ'_4 in this region is

$$\int_{-\infty}^{\infty} \int_{-\infty}^{\infty} \int_{-\infty}^{\infty} p(\xi_2, \xi_4, \xi_5, \xi_6, \xi_7) | \xi_4 \xi_6 - \xi_5 \xi_7 | dxdt d\xi_5 d\xi_6 d\xi_7. \quad (44)$$

Putting $\xi'_4 = 0$ and dropping the dash from ξ'_2 we have for the frequency of twinkles per unit distance and time

$$F_1(\xi_2) = \int_{-\infty}^{\infty} \int_{-\infty}^{\infty} \int_{-\infty}^{\infty} p(\xi_2, 0, \xi_5, \xi_6, \xi_7) | \xi_6 \xi_7 | d\xi_5 d\xi_6 d\xi_7. \quad (45)$$

Now the matrix of correlations for $(\xi_2, \xi_4, \xi_5, \xi_6, \xi_7)$ is

$$\begin{pmatrix} m_2 & 0 & 0 & -m'_3 & -m_4 \\ 0 & m_4 & m'_3 & 0 & 0 \\ 0 & m'_3 & m''_2 & 0 & 0 \\ -m'_3 & 0 & 0 & m''_4 & m'_5 \\ -m_4 & 0 & 0 & m'_5 & m_6 \end{pmatrix}. \quad (46)$$

241 *Statistical properties of a moving wave-form*

and so
$$p(\xi_2, \xi_4, \xi_5, \xi_6, \xi_7) = p(\xi_4, \xi_5) p(\xi_2, \xi_6, \xi_7), \quad (47)$$

where
$$p(\xi_4, \xi_5) = \frac{1}{2\pi \Delta_1^{\frac{1}{2}}} \exp \left[- (m_2'' \xi_4^2 - 2m_3' \xi_4 \xi_5 + m_4 \xi_5^2) / 2\Delta_1 \right], \quad (48)$$

$$\Delta_1 = m_2'' m_4 - m_3'^2, \quad (49)$$

and
$$p(\xi_2, \xi_6, \xi_7) = \frac{1}{(2\pi)^{\frac{3}{2}} \Delta^{\frac{1}{2}}} e^{-\frac{1}{2} M_{ij} \xi_i \xi_j}, \quad (50)$$

$$M_{ij} = \begin{pmatrix} m_2 & -m_3' & -m_4 \\ -m_3' & m_4'' & m_6 \\ -m_4 & m_6 & m_8 \end{pmatrix}^{-1}, \quad (51)$$

$$\Delta = |M_{ij}|^{-1}. \quad (52)$$

So we have

$$F_1 = \frac{1}{(2\pi)^{\frac{3}{2}} (\Delta_1 \Delta)^{\frac{1}{2}}} \int_{-\infty}^{\infty} \int_{-\infty}^{\infty} \int_{-\infty}^{\infty} e^{-m_4 \xi_5^2 / 2\Delta_1} e^{-\frac{1}{2} M_{ij} \xi_i \xi_j} |\xi_5 \xi_7| d\xi_5 d\xi_6 d\xi_7, \quad (53)$$

where i, j take values 2, 6, 7. The integration with regard to ξ_5 can be carried out immediately. We find

$$F_1 = \frac{2\Delta_1^{\frac{1}{2}}}{(2\pi)^{\frac{3}{2}} m_4 \Delta^{\frac{1}{2}}} \int_{-\infty}^{\infty} \int_{-\infty}^{\infty} e^{-\frac{1}{2} M_{ij} \xi_i \xi_j} |\xi_7| d\xi_6 d\xi_7. \quad (54)$$

Now if a_{ij} is any positive-definite (3×3) matrix we have, by standard methods,

$$\int_{-\infty}^{\infty} \int_{-\infty}^{\infty} e^{-\frac{1}{2} a_{ij} x_i x_j} |x_3| dx_2 dx_3 = 2(2\pi)^{\frac{1}{2}} A e^{-\frac{1}{2} B x_1^2} \left[e^{-\frac{1}{2} C x_1^2} + C x_1 \int_0^{C x_1} e^{-\frac{1}{2} x^2} dx \right], \quad (55)$$

where

$$\left. \begin{aligned} A &= \frac{a_{22}^{\frac{1}{2}}}{a_{22} a_{33} - a_{23}^2}, \\ B &= \frac{|a_{ij}|}{a_{22} a_{33} - a_{23}^2}, \\ C &= \frac{a_{22} a_{31} - a_{32} a_{21}}{a_{22}^{\frac{1}{2}} (a_{22} a_{33} - a_{23}^2)^{\frac{1}{2}}}. \end{aligned} \right\} \quad (56)$$

Substituting ξ_2, ξ_6, ξ_7 for x_1, x_2, x_3 in this result and writing

$$\xi_2 / m_2^{\frac{1}{2}} = \eta, \quad \frac{m_2 m_8 - m_4^2}{m_4^2} = \delta^2, \quad (57)$$

we find

$$F_1 = \frac{1}{\pi^2 m_2} \delta e^{-\frac{1}{2} \eta^2} \left[e^{-\frac{1}{2} \eta^2 / \delta^2} + (\eta / \delta) \int_0^{\eta / \delta} e^{-\frac{1}{2} x^2} dx \right], \quad (58)$$

or

$$F_1 = \frac{1}{\pi^2} s d F(\eta, \delta), \quad (59)$$

where

$$s = \frac{(m_2'' m_4)^{\frac{1}{2}}}{m_2}, \quad d^2 = \frac{m_2'' m_4 - m_3'^2}{m_2'' m_4} \quad (60)$$

and

$$F(\eta, \delta) = \delta e^{-\frac{1}{2} \eta^2} \left[e^{-\frac{1}{2} \eta^2 / \delta^2} + (\eta / \delta) \int_0^{\eta / \delta} e^{-\frac{1}{2} x^2} dx \right]. \quad (61)$$

Considering the terms in (59) we see that s is a scale factor, d discriminates between progressive and standing waves, and $F(\eta, \delta)$ is a function of η —the inclination of the surface relative to the r.m.s. slope $m_2^{\frac{1}{2}}$ —and of δ , which is a measure of the width of the spectrum regardless of direction of travel of the energy.

For example, let us consider a narrow band of swell with mean (absolute) wave number \bar{k} and frequency $\bar{\sigma}$. If a proportion q of the energy travels in the positive direction and $(1-q)$ in the negative direction we have

$$\left. \begin{aligned} m_2 &= \bar{k}^2 m_0, & m_4 &= \bar{k}^4 m_0, \\ m_2' &= \bar{k}^2 \bar{\sigma}^2 m_0, & m_3' &= \bar{k}^3 \bar{\sigma} (1-2q) m_0, \end{aligned} \right\} \quad (62)$$

and so
$$s = \bar{k} \bar{\sigma} = \frac{4\pi^2}{\lambda \bar{\tau}}, \quad (63)$$

where $\bar{\lambda}$ and $\bar{\tau}$ are the mean wave-length and period; also

$$d = 2q^{\frac{1}{2}}(1-q)^{\frac{1}{2}}. \quad (64)$$

d vanishes for $q = 0$ or 1 , i.e. for purely progressive waves, and is a maximum for $q = \frac{1}{2}$, i.e. for standing waves. It follows that for progressive waves there are no twinkles, as we should expect, since then the specular points will advance with uniform velocity (cf. § 2) and will have little tendency to vanish. On the other hand, for standing waves the range of surface gradients is changing frequently and we may expect considerable twinkling. This is confirmed by the vigorous twinkling in water waves when they are reflected from a fixed obstacle.

We may note that d is proportional to $q^{\frac{1}{2}}$, and so to the r.m.s. amplitude of the waves travelling in the positive direction. If a_1 and a_2 denote the r.m.s. amplitudes of the waves travelling in the two directions we have (for the narrow spectrum)

$$d \doteq \frac{2a_1 a_2}{a_1^2 + a_2^2} \quad (65)$$

Next consider the dependence of F_1 on the angle of observation. The form of $F(\eta, \delta)$ depends on the ratio η/δ . For $\eta/\delta \gg 1$, e.g. for narrow spectra and for moderate or large values of η , we have

$$F(\eta, \delta) = (\frac{1}{2}\pi)^{\frac{1}{2}} \eta e^{-\frac{1}{2}\eta^2}. \quad (66)$$

So the frequency of twinkles has a Rayleigh distribution with regard to angle of observation, with a maximum frequency at $\eta = 1$, when $\xi_2 =$ the r.m.s. gradient $m_2^{\frac{1}{2}}$. The maximum frequency is given by

$$F(\eta, \delta) = \left(\frac{\pi}{2e}\right)^{\frac{1}{2}}, \quad (67)$$

and so

$$F_1 = 4 \left(\frac{2\pi}{e}\right)^{\frac{1}{2}} q^{\frac{1}{2}} (1-q)^{\frac{1}{2}} \frac{1}{\lambda \bar{\tau}}. \quad (68)$$

Thus for narrow spectra the frequency of twinkles provides a method of determining both the r.m.s. gradient and the proportion of energy travelling in either direction.

Statistical properties of a moving wave-form

For broader spectra, or for angles of observation very near to the vertical, the above approximation to F breaks down, but we have

$$F(\eta, \delta) = \delta \quad (69)$$

very nearly, giving
$$F_1 = 8\delta \frac{q^{\frac{1}{2}}(1-q)^{\frac{1}{2}}}{\lambda \bar{\tau}}. \quad (70)$$

So the frequency of twinkles at the azimuth is roughly proportional to δ , the r.m.s. width of the spectrum.

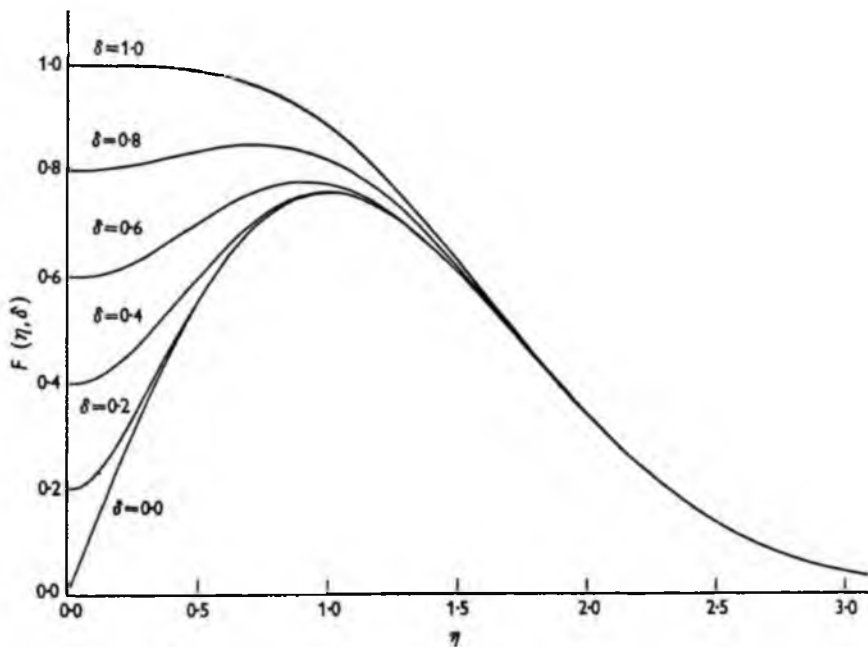


Fig. 2. Curves of $F(\eta, \delta)$, showing the frequency of twinkling as a function of the relative gradient η , for six different widths of spectrum δ .

To estimate the frequency of twinkles at intermediate values of η/δ we have plotted $F(\eta, \delta)$ against η for $\delta = 0.0, 0.2, 0.4, 0.6, 0.8, 1.0$ in Fig. 2.

The mean density of specular points being given by (40), the average lifetime L_1 of a specular point is

$$L_1 = \frac{N_1}{F_1} = \pi \left(\frac{m_2}{m_2^2} \right)^{\frac{1}{2}} \frac{1}{d} L(\eta, \delta), \quad (71)$$

where
$$L(\eta, \delta) = \delta^{-1} \left[e^{-\frac{1}{2}(\eta/\delta)^2} + (\eta/\delta) \int_0^{\eta/\delta} e^{-\frac{1}{2}x^2} dx \right]^{-1} \quad (72)$$
 and d is given by (60).

5. *Winkling and crinkling.* The analysis of twinkling, like that of specular points, involves essentially the function $\partial f/\partial x$ and its derivatives; f itself does not necessarily

enter. There is therefore a corresponding set of events involving the function f in place of $\partial f/\partial x$; the order of each derivative that occurs is to be reduced by one.

A twinkle is defined as the coalescence of two points of given gradient at a point of inflexion (zero rate of change of gradient). Thus the corresponding event of lower order is the coalescence of two points at a fixed level at a maximum or minimum, in other words, the passing of a maximum or minimum through the given level. If the level is the mean level, this entails the disappearance (or reappearance) of a pair of zeros; the part of the curve on one side of the mean level is, as it were, removed, or winkled out. Such an event we shall call a 'winkle'. The frequency F_0 of winks may be written down at once by analogy with the frequency of twinkles (equation (58)). For winks at a general level ξ_1 we have

$$F_0 = \frac{1}{\pi^2} \frac{\Delta_0^{\frac{1}{2}}}{m_0} F(\eta_0, \delta_0), \quad (73)$$

where now

$$\eta_0 = \xi_1/m_0^{\frac{1}{2}}, \quad \delta_0^2 = \frac{m_0 m_4 - m_2^2}{m_0 m_4} \quad (74)$$

and

$$\Delta_0 = m_0^2 m_2 - m_1'^2. \quad (75)$$

In particular, at the mean level we have

$$F_0 = \frac{1}{\pi^2} \frac{\Delta_0^{\frac{1}{2}} \delta_0}{m_0}. \quad (76)$$

The mean lifetime of a zero is

$$L_0 = \frac{N_0}{F_0} = \pi \frac{(m_0 m_2)^{\frac{1}{2}}}{\Delta_0^{\frac{1}{2}} \delta_0}. \quad (77)$$

The corresponding statistics for higher derivatives may also be interesting. For $\partial^2 f/\partial x^2$ the analogous event to a winkle or twinkle is the creation or annihilation of two points of inflexion, or more generally two new points having a given second derivative ξ_4 . The case where the given curvature is zero, and the points are points of inflexion, is probably most easy to visualize. The curve then develops an extra 'crinkle', which is accordingly the name that we give to such an event. The frequency of (generalized) crinkles is

$$F_2 = \frac{1}{\pi^2} \frac{\Delta_2^{\frac{1}{2}}}{m_4} F(\eta_2, \delta_2), \quad (78)$$

where

$$\eta_2 = \xi_4/m_4^{\frac{1}{2}}, \quad \delta_2^2 = \frac{m_4 m_8 - m_6^2}{m_8^2} \quad (79)$$

and

$$\Delta_2 = m_4^2 m_8 - m_6'^2. \quad (80)$$

The frequency of 'ordinary' crinkles is

$$F_2 = \frac{1}{\pi^2} \frac{\Delta_2^{\frac{1}{2}} \delta_2}{m_4}, \quad (81)$$

and the mean lifetime of a point of inflexion is

$$L_2 = \pi \frac{(m_4 m_8)^{\frac{1}{2}}}{\Delta_2^{\frac{1}{2}} \delta_2}. \quad (82)$$

REFERENCES

- (1) BARBER, N. F. *Ocean waves and swell* (Lecture, Institution of Civil Engineers, London, 1950, 22 pp.).
- (2) CRAMÉR, H. *Random variables and probability distributions* (*Camb. Tracts Math.* no. 36, 1937).
- (3) LONGUET-HIGGINS, M. S. On the statistical distribution of the heights of sea waves. *J. Mar. Res.* 9 (1952), 245-66.
- (4) RICE, S. O. The mathematical analysis of random noise. *Bell Syst. tech. J.* 23 (1944), 282-332; 24 (1945), 46-156.
- (5) WATTERS, J. K. Distribution of height in ocean waves. *N. Z. J. Sci. Tech.* B, 34 (1953), 409-22.

NATIONAL INSTITUTE OF OCEANOGRAPHY
WORMLEY

Reprinted from the *Proceedings of the Cambridge Philosophical Society*,
Volume 53, Part 1, pp. 230-233, 1957.

PRINTED IN GREAT BRITAIN

ON THE VELOCITIES OF THE MAXIMA IN A MOVING WAVE-FORM

By M. S. LONGUET-HIGGINS

Received 19 July 1956

In a recent paper (1) expressions were found for the statistical distributions of the velocities of the zero-crossings and of the maxima and minima of a random moving wave-form. In the present note it will be shown that these distributions are to some extent arbitrary, depending on how the points of observation are selected.

The same notation will be used and the same basic assumptions made as in (1). If

$$z = f(x, t) \quad (1)$$

represents the height of a moving wave-form, being a function both of the horizontal co-ordinate x and of the time t , then the joint-probability distribution of the three variables

$$\xi_1, \xi_2, \xi_3 = f, \frac{\partial f}{\partial x}, \frac{\partial f}{\partial t} \quad (2)$$

was shown in (1) to be

$$p(\xi_1, \xi_2, \xi_3) = p(\xi_1) p(\xi_2, \xi_3), \quad (3)$$

where

$$p(\xi_1) = \frac{1}{(2\pi m_0)^{\frac{1}{2}}} \exp(-\xi_1^2/2m_0), \quad (4)$$

$$p(\xi_2, \xi_3) = \frac{1}{2\pi\Delta_0^{\frac{1}{2}}} \exp[-(m_0'\xi_2^2 - 2m_1'\xi_2\xi_3 + m_2'\xi_3^2)/2\Delta_0], \quad (5)$$

$$\Delta_0 = m_2 m_0' - m_1'^2 \quad (6)$$

and m_0, m_0', m_1', m_2' are constants, being moments of the energy spectrum of f . The velocity of a point at a constant level $f = \xi_1$ is given by

$$c = -\frac{\partial f/\partial t}{\partial f/\partial x} = -\frac{\xi_3}{\xi_2}, \quad (7)$$

and from (5) it was concluded that the probability distribution of c is

$$p(c) = \frac{1}{\pi} \frac{\Delta_0'/m_2}{(c - \bar{c})^2 + \Delta_0'/m_2^2}, \quad (8)$$

where

$$\bar{c} = -\frac{m_1'}{m_2}. \quad (9)$$

This distribution is independent of the level ξ_1 and is a symmetrical distribution with mean \bar{c} . We shall denote it more specifically by $p^{(1)}(c)$.

However, the distribution of c depends upon the manner in which it is observed. If a point x and time t are taken at random, and if $c = -\xi_3/\xi_2$ is calculated for each x and t , then the distribution of c is indeed given by $p^{(1)}$. Moreover, if only those values

231 *Velocities of the maxima in a moving wave-form*

of c are counted for which $\xi_1 (= f)$ lies in the range $\xi'_1 < \xi_1 < \xi'_1 + d\xi_1$, then c has the same probability distribution (though the total frequency is naturally reduced), since by equation (2) ξ_2 and ξ_3 are statistically independent of ξ_1 . If, however, x and t are chosen not at random but so that $\xi_1 = \xi'_1$ exactly, that is, if only those points and instants are chosen at which the function f crosses a given level, then a different distribution for c results.

This somewhat paradoxical situation may be clarified by considering a simpler instance of the same behaviour. The probability distribution of ξ_1 itself, that is, the probability that ξ_1 will lie between the limits $\xi'_1, \xi'_1 + d\xi_1$ at any point and instant (x, t) , is given by

$$p(\xi'_1) d\xi_1 = \frac{1}{(2\pi m_0)^{\frac{1}{2}}} \exp(-\xi_1'^2/2m_0) d\xi_1. \quad (10)$$

However, the probability that ξ_1 will cross the level ξ'_1 in the range $(x, x+dx)$ and at time t is found by writing

$$d\xi_1 = df = \left| \frac{\partial f}{\partial x} \right| dx = |\xi_2| dx \quad (11)$$

in (10). Clearly this depends also on the gradient ξ_2 . Although ξ_1 will cross the level ξ'_1 on each 'occasion' when it lies in the range $(\xi'_1, \xi'_1 + d\xi_1)$, when this is sufficiently small, nevertheless it 'spends longer' in the range if the gradient ξ_2 happens to be small. To find the total probability $N(\xi'_1) dx$ for a crossing in the interval $(x, x+dx)$ it is necessary to integrate over all possible values of the gradient. Thus

$$N(\xi_1) dx = \int_{-\infty}^{\infty} p(\xi_1, \xi_2) |\xi_2| dx d\xi_2, \quad (12)$$

and since from (3)
$$p(\xi_1, \xi_2) = p(\xi_1) \frac{1}{(2\pi m_0)^{\frac{1}{2}}} \exp(-\xi_2^2/2m_0), \quad (13)$$

we obtain
$$N(\xi_1) = \frac{1}{\pi} \left(\frac{m_2}{m_0} \right)^{\frac{1}{2}} \exp(-\xi_1^2/2m_0) \quad (14)$$

(cf. (1), equation (32)).

We now apply this argument to find the distribution of c under the conditions stated. We require first the probability $p^{(2)}(\xi'_2, \xi'_3) d\xi_2 d\xi_3$ that $\xi'_2 < \xi_2 < \xi'_2 + d\xi_2, \xi'_3 < \xi_3 < \xi'_3 + d\xi_3$ when it is known that $\xi_1 = \xi'_1$ in $(x, x+dx)$, t being fixed. By the law of inverse probabilities,

$$p^{(2)}(\xi'_2, \xi'_3) = \frac{p^{(2)}(\xi_1 | \xi'_2, \xi'_3)}{N(\xi'_1)}, \quad (15)$$

where $p^{(2)}(\xi_1 | \xi'_2, \xi'_3) dx d\xi_2 d\xi_3$ denotes the probability that $\xi'_2 < \xi_2 < \xi'_2 + d\xi_2$, that $\xi'_3 < \xi_3 < \xi'_3 + d\xi_3$ and that $\xi_1 = \xi'_1$ in $(x, x+dx)$. But by the previous argument

$$p^{(2)}(\xi_1 | \xi'_2, \xi'_3) = |\xi_2| p(\xi_1, \xi_2, \xi_3), \quad (16)$$

where $p(\xi_1, \xi_2, \xi_3)$ is the ordinary joint-probability distribution of (ξ_1, ξ_2, ξ_3) . Substituting from (3) we have

$$p^{(2)}(\xi_2, \xi_3) = \frac{1}{2(2\pi)^{\frac{1}{2}} (m_2 \Delta_0)^{\frac{1}{2}}} |\xi_2| \exp[-(m_0^2 \xi_2^2 - 2m_1' \xi_2 \xi_3 + m_2 \xi_3^2)/2\Delta_0], \quad (17)$$

which may be compared with (5). To find the distribution of c , $= \xi_3/\xi_2$, we write

$$-\xi_3/\xi_2 = \eta_1, \quad \xi_2 = \eta_2, \quad (18)$$

$$\left| \frac{\partial(\xi_2, \xi_3)}{\partial(\eta_1, \eta_2)} \right| = |\eta_2| \quad (19)$$

in (17) and obtain

$$p^{(2)}(\eta_1, \eta_2) = \frac{1}{2(2\pi)^{\frac{1}{2}}} \frac{1}{(m_2 \Delta_0)^{\frac{1}{2}}} \eta_2^2 \exp[-(m_0'' + 2m_1' \eta_1 + m_2 \eta_1^2) \eta_2^2 / 2\Delta_0]. \quad (20)$$

On integrating with respect to η_2 from $-\infty$ to ∞ and writing $\eta_1 = c$ we find

$$p^{(2)}(c) = \frac{1}{2} \frac{\Delta_0/m_2^2}{[(c-\bar{c})^2 + \Delta_0/m_2^2]^{\frac{3}{2}}}, \quad (21)$$

\bar{c} being given by (9). Like $p^{(1)}(c)$ (equation (8)) this distribution is independent of ξ_1 and is symmetrical about the mean value \bar{c} . It differs from $p^{(1)}(c)$ only in having the index $\frac{3}{2}$ in the denominator, and in the normalizing constant. The width of the interquartile range is

$$2\sqrt{3}\Delta_0^{\frac{1}{2}}/m_2 \quad (22)$$

whereas that of $p^{(1)}(c)$ is

$$2\Delta_0^{\frac{1}{2}}/m_2. \quad (23)$$

The interpretation of the distribution of c is accordingly very similar to that given in (1), equations (26)–(30).

To find $p^{(2)}(c)$ we supposed that t was kept constant, and that c was to be considered at those points x for which f or ξ_1 passed through a certain value. In other words we have considered f as a function of x for fixed t . On the other hand, we may keep x constant and consider those instants t when f passes through a certain value, that is we may consider f as a function of t for fixed x . In this case the same argument leads to the following joint distribution for (ξ_2, ξ_3) :

$$p^{(3)}(\xi_2, \xi_3) = \frac{1}{2(2\pi)^{\frac{1}{2}}} \frac{1}{(m_0'' \Delta_0)^{\frac{1}{2}}} |\xi_3| \exp[-(m_0'' \xi_2^2 - 2m_1' \xi_2 \xi_3 + m_2 \xi_3^2) / 2\Delta_0], \quad (24)$$

and a similar substitution gives for the distribution of c :

$$p^{(3)}(c) = \frac{1}{2} \frac{\Delta_0/m_2^2}{[(c-\bar{c})^2 + \Delta_0/m_2^2]^{\frac{1}{2}}} \left(\frac{m_2}{m_0}\right)^{\frac{1}{2}} |c|. \quad (25)$$

This distribution is similar to $p^{(1)}(c)$ and $p^{(2)}(c)$ in being independent of ξ_1 and having a width of order $\Delta_0^{\frac{1}{2}}/m_2$. But it is no longer a symmetrical distribution, on account of the factor $|c|$.

From the examples given it is clear that the probability distribution $p(c)$ depends upon the manner of selection of the points to be observed. If we imagine the surface $z = f(x, t)$ drawn, the first case corresponds to taking the intersection of the surface by an arbitrary ordinate parallel to the z -axis, and the second and third cases correspond to taking the intersection of the surface by lines parallel to the x -axis and the t -axis respectively. Clearly we may choose lines of intersection in any arbitrary direction, or indeed, curves of intersection having any shape or orientation.

Velocities of the maxima in a moving wave-form

The second case considered may well be the most common in practical applications. Thus when studying water waves in a model tank photographs may be taken of the same wave profile at successive instants of time. The appropriate distribution is then $p^{(2)}(c)$.

In the paper (1) already quoted, the distribution of the velocities c of specular points was derived by direct analogy with the velocities of zeros. Here also the distribution depends on the manner of selecting the points (x, t) . If, as may be the case in practice, the specular points are studied by photographing points of reflected light from a fixed direction at successive instants, then the appropriate distribution will be that analogous to $p^{(2)}(c)$, that is to say,

$$p^{(2)}(c_1) = \frac{1}{2} \frac{\Delta_1/m_4^2}{[(c_1 - \bar{c}_1)^2 + \Delta_1/m_4^2]^{\frac{3}{2}}}, \quad (26)$$

where

$$\bar{c}_1 = -\frac{m_3'}{m_4} \quad (27)$$

and

$$\Delta_1 = m_4 m_2'' - m_3'^2, \quad (28)$$

rather than the distribution given by equation (34) of (1). Similarly for the velocities c_2 of the points of inflexion we have

$$p_2^{(2)}(c_2) = \frac{1}{2} \frac{\Delta_2/m_6^2}{[(c_2 - \bar{c}_2)^2 + \Delta_2/m_6^2]^{\frac{3}{2}}}, \quad (29)$$

where

$$\bar{c}_2 = -\frac{m_5'}{m_6} \quad (30)$$

and

$$\Delta_2 = m_6 m_4'' - m_5'^2. \quad (31)$$

It will be noticed that the frequency of 'twinkling', which is also treated in (1), is not subject to the same arbitrariness.

REFERENCE

- (1) LONGUET-HIGGINS, M. S. Statistical properties of a moving wave-form. *Proc. Camb. Phil. Soc.* 52 (1956), 234-45.

Reproduced with permission from *Phil. Trans. R. Soc. Lond. A* 249 (1957) 321–337.

[321]

THE STATISTICAL ANALYSIS OF A RANDOM, MOVING SURFACE

By M. S. LONGUET-HIGGINS

National Institute of Oceanography, Wormley

(Communicated by G. E. R. Deacon, F.R.S.—Received 29 March 1956—

Revised 31 July 1956)

The following statistical properties are derived for a random, moving, Gaussian surface: (1) the probability distribution of the surface elevation and of the magnitude and orientation of the gradient; (2) the average number of zero-crossings per unit distance along a line in an arbitrary direction; (3) the average length of the contours per unit area, and the distribution of their direction; (4) the average density of maxima and minima per unit area of the surface, and the average density of specular points (i.e. points where the two components of gradient take given values); (5) the probability distribution of the velocities of zero-crossings along a given line; (6) the probability distribution of the velocities of contours and of specular points; (7) the probability distribution of the envelope and phase angle, and hence (8) when the spectrum is narrow, the probability distribution of the heights of maxima and minima and the distribution of the intervals between successive zero-crossings along an arbitrary line. All the results are expressed in terms of the two-dimensional energy spectrum of the surface, and are found to involve the moments of the spectrum up to a finite order only. (1), (3), (4), (5) and (6) are discussed in detail for the special case of a narrow spectrum.

The converse problem is also studied and solved: given certain statistical properties of the surface, to find a convergent sequence of approximations to the energy spectrum.

The problems arise in connexion with the statistical analysis of the sea surface.

(More detailed summaries are given at the beginning of each part of the paper.)

CONTENTS

	PAGE		PAGE
INTRODUCTION	321	2-3. The length and direction of the contours	345
PART I. DESCRIPTION OF THE SURFACE	324	2-4. The density of maxima and minima	348
1-1. The representation of simple wave patterns	325	2-5. The velocities of zeros along a line	356
1-2. The representation of a surface having a continuous spectrum	327	2-6. The motion of the contours	359
1-3. Conditions for degeneracy	328	2-7. The velocities of specular points	362
1-4. The spectrum of the surface in an arbitrary direction	331	2-8. Properties of the envelope: the number of waves in a group	370
1-5. The wave envelope	333	2-9. The heights of maxima	374
1-6. A narrow spectrum	335	2-10. The intervals between successive zeros	376
PART II. STATISTICAL PROPERTIES	336	PART III. A METHOD OF DETERMINING THE ENERGY SPECTRUM	379
2-1. The distribution of surface elevation and gradient	338	3-1. To obtain $m_s(\theta)$	379
2-2. The number of zero-crossings along a line	342	3-2. To obtain m_{pq}	380
		3-3. To obtain E	382
		REFERENCES	386

INTRODUCTION

On observing waves in the open ocean, one is struck by their irregularity: no single wave retains its identity for long, the distance between neighbouring crests varies with time and place, and frequently it is difficult to assign to the waves any predominant direction or

orientation. Thus although the sea surface may, for some purposes, be treated as a uniform train of waves advancing in one direction only, such a representation is usually far from reality.

The first attempt to treat the sea surface as the sum of more than a finite number of simple sine-waves is due to Barber and his collaborators (1946), who used a harmonic analyzer to resolve a length of record, say of wave height or pressure at a fixed point, into its Fourier components. The physical basis for this procedure is that, if the waves are not too steep, the energy in any particular frequency band may be expected to be propagated independently of the rest of the spectrum, and with a velocity characteristic of its frequency. It was shown by Barber & Ursell (1948) that for ocean swell this is in fact nearly true.

Just as sea waves have no single frequency or wavelength, so they have no single direction. One must therefore consider the Fourier spectrum of the sea surface with regard to both frequency and direction or, what is equivalent, the spectrum with regard to wave-number in two horizontal directions. A two-dimensional Fourier analysis for sea waves was proposed by Longuet-Higgins & Barber (1946), who also suggested apparatus for finding a certain amount of information about the spectrum. Independently, Pierson (1952) has emphasized the importance of the distribution of energy with regard to direction when studying the generation and propagation of waves and swell. Thus waves from a limited storm area will decay more or less rapidly with distance according as the spread in direction of the energy is wide or narrow. Similarly, the angular distribution of the energy in a swell will be more or less concentrated according as the region in which it was generated subtends a wide or narrow angle at the point of observation.*

A very interesting problem now arises: the relation between the energy spectrum of the surface and its observable statistical properties. To take a simple example, suppose that we measure the surface elevation ζ at a fixed point: what is the r.m.s. value of ζ with regard to time; what is the average time interval between the maxima of ζ ; what proportion of the maxima have heights between two given values?

Questions of this kind have been studied theoretically by several authors, notably by Rice (1944, 1945) in connexion with the analysis of electrical noise currents. Rice considered the function

$$\zeta(t) = \sum_n c_n \cos(\sigma_n t + \epsilon_n), \quad (1)$$

which is the sum of a large number of sine-waves of different frequency $\sigma_n/2\pi$. The phases ϵ_n are random variables distributed uniformly in the interval $(0, 2\pi)$, and the amplitudes c_n are such that in any small interval of σ of width $d\sigma$,

$$\sum_n \frac{1}{2} c_n^2 = E(\sigma) d\sigma, \quad (2)$$

say (our notation is slightly different from Rice's). The function $E(\sigma)$ may be called the energy spectrum of ζ . It is the cosine transform of G. I. Taylor's correlation function

$$\psi(t) = \lim_{T \rightarrow \infty} \frac{1}{2T} \int_{-T}^T \zeta(t') \zeta(t'+t) dt' \quad (3)$$

* Some other applications of the two-dimensional spectrum may be mentioned. It has been used to calculate the seismic energy generated by sea waves, where the directional distribution of energy is essentially involved (Longuet-Higgins 1950). Eckart has used a two-dimensional analysis to calculate the scattering of sound from the sea surface (1953*a*) and the waves caused by a random distribution of pressure pulses (1953*b*). St Denis & Pierson (1953) have applied it to ship motion; see also Cartwright (1956).

(see Khintchine 1934). One can show that the method of harmonic analysis used by Barber & Ursell (1948) is essentially equivalent to making an estimate of \sqrt{E} , within limits of accuracy imposed by the finite length of the record (see Tukey 1949).

Using the above representation, Rice was able to derive many statistical properties of ζ , in particular the probability distribution of ζ itself (which is Gaussian), the average number of zero-crossings of ζ per unit time, the probability distribution of the maxima, and certain statistical properties of the envelope.

It was found by Rudnick (1950) that records of sea-wave pressure are in fact Gaussian (see also Pierson 1952). Barber (1950) considered the distribution of wave heights, that is, the difference in level between a crest and the preceding trough, and compared some observations with the 'random-walk' (or Rayleigh) distribution,* which is the theoretical distribution for a narrow-band spectrum. This distribution has been discussed in more detail by the present author (1952), who showed that the theoretical ratios of the mean wave height, the mean of the highest one-third of the waves, and the height of the highest of N waves were in close agreement with observation. Further observations are given by Watters (1953).

Some two-dimensional statistical properties of the sea surface have also been measured. By photographing the pattern and intensity of sunlight reflected from the sea surface, Cox & Munk (1954*a, b*) have deduced the statistical distribution of the two components of surface slope, in winds of different intensity. They find that the distribution differs only slightly from a normal distribution.† One may expect that for swell, which is usually less steep than waves under the action of the wind, the departures from the normal distribution will be still less.

For more than fifty years attempts have been made to construct contour maps of the sea surface. Some results, together with references to earlier work, are given by Schumacher (1952). At the present time some very extensive maps are being made as proposed by Marks (1954). These maps may well be suitable for statistical analysis.

On the theoretical side, Eckart (1946) has considered the intensity of light reflected from a random surface whose gradient and second derivatives are all distributed normally; and he has also calculated the first and second moments of the total curvature. However, no extensive theoretical study of the two-dimensional statistical properties of a random surface appears to have been made.

The purpose of the present paper is to study theoretically the statistical properties of a random, moving Gaussian surface, in relation to its two-dimensional spectrum.

In view of the observations mentioned above, there is reason to believe that some at least of the results are relevant to waves in the open ocean. The analysis may also apply to other geophysical phenomena, for example, to microseisms or perturbations of the ionosphere. In addition, however, the subject is of interest as a branch of geometry, and we shall develop it here on its own account, leaving the application of the results and comparison with observations to a separate study.

* So called because it was derived by Rayleigh in connexion with the theory of sound. See Rayleigh (1880; 1945, pp. 39-42).

† Schooley (1954) has made similar measurements for the river Anacostia. A different technique was used earlier by Duntley (1950) on Lake Winnipeg.

The paper is in three parts. Part I is mainly introductory; we define some convenient parameters for describing the surface: the *long-crestedness*, the *skewness*, the *carrier wave* and the *envelope*, and we find conditions for the surface to split up in various ways into one or more simpler systems of waves.

The chief results are contained in part II. Expressions are derived for the statistical distributions of the surface elevation and the magnitude and direction of the surface slope (§ 2.1); for the average number of zero-crossings of ζ along a line in an arbitrary direction (§ 2.2); for the average length of a given contour and for the distribution of its direction (§ 2.3); for the density of maxima and minima (humps and hollows) per unit area of the surface, and the density of specular points (points where the two components of surface gradient take given values) (§ 2.4); for the statistical distribution of the velocities of the zero-crossings of ζ along a given line (§ 2.5); for the statistical distributions of the velocities of the contours (§ 2.6) and of specular points (§ 2.7). In order to interpret the more complex results, the case when the energy spectrum is narrow, i.e. when the waves are more or less uniform in wavelength and direction, is studied in detail. In § 2.8 some properties of the wave envelope are considered, and from these are deduced the average number of waves in a group, the statistical distribution of the heights of maxima and the distribution of the spacing between successive zeros, all for a narrow spectrum.

In part III the converse problem is considered: given the statistical properties of the surface, to find its energy spectrum. To do this, use is made of a striking feature of the present distributions, that they depend only on the moments of the energy spectrum up to a finite order. Thus the average number of zero-crossings along a line involves only the moments of order 0 and 2. The average number of maxima and minima along a line involves only the moments of order 2 and 4. Properties depending on the motion of the surface involve the odd as well as the even moments. Hence, by considering the statistical properties of the surface along a line in a number of different directions, the moments of the two-dimensional spectrum up to, theoretically, any order can be deduced. From this it is possible to obtain a convergent sequence of approximations to the spectrum (§ 3.3).

Detailed summaries of the results will be found at the beginning of each part.

PART I. DESCRIPTION OF THE SURFACE

Section 1.1 introduces the representation of a simple wave pattern by a point in the wave-number diagram, and defines the concepts of *carrier wave* and *envelope*, which are afterwards to be extended to a surface with a continuous spectrum. The fundamental definition of a random surface in terms of its spectrum is given in § 1.2.

In § 1.3 conditions are found for the surface to degenerate in various ways. Thus, a simple condition for the surface to be 'long-crested' (i.e. for the energy to travel always in the same direction) is given by (1.3.3). A condition for the surface to consist of no more than two long-crested systems is given by (1.3.7), and a condition for no more than n such systems is given by (1.3.8). All these conditions are expressed in terms of the moments m_{pq} of the energy spectrum E , which are defined by (1.2.7). A condition for E to degenerate into a 'ring' spectrum, i.e. for the energy to have uniform wavelength though not necessarily constant direction, is given by (1.3.11). For standing waves, both (1.3.3) and (1.3.11) must be satisfied simultaneously. Necessary and sufficient conditions for the spectrum to be *narrow* so that the energy is uniform in both wavelength and direction, are given by (1.3.14). Necessary conditions for the existence of not more than two narrow bands of energy are given by (1.3.17) and (1.3.18).

STATISTICAL ANALYSIS OF A RANDOM, MOVING SURFACE 325

In §1.4 the curve of intersection of the surface by a perpendicular plane in an arbitrary direction O is considered. It is shown how the spectrum E_θ of this curve is related to the spectrum E of the surface. The *principal direction* is defined as the direction in which the second-order moment of E_θ , and so the r.m.s. wave-number, is a maximum. The minimum r.m.s. wave-number is in the perpendicular direction, and the ratios of the r.m.s. wave-numbers in these two directions is a convenient measure of the *long-crestedness* of the surface.

In §1.5 the *carrier wave* and the *wave envelope* are defined for a surface having a continuous spectrum. It is seen that in general the principal direction of the envelope is different from that of the wave surface, so that the waves form a 'staggered' or echelon pattern. The angle between the two principal directions is called the angle of *skewness*. It is proved that the envelope of the curve in which a vertical plane intersects the surface is the same as the curve in which the plane intersects the envelope.

In §1.6 some special properties of a narrow spectrum are deduced; in particular, that the long-crestedness equals the reciprocal of the r.m.s. angular deviation of energy from the principal direction.

1.1. *The representation of simple wave patterns*

Imagine a single long-crested wave of length λ travelling in a direction which makes an angle θ with the x axis (see figure 1a). The wave-number w along a line perpendicular to the crest is defined as

$$w = 2\pi/\lambda. \tag{1.1.1}$$

The wavelength and direction can be specified very conveniently by drawing a vector \overline{OP} from a fixed point O in a direction θ , such that the length of \overline{OP} equals w . Then if we consider a section of the surface along any line making an angle θ' with the x axis, it is clear that the wavelength along this section is increased in the ratio $\sec(\theta - \theta')$, so that the wave-number is multiplied by $\cos(\theta - \theta')$. In other words the corresponding wave-number is simply the projection of \overline{OP} on a line in that direction. In particular, the wave-numbers parallel to the two fixed directions (x, y) are the co-ordinates of the point P with respect of axes in these directions. The equation of the wave surface is then

$$\zeta = c \cos(ux + vy + \sigma t), \tag{1.1.2}$$

where

$$u, v = w \cos \theta, w \sin \theta, \tag{1.1.3}$$

and σ is a function of u and v . It will be assumed that σ depends only upon the wavelength, that is on $\sqrt{(u^2 + v^2)} = w$;

$$\sigma = \sigma(u, v) = \sigma(w). \tag{1.1.4}$$

We may take σ to be positive, so that the direction of propagation is opposite to \overline{OP} . It follows from (1.1.4) that

$$\sigma(-u, -v) = \sigma(u, v), \tag{1.1.5}$$

that is, waves of the same length but opposite in direction have equal and opposite velocities.

Consider now a pair of long-crested waves of equal amplitude c (figure 1b). If these are represented in the wave-number diagram by the vectors \overline{OP}_1 and \overline{OP}_2 , where $P_1 = (u_1, v_1)$ and $P_2 = (u_2, v_2)$, we have for the surface elevation

$$\zeta = c \cos(u_1 x + v_1 y + \sigma_1 t) + c \cos(u_2 x + v_2 y + \sigma_2 t). \tag{1.1.6}$$

This may be written

$$\zeta = 2c \cos(u'x + v'y + \sigma't) \cos(\bar{u}x + \bar{v}y + \bar{\sigma}t), \tag{1.1.7}$$

where

$$\begin{aligned} u' &= \frac{1}{2}(u_1 - u_2), & v' &= \frac{1}{2}(v_1 - v_2), & \sigma' &= \frac{1}{2}(\sigma_1 - \sigma_2), \\ \bar{u} &= \frac{1}{2}(u_1 + u_2), & \bar{v} &= \frac{1}{2}(v_1 + v_2), & \bar{\sigma} &= \frac{1}{2}(\sigma_1 + \sigma_2). \end{aligned} \tag{1.1.8}$$

If the wave-numbers (u_1, v_1) and (u_2, v_2) of the two original waves are nearly equal, the term

$$2c \cos(u'x + v'y + \sigma't) \quad (1.1.9)$$

in (1.1.7) represents a slowly varying amplitude which we may call the 'envelope' and

$$\cos(\bar{u}x + \bar{v}y + \bar{\sigma}t) \quad (1.1.10)$$

represents a 'carrier' wave of approximately the same wavelength and direction as the original waves. The carrier wave is represented in the wave-number diagram by the vector \vec{OM} , where M is the mid-point of P_1P_2 . The envelope is represented by \vec{MP}_1 or \vec{MP}_2 .

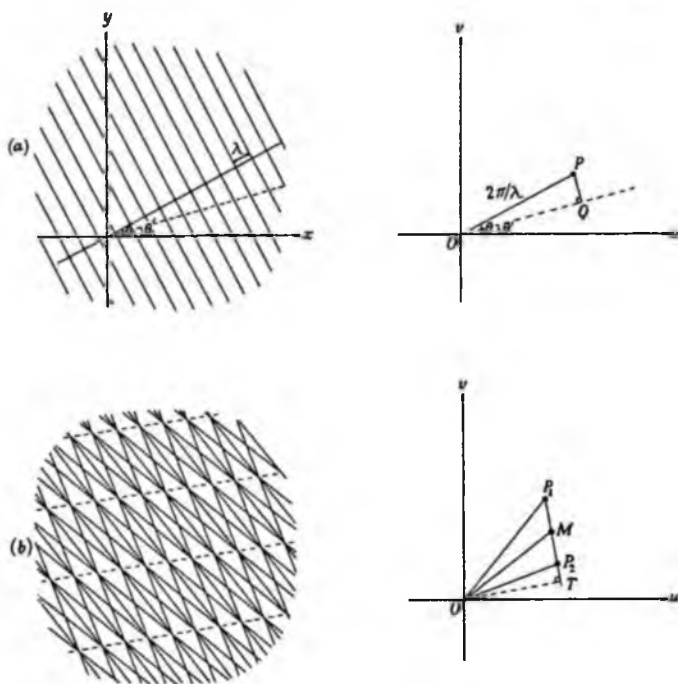


FIGURE 1. Representation in the wave-number plane of (a) a single long-crested wave and (b) the sum of two long-crested waves of different wavelength and direction.

For example, suppose that the two waves are in the same direction but of different wavelength. Then the vectors \vec{OP}_1 and \vec{OP}_2 are in the same direction and so also are \vec{OM} and \vec{MP}_2 . Thus the envelope has the same direction as the carrier wave; the crests are infinitely long.

Again, suppose that the two waves are of equal length but in different directions. Then the vectors \vec{OP}_1 and \vec{OP}_2 are of equal length but different direction. The carrier wave, represented by \vec{OM} , lies in the mean direction, but the direction of the envelope is now at right angles to the carrier wave. The result is a short-crested system of waves.

In the general case (figure 1 b) it will be seen that the wave crests are staggered, or form an echelon pattern one behind the other. The direction of this pattern is perpendicular to

STATISTICAL ANALYSIS OF A RANDOM, MOVING SURFACE 327

P_1P_2 . The wave-number perpendicular to P_1P_2 is given by the length OT of the perpendicular from O to P_1P_2 ; it is the direction in which the wave-numbers of the two component waves are equal.

The angle β between OM and P_1P_2 is a measure of the skewness of the waves.

The envelope (1.1.9) and the carrier (1.1.10) are not necessarily 'free' travelling waves, that is, they do not satisfy equations of the form of (1.1.4). Their representation in the wave-number diagram is valid only so far as the spatial periodicity is concerned. However, for a narrow spectrum \bar{u} , \bar{v} , $\bar{\sigma}$ are nearly equal to u_1 , v_1 , σ_1 respectively, and so the carrier wave does move with nearly the free-wave velocity, if the component waves are themselves free waves. But the envelope moves with a velocity whose components are

$$-\left(\frac{\sigma'}{u'}, \frac{\sigma'}{v'}\right) = -\left(\frac{\sigma_1 - \sigma_2}{u_1 - u_2}, \frac{\sigma_1 - \sigma_2}{v_1 - v_2}\right). \quad (1.1.11)$$

To a first approximation this is

$$-\left(\frac{\partial \sigma}{\partial u}, \frac{\partial \sigma}{\partial v}\right) = -\left(\frac{\partial w}{\partial u}, \frac{\partial w}{\partial v}\right) \frac{d\sigma}{dw} = -(\cos \theta, \sin \theta) \frac{d\sigma}{dw}, \quad (1.1.12)$$

which is the so-called group velocity. Thus in this special case the envelope moves with the group velocity of the carrier wave.

1.2. *The representation of a surface having a continuous spectrum*

We now assume that the surface possesses a continuous noise spectrum in two dimensions. Generalizing the representation used in equation (1) we write

$$\zeta(x, y, t) = \sum_n c_n \cos(u_n x + v_n y + \sigma_n t + \epsilon_n), \quad (1.2.1)$$

where it is supposed that the wave-numbers (u_n, v_n) are densely distributed throughout the u, v plane, i.e. there are an infinite number in any elementary area $du dv$. σ_n is a function of (u_n, v_n) :

$$\sigma_n = \sigma(u_n, v_n); \quad (1.2.2)$$

the amplitudes c_n are random variables such that in any element $du dv$ we may assume

$$\sum_n \frac{1}{2} c_n^2 = E(u, v) du dv; \quad (1.2.3)$$

the phases ϵ_n are distributed randomly and with equal probability in the interval $(0, 2\pi)$. The function $E(u, v)$ will be called the energy spectrum of ζ ; the mean-square value of ζ per unit area of the sea surface per unit time* is given by

$$\lim_{X, Y, T \rightarrow \infty} \frac{1}{8XYT} \int_{-X}^X \int_{-Y}^Y \int_{-T}^T \zeta^2 dx dy dt = \sum_n \frac{1}{2} c_n^2 = \int_{-\infty}^{\infty} \int_{-\infty}^{\infty} E(u, v) du dv. \quad (1.2.4)$$

Thus the contribution to the mean energy from an element $du dv$ is proportional to $E du dv$. We shall write

$$\int_{-\infty}^{\infty} \int_{-\infty}^{\infty} E(u, v) du dv = m_{00}, \quad (1.2.5)$$

* It is assumed that average values taken with respect to x, y or t are equivalent to average values with respect to the phases ϵ_n .

and in general for the (p, q) th moment of $E(u, v)$ about the origin we write

$$\int_{-\infty}^{\infty} \int_{-\infty}^{\infty} E(u, v) u^p v^q du dv = m_{pq}. \quad (1.2.6)$$

These quantities will occur repeatedly throughout the following analysis. It is assumed that they exist up to all orders required.

The function $E(u, v)$ is closely related to the correlation function $\psi(x, y, t)$ defined by

$$\psi(x, y, t) = \lim_{X, Y, T \rightarrow \infty} \frac{1}{8XYT} \int_{-X}^X \int_{-Y}^Y \int_{-T}^T \zeta(x', y', t') \zeta(x' + x, y' + y, t' + t) dx' dy' dt'. \quad (1.2.7)$$

On substituting from (1.2.1) in the above we find

$$\psi(x, y, t) = \sum_n \frac{1}{2} c_n^2 \cos(u_n x + v_n y + \sigma_n t), \quad (1.2.8)$$

which can be written

$$\psi(x, y, t) = \int_{-\infty}^{\infty} \int_{-\infty}^{\infty} E(u, v) \cos(ux + vy + \sigma t) du dv, \quad (1.2.9)$$

so that ψ is the cosine transform of E . The even moments m_{pq} are related very simply to the derivatives of ψ at the origin:

$$m_{pq} = (-1)^r \frac{\partial^{2r} \psi(0, 0, 0)}{\partial x^p \partial y^q} \quad (p + q = 2r). \quad (1.2.10)$$

1.3. Conditions for degeneracy

Some important features of the surface can be described immediately in terms of the moments. For example, to find a condition that the wave energy shall all travel in one direction, so that the spectrum is effectively one-dimensional, consider the integral

$$\int_{-\infty}^{\infty} \int_{-\infty}^{\infty} \int_{-\infty}^{\infty} \int_{-\infty}^{\infty} E(u_1, v_1) E(u_2, v_2) (u_1 v_2 - u_2 v_1)^2 du_1 dv_1 du_2 dv_2. \quad (1.3.1)$$

If the spectrum is one-dimensional, the product $E(u_1, v_1) E(u_2, v_2)$ is zero everywhere except when $u_1/v_1 = u_2/v_2$, when the squared factor vanishes. Therefore the integral vanishes. Conversely, if the spectrum is not one-dimensional there will be a contribution to the integral from some pairs of elements $du_1 dv_1, du_2 dv_2$ for which $u_1/v_1 \neq u_2/v_2$, and since the integrand is never negative the integral does not vanish. But on expanding the squared factor and separating the integrations with respect to u_1, v_1 and u_2, v_2 we find that (1.3.1) is equal to

$$2(m_{20} m_{02} - m_{11}^2) = 2 \begin{vmatrix} m_{20} & m_{11} \\ m_{11} & m_{02} \end{vmatrix} = 2\Delta_2, \quad (1.3.2)$$

say. Thus a necessary and sufficient condition for E to degenerate into a single one-dimensional spectrum is that

$$\Delta_2 = 0. \quad (1.3.3)$$

By similar reasoning, a condition for E to degenerate into two one-dimensional spectra (see figure 2a) is that

$$\int_{-\infty}^{\infty} \dots \int_{-\infty}^{\infty} E(u_1, v_1) E(u_2, v_2) E(u_3, v_3) \times (u_2 v_3 - u_3 v_2)^2 (u_3 v_1 - u_1 v_3)^2 (u_1 v_2 - u_2 v_1)^2 du_1 dv_1 du_2 dv_2 du_3 dv_3 \quad (1.3.4)$$

STATISTICAL ANALYSIS OF A RANDOM, MOVING SURFACE 329

shall vanish. The squared product may be written

$$\begin{vmatrix} u_1^2 & u_2^2 & u_3^2 \\ u_1 v_1 & u_2 v_2 & u_3 v_3 \\ v_1^2 & v_2^2 & v_3^2 \end{vmatrix}^2 = \epsilon_{ijk} u_i^2 u_j v_k^2 \begin{vmatrix} u_1^2 & u_2^2 & u_3^2 \\ u_1 v_1 & u_2 v_2 & u_3 v_3 \\ v_1^2 & v_2^2 & v_3^2 \end{vmatrix} \quad (1.3.5)$$

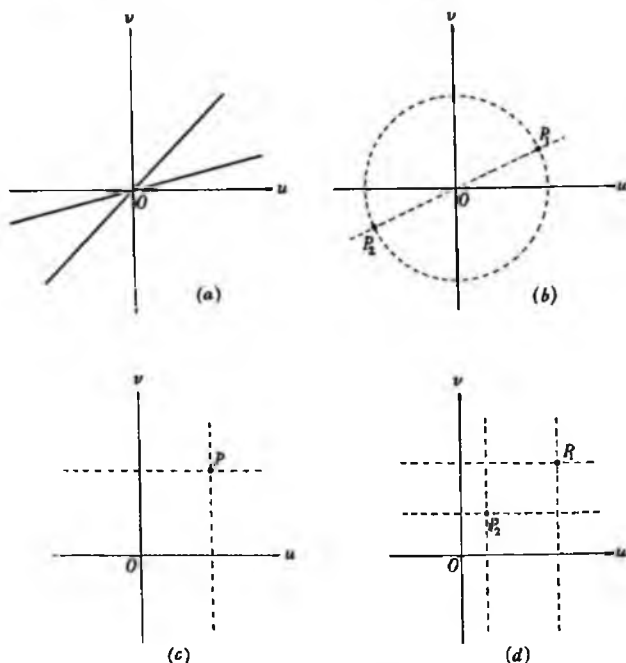


FIGURE 2. The form of the energy spectrum for (a) two intersecting long-crested systems of waves, (b) a system of standing waves, (c) a narrow band of waves, uniform in wavelength and direction and (d) two narrow bands of waves.

(where $\epsilon_{ijk} = \pm 1$ according as (i, j, k) is an even or odd permutation of $(1, 2, 3)$, and so the integral equals

$$6 \begin{vmatrix} m_{40} & m_{31} & m_{22} \\ m_{31} & m_{22} & m_{13} \\ m_{22} & m_{13} & m_{04} \end{vmatrix} = 6\Delta_4, \quad (1.3.6)$$

say. Thus E degenerates into not more than two one-dimensional spectra if and only if

$$\Delta_4 = 0. \quad (1.3.7)$$

There is an obvious generalization to any number of one-dimensional spectra: the condition that E degenerate into not more than n one-dimensional spectra is that

$$\Delta_{2n} = \begin{vmatrix} m_{2n,0} & m_{2n-1,1} & \cdots & m_{n,n} \\ m_{2n-1,1} & m_{2n-2,2} & \cdots & m_{n-1,n+1} \\ \vdots & \vdots & \ddots & \vdots \\ m_{nn} & m_{n-1,n+1} & \cdots & m_{0,2n} \end{vmatrix} = 0. \quad (1.3.8)$$

(In practice Δ_2, Δ_4 , etc., must be compared with quantities of the same dimensions. Thus Δ_{2n} may be compared with $(m_{20} + m_{02})^n$.)

A condition for E to degenerate into a 'ring' spectrum, such that all the energy corresponds to wave components of the same length but possibly different directions, is that

$$\int_{-\infty}^{\infty} \int_{-\infty}^{\infty} \int_{-\infty}^{\infty} \int_{-\infty}^{\infty} E(u_1, v_1) E(u_2, v_2) [(u_1^2 + v_1^2) - (u_2^2 + v_2^2)]^2 du_1 dv_1 du_2 dv_2 \quad (1.3.9)$$

shall vanish. This integral equals

$$2[(m_{40} + 2m_{22} + m_{04}) m_{00} - (m_{20} + m_{02})^2], \quad (1.3.10)$$

and so we must have

$$(m_{40} + 2m_{22} + m_{04}) m_{00} - (m_{20} + m_{02})^2 = 0. \quad (1.3.11)$$

The condition for the energy to be situated at two diametrically opposite points of the spectrum (giving a standing-wave pattern) is that (1.3.3) and (1.3.11) shall be satisfied simultaneously (see figure 2*b*).

A condition for the energy to be concentrated about a single point in the spectrum is that

$$\int_{-\infty}^{\infty} \int_{-\infty}^{\infty} \int_{-\infty}^{\infty} \int_{-\infty}^{\infty} E(u_1, v_1) E(u_2, v_2) [(u_1 - u_2)^2 + (v_1 - v_2)^2] du_1 dv_1 du_2 dv_2 \quad (1.3.12)$$

shall vanish. This is equivalent to the pair of conditions that

$$\int_{-\infty}^{\infty} \int_{-\infty}^{\infty} \int_{-\infty}^{\infty} \int_{-\infty}^{\infty} E(u_1, v_1) E(u_2, v_2) (u_1 - u_2)^2 du_1 dv_1 du_2 dv_2 \quad (1.3.13)$$

shall vanish, and a similar integral with factor $(v_1 - v_2)^2$. These are the conditions that the energy be concentrated on lines parallel to the v axis and the u axis respectively (see figure 2*c*)

On expanding the integrals we have

$$\begin{vmatrix} m_{20} & m_{10} \\ m_{10} & m_{00} \end{vmatrix} = 0, \quad \begin{vmatrix} m_{02} & m_{01} \\ m_{01} & m_{00} \end{vmatrix} = 0. \quad (1.3.14)$$

A condition for the energy to be concentrated about not more than two points in the spectrum (not necessarily opposite) is that

$$\int_{-\infty}^{\infty} \dots \int_{-\infty}^{\infty} E(u_1, v_1) E(u_2, v_2) E(u_3, v_3) \prod_{i \neq j} [(u_i - u_j)^2 + (v_i - v_j)^2] du_1 dv_1 du_2 dv_2 du_3 dv_3 \quad (1.3.15)$$

shall vanish. The term under the product sign may be written

$$(u_2 - u_3)^2 (u_3 - u_1)^2 (u_1 - u_2)^2 + (v_2 - v_3)^2 (v_3 - v_1)^2 (v_1 - v_2)^2 + \Sigma (u_2 - u_3)^2 (u_3 - u_1)^2 (v_1 - v_2)^2 + \Sigma (u_2 - u_3)^2 (v_3 - v_1)^2 (v_1 - v_2)^2. \quad (1.3.16)$$

Since all the terms are non-negative, each separately must vanish. The first two give the conditions

$$\begin{vmatrix} m_{40} & m_{30} & m_{20} \\ m_{30} & m_{20} & m_{10} \\ m_{20} & m_{10} & m_{00} \end{vmatrix} = 0, \quad \begin{vmatrix} m_{04} & m_{03} & m_{02} \\ m_{03} & m_{02} & m_{01} \\ m_{02} & m_{01} & m_{00} \end{vmatrix} = 0, \quad (1.3.17)$$

which are the conditions that the energy shall be at the intersections of two pairs of lines parallel to the v and u axes, i.e. at the corners of a rectangle (figure 2*d*). The remaining

conditions can also be expressed in terms of the moments. Thus the group of terms under the first summation sign in (1.3.16) leads to the condition

$$4 \begin{vmatrix} m_{30} & m_{20} & m_{11} \\ m_{21} & m_{11} & m_{02} \\ m_{20} & m_{10} & m_{01} \end{vmatrix} + 2 \begin{vmatrix} m_{30} & m_{20} & m_{22} \\ m_{20} & m_{10} & m_{12} \\ m_{10} & m_{00} & m_{02} \end{vmatrix} + \begin{vmatrix} m_{40} & m_{20} & m_{21} \\ m_{20} & m_{00} & m_{01} \\ m_{21} & m_{01} & m_{02} \end{vmatrix} = 0. \quad (1.3.18)$$

The last group of terms in (1.3.16) leads to a similar condition, the pair of suffixes in each of the moments m_{pq} being interchanged.

We have incidentally shown that each of the combinations of moments on the left-hand sides of equations (1.3.2), (1.3.6), (1.3.11), (1.3.14), (1.3.17) and (1.3.18) is never negative.

1.4. *The spectrum of the surface in an arbitrary direction*

Let us consider the curve in which the surface ζ is intersected by a perpendicular plane in direction θ , that is, the plane $x \sin \theta - y \cos \theta = 0$. The curve will represent a one-dimensional random function, whose spectrum E_θ with regard to the wave-number u' in this direction bears a simple relation to the original spectrum $E(u, v)$. We may call $E_\theta(u')$ the spectrum of the surface in the direction θ .

First, let x', y' denote co-ordinates in the x, y plane in directions parallel and perpendicular to the direction θ :

$$x' = x \cos \theta + y \sin \theta, \quad y' = -x \sin \theta + y \cos \theta. \quad (1.4.1)$$

Reciprocally, x, y are given in terms of x', y' by similar relations, but with the sign of θ reversed. On substituting in (1.2.1) we have

$$\zeta = \sum_n c_n \cos (u'_n x' + v'_n y' + \sigma'_n t + \epsilon_n), \quad (1.4.2)$$

where
$$u'_n = u_n \cos \theta + v_n \sin \theta, \quad v'_n = -u_n \sin \theta + v_n \cos \theta, \quad (1.4.3)$$

that is, the new wave-number u'_n is the co-ordinate, in the direction θ , of the point (u_n, v_n) , and v'_n is the co-ordinate at right angles. We have also

$$\sigma'_n = \sigma \{ \sqrt{(u_n^2 + v_n^2)} \} = \sigma \{ \sqrt{(u_n'^2 + v_n'^2)} \}. \quad (1.4.4)$$

On the curve of intersection we have $y' = 0$ and so

$$\zeta = \sum_n c_n \cos (u'_n x' + \sigma'_n t + \epsilon_n). \quad (1.4.5)$$

The spectrum $E_\theta(u')$ of this curve is defined as the function such that the energy corresponding to any small interval $(u', u' + du')$ is $E_\theta(u') du'$. Thus if $\sum_{du', v'}$ denotes summation over the strip $(u', u' + du')$,

$$E_\theta(u') du = \sum_{du', v'} \frac{1}{2} c_n^2 = du' \int_{-\infty}^{\infty} E(u, v) dv', \quad (1.4.6)$$

and therefore

$$E_\theta(u') = \int_{-\infty}^{\infty} E(u, v) dv'. \quad (1.4.7)$$

In other words, if we take a section of the surface in any direction θ , the spectrum $E_\theta(u')$ of this section is found by integrating $E(u, v)$ along the line through $P = (u' \cos \theta, u' \sin \theta)$ at right angles to OP .

From equation (1.4.7) there follow some simple and fundamental relations between the moments of the spectrum $E_\theta(u')$ and the moments of the original distribution $E(u, v)$. Let the n th moment of E_θ about the origin be denoted by $m_n(\theta)$. Then we have

$$m_n(\theta) = \int_{-\infty}^{\infty} E_\theta(u') u'^n du' = \int_{-\infty}^{\infty} \int_{-\infty}^{\infty} E(u, v) u'^n du' dv'. \quad (1.4.8)$$

Since
$$u' = u \cos \theta + v \sin \theta, \quad v' = -u \sin \theta + v \cos \theta \quad (1.4.9)$$

and
$$\frac{\partial(u', v')}{\partial(u, v)} = 1, \quad (1.4.10)$$

we have
$$m_n(\theta) = \int_{-\infty}^{\infty} \int_{-\infty}^{\infty} E(u, v) (u \cos \theta + v \sin \theta)^n du dv. \quad (1.4.11)$$

After expanding the binomial and integrating each term we find

$$m_n(\theta) = m_{n,0} \cos^n \theta + \binom{n}{1} m_{n-1,1} \cos^{n-1} \theta \sin \theta + \dots + m_{0,n} \sin^n \theta, \quad (1.4.12)$$

where m_{pq} is the (p, q) th moment of E about the origin (equation (1.2.6)) and $\binom{n}{r}$ denotes the binomial coefficient.

In particular we have
$$m_0(\theta) = m_{00}, \quad (1.4.13)$$

showing that the r.m.s. value of $\zeta(x')$ is independent of the direction θ and equals the r.m.s. value of $\zeta(x, y)$. Next,

$$m_1(\theta) = m_{10} \cos \theta + m_{01} \sin \theta. \quad (1.4.14)$$

If (\bar{u}, \bar{v}) denotes the centroid of the two-dimensional spectrum:

$$(\bar{u}, \bar{v}) = \left(\frac{m_{10}}{m_{00}}, \frac{m_{01}}{m_{00}} \right), \quad (1.4.15)$$

and if \bar{u}' denotes the mean wave-number of the spectrum of $\zeta(x')$ we have

$$\bar{u}' = \frac{m_1(\theta)}{m_0(\theta)} = \bar{u} \cos \theta + \bar{v} \sin \theta, \quad (1.4.16)$$

which can be expressed as
$$\bar{u}' = \bar{w} \cos(\theta - \bar{\theta}), \quad (1.4.17)$$

where
$$(\bar{w}, \bar{\theta}) = (\bar{w} \cos \bar{\theta}, \bar{w} \sin \bar{\theta}). \quad (1.4.18)$$

\bar{w} and $\bar{\theta}$ may be called the mean wave-number and mean direction of the two-dimensional spectrum. Thus the mean wave-number of $E_\theta(u')$ is the projection of the mean wave-number of $E(u, v)$ on to the line of the section. The physical significance of this result will become clearer in § 1.5.

The second moment $m_2(\theta)$ is particularly important. From (1.4.12) we have

$$m_2(\theta) = m_{20} \cos^2 \theta + 2m_{11} \cos \theta \sin \theta + m_{02} \sin^2 \theta. \quad (1.4.19)$$

The maxima and minima of this expression are given by

$$m_{2 \max}, m_{2 \min} = \frac{1}{2} [(m_{20} + m_{02}) \pm \sqrt{(m_{20} - m_{02})^2 + 4m_{11}^2}], \quad (1.4.20)$$

and these occur always in two directions at right angles, given by

$$\tan 2\theta_p = \frac{2m_{11}}{m_{20} - m_{02}}. \quad (1.4.21)$$

If θ_p corresponds to the maximum we have

$$m_2(\theta) = m_{2\max} \cos^2(\theta - \theta_p) + m_{2\min} \sin^2(\theta - \theta_p). \tag{1.4.22}$$

The direction θ_p corresponding to the maximum will be called the *principal direction* of the waves. Now

$$\left(\frac{m_2(\theta)}{m_{00}}\right)^{\frac{1}{2}} \tag{1.4.23}$$

is the r.m.s. wave-number in the direction θ . For a long-crested system of waves the r.m.s. wave-number is a maximum perpendicular to the crests and a minimum parallel to the crests. In general, therefore, a convenient measure of the *long-crestedness* is given by the ratio

$$\left(\frac{m_{2\max}}{m_{2\min}}\right)^{\frac{1}{2}}, \tag{1.4.24}$$

which we denote by $1/\gamma$. Thus we have

$$\gamma^2 = \frac{m_{2\min}}{m_{2\max}} = \frac{(m_{20} + m_{02}) - \sqrt{\{(m_{20} - m_{02})^2 + 4m_{11}^2\}}}{(m_{20} + m_{02}) + \sqrt{\{(m_{20} - m_{02})^2 + 4m_{11}^2\}}}. \tag{1.4.25}$$

When the condition (1.3.3) for a one-dimensional spectrum is satisfied we have

$$\gamma = 0, \quad 1/\gamma = \infty. \tag{1.4.26}$$

The two quantities $m_{2\max}$, $m_{2\min}$ are clearly invariant under a rotation of the axes. Hence we have also the invariants

$$m_{2\max} + m_{2\min} = m_{20} + m_{02} = m_2, \tag{1.4.27}$$

say, and

$$m_{2\max} m_{2\min} = m_{20} m_{02} - m_{11}^2 = \Delta_2. \tag{1.4.28}$$

1.5. The wave envelope

By analogy with §1.1 we define the mean wave-number as the centroid of the energy distribution:

$$\left. \begin{aligned} m_{00} \bar{u} &= \int_{-\infty}^{\infty} \int_{-\infty}^{\infty} E(u, v) u \, du \, dv = m_{10}, \\ m_{00} \bar{v} &= \int_{-\infty}^{\infty} \int_{-\infty}^{\infty} E(u, v) v \, du \, dv = m_{01} \end{aligned} \right\} \tag{1.5.1}$$

and we define also the mean frequency $\bar{\sigma}/2\pi$ by the analogous equation

$$m_{00} \bar{\sigma} = \int_{-\infty}^{\infty} \int_{-\infty}^{\infty} E(u, v) \sigma \, du \, dv = m'_{00}, \tag{1.5.2}$$

say. Now let (1.2.1) be written in the form

$$\zeta = \Re \sum_n c_n \exp \{i(u_n x + v_n y + \sigma_n t + \epsilon_n)\} \tag{1.5.3}$$

$$= \Re \left[\sum_n c_n \exp \{i[(u_n - \bar{u})x + (v_n - \bar{v})y + (\sigma_n - \bar{\sigma})t + \epsilon_n]\} \exp \{i(\bar{u}x + \bar{v}y + \bar{\sigma}t)\} \right], \tag{1.5.4}$$

where \Re denotes the real part. This expresses ζ as the product of a carrier wave

$$\exp \{i(\bar{u}x + \bar{v}y + \bar{\sigma}t)\}, \tag{1.5.5}$$

and a slowly varying amplitude function

$$\rho e^{i\phi} = \sum_n c_n \exp \{i[(u_n - \bar{u})x + (v_n - \bar{v})y + (\sigma_n - \bar{\sigma})t + \epsilon_n]\}, \tag{1.5.6}$$

which may be called the complex envelope. (ρ and ϕ are real functions of (x, y, t) , with $\rho \geq 0$.) Any other choice for the frequency of the carrier wave might have been taken; the mean wave-number has the unique property that the secular increase of ϕ with x and y is zero (as will be shown in § 2.8).

Comparing (1.5.3) and (1.5.4) we see that *the real part* of the amplitude function, i.e. $\rho \cos \phi$, has the same spectrum as ξ , only with the origin moved to (\bar{u}, \bar{v}) ; similarly for the imaginary part. (ρ itself, however, is a different type of function, being essentially positive.) The properties of the envelope, therefore, are defined by the moments of the energy distribution about the mean. Let

$$\int_{-\infty}^{\infty} \int_{-\infty}^{\infty} E(u, v) (u - \bar{u})^p (v - \bar{v})^q du dv = \mu_{pq}. \quad (1.5.7)$$

It is easily seen that

$$\mu_{00} = m_{00}, \quad \mu_{10} = \mu_{01} = 0, \quad (1.5.8)$$

and

$$\left. \begin{aligned} \mu_{20} &= m_{20} - \bar{u}^2 m_{00} = (m_{20} m_{00} - m_{10}^2) / m_{00}, \\ \mu_{11} &= m_{11} - \bar{u} \bar{v} m_{00} = (m_{11} m_{00} - m_{10} m_{01}) / m_{00}, \\ \mu_{02} &= m_{02} - \bar{v}^2 m_{00} = (m_{02} m_{00} - m_{01}^2) / m_{00}. \end{aligned} \right\} \quad (1.5.9)$$

The second moment about the mean in a direction θ is

$$\mu_2(\theta) = \mu_{20} \cos^2 \theta + 2\mu_{11} \cos \theta \sin \theta + \mu_{02} \sin^2 \theta, \quad (1.5.10)$$

and the principal direction of the envelope is given by

$$\tan 2\theta_e = \frac{2\mu_{11}}{\mu_{20} - \mu_{02}}. \quad (1.5.11)$$

The angle β between the principal direction of the envelope and the principal direction of the waves is given by

$$\tan 2\beta = \tan 2(\theta_e - \theta_p) = \frac{2\mu_{11}(m_{20} - m_{02}) - 2m_{11}(\mu_{20} - \mu_{02})}{(\mu_{20} - \mu_{02})(m_{20} - m_{02}) + 4\mu_{11}m_{11}}. \quad (1.5.12)$$

Thus β is a convenient measure of the *skewness* of the waves (see § 1.1).

Consider again the curve of intersection of the surface with a vertical plane in direction θ . We may see that the envelope of this curve is simply the intersection of the two-dimensional envelope with the vertical plane. For on the one hand we have from (1.5.6)

$$\rho e^{i\phi} = \sum_n c_n \exp \{i[(u'_n - \bar{u}') x' + (v'_n - \bar{v}') y' + (\sigma'_n - \bar{\sigma}) t + \epsilon_n]\}, \quad (1.5.13)$$

where u'_n and v'_n are given by (1.4.3) and

$$\bar{u}' = \bar{u} \cos \theta + \bar{v} \sin \theta, \quad \bar{v}' = -\bar{u} \sin \theta + \bar{v} \cos \theta. \quad (1.5.14)$$

The intersection of the envelope by the plane $y' = 0$ is therefore given by

$$\rho e^{i\phi} = \sum_n c_n \exp \{i[(u'_n - \bar{u}') x' + (\sigma'_n - \bar{\sigma}) t + \epsilon_n]\}. \quad (1.5.15)$$

On the other hand from (1.4.5) we may write

$$\xi(x', t) = \mathcal{A} \left[\sum_n c_n \exp \{i[(u'_n - \bar{u}') x' + (\sigma'_n - \bar{\sigma}) t + \epsilon_n]\} \exp \{i(\bar{u}' x' + \bar{v}' t)\} \right], \quad (1.5.16)$$

where \bar{u} is given by (1.5.14). But we saw in § 1.4 that \bar{u} is also the mean wave-number for the function $\zeta(x', t)$ and therefore $\exp\{i(\bar{u}x' + \bar{\sigma}t)\}$ is, by definition, the carrier wave for $\zeta(x', t)$ and (1.5.16) is the envelope; which proves the result.

1.6. A narrow spectrum

A case of special interest is when the energy is concentrated near a single point in the spectrum, so that the component waves are nearly constant in wavelength and direction. As we saw earlier, the conditions satisfied by the first-order and second-order moments are that the left-hand sides of equations (1.3.14) are small. In terms of the moments this implies $\mu_{20} + \mu_{02} \ll m_{20} + m_{02}$, or equivalently

$$\mu_{20} + \mu_{02} \ll (\bar{u}^2 + \bar{v}^2) m_{00}. \tag{1.6.1}$$

The envelope of the waves, as defined in the previous section, then has some special properties. If in (1.5.2) we expand $\sigma(u, v)$ in a Taylor series about (\bar{u}, \bar{v}) we have

$$\begin{aligned} m_{00}\bar{\sigma} &= \int_{-\infty}^{\infty} \int_{-\infty}^{\infty} E(u, v) \left[\sigma(\bar{u}, \bar{v}) + (u - \bar{u}) \frac{\partial}{\partial u} \sigma(\bar{u}, \bar{v}) + (v - \bar{v}) \frac{\partial}{\partial v} \sigma(\bar{u}, \bar{v}) \right] du dv \\ &= m_{00}\sigma(\bar{u}, \bar{v}) + \mu_{10} \frac{\partial}{\partial u} \sigma(\bar{u}, \bar{v}) + \mu_{01} \frac{\partial}{\partial v} \sigma(\bar{u}, \bar{v}), \end{aligned} \tag{1.6.2}$$

terms of higher order being negligible. Since $\mu_{10} = \mu_{01} = 0$ we have

$$\bar{\sigma} = \sigma(\bar{u}, \bar{v}). \tag{1.6.3}$$

In other words, the carrier wave is a free wave with the frequency and velocity appropriate to its wave-number. Further, in (1.5.6) we may write

$$\sigma_n - \bar{\sigma} = (u_n - \bar{u}) \frac{\partial \bar{\sigma}}{\partial \bar{u}} + (v_n - \bar{v}) \frac{\partial \bar{\sigma}}{\partial \bar{v}}, \tag{1.6.4}$$

so that
$$\rho e^{i\phi} = \sum_n \exp \{ i [(u_n - \bar{u}) (x + t \partial \bar{\sigma} / \partial \bar{u}) + (v_n - \bar{v}) (y + t \partial \bar{\sigma} / \partial \bar{v})] \}, \tag{1.6.5}$$

which is a function of $(x + t \partial \bar{\sigma} / \partial \bar{u})$ and $(y + t \partial \bar{\sigma} / \partial \bar{v})$ only. In other words, the envelope moves bodily with velocity

$$\left(-\frac{\partial \bar{\sigma}}{\partial \bar{u}}, -\frac{\partial \bar{\sigma}}{\partial \bar{v}} \right). \tag{1.6.6}$$

σ being a function of $w = (u^2 + v^2)^{\frac{1}{2}}$ only, this velocity is

$$-\left(\frac{\partial \bar{\sigma}}{\partial \bar{u}}, \frac{\partial \bar{\sigma}}{\partial \bar{v}} \right) \frac{d\bar{\sigma}}{dw} = -(\cos \theta, \sin \theta) \frac{d\bar{\sigma}}{dw}, \tag{1.6.7}$$

which is the group velocity of the carrier wave.

Let axes be chosen so that the u axis passes through the centroid (\bar{u}, \bar{v}) , making $\bar{v} = 0$. On expanding $u^p = \{\bar{u} + (u - \bar{u})\}^p$, by the binomial theorem we have

$$\begin{aligned} m_{pq} &= \int_{-\infty}^{\infty} \int_{-\infty}^{\infty} E(u, v) u^p v^q du dv \\ &= \int_{-\infty}^{\infty} \int_{-\infty}^{\infty} E(u, v) [\bar{u}^p + p\bar{u}^{p-1}(u - \bar{u}) + \dots + (u - \bar{u})^p] (v - \bar{v})^q du dv \\ &= \bar{u}^p \mu_{00} + p\bar{u}^{p-1} \mu_{1q} + \dots + \mu_{pq}. \end{aligned} \tag{1.6.8}$$

In particular, since $\mu_{10} = \mu_{01} = 0$, we have

$$\text{Thus (1.4.9) becomes } m_{20} = \bar{u}^2 \mu_{00} + \mu_{20}, \quad m_{11} = \mu_{11}, \quad m_{02} = \mu_{02}. \quad (1.6.9)$$

$$m_2(\theta) = \bar{u}^2 \mu_{00} \cos^2 \theta + (\mu_{20} \cos^2 \theta + 2\mu_{11} \cos \theta \sin \theta + \mu_{02} \sin^2 \theta). \quad (1.6.10)$$

Since $\mu_{11} \ll (\mu_{20} \mu_{02})^{\frac{1}{2}}$ it follows that all three moments μ_{20} , μ_{11} , μ_{02} are small compared with $\bar{u}^2 \mu_{00}$. Hence $m_2(\theta)$ has a maximum near $\theta = 0, \pi$ and a minimum near $\theta = \pm \frac{1}{2}\pi$. In other words, the principal direction lies along the axis of u . The long-crestedness γ^{-1} was defined as the ratio of the r.m.s. wave-numbers parallel and perpendicular to the principal directions. Thus

$$\gamma^2 = \frac{m_2(\frac{1}{2}\pi)}{m_2(0)} = \frac{\mu_{02}}{\bar{u}^2 \mu_{00}}. \quad (1.6.11)$$

Now in the neighbourhood of the centroid we have $v = \bar{u}\theta$ very nearly, so that

$$\mu_{02} = \int_{-\infty}^{\infty} \int_{-\infty}^{\infty} E(u, v) \bar{u}^2 \theta^2 du dv. \quad (1.6.12)$$

Hence

$$\gamma^2 \mu_{00} = \int_{-\infty}^{\infty} \int_{-\infty}^{\infty} E(u, v) \theta^2 du dv. \quad (1.6.13)$$

In other words, γ is the r.m.s. angular deviation of the energy from the mean direction.

Since the principal direction of the waves coincides with the u axis, the angle of skewness β is the angle between the u axis and the principal direction of the envelope, that is,

$$\tan 2\beta = \frac{\sum \mu_{11}}{\mu_{20} - \mu_{02}}. \quad (1.6.14)$$

It will be found convenient to introduce one further parameter for a narrow wave spectrum:

$$\nu = (\mu_{20} / \bar{u}^2 \mu_{00})^{\frac{1}{2}}. \quad (1.6.15)$$

ν is proportional to the r.m.s. width of the spectrum in the principal direction. We shall show in §2.8 that ν^{-1} is a measure of the average number of waves per 'group'.

PART II. STATISTICAL PROPERTIES

The fundamental statistical distributions of ξ and its derivatives are given in §2.1. The following three sections are devoted to properties of the surface not involving motion, and the next three sections to the distributions of velocities associated with these properties. Lastly, §§2.8 to 2.10 deal with the envelope of the surface and with properties which can be derived from it.

The distributions of the surface elevation ξ and of the two components of gradient $\partial\xi/\partial x$, $\partial\xi/\partial y$ are normal in one and two dimensions respectively (equations (2.1.8) and (2.1.12)). The greatest r.m.s. gradient is in the principal direction of the surface. The distribution of the magnitude α of the gradient regardless of direction is given by (2.1.31) and figure 3. For very short-crested waves the distribution is a Rayleigh distribution; for very long-crested waves it tends to a normal distribution, with an anomaly near $\alpha=0$, the shape of which is shown in figure 4. The probability distribution of the horizontal direction θ of the gradient is given by (2.1.37) and figure 5. It is shown that as the long-crestedness increases, the direction of the gradient becomes more and more certain to be near the principal direction.

In §2.2 is found the mean number of zeros of the surface along a horizontal line in an arbitrary direction θ . The number N_0 per unit distance is given by (2.2.5). Thus N_0 is a maximum when θ is in the principal direction, and a minimum in the direction at right angles. The ratio $N_{0\text{max}}/N_{0\text{min}}$

is equal to the long-crestedness γ^{-1} . The mean number of times that the surface crosses a line at arbitrary level is also found (2.2.12), and the mean number of crests and troughs of a plane section of the surface in any direction.

The average length of a contour of constant height drawn on the surface is derived in §2.3. The length \bar{l} per unit area is given by (2.3.16). The distribution of the direction θ of the normal to a particular contour, at points distributed uniformly along it, is given by (2.3.23). As in §2.1, when the waves become long-crested, the direction becomes concentrated near the principal direction.

Next (§2.4) the average density of maxima and minima of the surface per unit horizontal area is considered. It is shown that the average density of maxima, $D_{ma.}$, is equal to one-half of the average density of saddle-points, and to one-quarter of the total density of stationary points on the surface. The actual density is given by (2.4.51), in the general case. For a narrow spectrum, the density is given by (2.4.61) and table 1. $D_{ma.}$ depends not only on the long-crestedness but also on a parameter a representing the peakedness of the energy distribution with regard to direction.

Passing now to properties depending on the motion of the surface, we consider in §2.5 the velocity of the zeros of the surface along an arbitrary line. We find that the velocities have a probability distribution given by (2.5.15). This is symmetrical about a mean value depending on the first-order moments. Similarly, the velocities of maxima and minima of a plane section of the surface have a distribution given by (2.5.19). These distributions are studied in the special case of a narrow spectrum. The width of the distribution depends on both the width of the energy spectrum and on the dispersive properties of the medium.

The motion of a contour on the surface can be defined locally by the velocities of its points of intersection with lines parallel to the axes of x, y (§2.6). The distribution of the reciprocals of the velocities, which is simpler than that of the velocities themselves, is given by (2.6.21). The distribution is discussed in detail for the case of a narrow spectrum; the contours of constant probability are then concentric ellipses.

In §2.7 is considered the motion of the 'specular points' of the surface, that is, points where the gradient of the surface takes a certain value. (Such points on the sea surface are, to a distant observer, points of reflected sunlight.) The probability distribution of the two components of velocity is given by (2.7.31). In the special case of a narrow spectrum the mean velocity of the specular points is equal to the phase velocity of the carrier wave. The departures of the velocities from the mean velocity have a distribution given by (2.7.37). This expression has been computed for three different values of the peakedness a , and is shown in figure 12 a, b and c .

In §2.8 we consider some properties of the wave envelope, from which we derive some other useful distributions. The distribution of the envelope function itself is a Rayleigh distribution (2.8.6). The joint distribution of $\rho, \partial\rho/\partial x$ and $\partial\rho/\partial y$ is given by (2.8.15), from which it follows that the envelope possesses a number of properties analogous to the original surface. The envelope also controls the 'grouping' of the waves, and we find, taking a section of the surface in an arbitrary direction θ , that the average length of a group is $2/N$, where N is given by (2.8.26). Hence the average length of a group is least in the principal direction and greatest in the direction at right angles. We find the average number of waves in a group (2.8.27) and the condition that this shall be independent of the direction θ (2.8.28).

When the spectrum is narrow, the crests of the waves lie practically on the envelope, and so we are able to deduce that the probability distribution of the heights of crests is approximately a Rayleigh distribution (2.9.1). The distribution of the heights of maxima is found through the distribution of the heights of the maxima of the envelope (2.9.8). This distribution is shown in figure 13 for different values of peakedness a . The limiting case of two crossing swells ($a = 1$) is given by (2.8.12) and is also shown in figure 13.

Finally, in §2.10 is deduced the distribution of the intervals l between successive zero-crossings, or between the successive points of intersection of a straight line with a contour at fixed height. The distribution of l for waves of all heights is given by (2.10.18). However, if the waves are classified according to their height, the distribution of l is given by (2.10.23), and hence it is found that l is less scattered for the high waves than for the low waves. The degree of scattering is inversely proportional to the average number of waves in a group.

2.1. *The distribution of surface elevation and gradient*

Let ξ_1, \dots, ξ_n be n quantities, each the sum of a large number of independent variables whose expectation is zero. Then under certain general conditions (discussed by Rice 1944, 1945; see also Cramér 1937) the joint-probability distribution of ξ_1, \dots, ξ_n is normal in n dimensions:

$$p(\xi_1, \dots, \xi_n) = \frac{1}{(2\pi)^{n/2} \Delta^{1/2}} \exp\{-\frac{1}{2} M_{ij} \xi_i \xi_j\}, \quad (2.1.1)$$

where (M_{ij}) is the inverse matrix to

$$(\Xi_{ij}) = \begin{pmatrix} \overline{\xi_1^2} & \overline{\xi_1 \xi_2} & \dots & \overline{\xi_1 \xi_n} \\ \overline{\xi_2 \xi_1} & \overline{\xi_2^2} & \dots & \overline{\xi_2 \xi_n} \\ \vdots & \vdots & \ddots & \vdots \\ \overline{\xi_n \xi_1} & \overline{\xi_n \xi_2} & \dots & \overline{\xi_n^2} \end{pmatrix} \quad (2.1.2)$$

and

$$\Delta = |\Xi_{ij}|. \quad (2.1.3)$$

The elements of (Ξ_{ij}) are the mean products $\overline{\xi_i \xi_j}$ of the variables ξ_i and ξ_j , over the probability space of the independent components. (Ξ_{ij}) is a positive-definite matrix, for if $\alpha_1, \dots, \alpha_n$ are any n parameters not all zero

$$\alpha_i \alpha_j \overline{\xi_i \xi_j} = \overline{(\alpha_i \xi_i)^2} > 0. \quad (2.1.4)$$

Now according to equation (1.2.1), ζ and also its derivatives are variables of this type. Further, writing for brevity

$$u_n x + v_n y + \sigma_n t + \epsilon_n = \phi_n, \quad (2.1.5)$$

we have

$$\overline{\zeta^2} = \overline{(\sum_n c_n \cos \phi_n)^2} = \sum_n \frac{1}{2} c_n^2, \quad (2.1.6)$$

since the phases are random. Thus

$$\overline{\zeta^2} = \int_{-\infty}^{\infty} \int_{-\infty}^{\infty} E(u, v) du dv = m_{00}, \quad (2.1.7)$$

and accordingly the probability distribution of $\xi_1 = \zeta$, is

$$p(\xi_1) = \frac{1}{(2\pi)^{1/2} m_{00}^{1/2}} \exp\{-\xi_1^2/2m_{00}\}. \quad (2.1.8)$$

Similarly

$$\left. \begin{aligned} \overline{\left(\frac{\partial \zeta}{\partial x}\right)^2} &= \overline{(-\sum_n c_n u_n \sin \phi_n)^2} = \sum_n \frac{1}{2} c_n^2 u_n^2 = m_{20}, \\ \overline{\left(\frac{\partial \zeta}{\partial y}\right)^2} &= \overline{(\sum_n c_n v_n \sin \phi_n)^2} = \sum_n \frac{1}{2} c_n^2 v_n^2 = m_{02}, \\ \frac{\partial \zeta}{\partial x} \frac{\partial \zeta}{\partial y} &= \overline{(\sum_n c_n u_n \sin \phi_n)(\sum_n c_n v_n \sin \phi_n)} = \sum_n \frac{1}{2} c_n^2 u_n v_n = m_{11}. \end{aligned} \right\} \quad (2.1.9)$$

The matrix of correlations for

$$\xi_2, \xi_3 = \frac{\partial \zeta}{\partial x}, \frac{\partial \zeta}{\partial y} \quad (2.1.10)$$

is therefore

$$(\Xi_{ij}) = \begin{pmatrix} m_{20} & m_{11} \\ m_{11} & m_{02} \end{pmatrix}, \quad (2.1.11)$$

and the joint-probability distribution is

$$p(\xi_2, \xi_3) = \frac{1}{2\pi \Delta^{1/2}} \exp\{-(m_{02} \xi_2^2 - 2m_{11} \xi_2 \xi_3 + m_{20} \xi_3^2)/2\Delta\}, \quad (2.1.12)$$

$$\text{where} \quad \Delta_2 = \begin{vmatrix} m_{20} & m_{11} \\ m_{11} & m_{02} \end{vmatrix}. \quad (2.1.13)$$

The cross-correlations between ζ and $\partial\zeta/\partial x$, $\partial\zeta/\partial y$ are given by

$$\left. \begin{aligned} \overline{\zeta \frac{\partial\zeta}{\partial x}} &= \overline{\left(\sum_n c_n \cos \phi_n \right) \left(- \sum_n c_n u_n \sin \phi_n \right)} = 0, \\ \overline{\zeta \frac{\partial\zeta}{\partial y}} &= \overline{\left(\sum_n c_n \cos \phi_n \right) \left(- \sum_n c_n v_n \sin \phi_n \right)} = 0, \end{aligned} \right\} \quad (2.1.14)$$

so that ζ and $\partial\zeta/\partial x$, $\partial\zeta/\partial y$ are uncorrelated. The joint-probability distribution of

$$(\xi_1, \xi_2, \xi_3) = (\zeta, \partial\zeta/\partial x, \partial\zeta/\partial y) \quad (2.1.15)$$

$$\text{is therefore given by} \quad p(\xi_1, \xi_2, \xi_3) = p(\xi_1) p(\xi_2, \xi_3), \quad (2.1.16)$$

where $p(\xi_1)$ is given by (2.1.8) and $p(\xi_2, \xi_3)$ by (2.1.12).

In general we find, by repeated differentiation,

$$\left. \begin{aligned} \overline{\left(\frac{\partial^{p+q}\zeta}{\partial x^p \partial y^q} \right)^2} &= m_{2p, 2q} \\ \text{and} \quad \overline{\frac{\partial^{p+q}\zeta}{\partial x^p \partial y^q} \frac{\partial^{p'+q'}\zeta}{\partial x^{p'} \partial y^{q'}}} &= (-1)^{k(p+q-p'-q')} m_{p+p', q+q'} \quad \text{or} \quad 0, \end{aligned} \right\} \quad (2.1.17)$$

according as $(p+q-p'-q')$ is even or odd. For example, the derivatives of order $p+q=n$ are not correlated with those of order $p'+q'=n+1$; but they are correlated, negatively in general, with those of order $n+2$.

Slightly different results apply to derivatives involving the time t . We have from (1.2.1)

$$\frac{\partial\zeta}{\partial t} = - \sum_n c_n \sigma_n \sin(u_n x + v_n y + \sigma_n t + c_n), \quad (2.1.18)$$

and so the energy spectrum of $\partial\zeta/\partial t$ is $\sigma^2 E(u, v)$. The correlations between the derivatives of ζ and those of $\partial\zeta/\partial t$ are given in terms of the moments

$$\left. \begin{aligned} m'_{pq} &= \int_{-\infty}^{\infty} \int_{-\infty}^{\infty} \sigma E(u, v) u^p v^q du dv, \\ m''_{pq} &= \int_{-\infty}^{\infty} \int_{-\infty}^{\infty} \sigma^2 E(u, v) u^p v^q du dv \end{aligned} \right\} \quad (2.1.19)$$

of the functions $\sigma E(u, v)$ and $\sigma^2 E(u, v)$. As in (2.1.9) we have

$$\overline{\left(\frac{\partial\zeta}{\partial t} \right)^2} = m''_{00}, \quad \overline{\frac{\partial\zeta}{\partial t} \frac{\partial\zeta}{\partial x}} = m'_{10}, \quad \overline{\frac{\partial\zeta}{\partial t} \frac{\partial\zeta}{\partial y}} = m'_{01}, \quad (2.1.20)$$

and in general

$$\overline{\left(\frac{\partial^{p+q+1}\zeta}{\partial x^p \partial y^q \partial t} \right)^2} = m''_{2p, 2q} \quad (2.1.21)$$

$$\text{and} \quad \overline{\left(\frac{\partial^{p+q+1}\zeta}{\partial x^p \partial y^q \partial t} \right) \left(\frac{\partial^{p'+q'}\zeta}{\partial x^{p'} \partial y^{q'}} \right)} = (-1)^{k(p+q-p'-q'+1)} m'_{p+p', q+q'} \quad \text{or} \quad 0, \quad (2.1.22)$$

according as $(p+q-p'-q')$ is odd or even. Thus all the correlations of the spatial derivatives of $\partial\zeta/\partial t$ with the spatial derivatives of ζ are expressible in terms of the odd moments

of σE . The odd derivatives of $\partial \zeta / \partial t$ are all independent of the odd derivatives of ζ but are correlated with all the even derivatives; and vice versa.

Let us now consider more closely the pattern of surface slopes. If the magnitude of the surface slope is α and its direction is θ we have

$$(\xi_2, \xi_3) = \left(\frac{\partial \zeta}{\partial x}, \frac{\partial \zeta}{\partial y} \right) = (\alpha \cos \theta, \alpha \sin \theta), \quad (2.1.23)$$

and so

$$p(\alpha, \theta) = \left| \frac{\partial(\xi_2, \xi_3)}{\partial(\alpha, \theta)} \right| p(\xi_2, \xi_3) = \alpha p(\xi_2, \xi_3), \quad (2.1.24)$$

or from (2.1.12)

$$p(\alpha, \theta) = \frac{\alpha}{2\pi\Delta_2^{\frac{1}{2}}} \exp \{ -\alpha^2(m_{02} \cos^2 \theta - 2m_{11} \cos \theta \sin \theta + m_{20} \sin^2 \theta) / 2\Delta_2 \}. \quad (2.1.25)$$

If we take the x axis along the principal direction, so that m_{11} vanishes and $m_{20} \geq m_{02}$, then

$$p(\alpha, \theta) = \frac{\alpha^2}{2\pi\Delta_2^{\frac{1}{2}}} \exp \{ -\alpha^2(m_{02} \cos^2 \theta + m_{20} \sin^2 \theta) / 2\Delta_2 \}. \quad (2.1.26)$$

For a fixed value of θ , the r.m.s. slope is given by

$$\left[\frac{\int_0^\infty \alpha^2 p(\alpha, \theta) d\alpha}{\int_0^\infty p(\alpha, \theta) d\alpha} \right]^{\frac{1}{2}} = \left[\frac{2\Delta_2}{m_{02} \cos^2 \theta + m_{20} \sin^2 \theta} \right]^{\frac{1}{2}}. \quad (2.1.27)$$

The maximum r.m.s. slope, therefore, is in a direction $\theta = 0$, that is to say, in the principal direction. The minimum slope is in the direction at right angles to this.

The statistical distribution of the slope regardless of direction may be found by integrating $p(\alpha, \theta)$ with respect to θ from 0 to 2π . We find

$$p(\alpha) = \frac{\alpha}{\Delta_2^{\frac{1}{2}}} \exp \{ -\alpha^2(m_{20} + m_{02}) / 4\Delta_2 \} I_0[\alpha^2(m_{20} - m_{02}) / 4\Delta_2], \quad (2.1.28)$$

where

$$I_0(z) = \frac{1}{2\pi} \int_0^{2\pi} e^{-z \sin \theta} d\theta = J_0(iz), \quad (2.1.29)$$

I_0 being the Bessel function of order zero with imaginary argument (see Whittaker & Watson 1952, chap. 17). Writing

$$\eta = \frac{\alpha}{(m_{20} + m_{02})^{\frac{1}{2}}} = \frac{\alpha}{m} \quad (2.1.30)$$

for the relative slope, and $\gamma^{-1} = (m_{20}/m_{02})^{\frac{1}{2}}$ for the long-crestedness, we have

$$p(\eta) = \eta(\gamma + \gamma^{-1}) \exp \{ -\eta^2(\gamma + \gamma^{-1})^2 / 4 \} I_0[\eta^2(\gamma^2 - \gamma^{-2}) / 4]. \quad (2.1.31)$$

This distribution is shown in figure 3, for $\gamma = 1, \frac{1}{2}, \frac{1}{4}$ and 0. When $\gamma = 1$ we have, since $I_0(0) = 1$,

$$p(\eta) = 2\eta e^{-\eta^2}. \quad (2.1.32)$$

Thus for short-crested waves the slopes have a Rayleigh distribution. Now as z tends to infinity, $I_0(z) \sim (2\pi z)^{-\frac{1}{2}} e^z$ (Whittaker & Watson 1952, p. 373) and so when γ is small we have, for general values of η ,

$$p(\eta) \sim \left(\frac{2}{\pi} \right)^{\frac{1}{2}} e^{-\frac{1}{2}\eta^2}. \quad (2.1.33)$$

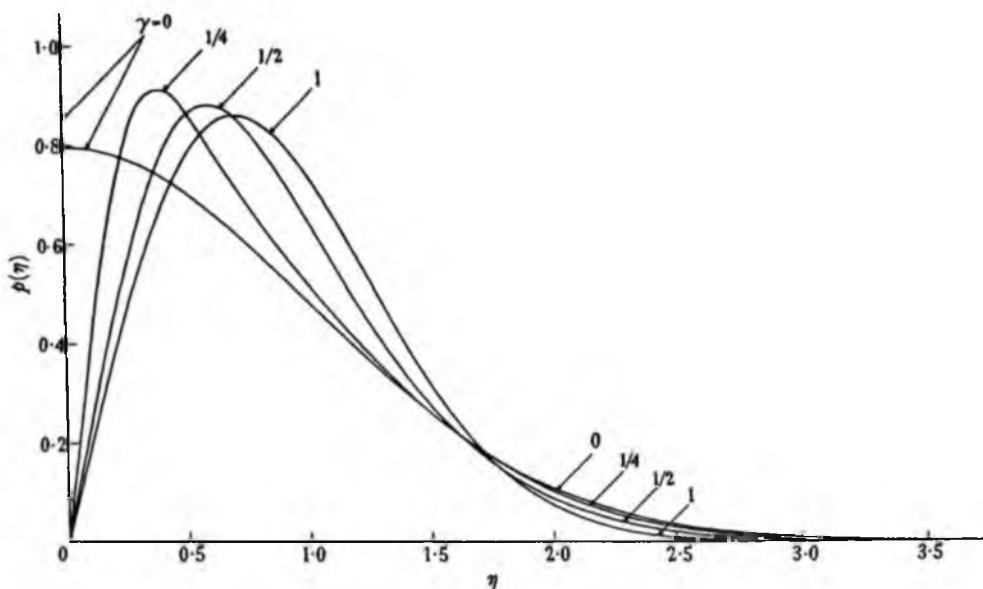


FIGURE 3. The probability distribution of the surface slope $\eta = \alpha / (m_{20}^2 + m_{02}^2)^{1/2}$, for different values of the long-crestedness.

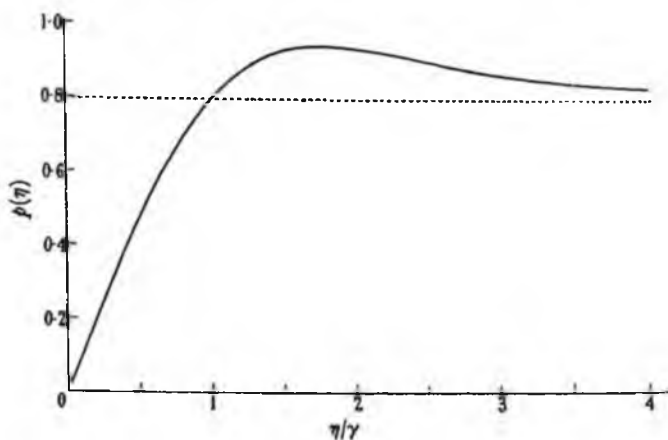


FIGURE 4. The limiting form of the slope distribution close to the origin, for a very long-crested surface.

In other words, for long-crested waves the slopes have in general a normal distribution (as we should expect, for since the slopes are nearly all in one plane, the distribution of α is the same as the distribution of $\partial\zeta/\partial x$, which is normal). However, for very small slopes, comparable with γm , we must use the approximation

$$p(\eta) = (\eta/\gamma) e^{-\eta^2/4\gamma^2} I_0(\eta^2/4\gamma^2), \quad = f(\eta/\gamma), \quad (2.1.34)$$

say. $f(\eta/\gamma)$ is plotted in figure 4. As $\eta/\gamma \rightarrow \infty$, so $f \rightarrow (2/\pi)^{\frac{1}{2}}$, which is the value of (2.1.33) at the origin. The anomalous distribution near the origin appears to arise from directions θ which are nearly perpendicular to the principal direction; since the crests are only of finite length, the chance of a very small slope in this direction is less than if the waves were two-dimensional. Nevertheless, the integral of (2.1.34) from 0 to ∞ is equal to 1, so that as the waves become infinitely long-crested the contribution to the integrated probability from the anomalous term is vanishingly small.

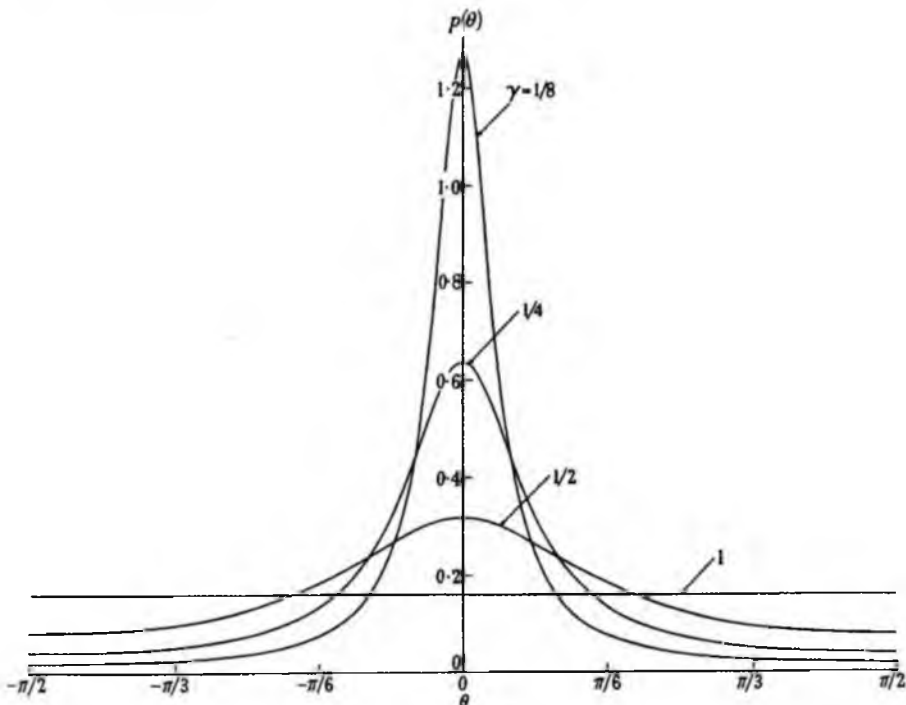


FIGURE 5. The probability distribution of the direction θ of the surface gradient for different values of the long-crestedness. $\theta = 0$ is the principal direction.

Even when the waves are not long-crested, still for large values of η

$$p(\eta) \sim \left(\frac{2}{\pi}\right)^{\frac{1}{2}} \frac{1}{(1-\gamma^2)^{\frac{1}{2}}} e^{-\frac{1}{2}\eta^2}. \quad (2.1.35)$$

Thus for large slopes the distribution always approaches a normal distribution ultimately, provided $\gamma < 1$.

The statistical distribution of the direction θ of the gradient is found by integrating (2.1.28) with respect to α from 0 to ∞ :

$$p(\theta) = \frac{\Delta^{\frac{1}{2}}}{2\pi(m_{02} \cos^2 \theta + m_{20} \sin^2 \theta)}. \quad (2.1.36)$$

or
$$p(\theta) = \frac{\gamma}{2\pi(\gamma^2 \cos^2 \theta + \sin^2 \theta)}. \quad (2.1.37)$$

STATISTICAL ANALYSIS OF A RANDOM, MOVING SURFACE 343

When $\gamma = 1$ (the waves are short-crested), $p(\theta)$ is independent of θ and there is no preferential direction for the slopes. As γ diminishes the slopes become more and more concentrated about the principal direction (see figure 5). When $\gamma \ll 1$ we have in general

$$p(\theta) = \frac{\gamma}{2\pi \sin^2 \theta},$$

which tends to zero as $\gamma \rightarrow 0$. But near the principal direction, i.e. when θ is comparable with γ , we have

$$p(\theta) = \frac{\gamma}{2\pi(\gamma^2 + \theta^2)},$$

a distribution whose width is proportional to γ . The integral of the distribution from $\theta/\gamma = -\infty$ to ∞ is equal to $\frac{1}{2}$. Thus the probability that θ is near zero is $\frac{1}{2}$, and so also is the probability that θ is near π . Hence it becomes almost certain that the gradient is nearly in the principal direction.

It should be noted that the probabilities so far discussed are for points distributed randomly and uniformly in the x, y plane. The corresponding probabilities for points selected so as to lie, for example, on a particular contour $\zeta = \text{constant}$, are different, as will be seen in § 2.3.

2.2. *The number of zero-crossings along a line*

As in § 1.4, let us consider the curve in which the surface is intersected by the vertical plane $x \sin \theta = y \cos \theta$. A point where this curve passes through the mean level ($\zeta = 0$) may be called a zero-crossing of ζ . We shall now consider the number of zero-crossings of ζ per unit distance x' measured along the line of intersection of the vertical plane and the mean level.

The mean number of zeros for a random function of a single variable has been derived by Rice (1944, 1945). We recall his argument briefly. ζ and $\partial\zeta/\partial x'$ are random functions which we shall denote by ξ_1 and ξ_2 respectively. Suppose that ζ passes through zero at some point x' in the interval $(x'_0, x'_0 + dx')$, and with gradient $\partial\zeta/\partial x'$ lying in the range $(\xi_2, \xi_2 + d\xi_2)$. Then at the point $x' = x'_0$ itself ζ lies in the range $(0, -\xi_2 dx')$, approximately, i.e. a range of height $d\xi_1 = |\xi_2| dx'$. The probability of this occurrence is

$$p(0, \xi_2) |\xi_2| dx' d\xi_2, \quad (2.2.1)$$

where $p(\xi_1, \xi_2)$ is the joint-probability distribution of (ξ_1, ξ_2) . The total probability of a zero in $(x'_0, x'_0 + dx')$ is found by integrating with respect to ξ_2 from $-\infty$ to ∞ . Hence the total number N_0 of zeros per unit distance is given by

$$N_0 = \int_{-\infty}^{\infty} p(0, \xi_2) |\xi_2| d\xi_2. \quad (2.2.2)$$

Now the matrix of correlations for (ξ_1, ξ_2) is

$$(\Xi_{ij}) = \begin{pmatrix} m_0 & 0 \\ 0 & m_2 \end{pmatrix}, \quad (2.2.3)$$

and so by (2.1.1)

$$p(\xi_1, \xi_2) = \frac{1}{2\pi(m_0 m_2)^{\frac{1}{2}}} \exp\{-\xi_1^2/2m_0 - \xi_2^2/2m_2\}. \quad (2.2.4)$$

On substituting in (2.2.2) and carrying out the integration we find

$$N_0 = \frac{1}{\pi} \left(\frac{m_2(\theta)}{m_0(\theta)} \right)^\dagger. \quad (2.2.5)$$

In other words πN_0 is equal to the r.m.s. wave-number in the direction θ . It follows at once from § 1.4 that

(1) the number of zeros is a maximum and a minimum for two directions at right angles, given by

$$\tan 2\theta_p = \frac{2m_{11}}{m_{20} - m_{02}}; \quad (2.2.6)$$

(2) the maximum and minimum values of N_0 are given by

$$N_{0\max.} N_{0\min.} = \frac{1}{\pi m_{00}^2} [(m_{20} + m_{02}) \pm \sqrt{\{(m_{20} - m_{02})^2 + 4m_{11}^2\}}]^\dagger; \quad (2.2.7)$$

(3) the number of zeros in a general direction θ is given by

$$N_0^2 = N_{0\max.}^2 \cos^2(\theta - \theta_p) + N_{0\min.}^2 \sin^2(\theta - \theta_p); \quad (2.2.8)$$

(4) the ratio $N_{0\min.}/N_{0\max.}$ is given by

$$\frac{N_{0\min.}}{N_{0\max.}} = \gamma, \quad (2.2.9)$$

where γ^{-1} is the long-crestedness; for a narrow spectrum $N_{0\min.}/N_{0\max.}$ equals the r.m.s. angular deviation of the energy from the mean direction.

There are similar relations for the mean number of crests and troughs along the curve, since these are simply zeros of the derivative $\partial\zeta/\partial x'$. The energy spectrum of $\partial\zeta/\partial x'$ is u'^2 times the energy spectrum of ζ . So the mean number N_1 of crests and troughs together is

$$N_1 = \frac{1}{\pi} \left(\frac{m_4(\theta)}{m_2(\theta)} \right)^\dagger \quad (2.2.10)$$

(the number of crests or troughs separately is half this). m_2 and m_4 can be expressed in terms of the two-dimensional moments of $E(u, v)$ by means of (1.4.12). m_4 is of the fourth degree in $\cos\theta$ and $\sin\theta$, and it is found that in general $N_1(\theta)$ has four maxima (in two pairs of opposite directions) and similarly four minima; these can be found, if necessary, in terms of the fourth-order moments $m_{40}, m_{31}, \dots, m_{04}$ and the second-order moments m_{20}, m_{11}, m_{02} .

In the same way the mean number N_2 of points of inflexion on the curve is

$$N_2 = \frac{1}{\pi} \left(\frac{m_6(\theta)}{m_4(\theta)} \right), \quad (2.2.11)$$

and the maxima and minima of N_2 are given in terms of the sixth-, fourth- and second-order moments of $E(u, v)$.

We may find similarly the average number of times that the curve of intersection crosses the level $\zeta = \xi_1$. For in (2.2.1) and (2.2.2) it is necessary only to replace $p(0, \xi_2)$ by $p(\xi_1, \xi_2)$. Since ξ_1 and ξ_2 are independent, this simply amounts to multiplying by a factor $\exp\{-\xi_1^2/2m_0\}$. So in the general case we have

$$N_0 = \frac{1}{\pi} \left(\frac{m_2(\theta)}{m_0(\theta)} \right)^\dagger \exp\{-\xi_1^2/2m_0(\theta)\}. \quad (2.2.12)$$

By similar reasoning, the number of times N_1 per unit distance that the curve has a gradient ξ_2 is given by

$$N_1 = \frac{1}{\pi} \left(\frac{m_4(\theta)}{m_2(\theta)} \right)^{\frac{1}{2}} \exp \{ -\xi_2^2 / 2m_2(\theta) \}, \quad (2 \cdot 2 \cdot 13)$$

and there are similar expressions corresponding to the higher derivatives of $\zeta(x')$.

2.3. The length and direction of the contours

Let us consider now a corresponding property in two dimensions. Imagine the surface contours $\zeta = \text{constant}$ to be drawn in the x, y plane. Contained in any region A of the plane there will be a certain length s of the contour $\zeta = \zeta_0$. The average length of contour, being proportional to the area A , may be denoted by $\bar{s}A$. The factor \bar{s} is now to be evaluated.

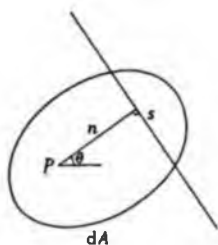


FIGURE 6. The length s of contour intercepted by a small element of area dA .

Let P be any fixed point in the plane, and dA the area of a small region surrounding P (see figure 6). Let s denote the length of a contour $\zeta = \zeta_0$ intercepted by the region dA , and let n denote the perpendicular distance of the contour from P . Suppose that the magnitude α and direction θ of the gradient are fixed. Then the height ζ of the surface at P is given by

$$|\zeta - \zeta_0| = \alpha n. \quad (2 \cdot 3 \cdot 1)$$

For the contour to cut the element of area, the perpendicular n and the height ζ must lie in certain small ranges (n_1, n_2) and (ζ_1, ζ_2) . If now α, θ are allowed to vary within small ranges $(\alpha, \alpha + d\alpha)$, $(\theta + d\theta)$, the expectation $\bar{s}_{\alpha, \theta} dA d\alpha d\theta$ of s over the area dA is given by

$$\bar{s}_{\alpha, \theta} dA d\alpha d\theta = \int_{\zeta_1}^{\zeta_2} s p(\zeta, \alpha, \theta) d\zeta d\alpha d\theta = \int_{n_1}^{n_2} s p(\zeta, \alpha, \theta) \alpha dn d\alpha d\theta, \quad (2 \cdot 3 \cdot 2)$$

where $p(\zeta, \alpha, \theta)$ denotes the joint distribution of ζ, α, θ at P . Since ζ, α, θ are nearly constant over the small range of integration of n we have

$$\bar{s}_{\alpha, \theta} dA = \alpha p(\zeta, \alpha, \theta) \int_{n_1}^{n_2} s dn = \alpha p(\zeta, \alpha, \theta) dA, \quad (2 \cdot 3 \cdot 3)$$

and so

$$\bar{s}_{\alpha, \theta} = \alpha p(\zeta, \alpha, \theta). \quad (2 \cdot 3 \cdot 4)$$

Integrating over all possible values of α, θ we have

$$\bar{s} = \int_0^{\infty} \int_0^{2\pi} \bar{s}_{\alpha, \theta} d\alpha d\theta = \int_0^{\infty} \int_0^{2\pi} \alpha p(\zeta, \alpha, \theta) d\alpha d\theta. \quad (2 \cdot 3 \cdot 5)$$

Now from § 2.1

$$p(\zeta, \alpha, \theta) = p(\zeta) p(\alpha, \theta), \quad (2 \cdot 3 \cdot 6)$$

where $p(\xi)$ is given by (2.1.8), with $\xi_1 = \xi$, and $p(\alpha, \theta)$ is given by (2.1.20). On substituting these values in (2.3.5) we have

$$\bar{s} = \frac{1}{(2\pi)^{\frac{1}{2}} (m_{00}\Delta_2)^{\frac{1}{2}}} \exp\{-\xi^2/2m_{00}\} \int_0^{2\pi} \int_0^{2\pi} \alpha^2 \exp\{-a^2(m_{02}\cos^2\theta + m_{20}\sin^2\theta)/2\Delta_2\} d\alpha d\theta. \quad (2.3.7)$$

(It has been supposed that the x axis is taken in the principal direction, so that m_{11} vanishes.) Integration with respect to α gives

$$\bar{s} = \frac{\Delta_2}{4\pi m_{00}^{\frac{1}{2}}} \exp\{-\xi^2/2m_{00}\} \int_0^{2\pi} \frac{d\phi}{(m_{02}\sin^2\phi + m_{20}\cos^2\phi)^{\frac{1}{2}}}, \quad (2.3.8)$$

where $\phi = \theta + \frac{1}{2}\pi$. That is to say

$$\bar{s} = \frac{m_{\epsilon 2}}{\pi(m_{00}m_{20})^{\frac{1}{2}}} \exp\{-\xi^2/2m_{00}\} \int_0^{\frac{1}{2}\pi} \frac{d\phi}{(1-k^2\sin^2\phi)^{\frac{1}{2}}}, \quad (2.3.9)$$

where

$$k^2 = 1 - \gamma^2. \quad (2.3.10)$$

Now since

$$\frac{d}{d\phi} \frac{k^2 \sin\phi \cos\phi}{(1-k^2\sin^2\phi)^{\frac{1}{2}}} = (1-k^2\sin^2\phi)^{-\frac{1}{2}} + \frac{k^2-1}{(1-k^2\sin^2\phi)^{\frac{3}{2}}}, \quad (2.3.11)$$

it follows, on integration between 0 and $\frac{1}{2}\pi$, that

$$(1-k^2) \int_0^{\frac{1}{2}\pi} \frac{d\phi}{(1-k^2\sin^2\phi)^{\frac{1}{2}}} = \int_0^{\frac{1}{2}\pi} (1-k^2\sin^2\phi)^{-\frac{1}{2}} d\phi = E(k), \quad (2.3.12)$$

where $E(k)$ is Legendre's complete elliptic integral of the first kind (Legendre 1811). Hence we have finally

$$\bar{s} = \frac{1}{\pi} \left(\frac{m_{20} + m_{02}}{m_{00}} \right)^{\frac{1}{2}} \exp\{-\xi^2/2m_{00}\} (1+\gamma^2)^{-\frac{1}{2}} E\{\sqrt{1-\gamma^2}\}. \quad (2.3.13)$$

In the special case of long-crested waves, when $\gamma = 0$, we have $E(1) = 1$ and further

$$m_{20} = m_2(0), \quad m_{02} = 0, \quad (2.3.14)$$

giving

$$\bar{s} = \frac{1}{\pi} \left(\frac{m_2(0)}{m_{00}} \right)^{\frac{1}{2}} \exp\{-\xi^2/2m_{00}\}. \quad (2.3.15)$$

Comparison with (2.2.12) shows what we might expect, namely, that the mean length of contour per unit area is equal to the mean number of crossings of the contour level per unit distance by a plane perpendicular to the wave crests.

In general (2.3.13) may be written

$$\bar{s} = \frac{1}{\pi} \left(\frac{m_{20} + m_{02}}{m_{00}} \right)^{\frac{1}{2}} \exp\{-\xi^2/2m_{00}\} f(\gamma), \quad (2.3.16)$$

where

$$f(\gamma) = (1+\gamma^2)^{-\frac{1}{2}} E\{\sqrt{1-\gamma^2}\}. \quad (2.3.17)$$

This function is shown in figure 7. At the two extreme values we have

$$f(0) = 1 \quad (2.3.18)$$

and

$$f(1) = \frac{\pi}{2\sqrt{2}} = 1.1107 \dots \quad (2.3.19)$$

STATISTICAL ANALYSIS OF A RANDOM, MOVING SURFACE 347

Throughout its whole range the function departs very little from unity. There is, however, a weak singularity at the origin, where

$$f(\gamma) = 1 + \frac{1}{2}\gamma^2 \left(\ln \frac{4}{\gamma} - \frac{3}{2} \right) + O(\gamma^2 \ln \gamma). \quad (2.3.20)$$

A very closely related distribution is that of the direction θ of the normal to a given contour. Let us suppose that θ is measured at points randomly and uniformly distributed along the contour. θ is also the direction of the surface gradient at the point of measurement. However, the distribution of θ for a given contour is quite distinct from the distribution of θ found in § 2.1, where it was supposed that the angle was measured, not on a particular contour but at points randomly distributed in the x, y plane.

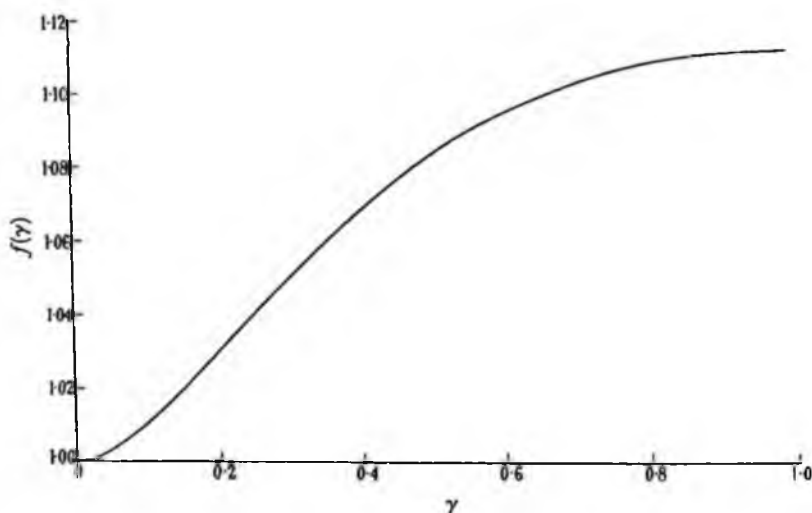


FIGURE 7. Graph of $f(\gamma) = (1 + \gamma^2)^{-1/2} E\{\sqrt{1 - \gamma^2}\}$.

To find the distribution $p(\theta)_\zeta$ for the contour $\zeta = \text{constant}$ we may note that the contribution of a given length of arc to the distribution of θ in the interval $(\theta, \theta + d\theta)$ is simply proportional to the expected length of arc for which θ lies between these limits, that is,

$$p(\theta)_\zeta d\theta \propto \int_0^\infty \bar{s}_{\alpha, \theta} d\alpha d\theta. \quad (2.3.21)$$

On normalizing the right-hand side by dividing by \bar{s} we have

$$p(\theta)_\zeta = \frac{1}{\bar{s}} \int_0^\infty \bar{s}_{\alpha, \theta} d\alpha = \frac{1}{\bar{s}} \int_0^\infty \alpha p(\zeta, \alpha, \theta) d\alpha. \quad (2.3.22)$$

Substituting from (2.3.6) and (2.3.13), and carrying out the integration we find

$$p(\theta)_\zeta = \frac{1}{4E\{\sqrt{1 - \gamma^2}\}} \frac{\gamma^2}{(\gamma^2 \cos^2 \theta + \sin^2 \theta)^{3/2}} \quad (2.3.23)$$

(where $\theta = 0$ is chosen as the principal direction). The form of this expression is somewhat similar to (2.1.37). When $\gamma = 1$ (for short-crested waves)

$$p(\theta)_{\zeta} = \frac{1}{2\pi}, \quad (2.3.24)$$

i.e. the contours have no preferential direction. As γ diminishes the distribution becomes more and more concentrated about the mean direction $\theta = 0$. When γ is small, we have for general directions

$$p(\theta)_{\zeta} = \frac{\gamma^2}{4 \sin^2 \theta}, \quad (2.3.25)$$

which tends to zero as $\gamma \rightarrow 0$. But near the mean direction, that is, when θ is comparable with γ ,

$$p(\theta)_{\zeta} = \frac{\gamma^2}{4(\gamma^2 + \theta^2)^{\frac{1}{2}}}. \quad (2.3.26)$$

The integral of this expression from $\theta/\gamma = -\infty$ to ∞ is equal to $\frac{1}{2}$. Thus the probability that θ is near zero is $\frac{1}{2}$, and so also is the probability that θ is near π . Hence it becomes highly probable that the direction of the contour is near the principal direction.

2.4. The density of maxima and minima

Let us consider now the problem of how many maxima and minima (humps and hollows) the surface possesses, on the average, per unit area.

At a maximum or a minimum the two components of gradient $\partial\zeta/\partial x$, $\partial\zeta/\partial y$ must vanish. But not all such points are maxima or minima; we may also have a col or saddle-point, where the surface tends to rise in one pair of opposite directions and fall in another pair of opposite directions. We shall prove the following theorem:

On a statistically uniform surface the average density of maxima per unit area plus the average density of minima is equal to the average density of saddle-points, or

$$D_{ma.} + D_{mi.} = D_{sa.} \quad (2.4.1)$$

Let a contour map of the surface be drawn, and let a direction ϕ be assigned to each contour, say to the right when facing up-hill. Thus at each point of the plane, except the stationary points, there is a unique direction ϕ . Consider now the variation of ϕ round a small closed curve C on the map (see figure 8). C may at first be so small as to contain no stationary point, in which case ϕ will return to its initial value after the circuit is completed (figure 8 a). If now C is expanded so as to enclose a single stationary point, ϕ will increase by 2π on completion of the circuit C if the stationary point is a maximum or a minimum (figure 8 b and c), and will decrease by 2π if the stationary point is a saddle-point (figure 8 d). As C is further increased in size, so as to enclose $d_{ma.}$ maxima, $d_{mi.}$ minima and $d_{sa.}$ saddle-points, say, the variation of ϕ round C will be $2\pi(d_{ma.} + d_{mi.} - d_{sa.})$, or $2\pi A(D_{ma.} + D_{mi.} - D_{sa.})$ approximately, where A is the area enclosed by C . But since the surface is statistically uniform, the variation of ϕ round C will increase proportionally to L at most, where L is the circumference of C .* On the other hand A increases like L^2 , supposing C is of constant shape. Thus $2\pi(D_{ma.} + D_{mi.} - D_{sa.})$ is proportional to L^{-1} at most, and letting L tend to infinity we see that $(D_{ma.} + D_{mi.} - D_{sa.})$ must vanish. This proves the result.

* In fact it may be shown that the increase is proportional only to $L^{\frac{1}{2}}$.

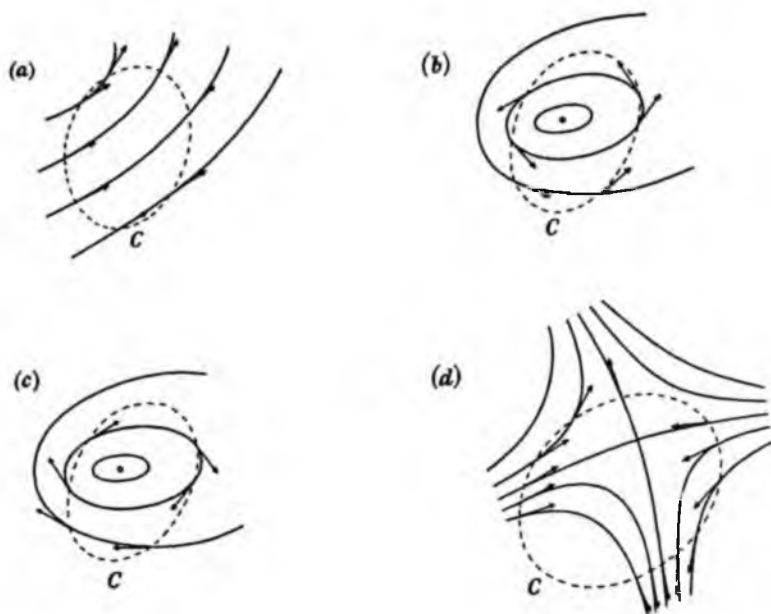


FIGURE 8. Illustrating the way in which the contour direction varies round a curve enclosing (a) no stationary point, (b) a maximum, (c) a minimum and (d) a saddle-point.

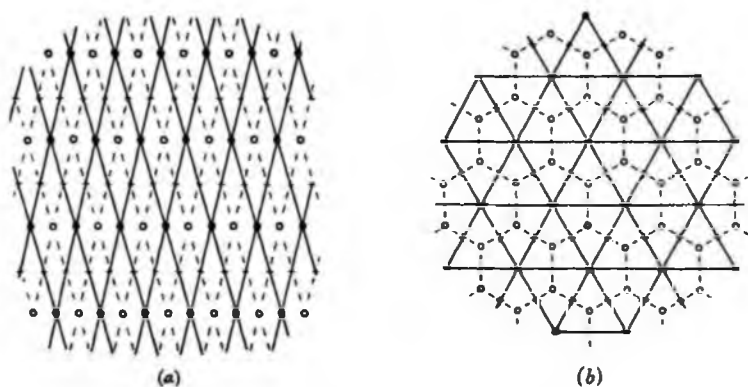


FIGURE 9. (a) Stationary points on a surface which consists of two intersecting wave systems. ● = a maximum, ○ = a minimum, + = a saddle-point. (b) Stationary points in a hexagonal pattern.

A simple example is shown in figure 9 *a*. The surface consists of two long-crested systems of waves of slowly varying amplitude. Where a crest from one system intersects a crest from the other system there is a maximum, and where two troughs intersect there is a minimum. But where a crest from one system intersects a trough from the other there is a saddle-point.

The pattern of saddle-points is similar and congruent to the pattern of maxima and minima together, so that (2.4.1) is satisfied.

On this surface the density of maxima is equal to the density of minima. But a case in which this is not so is illustrated in figure 9*b*. Here the maxima are at the centres of the cells of a hexagonal honeycomb, the minima are at the vertices and the saddle-points are half-way along the edges. There are twice as many maxima as minima, and three times as many saddle-points, so that

$$D_{ma.} = \frac{2}{3}D_{sa.}, \quad D_{mi.} = \frac{1}{3}D_{sa.}. \quad (2.4.2)$$

In general it can be shown that the stationary points must form a cellular pattern, and the theorem (2.4.1) then follows from Euler's relation $V + F = E + 2$ connecting the number of vertices V , faces F and edges E of a convex polyhedron (Euler 1752-3; Sommerville 1929, chap. ix).

The class of random surface represented by (1.2.1) satisfies the further relation

$$D_{ma.} = D_{mi.}. \quad (2.4.3)$$

For the phases ϵ_n of the component waves are randomly and uniformly distributed between 0 and 2π . The statistical properties of the surface are unaffected if a constant, π , is added to each phase. But this reverses the sign of ζ and converts maxima into minima, and vice versa.

From (2.4.1) and (2.4.3) it follows that

$$D_{sa.} = 2D_{ma.} = 2D_{mi.} \quad (2.4.4)$$

and if $D_{sta.}$ denotes the total density of stationary points per unit area of the surface

$$D_{sta.} = 2D_{sa.} = 4D_{ma.} = 4D_{mi.}. \quad (2.4.5)$$

In other words, of all the stationary points on the surface, one-quarter are maxima, one-quarter are minima, and the remaining half are saddle-points.

We proceed now to evaluate $D_{sta.}$ in terms of the energy spectrum of ζ . The variables entering the problem are

$$\frac{\partial \zeta}{\partial x}, \frac{\partial \zeta}{\partial y} = \xi_2, \xi_3 \quad (2.4.6)$$

and

$$\frac{\partial^2 \zeta}{\partial x^2}, \frac{\partial^2 \zeta}{\partial x \partial y}, \frac{\partial^2 \zeta}{\partial y^2} = \xi_4, \xi_5, \xi_6. \quad (2.4.7)$$

say. (ξ_2, ξ_3) is a pair of functions of (x, y) , and if (x, y) varies within a certain small region dA , $= (x, x + dx; y, y + dy)$, (ξ_2, ξ_3) will vary within a region $d\Sigma$ of area

$$|d\Sigma| = |J| |dA|, \quad (2.4.8)$$

where

$$J = \frac{\partial(\xi_2, \xi_3)}{\partial(x, y)} = \xi_4 \xi_6 - \xi_5^2. \quad (2.4.9)$$

The probability that a given point, say a stationary point, lies in dA is equal to the probability that (ξ_2, ξ_3) lies in the corresponding region $d\Sigma$, which is

$$\int_{-\infty}^{\infty} \int_{-\infty}^{\infty} \int_{-\infty}^{\infty} d\xi_4 d\xi_5 d\xi_6 \iint_{d\Sigma} d\xi_2 d\xi_3 p(\xi_2, \xi_3, \xi_4, \xi_5, \xi_6). \quad (2.4.10)$$

Since $(\xi_2, \xi_3) = (0, 0)$ somewhere in $d\Sigma$, $p(\xi_2, \xi_3, \xi_4, \xi_5, \xi_6)$ may be replaced by

$$p(0, 0, \xi_4, \xi_5, \xi_6)$$

when $d\mathcal{E}$ is sufficiently small, and since

$$\iint_{d\mathcal{E}} d\xi_2 d\xi_3 = |d\mathcal{E}|, \tag{2.4.11}$$

the above probability becomes

$$\int_{-\infty}^{\infty} \int_{-\infty}^{\infty} \int_{-\infty}^{\infty} d\xi_4 d\xi_5 d\xi_6 |d\mathcal{E}| p(0, 0, \xi_4, \xi_5, \xi_6). \tag{2.4.12}$$

On substituting from (2.4.8) we have for the probability of a stationary value of ζ in dA ,

$$D_{sta.} dA = \int_{-\infty}^{\infty} \int_{-\infty}^{\infty} \int_{-\infty}^{\infty} p(0, 0, \xi_4, \xi_5, \xi_6) | \xi_4 \xi_6 - \xi_5^2 | d\xi_4 d\xi_5 d\xi_6 dA. \tag{2.4.13}$$

For a true maximum of the surface we must have $\xi_4 \leq 0, \xi_5 \leq 0$ and $J \geq 0$; for a true minimum, $\xi_4 \geq 0, \xi_5 \geq 0$ and $J \leq 0$. Thus the true maxima and minima correspond to the region of the (ξ_4, ξ_5, ξ_6) space given by

$$J \equiv \xi_4 \xi_6 - \xi_5^2 \geq 0. \tag{2.4.14}$$

The boundary of this region is the surface $J = 0$, which is a cone with vertex at the origin. The remaining part of the (ξ_4, ξ_5, ξ_6) space corresponds to the saddle-points.

Now since the second derivatives ξ_4, ξ_5, ξ_6 are uncorrelated with the first derivatives ξ_2, ξ_3 (see § 2.1) it follows that

$$p(\xi_2, \xi_3, \xi_4, \xi_5, \xi_6) = p(\xi_2, \xi_3) p(\xi_4, \xi_5, \xi_6), \tag{2.4.15}$$

where $p(\xi_2, \xi_3)$ is given by (2.1.12) and $p(\xi_4, \xi_5, \xi_6)$ is the distribution for (ξ_4, ξ_5, ξ_6) independently of the other variables. The matrix of correlations is

$$(\Xi_{ij}) = \begin{pmatrix} m_{40} & m_{31} & m_{22} \\ m_{31} & m_{22} & m_{13} \\ m_{22} & m_{13} & m_{04} \end{pmatrix}, \tag{2.4.16}$$

and hence

$$p(\xi_4, \xi_5, \xi_6) = \frac{1}{(2\pi)^3 \Delta_4} \exp \left\{ -\frac{1}{2} M_{ij} \xi_{i+3} \xi_{j+3} \right\}, \tag{2.4.17}$$

where (M_{ij}) is the inverse matrix to (Ξ_{ij}) and

$$\Delta_4 = | \Xi_{ij} |. \tag{2.4.18}$$

Therefore, altogether we have for the density of stationary points

$$D_{sta.} = \frac{1}{(2\pi)^3 \Delta_4 \Delta_4} \int_{-\infty}^{\infty} \int_{-\infty}^{\infty} \int_{-\infty}^{\infty} \exp \left\{ -\frac{1}{2} M_{ij} \xi_{i+3} \xi_{j+3} \right\} | \xi_4 \xi_6 - \xi_5^2 | d\xi_4 d\xi_5 d\xi_6. \tag{2.4.19}$$

The density of maxima is given by a similar integral taken over the region $\xi_4 \leq 0, \xi_5 \leq 0, J \geq 0$. The density of saddle-points is given by the same integral taken over the region $J < 0$.

Since (Ξ_{ij}) is a positive-definite matrix, so also is its inverse (M_{ij}) , and there exists a real linear transformation

$$(\xi_4, \xi_5, \xi_6) = T(\eta_1, \eta_2, \eta_3) \tag{2.4.20}$$

which simultaneously reduces the exponent in (2.4.19) to the unit form

$$M_{ij} \xi_{i+3} \xi_{j+3} = \eta_1^2 + \eta_2^2 + \eta_3^2 \tag{2.4.21}$$

and J to a diagonal form

$$\xi_4 \xi_6 - \xi_5^2 = l_1 \eta_1^2 + l_2 \eta_2^2 + l_3 \eta_3^2. \tag{2.4.22}$$

The quantities l_1, l_2, l_3 are easily found, for they are the roots of

$$|\sigma_{ij} - lM_{ij}| = 0, \quad (2.4.23)$$

where (σ_{ij}) is the matrix of J :

$$(\sigma_{ij}) = \begin{pmatrix} 0 & 0 & \frac{1}{2} \\ 0 & -1 & 0 \\ \frac{1}{2} & 0 & 0 \end{pmatrix}. \quad (2.4.24)$$

On multiplying (2.4.23) by $|\Xi_{ij}| = |M_{ij}^{-1}|$, we have

$$|\Xi_{ij}\sigma_{jk} - l\delta_{ik}| = 0, \quad (2.4.25)$$

where δ_{ij} is the unit matrix of order 3. In other words l_1, l_2, l_3 are the latent roots of $(\Xi_{ij}\sigma_{jk})$:

$$\begin{vmatrix} \frac{1}{2}m_{22} - l & -m_{31} & \frac{1}{2}m_{40} \\ \frac{1}{2}m_{13} & -m_{22} - l & \frac{1}{2}m_{31} \\ \frac{1}{2}m_{04} & -m_{13} & \frac{1}{2}m_{22} - l \end{vmatrix} = 0. \quad (2.4.26)$$

On expanding the determinant we find

$$4l^3 - 3Hl - \Delta_4 = 0, \quad (2.4.27)$$

where

$$3H = m_{40}m_{04} - 4m_{31}m_{13} + 3m_{22}^2. \quad (2.4.28)$$

Hence

$$l_1 + l_2 + l_3 = 0 \quad (2.4.29)$$

and

$$l_1 l_2 l_3 = \frac{1}{4}\Delta_4 > 0. \quad (2.4.30)$$

It follows that one of the roots, say l_1 , is positive and the other two, say l_2, l_3 , are negative.

We write

$$l_1 > 0 > l_2 \geq l_3. \quad (2.4.31)$$

The solution of the cubic equation (2.4.27) is

$$(l_1, l_2, l_3) = H^{\frac{1}{3}}(\cos \psi_1, \cos \psi_2, \cos \psi_3), \quad (2.4.32)$$

where ψ_1, ψ_2, ψ_3 are the roots of

$$\cos 3\psi = \Delta_4/H^{\frac{1}{3}}. \quad (2.4.33)$$

The modulus of the transformation T is

$$\frac{\partial(\xi_4, \xi_5, \xi_6)}{\partial(\eta_1, \eta_2, \eta_3)} = |M_{ij}|^{-\frac{1}{2}} = \Delta_4^{\frac{1}{2}}. \quad (2.4.34)$$

We find then

$$D_{\text{stab.}} = \frac{1}{(2\pi)^{\frac{1}{2}} \Delta_4^{\frac{1}{2}}} I(l_1, l_2, l_3), \quad (2.4.35)$$

where

$$I(l_1, l_2, l_3) = \int_{-\infty}^{\infty} \int_{-\infty}^{\infty} \int_{-\infty}^{\infty} \exp\{-\frac{1}{2}(\eta_1^2 + \eta_2^2 + \eta_3^2)\} |l_1 \eta_1^2 + l_2 \eta_2^2 + l_3 \eta_3^2| d\eta_1 d\eta_2 d\eta_3. \quad (2.4.36)$$

The density of maxima is given by

$$D_{\text{ma.}} = \frac{1}{(2\pi)^{\frac{1}{2}} \Delta_4^{\frac{1}{2}}} I'(l_1, l_2, l_3), \quad (2.4.37)$$

where

$$I'(l_1, l_2, l_3) = \iiint \exp\{-\frac{1}{2}(\eta_1^2 + \eta_2^2 + \eta_3^2)\} |l_1 \eta_1^2 + l_2 \eta_2^2 + l_3 \eta_3^2| d\eta_1 d\eta_2 d\eta_3, \quad (2.4.38)$$

and V is the conical region

$$\eta_1 > 0, \quad l_1 \eta_1^2 + l_2 \eta_2^2 + l_3 \eta_3^2 > 0. \quad (2.4.39)$$

Clearly $4I' - I = \int_{-\infty}^{\infty} \int_{-\infty}^{\infty} \int_{-\infty}^{\infty} \exp\{-\frac{1}{2}(\eta_1^2 + \eta_2^2 + \eta_3^2)\} (l_1 \eta_1^2 + l_2 \eta_2^2 + l_3 \eta_3^2) d\eta_1 d\eta_2 d\eta_3,$
 $= (2\pi)^{\frac{3}{2}} (l_1 + l_2 + l_3), \quad (2.4.40)$

which vanishes, by (2.4.29). Thus

$$I = 4I', \quad D_{\text{sta}} = 4D_{\text{ma}}, \quad (2.4.41)$$

in agreement with (2.4.5).

The integral I' may be evaluated by means of the substitution

$$\left. \begin{aligned} \eta_1 &= l_1^{-\frac{1}{2}} r, \\ \eta_2 &= (-l_2)^{-\frac{1}{2}} r \sin \theta \cos \chi, \\ \eta_3 &= (-l_3)^{-\frac{1}{2}} r \sin \theta \sin \chi, \end{aligned} \right\} \quad (2.4.42)$$

where

$$0 < r < \infty, \quad 0 < \theta < \frac{1}{2}\pi, \quad 0 < \chi < 2\pi. \quad (2.4.43)$$

We have then

$$I' = \frac{1}{(l_1 l_2 l_3)^{\frac{1}{2}}} \int_0^{\infty} dr \int_0^{\frac{1}{2}\pi} d\theta \int_0^{2\pi} d\chi \exp\{-(1 + f \sin^2 \theta) r^2 / 2l_1\} r^4 \cos^3 \theta \sin \theta, \quad (2.4.44)$$

where

$$f = f(\chi) = -\frac{l_1}{l_2} \cos^2 \chi - \frac{l_1}{l_3} \sin^2 \chi. \quad (2.4.45)$$

Integration with respect to r gives

$$I' = 3(\frac{1}{2}\pi)^{\frac{1}{2}} \frac{l_1^{\frac{1}{2}}}{(l_2 l_3)^{\frac{1}{2}}} \int_0^{\frac{1}{2}\pi} d\theta \int_0^{2\pi} d\chi \frac{\cos^3 \theta \sin \theta}{(1 + f \sin^2 \theta)^{\frac{1}{2}}}. \quad (2.4.46)$$

Further integration with respect to θ gives

$$I' = 4(\frac{1}{2}\pi)^{\frac{1}{2}} \frac{l_1^{\frac{1}{2}}}{(l_2 l_3)^{\frac{1}{2}}} \int_0^{1/2\pi} d\chi \left[\frac{1}{f} - \frac{2}{f^2} + \frac{2}{f^2(1+f)} \right]. \quad (2.4.47)$$

This is an elliptic integral and may be evaluated by known methods (Legendre 1811). We find finally

$$I' = (8\pi)^{\frac{1}{2}} \left[(l_2 l_3)^{\frac{1}{2}} \left\{ \left(\frac{l_2 - l_1}{l_2} \right)^{\frac{1}{2}} E(k, \frac{1}{2}\pi) - \left(\frac{l_2}{l_2 - l_1} \right)^{\frac{1}{2}} F(k, \frac{1}{2}\pi) \right\} \right. \\ \left. - (l_1 + l_2 + l_3) \{ F(k', \phi) E(k, \frac{1}{2}\pi) + E(k', \phi) F(k, \frac{1}{2}\pi) - F(k', \phi) F(k, \frac{1}{2}\pi) - \frac{1}{2}\pi \} \right], \quad (2.4.48)$$

where E and F are the Legendre elliptic integrals of the first and second kind:

$$\left. \begin{aligned} E(k, \phi) &= \int_0^{\phi} (1 - k^2 \sin^2 \phi)^{\frac{1}{2}} d\phi, \\ F(k, \phi) &= \int_0^{\phi} (1 - k^2 \sin^2 \phi)^{-\frac{1}{2}} d\phi, \end{aligned} \right\} \quad (2.4.49)$$

and $k^2 = \frac{l_1(l_3 - l_2)}{l_3(l_1 - l_2)}, \quad k'^2 = 1 - k^2 = \frac{l_2(l_1 - l_3)}{l_3(l_1 - l_2)}, \quad \phi = \tan^{-1} \left(-\frac{l_3}{l_1} \right)^{\frac{1}{2}}. \quad (2.4.50)$

If we now make use of the condition (2.4.29) we find for the density of maxima

$$D_{\text{ma}} = \frac{1}{2\pi^2} \frac{(l_2 l_3)^{\frac{1}{2}}}{\Delta^{\frac{1}{2}}} \left[\left(\frac{l_2 - l_1}{l_2} \right)^{\frac{1}{2}} E(k, \frac{1}{2}\pi) - \left(\frac{l_2}{l_2 - l_1} \right)^{\frac{1}{2}} F(k, \frac{1}{2}\pi) \right]. \quad (2.4.51)$$

The density of stationary points D_{sta} is four times this value.

Equation (2.4.51) may also be written

$$D_{\text{ma}} = \frac{1}{2\pi^2} \frac{l_1}{\Delta_1^{\frac{1}{2}}} \Phi(-l_2/l_1), \quad (2.4.52)$$

where

$$\left. \begin{aligned} \Phi(\alpha) &= \{\alpha(1-\alpha)\}^{\frac{1}{2}} \left[\left(\frac{1+\alpha}{\alpha} \right)^{\frac{1}{2}} E(k, \frac{1}{2}\pi) - \left(\frac{\alpha}{1+\alpha} \right)^{\frac{1}{2}} F(k, \frac{1}{2}\pi) \right], \\ k^2 &= \frac{1-2\alpha}{1-\alpha^2} \quad (0 < \alpha \leq \frac{1}{2}). \end{aligned} \right\} \quad (2.4.53)$$

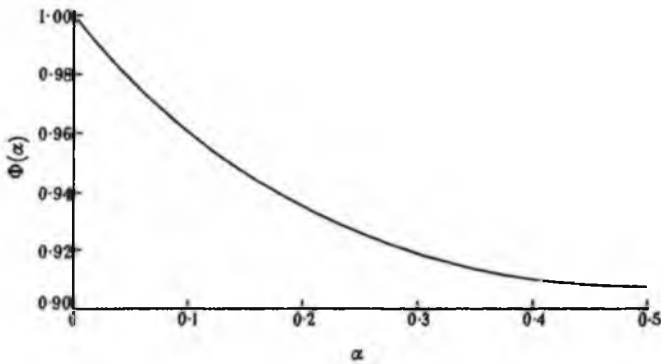


FIGURE 10. Graph of $\Phi(\alpha)$ (defined by (2.4.53)).

The form of $\Phi(\alpha)$ is shown in figure 10. When $\alpha \rightarrow 0$, $k^2 \rightarrow 1$ and $F(k, \frac{1}{2}\pi) \rightarrow \infty$ logarithmically. Hence $\alpha F(k, \frac{1}{2}\pi) \rightarrow 0$ and

$$\lim_{\alpha \rightarrow 0} \Phi(\alpha) = 1. \quad (2.4.54)$$

Also when $\alpha = \frac{1}{2}$, $k^2 = 0$ and so

$$\Phi\left(\frac{1}{2}\right) = (3^{\frac{1}{2}} - 3^{-\frac{1}{2}}) \pi/4 = 0.917 \dots \quad (2.4.55)$$

Throughout the whole of its range, Φ departs very little from unity.

A particularly interesting case is when the energy spectrum $E(u, v)$ is narrow. Let us take axes of (u, v) so that the u axis passes through the centroid (\bar{u}, \bar{v}) , making $\bar{v} = 0$. Then on substituting from (1.6.8 and 1.6.9) and retaining only the terms of highest order we find

$$\left. \begin{aligned} \Delta_2 &= \bar{u}^2 \mu_{00} \mu_{02}, \\ 3H &= \bar{u}^4 (\mu_{00} \mu_{04} + 3\mu_{02}^2), \\ \Delta_4 &= \bar{u}^6 (\mu_{00} \mu_{02} \mu_{04} - \mu_{00} \mu_{03}^2 - \mu_{02}^3). \end{aligned} \right\} \quad (2.4.56)$$

Now μ_{00} , μ_{02} , μ_{03} , μ_{04} are moments of the energy spectrum E_{\perp} of a section of the surface at right angles to the mean direction. We have

$$\mu_{02} = (\gamma \bar{u})^2 m_{00}, \quad \mu_{03} = b(\gamma \bar{u})^3 m_{00}, \quad \mu_{04} = a^2 (\gamma \bar{u})^4 m_{00}, \quad (2.4.57)$$

where γ^{-1} is the long-crestedness (defined in § 1.4), a^2 is a non-dimensional parameter (always greater than 1) which represents the peakedness of the spectrum E_{\perp} , and b is a

STATISTICAL ANALYSIS OF A RANDOM, MOVING SURFACE 355

measure of the asymmetry of E_{ψ} , about its mean (but is independent of the angle of skewness β). If we assume $\mu_{03} = 0$ and so $b = 0$, we have

$$\left. \begin{aligned} \Delta_2 &= (\gamma \bar{u}^2)^2 m_{00}^2, \\ H &= (\gamma \bar{u}^2)^4 m_{00}^2 (1 + a^2/3), \\ \Delta_4 &= (\gamma \bar{u}^2)^6 m_{00}^2 (a^2 - 1) \end{aligned} \right\} \quad (2.4.58)$$

and so from (2.4.32)

$$(l_1, l_2, l_3) = (\gamma \bar{u}^2)^2 m_{00} (1 + a^2/3)^{1/2} (\cos \psi_1, \cos \psi_2, \cos \psi_3), \quad (2.4.59)$$

where
$$\cos 3\psi = \frac{a^2 - 1}{(1 + a^2/3)^{1/2}}. \quad (2.4.60)$$

Thus from (2.4.52) we have
$$D_{\text{ma.}} = \gamma \bar{u}^2 C(a), \quad (2.4.61)$$

where
$$C(a) = \frac{1}{2\pi^2} (1 + a^2/3)^{1/2} \cos \psi_1 \Phi\left(-\frac{\cos \psi_2}{\cos \psi_1}\right), \quad (2.4.62)$$

which is a quantity depending only on the peakedness a . For a given peakedness, $D_{\text{ma.}}$ is proportional to the square of the wave-number of the carrier wave and inversely proportional to the long-crestedness γ^{-1} . To illustrate the effect of varying peakedness, $C(a)$ has been computed for a number of different values of a , including some interesting special cases. The results are given in table 1.

TABLE 1

a^2	$C(a)$	a^2	$C(a)$	a^2	$C(a)$
1	0.0507	4	0.0895	8	0.0880
$\frac{4}{3}$	0.0562	5	0.0747	9	0.0919
2	0.0578	6	0.0794	10	0.0956
3	0.0639	7	0.0838	20	0.1265

$a^2 = 1$ corresponds to a pair of intersecting wave trains, for then Δ_4 vanishes (by (2.4.54)), which is the condition for the spectrum to degenerate into two one-dimensional spectra (equation (1.3.7)). In the limit as $a^2 \rightarrow 1$ we find from (2.4.60) that

$$(\psi_1, \psi_2, \psi_3) = (\pm \frac{1}{3}\pi, \pm \frac{1}{3}\pi, \pm \frac{2}{3}\pi),$$

and hence

$$C = \frac{1}{2\pi^2} = 0.05066 \dots \quad (2.4.63)$$

This is what we should expect, for the wavelengths of the pattern in the u direction and the v direction are $2\pi/\bar{u}$ and $2\pi/\gamma\bar{u}$ respectively. Reference to figure 9 *a* will show that each maximum is at the centre of a parallelogram (bounded by troughs) whose diagonals are of length $2\pi/\bar{u}$ and $2\pi/\gamma\bar{u}$, and whose area is therefore $2\pi^2/\gamma\bar{u}^2$. The density of maxima is the reciprocal of this area, i.e. $\gamma\bar{u}^2/2\pi^2$.

The case $a^2 = \frac{4}{3}$ has been included, since this is the peakedness of a low-pass spectrum, when the wave energy is uniformly distributed with regard to direction over a narrow sector. $a^2 = 3$ corresponds to a normal distribution of energy with regard to direction. Another special case is $a^2 = 9$, when $(\psi_1, \psi_2, \psi_3) = (0, \pm \frac{2}{3}\pi, \pm \frac{2}{3}\pi)$, and so

$$C = \frac{1}{4\pi} (3^{1/2} - 3^{-1/2}) = 0.09189 \dots \quad (2.4.64)$$

Finally as $a \rightarrow \infty$ we find

$$C \sim \frac{a}{4\pi^2} \rightarrow \infty. \quad (2.4.65)$$

On the whole, however, the variation of C with a is slight. As a^2 increases from 0 to 10, C is less than doubled.

The density of *specular points*, i.e. points on the surface where the gradient takes a given value, not necessarily zero, may be found similarly. For it is only necessary to replace $p(0, 0, \xi_4, \xi_5, \xi_6)$ in equation (2.4.13) by $p(\xi_2, \xi_3, \xi_4, \xi_5, \xi_6)$, and, from equation (2.4.16), this amounts to multiplying by the exponential factor in (2.1.12). So the density D_{sp} of specular points with gradient (ξ_2, ξ_3) is given by

$$D_{sp} = 4D_{ma} \exp\{- (m_{02}\xi_2^2 - 2m_{11}\xi_2\xi_3 + m_{20}\xi_3^2)/2\Delta_2\}, \quad (2.4.66)$$

where D_{ma} is the density of maxima.

2.5. The velocities of zeros along a line

In this and the following two sections will be considered some statistical properties of the surface which depend on its motion, that is to say properties involving the time t .

Let $\zeta(x', t)$ denote the curve in which the surface is intersected by a fixed vertical plane in direction θ . Consider the movement of a point where the curve crosses a fixed level ζ . If x' and $x' + dx'$ are its co-ordinates at two successive instants of time t and $t + dt$, then we have

$$0 = d\zeta = \frac{\partial\zeta}{\partial x'} dx' + \frac{\partial\zeta}{\partial t} dt. \quad (2.5.1)$$

Therefore the velocity of the point is given by

$$c = \frac{dx'}{dt} = - \frac{\partial\zeta/\partial t}{\partial\zeta/\partial x'}. \quad (2.5.2)$$

Consider now the statistical distribution of c .

Let the variables ζ , $\partial\zeta/\partial x'$, $\partial\zeta/\partial t$ be denoted by ξ_1 , ξ_2 , ξ_3 respectively, so that $c = -\xi_3/\xi_2$, and let $p(\xi_1, \xi_2, \xi_3)$ denote the joint distribution of ξ_1, ξ_2, ξ_3 at an arbitrary point x' on the plane section. The probability distribution of ξ_2, ξ_3 at points x' where ξ_1 takes a given value will be denoted by $p(\xi_2, \xi_3)_{\xi_1}$. This may be found as follows. If $(x', x' + dx')$ is any fixed interval of distance, the probability of ξ_1 taking the given value in $(x', x' + dx')$ is

$$N_0(\xi_1) dx' \quad (2.5.3)$$

(evaluated in § 2.2). But if, at the point x' , the variables ξ_1, ξ_2, ξ_3 lie in certain ranges of width $d\xi_1, d\xi_2, d\xi_3$, then we have

$$d\xi_1 = |\xi_2| dx', \quad (2.5.4)$$

so that the probability of ξ_1 taking the given value in $(x', x' + dx')$ and of ξ_2, ξ_3 lying in the given range is

$$p(\xi_1, \xi_2, \xi_3) d\xi_1 d\xi_2 d\xi_3 = p(\xi_1, \xi_2, \xi_3) |\xi_2| dx' d\xi_2 d\xi_3. \quad (2.5.5)$$

The probability of ξ_2, ξ_3 lying in the ranges $d\xi_2, d\xi_3$ given that ξ_1 crosses the given level in $(x', x' + dx')$ is the quotient of (2.5.5) and (2.5.3). Hence

$$p(\xi_2, \xi_3)_{\xi_1} = \frac{p(\xi_1, \xi_2, \xi_3) |\xi_2|}{N_0(\xi_1)}. \quad (2.5.6)$$

STATISTICAL ANALYSIS OF A RANDOM, MOVING SURFACE 357

Now the matrix of correlations for ξ_1, ξ_2, ξ_3 is

$$(\Xi_{ij}) = \begin{pmatrix} m_0 & 0 & 0 \\ 0 & m_2 & m'_1 \\ 0 & m'_1 & m''_0 \end{pmatrix}, \quad (2.5.7)$$

and therefore

$$p(\xi_1, \xi_2, \xi_3) = \frac{1}{(2\pi)^{\frac{3}{2}} (m_0 \Delta_x)^{\frac{3}{2}}} \exp\{-\xi_1^2/2m_0\} \exp\{-(m_0 \xi_2^2 - 2m'_1 \xi_2 \xi_3 + m_2 \xi_3^2)/2\Delta_x\}, \quad (2.5.8)$$

where

$$\Delta_x = m_2 m''_0 - m_1'^2. \quad (2.5.9)$$

From this and (2.2.12) we have

$$p(\xi_2, \xi_3)_{\xi_1} = \frac{1}{2(2\pi)^{\frac{1}{2}} (m_2 \Delta_x)^{\frac{1}{2}}} |\xi_2| \exp\{-(m_0 \xi_2^2 - 2m'_1 \xi_2 \xi_3 + m_2 \xi_3^2)/2\Delta_x\}. \quad (2.5.10)$$

We require now the statistical distribution of $-\xi_3/\xi_2$. Writing

$$-\xi_3/\xi_2 = c, \quad \xi_3 = c' \quad (2.5.11)$$

in (2.5.10), so that

$$\frac{\partial(c, c')}{\partial(\xi_2, \xi_3)} = \frac{\xi_3}{\xi_2^2} = \frac{c^2}{c'}, \quad (2.5.12)$$

we have

$$p(c, c')_{\xi_1} = \frac{1}{2(2\pi)^{\frac{1}{2}} (m_2 \Delta_x)^{\frac{1}{2}}} \left| \frac{c'^2}{c^3} \right| \exp\{-(m_0/c^2 + 2m'_1/c + m_2) c'^2/2\Delta_x\}. \quad (2.5.13)$$

The distribution of c is found by integrating with respect to c' from $-\infty$ to ∞ . Thus

$$p(c)_{\xi_1} = \frac{1}{2} \frac{\Delta_x/m_2^{\frac{1}{2}}}{(m_0 + 2m'_1 c + m_2 c^2)^{\frac{3}{2}}}, \quad (2.5.14)$$

or

$$p(c)_{\xi_1} = \frac{1}{2} \frac{\Delta_x/m_2^{\frac{1}{2}}}{[(c - \bar{c})^2 + \Delta_x/m_2^2]^{\frac{3}{2}}}, \quad (2.5.15)$$

where

$$\bar{c} = -m'_1/m_2. \quad (2.5.16)$$

This distribution has a maximum or mode when $c = \bar{c}$ and is symmetrical about this mean value. The second moment of the distribution is divergent, but the interquartile range is given by

$$\frac{2}{\sqrt{3}} \frac{\Delta_x^{\frac{1}{2}}}{m_2}. \quad (2.5.17)$$

It will be seen that the distribution (2.5.15) is independent of the height ξ_1 at which the velocity is measured (provided this height is constant).

We may consider similarly the distribution of velocities of points on the curve having a given gradient (say, zero). The velocity of such a point is given by

$$c_1 = -\frac{\partial^2 \zeta / \partial x' \partial t}{\partial^2 \zeta / \partial x'^2}. \quad (2.5.18)$$

Hence the probability distribution is the same as for the velocities of zeros, except that the index of each of the moments is increased by two. Thus

$$p(c_1) = \frac{1}{2} \frac{\Delta_4/m_4^{\frac{1}{2}}}{[(c - \bar{c}_1)^2 + \Delta_4/m_4^2]^{\frac{3}{2}}}, \quad (2.5.19)$$

where

$$\Delta_4 = m_4 m''_2 - m_3'^2 \quad (2.5.20)$$

and

$$\bar{c}_1 = -m'_3/m_4. \quad (2.5.21)$$

This is a distribution with mean \bar{c}_1 and interquartile range equal to

$$\frac{2}{\sqrt{3}} \frac{\Delta_1^{\frac{1}{2}}}{m_4}. \quad (2.5.22)$$

Similar distributions can be written down for the velocities of points having given higher derivatives of ζ .

Let us interpret the above results for a narrow spectrum. Without loss of generality we may take the u axis to pass through the centroid. On expanding in a Taylor series about this point we have

$$\left. \begin{aligned} m_n &= u'^n \mu_{00} + \frac{1}{2} \left(\mu_{20} \frac{\partial^2}{\partial u^2} + 2\mu_{11} \frac{\partial^2}{\partial u \partial v} + \mu_{02} \frac{\partial^2}{\partial v^2} \right) u'^n + \dots, \\ m'_n &= u'^n \sigma \mu_{00} + \frac{1}{2} \left(\mu_{20} \frac{\partial^2}{\partial u^2} + 2\mu_{11} \frac{\partial^2}{\partial u \partial v} + \mu_{02} \frac{\partial^2}{\partial v^2} \right) (u'^n \sigma) + \dots, \\ m''_n &= u'^n \sigma^2 \mu_{00} + \frac{1}{2} \left(\mu_{20} \frac{\partial^2}{\partial u^2} + 2\mu_{11} \frac{\partial^2}{\partial u \partial v} + \mu_{02} \frac{\partial^2}{\partial v^2} \right) (u'^n \sigma^2) + \dots, \end{aligned} \right\} \quad (2.5.23)$$

where u' , v' and σ are to be evaluated at $(\bar{u}, 0)$. Suppose that $\theta = 0$, that is, let the plane of intersection be taken parallel to the principal direction. Then $u' = u$ and, σ being a function of $(u^2 + v^2)$ only,

$$\frac{\partial \sigma}{\partial v} = 0, \quad \frac{\partial^2 \sigma}{\partial u \partial v} = 0. \quad (2.5.24)$$

From (2.5.16) and (2.5.21) we find first

$$\bar{c} = \bar{c}_1 = -\sigma/\mu, \quad (2.5.25)$$

showing that the mean velocities of zeros and of specular points are equal to the phase velocity of the carrier wave. Also from (2.5.9) and (2.5.20)

$$\left. \begin{aligned} \Delta_2 &= \mu_{00} \mu_{20} u^2 (\sigma/u - \partial \sigma / \partial u)^2, \\ \Delta_4 &= \mu_{00} \mu_{20} u^6 (\sigma/u - \partial \sigma / \partial u)^2, \end{aligned} \right\} \quad (2.5.26)$$

so that

$$\frac{\Delta_2^{\frac{1}{2}}}{m_2} = \frac{\Delta_4^{\frac{1}{2}}}{m_4} = \left(\frac{\mu_{20}}{\mu_{00}} \right)^{\frac{1}{2}} \frac{\sigma/u - \partial \sigma / \partial u}{u}. \quad (2.5.27)$$

Thus the interquartile ranges of both the velocities of zeros and the velocities of specular points are equal to

$$\frac{2}{\sqrt{3}} \nu (\bar{c} - \Gamma), \quad (2.5.28)$$

where ν is defined by (1.6.15) and $\Gamma = \partial \sigma / \partial u$ is the group velocity of the carrier wave. Thus we see that the width of the velocity distribution depends both on the r.m.s. width of the spectrum (given by νu) and also on the dispersive properties of the medium. If the medium is non-dispersive, $\Gamma = \bar{c}$ and so (2.5.28) vanishes. This is what we should expect, since in a non-dispersive medium a long-crested disturbance advances without change of form and the zeros and specular points move with uniform velocity in the direction of wave propagation.

For gravity waves in deep water the group velocity is half the wave velocity and so the interquartile range equals $\nu \bar{c} / \sqrt{3}$.

2.6. *The motion of the contours*

Consider first how to define this motion. Let P be a point in the plane lying on the contour $\zeta = \text{constant}$. A moment later the contour at the same level will have moved to a new position, say QSR (see figure 11 *a*). If PQ and PR are axes parallel to Ox and Oy , the rates at which PQ and PR are increasing, which we denote by c_x and c_y , define the local displacement of the contour uniquely, and we have

$$(c_x, c_y) = \left(-\frac{\partial \zeta / \partial t}{\partial \zeta / \partial x}, -\frac{\partial \zeta / \partial t}{\partial \zeta / \partial y} \right). \quad (2.6.1)$$

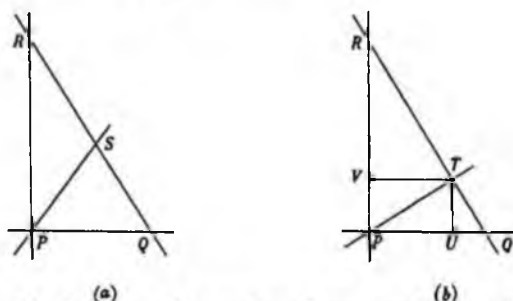


FIGURE 11. Definition of the motion of a contour (*a*) by its intercept on an arbitrary line, (*b*) by its normal displacement.

However, if we take a line through P in an arbitrary direction θ , and if this line intersects the displaced contour in S (figure 11), then it may be shown that

$$\frac{1}{PS} = \frac{1}{PQ} \cos \theta + \frac{1}{PR} \sin \theta, \quad (2.6.2)$$

and so if c is the rate at which the intercept PS is increasing

$$\frac{1}{c} = \frac{1}{c_x} \cos \theta + \frac{1}{c_y} \sin \theta. \quad (2.6.3)$$

This shows that the reciprocal quantity $(1/c_x, 1/c_y)$ is transformed like a vector, but not (c_x, c_y) itself. It is therefore more appropriate, and in fact more convenient, to consider the distribution of

$$(\kappa_x, \kappa_y) = (1/c_x, 1/c_y) = \left(-\frac{\partial \zeta / \partial x}{\partial \zeta / \partial t}, -\frac{\partial \zeta / \partial y}{\partial \zeta / \partial t} \right), \quad (2.6.4)$$

rather than the distribution of (c_x, c_y) . However, each may be derived from the other by a simple substitution. For since

$$\frac{\partial(\kappa_x, \kappa_y)}{\partial(c_x, c_y)} = \frac{1}{c_x^2 c_y^2} = \kappa_x^2 \kappa_y^2, \quad (2.6.5)$$

we have

$$\rho(c_x, c_y) = \frac{1}{c_x^2 c_y^2} \rho(\kappa_x, \kappa_y). \quad (2.6.6)$$

The distribution of the velocities of the contours normal to themselves can also be found. In figure 11 *b*, T is the foot of the perpendicular from P to QR , and TU , TV are drawn perpendicular to PQ , PR . It can be shown that

$$PU = \frac{PQ PR^2}{QR^2}, \quad PV = \frac{PQ^2 PR}{QR^2}, \quad (2.6.7)$$

360

M. S. LONGUET-HIGGINS ON THE

and hence the components of the normal velocity are

$$(q_x, q_y) = \left(\frac{c_x c_y^2}{c_x^2 + c_y^2}, \frac{c_x^2 c_y}{c_x^2 + c_y^2} \right) = \left(\frac{\kappa_x}{\kappa_x^2 + \kappa_y^2}, \frac{\kappa_y}{\kappa_x^2 + \kappa_y^2} \right). \quad (2.6.8)$$

Solving, we have

$$(\kappa_x, \kappa_y) = \left(\frac{q_x}{q_x^2 + q_y^2}, \frac{q_y}{q_x^2 + q_y^2} \right), \quad \frac{\partial(\kappa_x, \kappa_y)}{\partial(q_x, q_y)} = -\frac{1}{(q_x^2 + q_y^2)^2}, \quad (2.6.9)$$

and so

$$p(q_x, q_y) = \frac{1}{(q_x^2 + q_y^2)^2} p(\kappa_x, \kappa_y). \quad (2.6.10)$$

Let us write

$$\xi_i, \frac{\partial \xi}{\partial x}, \frac{\partial \xi}{\partial y}, \frac{\partial \xi}{\partial l} = \xi_1, \xi_2, \xi_3, \xi_4, \quad (2.6.11)$$

and let $p(\xi_1, \xi_2, \xi_3, \xi_4)$ denote the joint distribution of $\xi_1, \xi_2, \xi_3, \xi_4$ at an arbitrary point P in the (x, y) plane. We require the joint distribution of ξ_2, ξ_3, ξ_4 at points distributed uniformly along the contour $\xi_1 = \text{constant}$. Let this be denoted by $p(\xi_2, \xi_3, \xi_4)_{\xi_1}$. To find this distribution let dA be a small area surrounding P . If ξ_2, ξ_3, ξ_4 at P are restricted to lie in certain ranges of width $d\xi_2, d\xi_3, d\xi_4$, the contribution of the area dA to the distribution over these ranges is, by the argument of § 2.3,

$$p(\xi_1, \xi_2, \xi_3, \xi_4) \alpha dA d\xi_2 d\xi_3 d\xi_4, \quad (2.6.12)$$

where $\alpha = (\xi_2^2 + \xi_3^2)^{\frac{1}{2}}$. But the total expectation of contour length over the area dA is $3dA$ (see § 2.3). Hence we have

$$p(\xi_2, \xi_3, \xi_4)_{\xi_1} = \frac{(\xi_2^2 + \xi_3^2)^{\frac{1}{2}} p(\xi_1, \xi_2, \xi_3, \xi_4)}{3}. \quad (2.6.13)$$

Now by § 2.1, the elevation ξ_1 is uncorrelated with the first derivatives ξ_2, ξ_3, ξ_4 . Therefore

$$p(\xi_1, \xi_2, \xi_3, \xi_4) = p(\xi_1) p(\xi_2, \xi_3, \xi_4), \quad (2.6.14)$$

where $p(\xi_1)$ is given by (2.1.8). The matrix of correlations for (ξ_2, ξ_3, ξ_4) is

$$(\Xi_{ij}) = \begin{pmatrix} m_{20} & m_{11} & m'_{10} \\ m_{11} & m_{02} & m'_{01} \\ m'_{10} & m'_{01} & m''_{00} \end{pmatrix}. \quad (2.6.15)$$

Hence

$$p(\xi_2, \xi_3, \xi_4) = \frac{1}{(2\pi)^{\frac{3}{2}} \Delta_{\frac{1}{2}}} \exp\{-\frac{1}{2} M_{ij} \xi_{i+1} \xi_{j+1}\}, \quad (2.6.16)$$

where (M_{ij}) is the inverse matrix to (Ξ_{ij}) and where $\Delta_{\frac{1}{2}} = |\Xi_{ij}|$. On substituting these values in (2.6.13) we have

$$p(\xi_2, \xi_3, \xi_4)_{\xi_1} = \frac{1}{4\pi(m_{20} + m_{02})^{\frac{1}{2}} \Delta_{\frac{1}{2}}} \frac{(1 + \gamma^2)^{\frac{1}{2}}}{E\{\sqrt{(1 - \gamma^2)}\}} (\xi_2^2 + \xi_3^2)^{\frac{1}{2}} \exp\{-\frac{1}{2} M_{ij} \xi_{i+1} \xi_{j+1}\}. \quad (2.6.17)$$

Writing now

$$\kappa_x = -\xi_2/\xi_4, \quad \kappa_y = -\xi_3/\xi_4, \quad \kappa = \xi_4 \quad (2.6.18)$$

so that

$$\frac{\partial(\kappa_x, \kappa_y, \kappa)}{\partial(\xi_2, \xi_3, \xi_4)} = \frac{1}{\xi_4^2} = \frac{1}{\kappa^2}, \quad (2.6.19)$$

we have

$$p(\kappa_x, \kappa_y, \kappa)_{\xi_1} = \frac{1}{4\pi \Delta_{\frac{1}{2}} (m_{20} + m_{02})^{\frac{1}{2}} E\{\sqrt{(1 - \gamma^2)}\}} |\kappa^3| (\kappa_x^2 + \kappa_y^2)^{\frac{1}{2}} \times \exp\{-\frac{1}{2} \kappa^2 (M_{11} \kappa_x^2 + 2M_{12} \kappa_x \kappa_y + M_{22} \kappa_y^2 - 2M_{13} \kappa_x - 2M_{23} \kappa_y + M_{33})\}. \quad (2.6.20)$$

To obtain the distribution of κ_x, κ_y , we eliminate κ by integrating from $-\infty$ to ∞ ; thus

$$p(\kappa_x, \kappa_y)_{\xi} = \frac{1}{\pi \Delta \frac{1}{2} (m_{20} + m_{02})^{\frac{1}{2}} E\{\sqrt{(1-\gamma^2)}\}} \frac{(\kappa_x^2 + \kappa_y^2)^{\frac{1}{2}}}{R^2}, \tag{2.6.21}$$

where $R = M_{11}\kappa_x^2 + 2M_{12}\kappa_x\kappa_y + M_{22}\kappa_y^2 - 2M_{13}\kappa_x - 2M_{23}\kappa_y + M_{33}$. (2.6.22)

We may also write

$$R = M_{11}(\kappa_x - \bar{\kappa}_x)^2 + 2M_{12}(\kappa_x - \bar{\kappa}_x)(\kappa_y - \bar{\kappa}_y) + M_{22}(\kappa_y - \bar{\kappa}_y)^2 + M, \tag{2.6.23}$$

where $\left. \begin{aligned} \bar{\kappa}_x &= \frac{M_{13}M_{22} - M_{12}M_{23}}{M_{11}M_{22} - M_{12}^2} = -\frac{m'_{10}}{m_{00}}, \\ \bar{\kappa}_y &= \frac{M_{11}M_{23} - M_{12}M_{13}}{M_{11}M_{22} - M_{12}^2} = -\frac{m'_{01}}{m_{00}}, \\ M &= M_{33} - (M_{11}\bar{\kappa}_x^2 + 2M_{12}\bar{\kappa}_x\bar{\kappa}_y + M_{22}\bar{\kappa}_y^2) = \frac{1}{m_{00}}. \end{aligned} \right\} \tag{2.6.24}$

The denominator R is thus a symmetrical expression with a maximum at

$$(\bar{\kappa}_x, \bar{\kappa}_y) = \left(-\frac{m'_{10}}{m_{00}}, -\frac{m'_{01}}{m_{00}} \right). \tag{2.6.25}$$

The distribution (2.6.22) itself is not in general symmetrical. However, when the spectrum is narrow, R is appreciable only in the neighbourhood of $(\bar{\kappa}_x, \bar{\kappa}_y)$, giving

$$p(\kappa_x, \kappa_y)_{\xi} = \frac{1}{\pi m \Delta \frac{1}{2}} \frac{(\bar{\kappa}_x^2 + \bar{\kappa}_y^2)^{\frac{1}{2}}}{R^2}, \tag{2.6.26}$$

approximately. The curves of constant probability are then the ellipses $R = \text{constant}$. The major axis of each ellipse makes an angle ϖ with the x axis given by

$$\tan 2\varpi = \frac{2M_{12}}{M_{11} - M_{22}}. \tag{2.6.27}$$

Since $p(\kappa_x, \kappa_y)_{\xi}$ is proportional to R^{-2} , it may be shown that the fraction of the distribution lying *outside* the ellipse is proportional to R^{-1} . At the centre, $R = M$. Therefore the ellipse enclosing just half the distribution is

$$R = 2M. \tag{2.6.28}$$

The semi-axes of this ellipse are of length

$$r_1, r_2 = \left[\frac{2M}{(M_{11} + M_{22}) \pm \sqrt{\{(M_{11} - M_{22})^2 + 4M_{12}^2\}}} \right]^{\frac{1}{2}}. \tag{2.6.29}$$

To interpret these results, let the u axis be taken so as to pass through the centroid (\bar{u}, \bar{v}) of the energy spectrum. The spectrum being narrow, we may expand in a Taylor series about $(\bar{u}, 0)$ thus:

$$\left. \begin{aligned} m_{00}'' &= \sigma^2 \mu_{00} + \frac{1}{2} \left(\mu_{20} \frac{\partial^2}{\partial u^2} + \mu_{02} \frac{\partial^2}{\partial v^2} \right) \sigma^2 + \dots, \\ m_{10}' &= u \sigma \mu_{00} + \frac{1}{2} \left(\mu_{20} \frac{\partial^2}{\partial u^2} + \mu_{02} \frac{\partial^2}{\partial v^2} \right) (u \sigma) + \dots, \\ m_{01}' &= \mu_{11} \frac{\partial^2}{\partial u \partial v} (v \sigma) + \dots \end{aligned} \right\} \tag{2.6.30}$$

where $u = \bar{u}$. Making use of (1.6.9) we obtain

$$\left. \begin{aligned} M_{11} &= \frac{\mu_{02}}{\mu_{20}\mu_{02} - \mu_{11}^2} \frac{(\sigma/u)^2}{(\sigma/u - \partial\sigma/\partial u)^2}, \\ M_{12} &= \frac{\mu_{11}}{\mu_{20}\mu_{02} - \mu_{11}^2} \frac{\sigma/u}{\sigma/u - \partial\sigma/\partial u}, \\ M_{22} &= \frac{\mu_{20}}{\mu_{20}\mu_{02} - \mu_{11}^2}, \\ \Delta_3 &= \mu_{00}(\mu_{20}\mu_{02} - \mu_{11}^2) u^2 (\sigma/u - \partial\sigma/\partial u)^2. \end{aligned} \right\} \quad (2.6.31)$$

Hence

$$(\bar{x}, \bar{y}) = \left(-\frac{u}{\sigma}, 0 \right), \quad (2.6.32)$$

and

$$\tan 2\varpi = \frac{2\mu_{11} \sigma/u (\sigma/u - \partial\sigma/\partial u)}{\mu_{20}(\sigma/u - \partial\sigma/\partial u)^2 - \mu_{02}(\sigma/u)^2}, \quad (2.6.33)$$

showing that the centre of the distribution is the inverse of the phase velocity, and that $\tan 2\varpi$, like $\tan 2\beta$, is proportional to μ_{11} (cf. equation (1.6.14)). When the spectrum is symmetrical the semi-axes of the distribution are given by

$$r_1 = \left(\frac{\mu_{20}}{\mu_{00}} \right)^{\frac{1}{2}} \left| \frac{\sigma/u - \partial\sigma/\partial u}{\sigma^2/u} \right|, \quad r_2 = \left(\frac{\mu_{02}}{\mu_{00}} \right)^{\frac{1}{2}} \frac{1}{\sigma}, \quad (2.6.34)$$

that is,

$$r_1 = |\nu\kappa(1 - \Gamma\bar{\kappa})|, \quad r_2 = |\gamma\bar{\kappa}|, \quad (2.6.35)$$

where $\kappa = -u/\sigma$, is the mean reciprocal velocity; $\Gamma = -\partial\sigma/\partial u$, is the corresponding group velocity; $\nu = (\mu_{20}/\mu_{00}u^2)^{\frac{1}{2}}$ and $\gamma = (\mu_{02}/\mu_{00}u^2)^{\frac{1}{2}}$. This shows that $r_2/\bar{\kappa}$, which represents the width of the distribution perpendicular to the principal direction of the waves, depends only on the long-crestedness γ^{-1} and is proportional to γ . On the other hand, $r_1/\bar{\kappa}$, which represents the width of the distribution parallel to the principal direction, depends not only on the r.m.s. width of the spectrum, represented by ν , but also on the dispersive properties of the medium. For gravity waves in deep water $\Gamma\bar{\kappa} = \frac{1}{2}$ and so

$$r_1 = \frac{1}{2} |\nu\bar{\kappa}|. \quad (2.6.36)$$

2.7. The velocities of specular points

A specular point on the surface is defined as a point where the two components of the gradient take given values. Such points would be indicated to a distant observer as the points where light was reflected from a distant source. In § 2.4 we deduced the mean density of such points per unit area; let us now consider the statistical distribution of their velocities.

If (x, y) are the co-ordinates at time t of a point whose components of gradient

$$\frac{\partial\zeta}{\partial x}, \frac{\partial\zeta}{\partial y} = \xi_2, \xi_3 \quad (2.7.1)$$

are fixed. At a subsequent time $t + dt$ the point will have moved to a position $(x + dx, y + dy)$, where

$$\left. \begin{aligned} 0 &= d\left(\frac{\partial\zeta}{\partial x}\right) = \frac{\partial^2\zeta}{\partial x^2} dx + \frac{\partial^2\zeta}{\partial x\partial y} dy + \frac{\partial^2\zeta}{\partial x\partial t} dt, \\ 0 &= d\left(\frac{\partial\zeta}{\partial y}\right) = \frac{\partial^2\zeta}{\partial x\partial y} dx + \frac{\partial^2\zeta}{\partial y^2} dy + \frac{\partial^2\zeta}{\partial y\partial t} dt. \end{aligned} \right\} \quad (2.7.2)$$

STATISTICAL ANALYSIS OF A RANDOM, MOVING SURFACE 363

The ratios
$$\frac{dx}{dt}, \frac{dy}{dt} = c_x, c_y \quad (2.7.3)$$

are the required velocities. Writing

$$\left. \begin{aligned} \frac{\partial^2 \xi}{\partial x^2}, \frac{\partial^2 \xi}{\partial x \partial y}, \frac{\partial^2 \xi}{\partial y^2} &= \xi_4, \xi_5, \xi_6, \\ \frac{\partial^2 \xi}{\partial x \partial t}, \frac{\partial^2 \xi}{\partial y \partial t} &= \xi_7, \xi_8 \end{aligned} \right\} \quad (2.7.4)$$

in (2.7.2) we have

$$\left. \begin{aligned} \xi_4 c_x + \xi_5 c_y &= -\xi_7, \\ \xi_6 c_x + \xi_8 c_y &= -\xi_8. \end{aligned} \right\} \quad (2.7.5)$$

Since the velocities c_x, c_y are given in terms of ξ_4, \dots, ξ_8 , we require first the joint distribution $p(\xi_4, \dots, \xi_8)_{\xi_2, \xi_3}$ of these quantities at points where ξ_2, ξ_3 take the given values.

Let dA denote any small area of the x, y plane, and P a neighbouring point. As usual, $p(\xi_2, \dots, \xi_8)$ will denote the ordinary distribution of ξ_2, \dots, ξ_8 at P . Now if ξ_2, ξ_3 take the given values at some point in dA , and ξ_4, \dots, ξ_8 are fixed, then (ξ_2, ξ_3) at P lies within a certain region $d\Sigma$ of area

$$d\Sigma = |\xi_4 \xi_6 - \xi_5^2| dA \quad (2.7.6)$$

(cf. § 2.4). Hence the probability that ξ_2, ξ_3 take the given values in dA and that ξ_4, \dots, ξ_8 lie in ranges of width $d\xi_4, \dots, d\xi_8$ respectively is

$$p(\xi_2, \xi_3, \dots, \xi_8) |\xi_4 \xi_6 - \xi_5^2| dA d\xi_4 d\xi_5 \dots d\xi_8. \quad (2.7.7)$$

But the total probability of ξ_2, ξ_3 taking the given values in dA is

$$D_{sp} dA, \quad (2.7.8)$$

where D_{sp} is the density of specular points with gradient (ξ_2, ξ_3) . Therefore the probability that $\xi_4 \dots \xi_8$ lie in their respective ranges given that there is a specular point in dA is the quotient of (2.7.7) and (2.7.8), that is

$$\frac{p(\xi_2, \dots, \xi_8) |\xi_4 \xi_6 - \xi_5^2| d\xi_4 \dots d\xi_8}{D_{sp}}. \quad (2.7.9)$$

In other words
$$p(\xi_4, \dots, \xi_8)_{\xi_2, \xi_3} = \frac{p(\xi_2, \dots, \xi_8) |\xi_4 \xi_6 - \xi_5^2|}{D_{sp}}. \quad (2.7.10)$$

Now the first derivatives ξ_2, ξ_3 are statistically independent of the second derivatives $\xi_4 \dots \xi_8$. Therefore

$$p(\xi_2, \dots, \xi_8) = p(\xi_2, \xi_3) p(\xi_4, \dots, \xi_8), \quad (2.7.11)$$

where $p(\xi_2, \xi_3)$ is the ordinary distribution of ξ_2, ξ_3 given by (2.1.12) and $p(\xi_4, \dots, \xi_8)$ is the ordinary distribution of ξ_4, \dots, ξ_8 . The matrix of correlations for ξ_4, \dots, ξ_8 is

$$(\Xi_{ij}) = \begin{pmatrix} m_{40} & m_{31} & m_{22} & m'_{30} & m'_{21} \\ m_{31} & m_{22} & m_{13} & m'_{21} & m'_{12} \\ m_{22} & m_{13} & m_{04} & m'_{12} & m'_{03} \\ \hline m'_{30} & m'_{21} & m'_{12} & m''_{20} & m''_{11} \\ m'_{21} & m'_{12} & m'_{03} & m''_{11} & m''_{02} \end{pmatrix}, \quad (2.7.12)$$

364

M. S. LONGUET-HIGGINS ON THE

and so
$$p(\xi_4, \dots, \xi_8) = \frac{1}{(2\pi)^{\frac{1}{2}} \Delta_3^{\frac{1}{2}}} \exp\{-\frac{1}{2} M_{ij} \xi_{i+3} \xi_{j+3}\}, \quad (2.7.13)$$

where (M_{ij}) is the inverse matrix to (Ξ_{ij}) and where

$$\Delta_3 = |\Xi_{ij}|. \quad (2.7.14)$$

Substituting in (2.7.10) we have then

$$p(\xi_4, \dots, \xi_8)_{\xi_4, \xi_5} = \frac{1}{4(2\pi)^{\frac{1}{2}} (\Delta_2 \Delta_3)^{\frac{1}{2}} D_{ma}} |\xi_4 \xi_6 - \xi_5^2| \exp\{-\frac{1}{2} M_{ij} \xi_{i+3} \xi_{j+3}\}, \quad (2.7.15)$$

where D_{ma} is given by (2.4.51).

The distribution of the velocities c_x, c_y is now obtained from the relations (2.7.5). If we write also

$$c_1, c_2, c_3 = \xi_4, \xi_5, \xi_6 \quad (2.7.16)$$

and transform to the variables c_x, c_y, c_1, c_2, c_3 we have

$$\frac{\partial(\xi_4, \dots, \xi_8)}{\partial(c_x, c_y, c_1, c_2, c_3)} = \xi_4 \xi_6 - \xi_5^2 = c_1 c_3 - c_2^2. \quad (2.7.17)$$

Hence
$$p(c_x, c_y, c_1, c_2, c_3)_{\xi_4, \xi_5} = \frac{1}{4(2\pi)^{\frac{1}{2}} (\Delta_2 \Delta_3)^{\frac{1}{2}} D_{ma}} (c_1 c_3 - c_2^2)^2 \exp\{-\frac{1}{2} N_{ij} c_i c_j\}, \quad (2.7.18)$$

where (N_{ij}) is the (3×3) matrix whose elements are

$$\left. \begin{aligned} N_{11} &= M_{44} c_x^2 && -2M_{41} c_x && +M_{11}, \\ N_{22} &= M_{55} c_y^2 + 2M_{45} c_x c_y + M_{44} c_y^2 - 2M_{52} c_x && -2M_{42} c_y && +M_{22}, \\ N_{33} &= && M_{55} c_y^2 && -2M_{53} c_y && +M_{33}, \\ N_{23} &= && M_{55} c_x c_y + M_{45} c_y^2 - M_{53} c_x && - (M_{43} + M_{52}) c_y + M_{23}, \\ N_{31} &= && M_{45} c_x c_y && - M_{43} c_x && - M_{51} c_y && +M_{31}, \\ N_{12} &= M_{45} c_x^2 + M_{44} c_x c_y && - (M_{42} + M_{51}) c_x - M_{41} c_y && +M_{12}. \end{aligned} \right\} \quad (2.7.19)$$

On eliminating c_1, c_2, c_3 by integration between $\pm\infty$ we have

$$p(c_x, c_y)_{\xi_4, \xi_5} = \frac{1}{4(2\pi)^{\frac{1}{2}} (\Delta_2 \Delta_3)^{\frac{1}{2}} D_{ma}} \int_{-\infty}^{\infty} \int_{-\infty}^{\infty} \int_{-\infty}^{\infty} (c_1 c_3 - c_2^2)^2 \exp\{-\frac{1}{2} N_{ij} c_i c_j\} dc_1 dc_2 dc_3. \quad (2.7.20)$$

The matrix (N_{ij}) is positive-definite. For, if any real values of c_1, c_2, c_3 , not all zero existed which made the quadratic form $N_{ij} c_i c_j$ zero or negative, a corresponding set of values of $\xi_4 \dots \xi_8$ could be found from (2.7.5) which made $M_{ij} \xi_{i+3} \xi_{j+3}$ zero or negative. But this is impossible, since (M_{ij}) is positive-definite. Therefore (N_{ij}) is positive-definite. Therefore by a real linear transformation of variables $c_1, c_2, c_3 \rightarrow \eta_1, \eta_2, \eta_3$ we have

$$\left. \begin{aligned} N_{ij} c_i c_j &= \eta_1^2 + \eta_2^2 + \eta_3^2, \\ c_1 c_3 - c_2^2 &= \mathbf{l}_1 \eta_1^2 + \mathbf{l}_2 \eta_2^2 + \mathbf{l}_3 \eta_3^2, \end{aligned} \right\} \quad (2.7.21)$$

where $\mathbf{l}_1, \mathbf{l}_2, \mathbf{l}_3$ are roots of the equation

$$|\sigma_{ij} - \mathbf{l} N_{ij}| = 0. \quad (2.7.22)$$

As in § 2.4 we have then

$$p(c_x, c_y)_{\xi_4, \xi_5} = \frac{1}{4(2\pi)^{\frac{1}{2}} (\Delta_2 \Delta_3 |N_{ij}|)^{\frac{1}{2}} D_{ma}} \mathbf{I}(\mathbf{l}_1, \mathbf{l}_2, \mathbf{l}_3), \quad (2.7.23)$$

where

$$I(l_1, l_2, l_3) = \int_{-\infty}^{\infty} \int_{-\infty}^{\infty} \int_{-\infty}^{\infty} (l_1 \eta_1^2 + l_2 \eta_2^2 + l_3 \eta_3^2)^2 \exp\{-\frac{1}{2}(\eta_1^2 + \eta_2^2 + \eta_3^2)\} d\eta_1 d\eta_2 d\eta_3. \quad (2.7.24)$$

This integral is much easier to evaluate than the similar integral $I(l_1, l_2, l_3)$ of equation (2.4.36) on account of the factor in the integrand being squared. In fact we have immediately

$$\begin{aligned} I(l_1, l_2, l_3) &= (2\pi)^{\frac{3}{2}} [3(l_1^2 + l_2^2 + l_3^2) + 2(l_2 l_3 + l_3 l_1 + l_1 l_2)]. \\ &= (2\pi)^{\frac{3}{2}} [3(l_1 + l_2 + l_3)^2 - 4(l_2 l_3 + l_3 l_1 + l_1 l_2)]. \end{aligned} \quad (2.7.25)$$

Therefore
$$p(c_x, c_y)_{\xi_1, \xi_2} = \frac{1}{16\pi^2 (\Delta_2 \Delta_3)^{\frac{1}{2}} D_{\max}} [3(\sum_i l_i)^2 - 4 \sum_{i \neq j} l_i l_j]. \quad (2.7.26)$$

Equation (2.7.22) on expansion becomes

$$N^3 - (\frac{1}{2}n_{13} - n_{22} + \frac{1}{2}n_{31})^2 + (\frac{1}{2}N_{13} - \frac{1}{4}N_{22} + \frac{1}{2}N_{31})^2 - \frac{1}{2} = 0, \quad (2.7.27)$$

where
$$N = |N_{ij}| \quad (2.7.28)$$

and
$$n_{13} = N_{21} N_{32} - N_{22} N_{31} = n_{31}, \quad n_{22} = N_{11} N_{33} - N_{22}^2. \quad (2.7.29)$$

Therefore
$$\sum_i l_i = \frac{n_{13} - n_{22}}{N}, \quad \sum_{i \neq j} l_i l_j = \frac{N_{13} - \frac{1}{4}N_{22}}{N}, \quad (2.7.30)$$

and so finally

$$p(c_x, c_y)_{\xi_1, \xi_2} = \frac{1}{16\pi^2 (\Delta_2 \Delta_3)^{\frac{1}{2}} D_{\max}} \frac{3(n_{13} - n_{22})^2 + (N_{22} - 4N_{13}) N}{N^{\frac{3}{2}}}. \quad (2.7.31)$$

It will be seen that in general the quantities N_{ij} , n_{ij} and N which occur in this expression are polynomials in c_x , c_y of degree 2, 4 and 6 respectively.

As before, we may study this distribution in the special case when the energy spectrum is narrow and has symmetry about the principal direction. Taking the u axis along the line of symmetry we have $m_{pq} = 0$ whenever q is odd, and so

$$(\Xi_{ij}) = \begin{pmatrix} m_{40} & 0 & m_{22} & m'_{30} & 0 \\ 0 & m_{22} & 0 & 0 & m'_{12} \\ m_{22} & 0 & m_{04} & m'_{12} & 0 \\ m'_{30} & 0 & m'_{12} & m''_{20} & 0 \\ 0 & m'_{12} & 0 & 0 & m''_{02} \end{pmatrix}. \quad (2.7.32)$$

The reciprocal matrix (M_{ij}) is given by

$$(M_{ij}) = \begin{pmatrix} A_{11} & 0 & A_{12} & A_{13} & 0 \\ 0 & B_{11} & 0 & 0 & B_{12} \\ A_{21} & 0 & A_{22} & A_{23} & 0 \\ A_{31} & 0 & A_{32} & A_{33} & 0 \\ 0 & B_{21} & 0 & 0 & B_{22} \end{pmatrix}, \quad (2.7.33)$$

where
$$(A_{ij}) = \begin{pmatrix} m_{40} & m_{22} & m'_{30} \\ m_{22} & m_{04} & m'_{12} \\ m'_{30} & m'_{12} & m''_{20} \end{pmatrix}^{-1}, \quad (B_{ij}) = \begin{pmatrix} m_{22} & m'_{12} \\ m'_{12} & m''_{02} \end{pmatrix}^{-1}. \quad (2.7.34)$$

Since the spectrum is narrow, each coefficient may be expanded in a Taylor series about the centroid (\bar{u} , 0). Thus

$$\left. \begin{aligned} m_{40} &= \mu_{00} u^4 + \frac{1}{2} \mu_{20} \frac{\partial^2}{\partial u^2} (u^4) + \dots, \\ m_{22} &= \mu_{02} u^2 + \mu_{12} \frac{\partial}{\partial u} (u^2) + \frac{1}{2} \mu_{22} \frac{\partial^2}{\partial u^2} (u^2), \\ m_{04} &= \mu_{04}, \\ m'_{30} &= \mu_{00} u^3 \sigma + \frac{1}{2} \left(\mu_{20} \frac{\partial^2}{\partial u^2} + \mu_{02} \frac{\partial^2}{\partial v^2} \right) (u^3 \sigma) + \dots, \\ m'_{12} &= \mu_{02} u \sigma + \mu_{12} \frac{\partial}{\partial u} (u \sigma) + \frac{1}{2} \left(\mu_{22} \frac{\partial^2}{\partial u^2} + \mu_{04} \frac{\partial^2}{\partial v^2} \right) (u \sigma) + \dots, \\ m''_{20} &= \mu_{00} u^2 \sigma^2 + \frac{1}{2} \left(\mu_{20} \frac{\partial^2}{\partial u^2} + \mu_{02} \frac{\partial^2}{\partial v^2} \right) (u^2 \sigma^2) + \dots, \\ m''_{02} &= \mu_{02} \sigma^2 + \mu_{12} \frac{\partial}{\partial u} (\sigma^2) + \frac{1}{2} \left(\mu_{22} \frac{\partial^2}{\partial u^2} + \mu_{04} \frac{\partial^2}{\partial v^2} \right) (\sigma^2) + \dots, \end{aligned} \right\} \quad (2.7.35)$$

where $u = \bar{u}$ and $\sigma = \sigma(\bar{u}, 0)$. Thus we find for the determinants of $(A_{ij})^{-1}$ and $(B_{ij})^{-1}$

$$\left. \begin{aligned} |A_{ij}|^{-1} &= \delta_3 u^3 (\sigma/u - \partial\sigma/\partial u)^2, \\ |B_{ij}|^{-1} &= \delta_2 u^2 (\sigma/u - \partial\sigma/\partial u)^2, \end{aligned} \right\} \quad (2.7.36)$$

where

$$\delta_3 = \begin{vmatrix} \mu_{00} & 0 & \mu_{02} \\ 0 & \mu_{20} & \mu_{12} \\ \mu_{02} & \mu_{12} & \mu_{04} \end{vmatrix}, \quad \delta_2 = \begin{vmatrix} \mu_{02} & \mu_{12} \\ \mu_{12} & \mu_{22} \end{vmatrix}. \quad (2.7.37)$$

(Each zero term in δ_3 could be replaced by μ_{10} .) Further, on evaluating (A_{ij}) and (B_{ij}) and substituting in (2.7.19) we find eventually

$$(N_{ij}) = \frac{1}{u^4} \begin{pmatrix} \alpha_{22} u^2 q_1^2 + 2\alpha_{12} u q_1 + \alpha_{11} & \alpha_{22} u^2 q_1 q_2 + \alpha_{12} u q_2 & \alpha_{23} u^3 q_1 + \alpha_{13} u^2 \\ \alpha_{22} u^2 q_1 q_2 + \alpha_{12} u q_2 & \alpha_{22} u^2 q_2^2 + \beta_{22} u^4 q_1^2 + 2\beta_{12} u^3 q_1 + \beta_{11} u^2 & \alpha_{23} u^3 q_2 + \beta_{32} u^4 q_1 q_2 + \beta_{12} u^3 q_2 \\ \alpha_{23} u^3 q_1 + \alpha_{13} u^2 & \alpha_{23} u^3 q_2 + \beta_{22} u^4 q_1 q_2 + \beta_{12} u^3 q_2 & \alpha_{33} u^4 + \beta_{22} u^4 q_2^2 \end{pmatrix} \quad (2.7.38)$$

where α_{ij} and β_{ij} are the (i, j) th elements of the reciprocal matrices of δ_3 and δ_2 respectively, and

$$q_1, q_2 = \frac{c_x + \sigma/u}{\sigma/u - \partial\sigma/\partial u}, \frac{c_y}{\sigma/u - \partial\sigma/\partial u}. \quad (2.7.39)$$

Thus q_1, q_2 are non-dimensional quantities proportional to the departures of c_x, c_y from their mean values $(-\sigma/u, 0)$. In deriving (2.7.38) it has been assumed that q_1 is of the same order of magnitude as γ , $(\mu_{02}/u^2 \mu_{00})^{1/2}$, but that q_2 is of order 1; this makes the matrix (N_{ij}) more homogeneous. Before proceeding further we may make the additional restrictions

$$\mu_{12} = 0, \quad \mu_{22} = \mu_{20} \mu_{02} / \mu_{00}, \quad (2.7.40)$$

and we may write $\mu_{20} = \nu^2 u^2 \mu_{00}$, $\mu_{02} = \gamma^2 u^2 \mu_{00}$, $\mu_{04} = a^2 \gamma^4 u^4 \mu_{00}$, $(2.7.41)$

where ν , γ and a have the same meanings as before, namely, ν^{-1} is a measure of the average length of a group of waves, γ^{-1} is the long-crestedness and a is the peakedness of the spectrum in the ν direction. Then (2.7.38) reduces to

$$(N_{ij}) = \frac{1}{u^4 \mu_{00}} \begin{pmatrix} (\xi^2 + d^2 + 1) & \xi\eta/\gamma & -d^2/\gamma^2 \\ \xi\eta/\gamma & (\xi^2 + \eta^2 + 1)/\gamma^2 & \xi\eta/\gamma^3 \\ -d^2/\gamma^2 & \xi\eta/\gamma^3 & (\xi^2 + \eta^2)/\gamma^4 \end{pmatrix}, \tag{2.7.42}$$

where $\xi = q_1/\nu$, $\eta = \gamma q_2/\nu$, $d^2 = 1/(a^2 - 1)$. (2.7.43)

Clearly the (i, j) th term of (N_{ij}) is of order $1/\gamma^{i+j}$. Therefore

$$I_1, I_2, I_3 = \gamma^2 u^4 \mu_{00} (I'_1, I'_2, I'_3) \tag{2.7.44}$$

where I'_1, I'_2, I'_3 are the corresponding roots of the equation

$$|\sigma_{ij} - I' N'_{ij}| = 0 \tag{2.7.45}$$

and (N'_{ij}) is the non-dimensional matrix

$$(N'_{ij}) = \begin{pmatrix} \xi^2 + d^2 + 1 & \xi\eta & -d^2 \\ \xi\eta & \xi^2 + \eta^2 + 1 & \xi\eta \\ -d^2 & \xi\eta & \eta^2 + d^2 \end{pmatrix}. \tag{2.7.46}$$

Also $|N_{ij}| = |N'_{ij}| / (\gamma^6 u^{12} \mu_{00}^3)$. (2.7.47)

So from equation (2.7.26)

$$p(c_x, c_y)_{\xi_1, \xi_2} = \frac{\gamma^7 u^{14} \mu_{00}^3}{16\pi^2 (\Delta_2 \Delta_5)^{\frac{1}{2}} D_{ma}} \frac{3(\sum_i I_i')^2 - 4 \sum_{i \neq j} I_i' I_j'}{|N'_{ij}|^{\frac{1}{2}}}. \tag{2.7.48}$$

It is convenient to state the solution in terms of the non-dimensional variables

$$\xi, \eta = \frac{c_x + \sigma/u}{\nu(\sigma/u - \partial\sigma/\partial u)}, \frac{\gamma c_y}{\nu(\sigma/u - \partial\sigma/\partial u)}, \tag{2.7.49}$$

so that

$$p(\xi, \eta)_{\xi_1, \xi_2} = \frac{\nu^2 (\sigma/u - \partial\sigma/\partial u)^2}{\gamma} p(c_x, c_y)_{\xi_1, \xi_2}. \tag{2.7.50}$$

First, on expanding the left-hand side of (2.7.45) we have

$$N' I'^3 + \eta^2 I'^2 - [\frac{1}{2}(\xi^2 + \eta^2 + 1) + d^2] I' - \frac{1}{2} = 0, \tag{2.7.51}$$

where $N' = |N'_{ij}| = (\xi^2 + \eta^2 + 1) \eta^2 + \{(\xi + \eta)^2 + 1\} \{(\xi - \eta)^2 + 1\} d^2$, (2.7.52)

giving $\sum_i I_i' = -\eta^2/N'$, $\sum_{i \neq j} I_i' I_j' = -[\frac{1}{2}(\xi^2 + \eta^2 + 1) + d^2]/N'$. (2.7.53)

Secondly, from (2.4.58), (2.7.36) and (2.7.37),

$$\Delta_2 = \gamma^2 u^4 \mu_{00}^2, \quad \Delta_5 = |A_{ij}^{-1}| |B_{ij}^{-1}| = \delta_2 \delta_3 u^8 (\sigma/u - \partial\sigma/\partial u)^4, \tag{2.7.54}$$

and $\delta_2 \delta_3 = \mu_{20} \mu_{22} \mu_{02} (\mu_{00} \mu_{04} - \mu_{02}^2) = \nu^4 \gamma^8 u^{12} \mu_{00}^2 (a^2 - 1)$. (2.7.55)

Thirdly from (2.4.61) $D_{ma} = \gamma u^2 C(a)$. (2.7.56)

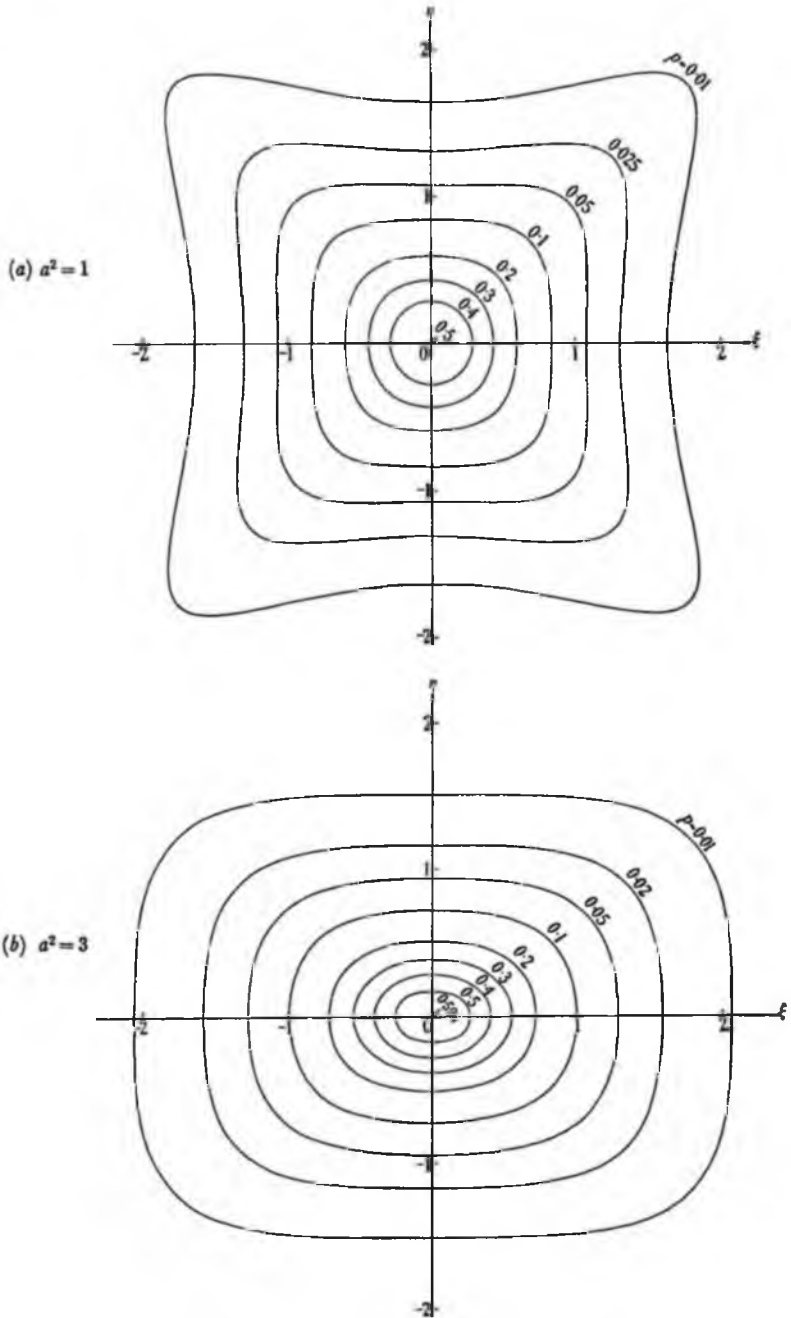


FIGURE 12

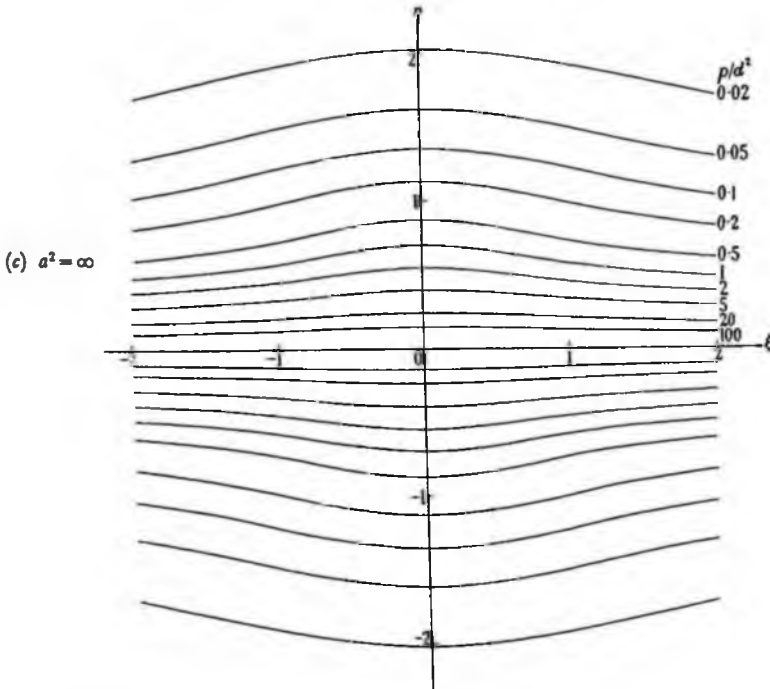


FIGURE 12. The probability distribution of the velocities of specular points, for a narrow spectrum

Therefore, altogether we have

$$p(\xi, \eta)_{\xi, \eta} = \frac{d}{16\pi^2 C(a)} \frac{3\eta^4 + [(\xi^2 + \eta^2 + 1) + 4d^2] N'}{N'^{\frac{1}{2}}}, \tag{2.7.57}$$

where $C(a)$ is given by (2.4.62) and N' by (2.7.52).

Two special cases are of interest. Suppose first that the surface consists of two systems of long-crested waves, intersecting at a small angle 2γ . As we saw in § 2.4, this corresponds to the limiting case when $a \rightarrow 1$ and $d \rightarrow \infty$. Equation (2.7.57) then becomes

$$p(\xi, \eta)_{\xi, \eta} = \frac{1}{2} \frac{1}{\{(\xi + \eta)^2 + 1\}^{\frac{1}{2}} \{(\xi - \eta)^2 + 1\}^{\frac{1}{2}}}. \tag{2.7.58}$$

The distribution is shown in figure 12 a. There are two ridges of high probability, in the directions $\xi = \pm \eta$, that is

$$c_x + \sigma/u = \pm \gamma c_y, \tag{2.7.59}$$

or when the vector difference between the specular velocity (c_x, c_y) and the mean velocity $(-\sigma/u, 0)$ is in the direction of the crests of one of the two wave systems.

This particular case may also be derived quite simply as follows. We have seen that the velocities of specular points have the same probability distribution as the velocities of the maxima only. Now with two intersecting systems of long-crested waves, the maxima occur at the points of intersection of the crests of the two systems, and at no other points (see

figure 9 a). If the point of intersection of two crests has components of velocity c_x , c_y parallel and perpendicular to the mean direction, then the rates of advance of the crests in the two systems of waves are

$$c_1^{(1)} = c_x \cos \gamma + c_y \sin \gamma, \quad c_1^{(2)} = c_x \cos \gamma - c_y \sin \gamma, \quad (2.7.60)$$

where 2γ is the angle between the two wave systems. But the distribution of c_1 for a long-crested system of waves was found in § 2.5 to be

$$p(c_1) = \frac{1}{2} \frac{\nu^2 (\sigma/u - \partial\sigma/\partial u)^2}{[(c_1 + \sigma/u)^2 + \nu^2 (\sigma/u - \partial\sigma/\partial u)^2]^{\frac{3}{2}}}, \quad (2.7.61)$$

where u is measured in the direction of propagation. Since the two systems are independent,

$$p(c_1^{(1)}, c_1^{(2)}) = p(c_1^{(1)}) p(c_1^{(2)}) \quad (2.7.62)$$

When the angle of separation 2γ is small, ν and u are effectively the same for the two systems and for the combined system. Thus

$$\left. \begin{aligned} c_1^{(1)} + \sigma/u &= (c_x + \sigma/u) + \gamma c_y = (\xi + \eta) \nu (\sigma/u - \partial\sigma/\partial u), \\ c_1^{(2)} + \sigma/u &= (c_x + \sigma/u) - \gamma c_y = (\xi - \eta) \nu (\sigma/u - \partial\sigma/\partial u). \end{aligned} \right\} \quad (2.7.63)$$

Further,

$$p(\xi, \eta)_{\xi_1, \xi_2} = \left| \frac{\partial(c_1^{(1)}, c_1^{(2)})}{\partial(\xi, \eta)} \right| p(c_1^{(1)}, c_1^{(2)})_{\xi_1, \xi_2}, \quad (2.7.64)$$

and so

$$p(\xi, \eta)_{\xi_1, \xi_2} = 2\nu^2 (\sigma/u - \partial\sigma/\partial u)^2 p(c_1^{(1)}) p(c_1^{(2)}), \quad (2.7.65)$$

from which (2.7.58) follows.

A second case of interest is that of infinite peakedness: $a \rightarrow \infty$ and $d \rightarrow 0$. For large values of a , (2.7.57) becomes

$$p(\xi, \eta)_{\xi_1, \xi_2} = \frac{1}{4a^2} \frac{3\eta^2 + (\xi^2 + \eta^2 + 1)^2}{\eta^3 (\xi^2 + \eta^2 + 1)^{\frac{3}{2}}}. \quad (2.7.66)$$

This distribution is shown in figure 12 c. There is only one ridge of high probability, namely, that in the principal direction of the waves. The expression is valid only asymptotically, as is shown by the presence of the factor $1/4a^2$ and the fact that $\iint p(\xi, \eta)_{\xi_1, \xi_2} d\xi d\eta$ diverges.

An intermediate case, $a^2 = 3$, $d^2 = \frac{1}{2}$, is shown in figure 12 b. This corresponds to a distribution of energy distributed normally with regard to direction, over a narrow range.

2.8. Properties of the envelope: the number of waves in a group

We shall now consider briefly some statistical properties of the envelope of the wave surface, as defined in § 1.5. The envelope function ρ is essentially different from the surface elevation ζ , in that ρ is always positive whereas ζ has a mean value zero. Nevertheless, many of the properties of ρ will be seen to be analogous to corresponding properties of ζ .

It is convenient to introduce the auxiliary variables

$$\left. \begin{aligned} \xi_1 &= \rho \cos \phi = \sum_n c_n \cos \{ (u_n - \bar{u})x + (v_n - \bar{v})y + (\sigma_n - \bar{\sigma})t + \epsilon_n \}, \\ \xi_2 &= \rho \sin \phi = \sum_n c_n \sin \{ (u_n - \bar{u})x + (v_n - \bar{v})y + (\sigma_n - \bar{\sigma})t + \epsilon_n \}, \end{aligned} \right\} \quad (2.8.1)$$

which are the real and imaginary parts of the complex envelope function $\rho e^{i\phi}$ (see equation (1.5.6)). ξ_1, ξ_2 have the same form as ζ , each being the sum of an infinite number of sinusoidal

STATISTICAL ANALYSIS OF A RANDOM, MOVING SURFACE 371

components with random phase. In fact, the energy spectrum of ξ_1, ξ_2 is the same as that of ξ , but with the origin moved to the mean wave-number (\bar{u}, \bar{v}) . Thus ξ_1, ξ_2 are normally distributed with mean value zero. Since

$$\overline{\xi_1^2} = \overline{\xi_2^2} = m_{00}, \quad \overline{\xi_1 \xi_2} = 0, \quad (2.8.2)$$

we have
$$p(\xi_1, \xi_2) = \frac{1}{2\pi m_{00}} \exp\{- (\xi_1^2 + \xi_2^2)/2m_{00}\}. \quad (2.8.3)$$

We now transform back to the variables ρ, ϕ . From (2.8.1)

$$\xi_1^2 + \xi_2^2 = \rho^2, \quad \frac{\partial(\xi_1, \xi_2)}{\partial(\rho, \phi)} = \rho, \quad (2.8.4)$$

and so
$$p(\rho, \phi) = \frac{1}{2\pi m_{00}} \rho \exp\{-\rho^2/2m_{00}\}. \quad (2.8.5)$$

This is independent of the phase angle ϕ . The distribution of ρ alone is found by integrating with respect to ϕ from 0 to 2π :

$$p(\rho) = \frac{1}{m_{00}} \rho \exp\{-\rho^2/2m_{00}\}, \quad (2.8.6)$$

which is the well-known Rayleigh distribution.

The joint distribution of ρ, ϕ and their first-order derivatives with respect to x, y may be found as follows. Let

$$\xi_3, \xi_4 = \frac{\partial \xi_1}{\partial x}, \frac{\partial \xi_1}{\partial y}; \quad \xi_5, \xi_6 = \frac{\partial \xi_2}{\partial x}, \frac{\partial \xi_2}{\partial y}. \quad (2.8.7)$$

The matrix of correlations for ξ_1, \dots, ξ_6 is

$$(\Xi_{ij}) = \begin{pmatrix} \mu_{00} & 0 & 0 & 0 & \mu_{10} & \mu_{01} \\ 0 & \mu_{00} & -\mu_{10} & -\mu_{01} & 0 & 0 \\ \hline 0 & -\mu_{10} & \mu_{20} & \mu_{11} & 0 & 0 \\ 0 & -\mu_{01} & \mu_{11} & \mu_{02} & 0 & 0 \\ \mu_{10} & 0 & 0 & 0 & \mu_{20} & \mu_{11} \\ \mu_{01} & 0 & 0 & 0 & \mu_{11} & \mu_{02} \end{pmatrix}, \quad (2.8.8)$$

where μ_{pq} is the (p, q) th moment of $E(u, v)$ about (\bar{u}, \bar{v}) . But since (\bar{u}, \bar{v}) is the centroid of E , the first-order moments μ_{10}, μ_{01} vanish. Hence $\xi_3, \xi_4, \xi_5, \xi_6$ are independent of ξ_1, ξ_2 , and

$$p(\xi_1, \dots, \xi_6) = p(\xi_1, \xi_2) p(\xi_3, \dots, \xi_6), \quad (2.8.9)$$

where

$$p(\xi_3, \dots, \xi_6) = \frac{1}{(2\pi)^2 \delta} \exp\{-[\mu_{02}(\xi_3^2 + \xi_5^2) - 2\mu_{11}(\xi_3 \xi_4 + \xi_5 \xi_6) + \mu_{20}(\xi_4^2 + \xi_6^2)]/2\delta\}, \quad (2.8.10)$$

and we have written

$$\delta = \begin{vmatrix} \mu_{20} & \mu_{11} \\ \mu_{11} & \mu_{02} \end{vmatrix}. \quad (2.8.11)$$

Now since

$$\xi_3 = \frac{\partial}{\partial x}(\rho \cos \phi) = \rho_x \cos \phi - \rho \phi_x \sin \phi, \quad (2.8.12)$$

etc.,

we have
$$\frac{\partial(\xi_1, \xi_2, \xi_3, \xi_4, \xi_5, \xi_6)}{\partial(\rho, \phi, \rho_x, \phi_x, \rho_y, \phi_y)} = -\rho^3, \quad (2.8.13)$$

and hence

$$p(\rho, \phi, \rho_x, \phi_x, \rho_y, \phi_y) = \frac{1}{(2\pi)^3 m_{00} \delta} \rho^3 \exp\{-\rho^2/2m_{00}\} \\ \times \exp\{-(\mu_{02}\rho_x^2 - 2\mu_{11}\rho_x\rho_y + \mu_{20}\rho_y^2)/2\delta\} \exp\{-\rho^2\{\mu_{02}\phi_x^2 - 2\mu_{11}\phi_x\phi_y + \mu_{20}\phi_y^2\}/2\delta\}. \quad (2.8.14)$$

From this distribution some immediate conclusions may be drawn. First, by integrating with respect to ϕ (from 0 to 2π) and ϕ_x, ϕ_y (from $-\infty$ to ∞) we obtain the joint distribution of ρ, ρ_x and ρ_y . Thus

$$p(\rho, \rho_x, \rho_y) = p(\rho) p(\rho_x, \rho_y), \quad (2.8.15)$$

where $p(\rho)$ is given by (2.8.6) and

$$p(\rho_x, \rho_y) = \frac{1}{2\pi\delta^{\frac{1}{2}}} \exp\{-(\mu_{02}\rho_x^2 - 2\mu_{11}\rho_x\rho_y + \mu_{20}\rho_y^2)/2\delta\}. \quad (2.8.16)$$

This shows that ρ_x, ρ_y are statistically independent of ρ , just as $\partial\zeta/\partial x, \partial\zeta/\partial y$ are independent of ζ . Further, the distribution (2.8.16) is formally identical with (2.1.12), if the moments μ_{pq} about the centroid are substituted for the moments m_{pq} about the origin. We deduce immediately that

(1) the steepest r.m.s. gradient of the envelope is in the principal direction of the envelope, and the gentlest r.m.s. gradient of the envelope is in the direction at right angles;

(2) the most probable direction of contours of the envelope is perpendicular to the principal direction of the envelope, and the least probable direction is parallel to the principal direction.

We see from (2.8.14) that the mean values of ϕ_x and ϕ_y are zero. It follows that *the phase angle ϕ of the envelope has zero secular increase in any horizontal direction*. Now the phase angle of ζ is the sum of the phase angles of the envelope and of the carrier wave. Hence *the phase angle of ζ increases at the same average rate as that of the carrier wave*, in any horizontal direction. This property is the result of our having chosen the centroid (\bar{u}, \bar{v}) of the energy distribution as the wave-number of the carrier wave (§ 1.5).

By integrating (2.8.14) with respect to ρ_x, ρ_y and ϕ we obtain

$$p(\rho, \phi_x, \phi_y) = \frac{1}{2\pi m_{00} \delta^{\frac{1}{2}}} \rho^3 \exp\{-\rho^2/2m_{00}\} \exp\{-\rho^2(\mu_{02}\phi_x^2 - 2\mu_{11}\phi_x\phi_y + \mu_{20}\phi_y^2)/2\delta\}. \quad (2.8.17)$$

This shows that ϕ_x and ϕ_y are *not* statistically independent of ρ . In fact the standard deviation of (ϕ_x, ϕ_y) (defined as the square root of the mean value of $(\phi_x^2 + \phi_y^2)$) is

$$(\overline{\phi_x^2 + \phi_y^2})^{\frac{1}{2}} = \frac{1}{\rho} (\mu_{20} + \mu_{02})^{\frac{1}{2}}, \quad (2.8.18)$$

which is inversely proportional to ρ . Roughly, this means that the higher waves are more regular than the lower waves (cf. § 2.10). The joint distribution of ϕ_x and ϕ_y alone is found from (2.8.17) to be

$$p(\phi_x, \phi_y) = \frac{1}{\pi} \frac{m_{00}/\delta^{\frac{1}{2}}}{[1 + (\mu_{02}\phi_x^2 - 2\mu_{11}\phi_x\phi_y + \mu_{20}\phi_y^2)/m_{00}\delta]^2}. \quad (2.8.19)$$

It will be useful to consider also the statistical properties of the envelope of the curve in which the surface is intersected by a vertical plane in a direction θ . When $\theta = 0, x = x'$, the

STATISTICAL ANALYSIS OF A RANDOM, MOVING SURFACE 373

distribution of ρ , ϕ , ρ_x , ϕ_x may be found from (2.8.14) by integration with respect to ρ_y and ϕ_y . On replacing μ_{20} by $\mu_2(\theta)$ and x by x' we have in the general case

$$p(\rho, \phi, \rho_x, \phi_x) = \frac{1}{(2\pi)^2 m_{00} \mu_2} \rho^2 \exp\{-\rho^2/2m_{00}\} \exp\{-(\rho_x^2 + \rho^2 \phi_x^2)/2\mu_2\}. \quad (2.8.20)$$

Alternatively, the distribution may be derived from first principles by the method used to obtain (2.8.14). The joint distribution of ρ and ρ_x is found by further integration with respect to ϕ and ϕ_x :

$$p(\rho, \rho_x) = \frac{1}{(2\pi)^{\frac{1}{2}} m_{00} \mu_2} \rho \exp\{-\rho^2/2m_{00}\} \exp\{-\rho_x^2/2\mu_2\}. \quad (2.8.21)$$

Similarly the joint distribution of ρ , ϕ and ϕ_x is

$$p(\rho, \phi, \phi_x) = \frac{1}{(2\pi)^{\frac{3}{2}} m_{00} \mu_2^{\frac{1}{2}}} \rho^2 \exp\{-\rho^2/2m_{00}\} \exp\{-\rho^2 \phi_x^2/2\mu_2\}, \quad (2.8.22)$$

and the distribution of ϕ and ϕ_x is

$$p(\phi, \phi_x) = \frac{(m_{00}/\mu_2)^{\frac{1}{2}}}{4\pi(1 + \phi_x^2 m_{00}/\mu_2)^{\frac{1}{2}}}. \quad (2.8.23)$$

From these distributions one can state immediately some general conclusions for the one-dimensional envelope analogous to those for the two-dimensional envelope of surface. Thus ρ_x , but not ϕ_x , is independent of ρ ; the mean secular increase of ϕ with x' is zero; the standard deviation of ϕ_x is inversely proportional to ρ .

When the spectrum is fairly narrow, the envelope follows closely the crests of the waves. In any particular plane section the waves will appear in groups, and a rough measure of the average length of a group is given by $2/\mathbf{N}$, where \mathbf{N} is the average number of times per unit distance that the envelope crosses an arbitrary level ρ . Now by the argument of § 2.2,

$$\mathbf{N}(\rho) = \int_{-\infty}^{\infty} p(\rho, \rho_x) |\rho_x| d\rho_x. \quad (2.8.24)$$

On substituting from (2.8.23) and carrying out the integration we have

$$\mathbf{N}(\rho) = \left(\frac{2}{\pi}\right)^{\frac{1}{2}} \frac{\mu_2^{\frac{1}{2}}}{m_{00}} \rho \exp\{-\rho^2/2m_{00}\}. \quad (2.8.25)$$

For definiteness we may take the largest possible value of \mathbf{N} , which occurs when $\rho = m_{00}^{\frac{1}{2}}$, giving

$$\mathbf{N} = \left(\frac{2}{\pi}\right)^{\frac{1}{2}} \left(\frac{\mu_2}{m_{00}}\right)^{\frac{1}{2}}. \quad (2.8.26)$$

Now by § 1.5 $\mu_2(\theta)$ is greatest when θ defines the principal direction. It follows that *the average length of a group of waves is least in the principal direction and greatest in the direction at right angles.*

A rough measure of the number of waves in each group is given by N_0/\mathbf{N} , where N_0 is the number of zero-crossings of ζ in the direction θ (see § 2.2). When $\rho = m_{00}^{\frac{1}{2}}$ we have

$$\frac{N_0}{\mathbf{N}} = \left(\frac{e}{2\pi}\right)^{\frac{1}{2}} \left(\frac{m_2}{\mu_2}\right)^{\frac{1}{2}} = \left(\frac{e}{2\pi}\right)^{\frac{1}{2}} \left[\frac{m_{20} \cos^2 \theta + 2m_{11} \cos \theta \sin \theta + m_{02} \sin^2 \theta}{\mu_{20} \cos^2 \theta + 2\mu_{11} \cos \theta \sin \theta + \mu_{02} \sin^2 \theta} \right]^{\frac{1}{2}}. \quad (2.8.27)$$

In general this number will vary with the direction θ , but it may also be constant. The condition for constancy is

$$\mu_{20}^2 \mu_{11} : \mu_{02} = m_{20}^2 m_{11} : m_{02}. \quad (2.8.28)$$

When this condition is satisfied the number of waves in a group is independent of the direction.

If we write
$$\nu'(\theta) = \frac{m_{00}}{m_1(\theta)} \left(\frac{\mu_2(\theta)}{m_{00}} \right)^{\frac{1}{2}}, \tag{2.8.29}$$

so that (for a narrow spectrum)

$$\nu'(\theta) \approx \left(\frac{\mu_2(\theta)}{m_2(\theta)} \right)^{\frac{1}{2}} = \left(\frac{2\pi}{\epsilon} \right)^{\frac{1}{2}} \frac{N}{N_0}, \tag{2.8.30}$$

it is clear that ν' is inversely proportional to the number of waves in a group. In particular, when the section is taken in the direction $\theta = 0$ we have

$$\nu'(0) = \left(\frac{\mu_{20}}{i^2 m_{00}} \right)^{\frac{1}{2}} = \nu, \tag{2.8.31}$$

where ν is the parameter defined in § 1.6. Now $\theta = 0$ was taken there to be the mean direction, and also the principal direction. It follows that ν is inversely proportional to the number of waves in a group corresponding to a vertical section taken in the principal direction.

2.9. The heights of maxima

Throughout this and the following section it will be assumed that the spectrum is narrow. We shall see that from the properties of the envelope one can then derive some interesting statistical properties that are otherwise difficult to obtain.

Consider first the distribution of the heights ξ of the crests. A crest may be defined as the locus of the maxima of all vertical sections of the surface parallel to the mean direction θ . Now when the spectrum is narrow, the waves will be long-crested and regular, and the crests will lie almost on the envelope. Further, the crests will be spaced at more or less equal intervals in the x, y plane. It follows that the distribution of the crest heights is practically the same as the distribution of the envelope function ρ . So from (2.8.6)

$$\rho(\xi) = \frac{\xi}{m_{00}} \exp \{ -\xi^2 / 2m_{00} \}. \tag{2.9.1}$$

In other words, ξ has a Rayleigh distribution.

Consider, on the other hand, the distribution of the heights of the maxima. A maximum of the surface is simultaneously a maximum perpendicular and parallel to the mean direction. The distribution of maxima of the surface therefore approximates to the distribution of the maxima of the envelope of a section at right angles to the mean direction.

Now the distribution of the maxima of the envelope of a single random variable has been studied by Rice (1944, 1945). Making the simplifying assumption that $\mu_1 = \mu_3 = 0$ (in our case $\mu_1 = 0$ anyway), he obtains for the joint distribution of x' and the height R of a maximum

$$\rho(x', R) = \frac{1}{4\pi^{\frac{1}{2}} \mu_0} (a^2 - 1)^{\frac{1}{2}} z^{\frac{1}{2}} e^{-a^2 z^2} \sum_{n=0}^{\infty} \frac{A_n z^n}{(\frac{1}{2}n + \frac{3}{4})!}, \tag{2.9.2}$$

where

$$a^2 = \frac{\mu_0 \mu_4}{\mu_2^2}, \quad z = \frac{R}{[2(a^2 - 1) \mu_0]^{\frac{1}{2}}}, \tag{2.9.3}$$

and

$$A_n = \sum_{m=0}^n \frac{(\frac{1}{2}) (\frac{3}{2}) \dots (m - \frac{1}{2})}{m!} (n - m + 1) (\frac{3}{2} - \frac{1}{2} a^2)^m \tag{2.9.4}$$

(the term corresponding to $m = 0$ in (2.9.4) is $n + 1$). To obtain the probability density of R alone we must normalize (2.9.2) by dividing by the number N of maxima per unit distance x' . N is found by integrating with respect to R from 0 to ∞ . We have

$$N = \frac{1}{4(2\pi)^{\frac{1}{2}}} \frac{(\mu_2)^{\frac{1}{2}} (a^2 - 1)^2}{(\mu_0)^{\frac{1}{2}} a^{\frac{1}{2}}} \sum_{n=0}^{\infty} \frac{(\frac{1}{2}n + \frac{1}{2})! A_n}{(\frac{1}{2}n + \frac{3}{2})! a^n} \quad (2.9.5)$$

(Rice 1945, p. 83).

This may be checked immediately by comparison with our previous work. For, since the maxima occur only at the crests of the waves, which are more or less evenly spaced at distance $2\pi/\bar{u}$ apart, it follows that the mean density of maxima per unit area is $N\bar{u}/2\pi$ approximately. On replacing $(\mu_2/\mu_0)^{\frac{1}{2}}$ by $\gamma\bar{u}$, where γ^{-1} is the long-crestedness, we have

$$D_{ma.} = \frac{N\bar{u}}{2\pi} = \frac{1}{4(2\pi)^{\frac{1}{2}}} \frac{(a^2 - 1)^2}{a^{\frac{1}{2}}} \sum_{n=0}^{\infty} \frac{(\frac{1}{2}n + \frac{1}{2})! A_n}{(\frac{1}{2}n + \frac{3}{2})! a^n} \gamma\bar{u}^2. \quad (2.9.6)$$

This expression should agree with (2.3.57). Rice summed the series in (2.9.6) for $a^2 = 3$ (the normal distribution) and found it to be about 3.97. With this value (2.9.6) becomes

$$D_{ma.} = 0.0638\gamma\bar{u}^2, \quad (2.9.7)$$

which is in agreement with the more accurate value $D_{ma.} = 0.0639\gamma\bar{u}^2$ given by (2.3.57) and table 1.

The distribution of the heights of maxima may be stated in terms of the non-dimensional parameter $\eta = R/\mu_0^{\frac{1}{2}} = R/m_{00}^{\frac{1}{2}}$. On dividing $p(x', R)$ by $N\mu_0^{\frac{1}{2}}$, we find

$$p(\eta) = \frac{1}{2^{\frac{1}{2}}(1-a^2)^{\frac{1}{2}}} \eta^{\frac{1}{2}} \exp\{-\eta^2/2(1-a^2)\} \sum_{n=0}^{\infty} \frac{A_n [\eta^2/2(a^2-1)]^{\frac{1}{2}n}}{(\frac{1}{2}n + \frac{1}{2})!} \bigg/ \sum_{n=0}^{\infty} \frac{(\frac{1}{2}n + \frac{1}{2})! A_n}{(\frac{1}{2}n + \frac{3}{2})! a^n}. \quad (2.9.8)$$

This distribution has been computed for $a^2 = 2, 3, 5, 9$, and the curves are shown in figure 13.

When $a^2 \neq 1$ the above series becomes unsuitable for computation, but we may obtain a solution by an independent method as follows. $a^2 = 1$ corresponds to two narrow bands of energy of slightly different frequency. These form beats, and the maxima of the envelope occur when the two wave bands are in phase. The height of the envelope R is then the sum of the amplitudes ρ_1, ρ_2 of the two wave trains at that point. But the amplitude of each wave train has a Rayleigh distribution:

$$p(\rho_1) = \frac{2\rho_1}{m_{00}} \exp\{-\rho_1^2/m_{00}\}, \quad p(\rho_2) = \frac{2\rho_2}{m_{00}} \exp\{-\rho_2^2/m_{00}\} \quad (2.9.9)$$

(the mean energy for each wave train being $\frac{1}{2}m_{00}$). The distribution of the sum of these is

$$p(R) = \int_0^R p(\rho_1) p(\rho_2) d\rho_1, \quad (2.9.10)$$

where $\rho_2 = R - \rho_1$. In terms of non-dimensional variables we have

$$p(\eta) = 2 \int_0^{\eta} \xi e^{-\xi^2} (\eta - \xi) e^{-(\eta - \xi)^2} d\xi. \quad (2.9.11)$$

On evaluating the integral we have

$$p(\eta) = e^{-\frac{1}{2}\eta^2} [\eta e^{-\frac{1}{2}\eta^2} + (\eta^2 - 1) \int_0^{\eta} e^{-\frac{1}{2}t^2} dt], \quad (2.9.12)$$

which is the distribution shown in figure 13 for $a^2 = 1$.

It can be seen independently that this is the appropriate distribution for two long-crested systems of waves intersecting at an angle. For the maxima of the combine system occur at the points of intersection of the crests of the two long-crested systems. The height of a maximum is the sum of the heights of the crests of the two systems. Consequently η is the sum of two variables each having a Rayleigh distribution.

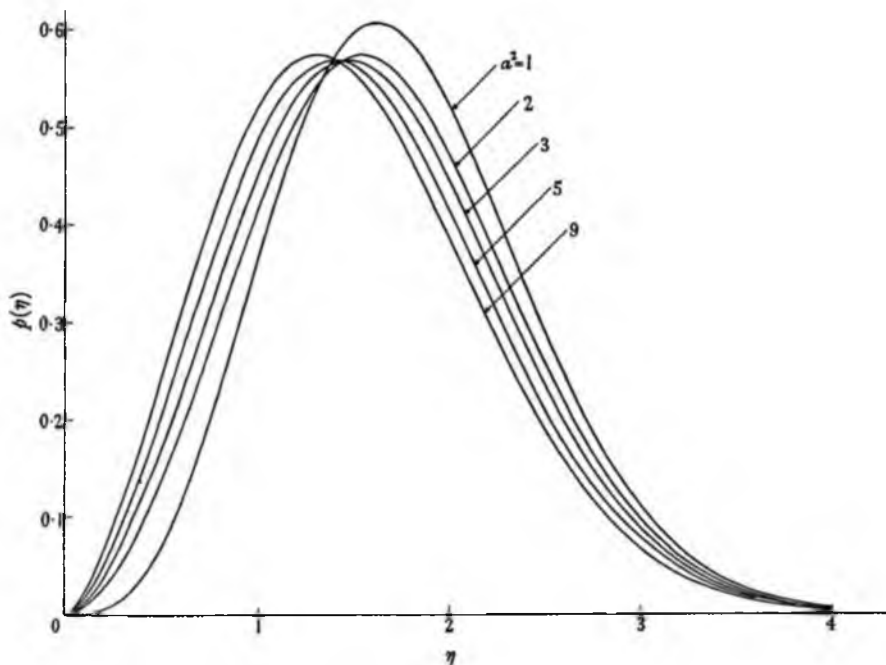


FIGURE 13. The probability distribution of the heights of maxima, for a narrow spectrum ($a^2 = 1, 2, 3, 5, 9$).

2.10. *The intervals between successive zeros*

Finally, let us consider the distribution of the intervals l between successive zeros of the surface, along a line drawn in an arbitrary direction θ . An approximate expression for the distribution of intervals for a one-dimensional function has been derived by Rice (1945, § 3.4) after a series of approximations assuming that the spectrum is narrow. It will now be shown how the same distribution can be derived very simply using the properties of the phase angle ϕ . Further, the distribution will be derived for a section of the surface in an arbitrary direction θ , and for waves of any particular amplitude ρ .

For simplicity we may take initially $\theta = \theta_p = 0$ and $x' = x$, and we may generalize to arbitrary values of θ at a suitable stage. The equation of the curve at an arbitrary time, say $t = 0$, may be written

$$\zeta = \mathcal{R}\rho e^{i\chi}, \quad (2.10.1)$$

where

$$\chi = \bar{u}x + \phi, \quad \chi_x = \bar{u} + \phi_x. \quad (2.10.2)$$

STATISTICAL ANALYSIS OF A RANDOM, MOVING SURFACE 377

and $\bar{u} = m_1/m_0$. Like ϕ , χ is a multivalued function of x , having branches separated by multiples of 2π . Since

$$\frac{\partial(\chi, \chi_x)}{\partial(\phi, \phi_x)} = 1, \quad (2\cdot10\cdot3)$$

we have from (2·8·23)

$$p(\chi, \chi_x) = p(\phi, \phi_x) = \frac{(m_0/\mu_2)^{\frac{1}{2}}}{4\pi(1 + (\chi_x - \bar{u})^2 m_0/\mu_2)^{\frac{1}{2}}}. \quad (2\cdot10\cdot4)$$

Now χ has a zero-crossing when and only when $\chi = n\pi$, where n is an integer. By the same reasoning as in §2·2, the probability of χ taking the value $2r\pi$ in $(x, x + dx)$ is

$$H(\chi) dx = \int_{-\infty}^{\infty} p(\chi, \chi_x) |\chi_x| dx d\chi_x = \frac{1}{2\pi} \left(\frac{m_2}{m_0}\right)^{\frac{1}{2}} dx. \quad (2\cdot10\cdot5)$$

The probability of χ taking the value $(2r+1)\pi$ is the same. Therefore the total probability of a zero in $(x, x + dx)$ is twice this value, or

$$\frac{1}{\pi} \left(\frac{m_2}{m_0}\right)^{\frac{1}{2}} dx, \quad (2\cdot10\cdot6)$$

in agreement with (2·3·5).

Let l denote the interval between successive zeros. The average value l of the distribution of l may be written down immediately; for it is simply the reciprocal of the average number of zeros per unit distance, i.e.

$$l = \pi \left(\frac{m_0}{m_2}\right)^{\frac{1}{2}} = \frac{\pi}{\bar{u}} (1 + \nu^2)^{\frac{1}{2}}, \quad (2\cdot10\cdot7)$$

where ν is defined by (2·8·31). When the spectrum is narrow (ν is small) we have

$$l = \pi/\bar{u}, \quad (2\cdot10\cdot8)$$

approximately.

Let us now consider the whole distribution of l , on the assumption that ν is small. In the first place we may note that where χ crosses any level $n\pi$ it nearly always has an up-crossing. For the probability of a down-crossing ($\chi_x < 0$) in the interval $(x, x + dx)$ is given by

$$\int_{-\infty}^0 p(\chi, \chi_x) |\chi_x| dx d\chi_x = \frac{1}{4\pi} \left(\frac{m_2}{m_0}\right)^{\frac{1}{2}} [1 - (1 + \nu^2)^{-\frac{1}{2}}] dx, \quad (2\cdot10\cdot9)$$

and the proportion of down-crossings is therefore

$$\frac{1}{2} [1 - (1 + \nu^2)^{-\frac{1}{2}}] \doteq \frac{1}{4} \nu^2, \quad (2\cdot10\cdot10)$$

which is negligible. If each crossing of $2r\pi$ or $(2r+1)\pi$ is an up-crossing, it follows that between any two successive zeros x_1 and x_2 , χ must increase by π . Hence

$$\pi = \chi(x_2) - \chi(x_1) = [l\chi_x + \frac{1}{2}l^2\chi_{xx} + \dots], \quad (2\cdot10\cdot11)$$

where we have expanded in a Taylor series about $x = x_1$. It can be shown that χ_{xx} is of order ν^2 , and so to our present order of approximation

$$l = \pi/\chi_x. \quad (2\cdot10\cdot12)$$

Now the distribution of χ_x , at points where χ takes a particular value, is given by

$$p(\chi_x)_\chi = \frac{p(\chi, \chi_x) |\chi_x|}{H(\chi)}, \quad (2\cdot10\cdot13)$$

where $H(\chi)$ is given by (2.10.5). That is to say

$$p(\chi_x)_x = \frac{1}{2} \left(\frac{m_0}{m_2} \right)^{\frac{1}{2}} \frac{|\chi_x| (m_0/\mu_2)^{\frac{1}{2}}}{[1 + (\chi_x - \bar{u})^2 m_0/\mu_2]^{\frac{1}{2}}}. \quad (2.10.14)$$

On substituting from (2.10.12) we have, when $l > 0$,

$$p(l) = \frac{1}{2\pi} \left(\frac{m_0}{m_2} \right)^{\frac{1}{2}} \frac{\bar{u}^2/\nu}{[l^2/l^2 + (l/l-1)^2/\nu^2]^{\frac{1}{2}}}, \quad (2.10.15)$$

where l is given by the approximate relation (2.10.8). Clearly $p(l)$ is appreciable only when l differs from l by an amount of order ν . Writing

$$\xi = (l-l)/l \quad (2.10.16)$$

for the relative departure of l from its mean value, we have finally for the approximate distribution of ξ in the neighbourhood of the mean

$$p(\xi) = \frac{1}{2\nu(1+\xi^2/\nu^2)^{\frac{1}{2}}}. \quad (2.10.17)$$

This is similar to the approximate distribution found by Rice (1945, p. 63) by a rather longer method.

In the general case when the line drawn on the surface is in an arbitrary direction θ , ν may be replaced by $\nu'(\theta)$. Thus we have in general

$$p(\xi) = \frac{1}{2\nu'(1+\xi^2/\nu'^2)^{\frac{1}{2}}}. \quad (2.10.18)$$

The second moment of this distribution is divergent, but a convenient measure of its spread is the width of the interquartile range, given by

$$\frac{2}{\sqrt{3}} \nu'. \quad (2.10.19)$$

So we may say that *the width of the distribution of ξ is inversely proportional to the average number of waves in a group*. The width of the distribution of l is given by the above expression multiplied by l , that is to say

$$\frac{2\pi m_0^{\frac{1}{2}} \bar{u}^{\frac{1}{2}}}{\sqrt{3} m_1^{\frac{1}{2}}}. \quad (2.10.20)$$

To find the distribution of intervals l for waves of a given amplitude (say with amplitude lying between ρ and $\rho + d\rho$), we may start from the distribution of (ϕ, ϕ_x) for values of ρ lying between these limits. This is given by

$$p_\rho(\phi, \phi_x) = \frac{p(\rho, \phi, \phi_x)}{p(\rho)} = \frac{1}{(2\pi)^{\frac{1}{2}} \mu_1^{\frac{1}{2}}} \rho \exp\{-\rho^2 \phi_x^2 / 2\mu_2\} \quad (2.10.21)$$

from (2.8.6) and (2.8.22). Hence

$$p_\rho(\chi, \chi_x) = \frac{1}{(2\pi)^{\frac{1}{2}} \mu_1^{\frac{1}{2}}} \rho \exp\{-\rho^2 (\chi_x - \bar{u})^2 / 2\mu_2\}. \quad (2.10.22)$$

On carrying out the same calculation with $p_\rho(\chi, \chi_x)$ in place of $p(\chi, \chi_x)$ we find, with ξ given by (2.10.16), that

$$p_\rho(\xi) = \frac{1}{(2\pi)^{\frac{1}{2}} \nu' m_{00}^{\frac{1}{2}}} \rho \exp\{-\rho^2 \xi^2 / 2\nu'^2 m_{00}\}. \quad (2.10.23)$$

This is a normal distribution for ξ , with mean value zero and standard deviation

$$\frac{v' m_{00}^{\frac{1}{2}}}{\rho} \tag{2.10.24}$$

The mean and standard deviation of l are equal to l and $v' m_{00}^{\frac{1}{2}} l / \rho$ respectively. Hence we may say that *the expectation of l is independent of the height of the waves* (to the present order of approximation) and also *the width of the distribution of l is inversely proportional to the wave height*. If we take this width as a measure of the irregularity of the waves as regards their intervals, we may also say that *the lower the waves, the less regular are their intervals*.

PART III. A METHOD OF DETERMINING THE ENERGY SPECTRUM

In the two previous parts of this paper we have derived some statistical properties of a random surface in terms of its energy spectrum $E(u, v)$. In this part we solve the converse problem: given the statistical properties, to find the energy spectrum.

The best method of determining E depends to some extent upon which properties can be measured most conveniently. We assume that it is possible to obtain the height $\zeta(x')$ of the surface along a line in an arbitrary direction θ . (In the case of the sea surface one may imagine the observations to be made by an aircraft flying on a fixed course at high speed and constant altitude and recording by radar its height above the waves.) We also assume that $\partial\zeta(x')/\partial t$ can be measured (by a pair of radar sets, or otherwise).

In §3.1 it is shown how from the statistical analysis of such measurements the moments $m_n(\theta)$, for each value of θ , can be deduced. In §3.2 it is shown how to obtain the two-dimensional moments m_{pq} from the moments $m_n(\theta)$; and in §3.3 how to obtain the energy spectrum from the moments m_{pq} .

3.1. To obtain $m_n(\theta)$

We saw in §2.2 that the number of zeros of $\zeta(x')$ per unit horizontal distance x' is given by

$$N_0 = \frac{1}{\pi} \left(\frac{m_2(\theta)}{m_0(\theta)} \right)^{\frac{1}{2}}, \tag{3.1.1}$$

and in general the number of zeros of the r th derivative of ζ is given by

$$N_r = \frac{1}{\pi} \left(\frac{m_{2r+2}(\theta)}{m_{2r}(\theta)} \right)^{\frac{1}{2}}. \tag{3.1.2}$$

Now from the record of ζ , the numbers N_0, N_1 , etc., may be determined by simple counting of zeros, maxima and minima, points of inflexion, and so on. $m_0(\theta)$ can be determined as the r.m.s. value of ζ along the curve. From (3.1.1) we have

$$m_2(\theta) = \pi^2 N_0^2 m_0(\theta) \tag{3.1.3}$$

and from (3.1.2)

$$m_{2r+2}(\theta) = \pi^2 N_r^2 m_{2r}(\theta). \tag{3.1.4}$$

So $m_{2r}, m_{4r}, \dots, m_{2r+2}$ can be determined in succession, or else directly from

$$m_{2r+2}(\theta) = \pi^{2r+2} N_0^2 N_1^2 \dots N_r^2 m_0(\theta). \tag{3.1.5}$$

To obtain the moments of odd order we have to use some property involving the motion of the surface. We take the distribution of the velocities of zeros of $\zeta(x')$, which was derived in §2.5. It was shown that the mean velocity of the zeros of ζ is given by

$$\bar{v} = - \frac{m'_1(\theta)}{m_2(\theta)}, \tag{3.1.6}$$

and that the mean velocity of points where the r th derivative vanishes is

$$\bar{z}_r = -\frac{m'_{2r+1}(\theta)}{m_{2r+2}(\theta)}. \quad (3.1.7)$$

Now $m'_{2r+2}(\theta)$ is already known, from equation (3.1.5), so from

$$m'_{2r+1}(\theta) = -\bar{z}_r m_{2r+2}(\theta) \quad (3.1.8)$$

we may determine $m'_{2r+1}(\theta)$.

It is true that the odd moments $m'_{2r+1}(\theta)$ correspond not to the original function $E(u, v)$ but to $\sigma(u, v) E(u, v)$. However, we shall show in § 3.3 how this difficulty can be overcome.

3.2. To obtain m_{pq}

In § 1.4 we saw that $m_n(\theta)$ is related to the moments m_{pq} ($p+q=n$) by the equation

$$m_n(\theta) = m_{n,0} \cos^n \theta + \binom{n}{1} m_{n-1,1} \cos^{n-1} \theta \sin \theta + \dots + m_{0,n} \sin^n \theta. \quad (3.2.1)$$

The expression on the right-hand side is a trigonometric polynomial of degree n , with coefficients which are linear combinations of the moments. Therefore we may expect to solve for m_{pq} by taking the Fourier components of $m_n(\theta)$, that is, by considering the quantities

$$a_{n,l} = \frac{1}{\pi} \int_0^{2\pi} m_n(\theta) e^{il\theta} d\theta. \quad (3.2.2)$$

Going back to equation (1.4.11), we have

$$\begin{aligned} a_{n,l} &= \frac{1}{\pi} \int_0^{2\pi} \int_{-\infty}^{\infty} \int_{-\infty}^{\infty} E(u, v) (u \cos \theta_1 + v \sin \theta_1)^n du dv e^{il\theta_1} d\theta_1 \\ &= \frac{1}{\pi} \int_0^{2\pi} \int_{-\infty}^{\infty} \int_{-\infty}^{\infty} E(u, v) \{w \cos(\theta - \theta_1)\}^n du dv e^{il\theta_1} d\theta_1, \end{aligned} \quad (3.2.3)$$

where $(w \cos \theta, w \sin \theta) = (u, v)$. On writing $\theta_1 - \theta = \theta_2$ and reversing the order of integration we have

$$\begin{aligned} a_{n,l} &= \frac{1}{\pi} \int_{-\infty}^{\infty} \int_{-\infty}^{\infty} \int_0^{2\pi} E(u, v) w^n \cos^n \theta_2 e^{i(l\theta + \theta_2)} d\theta_2 du dv \\ &= \gamma_{n,l} \int_{-\infty}^{\infty} \int_{-\infty}^{\infty} E(u, v) w^n e^{il\theta} du dv, \end{aligned} \quad (3.2.4)$$

where $\gamma_{n,l}$ is a numerical constant:

$$\gamma_{n,l} = \frac{1}{\pi} \int_0^{2\pi} \cos^n \theta_2 e^{il\theta_2} d\theta_2 = \begin{cases} 2^{1-n} \binom{n}{r} & \text{when } n-l = 2r > 0 \\ 0 & \text{otherwise.} \end{cases} \quad (3.2.5)$$

Now

$$\begin{aligned} m_{pq} &= \int_{-\infty}^{\infty} \int_{-\infty}^{\infty} E(u, v) u^p v^q du dv \\ &= \int_{-\infty}^{\infty} \int_{-\infty}^{\infty} E(u, v) w^n \cos^p \theta \sin^q \theta du dv \\ &= \int_{-\infty}^{\infty} \int_{-\infty}^{\infty} E(u, v) w^n \frac{1}{2^n i^q} (e^{i\theta} + e^{-i\theta})^n (e^{i\theta} - e^{-i\theta})^q du dv \\ &= \int_{-\infty}^{\infty} \int_{-\infty}^{\infty} E(u, v) w^n \left[e^{in\theta} + \binom{p}{1} \binom{q}{1} e^{i(n-2)\theta} + \binom{p}{2} \binom{q}{2} e^{i(n-4)\theta} + \dots + (-1)^q e^{-in\theta} \right] du dv, \end{aligned} \quad (3.2.6)$$

where $\binom{p}{r} \binom{q}{r}$ is the coefficient of x^r in the expansion of $(1+x)^p (1-x)^q$. In full,

$$\binom{p}{r} \binom{q}{r} = \binom{p}{r} - \binom{p}{r-1} \binom{q}{1} + \binom{p}{r-2} \binom{q}{2} - \dots + (-1)^r \binom{q}{r}, \tag{3.2.7}$$

where $\binom{p}{0} = 1$ and $\binom{p}{r} = 0$ for $r > p$. From (3.2.4) and (3.2.6) we have

$$m_{pq} = \frac{1}{2i^q} \left[a_{n,n} + \binom{p}{1} \binom{q}{1} / \binom{n}{1} a_{n,n-2} + \binom{p}{2} \binom{q}{2} / \binom{n}{2} a_{n,n-4} + \dots + (-1)^q a_{n,n} \right]. \tag{3.2.8}$$

TABLE 2. FUNCTIONS $C_{pq}(\theta)$

$C_{00} = \frac{1}{2}$ $\begin{cases} C_{20} = \cos 2\theta + \frac{1}{2} \\ C_{11} = \sin 2\theta \\ C_{02} = -\cos 2\theta + \frac{1}{2} \end{cases}$ $\begin{cases} C_{40} = \cos 4\theta + \cos 2\theta + \frac{1}{2} \\ C_{31} = \sin 4\theta + \frac{1}{2} \sin 2\theta \\ C_{22} = -\cos 4\theta + \frac{1}{2} \\ C_{13} = -\sin 4\theta + \frac{1}{2} \sin 2\theta \\ C_{04} = \cos 4\theta - \cos 2\theta + \frac{1}{2} \end{cases}$	$\begin{cases} C_{10} = \cos \theta \\ C_{01} = \sin \theta \end{cases}$ $\begin{cases} C_{30} = \cos 3\theta + \cos \theta \\ C_{21} = \sin 3\theta + \frac{1}{2} \sin \theta \\ C_{12} = -\cos 3\theta + \frac{1}{2} \cos \theta \\ C_{03} = -\sin 3\theta + \sin \theta \end{cases}$ $\begin{cases} C_{50} = \cos 5\theta + \cos 3\theta + \cos \theta \\ C_{41} = \sin 5\theta + \frac{3}{2} \sin 3\theta + \frac{1}{2} \sin \theta \\ C_{32} = -\cos 5\theta - \frac{1}{2} \cos 3\theta + \frac{1}{2} \cos \theta \\ C_{23} = -\sin 5\theta + \frac{1}{2} \sin 3\theta + \frac{1}{2} \sin \theta \\ C_{14} = \cos 5\theta - \frac{3}{2} \cos 3\theta + \frac{1}{2} \cos \theta \\ C_{05} = \sin 5\theta - \sin 3\theta + \sin \theta \end{cases}$
---	--

So on substitution from (3.2.2)

$$m_{pq} = \frac{1}{\pi} \int_0^{2\pi} m_n(\theta) C_{pq}(\theta) d\theta, \tag{3.2.9}$$

where
$$C_{pq}(\theta) = \frac{1}{2i^q} \left[e^{in\theta} + \binom{p}{1} \binom{q}{1} / \binom{n}{1} e^{i(n-2)\theta} + \dots + (-1)^n e^{-in\theta} \right]. \tag{3.2.10}$$

The quantities $m_n(\theta)$ being known, this determines the moments m_{pq} . The first few functions $C_{pq}(\theta)$ are listed in table 2.

Incidentally, when the spectrum $E(u, v)$ has circular symmetry, $m_n(\theta)$ is independent of θ and so from (3.2.9)

$$m_{pq}(\theta) = \begin{cases} (-1)^{\frac{1}{2}q} \binom{p}{\frac{1}{2}n} \binom{q}{\frac{1}{2}n} / \binom{n}{\frac{1}{2}n} m_n & \text{when } p, q \text{ are both even} \\ 0 & \text{otherwise.} \end{cases} \tag{3.2.11}$$

In particular
$$m_{20} = m_{02} = m_{22}, \quad m_{40} = m_{04} = m_{44}, \quad m_{22} = \frac{1}{3} m_{44}, \tag{3.2.12}$$

and so the condition (1.3.11) for a narrow ring spectrum reduces to

$$\frac{3}{2} m_4 m_0 - 4 m_2^2 = 0 \tag{3.2.13}$$

or
$$\frac{m_4 m_0}{m_2^2} = \frac{3}{2}. \tag{3.2.14}$$

As a corollary, we see that $m_4 m_0 / m_2^2$ is never less than $\frac{3}{2}$.

3.3. To obtain $E(u, v)$

We have so far obtained the even moments m_{pq} of $E(u, v)$ and the odd moments m'_{pq} of $\sigma(u, v) E(u, v)$. Now consider the function

$$F(u, v) = \frac{1}{2}[E(u, v) + E(-u, -v)]. \quad (3.3.1)$$

This is clearly an even function of (u, v) , since $F(-u, -v) = F(u, v)$. Therefore its odd moments vanish. But its even moments are the same as those of $E(u, v)$. Therefore both the odd and even moments of $F(u, v)$ are known. Similarly

$$G(u, v) = \frac{1}{2}[\sigma(u, v) E(u, v) - \sigma(-u, -v) E(-u, -v)] \quad (3.3.2)$$

is clearly an odd function of (u, v) , since $G(-u, -v) = -G(u, v)$, and so its even moments vanish. But since $\sigma(-u, -v) = \sigma(u, v)$ (equation (1.1.5)) the odd moments of G are equal to those of $\sigma(u, v) E(u, v)$. Therefore both the odd and even moments of G are known. If F and G can both be determined from their moments we may then determine E , from the identity

$$E(u, v) = F(u, v) + G(u, v)/\sigma(u, v). \quad (3.3.3)$$

We have then simply to consider how to determine F and G from their moments.*

Formally, if the moments were known to all orders, the problem would be solved. For since the even moments m_{pq} are equivalent to the derivatives of the correlation function $\psi(x, y, 0)$ (equation (1.2.10)) we have

$$\psi(x, y, 0) = \sum_{p+q=2r} (-1)^r \frac{m_{pq}}{p! q!} x^p y^q. \quad (3.3.4)$$

But by (1.2.9), $\psi(x, y, 0)$ is the cosine transform of $E(u, v)$ and so of $F(u, v)$. Hence

$$F(u, v) = \frac{1}{(2\pi)^2} \int_{-\infty}^{\infty} \int_{-\infty}^{\infty} \psi(x, y, 0) \cos(ux + vy) dx dy. \quad (3.3.5)$$

Similarly, if we define a function

$$\psi'(x, y, 0) = \sum_{p+q=2r} (-1)^{r+1} \frac{m'_{pq}}{p! q!} x^p y^q, \quad (3.3.6)$$

we have

$$G(u, v) = \frac{1}{(2\pi)^2} \int_{-\infty}^{\infty} \int_{-\infty}^{\infty} \psi'(x, y, 0) \sin(ux + vy) dx dy. \quad (3.3.7)$$

In practice, however, only a finite number of moments can be obtained, and if (3.3.4) is replaced by only a finite number of terms of the series, (3.3.5) does not converge. The problem then is to find a convergent sequence of approximations to F and G , each approximation depending on the moments of the function up to a finite order.

It was shown by Weierstrass (1885) that a function of a single variable may be approximated over a finite range by a polynomial, and that this may be done in a variety of different ways. A simple method is given by Courant & Hilbert (1953, §4), which we generalize to two dimensions as follows. Consider the function†

$$g_n(u, v) = (1 - u^2 - v^2)^n. \quad (3.3.8)$$

* For a discussion of whether a function is uniquely determined by its moments, see Kendall (1952, chap. 4).

† This is different from the generalization suggested in Courant & Hilbert (1953, p. 68), and leads to a more homogeneous approximation.

STATISTICAL ANALYSIS OF A RANDOM, MOVING SURFACE 383

As n tends to infinity, g_n tends to zero for all values of (u, v) inside the circle $u^2 + v^2 = 1$ except the origin. Further, if S is any smaller circle of radius $\delta < 1$,

$$\iint_S g_n(u, v) \, du \, dv = \int_0^\delta \int_0^{2\pi} (1 - w^2)^n \, w \, dw \, d\theta = \frac{\pi}{n+1} [1 - (1 - \delta^2)^{n+1}], \tag{3.3.9}$$

which also tends to zero. However, the dominant part of the above integral is contributed by the neighbourhood of the origin, that is, if S' is any interior circle of fixed radius δ' , however small, almost the entire contribution to the integral comes from S' :

$$\lim_{n \rightarrow \infty} \frac{\iint_{S'} g_n(u, v) \, du \, dv}{\iint_S g_n(u, v) \, du \, dv} = \lim_{n \rightarrow \infty} \frac{1 - (1 - \delta'^2)^{n+1}}{1 - (1 - \delta^2)^{n+1}} = 1. \tag{3.3.10}$$

Now suppose that $f(u, v)$ is any continuous function of two variables that we wish to approximate in the region S , $(u^2 + v^2)^{\frac{1}{2}} < \frac{1}{2}$. Then if (u, v) is any interior point of S , the function

$$f_n(u, v) = \frac{\iint_S f(u_1, v_1) [1 - (u - u_1)^2 - (v - v_1)^2]^n \, du_1 \, dv_1}{\iint_S [1 - u_1^2 - v_1^2]^n \, du_1 \, dv_1} \tag{3.3.11}$$

is a weighted mean of $f(u, v)$, with weighting function $g_n(u - u_1, v - v_1)$ centred on (u, v) . And since the neighbourhood of (u, v) contributes almost all the weight when n is large we see that

$$\lim_{n \rightarrow \infty} f_n(u, v) = f(u, v). \tag{3.3.12}$$

The convenience of this approximation lies in the fact that $f_n(u, v)$ is a polynomial in (u, v) of degree $2n$, and with coefficients that are definite integrals taken over S . Further, if we assume that $f(u, v)$ is negligible or zero outside S the coefficients in $f_n(u, v)$ are simply combinations of the moments of f of order not greater than $2n$.

To apply the representation in the present case let us assume that $E(u, v)$ is negligible when $(u^2 + v^2)^{\frac{1}{2}} > \frac{1}{2}w_0$, say. In other words, we assume a cut-off at high wave-numbers (some such assumption is in any case necessary in order to ensure the uniqueness of the solution.) Then we take as an approximation to $F(u, v)$

$$F_n(u, v) = \frac{n+1}{\pi w_0^2} \iint_{S_1} F(u_1, v_1) [1 - (u - u_1)^2/w_0^2 - (v - v_1)^2/w_0^2]^n \, du_1 \, dv_1, \tag{3.3.13}$$

where S_1 is the region $(u_1^2 + v_1^2)^{\frac{1}{2}} \leq \frac{1}{2}w_0$. Similarly we take

$$G_n(u, v) = \frac{n+1}{\pi w_0^2} \iint_{S_1} G(u_1, v_1) [1 - (u - u_1)^2/w_0^2 - (v - v_1)^2/w_0^2]^n \, du_1 \, dv_1, \tag{3.3.14}$$

and finally
$$E_n(u, v) = F_n(u, v) + G_n(u, v)/\sigma(u, v). \tag{3.3.15}$$

On expanding the polynomial expressions in (3.3.13) and (3.3.14) and carrying out the integrations we find, say, for $n = 2$,

$$F_2(u, v) = \frac{3}{\pi} [m_{00}(w_0^2 - u^2 - v^2) - 2(m_{20} + m_{02})(w_0^2 - u^2 - v^2)w_0^2 + (m_{40} + m_{04} + 2m_{22})w_0^4] \tag{3.3.16}$$

384

M. S. LONGUET-HIGGINS ON THE

and

$$G_2(u, v) = \frac{3}{\pi} [4(m'_{10}u + m'_{01}v)(w_0^2 - u^2 - v^2)w_0 - 4\{(m'_{30} + m'_{12})u + (m'_{21} + m'_{03})v\}w_0^3], \quad (3.3.17)$$

so that F_2 and G_2 are expressible as polynomials in (u, v) having as coefficients the moments of E up to degree 4. Approximations of higher order may be written down at will.

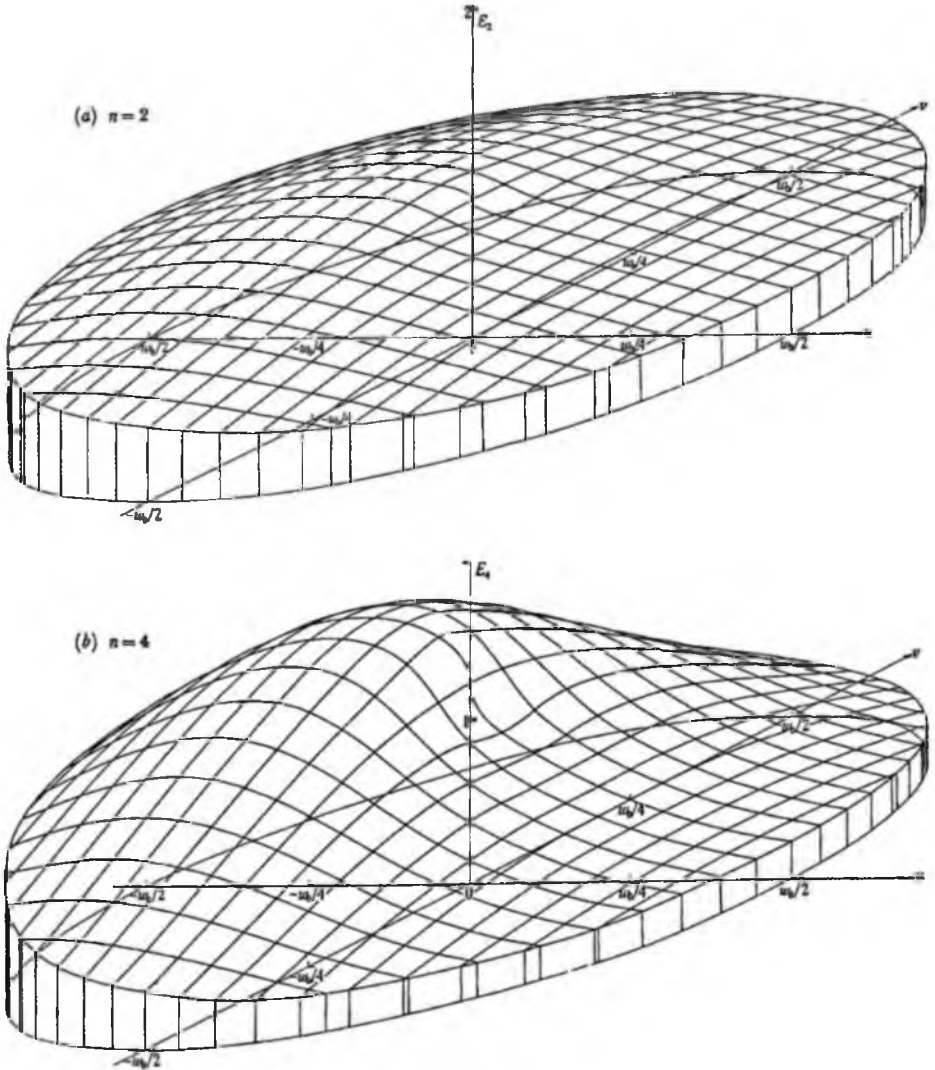


FIGURE 14

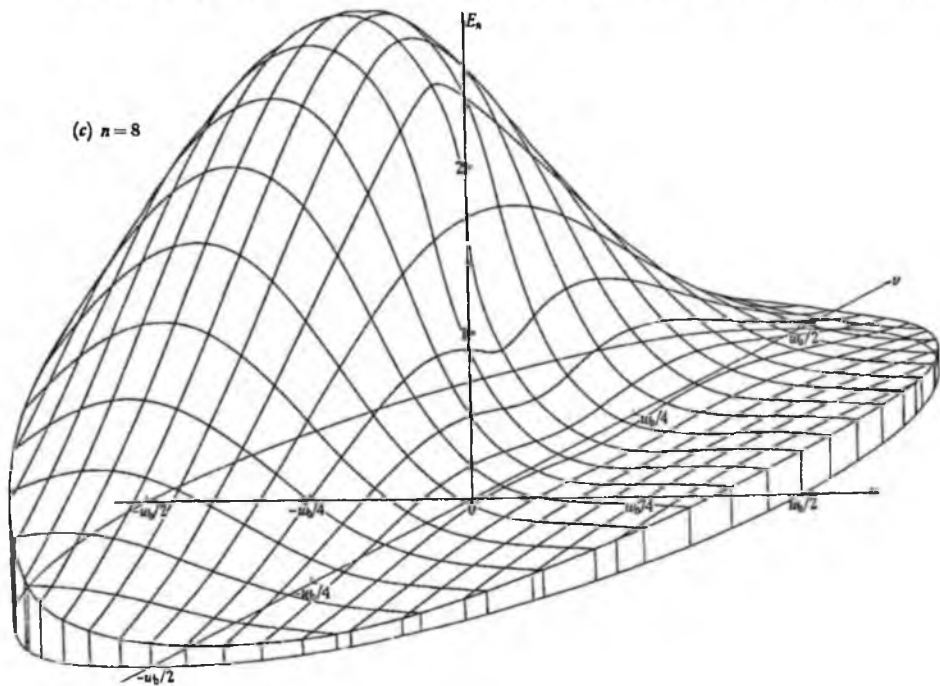


FIGURE 14. Successive approximations $E_n(u, v) = W_n(u, v; w_0/4, 0)$.

We have seen that F_n and G_n are essentially weighted averages of F and G by a weighting function proportional to $g_n[(u-u_1)/w_0, (v-v_1)/w_0]$. The weighting function corresponding to E_n is somewhat different owing to the presence of the factor $\sigma(u, v)$ in (3.3.15). In fact we have from (3.3.1) and (3.3.2)

$$\begin{aligned}
 E_n(u, v) = & \frac{n+1}{2\pi w_0^2} \iint_{S_1} E(u_1, v_1) \left[1 + \frac{\sigma(u_1, v_1)}{\sigma(u, v)} \right] \left[1 - \left(\frac{u-u_1}{w_0} \right)^2 - \left(\frac{v-v_1}{w_0} \right)^2 \right]^n du_1 dv_1 \\
 & + \frac{n+1}{2\pi w_0^2} \iint_{S_1} E(-u_1, -v_1) \left[1 - \frac{\sigma(u_1, v_1)}{\sigma(u, v)} \right] \left[1 - \left(\frac{u+u_1}{w_0} \right)^2 - \left(\frac{v+v_1}{w_0} \right)^2 \right]^n du_1 dv_1. \quad (3.3.18)
 \end{aligned}$$

On changing the sign of (u_1, v_1) in the second integral we have

$$E(u, v) = \frac{1}{w_0^2} \iint_{S_1} E(u_1, v_1) W'_n(u, v; u_1, v_1) du_1 dv_1, \quad (3.3.19)$$

where

$$\begin{aligned}
 W'_n(u, v; u_1, v_1) = & \frac{n+1}{2\pi} \left[1 + \frac{\sigma(u_1, v_1)}{\sigma(u, v)} \right] \left[1 - \left(\frac{u-u_1}{w_0} \right)^2 - \left(\frac{v-v_1}{w_0} \right)^2 \right]^n \\
 & + \frac{n+1}{2\pi} \left[1 - \frac{\sigma(u_1, v_1)}{\sigma(u, v)} \right] \left[1 - \left(\frac{u+u_1}{w_0} \right)^2 - \left(\frac{v+v_1}{w_0} \right)^2 \right]^n. \quad (3.3.20)
 \end{aligned}$$

W_n is not a function of $(u-u_1)$ and $(v-v_1)$ alone. However, the second half of (3.3.20) only gives a contribution when $(u, v_1) \doteq (u, v)$, and then this is small owing to the presence of the factor $[1 - \sigma(u_1, v_1)/\sigma(u, v)]$.

To obtain an idea of the accuracy of successive approximations we may consider the case of a narrow spectrum, when $E(u, v)$ is appreciably large only in the neighbourhood of a single point, say $(-\frac{1}{2}w_0, 0)$. Then

$$E_n(u, v) = W_n(u, v; -\frac{1}{2}w_0, 0). \quad (3.3.21)$$

W_n has been computed for $n = 2, 4, 8$ assuming that, as for gravity waves on deep water,

$$\sigma(u, v) \propto (u^2 + v^2)^{\frac{1}{2}}. \quad (3.3.22)$$

The results are shown in figure 14 *a, b* and *c*. It will be seen how the functions become progressively more peaked as the degree of the approximation is raised. When $n = 8$ the area in which W_n exceeds half its maximum value has a radius of about $0.3w_0$. For large values of n we have, in the neighbourhood of (u_1, v_1) ,

$$W_n \doteq \frac{n}{\pi} \exp \{-n[(u-u_1)^2 + (v-v_1)^2]/w_0^2\}, \quad (3.3.23)$$

and so the 'radius' of W_n is proportional to $n^{-\frac{1}{2}}$. It will be seen then that E_n converges to E rather slowly. In order to distinguish parts of the spectrum separated by a distance δ , it is necessary to take n to be of order $(w_0/\delta)^2$.

I am indebted to Mr D. E. Cartwright for advice in evaluating the elliptic integral (2.4.47) and to Mr E. A. Steer and Miss S. A. Yeo for assistance with the computation for figures 12 and 13.

REFERENCES

- Barber, N. F., Ursell, F., Darbyshire, J. & Tucker, M. J. 1946 A frequency analyser used in the study of ocean waves. *Nature, Lond.*, **158**, 329-332.
- Barber, N. F. & Ursell, F. 1948 The generation and propagation of ocean waves and swell. I. Wave periods and velocities. *Phil. Trans. A*, **140**, 527-560.
- Barber, N. F. 1950 *Ocean waves and swell*. Lecture, Institution of Civil Engineers, London, 22 pp.
- Cartwright, D. E. 1956 On determining the directions of waves from a ship at sea. *Proc. Roy. Soc. A*, **234**, 382-387.
- Courant, R. & Hilbert, D. 1953 *Methods of mathematical physics*. 1st English edition. New York: Interscience Publishers, Inc.
- Cox, C. & Munk, W. 1954*a* Measurement of the roughness of the sea surface from photographs of the sun's glitter. *J. Opt. Soc. Amer.* **44**, 838-850.
- Cox, C. & Munk, W. 1954*b* Statistics of the sea surface derived from the sun's glitter. *J. Mar. Res.* **13**, 198-227.
- Cramér, H. 1937 *Random variables and probability distributions*. Cambridge Mathematical Tract, no. 36. Cambridge University Press.
- Duntley, S. Q. 1950 The visibility of submerged objects. Part I. Optical effects of water waves. Report, Visibility Lab., Mass. Inst. Techn.
- Eckart, C. 1946 *The sea surface and its effect on the reflection of sound and light*. University of California, Division of War Research, Report M407 (unpublished).
- Eckart, C. 1953*a* The scattering of sound from the sea surface. *J. Acoust. Soc. Amer.* **25**, 566-570.

STATISTICAL ANALYSIS OF A RANDOM, MOVING SURFACE 387

- Eckart, C. 1953^b The generation of wind waves on a water surface. *J. Appl. Phys.* 24, 1485-1494.
- Eckart, C. 1953^c Relation between time averages and ensemble averages in the statistical dynamics of continuous media. *Phys. Rev.* 91, 784-790.
- Euler, L. 1752-3 *Elementa doctrinae solidorum*. *Nov. Comment. Acad. Sci. Imp. Petropol.* 4, 109-160.
- Kendall, M. G. 1952 *The advanced theory of statistics*, vol. 1. London: Griffin. 457 pp.
- Khintchine, A. 1934 Korrelationstheorie der stationären stochastischen Prozesse. *Math. Ann.* 109, 604-615.
- Legendre, A. M. 1811 *Exercices de calcul integrale*, t. 1. Paris: Courcier. 386 pp.
- Longuet-Higgins, M. S. & Barber, N. F. 1946 Four theoretical notes on the estimation of sea conditions. Admiralty Research Laboratory, Teddington, Report N1-N4 103.30/W (unpublished).
- Longuet-Higgins, M. S. 1950 A theory of the origin of microseisms. *Phil. Trans. A*, 243, 1-35.
- Longuet-Higgins, M. S. 1952 On the statistical distribution of the heights of sea waves. *J. Mar. Res.* 9, 245-266.
- Marks, W. 1954 The use of a filter to sort out directions in a short-crested gaussian sea surface. *Trans. Amer. Geophys. Un.* 35, 758-766.
- Pierson, W. J. 1952 *A unified mathematical theory for the analysis, propagation and refraction of storm generated ocean surface waves, Part I*. Report, Dept. of Meteorology, N.Y. Univ., 336 pp.
- Rayleigh, Lord 1880 On the resultant of a large number of vibrations of the same pitch and of arbitrary phase. *Phil. Mag.* 10, 73-78.
- Rayleigh, Lord 1945 *The theory of sound*, 1st American edition. New York: Dover Publications.
- Rice, S. O. 1944 The mathematical analysis of random noise. *Bell Syst. Tech. J.* 23, 282-332.
- Rice, S. O. 1945 The mathematical analysis of random noise. *Bell. Syst. Tech. J.* 24, 46-156.
- Rudnick, P. 1950 Correlograms for Pacific Ocean waves. *Proc. 2nd Berkeley Symposium on Mathematical Statistics and Probability*, pp. 627-638, University of California Press.
- St Denis, M. & Pierson, W. J. 1953 On the motions of ships in confused seas. *Trans. Soc. Nav. Archit., N.Y.*, 61, 1-65.
- Schumacher, A. 1952 Results of exact wave measurements (by stereophotogrammetry) with special reference to more recent theoretical investigations. Symposium on Gravity Waves, Washington, June 1951. *Nat. Bur. Stand. Circ.* no. 521, U.S. Govt. Printing Office.
- Schooley, A. H. 1954 A simple optical method for measuring the statistical distribution of water surface slopes. *J. Opt. Soc. Amer.* 44, 37-40.
- Sommerville, D. M. Y. 1929 *An introduction to the geometry of n dimensions*. London: Methuen. 196 pp.
- Taylor, G. I. 1922 Diffusion by continuous movements. *Proc. Lond. Math. Soc.* (2), 20, 196-212.
- Tukey, J. W. 1949 *The sampling theory of power spectrum estimates*. Symposium on application of autocorrelation analysis to physical problems, Woods Hole, Mass., June 1949. Office of Naval Research, Washington, D.C.
- Tukey, J. W. & Hamming, R. W. 1949 *Measuring noise color*. Bell Telephone Laboratories Internal Memorandum, MM 49.
- Watters, J. K. 1953 Distribution of height in ocean waves. *N.Z. J. Sci. Tech.* B, 34, 409-422.
- Weierstrass, K. T. W. 1885 Über die analytische Darstellbarkeit sogenannter willkürlicher Funktionen reeller Argumente. *S.B. Akad. Wiss. Berl.* 633-639, 789-805.
- Weierstrass, K. T. W. 1903 *Werke*, vol. 3, 1-37. Berlin.
- Whittaker, E. T. & Watson, G. N. 1952 *Modern analysis*. 4th edition. Cambridge University Press.

Reproduced with permission from *Phil. Trans. R. Soc. Lond. A* 250 (1957) 157-174.

[157]

STATISTICAL PROPERTIES OF AN ISOTROPIC RANDOM SURFACE

By M. S. LONGUET-HIGGINS

National Institute of Oceanography, Wormley

(Communicated by G. E. R. Deacon, F.R.S.—Received 26 February 1957)

CONTENTS

	PAGE		PAGE
INTRODUCTION	157	The number of zeros per unit distance	163
1. PARAMETERS FOR THE SURFACE	158	The length and direction of contours	164
The energy spectrum	158	The density of maxima and minima	165
Moments of the spectrum	158	The velocities of zeros	166
Invariants of the spectrum	160	The motion of the contours	167
A ring spectrum	161	The velocities of specular points	168
2. STATISTICAL PROPERTIES	162	3. ON THE UNIQUENESS OF THE SPECTRUM	170
The distribution of surface elevation		APPENDIX	173
and gradient	162	REFERENCES	174

A number of statistical properties of a random, moving surface are obtained in the special case when the surface is Gaussian and isotropic. The results may be stated with special simplicity for a 'ring' spectrum when the energy in the spectrum is confined to one particular wavelength $\bar{\lambda}$. In particular, the average density of maxima per unit area equals $\pi/(2\sqrt{3}\bar{\lambda}^2)$, and the average length, per unit area, of the contour drawn at the mean level equals $\pi/(\sqrt{2}\bar{\lambda})$.

INTRODUCTION

Some of the statistical properties of a random, moving surface have been studied in a recent paper (Longuet-Higgins 1957) † in connexion with the analysis of sea waves. The surface was there assumed to have a correlation function of general form. In the present paper we shall discuss the special case when the surface is isotropic, that is to say, its statistical properties are independent of direction.

Although the corresponding properties of an isotropic spectrum are simpler than for a spectrum of general form, to derive them from first principles would in most cases take almost as long. In what follows, therefore, free use will be made of the more general results already obtained in (A).

The paper falls into two main sections. The first defines the parameters used to describe the surface, and discusses the relations between them. The second and main section derives various statistical properties: the distributions of elevation and gradient; the mean number of zeros along a line in arbitrary direction; the average length of contour per unit area, and the average density of maxima and minima per unit area. All these properties are independent of the motion. Next are considered the statistical distributions of the velocities of zeros, of contours and of specular points on the surface (i.e. points where the components

† This will subsequently be referred to as (A).

of the gradient take given values). The results are discussed in detail when the surface has a 'ring' spectrum, that is to say, when the energy is confined to one particular wavelength, while distributed uniformly with regard to direction.

In a final section the question is discussed of how far the spectrum is determined by its statistical properties.

1. PARAMETERS FOR THE SURFACE

The energy spectrum

The surface under consideration is assumed to be representable as the sum of an infinity of long-crested waves:

$$\zeta(x, y, t) = \sum_n c_n \cos(u_n x + v_n y + \sigma_n t + \epsilon_n), \quad (1)$$

where x and y are horizontal co-ordinates and t denotes the time. The summation is over a set of wave numbers (u_n, v_n) distributed densely throughout the (u, v) plane. The frequency σ_n of each wave component depends only on the wavelength $2\pi/w_n$, where

$$w_n = (u_n^2 + v_n^2)^{\frac{1}{2}}, \quad (2)$$

and the phases ϵ_n are randomly distributed in the interval $(0, 2\pi)$. The amplitudes c_n are such that, over any element $du dv$

$$\sum_n \frac{1}{2} c_n^2 = E(u, v) du dv. \quad (3)$$

The function $E(u, v)$ is called the energy spectrum of ζ . Formally, it is the cosine transform of the correlation function $\psi(x, y)$ defined by

$$\psi(x, y) = \lim_{X, Y, T \rightarrow \infty} \frac{1}{8XYT} \int_{-X}^X \int_{-Y}^Y \int_{-T}^T \zeta(x', y', t') \zeta(x+x', y+y', t') dx' dy' dt'. \quad (4)$$

In the special case considered in the present paper $E(u, v)$ is assumed to have circular symmetry about the origin, i.e.

$$E(u, v) = E(w), \quad (5)$$

say, where

$$w = (u^2 + v^2)^{\frac{1}{2}}. \quad (6)$$

Moments of the spectrum

Parameters which frequently occur in the analysis of the general two-dimensional spectrum are the moments m_{pq} , m'_{pq} and m''_{pq} defined by

$$\left. \begin{aligned} m_{pq} &= \int_{-\infty}^{\infty} \int_{-\infty}^{\infty} E(u, v) u^p v^q du dv, \\ m'_{pq} &= \int_{-\infty}^{\infty} \int_{-\infty}^{\infty} E(u, v) \sigma(u, v) u^p v^q du dv, \\ m''_{pq} &= \int_{-\infty}^{\infty} \int_{-\infty}^{\infty} E(u, v) \sigma^2(u, v) u^p v^q du dv. \end{aligned} \right\} \quad (7)$$

For example, m_{00} defines the total energy of the surface per unit area. It is assumed that the moments exist up to all orders required.

If we consider the intersection of the surface by a vertical plane in an arbitrary direction θ (that is, the plane $x \sin \theta = y \cos \theta$) the resulting curve has a one-dimensional spectrum

PROPERTIES OF AN ISOTROPIC RANDOM SURFACE 159

which we may denote by $E_\theta(u')$, where u' is the wave number measured in the direction θ . The moments of this function are defined by

$$m_n(\theta) = \int_{-\infty}^{\infty} E_\theta(u') u'^n du'. \quad (8)$$

The moments $m'_n(\theta)$ and $m''_n(\theta)$ are, by definition, related to $E\sigma$ and $E\sigma^2$ in the same way that $m_n(\theta)$ is related to E . A simple relationship exists between $m_n(\theta)$ and the moments m_{pq} of the two-dimensional spectrum. On the one hand

$$m_n(\theta) = m_{n,0} \cos^n \theta + \binom{n}{1} m_{n-1,1} \cos^{n-1} \theta \sin \theta + \dots + m_{0,n} \sin^n \theta \quad (9)$$

((A), equation (1.4.12)); on the other hand

$$m_{pq} = \frac{1}{\pi} \int_0^{2\pi} m_n(\theta) C_{pq}(\theta) d\theta, \quad (10)$$

where
$$C_{pq}(\theta) = \frac{1}{2i^q} \left[e^{in\theta} + \binom{p}{1} \binom{q}{1} \left/ \binom{n}{1} \right. e^{i(n-2)\theta} + \dots + (-1)^n e^{-in\theta} \right] \quad (11)$$

and $\binom{p}{r} \binom{q}{r}$ denotes the coefficient of x^r in the expansion of $(1+x)^p (1-x)^q$ (see (A), § 3.2).

When the spectrum has circular symmetry, $m_n(\theta)$ is independent of θ and hence

$$m_{pq} = \begin{cases} (-1)^{iq} \binom{p}{\frac{1}{2}n} \binom{q}{\frac{1}{2}n} \left/ \binom{n}{\frac{1}{2}n} \right. m_n, & p, q \text{ both even;} \\ 0 & \text{otherwise.} \end{cases} \quad (12)$$

Similar relations hold between $m'_n(\theta)$ and m'_{pq} , and between $m''_n(\theta)$ and m''_{pq} .

It is possible to describe the statistical properties of the surface in terms of the moments $m_n(\theta)$, $m'_n(\theta)$ and $m''_n(\theta)$. Nevertheless, for an isotropic spectrum it is more convenient to use the radial moments, defined by

$$M_n = \int_{-\infty}^{\infty} \int_{-\infty}^{\infty} E(u, v) w^n du dv \quad (13)$$

$$\begin{aligned} &= \int_0^{\infty} \int_0^{2\pi} E(w) w^n w dw d\theta \\ &= 2\pi \int_0^{\infty} E(w) w^{n+1} dw, \end{aligned} \quad (14)$$

and, similarly,

$$M'_n = \int_{-\infty}^{\infty} \int_{-\infty}^{\infty} \sigma(u, v) E(u, v) w^n du dv \quad (15)$$

$$= 2\pi \int_0^{\infty} \sigma(w) E(w) w^{n+1} dw \quad (16)$$

and

$$M''_n = \int_{-\infty}^{\infty} \int_{-\infty}^{\infty} \sigma^2(u, v) E(u, v) w^n du dv \quad (17)$$

$$= 2\pi \int_0^{\infty} \sigma^2(w) E(w) w^{n+1} dw. \quad (18)$$

The relation of M_n to $m_n(\theta)$, when n is even, can be found as follows. We have

$$M_{2r} = \int_{-\infty}^{\infty} \int_{-\infty}^{\infty} E(u, v) (u^2 + v^2)^r \, du \, dv \tag{19}$$

$$\begin{aligned} &= m_{2r,0} + \binom{r}{1} m_{2r-2,2} + \binom{r}{2} m_{2r-4,4} + \dots + m_{0,2r} \\ &= \left[\binom{2r}{r} \binom{0}{r} - \binom{r}{1} \binom{2r-2}{r} \binom{2}{r} + \dots + (-1)^r \binom{0}{r} \binom{2r}{r} \right] m_{2r}(\theta) / \binom{2r}{r} \end{aligned} \tag{20}$$

from equation (12). The expression in square brackets is the coefficient of x^r in

$$\begin{aligned} (1+x)^{2r} - \binom{r}{1} (1+x)^{2r-2} (1-x)^2 + \dots + (-1)^r (1-x)^{2r} &= [(1+x)^2 - (1-x)^2]^r \\ &= [4x]^r. \end{aligned} \tag{21}$$

Hence
$$M_{2r} = 2^{2r} m_{2r}(\theta) / \binom{2r}{r} = \frac{2 \cdot 4 \cdot 6 \dots 2r}{1 \cdot 3 \cdot 5 \dots (2r-1)} m_{2r} \tag{22}$$

Similarly, we have
$$M'_{2r} = \frac{2 \cdot 4 \cdot 6 \dots 2r}{1 \cdot 3 \cdot 5 \dots (2r-1)} m'_{2r} \tag{23}$$

and
$$M''_{2r} = \frac{2 \cdot 4 \cdot 6 \dots 2r}{1 \cdot 3 \cdot 5 \dots (2r-1)} m''_{2r} \tag{24}$$

In particular,
$$M_0 = m_0, \quad M_2 = 2m_2, \quad M_4 = \frac{8}{3}m_4. \tag{25}$$

For an isotropic spectrum the odd moments vanish identically:

$$m_{2r+1}(\theta) = m'_{2r+1}(\theta) = m''_{2r+1}(\theta) = 0. \tag{26}$$

The odd moments $M_{2r+1}, M'_{2r+1}, M''_{2r+1}$ do not occur in the present analysis.

Invariants of the spectrum

The following determinants are fundamental for the analysis of the general spectrum:

$$\Delta_0 = m_{00}, \tag{27}$$

$$\Delta_2 = \begin{vmatrix} m_{20} & m_{11} \\ m_{11} & m_{02} \end{vmatrix}, \tag{28}$$

$$\Delta_3 = \begin{vmatrix} m_{40} & m_{31} & m_{22} \\ m_{31} & m_{22} & m_{13} \\ m_{22} & m_{13} & m_{04} \end{vmatrix}, \tag{29}$$

and, more generally,

$$\Delta_{2r} = \begin{vmatrix} m_{2r,0} & m_{2r-1,1} & \dots & m_{r,r} \\ m_{2r-1,1} & m_{2r-2,2} & \dots & m_{r-1,r+1} \\ \vdots & \vdots & \ddots & \vdots \\ m_{r,r} & m_{r-1,r+1} & \dots & m_{0,2r} \end{vmatrix}. \tag{30}$$

The vanishing of Δ_{2r} is a necessary condition for the spectrum to consist of not more than r one-dimensional spectra (see (A), §1.3).

PROPERTIES OF AN ISOTROPIC RANDOM SURFACE

161

Substitution from (12) and (25) shows that for an isotropic spectrum

$$\left. \begin{aligned} \Delta_0 &= m_0 = M_0, \\ \Delta_2 &= m_2^2 = \frac{1}{4}M_2^2, \\ \Delta_4 &= \frac{8}{3}m_4^3 = \frac{1}{3}M_4^3. \end{aligned} \right\} \quad (31)$$

It can be proved (see Appendix) that, for all integers $r \geq 0$,

$$\Delta_{2r} = \frac{1}{2^{r(r+1)}} M_{2r}^{r+1}. \quad (32)$$

As we should expect, Δ_{2r} vanishes only when M_{2r} vanishes, since an isotropic spectrum can be the sum of a finite number of one-dimensional spectra only in the trivial case when all the energy is concentrated at the origin.

Since, in an isotropic spectrum, $m_2(\theta)$ is independent of θ , we have $m_{2 \max.} = m_{2 \min.}$. Thus the long-crestedness γ^{-1} is given by

$$\gamma^{-1} = \left(\frac{m_{2 \max.}}{m_{2 \min.}} \right)^{\frac{1}{2}} = 1. \quad (33)$$

The invariant quantity $(m_{20} + m_{02})$, which is independent of the direction of the co-ordinate axes in the general case, has (from equations (12) and (25)) the value

$$m_{20} + m_{02} = M_2. \quad (34)$$

Another invariant that we shall require is the quadratic expression

$$3H = m_{40}m_{04} - 4m_{31}m_{13} + 3m_{22}^2. \quad (35)$$

Substitution from (12) gives

$$3H = \frac{3}{8}m_4^2, \quad (36)$$

and so from (25)

$$H = \frac{1}{16}M_4^2. \quad (37)$$

Therefore for an isotropic spectrum

$$\frac{\Delta_4^2}{H^3} = 1. \quad (38)$$

A ring spectrum

When the surface is isotropic it is impossible for the spectrum to be 'narrow' in the sense that the energy is concentrated with respect to both wavelength and direction (except in the trivial case when all the energy is at the origin). However, an interesting special case is when the energy has predominantly one wavelength λ , that is, when it is concentrated in a narrow annular region in the (u, v) plane, with centre the origin. If $\bar{w} = 2\pi/\lambda$ denotes the mean radius of the annulus we have approximately

$$M_n = \bar{w}^n M_0, \quad (39)$$

and hence

$$M_0 M_4 = M_2^2 \quad (40)$$

or

$$m_0 m_4 = \frac{3}{2} m_2^2. \quad (41)$$

Now from (14)

$$M_0 M_4 - M_2^2 = \iiint \iiint E(u_1, v_1) E(u_2, v_2) (w_1^4 - w_1^2 w_2^2) du_1 dv_1 du_2 dv_2, \quad (42)$$

and hence

$$2(M_0 M_4 - M_2^2) = \iiint \iiint E(u_1, v_1) E(u_2, v_2) (w_1^4 - w_2^2)^2 du_1 dv_1 du_2 dv_2. \quad (43)$$

This quantity is always positive or zero and vanishes only when $E(u, v)$ is a ring spectrum. Further, in the isotropic case,

$$2(M_0 M_4 - M_2^2) = 4\pi^2 \int_0^\infty \int_0^\infty E(w_1) E(w_2) (w_1^2 - w_2^2)^2 dw_1 dw_2, \quad (44)$$

which, for a nearly annular spectrum, is proportional to the square of the width of the annulus. A convenient parameter for specifying the width of the annulus is therefore

$$\delta = \frac{(M_0 M_4 - M_2^2)^{\frac{1}{2}}}{M_2}. \quad (45)$$

2. STATISTICAL PROPERTIES

The distribution of surface elevation and gradient

The statistical distribution of the surface elevation ζ ($= \xi_1$) is given by equation (2.1.8) of (A). Substituting $m_0 = M_0$ we have

$$p(\xi_1) = \frac{1}{(2\pi M_0)^{\frac{1}{2}}} \exp(-\xi_1^2/2M_0). \quad (46)$$

This is a Gaussian distribution, with mean-square value

$$\overline{\xi_1^2} = M_0. \quad (47)$$

The joint distribution of the two components of gradient

$$\frac{\partial \zeta}{\partial x}, \frac{\partial \zeta}{\partial y}, = \xi_1, \xi_2, \quad (48)$$

is given by

$$p(\xi_2, \xi_3) = \frac{1}{2\pi \Delta_1^{\frac{1}{2}}} \exp[-(m_{02}\xi_2^2 - 2m_{11}\xi_2\xi_3 + m_{20}\xi_3^2)/2\Delta_2] \quad (49)$$

in the general case (see (A), equation (2.1.12)). On substituting from (12) and (31) we have

$$p(\xi_2, \xi_3) = \frac{1}{\pi M_2} \exp[-(\xi_2^2 + \xi_3^2)/M_2], \quad (50)$$

a symmetrical Gaussian distribution in two dimensions. The distributions of ξ_1 and (ξ_2, ξ_3) are statistically independent (see (A), § 2.1).

Let us write

$$(\xi_2, \xi_3) = (\alpha \cos \theta, \alpha \sin \theta), \quad \frac{\partial(\xi_2, \xi_3)}{\partial(\alpha, \theta)} = \alpha \quad (51)$$

in (50), so that α and θ denote the magnitude and direction of the surface gradient. Then we have for the joint distribution of α and θ

$$p(\alpha, \theta) = \frac{\alpha}{\pi M_2} \exp(-\alpha^2/M_2), \quad (52)$$

which is of course independent of θ . The mean-square slope of the surface is given by

$$\overline{\alpha^2} = M_2. \quad (53)$$

PROPERTIES OF AN ISOTROPIC RANDOM SURFACE

163

The distribution of the slope α , regardless of θ , is a Rayleigh distribution:

$$p(\alpha) = \frac{2\alpha}{M_2} \exp(-\alpha^2/M_2). \quad (64)$$

The distribution of θ , regardless of α , is a constant:

$$p(\theta) = \frac{1}{2\pi}. \quad (65)$$

The number of zeros per unit distance

If we consider the curve of intersection of the surface by a vertical plane in the direction θ , we may count the number N_0 of zeros of this curve per unit horizontal distance. From (A), equation (2.2.5), N_0 is given by

$$N_0 = \frac{1}{\pi} \left(\frac{m_2(\theta)}{m_0(\theta)} \right)^{\frac{1}{2}} = \frac{1}{\pi} \left(\frac{M_2}{2M_0} \right)^{\frac{1}{2}}. \quad (66)$$

Similarly from equation (2.2.10) of (A) the number of maxima and minima of the curve per unit distance is given by

$$N_1 = \frac{1}{\pi} \left(\frac{m_4(\theta)}{m_2(\theta)} \right)^{\frac{1}{2}} = \frac{1}{\pi} \left(\frac{3M_4}{4M_2} \right)^{\frac{1}{2}}. \quad (67)$$

In general, the number of zeros, per unit distance, of the r th derivative of the curve is given by

$$N_r = \frac{1}{\pi} \left(\frac{m_{2r+2}(\theta)}{m_{2r}(\theta)} \right)^{\frac{1}{2}} = \frac{1}{\pi} \left(\frac{2r+1}{2r+2} \frac{M_{2r+2}}{M_{2r}} \right)^{\frac{1}{2}}. \quad (68)$$

Also from (2.2.12) and (2.2.13) of (A) the number of points per unit distance where the curve crosses the arbitrary level $\zeta = \xi_1$ is

$$N_0(\xi_1) = \frac{1}{\pi} \left(\frac{M_2}{2M_0} \right)^{\frac{1}{2}} \exp(-\xi_1^2/2M_0), \quad (69)$$

and the number of times when the gradient of the curve takes the arbitrary value ξ_2 is

$$N_0(\xi_2) = \frac{1}{\pi} \left(\frac{3M_4}{4M_2} \right)^{\frac{1}{2}} \exp(-\xi_2^2/M_2). \quad (69)$$

For a ring spectrum, we have

$$N_0 = \frac{\overline{w}}{\pi} \left(\frac{1}{2} \right)^{\frac{1}{2}} = \frac{2}{\lambda} \left(\frac{1}{2} \right)^{\frac{1}{2}}, \quad (61)$$

$$N_1 = \frac{\overline{w}}{\pi} \left(\frac{3}{4} \right)^{\frac{1}{2}} = \frac{2}{\lambda} \left(\frac{3}{4} \right)^{\frac{1}{2}}, \quad (62)$$

and, in general,

$$N_r = \frac{\overline{w}}{\pi} \left(\frac{2r+1}{2r+2} \right)^{\frac{1}{2}} = \frac{2}{\lambda} \left(\frac{2r+1}{2r+2} \right)^{\frac{1}{2}}, \quad (63)$$

where

$$\lambda = \frac{2\pi}{\overline{w}} \quad (64)$$

denotes the characteristic wavelength of the spectrum. For a long-crested wave of the same wavelength, the number of zero crossings per unit distance would be $2/\lambda$ in a direction at right angles to the crests, and zero in a direction parallel to the crests. Equation (63) shows that, for an isotropic spectrum, N_r is always less than the maximum value $2/\lambda$. On the other hand, for large values of r , N_r approaches this value.

The length and direction of contours

Let contours be drawn on the surface at the level $\zeta = \xi_1 = \text{constant}$; the length of contour lying in any given horizontal area will be, on the average, proportional to that area. The mean length \bar{s} per unit area is shown in (A), § 2.3, to be given by

$$\bar{s}(\xi_1) = \frac{1}{\pi} \left(\frac{m_{20} + m_{02}}{m_{00}} \right)^{\frac{1}{2}} \frac{E(\sqrt{(1-\gamma^2)})}{\sqrt{(1+\gamma^2)}} \exp(-\xi_1^2/2m_0), \quad (65)$$

where γ^{-1} denotes the long-crestedness and $E(k)$ is the Legendre elliptic integral of the first kind. For an isotropic spectrum we have

$$\gamma = 1, \quad E(\sqrt{(1-\gamma^2)}) = \frac{1}{2}\pi, \quad (66)$$

and hence

$$\bar{s}(\xi_1) = \frac{1}{2\sqrt{2}} \left(\frac{M_2}{M_0} \right)^{\frac{1}{2}} \exp(-\xi_1^2/2M_0). \quad (67)$$

The distribution of contour direction for an isotropic spectrum is of course uniform.

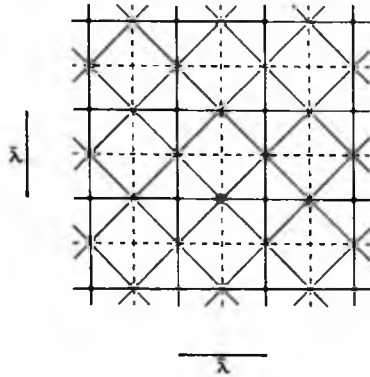


FIGURE 1. The pattern formed by two systems of regular waves intersecting at right angles.
 —, crests of the individual wave systems; ----, troughs of the individual wave systems;
 —, contours of mean level in the combined system; ●, maxima of the combined system.

For a ring spectrum the average length of contour becomes

$$\bar{s}(\xi_1) = \frac{\bar{w}}{2\sqrt{2}} \exp(-\xi_1^2/2M_0), \quad (68)$$

and in particular at the mean level $\zeta = 0$ we have

$$\bar{s}(0) = \frac{\bar{w}}{2\sqrt{2}} = \frac{\pi}{\sqrt{2}} \frac{1}{\lambda} = 2.22 \dots \frac{1}{\lambda}. \quad (69)$$

This result may be compared with the simple pattern made by two regular sine waves of equal wavelength λ and of equal amplitude intersecting at right angles (see figure 1). It is easy to see that the contours of zero level run diagonally, making angles of $\frac{1}{4}\pi$ with the directions of the two sine waves. The distance between adjacent parallel contours is $\lambda/\sqrt{2}$. The mean length of contour for each diagonal direction is therefore $\sqrt{2}\lambda$, and the total mean length is twice this, or

$$\bar{s}(0) = 2\sqrt{2} \frac{1}{\lambda} = 2.83 \dots \frac{1}{\lambda}. \quad (70)$$

PROPERTIES OF AN ISOTROPIC RANDOM SURFACE

165

This is somewhat greater than in the isotropic case. However, $\bar{s}(\xi_1)$ falls off in a different fashion in the two cases; clearly for the two intersecting waves $\bar{s}(\xi_1)$ vanishes when ξ_1 exceeds twice the amplitude of each wave.

The density of maxima and minima

A very interesting problem is that of the density of maxima, minima or stationary points per unit horizontal area. It is shown in (A) that for any statistically uniform surface the density of maxima D_{ma} together with the density of minima D_{mi} equals the density of saddle points D_{sa} . Also that for the special surface represented by equation (1), $D_{ma} = D_{mi}$. It follows that

$$D_{ma} = D_{mi} = \frac{1}{4}D_{sta.}, \quad D_{sa} = \frac{1}{2}D_{sta.}, \quad (71)$$

where $D_{sta.}$ denotes the total density of stationary points. The density of specular points, that is, points where the two components of gradient take given values ξ_2, ξ_3 is given by

$$D_{sp.} = D_{sta.} [-(\xi_2^2 + \xi_3^2) / M_2] \quad (72)$$

for an isotropic surface (cf. (A), equation (2.4.66)).

The evaluation of D_{ma} in terms of the energy spectrum of the surface is given by

$$D_{ma} = \frac{1}{2\pi^2} \frac{l_1}{\Delta_4^2} \Phi(-l_2/l_1), \quad (73)$$

where $l_1 \geq 0 \geq l_2 \geq l_3$, these being the three roots (always real) of the cubic equation

$$4l^3 - 3Hl - \Delta_4 = 0, \quad (74)$$

and where Φ is a function involving complete elliptic integrals (see (A), equation (2.4.53)). Substituting for Δ_4 and H from (31) and (48) we have

$$64l^3 - 3M_4l - M_4^3 = 0, \quad (75)$$

and so

$$(l_1, l_2, l_3) = (\frac{1}{4}M_4, -\frac{1}{8}M_4, -\frac{1}{8}M_4). \quad (76)$$

Since, from equation (2.5.55) of (A),

$$\Phi(\frac{1}{2}) = \frac{\pi}{2\sqrt{3}}, \quad (77)$$

we have

$$D_{ma} = \frac{1}{2\pi^2} \frac{M_4}{2M_2} \frac{\pi}{2\sqrt{3}} = \frac{1}{8\sqrt{3}} \frac{M_4}{\pi M_2}. \quad (78)$$

In particular, for a ring spectrum,

$$D_{ma} = \frac{1}{8\sqrt{3}} \frac{1}{\pi \bar{\omega}^2} = \frac{\pi}{2\sqrt{3}} \frac{1}{\lambda^2} = 0.907 \dots \frac{1}{\lambda^2}. \quad (79)$$

This may be compared with the corresponding result for two regular sine waves of equal wavelength λ , and equal amplitude, crossing at right angles; in that case

$$D_{ma} = \frac{1}{\lambda^2} \quad (80)$$

simply. So the density of maxima in the isotropic case is slightly less than for the two intersecting sine waves.

The velocities of zeros

If a plane section of the surface be taken in a direction θ as before, we may consider the distribution of the velocities of points on this curve which lie at a given level, say $\zeta = \xi_1$. This would be equivalent to drawing a contour map of the surface and finding the velocities of the intersections of the contours $\zeta = \xi_1$ with a fixed line in direction θ .

For a general spectrum, the distribution of the velocity is given by

$$p(c)_{\xi_1} = \frac{1}{2} \frac{\Delta_{2'} / m_2^{\frac{1}{2}}}{(m_0^2 + 2m_1'c + m_2c^2)^{\frac{1}{2}}} \quad (81)$$

(see (A), equation (2.5.14)), where

$$\Delta_{2'} = m_0^2 m_2 - m_1'^2. \quad (82)$$

For an isotropic spectrum we have

$$\left. \begin{aligned} m_0 &= M_0, & m_1' &= 0, \\ m_0^2 &= M_0^2, & m_2 &= \frac{1}{2} M_2, \end{aligned} \right\} \quad (83)$$

giving

$$p(c)_{\xi_1} = \frac{M_0^2 / M_2}{(c^2 + 2M_0^2 / M_2)^{\frac{1}{2}}}. \quad (84)$$

This distribution is symmetrical about the origin, as we should expect. Its second moment and standard deviation are infinite, but a measure of its width is the interquartile range, given by

$$2 \sqrt{\left(\frac{2}{3}\right) \left(\frac{M_0^2}{M_2}\right)^{\frac{1}{2}}}. \quad (85)$$

For a ring spectrum this becomes

$$2 \sqrt{\left(\frac{2}{3}\right) \frac{\bar{\sigma}}{\bar{w}}} = 2 \sqrt{\left(\frac{2}{3}\right) \bar{c}}, \quad (86)$$

where \bar{c} is the phase velocity of the component waves.

It will be noticed that the distribution of c is independent of the particular contour $\zeta = \xi_1$ at which the velocity is measured.

Similarly, we may consider the velocities c_1 of the maxima and minima of the curve. From equation (2.5.19) of (A) we find for the distribution of c_1

$$p(c_1) = \frac{2M_0^2 / 3M_4}{(c^2 + 4M_0^2 / 3M_4)^{\frac{1}{2}}}. \quad (87)$$

This is of the same form as $p(c)$ but with an interquartile range of width

$$\frac{4}{3} \left(\frac{M_0^2}{M_4}\right)^{\frac{1}{2}}. \quad (88)$$

For a ring spectrum this becomes

$$\frac{4}{3} \frac{\bar{\sigma}}{\bar{w}} = \frac{4}{3} \bar{c}. \quad (89)$$

The distributions of the velocities of higher derivatives of the curve may be found in a similar way.

PROPERTIES OF AN ISOTROPIC RANDOM SURFACE

The motion of the contours

The motion of a contour may be defined as follows. Let P be a fixed point through which the contour passes at a given time, and let straight lines be drawn through P parallel to the axes Ox , Oy . The intersections of the contour with these two lines will move with velocities c_x , c_y , say, which determine completely the local motion of the contour. If any other fixed line is drawn through P in a direction θ , and if c is the speed of the contour intersection along it, then it can be shown that

$$\frac{1}{c} = \frac{1}{c_x} \cos \theta + \frac{1}{c_y} \sin \theta. \quad (90)$$

The reciprocals $1/c_x$, $1/c_y$ will be denoted by κ_x , κ_y respectively.

Alternatively we may consider the components q_x , q_y of the velocity of the contour normal to itself at P . Between (κ_x, κ_y) and (q_x, q_y) there is a reciprocal relationship:

$$\left. \begin{aligned} (q_x, q_y) &= \left(\frac{\kappa_x}{\kappa_x^2 + \kappa_y^2}, \frac{\kappa_y}{\kappa_x^2 + \kappa_y^2} \right), \\ (\kappa_x, \kappa_y) &= \left(\frac{q_x}{q_x^2 + q_y^2}, \frac{q_y}{q_x^2 + q_y^2} \right) \end{aligned} \right\} \quad (91)$$

(see (A), § 2.6).

The statistical distribution of (κ_x, κ_y) is given by equation (2.6.21) of (A). In the general case,

$$p(\kappa_x, \kappa_y)_{\xi_1} = \frac{1}{\pi \Delta_3^{\frac{1}{2}} (m_{20} + m_{02})^{\frac{1}{2}}} \frac{\sqrt{(1 + \gamma^2)} (\kappa_x^2 + \kappa_y^2)^{\frac{1}{2}}}{E(\sqrt{(1 - \gamma^2)}) R}, \quad (92)$$

where

$$\Delta_3 = \begin{vmatrix} m_{20} & m_{11} & m'_{10} \\ m_{11} & m_{02} & m'_{01} \\ m'_{10} & m'_{01} & m''_{00} \end{vmatrix}, \quad (93)$$

γ^{-1} is the long-crestedness, E is the Legendre elliptic integral of the first kind, and

$$R = M_{11}\kappa_x^2 + 2M_{12}\kappa_x\kappa_y + M_{22}\kappa_y^2 - 2M_{13}\kappa_x - 2M_{23}\kappa_y + M_{33}, \quad (94)$$

in which (M_{ij}) is the matrix inverse to that of Δ_3 . In the isotropic case we have

$$\Delta_3 = \begin{vmatrix} \frac{1}{2}M_2 & 0 & 0 \\ 0 & \frac{1}{2}M_2 & 0 \\ 0 & 0 & M_0'' \end{vmatrix}, \quad (95)$$

and so

$$R = \frac{2}{M_2} (\kappa_x^2 + \kappa_y^2) + \frac{1}{M_0''}. \quad (96)$$

Setting also $\gamma = 1$ in (92) we have

$$p(\kappa_x, \kappa_y)_{\xi_1} = \frac{2}{\pi^2} \left(\frac{M_2}{2M_0''} \right)^{\frac{1}{2}} \frac{(\kappa_x^2 + \kappa_y^2)^{\frac{1}{2}}}{[(\kappa_x^2 + \kappa_y^2) + M_2/2M_0'']^2}, \quad (97)$$

whence also

$$p(q_x, q_y)_{\xi_1} = \frac{2}{\pi^2} \left(\frac{2M_0''}{M_2} \right)^{\frac{1}{2}} \frac{(q_x^2 + q_y^2)^{-\frac{1}{2}}}{[(q_x^2 + q_y^2) + 2M_0''/M_2]^2}. \quad (98)$$

These are symmetrical distributions, independent of direction in the horizontal plane.

If we write

$$(q_x, q_y) = (q \cos \theta, q \sin \theta), \quad (99)$$

so that q is the absolute value of the normal velocity, we have

$$p(q)_{\xi_1} = 2\pi p(q, \theta)_{\xi_1} = 2\pi q p(q_x, q_y)_{\xi_1} \tag{100}$$

or from (98)

$$p(q)_{\xi_1} = \frac{4}{\pi} \left(\frac{2M_0}{M_2} \right)^{\frac{1}{2}} \frac{1}{(q^2 + 2M_0^2/M_2^2)^2} \tag{101}$$

This distribution has a mode at the origin $q = 0$. The mean-square value of the velocity is given by

$$\bar{q}^2 = \frac{2M_0^2}{M_2} \tag{102}$$

For a ring spectrum,

$$\bar{q}^2 = \frac{2\bar{v}^2}{w^2} = 2\bar{v}^2, \tag{103}$$

where \bar{v} is the velocity of a component sine wave in the spectrum.

The velocities of specular points

As defined above, a specular point is a point that would be seen by a distant observer as a point of reflexion of a distant source of light. We may imagine such a point to be followed continuously. If its velocity is denoted by (c_x, c_y) then the distribution of (c_x, c_y) is shown in (A), § 2.7, to depend upon the matrix

$$(\Xi_{ij}) = \begin{pmatrix} m_{40} & m_{31} & m_{22} & m'_{30} & m'_{21} \\ m_{31} & m_{22} & m_{13} & m'_{21} & m'_{12} \\ m_{22} & m_{13} & m_{04} & m'_{12} & m'_{03} \\ \hline m'_{30} & m'_{21} & m'_{12} & m''_{20} & m''_{11} \\ m'_{21} & m'_{12} & m'_{03} & m''_{11} & m''_{02} \end{pmatrix} \tag{104}$$

If (M_{ij}) denotes the inverse of this matrix, then it is found that

$$f(c_x, c_y)_{\xi_1, \xi_2} = \frac{1}{16\pi^2 (\Delta_2 \Delta_5)^{\frac{1}{2}} D_{\text{max}}} \frac{3(n_{13} - n_{22})^2 + N(N_{22} - 4N_{31})}{N^{\frac{1}{2}}} \tag{105}$$

where (N_{ij}) is the symmetric 3×3 matrix whose components are

$$\left. \begin{aligned} N_{11} &= M_{44} c_x^2 && -2M_{41} c_x && +M_{11}, \\ N_{22} &= M_{35} c_y^2 + 2M_{45} c_x c_y + M_{44} c_y^2 - 2M_{52} c_x && -2M_{42} c_y && +M_{22}, \\ N_{33} &= && M_{55} c_y^2 && -2M_{53} c_y && +M_{33}, \\ N_{23} &= && M_{35} c_x c_y + M_{45} c_y^2 - M_{53} c_x && -(M_{43} + M_{52}) c_y + M_{23}, \\ N_{31} &= && M_{45} c_x c_y && -M_{43} c_x && -M_{51} c_y && +M_{31}, \\ N_{12} &= M_{45} c_x^2 + M_{44} c_x c_y && -(M_{42} + M_{51}) c_x - M_{41} c_y && +M_{12} \end{aligned} \right\} \tag{106}$$

and where

$$\Delta_2 = \begin{vmatrix} m_{20} & m_{11} \\ m_{11} & m_{02} \end{vmatrix}, \quad \Delta_5 = |\Xi_{ij}|, \quad N = |N_{ij}|, \tag{107}$$

$$\left. \begin{aligned} n_{13} &= N_{21} N_{32} - N_{22} N_{31}, \\ n_{22} &= N_{11} N_{33} - N_{13}^2. \end{aligned} \right\} \tag{108}$$

PROPERTIES OF AN ISOTROPIC RANDOM SURFACE

169

(D_{ma} denotes the density of maxima.) For an isotropic spectrum these expressions are considerably simplified. Thus (Ξ_{ij}) becomes

$$(\Xi_{ij}) = \begin{pmatrix} \frac{3}{8}M_4 & 0 & \frac{1}{8}M_4 & 0 & 0 \\ 0 & \frac{1}{8}M_4 & 0 & 0 & 0 \\ \frac{1}{8}M_4 & 0 & \frac{3}{8}M_4 & 0 & 0 \\ \hline 0 & 0 & 0 & \frac{1}{2}M_2'' & 0 \\ 0 & 0 & 0 & 0 & \frac{1}{2}M_2'' \end{pmatrix}, \quad (109)$$

and so

$$(M_{ij}) = \begin{pmatrix} \frac{3}{M_4} & 0 & -\frac{1}{M_4} & 0 & 0 \\ 0 & \frac{8}{M_4} & 0 & 0 & 0 \\ -\frac{1}{M_4} & 0 & \frac{3}{M_4} & 0 & 0 \\ \hline 0 & 0 & 0 & \frac{2}{M_2''} & 0 \\ 0 & 0 & 0 & 0 & \frac{2}{M_2''} \end{pmatrix}. \quad (110)$$

Hence we have

$$(N_{ij}) = \frac{1}{M_4} \begin{pmatrix} 2\xi^2 + 3 & 2\xi\eta & -1 \\ 2\xi\eta & 2(\xi^2 + \eta^2) + 8 & 2\xi\eta \\ -1 & 2\xi\eta & 2\eta^2 + 3 \end{pmatrix}, \quad (111)$$

where

$$(\xi, \eta) = \left(\frac{M_4}{M_2''}\right)^{\frac{1}{2}} (c_x, c_y). \quad (112)$$

After some reduction we find from (105)

$$p(c_x, c_y)_{\xi_1, \xi_2} = \frac{4\sqrt{3} M_4 (\alpha^2 + 4) (3\alpha^2 + 4) (\alpha^2 + 6) + 6\alpha^4}{\pi M_2'' [(\alpha^2 + 4) (3\alpha^2 + 4)]^{\frac{1}{2}}}, \quad (113)$$

where

$$\alpha^2 = \xi^2 + \eta^2 = \frac{M_4}{M_2''} (c_x^2 + c_y^2). \quad (114)$$

To find the distribution of the non-dimensional velocity α we may write

$$(\xi, \eta) = (\alpha \cos \theta, \alpha \sin \theta), \quad (115)$$

and so

$$p(\alpha) = 2\pi\alpha p(\xi, \eta) = 2\pi\alpha \frac{M_4''}{M_4^2} p(c_x, c_y), \quad (116)$$

giving

$$p(\alpha) = 8\sqrt{3}\alpha \frac{(\alpha^2 + 4) (3\alpha^2 + 4) (\alpha^2 + 6) + 6\alpha^4}{[(\alpha^2 + 4) (3\alpha^2 + 4)]^{\frac{1}{2}}}. \quad (117)$$

The form of the distribution is shown in figure 2. There is a single maximum, at $\alpha = 0.72$ approximately. At infinity $p(\alpha)$ is $O(\alpha^{-3})$, so that the second moment diverges. The median value (dividing the distribution into two equal parts) is at

$$\alpha = 1.240 \dots = \alpha_m, \quad (118)$$

say. The value α_m has the following significance: if the positions of the specular points are noted at two successive instants t and $t + dt$, half of the points may be observed to have moved through distances greater than

$$\left(\frac{M_2'}{M_4'}\right)^{\frac{1}{2}} \alpha_m dt \quad (119)$$

from their original positions.

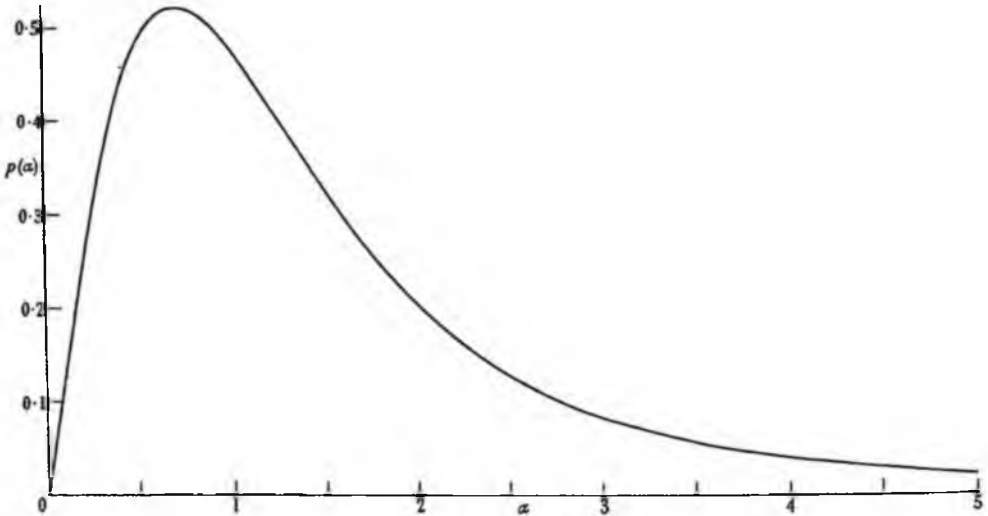


FIGURE 2. Graph of $p(\alpha)$, showing the form of the probability distribution of the absolute velocities of specular points.

For a ring spectrum this median distance is

$$\alpha_m \bar{v} dt, \quad (120)$$

where \bar{v} is the velocity corresponding to the wave number \bar{v} .

3. ON THE UNIQUENESS OF THE SPECTRUM

Suppose we are given certain of the statistical properties discussed in § 2, the question arises whether these determine the spectrum uniquely, or to what extent the properties may be shared by other spectra.

The correlation function $\psi(x, y)$, if known for all values of x and y , would suffice to determine $E(u, v)$ under general conditions; for E is simply the cosine transform of ψ . However, the properties discussed above are purely local, that is to say, they involve the behaviour of the surface at one point and its immediate neighbourhood. We have seen that these properties depend only on the moments M_{2r}, M_{2r}' , of the spectrum (which are the derivatives of ψ at the origin). In fact M_{2r} is the r th moment with respect to $\beta (= w^2)$, of the function

$$F(\beta) = F(w^2) = \pi E(w) \quad (121)$$

defined over $0 < \beta < \infty$.

PROPERTIES OF AN ISOTROPIC RANDOM SURFACE

171

The properties which depend on moments M_{2r} , up to order $r = s$ will be said to be of order $2s$. If all the properties of order up to $2s$ are known, the moments up to order $2s$ may all be determined. For example, from (47) and (59) we have

$$\left. \begin{aligned} M_0 &= \bar{\zeta}^2, \\ \frac{M_{2r+2}}{M_{2r}} &= \frac{2r+2}{2r+1} \pi^2 N_r^2 \quad (r = 0, 1, 2, \dots), \end{aligned} \right\} \quad (122)$$

and therefore

$$M_{2r} = \frac{2 \cdot 4 \cdot 6 \cdots 2r}{1 \cdot 3 \cdot 5 \cdots (2r-1)} \pi^{2r} \bar{\zeta}^2 N_0^2 N_1^2 \cdots N_{r-1}^2. \quad (123)$$

Suppose first that the moments of F exist and are known up to infinite order. This does not determine F uniquely in general (see Kendall 1952, chap. 4), but if certain restrictions are placed upon F for large values of β —for example, if E is exponentially small at infinity—then only one function with these moments can exist.

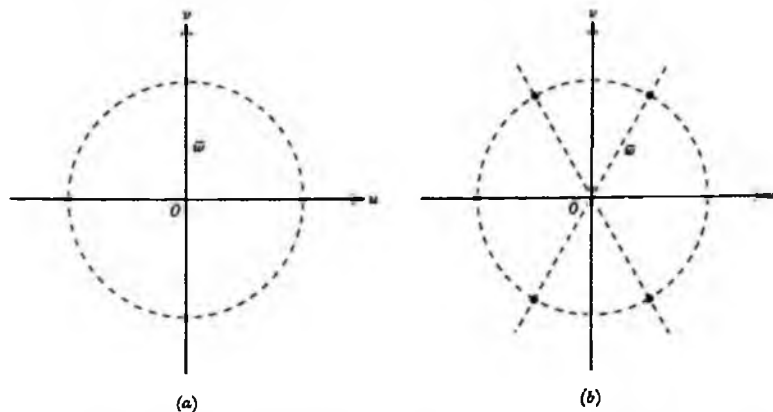


FIGURE 3. Examples of spectra whose statistical properties are isotropic (a) to order 2, (b) to order 4.

In practice we may know, or be concerned with, properties up to a finite order $2s$ only. Except in special cases, if the moments are known up to a finite order only, infinitely many functions may be found having these same moments. A particularly simple function is one consisting of the sum of delta functions. It can be shown (Stieltjes 1894, chap. 1) that if the moments M_{2r} are specified for $r = 0, 1, \dots, s$, then a function F^* , the sum of not more than $[\frac{1}{2}s + 1]$ positive delta functions, may be found having these same moments and lying in the range $0 \leq \beta < \infty$. Hence a combination of not more than $[\frac{1}{2}s + 1]$ ring spectra may be found which has the required statistical properties, to order $2s$.

One can also find non-isotropic spectra with the same statistical properties. Consider, for example, a surface which is the sum of two pairs of long-crested, incoherent systems of waves, of equal wavelength and mean-square amplitude, intersecting at right angles (figure 3a). The spectrum function has the same moments $m_{00}, m_{20}, m_{11}, m_{02}$ as an isotropic ring spectrum of the same radius \bar{w} , for if

$$m_{00} = M_0, \quad (124)$$

$$\text{then } (m_{20}, m_{11}, m_{02}) = (\frac{1}{2}\bar{w}^2 M_0, 0, \frac{1}{2}\bar{w}^2 M_0). \quad (125)$$

Now by equation (9) both $m_0(\theta)$ and $m_2(\theta)$ depend only on these moments; thus they are the same as for a ring spectrum, and so independent of θ . Hence the number N_0 of zeros per unit distance, which is given by equation (56), is also independent of the direction θ . Similarly, all properties depending only on moments of order 0 and 2 will appear as isotropic, including the distributions of surface slopes and of contour direction.

More generally, if we consider a surface which is the sum of $s+1$ pairs of long-crested waves travelling in directions $\theta = j\pi/(s+1)$ uniformly spaced between 0 and 2π , then all the moments m_{pq} of order $p+q \leq 2s$ are the same as for a ring spectrum. Hence N_0, N_1, \dots, N_{s-1} are all independent of θ , and so are all properties of order less than or equal to $2s$.

The case $s=2$ is shown in figure 3*b*. For this surface both the number N_0 of zeros and the number N_1 of maxima and minima in a direction θ are independent of θ .

The general theorem may be quite simply proved as follows. Consider any spectrum in which the energy is all concentrated on the circle $w = \bar{w}$, and in which the distribution of energy with regard to θ is given by some function $G(\theta)$. The (p, q) th moment of the spectrum is then

$$m_{pq} = \int_0^{2\pi} u^p v^q G(\theta) d\theta, \quad (126)$$

where $(u, v) = (\bar{w} \cos \theta, \bar{w} \sin \theta)$. That is to say,

$$m_{pq} = \int_0^{2\pi} \bar{w}^{p+q} \cos^p \theta \sin^q \theta G(\theta) d\theta. \quad (127)$$

The product $\cos^p \theta \sin^q \theta$ can be expressed as a trigonometric series in θ containing terms in $\cos n\theta$ and $\sin n\theta$, where n does not exceed $p+q$. Suppose then that the Fourier series for $G(\theta)$ is of the form

$$G(\theta) = \bar{G} + \sum_{n=1}^{\infty} [A_n \cos n\theta + B_n \sin n\theta], \quad (128)$$

where

$$\left. \begin{aligned} A_1 = A_2 = \dots = A_{2s+1} = 0, \\ B_1 = B_2 = \dots = B_{2s+1} = 0. \end{aligned} \right\} \quad (129)$$

Then if $p+q \leq (2s+1)$ all terms in (126) will vanish except those arising from the constant term \bar{G} . This gives

$$m_{pq} = \int_0^{2\pi} \bar{w}^{p+q} \cos^p \theta \sin^q \theta \bar{G} d\theta. \quad (130)$$

In other words, m_{pq} is the same as for a ring spectrum. Now when the spectrum consists of s uniformly spaced pairs of wave systems we have

$$G(\theta) = \frac{\pi \bar{G}}{s+1} \sum_{j=1}^{2s+2} \delta\left(\theta - \frac{j\pi}{s+1}\right), \quad (131)$$

where $\delta(\theta)$ denotes the Dirac delta function. So

$$A_n = \frac{1}{\pi} \int_0^{2\pi} G(\theta) \cos n\theta d\theta = \frac{\bar{G}}{s+1} \sum_{j=1}^{2s+2} \cos \frac{jn\pi}{s+1}, \quad (132)$$

which vanishes when $n = 1, 2, \dots, (2s+1)$; and similarly for B_n . Thus the conditions (128) are satisfied.

PROPERTIES OF AN ISOTROPIC RANDOM SURFACE

173

As a corollary it follows that any spectrum which is periodic in θ with period $\pi/(s+1)$ will have isotropic properties up to order $2s+1$. For the spectrum may be considered as the sum of regular systems of point spectra of the type just discussed.

APPENDIX

Proof of equation (32)

Substitution from (7) into (30) gives

$$\Delta_{2r} = \int_{-\infty}^{\infty} \int_{-\infty}^{\infty} \dots \int_{-\infty}^{\infty} \int_{-\infty}^{\infty} E(u_1, v_1) \dots E(u_{r+1}, v_{r+1})$$

$$\times \begin{vmatrix} u_1^{2r} & u_2^{2r-1} v_2 & \dots & u_{r+1}^{2r} v_{r+1} \\ u_1^{2r-1} v_1 & u_2^{2r-2} v_2^2 & \dots & u_{r+1}^{2r-1} v_{r+1}^2 \\ \vdots & \vdots & & \vdots \\ u_1 v_1 & u_2^{r-1} v_2^{r+1} & \dots & v_{r+1}^{2r} \end{vmatrix} du_1 dv_1 \dots du_{r+1} dv_{r+1} \quad (\text{A } 1)$$

$$= \int_{-\infty}^{\infty} \int_{-\infty}^{\infty} \dots \int_{-\infty}^{\infty} \int_{-\infty}^{\infty} E(u_1, v_1) \dots E(u_{r+1}, v_{r+1})$$

$$\times \begin{vmatrix} 1 & 1 & \dots & 1 \\ v_1/u_1 & v_2/u_2 & \dots & (v_{r+1}/u_{r+1}) \\ \vdots & \vdots & & \vdots \\ (v_1/u_1)^r & (v_2/u_2)^r & \dots & (v_{r+1}/u_{r+1})^r \end{vmatrix}$$

$$\times (u_1/v_1)^r (u_2/v_2)^{r-1} \dots (u_{r+1}/v_{r+1})^0$$

$$\times (u_1 v_1 \dots u_{r+1} v_{r+1})^r du_1 dv_1 \dots du_{r+1} dv_{r+1}. \quad (\text{A } 2)$$

The value of Δ_{2r} is unaltered by permuting the suffixes 1, 2, ..., $(r+1)$ among themselves. Thus, adding all the $(r+1)!$ different permutations we have

$$(r+1)! \Delta_{2r} = \int_{-\infty}^{\infty} \int_{-\infty}^{\infty} \dots \int_{-\infty}^{\infty} \int_{-\infty}^{\infty} E(u_1, v_1) \dots E(u_{r+1}, v_{r+1})$$

$$\times \begin{vmatrix} 1 & \dots & 1 \\ \vdots & & \vdots \\ (v_1/u_1)^r & \dots & (v_{r+1}/u_{r+1})^r \end{vmatrix} \times \begin{vmatrix} 1 & \dots & 1 \\ \vdots & & \vdots \\ (u_1/v_1)^r & \dots & (u_{r+1}/v_{r+1})^r \end{vmatrix}$$

$$\times (u_1 v_1 u_2 v_2 \dots u_{r+1} v_{r+1})^r du_1 dv_1 \dots du_{r+1} dv_{r+1}$$

$$= \int_{-\infty}^{\infty} \int_{-\infty}^{\infty} \dots \int_{-\infty}^{\infty} \int_{-\infty}^{\infty} E(u_1, v_1) \dots E(u_{r+1}, v_{r+1})$$

$$\times \prod_{p>q} (u_p/v_p - u_q/v_q) \prod_{p>q} (v_p/u_p - v_q/u_q)$$

$$\times (u_1 v_1 \dots u_{r+1} v_{r+1})^r du_1 dv_1 \dots du_{r+1} dv_{r+1}. \quad (\text{A } 3)$$

Now writing

$$\left. \begin{aligned} (u_p, v_p) &= (w_p \cos \theta_p, w_p \sin \theta_p), \\ E(u_p, v_q) &= E(w_p), \end{aligned} \right\} \quad (\text{A } 4)$$

in the above, we have

$$\begin{aligned}
 (r+1)! \Delta_{2r} &= \int_0^\infty \int_0^{2\pi} \dots \int_0^\infty \int_0^{2\pi} E(w_1) \dots E(w_{r+1}) \\
 &\quad \times \prod_{p>q} \sin^2(\theta_p - \theta_q) w_1^{r+1} \dots w_{r+1}^1 dw_1 d\theta_1 \dots dw_{r+1} d\theta_{r+1} \\
 &= \left(\frac{M_{2r}}{2\pi}\right)^{r+1} \int_0^{2\pi} \dots \int_0^{2\pi} \prod_{p>q} \sin^2(\theta_p - \theta_q) d\theta_1 \dots d\theta_{r+1}. \tag{A 5}
 \end{aligned}$$

The multiple integral may be evaluated as follows. Since

$$\sin^2(\theta_p - \theta_q) = \frac{1}{4}(e^{2i\theta_p} - e^{2i\theta_q})(e^{-2i\theta_p} - e^{-2i\theta_q}), \tag{A 6}$$

we have

$$\begin{aligned}
 &\prod_{p>q} \sin^2(\theta_p - \theta_q) \\
 &= \frac{1}{2^{r(r+1)}} \begin{vmatrix} 1 & 1 & \dots & 1 \\ e^{2i\theta_1} & e^{2i\theta_2} & \dots & e^{2i\theta_{r+1}} \\ \vdots & \vdots & \ddots & \vdots \\ e^{2ri\theta_1} & e^{2ri\theta_2} & \dots & e^{2ri\theta_{r+1}} \end{vmatrix} \times \begin{vmatrix} 1 & 1 & \dots & 1 \\ e^{-2i\theta_1} & e^{-2i\theta_2} & \dots & e^{-2i\theta_{r+1}} \\ \vdots & \vdots & \ddots & \vdots \\ e^{-2ri\theta_1} & e^{-2ri\theta_2} & \dots & e^{-2ri\theta_{r+1}} \end{vmatrix}. \tag{A 7}
 \end{aligned}$$

A typical term in the expansion of the first determinant is

$$1 \cdot e^{2i\theta_1} \cdot e^{4i\theta_2} \cdot \dots \cdot e^{2ri\theta_{r+1}}, \tag{A 8}$$

which, when multiplied into the second determinant, gives

$$\begin{vmatrix} 1 & e^{2i\theta_2} & \dots & e^{2ri\theta_{r+1}} \\ e^{-2i\theta_1} & 1 & \dots & e^{2(r-1)i\theta_{r+1}} \\ \vdots & \vdots & \ddots & \vdots \\ e^{-2ri\theta_1} & e^{-2(r-1)i\theta_2} & \dots & 1 \end{vmatrix}. \tag{A 9}$$

The integral of this determinant over the given ranges of $\theta_1, \dots, \theta_{r+1}$ is

$$\begin{vmatrix} 2\pi & 0 & \dots & 0 \\ 0 & 2\pi & \dots & 0 \\ \vdots & \vdots & \ddots & \vdots \\ 0 & 0 & \dots & 2\pi \end{vmatrix} = (2\pi)^{r+1}. \tag{A 10}$$

Since the first determinant in (A 7) contributes altogether $(n+1)!$ such terms we have

$$\int_0^{2\pi} \dots \int_0^{2\pi} \prod_{p>q} \sin^2(\theta_p - \theta_q) d\theta_1 \dots d\theta_{r+1} = \frac{(r+1)! (2\pi)^{r+1}}{2^{r(r+1)}}. \tag{A 11}$$

From this and (A 5) the result follows.

REFERENCES

Kendall, M. G. 1952 *The advanced theory of statistics* (5th ed.), vol. 1. London: Griffin and Co.
 Longuet-Higgins, M. S. 1957 The statistical analysis of a random, moving surface. *Phil. Trans. A*, 249, 321-387.
 Stieltjes, J. 1894 Recherches sur les fractions continues. *Ann. Fac. Sci. Toulouse*, 8, 1-122. [Reprinted in *Oeuvres*, 2, 402-523, Groningen, 1918.]

REPRINTED FROM THE
 PROCEEDINGS OF THE PHYSICAL SOCIETY, B, VOL. LXX, p. 559, 1957
 All Rights Reserved
 PRINTED IN GREAT BRITAIN

A Statistical Distribution arising in the Study of the Ionosphere

By M. S. LONGUET-HIGGINS

National Institute of Oceanography, Wormley, Surrey

MS. received 7th February 1957

Abstract. An approximate distribution is deduced for the directions of the 'lines of maxima' on a random surface. The theoretical distribution is found to be in good agreement with some experimental results obtained previously by Briggs and Page.

§ 1. INTRODUCTION

THE analysis of fading patterns of radio waves reflected from the ionosphere gives rise to some interesting statistical problems. Among these is one studied by Briggs and Page (1955) which may be stated as follows.

Suppose we are given a two-dimensional surface whose height represents, say, the intensity $f(x, y)$ of a beam of reflected radiation as a function of two horizontal coordinates x and y . Let two parallel sections of the surface be taken, along the lines $y = y_0$ and $y = y_0 + \delta$. Consider the maxima of the sections along these lines. If the lines are sufficiently close (δ sufficiently small) the maxima of the two functions will correspond in pairs, the members of a pair being slightly shifted relative to one another. If the line joining a pair of maxima makes an angle α with the y -axis the problem is to find the statistical distribution of $\tan \alpha$.

Lacking a theoretical solution, Briggs and Page constructed pairs of random sequences to represent the functions $f(x, y_0)$ and $f(x, y_0 + \delta)$. These sequences were arranged so as to be normally distributed with zero mean and unit standard deviation. Further, their auto-correlograms and cross-correlograms were also of normal form. The observed distribution of $\tan \alpha$ for the pairs of sequences is indicated by the experimental points in the figure, which are transcribed from Fig. 3 of Briggs and Page (1955).

The theoretical problem, however, is similar to many that have been treated in connection with the analysis of the sea surface (see Longuet-Higgins 1957 a, b) and in this note we shall present a solution. It will be shown that, provided only the joint distribution of $f(x, y)$ and its derivatives is normal (a condition satisfied in very general circumstances) the probability distribution of $\tan \alpha$ is given by

$$p(\tan \alpha) = \frac{A^2}{2[A^2 + (\tan \alpha - B)^2]^{3/2}}, \quad \dots\dots(1)$$

where A and B are constants which depend only on the form of the correlogram of f . When the surface is isotropic, so that its correlogram has circular symmetry, we have

$$A^2 = 1/3, \quad B = 0$$

and so

$$p(\tan \alpha) = \frac{1}{6[\frac{1}{3} + \tan^2 \alpha]^{3/2}} \quad \dots\dots(2)$$

In the case treated by Briggs and Page we have apparently (see § 5 below)

$$A^2 = 2/3, \quad B = 0$$

and so

$$p(\tan \alpha) = \frac{1}{3[\frac{2}{3} + \tan^2 \alpha]^{3/2}}. \quad \dots (3)$$

This curve is shown by the dotted line in the figure. It will be seen that the agreement is fairly close. Moreover, the curve is in adequate agreement at the tails of the distribution, in contrast with the normal frequency curve tentatively suggested by Briggs and Page.

§ 2. THE DERIVATION OF $p(\tan \alpha)$

Suppose that two corresponding maxima are separated by intervals dx and dy in the x and y directions. Then, since the gradient $\partial f/\partial x$ vanishes at both maxima we have

$$\frac{\partial f}{\partial x}(x + dx, y + dy) - \frac{\partial f}{\partial x}(x, y) = 0$$

or

$$\frac{\partial^2 f}{\partial x^2} dx + \frac{\partial^2 f}{\partial x \partial y} dy = 0$$

approximately, and therefore

$$\tan \alpha = \frac{dx}{dy} = - \frac{\partial^2 f / \partial x \partial y}{\partial^2 f / \partial x^2}. \quad \dots (4)$$

Clearly this formula also holds for any pair of points having the *same* gradient not necessarily zero.

Now, let us assume that f is a stationary random function whose partial derivatives up to the second order are distributed normally.

Writing for convenience

$$\frac{\partial f}{\partial x}, \quad \frac{\partial^2 f}{\partial x^2}, \quad \frac{\partial^2 f}{\partial x \partial y} = \xi_1, \xi_2, \xi_3$$

we have for the probability-density of (ξ_1, ξ_2, ξ_3)

$$p(\xi_1, \xi_2, \xi_3) = \frac{1}{(2\pi)^{3/2} |\Xi_{ij}|^{1/2}} \exp \left[-\frac{1}{2} \sum_{i,j} M_{ij} \xi_i \xi_j \right], \quad \dots (5)$$

where (M_{ij}) is the reciprocal of the matrix of mean values

$$(\Xi_{ij}) = (\overline{\xi_i \xi_j}).$$

In fact, if $\psi(X, Y)$ denotes the correlation function

$$\psi(X, Y) = \overline{f(x, y) f(x + X, y + Y)} \quad \dots (6)$$

we have by repeated differentiation

$$\left. \begin{aligned} \overline{\xi_1^2} &= - \frac{\partial^2 \psi}{\partial X^2}(0, 0) = m_{20}, \quad \text{say,} \\ \overline{\xi_2^2} &= \frac{\partial^4 \psi}{\partial X^4}(0, 0) = m_{40}, \\ \overline{\xi_3^2} &= \frac{\partial^4 \psi}{\partial X^2 \partial Y^2}(0, 0) = m_{22}, \end{aligned} \right\} \dots (7)$$

and also

$$\left. \begin{aligned} \overline{\xi_2 \xi_3} &= \frac{\partial^2 \psi}{\partial X^2 \partial Y} (0, 0) = m_{31} \\ \overline{\xi_1 \xi_2} &= \overline{\xi_1 \xi_3} = 0. \end{aligned} \right\} \dots\dots (8)$$

So

$$(\Xi_{ij}) = \begin{bmatrix} m_{20} & 0 & 0 \\ 0 & m_{40} & m_{31} \\ 0 & m_{31} & m_{22} \end{bmatrix}$$

and

$$p(\xi_1, \xi_2, \xi_3) = p(\xi_1) p(\xi_2, \xi_3), \dots\dots (9)$$

where

$$\left. \begin{aligned} p(\xi_1) &= \frac{1}{(2\pi m_{20})^{1/2}} \exp(-\xi_1^2/2m_{20}), \\ p(\xi_2, \xi_3) &= \frac{1}{(2\pi\Delta)^{1/2}} \exp[-(m_{22}\xi_2^2 - 2m_{31}\xi_2\xi_3 + m_{40}\xi_3^2)/2\Delta], \\ \Delta &= m_{40}m_{22} - m_{31}^2 \end{aligned} \right\} \dots\dots (10)$$

$p(\xi_1)$ and $p(\xi_2, \xi_3)$ are the distributions of ξ_1 and of (ξ_2, ξ_3) separately, and equation (9) shows that they are statistically independent.

We wish now to find the distribution of the quantity

$$\eta = \tan \alpha = -\xi_3/\xi_2$$

at the points where the gradient ξ_1 vanishes. First let us find the joint distribution of (ξ_2, ξ_3) at such points; we shall denote this by $p(\xi_2, \xi_3)_{\xi_1}$. Now since ξ_2 and ξ_3 are statistically independent of ξ_1 , the distribution of (ξ_2, ξ_3) for points on the x -axis such that $0 < \xi_1 < d\xi_1$ is the same as the ordinary distribution $p(\xi_2, \xi_3)$ for points distributed randomly and uniformly with regard to x . But near any particular zero of ξ_1 the function ξ_1 remains in the interval $0 < \xi_1 < d\xi_1$ for a distance dx inversely proportional to $|\partial\xi_1/\partial x| = |\xi_3|$. Hence we have

$$p(\xi_2, \xi_3) = C|\xi_2|^{-1} p(\xi_2, \xi_3)_{\xi_1}$$

or

$$p(\xi_2, \xi_3)_{\xi_1} = C^{-1}|\xi_2| p(\xi_2, \xi_3),$$

where C is a normalizing constant. This gives

$$p(\xi_2, \xi_3)_{\xi_1} = \frac{1}{2(2\pi\Delta m_{40})^{1/2}} |\xi_2| \exp[-m_{22}\xi_2^2 - 2m_{31}\xi_2\xi_3 + m_{40}\xi_3^2/2\Delta]. \dots\dots (11)$$

To find the distribution of η we now put

$$(-\xi_3/\xi_2, \xi_2) = (\eta, \eta'), \quad \frac{\partial(\xi_2, \xi_3)}{\partial(\eta, \eta')} = \eta',$$

giving

$$p(\eta, \eta')_{\xi_1} = \frac{1}{2(2\pi\Delta m_{40})^{1/2}} \eta'^2 \exp[-\eta'^2(m_{22} + 2m_{31}\eta + m_{40}\eta'^2)/2\Delta]. \dots\dots (12)$$

On eliminating η' by integration over the whole range $(-\infty, \infty)$ we find

$$p(\eta)_{\xi_1} = \frac{\Delta/m_{40}^{1/2}}{2[m_{22} + 2m_{31}\eta + m_{40}\eta^2]^{3/2}}$$

or

$$p(\eta)_{\xi_1} = \frac{1}{2[A^2 + (\eta - B)^2]^{3/2}}, \dots\dots (13)$$

where

$$A = \frac{\Delta^{1/2}}{m_{40}}, \quad B = -\frac{m_{31}}{m_{40}}. \dots\dots (14)$$

This is the result stated in equation (1).

We have included in this distribution all points at which the gradient vanishes, i.e. both maxima and minima. However, since $p(\eta, \eta')_{\xi_1}$ is symmetrical about the origin, the contributions to $p(\eta)_{\xi_1}$ from the maxima ($\eta' < 0$) are equal to the contributions from the minima ($\eta' > 0$). So, after introducing the appropriate normalizing constant, we see that equation (1) represents the distribution of $\tan \alpha$ for the maxima alone, and also for the minima.

Clearly $p(\eta)_{\xi_1}$ is a symmetrical distribution centred on $\eta = B$ and falling off like η^{-3} for large values of η . Thus the standard deviation is infinite. But a convenient measure of the width of the distribution is the interquartile range, which is

$$\frac{2}{\sqrt{3}} A = 1.155 \dots A. \quad \dots (15)$$

The width of the distribution at a level equal to half its maximum height is

$$2\sqrt{(4^{1/3} - 1)}A = 1.532 \dots A. \quad \dots (16)$$

§ 3. REMARK

We have seen that the angle α can be defined at all points of the curve, being the angle made with the y -axis by lines of constant $\partial f / \partial x$. The distribution of $\tan \alpha$ for points where $\partial f / \partial x$ takes any particular value ξ_1 other than zero is also given by equation (1); this follows from the fact that $p(\xi_2, \xi_3)_{\xi_1}$ is independent of ξ_1 itself.

However, if instead of the distribution of $\tan \alpha$ at points of given gradient we wish to find the distribution of $\tan \alpha$ at points randomly and uniformly distributed with regard to x , then we have only to replace $p(\xi_2, \xi_3)_{\xi_1}$ in the foregoing analysis by the ordinary distribution $p(\xi_2, \xi_3)$. As a consequence we find the following distribution for $\tan \alpha$:

$$p^\omega(\tan \alpha) = \frac{1}{\pi} \frac{1}{A^2 + (\tan \alpha - B)^2}, \quad \dots (17)$$

where A and B have their former meanings. This expression is similar in form to the previous distribution, having a mean value B and a width proportional to A . However, the two distributions are not to be confused, and in fact the former distribution (1) is the one which is appropriate in the present case, considering the method of observing the data. For a further discussion of these distributions, which arise also in the analysis of moving waveforms, the reader is referred to Longuet-Higgins (1957 b).

§ 4. AN ISOTROPIC SURFACE

Assuming that the derivatives of the correlation function $\psi(X, Y)$ at the origin exist up to the fourth order, we have in general

$$\begin{aligned} \psi(X, Y) = & C_{00} + (C_{10}X + C_{01}Y) \\ & + (C_{20}X^2 + C_{11}XY + C_{02}Y^2) \\ & + (C_{30}X^3 + C_{21}X^2Y + C_{12}XY^2 + C_{03}Y^3) \\ & + (C_{40}X^4 + C_{31}X^3Y + C_{22}X^2Y^2 + C_{13}XY^3 + C_{04}Y^4) \\ & + R \end{aligned}$$

where

$$C_{pq} = \frac{1}{p!q!} \frac{\partial^{p+q}\psi}{\partial X^p \partial Y^q} (0, 0)$$

and R is a remainder term of higher order. Suppose now that the surface is isotropic. Then from the two conditions

$$\begin{aligned} \psi(X, Y) &= \psi(-X, Y) \\ \psi(X, Y) &= \psi(X, -Y) \end{aligned}$$

we see that C_{pq} vanishes whenever p is odd and whenever q is odd, respectively. The remaining terms in the expansion of ψ are integral powers of both X^2 and Y^2 . Further, since the surface is isotropic, $\psi(X, Y)$ is a function of $X^2 + Y^2$ only. The only polynomial of the $2n$ th degree having this form is $(X^2 + Y^2)^n$. Hence

$$\psi(X, Y) = D_0 + D_1(X^2 + Y^2) + D_2(X^4 + 2X^2Y^2 + Y^4) + R,$$

where D_0, D_1 and D_2 are constants. This gives

$$\left. \begin{aligned} m_{40} &= \frac{\partial^4 \psi}{\partial X^4}(0, 0) = 24D_2 \\ m_{31} &= \frac{\partial^4 \psi}{\partial X^3 \partial Y}(0, 0) = 0 \\ m_{22} &= \frac{\partial^4 \psi}{\partial X^2 \partial Y^2}(0, 0) = 8D_2 \end{aligned} \right\}$$

and so

$$A^2 = \frac{\Delta}{m_{40}^3} = \frac{1}{3}; \quad B = 0. \quad \dots\dots(18)$$

With these values of A and B the distribution (13) becomes

$$p(\tan \alpha) = \frac{1}{6[\frac{1}{3} + \tan^2 \alpha]^{3/2}}. \quad \dots\dots(19)$$

Thus $p(\tan \alpha)$ has a mean value zero and an interquartile range $2/3$. The width of the distribution at half the maximum level is $0.884\dots$

The conditions (18), although necessary for an isotropic surface, are not sufficient. For example, a surface consisting of three long-crested but incoherent wave systems whose directions make angles $0, 2\pi/3, 4\pi/3$ with a fixed direction would also satisfy the same conditions. The surface would therefore give rise to the same distribution of $\tan \alpha$ as does an isotropic surface.

§ 5. THE SURFACE STUDIED BY BRIGGS AND PAGE (1955)

To represent the two functions $f(x, y_0)$ and $f(x, y_0 + \delta)$ Briggs and Page first constructed two sequences of numbers

$$P_i = \sum_{j=-\infty}^{\infty} a_j \xi_{i+j}; \quad Q_i = \sum_{j=-\infty}^{\infty} a_j \eta_{i+j} \quad \dots\dots(20)$$

where ξ_i and η_i ($i = \dots -2, -1, 0, 1, 2, \dots$) were two sets of mutually independent random normal deviates (each with zero mean and unit standard deviation) and where the a_j were fixed weighting constants given by

$$a_j = \text{constant} \times \exp(-j^2/\sigma^2). \quad \dots\dots(21)$$

It can be shown that under these circumstances each of the sequences P_i, Q_i is normally distributed, and further that their auto-correlations and cross-correlations are given by

$$\left. \begin{aligned} \frac{P_i P_{i+n}}{P_i Q_{i+n}} &= \frac{Q_i Q_{i+n}}{P_i Q_{i+n}} = \text{constant} \times \exp(-n^2/2\sigma^2), \quad (n \text{ even}) \\ \frac{P_i Q_{i+n}}{P_i Q_{i+n}} &= 0. \end{aligned} \right\} \dots\dots(22)$$

The constant in (22) is taken to be unity. The authors then represent $f(x, y_0)$ by the series P_i and $f(x, y_0 + \delta)$ by the series

$$R_i = \rho P_i + (1 - \rho^2)^{1/2} Q_i,$$

where ρ is a constant, equal to $\exp(-\delta^2/\sigma^2)$. It can easily be seen that

$$\left. \begin{aligned} \overline{R_i R_{i+n}} &= \exp(-n^2/2\sigma^2), \\ \overline{P_i R_{i+n}} &= \exp(-n^2/2\sigma^2). \end{aligned} \right\}$$

Thus

$$\left. \begin{aligned} \overline{f(x, y_0) f(x+n, y_0)} &= \exp(-n^2/2\sigma^2), \\ \overline{f(x, y_0 + \delta) f(x+n, y_0 + \delta)} &= \exp(-n^2/2\sigma^2), \\ \overline{f(x, y_0) f(x+n, y_0 + \delta)} &= \exp[-(n^2 + 2\delta^2)/2\sigma^2]. \end{aligned} \right\} \dots\dots (23)$$

so that, in so far as the two functions are concerned, they behave like sections of a surface having a correlation function

$$\psi(X, Y) = \exp[-(X^2 + 2Y^2)/2\sigma^2]. \dots\dots (24)$$

For this surface we have clearly

$$\left. \begin{aligned} m_{40} &= \frac{\partial^4 \psi}{\partial X^4} (0, 0) = \frac{3}{\sigma^4}, \\ m_{31} &= \frac{\partial^4 \psi}{\partial X^3 \partial Y} (0, 0) = 0, \\ m_{22} &= \frac{\partial^4 \psi}{\partial X^2 \partial Y^2} (0, 0) = \frac{2}{\sigma^4}, \end{aligned} \right\} \dots\dots (25)$$

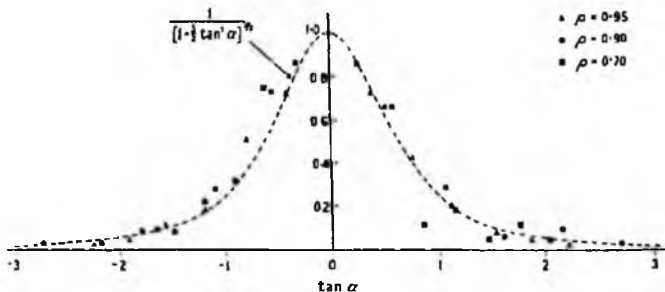
giving

$$A^2 = 2/3, \quad B = 0.$$

The corresponding curve is

$$\rho(\tan \alpha) = \frac{1}{3[\frac{2}{3} + \tan^2 \alpha]^{3/2}} = \frac{(3/8)^{1/2}}{[1 + \frac{2}{3} \tan^2 \alpha]^{3/2}}. \dots\dots (27)$$

The experimental points of Briggs and Page are shown in the figure. These were not normalized, but were reduced so that the maximum ordinate, for each value of ρ , was equal to unity. The broken curve in the figure corresponds to the distribution (27) multiplied by a factor $(8/3)^{1/2}$ to bring the maximum ordinate also to unity. It will be seen that there is reasonably good agreement.



The theoretical curve of equation (27) (with vertical scale multiplied by $(8/3)^{1/2}$) compared with the experimental points of Briggs and Page.

It should be noted that in their paper Briggs and Page assumed that $P_i P_{i+n}$ was proportional to $\exp(-n^2/\sigma^2)$, omitting the factor 2 in equation (22)†. Consequently, they assumed the correlation function to be of the form

$$\psi(X, Y) = \exp[-(X^2 + Y^2)/2\sigma^2],$$

which would represent an isotropic surface. In fact an isotropic correlogram could have been obtained by assuming

$$\rho = \exp(-\delta^2/\sigma^2)$$

and by plotting the frequency curves in Fig. 3 of their paper against the parameter $(\Delta/\sigma)(-2 \log \rho)^{1/2}$ instead of against $(\Delta/\sigma)(-\log \rho)^{1/2}$.

§ 6. CONCLUSIONS

The distribution of $\tan \alpha$ for a random, normal surface is in general given by equation (13), where $\eta = \tan \alpha$ and A and B are constants depending on the correlation function of the surface. This is in agreement with the experimental distribution found by Briggs and Page.

For an isotropic surface the distribution of $\tan \alpha$ is given by equation (19).

ACKNOWLEDGMENT

I am indebted to Mr J. A. Ratcliffe for drawing my attention to this problem.

REFERENCES

- BRIGGS, B. H., and PAGE, E. S., 1955, *Report of the 1954 Conference on The Physics of the Ionosphere* (London: Physical Society), p. 119.
 LONGUET-HIGGINS, M. S., 1957 a, *Phil. Trans. Roy. Soc. A*, **249**, 321; 1957 b, *Proc. Camb. Phil. Soc.*, **53**, 23.

† Dr. Briggs has kindly confirmed this in a personal communication.

*Reprinted without change of pagination from the
Proceedings of the Royal Society, A, volume 246, pp. 98-118, 1958*

On the intervals between successive zeros of a random function

BY M. S. LONGUET-HIGGINS

National Institute of Oceanography, Wormley, Surrey

(Communicated by G. E. R. Deacon, F.R.S.—Received 13 February 1958)

A new approach is suggested to the problem of the statistical distribution of the intervals between successive zeros of a random, Gaussian function. Hence is derived a sequence of approximations $p_n(\tau)$ ($n=3, 4, 5, \dots$) to the desired probability density $p(\tau)$. The third approximation p_3 is already correct to order τ^4 , and has the correct limiting form in the case of a narrow spectrum. The analysis also gives rise to an alternative approximation $p_n^*(\tau)$, less accurate for small values of τ , but possibly more accurate for larger values. Numerical computation of both p_3 , p_4 , p_5 and p_3^* , p_4^* , p_5^* is carried out for a low-pass spectrum, and the results are compared with observation.

INTRODUCTION

Let f denote a stationary random function of the time t , with mean value zero. What is the statistical distribution of the interval τ between two successive zeros of f , or between two successive maxima or minima?

The problem arises in connexion with the analysis of the sea surface, where $f(t)$ may represent, for example, the height of the surface above a fixed point. It has also been considered by Rice (1945) in connexion with the analysis of noise in electrical circuits.

As in a recent paper (1956), f will be assumed to be representable as the sum of an infinity of sine waves in random relative phase, and its energy spectrum will be assumed a continuous function of the frequency. Under general conditions (see Rice 1944) the statistical distribution of f itself is then normal.

The distribution of τ (which we denote by $p(\tau)$) has a mean value which is easily found; it is reciprocal of the average number N_0 of zero-crossings per unit time, and Rice (1944, 1945) has shown this to be given by

$$N_0 = \frac{1}{\pi} \left(\frac{-\dot{\psi}_0}{\psi_0} \right)^{\frac{1}{2}}, \quad (0.1)$$

where ψ_r denotes the correlation function of f , as defined in §1 below.

To find the complete distribution of τ is somewhat more difficult. In certain limiting cases $p(\tau)$ is known: for example, when τ is small an approximate expression has been given by Rice (1945, p. 59) and when τ is very large it may be shown that $p(\tau)$ decreases exponentially (Kuznetsov, Stratonovich & Tikhonov 1954). Further, in the important case of a narrow spectrum, when f appears as a sine wave of slowly varying amplitude and phase, Rice gave an approximation to $p(\tau)$ valid for a limited range of τ around the mean value $\bar{\tau}$ (1945, p. 63). It is interesting to note that the same approximation may be derived by two alternative methods, either through the distribution of f''/f (Longuet-Higgins 1956) or through the distribution of the phase angle of f (Longuet-Higgins 1957, §2.10).

The purpose of the present paper is to describe a fresh approach to the problem, by which successive approximations to $p(\tau)$ may be calculated. The method depends upon a simple relation (equation (2.1) below) between $p(\tau)$ and the function $U(\tau)$, defined as the probability that f is entirely positive over a fixed time interval of length τ . Since $U(\tau)$ may be approximated by the probability $U_n(\tau)$ that f be positive at n suitably chosen points in the interval (where n is sufficiently great), we thus obtain a set of successive approximations to $p(\tau)$, depending on n .

It is found that the third approximation $p_3(\tau)$ already has the correct gradient, curvature and derivatives up to the fourth order at the origin; moreover, it tends to the correct limiting form when the energy spectrum is narrow. The next two approximations, $p_4(\tau)$ and $p_5(\tau)$ can be evaluated without difficulty, though higher approximations require one or more additional integrations to be performed. Numerical computation of p_3 , p_4 and p_5 is carried out for the case when f has a low-pass spectrum. The results are compared with experimental data, with encouraging agreement.

An alternative approximation $p_n^*(\tau)$ is also derived which is less accurate than p_n for small values of τ , but more accurate for larger values.

1. DEFINITIONS

We assume that $f(t)$ may be represented in the form

$$f(t) = \sum_n c_n \cos(\sigma_n t + \epsilon_n), \quad (1.1)$$

where the frequencies σ_n of the individual sine waves are distributed densely in the interval $(0, \infty)$; the phases ϵ_n are randomly and uniformly distributed in $(0, 2\pi)$ and the amplitudes c_n are such that over a small interval of frequency $(\sigma, \sigma + d\sigma)$

$$\sum_n \frac{1}{2} c_n^2 = E(\sigma) d\sigma, \quad (1.2)$$

where $E(\sigma)$ is a continuous function which will be called the energy spectrum of f . The moments of E about the origin, given by

$$m_r = \int_0^\infty E(\sigma) \sigma^r d\sigma \quad (r = 0, 1, 2, \dots) \quad (1.3)$$

are assumed to exist up to all orders required.

The correlation function of f , defined by

$$\psi(\tau) = \overline{f(t) f(t + \tau)}, \quad (1.4)$$

where a bar denotes a mean value with respect to the phases or with respect to t , exists and is related to the spectrum by

$$\psi(\tau) = \int_0^\infty E(\sigma) \cos \sigma \tau d\sigma. \quad (1.5)$$

The derivatives of ψ at the origin are given by

$$\frac{d^r \psi}{d\tau^r} = \begin{cases} (-1)^{\frac{1}{2}r} m_r & r \text{ even,} \\ 0 & r \text{ odd.} \end{cases} \quad (1.6)$$

Thus if we write (in Rice's notation)

$$\psi(\tau) = \psi_r, \quad d\psi_r/d\tau = \psi'_r, \quad (1.7)$$

we have
$$\psi_0 = m_0, \quad \psi'_0 = 0, \quad \psi''_0 = -m_2, \quad \text{etc.} \quad (1.8)$$

The mean frequency in the spectrum may be defined by

$$\bar{\sigma} = m_1/m_0 \quad (1.9)$$

and the r th moment about the mean is then

$$\mu_r = \int_0^\infty E(\sigma) (\sigma - \bar{\sigma})^r d\sigma = m_r - \binom{r}{1} m_{r-1} \bar{\sigma} + \dots (-1)^r m_0 \bar{\sigma}^r. \quad (1.10)$$

In particular,
$$\mu_0 = m_0, \quad \mu_1 = 0, \quad \mu_2 = m_2 - m_0 \bar{\sigma}^2 = m_0 \bar{\sigma}^2 \delta^2, \quad (1.11)$$

where
$$\delta^2 = \frac{m_0 m_2 - m_1^2}{m_1^2}. \quad (1.12)$$

δ^2 is a non-dimensional parameter proportional to the variance of $E(\sigma)$; it may be expressed also in the form

$$\delta^2 = \frac{1}{2m_1^2} \int_0^\infty \int_0^\infty E(\sigma_1) E(\sigma_2) (\sigma_1 - \sigma_2)^2 d\sigma_1 d\sigma_2. \quad (1.13)$$

When $\delta \ll 1$ the spectrum will be said to be *narrow*, and we see that in that case the energy is concentrated in a narrow range surrounding the mean frequency $\bar{\sigma}$. The correlation function may then be expanded asymptotically in the following way. In (1.5) let the term $\cos \sigma \tau$ be written

$$\begin{aligned} \cos \sigma \tau &= \cos (\sigma - \bar{\sigma}) \tau \cos \bar{\sigma} \tau - \sin (\sigma - \bar{\sigma}) \tau \sin \bar{\sigma} \tau \\ &= \left[1 - \frac{(\sigma - \bar{\sigma})^2 \tau^2}{2!} + \dots \right] \cos \bar{\sigma} \tau - \left[\frac{(\sigma - \bar{\sigma}) \tau}{1!} - \dots \right] \sin \bar{\sigma} \tau. \end{aligned} \quad (1.14)$$

On multiplying by $E(\sigma)$ and integrating term by term we have

$$\psi(\tau) = \left[\mu_0 - \mu_2 \frac{\tau^2}{2!} + \dots \right] \cos \bar{\sigma} \tau - \left[\frac{\mu_1 \tau}{1!} - \dots \right] \sin \bar{\sigma} \tau. \quad (1.15)$$

In the second bracket, μ_1 vanishes. Then assuming that μ_r is of order δ^r and neglecting $(\delta \bar{\sigma} \tau)^3$ we have

$$\psi(\tau) = A_r \cos \bar{\sigma} \tau, \quad (1.16)$$

where
$$A_r = \mu_0 - \frac{1}{2} \mu_2 \tau^2 = \psi_0 (1 - \frac{1}{2} \bar{\sigma}^2 \tau^2 \delta^2). \quad (1.17)$$

In other words, the correlation function then approximates to a sine wave of period $2\pi/\bar{\sigma}$ and of slowly varying amplitude A_r .

It has been mentioned that the distribution of f is in general normal. Thus if t_1, \dots, t_n are n given values of t , and if $f(t_1) \dots f(t_n)$ are denoted for short by ξ_1, \dots, ξ_n , then the joint-probability density of $\xi_1 \dots \xi_n$ is of the form

$$p(\xi_1, \dots, \xi_n) = \frac{1}{(2\pi)^{n/2} \Delta_n^{1/2}} \exp \left[-\frac{1}{2} \sum_{i,j} M_{ij} \xi_i \xi_j \right]. \quad (1.18)$$

In this expression the matrix (M_{ij}) is the inverse of the matrix of mean values (Ξ_{ij}) , given by

$$\Xi_{ij} = \overline{\xi_i \xi_j} = \overline{f(t_i) f(t_j)} = \psi(t_i - t_j) = \psi_{ij}, \quad (1.19)$$

say; and

$$\Delta_n = |(\psi_{ij})| = |(M_{ij})|^{-1}. \quad (1.20)$$

It may be shown that (M_{ij}) is positive-definite (see, for example, Longuet-Higgins 1957).

2. A RELATION FOR $p(\tau)$

Our method depends upon the following lemma: let $U(\tau)$ denote the probability that f is positive over an arbitrary time-interval of length τ ; then the distribution of the intervals between successive zeros is given by

$$p(\tau) = \frac{2}{N_0} \frac{d^2 U}{d\tau^2}, \quad (2.1)$$

where N_0 denotes the average number of zero crossings per unit time (equation (0.1)).

To prove this, let t' , t'' be any two instants of time separated by an interval $\tau = t'' - t'$. Then we have

$$U(t'' - t') = \text{prob} \{f > 0 \text{ at all points in } (t', t'')\}. \quad (2.2)$$

Now let

$$V(t'' - t') dt'' = \text{prob} \left\{ \begin{array}{l} f > 0 \quad \text{at all points in } (t', t'') \\ f = 0 \quad \text{at some point in } (t'', t'' + dt'') \end{array} \right\} \quad (2.3)$$

then

$$U(t'' - t') = U(t'' + dt'' - t') + V(t'' - t') dt'', \quad (2.4)$$

for the possibilities represented in the right-hand side are mutually exclusive and together exhaust the possibilities represented on the left-hand side. Taking the limit as dt'' tends to zero we have

$$V(t'' - t') = -\frac{\partial}{\partial t''} U(t'' - t'). \quad (2.5)$$

Similarly, if we define

$$W(t'' - t') dt' dt'' = \text{prob} \left\{ \begin{array}{l} f = 0 \quad \text{at some point in } (t', t' + dt') \\ f > 0 \quad \text{at all points in } (t' + dt', t'') \\ f = 0 \quad \text{at some point in } (t'', t'' + dt'') \end{array} \right\}, \quad (2.6)$$

we have

$$V(t'' - t' - dt') = V(t'' - t') + W(t'' - t') dt' \quad (2.7)$$

and so

$$W(t'' - t') = \frac{\partial}{\partial t'} V(t'' - t'), \quad (2.8)$$

or

$$W(t'' - t') = -\frac{\partial^2}{\partial t' \partial t''} U(t'' - t'). \quad (2.9)$$

Now $p(t'' - t') dt''$ is, by definition, the probability that $f > 0$ at all points in (t', t'') and that $f = 0$ at some point in $(t'', t'' + dt'')$, given that t' is an up-crossing of f , or alternatively given that there is an up-crossing at some point in $(t', t' + dt')$, no matter where. (The probability of two or more zero-crossings in $(t', t' + dt')$ becomes

negligible as $dt' \rightarrow 0$.) But the prior probability of an up-crossing in $(t', t' + dt')$ is $\frac{1}{2}N_0 dt'$. Hence, by the rule of inverse probabilities,

$$p(t'' - t') dt'' = \frac{W(t'' - t') dt' dt''}{\frac{1}{2}N_0 dt'}, \tag{2.10}$$

giving

$$p(t'' - t') = -\frac{2}{N_0} \frac{\partial^2}{\partial t' \partial t''} U(t'' - t'). \tag{2.11}$$

On substituting $t'' - t' = \tau$, we have the relation (2.1).

The relation is proved, in the first place, only when τ denotes the interval between an up-crossing and the next down-crossing. But since $f(t)$ is symmetrical about zero, the relation holds also for the interval between a down-crossing and the next up-crossing, and so when τ denotes the interval between any two successive zeros.

The relation between $p(\tau)$ and $U(\tau)$ is sketched in figure 1, assuming a fairly narrow spectrum. $U(\tau)$ is always a positive function, tending to zero at infinity. Also, since there is an even chance that in any given small interval of time f will be positive we have $U(0) = \frac{1}{2}$. At the origin $p(\tau)$ vanishes (as will be shown), and has a finite gradient. Hence the curvature of $U(\tau)$ is zero at the origin.

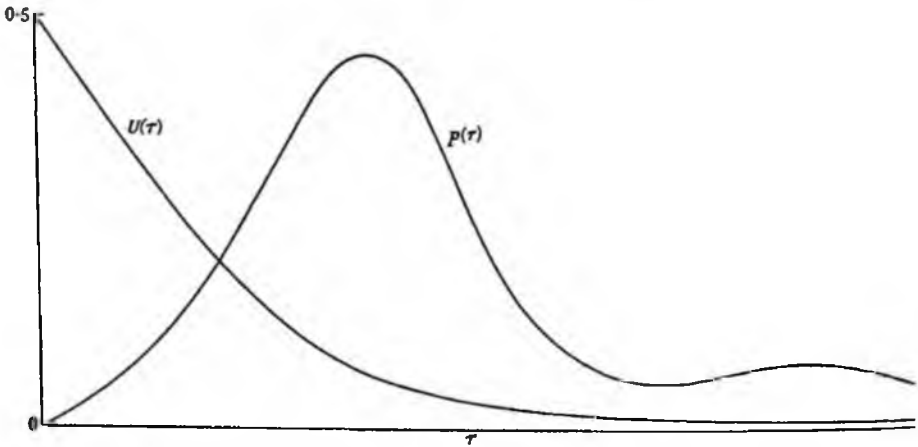


FIGURE 1. The relation between $p(\tau)$ and $U(\tau)$ for a typical random function.

Since $p(\tau)$ can never be negative it is clear from (2.1) that the curvature of $U(\tau)$ is always positive or zero.

3. AN EXPRESSION FOR $U(\tau)$

By the preceding lemma our problem is now reduced to the evaluation of $U(\tau)$.

Taking n points t_1, t_2, \dots, t_n between t' and t'' , with $t_1 = t'$ and $t_n = t''$, let

$$U_n(t_1, \dots, t_n) = \text{prob}\{f(t_1) > 0, \dots, f(t_n) > 0\}. \tag{3.1}$$

Then if n tends to infinity in such a way that the largest interval between the points tends to zero it is reasonable to assume (if $f(t)$ is continuous) that

$$\lim_{n \rightarrow \infty} U_n(t_1, \dots, t_n) = U(t'' - t'). \tag{3.2}$$

104

M. S. Longuet-Higgins

An expression for U_n may be written down immediately. For

$$U_n = \int_0^\infty \dots \int_0^\infty p(\xi_1, \dots, \xi_n) d\xi_1 \dots d\xi_n, \quad (3.3)$$

where ξ_i denotes $f(t_i)$. So from equation (1.18)

$$U_n = \frac{|(M_{ij})|^{\frac{1}{2}}}{(2\pi)^{\frac{1}{2}n}} \int_0^\infty \dots \int_0^\infty \exp[-\frac{1}{2} \sum_{ij} M_{ij} \xi_i \xi_j] d\xi_1 \dots d\xi_n. \quad (3.4)$$

Since (M_{ij}) is positive-definite we may, by a real linear substitution

$$\xi_i = \sum_{j=1}^n a_{ij} \eta_j, \quad (3.5)$$

transform the integral into the form

$$U_n = \frac{1}{(2\pi)^{\frac{1}{2}n}} \int_V \dots \int_V \exp[-\frac{1}{2}(\eta_1^2 + \dots + \eta_n^2)] d\eta_1 \dots d\eta_n, \quad (3.6)$$

where V denotes the solid angle

$$\sum_{j=1}^n a_{ij} \eta_j \geq 0. \quad (3.7)$$

This in turn may be written

$$U_n = \frac{1}{(2\pi)^{\frac{1}{2}n}} \int_0^\infty \exp[-\frac{1}{2}r^2] r^{n-1} dr S_n, \quad (3.8)$$

where $r^2 = \eta_1^2 + \dots + \eta_n^2$ and S_n (or S) is the region of the unit hypersphere

$$\eta_1^2 + \dots + \eta_n^2 = 1$$

bounded by the hyperplanes $\sum a_{ij} \eta_j = 0$. Integration with respect to r gives

$$U_n = \frac{(\frac{1}{2}n-1)!}{2\pi^{\frac{1}{2}n}} S_n. \quad (3.9)$$

4. PROPERTIES OF S_n

When $n = 2$ or 3 , S_n denotes the angle contained by two straight lines, or the solid angle contained by three given planes, respectively. For general values of n , S_n is obviously a function of the $\frac{1}{2}n(n-1)$ angles between the n bounding hyperplanes of (3.7). Denoting the *interior* angle between the i th and j th hyperplanes by θ_{ij} we have

$$\cos \theta_{ij} = - \frac{\sum_k a_{ik} a_{kj}}{(\sum_k a_{ik}^2)^{\frac{1}{2}} (\sum_k a_{kj}^2)^{\frac{1}{2}}} = - \frac{\psi_{ij}}{(\psi_{ii} \psi_{jj})^{\frac{1}{2}}} \quad (4.1)$$

and so

$$\theta_{ij} = \cos^{-1}(-\psi_{ij}/\psi_0) \quad (0 \leq \theta_{ij} \leq \pi). \quad (4.2)$$

In the case $n = 2$,

$$S_n = S_2 = \theta_{12} \quad (4.3)$$

and when $n = 3$ the well-known formula for the area of a spherical triangle gives

$$S_n = S_3 = \theta_{23} + \theta_{31} + \theta_{12} - \pi. \quad (4.4)$$

Schlaefli (1858) has shown that in general S_n may be expressed in terms of functions of the type $S_{n-1}, S_{n-2}, \dots, S_2$ whenever n is odd, but not when n is even. There is in fact no reduction formula for S_n which is valid for all integral values of n , although for particular values of the angles θ_{ij} it is sometimes possible to express S_n in finite terms (see Schlaefli 1860; Coxeter 1935; Anis & Lloyd 1953).

However, there exists a fundamental differential relation, first proved by Schlaefli (1858; see also Plackett 1954), namely

$$\frac{\partial S_n}{\partial \theta_{pq}} = \frac{1}{n-2} S^{(pq)} \quad (n \geq 4), \tag{4.5}$$

where $S^{(pq)}$ denotes the simplex S_{n-2} corresponding to the $(n-2) \times (n-2)$ matrix $M_{ij}^{(pq)}$ which is derived from (M_{ij}) by deleting the p th and q th rows and columns.

The relation (4.5) reduces the number of consecutive integrations to be performed in evaluating S_n to $\frac{1}{2}n$ or $\frac{1}{2}(n-1)$ according as n is even or odd. S_2 involves essentially one integration since

$$\theta_{12} = \cos^{-1}(-\psi_{12}/\psi_0) = \int_{-\psi_{12}/\psi_0}^1 \frac{dx}{(1-x^2)^{\frac{1}{2}}}. \tag{4.6}$$

We shall make frequent use of (4.5) in the following work.

From the definition of $S^{(pq)}$ it will be seen that the (r, s) th angle of $S^{(pq)}$ is given by

$$\cos \theta_{rs}^{(pq)} = - \frac{\begin{vmatrix} p & q & r \\ p & q & s \end{vmatrix}}{\begin{vmatrix} p & q & r \\ p & q & r \end{vmatrix} \begin{vmatrix} p & q & s \\ p & q & s \end{vmatrix}^{\frac{1}{2}}} \quad (0 \leq \theta_{rs}^{(pq)} \leq \pi), \tag{4.7}$$

where $\begin{vmatrix} p & q & r \\ p & q & s \end{vmatrix}$ denotes the 3×3 determinant

$$\begin{vmatrix} p & q & r \\ p & q & s \end{vmatrix} = \begin{vmatrix} \psi_{pp} & \psi_{pq} & \psi_{ps} \\ \psi_{qp} & \psi_{qq} & \psi_{qs} \\ \psi_{rp} & \psi_{rq} & \psi_{rs} \end{vmatrix}. \tag{4.8}$$

5. APPROXIMATING TO $p(\tau)$

From (2.1) and (2.11) it follows that

$$p(t'' - t') = - \frac{2}{N_0} \frac{\partial^2}{\partial t_1 \partial t_n} \lim_{n \rightarrow \infty} U_n(t_1 \dots t_n) \tag{5.1}$$

or
$$p(\tau) = \frac{2}{N_0} \frac{d^2}{d\tau^2} \lim_{n \rightarrow \infty} U_n(t_1 \dots t_n). \tag{5.2}$$

Assuming that the order of differentiation and of letting n tend to infinity may be reversed, we have either

$$p(\tau) = \lim_{n \rightarrow \infty} p_n(\tau), \tag{5.3}$$

or
$$p(\tau) = \lim_{n \rightarrow \infty} p_n^*(\tau), \tag{5.4}$$

where
$$p_n(\tau) = - \frac{2}{N_0} \frac{\partial^2}{\partial t_1 \partial t_n} U_n(t_1 \dots t_n) \tag{5.5}$$

and
$$p_n^*(\tau) = \frac{2}{N_0} \frac{d^2}{d\tau^2} U_n(t_1 \dots t_n). \tag{5.6}$$

We have therefore two alternative approximations to $p(\tau)$, namely $p_n(\tau)$ and $p_n^*(\tau)$. In the first of these, $U_n(t_1, \dots, t_n)$ is differentiated partially with respect to t_1 and t_n only, t_2, \dots, t_{n-1} being kept constant. In the second, each of $t_1 \dots t_n$ is considered to be a function of τ , and in fact the most natural assumption is that the t_i are all equally spaced:

$$t_i = \frac{i\tau}{n-1}. \quad (5.7)$$

Differentiation with respect to τ then involves all the points.

We shall examine both types of approximation and compare their merits.

6. $p_n(\tau)$

From (5.5), (3.9) and (0.1) we have

$$p_n(\tau) = -\frac{(\frac{1}{2}n-1)!}{\pi^{\frac{1}{2}n-1}} \left(\frac{\psi_0}{-\psi_0''}\right)^{\frac{1}{2}} \frac{\partial^2 S_n}{\partial t_1 \partial t_n}. \quad (6.1)$$

The first interesting case is $n = 3$. Substituting from (4.4) we have

$$p_3(\tau) = -\frac{1}{2} \left(\frac{\psi_0}{-\psi_0''}\right)^{\frac{1}{2}} \frac{\partial^2}{\partial t_1 \partial t_3} (\theta_{23} + \theta_{31} + \theta_{12} - \pi). \quad (6.2)$$

Since θ_{ij} depends only on t_i and t_j and since

$$\theta_{13} = \cos^{-1} \left(\frac{-\psi_{13}}{\psi_0}\right) = \cos^{-1} \left(\frac{-\psi_\tau}{\psi_0}\right), \quad (6.3)$$

it follows that

$$p_3(\tau) = \frac{1}{2} \left(\frac{\psi_0}{-\psi_0''}\right)^{\frac{1}{2}} \frac{d^2}{d\tau^2} \cos^{-1} \left(\frac{-\psi_\tau}{\psi_0}\right). \quad (6.4)$$

On performing the differentiation we have

$$p_3(\tau) = \frac{1}{2} \left(\frac{\psi_0}{-\psi_0''}\right)^{\frac{1}{2}} \frac{d}{d\tau} \frac{\psi_\tau'}{(\psi_0^2 - \psi_\tau^2)^{\frac{1}{2}}} \quad (6.5)$$

$$= \frac{1}{2} \left(\frac{\psi_0}{-\psi_0''}\right)^{\frac{1}{2}} \frac{\psi_\tau''(\psi_0^2 - \psi_\tau^2) - \psi_\tau \psi_\tau'^2}{(\psi_0^2 - \psi_\tau^2)^{\frac{3}{2}}}. \quad (6.6)$$

It will be noticed that this distribution is quite independent of the choice of the middle ordinate t_2 . We now examine some of the properties of the distribution.

Small values of τ . By straightforward expansion of ψ in powers of τ we find

$$p_3(\tau) = \frac{1}{8} \frac{\psi_0 \psi_0^{4\tau} - \psi_0^{2\tau}}{-\psi_0 \psi_0''} \tau + O(\tau^3). \quad (6.7)$$

Thus p_3 vanishes when $\tau = 0$, and the gradient there is

$$\left(\frac{dp_3}{d\tau}\right)_{\tau=0} = \frac{1}{8} \frac{\psi_0 \psi_0^{4\tau} - \psi_0^{2\tau}}{-\psi_0 \psi_0''}. \quad (6.8)$$

This agrees with Rice's approximation (1945, p. 59). Now from (1.8) and (1.3) we have

$$\psi_0 \psi_0^{4\tau} - \psi_0^{2\tau} = m_0 m_4 - m_2^2 \quad (6.9)$$

$$= \frac{1}{2} \int_0^\infty \int_0^\infty E(\sigma_1) E(\sigma_2) (\sigma_1^2 - \sigma_2^2)^2 d\sigma_1 d\sigma_2 \quad (6.10)$$

$$= \frac{1}{2} \int_0^\infty \int_0^\infty E(\sigma_1) E(\sigma_2) (\sigma_1 + \sigma_2)^2 (\sigma_1 - \sigma_2)^2 d\sigma_1 d\sigma_2, \quad (6.11)$$

showing that, when the spectrum is narrow, the above quantity is almost proportional to δ^2 , the variance of the spectrum (cf. (1.13)). Hence, the narrower the spectrum the smaller is the gradient at the origin.

In general, the gradient at the origin is closely related to the parameter ϵ^2 defined by

$$\epsilon^2 = \frac{m_0 m_4 - m_2^2}{m_0 m_4} \quad (6.12)$$

(see Cartwright & Longuet-Higgins 1956). In fact

$$\left(\frac{dp_3}{d\tau}\right)_{\tau=0} = \frac{1}{8} \frac{m_0 m_4 - m_2^2}{m_0 m_2} = \frac{1}{8} \pi^2 N_0^2 \frac{\epsilon^2}{1 - \epsilon^2} \quad (6.13)$$

(where N_0 denotes the number of zero-crossings per unit time. It is shown, in the paper just referred to, that ϵ lies between 0 and 1, and its exact value, together with the value of m_0 , determines the statistical distribution of the heights of the maxima of $f(t)$).

A narrow spectrum. We have seen in § 1 that for a narrow spectrum

$$\psi_\tau = \psi_0(1 - \frac{1}{2}\delta^2\bar{\sigma}^2\tau^2) \cos \bar{\sigma}\tau + O(\delta^3\bar{\sigma}^4\tau^4). \quad (6.14)$$

It follows that

$$\psi'_0 = -\psi_0\bar{\sigma}^2(1 + \delta^2) \quad (6.15)$$

and therefore, from (0.1),

$$N_0 = \frac{\bar{\sigma}}{\pi}(1 + \delta^2)^{\frac{1}{2}}. \quad (6.16)$$

The mean interval $\bar{\tau}$ is therefore given by

$$\bar{\tau} = \frac{1}{N_0} \doteq \frac{\pi}{\bar{\sigma}}, \quad (6.17)$$

neglecting δ^2 . In the neighbourhood of this mean interval let us write

$$\bar{\sigma}\tau = \pi + \eta, \quad (6.18)$$

where η is of order δ . Then from (6.14) we have

$$\psi_\tau = \psi_0[1 - \frac{1}{2}(\eta^2 + \pi^2\delta^2)] + O(\delta^3) \quad (6.19)$$

and so (6.7) becomes

$$p_3(\tau) \doteq \frac{1}{2\bar{\tau}\delta} \frac{1}{(1 + \eta^2/\pi^2\delta^2)^{\frac{1}{2}}} \quad (6.20)$$

(terms of order δ^2 are neglected). This expression is equivalent to the expression obtained by Rice (1945, p. 63) for a narrow spectrum and also to the results found by two independent methods (Longuet-Higgins 1957, § 2.10 and 1958). The distribution is symmetrical, about $\eta = 0$ or $\tau = \pi/\bar{\sigma}$, and it diminishes like $(\eta^2 + \pi^2\delta^2)^{-\frac{1}{2}}$.

Large values of τ . Assuming that ψ_τ and its derivatives tend to zero at infinity, we have

$$p_3(\tau) \rightarrow 0 \quad (\tau \rightarrow \infty), \quad (6.21)$$

unlike Rice's approximation, which tends to a positive value (1954, p. 60). However, neither approximation can be considered valid when τ is large.

In fact, $p_n(\tau)$ cannot be expected to give a good approximation to $p(\tau)$ when τ is greater than about $(n-1)\bar{\tau}$; for U_n is only an approximation to U provided that the

probability of f being negative between two positive ordinates ξ_i, ξ_{i+1} can be neglected; and this is not so when $(t_{i+1} - t_i)$ is greater than $\bar{\tau}$.

Therefore we shall not be surprised to find $p_3(\tau)$ becoming erratic or even negative when τ is greater than about $2\bar{\tau}$.

Higher approximations

Returning to the general formula for p_n (equation (6.1)) we see that, since S_n is a function of the angles θ_{ij} ,

$$\frac{\partial S}{\partial t_1} = \sum_{i < j} \frac{\partial S}{\partial \theta_{ij}} \frac{\partial \theta_{ij}}{\partial t_1}. \quad (6.22)$$

Since θ_{ij} is a function of $(t_i - t_j)$ only, the above reduces to

$$\frac{\partial S}{\partial t_1} = \sum_{j=2}^n \frac{\partial S}{\partial \theta_{1j}} \frac{\partial \theta_{1j}}{\partial t_1}, \quad (6.23)$$

or

$$\frac{\partial S}{\partial t_1} = \frac{1}{n-2} \sum_{j=2}^n S^{(1j)} \frac{\partial \theta_{1j}}{\partial t_1}, \quad (6.24)$$

by (4.5). Hence

$$\frac{\partial^2 S}{\partial t_1 \partial t_n} = \frac{1}{n-2} S^{(1n)} \frac{\partial \theta_{1n}}{\partial t_1 \partial t_n} + \frac{1}{n-2} \sum_{j=2}^n \frac{\partial S^{(1j)}}{\partial t_n} \frac{\partial \theta_{1j}}{\partial t_1} \quad (6.25)$$

and so, from (6.1),

$$p_n(\tau) = \frac{(\frac{1}{2}n-2)!}{\pi^{\frac{1}{2}n-1}} S^{(1n)} p_3(\tau) - \frac{(\frac{1}{2}n-2)!}{2\pi^{\frac{1}{2}n-1}} \left(\frac{\psi_0}{-\psi_0} \right)^{\frac{1}{2}} \sum_{j=2}^n \frac{\partial S^{(1j)}}{\partial t_n} \frac{\partial \theta_{1j}}{\partial t_1}. \quad (6.26)$$

When τ is small it can be shown (see the appendix) that the dihedral angles $\theta_{ij}^{(1n)}$ of the spherical simplex $S^{(1n)}$ all approach π ; hence $S^{(1n)}$ approaches half the content of a hypersphere in $(n-2)$ dimensions, that is

$$S^{(1n)} = \frac{\pi^{\frac{1}{2}n-1}}{(\frac{1}{2}n-2)!} + O(\tau). \quad (6.27)$$

Thus the first term on the right of (6.26) becomes

$$p_3(\tau) + O(\tau^2) \quad (6.28)$$

(since p_3 itself is $O(\tau)$ at the origin). In the second group of terms we have

$$\frac{\partial \theta_{1j}}{\partial t_1} = - \frac{\psi'_{1j}}{(\psi_0^2 - \psi_{1j}^2)^{\frac{1}{2}}} = \left(\frac{-\psi_0''}{\psi_0} \right)^{\frac{1}{2}} + O(\tau^2) \quad (6.29)$$

and so

$$\sum_{j=2}^n \frac{\partial S^{(1j)}}{\partial t_n} \frac{\partial \theta_{1j}}{\partial t_1} = \left(\frac{-\psi_0''}{\psi_0} \right)^{\frac{1}{2}} \sum_{j=2}^n \frac{\partial S^{(1j)}}{\partial t_n} + O(\tau^2). \quad (6.30)$$

It is shown in the appendix that

$$\sum_{j=2}^n \frac{\partial S^{(1j)}}{\partial t_n} = O(\tau^2) \quad (6.31)$$

and so finally

$$p_n(\tau) = p_3(\tau) + O(\tau^2), \quad (6.32)$$

from which we conclude that $p_3(\tau)$ has both the correct value and the correct gradient at the origin.†

† Also the correct curvature. For $p_n(\tau)$ involves only odd powers of τ , all coefficients of even powers being zero.

We saw in §4 that S_n can be evaluated in terms of known functions up to and including $n = 3$. Since $S^{(2)}$ is of degree $(n-2)$, it follows from (6.26) that $p_n(\tau)$ may be evaluated as far as $n = 5$.

Thus for $n = 4$, for example, we find

$$p_4(\tau) = \frac{\gamma}{\pi} p_3(\tau) - \frac{1}{2\pi} \left(\frac{\psi_0}{-\psi_0'} \right)^{\frac{1}{2}} \left[\frac{\partial \alpha \partial \theta_{12}}{\partial t_4 \partial t_1} + \frac{\partial \beta \partial \theta_{13}}{\partial t_4 \partial t_1} + \frac{\partial \gamma \partial \theta_{14}}{\partial t_4 \partial t_1} \right], \quad (6.33)$$

$$\left. \begin{aligned} \text{where } \alpha &= \theta_{34}^{(10)} = \cos^{-1} \left[- \left(1 \ 2 \ 3 \right) / \sqrt{\left(\left(1 \ 2 \ 3 \right) \left(1 \ 2 \ 4 \right) \right)} \right], \\ \beta &= \theta_{24}^{(13)} = \cos^{-1} \left[- \left(1 \ 3 \ 2 \right) / \sqrt{\left(\left(1 \ 3 \ 2 \right) \left(1 \ 3 \ 4 \right) \right)} \right], \\ \gamma &= \theta_{23}^{(14)} = \cos^{-1} \left[- \left(1 \ 4 \ 2 \right) / \sqrt{\left(\left(1 \ 4 \ 2 \right) \left(1 \ 4 \ 3 \right) \right)} \right]. \end{aligned} \right\} \quad (6.34)$$

In carrying through the computation certain relations between the determinants $\begin{pmatrix} p & q & r \\ & & s \end{pmatrix}$ are found useful. These arise from the fact that each determinant depends only on the correlations $\psi_{pq}, \psi_{ps}, \dots$ and therefore on the magnitudes $|p-q|, |p-s|, \dots$. Thus we have

$$\begin{pmatrix} p & q & r \\ & & s \end{pmatrix} = \begin{pmatrix} q & p & r \\ & & s \end{pmatrix} = \begin{pmatrix} p & q & s \\ & & r \end{pmatrix} \quad (6.35)$$

and

$$\begin{pmatrix} p & q & r \\ & & r \end{pmatrix} = \begin{pmatrix} p & r & q \\ & & q \end{pmatrix} = \begin{pmatrix} r & q & p \\ & & p \end{pmatrix}. \quad (6.36)$$

If, for convenience, the points t_i are equally spaced at intervals of $\tau/(n-1)$ apart, we also have relations such as

$$\begin{pmatrix} p & q & r \\ & & s \end{pmatrix} = \begin{pmatrix} p+1 & q+1 & r+1 \\ & & s+1 \end{pmatrix} = \begin{pmatrix} n-p & n-q & n-r \\ & & n-s \end{pmatrix} \quad (6.37)$$

which greatly reduce the number of quantities to be calculated.

The computation of p_n for $n = 3, 4, 5$ has been carried through for the case of a low-pass spectrum:

$$E(\sigma) = \begin{cases} 1 & (0 < \sigma < 1), \\ 0 & (1 < \sigma). \end{cases} \quad (6.38)$$

The correlation function in this case assumes the simple form

$$\frac{\psi_\tau}{\psi_0} = \frac{\sin \tau}{\tau}. \quad (6.39)$$

The results for p_n are shown in figure 2. It will be seen that p_3, p_4 and p_5 all lie very close together up to about $\tau = 3.5$, suggesting that the third approximation is accurate up to this point. In fact the numerical results show that $(p_4 - p_3)$ and $(p_5 - p_4)$ both behave like τ^5 near the origin, so that p_3 is very probably correct as far as the term in τ^4 .

As we should expect, p_3 begins to differ appreciably from the next two approximations when τ exceeds π , that is, half the cut-off period 2π . When $\tau > 6$, p_3 becomes

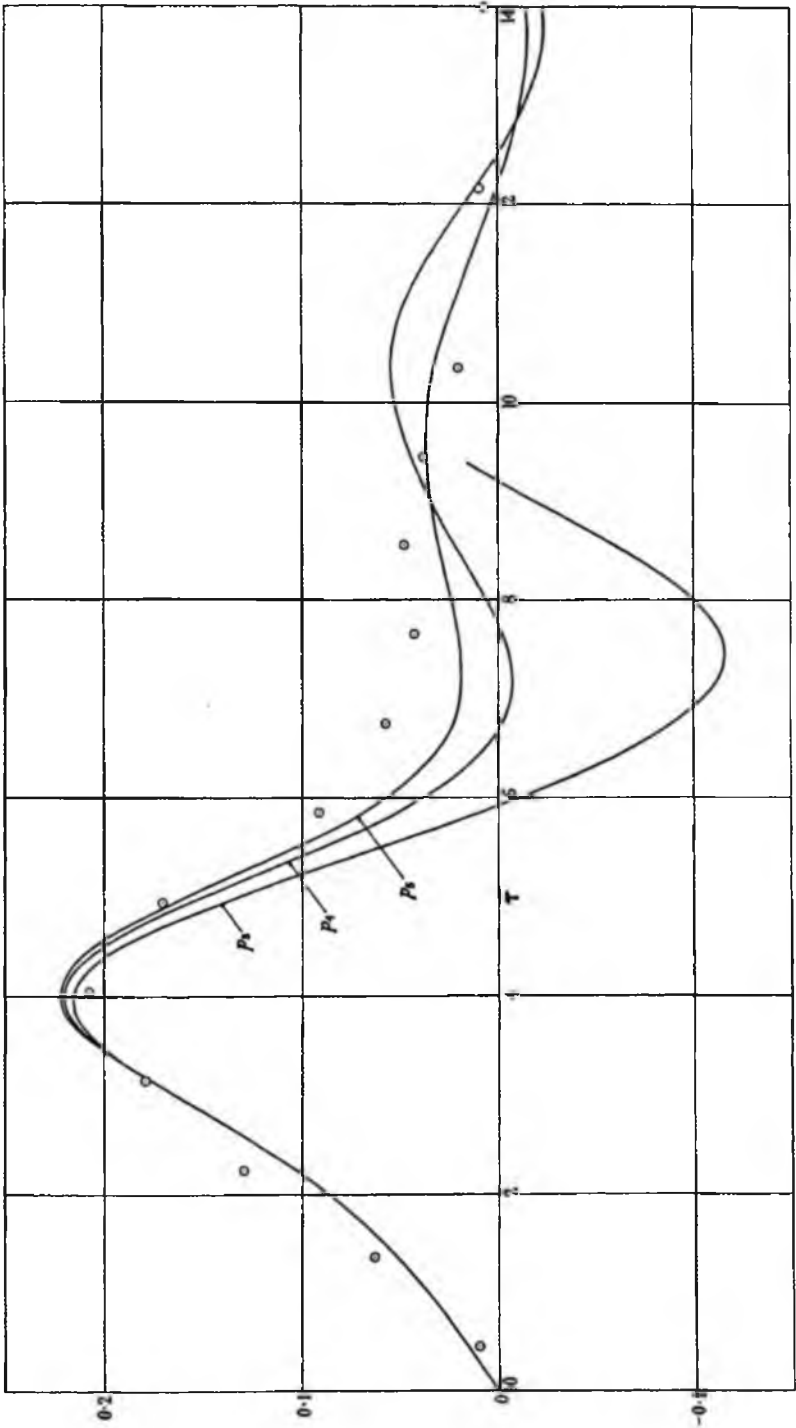


FIGURE 2. Graphs of $p_1(\tau)$, $p_2(\tau)$ and $p_3(\tau)$ for a low-pass spectrum with out-off period 2π . Experimental data (O) are shown for comparison.

negative, which is of course impossible. p_4 also becomes negative at about $\tau = 7.3$, though to a lesser extent. However, p_5 is positive until $\tau = 12.5$ and shows the interesting phenomenon of a second maximum at about $\tau = 10$, also observed experimentally. The observations of Campbell quoted by Rice are also shown in the figure. It should be borne in mind that in the observational material the cut-off frequency was not well defined, and that this has probably affected the position of the two maxima; the presence of any additional energy beyond the theoretical cut-off frequency might be expected to increase the number of short intervals in the distribution and so to shift both observed maxima towards the left. The theoretical cut-off frequency was chosen so that the first maximum of ψ_τ coincided with the observed maximum, but the correct position of the second maximum is somewhat uncertain.

7. $p_n^*(\tau)$

From equations (5.6) we have in general

$$p_n^*(\tau) = \frac{(\frac{1}{2}n-1)!}{\pi^{\frac{1}{2}n-1}} \left(\frac{\psi_0}{-\psi_0'} \right)^{\frac{1}{2}} \frac{d^2 S_n}{d\tau^2}. \quad (7.1)$$

When $n = 3$ this becomes

$$p_3^*(\tau) = \frac{1}{2} \left(\frac{\psi_0}{-\psi_0'} \right)^{\frac{1}{2}} \frac{d^2}{d\tau^2} (\theta_{23} + \theta_{31} + \theta_{13} - \pi). \quad (7.2)$$

In contrast to the previous case, all three angles θ_{23} , θ_{31} , θ_{13} make non-zero contributions. Supposing that the points t_1 , t_2 , t_3 are equally spaced, then $t_2 - t_1$ and $t_3 - t_2$ are both equal to $\frac{1}{2}\tau$ and hence

$$p_3^*(\tau) = p_3(\tau) + \frac{1}{2}p_3(\frac{1}{2}\tau), \quad (7.3)$$

where $p_3(\tau)$ is the approximation considered in § 6.

Gradient at the origin. On differentiating with respect to τ and putting $\tau = 0$ we find

$$\left(\frac{dp_3^*}{d\tau} \right)_{\tau=0} = \frac{5}{4} \left(\frac{dp_3}{d\tau} \right)_{\tau=0}. \quad (7.4)$$

Therefore, the gradient of p_3^* at the origin is not equal to the true gradient, but exceeds it by 25%.

A narrow spectrum. On making the same approximations as before we find, when τ is in the neighbourhood of $\bar{\tau}$, that $p_3(\frac{1}{2}\tau)$ is small; hence

$$p_3^*(\tau) \doteq p_3(\tau) \quad (7.5)$$

and the approximations have the same limiting form for a narrow spectrum.

At infinity, p_3^* like p_3 tends to zero.

Computation of p_3^* for a low-pass spectrum shows (figure 3) that although the approximation is not so good as p_3 near the origin, yet it is somewhat better for values of τ greater than about 4.

Higher approximations of the same type may be obtained by computing

$$\frac{dS_n}{d\tau} = \sum_{i < j} \frac{\partial S}{\partial \theta_{ij}} \frac{d\theta_{ij}}{d\tau} = \frac{1}{n-2} \sum_{i < j} S^{(ij)} \frac{-\psi'_{ij}}{(\psi_0^2 - \psi_{ij}^2)^{\frac{1}{2}}} \quad (7.6)$$

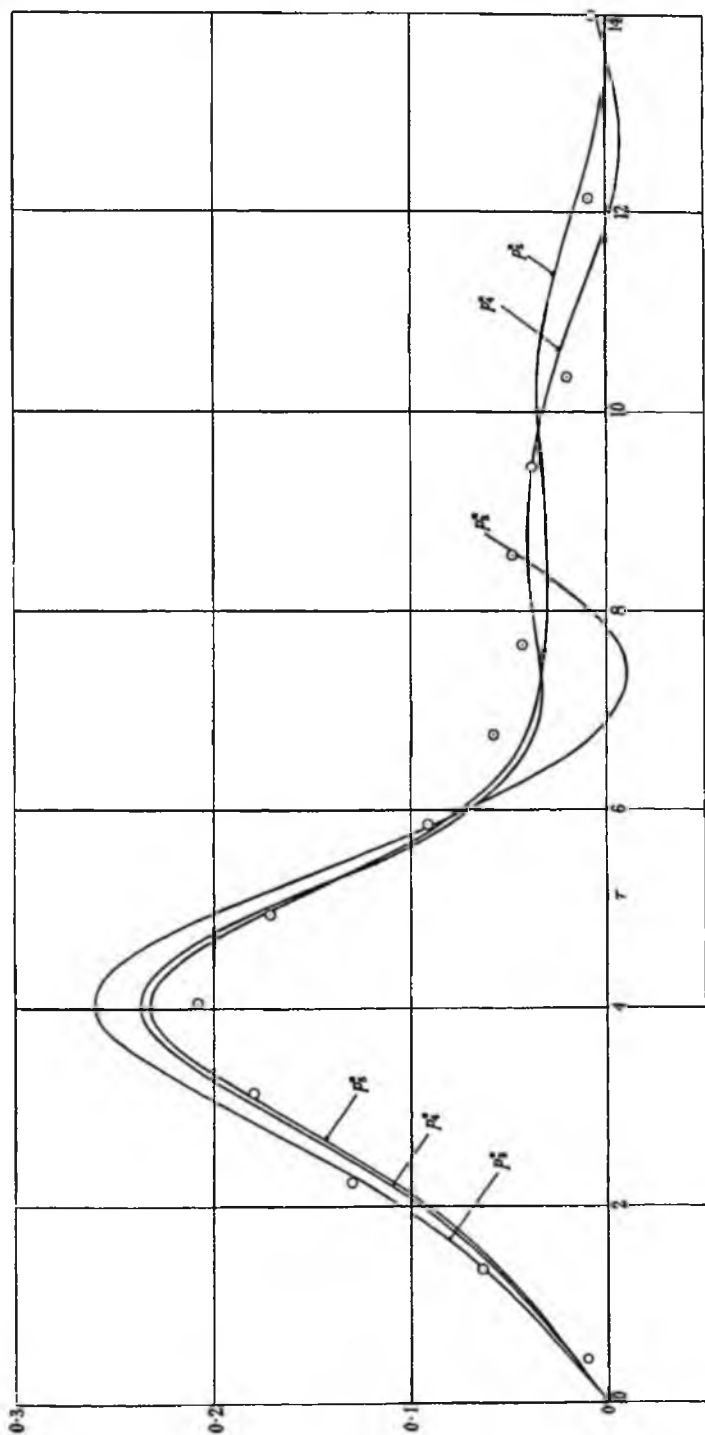


FIGURE 3. Graphs of $p_1^2(\tau)$, $p_2^2(\tau)$ and $p_3^2(\tau)$ for the same spectrum as in figure 2 (and with the same experimental data).

at regular intervals of τ and then differentiating numerically in equation (7.1). Since $S^{(n)}$ is of degree $n - 2$, this may be done up to and including $n = 5$.

The above procedure was carried out for a low-pass spectrum (given by (6.38)) and the results are shown in figure 3. It will be seen that the gradient of p_4^* and p_5^* at the origin differs from the gradient of p_3^* , and all in fact differ from the correct gradient. On the other hand, none of the approximations p_n^* becomes as negative as the corresponding approximation p_n , and from the observed points (which are the same as in figure 2) it appears that, for the larger values of τ , p_n^* is somewhat more accurate than p_n .

8. CONCLUSIONS

Two sequences of approximations to $p(\tau)$ have been derived, namely $p_n(\tau)$ and $p_n^*(\tau)$. Of these, the sequence $p_n(\tau)$ is the better approximation near the origin. Indeed the third approximation $p_3(\tau)$ is remarkably accurate over the lower half of the distribution, so that we have

$$p(\tau) \doteq \frac{1}{2\pi N_0} \frac{d^2}{d\tau^2} \cos^{-1} \left(\frac{-\psi_\tau}{\psi_0} \right) \quad (\tau \leq \tau_m), \tag{8.1}$$

where τ_m denotes the median value of τ . The alternative sequence $p_n^*(\tau)$, however, appears to be more accurate for larger values of τ , and for a low-pass spectrum p_4^* and p_5^* give secondary maxima in accordance with observation. Both types of approximation tend to the correct form when the spectrum becomes narrow.

To compute higher approximations it would be necessary to carry out numerically some further steps of integration; though rather long, this might be done on the lines suggested by Plackett (1954).

From equation (8.1) some simple conclusions may be drawn. On integrating from the limit $\tau = 0$ (that is to say over the range of τ for which the approximation is most accurate) we have

$$\int_0^\tau p(\tau) d\tau \doteq \frac{1}{2\pi N_0} \left[\frac{d}{d\tau} \cos^{-1} \left(\frac{-\psi_\tau}{\psi_0} \right) \right]_0^\tau. \tag{8.2}$$

The expression on the right, evaluated at $\tau = 0$, is

$$\lim_{\tau \rightarrow 0} \frac{\psi'_\tau}{(\psi_0^2 - \psi_\tau^2)^{\frac{1}{2}}} = \left(\frac{-\psi'_0}{\psi_0} \right)^{\frac{1}{2}} = \pi N_0 \tag{8.3}$$

and so

$$\frac{1}{2\pi N_0} \frac{d}{d\tau} \cos^{-1} \left(\frac{-\psi_\tau}{\psi_0} \right) \doteq \frac{1}{2} \int_0^\tau p(\tau) d\tau. \tag{8.4}$$

At the first minimum of ψ_τ , we have $\psi'_\tau = 0$, and so the left-hand side vanishes, giving

$$\int_0^{\tau_m} p(\tau) d\tau = \frac{1}{2}. \tag{8.5}$$

In other words, $\tau = \tau_m$, the median of the distribution; or *the median of $p(\tau)$ is approximately at the first minimum of the correlation function ψ_τ .*

Further, from (8.4)

$$\frac{1}{2\pi N_0} \frac{d}{d\tau} \cos^{-1} \left(\frac{\psi_\tau}{\psi_0} \right) \doteq \int_{\tau_m}^\tau p(\tau) d\tau = F(\tau), \tag{8.6}$$

where $F(\tau)$ is the distribution function of τ measured from the median. Hence

$$\psi_r/\psi_0 \doteq \cos \left[2\pi N_0 \int_0^r F(\tau) d\tau \right]. \quad (8.7)$$

This serves to give ψ_r/ψ_0 very simply in terms of $F(\tau)$, which in turn may be found from the observed distribution of τ .

Thus by measuring the distribution of intervals between zeros we have a simple Monte Carlo method to determine the correlation function ψ_r . The method is valid for values of τ less than the median of the distribution.

APPENDIX. THE BEHAVIOUR OF p_n NEAR THE ORIGIN

To prove the assertions which were made in § 6 regarding the behaviour of $p_n(\tau)$ at the origin, we must examine the nature of $S^{(n)}$ and $\Sigma \partial S^{(n)} / \partial t_n$ for small values of τ .

From (4.7) the (r, s) th angle of $S^{(n)}$ is given by

$$\cos \theta_{rs}^{(n)} = - \frac{\begin{vmatrix} \psi_{11} & & \\ & \psi_{ii} & \\ & & \psi_{rs} \end{vmatrix}}{\begin{vmatrix} \psi_{11} & & \\ & \psi_{ii} & \\ & & \psi_{rr} \end{vmatrix} \begin{vmatrix} \psi_{11} & & \\ & \psi_{ii} & \\ & & \psi_{rs} \end{vmatrix}} \quad (A 1)$$

(where for convenience only the diagonal element of each determinant is written).

Now

$$\psi_{ij} = \psi(t_i - t_j) = \psi \left(\frac{i-j}{n-1} \tau \right) \quad (A 2)$$

a function which, by hypothesis, may be expanded in even powers of τ . Thus we may apply the following lemma: If $F(x)$ is any function expansible in a power series about $x = 0$, and if $x_1, \dots, x_n, y_1, \dots, y_n$ are proportional to τ , the first term in the expansion of

$$\begin{vmatrix} F(x_1 - y_1) & F(x_1 - y_2) & \dots & F(x_1 - y_n) \\ F(x_2 - y_1) & F(x_2 - y_2) & \dots & F(x_2 - y_n) \\ \vdots & \vdots & \ddots & \vdots \\ F(x_n - y_1) & F(x_n - y_2) & \dots & F(x_n - y_n) \end{vmatrix} \quad (A 3)$$

$$\text{is } \frac{\prod_{i < j} (x_i - x_j)(y_j - y_i)}{[1! 2! \dots (n-1)!]^2} \begin{vmatrix} F(0) & F'(0) & \dots & F^{(n-1)}(0) \\ F'(0) & F''(0) & \dots & F^{(n)}(0) \\ \vdots & \vdots & \ddots & \vdots \\ F^{(n-1)}(0) & F^{(n)}(0) & \dots & F^{(2n-2)}(0) \end{vmatrix} \quad (A 4)$$

For example

$$\begin{vmatrix} \psi_{11} & & \\ & \psi_{ii} & \\ & & \psi_{rs} \end{vmatrix} \doteq \frac{1}{4} (t_1 - t_i)(t_1 - t_r)(t_i - t_r) \cdot (t_i - t_1)(t_s - t_1)(t_s - t_i) \begin{vmatrix} \psi_0 & 0 & \psi_0'' \\ 0 & \psi_0'' & 0 \\ \psi_0'' & 0 & \psi_0^{(4)} \end{vmatrix} \quad (A 5)$$

the remainder being of order τ^8 . Applying this in (A 1) we find

$$\cos \theta_{rs}^{(n)} = - \frac{(t_1 - t_r)(t_1 - t_s)(t_i - t_r)(t_i - t_s)}{(t_1 - t_r)(t_1 - t_s)(t_i - t_r)(t_i - t_s)} \quad (A 6)$$

According as i does or does not lie between r, s we have

$$\cos \theta_{rs}^{(i)} = \pm 1; \quad \theta_{rs}^{(i)} = 0 \quad \text{or} \quad \pi. \tag{A 7}$$

Hence the first of our assertions is proved.

To examine $\Sigma \partial S^{(i)} / \partial t_n$ (which we denote by Q), we have first

$$\sin^2 \theta_{rs}^{(i)} = \frac{\begin{vmatrix} \psi_{11} & & & \\ & \psi_{ii} & & \\ & & \psi_{rr} & \\ & & & \psi_{ss} \end{vmatrix} \begin{vmatrix} \psi_{11} & & & \\ & \psi_{ii} & & \\ & & \psi_{rr} & \\ & & & \psi_{ss} \end{vmatrix} - \begin{vmatrix} \psi_{11} & & & \\ & \psi_{ii} & & \\ & & \psi_{rr} & \\ & & & \psi_{rs} \end{vmatrix} \begin{vmatrix} \psi_{11} & & & \\ & \psi_{ii} & & \\ & & \psi_{rr} & \\ & & & \psi_{ss} \end{vmatrix}}{\begin{vmatrix} \psi_{11} & & & \\ & \psi_{ii} & & \\ & & \psi_{rr} & \\ & & & \psi_{ss} \end{vmatrix} \begin{vmatrix} \psi_{11} & & & \\ & \psi_{ii} & & \\ & & \psi_{rr} & \\ & & & \psi_{ss} \end{vmatrix}}. \tag{A 8}$$

By Jacobi's theorem on the minors of a determinant the numerator may be written

$$\begin{vmatrix} \psi_{11} & & & \\ & \psi_{ii} & & \\ & & \psi_{rr} & \\ & & & \psi_{ss} \end{vmatrix} \begin{vmatrix} \psi_{11} & & & \\ & \psi_{ii} & & \\ & & \psi_{rr} & \\ & & & \psi_{ss} \end{vmatrix} \tag{A 9}$$

and on using the lemma we find

$$\sin^2 \theta_{rs}^{(i)} = \frac{(t_r - t_s)^2}{9} \frac{\psi_0 \psi_0'' \psi_0^{r1} - \psi_0^{r2}}{-\psi_0'' (\psi_0 \psi_0^{r1} - \psi_0^{r2})}. \tag{A 10}$$

Since $\theta_{rs}^{(i)}$ lies between 0 and π by definition, we have, assuming $r < s$ and so $t_r < t_s$,

$$\sin \theta_{rs}^{(i)} = G(t_r - t_s), \tag{A 11}$$

where

$$G = \frac{1}{3} \left[\frac{\psi_0 (\psi_0'' \psi_0^{r1} - \psi_0^{r2})}{-\psi_0'' (\psi_0 \psi_0^{r1} - \psi_0^{r2})} \right]^{\frac{1}{2}}. \tag{A 12}$$

Hence†

$$\theta_{rs}^{(i)} = \begin{cases} G(t_s - t_r) + O(\tau^3) & (r < i < s), \\ \pi - G(t_s - t_r) + O(\tau^3) & (i < r < s). \end{cases} \tag{A 13}$$

Writing $s = n$ we have

$$\frac{\partial \theta_{rs}^{(i)}}{\partial t_n} = \begin{cases} G + O(\tau^2) & (r < i), \\ -G + O(\tau^2) & (i < r); \end{cases} \tag{A 14}$$

and writing $i = n$ (so that neither r nor $s = n$) we have

$$\frac{\partial \theta_{rs}^{(i)}}{\partial t_n} = O(\tau^2). \tag{A 15}$$

It follows from the last equation that

$$\frac{\partial S^{(i)}}{\partial t_n} = \sum_{r < s} \frac{\partial S^{(i)}}{\partial \theta_{rs}^{(i)}} \frac{\partial \theta_{rs}^{(i)}}{\partial t_n} = O(\tau^2) \tag{A 16}$$

and hence, neglecting terms of order τ^2 ,

$$Q = \sum_{j=2}^n \frac{\partial S^{(j)}}{\partial t_n} = \sum_{j=2}^{n-1} \frac{\partial S^{(j)}}{\partial t_n} = \sum_{\substack{j=2 \\ i \neq j}}^{n-1} \frac{\partial S^{(j)}}{\partial \theta_{in}^{(j)}} \frac{\partial \theta_{in}^{(j)}}{\partial t_n}. \tag{A 17}$$

† A geometrical interpretation of this result is given in another paper (in preparation).

116

M. S. Longuet-Higgins

When $n = 4$ we have simply $S^{(4)} = \theta_{24}^{(1)}$ (A 18)

and so $Q = \frac{\partial \theta_{24}^{(12)}}{\partial t_4} + \frac{\partial \theta_{24}^{(13)}}{\partial t_2} = G - G = 0$. (A 19)

When $n = 5$, we have $S^{(5)} = \theta_{kl}^{(1)} + \theta_{ks}^{(2)} + \theta_{ls}^{(3)} - \pi$, (A 20)

where i, k, l denote 2, 3, 4 in any order. Then

$$Q = \sum_{\substack{i,j=2 \\ i+j}}^4 \frac{\partial \theta_{ij}^{(2)}}{\partial t_5} = 0, \quad (\text{A 21})$$

since for every pair (i, j) with $i < j$ there is another pair (j, i) and these give contributions $\pm G$ which cancel. So again Q vanishes.

When $n \geq 6$ we have from (4.5) and (A 17)

$$Q = \frac{1}{n-4} \sum_{\substack{i,j=2 \\ i+j}}^{n-1} S^{(i+j)} \frac{\partial \theta_{in}^{(1)}}{\partial t_n} \quad (\text{A 22})$$

with an obvious notation. To show that this expression is of order τ^2 we may examine the dihedral angles $\theta_{rs}^{(i+j)}$ of $S^{(i+j)}$. These are given by

$$\cos \theta_{rs}^{(i+j)} = \frac{\begin{vmatrix} \psi_{11} & & & & \\ & \psi_{ii} & & & \\ & & \psi_{jj} & & \\ & & & \psi_{nn} & \\ & & & & \psi_{rs} \end{vmatrix}}{\begin{vmatrix} \psi_{11} & & & & \\ & \psi_{ii} & & & \\ & & \psi_{jj} & & \\ & & & \psi_{nn} & \\ & & & & \psi_{rr} \end{vmatrix}^{\frac{1}{2}} \begin{vmatrix} \psi_{11} & & & & \\ & \psi_{ii} & & & \\ & & \psi_{jj} & & \\ & & & \psi_{nn} & \\ & & & & \psi_{ss} \end{vmatrix}^{\frac{1}{2}}} \quad (\text{A 23})$$

Using the lemma, we find that when $\tau = 0$

$$\theta_{rs}^{(i+j)} = 0 \quad \text{or} \quad \pi, \quad (\text{A 24})$$

according as the pair (r, s) does, or does not, separate the pair (i, j) . Now if any one of the angles $\theta_{rs}^{(i+j)}$ vanishes, then $S^{(i+j)}$ vanishes. The only cases in which this is not possible is when i, j are consecutive, or if $(i, j) = (2, n-1)$ or $(n-1, 2)$; then $S^{(i+j)}$ equals half the surface of a hypersphere in $(n-4)$ dimensions. In all cases, interchanging i and j leaves the value of $S^{(i+j)}$ unaltered, but reverses the sign of $\partial \theta_{in}^{(1)} / \partial t_n$ and so the sum (A 22) vanishes, when $\tau = 0$. To the first order, therefore, this expression equals

$$Q = \sum_{k=1}^n Q_k t_k, \quad (\text{A 25})$$

where

$$Q_k = \frac{1}{n-4} \sum_{i,j=2}^{n-1} \frac{\partial S^{(i+j)}}{\partial t_k} \frac{\partial \theta_{in}^{(1)}}{\partial t_n} \quad (\text{A 26})$$

$$= \frac{1}{n-4} \sum_{i,j=2}^{n-1} \sum_{r < s} \frac{\partial S^{(i+j)}}{\partial \theta_{rs}^{(i+j)}} \frac{\partial \theta_{rs}^{(i+j)}}{\partial t_k} \frac{\partial \theta_{in}^{(1)}}{\partial t_n}. \quad (\text{A 27})$$

Now by considering $\sin \theta_{rs}^{(i,jn)}$ as before we find that

$$\theta_{rs}^{(i,jn)} \doteq \begin{cases} H(t_s - t_r) & \text{if } (r, s) \text{ separate } (i, j), \\ \pi - (t_s - t_r) & \text{if not;} \end{cases} \quad (A 28)$$

where H is a positive constant, and therefore

$$\left. \begin{aligned} \frac{\partial \theta_{rs}^{(i,jn)}}{\partial t_r} &\doteq \begin{cases} -H & \text{if } (r, s) \text{ separate } (i, j), \\ H & \text{if not;} \end{cases} \\ \frac{\partial \theta_{rs}^{(i,jn)}}{\partial t_s} &\doteq \begin{cases} H & \text{if } (r, s) \text{ separate } (i, j), \\ -H & \text{if not;} \end{cases} \end{aligned} \right\} \quad (A 29)$$

(terms of order τ^2 being neglected). Further

$$\frac{\partial \theta_{rs}^{(i,jn)}}{\partial t_k} = O(\tau^2) \quad (k \neq r, s). \quad (A 30)$$

When $n = 6$ we have

$$S^{(i,jn)} = \theta_{rs}^{(i,jn)} \quad (A 31)$$

and so

$$Q_k = \frac{1}{2} \sum_{i,j=2}^5 \sum_{r < s} \frac{\partial \theta_{rs}^{(i,jn)}}{\partial t_k} \frac{\partial \theta_{rs}^{(i,jn)}}{\partial t_k}. \quad (A 32)$$

Interchanging i and j has no effect in the first term, but reverses the sign of the second, and so on summation

$$Q_k = 0. \quad (A 33)$$

Similarly when $n = 7$. When $n \geq 8$ we have by (4.5)

$$Q_k = \frac{1}{(n-4)(n-6)} \sum_{i,j=2}^{n-1} \sum_{r < s} S^{(i,jrn)} \frac{\partial \theta_{rs}^{(i,jn)}}{\partial t_k} \frac{\partial \theta_{rs}^{(i,jn)}}{\partial t_k}. \quad (A 34)$$

By the same argument as before, the (p, q) th angle of $S^{(i,jrn)}$ approximates to 0 or π . The only non-zero $S^{(i,jrn)}$ are those all of whose angles are π , and these are unchanged by interchanging i and j . But $\partial \theta_{rs}^{(i,jn)} / \partial t_k$ is unaltered also, whereas $\partial \theta_{rs}^{(i,jn)} / \partial t_n$ is reversed in sign. Therefore, the terms in the summation again cancel in pairs and

$$Q_k = 0. \quad (A 35)$$

This shows that Q is of order τ^2 , as was to be proved.

I am indebted to Miss D. Greenwood and Miss D. B. Catton for assistance with the numerical computation for figures 2 and 3.

REFERENCES

Anis, A. A. & Lloyd, E. H. 1953 On the range of partial sums of a finite number of normal variates. *Biometrika*, **40**, 35-42.
 Cartwright, D. E. & Longuet-Higgins, M. S. 1956 The statistical distribution of the maxima of a random function. *Proc. Roy. Soc. A*, **237**, 212-232.
 Coxeter, H. S. M. 1935 The functions of Schlafli and Lobatschewsky. *Quart. J. Math.* **6**, 13-29.
 Kuznetsov, P. L., Statonovich, R. L. & Tikhonov, V. I. 1954 On the duration of the exceedences of a random function. *J. Tech. Phys. Moscow*, **24**, 103-112. English translation by N. R. Goodman, Scientific Paper no. 5, Eng. Stat. Group, N.Y.U. Coll. of Eng., 1956.

Longuet-Higgins, M. S. 1956 Les énergies de la mer. *C.R., IVèmes Journées de l'Hydraulique*, t. 1, pp. 118-119. La Houille Blanche, Grenoble.

Longuet-Higgins, M. S. 1957 The statistical analysis of a random, moving surface. *Phil. Trans. A*, 249, 321-287.

Plackett, R. L. 1954 A reduction formula for multivariate integrals. *Biometrika*, 41, 351-360.

Rice, S. O. 1944 The mathematical analysis of random noise. *Bell Syst. Tech. J.* 23, 282-332.

Rice, S. O. 1945 The mathematical analysis of random noise. *Bell Syst. Tech. J.* 24, 46-156.

Schlaefli, L. 1858 On the multiple integral $\int dz dy \dots dz$ whose limits are

$$p_1 = a_1x + b_1y + \dots + c_1z > 0, \quad p_2 > 0, \dots, p_n > 0 \quad \text{and} \quad x^2 + y^2 + \dots + z^2 < 1.$$

Quart. J. Pure Appl. Math. 2, 289-301.

Schlaefli, L. 1860 On the multiple integral $\int dx dy \dots dz$ whose limits are

$$p_1 = a_1x + b_1y + \dots + c_1z > 0, \quad p_2 > 0, \dots, p_n > 0 \quad \text{and} \quad x^2 + y^2 + \dots + z^2 < 1.$$

Quart. J. Pure Appl. Math. 3, 54-68 and 97-107.

Reprinted from the *Proceedings of the Cambridge Philosophical Society*,
Volume 54, Part 4, pp. 439-453, 1958.

PRINTED IN GREAT BRITAIN

THE STATISTICAL DISTRIBUTION OF THE CURVATURE OF A RANDOM GAUSSIAN SURFACE

By M. S. LONGUET-HIGGINS

Received 16 December 1957

ABSTRACT. The distribution of the total (or 'second') curvature of a stationary random Gaussian surface is derived on the assumption that the squares of the surface slopes are negligible. The distribution is found to depend on only two parameters, derivable from the fourth moments of the energy spectrum of the surface. Each distribution function satisfies a linear differential equation of the third order, and the distribution is asymmetrical with positive skewness, in general. A special case of zero skewness occurs when the surface consists of two intersecting systems of long-crested waves.

1. *Introduction.* The study of a random, Gaussian surface with a continuous energy spectrum is of interest in physics as providing a realistic model for ocean swell and for other geophysical phenomena (5), (7). Where optical properties of the sea surface are involved, it becomes important to know the statistical distribution of the total curvature at a point on the surface; for the curvature determines the relative intensity of a reflected beam of light and the size of the reflected image of a distant object (see (2), (3), (5)).

It will be recalled that there are two invariant measures of curvature for a surface, the mean curvature J , which is the sum of the principal curvatures κ_a , κ_b , and the total curvature Ω , which is the product of κ_a and κ_b . If the slope of the surface is so small that its square is negligible, then J and Ω are given by

$$\left. \begin{aligned} J &= \kappa_a + \kappa_b = \frac{\partial^2 \zeta}{\partial x^2} + \frac{\partial^2 \zeta}{\partial y^2}, \\ \Omega &= \kappa_a \kappa_b = \frac{\partial^2 \zeta}{\partial x^2} \frac{\partial^2 \zeta}{\partial y^2} - \left(\frac{\partial^2 \zeta}{\partial x \partial y} \right)^2, \end{aligned} \right\} \quad (1.1)$$

where ζ denotes the height of the surface and x , y are rectangular coordinates in a horizontal plane.

The statistical distribution of J is normal, as was remarked by Cox and Munk (3). The distribution of Ω , on the other hand, is known not to be normal, though its functional form has not yet been found.* The main object of the present paper is to obtain the distribution of Ω , in terms of the energy spectrum of the surface. We shall show that the distribution is in fact strikingly non-normal.

2. *The distribution of ζ and its derivatives.* The surface that we shall consider is one given by

$$\zeta = \sum_n c_n \cos(u_n x + v_n y + \epsilon_n), \quad (2.1)$$

where x , y are horizontal coordinates, u_n , v_n are wave-numbers with respect to x , y , and c_n , ϵ_n are amplitude and phase constants. The two-dimensional wave-numbers

* Eckart (5) assumed that Ω was distributed normally, but only for the purpose of a rough analysis.

(u_n, v_n) are assumed to be densely distributed throughout the wave-number plane, so that in any small region dS of the plane there are an infinite number of points (u_n, v_n) . The phases ϵ_n are assumed to be randomly and uniformly distributed between 0 and 2π , and the amplitudes c_n are such that over any region dS

$$\sum_{dS} \frac{1}{2} c_n^2 = E(u, v) dS, \quad (2.2)$$

where $E(u, v)$ is a continuous function* which will be called the energy spectrum of ζ .

The expression under the summation sign in (2.1) represents a long-crested wave of length

$$\frac{2\pi}{(u_n^2 + v_n^2)^{\frac{1}{2}}} = \frac{2\pi}{w_n} \quad (2.3)$$

and in a direction

$$\theta_n = \tan^{-1} \frac{v_n}{u_n}. \quad (2.4)$$

Thus ζ is represented as the sum of an infinite number of sine-waves of different wave-lengths and directions and in random relative phase (cf. (7)).

It is convenient to write ϕ_n for the total phase,

$$\phi_n = u_n x + v_n y + \epsilon_n, \quad (2.5)$$

so that

$$\zeta = \sum_n c_n \cos \phi_n. \quad (2.6)$$

Since ϵ_n is randomly distributed, so also is ϕ_n . We shall seek statistical averages over the field of values of ϵ_n , and clearly this will be equivalent to averaging over all possible values of ϕ_n . We assume an ergodic theorem, namely, that these averages are the same as would result from averaging with respect to x and y . All such averages will be denoted by a bar.

For example, the mean square value of ζ per unit area of the surface is

$$\begin{aligned} \bar{\zeta}^2 &= \overline{\left(\sum_n c_n \cos \phi_n \right) \left(\sum_m c_m \cos \phi_m \right)} \\ &= \overline{\sum_{n,m} \frac{1}{2} c_n c_m [\cos(\phi_n + \phi_m) + \cos(\phi_n - \phi_m)]} \\ &= \sum_n \frac{1}{2} c_n^2, \end{aligned} \quad (2.7)$$

since only the second term, when $m = n$, gives a non-zero contribution to the average. By (2.2) we may also write

$$\bar{\zeta}^2 = \int_{-\infty}^{\infty} \int_{-\infty}^{\infty} E(u, v) du dv \quad (2.8)$$

which shows that the total contribution to the mean square value of ζ from any element of the (u, v) -plane is proportional to $E(u, v)$.

* We here generalize to two dimensions the representation used by Rice (9). A more rigorous though less intuitive definition of ζ as a stationary continuous process can of course be given (see for example Doob (4), Chapter 11).

Statistical distribution of curvature of a random Gaussian surface 441

It will be convenient also to write m_{pq} for the (p, q) th moment of the energy about the origin

$$m_{pq} = \sum \frac{1}{2} c_n^2 u_n^p v_n^q = \int_{-\infty}^{\infty} E(u, v) u^p v^q du dv. \quad (2.9)$$

It can be shown that m_{pq} is related to the derivatives of the correlation function at the origin (see, for example, (7)).

Consider now the derivatives of ζ on which Ω depends. We have

$$\left. \begin{aligned} \xi_1 &= \frac{\partial^2 \zeta}{\partial x^2} = - \sum_n c_n u_n^2 \cos \phi_n, \\ \xi_2 &= \frac{\partial^2 \zeta}{\partial x \partial y} = - \sum_n c_n u_n v_n \cos \phi_n, \\ \xi_3 &= \frac{\partial^2 \zeta}{\partial y^2} = - \sum_n c_n v_n^2 \cos \phi_n. \end{aligned} \right\} \quad (2.10)$$

Since ξ_1, ξ_2, ξ_3 are each the sum of a large number of contributions of independent phase, their joint distribution, under certain general conditions, is normal. Also the matrix of averages $(\overline{\xi_i \xi_j})$ is given by

$$(\overline{\xi_i \xi_j}) = \begin{pmatrix} m_{40} & m_{21} & m_{22} \\ m_{21} & m_{22} & m_{13} \\ m_{22} & m_{13} & m_{04} \end{pmatrix} = (\overline{\Xi_{ij}}), \quad (2.11)$$

where m_{pq} is given by (2.9). Hence, the probability distribution of (ξ_1, ξ_2, ξ_3) is given by

$$p(\xi_1, \xi_2, \xi_3) = \frac{1}{(2\pi)^{\frac{3}{2}} \Delta^{\frac{1}{2}}} \exp \left[-\frac{1}{2} \sum_{ij} M_{ij} \xi_i \xi_j \right], \quad (2.12)$$

where

$$(M_{ij}) = (\overline{\Xi_{ij}})^{-1} \quad (2.13)$$

and

$$\Delta = |(\overline{\Xi_{ij}})|. \quad (2.14)$$

3. *The distribution of J.* We have

$$J = \xi_1 + \xi_3 = - \sum_n c_n (u_n^2 + v_n^2) \cos \phi_n. \quad (3.1)$$

Therefore J , being the sum of two variates with a normal joint-distribution, is itself distributed normally. Alternatively, we may remark that J is of the same form as ζ , being the sum of an infinite number of components in random phase; hence (under appropriate conditions) its distribution is normal. The variance of J can be written down at once, for on replacing c_n in equation (2.7) by $-c_n(u_n^2 + v_n^2)$ we have

$$J^2 = \sum_n \frac{1}{2} c_n^2 (u_n^2 + v_n^2)^2 = \int_{-\infty}^{\infty} \int_{-\infty}^{\infty} E(u, v) (u^2 + v^2)^2 du dv. \quad (3.2)$$

Expanding the squared factor and integrating each term we find

$$J^2 = m_{40} + 2m_{22} + m_{04} = D, \quad (3.3)$$

say. The distribution of J is then given by

$$p(J) = \frac{1}{(2\pi D)^{\frac{1}{2}}} e^{-J^2/2D}. \quad (3.4)$$

4. *Moments for $p(\Omega)$.* The distribution of Ω , which involves squares and products of normally distributed variables, is essentially more complicated than that of J . But the first few moments of $p(\Omega)$ may be quickly calculated. From (2.10) we have

$$\begin{aligned}\Omega &= \xi_1 \xi_3 - \xi_2^2 \\ &= \left(\sum_n c_n u_n^2 \cos \phi_n \right) \left(\sum_m c_m v_m^2 \cos \phi_m \right) - \left(\sum_n c_n u_n v_n \cos \phi_n \right) \left(\sum_m c_m u_m v_m \cos \phi_m \right) \\ &= \sum_{n,m} c_n c_m (u_n v_m - u_m v_n)^2 \cos \phi_n \cos \phi_m.\end{aligned}\quad (4.1)$$

Interchanging the suffixes n, m and adding gives

$$\Omega = \frac{1}{2} \sum_{n,m} c_n c_m (u_n v_m - u_m v_n)^2 \cos \phi_n \cos \phi_m \quad (4.2)$$

$$= \frac{1}{8} \sum_{n,m} c_n c_m (u_n v_m - u_m v_n)^2 \cos (\pm \phi_n \pm \phi_m), \quad (4.3)$$

where the last summation is to be taken over all combinations of positive and negative signs, as well as over n and m . On taking mean values in the last equation, all the cosine terms vanish except those for which $m = n$ and the signs of ϕ_n and ϕ_m are opposite. But when $m = n$ the squared term vanishes, giving a zero contribution to the sum in this case also. Thus

$$\bar{\Omega} = 0. \quad (4.4)$$

To calculate the second moment we have from (4.2)

$$\Omega^2 = \frac{1}{4} \sum_{n,m} \sum_{n',m'} c_n c_m c_{n'} c_{m'} (u_n v_m - u_m v_n)^2 (u_{n'} v_{m'} - u_{m'} v_{n'})^2 \cos \phi_n \cos \phi_m \cos \phi_{n'} \cos \phi_{m'}. \quad (4.5)$$

$$= \frac{1}{84} \sum_{n,m} \sum_{n',m'} c_n c_m c_{n'} c_{m'} (u_n v_m - u_m v_n)^2 (u_{n'} v_{m'} - u_{m'} v_{n'})^2 \cos (\pm \phi_n \pm \phi_m \pm \phi_{n'} \pm \phi_{m'}). \quad (4.6)$$

To obtain a non-zero contribution to the mean value, the phases ϕ_n , etc., must cancel in pairs. The only such pairs giving non-zero contributions are $n' = n$, $m' = m$ and $n' = m$, $m' = n$, the signs being both positive or both negative. Hence

$$\bar{\Omega}^2 = \frac{1}{8} \sum_{n,m} c_n^2 c_m^2 (u_n v_m - u_m v_n)^4 \quad (4.7)$$

$$= \frac{1}{2} \iiint \iiint E(u, v) E(u', v') (uv' - u'v)^4 du dv du' dv'. \quad (4.8)$$

On expanding the binomial term and evaluating the integrals we find

$$\begin{aligned}\bar{\Omega}^2 &= \frac{1}{2} (m_{40} m_{04} - 4m_{31} m_{13} + 6m_{22}^2 - 4m_{13} m_{31} + m_{04} m_{40}) \\ &= (m_{40} m_{04} - 4m_{31} m_{13} + 3m_{22}^2)\end{aligned}\quad (4.9)$$

$$= 3H, \quad (4.10)$$

say. Since E is non-negative we see from the integral expression (4.8) that $\bar{\Omega}^2$ can vanish only if $E(u, v)$ and $E(u', v')$ vanish at all points for which $(uv' - u'v)$ does not vanish, that is, if all the energy is concentrated along a single line through the origin.

Statistical distribution of curvature of a random Gaussian surface 443

In other words, the spectrum must be uni-directional and the surface perfectly long-crested. It may also be seen intuitively that $\bar{\Omega}^2$ must vanish in this case, since at each point of the surface one of the principal curvatures is zero and so Ω , which equals the product of the principal curvatures, vanishes everywhere.

Similarly for the third moment consider

$$\Omega^3 = \frac{1}{2^3} \sum_{n,m} \sum_{n',m'} \sum_{n'',m''} (u_n v_m - u_m v_n)^2 (u_{n'} v_{m'} - u_{m'} v_{n'})^2 (u_{n''} v_{m''} - u_{m''} v_{n''})^2 \times c_n c_m c_{n'} c_{m'} c_{n''} c_{m''} \cos(\pm \phi_n \pm \phi_m \pm \phi_{n'} \pm \phi_{m'} \pm \phi_{n''} \pm \phi_{m''}). \quad (4.11)$$

Again, the phases must cancel in pairs, but any combination containing pairs (n, m) , (n', m') or (n'', m'') gives zero contribution. We find there are eight possible combinations of the six phases, and for each of these there are eight combinations of sign. Hence

$$\bar{\Omega}^3 = \frac{1}{8} \sum_{n,n',n''} (u_n v_n - u_n v_n)^2 (u_{n'} v_{n'} - u_{n'} v_{n'})^2 (u_{n''} v_{n''} - u_{n''} v_{n''})^2 c_n^2 c_{n'}^2 c_{n''}^2 = \iiint \iiint \iiint (uv' - u'v)^2 (u'v'' - u''v')^2 (u''v - uv'')^2 \times E(u, v) E(u', v') E(u'', v'') du dv du' dv' du'' dv''. \quad (4.12)$$

On expanding the squared factors we find (as in (7), § 1.3) that

$$\bar{\Omega}^3 = 6 \begin{vmatrix} m_{40} & m_{31} & m_{22} \\ m_{31} & m_{22} & m_{13} \\ m_{22} & m_{13} & m_{04} \end{vmatrix} = 6\Delta, \quad (4.14)$$

say. The integrand in (4.13) is never negative and so

$$\bar{\Omega}^3 \geq 0. \quad (4.15)$$

From (4.13) it also follows that $\bar{\Omega}^3$ vanishes only if the energy is concentrated on not more than two lines through the origin; if there are appreciable amounts of energy in three or more different directions, then the integral is positive. Hence, we may say that the skewness of the distribution vanishes only when the surface degenerates into one or two systems of long-crested waves.

5. *The characteristic function of Ω .* The comparative simplicity of the first few moments of Ω suggests that the complete distribution $p(\Omega)$ may be derived most simply from its characteristic function

$$\phi(t) = \int_{-\infty}^{\infty} p(\Omega) e^{i\Omega t} d\Omega \quad (5.1)$$

$$= \mu_0 + \frac{it}{1!} \mu_1 + \frac{(it)^2}{2!} \mu_2 + \dots, \quad (5.2)$$

where μ_r denotes the r th moment.

Now it can be shown (see (7), § 2.1) that the matrix (Ξ_{ij}) of equation (2.11) is positive-definite; hence by a real linear transformation of variables

$$\xi_i = \sum_j a_{ij} \eta_j \quad (i = 1, 2, 3) \quad (5.3)$$

444

M. S. LONGUET-HIGGINS

the exponent in (2.12) can be reduced to the unit form and simultaneously Ω to a diagonal form. Thus

$$\left. \begin{aligned} \sum_{i,j} M_{ij} \xi_i \xi_j &= \eta_1^2 + \eta_2^2 + \eta_3^2, \\ \Omega &= \xi_1 \xi_2 - \xi_3^2 = l_1 \eta_1^2 + l_2 \eta_2^2 + l_3 \eta_3^2, \end{aligned} \right\} \quad (5.4)$$

where l_1, l_2, l_3 are the roots of

$$|\sigma_{ij} - lM_{ij}| = 0 \quad (5.5)$$

and (σ_{ij}) is the matrix of Ω :

$$(\sigma_{ij}) = \begin{pmatrix} 0 & 0 & \frac{1}{2} \\ 0 & -1 & 0 \\ \frac{1}{2} & 0 & 0 \end{pmatrix}. \quad (5.6)$$

On multiplying each side of (5.5) by

$$\Delta = |(\Xi_{ij})| = |(M_{ij})|^{-1} \quad (5.7)$$

we have

$$|(\sigma_{ij})(\Xi_{jk}) - l(\delta_{ik})| = 0, \quad (5.8)$$

where $(\delta_{i,k})$ is the unit matrix. In other words

$$\begin{vmatrix} \frac{1}{2}m_{22} - l & -m_{31} & \frac{1}{2}m_{40} \\ \frac{1}{2}m_{13} & -m_{22} - l & \frac{1}{2}m_{31} \\ \frac{1}{2}m_{04} & -m_{13} & \frac{1}{2}m_{22} - l \end{vmatrix} = 0. \quad (5.9)$$

On expanding the determinant we obtain

$$4l^3 - 3Hl - \Delta = 0, \quad (5.10)$$

where H and Δ are the combinations of moments given by (4.10) and (4.14). Since the roots l_1, l_2, l_3 of the cubic (5.10) are all real we must have

$$\frac{\Delta^2}{H^3} \leq 1 \quad (5.11)$$

and further

$$\left. \begin{aligned} l_1 + l_2 + l_3 &= 0, \\ l_2 l_3 + l_2 l_1 + l_1 l_2 &= -\frac{3}{4}H \leq 0, \\ l_1 l_2 l_3 &= \frac{1}{4}\Delta \geq 0. \end{aligned} \right\} \quad (5.12)$$

The first and third of these equations together show that in general one of the roots is positive and the other two are negative. We shall write

$$l_1 \geq 0 \geq l_2 \geq l_3. \quad (5.13)$$

Now the probability distribution of η_1, η_2, η_3 is given by

$$p(\eta_1, \eta_2, \eta_3) = \left| \frac{\partial(\xi_1, \xi_2, \xi_3)}{\partial(\eta_1, \eta_2, \eta_3)} \right| p(\xi_1, \xi_2, \xi_3) = |(a_{ij})| p(\xi_1, \xi_2, \xi_3), \quad (5.14)$$

where $|(a_{ij})|$ is a constant independent of η_1, η_2, η_3 . So on substituting from (2.12) and normalizing the distribution we have

$$p(\eta_1, \eta_2, \eta_3) = \frac{1}{(2\pi)^{\frac{3}{2}}} \exp[-\frac{1}{2}(\eta_1^2 + \eta_2^2 + \eta_3^2)]. \quad (5.15)$$

Statistical distribution of curvature of a random Gaussian surface 445

Integration with respect to two of the variables gives

$$p(\eta_1) = \frac{1}{(2\pi)^{\frac{1}{2}}} e^{-\frac{1}{2}\eta_1^2} \quad (5.16)$$

and so

$$p(\eta_1, \eta_2, \eta_3) = p(\eta_1)p(\eta_2)p(\eta_3), \quad (5.17)$$

showing that η_1, η_2, η_3 are statistically independent variables. Hence Ω , by (5.4), is the sum of the statistically independent variables $l_1\eta_1^2, l_2\eta_2^2, l_3\eta_3^2$ and the characteristic function of Ω is, by a well-known property, the product of the characteristic functions for these variables. From (5.16) we have for the distribution of $\chi_1 = l_1\eta_1^2$,

$$p(\chi_1) = \begin{cases} 0 & (\chi_1 < 0), \\ \frac{1}{(2\pi l_1)^{\frac{1}{2}}} \frac{1}{\chi^{\frac{1}{2}}} e^{-x_1/2l_1} & (\chi_1 > 0). \end{cases} \quad (5.18)$$

Hence, the characteristic function for χ_1 is given by

$$\phi_1(t) = \int_{-\infty}^{\infty} p(\chi_1) e^{i\chi_1 t} d\chi_1 = (1 - 2il_1 t)^{-\frac{1}{2}}. \quad (5.19)$$

We find similar expressions for the characteristic functions $\phi_2(t), \phi_3(t)$ of χ_2 and χ_3 . Therefore the characteristic function of Ω is given by

$$\begin{aligned} \phi(t) &= \phi_1(t)\phi_2(t)\phi_3(t) \\ &= [(1 - 2il_1 t)(1 - 2il_2 t)(1 - 2il_3 t)]^{-\frac{1}{2}} \\ &= (1 + 3Ht^2 + 2i\Delta t^3)^{-\frac{1}{2}}, \end{aligned} \quad (5.20)$$

where we have used equations (5.12). On expanding in powers of t and equating with (5.2), we find

$$\left. \begin{aligned} \mu_0 &= 1, & \mu_1 &= 0, \\ \mu_2 &= 3H, & \mu_3 &= 6\Delta, \\ \mu_4 &= 81H^2, & \mu_5 &= 540H\Delta, \end{aligned} \right\} \quad (5.21)$$

etc. The values of μ_1, μ_2, μ_3 will be seen to agree with those found in § 4.

6. *The distribution of Ω .* The distribution of Ω may now be obtained by inverting the Fourier transform (3.1). Thus

$$p(\Omega) = \frac{1}{2\pi} \int_{-\infty}^{\infty} \phi(t) e^{-i\Omega t} dt \quad (6.1)$$

$$\begin{aligned} &= \frac{1}{2\pi} \int_{-\infty}^{\infty} \frac{e^{-i\Omega t}}{(1 + 3Ht^2 + 2i\Delta t^3)^{\frac{1}{2}}} dt \\ &= \frac{1}{2\pi} \int_{-i\infty}^{i\infty} \frac{e^{-i(\Omega/3H)\alpha}}{(1 - \alpha^2 - \lambda\alpha^3)^{\frac{1}{2}}} \frac{d\alpha}{i\sqrt{(3H)^{\frac{1}{2}}}}, \end{aligned} \quad (6.2)$$

where we have written

$$\alpha = i(3H)^{\frac{1}{2}} t \quad (6.3)$$

and

$$\lambda = \frac{2\Delta}{(3H)^{\frac{3}{2}}}. \quad (6.4)$$

Introducing the non-dimensional variable

$$\omega = \frac{\Omega}{(3H)^{\frac{1}{2}}} = \frac{\Omega}{(\bar{\Omega}^2)^{\frac{1}{2}}} \quad (6.5)$$

we have

$$p(\Omega) = \frac{1}{(3H)^{\frac{1}{2}}} f(\omega), \quad (6.6)$$

where

$$f(\omega) = \frac{1}{2\pi} \int_{-i\infty}^{i\infty} \frac{e^{-\omega\alpha}}{(\lambda\alpha^3 + \alpha^2 - 1)^{\frac{1}{2}}} d\alpha = f(\omega, \lambda). \quad (6.7)$$

This is the formal solution of the problem, showing that, apart from the scale-factor $(3H)^{\frac{1}{2}}$, the distribution of Ω depends on only one other parameter λ , given by (6.4). We have seen from § 4 and from equation (5.11) that $\Delta/H^{\frac{3}{2}}$ is positive and less than unity, in general; and we shall see in § 8 that $\Delta/H^{\frac{3}{2}}$ may take either of the extreme values 0 or 1. Hence the range of λ is

$$0 \leq \lambda \leq 2/3\sqrt{3}. \quad (6.8)$$

7. *The evaluation of $f(\omega, \lambda)$.* Let us examine more closely the function $f(\omega, \lambda)$ defined by (6.7). Clearly the integrand has branch-points at the three roots $\alpha_1, \alpha_2, \alpha_3$ of the cubic

$$\lambda\alpha^3 + \alpha^2 - 1 = 0. \quad (7.1)$$

The roots are all real; in fact, by comparison with (3.10) we have

$$(\alpha_1, \alpha_2, \alpha_3) = \frac{(3H)^{\frac{1}{2}}}{2} \left(\frac{1}{l_1}, \frac{1}{l_2}, \frac{1}{l_3} \right) \quad (7.2)$$

and hence

$$\alpha_1 \geq 0 \geq \alpha_2 \geq \alpha_3. \quad (7.3)$$

The situation is as shown in Fig. 1, one of the branch-points lying to the right of the contour of integration, the other two to the left.

When $\omega > 0$ the path of integration may be deformed so as to run from ∞ to α_1 along the lower side of the real axis and from α_1 to ∞ on the upper side, giving

$$f(\omega) = \frac{1}{\pi} \int_{\alpha_1}^{\infty} \frac{e^{-\omega\alpha}}{\sqrt{\{\lambda(\alpha - \alpha_1)(\alpha - \alpha_2)(\alpha - \alpha_3)\}}} d\alpha. \quad (7.4)$$

Similarly, when $\omega < 0$ the path may be deformed into a closed contour surrounding the branch-points α_2 and α_3 . Taking this to lie along the real axis in each direction, we have

$$f(\omega) = \frac{1}{\pi} \int_{\alpha_3}^{\alpha_2} \frac{e^{-\omega\alpha}}{\sqrt{\{\lambda(\alpha - \alpha_1)(\alpha - \alpha_2)(\alpha - \alpha_3)\}}} d\alpha. \quad (7.5)$$

At the two extreme values of λ , $f(\omega)$ may be expressed in terms of known functions as follows:

(i) $\lambda = 0$. One of the roots of (7.1), namely α_2 , goes to $-\infty$, and we have from (6.7)

$$f(\omega) = \frac{1}{2\pi} \int_{-i\infty}^{i\infty} \frac{e^{-\omega\alpha}}{(\alpha^2 - 1)^{\frac{1}{2}}} d\alpha = \frac{1}{\pi} K_0(\omega), \quad (7.6)$$

Statistical distribution of curvature of a random Gaussian surface 447

where K_0 denotes the modified Bessel function with imaginary argument ((10), § 3.7). The function is symmetrical about the origin, where it has a logarithmic singularity:

$$f(\omega) \sim \frac{1}{\pi} \log \frac{2}{|\omega|}. \quad (7.7)$$

For large values of $|\omega|$ we find, from the asymptotic expression for $K_0(z)$,

$$f(\omega) \sim \frac{1}{\sqrt{(2\pi|\omega|)}} e^{-|\omega|}. \quad (7.8)$$

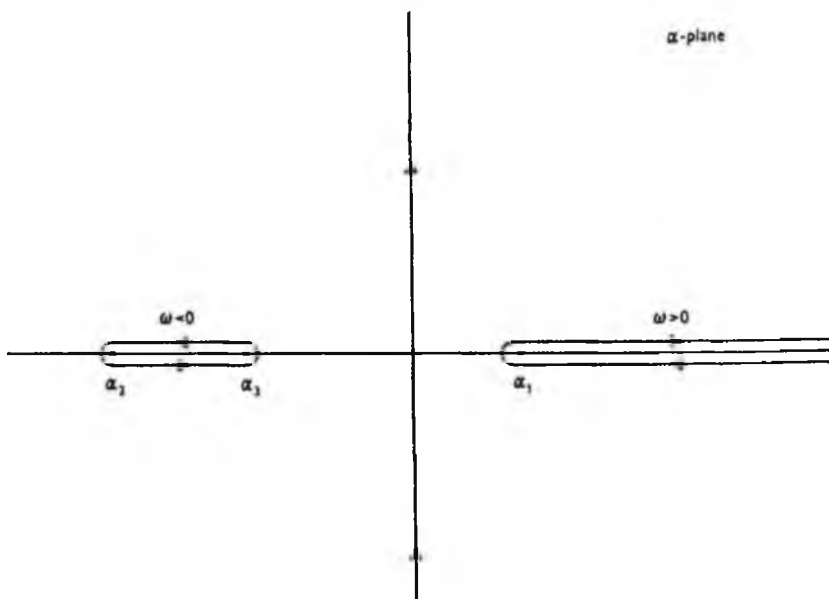


Fig. 1. Contours of integration for $f(\omega)$.

(ii) $\lambda = 2/3\sqrt{3}$. Two of the roots of (5.1), namely, α_2 and α_3 , coincide and we have

$$\alpha_1 = \frac{1}{2}\sqrt{3}, \quad \alpha_2 = \alpha_3 = -\sqrt{3}. \quad (7.9)$$

When $\omega > 0$ we have from (7.4), writing $\alpha + \sqrt{3} = \alpha'$,

$$f(\omega) = \frac{1}{\pi\sqrt{3}} \frac{3\sqrt{3}}{2} e^{-\sqrt{3}\omega} \int_{\frac{1}{2}\sqrt{3}}^{\infty} \frac{e^{-\omega\alpha'}}{\alpha' \sqrt{(\alpha' - \frac{1}{2}\sqrt{3})^2}} d\alpha'. \quad (7.10)$$

The above integral may be transformed ((6), equation (4.3), (8)), into the form

$$f(\omega) = \frac{1}{\sqrt{\pi}} e^{\sqrt{3}\omega} \int_{\frac{1}{2}\sqrt{3}\omega}^{\infty} \frac{e^{-t}}{\sqrt{t}} dt = e^{\sqrt{3}\omega} \operatorname{erfc} \left(\sqrt{\frac{3\sqrt{3}\omega}{2}} \right). \quad (7.11)$$

On the other hand when $\omega \leq 0$ we have

$$f(\omega) = \frac{1}{2\pi\sqrt{3}} \frac{3\sqrt{3}}{2} \int_0^{\infty} \frac{e^{-\omega\alpha}}{(\alpha + \sqrt{3})(\alpha - \sqrt{3}/2)^{\frac{1}{2}}} d\alpha, \quad (7.12)$$

where C is a contour enclosing the point $-\sqrt{3}$. On evaluating the residue at this point we find simply

$$f(\omega) = e^{\sqrt{3}\omega}. \quad (7.13)$$

Thus altogether

$$f(\omega) = e^{\sqrt{3}\omega} \times \begin{cases} 1, & (\omega < 0) \\ \operatorname{erfc}\left(\sqrt{\frac{3}{2}}\sqrt{3}\omega\right), & (\omega > 0) \end{cases} \quad (7.14)$$

For large positive values of ω we have, from the asymptotic expansion of the error function,

$$f(\omega) \sim \sqrt{\frac{2}{3\sqrt{3}\pi\omega}} e^{-\sqrt{3}\omega}. \quad (7.15)$$

We come now to the intermediate case:

(iii) $0 < \lambda < 2/3\sqrt{3}$. On differentiating under the integral sign in (6.7) and integrating by parts, we find that $f(\omega)$ is a solution of the third-order equation

$$-\lambda f''' + f'' - f = \frac{1}{\omega} \left(\frac{3}{2} \lambda f'' - f' \right) \quad (7.16)$$

(where a prime denotes differentiation with respect to ω). This has a regular singularity at the origin, with exponents 0, 1 and $\frac{1}{2}$. (In the case $\lambda = 0$ the equation reduces to a second-order differential equation of Bessel type.)

$f(\omega)$ is not expressible in terms of known functions,* except for particular values of ω . Thus from (7.5) we may deduce, by means of the substitution $\alpha = \alpha_2 \cos^2 \phi + \alpha_3 \sin^2 \phi$, that

$$f(0) = \frac{2}{\pi \sqrt{\lambda(\alpha_1 - \alpha_2)}} K\left(\sqrt{\frac{\alpha_3 - \alpha_2}{\alpha_1 - \alpha_2}}\right), \quad (7.17)$$

where $K(k)$ denotes the Legendre complete elliptic integral of the first kind. Similarly, by differentiating (7.5) under the integral sign we find for the gradient to the left of the origin

$$f'(-0) = \frac{2}{\pi \sqrt{\lambda(\alpha_1 - \alpha_2)}} \left[(\alpha_1 - \alpha_2) E\left(\sqrt{\frac{\alpha_3 - \alpha_2}{\alpha_1 - \alpha_2}}\right) - \alpha_1 K\left(\sqrt{\frac{\alpha_3 - \alpha_2}{\alpha_1 - \alpha_2}}\right) \right], \quad (7.18)$$

where $E(k)$ denotes the Legendre integral of the second kind. From (7.4) we see that the gradient to the right of the origin is infinite; in fact

$$f'(\omega) \sim -\frac{1}{\pi \sqrt{\lambda}} \int_A^\infty \frac{e^{-\omega\alpha}}{\sqrt{\alpha}} d\alpha \sim -\frac{1}{\sqrt{\pi \lambda \omega}} \quad (7.19)$$

(A denotes some constant greater than α_1).

A discontinuity of this kind is consistent with the nature of the differential equation (7.16) near the origin.

The asymptotic behaviour of the function for large positive values of ω may be derived from (7.4) by expanding in a Taylor series about α_1 and using Watson's lemma. This gives, as a first term

$$f(\omega) \sim \frac{e^{-\alpha_1 \omega}}{\sqrt{\{\pi \lambda (\alpha_1 - \alpha_2) (\alpha_1 - \alpha_3)\}}} \quad (\omega > 0). \quad (7.20)$$

* A different solution of (7.16), expressible as a generalized Humbert series, would be obtained by taking the path of integration to the right of all the branch points (see (6), p. 13).

Statistical distribution of curvature of a random Gaussian surface 449

Similarly, for large negative values of ω the integral (7.5) gives

$$f(\omega) \sim \frac{e^{-\alpha_2 \omega}}{\sqrt{\{\pi\lambda(\alpha_1 - \alpha_3)(\alpha_2 - \alpha_3)\omega\}}} \quad (\omega < 0). \tag{7.21}$$

Since
$$\frac{1}{\alpha_1} + \frac{1}{\alpha_2} + \frac{1}{\alpha_3} = 0 \tag{7.22}$$

we see that $\alpha_1 < -\alpha_3$, and so the function tends to zero less strongly on the positive side of the origin than on the negative side. This accounts for the positive coefficient of skewness noted previously.

The r th moment of $f(\omega)$ about the origin is given by

$$\nu_r = \frac{\mu_r}{(3H)^{1/r}}, \tag{7.23}$$

where μ_r is the corresponding moment for $p(\Omega)$. From (5.21) we have

$$\left. \begin{aligned} \nu_0 &= 1, & \nu_1 &= 0, \\ \nu_2 &= 1, & \nu_3 &= 3\lambda, \\ \nu_4 &= 9, & \nu_5 &= 90\lambda. \end{aligned} \right\} \tag{7.24}$$

Thus $\nu_0, \nu_1, \nu_2, \nu_4$ are all independent of λ . The coefficient of skewness (ν_3/ν_2^3) is proportional to λ while the kurtosis (ν_4/ν_2^2) is constant and equal to 9 (compared with 3 for the normal distribution). Higher moments than the fifth are, in general, polynomials in λ .

Numerical computation of $f(\omega)$ has been carried out by D. B. Catton, and B. G. Millis at the Mathematical Laboratory, Cambridge, and the computation is described in an adjoining paper (1). In Fig. 2, the form of $f(\omega)$ is shown graphically for

$$\lambda = 2/3\sqrt{3} \times (0, 0.2, 0.5 \text{ and } 1).$$

The skewness of the curves, and the singularities at $\omega = 0$, are apparent.

8. *The significance of λ .* Lastly let us consider the significance of the parameter

$$\lambda = \frac{2}{3^{\frac{1}{2}}} \frac{\Delta}{H^{\frac{1}{2}}} \tag{8.1}$$

in terms of the spectrum of the surface. Of particular interest to us are the conditions under which $\Delta/H^{\frac{1}{2}}$ may take the extreme values 0 and 1.

In equations (4.8) and (4.13) we may transform to polar coordinates by the substitution

$$(u, v) = (w \cos \theta, w \sin \theta) \tag{8.2}$$

so that w, θ represent the wave-number and the direction, respectively, of a typical wave component in the spectrum. Using (4.10) and (4.14) we have then

$$H = \frac{1}{6} \int_0^\infty \int_0^\infty dw dw' \int_0^{2\pi} \int_0^{2\pi} d\theta d\theta' E(u, v) E(u', v') w^5 w'^5 \sin^4(\theta - \theta') \tag{8.3}$$

and

$$\begin{aligned} \Delta = \frac{1}{6} \int_0^\infty \int_0^\infty \int_0^\infty dw dw' dw'' \int_0^{2\pi} \int_0^{2\pi} \int_0^{2\pi} d\theta d\theta' d\theta'' E(u, v) E(u', v') E(u'', v'') \\ \times w^5 w'^5 w''^5 \sin^2(\theta' - \theta'') \sin^2(\theta'' - \theta) \sin^2(\theta' - \theta''). \end{aligned} \tag{8.4}$$

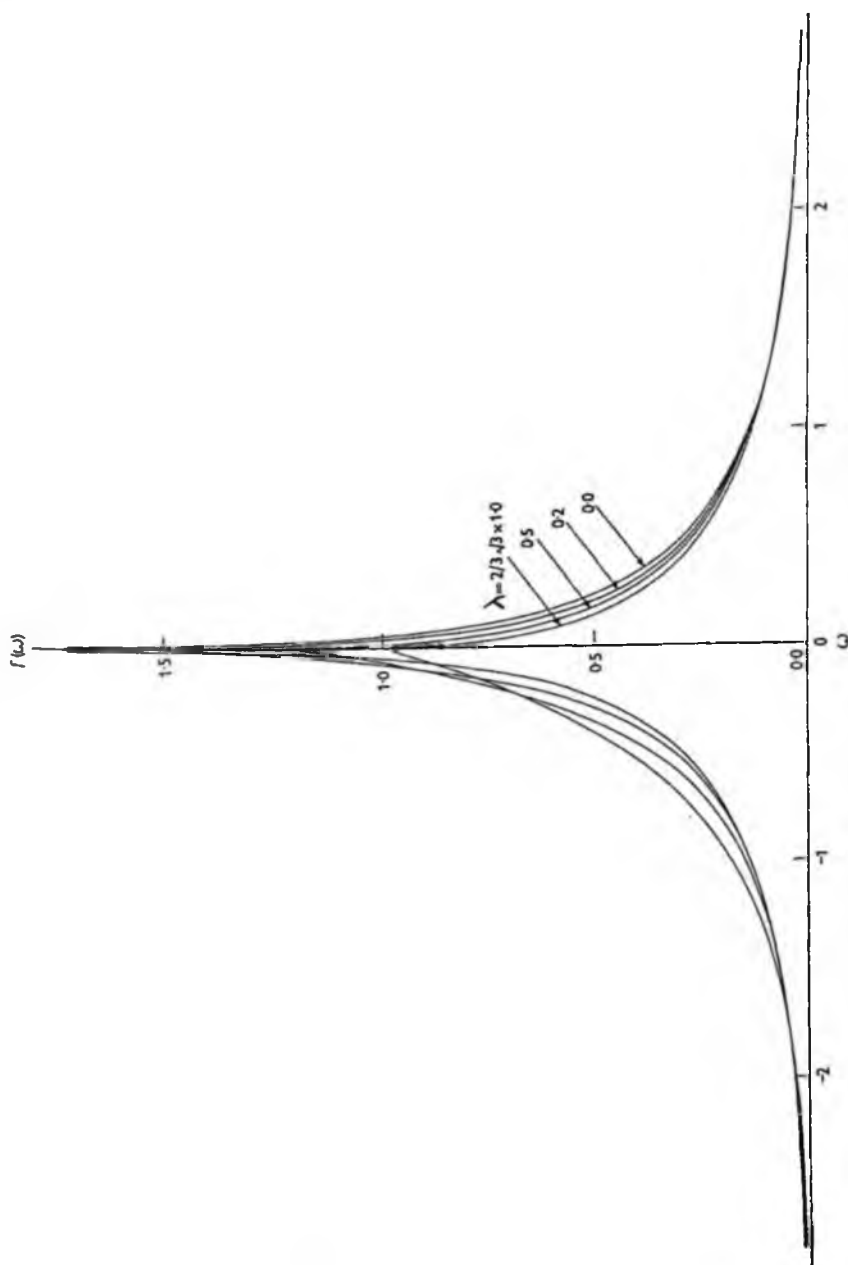


Fig. 2. Graph of $f(\omega)$ for four different values of λ , showing the form of the distribution of Ω .

Statistical distribution of curvature of a random Gaussian surface 451

We have already seen that if the energy is concentrated in two distinct directions $\theta = \theta_1, \theta_2$ then Δ vanishes but not H and so

$$\frac{\Delta}{H^{\frac{1}{2}}} = 0. \quad (8.5)$$

If all the energy is concentrated in a single direction then both H and Δ vanish, and the ratio $\Delta/H^{\frac{1}{2}}$ is indeterminate. However, this case may be examined by considering a spectrum of finite angular width tending to zero; and it will be shown that $\Delta/H^{\frac{1}{2}}$ may, for a narrow spectrum, take any value between 0 and 1.

Suppose, for example, that the spectrum $E(u, v)$ has the form

$$E(u, v) = W(w) \Theta(\theta), \quad (8.6)$$

where W is a function of w only and Θ is a function of θ only, then from (8.3) and (8.4) we have

$$H = \frac{1}{2} M^2 \int_0^{2\pi} \int_0^{2\pi} \Theta(\theta) \Theta(\theta') \sin^4(\theta - \theta') d\theta d\theta' \quad (8.7)$$

and

$$\Delta = \frac{1}{2} M^3 \int_0^{2\pi} \int_0^{2\pi} \int_0^{2\pi} \Theta(\theta) \Theta(\theta') \Theta(\theta'') \sin^2(\theta' - \theta'') \sin^2(\theta'' - \theta) \sin^2(\theta - \theta') d\theta d\theta' d\theta'', \quad (8.8)$$

where

$$M = \int_0^{\infty} W(w) w^5 dw. \quad (8.9)$$

If the energy is all confined to one narrow range of direction, then, over the important region of integration, $\sin(\theta' - \theta'')$, $\sin(\theta'' - \theta)$ and $\sin(\theta - \theta')$ may be replaced by $(\theta - \theta'')$, $(\theta'' - \theta)$ and $(\theta - \theta')$, respectively. Hence we find

$$H = \frac{1}{2} M^2 (t_4 t_0 - 4t_3 t_1 + 6t_2^2 - 4t_1 t_3 + t_0 t_4) \quad (8.10)$$

and

$$\Delta = M^3 \begin{vmatrix} t_0 & t_1 & t_2 \\ t_1 & t_2 & t_3 \\ t_2 & t_3 & t_4 \end{vmatrix}, \quad (8.11)$$

where t_n denotes the n th moment of Θ ,

$$t_n = \int \Theta(\theta) \theta^n d\theta. \quad (8.12)$$

Assuming that $t_1 = t_3 = 0$ (as for a symmetrical distribution) we find

$$\frac{\Delta}{H^{\frac{1}{2}}} = \frac{a^2 - 1}{(a^2/3 + 1)^{\frac{1}{2}}}, \quad (8.13)$$

where

$$a^2 = \frac{t_0 t_4}{t_2^2}. \quad (8.14)$$

The parameter a^2 represents the 'peakedness' of the energy spectrum with regard to direction. The minimum value of a^2 is unity, attained when Θ consists of two close but separate concentrations of energy

$$\Theta = \delta(\theta - \theta_1) + \delta(\theta - \theta_2). \quad (8.15)$$

This is when the surface $\zeta(x, y)$ really consists of two distinct systems of long-crested waves intersecting at a small angle $(\theta_1 - \theta_2)$; and $\Delta/H^{\frac{1}{2}}$ has the value zero, as we should expect.

For a uniform distribution of energy over a narrow sector, $a^2 = \frac{3}{2}$ and so

$$\frac{\Delta}{H^{\frac{1}{2}}} = \frac{3\sqrt{6}}{40} = 0.194 \dots \quad (8.16)$$

For a normal distribution, $a^2 = 3$ and so

$$\frac{\Delta}{H^{\frac{1}{2}}} = \frac{1}{\sqrt{2}} = 0.707 \dots \quad (8.17)$$

The maximum value of λ is attained when $a^2 = 9$ and

$$\frac{\Delta}{H^{\frac{1}{2}}} = 1. \quad (8.18)$$

By further concentrating the energy around the central direction, a^2 may be made to increase indefinitely and so

$$\frac{\Delta}{H^{\frac{1}{2}}} \rightarrow 0 \quad (8.19)$$

once more.

A quite different case in which λ attains its maximum value is when the surface is isotropic. For then

$$E(u, v) = W(w) \times \text{constant} \quad (8.20)$$

and on writing $\Theta = (2\pi)^{-1}$ in (6.7) and (6.8) we have

$$H = \frac{1}{16}M^2, \quad \Delta = \frac{1}{64}M^3 \quad (8.21)$$

and so

$$\frac{\Delta^2}{H^3} = 1. \quad (8.22)$$

Lastly, since H and Δ depend only on moments of order 4, the same value of λ will be found for any two surfaces whose spectra have the same fourth-order moments. Thus the maximum value of λ is attained by any spectrum having n -fold rotational symmetry about the origin, where $n = 3, 5, 6, 7, \dots$, for this will have the same fourth-order moments as an isotropic spectrum (see (8)).

9. *Conclusions.* Unlike the mean curvature J , the total curvature Ω has a non-normal distribution; it is skew in general, and has a discontinuity in gradient at the origin (see Fig. 2). The distribution depends on only two parameters H and Δ , given in terms of the energy spectrum of the surface by equations (8.3) and (8.4). The scale of the distribution is proportional to $(3H)^{\frac{1}{2}}$ which equals the r.m.s. value of Ω . The skewness of the distribution is proportional to λ , $= 2\Delta/(3H)^{\frac{3}{2}}$. The analytical expression for $p(\Omega)$ is given by equation (6.6).

If D denotes the r.m.s. value of J (see equation (3.3)) then

$$\frac{H}{D^2} = 0$$

Statistical distribution of curvature of a random Gaussian surface 453

when and only when the original surface degenerates into a single system of long-crested waves; and

$$\frac{\Delta}{D^3} = 0, \quad \frac{H}{D^2} \neq 0,$$

when and only when the surface consists of two systems of long-crested waves intersecting at a non-zero angle. In this case λ clearly vanishes. The maximum value of λ , which equals $2/3\sqrt{3}$, may be taken in a variety of circumstances, for example if the surface is isotropic.

In the present paper $p(\Omega)$ was found by evaluating the characteristic function of Ω and then taking the Fourier transform of the result so as to obtain the function in the form of an integral. It may be mentioned that the same method would serve to determine the distribution of a general quadratic form in n normally distributed variables, and that the frequency function would satisfy a linear differential equation of the n th degree.

In a subsequent paper we shall apply the present results by deducing the distribution of image sizes of a distant object reflected in the surface.

REFERENCES

- (1) CATTON, D. B. and MILLIS, B. G. Numerical evaluation of the integral

$$\frac{1}{2\pi} \int_{-i\infty}^{i\infty} (\lambda\alpha^3 + \alpha^2 - 1)^{-1} e^{-\alpha\omega} d\alpha. \quad \textit{Proc. Camb. Phil. Soc.} \text{ 54 (1958), 454-82.}$$

- (2) COX, C. and MUNK, W. Measurement of the roughness of the sea surface from photographs of the sun's glitter. *J. Opt. Soc. Amer.* 44 (1954), 838-50.
 (3) COX, C. and MUNK, W. Slopes of the sea surface deduced from photographs of sun glitter, *Bull. Scripps Instn Oceanogr.* 6 (1956), 401-88.
 (4) DOOB, J. L. *Stochastic processes* (New York, 1953).
 (5) ECKART, C. *The sea surface and its effect on the reflection of sound and light* (University of California, Division of Wave Research, Report 01.75, 1946).
 (6) ERDELYI, A. *et al. Tables of integral transforms*, Vol. I (New York, 1954).
 (7) LONGUET-HIGGINS, M. S. The statistical analysis of a random, moving surface. *Phil. Trans. A*, 249 (1957), 321-87.
 (8) LONGUET-HIGGINS, M. S. Statistical properties of an isotropic random surface. *Phil. Trans. A*, 250 (1957), 157-74.
 (9) RICE, S. O. Mathematical analysis of random noise. *Bell System Tech. J.* 24 (1945), 46-156.
 (10) WATSON, G. N. *A treatise on the theory of Bessel functions*, 2nd ed. (Cambridge, 1952).

NATIONAL INSTITUTE OF OCEANOGRAPHY
WORMLEY

Reprinted from the *Proceedings of the Cambridge Philosophical Society*,
Volume 55, Part 1, pp. 91-100, 1959.

PRINTED IN GREAT BRITAIN

THE DISTRIBUTION OF THE SIZES OF IMAGES REFLECTED IN A RANDOM SURFACE

By M. S. LONGUET-HIGGINS

Received 25 July 1958

1. *Introduction.* It has been shown recently that a fruitful method of studying the formation of waves on the sea surface is through the average intensity of reflected sunlight, as seen from different angles ((3), (4)). This gives, in effect, the statistical distribution of the components of surface slope.

Following the same line of thought, we may inquire what information could be derived from the distribution of the sizes of the reflected images of the sun. The size of an image depends essentially on the total curvature of the surface at the point of reflexion (see § 2).

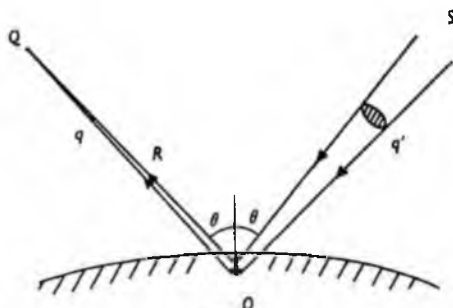


Fig. 1

As a physical model for the sea surface it is reasonable to assume in the first place a Gaussian surface, that is to say one whose elevation ζ and derivatives $\partial^p \zeta / \partial x^p \partial y^q$ are distributed normally. The model has given satisfactory results for the distribution of wave heights (1) and of surface slopes (4) and it is reasonable therefore to try it next for properties depending on the curvature.

The statistical distribution of the total curvature Ω for such a surface has been evaluated in a recent paper (7), and has been shown to depend upon two parameters H and λ derivable from the spectrum of the surface. It will be shown in the present paper that the distribution of image sizes depends upon the same parameters, but that its form is almost independent of λ . Hence, from the observed distribution the parameter H could be accurately found, but not λ . The information given by H is discussed in some detail in § 6.

2. *Geometrical relations.* Suppose that light from a distant object S , after reflexion from a surface near O , is received at a point Q distant R from O (see Fig. 1). The projected area of the image at O is given by

$$I = R^2 q, \quad (2.1)$$

where q denotes the solid angle subtended by the beam at Q . The incident rays SQ do not in general meet in a point, but it may be shown* that the solid angle q' formed by the incident rays is related to the solid angle q by the expression

$$-q'/q = 1 + 2R(\kappa_1 \sec \theta + \kappa_2 \cos \theta) + 4R^2\Omega, \quad (2.2)$$

where κ_1 and κ_2 denote the curvatures of the surface in the plane of the ray and perpendicular to it, θ denotes the angle of incidence and Ω denotes the total curvature. (Ω may be defined as the product of the two principal curvatures κ_a and κ_b at O .) The negative sign in (2.2) signifies that the sense of rotation of the image is reversed. Provided $R\kappa_a$ and $R\kappa_b$ are both large, we have

$$|q'/q| = 4R^2 |\Omega|, \quad (2.3)$$

a relation which is independent of θ . Combining (2.1) and (2.3) gives

$$I = \frac{q'}{4|\Omega|}. \quad (2.4)$$

If q' is fixed (as for a distant object, large compared with I), then I is inversely proportional to $|\Omega|$.

3. *Definitions.* If the surface is represented in the form

$$z = \zeta(x, y), \quad (3.1)$$

where (x, y) are horizontal coordinates and z is measured vertically upwards, the total curvature Ω is given by

$$\Omega = \left[\frac{\partial^2 \zeta}{\partial x^2} \frac{\partial^2 \zeta}{\partial y^2} - \left(\frac{\partial^2 \zeta}{\partial x \partial y} \right)^2 \right] / \left[1 + \left(\frac{\partial \zeta}{\partial x} \right)^2 + \left(\frac{\partial \zeta}{\partial y} \right)^2 \right] \quad (3.2)$$

(see (10), § 33). If the squares of $\partial \zeta / \partial x$ and $\partial \zeta / \partial y$ are supposed negligible this reduces to

$$\Omega = \frac{\partial^2 \zeta}{\partial x^2} \frac{\partial^2 \zeta}{\partial y^2} - \left(\frac{\partial^2 \zeta}{\partial x \partial y} \right)^2. \quad (3.3)$$

As in a recent paper (7), it will be assumed that ζ is given by

$$\zeta(x, y) = \sum_n c_n \cos(u_n x + v_n y + \epsilon_n), \quad (3.4)$$

where u_n and v_n are wave numbers densely distributed in the wave-number plane, and where c_n and ϵ_n are amplitude and phase constants. The ϵ_n are supposed randomly and uniformly distributed between 0 and 2π , and the c_n are such that in any small region $du dv$ of the (u, v) plane

$$\sum_n \frac{1}{2} c_n^2 = E(u, v) du dv, \quad (3.5)$$

where $E(u, v)$ is a continuous function. $E(u, v)$ will be called the energy spectrum of the surface.

* This relation may be derived from first principles, or from a more general formula given by Primakoff and Keller (8), equation (42).

Sizes of images reflected in a random surface 93

Under certain general conditions (see (9), § 2·10) it follows that the joint distribution of ζ and its derivatives is normal, and it has been shown (7) that in that case the distribution of Ω is given by

$$p(\Omega) = \frac{1}{(3H)^{\frac{1}{2}}} f\left(\frac{\Omega}{(3H)^{\frac{1}{2}}}, \frac{2\Delta}{(3H)^{\frac{1}{2}}}\right), \quad (3\cdot6)$$

where H, Δ are constants given in terms of $E(u, v)$ by

$$H = \frac{1}{6} \iiint E(u, v) E(u', v') (uv' - u'v)^2 du dv du' dv', \quad (3\cdot7)$$

$$\Delta = \frac{1}{6} \iiint \dots \iiint E(u, v) E(u', v') E(u'', v'') (u'v'' - u''v')^2 (u''v - uv'')^2 \\ \times (uv' - u'v'')^2 du dv du' dv' du'' dv'' \quad (3\cdot8)$$

and where
$$f(\omega, \lambda) = \frac{1}{2\pi} \int_{-i\omega}^{i\omega} \frac{e^{-\alpha\omega}}{(\lambda\alpha^3 + \alpha^2 - 1)^{\frac{1}{2}}} d\alpha. \quad (3\cdot9)$$

This last function has been discussed in (7) and evaluated numerically by Catton and Millis (2). Graphs are given in (7). The non-dimensional parameter

$$\lambda = \frac{2\Delta}{(3H)^{\frac{1}{2}}} \quad (3\cdot10)$$

is restricted by the condition that

$$0 \leq \frac{\Delta}{H^{\frac{1}{2}}} \leq 1. \quad (3\cdot11)$$

Now $p(\Omega)$ is the distribution of Ω for points on the surface selected at random in the (x, y) -plane. In practice, however, the surface is viewed from a particular angle, and the images are seen only at those points on the surface (called specular points) where the surface has the particular slope required to reflect the light into the observer's eye. What we seek, therefore, is the distribution of Ω at specular points, which distribution we shall denote by $p^*(\Omega)$. It turns out that $p^*(\Omega)$, although different in form from $p(\Omega)$, is very closely related.

4. *The distribution of Ω at specular points.* As in (7) let us write for short

$$\frac{\partial^2 \zeta}{\partial x^2}, \frac{\partial^2 \zeta}{\partial x \partial y}, \frac{\partial^2 \zeta}{\partial y^2} = \xi_1, \xi_2, \xi_3 \quad (4\cdot1)$$

and also
$$\frac{\partial \xi}{\partial x}, \frac{\partial \xi}{\partial y} = \xi_4, \xi_5. \quad (4\cdot2)$$

The problem then is to find the distribution of

$$\Omega = \xi_1 \xi_3 - \xi_2^2 \quad (4\cdot3)$$

at those points where ξ_4, ξ_5 take particular values.

Let $p(\xi_1, \xi_2, \xi_3, \xi_4, \xi_5)$ denote the probability density of ξ_1, \dots, ξ_5 at an arbitrary point P in the (x, y) -plane, and let dA denote a small area of the (x, y) -plane surrounding

P. If ξ_4, ξ_5 take the specified values somewhere in dA then (ξ_4, ξ_5) at *P* itself must lie within a certain region of the (ξ_4, ξ_5) -plane having an area

$$\left| \frac{\partial(\xi_4, \xi_5)}{\partial(x, y)} \right| dA = |\xi_1 \xi_3 - \xi_2^2| dA = |\Omega| dA. \quad (4.4)$$

So the probability that ξ_4, ξ_5 take the given values in dA and that ξ_1, ξ_2, ξ_3 also lie in the ranges $d\xi_1, d\xi_2, d\xi_3$ is

$$p(\xi_1, \dots, \xi_5) d\xi_1 d\xi_2 d\xi_3 |\Omega| dA \quad (4.5)$$

The total probability of ξ_4, ξ_5 taking the specified values in dA is

$$\int_{-\infty}^{\infty} d\xi_1 \int_{-\infty}^{\infty} d\xi_2 \int_{-\infty}^{\infty} d\xi_3 p(\xi_1, \dots, \xi_5) |\Omega| dA = D_{sp} dA, \quad (4.6)$$

(where D_{sp} denotes the average density of specular points with gradient (ξ_4, ξ_5) , per unit horizontal area). Therefore the probability that ξ_1, ξ_2, ξ_3 lie in their respective ranges given that there is a specular point in dA is the quotient of (4.5) and (4.6), that is to say

$$\frac{p(\xi_1, \dots, \xi_5) |\Omega|}{D_{sp}} d\xi_1 d\xi_2 d\xi_3. \quad (4.7)$$

In other words, the probability distribution of (ξ_1, ξ_2, ξ_3) at such points is given by

$$p^*(\xi_1, \xi_2, \xi_3) = \frac{p(\xi_1, \dots, \xi_5) |\Omega|}{D_{sp}}. \quad (4.8)$$

It may easily be shown (see (5) § 2.1) that the first derivatives ξ_4, ξ_5 are statistically independent of the second derivatives ξ_1, ξ_2, ξ_3 so that

$$p(\xi_1, \dots, \xi_5) = p(\xi_1, \xi_2, \xi_3) p(\xi_4, \xi_5), \quad (4.9)$$

where $p(\xi_4, \xi_5)$ denotes the probability distribution of (ξ_4, ξ_5) . Hence $p(\xi_4, \xi_5)$ is a factor in both the numerator and denominator of (4.8) and we have

$$p^*(\xi_1, \xi_2, \xi_3) = \frac{|\Omega| p(\xi_1, \xi_2, \xi_3)}{M}, \quad (4.10)$$

where M denotes the normalizing constant

$$M = \int_{-\infty}^{\infty} \int_{-\infty}^{\infty} \int_{-\infty}^{\infty} |\Omega| p(\xi_1, \xi_2, \xi_3) d\xi_1 d\xi_2 d\xi_3. \quad (4.11)$$

Now the distribution of Ω at those points where the gradient is specified is given by

$$p^*(\Omega) d\Omega = \iiint_{d\Omega} p^*(\xi_1, \xi_2, \xi_3) d\xi_1 d\xi_2 d\xi_3 \quad (4.12)$$

where the triple integral is taken over the space between the two adjacent surfaces

$$\xi_1 \xi_3 - \xi_2^2 = \Omega, \quad \Omega + d\Omega. \quad (4.13)$$

Similarly for the previous distribution $p(\Omega)$ we have

$$p(\Omega) d\Omega = \iiint_{d\Omega} p(\xi_1, \xi_2, \xi_3) d\xi_1 d\xi_2 d\xi_3. \quad (4.14)$$

Sizes of images reflected in a random surface

95

But on substituting from (4.10) into (4.12) we see that over the region of integration the factor $|\Omega|$ is constant (to the first order). Hence

$$p^*(\Omega) = \frac{|\Omega|}{M} p(\Omega), \quad (4.15)$$

where $p(\Omega)$ is the distribution previously evaluated. Writing

$$\frac{\Omega}{(3H)^{\frac{1}{2}}} = \omega, \quad (4.16)$$

we have

$$p^*(\Omega) = \frac{1}{M} |\omega| f(\omega, \lambda), \quad (4.17)$$

where f is given by equation (3.9).

The constant M is related to the density of specular points per unit area of the surface and has been evaluated in (5), § 2.4. The result is

$$M = \frac{4}{\pi} (l_2 l_3)^{\frac{1}{2}} \left[\left(\frac{l_2 - l_1}{l_2} \right)^{\frac{1}{2}} E(k) - \left(\frac{l_2}{l_2 - l_1} \right)^{\frac{1}{2}} K(k) \right], \quad (4.18)$$

where $K(k)$ and $E(k)$ are the complete elliptic integrals of modulus

$$k = \sqrt{\frac{l_1(l_3 - l_2)}{l_3(l_1 - l_2)}} \quad (4.19)$$

and l_1, l_2, l_3 are the roots of the cubic equation

$$4l^3 - 3Hl - \Delta = 0 \quad (4.20)$$

in descending order.

To evaluate this expression numerically it is convenient to write

$$l_1, l_2, l_3 = \frac{1}{2}(3H)^{\frac{1}{2}}(\beta_1, \beta_2, \beta_3) \quad (4.21)$$

so that $\beta_1, \beta_2, \beta_3$ are the roots of

$$\beta^3 - \beta - \lambda = 0. \quad (4.22)$$

We have then

$$M = (2/\pi)(3H)^{\frac{1}{2}} \beta_1 \Phi(-\beta_2/\beta_1). \quad (4.23)$$

where

$$\Phi(t) = t^{\frac{1}{2}}(1-t)^{\frac{1}{2}} \left[\left(\frac{1+t}{t} \right)^{\frac{1}{2}} E(k) - \left(\frac{t}{1+t} \right)^{\frac{1}{2}} K(k) \right],$$

$$k = \sqrt{\frac{1-2t}{1-t^2}}. \quad (4.24)$$

The function Φ is shown graphically in Fig. 10 of (5). It is a very slowly varying function with a maximum value $\Phi(0) = 1$ (corresponding to $\lambda = 0$) and a minimum value $\Phi(\frac{1}{2}) = 0.907\dots$ (corresponding to $\lambda = 2/3^{\frac{1}{2}}$). Altogether we have

$$p^*(\Omega) = \frac{N}{(3H)^{\frac{1}{2}}} |\omega| f(\omega, \lambda), \quad (4.25)$$

where

$$N = \frac{\pi}{2\beta_1 \Phi(-\beta_2/\beta_1)}. \quad (4.26)$$

Values of N are given in Table 1 for some values of λ equally spaced over the range $0 \leq \lambda \leq 2/3^{\frac{1}{2}}$. It will be seen that N differs very little from 1.5 over the whole range.

5. *The distribution of $|\Omega|^{-1}$.* Since the apparent image size I is inversely proportional to $|\Omega|$, we consider now the statistical distribution of $|\Omega|^{-1}$ at specular points. Writing

$$\Omega^{-1} = \Psi \quad (5.1)$$

we have
$$p^*(\Psi) = \left| \frac{d\Omega}{d\Psi} \right| p^*(\Omega) = N(3H)^{\frac{1}{2}} |\omega|^3 f(\omega) \quad (5.2)$$

from (4.25); or if
$$\psi = \frac{1}{\omega} = \frac{(3H)^{\frac{1}{2}}}{\Omega} = (3H)^{\frac{1}{2}} \Psi \quad (5.3)$$

then
$$p^*(\Psi) = N(3H)^{\frac{1}{2}} \psi^{-3} f(\psi^{-1}). \quad (5.4)$$

The distribution of $|\Psi| = |\Omega|^{-1}$ is found by adding the two distributions for positive and negative values of Ψ . Thus

$$p^*(|\Psi|) = (3H)^{\frac{1}{2}} g(|\psi|), \quad (5.5)$$

where
$$g(|\psi|) = N |\psi|^{-3} [f(\psi) + f(-\psi)]. \quad (5.6)$$

Then the distribution of apparent image sizes is given by

$$p^*(I) = \frac{4(3H)^{\frac{1}{2}}}{q'} g(|\psi|) \quad (5.7)$$

from equation (2.4).

Table 1

$\lambda \times 3^{\frac{1}{2}}/2$	N	$\lambda \times 3^{\frac{1}{2}}/2$	N
0.0	1.571	0.6	1.534
0.1	1.568	0.7	1.525
0.2	1.563	0.8	1.517
0.3	1.557	0.9	1.509
0.4	1.550	1.0	1.500
0.5	1.542	—	—

The form of $g(|\psi|)$ is shown in Fig. 2 for the two extreme values of λ . The tables of $f(\omega)$ given in (2), and the graphs in (7), show that the curves for intermediate values of λ lie mainly between those for the two extreme values. But the whole family of curves lie so close together that for the sake of clarity only those for the extreme values of λ are shown.

A striking feature of the distributions is the very sharp cut-off at about $|\psi| = 0.1$. For large values of $|\omega|$ we have from § 7 of (7)

$$f(\omega) + f(-\omega) \sim C_1 \omega^{-\frac{1}{2}} e^{-C_2|\omega|}, \quad (5.8)$$

where C_1 and C_2 are constant; therefore for small values of $|\psi|$

$$g(|\psi|) \sim C_3 |\psi|^{-\frac{1}{2}} e^{-C_4/|\psi|}. \quad (5.9)$$

The average value of $|\psi|$ is very simple: we have

$$\int_0^{\infty} g(|\psi|) |\psi| d\psi = \int_{-\infty}^{\infty} N \psi^{-2} f(\psi) d\psi = \int_{-\infty}^{\infty} N f(\omega) d\omega = N, \quad (5.10)$$

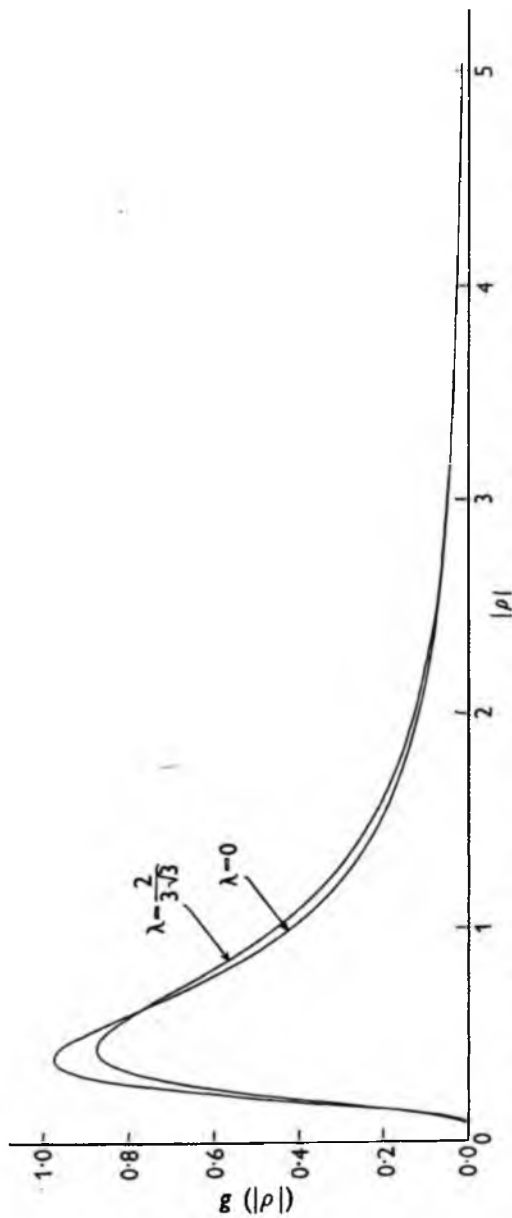


Fig. 2. Graph of $g(|\psi|)$ for the two extreme values of λ , showing the form of the distribution of image sizes.

since $f(\omega)$ itself is a probability distribution. From Table 1 we see that N lies between 1.5 and about 1.571 (that is to say $\frac{1}{2}\pi$). This mean value is somewhat greater than might be expected from Fig. 2, owing, no doubt, to the long 'tail' on the positive side of the distribution.

The second moment of $g(|\psi|)$, and all higher moments, are infinite.

From (5.10) it follows that the mean value of $|\Omega|^{-1}$ is given by

$$\text{av. } |\Omega|^{-1} = \text{av. } \frac{|\psi|}{(3H)^{\frac{1}{2}}} = \frac{N}{(3H)^{\frac{1}{2}}} \quad (5.11)$$

and the mean value of I is given by

$$\text{av. } I = \text{av. } \frac{g'}{4|\Omega|} = \frac{Ng'}{4(3H)^{\frac{1}{2}}}. \quad (5.12)$$

6. *Discussion and conclusions.* We have seen that the distribution of image sizes depends fundamentally on two parameters, H and λ , determined by the energy spectrum of the surface. The quantity $(3H)^{-\frac{1}{2}}$, which defines the scale of the distribution, is related to the spectrum of the surface by equation (3.7). We see that H is always positive (unless the surface degenerates into a single system of long-crested waves, in which case equation (2.3) becomes inapplicable). The parameter λ may lie anywhere between 0 and $2/3^{\frac{1}{2}}$ (see (7), § 8). The lower value $\lambda = 0$ is characteristic of two intersecting systems of long-crested waves; the upper value $\lambda = 2/3^{\frac{1}{2}}$ may occur in a variety of circumstances, for example, if the surface is isotropic, or if the angular spread of energy is small and has a certain 'peakedness' (see (7), § 8).

On the other hand, it has been shown in the present paper that the form of the distribution of image sizes is not critically dependent on λ , and that the distributions corresponding to different values of λ are very alike, even those corresponding to the two extreme values 0 and $2/3^{\frac{1}{2}}$.

Suppose then that the distribution of image sizes is observed; what information about the spectrum can be deduced? Clearly, the value of λ could not be determined accurately without very many observations. On the other hand, H could be determined quite reliably, for example, from equation (5.12), since N is very nearly equal to 1.5. Alternatively, H could be found from the position of the sharp cut-off at the lower end of the distribution.

The information given by H is summarized in equation (3.7). Let us transform to polar coordinates w, θ by the substitution

$$u, v = \omega \cos \theta, \omega \sin \theta, \quad (5.1)$$

so that w and θ denote the wave number $(u^2 + v^2)^{\frac{1}{2}}$ and direction $\tan^{-1} v/u$, respectively, for the distribution of energy in the spectrum. Then we have

$$H = \frac{1}{6} \int_0^\infty \int_0^\infty dw dw' \int_0^{2\pi} \int_0^{2\pi} d\theta d\theta' E(u, v) E(u', v') \omega^5 w'^5 \sin^4(\theta - \theta'). \quad (6.2)$$

If we assume that the spectrum has the form

$$E(u, v) = W(w) \Theta(\theta), \quad (6.3)$$

Sizes of images reflected in a random surface

99

where W is a function of w only and Θ is a function of θ only, then

$$H = \frac{1}{8} D^2 \int_0^{2\pi} \int_0^{2\pi} \Theta(\theta) \Theta(\theta') \sin^{-4}(\theta - \theta') d\theta d\theta', \quad (6.4)$$

where
$$D = \int_0^{\infty} W(w) w^5 dw. \quad (6.5)$$

D is essentially the fourth moment of the distribution with regard to wave number; for this is given by

$$M_4 = \int_{-\infty}^{\infty} \int_{-\infty}^{\infty} E(u, v) w^4 du dv = \int_0^{\infty} \int_0^{2\pi} \omega(w) \Theta(\theta) w^5 dw d\theta = D \quad (6.6)$$

provided that Θ is normalized:

$$\int_0^{2\pi} \Theta(\theta) d\theta = 1. \quad (6.7)$$

In particular, when the energy is confined to a narrow range of wavelengths, corresponding to a wave-number \bar{w} we have

$$D = M_4 = \bar{w}^4 M_0, \quad (6.8)$$

where M_0 is the moment of order zero, equal to the total energy in the surface per unit area (6).

When the surface is isotropic (which must be established by other means) then $\Theta = \text{constant} = (2\pi)^{-1}$, and so from (6.4)

$$H = \frac{1}{18} D^2. \quad (6.9)$$

If, on the other hand, the spectrum is fairly narrow in direction, then on replacing $\sin(\theta - \theta')$ by $(\theta - \theta')$ in (6.4) we have

$$H = \frac{1}{8} (t_4 t_0 - 4t_3 t_1 + 6t_2^2 - 4t_1 t_3 + t_0 t_4) \quad (6.10)$$

where t_n denotes the n th angular moment of the distribution:

$$t_n = \int \Theta(\theta) \theta^n d\theta \quad (6.11)$$

Assuming $t_1 = t_3 = 0$ as for a symmetrical distribution, and writing (as in (5))

$$\frac{t_2}{t_0} = \gamma^2, \quad \frac{t_0 t_4}{t_2^2} = \alpha^2 \quad (6.12)$$

we obtain
$$H = M_4^2 \gamma^2 (1 + \frac{1}{3} \alpha^2). \quad (6.13)$$

Here γ denotes the r.m.s. angular spread of the spectrum and α^2 denotes its 'peakedness'. For a normal distribution, $\alpha^2 = 3$ and so

$$H = 2\gamma^2 M_4^2. \quad (6.14)$$

If γ is determined independently, as for example in (5), then (6.14) provides us with a means of estimating M_4 .

REFERENCES

- (1) CARTWRIGHT, D. E. and LONGUET-HIGGINS, M. S. The statistical distribution of the maxima of a random function. *Proc. Roy. Soc. A*, 237 (1956), 212-32.
 (2) CATTON, DIANA and MILLIS, B. G. Numerical evaluation of the integral

$$\frac{1}{2\pi} \int_{-i\infty}^{i\infty} (\lambda\alpha^2 + \alpha^2 - 1)^{-\frac{1}{2}} e^{-z\alpha} d\alpha.$$

Proc. Camb. Phil. Soc. 54 (1958), 454-62.

- (3) COX, C. and MUNK, W. Measurement of the roughness of the sea surface from photographs of the sun's glitter. *J. Opt. Soc. Amer.* 44 (1954), 838-50.
 (4) COX, C. and MUNK, W. Slopes of the sea surface deduced from photographs of sun glitter. *Bull. Scripps Instn Oceanogr.* 6 (1956), 401-88.
 (5) LONGUET-HIGGINS, M. S. The statistical analysis of a random, moving surface. *Phil. Trans. Roy. Soc. A*, 249 (1957), 321-87.
 (6) LONGUET-HIGGINS, M. S. Statistical properties of an isotropic random surface. *Phil. Trans. Roy. Soc. A*, 250 (1957), 157-74.
 (7) LONGUET-HIGGINS, M. S. The statistical distribution of the curvature of a random gaussian surface. *Proc. Camb. Phil. Soc.* 54 (1958), 439-53.
 (8) PRIMAKOFF, H. and KELLER, J. B. Reflection and transmission of sound by thin curved shells. *J. Acoust. Soc. Amer.* 19 (1947), 820-32.
 (9) RICE, S. O. Mathematical analysis of random noise. *Bell. Syst. Tech. J.* 23 (1944), 282-332.
 (10) WEATHERBURN, C. E. *Differential geometry of three dimensions*, vol. 1 (Cambridge, 1939).

NATIONAL INSTITUTE OF OCEANOGRAPHY
 WORMLEY

Reprinted from the *Proceedings of the Cambridge Philosophical Society*,
Volume 56, Part 1, pp. 27-40, 1960.

PRINTED IN GREAT BRITAIN

THE FOCUSING OF RADIATION BY A RANDOM SURFACE WHEN THE SOURCE IS AT A FINITE DISTANCE

By M. S. LONGUET-HIGGINS

Received 13 June 1959

1. *Introduction and summary.* Imagine a nearly horizontal, statistically uniform, random surface $\zeta(x, y)$, Gaussian in the sense that the second derivatives $\partial^2\zeta/\partial x^2$, $\partial^2\zeta/\partial x\partial y$, $\partial^2\zeta/\partial y^2$ have a normal joint distribution. The problem considered is the statistical distribution of the quantity

$$F = \begin{vmatrix} 1 + \nu \frac{\partial^2\zeta}{\partial x^2} & \nu \frac{\partial^2\zeta}{\partial x\partial y} \\ \nu \frac{\partial^2\zeta}{\partial x\partial y} & 1 + \nu \frac{\partial^2\zeta}{\partial y^2} \end{vmatrix} = 1 + \nu J + \nu^2 \Omega, \quad (1.1)$$

where J and Ω denote the mean curvature and total curvature of the surface, respectively, and ν is a constant parameter.

In a previous paper (2) the distribution of J and Ω separately was determined; the distribution of F reduces to that of $\nu^2\Omega$ as ν tends to infinity. The previous results were applicable to the focusing of radiation reflected by the surface when the source of radiation and the observer were both at infinite distance from the surface. The present results apply to a source or observer at finite distance, provided that the radiation falls nearly vertically.

The problem is solved completely when the surface is statistically isotropic; typical curves for the distribution of F are shown in Fig. 2. The family of curves depends upon a single parameter A proportional to the square of ν (i.e. height above the surface) and to the mean-square value of J , the mean curvature.

From this distribution we deduce the distribution of the sizes of images reflected in the surface (see Fig. 4), which is also equivalent to the distribution of the intensity, provided the radiation from each image is considered separately.

The general distribution for an anisotropic surface depends in addition on three further parameters of the surface B_1 , B_2 , B_3 (and no others). It is shown that in the extreme case when $A \ll 1$ the other three parameters do not affect the distribution, while if $A \gg 1$ only one of the three enters the solution, and then as a simple scale-factor. So from the form of the distribution, together with the observed distribution of image-size or intensity, it may be possible to determine the parameter A with a fair degree of certainty.

2. *Parameters of the surface.* In the notation of (2) the joint distribution of

$$(\xi_1, \xi_2, \xi_3) = \left(\frac{\partial^2\zeta}{\partial x^2}, \frac{\partial^2\zeta}{\partial x\partial y}, \frac{\partial^2\zeta}{\partial y^2} \right) \quad (2.1)$$

is given by

$$p(\xi_1, \xi_2, \xi_3) = \frac{1}{(2\pi)^{\frac{3}{2}} \Delta^{\frac{1}{2}}} \exp \left[-\frac{1}{2} \sum_{ij} M_{ij} \xi_i \xi_j \right], \quad (2.2)$$

where

$$(M_{ij}) = \begin{pmatrix} m_{40} & m_{31} & m_{22} \\ m_{31} & m_{22} & m_{13} \\ m_{22} & m_{13} & m_{04} \end{pmatrix}^{-1} = \Xi^{-1} \quad (2.3)$$

say;

$$\Delta = |\Xi|, \quad (2.4)$$

and the quantities m_{pq} are moments of the energy spectrum $E(u, v)$ of the surface $\zeta(x, y)$:

$$m_{pq} = \int_{-\infty}^{\infty} \int_{-\infty}^{\infty} E(u, v) u^p v^q du dv. \quad (2.5)$$

(They are also derivatives of the correlation function of $\zeta(x, y)$.) In the above integral the quantities u, v correspond to wave-numbers in the x, y directions, and evidently the quantities m_{pq} depend on the particular orientation chosen for the axes of x, y . The physical problem, however, is independent of choice of axes. So we shall expect to be concerned with parameters that are invariant with respect to rotation of the axes of x, y . With the aid of polar coordinates, defined by

$$\left. \begin{aligned} (u, v) &= (w \cos \theta, w \sin \theta), \\ (u', v') &= (w' \cos \theta', w' \sin \theta'), \\ (u'', v'') &= (w'' \cos \theta'', w'' \sin \theta''), \end{aligned} \right\} \quad (2.6)$$

such invariants may be written down at will. For example,

$$\left. \begin{aligned} D &= \iint E(u, v) w^4 du dv, \\ 2G &= \iiint E(u, v) E(u', v') w^4 w'^4 \sin^2(\theta - \theta') du dv du' dv', \\ 6H &= \iiint E(u, v) E(u', v') w^4 w'^4 \sin^4(\theta - \theta') du dv du' dv', \\ 6\Delta &= \iiint E(u, v) E(u', v') E(u'', v'') w^4 w'^4 w''^4 \\ &\quad \times \sin^2(\theta' - \theta'') \sin^2(\theta'' - \theta) \sin^2(\theta - \theta') du dv du' dv' du'' dv''. \end{aligned} \right\} \quad (2.7)$$

(The physical significance of H, Δ is discussed more fully in (3).) By substituting from equation (2.6) and separating the various terms we have identically

$$\left. \begin{aligned} D &= m_{40} + 2m_{22} + m_{04}, \\ G &= (m_{40} + m_{22})(m_{22} + m_{04}) - (m_{31} + m_{13})^2, \\ 3H &= m_{40} m_{04} - 4m_{31} m_{13} + 3m_{22}^2, \\ \Delta &= \begin{vmatrix} m_{40} & m_{31} & m_{22} \\ m_{31} & m_{22} & m_{13} \\ m_{22} & m_{13} & m_{04} \end{vmatrix}. \end{aligned} \right\} \quad (2.8)$$

Focusing of radiation by a random surface

29

Now the five moments m_{40} , m_{31} , m_{22} , m_{13} , m_{04} are independent. Rotation of the axes represents one degree of freedom, and one therefore expects just four independent invariant combinations of the moments, unchanged by rotation of the axes. Four such independent combinations are in fact D , G , H and Δ . Another invariant which will occur in the following, namely

$$\begin{aligned} G' &= \frac{1}{2} \iint E(u, v) E(u', v') w^4 w'^4 \sin^2(\theta - \theta') \cos^2(\theta + \theta') du dv du' dv' \\ &= m_{22}(m_{40} - 2m_{22} + m_{04}) - (m_{31} - m_{13})^2, \end{aligned} \quad (2-9)$$

is expressible in terms of the other four. Evidently

$$G' = G - 3H. \quad (2-10)$$

In the special case when the surface is *isotropic* all the above parameters are expressible in terms of one only, say D . For then $E(u, v)$ is a function of w only; on replacing $du dv$ by $w dw d\theta$ and carrying out the integrations with respect to θ we find

$$G = \frac{1}{4}D^2, \quad H = \frac{1}{16}D^2, \quad \Delta = \frac{1}{4}D^2, \quad (2-11)$$

and hence

$$G' = \frac{1}{16}D^2. \quad (2-12)$$

If on the other hand the surface consists of two intersecting systems of long-crested waves crossing at an angle θ_0 , and if $D = D^{(1)}, D^{(2)}$ for the two systems individually, then in the combined system we have

$$\left. \begin{aligned} D &= D^{(1)} + D^{(2)}, \\ G &= D^{(1)}D^{(2)} \sin^2 \theta_0, & 3H &= D^{(1)}D^{(2)} \sin^4 \theta_0, \\ G' &= D^{(1)}D^{(2)} \sin^2 \theta_0 \cos^2 \theta_0, & \Delta &= 0. \end{aligned} \right\} \quad (2-13)$$

In the particular case when $D^{(1)} = D^{(2)} = \frac{1}{2}D$ (i.e. mean-square curvatures are equal for the two systems) then

$$G = \frac{1}{4}D^2 \sin^2 \theta_0, \quad H = \frac{1}{12}D^2 \sin^4 \theta_0, \quad G' = \frac{1}{16}D^2 \sin^2 2\theta_0. \quad (2-14)$$

3. *The distribution of F.* From the definition of F we have

$$F = 1 + \nu(\xi_1 + \xi_2) + \nu^2(\xi_1 \xi_2 - \xi_3^2), \quad (3-1)$$

where the joint distribution of (ξ_1, ξ_2, ξ_3) is given by (2-2). By a real linear transformation

$$\xi_i = \sum_j a_{ij} \eta_j \quad (3-2)$$

we may make

$$\left. \begin{aligned} \sum_j M_{ij} \xi_i \xi_j &= \eta_1^2 + \eta_2^2 + \eta_3^2, \\ \xi_1 \xi_2 - \xi_3^2 &= l_1 \eta_1^2 + l_2 \eta_2^2 + l_3 \eta_3^2, \end{aligned} \right\} \quad (3-3)$$

say. Then the joint distribution of η_1, η_2, η_3 is

$$p(\eta_1, \eta_2, \eta_3) = \frac{1}{(2\pi)^{\frac{3}{2}}} \exp \left[-\frac{1}{2}(\eta_1^2 + \eta_2^2 + \eta_3^2) \right] \quad (3-4)$$

and we have

$$F = \chi_1 + \chi_2 + \chi_3 + \chi_4. \quad (3-5)$$

30

M. S. LONGUET-HIGGINS

where

$$\left. \begin{aligned} \chi_j &= l_j \left(v \eta_j + \frac{a_{1j} + a_{3j}}{2l_j} \right)^2 \quad (j = 1, 2, 3), \\ \chi_4 &= 1 - \sum_{j=1}^3 \frac{(a_{1j} + a_{3j})^2}{4l_j}. \end{aligned} \right\} \quad (3.6)$$

This expresses F as the sum of functions χ_j whose characteristic functions

$$\phi_j(t) = \int_{-\infty}^{\infty} p(\chi_j) e^{i\chi_j t} d\chi_j \quad (3.7)$$

are known. In fact we have

$$\left. \begin{aligned} \phi_j(t) &= (1 - 2l_j i\nu^2 t)^{-1} \exp \left[\frac{it(a_{1j} + a_{3j})^2}{4l_j(1 - 2l_j i\nu^2 t)} \right] \quad (j = 1, 2, 3), \\ \phi_4(t) &= \exp \left[it - it \sum_{j=1}^3 \frac{it(a_{1j} + a_{3j})^2}{4l_j(1 - 2l_j i\nu^2 t)} \right]. \end{aligned} \right\} \quad (3.8)$$

The characteristic function of F is the product of the characteristic functions ϕ_j , that is

$$\phi(t) = \frac{\exp \left[it + \frac{1}{2}(it)^2 \nu^2 \sum (a_{1j} + a_{3j})^2 / (1 - 2l_j i\nu^2 t) \right]}{[(1 - 2l_1 i\nu^2 t)(1 - 2l_2 i\nu^2 t)(1 - 2l_3 i\nu^2 t)]^{\frac{1}{2}}}. \quad (3.9)$$

Now from (2), equations (5.12) we have

$$l_1 + l_2 + l_3 = 0, \quad l_2 l_3 + l_3 l_1 + l_1 l_2 = -\frac{3}{4}H, \quad l_1 l_2 l_3 = \frac{1}{4}\Delta; \quad (3.10)$$

and it may also be shown (see Appendix) that

$$\sum_j (a_{1j} + a_{3j})^2 = D, \quad \sum_j l_j^{-1} (a_{1j} + a_{3j})^2 = 4, \quad \sum_j l_j (a_{1j} + a_{3j})^2 = G. \quad (3.11)$$

By means of these relations $\phi(t)$ is reduced to

$$\phi(t) = \frac{\exp \left[it \frac{1 + \frac{1}{2}D(i\nu^2 t) + G'(i\nu^2 t)^2}{1 - 3H(i\nu^2 t)^2 - 2\Delta(i\nu^2 t)^3} \right]}{[1 - 3H(i\nu^2 t)^2 - 2\Delta(i\nu^2 t)^3]^{\frac{1}{2}}}. \quad (3.12)$$

The probability distribution of F is now found from

$$p(F) = \frac{1}{2\pi} \int_{-\infty}^{\infty} \phi(t) e^{iFt} dt. \quad (3.13)$$

Writing

$$\frac{1}{2} \nu^2 D = A, \quad (3.14)$$

$$\frac{G'}{D^2} = \frac{1}{16} B_1, \quad \frac{H}{D^2} = \frac{1}{16} B_2, \quad \frac{\Delta}{D^3} = \frac{1}{64} B_3, \quad (3.15)$$

(so that in the isotropic case B_1, B_2, B_3 will reduce to unity) and changing the variable of integration to

$$\alpha = Ait, \quad (3.16)$$

we have finally

$$p(F) = \frac{1}{2\pi A} \int_{-\infty}^{\infty} \frac{\exp \left[\frac{\alpha}{A} \left(\frac{1 + 2\alpha + B_1 \alpha^2}{1 - 3B_2 \alpha^2 - 2B_3 \alpha^3} - F \right) \right]}{[2B_2 \alpha^3 + 3B_3 \alpha^2 - 1]^{\frac{1}{2}}} d\alpha, \quad (3.17)$$

where that value of the square root is taken which has negative real part at $\alpha = -i\infty$.

Focusing of radiation by a random surface

31

4. *Discussion: the isotropic case.* For general values of the ratios B_1, B_2, B_3 the distribution $p(F)$ is not expressible in terms of known functions, as may be shown even in the special case when A is large (see (2)). However, if the surface is isotropic we have from (2.11) and (3.15)

$$B_1 = B_2 = B_3 = 1, \quad (4.1)$$

giving

$$p(F) = \frac{1}{2\pi A} \int_{-i\infty}^{i\infty} \frac{\exp\left[\frac{\alpha}{A} \left(\frac{1}{1-2\alpha} - F\right)\right]}{(\alpha+1)(2\alpha-1)^{\frac{1}{2}}} d\alpha. \quad (4.2)$$

This function has different forms for positive F and for negative F . When F is negative the contour of integration may be completed by a semi-circle of infinite radius in the left half-plane, since the integrand satisfies Jordan's lemma (see (5)). Hence

$$p(F) = 2\pi i \times \{\text{residue of integrand at } \alpha = -1\} = \frac{1}{A\sqrt{3}} e^{(F-1)A}. \quad (4.3)$$

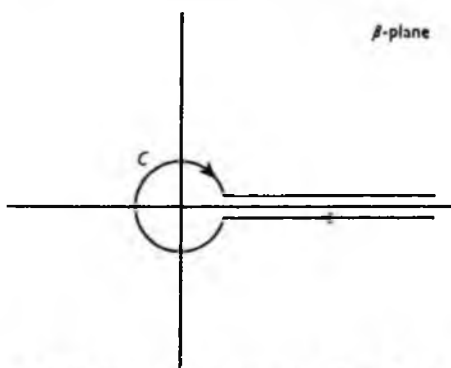


Fig. 1. Contour of integration when $F > 0$.

When F is positive, we may proceed as follows. Write $F/A = \psi$. Then on multiplying $p(F)$ by $e^{-\psi}$ and differentiating under the integral sign we have

$$-\frac{d}{d\psi} [e^{-\psi} p(F)] = \frac{1}{2\pi A} \int_{-i\infty}^{i\infty} \frac{\exp\left[\frac{\alpha}{A} \left(\frac{1}{1-2\alpha}\right) - (\alpha+1)\psi\right]}{(2\alpha-1)^{\frac{1}{2}}} d\alpha. \quad (4.4)$$

On setting $2\alpha - 1 = 2\psi^{-1}\beta$ the above expression becomes

$$\frac{1}{2\pi A(2\psi)^{\frac{1}{2}}} \exp\left[-\frac{1}{2A} - \frac{3\psi}{2}\right] \int_C \exp\left[-\left(\frac{\psi}{A\beta} + \beta\right)\right] \frac{d\beta}{\beta^{\frac{1}{2}}}, \quad (4.5)$$

where the contour C may now be deformed as in Fig. 1. The integral may be recognized as a Bessel function of order $-\frac{1}{2}$ (see for example (5), Chapter 17) or directly as the hyperbolic cosine

$$2\pi^{\frac{1}{2}} \cosh(\psi/A)^{\frac{1}{2}}. \quad (4.6)$$

After substitution in (4.4) and integration with respect to ψ from ψ to ∞ we have

$$e^{-\psi} p(F) = \frac{1}{(2\pi)^{\frac{1}{2}} A} e^{-1/2A} \int_{F/A}^{\infty} e^{-\psi} \cosh\left(\frac{\psi}{A}\right)^{\frac{1}{2}} \frac{d\psi}{\psi^{\frac{1}{2}}}. \quad (4.7)$$

The substitution $z^2 = 3\psi/2$ gives

$$e^{-\psi} p(F) = \frac{1}{(3\pi)^{\frac{1}{2}} A} e^{-1/2A} \int_{(3F/2A)^{\frac{1}{2}}}^{\infty} e^{-z^2} [e^{(2/3A)^{\frac{1}{2}} z} + e^{-(2/3A)^{\frac{1}{2}} z}] dz. \quad (4.8)$$

$$= \frac{1}{2\sqrt{3}A} e^{-1/3A} \left[\operatorname{erfc} \left\{ \left(\frac{3F}{2A} \right)^{\frac{1}{2}} + \left(\frac{1}{6A} \right)^{\frac{1}{2}} \right\} + \operatorname{erfc} \left\{ \left(\frac{3F}{2A} \right)^{\frac{1}{2}} - \left(\frac{1}{6A} \right)^{\frac{1}{2}} \right\} \right], \quad (4.9)$$

where
$$\operatorname{erfc}(x) = \frac{2}{\pi^{\frac{1}{2}}} \int_x^{\infty} e^{-z^2} dz. \quad (4.10)$$

Multiplying by e^{ψ} and combining this result with that for negative F , we have altogether

$$p(F) = \frac{1}{\sqrt{3}A} e^{(F-1)\nu A} \times \begin{cases} 1 & (F < 0), \\ \frac{1}{2} \left[\operatorname{erfc} \left\{ \left(\frac{3F}{2A} \right)^{\frac{1}{2}} + \left(\frac{1}{6A} \right)^{\frac{1}{2}} \right\} + \operatorname{erfc} \left\{ \left(\frac{3F}{2A} \right)^{\frac{1}{2}} - \left(\frac{1}{6A} \right)^{\frac{1}{2}} \right\} \right] & (F > 0). \end{cases} \quad (4.11)$$

Limiting forms. For small values of the parameter A the arguments of the error functions are large. Since, as $x \rightarrow \infty$,

$$\operatorname{erfc}(x) \sim \frac{1}{\pi^{\frac{1}{2}}} \frac{e^{-x^2}}{x} \quad (4.12)$$

we find
$$p(F) \sim \left(\frac{1}{8\pi A} \right)^{\frac{1}{2}} e^{-(F-1)^2/2A}. \quad (4.13)$$

In other words F is almost normally distributed about $F = 1$ with variance $4A$. This is what we should expect since for small A (that is, in effect for small ν) we have from equation (1.1)

$$F \doteq 1 + \nu J \quad (4.14)$$

and it is well known that the distribution of J is normal, with variance D . (The probability of negative F is negligible.)

On the other hand for large values of A we have, writing

$$F = A\psi, \quad p(\psi) = Ap(F), \quad (4.15)$$

the limiting form

$$p(\psi) = \frac{1}{\sqrt{3}} e^{\psi} \times \begin{cases} 1 & (\psi < 0), \\ \operatorname{erfc} \left(\frac{3}{2} \psi \right)^{\frac{1}{2}} & (\psi > 0). \end{cases} \quad (4.16)$$

This is in agreement with the distribution of the total curvature for an isotropic surface found previously (2). In fact for large values of A

$$F \doteq \nu^2 \Omega, \quad (4.17)$$

while for isotropy
$$A = \frac{1}{2} \nu^2 D = \nu^2 H^{\frac{1}{2}}, \quad (4.18)$$

so that
$$\psi = \frac{F}{A} \doteq \frac{\Omega}{H^{\frac{1}{2}}} = \sqrt{3} \omega. \quad (4.19)$$

The distribution of ω , as given by equation (7.14) of (2), will be seen to agree with (4.16) above.

Focusing of radiation by a random surface

33

For general values of A the distributions $p(F)$, given by (4.11), may still be computed numerically, for example, by means of the excellent tables in (4). Some typical curves are shown in Fig. 2. The transition from the normal probability curve to the skew curve appropriate to the distribution (4.16) can be clearly seen.

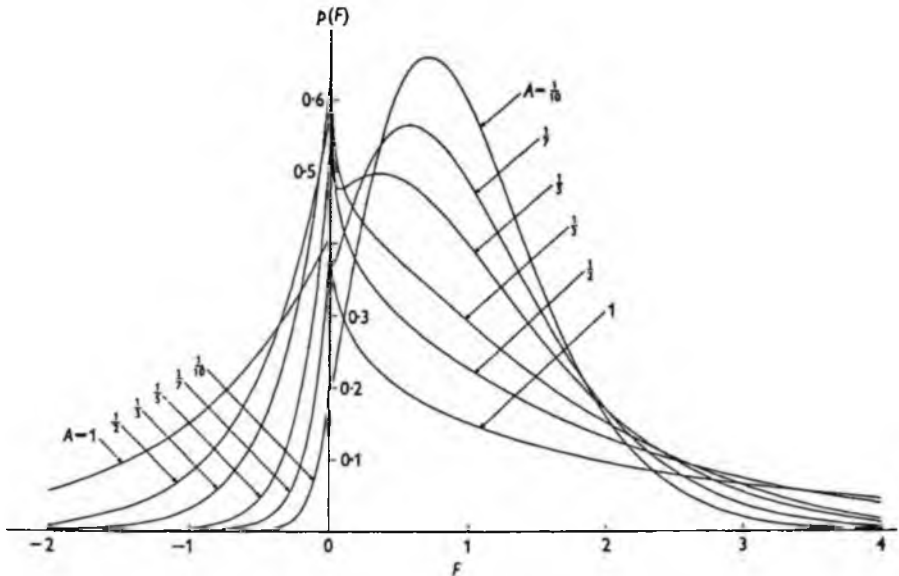


Fig. 2. The statistical distribution of F for an isotropic surface.

The value of $p(F)$ at the origin is simply

$$p(0) = \frac{1}{\sqrt{3}A} e^{-1/3A}, \quad (4.20)$$

which has a maximum value $\sqrt{3}e^{-1}$ attained when $A = \frac{1}{3}$. The probability of negative F is given by

$$\int_{-\infty}^0 p(F) dF = \frac{1}{\sqrt{3}} e^{-1/3A}, \quad (4.21)$$

which diminishes very rapidly as A decreases beyond about 0.1.

5. *Applications.* Imagine a source of radiation at a point O , height h_1 above or below a nearly horizontal surface, as in Fig. 3 (a). The radiation is reflected from the surface at a typical point P and received at a corresponding point Q on a horizontal plane distant h_2 from the mean surface level. It is supposed that OP and PQ are both nearly vertical. If x, y denote the horizontal coordinates of P , and x', y' the coordinates of Q relative to O as origin, then we have

$$\begin{aligned} x' &= (1 + h_2/h_1) \left(x + h_1 \frac{\partial \xi}{\partial x} \right), \\ y' &= (1 + h_2/h_1) \left(y + h_1 \frac{\partial \xi}{\partial y} \right), \end{aligned} \quad (5.1)$$

where $z = \zeta(x, y)$ is the equation of the surface. If now the point P describes a small closed circuit of area da , the corresponding point Q describes a circuit of area da' where

$$\frac{da'}{da} = \left| \frac{\partial(x', y')}{\partial(x, y)} \right| = (1 + h_2/h_1)^2 |F|. \quad (5.2)$$

Here F is given by equation (1.1) with h_1 replacing ν . Hence the area of the image of the source at P , as seen from Q is proportional to $|F|^{-1}$. In fact, since $F = 1$ for a flat surface, the image area is simply

$$a = a_0 |F|^{-1}, \quad (5.3)$$

where a_0 is the area of the image reflected by a plane surface at P .

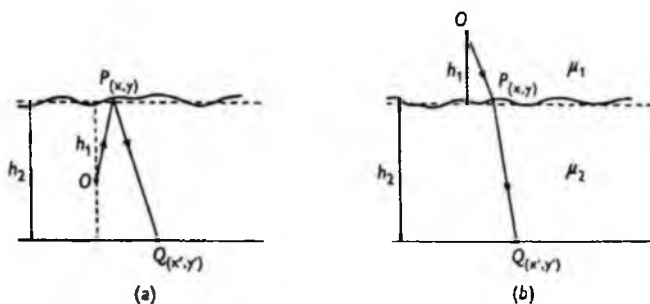


Fig. 3. Definition of parameters for (a) reflexion and (b) refraction.

Similarly, if I_0 denote the intensity of radiation at Q supposing the curvature to be zero, the intensity at Q due to radiation received from the neighbourhood of P is

$$I = I_0 |F|^{-1}. \quad (5.4)$$

(If, however, more than one image is seen at Q , say from P_1, P_2, \dots, P_N then the total intensity will be the sum of such expressions evaluated at P_1, P_2, \dots, P_N .)

Suppose now that we wish to find the statistical distribution of the image-sizes, as seen from an arbitrary point $Q(x', y')$. We have already obtained the statistical distribution of F at a fixed point $P(x, y)$, for an ensemble of surfaces; and assuming the surface is ergodic with respect to space and time, this distribution $p(F)$ is the same as would be obtained by random sampling of a particular surface $\zeta(x, y)$ at points distributed uniformly with regard to x, y (and not too far from the origin). But we require the distribution $p^*(F)$ for points Q uniformly spaced in the (x', y') -plane. The concentration of sampling points $Q(x', y')$ differs from that of the corresponding points $P(x, y)$ by a factor

$$\left| \frac{\partial(x', y')}{\partial(x, y)} \right| = (1 + h_2/h_1)^2 |F| \quad (5.5)$$

and hence we have

$$p^*(F) = c |F| p(F), \quad (5.6)$$

where c is a pure constant, which may be found by the condition that

$$1 = \int_{-\infty}^{\infty} p^*(F) dF = c \int_{-\infty}^{\infty} |F| p(F) dF. \quad (5.7)$$

Focusing of radiation by a random surface

35

In the case of an isotropic surface it is found without difficulty that

$$\int_{-\infty}^{\infty} |F| p(F) dF = 1 + \frac{2A}{\sqrt{3}} e^{-1/3A} \quad (5.8)$$

and hence

$$c = \left[1 + \frac{2A}{\sqrt{3}} e^{-1/3A} \right]^{-1}. \quad (5.9)$$

This distribution of $\vartheta = |F|^{-1}$ is given by

$$p^*(\vartheta) = \left| \frac{dF}{d\vartheta} \right| [p^*(F) + p^*(-F)], \quad (5.10)$$

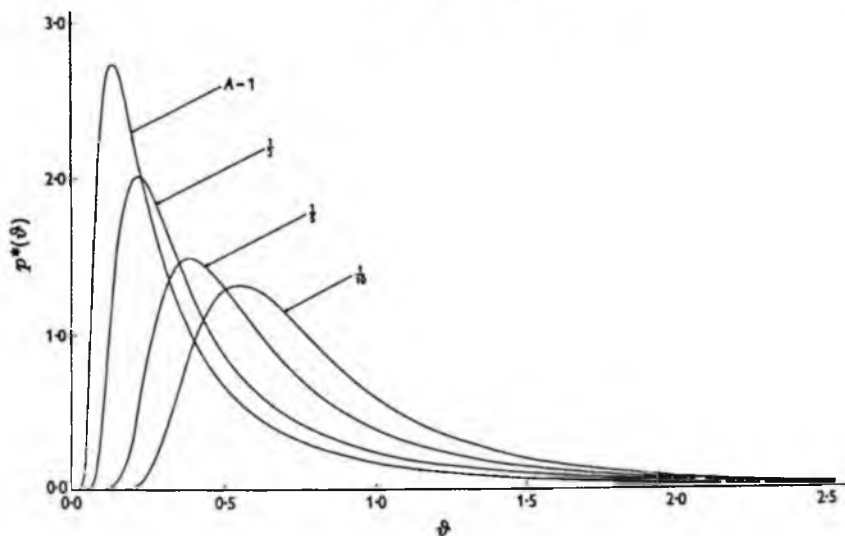


Fig. 4. The statistical distribution of $\vartheta = |F|^{-1}$, giving the distribution of image sizes.

where $F = \vartheta^{-1}$ and $p^*(F)$ is given by equation (5.6): that is

$$p^*(\vartheta) = c |F|^2 [p^*(F) + p^*(-F)]_{F=\vartheta^{-1}}. \quad (5.11)$$

The mean value of this distribution is given by

$$\bar{\vartheta} = \int_0^{\infty} \vartheta p^*(\vartheta) d\vartheta = c \int_{-\infty}^{\infty} p(F) dF = c, \quad (5.12)$$

some values of which are given in Table 1. All higher moments are infinite.

The family of distributions is shown in Fig. 4, for various values of the parameter A . Two limiting forms may be noted: when $A \ll 1$

$$p(\vartheta) \sim \left(\frac{1}{8\pi A} \right) e^{-\vartheta - 1/3A}, \quad (5.13)$$

that is to say a normal distribution centred on $\vartheta = 1$. Secondly when $A \gg 1$ we have

$$p(\vartheta) \sim \frac{1}{2A^2} \left[e^{-1/4A\vartheta} + e^{1/4A\vartheta} \operatorname{erfc} \left(\frac{3}{2A\vartheta} \right)^{1/2} \right], \quad (5.14)$$

which will be found to be identical with the distribution of image-sizes for distant points, as given in (3).

M. S. LONGUET-HIGGINS

Table 1. Mean values of ϑ

A	$\bar{\vartheta}$	A	$\bar{\vartheta}$
0	1.0000	$\frac{1}{2}$	0.8760
$\frac{1}{10}$	0.9959	$\frac{1}{2}$	0.7714
$\frac{1}{5}$	0.9842	1	0.5472
$\frac{1}{2}$	0.9582	2	0.3384
—	—	∞	$A \times 0.8660$

The distributions clearly become less symmetrical as the parameter A increases. The conventional measures of skewness (see for example (1)) are inapplicable since the higher moments of the distribution are infinite. However, the curves generally have a very sharp cut-off on the lower side, and a convenient measure of the skewness is given by

$$\beta = \vartheta^{(1,20)} / \bar{\vartheta}, \quad (5.15)$$

where $\bar{\vartheta}$ is the mean and $\vartheta^{(1,20)}$ the value of ϑ such that 5% of the distribution lies to the left of it:

$$\int_0^{\vartheta^{(1,20)}} p(\vartheta) d\vartheta = \frac{1}{20}. \quad (5.16)$$

Values of β have been determined graphically and are shown in figure 5 against the parameter $A^{\frac{1}{2}}$.

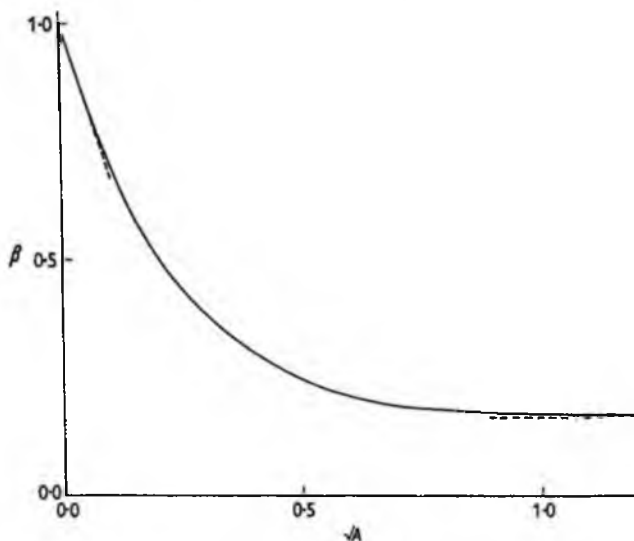


Fig. 5. Skewness of the curves in Fig. 4, as a function of \sqrt{A} .

A precisely similar reasoning will apply when the source O and the receiver Q are on opposite sides of a surface bounding two refracting media, of indices μ_1 and μ_2 (see Fig. 3(b)). Then with the same notation we have

$$\left. \begin{aligned} x' &= \left(1 + \frac{\mu_2 h_2}{\mu_1 h_1} \right) \left(x + \frac{(\mu_2 - \mu_1) h_1 h_2}{\mu_1 h_1 + \mu_2 h_2} \frac{\partial \zeta}{\partial x} \right), \\ y' &= \left(1 + \frac{\mu_2 h_2}{\mu_1 h_1} \right) \left(y + \frac{(\mu_2 - \mu_1) h_1 h_2}{\mu_1 h_1 + \mu_2 h_2} \frac{\partial \zeta}{\partial y} \right), \end{aligned} \right\} \quad (5.17)$$

Focusing of radiation by a random surface

37

and the analysis proceeds exactly as before, but with

$$\nu = \frac{(\mu_2 - \mu_1) h_1 h_2}{\mu_1 h_1 + \mu_2 h_2}. \quad (5.18)$$

The same analytical function (5.11) clearly describes the distribution of the intensity I in the plane of Q provided, however, that the radiation from each image is considered separately. When there is an appreciable chance that more than one image may be seen at a time, then the sum of the intensities has a difference law of distribution. In this case, however, at least one of the images must correspond to a negative value of F . The present distribution will therefore apply to the total intensity only when the probability of negative F , given by equation (4.21), is negligible.

6. *Anisotropic surfaces.* Generally, as we have seen, the distribution of $|F|^{-1}$ depends upon four independent parameters A, B_1, B_2, B_3 ; we have so far fully evaluated only the distribution for an isotropic surface, which depends on A alone. To what extent are the results applicable to anisotropic surfaces?

Some kind of answer can be given in the two extreme cases $A \ll 1$ and $A \gg 1$. In the former case we have seen that $F \doteq 1 + \nu J$, and, since the distribution of J depends always on one parameter D , it follows that the distribution of F (and likewise of $|F|^{-1}$) depends only on A . Hence for small values of A the above distributions are independent of the other three parameters, and are valid generally.

When on the other hand $A \gg 1$, it has been shown in a previous paper (3) that the distribution of $|F|^{-1}$ depends on two parameters. One of these,

$$\nu^2 H^{\frac{1}{2}} = B_2^{\frac{1}{2}} A, \quad (6.1)$$

determines the scale of the distribution. The other,

$$H^{\frac{1}{2}}/\Delta = B_2^{\frac{1}{2}}/B_3, \quad (6.2)$$

hardly affects the distribution of $|F|^{-1}$ at all, so that for practical purposes the only variable parameter is $B_2^{\frac{1}{2}} A$. For an isotropic surface B_2 takes the value 1. Thus the above results (for large A) are applicable provided only that A is replaced by $B_2^{\frac{1}{2}} A$, that is, the scale of the distribution is stretched by a factor $B_2^{\frac{1}{2}}$.

From the definitions (3.15) we have

$$B_2^{\frac{1}{2}} = 4H^{\frac{1}{2}}/D, \quad (6.3)$$

which may vary considerably, but is generally of order 1. For example, if the surface consists of two long-crested systems of waves intersecting at an angle θ_0 we have from (2.14)

$$B_2^{\frac{1}{2}} = \left(\frac{2}{3}\right)^{\frac{1}{2}} \sin \theta_0. \quad (6.4)$$

It is curious that when $\theta_0 = \sin^{-1} \left(\frac{3}{4}\right)^{\frac{1}{2}} = \frac{1}{2}\pi$

(that is, the two systems intersect at an angle of 60°), then $B_2 = 1$ and the limiting form for $p^*(\vartheta)$ is valid without any change of scale.

7. *Conclusions.* It has been shown that the random surface $\zeta(x, y)$ is fully characterized, for the present purpose, by four independent parameters D, G, H and Δ . The distribution of F is found to depend on all four of these, which, when combined with ν ,

M. S. LONGUET-HIGGINS

give four non-dimensional parameters A, B_1, B_2, B_3 for the distribution (§ 3). However, when the surface is isotropic the number of parameters is reduced to one, and the distribution is dependent on the parameter A only. Moreover, the distribution of F is then expressible in terms of known analytical functions.

For very small values of A the distribution tends always to a normal curve, irrespective of the values of B_1, B_2, B_3 ; for large values of A the distribution tends to a form which depends only on the scale-factor $B_2^{\frac{1}{2}}A$ (which equals unity both for an isotropic surface and for two long-crested systems of waves intersecting at an angle of 60°). Hence the form of the distribution, apart from its scale, may depend mainly on A throughout the whole of its range, so that the curves computed for the isotropic case are typical. From the skewness of these curves the parameter A can be fairly well estimated provided $A < 1$. When A increases beyond 1 it becomes easier to estimate $3B_2A^2$, the mean-square value of $v^2\Omega$.

APPENDIX

Proof of equations (3.11)

Let us introduce new variables $\zeta_1, \zeta_2, \zeta_3$, linearly dependent on ξ_1, ξ_2, ξ_3 , by

$$\zeta_i = \sum_j T_{ij} \xi_j, \quad (\text{A } 1)$$

where

$$(T_{ij}) = \begin{pmatrix} 1 & 0 & 1 \\ 0 & 1 & 0 \\ 1 & 0 & -1 \end{pmatrix}. \quad (\text{A } 2)$$

In matrix notation this can be written $\xi = T\zeta$. Inverting, we have

$$\zeta = T^{-1}\xi = T^{-1}a\eta = b\eta, \quad (\text{A } 3)$$

where a denotes the matrix (a_{ij}) , and $b = T^{-1}a$. Since

$$T^{-1} = \begin{pmatrix} \frac{1}{2} & 0 & \frac{1}{2} \\ 0 & 1 & 0 \\ \frac{1}{2} & 0 & -\frac{1}{2} \end{pmatrix} \quad (\text{A } 4)$$

this gives in particular

$$b_{11} = \frac{1}{2}(a_{11} + a_{31}), \quad b_{12} = \frac{1}{2}(a_{12} + a_{32}), \quad b_{13} = \frac{1}{2}(a_{13} + a_{33}), \quad (\text{A } 5)$$

and our object is now to prove

$$b_{11}^2 + b_{12}^2 + b_{13}^2 = \frac{1}{4}D, \quad (\text{A } 6)$$

$$l_1^{-1}b_{11}^2 + l_2^{-1}b_{12}^2 + l_3^{-1}b_{13}^2 = 1, \quad (\text{A } 7)$$

$$l_1 b_{11}^2 + l_2 b_{12}^2 + l_3 b_{13}^2 = \frac{1}{4}G. \quad (\text{A } 8)$$

With the above transformation we have

$$\left. \begin{aligned} \xi_1 \xi_1 - \xi_2^2 &= \zeta_1^2 - \zeta_2^2 - \zeta_3^2, \\ \sum_{ij} M_{ij} \xi_i \xi_j &= \sum_{ij} N_{ij} \zeta_i \zeta_j, \end{aligned} \right\} \quad (\text{A } 9)$$

Focusing of radiation by a random surface

39

where

$$\mathbf{N} = \mathbf{T}'\mathbf{M}\mathbf{T} \quad (\text{A } 10)$$

and so

$$\mathbf{N}^{-1} = \mathbf{T}^{-1}\mathbf{E}'\mathbf{T}^{-1'}, \quad (\text{A } 11)$$

where \mathbf{E} is given by (2.3). Writing $\mathbf{N}^{-1} = \mathbf{H}$ we have

$$\mathbf{H} = \begin{pmatrix} \frac{1}{2}(m_{40} + 2m_{22} + m_{04}) & \frac{1}{2}(m_{31} + m_{13}) & \frac{1}{2}(m_{40} - m_{04}) \\ \frac{1}{2}(m_{31} + m_{13}) & m_{22} & \frac{1}{2}(m_{31} - m_{13}) \\ \frac{1}{2}(m_{40} - m_{04}) & \frac{1}{2}(m_{31} - m_{13}) & \frac{1}{2}(m_{40} - 2m_{22} + m_{04}) \end{pmatrix}. \quad (\text{A } 12)$$

Now from (3.3) and (A 9)

$$\left. \begin{aligned} \sum_{ij} N_{ij} \zeta_i \zeta_j &= \eta_1^2 + \eta_2^2 + \eta_3^2, \\ \zeta_1^2 - \zeta_2^2 - \zeta_3^2 &= l_1 \eta_1^2 + l_2 \eta_2^2 + l_3 \eta_3^2. \end{aligned} \right\} \quad (\text{A } 13)$$

From the first of these equations,

$$\mathbf{b}'\mathbf{N}\mathbf{b} = \mathbf{I}, \quad (\text{A } 14)$$

where \mathbf{I} denotes the unit matrix. So on taking inverse matrices

$$\mathbf{b}^{-1}\mathbf{H}\mathbf{b}^{-1'} = \mathbf{I} \quad (\text{A } 15)$$

and hence

$$\mathbf{H} = \mathbf{b}\mathbf{b}'. \quad (\text{A } 16)$$

In particular

$$H_{11} = b_{11}^2 + b_{12}^2 + b_{13}^2. \quad (\text{A } 17)$$

Since from (2.8) and (A 12) we have $H_{11} = \frac{1}{2}D$, this proves (A 6).

Similarly from the second of equations (A 13) we have

$$\mathbf{b}'\mathbf{K}\mathbf{b} = \mathbf{L}, \quad (\text{A } 18)$$

where

$$\mathbf{K} = \begin{pmatrix} 1 & 0 & 0 \\ 0 & -1 & 0 \\ 0 & 0 & -1 \end{pmatrix}, \quad \mathbf{L} = \begin{pmatrix} l_1 & 0 & 0 \\ 0 & l_2 & 0 \\ 0 & 0 & l_3 \end{pmatrix}; \quad (\text{A } 19)$$

and so by the same procedure

$$\mathbf{K}^{-1} = \mathbf{b}\mathbf{L}^{-1}\mathbf{b}'. \quad (\text{A } 20)$$

The leading element of this matrix relationship gives us (A 7).

To prove (A 8) we note that from (3.2) and (3.3)

$$\mathbf{a}'\mathbf{M}\mathbf{a} = \mathbf{I}, \quad \mathbf{a}'\sigma\mathbf{a} = \mathbf{L}, \quad (\text{A } 21)$$

where

$$\sigma = \begin{pmatrix} 0 & 0 & \frac{1}{2} \\ 0 & -1 & 0 \\ \frac{1}{2} & 0 & 0 \end{pmatrix}. \quad (\text{A } 22)$$

From the first of (A 21),

$$\mathbf{a}' = \mathbf{a}^{-1}\mathbf{M}^{-1} = \mathbf{a}^{-1}\mathbf{E}; \quad (\text{A } 23)$$

and so from the second

$$\mathbf{L} = \mathbf{a}^{-1}\mathbf{E}\sigma\mathbf{E}'\mathbf{a}^{-1'}, \quad (\text{A } 24)$$

giving

$$\mathbf{b}\mathbf{L}\mathbf{b}' = \mathbf{b}\mathbf{a}^{-1}\mathbf{E}\sigma\mathbf{E}'\mathbf{a}^{-1'}\mathbf{b}' = \mathbf{S}\sigma\mathbf{S}', \quad (\text{A } 25)$$

where

$$\mathbf{S} = \mathbf{b}\mathbf{a}^{-1}\mathbf{E} = \mathbf{T}^{-1}\mathbf{E}. \quad (\text{A } 26)$$

From (2.3) and (A 4) we have

$$S = \begin{pmatrix} \frac{1}{2}(m_{40} + m_{22}) & \frac{1}{2}(m_{31} + m_{13}) & \frac{1}{2}(m_{22} + m_{04}) \\ m_{31} & m_{22} & m_{13} \\ \frac{1}{2}(m_{40} - m_{22}) & \frac{1}{2}(m_{31} - m_{13}) & \frac{1}{2}(m_{22} - m_{04}) \end{pmatrix}. \quad (\text{A } 27)$$

On taking the leading element in equation (A 25) we obtain the desired relation.

REFERENCES

- (1) KENDALL, M. G. and STUART, A. *The advanced theory of statistics*, vol. I. (London, 1958).
- (2) LONGUET-HIGGINS, M. S. The statistical distribution of the curvature of a random Gaussian surface. *Proc. Camb. Phil. Soc.* 54 (1958), 439-53.
- (3) LONGUET-HIGGINS, M. S. The distribution of the sizes of images reflected in a random surface. *Proc. Camb. Phil. Soc.* 55 (1959), 91-100.
- (4) LOWAN, A. N. Tables of normal probability functions. *N.B.S. Appl. Math. Ser.*, 23 (Washington, 1953).
- (5) WHITTAKER, E. T. and WATSON, G. N. *A course of modern analysis*, 4th ed. (Cambridge, 1952).

NATIONAL INSTITUTE OF OCEANOGRAPHY

WORMLEY

SURREY

Reflection and Refraction at a Random Moving Surface.

I. Pattern and Paths of Specular Points

M. S. LONGUET-HIGGINS

National Institute of Oceanography, England

(Received January 25, 1960)

Light falling from a point source on a ruffled surface produces a pattern of images, which move about over the surface. The image points correspond to the maxima, minima, and saddle points of a certain function. It is shown that the images are generally created in pairs, a maximum with a saddle point or a minimum with a saddle point, and that the total numbers of maxima, minima, and saddle points satisfy the relation

$$N_{\max} + N_{\min} = N_{\text{saddle}} + 1.$$

The process of creation or annihilation of images is studied in detail, and also the tracks of the image points, in certain special cases. It is shown that closed tracks may be common. This is confirmed by photography of the sea surface.

1. INTRODUCTION

WHEN light from a fixed source falls upon a wavelike surface, such as the surface of a lake when ruffled by the wind, an observer may see a number of dancing images of the source reflected at different points in the surface; these points are sometimes called the "specular points."¹ Similarly, an observer beneath the surface would also see a number of moving images, depending upon the refractive index and the positions of the source and observer.

The number of images seen by the observer is not constant. The images move, and two specular points may come together and disappear or, on the other hand, two such points may suddenly appear where there were none before. Such an event, namely, the creation or the annihilation of two specular points may be called a "twinkle."²

It can be shown that at a "twinkle" the intensity of the image becomes exceptionally bright; the light is partially focused on the observer, so that the latter sees a bright flash. Correspondingly, if the reflected or refracted light is allowed to illuminate a fixed surface parallel to the mean wave surface, the intensity of illumination on the fixed surface fluctuates, and lines of especially bright illumination may be seen, for example, on the bottom of a shallow lake or sea. At the instant when one such line sweeps across a point Q in the plane, an observer at Q will see a "twinkle." A particular case of this phenomenon when the water surface is perfectly regular and sinusoidal and the source is at infinite distance has been considered by Shenck.³

It is well known, however, that water waves generated by wind are not perfectly regular but have a certain degree of randomness arising from the character of their origin. For example, the slopes of wind waves are known to have a statistical distribution which is ap-

proximately Gaussian.⁴ It is sometimes convenient to assume that the water surface is the sum of an infinite number of long-crested waves of different wavelengths and directions, whose phases have been chosen at random from the interval $(0, 2\pi)$; under suitable conditions, this leads to a Gaussian distribution of the elevation, slopes, and higher derivatives.⁴

The purpose of the present paper is to study the pattern of specular points in a random surface, to show how specular points may be added or subtracted at a "twinkle," and to examine the paths of specular points such as would be revealed by a time exposure of the surface. It is not here assumed that the surface is Gaussian but only that it has a certain degree of randomness so that special and unlikely cases (with probability zero) can be ignored. In subsequent papers the Gaussian assumption will be explicitly made, and the average numbers of specular points, as well as the mean number of twinkles per unit time, will be determined in terms of the spectrum of the surface.

First, in Sec. 2, we consider the pattern of specular points on the surface at a typical instant. Some of these points are "maxima," some are "minima," and some "saddle points." A simple relation between the number of each kind, namely,

$$N_{\max} + N_{\min} = N_{\text{saddle}} + 1 \quad (1.1)$$

is established.

It is then shown that as the surface moves, the specular points are generally created in pairs—a maximum with a saddle point or else a minimum with a saddle point. The way in which these fit into the previous pattern is also considered.

Ordinarily, a specular point, as it moves about on the surface, has a finite velocity; but we find that at the beginning and end of its life (that is to say when it is created or destroyed with another specular point), the

¹ C. Cox and W. Munk, *J. Opt. Soc. Am.* 44, 838 (1954).

² M. S. Longuet-Higgins, *Proc. Cambridge Phil. Soc.* 56, 234 (1956).

³ H. Shenck, *J. Opt. Soc. Am.* 47, 653 (1957).

⁴ M. S. Longuet-Higgins, *Phil. Trans. Roy. Soc. London* A247, 321 (1957).

velocity becomes infinite—in such a way, however, that the total distance traveled by the point is finite.

Typical tracks of specular points are considered in Sec. 6. When the surface consists of certain kinds of wave systems, it is shown that closed tracks will be common. A photograph of such tracks on the sea surface is reproduced in Fig. 9.

2. CONDITIONS AT A SPECULAR POINT

Let the equation of the surface in rectangular coordinates be

$$z = \zeta(x, y, t), \quad (2.1)$$

where the z axis is directed vertically upward. If the light source O and the point of observation Q are at $(0, 0, h_1)$ and $(0, 0, h_2)$, respectively (both above the surface), then the conditions for a point P at (x, y, ζ) to be a specular point are

$$\partial \zeta / \partial x = -\kappa x, \quad \partial \zeta / \partial y = -\kappa y, \quad (2.2)$$

where

$$\kappa = \frac{1}{2} \left[(1/h_1) + (1/h_2) \right], \quad (2.3)$$

it being supposed that $\kappa \zeta$ and $\partial \zeta / \partial x$, $\partial \zeta / \partial y$ are all small quantities. Similarly, if Q is situated at a distance h_2 below the surface and μ_1, μ_2 are the refractive indices for the two media above and below, we again have Eq. (2.2), but with

$$\kappa = (\mu_1 h_1 + \mu_2 h_2) / (\mu_2 - \mu_1) h_1 h_2. \quad (2.4)$$

It follows from (2.2) that the specular points correspond to the solutions of the equations

$$\partial f / \partial x = 0, \quad \partial f / \partial y = 0, \quad (2.5)$$

where

$$f(x, y, t) = \zeta(x, y, t) + \frac{1}{2} \kappa (x^2 + y^2), \quad (2.6)$$

that is to say, they are the stationary points of the function f .

Let us first consider the surface as "frozen" at one particular time t , so that f is a function of x, y only. The form of the surface in the neighborhood of a specular point is well known. Shifting the origin of x, y to the point P and assuming that $\zeta(x, y)$ is differentiable up to the second order, we have

$$f(x, y) = \frac{1}{2} (a_{20}x^2 + 2a_{11}xy + a_{02}y^2) + R, \quad (2.7)$$

where R is a remainder of higher order than the second. We may write

$$\Omega_f = (\partial^2 f / \partial x^2)(\partial^2 f / \partial y^2) - (\partial^2 f / \partial x \partial y)^2 = a_{20}a_{02} - a_{11}^2 \quad (2.8)$$

for the discriminant of the quadratic form in (2.7); Ω_f also equals the "total" curvature of the surface $z = f$ at P . There are generally two distinct cases: either

(1) $\Omega_f > 0$; the quadratic form in (2.7) is always of the same sign, and f has a maximum or a minimum according as $a_{20} \leq 0$; the contours $f = \text{constant}$ are ellipses as in Figs. 1(a) and 1(c). Alternatively,



FIG. 1. The full lines indicate contours of $f(x, y, t)$ in the neighborhood of an ordinary specular point: (a) a maximum, (b) a saddle point, (c) a minimum. The broken lines and arrows indicate directions of steepest ascent.

(2) $\Omega_f < 0$; the quadratic form is indefinite, and the contours of f are hyperbolic, as in Fig. 1(b).

Of special interest to us are the paths of steepest ascent on the surface; these are the orthogonal trajectories of the contour lines shown in Fig. 2. It is evident that in case (1) a path of steepest descent may either leave or enter P in any direction whatsoever, and there is a continuous family of such paths. In case (2) on the other hand, the orthogonal trajectories are rectangular hyperbolas with center P and so can never pass through P itself, with the exception of the hyperbola of zero "radius," that is, the line pair which forms the asymptotes of all the other paths. Thus, at a saddle point only two pairs of directions exist from which a path of steepest ascent may enter or leave the point, compared with a continuous family of directions for a maximum or minimum.

We have purposely not investigated the special case $\Omega_f = 0$ at present, because if the surface is "frozen" the probability of such points occurring is nil; only when the surface is allowed to move, that is to say, it is given an extra degree of freedom, is there a finite probability that Ω_f will pass through zero in a given length of time.

3. PATTERN OF SPECULAR POINTS

It is sufficient, then, so long as the surface is "frozen," to suppose that the stationary points are either maxima, minima, or saddle points; any other cases have a total probability zero.

We now give a chain of reasoning which suggests that all the minima on the surface may be joined by a network of paths so that each mesh contains one maximum and each segment contains one saddle point.

Consider the form of $z = f(x, y)$ as the radius $r = (x^2 + y^2)^{1/2}$ tends to infinity. In Eq. (2.6) the constant κ is positive. If we suppose that $\zeta(x, y)$ is Gaussian, so that the probability of large negative values is exponentially small, then it will follow that as $r \rightarrow \infty$, $f(x, y)$ almost always tends to infinity also.

Further, if the first and second derivatives of ζ are also Gaussian (and certainly if the slopes are bounded) we may expect that the paths of steepest ascent on the surface will, outside a circle of given radius r_0 , all tend to infinity, except for a set of surfaces having probability

ϵ , where ϵ tends to 0 as $\tau_0 \rightarrow \infty$. We assume, therefore, that beyond a given radius all paths are directed outward to a "maximum at infinity," it being understood that we are neglecting a set of cases of vanishing total probability.

We shall also assume that there is only a finite number of stationary points at any time throughout the whole plane.

Starting from a typical point P on the surface (not a stationary point), let us follow the path of steepest ascent from P ; this will climb until it reaches a stationary point or else goes to infinity. Generally, the path will not encounter a saddle point, since to each saddle point there are only two paths of steepest ascent; therefore, it will generally reach a maximum A (which may be the "maximum at infinity"). Moreover, if P is a point in the neighborhood of P , the path of steepest ascent from P' will generally arrive at the same maximum A . Hence P lies in a continuous region, all points of which are connected to A by paths of steepest ascent. From Fig. 1(a), every maximum is surrounded by such a region.

In this way the whole plane, with the exceptions of the minima and of the paths passing through the saddle points, is divided into regions, one region for each maximum.

Let us now go to a typical minimum B and follow the line of steepest ascent, starting out from B in an arbitrary direction θ . This path, for the same reason, generally leads to a maximum $A(\theta)$. Moreover, all paths adjacent to the first path, that is starting in slightly different directions $\theta + d\theta$, generally arrive at A also.

Suppose now there exist two different directions θ_1 and θ_2 for which the paths of steepest ascent arrive at different maxima A_1 and A_2 [Fig. 2(a)]. By varying θ continuously from θ_1 to θ_2 we must encounter a direction θ_3 for which the path bifurcates, one branch going to A_1 and one to A_2 (where A_2 may be the same as A_1). The point of bifurcation cannot be an ordinary point or a maximum or minimum; it must therefore be a saddle point C , say.

Now the path from B to C must form a part of the boundary of the region surrounding A_1 (for a slight

variation of θ produces a path leading to A_1 on the one side or to A_2 on the other). Further, if the path BC is continued beyond the saddle point C and down the other side it must eventually reach a stationary point, which is either a minimum or another saddle point. A saddle point is ruled out, as being of vanishing probability. So in almost all cases the path ends in another minimum B' , say.

On continuing in this way round the maximum A_1 we have a succession of minima B, B', B'' , and we eventually arrive back at B , having toured A_1 just once. It is quite possible for B' to coincide with B , as in Fig. 2(b).

Proceeding to the contiguous region which surrounds A_2 , say, we may make a similar circuit. So eventually we fill up the whole plane with a network of paths, each mesh of the net containing just one maximum. The minima lie at the corners of the mesh, and along each segment between two adjacent minima there is one saddle point.

In fact, the network of minima may be considered as the Schlegel diagram of a polyhedron⁴ in which the faces correspond to the maxima, the vertices correspond to the minima, and the edges correspond to the saddle points—with the difference, however, that it is allowable to have one "vertex" joined to the rest of the network by a single "edge," as in Fig. 2(b).

The dual network, formed by lines joining the maxima, and passing through the saddle points, is easily constructed.

Both the original network and its dual satisfy Euler's theorem^{5,7}:

$$N_{\text{faces}} + N_{\text{vertices}} = N_{\text{edges}} + 2 \quad (3.1)$$

(where N_{faces} denotes the number of faces, etc.). One "face" in the original network corresponds to the maximum at infinity. On omitting this, we have

$$N_{\text{max}} + N_{\text{min}} = N_{\text{sc}} + 1, \quad (3.2)$$

where N_{max} , N_{min} , and N_{sc} denote the total numbers of maxima, minima, and saddle points, respectively.

It may be noted that the surface can be divided in another way, into regions where Ω_f is positive (elliptic regions) on the one hand and regions where Ω_f is negative (hyperbolic regions) on the other. The maxima and minima all lie in elliptic regions, and saddle points in hyperbolic regions. The boundaries between these, that is to say, the loci of points for which $\Omega_f = 0$, are called the *parabolic lines*.

4. CONDITIONS AT A TWINKLE

From now on we shall allow the surface to be in motion, so that individual specular points move about

⁴ H. S. M. Coxeter, *Regular Polytopes* (Methuen and Company, Ltd., London, 1948), p. 321.

⁵ L. Euler, *Nov. Comment. Acad. Sci. Imp. Petropol.* 4, 109 (1752-1753).

⁷ D. M. Y. Sommerville, *An Introduction to the Geometry of n Dimensions* (Methuen and Company, Ltd., London, 1929), p. 196.

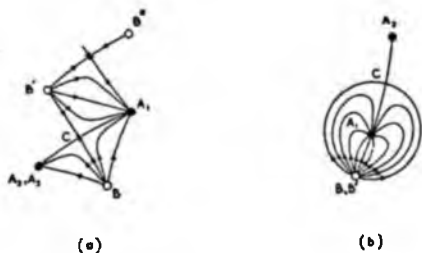


FIG. 2. Configurations of stationary points. (●) = maximum, (○) = minimum, (×) = saddle point

on the surface. Let us follow one such point. Its coordinates are given by the conditions that

$$\partial f/\partial x=0, \quad \partial f/\partial y=0, \quad (4.1)$$

and on taking the differential of these equations with respect to both x, y and t we have

$$\begin{aligned} (\partial^2 f/\partial x^2)dx + (\partial^2 f/\partial x\partial y)dy + (\partial^2 f/\partial x\partial t)dt &= 0, \\ (\partial^2 f/\partial x\partial y)dx + (\partial^2 f/\partial y^2)dy + (\partial^2 f/\partial y\partial t)dt &= 0. \end{aligned} \quad (4.2)$$

Equations (4.2) may be solved uniquely for the ratios dx/dt and dy/dt , provided that

$$\Omega_f = (\partial^2 f/\partial x^2)(\partial^2 f/\partial y^2) - (\partial^2 f/\partial x\partial y)^2 \neq 0. \quad (4.3)$$

In other words, after a short time dt , each specular point will move to a well-defined new position, provided that Ω_f is not zero. A necessary condition, therefore, for the creation or annihilation of a specular point (which we call a "twinkle") is the vanishing of Ω_f .

Let us shift the origin of coordinates to the position of the twinkle, at which time we also take $t=0$. If the surface is continuous and differentiable up to the third order, $f(x, y, t)$ may be expanded in the Taylor series

$$f(x, y, t) = \sum_{i,j,k=0}^3 \frac{a_{ijk}}{i!j!k!} x^i y^j t^k + R, \quad (4.4)$$

where

$$a_{ijk} = (\partial^{i+j+k} f/\partial x^i \partial y^j \partial t^k)_{x=y=t=0} \quad (4.5)$$

and R is a higher-order remainder. Since the origin is at

$$a_{000} = 0, \quad (4.6)$$

and the conditions (4.1) at $t=0$ give also

$$a_{100} = a_{010} = 0. \quad (4.7)$$

Further, by a rotation of the axes of x, y we may make

$$a_{110} = 0. \quad (4.8)$$

The condition that Ω_f shall vanish now gives

$$a_{200}a_{020} = 0, \quad (4.9)$$

whence either a_{200} or a_{020} must vanish also. By naming the axes appropriately we make

$$a_{200} = 0. \quad (4.10)$$

Lastly, the terms independent of x, y do not alter the form of the surface near P , except to raise or lower it bodily by a small amount. So without loss of generality, we assume

$$a_{001} = a_{002} = a_{003} = 0. \quad (4.11)$$

The resulting expression for f in the neighborhood of the twinkle is

$$\begin{aligned} f(x, y, t) = & \frac{1}{2}a_{020}y^2 + \frac{1}{2}(a_{200}x^2 + 3a_{210}x^2y + 3a_{110}xy^2 + a_{020}y^2) \\ & + (a_{101}x + a_{011}y)t + \frac{1}{2}(a_{201}x^2 + 2a_{111}xy + a_{011}y^2)t \\ & + \frac{1}{2}(a_{102}x + a_{012}y)t^2 + R. \end{aligned} \quad (4.12)$$

The coordinates of a specular point in the neighborhood are found by substituting this expression in (4.1), which gives

$$\begin{aligned} \frac{1}{2}(a_{200}x^2 + 2a_{210}xy + a_{120}y^2) + a_{101}t + \dots &= 0, \\ a_{010}y + \frac{1}{2}(a_{210}x^2 + 2a_{120}xy + a_{020}y^2) + a_{011}t + \dots &= 0, \end{aligned} \quad (4.13)$$

whence it is clear that x is of order $|t|^{1/2}$ and y of order t . In fact, on retaining only the lowest powers of t in each case, we have

$$x = \pm \left(\frac{-2a_{101}t}{a_{200}} \right)^{1/2}, \quad y = \frac{a_{210}a_{101} - a_{200}a_{011}}{a_{200}a_{020}}t. \quad (4.14)$$

The interpretation is interesting. If a_{100}/a_{200} is positive, two solutions exist when $t < 0$ and none when $t > 0$; hence, two specular points are simultaneously annihilated. If, on the other hand, a_{100}/a_{200} is negative, no solution exists for $t < 0$ and two solutions exist for $t > 0$; therefore, two specular points are simultaneously created.

The path of the points is found by eliminating t from (4.14):

$$(a_{210}a_{100} - a_{200}a_{010})x^2 + 2a_{100}a_{010}y = 0, \quad (4.15)$$

which is a parabola with axis $y=0$. The velocity of the specular points near the vertex of the parabola is given by

$$\frac{dx}{dt} = \pm \left(\frac{-a_{101}}{2a_{200}t} \right)^{1/2}, \quad \frac{dy}{dt} = \frac{a_{210}a_{101} - a_{200}a_{011}}{a_{100}a_{020}}, \quad (4.16)$$

showing that the x component of velocity tends to infinity as $|t| \rightarrow 0$, as was expected.

Consider now the locus of "parabolic points," that is to say, points for which the total curvature, given by

$$\Omega_f = (\partial^2 f/\partial x^2)(\partial^2 f/\partial y^2) - (\partial^2 f/\partial x\partial y)^2 \quad (4.17)$$

vanishes. Substitution from (4.12) gives this locus as

$$a_{200}x + a_{210}y + a_{201}t = 0 \quad (4.18)$$

(terms of higher order being neglected). This is a straight line making an angle

$$\tan^{-1}(a_{210}/a_{200}) \quad (4.19)$$

with the path of the specular points, and passing within a distance of order t from the origin. But the x coordinates of the specular points are of order $t^{1/2}$. Hence, the two specular points lie generally on either side of the parabolic line $\Omega_f=0$.

Now the parabolic line is a boundary separating points for which $\Omega_f < 0$ from those for which $\Omega_f > 0$. It follows that one of the two specular points is a saddle point and the other is a maximum or a minimum.

In other words, specular points are generally created or annihilated in pairs; a maximum together with a saddle point or a minimum together with a saddle

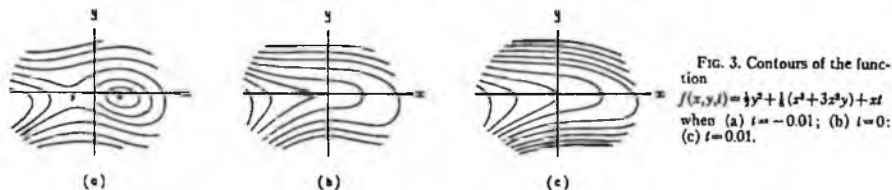


FIG. 3. Contours of the function $f(x, y, t) = \frac{1}{2}y^2 + \frac{1}{2}(x^2 + 3x^2y) + xt$ when (a) $t = -0.01$; (b) $t = 0$; (c) $t = 0.01$.

point. It is evident that this process preserves the relation (3.2).

The form of the surface at the twinkle itself (time $t=0$) is found from (4.12):

$$f(x, y, 0) = \frac{1}{2}a_{020}y^2 + \frac{1}{8}(a_{300}x^2 + 3a_{210}x^2y + 3a_{120}xy^2 + a_{030}y^3) + \dots \quad (4.20)$$

By the linear transformation

$$\begin{aligned} x + (a_{210}/a_{300})y &= \xi \\ y &= \eta \end{aligned} \quad (4.21)$$

(a change to oblique axes), the equation becomes

$$f(x, y, 0) = \frac{1}{2}a_{300}\xi^2 + \frac{1}{2}a_{020}\eta^2(1 + A\xi + B\eta) + \dots, \quad (4.22)$$

where A and B are constants; or, since ξ and η are small near the origin,

$$f = \frac{1}{2}a_{020}\eta^2 + \frac{1}{2}a_{300}\xi^2 + \dots \quad (4.23)$$

The contour through the origin ($f=0$) is thus a semi-cubical parabola with a cusp lying to the left or right of the origin, according as a_{020}/a_{300} is positive or negative. The tangent at the cusp is the line $\eta=0$, i.e., the x axis.

The essential features of the surface before and after a twinkle are illustrated by the contour

$$f(x, y, t) = \frac{1}{2}y^2 + \frac{1}{2}(x^2 + 3x^2y) + xt, \quad (4.24)$$

whose contours are plotted in Fig. 3 for $t = -0.01, 0$, and 0.01 . Two specular points—a minimum and a saddle point—are shown in the process of annihilation.

A geometrical interpretation may be given as follows. At each point on the surface there are two principal

curvatures, κ_a and κ_b , say, and the total curvature Ω_t is the product of these. At a maximum or minimum, κ_a and κ_b are of the same sign, while at a saddle point they are of opposite signs. At a twinkle, when Ω_t vanishes, one of the principal curvatures also vanishes (in the foregoing example this curvature is in the x direction). That is to say, one of the principal sections of the surface has a point of inflexion. It is not difficult to see, by considering the corresponding two-dimensional problem⁴ that, at a point of inflexion, two specular points must coincide and that their velocities become infinite.

If the source of light is of small but still finite dimensions, each image on the surface covers a small area. It can be shown that as the two specular points approach each other, the images become elongated along their direction of travel (that is to say in the x direction). During this process the area of the image is greatly enlarged, so that an observer sees a bright flash.⁶ However, the brighter the image, the faster it is moving, and it can be shown that the total intensity of light (integrated with respect to time) which is received from any small part of the track remains finite. Hence a time exposure of the whole track shows no particular increase in brightness at the twinkle itself.

In what has been said we have purposely ignored the possibility of such special cases as $a_{020}=0$ or $a_{300}=0$. These situations, besides being of zero probability, may be considered as coincidences of the kind of twinkle just described. For example, if $a_{010}=0$, then we have for the coordinates of the specular points the equations

$$\begin{aligned} \frac{1}{2}(a_{300}x^2 + 2a_{210}xy + a_{130}y^2) + a_{010}t + \dots &= 0 \\ \frac{1}{2}(a_{210}x^2 + 2a_{120}xy + a_{030}y^2) + a_{010}t + \dots &= 0, \end{aligned} \quad (4.25)$$

which represent two concentric conics. Generally, there are either four real intersections or none, giving four specular points in the neighborhood or none. If either conic is real when $t < 0$ it will be imaginary when $t > 0$. So we may distinguish the following cases: (1) both conics are simultaneously real and intersecting: then four specular points are simultaneously created or annihilated; (2) both conics are simultaneously real but nonintersecting: this gives an isolated flash at $t=0$; (3) one conic is real, the other imaginary: again there is an isolated flash at $t=0$. In case (1) the event can be regarded as the simultaneous creation of two

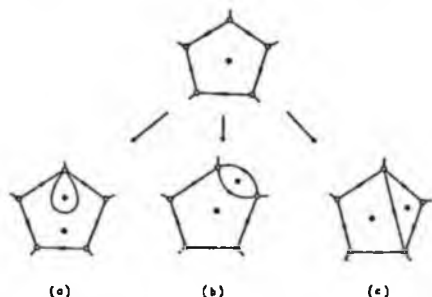


FIG. 4. Modifications of the pattern of stationary points by the addition of a maximum and a saddle point.

⁴ At an ordinary point the total brightness is proportional to $|\Omega_t|^{-1}$, but when Ω_t vanishes this approximation breaks down.

pairs of specular points (or their simultaneous destruction). In cases (2) and (3) the event can be regarded as the simultaneous creation and annihilation of the same pair of specular points; their life ends as soon as it has begun.

5. CHANGING THE PATTERN OF SPECULAR POINTS

Let us now consider how two new specular points may be fitted into an already existing pattern.

We have seen that specular points are generally born in pairs at a parabolic line. Let us consider first the addition of a saddle point and a *maximum*.

The saddle point must lie on a path joining two minima. Since the minima are to be preserved, the only way to create a new path is to join up two already existing minima—these must therefore belong to the same mesh. The mesh being thus divided into two parts, a new maximum is created at the same time.

Three possible ways of dividing the mesh are illustrated in Figs. 4(a)–4(c). These ways correspond to the

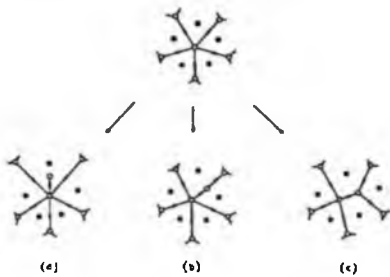


FIG. 5. Modifications of the pattern of stationary points by the addition of a minimum and a saddle point.

joining of one minimum to itself, to an adjacent minimum, or to one of the other minima of the same mesh.

The addition of a new *minimum* may be regarded in a precisely similar way but from the point of view of the dual network (see Sec. 3). Modifying the dual as in Figs. 4(a)–4(c) and then returning to the original we obtain the three types of division shown in Figs. 5(a)–5(c).

The destruction of two specular points consists of any such step in reverse.

Since a complete network may be built up from a single minimum or may be reduced to a single minimum by a combination of such steps, it follows that any pattern of specular points may be converted into any other by the steps described.

6. PATHS OF SPECULAR POINTS

If $z = \zeta(x, y, t)$ is a Gaussian surface, the tracks of the specular points are generally complicated. However, in

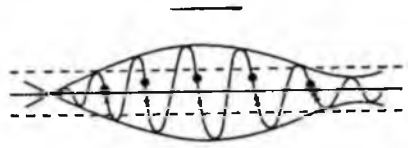


FIG. 6. The formation of specular lines on a moving waveform.

some special cases purely qualitative considerations may help in understanding certain features of the observed tracks.

Consider the special case when the surface consists of two systems of long-crested waves crossing at right angles. We have

$$\zeta(x, y, t) = \zeta_1(x, t) + \zeta_2(y, t), \tag{6.1}$$

and the conditions for a specular point reduce to

$$\partial \zeta_1 / \partial x = -kx, \quad \partial \zeta_2 / \partial y = -ky, \tag{6.2}$$

which is to say that a specular point in the combined system is the intersection of two *specular lines*, one from each of the long-crested systems individually.

Let us further suppose that each of the systems ζ_1 and ζ_2 consists of a fairly narrow band of wavelengths, and that the distances of the source and observer from the surface are great compared with the mean wavelength λ . Then the condition for a specular line in the system ζ_1 (say) is that the gradient $\partial \zeta_1 / \partial x$ shall take the value $-kx$, which value is almost constant over a few wavelengths.

Consider now a progressive train of waves in a dispersive medium such as water (Fig. 6). The envelope of such a wave train will move forward with the group velocity of the waves, and if, as in water, the phase velocity exceeds the group velocity,¹ the individual waves will grow at the rear of the group, move forward through the group and eventually die out at the front. At the instant when the wave amplitude rises through the value $k|x|\lambda/2\pi$, two specular lines suddenly appear, and when the amplitude falls below this value, they disappear together. The specular lines are thus carried along through a distance comparable to the length

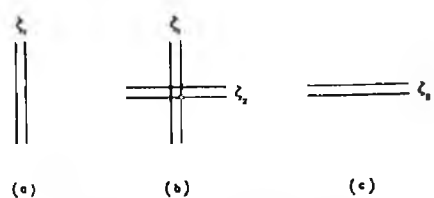


FIG. 7. The formation of specular points by two intersecting wave systems.

¹ This is for gravity waves. For surface-tension waves the reverse is true, but a similar argument applies.

of the group, which equals $n\lambda$, where n is the number of waves in the group.

Consider on the other hand a standing wave train. The wavelength is nearly uniform but the amplitude fluctuates rapidly, twice per complete cycle. Specular lines will appear (in pairs) and disappear again within half a cycle. The distance that they traverse is, by contrast with the previous case, only a fraction of λ .

Figure 7 illustrates the combined effect of the two intersecting systems. In Fig. 7(a) a pair of specular lines exists in system ζ_1 , but not in system ζ_2 ; then (b) a pair appears also in the system ζ_2 ; this generates simultaneously two pairs of specular points (of which one pair is a maximum and a saddle point, the other a minimum and a saddle point). The pairs of points quickly separate in the y direction. Then either (c) the specular lines of ζ_1 vanish first or (a) the specular lines of ζ_2 .

Typical tracks of the points are shown in Fig. 8. In Figs. 8(a) and 8(b), both systems ζ_1 and ζ_2 are progressive. In case (c), ζ_1 is a progressive wave but ζ_2 a standing wave; in case (d), both ζ_1 and ζ_2 are standing waves. The directions of movement are shown by arrows.

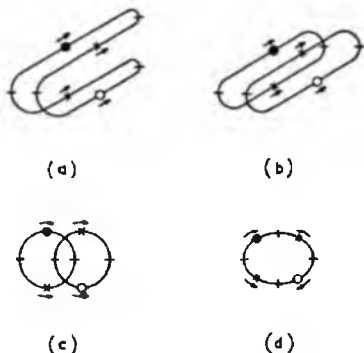


FIG. 8. Possible tracks of specular points (the arrows indicate directions of motion).

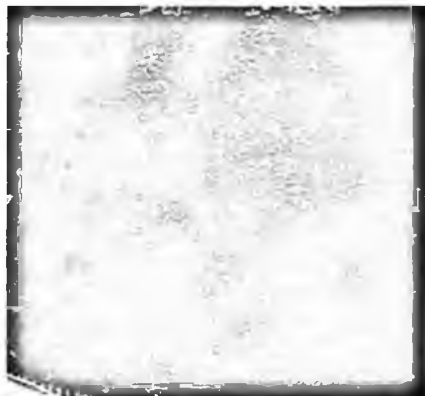


FIG. 9. A time exposure of the sea surface, showing tracks formed by images of the sun. The photograph was taken at mid-day, the camera being inclined at about 45° to the horizontal. (Triex XXX plate film was used, with a red filter.)

A time exposure (0.2 sec) of the pattern of sunlight reflected in the sea surface, taken a few feet above the water, is shown in Fig. 9. It seems from the photograph that the existence of closed tracks is quite common. Probably some waves were being reflected from the structure in the foreground, thus producing standing waves.

In Figs. 8(c) and 8(d) we saw that a closed track may correspond to two or four nearly simultaneous twinkles. Thus the closed tracks will enhance strongly the glittering appearance of the sea surface.

ACKNOWLEDGMENT

I am much indebted to Timothy Rhodes for a vacation on Beach Island, Maine, which first stimulated consideration of this problem. For the photograph in Fig. 9, I am indebted to Harlow G. Farmer of the Woods Hole Oceanographic Institution.

Reflection and Refraction at a Random Moving Surface.

II. Number of Specular Points in a Gaussian Surface

M. S. LONGUET-HIGGINS

National Institute of Oceanography, England

(Received January 25, 1960)

The number of specular points reflected in a random Gaussian surface is determined theoretically under the following alternative conditions: (1) when the surface is perfectly long crested (two-dimensional); (2) when the surface is three-dimensional but isotropic; (3) for quite general surfaces, provided that the observer and the source of radiation are both at a great distance from the surface.

The results can be applied to the similar problem when the surface forms the boundary of two refracting media.

1. INTRODUCTION

SUPPOSE that light from a point source falls upon a wavelike surface such as the surface of a lake or sea. An observer may see many distinct images of the source reflected in the surface at the specular points. Following a previous paper¹ we shall here determine the average number of reflections seen by the observer, as a function of the wave-energy spectrum of the surface and of the positions of observer and light source.

It will be supposed in this paper that the surface is Gaussian, that is to say, the probability distribution of the surface slopes and their derivatives is jointly normal. Such an assumption is convenient mathematically and may approximate to naturally occurring surfaces under some conditions; for example, it may apply to water surfaces where the slope is not too great, so that the waves do not approach breaking point. Ocean swell or shorter wind waves passing through "slicks" may come under this heading. Very steep wind waves, however, can be markedly non-Gaussian.²

When both source and observer are at infinite distance from the surface, the specular points in any finite region are those points where the surface has a particular gradient. The average number of specular points per unit area in this case has been evaluated previously.¹ Here we shall treat the more general case when both the source O and observer Q may be at a finite distance from the surface; but we restrict the discussion to cases where OQ is nearly perpendicular to the surface level.

With very slight modification the solution can be applied to the case when O and Q are on opposite sides of the surface, and the latter forms the boundary between two media of different refractive index: for example, how many images can an observer above water see when a light source is situated below water level, or vice versa?

The problem is first solved in the two-dimensional case when, strictly speaking, the source O is a line

¹ M. S. Longuet-Higgins, *J. Opt. Soc. Am.* 50, 838 (1960).
² A. F. Schooley, *Trans. Am. Geophys. Union* 36, 273 (1955).
³ M. S. Longuet-Higgins, *Phil. Trans. Roy. Soc. London* A249, 321 (1957).

source and Q is a line receiver. The full three-dimensional problem is solved formally in Sec. 3 and is explicitly evaluated in Sec. 4 for the special case when the surface is *isotropic* (its statistical properties are independent of azimuthal direction). The mean number N of images is given by Eq. (4.11), in which A is a parameter proportional to the mean-square curvature of the surface and to the square of the distances of source and observer from the surface.

In Sec. 5 the solution is given for the case when the surface consists of two sets of long-crested waves (both Gaussian) intersecting at right angles. The number N is then given by Eq. (5.7). This and the isotropic case are compared in Fig. 2.

Finally, the solution is given for large values of A (corresponding to the source and observer at great distances) and an arbitrary form of the wave spectrum. In particular it is shown that if the surface consists of two wave systems intersecting at an arbitrary angle θ_0 , then the number of images is proportional to $\sin\theta_0$ [see Eq. (6.9)]. The mean number of images is equal to the mean number for an isotropic surface of the same rms curvature provided that $\theta_0 = 66^\circ 30'$.

2. TWO-DIMENSIONAL CASE

Let (x, z) be rectangular coordinates, with z vertically upward, and let $O = (0, h_1)$ and $Q = (0, h_2)$ denote the positions of the source of light and of the observer, respectively, at heights h_1 and h_2 above the mean surface level. Further, let $P = (x, t)$ denote a typical point upon the surface $z = f(x)$. It is easily seen¹ that for P to be an image point we must have, at P ,

$$\partial f / \partial x = -kx, \quad (2.1)$$

where

$$k = \frac{1}{2} [(1/h_1) + (1/h_2)], \quad (2.2)$$

provided that kx and $\partial f / \partial x$ are both small quantities.

In the case of refraction, if h_1 and h_2 denote the distances of O and Q above and below the surface, and if μ_1 and μ_2 denote the refractive indices, then Eq. (2.1) must hold, but with

$$k = (\mu_1 h_1 + \mu_2 h_2) / (\mu_1 - \mu_2) h_1 h_2. \quad (2.3)$$

On writing, for brevity,

$$(1/x)(\partial \xi_1 / \partial x) = \xi_1, \quad \partial^2 \xi_1 / \partial x^2 = \xi_2, \quad (2.4)$$

we seek first the probability that, at some point in a given small interval $(x, x+dx)$, ξ_1 takes precisely the value $-\kappa$. Let us denote by $p(\xi_1, \xi_2)$ the joint probability density of ξ_1 and ξ_2 ; thus $p(\xi_1, \xi_2)d\xi_1 d\xi_2$ gives the probability that ξ_1, ξ_2 lie in given small intervals of width $d\xi_1, d\xi_2$. But $\xi_1 = -\kappa$ in $(x, x+dx)$ if and only if ξ_1 at x lies within a range of width

$$|d\xi_1| = |\partial \xi_1 / \partial x| dx = (1/|x|) |\xi_1 - \xi_2| dx \quad (2.5)$$

approximately, ξ_2 being kept constant. Hence the probability of a specular point in $(x, x+dx)$ is

$$N_x dx = \int_{-\infty}^{\infty} p(\xi_1, \xi_2) \frac{1}{|x|} |\xi_1 - \xi_2| dx d\xi_2, \quad (2.6)$$

and the total expectation of specular points over the whole range $-\infty < x < \infty$ is given by

$$N = \int_{-\infty}^{\infty} N_x dx. \quad (2.7)$$

As a model for the surface we may take the representation used by Rice,⁴ and suppose that

$$\zeta(x) = \sum_{n=1}^{n_0} c_n \cos(k_n x + \epsilon_n), \quad (2.8)$$

where the k_n denote constant wave numbers, the phases ϵ_n are randomly distributed in $(0, 2\pi)$, and where, in the end, n_0 tends to infinity and the c_n tend to zero in such a way that over any small interval of wave number $(k, k+dk)$, we have

$$\sum \frac{1}{2} c_n^2 = E(k) dk, \quad (2.9)$$

where E is a continuous function of k , known as the energy or power spectrum of $\zeta(x)$. The function $\zeta(x)$ may also be expressed as a stochastic integral.⁶

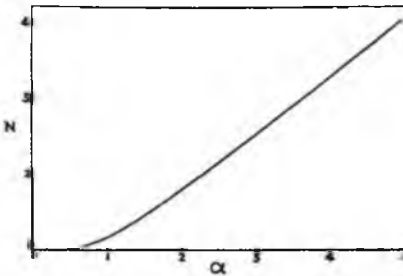


FIG. 1. The mean number of images N , as a function of the parameter α , defined by Eq. (2.15).

⁴ S. O. Rice, Bell System Tech. J. 23, 282 (1944); 24, 46 (1945).
⁶ J. L. Doob, *Stochastic Processes* (John Wiley & Sons, Inc., New York, 1953).

Under general conditions to be satisfied by the amplitudes c_n , the distribution of ζ and its derivatives is Gaussian: We shall assume that this is so at least as far as the second derivative ξ_1 . Now the matrix of mean values for the ξ_i is⁴

$$\langle (\xi_i \xi_j)_{x_0} \rangle = \begin{pmatrix} m_2/x^2 & 0 \\ 0 & m_4 \end{pmatrix}, \quad (2.10)$$

where

$$m_r = \int_0^{\infty} E(k) k^r dr \quad (2.11)$$

and hence we have

$$p(\xi_1, \xi_2) = \frac{|x|}{2\pi(m_2 m_4)^{1/2}} \exp[-\frac{1}{2}(\xi_1^2 x^2/m_2 + \xi_2^2/m_4)]. \quad (2.12)$$

On substituting into (2.7) and writing $\xi_1 = -\kappa$, we have

$$N = \frac{1}{2\pi(m_2 m_4)^{1/2}} \int_{-\infty}^{\infty} \int_{-\infty}^{\infty} |\xi_2 + \kappa| \times \exp[-\frac{1}{2}(\xi_1^2 x^2/m_2 + \xi_2^2/m_4)] dx d\xi_2. \quad (2.13)$$

The preceding integral is easily evaluated and we find

$$N = \left(\frac{2}{\pi}\right)^{1/2} \left[\alpha \exp(-\frac{1}{2}\alpha^2) + \int_0^{\alpha} \exp(-\frac{1}{2}s^2) ds \right], \quad (2.14)$$

where

$$\alpha = m_4^{1/2}/\kappa. \quad (2.15)$$

From (2.2) it will be seen that when $h_1 = h_2$, then $1/\kappa$ represents the distance of the observer from the mean surface [Eq. (2.2)]. Also, $m_4^{1/2}$ equals the root-mean-square value of the curvature ξ_2 [from (2.10)]. The nondimensional quantity is the product of these two. For small values of α (which therefore correspond to sources or observers very close to the surface), we have

$$N = 1, \quad (2.16)$$

as we might expect; only one image can be seen. For large α , on the other hand, we find

$$N \sim (2/\pi)\alpha, \quad (2.17)$$

that is to say, the total number of image points increases almost linearly with distance from the surface.

The number N as a function of α is plotted in Fig. 1.

3. THREE-DIMENSIONAL CASE: GENERAL SOLUTION

The formulation of the problem in three dimensions is very similar. If $z = \zeta(x, y)$ denotes the equation of the surface, and if h_1, h_2 denote the distances of O, Q from the mean surface level, then the conditions to be satisfied by an image point $P(x, y, \zeta)$ are

$$\partial \zeta / \partial x = -x\alpha, \quad \partial \zeta / \partial y = -y\alpha, \quad (3.1)$$

where κ is defined by (2.2) or (2.3) according to the physical situation. On writing

$$(1/x)(\partial\zeta/\partial x), (1/y)(\partial\zeta/\partial y) = \xi_1, \xi_3, \\ \partial^2\zeta/\partial x^2, \partial^2\zeta/\partial x\partial y, \partial^2\zeta/\partial y^2 = \xi_2, \xi_4, \xi_5, \quad (3.2)$$

we seek the probability that $(\xi_1, \xi_2) = (-\kappa, -\kappa)$ at some point in a given small region $dxdy$. This probability is

$$N_{xy}dxdy = \int_{-\infty}^{\infty} \int_{-\infty}^{\infty} \int_{-\infty}^{\infty} \rho(\xi_1, \dots, \xi_5) \left| \frac{\partial(\xi_1, \xi_2)}{\partial(x, y)} \right| \\ \times d\xi_1 d\xi_2 d\xi_3 d\xi_4 d\xi_5, \quad (3.3)$$

where

$$\frac{\partial(\xi_1, \xi_2)}{\partial(x, y)} = \begin{vmatrix} (1/x)(\xi_1 - \xi_1) & (1/x)\xi_4 \\ (1/y)\xi_4 & (1/y)(\xi_5 - \xi_2) \end{vmatrix} \\ = -\frac{1}{xy} [(\xi_3 + \kappa)(\xi_5 + \kappa) - \xi_4^2]. \quad (3.4)$$

The total expectation of image points is then

$$N = \int_{-\infty}^{\infty} \int_{-\infty}^{\infty} N_{xy}dxdy. \quad (3.5)$$

We adopt the same model of the surface as in previous studies.^{1,6} It is supposed that

$$\zeta(x, y) = \sum_{n=1}^{\infty} c_n \cos(u_n x + v_n y + \epsilon_n), \quad (3.6)$$

where u_n and v_n denote constant wave numbers, the phases ϵ_n are randomly distributed in $(0, 2\pi)$, and where, in the limit, as $n_0 \rightarrow \infty$ we have, over an arbitrary small area $dudv$,

$$\sum_{n=1}^{\infty} c_n^2 = E(u, v)dudv. \quad (3.7)$$

Here $E(u, v)$ is assumed to be a continuous function—the spectrum of $\zeta(x, y)$.

As before, we assume that ζ and its derivatives up to the second order are distributed normally. The matrix of mean values for the ξ_i is easily shown to be

$$\langle (\xi_i \xi_j)_{xy} \rangle = \begin{vmatrix} m_{10}/x^2 & m_{11}/xy & 0 & 0 & 0 \\ m_{11}/xy & m_{00}/y^2 & 0 & 0 & 0 \\ 0 & 0 & m_{10} & m_{11} & m_{12} \\ 0 & 0 & m_{11} & m_{22} & m_{12} \\ 0 & 0 & m_{12} & m_{12} & m_{04} \end{vmatrix}, \quad (3.8)$$

where

$$m_{pq} = \int_{-\infty}^{\infty} \int_{-\infty}^{\infty} E(u, v) u^p v^q dudv. \quad (3.9)$$

Hence we have

$$\rho(\xi_1, \dots, \xi_5) = \rho(\xi_1, \xi_2) \rho(\xi_3, \xi_4, \xi_5), \quad (3.10)$$

where

$$\rho(\xi_1, \xi_2) = \frac{|xy|}{2\pi(m_{10}m_{02} - m_{11}^2)^{\frac{1}{2}}} \\ \times \exp\left[-\frac{m_{02}x^2\xi_1^2 - 2m_{11}xy\xi_1\xi_2 + m_{20}\xi_2^2}{2(m_{10}m_{02} - m_{11}^2)^{\frac{1}{2}}}\right], \quad (3.11)$$

$$\rho(\xi_3, \xi_4, \xi_5) = \frac{|M_{ij}|^{\frac{1}{2}}}{(2\pi)^{\frac{3}{2}}} \exp\left[-\frac{1}{2} \sum_{i,j=3,4,5} M_{ij}\xi_i\xi_j\right],$$

and (M_{ij}) is the matrix inverse to

$$(\Xi_{ij}) = \begin{vmatrix} m_{40} & m_{41} & m_{42} \\ m_{31} & m_{32} & m_{33} \\ m_{22} & m_{12} & m_{04} \end{vmatrix} = (M_{ij})^{-1}. \quad (3.12)$$

On substituting the expression (3.3) into Eq. (3.5) and setting $\xi_1 = \xi_2 = -\kappa$, we find that the integration with respect to x, y may be carried out immediately, and hence

$$N = \frac{|M_{ij}|^{\frac{1}{2}}}{(2\pi)^{\frac{3}{2}} \kappa^2} \int_{-\infty}^{\infty} \int_{-\infty}^{\infty} \int_{-\infty}^{\infty} |(\xi_3 + \kappa)(\xi_5 + \kappa) - \xi_4^2| \\ \times \exp\left[-\frac{1}{2} \sum_{i,j=3,4,5} M_{ij}\xi_i\xi_j\right] d\xi_3 d\xi_4 d\xi_5. \quad (3.13)$$

It is the evaluation of this integral which now concerns us.

By means of the linear transformation

$$\xi_i = \sum_{j=1}^3 a_{ij}\eta_j, \quad i=3, 4, 5, \quad (3.14)$$

it is possible to reduce the quadratic forms in (3.13) simultaneously so that

$$\sum M_{ij}\xi_i\xi_j = \eta_1^2 + \eta_2^2 + \eta_3^2, \\ \xi_3\xi_5 - \xi_4^2 = l_1\eta_1^2 + l_2\eta_2^2 + l_3\eta_3^2. \quad (3.15)$$

The constants l_1, l_2, l_3 may be shown⁷ to be the roots of the cubic equation

$$4l^3 - 3Hl - \Delta = 0, \quad (3.16)$$

where H and Δ are certain invariant combinations of the moments m_{pq} . Thus

$$3H = m_{40}m_{04} - 4m_{41}m_{14} + 3m_{42}^2, \\ \Delta = |(\Xi_{ij})| = |(M_{ij})|^{-1}. \quad (3.17)$$

From (3.16) we have

$$l_1 + l_2 + l_3 = 0, \\ l_1^2 + l_2^2 + l_3^2 + l_1l_2 = -\frac{3}{2}H, \\ l_1l_2l_3 = \frac{1}{2}\Delta. \quad (3.18)$$

⁷ M. S. Longuet-Higgins, Proc. Cambridge Phil. Soc. (to be published).

It can further be shown⁴ that

$$(a_{31} + a_{61})^2 + (a_{32} + a_{62})^2 + (a_{33} + a_{63})^2 = D, \tag{3.19}$$

$$(a_{31} + a_{61})^2/l_1 + (a_{32} + a_{62})^2/l_2 + (a_{33} + a_{63})^2/l_3 = 4,$$

where

$$D = m_{40} + 2m_{22} + m_{04}, \tag{3.20}$$

another invariant of the surface. The first factor in the integrand of (3.13) may be written as

$$(\xi_3 \xi_4 - \xi_4^2) + \kappa(\xi_3 + \xi_4) + \kappa^2$$

$$= (l_1 \eta_1^2 + l_2 \eta_2^2 + l_3 \eta_3^2) + \kappa \sum_{j=1}^3 (a_{3j} + a_{6j}) \eta_j + \kappa^2$$

$$= \sum_{j=1}^3 l_j \{ \eta_j + \kappa(a_{3j} + a_{6j})/2l_j \}^2, \tag{3.21}$$

by the second of equations (3.19). Since the modulus of the transformation (3.14) is

$$\partial(\xi_3, \xi_4, \xi_5) / \partial(\eta_1, \eta_2, \eta_3) = |(a_{ij})| = |(M_{ij})|, \tag{3.22}$$

Eq. (3.13) becomes

$$N = \frac{1}{(2\pi)^3 \kappa^2} \int_{-\infty}^{\infty} \int_{-\infty}^{\infty} \int_{-\infty}^{\infty} \left| \sum_{j=1}^3 l_j (\eta_j + y_j) \right|$$

$$\times \exp\left[-\frac{1}{2} \sum_{j=1}^3 \eta_j^2\right] d\eta_1 d\eta_2 d\eta_3 \tag{3.23}$$

in which we have put, for brevity,

$$y_j = \kappa(a_{3j} + a_{6j}) / (2l_j). \tag{3.24}$$

Now the corresponding triple integral without the modulus sign equals

$$\frac{1}{(2\pi)^3 \kappa^2} \sum_{j=1}^3 l_j (1 + y_j^2) (2\pi)^3 = 1 \tag{3.25}$$

by (3.18) and (3.19). On adding this quantity to each side of (3.23), we have

$$N + 1 = \frac{2}{(2\pi)^3 \kappa^2} \int \int \int \left[\sum_{j=1}^3 l_j (\eta_j + y_j)^2 \right]$$

$$\times \exp\left[-\frac{1}{2} \sum_{j=1}^3 \eta_j^2\right] d\eta_1 d\eta_2 d\eta_3, \tag{3.26}$$

where the integration is over that region of η space for which the first factor in square brackets is positive.

Now Δ being a positive quantity it follows from (3.18) that one of the roots l_j is positive (let it be l_1 , say) and that the other two are negative in general. So over the region of integration we may make the substitution

$$l_1^{1/2}(\eta_1 + y_1) = r,$$

$$(-l_2)^{1/2}(\eta_2 + y_2) = r \sin\theta \cos\phi, \tag{3.27}$$

$$(-l_3)^{1/2}(\eta_3 + y_3) = r \sin\theta \sin\phi.$$

The ranges of the variables are

$$-\infty < r < \infty, \quad 0 \leq \theta \leq \pi/2, \quad 0 \leq \phi < 2\pi, \tag{3.28}$$

and the modulus of transformation is

$$\partial(\eta_1, \eta_2, \eta_3) / \partial(r, \theta, \phi) = (l_1 l_2 l_3)^{-1/2} \cos\theta \sin\theta. \tag{3.29}$$

So, on using (3.17), we have

$$N + 1 = \frac{2^4}{\pi^3 \kappa^2 \Delta^3} \int_{-\infty}^{\infty} dr \int_0^{\pi/2} d\theta \int_0^{2\pi} d\phi r^4 \cos^2\theta \sin\theta$$

$$\times \exp\left[-\frac{1}{2}(Pr^2 + 2Qr + R)\right], \tag{3.30}$$

where we have written

$$P = l_1^{-1} - l_2^{-1} \sin^2\phi \cos^2\theta - l_3^{-1} \sin^2\theta \sin^2\phi,$$

$$Q = y_1 l_1^{-1} + y_2 (-l_2)^{-1} \sin\theta \cos\phi$$

$$+ y_3 (-l_3)^{-1} \sin\theta \sin\phi, \tag{3.31}$$

$$R = y_1^2 + y_2^2 + y_3^2.$$

The integration with respect to r can be carried out immediately, giving

$$N + 1 = \frac{2e^{-4R}}{\pi^2 \kappa^2 \Delta^3} \int_0^{\pi/2} d\theta \int_0^{2\pi} d\phi \cos^2\theta \sin\theta$$

$$\times (3P^2 + 6Q^2P + Q^4) P^{-3/2} \exp(Q^2/2P). \tag{3.32}$$

4. ISOTROPIC CASE

In general, the integral (3.32) cannot be expressed in terms of known functions. We therefore specialize to the case when the surface is isotropic, that is to say, its statistical properties are independent of direction on the surface. In that case the spectrum $E(u, v)$ is a function of $(u^2 + v^2)$ only, and it has been shown⁴ that

$$H = (1/16)D^3, \quad \Delta = (1/64)D^3. \tag{4.1}$$

The roots of (3.16) are then

$$l_1, l_2, l_3 = \frac{1}{2}D, -\frac{1}{2}D, -\frac{1}{2}D. \tag{4.2}$$

Equations (3.19) then give

$$(a_{31} + a_{61})^2 = D,$$

$$(a_{31} + a_{61})^2 + (a_{32} + a_{62})^2 = 0, \tag{4.3}$$

whence it is clear that both squared terms in the second equation must be zero. So, from (3.24),

$$y_1, y_2, y_3 = \kappa l_1^{-1}, 0, 0, \tag{4.4}$$

and hence from (3.28)

$$P = 4D^{-1}(1 + 2 \sin^2\theta),$$

$$Q = 4D^{-1}\kappa, \tag{4.5}$$

$$R = 4D^{-1}\kappa^2.$$

We see then that the integrand in (3.32) is independent of ϕ , so that integration with respect to ϕ amounts to

multiplying by 2π . On writing, for brevity,

$$D/(4\kappa^2) = A, \tag{4.6}$$

we find

$$N+1 = \frac{4}{A} \int_0^{\pi/2} d\theta \cdot \cos^2\theta \sin\theta \exp\left[\frac{\sin^2\theta}{A(1+2\sin^2\theta)} \right] \\ \times [3A^2(1+2\sin^2\theta)^3 + 6A(1+2\sin^2\theta) + 1] \\ \times (1+2\sin^2\theta)^{-3/2}. \tag{4.7}$$

The substitution

$$1+2\sin^2\theta = s^{-2} \tag{4.8}$$

reduces this integral to the form

$$N+1 = \frac{1}{A} \int_{1/\sqrt{3}}^1 (3s^2-1)(3A^2+6As^2+s^4) \\ \times \exp[(s^2-1)/2A] ds, \tag{4.9}$$

which can easily be evaluated by integrating by parts. The result is

$$N+1 = 2 + (2A/\sqrt{3})e^{-(3A^{-1})}, \tag{4.10}$$

so that

$$N = 1 + (2A/\sqrt{3})e^{-(4A^{-1})}. \tag{4.11}$$

The interpretation of this result is very similar to the two-dimensional case discussed in Sec. 3. The parameter A defined by (4.6) is proportional to κ^{-2} , that is to say, to the square of the distance of the observer from the surface, and also to D , which by (3.20) represents the average square of the "mean curvature"; for this is

$$\left\langle \left(\frac{\partial^2 \zeta}{\partial x^2} + \frac{\partial^2 \zeta}{\partial y^2} \right)^2 \right\rangle_{av} = \langle (\xi_1 + \xi_2)^2 \rangle_{av} = \langle \xi_1^2 \rangle_{av} \\ + 2\langle \xi_1 \xi_2 \rangle_{av} + \langle \xi_2^2 \rangle_{av} = m_{40} + 2m_{22} + m_{04} \tag{4.12}$$

by (3.8). When the point of observation is very close to the surface (A is small), we find

$$N \sim 1 \tag{4.13}$$

as before, and at great distances

$$N \sim 2A/\sqrt{3}, \tag{4.14}$$

that is to say, the number of points increases as the square of the distance from the surface. N is graphed against A in Fig. 2, curve (a).

5. TWO LONG-CRESTED SYSTEMS

Another special case for which a complete solution may be given is when the surface consists of two systems of long-crested waves intersecting at right angles.

If the axes of x and y are chosen to be parallel to the two systems, respectively, we have then

$$\zeta(x,y) = \zeta_1(x) + \zeta_2(y) \tag{5.1}$$

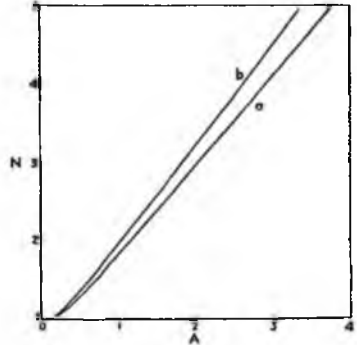


FIG. 2. The mean number of images as a function of A , defined by Eq. (4.6): (a) an isotropic surface, (b) a surface consisting of two long-crested systems at right angles.

and it is clear that the two conditions for a specular point [Eqs. (3.1)] are satisfied if and only if

$$\partial \zeta_1 / \partial x = -\kappa x, \quad \partial \zeta_2 / \partial y = -\kappa y. \tag{5.2}$$

Thus, specular points occur only when they would occur (in the two-dimensional sense) for each of the two long-crested systems simultaneously; whence it follows that the total number of specular points is the product of the number for the two systems individually:

$$N = N^{(1)}N^{(2)}, \tag{5.3}$$

where

$$N^{(i)} = \left(\frac{2}{\pi} \right)^{1/2} \left[\alpha_i \exp\left[-\left(\frac{1}{2} \alpha_i^{-2} \right) \right] \right. \\ \left. + \int_{\frac{1}{2} \alpha_i^{-2}}^{\infty} \exp\left(-\frac{1}{2} z^2 \right) dz \right] \tag{5.4}$$

and α_1, α_2 are the nondimensional parameters for the two systems.

The energy in the spectrum E must be regarded as being concentrated along the two axes of u, v , and negligible elsewhere. The moments m_{pq} of equation (3.9) are then zero whenever $pq \neq 0$, and the two parameters α_1, α_2 are given by

$$\alpha_1 = m_{40}^{1/4} / \kappa, \quad \alpha_2 = m_{04}^{1/4} / \kappa. \tag{5.5}$$

In the case when the two systems have equal mean-square curvature, i.e., $m_{40} = m_{04}$, then

$$\alpha_1 = \alpha_2 = \left(\frac{1}{2} D \right)^{1/4} / \kappa = (2A)^{1/4}, \tag{5.6}$$

where D and A are given by (3.19) and (4.6). Hence,

$$N = \frac{2}{\pi} \left[(2A)^{1/2} e^{-(1/2)A^{-1}} + \int_{\frac{1}{2}A^{-1}}^{\infty} \exp\left(-\frac{1}{2} z^2 \right) dz \right]. \tag{5.7}$$

This function is shown in Fig. 2, curve (b), and it will be seen that the results are not very different from the

isotropic case [curve (a)]. For large values of A , we find

$$N \sim 4A/\pi. \tag{5.8}$$

6. CASE $\kappa \rightarrow 0$

Further, it is possible to determine the behavior of N at great distances from the surface for quite general forms of the energy spectrum E . For when $\kappa \rightarrow 0$, we have, from (3.26),

$$N \sim \frac{2}{(2\pi)^4 \kappa^2} \int \int \int [\sum_{j=1}^3 l_j \eta_j^2] \times \exp[-\frac{1}{2} \sum_{j=1}^3 \eta_j^2] d\eta_1 d\eta_2 d\eta_3. \tag{6.1}$$

The preceding integral has been evaluated previously (footnote reference 3, Sec. 2.4; the integral equals $2I'$). The result is

$$N \sim \frac{4}{\pi \kappa^2} (l_1 l_2)^{1/2} \left[\left(\frac{l_2 - l_1}{l_1} \right)^{1/2} E(k) - \left(\frac{l_2}{l_2 - l_1} \right)^{1/2} F(k) \right], \tag{6.2}$$

where

$$E(k) = \int_0^{\pi/2} (1 - k^2 \sin^2 \phi)^{1/2} d\phi \tag{6.3}$$

$$F(k) = \int_0^{\pi/2} (1 - k^2 \sin^2 \phi)^{-1/2} d\phi$$

and

$$k^2 = l_1(l_1 - l_2)/l_2(l_1 - l_2). \tag{6.4}$$

This can also be written

$$N \sim (A/\pi) (l_1/D) \Phi(-l_2/l_1), \tag{6.5}$$

where

$$\Phi(\rho) = (\rho(1-\rho))^{1/2} \left[\left(\frac{1+\rho}{\rho} \right)^{1/2} E(k) - \left(\frac{\rho}{1+\rho} \right)^{1/2} F(k) \right], \tag{6.6}$$

$$\rho = -l_2/l_1, \quad k^2 = (1-2\rho)/(1-\rho^2).$$

The function Φ is plotted in Fig. 10 of footnote reference 3. It is a very slowly varying function and lies always between 0.917 and 1.

For example, when the surface consists of two equal long-crested systems of waves intersecting at an arbitrary angle θ_0 , it can be shown (see footnote reference 6) that

$$H = \frac{1}{4} D^2 \sin^2 \theta_0, \quad \Delta = 0, \tag{6.7}$$

and so from (3.16),

$$l_1, l_2, l_3 = \frac{1}{2} D \sin \theta_0, 0, -\frac{1}{2} D \sin \theta_0. \tag{6.8}$$

It follows that $\rho = 0$ and $\Phi(\rho) = 1$, whence

$$N \sim (4A/\pi) \sin \theta_0. \tag{6.9}$$

When $\theta_0 = \pi/2$, i.e., the systems are perpendicular, we regain Eq. (5.8).

On the other hand, when the surface is isotropic, we see from (4.2) that $\rho = \frac{1}{2}$ and so $\Phi(\rho) = \pi/2\sqrt{3}$. Hence

$$N \sim D/2\sqrt{3} \kappa^2 = 2A/\sqrt{3} \tag{6.10}$$

in agreement with (4.14).

We may compare an isotropic surface with a surface consisting of two intersecting long-crested systems having the same mean-square curvature D . From Eqs. (6.9) and (6.10) we see that they will give equal numbers of image points provided the angle of intersection θ_0 is

$$\sin^{-1}(\pi/2\sqrt{3}) = 66^\circ 30'. \tag{6.11}$$

7. CONCLUSIONS

The average number of specular reflections seen by an observer at distance h from an isotropic Gaussian surface is given by Eq. (4.11), in which $A = \frac{1}{2} k^2 D$ and D denotes the mean-square curvature. This number increases from 1 at small distances to a value proportional to h^2 at great distances.

For two long-crested systems of waves intersecting at right angles, the number of images is given by Eq. (5.7). The two solutions are shown as functions of A in Fig. 2.

Finally a solution can always be found for large values of h ; it is given by Eq. (6.5). In particular, when the surface consists of two long-crested systems of waves intersecting at an angle θ_0 , the total number of images is given by Eq. (6.9).

Reflection and Refraction at a Random Moving Surface.

III. Frequency of Twinkling in a Gaussian Surface

M. S. LONGUET-HIGGINS
National Institute of Oceanography, England
 (Received January 25, 1960)

When light is reflected or refracted at a moving Gaussian surface, the observer sees a number of moving images of the source, which appear or disappear generally in pairs; such an event is called a "twinkle." In the present paper the number of twinkles per unit time is evaluated in terms of the frequency spectrum of the surface and the distance of the source O and observer Q , on the assumption that the surface is Gaussian and that OQ is perpendicular to the mean surface level.

A solution is found first for a single system of long-crested (or

two-dimensional) waves, and then extended to the case of two such systems intersecting at right angles.

The rate of twinkling is found to depend, apart from a scale factor, on two parameters of the surface, one of which, α , increases steadily with the distance of O or Q from the surface; the other, d , discriminates between waves of standing type and waves of progressive type. Over a considerable range of α , the rate of twinkling is almost independent of d , but for large values of α the rate is much greater for standing waves than for progressive waves; waves of intermediate type are included in the analysis.

1. INTRODUCTION

IN two previous papers^{1,2} we have studied the pattern of reflections of a point-source in a random, moving surface, and have determined the average number of distinct images seen by an observer in the case when the surface slopes and curvature have a Gaussian distribution. It was shown¹ that the specular points (that is, images of the point source) are generally created or annihilated in pairs, such an event being called a "twinkle." In this paper our purpose is to evaluate the frequency of twinkling, that is to say the average number of twinkles per unit time over the whole surface. This number π is to be expressed in terms of the wave energy spectrum of the surface.

It can be shown that at a twinkle the intensity of radiation seen by the observer is greatly increased, so that the observer sees a bright flash. (This may be analogous to some sudden increases in the recorded intensity of radio waves reflected from the ionosphere.³) In the language of ray optics, the surface momentarily focuses the radiation at the point of observation. Corresponding to the principal radii of curvature, there are generally two focal points along a reflected ray, and the flash occurs when one of these coincides with the observer.

An exactly similar effect is produced when the surface is the boundary of a refracting medium (such as water) and the source of light is observed from a point on the far side of the surface; an observer below the water surface will see a pattern of images of the light source; these are created and destroyed in a manner analogous to the reflected images.

Another way of looking at the phenomenon is as follows. Suppose that the radiation, after passing through the surface, illuminates a horizontal plane at some fixed distance below the mean surface level—

as sunlight falling on the sea bed in shallow water. If the plane is not too near to the surface it can be seen to be covered with a pattern of bright lines—the loci of those points where a twinkle may be momentarily observed. The rate of twinkling is then the average number of times that one of these lines sweeps through a fixed point in the plane.

The general problem, for a Gaussian surface with arbitrary frequency spectrum, appears to be complicated. Our approach will be to solve first the analogous problem in two dimensions (when the surface is long-crested and the light source is a line parallel to the crests); then we may deduce the solution for a surface which consists of two such long-crested systems intersecting at right angles.

It is found that apart from a scale factor the rate of twinkling depends upon two parameters of the surface. The first of these, α , is proportional to the distance of the observer from the surface and to the rms curvature of the surface. The second, d , is small for waves of progressive type and increases to a maximum for waves of standing type. Over much of the range of α the rate of twinkling is found to be nearly independent of d ; for larger values of α , however, the rate of twinkling increases with d , and is much greater for standing waves than for progressive waves.

2. GEOMETRICAL CONDITIONS

If $z = \zeta(x, y, t)$ denotes the equation of the surface in rectangular coordinates, z being directed vertically upward, then it can be shown¹ that the condition for a specular point, when source and observer lie on the x axis, is

$$\partial f / \partial x = 0, \quad \partial f / \partial y = 0, \quad (2.1)$$

where

$$f(x, y, t) = \zeta(x, y, t) + \frac{1}{2}\kappa(x^2 + y^2) \quad (2.2)$$

and κ is a constant. In the reflection problem, if h_1 and h_2 denote the heights of source and observer above the mean surface level, then

$$\kappa = \frac{1}{2}[(1/h_1) + (1/h_2)]. \quad (2.3)$$

¹ M. S. Longuet-Higgins, *J. Opt. Soc. Am.* **50**, 838 (1960), paper I of this series.

² M. S. Longuet-Higgins, *J. Opt. Soc. Am.* **50**, 845 (1960), paper II of this series.

³ J. D. Whitehead, *J. Terrest. Atm. Phys.* **9**, 269 (1956).

In the refraction problem, if h_1 and h_2 denote the distances of source and observer above and below the surface, and if μ_1 and μ_2 are the refractive indices of the two media, then

$$\kappa = (\mu_1 h_1 + \mu_2 h_2) / [(\mu_2 - \mu_1) h_1 h_2]. \quad (2.4)$$

The condition for a twinkle is that, besides Eqs. (2.1),

$$(\partial^2 f / \partial x^2)(\partial^2 f / \partial y^2) - (\partial^2 f / \partial x \partial y)^2 = 0 \quad (2.5)$$

shall also be satisfied; that is the vanishing of the total curvature of the surface $z = f$.

In the corresponding one-dimensional case, when the situation is independent of the y coordinate the conditions are simply that

$$\partial f / \partial x = 0, \quad \partial^2 f / \partial x^2 = 0, \quad (2.6)$$

where

$$f(x, t) = \zeta(x, t) + \frac{1}{2} \kappa x^2. \quad (2.7)$$

3. TWO-DIMENSIONAL CASE: STATISTICAL MODEL

We take as a model for the surface the function

$$\zeta(x, t) = \sum_{n=1}^{n_0} c_n \cos(k_n x + \sigma_n t + \epsilon_n), \quad (3.1)$$

where the phase constants ϵ_n are supposed to be distributed randomly and uniformly over $(0, 2\pi)$, the wave numbers k_n , σ_n are distributed over the intervals $(-\infty, \infty)$ and $(0, \infty)$, and where n_0 at last tends to infinity in such a way that over any small intervals $(k, k + dk)$, $(\sigma, \sigma + d\sigma)$,

$$\sum_n \frac{1}{2} c_n^2 = E(k, \sigma) dk d\sigma, \quad (3.2)$$

where $E(k, \sigma)$ is a continuous function of k , σ (the spectrum function). Such a model is a generalization of that employed for a time-independent surface.²

Under certain conditions the distribution of ζ and its derivatives at a given point x and time t is Gaussian. On writing, for brevity,

$$\begin{aligned} \partial \zeta / \partial x, \quad \partial^2 \zeta / \partial x^2, \quad \partial^2 \zeta / \partial x \partial t, \\ \partial^3 \zeta / \partial x^3 = \xi_1, \xi_2, \xi_3, \xi_4, \end{aligned} \quad (3.3)$$

we have for the matrix of mean values of the products:

$$\langle (\xi_i \xi_j)_{x,t} \rangle = \begin{pmatrix} m_1 & 0 & 0 & -m_4 \\ 0 & m_2 & m_3' & 0 \\ 0 & m_3' & m_2' & 0 \\ -m_4 & 0 & 0 & m_4 \end{pmatrix}, \quad (3.4)$$

where

$$\begin{aligned} m_1 &= \int_{-\infty}^{\infty} \int_0^{\infty} E(k, \sigma) k^2 dk d\sigma, \\ m_2 &= \int_{-\infty}^{\infty} \int_0^{\infty} E(k, \sigma) k^2 \sigma dk d\sigma, \\ m_3' &= \int_{-\infty}^{\infty} \int_0^{\infty} E(k, \sigma) k^2 \sigma^2 dk d\sigma, \\ m_4 &= \int_{-\infty}^{\infty} \int_0^{\infty} E(k, \sigma) k^3 \sigma^2 dk d\sigma. \end{aligned} \quad (3.5)$$

The probability density of $\xi_1, \xi_2, \xi_3, \xi_4$ is therefore given by

$$p(\xi_1, \xi_2, \xi_3, \xi_4) = \frac{|(M_{ij})|^{-1}}{4\pi^2} \exp[-\frac{1}{2} \sum_{i,j} M_{ij} \xi_i \xi_j], \quad (3.6)$$

where (M_{ij}) is the matrix inverse to (3.4). The occurrence of zeros in the matrix implies that the distributions of ξ_1, ξ_4 and of ξ_2, ξ_3 are independent. In fact,

$$p(\xi_1, \xi_2, \xi_3, \xi_4) = p(\xi_1, \xi_4) p(\xi_2, \xi_3), \quad (3.7)$$

where

$$p(\xi_1, \xi_4) = \frac{1}{2\pi(m_1 m_4 - m_4^2)^{1/2}} \times \exp\left[-\frac{m_1 \xi_1^2 + 2m_4 \xi_1 \xi_4 + m_4 \xi_4^2}{2(m_1 m_4 - m_4^2)}\right]$$

$$p(\xi_2, \xi_3) = \frac{1}{2\pi(m_2 m_2' - m_3'^2)^{1/2}} \times \exp\left[-\frac{m_2 \xi_2^2 - 2m_3' \xi_2 \xi_3 + m_2 \xi_3^2}{2(m_2 m_2' - m_3'^2)}\right] \quad (3.8)$$

It will be convenient to write

$$\eta_1, \eta_2, \eta_3, \eta_4 = \partial f / \partial x, \partial^2 f / \partial x^2, \partial^2 f / \partial x \partial t, \partial^3 f / \partial x^3 = (\xi_1 + \kappa x), (\xi_2 + \kappa), \xi_3, \xi_4, \quad (3.9)$$

so that the probability density of $\eta_1, \eta_2, \eta_3, \eta_4$ at a fixed value of x, t is given by

$$p(\eta_1, \eta_2, \eta_3, \eta_4) = p(\xi_1, \xi_2, \xi_3, \xi_4), \quad (3.10)$$

where

$$\xi_1, \xi_2, \xi_3, \xi_4 = (\eta_1 - \kappa x), (\eta_2 - \kappa), \eta_3, \eta_4. \quad (3.11)$$

4. EVALUATION OF THE PROBABILITY

We wish now to find the probability that in a given small interval of time $(t, t + dt)$, and in $-\infty < x < \infty$, the conditions

$$\eta_1 = 0, \quad \eta_2 = 0 \quad (4.1)$$

shall be satisfied. Let this probability be $n dt$ (clearly, n is the mean number of "flashes" per unit time). We first seek the probability of (4.1) being satisfied in a small interval $(t, t + dt)$ and in $(x, x + dx)$; if this probability is denoted by $n_x dx dt$, then clearly

$$n = \int_{-\infty}^{\infty} n_x dx. \quad (4.2)$$

The advantage of dealing first with n_x is that for fixed x the distributions of $\eta_1, \eta_2, \eta_3, \eta_4$ are invariant.⁴

Now the probability $p(\eta_1, \eta_2) d\eta_1 d\eta_2$ represents the probability that η_1, η_2 lie within the limits $\eta_1 + d\eta_1$ and $\eta_2 + d\eta_2$ at certain fixed values of x, t . On the

⁴ n_x has been evaluated previously in the case when the source and observer are at infinite distance. See M. S. Longuet-Higgins, Proc. Cambridge Phil. Soc. 56, 234 (1956).

other hand if η_1, η_2 take the given values (4.1) in a given range $(x, x+dx)$ and interval $(t, t+dt)$ then (η_1, η_2) at (x, t) itself may vary within a region of measure

$$\left| \frac{\partial(\eta_1, \eta_2)}{\partial(x, t)} \right| = \left\| \begin{matrix} \partial^2 f / \partial x^2 & \partial^2 f / \partial x^2 \\ \partial^2 f / \partial x \partial t & \partial^2 f / \partial x^2 \partial t \end{matrix} \right\| dx dt, \quad (4.3)$$

which in the neighborhood of the points (4.1) reduces to $|\eta_1 \eta_2| dx dt$ simply. Hence the probability $n dx dt$ is given by

$$n dx dt = \int_{-\infty}^{\infty} \int_{-\infty}^{\infty} \rho(\eta_1, \eta_2, \eta_3, \eta_4) |\eta_3 \eta_4| dx dt d\eta_3 d\eta_4, \quad (4.4)$$

and the required probability $n dt$ is given by

$$n = \int_{-\infty}^{\infty} \int_{-\infty}^{\infty} \int_{-\infty}^{\infty} \rho(\eta_1, \eta_2, \eta_3, \eta_4) |\eta_3 \eta_4| dx d\eta_3 d\eta_4. \quad (4.5)$$

Now x is involved only in η_1 , so that the integration with respect to x may be carried out immediately. Replacing η_2 at the same time by 0, we have, from (3.10),

$$n = \frac{1}{(2\pi)^{1/2} m_1} \int_{-\infty}^{\infty} \exp(-\eta_1^2 / 2m_1) |\eta_1| d\eta_1 \times \frac{1}{2\pi(m_1 m_2'' - m_2'^2)^{1/2}} \times \int_{-\infty}^{\infty} \exp\left[-\frac{m_2'' k^2 + 2m_2' k \eta_1 + m_1 \eta_1^2}{2(m_1 m_2'' - m_2'^2)}\right] d\eta_1, \quad (4.6)$$

The remaining integrals present no difficulty, and give the following:

$$n = \frac{2^{1/2} m_1^{1/2} (m_1 m_2'' - m_2'^2)^{1/2}}{\pi^{1/2} m_1} \exp(-\kappa^2 / 2m_1) \times \left[\exp(-\frac{1}{2}\phi^2) + \phi \int_0^{\infty} \exp(-\frac{1}{2}z^2) dz \right], \quad (4.7)$$

where

$$\phi = \kappa m_2' / [m_1^{1/2} (m_1 m_2'' - m_2'^2)^{1/2}]. \quad (4.8)$$

If we now define the dimensionless quantities

$$\alpha = m_1^{1/2} / \kappa, \quad (4.9)$$

$$d = [(m_1 m_2'' - m_2'^2) / m_1 m_2'']^{1/2}, \quad (4.10)$$

then (4.7) can be written in the final form

$$n = [(m_1 m_2'')^{1/2} / m_1] f(\alpha, d), \quad (4.11)$$

where

$$f(\alpha, d) = \frac{2^{1/2}}{\pi^{1/2}} \alpha d \exp(-2\alpha^2) \times \left[\exp(-\frac{1}{2}\phi^2) + \phi \int_0^{\infty} \exp(-\frac{1}{2}z^2) dz \right] \quad (4.12)$$

and

$$\phi = (1 - d^2)^{1/2} / \alpha d.$$

Since the error integral on the right-hand side is a tabulated function,⁶ this completes the formal solution of the problem.

5. DISCUSSION

In Eq. (4.11) the first factor on the right-hand side has the dimensions of (time)⁻¹. If the spectrum contains a single narrow band of frequencies centered on a mean wavelength λ and period τ , then

$$(m_1 m_2'')^{1/2} / m_1 = 2\pi / \tau, \quad (5.1)$$

approximately. This factor, therefore, essentially determines the time scale.

Of the remaining two parameters α, d , the first is inversely proportional to κ , and so increases linearly with the distances of O and Q from the surface. Also, α is proportional to $m_1^{1/2}$, the root-mean-square value of the "curvature" $\partial^2 f / \partial x^2$.

The parameter d is a function of the frequency spectrum $E(k, \sigma)$ only. Now, since

$$2(m_1 m_2'' - m_2'^2) = \int_{-\infty}^{\infty} \int_{-\infty}^{\infty} \int_{-\infty}^{\infty} \int_{-\infty}^{\infty} E(k_1, \sigma_1) E(k_2, \sigma_2) \times (k_1^2 k_2^2 \sigma_2^2 + k_2^2 k_1^2 \sigma_1^2 - 2k_1^2 k_2^2 \sigma_1 \sigma_2) \times dk_1 d\sigma_1 dk_2 d\sigma_2, \quad (5.2)$$

and since the factor in the integrand is a perfect square, we have

$$m_1 m_2'' - m_2'^2 \geq 0,$$

whence

$$0 \leq d \leq 1.$$

The lower limit of d is approached whenever the spectrum of the surface is narrow; the surface then has the appearance of a progressive wave of slowly varying amplitude and phase. The upper limit of d is attained when $m_2' = 0$, which occurs, for example, if the spectrum function $E(k, \sigma)$ is symmetrical with respect to k : $E(k, \sigma) = E(-k, \sigma)$, while σ is an even function of k ; the surface then has the appearance of a standing-wave pattern of varying phase and amplitude. Thus the parameter d discriminates between progressive and standing waves.

The function $f(\alpha, d)$ is shown in Fig. 1 for various

⁶ A. N. Lowan, "Tables of normal probability functions," Natl. Bur. Standards, Appl. Math. Ser. 23 (1953).

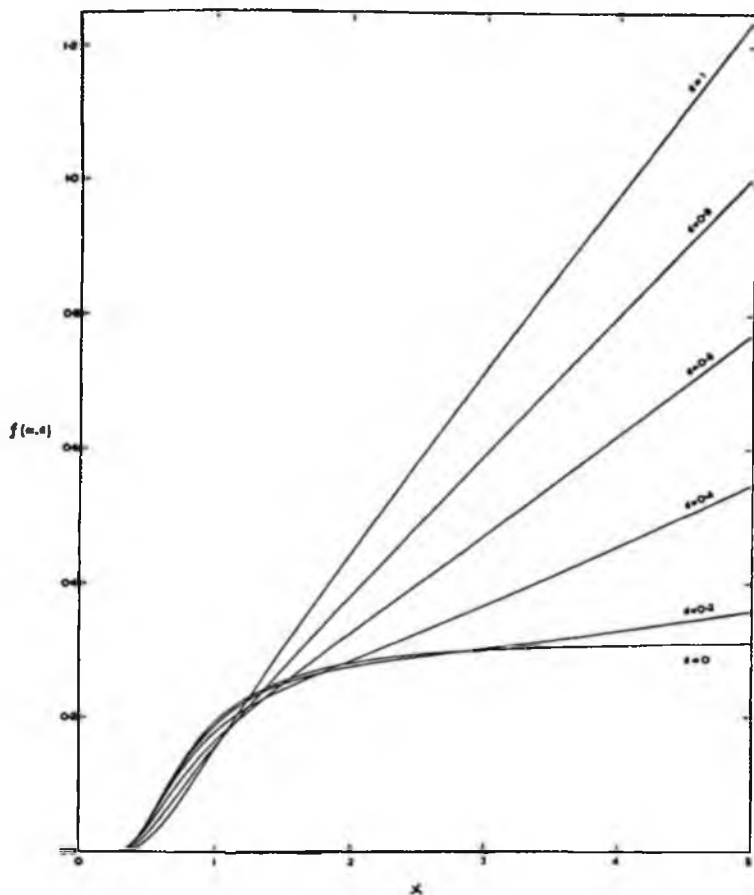


FIG. 1. Graphs of $f(\alpha, d)$ showing the rate of twinkling as a function of α (proportional to distance from surface) for various values of d .

values of the parameter d . Two limiting forms may be noted: as $d \rightarrow 0$

$$f(\alpha, d) \rightarrow (1/\pi) \exp(-2\alpha^2)^{-1}, \quad (5.3)$$

and when $d \rightarrow 1$

$$f(\alpha, d) \rightarrow (2^{1/2}/\pi^{1/2}) \alpha \exp(-2\alpha^2)^{-1}. \quad (5.4)$$

Although these two functions behave very differently at infinity it is remarkable that when $\alpha < 1.5$, they lie quite close together, as indeed does the whole family of functions; over the range $0 < \alpha < 1.5$, $f(\alpha, d)$ may for some purposes be taken as independent of d .

All the functions have an extremely sharp cutoff at about $\alpha = 0.3$, because of the factor $\exp(-2\alpha^2)^{-1}$. Hence the rate of twinkling falls off suddenly as the observer approaches the surface.

On the other hand, for large values of α , and when $d > 0$, we have

$$f(\alpha, d) \sim (2^{1/2}/\pi^{1/2}) \alpha d, \quad (5.5)$$

that is to say, π increases linearly with distance from the surface, as we might expect. The limiting case $d = 0$, when $f(\alpha, d) \rightarrow 1/\pi$ as $\alpha \rightarrow \infty$, is never in fact attained, because the bandwidth of the spectrum is never quite zero.

6. THREE-DIMENSIONAL PROBLEM

The general problem in three dimensions, when stated analytically, involves the evaluation of multiple integrals of high order. A useful simplification, however, results whenever the surface consists of two systems of long-crested waves (both Gaussian) intersecting at

right angles; for then by choosing the axes appropriately, we have

$$\zeta(x, y, t) = \zeta_1(x, t) + \zeta_2(y, t), \tag{6.1}$$

and the conditions (2.1) and (2.5) reduce to

$$\partial f_1 / \partial x = 0, \quad \partial f_2 / \partial x = 0, \quad (\partial^2 f_1 / \partial x^2)(\partial^2 f_2 / \partial y^2) = 0, \tag{6.2}$$

where

$$\begin{aligned} f_1(x, t) &= \zeta_1(x, t) + \frac{1}{2}\alpha x^2, \\ f_2(x, t) &= \zeta_2(x, t) + \frac{1}{2}\alpha y^2. \end{aligned} \tag{6.3}$$

Equations (6.2) show that a twinkle will occur in the combined system if a specular point in the one system ($\partial f_1 / \partial x = 0$) is combined with a twinkle in the other ($\partial f_2 / \partial y = 0, \partial^2 f_2 / \partial y^2 = 0$), or vice versa. Hence the total rate of twinkling is given by

$$n = n^{(1)}N^{(2)} + n^{(2)}N^{(1)}, \tag{6.4}$$

where $N^{(1)}$ and $N^{(2)}$ denote the numbers of specular points in the two systems, respectively, and $n^{(1)}$ and $n^{(2)}$ denote the rates of twinkling. Now $N^{(1)}$ has been

evaluated in a previous paper,¹ in fact, for a long-crested system of waves,

$$N^{(1)} = \left(\frac{2}{\pi}\right) \left[\alpha \exp(-2\alpha^2)^{-1} + \int_0^{1/\alpha} \exp(-\frac{1}{2}\pi^2 z^2) dz \right], \tag{6.5}$$

where α is the same parameter as before [Eq. (4.9)]. N is a function which increases steadily from unity at small values of α to the asymptotic value

$$N \sim (2/\pi)^{1/2} \alpha \tag{6.6}$$

for large values of α .

If the frequency characteristics of the two systems happen to be similar, then $N^{(1)} = N^{(2)}$ and $n^{(1)} = n^{(2)}$ and we have, from (6.4),

$$n = 2n^{(1)}N^{(1)}. \tag{6.7}$$

This can be expressed in terms of the parameter

$$A = \frac{1}{2}\alpha^2 = \frac{1}{2}\pi^2 D, \tag{6.8}$$

where D represents the mean-square value of the mean curvature of the surface (see footnote reference 1).

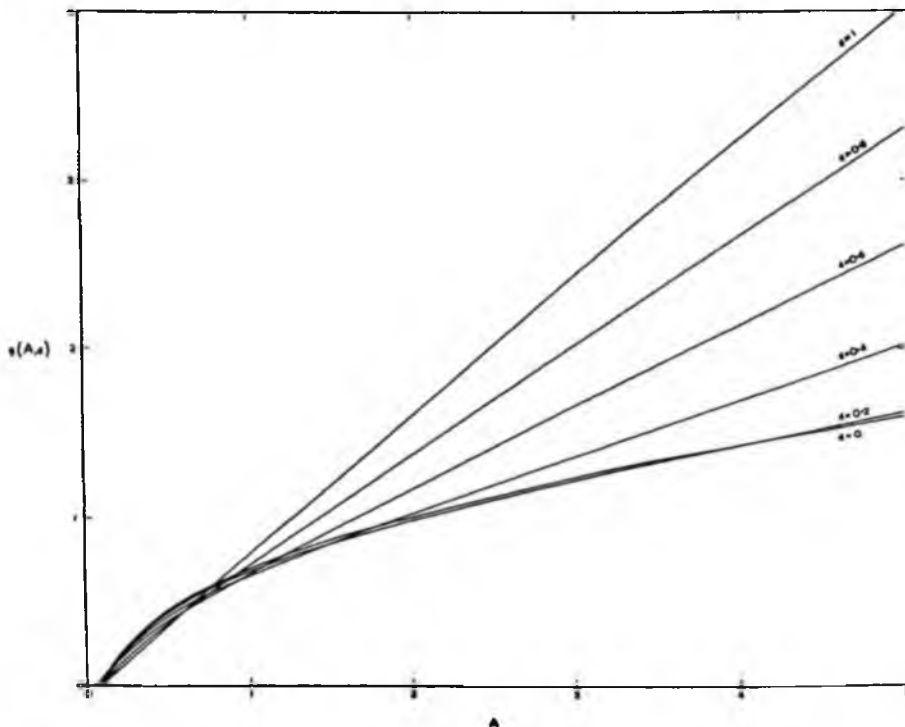


FIG. 2. Graphs of $g(A, d)$, showing the rate of twinkling for two intersecting systems as a function of A (proportional to the square of the distance from the surface) for various values of d .

Thus,

$$n = [(m\alpha m_1'')^2 / m_1] g(A, d). \quad (6.9)$$

The function $g(A, d)$ is shown in Fig. 2.

The interpretation of this result is similar to the two-dimensional case. A is proportional to the square of the distance from the origin and to the mean-square curvature, while d discriminates between standing waves and progressive waves. The function $g(A, d)$ is nearly independent of d for $0 < A < 1$, while for large values of A (that is, great distances from the origin), we have

$$g(A, d) \doteq (8/\pi^2) A d. \quad (6.10)$$

Thus, the rate of twinkling is more vigorous for standing waves $d=1$ than for progressive waves $d \ll 1$.

A rather general result may be deduced from Eq. (6.4). Consider the mean lifetime of a specular point. Since each specular point involves two twinkles, one at the beginning and one at the end of its life, and since two specular points are involved in a twinkle it follows that the mean lifetime of a specular point is given by

$$L = N/n, \quad (6.11)$$

and similarly in the two long-crested systems the mean lifetime of a specular *line* is given by

$$L^{(0)} = N^{(0)}/n^{(0)}, \quad L^{(1)} = N^{(1)}/n^{(1)}. \quad (6.12)$$

Now, since a specular point in the combined system is always the intersection of two specular lines, one from each of the two systems, we have

$$N = N^{(0)} N^{(1)}. \quad (6.13)$$

On dividing each side of Eq. (6.4) by the corresponding side of (6.13), we find

$$1/L = (1/L^{(0)}) + (1/L^{(1)}). \quad (6.14)$$

Hence, the lifetime of a specular point in the combined system is always less than the lifetime of a specular line in either long-crested system. When the two long-crested systems are similar, $L^{(0)} = L^{(1)}$, and hence

$$1/L = 2/L^{(0)}, \quad (6.15)$$

that is, the mean lifetime in the combined system is exactly half that in either system individually.

[557]

THE DISTRIBUTION OF INTERVALS BETWEEN ZEROS OF A STATIONARY RANDOM FUNCTION

BY M. S. LONGUET-HIGGINS

National Institute of Oceanography, Wormley

(Communicated by G. E. R. Deacon, F.R.S.—Received 21 August 1961)

CONTENTS

	PAGE		PAGE
INTRODUCTION	558	4.2. The cases $n = 1, 2$ and 3	573
1. GENERAL RELATIONS BETWEEN $P_m(\tau)$, $\rho(n, \tau)$ AND $W(S)$	559	4.3. General values of n	574
1.1. Generalization of a result of McFadden	560	4.4. Asymptotic behaviour of $P_m(\tau)$	576
1.2. Series for $P_m(\tau)$	562	4.5. Approximations to $P_m(0)$	577
1.3. Relation to a series of Rice	563	4.6. Disproof of the 'exponential hypothesis'	578
1.4. Series for $\rho(n, \tau)$	564	4.7. Further estimates of $P_m(0)$	578
2. EVALUATION OF $W(S)$ FOR GAUSSIAN PROCESSES	565	4.8. Asymptotic behaviour of $\rho(n, \tau)$	579
2.1. A general expression for $W(S)$	565	5. A COMPARISON OF DIFFERENT APPROXI- MATIONS TO $P_0(\tau)$	580
2.2. The cases $n = 1, 2$ and 3	567	5.1. Rice's approximation (1945)	580
2.3. General values of n	568	5.2. The approximation $P_0^{(1)}$	580
3. ASYMPTOTIC EXPANSIONS NEAR THE ORIGIN: ψ_τ REGULAR	569	5.3. The 'multiply conditioned' approximations	581
3.1. Expansion of $W(S)$	569	5.4. McFadden's first approximation	582
3.2. Evaluation of $P_m(\tau)$	570	5.5. $\beta_n(\tau)$ and $\beta_n^*(\tau)$	583
3.3. Evaluation of $\rho(n, \tau)$	571	5.6. McFadden's second approximation	586
4. ASYMPTOTIC EXPANSIONS NEAR THE ORIGIN: A SINGULAR CASE	572	5.7. The 'narrow-band' approximation	587
4.1. Expansion of $W(S)$	572	5.8. Numerical computations	588
		REFERENCES	599

The probability density P_m of the spacing between the i th zero and the $(i+m+1)$ th zero of a stationary, random function $f(t)$ (not necessarily Gaussian) is expressed as a series, of a type similar to that given by Rice (1945) but more rapidly convergent. The partial sums of the series provide upper and lower bounds successively for P_m . The series converges particularly rapidly for small spacings τ . It is shown that for fixed values of τ , the density $P_m(\tau)$ diminishes more rapidly than any negative power of m .

The results are applied to Gaussian processes; then the first two terms of the series for $P_m(\tau)$ may be expressed in terms of known functions. Special attention is paid to two cases:

(1) In the 'regular' case the covariance function $\psi(t)$ is expressible as a power series in t ; then $P_m(\tau)$ is of order $\tau^{1(m+2(m+3))^{-2}}$ at the origin, and in particular $P(\tau)$ is of order τ (adjacent zeros have a strong mutual repulsion). The first two terms of the series give the value of $P_0(\tau)$ correct to τ^{16} .

(2) In a singular case, the covariance function $\psi(t)$ has a discontinuity in the third derivative. This happens whenever the frequency spectrum of $f(t)$ is $O(\text{frequency})^{-4}$ at infinity. Then $P_m(\tau)$ is

shown to tend to a positive value $P_m(0)$ as $\tau \rightarrow 0$ (neighbouring zeros are less strongly repelled). Upper and lower bounds for $P_m(0)$ ($m = 0, 1, 2, 3$) are given, and it is shown that $P_0(0)$ is in the neighbourhood of $1.155\psi''/(-6\psi')$. The conjecture of Favreau, Low & Pfeffer (1956) according to which in one case $P_0(\tau)$ is a negative exponential, is disproved.

In a final section, the accuracy of other approximations suggested by Rice (1945), McFadden (1958), Ehrenfeld *et al.* (1958) and the present author (1958) are compared and the results are illustrated by computations, the frequency spectrum of $f(t)$ being assumed to have certain ideal forms: a low-pass spectrum, band-pass spectrum, Butterworth spectrum, etc.

INTRODUCTION

The problem of finding the statistical distribution of the intervals τ between zeros of a stationary, random function $f(t)$ is one with many physical applications, for example, to noise in electrical circuits (Rice 1944, 1945; McFadden 1956, 1958), sea waves (Ehrenfeld *et al.* 1958), microseisms (Longuet-Higgins 1953) or irregularities in the ionosphere (Briggs & Page 1955; Longuet-Higgins 1957). Yet in one most useful case, when $f(t)$ itself is Gaussian, only approximate solutions to the problem have been found. One such solution was given in a previous paper (1958). In the present paper the solution is expressed in the form of a series, in which each term is an integral of the joint probability

$$W(+, -, -, \dots, -) dt_1 \dots dt_n$$

that $f(t)$ have an up-crossing in the infinitesimal interval $(t_i, t_i + dt_i)$ and a down-crossing in the remaining $(n-1)$ intervals $(t_i, t_i + dt_i)$ ($i = 2, 3, \dots, n$). The series is somewhat similar to one given earlier by Rice (1945) but converges more rapidly. Moreover, successive partial sums of the series provide upper and lower bounds to the required distribution $P_0(\tau)$. The present series leads to a much more accurate estimate of the behaviour of P_0 near the origin $\tau = 0$ and to a systematic comparison of other approximations that have been previously proposed.

Following Rice (1945), the probability density of the interval between the i th and the $(i+m+1)$ th zero of $f(t)$ is denoted by $P_m(\tau)$; and the probability of exactly n zeros occurring in the interval $(t, t+\tau)$ is denoted by $p(n, \tau)$. In § 1 of this paper, some relations between the W and the $P_m(\tau)$ are proved, and series are obtained for both $P_m(\tau)$ and $p(n, \tau)$ in terms of the W . One result is to show that $P_m(\tau)$ decreases with m more rapidly than any negative power of m . The relations are quite general, and no assumption is made as to the Gaussian character of $f(t)$. It is assumed only that $f(t)$ is statistically stationary; that $-f(t)$ is statistically equivalent to $f(t)$ (i.e. that $f(t)$ is statistically symmetric with regard to the axis $f = 0$); and that the various quantities defined actually exist.

In § 2 we obtain explicit expressions for the W in terms of the covariance function of $f(t)$, which is denoted by $\psi(t)$. By using some recent results of Kamat (1953) and Nabeya (1952) it is shown that $W(+, -, -)$ can in fact be expressed in terms of known functionals of $\psi(t)$, a fact not apparently used previously. Moreover, in special cases the W can be evaluated for any integral n .

The results are applied in § 3 to the case when $\psi(t)$ is itself a regular function at $t = 0$ (implying the differentiability of $f(t)$ up to all orders). Thus it is shown that for small intervals $|t_i - t_j|$

$$W(+, -, +, \dots, (-)^{n-1}) \sim C_n \prod_{i < j} (t_j - t_i),$$

INTERVALS BETWEEN ZEROS OF A RANDOM FUNCTION 559

where C_n is a constant independent of the t_i . Hence the asymptotic behaviour of $P_m(\tau)$ and $p(n, \tau)$ for small τ is obtained. In particular it is shown that

$$P_m(\tau) \propto \tau^{\frac{1}{2}(m+2)(m+3)-2}$$

and

$$p(n, \tau) \propto \tau^{\frac{1}{2}n(n+1)}.$$

The power of τ increases rapidly with m or n , indicating a strong 'mutual repulsion' of neighbouring zeros of $f(t)$.

A very interesting singular case is studied in § 4, when the covariance function $\psi(t)$, instead of being regular at $t = 0$, has a finite discontinuity in the third derivative $f'''(t)$. This occurs, for example, whenever the spectral density of $f(t)$ is proportional to (frequency)⁻⁴ at high frequencies, and some examples have been studied experimentally by Favreau, Low & Pfeffer (1956). In contrast to the regular case, it is shown that, for small spacings $|t_i - t_j|$,

$$W(+, -, +, \dots, (-)^{n-1}) \sim \frac{F(t_1, t_2, \dots, t_n)}{(t_3 - t_1)(t_4 - t_2) \dots (t_n - t_{n-2})} \quad (n \geq 2),$$

where $F(t_1, t_2, \dots, t_n)$ is a function of the $(t_i - t_j)$ lying between positive upper and lower bounds. It follows now that

$$P_m(\tau) \propto \tau^0 \quad (m \geq 0),$$

and

$$p(n, \tau) \propto \tau^2 \quad (n \geq 2),$$

so that, as $\tau \rightarrow 0$, $P_m(\tau)$ tends to a value $P_m(0)$ independent of τ .

Moreover, upper and lower bounds for $P_m(0)$ can be found. Thus

$$1.147\alpha < P_0(0) < 1.218\alpha,$$

where $\alpha = \psi''(0+) / \{-6\psi''(0)\}$. This result enables us to disprove rigorously the 'exponential hypothesis' of Favreau *et al.* (1956), whereby the distribution of intervals τ for the function whose spectrum is $(1 + \sigma^2)^{-2}$ is conjectured to be $\pi^{-1} e^{-\tau/\pi}$. For this would make

$$P_0(0) = 3\pi^{-1}\alpha = 0.955\alpha,$$

in contradiction to the above inequality.

Some rough work shows that a close approximation to $P_0(\tau)$ is probably

$$P_0(0) \doteq 1.155\alpha.$$

Lastly in § 5 we use the asymptotic expansions of $P_m(\tau)$, $p(n, \tau)$ and the W to compare the accuracy of the approximations proposed by Rice (1945), McFadden (1956, 1958), Ehrenfeld *et al.* (1958) and the present author (1958), especially in the neighbourhood of the origin. Numerical computation of the various approximations is also compared with experimental results of Blötekjaer (1958) and other authors.

1. GENERAL RELATIONS BETWEEN $P_m(\tau)$, $p(n, \tau)$ AND $W(S)$

Let $W(+, +, \dots, +) dt_1 \dots dt_n$ denote the probability that the function $f(t)$ have an up-crossing (zero-crossing with positive gradient) in each of the intervals

$$(t_i, t_i + dt_i) \quad (i = 1, \dots, n);$$

by substituting a minus sign for any plus sign in $W(+, +, \dots, +)$ we denote the corresponding probability for a down-crossing. Thus $W(+, -, +, \dots, (-)^{n-1}) dt_1 \dots dt_n$ denotes the probability of alternate up-crossings and down-crossings in $(t_i, t_i + dt_i)$, the first being

an up-crossing. It will be seen later that the W may in many cases be evaluated explicitly in terms of the covariance function of the random process $f(t)$.

In this section we shall derive some quite general relations between $P_m(\tau)$, $p(n, \tau)$ and the W , which are valid not only for Gaussian but for non-Gaussian processes.

1.1. Generalization of a result of McFadden

It was pointed out by McFadden (1958) that

$$\frac{W(+, -)}{W(+)} = P_0(\tau) + P_2(\tau) + P_4(\tau) + \dots, \quad (1.1.1)$$

$$\frac{W(+, +)}{W(+)} = P_1(\tau) + P_3(\tau) + P_5(\tau) + \dots, \quad (1.1.2)$$

where $\tau = (t_2 - t_1)$. The proof is very simple: the left-hand side of (1.1.1), when multiplied by dt_2 , represents the probability that f has a down-crossing in $(t_2, t_2 + dt_2)$ given that it has an up-crossing at t_1 . This down-crossing must be either the next zero of f , or the next but two, and so on. These mutually exclusive events correspond to the individual terms on the right of (1.1.1); hence the identity. A similar argument proves (1.1.2).

Corresponding to (1.1.1) and (1.1.2) we may establish the following three relations:

$$\int_{t_1 < t_2 < t_3} \frac{W(+, -, -)}{W(+)} dt_2 = P_1(\tau) + 2P_3(\tau) + 3P_5(\tau) + \dots, \quad (1.1.3)$$

$$\int_{t_1 < t_2 < t_3} \frac{W(+, -, +)}{W(+)} dt_2 = P_2(\tau) + 2P_4(\tau) + 3P_6(\tau) + \dots, \quad (1.1.4)$$

$$\int_{t_1 < t_2 < t_3} \frac{W(+, +, +)}{W(+)} dt_2 = P_3(\tau) + 2P_5(\tau) + 3P_7(\tau) + \dots, \quad (1.1.5)$$

where $\tau = (t_3 - t_1)$. To prove (1.1.3), for example, consider

$$\frac{W(+, -, +)}{W(+)} dt_2 dt_3.$$

This represents the probability that f has a down-crossing in $(t_2, t_2 + dt_2)$ and an up-crossing in $(t_3, t_3 + dt_3)$, given that it has an up-crossing at t_1 . Now the up-crossing in $(t_3, t_3 + dt_3)$ is either the second zero after t_1 or the fourth or the sixth, etc. Suppose it is the $(2r)$ th. Then the down-crossing in $(t_2, t_2 + dt_2)$ is either the first zero after t_1 or the third or the fifth, up to the $(2r-1)$ th. But if the probabilities are each integrated with respect to t_2 from t_1 to t_3 each gives precisely $P_{2r-1} dt_3$. The r possibilities together contribute $rP_{2r-1} dt_3$. Hence the series (1.1.3); and similarly for (1.1.4) and (1.1.5).

We now prove the following general theorem. Let S denote any sequence of n signs, plus or minus, the first sign being $+$, and let s denote the number of times that the sequence changes sign. (For example, if $S = (+, -, +, -)$ then $s = 3$.) Then the expression $X(S)$ defined by

$$X(S) \equiv \int \dots \int_{t_1 < t_2 < \dots < t_n} \frac{W(S)}{W(+)} dt_2 \dots dt_{n-1} \quad (1.1.6)$$

is the sum of the series

$$X(S) = \sum_{r=0}^{\infty} \binom{n-2+r}{r} P_{2n-3-s+2r}(\tau), \quad (1.1.7)$$

where $\tau = (t_n - t_1)$ and $\binom{p}{q}$ denotes the coefficient of x^q in $(1+x)^p$.

INTERVALS BETWEEN ZEROS OF A RANDOM FUNCTION 561

Proof. The integrand in (1.1.6) represents the probability that the $(n-1)$ intervals $(t_i, t_i + dt_i)$ ($i = 2, 3, \dots, n$), contain zero-crossings of $f(t)$ with gradients of the appropriate sign, given that f vanishes at t_1 . Suppose that the last interval $(t_n, t_n + dt_n)$ contains the $(k+1)$ th zero of f after t_1 . The remaining $(n-2)$ intervals $(t_2, t_2 + dt_2), \dots, (t_{n-1}, t_{n-1} + dt_{n-1})$ must contain $(n-2)$ of the remaining k zeros between t_1 and t_n . Each distinct way of choosing these $(n-2)$ zeros contributes a term $P_k(\tau)$ to the integral $X(S)$. Hence

$$X(S) = \sum_k c_k P_k(\tau),$$

where c_k denotes the number of distinct ways of choosing the sequence S from a sequence S' of $(k+2)$ signs, alternately $+$ and $-$, so that the first and last signs of S' correspond to those of S .

Now between each pair of successive signs of S that are both $+$ (or both $-$) there must be an odd number of signs of S . From the definition of s there are $(n-1-s)$ such cases, and so

$$k+2 = n + (n-1-s) + 2r,$$

where $r = 0, 1, 2, \dots$. The remaining r pairs of signs of S' may occur anywhere in the $(n-1)$ gaps between the signs of S . The number of distinct ways of disposing of these is

$$c_k = \binom{n-2+r}{r}.$$

On combining the last three equations we obtain (1.1.7).

It follows from the theorem that in the sequence S the only two relevant parameters are n and s . So we may write

$$X(S) = X_{n,s} \quad (1.1.8)$$

The following special cases will be useful. When $S = (+, +, \dots, +)$ then $s = 0$ and

$$X_{n,0} = \sum_{r=0}^{\infty} \binom{n-2+r}{r} P_{2n-3+2r} \quad (1.1.9)$$

When $S = (+, -, -, \dots, -)$ then $s = 1$ and

$$X_{n,1} = \sum_{r=0}^{\infty} \binom{n-2+r}{r} P_{2n-4+2r} \quad (1.1.10)$$

When $S = (+, -, +, \dots, (-)^{n-1})$ then $s = (n-1)$ and

$$X_{n,n-1} = \sum_{r=0}^{\infty} \binom{n-2+r}{r} P_{n-2+2r} \quad (1.1.11)$$

From these series there follows also a useful result on the order of magnitude of $P_m(\tau)$ for large values of m (when τ is fixed). For the binomial coefficient in each case is

$$\binom{n-2+r}{r} = \frac{(n-2+r)(n-3+r)\dots(1+r)}{(n-2)!} = O(\tau^{n-2})$$

as t tends to infinity. But if the series converges the individual terms must each tend to zero. So from (1.1.9), for example,

$$\lim_{r \rightarrow \infty} r^{n-2} P_{2n-3+2r} = 0.$$

In this expression the factor r^{n-2} may be replaced by $(2n-3+2r)^{n-2}$ without altering the limit. So

$$\lim_{m \rightarrow \infty} m^{n-2} P_m = 0 \quad (1.1.12)$$

if m tends to infinity through the odd values; and similarly for the even values.

Thus $P_m(\tau)$ tends to zero more rapidly than $m^{-(n-2)}$, τ being kept constant. Provided, then, that the $X_{n,s}$ exist for all values of n , it follows that $P_m(\tau)$ tends to zero more rapidly than any negative power of m .

1.2. Series for $P_m(\tau)$

Equations (1.1.1) to (1.1.5) may be written

$$\left. \begin{aligned} P_0 &= X(+, -) - (P_2 + P_4 + P_6 + \dots), \\ P_1 &= X(+, +) - (P_3 + P_5 + P_7 + \dots), \end{aligned} \right\} \quad (1.2.1)$$

and†

$$\left. \begin{aligned} P_1 &= X(+, -, +) - (2P_3 + 3P_5 + 4P_7 + \dots), \\ P_2 &= X(+, -, -) - (2P_4 + 3P_6 + 4P_8 + \dots), \\ P_3 &= X(+, +, +) - (2P_5 + 3P_7 + 4P_9 + \dots). \end{aligned} \right\} \quad (1.2.2)$$

Rice (1945) and McFadden (1958) neglected P_2, P_3, \dots and took as an approximation

$$\left. \begin{aligned} P_0 &\doteq X(+, -), \\ P_1 &\doteq X(+, +). \end{aligned} \right\} \quad (1.2.3)$$

However, by eliminating P_2 and P_3 from the right-hand side of (1.2.1) by means of equations (1.2.2) we have

$$\left. \begin{aligned} P_0 &= X(+, -) - X(+, -, -) + (P_4 + 2P_6 + 3P_8 + \dots), \\ P_1 &= X(+, +) - X(+, +, +) + (P_5 + 2P_7 + 3P_9 + \dots) \end{aligned} \right\} \quad (1.2.4)$$

so that a higher approximation, neglecting only P_4, P_5, \dots is given by

$$\left. \begin{aligned} P_0 &\doteq X(+, -) - X(+, -, -), \\ P_1 &\doteq X(+, +) - X(+, +, +). \end{aligned} \right\} \quad (1.2.5)$$

It is easy to show that these approximations are the first in an infinite sequence. Equations (1.1.10), which involve only the even P_m , may be solved for P_0 by multiplying the first equation ($n=2$) by 1, the next by -1 , and so on up to $n=N$, and adding. On the right-hand side the coefficient of P_{2i} , when $i \leq N$, is

$$\binom{i}{0} - \binom{i}{1} + \binom{i}{2} - \dots + (-1)^i \binom{i}{i} = \begin{cases} 1 & (i=0), \\ 0 & (0 < i \leq N), \end{cases}$$

and when $i > N$ it is

$$\binom{i}{0} - \binom{i}{1} + \binom{i}{2} - \dots + (-1)^N \binom{i}{N} = (-1)^{N+1} \binom{i-1}{N}.$$

Hence $X_{2,1} - X_{3,1} + X_{4,1} - \dots + (-1)^N X_{N+2,1}$

$$= P_0 + (-1)^N \left[P_{2N+2} + \binom{N+1}{1} P_{2N+4} + \binom{N+2}{2} P_{2N+6} + \dots \right]. \quad (1.2.6)$$

† The five equations (1.1.1) to (1.1.5), regarded as equations for the P_m , are not independent, for we have the identical relation

$$X(+, -, +) - X(+, +, +) = X(+, +).$$

Thus provided the expression in square brackets tends to zero we have

$$P_0 = X_{2,1} - X_{3,1} + X_{4,1} - \dots, \tag{1.2.7}$$

and similarly

$$P_1 = X_{2,0} - X_{3,0} + X_{4,0} - \dots \tag{1.2.8}$$

The approximations (1.2.3) and (1.2.5) correspond to the first two partial sums of these series.

Moreover, the remainder after $(N+1)$ terms of the series is

$$(-1)^{N+1} \left[P_{2N+2} + \binom{N+1}{1} P_{2N+4} + \binom{N+2}{2} P_{2N+6} + \dots \right] \tag{1.2.9}$$

which, since the P are all positive, has the same sign as $(-1)^{N+1}$. Hence the sums of the series (1.2.7) and (1.2.8) lie between any two successive partial sums.

The corresponding series for P_{2r} and P_{2r+1} ($r \geq 0$) are found from (1.1.10) and (1.1.9) to be

$$\left. \begin{aligned} P_{2r} &= \sum_{i=0}^{\infty} (-1)^i \binom{r+i}{i} X_{r+2+i,1}, \\ P_{2r+1} &= \sum_{i=0}^{\infty} (-1)^i \binom{r+i}{i} X_{r+2+i,0} \end{aligned} \right\} \tag{1.2.10}$$

(the coefficients in the two series being identical). The solution of (1.1.11) for P_m is

$$P_m = (m+1) \sum_{i=0}^{\infty} (-1)^i \frac{(m+2i)!}{i!(m+i+1)!} X_{m+2+2i} \tag{1.2.11}$$

for all $m \geq 0$, where X_n is written more shortly for $X_{n,n-1}$. The solutions are valid provided each series is absolutely convergent.

1.3. Relation to a series of Rice

It is interesting to compare the series (1.2.7) for $P_0(\tau)$ with one stated by Rice (1945, equation (3.4-11)). His series may be written

$$P_0 = Y_2 - Y_3 + Y_4 - \dots, \tag{1.3.1}$$

where
$$Y_n = \frac{1}{(n-2)!} \int_{t_1}^{t_2} \dots \int_{t_1}^{t_n} \frac{W(\pm, \pm, \dots, \pm)}{W(\pm)} dt_2 \dots dt_{n-1} \tag{1.3.2}$$

and $W(\pm, \pm, \dots, \pm) dt_1 \dots dt_n$ denotes the probability of a zero-crossing in each of the intervals $(t_i, t_i + dt_i)$ irrespective of the sign of $f'(t)$.

Now from the point of view of calculation Y_n is of a similar complexity to $X_{n,1}$, since each involves an $(n-2)$ -fold integration of a probability density such as $W(S)$. On the other hand in the series (1.3.1) the first term neglected after N terms is Y_{N+3} , which is of order P_{N+1} (see below), whereas the remainder after N terms in the series (1.2.7) is only of order P_{2N+2} . Clearly then (1.2.7) is more rapidly convergent than (1.3.1).

The reason for this difference is apparently that in deriving (1.2.7) we have made use of the continuity of $f'(t)$ which implies that up-crossings and down-crossings follow one another alternately. In (1.3.1) no such property is used.

For completeness we now express Y_n in terms of the $P_m(\tau)$.

Since $-f(t)$ is assumed statistically equivalent to $f(t)$, the integrand in (1.3.2) may be replaced by $W(+, \pm, \pm, \dots, \pm)/W(+)$; and further by the symmetry of the integrand with respect to t_2, t_3, \dots, t_{n-1} we have

$$Y_n = \int \dots \int_{t_1 < t_2 < \dots < t_n} \frac{W(+, \pm, \pm, \dots, \pm)}{W(+)} dt_2 \dots dt_{n-1}.$$

Now $W(+, \pm, \pm, \dots, \pm)$ can be considered as the sum of 2^{n-1} expressions of the form $W(S)$, where S is a sequence of n signs such as was defined in § 1.1. Corresponding to any given value of s there are $\binom{n-1}{s}$ such sequences S . Hence

$$Y_n = \sum_{s=0}^{n-1} \binom{n-1}{s} X_{n,s}.$$

But $X_{n,s}$, or $X(S)$ is given by (1.1.7). Thus

$$Y_n = \sum_{s=0}^{n-1} \sum_{r=0}^{\infty} \binom{n-1}{s} \binom{n-2+r}{r} P_{n-2+s+2r}.$$

The coefficient of P_{n-2+i} may be summed by comparing coefficients of x^i in the expansion of the identity

$$(1+x)^{n-1} (1-x^2)^{-(n-1)} \equiv (1-x)^{-(n-1)}$$

in powers of x . Hence

$$Y_n = \sum_{i=0}^{\infty} \binom{n-2+i}{i} P_{n-2+i} \tag{1.3.3}$$

The first term in this series is P_{n-2} , which proves our statement concerning the order of magnitude of Y_{N+3} made above.

The solution of equations (1.3.3) for the P_m is

$$P_m = \sum_{i=0}^{\infty} (-1)^i \binom{m+1}{i} Y_{m+2+i} \tag{1.3.4}$$

of which (1.3.1) is the special case when $m = 0$.

1.4. Series for $p(n, \tau)$

McFadden (1958) has shown that $p(n, \tau)$ (the probability of exactly n zeros in the interval $(t, t+\tau)$) is related to $P_m(\tau)$ by the following set of equations:†

$$\left. \begin{aligned} p''(0, \tau) &= 2W(+) P_0, \\ p''(1, \tau) &= 2W(+) (P_1 - 2P_0), \\ p''(n, \tau) &= 2W(+) (P_n - 2P_{n-1} + P_{n-2}) \quad (n \geq 2), \end{aligned} \right\} \tag{1.4.1}$$

where a prime denotes differentiation with respect to τ . On substitution for P_n, P_{n-1}, P_{n-2} from equations (1.2.11) we have in the general case

$$p''(n, \tau) = 2W(+) \sum_{i=0}^{\infty} C_{n,i} X_{n+i}, \tag{1.4.2}$$

† The first of these relations is apparently due to Kohlenberg (1953).

where

$$C_{n,0} = 1$$

$$\left. \begin{aligned} C_{n,2r} &= (-1)^{r+1} (2r - n^2 + n) \frac{(n - 2 + 2r)!}{r! (n+r)!} \quad (r \geq 1), \\ C_{n,2r+1} &= (-1)^{r+1} 2n \frac{(n - 1 + 2r)!}{r! (n+r)!} \quad (r \geq 0). \end{aligned} \right\} \quad (1.4.3)$$

Now by definition

$$X_n = \int \dots \int_{t_1 < t_2 < \dots < t_n} \frac{W(+, -, +, \dots, (-)^{n-1})}{W(+)} dt_1 \dots dt_n \quad (1.4.4)$$

which is a function of $\tau = (t_n - t_1)$. Hence

$$X_n(\tau) = \frac{1}{W(+)} I_n'(\tau), \quad (1.4.5)$$

where

$$I_n = \int \dots \int_{0 < t_1 < \dots < t_n < \tau} W(+, -, +, \dots, (-)^{n-1}) dt_1 \dots dt_n. \quad (1.4.6)$$

On substituting in (1.4.2) and integrating twice with respect to τ from $\tau = 0$ we have

$$p(n, \tau) = 2 \sum_{r=0}^{\infty} C_{n,r} I_{n+r}(\tau) \quad (1.4.7)$$

provided the constants of integration vanish. The first term in this expansion is $2I_n$.

Let $R(t)$ denote the covariance function of the function $\xi(t)$ which equals 1 when $f(t) > 0$ and -1 when $f(t) < 0$. Rice (1944) showed that

$$R(t) = p(0, \tau) - p(1, \tau) + p(2, \tau) - \dots$$

By differentiating twice and using equations (1.4.1) one obtains

$$R''(\tau) = 8W(+)(P_0 - P_1 + P_2 - \dots) \quad (1.4.8)$$

(McFadden 1958). From the first two equations of § 1.1 it follows that

$$R''(\tau) = 8[W(+, -) - W(+, +)]. \quad (1.4.9)$$

2. EVALUATION OF $W(S)$ FOR GAUSSIAN PROCESSES

We now specialize the discussion to the case when $f(t)$ is Gaussian, and seek some explicit formulae for $W(S)$ in terms of the covariance function of $f(t)$.

2.1. A general expression for $W(S)$

Consider first the probability $W(+, +, \dots, +) dt_1 \dots dt_n$ that $f(t)$ should have a zero up-crossing in each of the small intervals $(t_i, t_i + dt_i)$ ($i = 1, \dots, n$). For convenience write

$$f(t_i) = \xi_i, \quad f'(t_i) = \eta_i \quad (i = 1, \dots, n),$$

and let $p(\xi_1, \dots, \xi_n; \eta_1, \dots, \eta_n)$ denote the joint probability density of the ξ_i and η_i . Thus

$$p(\xi_1, \dots, \xi_n; \eta_1, \dots, \eta_n) d\xi_1 \dots d\xi_n, d\eta_1 \dots d\eta_n \quad (2.1.1)$$

is the probability that the ξ_i and η_i lie in given intervals $(\xi_i, \xi_i + d\xi_i)$, $(\eta_i, \eta_i + d\eta_i)$. Now if $f(t)$ has a zero-crossing in $(t_i, t_i + dt_i)$, with gradient η_i , then $f(t_i)$ must lie in a small range of values of extent $|\eta_i| dt_i$. Thus to obtain the probability $W(+, +, \dots, +) dt_1 \dots dt_n$ we replace

$d\xi_i$ in (2.1.1) by $|\eta_i| d\eta_i$ and integrate over all positive values of the η_i . After dividing by $d\tau_1 \dots d\tau_n$ we have

$$W(+, +, \dots, +) = \int_0^\infty \dots \int_0^\infty |\eta_1 \dots \eta_n| \rho(0, \dots, 0; \eta_1, \dots, \eta_n) d\eta_1 \dots d\eta_n. \quad (2.1.2)$$

For the covariance function of $f(t)$ we write

$$\overline{f(t)f(t+\tau)} = \psi(\tau).$$

The function $\psi(\tau)$ (or ψ_τ) is considered as given: it is the cosine transform of the spectral density of $f(t)$.

Then the covariance matrix of the $2n$ variables $\xi_1, \dots, \xi_n; \eta_1, \dots, \eta_n$ is

$$(\lambda_{ij}) = \begin{pmatrix} \psi_{11} & \dots & \psi_{1n} & \psi'_{11} & \dots & \psi'_{1n} \\ & & \vdots & \vdots & & \vdots \\ \psi_{n1} & \dots & \psi_{nn} & \psi'_{n1} & \dots & \psi'_{nn} \\ -\psi'_{11} & \dots & -\psi'_{1n} & -\psi''_{11} & \dots & -\psi''_{1n} \\ & & & \vdots & & \vdots \\ -\psi'_{n1} & \dots & -\psi'_{nn} & -\psi''_{n1} & \dots & -\psi''_{nn} \end{pmatrix}, \quad (2.1.3)$$

where $\psi_{ij} = \psi(t_i - t_j)$ and a prime denotes differentiation.

By the Gaussian hypothesis we have

$$\rho(\xi_1, \dots, \xi_n; \eta_1, \dots, \eta_n) = \frac{1}{(2\pi)^n \Delta^{\frac{1}{2}}} \exp \left[-\frac{1}{2} \sum_{i,j=1}^{2n} L_{ij} \xi_i \xi_j \right], \quad (2.1.4)$$

where $\xi_{n+i} = \eta_i$ and

$$\Delta = |(L_{ij})|, \quad (L_{ij}) = (\lambda_{ij})^{-1}. \quad (2.1.5)$$

Substitution in (2.1.2) gives

$$W(+, +, \dots, +) = \frac{1}{(2\pi)^n \Delta^{\frac{1}{2}}} \int_0^\infty \dots \int_0^\infty |\eta_1 \dots \eta_n| \exp \left[-\frac{1}{2} \sum_{i,j=1}^n L_{n+i, n+j} \eta_i \eta_j \right] d\eta_1 \dots d\eta_n.$$

The summation in the last equation involves only the last n rows and columns of (L_{ij}) . It is convenient to denote the inverse of this matrix by (μ_{ij})

$$(\mu_{ij}) = \begin{pmatrix} L_{n+1, n+1} & \dots & L_{n+1, 2n} \\ \vdots & & \vdots \\ L_{2n, n+1} & \dots & L_{2n, 2n} \end{pmatrix}^{-1}. \quad (2.1.7)$$

By Jacobi's theorem the (r, s) th element of this matrix is the bordered determinant

$$\mu_{r,s} = \begin{vmatrix} \psi_{11} & \dots & \psi_{1n} & \psi'_{1s} \\ \vdots & & \vdots & \vdots \\ \psi_{n1} & \dots & \psi_{nn} & \psi'_{ns} \\ -\psi'_{r1} & \dots & -\psi'_{rn} & -\psi''_{rs} \end{vmatrix} \div D, \quad (2.1.8)$$

where

$$D = \begin{vmatrix} \psi_{11} & \dots & \psi_{1n} \\ \vdots & & \vdots \\ \psi_{n1} & \dots & \psi_{nn} \end{vmatrix}. \quad (2.1.9)$$

The determinant of (μ_{ij}) is given by

$$|(\mu_{ij})| = \Delta/D. \quad (2.1.10)$$

(μ_{ij}) will be recognized as the covariance matrix of (η_1, \dots, η_n) given that

$$\xi_1 = \xi_2 = \dots = \xi_n = 0.$$

For, if $p(\eta_1, \dots, \eta_n | \xi_1, \dots, \xi_n)$ denotes the conditional distribution of (η_1, \dots, η_n) for given values of (ξ_1, \dots, ξ_n) we have

$$p(\eta_1, \dots, \eta_n | \xi_1, \dots, \xi_n) = \frac{p(\xi_1, \dots, \xi_n; \eta_1, \dots, \eta_n)}{p(\xi_1, \dots, \xi_n)},$$

where $p(\xi_1, \dots, \xi_n)$ is the distribution of (ξ_1, \dots, ξ_n) only

$$p(\xi_1, \dots, \xi_n) = \frac{1}{(2\pi)^{\frac{1}{2}n} D^{\frac{1}{2}}} \exp \left[-\frac{1}{2} \sum_{i,j=1}^n M_{ij} \xi_i \xi_j \right],$$

where (M_{ij}) is the inverse of (ψ_{ij}) . Hence when the ξ_i vanish we have, using (2·1·10),

$$p(\eta_1, \dots, \eta_n | 0, \dots, 0) = \frac{1}{(2\pi)^{\frac{1}{2}n} |(\mu_{ij})|^{\frac{1}{2}}} \exp \left[-\frac{1}{2} \sum_{i,j=1}^n L_{n+i, n+j} \eta_i \eta_j \right] = Z(\eta, \mu),$$

say. With this notation (2·1·6) may be written

$$W(+, +, \dots, +) = \frac{1}{(2\pi)^{\frac{1}{2}n} D^{\frac{1}{2}}} \int_0^\infty \dots \int_0^\infty |\eta_1 \dots \eta_n| Z(\eta, \mu) d\eta_1 \dots d\eta_n. \tag{2·1·11}$$

It is convenient to introduce the normalized covariance matrix (ν_{ij}) whose (i, j) th element is

$$\nu_{ij} = \frac{\mu_{ij}}{(\mu_{ii} \mu_{jj})^{\frac{1}{2}}}. \tag{2·1·12}$$

Then on writing

$$\zeta_i = (\mu_{ii})^{-\frac{1}{2}} \eta_i$$

in equation (2·1·11) so that (ν_{ij}) is the covariance matrix of the new variables ζ_i , we have

$$W(+, +, \dots, +) = \frac{(\mu_{11} \mu_{22} \dots \mu_{nn})^{\frac{1}{2}}}{(2\pi)^{\frac{1}{2}n} D^{\frac{1}{2}}} J_n, \tag{2·1·13}$$

where

$$J_n = \int_0^\infty \dots \int_0^\infty \zeta_1 \dots \zeta_n Z(\zeta, \nu) d\zeta_1 \dots d\zeta_n. \tag{2·1·14}$$

Now $Z(\zeta, \nu)$ is the ordinary normal probability density in the n variables ζ_i , with covariance matrix (ν_{ij}) . Since the diagonal elements have been normalized (by equation (2·1·12)), J_n is a function only of the off-diagonal element ν_{ij} ($i \neq j$).

Suppose that one of the zeros in the sequences (say the k th zero) is to be a down-crossing instead of an up-crossing. Then in calculating the corresponding probability density W we need only to take the range of integration of η_k in (2·1·2) from $-\infty$ to 0 instead of 0 to ∞ . Equivalently, we may simply reverse the sign of the $(n+k)$ th row and column of L_{ij} , and hence the k th row and column of (μ_{ij}) and of (ν_{ij}) .

Hence to find $W(+, -, +, \dots, (-)^{n-1})$, in which each alternate zero-crossing is a down-crossing, we have to multiply $L_{n+i, n+j}$ by $(-1)^{i+j}$ and hence also multiply μ_{ij} and ν_{ij} by $(-1)^{i+j}$.

2·2. The cases $n = 1, 2$ and 3

The case $n = 1$ is trivial, for then $Z(\zeta, \nu)$ is the normal distribution for a single variate and

$$J_1 = \int_0^\infty \zeta \frac{e^{-\frac{1}{2}\zeta^2}}{(2\pi)^{\frac{1}{2}}} d\zeta = \frac{1}{(2\pi)^{\frac{1}{2}}}.$$

568

M. S. LONGUET-HIGGINS

Since in (2.1.8) ψ'_{11} vanishes we have $\mu_{11} = -\psi''_{11} = -\psi''_0$ and so from (2.1.13)

$$W(+)=\left(\frac{\mu_{11}}{2\pi D}\right)^{\frac{1}{2}} J_1 = \frac{1}{2\pi} \left(\frac{-\psi''_0}{\psi_0}\right)^{\frac{1}{2}} \quad (2.2.1)$$

as is well known (Kac 1943).

Also well known is the case $n = 2$, when

$$J_2 = \frac{1}{2\pi} [(1-\nu_{12}^2)^{\frac{1}{2}} + \nu_{12} \cos^{-1}(-\nu_{12})]$$

(the angle being chosen so as to lie between 0 and π). This gives

$$W(+,+) = \frac{(\mu_{11}\mu_{22})^{\frac{1}{2}}}{4\pi^2(\psi_0^2 - \psi_{12}^2)^{\frac{1}{2}}} [(1-\nu_{12}^2)^{\frac{1}{2}} + \nu_{12} \cos^{-1}(-\nu_{12})] \quad (2.2.2)$$

(Rice 1945, § 3.10). By changing the sign of ν_{12} we have

$$W(+,-) = \frac{(\mu_{11}\mu_{22})^{\frac{1}{2}}}{4\pi^2(\psi_0^2 - \psi_{12}^2)^{\frac{1}{2}}} [(1-\nu_{12}^2)^{\frac{1}{2}} - \nu_{12} \cos^{-1}(\nu_{12})]. \quad (2.2.3)$$

Not so well known is the case $n = 3$. However, J_3 may be derived from some integrals calculated quite recently by Nabeya (1952) and Kamat (1953). One obtains

$$J_3 = \frac{1}{(2\pi)^{\frac{3}{2}}} [|(v_{ij})|^{\frac{1}{2}} + (s_1\alpha_1 + s_2\alpha_2 + s_3\alpha_3)],$$

where

$$s_1 = \cos^{-1} \frac{\nu_{31}\nu_{12} - \nu_{23}}{(1-\nu_{31}^2)^{\frac{1}{2}}(1-\nu_{23}^2)^{\frac{1}{2}}}, \quad \alpha_1 = \nu_{31}\nu_{12} + \nu_{23}.$$

(s_2, s_3 , etc., are obtained by cyclic permutation of the ν_{ij}). These angles are also to be taken in the range $(0, \pi)$. So from (2.1.13) we find

$$\left. \begin{aligned} W(+,+,+) &= \frac{(\mu_{11}\mu_{22}\mu_{33})^{\frac{1}{2}}}{8\pi^3 D^{\frac{3}{2}}} [|(v_{ij})|^{\frac{1}{2}} + (s_1\alpha_1 + s_2\alpha_2 + s_3\alpha_3)], \\ W(+,-,+) &= \frac{(\mu_{11}\mu_{22}\mu_{33})^{\frac{1}{2}}}{8\pi^3 D^{\frac{3}{2}}} [|(v_{ij})|^{\frac{1}{2}} + (s_1 - \pi)\alpha_1 + s_2\alpha_2 + (s_3 - \pi)\alpha_3], \\ W(+,-,-) &= \frac{(\mu_{11}\mu_{22}\mu_{33})^{\frac{1}{2}}}{8\pi^3 D^{\frac{3}{2}}} [|(v_{ij})|^{\frac{1}{2}} + s_1\alpha_1 + (s_2 - \pi)\alpha_2 + (s_3 - \pi)\alpha_3]. \end{aligned} \right\} \quad (2.2.4)$$

2.3. General values of n

When $n > 3$, the integral J_n cannot be expressed in terms of known functions, in general. However, two particular cases in which this is possible may be stated here for later use.

First, if the covariances ν_{ij} all vanish when $i \neq j$, then ζ_1, \dots, ζ_n are statistically independent variates and

$$J_n = \left[\int_0^\infty \zeta \frac{e^{-\frac{1}{2}\zeta^2}}{(2\pi)^{\frac{1}{2}}} d\zeta \right]^n = \frac{1}{(2\pi)^{\frac{n}{2}}}$$

giving

$$W = \frac{1}{(2\pi)^n} \frac{(\mu_{11} \dots \mu_{nn})^{\frac{1}{2}}}{D^{\frac{1}{2}}}. \quad (2.3.1)$$

Secondly, if all the covariances ν_{ij} are unity, then ζ_1, \dots, ζ_n all reduce to the same Gaussian variate, giving

$$J_n = \int_0^\infty \zeta^n \frac{e^{-\frac{1}{2}\zeta^2}}{(2\pi)^{\frac{1}{2}}} d\zeta = \frac{1}{(2\pi)^{\frac{1}{2}}} 2^{\frac{1}{2}(n-1)} \left(\frac{n-1}{2}\right)!$$

Hence

$$W = \frac{1}{2\pi^{\frac{1}{2}(n+1)}} \left(\frac{n-1}{2}\right)! \frac{(\mu_{11} \dots \mu_{nn})^{\frac{1}{2}}}{D^{\frac{1}{2}}}. \quad (2.3.2)$$

3. ASYMPTOTIC EXPANSIONS NEAR THE ORIGIN: ψ REGULAR

In this section we evaluate the probabilities defined earlier, for small time intervals τ . It will be assumed that the covariance function $\psi(t)$ is regular at the origin

$$\psi(t) = \psi_0 + \frac{\psi_0''}{2!} t^2 + \frac{\psi_0^{iv}}{4!} t^4 + \dots$$

(coefficients of the odd powers vanish, since $\psi(t)$ is an even function of t).

3.1. Expansion of $W(S)$

Our first object is to obtain a multiple power series in the t_i for the probability density $W(S)$. Since W depends only on the covariance matrix (λ_{ij}) of equation (2.1.3), it is evidently a function of the time differences $(t_i - t_j)$. We shall see that the leading terms in W are homogeneous and of degree $\frac{1}{2}n(n-1)$ in the $(t_i - t_j)$.

We use the following lemma: if $F(x)$ is any function of x regular at $x = 0$, then the leading term in the expansion of

$$\begin{vmatrix} F(x_1 + y_1) & \dots & F(x_1 + y_n) \\ \vdots & & \vdots \\ F(x_n + y_1) & \dots & F(x_n + y_n) \end{vmatrix}$$

in powers of the x_i and y_i is

$$\begin{vmatrix} F(0) & F'(0) & \dots & F^{(n-1)}(0) \\ F'(0) & F''(0) & \dots & F^{(n)}(0) \\ \vdots & \vdots & & \vdots \\ F^{(n-1)}(0) & F^{(n)}(0) & \dots & F^{(2n-2)}(0) \end{vmatrix} \frac{\prod_{i < j} (x_j - x_i)(y_j - y_i)}{[1! 2! \dots (n-1)!]^2}.$$

To prove this, first express each term as a Taylor series in the x_i

$$F(x_i + y_i) = F(y_i) + x_i F'(y_i) + \frac{x_i^2}{2!} F''(y_i) + \dots$$

Subtract the first row of the determinant from the remaining rows, taking out the factors $(x_2 - x_1), \dots, (x_n - x_1)$; then subtract the second row from the rows beneath it, taking out the factors $(x_3 - x_2), \dots, (x_n - x_2)$; and so on. In the result write

$$F^{(0)}(y_j) = F^{(0)}(0) + y_j F^{(1)}(0) + \frac{y_j^2}{2!} F^{(2)}(0) + \dots$$

and proceed similarly with the columns. This gives the result.

Setting $F = \psi$, $x_i = t_i$ and $y_i = -t_i$ in the lemma we find, from (2.1.9),

$$D \sim D_n \frac{\prod_{i < j} (t_j - t_i)^2}{[1! 2! \dots (n-1)!]^2}, \tag{3.1.1}$$

where
$$D_m = (-1)^{\frac{1}{2}m(m-1)} \begin{vmatrix} \psi_0 & \psi_0' & \dots & \psi_0^{(m-1)} \\ \psi_0' & \psi_0'' & \dots & \psi_0^{(m)} \\ \vdots & \vdots & & \vdots \\ \psi_0^{(m-1)} & \psi_0^{(m)} & \dots & \psi_0^{(2m-2)} \end{vmatrix}. \tag{3.1.2}$$

It will be noticed that since the odd derivatives of ψ all vanish, every alternate element of D_m is zero, so that D_m may be factorized into two determinants

$$D_m = (-1)^{\frac{1}{2}m(m-1)} \begin{vmatrix} \psi_0 & \psi_0'' & \dots \\ \psi_0'' & \psi_0^{(4)} & \dots \\ \vdots & \vdots & \ddots \end{vmatrix} \times \begin{vmatrix} \psi_0'' & \psi_0^{(4)} & \dots \\ \psi_0^{(4)} & \psi_0^{(6)} & \dots \\ \vdots & \vdots & \ddots \end{vmatrix}.$$

By a similar method we may evaluate the leading term in μ_{rs} (equation (2.1.8)). One finds in fact

$$\mu_{rs} \sim \frac{D_{n+1} \prod_{i \neq r} (t_r - t_i) \prod_{j \neq s} (t_s - t_j)}{D_n (n!)^2}. \tag{3.1.3}$$

Hence

$$\nu_{rs} = \frac{\mu_{rs}}{(\mu_{rr} \mu_{ss})^{\frac{1}{2}}} \sim \pm 1$$

according as μ_{rs} is positive or negative. Now since (ψ_{ij}) is a positive-definite matrix its determinant D must be positive, so that by (3.1.1) D_m is positive also. On the other hand when $t_1 < t_2 < \dots < t_n$ the product $\prod_{i < r} (t_r - t_i)$ has the same sign as $(-1)^{r+s}$, and so μ_{rs} has the same sign as $(-1)^{r+s}$. It follows that

$$\nu_{rs} \sim (-1)^{r+s}.$$

Now to calculate $W(+, -, +, \dots, (-)^{n-1})$ we recall that ν_{rs} was to be multiplied by $(-1)^{r+s}$. The elements of the corresponding covariance matrix thus all become equal to unity, in the limit, and so (2.3.2) applies. On substituting for μ_{ij} and D we find

$$W(+, -, +, \dots, (-)^{n-1}) \sim C_n \prod_{i < j} (t_j - t_i), \tag{3.1.4}$$

where

$$C_n = \frac{1! 2! \dots (n-1)! (n-1)!}{2^n \frac{1}{2} (n!)^n} \left(\frac{D_{n+1}}{D_n} \right)^{\frac{1}{2}}. \tag{3.1.5}$$

In particular when $n = 1$ and 2 we have the known results

$$W(+) = \frac{1}{2\pi} \frac{D_2^{\frac{1}{2}}}{D_1} \tag{3.1.6}$$

and

$$W(+, -) \sim \frac{1}{16\pi} \frac{D_3}{D_2^{\frac{1}{2}}} (t_2 - t_1) \tag{3.1.7}$$

(cf. Rice 1945, § 3.4).

3.2. Evaluation of $P_m(\tau)$

The integral I_n defined by (1.4.6) can now be evaluated. We use the identity

$$\int \dots \int_{0 < t_1 < t_2 < \dots < t_n < \tau} \prod_{i < j} (t_j - t_i) dt_1 \dots dt_n = \frac{[1! 2! 3! \dots (n-1)!]^2}{1! 3! 5! \dots (2n-1)!} \tau^{\frac{1}{2}n(n+1)}, \tag{3.2.1}$$

a proof of which is given, for example, by Mehta (1960). From (1.4.6) and (3.1.4) we have then

$$I_n \sim \frac{[1! 2! 3! \dots (n-1)!]^2}{1! 3! 5! \dots (2n-1)!} C_n \tau^{\frac{1}{2}n(n+1)}, \tag{3.2.2}$$

which is of order $\tau^{\frac{1}{2}n(n+1)}$. From this it follows that

$$X_n = \frac{1}{W(+)} I_n^n = O(\tau^{\frac{1}{2}n(n+1)-2}). \tag{3.2.3}$$

INTERVALS BETWEEN ZEROS OF A RANDOM FUNCTION 571

Since the power of τ increases with n , one sees that $P_m(\tau)$ is given asymptotically by the first term in the series (1.2.11), i.e.

$$P_m(\tau) \sim X_{m+2}. \tag{3.2.4}$$

From the last three equations and (3.1.5) we have

$$P_m(\tau) \sim \frac{[1! 2! 3! \dots (m+1)!]^2 C_{m+2}}{1! 3! 5! \dots (2m+3)! C_1} \frac{d^2}{d\tau^2} \tau^{4(m+2)(m+3)}. \tag{3.2.5}$$

In particular

$$\left. \begin{aligned} P_0(\tau) &\sim \frac{C_2}{C_1} \tau = \frac{1}{8} \frac{D_1^\dagger D_3}{D_2^2} \tau, \\ P_1(\tau) &\sim \frac{C_3}{C_1} \tau^4 = \frac{1}{648\pi} \frac{D_1^\dagger D_3^\dagger}{D_2^\dagger D_3^2} \tau^4, \end{aligned} \right\} \tag{3.2.6}$$

in agreement with Rice (1945) and Palmer (1956), respectively. In general we have

$$P_m(\tau) = O(\tau^{4(m+2)(m+3)-2}), \tag{3.2.7}$$

a power of τ that increases very rapidly with m .

3.3. Evaluation of $p(n, \tau)$

When $n = 0$ and 1 we have trivially

$$p(0, \tau) \sim 1 \tag{3.3.1}$$

and
$$p(1, \tau) \sim 2W(+)\tau = \frac{1}{\pi} \frac{D_1^\dagger}{D_2} \tau \tag{3.3.2}$$

from (3.1.6).

When $n \geq 2$, both I_n and I'_n vanish at $\tau = 0$, and therefore (1.4.5) is valid provided both $p(n, 0)$ and $p'(n, 0)$ are zero. Both conditions are satisfied if we assume $p(n, \tau) = O(\tau^{1+\epsilon})$, where $\epsilon > 0$. In the series (1.4.7) the terms $I_{n+i}(\tau)$ are proportional to increasing powers of τ and hence $p(n, \tau)$ is given asymptotically by the first term

$$p(n, \tau) \sim 2I_n, \tag{3.3.3}$$

or on substitution from (3.2.2)

$$p(n, \tau) \sim 2 \frac{[1! 2! 3! \dots (n-1)!]^2}{1! 3! 5! \dots (2n-1)!} C_n \tau^{4n(n+1)} \quad (n \geq 2). \tag{3.3.4}$$

For example

$$\left. \begin{aligned} p(2, \tau) &\sim \frac{1}{3} C_2 \tau^3 = \frac{1}{48\pi} \frac{D_3}{D_2^2} \tau^3, \\ p(3, \tau) &\sim \frac{1}{50} C_3 \tau^6 = \frac{1}{19\,440\pi^2} \frac{D_1^\dagger}{D_3^2} \tau^6. \end{aligned} \right\} \tag{3.3.5}$$

Since $p(2, \tau)$ is of order τ^3 and not τ^2 we see that neighbouring zeros of $f(t)$ are not independent of one another. The effect may be called a 'mutual repulsion' of the zeros. It is connected with the property, seen in the previous section, that $P_0(\tau) \rightarrow 0$ as $\tau \rightarrow 0$, that is to say, small intervals τ are unlikely.

Moreover, as n increases, so the power of τ in $p(n, \tau)$ increases very rapidly.

A heuristic argument for the rapidly increasing power of τ may be given as follows. If $f(t)$ is to have n zeros in $(t, t+\tau)$ then by Rolle's theorem $f'(t)$ must have at least $(n-1)$ zeros in the same interval, and further $f''(t)$ must have at least $(n-2)$ zeros, and so on, till finally $f^{(n-1)}(t)$ must have at least one zero in the interval. Therefore (assuming the existence

of $f^{(n)}$, $f^{(n-1)}$ must be of order τ throughout the interval, and by integration $f^{(n-2)}$, $f^{(n-3)}$, ..., f must be of order τ^2 , τ^3 , ..., τ^n , respectively. That is to say, $f^{(n-1)}$, $f^{(n-2)}$, ..., f at some fixed point in the interval, must lie within ranges $\delta f^{(n-1)}$, $\delta f^{(n-2)}$, ..., δf of order τ , τ^2 , ..., τ^n , respectively. The probability of such an event is of order

$$\delta f^{(n-1)} \delta f^{(n-2)} \dots \delta f = O(\tau^{1+2+\dots+n}) = O(\tau^{\frac{1}{2}n(n+1)}).$$

4. ASYMPTOTIC EXPANSIONS NEAR THE ORIGIN: A SINGULAR CASE

We shall now seek expansions at the origin in a very interesting singular case. Instead of the Taylor series for $\psi(t)$ (equation (3.1)), suppose now that $\psi(t)$ has an expansion of the form

$$\psi(t) = \psi_0 + \frac{\psi_0''}{2!} t^2 + \frac{\psi_0'''}{3!} |t|^3 + \dots \quad (4.1)$$

In other words, the third derivative of $\psi(t)$ possesses a finite discontinuity at the origin.† Some examples of such functions were studied experimentally by Favreau *et al.* (1956), and McFadden (1958) has considered them theoretically. They occur whenever the spectral density of $f(t)$ is of order (frequency)⁻⁴ at high frequencies.

4.1. Expansion of $W(S)$

If the procedure of § 3.1 is attempted it is found that altogether fewer factors can be extracted from the determinants. For example, to evaluate D , defined by (2.1.9), we begin by subtracting row $(n-1)$ from row n of the determinant, then row $(n-2)$ from row $(n-1)$, and so on, in turn extracting the factors $(t_n - t_{n-1})$, $(t_{n-1} - t_{n-2})$, ..., $(t_2 - t_1)$; and similarly for the columns. The process is then repeated as far as row 2 only, and without extracting any factors. The leading term in the determinant is then seen to be

$$D \sim -\psi_0 \psi_0'' c^{n-2} (\tau_1 \tau_2 \dots \tau_{n-1})^2 |\mathbf{A}| \quad (n > 2), \quad (4.1.1)$$

$$\text{where we have written} \quad \frac{1}{2} \psi_0'' = c, \quad t_{i+1} - t_i = \tau_i, \quad (4.1.2)$$

and where \mathbf{A} is the $(n-2) \times (n-2)$ square matrix

$$\mathbf{A} = \begin{pmatrix} 4(\tau_1 + \tau_2) & 2\tau_2 & 0 & \dots & 0 \\ 2\tau_2 & 4(\tau_2 + \tau_3) & 2\tau_3 & \dots & 0 \\ 0 & 2\tau_3 & 4(\tau_3 + \tau_4) & \dots & 0 \\ \vdots & \vdots & \dots & \vdots & \vdots \\ 0 & 0 & 0 & \dots & 4(\tau_{n-2} + \tau_{n-1}) \end{pmatrix}. \quad (4.1.3)$$

When $n = 2$, $|\mathbf{A}|$ is replaced by unity in equation (4.1.1).

Instead of calculating (μ_{rs}) directly, it is rather more convenient to determine first $(L_{n+i, n+j})$. Now (L_{ij}) is the reciprocal of the covariance matrix (λ_{ij}) , given by (2.1.3). The determinant of (λ_{ij}) is found, by a process similar to the above, to be

$$\Delta \sim -\psi_0 \psi_0'' c^{2n-2} (\tau_1 \tau_2 \dots \tau_{n-1})^2 |\mathbf{E}|, \quad (4.1.4)$$

where \mathbf{E} denotes the $(2n-2) \times (2n-2)$ square matrix made up as follows:

$$\mathbf{E} = \begin{pmatrix} \mathbf{A} & \mathbf{C} \\ \mathbf{C}^* & \mathbf{B} \end{pmatrix}$$

† The existence of $\psi''(t)$ is sufficient to ensure the joint distribution of $f(t)$ and $f'(t)$ as in § 2. If the expansion of $\psi(t)$ contains a term in $|t|$ then the mean density of zeros no longer exists in the usual sense. Such a case was considered by Siebert (1951). See also Rice (1958, § 9).

in which A is given by (4.1.3), B is the $n \times n$ matrix

$$B = \begin{pmatrix} 4\tau_1 & -2\tau_1 & 0 & 0 & \dots & 0 \\ -2\tau_1 & 4\tau_1 & 0 & 0 & \dots & 0 \\ 0 & 0 & 4\tau_2 & 0 & \dots & 0 \\ 0 & 0 & 0 & 4\tau_3 & \dots & 0 \\ \vdots & \vdots & \vdots & \vdots & \ddots & \vdots \\ 0 & 0 & 0 & 0 & \dots & 4\tau_{n-1} \end{pmatrix}$$

and C is the $(n-2) \times n$ matrix

$$C = \begin{pmatrix} -2\tau_1 & 4\tau_1 & 2\tau_2 & 0 & \dots & 0 & 0 & 0 \\ 0 & 0 & 4\tau_2 & 2\tau_3 & \dots & 0 & 0 & 0 \\ 0 & 0 & 0 & 4\tau_3 & \dots & 0 & 0 & 0 \\ \vdots & \vdots & \vdots & \vdots & \ddots & \vdots & \vdots & \vdots \\ 0 & 0 & 0 & 0 & \dots & 4\tau_{n-3} & 2\tau_{n-2} & 0 \\ 0 & 0 & 0 & 0 & \dots & 0 & 4\tau_{n-2} & 2\tau_{n-1} \end{pmatrix}$$

(C^* denotes the transpose of C). By subtracting the $(n-1+i)$ th row of E from the i th row ($i = 1, 2, \dots, (n-2)$), and similarly for the columns we find

$$|E| = 12^{n-1}(\tau_1 \tau_2 \dots \tau_{n-1})^2$$

and so
$$\Delta \sim 12^{n-1}(-\psi_0 \psi_0') c^{2n-2}(\tau_1 \tau_2 \dots \tau_{n-1})^4. \quad (4.1.5)$$

The quantities $\Delta L_{n+i, n+j}$ involve the cofactors of the last n rows and columns of (λ_{ij}) and hence of E . Hence we find

$$(L_{n+i, n+j}) \sim \frac{1}{3c} \begin{pmatrix} u_1 & \frac{1}{2}u_1 & 0 & \dots & 0 & 0 \\ \frac{1}{2}u_1 & (u_1 + u_2) & \frac{1}{2}u_2 & \dots & 0 & 0 \\ 0 & \frac{1}{2}u_2 & (u_2 + u_3) & \dots & 0 & 0 \\ \vdots & \vdots & \vdots & \ddots & \vdots & \vdots \\ 0 & 0 & 0 & \dots & (u_{n-2} + u_{n-1}) & \frac{1}{2}u_{n-1} \\ 0 & 0 & 0 & \dots & \frac{1}{2}u_{n-1} & u_{n-1} \end{pmatrix}, \quad (4.1.6)$$

where

$$u_i = \frac{1}{\tau_i} = \frac{1}{t_{i+1} - t_i}. \quad (4.1.7)$$

4.2. The cases $n = 1, 2$ and 3

In the special case $n = 1$ the above expansions do not apply, but the well-known result

$$W(+)=\frac{1}{2\pi}\left(\frac{-\psi_0''}{\psi_0'}\right)^{\frac{1}{2}} \quad (4.2.1)$$

is easily derived as in §2.

When $n = 2$ we have

$$(L_{n+i, n+j}) \sim \frac{1}{3c} \begin{pmatrix} u_1 & \frac{1}{2}u_1 \\ \frac{1}{2}u_1 & u_1 \end{pmatrix}$$

and so by inversion

$$(\mu_{ij}) \sim c \begin{pmatrix} 4\tau_1 & -2\tau_1 \\ -2\tau_1 & 4\tau_1 \end{pmatrix}$$

574

M. S. LONGUET-HIGGINS

giving $\nu_{12} \sim -\frac{1}{2} = \cos^{-1}(\frac{2}{3}\pi)$. Thus from (2.2.2) and (2.2.3)

$$\left. \begin{aligned} W(+, +) &\sim \frac{1}{\pi^2} \left(\frac{\sqrt{3}}{2} - \frac{\pi}{6} \right) \frac{c}{(-\psi_0 \psi_0'')^{\frac{1}{2}}} \\ W(+, -) &\sim \frac{1}{\pi^2} \left(\frac{\sqrt{3}}{2} + \frac{\pi}{3} \right) \frac{c}{(-\psi_0 \psi_0'')^{\frac{1}{2}}} \end{aligned} \right\} \quad (4.2.2)$$

When $n = 3$ we have $(L_{n+i, n+j}) \sim \frac{1}{3c} \begin{pmatrix} u_1 & \frac{1}{2}u_1 & 0 \\ \frac{1}{2}u_1 & (u_1 + u_2) & \frac{1}{2}u_2 \\ 0 & \frac{1}{2}u_2 & u_2 \end{pmatrix}$

and so $(\mu_{ij}) \sim \frac{c}{\tau_1 + \tau_2} \begin{pmatrix} \tau_1(3\tau_1 + 4\tau_2) & -2\tau_1\tau_2 & \tau_1\tau_2 \\ -2\tau_1\tau_2 & 4\tau_1\tau_2 & -2\tau_1\tau_2 \\ \tau_1\tau_2 & -2\tau_1\tau_2 & (4\tau_1 + 3\tau_2)\tau_2 \end{pmatrix}$.

Thus $\nu_{23}, \nu_{31}, \nu_{12} = -\left(\frac{\tau_2}{3\tau_1 + 4\tau_2}\right)^{\frac{1}{2}}, \left(\frac{\tau_1\tau_2}{(3\tau_1 + 4\tau_2)(4\tau_1 + 3\tau_2)}\right)^{\frac{1}{2}}, -\left(\frac{\tau_1}{4\tau_1 + 3\tau_2}\right)^{\frac{1}{2}}$.

Writing for short $\left. \begin{aligned} \frac{\tau_1}{\tau_1 + \tau_2} &= \frac{l_2 - l_1}{l_3 - l_1} = x, \\ \frac{\tau_2}{\tau_1 + \tau_2} &= \frac{l_3 - l_2}{l_3 - l_1} = y, \end{aligned} \right\} \quad (4.2.3)$

so that $x + y = 1$, we find from (2.2.4)

$$W(S) = \frac{1}{8\pi^3} \frac{c}{(-\psi_0 \psi_0'')^{\frac{1}{2}}} \frac{1}{l_3 - l_1} Q^{(S)}, \quad (4.2.4)$$

where

$$\left. \begin{aligned} Q^{(+, +, +)} &= 3 - \frac{(5-2x)x^{\frac{1}{2}}}{(4-x)^{\frac{1}{2}}} \cos^{-1}\left(\frac{x^{\frac{1}{2}}}{2}\right) + \pi(xy)^{\frac{1}{2}} - \frac{(5-2y)y^{\frac{1}{2}}}{(4-y)^{\frac{1}{2}}} \cos^{-1}\left(\frac{y^{\frac{1}{2}}}{2}\right), \\ Q^{(+, -, +)} &= 3 + \frac{(5-2x)x^{\frac{1}{2}}}{(4-x)^{\frac{1}{2}}} \cos^{-1}\left(\frac{-x^{\frac{1}{2}}}{2}\right) + \pi(xy)^{\frac{1}{2}} + \frac{(5-2y)y^{\frac{1}{2}}}{(4-y)^{\frac{1}{2}}} \cos^{-1}\left(\frac{-y^{\frac{1}{2}}}{2}\right), \\ Q^{(+, -, -)} &= 3 - \frac{(5-2x)x^{\frac{1}{2}}}{(4-x)^{\frac{1}{2}}} \cos^{-1}\left(\frac{x^{\frac{1}{2}}}{2}\right) - \pi(xy)^{\frac{1}{2}} + \frac{(5-2y)y^{\frac{1}{2}}}{(4-y)^{\frac{1}{2}}} \cos^{-1}\left(\frac{-y^{\frac{1}{2}}}{2}\right). \end{aligned} \right\} \quad (4.2.5)$$

These three functions are plotted in figure 1. $Q^{(+, +, +)}$ and $Q^{(+, -, +)}$ are symmetrical about the mid-point $x = \frac{1}{2}$, as would be expected, whereas $Q^{(+, -, -)}$ is asymmetrical.

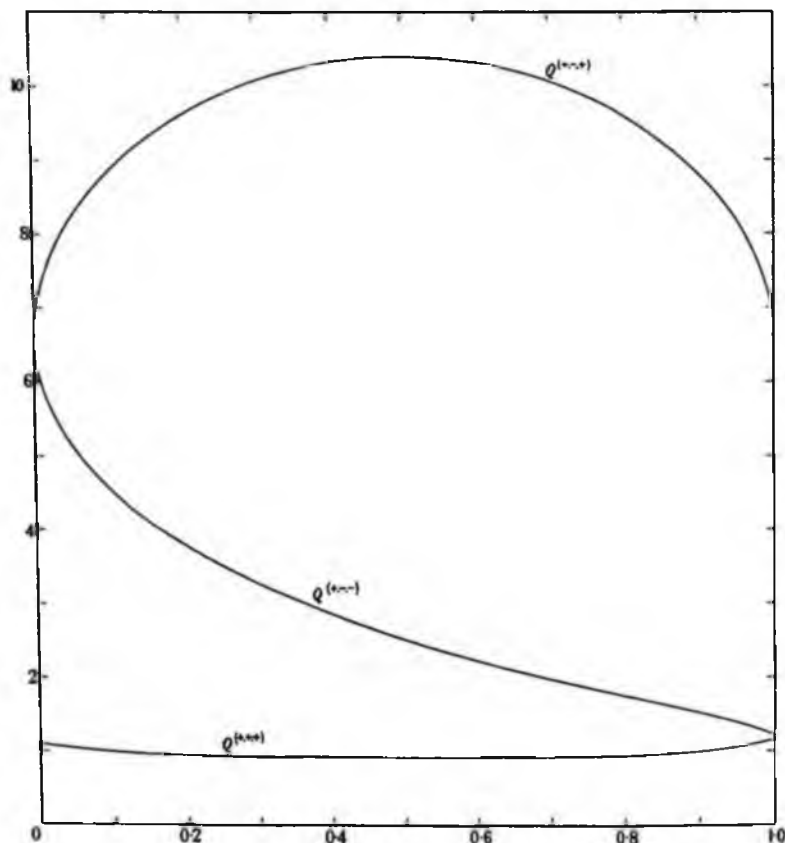
The probability density of a down-crossing at t_2 given up-crossings at t_1 and t_3 is proportional to $Q^{(+, -, +)}$. Figure 1 then shows that the probability density is a maximum when t_2 is mid-way between the two ends of the interval. On the other hand the curve for $Q^{(+, +, +)}$ shows that given up-crossings at both t_1 and t_3 the probability density of an up-crossing at an intermediate point t_2 is fairly insensitive to the position of t_2 . At the mid-point, the density is actually a minimum.

4.3. General values of n

Exact expressions do not appear to exist in general, but upper and lower bounds for $W(S)$ may be obtained in the following way.

In equation (2.1.6) write

$$\eta_i = \frac{x_i}{(L_u)^{\frac{1}{2}}}, \quad l_{ij} = \frac{L_{ij}}{(L_u L_{jj})^{\frac{1}{2}}}. \quad (4.3.1)$$

FIGURE 1. Graphs of $Q^{(+,+,+)}$, $Q^{(+,-,+)}$ and $Q^{(+,-,-)}$.

This gives
$$W(+, +, \dots, +) = \frac{1}{(2\pi)^n \Delta^{\frac{1}{2}} L_{11} L_{22} \dots L_{nn}} \Phi(1) \quad (4.3.2)$$

where
$$\Phi(1) = \int_0^{\infty} \dots \int_0^{\infty} x_1 x_2 \dots x_n \exp\left[-\frac{1}{2} \sum_{i,j=1}^n L_{ij} x_i x_j\right]. \quad (4.3.3)$$

Using the asymptotic formulae for Δ and L_{ij} (equations (4.1.4) and (4.1.6)) we have

$$W(+, +, \dots, +) \sim \frac{1}{(2\pi)^n} \frac{3^n}{12^{k(n-1)}} \frac{c}{(-\psi_0 \psi_0'')^{\frac{1}{2}} (\tau_1 + \tau_2) (\tau_2 + \tau_3) \dots (\tau_{n-2} + \tau_{n-1})} \Phi(1) \quad (4.3.4)$$

and
$$(l_{ij}) = \begin{pmatrix} 1 & \frac{1}{2} \left(\frac{u_1}{u_1 + u_2}\right)^{\frac{1}{2}} & 0 & \dots & 0 \\ \frac{1}{2} \left(\frac{u_1}{u_1 + u_2}\right)^{\frac{1}{2}} & 1 & \frac{1}{2} \left(\frac{u_2}{u_1 + u_2}\right)^{\frac{1}{2}} \left(\frac{u_2}{u_2 + u_3}\right)^{\frac{1}{2}} & \dots & 0 \\ 0 & \frac{1}{2} \left(\frac{u_2}{u_1 + u_2}\right)^{\frac{1}{2}} \left(\frac{u_2}{u_2 + u_3}\right)^{\frac{1}{2}} & 1 & \dots & 0 \\ \vdots & \vdots & \vdots & \ddots & \vdots \\ 0 & 0 & 0 & \dots & 1 \end{pmatrix}. \quad (4.3.5)$$

It is now easy to find bounds for Φ . For since $u_i > 0$, all the elements of (l_{ij}) adjacent to the diagonal lie between 0 and $\frac{1}{2}$. Therefore, the x_i being non-negative,

$$\sum_i x_i^2 \leq \sum_{i,j} l_{ij} x_i x_j \leq \sum_i x_i^2 + \sum x_i x_{i+1}. \quad (4.3.6)$$

In the right-hand inequality substitute

$$x_i x_j \leq \frac{1}{2}(x_i^2 + x_j^2)$$

giving

$$\sum x_i^2 \leq \sum_{i,j} l_{ij} x_i x_j \leq 2 \sum_i x_i^2.$$

Thus from (4.3.3)

$$1 \geq \Phi \geq 1/2^n. \quad (4.3.7)$$

These bounds may now be substituted in (4.3.4).

For $W(S)$, when the signs of S are not all +, one or more of the l_{ij} may be reversed in sign. Hence the left-hand inequality in (4.3.6) is not valid but may be replaced by

$$\sum_i x_i^2 - \sum_i x_i x_{i+1} \leq \sum_{i,j} x_i x_{i+1}.$$

Now it can be shown that

$$\lambda \sum_i x_i^2 \leq \sum_i x_i^2 - \sum_i x_i x_{i+1},$$

where λ is the smallest root of the equation

$$\begin{vmatrix} (1-\lambda) & -\frac{1}{2} & 0 & \dots & 0 \\ -\frac{1}{2} & (1-\lambda) & -\frac{1}{2} & \dots & 0 \\ 0 & -\frac{1}{2} & (1-\lambda) & \dots & 0 \\ \vdots & \vdots & \vdots & \ddots & \vdots \\ 0 & 0 & 0 & \dots & (1-\lambda) \end{vmatrix} = 0,$$

that is to say

$$\lambda = 2 \sin^2 \{ \pi / 2(n+1) \}.$$

Since, then, in all possible cases

$$\lambda \sum_i x_i^2 \leq \sum_{i,j} l_{ij} x_i x_j \leq 2 \sum_i x_i^2$$

we have

$$\frac{1}{2^n \sin^{2n} \{ \pi / 2(n+1) \}} \geq \Phi \geq \frac{1}{2^n}. \quad (4.3.6)$$

Our general result then is that

$$W(S) \sim \frac{1}{(2\pi)^n} \left(\frac{3}{4} \right)^{in} \frac{c}{(-\psi_0 \psi_0')^{\frac{1}{2}}} \frac{2\sqrt{3}\Phi}{(t_3-t_1)(t_4-t_2)\dots(t_n-t_{n-2})}, \quad (4.3.7)$$

where Φ is a function of the t_i lying between the bounds (4.3.6).

4.4. Asymptotic behaviour of $P_n(\tau)$

By the mean-value theorem for integrals, the integral X_n of (1.4.4) can be expressed as

$$X_n \sim \frac{1}{(2\pi)^{n-1}} \left(\frac{3}{4} \right)^{in} \frac{c}{-\psi_0'} 2\sqrt{3}\Phi' K_n, \quad (4.4.1)$$

where

$$K_n = \int \dots \int_{t_1 < t_2 < \dots < t_n} \frac{dt_2 \dots dt_{n-1}}{(t_3-t_1)(t_4-t_2)\dots(t_n-t_{n-2})} \quad (4.4.2)$$

INTERVALS BETWEEN ZEROS OF A RANDOM FUNCTION 577

and Φ' is some value of Φ within the bounds (4.3.6). It can be shown that K_n is finite, and since the denominator of the integrand is homogeneous and of degree $(n-2)$, K_n is independent of $(t_n - t_1)$, or τ . In fact when $n = 2, 3, 4, 5, \dots$

$$K_n = 1, 1, \frac{1}{2}\pi^2, \frac{1}{3}\pi^2, \dots \quad (4.4.3)$$

Thus, as $\tau \rightarrow 0$, X_n tends asymptotically to a positive value independent of τ . From the expansion (1.2.11) it now appears that, for each value of m , $P_m(\tau)$ tends asymptotically to a limiting value $P_m(0)$.

This behaviour of $P_m(\tau)$ is in marked contrast to the corresponding behaviour when $\psi(t)$ is a regular function. Then, as was seen in §3.2, $P_m(\tau)$ is proportional to an increasing power of τ as m increases. A further discussion will be given in connexion with $p(n, \tau)$ (see §4.8). Meanwhile, however, we shall establish some close inequalities for $P_m(0)$ when $m = 1, 2$.

4.5. Approximations to $P_m(0)$

From the results of §4.2 we may evaluate $X(S)$ explicitly when $n = 2$ and 3. Thus from (4.2.1) and (4.2.2) we have

$$\left. \begin{aligned} X(+, -) &\sim \left(\frac{\sqrt{3}}{\pi} + \frac{2}{3} \right) \alpha \\ X(+, +) &\sim \left(\frac{\sqrt{3}}{\pi} - \frac{1}{3} \right) \alpha \end{aligned} \right\} \quad (4.5.1)$$

where we have written for short $\alpha = \frac{c}{-\psi_0''} = \frac{\psi_0''}{-6\psi_0''}$. (4.5.2)

Further, on integrating the expressions (4.2.4) with respect to t_2 over $t_1 < t_2 < t_3$ we find

$$\left. \begin{aligned} X(+, -, +) &\sim \left(\frac{3}{8\pi^2} + \frac{2}{\sqrt{3}\pi} - \frac{47}{288} \right) \alpha, \\ X(+, -, -) &\sim \left(\frac{3}{8\pi^2} + \frac{1}{2\sqrt{3}\pi} - \frac{17}{288} \right) \alpha, \\ X(+, +, +) &\sim \left(\frac{3}{8\pi^2} - \frac{1}{\sqrt{3}\pi} + \frac{49}{288} \right) \alpha. \end{aligned} \right\} \quad (4.5.3)$$

The identity $X(+, -, +) - X(+, +, +) = X(+, +)$ can be readily verified.

Equations (1.2.1) and (1.2.2) give, in the limit when $\tau \rightarrow 0$

$$\left. \begin{aligned} P_0 &= 1.217\,996\alpha - (P_2 + P_4 + P_6 + \dots), \\ P_1 &= 0.217\,996\alpha - (P_3 + P_5 + P_7 + \dots) \end{aligned} \right\} \quad (4.5.4)$$

and $\left. \begin{aligned} P_2 &= 0.070\,856\alpha - (2P_4 + 3P_6 + 4P_8 + \dots), \\ P_3 &= 0.024\,358\alpha - (2P_5 + 3P_7 + 4P_9 + \dots) \end{aligned} \right\} \quad (4.5.5)$

whence also $\left. \begin{aligned} P_0 &= 1.147\,139\alpha + (P_4 + 2P_6 + 3P_8 + \dots), \\ P_1 &= 0.193\,638\alpha + (P_5 + 2P_7 + 3P_9 + \dots). \end{aligned} \right\} \quad (4.5.6)$

Hence the inequalities $\left. \begin{aligned} 1.147\alpha &< P_0(0) < 1.218\alpha, \\ 0.193\alpha &< P_1(0) < 0.218\alpha, \end{aligned} \right\} \quad (4.5.7)$

and $\left. \begin{aligned} 0 &< P_2(0) < 0.071\alpha, \\ 0 &< P_3(0) < 0.025\alpha. \end{aligned} \right\} \quad (4.5.8)$

4.6. *Disproof of the 'exponential hypothesis'*

We now apply the inequalities of the previous section to a particular case which was studied experimentally by Favreau *et al.* (1956). This is the Gaussian process $f(t)$ whose spectral density is given by

$$E \propto 1/(1 + \sigma^2)^2, \quad (4.6.1)$$

where $\sigma = \text{frequency}$. The covariance function ψ_τ , being the cosine transform of E , has the form

$$\psi(t) \propto (1 + |t|) e^{-|t|} = 1 - \frac{1}{2}t^2 + \frac{1}{6}|t|^3 - \dots$$

and so is of the form (4.1).

The experimental results showed that the distribution of zero-crossing intervals $P_0(\tau)$ was quite close to a negative exponential. Since the mean of the distribution must be

$$\frac{1}{2W(+)} = \frac{1}{\pi} \left(\frac{\psi_0}{-\psi_0''} \right)^{\frac{1}{2}} = \frac{1}{\pi},$$

the only possible exponential law is

$$P_0(\tau) = (1/\pi) e^{-\tau/\pi}$$

which makes $P_0(0) = 1/\pi$, or, since

$$\alpha = \psi_0''/(-6\psi_0''') = \frac{1}{3}$$

in this case,

$$P_0(0) = 3\alpha/\pi = 0.955 \dots \alpha. \quad (4.6.2)$$

McFadden (1956) doubted the conjecture but was unable to disprove it (McFadden's assumption that $p''(n, \tau) = 0$ when $n \geq 4$ is actually incorrect), since the only inequalities then available to him were the right-hand inequalities of (4.5.7). However, the left-hand inequality

$$1.147\alpha < P_0(0)$$

is definitely contradictory to (4.6.2). Thus the exponential hypothesis is disproved.

It may be pointed out that because of certain limitations in the experiments (indicated by Favreau *et al.*), the value of $P_0(\tau)$ is liable to be underestimated at the small values of τ ; so that it is not surprising that the experiments suggested a too low value of $P_0(0)$.

4.7. *Further estimates of $P_m(0)$*

If P_4, P_5, \dots are neglected in equations (4.5.5) and (4.5.6), the resulting estimates of P_0, P_1, P_2 and P_3 show that P_2/P_1 and P_3/P_2 are about equal to $1/3$. Now in § 1.1 it was shown that $P_m(\tau)$ tended to zero with m more rapidly than any negative power of m . It is consistent with this result to conjecture that the ratio P_{m+1}/P_m tends to a constant value. If we take roughly

$$\left. \begin{aligned} P_4(0) &\doteq \frac{1}{3}P_3(0) \doteq 0.006\alpha, \\ P_5(0) &\doteq \frac{1}{3}P_4(0) \doteq 0.002\alpha, \\ P_6(0) &\doteq \frac{1}{3}P_5(0) \doteq 0.001\alpha, \end{aligned} \right\} \quad (4.7.1)$$

then on substituting in equations (4.5.5) and (4.5.6) we find as possibly closer approximations

$$\left. \begin{aligned} P_0(0) &\doteq 1.155\alpha, \\ P_1(0) &\doteq 0.186\alpha, \\ P_2(0) &\doteq 0.055\alpha, \\ P_3(0) &\doteq 0.017\alpha. \end{aligned} \right\} \quad (4.7.2)$$

4.8. Asymptotic behaviour of $p(n, \tau)$

As in § 3.3 we have

$$p(0, \tau) \sim 1, \quad p(1, \tau) \sim \frac{1}{\pi} \left(\frac{-\psi_0''}{\psi_0'} \right) \tau. \quad (4.8.1)$$

When $n \geq 2$ we have from (1.4.1) by integration

$$p(n, \tau) = \int_0^\tau dr' \int_0^{r'} dr'' 2W(+)[P_n(r'') - 2P_{n-1}(r'') + P_{n-2}(r'')]$$

provided that $p(n, 0)$ and $p'(n, 0)$ are both zero. This will be satisfied provided

$$p(n, \tau) = O(\tau^{1+\epsilon}), \quad \text{where } \epsilon > 0.$$

Now we have seen earlier that in the singular case $P_m(\tau)$ tends to a positive value $P_m(0)$ as $\tau \rightarrow 0$. Hence by integration

$$p(n, \tau) \sim W(+)[P_n(0) - 2P_{n-1}(0) + P_{n-2}(0)]\tau^2 \quad (4.8.2)$$

as $\tau \rightarrow 0$.

From (4.5.8) and (4.5.9) we have the strict inequalities

$$\left. \begin{aligned} 0.711\beta\tau^2 < p(2, \tau) < 0.903\beta\tau^2, \\ 0.051\beta\tau^2 < p(3, \tau) < 0.243\beta\tau^2, \end{aligned} \right\} \quad (4.8.3)$$

where

$$\beta = W(+)\alpha = \frac{1}{12\pi} \frac{\psi_0''}{(-\psi_0'\psi_0')^{\frac{1}{2}}}. \quad (4.8.4)$$

The rough estimates (4.7.2) would yield

$$\left. \begin{aligned} p(2, \tau) &\doteq 0.818\beta\tau^2, \\ p(3, \tau) &\doteq 0.103\beta\tau^2. \end{aligned} \right\} \quad (4.8.5)$$

Equation (4.8.2) shows that, in contrast to the regular case, $p(n, \tau)$ is of order τ^2 for all values of n greater than or equal to 2; there is no longer a strong mutual repulsion of the zeros.

Again, a heuristic argument suggests that this result is not unreasonable. Since ψ_τ'' has no continuous derivative at the origin, the second derivative of f is, in this case, non-existent almost everywhere (cf. Bartlett 1955, chapter 5) and the first derivative $f'(t)$ may be expected to behave like a random-walk process in which the standard deviation of

$$[f'(t_1) - f'(t_2)]$$

increases like $|t_1 - t_2|^{\frac{1}{2}}$ for small time-differences. Now in the fixed interval $(0, \tau)$, if f has two or more zeros, f'' has at least one. So f' is of order $\tau^{\frac{1}{2}}$ in the interval while f , by integration, is of order $\tau^{\frac{3}{2}}$. That is to say f and f' lie within intervals δf and $\delta f'$ of order $\tau^{\frac{3}{2}}$ and $\tau^{\frac{1}{2}}$, respectively. Since the joint probability density of f and f' at some fixed point t in the interval exists by hypothesis it follows that $p(n, \tau)$ is of order

$$\delta f \cdot \delta f' = O(\tau^{\frac{3}{2}}\tau^{\frac{1}{2}}) = O(\tau^2).$$

One consequence of (4.8.2) is that, given the existence of two zeros in the interval $(0, \tau)$, the probability of $(n-2)$ further zeros in the same interval is of order $\tau^2/\tau^2 = 1$. Roughly speaking, we may say that the first two zeros serve to 'pin down' the function f and its derivative so that the probability of any further number of zeros in the interval is

finite, no matter how short the interval is. However, the probability density of, say, a third zero lying somewhere between the first two depends upon the situation of the third zero relative to the first two, as was seen from the curves of figure 1.

5. A COMPARISON OF DIFFERENT APPROXIMATIONS TO $P_0(\tau)$

In the following we shall compare the accuracy of the approximations suggested by Rice (1945), McFadden (1956, 1958), Ehrenfeld *et al.* (1958), and Longuet-Higgins (1958; this paper is referred to as (I)), with the approximations suggested in the present paper. Discussion is purposely restricted to those methods of approximation on the basis of which numerical computation has been, or readily could be, carried out.

Two different aspects of the approximations are first considered: (a) their accuracy for small values of τ , both in the regular and singular case of §§ 3 and 4, and (b) their accuracy for large values of τ . The results are tabulated in table 1.

Then the 'narrow spectrum' approximation is considered in § 5.8, and lastly the approximations are compared numerically with experimental results obtained by analogue methods when the spectrum of $f(t)$ has certain ideal forms.

5.1. Rice's approximation (1945)

This has been used as a starting point for several of the later approximations. It is

$$P_0(\tau) \doteq \frac{W(+, -)}{W(+)} = X(+, -), \quad (5.1.1)$$

in our notation. The right-hand side, being the first term in the series (1.2.7) may also be written as $P_0^{(1)}$, where $P_0^{(N)}$ is the sum of N terms. As we have seen, the calculation of $W(+, -)$ involves the evaluation of a bivariate normal integral.

From equation (1.1.1) the error in $P_0^{(1)}$ is equal to

$$P_2 + P_4 + P_6 + \dots, \quad (5.1.2)$$

which is always positive. Thus $P_0^{(1)}$ always exceeds P_0 .

(a) *Small values of τ .* In the *regular* case the highest term in the remainder is

$$P_2 \sim \frac{1}{2} \frac{C_4}{C_1} \tau^8. \quad (5.1.3)$$

Thus $P_0^{(1)}$ is correct to order τ^7 near the origin. In the *singular* case equations (4.7.1) and (4.7.2) give

$$P_2 + P_4 + P_6 + \dots = 0.062\alpha, \quad (5.1.4)$$

an error of about 5%.

(b) *Large values of τ .* When τ is so large that $f(t)$ and $f(t + \tau)$ are uncorrelated then we have

$$P_0^{(1)} = \frac{W(+, -)}{W(+)} \sim W(-) = W(+). \quad (5.1.5)$$

P_0 , on the other hand, must tend to zero, in order that $\int P_0(\tau) d\tau$ shall converge. Thus (5.1.5) represents also the error in $P_0^{(1)}$.

5.2. The approximation $P_0^{(2)}$

The approximation discussed in the present paper, namely

$$P_0^{(2)} = \frac{W(+, -)}{W(+)} - \int_{t_1 < t_2 < t_3} \frac{W(+, -, -)}{W(+)} dt_2 = X(+, -) - X(+, -, -), \quad (5.2.1)$$

appears as a natural second approximation to P_0 . Its evaluation involves the single integration of $W(+, -, -)/W(+)$, which, as we have seen in § 2.2, is expressible in terms of known functions. Higher approximations

$$P_0^{(N)} = X_{2,1} - X_{3,1} + X_{4,1} - \dots (-)^{N+1} X_{N+1,1}$$

will each involve additional integrations, in general.

Equation (1.2.4) shows that the error in $P_0^{(2)}$ is equal to

$$-(P_4 + 2P_6 + 3P_8 + \dots) \tag{5.2.2}$$

which is always negative. Thus $P_0^{(2)}$ is always a lower bound for P_0 .

(a) *Small values of τ .* In the regular case the highest term in the remainder is

$$-P_4 \sim -\frac{8}{21 \cdot (11)!} \frac{C_8}{C_1} \tau^{19}. \tag{5.2.3}$$

Thus $P_0^{(2)}$ is correct to order τ^{18} near the origin. In the singular case equations (4.7.1) give

$$-(P_4 + 2P_6 + \dots) \doteq -0.008\alpha, \tag{5.2.4}$$

an error of 0.7%.

It is clear that near the origin this approximation leaves little to be desired.

(b) *Large values of τ .* Asymptotically we have

$$\frac{W(+, -, -)}{W(+)} \sim W(+)^2$$

and hence

$$P_0^{(2)} \sim -W(+)^2 \tau \tag{5.2.5}$$

which is $O(\tau)$ at infinity. It is clear that the approximation fails radically for large values of τ .

Indeed it will be seen generally that the approximation of P_0 by $P_0^{(N)}$ is analogous, for large τ , to the approximation of e^{-x} by a finite number of terms of its power series; the convergence of the approximation is non-uniform over $(0, \infty)$.

5.3. The 'multiply conditioned' approximations

In § 3.10 of his original paper (1945) Rice suggested that the approximation (5.1.1) might be improved by including in the probability density $W(+, -)$ the condition that $f(t)$ be positive at one or more given points of the range (t_1, t_2) . The inclusion of just one extra point leads to a threefold normal integral that can be expressed in closed form. The inclusion of more than one point leads to fourfold and higher integrals.

The suggestion was taken up by Ehrenfeld *et al.* (1958), who refer to such approximations as 'multiply conditioned' approximations. Thus (5.1.1) is denoted by MC-0; with one condition at the mid-point of the range the approximation is MC-1, and so on. Clearly all such approximations are, like MC-0, upper bounds for the true value P_0 .

(a) *Small values of τ .* The error in MC-1 is just equal to the probability density of a down-crossing at $t = \tau$ plus a zero in $(0, \tau)$, given that $f(0) = 0$ and $f(\frac{1}{2}\tau) > 0$. Now if $f(\frac{1}{2}\tau) > 0$, there must be at least two zeros in the interval $(0, \frac{1}{2}\tau)$ and/or at least two zeros in $(\frac{1}{2}\tau, \tau)$. If we ignore $p(5, \tau)$, $p(6, \tau)$, etc., relative to $p(4, \tau)$, the error is clearly

$$\Sigma \int \int_{0 < t_4 < t_3 < \frac{1}{2}\tau} \frac{W(+, -, +, -)}{W(+)} dt_2 dt_3. \tag{5.3.1}$$

In the regular case, the neglect of $\rho(5, \tau)$, etc., is justified by § 3.3, and we have from (3.1.4)

$$\frac{W(+, -, +, -)}{W(+)} \sim \frac{C_4}{C_1} t_2 t_3 \tau (t_3 - t_2) (\tau - t_2) (\tau - t_3).$$

Substituting in (5.3.1) we find for the error

$$\frac{39}{8!} \frac{C_4}{C_1} \tau^8. \quad (5.3.2)$$

This may be compared with (5.1.3). Clearly the order of the error is the same as in MC-0, but is less by the ratio

$$\frac{39 \times 280}{8!} = \frac{13}{48}.$$

In the *singular* case the limiting value of MC-1 as $\tau \rightarrow 0$ was calculated by Rice (1958) in the case of the spectrum $(1 + \sigma^2)^{-2}$ (cf. § 4.8 above), with the result

$$\text{MC-1} \sim \frac{1.251}{\pi} = 1.195\alpha,$$

since $\alpha = 1/3$ in this case. From (4.7.2) the error appears to be

$$1.195\alpha - 1.155\alpha = 0.040\alpha \quad (5.3.2)$$

or about 3% of $P_0(0)$. Compared with MC-0, the error is reduced by about one-third.

In the case of the higher multiply-conditioned solutions, if the subintervals of $(0, \tau)$ are denoted by $(t^{(0)}, t^{(i+1)})$ (with $t^{(0)} = 0$) then the expression corresponding to (5.3.1) is

$$\sum_i \int_{t^{(0)} < t_1 < t_2 < t^{(i+1)}} \frac{W(+, -, +, -)}{W(+)} dt_2 dt_1.$$

Since W is of order τ^6 it follows that the error is always of order τ^8 .

(b) *Large values of τ* . When the interval τ is sufficiently large, the sign of $f(\frac{1}{2}\tau)$ becomes independent of the other conditions, and the probability of $f(\frac{1}{2}\tau)$ being positive is one-half. Hence

$$\text{MC-1} \sim \frac{1}{2} \text{MC-0} \sim \frac{1}{2} W(+). \quad (5.3.3)$$

Thus the error is reduced relative to MC-0 by one-half.

Generally, if the N 'conditioned' points in the multiply conditioned approximation MC- N are spaced so that their separation tends to infinity with τ , then

$$\text{MC-}N \sim \frac{1}{2^N} \text{MC-0} \sim \frac{1}{2^N} W(+). \quad (5.3.4)$$

5.4. McFadden's first approximation

McFadden (1956) gave the following approximation to $P_0(\tau)$, valid for small intervals τ

$$P_0(\tau) \approx \frac{R^*(\tau)}{8W(\tau)} = F(\tau),$$

say. Here $R^*(\tau)$ denotes the correlation function of the 'clipped' form of $f(t)$, defined in § 1.4. From (1.4.8),

$$F(\tau) = P_0 - P_1 + P_2 - P_3 + \dots = X(+, -) - X(+, +). \quad (5.4.1)$$

The approximation is equivalent to neglecting P_1, P_2, \dots in the above series; thus it is actually of a lower order of accuracy than $P_0^{(1)}$.

In the Gaussian case we have the well-known formula

$$R(\tau) = \frac{2}{\pi} \sin^{-1} \left(\frac{\psi(\tau)}{\psi_0} \right)$$

and so

$$F(\tau) = \frac{1}{2} \left(\frac{\psi_0}{-\psi_0} \right)^{\frac{1}{2}} \frac{d^2}{d\tau^2} \cos^{-1} \left(\frac{-\psi(\tau)}{\psi_0} \right). \tag{5.4.2}$$

(a) *Small values of τ .* In the regular case the error is of order

$$-P_1(\tau) \sim -\frac{1}{6} \frac{C_3}{C_1} \tau \tag{5.4.3}$$

and in the singular case we find by expansion in powers of τ

$$F(\tau) \sim -\psi_0''/6\psi_0'' = \alpha.$$

By comparison with (4.7.2) the error is

$$-0.155\alpha. \tag{5.4.4}$$

(b) *Large values of τ .* In (5.4.1) each of the terms $X(+, -), X(+, +)$ tends to 0, and so $F(\tau)$ tends to 0. The error thus vanishes.

5.5. $p_r(\tau)$ and $p_r^*(\tau)$

The sequence of approximations proposed in (I) depends on writing the first of equations (1.4.1) in the form

$$P_0(\tau) = -\frac{1}{W(+)} \frac{\partial^2}{\partial t_1 \partial t_n} U(t_n - t_1),$$

or

$$P_0(\tau) = \frac{1}{W(+)} \frac{d^2}{d\tau^2} U(\tau),$$

where $U(\tau) = \frac{1}{2} p(0, \tau)$, is the probability that $f(t)$ be positive throughout the interval $(0, \tau)$. Let $U(\tau)$ be replaced by the probability $U_r(t^{(1)}, \dots, t^{(r)})$ that $f(t)$ be positive at r suitably spaced points in $(0, \tau)$. (For convenience it is supposed that the points are equally spaced and that $t^{(1)}, t^{(r)}$ are at the end-points.) As the number r of points is increased, U_r becomes an increasingly good approximation to U . The corresponding approximations to $P_0(\tau)$ are defined by

$$p_r(\tau) = -\frac{1}{W(+)} \frac{\partial^2}{\partial t^{(1)} \partial t^{(r)}} U_r(t^{(1)}, \dots, t^{(r)}) \tag{5.5.1}$$

and

$$p_r^*(\tau) = \frac{1}{W(+)} \frac{d^2}{d\tau^2} U_r(\tau). \tag{5.5.2}$$

It turns out that in the Gaussian case $p_3(\tau)$ is identical with $F(\tau)$ given by equation (5.4.2). Generally, although U_r involves an r -fold normal integral, the approximations p_r and p_r^* , which depend on the derivatives of U_r , involve only $(r-2)$ -fold normal integrals. Thus p_3, p_4, p_5 and p_3^*, p_4^*, p_5^* can all be evaluated in terms of elementary functions.

(a) *Small values of τ .* The difference $(U_r - U)$ is equal to the probability that $f(t)$ be positive at each of the points $t^{(i)}$, and have a zero-crossing at some point in the interval $(0, \tau)$. Hence

$f(t)$ must have two, four or more zeros in at least one of the subintervals $(t^{(i)}, t^{(i+1)})$ (the first such zero a down-crossing) and certainly not one, three or five zeros in any of the remaining subintervals. If we neglect $p(4, \tau)$ relative to $p(2, \tau)$ and $p(3, \tau)$ the probability of such an event for the subinterval $(t^{(i)}, t^{(i+1)})$ is

$$\iint_{t^{(i)} < t_1 < t_2 < t^{(i+1)}} W(-, +) dt_1 dt_2 - \iiint_{t^{(i)} < t_1 < t_2; t^{(i)} < t_3 < t^{(i+1)}} W(+, -, +) dt_1 dt_2 dt_3 \\ - \iiint_{t^{(i)} < t_1 < t_2 < t^{(i+1)}; t_3 < t_4 < t^{(i+1)}} W(-, +, -) dt_1 dt_2 dt_3. \quad (5.5.3)$$

Again, if $p(4, \tau)$ is neglected the probability of a pair of zeros in more than one of the subintervals is negligible, so that the events are mutually independent. So $(U_r - U)$ is equal to the sum of $(r-1)$ expressions like (5.5.3).

On differentiating (5.5.3) partially with respect to both $t^{(i)}$ and $t^{(i+1)}$ the first integral vanishes identically whenever $r > 2$; the other integrals also vanish except when $i = 1$ or $(r-1)$. Hence we have

$$p_r(\tau) - P_0(\tau) \sim \frac{2}{W(+)} \frac{\partial^2}{\partial t^{(1)} \partial t^{(r)}} \iiint_{t^{(1)} < t_1 < t_2; t^{(r-1)} < t_3 < t^{(r)}} W(+, -, +) dt_1 dt_2 dt_3.$$

Substituting for $W(+, -, +)$ from (3.1.4) we find

$$p_r(\tau) - P_0(\tau) = -\frac{1}{3}(C_3/C_1) (t^{(r)} - t^{(1)}) (t^{(r)} - t^{(r-1)}) (t^{(r)} + 2t^{(r-1)} - 3t^{(1)}).$$

Now putting $(t^{(r)} - t^{(1)}) = \tau$ and $(t^{(r)} - t^{(r-1)}) = \tau/(r-1)$ we obtain for the error in p_r ,

$$-\frac{(3r-5)}{3(r-1)^2} \frac{C_3}{C_1} \tau^4. \quad (5.5.4)$$

Thus $p_r(\tau)$ is correct to order τ^3 (not τ^4 , as was stated in (I)). In particular when $r = 3, 4, 5$ the errors are, respectively,

$$-\frac{1}{6} \frac{C_3}{C_1} \tau^4, \quad -\frac{7}{81} \frac{C_3}{C_1} \tau^4, \quad -\frac{5}{96} \frac{C_3}{C_1} \tau^4. \quad (5.5.5)$$

The case $r = 3$ is in agreement with (5.4.3).

On the other hand p_r^* involves the first term in (5.5.3) which is of a lower order. Thus

$$U_r - U = (r-1) \iint_{0 < t_1 < t_2 < \tau/(r-1)} W(+, -) dt_1 dt_2 + O(\tau^4).$$

On substituting in (5.5.2) and using (3.2.4) we find

$$p_r^*(\tau) - P_0(\tau) = \frac{1}{r-1} P_0 \left(\frac{\tau}{r-1} \right) + O(\tau^4).$$

Therefore at $\tau = 0$

$$\left. \begin{aligned} p_r^* &= \left(1 + \frac{1}{r-1} \right) P_0 = 0, \\ \frac{dp_r^*}{d\tau} &= \left(1 + \frac{1}{(r-1)^2} \right) \frac{dP_0}{d\tau}, \\ \frac{d^2 p_r^*}{d\tau^2} &= \left(1 + \frac{1}{(r-1)^3} \right) \frac{d^2 P_0}{d\tau^2}, \\ \frac{d^3 p_r^*}{d\tau^3} &= \left(1 + \frac{1}{(r-1)^4} \right) \frac{d^3 P_0}{d\tau^3}. \end{aligned} \right\}$$

For example, when $r = 3$ we have

$$\frac{d\rho_3^*}{d\tau} = \frac{5}{4} \frac{dP_0}{d\tau},$$

a relation proved independently in (I). For $r \geq 3$, since $P_0(\tau) \sim (C_2/C_1)\tau$, the error in $\rho_r^*(\tau)$ is

$$\frac{1}{(r-1)^2} \frac{C_2}{C_1} \tau. \quad (5.5.6)$$

In the singular case we make a straightforward expansion of $\rho_r(\tau)$ in powers of τ . The calculations lead eventually to the following, when $r = 3, 4, 5$

$$\rho_3(0) = \alpha,$$

$$\rho_4(0) = \frac{1}{\pi} \left[\cos^{-1} \left(\frac{-7}{8} \right) + \frac{8}{3\sqrt{15}} \right] \alpha = 1.0583\alpha,$$

$$\begin{aligned} \rho_5(0) &= \frac{1}{2\pi} \left[2 \cos^{-1} \left(\frac{-11}{12} \right) - \cos^{-1} \left(\frac{7}{9} \right) + \frac{1}{16} \left(\frac{83}{\sqrt{23}} + 11\sqrt{2} \right) \right] \alpha \\ &= 1.0879\alpha. \end{aligned}$$

The corresponding expansions of $\rho_r^*(\tau)$ lead to

$$\rho_3^*(0) = 1.5\alpha,$$

$$\begin{aligned} \rho_4^*(0) &= \frac{\alpha}{9\pi} \left[\cos^{-1} \left(\frac{-1}{4} \right) + 2 \cos^{-1} \left(\frac{-3\sqrt{3}}{4\sqrt{2}} \right) + 8 \cos^{-1} \left(\frac{\sqrt{3}}{2\sqrt{2}} \right) + 9 \cos^{-1} \left(\frac{-7}{8} \right) \right] \\ &= 1.3551\alpha, \end{aligned}$$

$$\begin{aligned} \rho_5^*(0) &= \frac{\alpha}{16\pi} \left[\left(\cos^{-1} \frac{-7}{8\sqrt{2}} + \cos^{-1} \frac{-5}{3\sqrt{3}} + \cos^{-1} \frac{-1}{4} + \cos^{-1} \frac{1}{2\sqrt{6}} \right) + 16 \cos^{-1} \left(\frac{-11}{12} \right) \right. \\ &\quad \left. - 2 \left(\cos^{-1} \frac{3\sqrt{3}}{4\sqrt{2}} + \cos^{-1} \frac{1}{3} \right) + 4 \left(\cos^{-1} \frac{3}{4\sqrt{2}} - \cos^{-1} \frac{13}{8\sqrt{3}} \right) \right. \\ &\quad \left. + 8 \left(\cos^{-1} \frac{3}{2\sqrt{2}} - \cos^{-1} \frac{7}{9} \right) + 9 \left(\cos^{-1} \frac{5}{4\sqrt{3}} + \cos^{-1} \frac{1}{3} + \cos^{-1} \frac{7}{8} \right) \right] \\ &= 1.2899\alpha. \end{aligned}$$

These results are plotted in figure 2 against the abscissa $1/(r-1)$, and taking $\alpha = 1$. The point labelled $P_0^{(\infty)}$ and plotted at $r = \infty$ corresponds to the estimate $P_0 \doteq 1.155\alpha$ of § 4.7. It will be seen that ρ_r and ρ_r^* both approach $P_0^{(\infty)}$, the one from below and the other from above.

For comparison, the other approximations to $P_0(0)$ discussed above have been plotted in the same diagram. Because they are of comparable complexity, MC-0 and MC-1 have been plotted on the same ordinates as ρ_4 and ρ_5 , respectively. $P_0^{(2)}$, which involves the single integration of a known function (corresponding to a fourfold integration) is plotted level with $r = 6$. It is obviously the closest approximation.

(b) *Large values of τ .* As $\tau \rightarrow \infty$ so $U_r(\tau)$ tends to zero; for the probability that $f(t)$ remain of constant sign throughout the infinite interval becomes vanishingly small. Hence also ρ_r and ρ_r^* tend to zero at infinity, and the error in both ρ_r and ρ_r^* is vanishingly small.

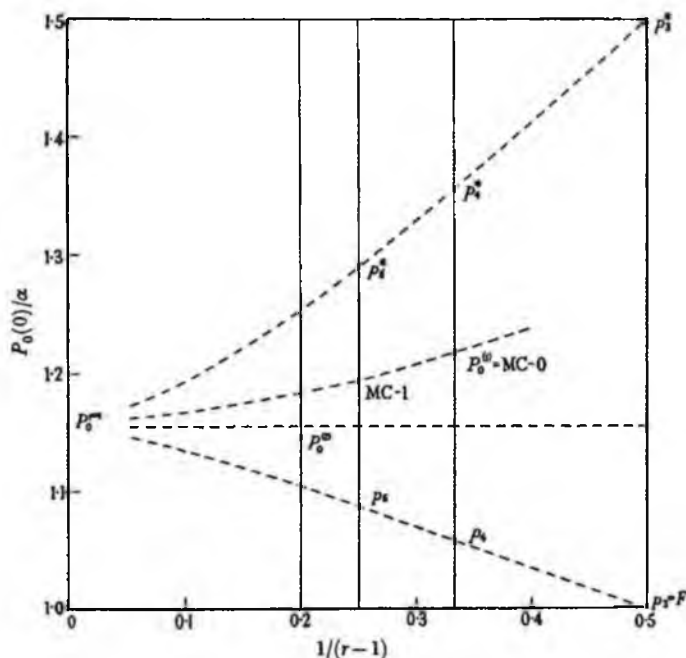


FIGURE 2. Approximations to $P_0(0)$ in the singular case.

5.6. McFadden's second approximation

A quite different method was suggested in a later paper by McFadden (1958). On the assumption that a given interval τ is independent of the sums of the previous $(2m+2)$ intervals ($m = 0, 1, 2, \dots$) McFadden derived the integral equation

$$P_0(\tau) = X(+, -) - X(+, +) * P_0(\tau). \quad (5.6.1)$$

$X(+, -)$ and $X(+, +)$ are as in § 1.1 and a star * denotes convolution:

$$F_1(\tau) * F_2(\tau) = \int_0^\tau F_1(\tau') F_2(\tau - \tau') d\tau'.$$

The solution of this (approximate) integral equation may be denoted by $\text{McF}(\tau)$.

(a) *Small values of τ .* In the regular case, $X(+, +) \sim P_1$ (by (1.2.1)) and so the second term in (5.6.1) is, by (3.2.6),

$$-X(+, +) * P_1(\tau) \sim -\frac{C_2 C_4}{6C_1^2} \int_0^\tau \tau'^4 (\tau - \tau') d\tau' = -\frac{1}{180} \frac{C_2 C_4}{C_1^2} \tau^6.$$

But we saw that $X(+, -)$, or $P_0^{(1)}$ is correct to order τ^7 , so that the major part of the error is in fact due to the second term. This corresponds to the fact that for small intervals at least the assumption of independence is invalid (Palmer 1956).

In the singular case the second term is zero at the origin and so

$$\text{McF}(\tau) = X(+, -) = 1.218\alpha.$$

The error is therefore the same as in $P_0^{(1)}$ (see equation (5.1.4)).

INTERVALS BETWEEN ZEROS OF A RANDOM FUNCTION 587

(b) Large values of τ . Since $X(+, -)$ and $X(+, +)$ both become equal to $W(+)$ at infinity. The solution to the limiting equation

$$F(\tau) \doteq W(+)-W(+)\int_0^\tau F(\tau-\tau')d\tau'$$

is $F(\tau) \doteq W(+)\text{e}^{-W(+)\tau}$,

a negative exponential. Hence we expect $\text{McF}(\tau)$ to tend to zero exponentially at infinity.

The results of §§ 5.1 and 5.6 are summarized in table 1.

TABLE 1. COMPARISON OF DIFFERENT APPROXIMATIONS TO $P_0(\tau)$
error for small τ

approximation	regular case	singular case	error for large τ
$P_0^{(0)} = \text{MC-0}$	$\frac{1}{280} C_1 \tau^2$	0.062α	$W(+)$
$P_0^{(2)}$	$-\frac{8}{21 \cdot (11)!} C_1^6 \tau^{19}$	-0.008α	$-W(+)^2 \tau$
MC-1	$\frac{39}{81} C_1 \tau^3$	0.040α	$\frac{1}{2}W(+)$
$p_3 = F$	$-\frac{1}{6} C_1 \tau^4$	-0.155α	$o(1)$
p_4	$-\frac{7}{81} C_1 \tau^4$	-0.097α	$o(1)$
p_5	$-\frac{5}{96} C_1 \tau^4$	-0.087α	$o(1)$
p_3^*	$\frac{1}{4} C_1 \tau$	0.345α	$o(1)$
p_4^*	$\frac{1}{9} C_1 \tau$	0.200α	$o(1)$
p_5^*	$\frac{1}{16} C_1 \tau$	0.135α	$o(1)$
McF	$-\frac{1}{180} C_2 C_1 \tau^6$	0.062α	$o(1)$

5.7. The narrow-band approximation

Let $E(\sigma)$ denote the spectral density of $f(t)$, related to $\psi(t)$ by the equations

$$\left. \begin{aligned} E(\sigma) &= \frac{2}{\pi} \int_0^\infty \psi(t) \cos \sigma t dt, \\ \psi(t) &= \int_0^\infty E(\sigma) \cos \sigma t d\sigma. \end{aligned} \right\}$$

The mean frequency of the spectrum is defined as $\bar{\sigma} = m_1/m_0$, where

$$m_r = \int_0^\infty E(\sigma) \sigma^r d\sigma$$

is the r th moment of the spectrum. It is convenient to write also

$$\mu_r = \int_0^\infty E(\sigma) (\sigma - \bar{\sigma})^r d\sigma.$$

The spectrum is said to be *narrow* if

$$\frac{\mu_2}{\bar{\sigma}^2 \mu_0} = \delta^2 \ll 1$$

and it can be shown (I) that in that case $\psi(t)$ has the form

$$\psi(t) = A(t) \cos \bar{\sigma}t + O(\delta \bar{\sigma}t)^3, \quad (5.7.1)$$

where $A(t)$ is a slowly varying function of t

$$A(t) = \mu_0 - \frac{1}{2} \mu_2 t^2 = \psi_0 (1 - \frac{1}{2} \delta^2 \bar{\sigma}^2 t^2).$$

Under these conditions one expects $f(t)$ to have the form of a sine wave of almost constant frequency $\bar{\sigma}$ and slowly varying amplitude, so that the greater part of the distribution $P_0(\tau)$ lies within the neighbourhood of $\tau_0 = \pi/\bar{\sigma}$. In fact the approximation $F(\tau)$ of equation (5.4.2) reduces to

$$F(\tau) \doteq \frac{1}{2\delta\tau_0 [1 + (\tau - \tau_0)^2 / (\delta\tau_0)^2]^{\frac{1}{2}}} \quad (5.7.2)$$

provided $(\tau - \tau_0)$ is comparable with $\delta\tau_0$. It can be shown that all the other approximations discussed in this paper have the same limiting form as $\delta \rightarrow 0$. This approximation will be called the narrow-band approximation and will be denoted by $NB(\tau)$. It has the following properties:

- (1) It is symmetrical about the mean point $\tau = \tau_0$.
- (2) For large values of $(\tau - \tau_0)$ it is of order $|\tau - \tau_0|^{-3}$, and so has no second moment.
- (3) The maximum probability density is

$$NB(\tau_0) = \frac{1}{2\delta\tau_0}.$$

- (4) The width of the curve where it reaches half its maximum height is given by

$$2 \times (2^{\frac{1}{2}} - 1)^{\frac{1}{2}} \delta\tau_0 = 1.533\delta\tau_0.$$

- (5) The cumulative distribution function is

$$\int_{-\infty}^{\tau} NB(\tau) d\tau = \frac{(\tau - \tau_0) / (\delta\tau_0)}{2[1 + (\tau - \tau_0)^2 / (\delta\tau_0)^2]^{\frac{1}{2}}} + \frac{1}{2}.$$

- (6) Hence the quartiles are given by

$$\frac{\tau - \tau_0}{\delta\tau_0} = \frac{1}{\sqrt{3}} = 0.5774$$

and the interquartile range is

$$1.155\delta\tau_0.$$

5.8. Numerical computations

In this last section, the various approximations to $P_0(\tau)$ described in §§ 5.1 to 5.7 are compared by numerical computation over values of τ not necessarily very small or very large. Where possible, the results are compared with those obtained experimentally by analogue methods (Favreau *et al.* 1956; Blötekjaer 1958).

Only these approximations are shown which are the highest of their type at present available. For example, MC-0 is not shown if MC-1 is available, and p_3, p_4 are not shown if p_5 is available.

INTERVALS BETWEEN ZEROS OF A RANDOM FUNCTION 589

Figures 3 to 7 show the approximations $p_5, p_5^*, P_0^{(2)}$, McF and MC-0 (or MC-1) for spectra of the form

$$E(\sigma) = \sigma^{2n}/(1 + \sigma^2)^m$$

(see table 2). In two cases (figures 3 and 6) the spectra are $O(\sigma^{-4})$ at infinity so that ψ has the singularity discussed in § 4. Figure 3 corresponds to the case discussed in § 4.6, where it was shown that $P_0(\tau)$ is not a negative exponential, as the observations might suggest.

The experimental results of Favreau *et al.* are indicated in figure 3 by the plotted points (the vertical lines indicate the estimated uncertainty of the observations); in figures 4 to 7 the experimental values (Favreau *et al.*) are shown by broken curves.

The curves which form lower and upper bounds of P_0 —namely $P_0^{(2)}$ and MC-0 or MC-1—are drawn rather more heavily than the others. From figures 3, 6 and 7 it will be seen that at small values of τ the experimental points lie considerably below the theoretical lower bound. This implies that in some other parts of the curve the experimental points must be too high, since the total area under each curve must be unity.

TABLE 2

figure	$E(\sigma)$	$\psi(t)$
3	$(1 + \sigma^2)^{-2}$	$e^{- t }(1 + t)$
4	$(1 + \sigma^2)^{-3}$	$e^{- t }(1 + t + \frac{1}{2}t^2)$
5	$(1 + \sigma^2)^{-5}$	$e^{- t }(1 + t + \frac{3}{2}t^2 + \frac{5}{24}t^3 + \frac{1}{16}t^4)$
6	$\sigma^4(1 + \sigma^2)^{-4}$	$e^{- t }(1 + t - 2t^2 + \frac{1}{2} t ^3)$
7	$\sigma^4(1 + \sigma^2)^{-5}$	$e^{- t }(1 + t - \frac{3}{2}t^2 - \frac{1}{2} t ^3 + \frac{1}{2}t^4)$

Nevertheless, there is substantial agreement between the experimental points and the three approximations $p_5^*, P_0^{(2)}$ and McF. For all except small values of τ the agreement with p_5 is less good than with p_5^* .

Figure 8 shows a similar study in the case of the Butterworth spectrum

$$E(\sigma) = 1/(1 + \sigma^{14}),$$

which has a fairly sharp cut-off at about $\sigma = 1$. The plotted points are those of Favreau *et al.* (1956). Evidently the agreement between the observations and the theoretical curves $p_5^*, P_0^{(2)}$ and McF is quite close. In the range $6 < \tau < 8$, where $P_0^{(2)}$ is the uppermost of the three curves $P_0^{(2)}$ must also be the closest approximation, since it is a lower bound.

For the low-pass spectrum

$$E(\sigma) = \begin{cases} 1 & (0 < \sigma < 1), \\ 0 & (1 < \sigma < \infty), \end{cases}$$

the best experimental results available appear to be those of Blötekjaer (1958), which are represented by the broken curve (B) in figure 9. It will be seen that the agreement with McF is fairly good, with p_5^* somewhat better, and with $P_0^{(2)}$ very close indeed, as far as $\tau = 14$.

For the band-pass spectrum

$$E(\sigma) = \begin{cases} 0 & (0 < \sigma < \sigma_1), \\ 1 & (\sigma_1 < \sigma < 1), \\ 0 & (1 < \sigma < \infty), \end{cases}$$

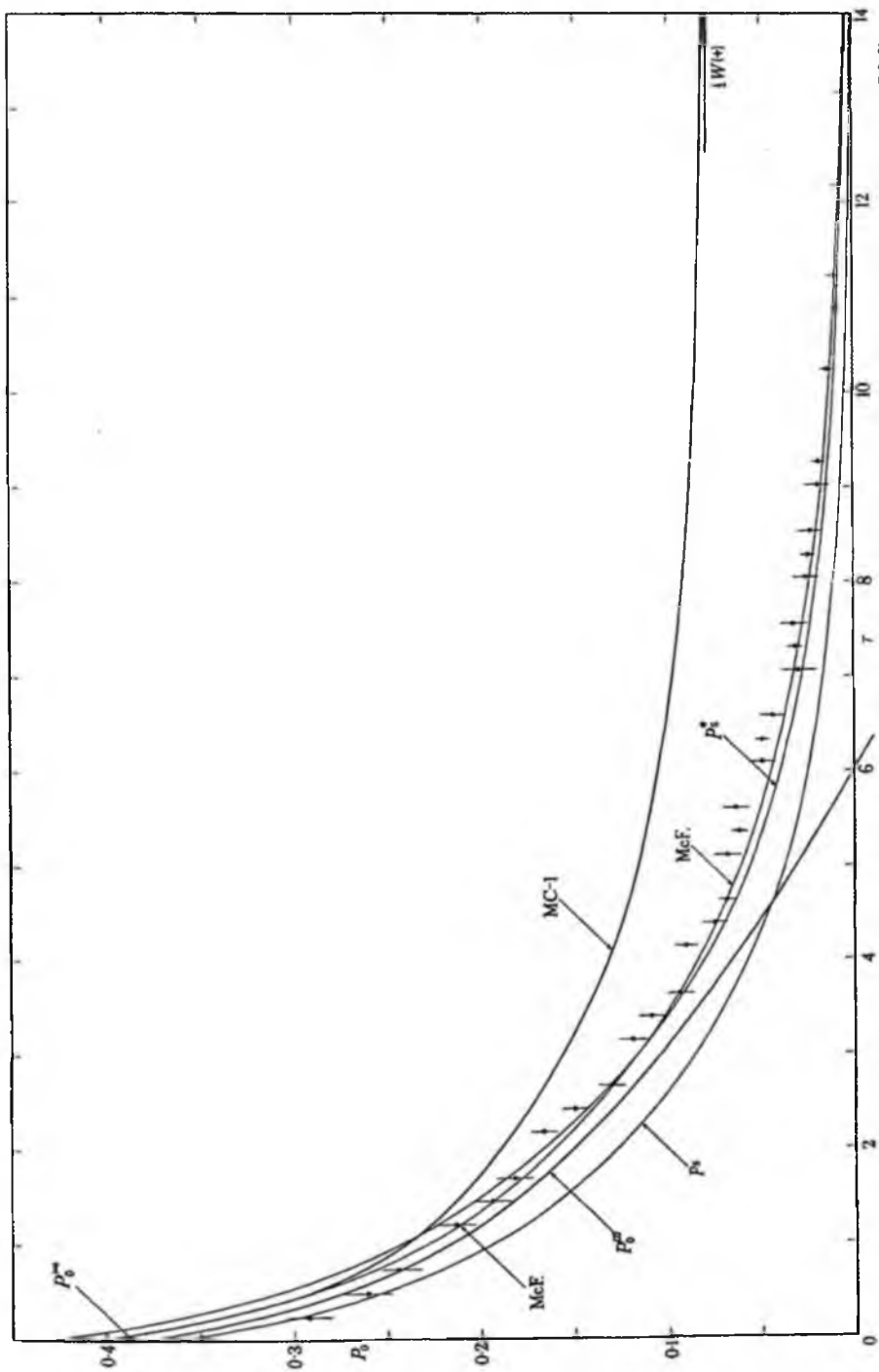


FIGURE 3. Approximations to $P_0(\tau)$ for the spectrum $E = (1 + \sigma^2)^{-2}$. The plotted points are the experimental results of Favreau, Low and Pfeiffer.

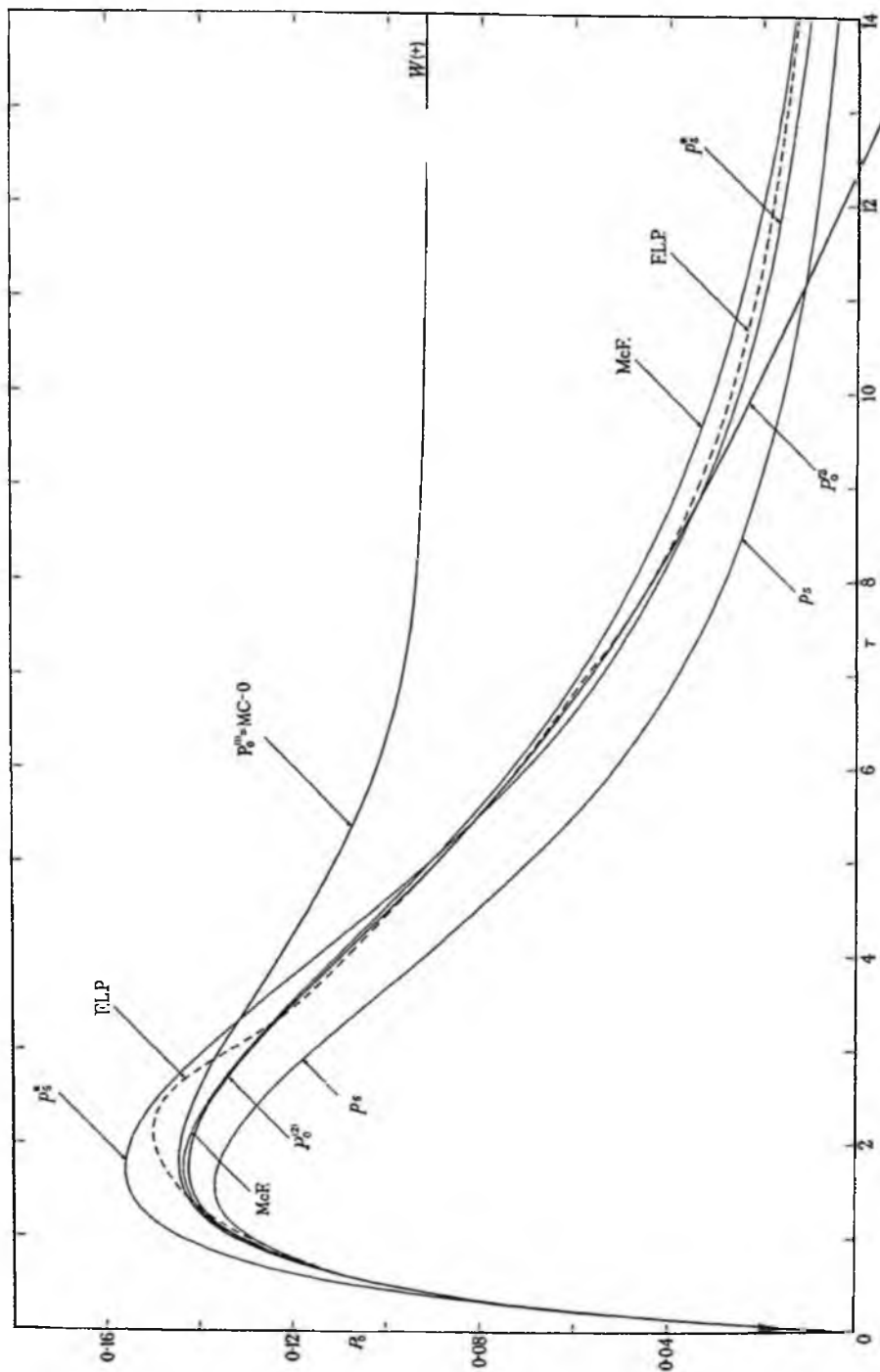


FIGURE 4. Approximations to $P_0(\tau)$ for the spectrum $E = (1 + \sigma^2)^{-1}$.

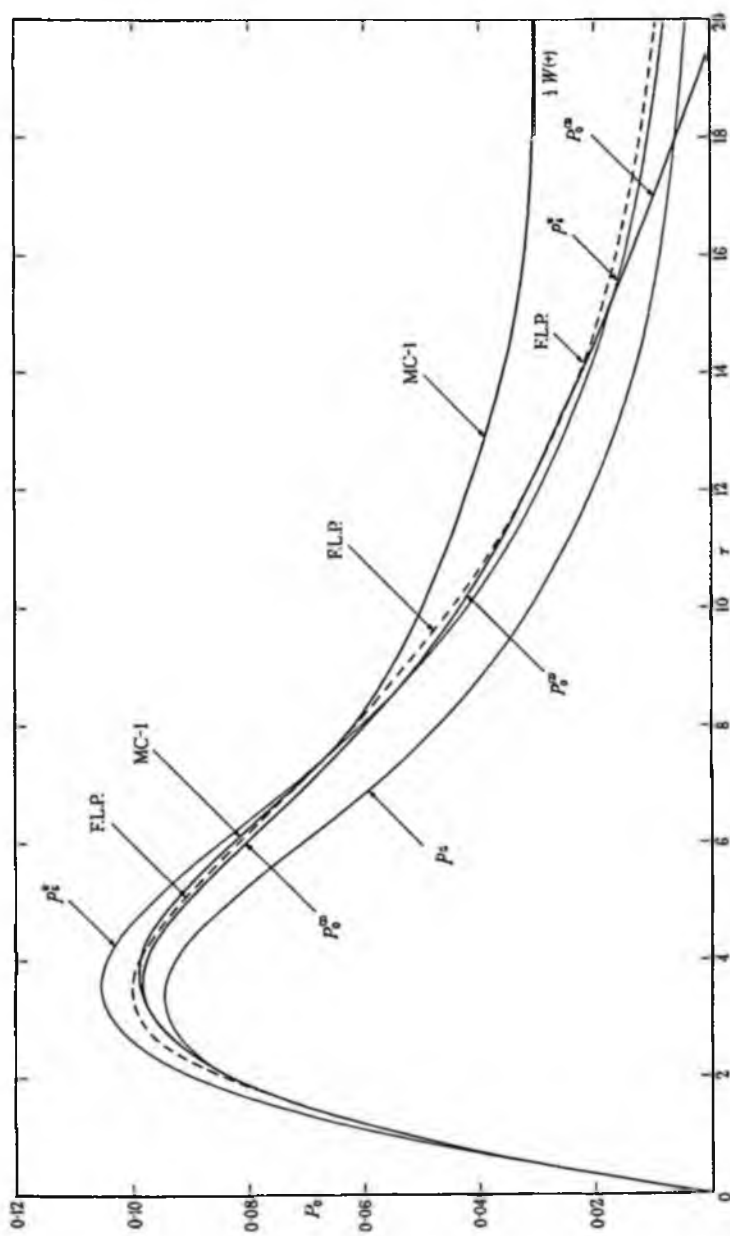


FIGURE 6. Approximations to $P_0(\tau)$ for the spectrum $E = (1 + \sigma^2)^{-2}$.

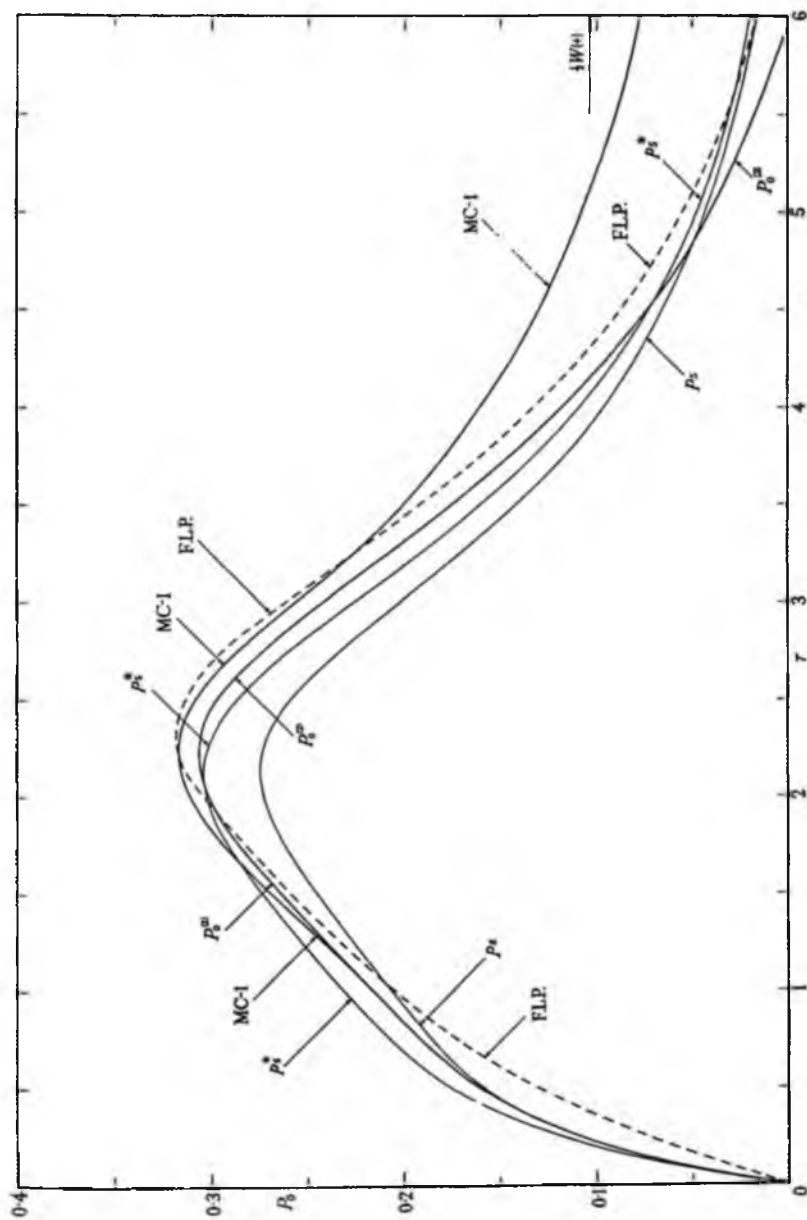


FIGURE 7. Approximations to $F_0(\tau)$ for the spectrum $E = \sigma^2(1 + \sigma^2)^{-1}$.

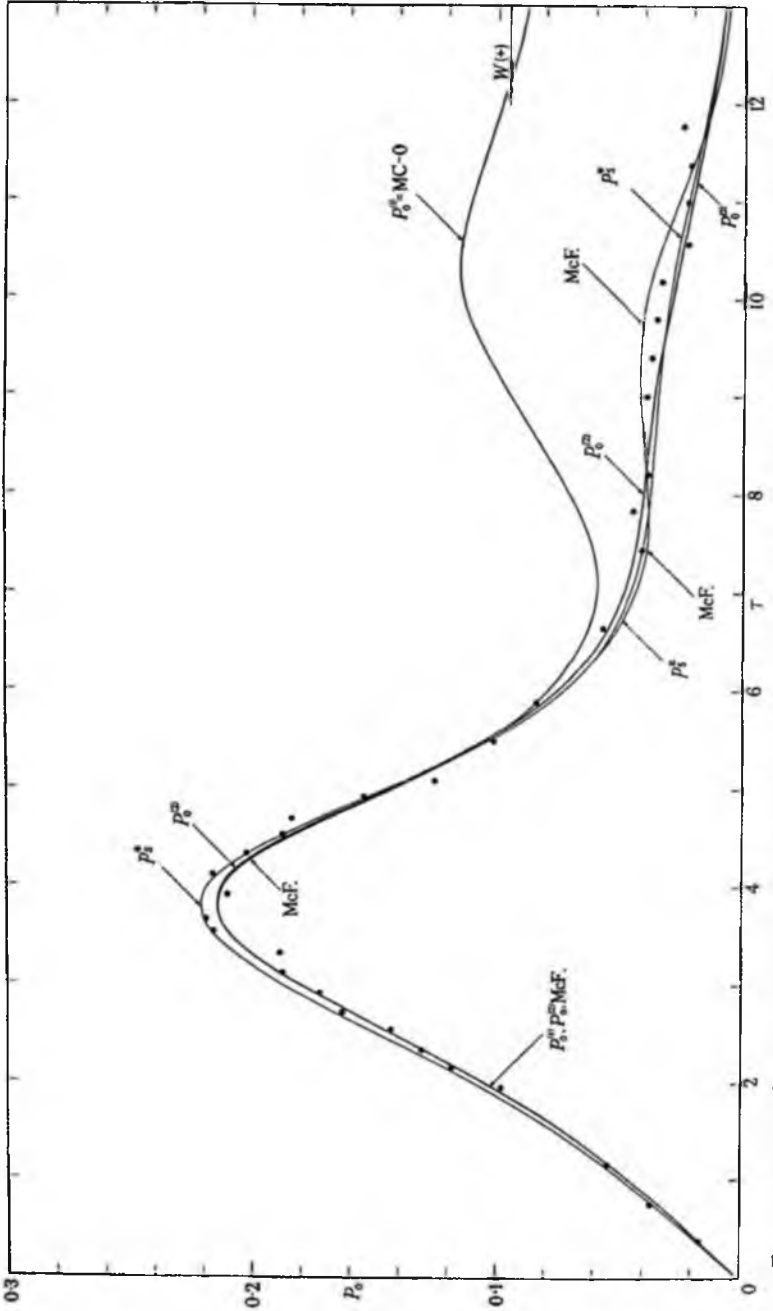


FIGURE 8. Approximations to $P_0(\tau)$ for the spectrum $E = (1 + \sigma^4)^{-1}$. The plotted points are the experimental results of Favreau, Low & Picferrer.

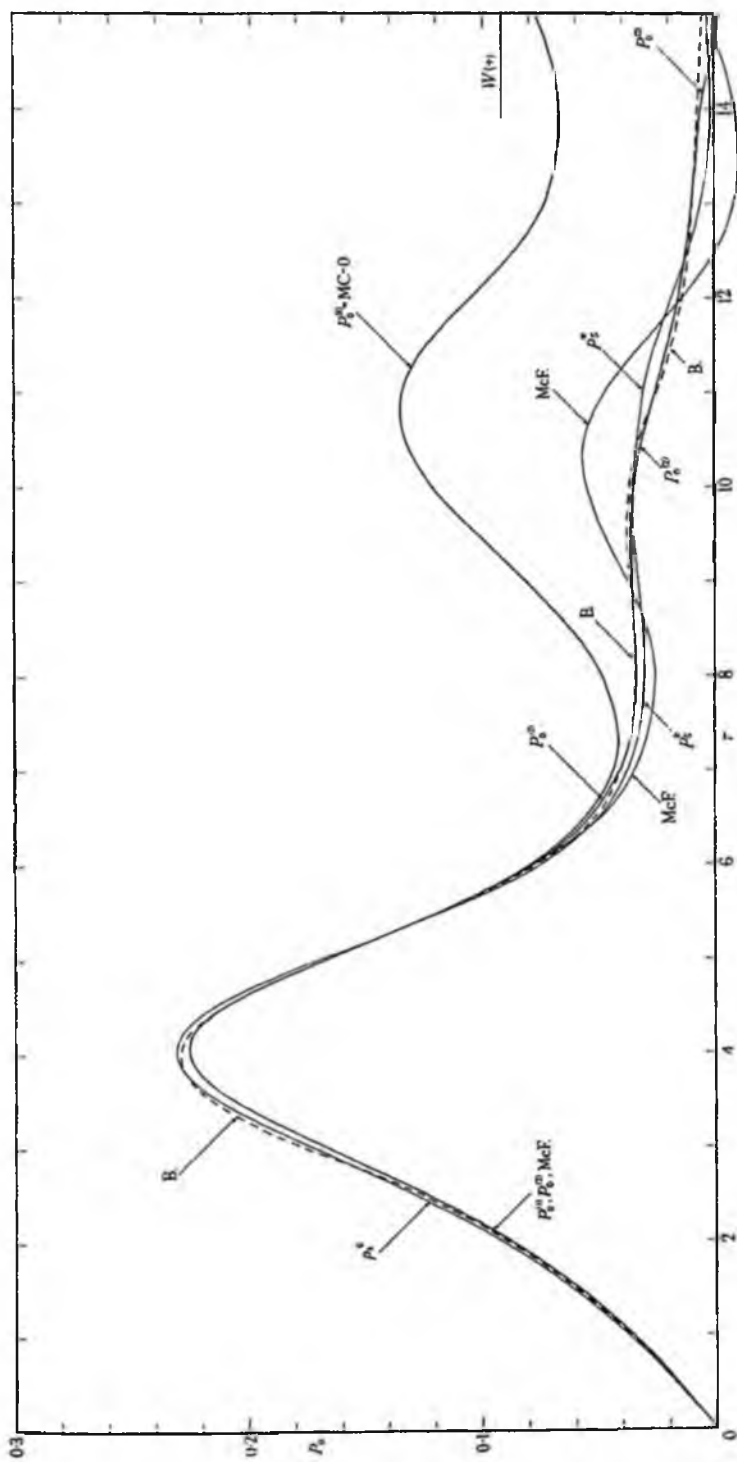


FIGURE 9. Approximations to $P_0(\tau)$ for a low-pass spectrum (cut-off at $\sigma = 1$).

$P_0^{(2)}$ can be expected to be an even closer approximation than that for the low-pass spectrum, since some of the low frequencies will have been eliminated. Accordingly $P_0^{(2)}$ has been plotted in figure 10 for $\sigma_1 = 0, \frac{1}{2}, \frac{2}{3}$ and $\frac{3}{4}$. It will be seen that as σ_1 approaches 1 and the spectrum becomes narrower so the distribution also becomes narrower and the height of

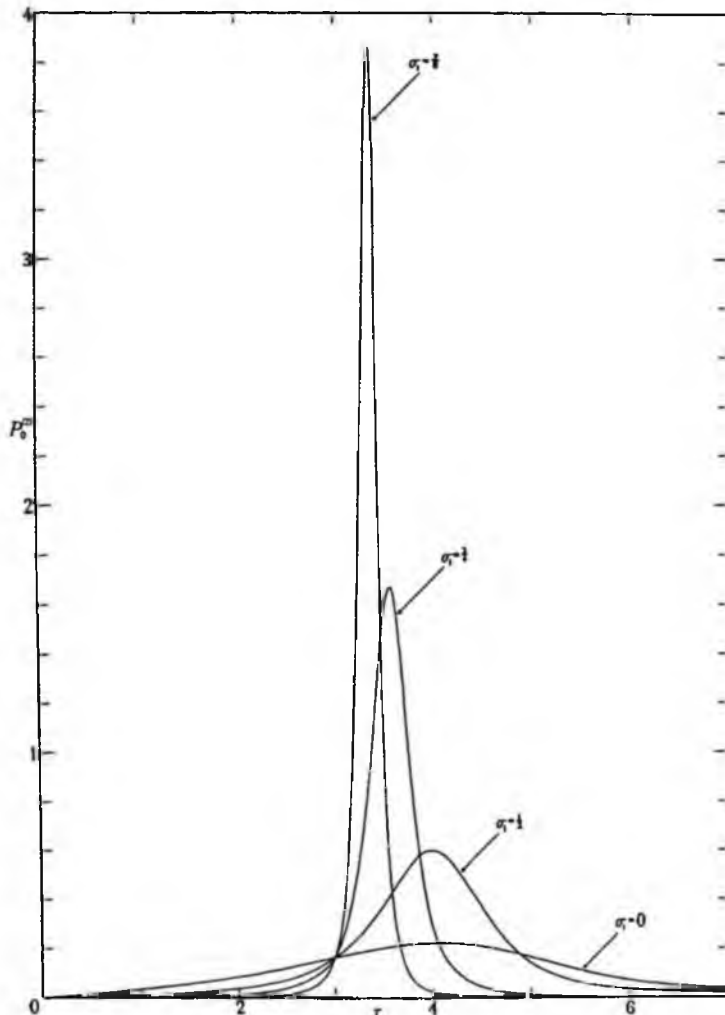


FIGURE 10. Computed values of $P_0(\tau)$ for a band-pass spectrum (low and high cut-offs at σ_1 and 1, respectively).

the maximum probability density is increased. The position and height of the maximum, and the width of the curve at half the maximum height are shown by the full curves (a), (b) and (c) in figure 11. (For plotting these curves the distributions $P_0^{(2)}$ for $\sigma_1 = 0.1, 0.2, 0.3, 0.4$ and 0.6 were also computed.)

A comparison may be made with the narrow-band approximation of § 5.7, which gives for the abscissa of the maximum

$$\tau_0 = 2\pi(1 + \sigma_1)^{-1}$$

and for the height and width of the distribution $(2\delta\tau_0)^{-1}$ and $1.533\delta\tau_0$ respectively, where

$$\delta\tau_0 = \frac{2\pi}{\sqrt{3}} \frac{1 - \sigma_1}{(1 + \sigma_1)^2}.$$

These values are represented by the broken curves in figure 11. It will be seen that for $\sigma_1 > \frac{1}{2}$ the narrow band approximation agrees well with $P_0^{(2)}$ but there are noticeable divergences when $\sigma_1 < \frac{1}{2}$.

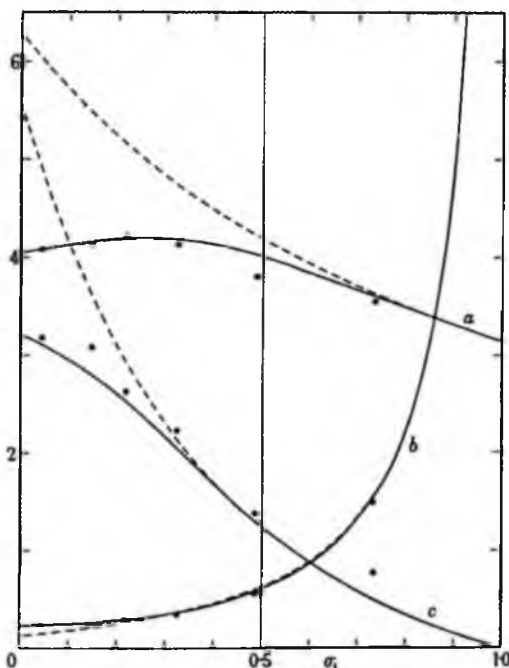


FIGURE 11. Characteristics of the distribution of intervals in a band-pass spectrum. (a) Abscissa of maximum; (b) ordinate of maximum; (c) width of distribution at half the maximum height. The full curves represent $P_0^{(2)}$; the broken curves the narrow-band approximation. Plotted points correspond to experimental curves of Blotekjaer (1958).

In the same figure some experimental results due to Blotekjaer (1958) have been inserted. As one would expect, they agree with $P_0^{(2)}$ rather than with NB. In particular one may note the slight negative trend in curve (a) as σ_1 approaches zero.

The author is indebted to S. O. Rice, D. S. Palmer and J. A. McFadden for stimulating correspondence, and to the latter especially for useful comments. A reference to the work of M. L. Mehta was provided by F. J. Dyson. The computations on ρ , and ρ^* were carried

out by Miss D. B. Catton on the DEUCE at the Royal Aircraft Establishment, Farnborough; the computations on $P_0^{(2)}$ were carried out at the Mathematical Laboratory, Cambridge, by Mrs M. O. Mutch and Mr P. F. Swinnerton-Dyer.

REFERENCES

- Bartlett, M. S. 1955 *Stochastic processes*. Cambridge University Press.
- Bløtekjaer, K. 1958 An experimental investigation of some properties of band-pass limited Gaussian noise. *Trans. Inst. Rad. Engrs*, IT-4, 100-102.
- Briggs, B. H. & Page, E. S. 1955 *Report of the 1954 Conference on the Physics of the Ionosphere*, p. 119. London: Physical Society.
- Ehrenfeld, S., Goodman, N. R., Kaplan, S., Mehr, E., Pierson, W. J., Stevens, R. & Tick, L. J. 1958 Theoretical and observed results for the zero and ordinate crossing problems of stationary Gaussian noise with application to pressure records of ocean waves. *N.Y. Univ., Coll. Eng., Tech. Rep.* no. 1, Dec. 1958.
- Favreau, R. R., Low, H. & Pfeffer, I. 1956 Evaluation of complex statistical functions by an analog computer. *Inst. Rad. Eng. Nat. Convention Record* 1956, pt. 4, pp. 31-37.
- Kac, M. 1943 On the distribution of values of trigonometric sums with linearly independent frequencies. *Amer. J. Math.* 65, 609-615.
- Kamat, A. R. 1953 Absolute moments of the multivariate normal distribution. *Biometrika*, 40, 20-34.
- Kohlenberg, A. 1953 Notes on the zero distribution of Gaussian noise. *Mass. Inst. Tech. Lincoln Lab., Tech. Mem.* no. 44.
- Longuet-Higgins, M. S. 1953 Contribution to Discussion, Symposium on Microseisms. *U.S. Nat. Acad. Sci. Publ.* 306, p. 124.
- Longuet-Higgins, M. S. 1957 A statistical distribution arising in the study of the ionosphere. *Proc. Phys. Soc. B*, 70, 559-565.
- Longuet-Higgins, M. S. 1958 On the intervals between successive zeros of a random function. *Proc. Roy. Soc. A*, 246, 99-118.
- McFadden, J. A. 1956 The axis-crossing intervals of random functions. *Trans. Inst. Rad. Engrs*, IT-2, 146-150.
- McFadden, J. A. 1958 The axis-crossing intervals of random functions. II. *Trans. Inst. Rad. Engrs*, IT-4, 14-24.
- Mehta, M. L. 1960 On the statistical properties of the level-spacings in nuclear spectra. *Nucl. Phys.* 18, 395-419.
- Nabeya, S. 1952 Absolute moments in 3-dimensional normal distribution. *Ann. Inst. Stat. Math.* 4, 15-29.
- Palmer, D. S. 1956 Properties of random functions. *Proc. Camb. Phil. Soc.* 52, 672-686.
- Rice, S. O. 1944 The mathematical analysis of random noise. *Bell Syst. Tech. J.* 23, 282-332.
- Rice, S. O. 1945 The mathematical analysis of random noise. *Bell Syst. Tech. J.* 24, 46-156.
- Rice, S. O. 1958 Distribution of the duration of fades in radio transmission: Gaussian noise model. *Bell Syst. Tech. J.* 37, 581-635.
- Siebert, A. J. F. 1951 On the first passage-time probability problems. *Phys. Rev.* 81, 617-623.

Reproduced by permission from *Time Series Analysis*
 edited by M. Rosenblatt & published by John Wiley & Sons Inc., 1963

CHAPTER 4

Bounding Approximations to the Distribution of Intervals between Zeros of a Stationary Gaussian Process

M. S. Longuet-Higgins, National Institute of
 Oceanography, Wormley, England
 Appendix, F. J. Dyson, Institute for Advanced Study, Princeton

ABSTRACT

Let $P(\tau)$ denote the probability density of zero-crossing intervals in a stationary gaussian process. This chapter discusses a rapidly convergent sequence of approximations which form successively upper and lower bounds to $P(\tau)$. Particular attention is paid to processes whose covariance $\psi(t)$ has the form $\psi(t) = a - bt^2 + c|t^3| + \dots$ for small t . Close bounds are obtained on the initial value $P(0)$. It is shown that

$$1.155,6\alpha < P(0) < 1.158,0\alpha$$

where $\alpha = c/2b$. Similar bounds are obtained for the related quantities $P_m(\tau)$ and $p(n, \tau)$. An alternative approach to the evaluation of $P_m(0)$ is described in Appendix 2 by F. J. Dyson.

1. INTRODUCTION

Let $f(t)$ denote a continuous, stationary, gaussian random function of a continuous parameter t . It is supposed that $f(t)$ is ergodic and has the mean value zero. The covariance function

$$\psi(t') = \overline{f(t)f(t+t')}$$

is known, or, equivalently, the spectral density

$$E(\sigma) = \frac{1}{2\pi} \int_{-\infty}^{\infty} \psi(t) \cos \sigma t dt.$$

A classical problem [1] is to find the probability density $P(\tau)$ of the intervals τ between successive zeros of $f(t)$. The solution is required both as a function of τ and as a functional of the covariance $\psi(t)$ *.

* $\psi(t)$ is also written as ψ_t . It is assumed that the probability density $P(t)$ exists, which implies the existence of ψ_0' .

A recent bibliography on this and related problems will be found in reference [2]. It appears that no exact solution to the general problem is known, though a number of approximations have been suggested. Rice [1] evaluated the probability density (p.d.) $W(+)$ of a single zero at t_1 :

$$W(+) = \frac{1}{2\pi} \left(\frac{-\psi_0'''}{\psi_0} \right)^{3/4}, \quad (1)$$

which gives the expected number of zeros per unit time:

$$N = 2W(+) = \frac{1}{\pi} \left(\frac{-\psi_0'''}{\psi_0} \right)^{3/4},$$

hence the mean value of the distribution of τ

$$\int_0^\infty \tau P(\tau) d\tau = \frac{1}{N} = \pi \left(\frac{\psi_0}{-\psi_0'''} \right)^{3/4}.$$

Rice also evaluated the joint p.d. $W(+, -)$ of an up-crossing at t_1 and a down-crossing at t_2 and suggested the approximation

$$\frac{W(+, -)}{W(+)} \doteq P(\tau), \quad \tau = t_2 - t_1. \quad (2)$$

The expression on the left represents the p.d. of a down-crossing at t_2 , given an up-crossing at t_1 , regardless of any zero-crossings between. It therefore includes the probability of $f(t)$ becoming negative at some intermediate points, so that strictly (2) represents an upper bound to $P(\tau)$.

As a closer approximation, Rice suggested including the condition that $f(t)$ be positive at some intermediate point, say $t = t_1 + \frac{1}{2}\tau$. The expressions involved are then threefold normal integrals which can be evaluated in finite terms. The conditions that $f(t)$ be positive at other points may be added, introducing integrals of higher order. Some computations have been carried out by Ehrenfeld et al. [3], who denote by $MC-n$ the probability density $W(+, -)/W(+)$ with n conditioned points added. Thus Rice's approximation is $MC-0$. Since there is the possibility of $f(t)$ becoming negative between the conditioned points, $MC-n$ is always an upper bound to $P(\tau)$.

Other approximations to $P(\tau)$ have been proposed in [3], [4] and [5], but none of these constitutes a strict upper or lower bound.

However, recently [6] a sequence of approximations was suggested, which form successive upper and lower bounds to $P(\tau)$; (2) is the first of this sequence. Moreover, the second approximation, which is a lower bound, may be computed without difficulty. It was shown that if $\psi(t)$ is a regular function at $t = 0$ then the second approximation is correct to a very high order in powers of τ . The second approximation also yields a positive lower bound to $P(0)$ in the singular case in which $\psi'''(t)$ has a finite discontinuity at $t = 0$.

The purpose of this chapter is to give a simplified account of the results in reference [6] (with detailed proofs omitted) and to obtain closer limits on the values of $P(0)$ in the singular case. An alternative and closely related approach to the same problem is discussed in Appendix 2 by F. J. Dyson.

2. THE SEQUENCE $P_0^{(N)}$

Imagine the zeros of a particular function $f(t)$, numbered in order of increasing t , and let

$P_m(\tau)$ = p.d. of the interval between the i th and $(i + m + 1)$ th zeros.

Thus $P_0(\tau)$ is the probability density of the interval between successive zeros of $f(t)$, that is, $P_0(\tau) = P(\tau)$. Further, if $t_1 < t_2 < \dots < t_n$ are any n points and S is any sequence of n signs, + or -, we denote by $W(S) dt_1 \dots dt_n$ the probability of zero-crossings in the intervals $(t_1, t_1 + dt_1), \dots, (t_n, t_n + dt_n)$ with gradients specified by S ; that is,

$W(S)$ = p.d. of zero-crossings at t_1, \dots, t_n , with signs S .

The following relations were stated by McFadden [4]: if $\tau = (t_2 - t_1)$,

$$\begin{aligned} \frac{W(+, -)}{W(+)} &= P_0 + P_2 + P_4 + \dots \\ \frac{W(+, +)}{W(+)} &= P_1 + P_3 + P_5 + \dots \end{aligned} \quad (3)$$

The interpretation of the first equation, for example, is simple: t_2 is either the first zero after t_1 or the third or the fifth, and so on. These mutually exclusive possibilities are represented by the individual terms in the series.

In [6] these relations were generalized as follows: let S denote any sequence of + or - signs and let

$$X(S) = \int_{t_1 < t_2 < \dots < t_n} \dots \int \frac{W(S)}{W(+)} dt_2 \dots dt_{n-1}, \quad (4)$$

so that, for example, $X(+, -) = W(+, -)/W(+)$. Then it may be shown that

$$X(S) = \sum_{r=0}^{\infty} \binom{n-2+r}{n-2} P_{2n-3-s+2r}, \quad \tau = t_n - t_1, \quad (5)$$

where s denotes the number of times that the sequence S changes sign. Equations (3) are the special cases $n = 2$ and $s = 1, 0$. Since $X(S)$ depends on the sequence S only through n and s , it may be written in a shorter form: $X(S) = X_{n,s}$.

Since $X_{n,s}$ can be evaluated, at least in principle, (5) may be regarded as a set of simultaneous equations for the P_m . These are not all independent, for by a property of the binomial coefficients there follows the identity

$$X_{n,s+2} - X_{n,s} = X_{n-1,s}. \quad (6)$$

Thus it will be seen that $X_{n,0}$ and $X_{n,1}$ ($n = 2, 3, \dots$) form a complete set on which all the other $X_{n,s}$ depend.

Equations (5) can now be solved for the P_m :

$$P_0 = X_{2,1} - X_{3,1} + X_{4,1} - \dots \quad (7)$$

$$P_1 = X_{2,0} - X_{3,0} + X_{4,0} - \dots \quad (8)$$

and, in general,

$$P_{2r} = \sum_{i=0}^{\infty} (-1)^i \binom{r+i}{i} X_{r+2+i,1} \quad (9)$$

$$P_{2r+1} = \sum_{i=0}^{\infty} (-1)^i \binom{r+i}{i} X_{r+2+i,0}.$$

These series have the convenient property that the remainder after n terms has the same sign as the first term neglected. For example,

$$P_0 = X_{2,1} - X_{3,1} + \dots + (-1)^{N+1} X_{N+1,1} + R^{(N)}, \quad (10)$$

where

$$R^{(N)} = (-1)^N \left[P_{2N} + \binom{N}{1} P_{2N+2} + \binom{N+1}{2} P_{2N+4} + \dots \right]. \quad (11)$$

Since the P_m are all nonnegative, $R^{(N)}$ has the same sign as $(-1)^N$. Hence the partial sum

$$P_0^{(N)} = X_{2,1} - X_{3,1} + X_{4,1} - \dots + (-1)^{N+1} X_{N+1,1} \quad (12)$$

is an upper or lower bound to P_0 according as N is odd or even.

It will be noted also that the first term in the remainder $R^{(N)}$ is $(-1)^N P_{2N}$. In a somewhat similar series stated by Rice [1], namely,

$$P_0 = Y_2 - Y_3 + Y_4 - \dots, \quad (13)$$

where

$$Y_n = \frac{1}{(n-2)!} \int_{t_1}^{t_n} \dots \int_{t_1}^{t_n} \frac{W(\pm, \dots, \pm)}{W(\pm)} dt_2 \dots dt_{n-1} \quad (14)$$

and $W(\pm, \dots, \pm)$ is the p.d. of zero-crossings at t_1, \dots, t_n regardless of sign, the remainder after N terms is of order P_N . Hence the series (7) converges more rapidly than the series (13).*

* Since the binomial coefficient $\binom{n-2+r}{n-2}$ is $O(r^n)$ as $r \rightarrow \infty$, keeping n fixed, the convergence of (5) implies that $m^n P_m \rightarrow 0$ as $m \rightarrow \infty$, for fixed n . Thus $P_m(r)$ decreases with m more rapidly than any negative power of m .

3. EXPLICIT FORMULAS FOR $P_0^{(1)}$ AND $P_0^{(2)}$

As is well known [1], $W(S)$ may be expressed in the form

$$W(S) = \int_0^{\pm\infty} \cdots \int_0^{\pm\infty} p(0, \dots; \eta_1, \dots, \eta_n) |\eta_1 \cdots \eta_n| d\eta_1 \cdots d\eta_n \quad (15)$$

where $\xi_i = f(t_i)$, $\eta_i = f'(t_i)$ and $p(\xi_1, \dots, \xi_n; \eta_1, \dots, \eta_n)$ is the joint p.d. of the ξ_i and η_i . Hence for Gaussian processes

$$W(S) = \int_0^{\pm\infty} \cdots \int_0^{\pm\infty} \frac{1}{(2\pi)^n \Delta^{1/2}} \exp \left[-\frac{1}{2} \sum_{i,j=1}^n L_{n+i,n+j} \eta_i \eta_j \right] |\eta_1 \cdots \eta_n| d\eta_1 \cdots d\eta_n, \quad (16)$$

where L_{ij} and Δ depend on the covariance function $\psi(t)$. Thus $W(S)$ is expressed as an n -fold normal integral, which can be evaluated explicitly in terms of known functions when $n \leq 3$. When $n > 3$, the integrals involve the functions of Schlaefli and Lobatchevsky, which are known only for certain values of the arguments.

When $n = 1, 2, 3$, the explicit expressions for $W(S)$ are as follows ([6], Section 2). Let ψ_{ij} denote $\psi(t_i - t_j)$ and let

$$D = \begin{vmatrix} \psi_{11} & \cdots & \psi_{1n} \\ \vdots & & \vdots \\ \psi_{n1} & \cdots & \psi_{nn} \end{vmatrix}$$

$$\mu_{rs} = \begin{vmatrix} \psi_{11} & \cdots & \psi_{1n} & \psi'_{1s} \\ \vdots & & \vdots & \vdots \\ \psi_{n1} & \cdots & \psi_{nn} & \psi'_{ns} \\ -\psi'_{r1} & \cdots & -\psi'_{rn} & -\psi''_{rs} \end{vmatrix} \div D.$$

Also let

$$\nu_{rs} = \frac{\mu_{rs}}{(\mu_{rr}\mu_{ss})^{1/2}}.$$

Then, when $n = 1$, we have

$$W(+, +) = \frac{\mu_{11}^{1/2}}{2\pi D^{1/2}} = \frac{1}{2\pi} \left(\frac{-\psi''_0}{\psi_0} \right)^{1/2}. \quad (17)$$

When $n = 2$,

$$W(+, +) = \frac{(\mu_{11}\mu_{22})^{1/2}}{4\pi^2 D^{1/2}} [(1 - \nu_{12}^2)^{1/2} + \nu_{12} \cos^{-1}(-\nu_{12})],$$

$$W(+, -) = \frac{(\mu_{11}\mu_{22})^{1/2}}{4\pi^2 D^{1/2}} [(1 - \nu_{12}^2)^{1/2} - \nu_{12} \cos^{-1}(\nu_{12})], \quad (18)$$

68 ZEROS OF PROCESSES AND RELATED QUESTIONS

the angles being chosen to be between 0 and π . When $n = 3$, we find

$$W(+, +, +) = \frac{(\mu_{11}\mu_{22}\mu_{33})^{3/4}}{8\pi^3 D^{3/4}} [|(\nu_{ij})|^{3/4} + (\alpha_1 s_1 + \alpha_2 s_2 + \alpha_3 s_3)]$$

$$W(+, -, +) = \frac{(\mu_{11}\mu_{22}\mu_{33})^{3/4}}{8\pi^3 D^{3/4}} [|(\nu_{ij})|^{3/4} + \alpha_1(s_1 - \pi) + \alpha_2 s_2 + \alpha_3(s_3 - \pi)] \quad (19)$$

$$W(+, -, -) = \frac{(\mu_{11}\mu_{22}\mu_{33})^{3/4}}{8\pi^3 D^{3/4}} [|(\nu_{ij})|^{3/4} + \alpha_1 s_1 + \alpha_2(s_2 - \pi) + \alpha_3(s_3 - \pi)],$$

where

$$\begin{aligned} \alpha_1 &= \nu_{31}\nu_{12} + \nu_{23} \\ s_1 &= \cos^{-1} \frac{\nu_{31}\nu_{12} - \nu_{23}}{(1 - \nu_{31}^2)^{1/2}(1 - \nu_{23}^2)^{1/2}} \end{aligned} \quad (20)$$

α_2, α_3 , etc., being obtained by cyclic permutation of the indices.

Hence the approximations

$$\begin{aligned} P_0^{(1)} &= X_{2,1} = \frac{W(+, -)}{W(+)} \\ P_0^{(2)} &= X_{2,1} - X_{3,1} = \frac{W(+, -)}{W(+)} - \int_{t_1}^{t_2} \frac{W(+, -, -)}{W(+)} dt_2 \end{aligned} \quad (21)$$

may be computed without difficulty. Figure 1 shows the results for the low-pass spectrum

$$E(\sigma) = \begin{pmatrix} 1, & \sigma < 1 \\ 0, & \sigma > 1 \end{pmatrix} \quad (22)$$

when

$$\psi(t) = \frac{\sin t}{t}$$

It will be seen that $P_0^{(2)}$ lies quite close to the experimental curve of Blötekjaer [7], as far as $\tau = 14$, when it leaves the curve and goes negative. In Figure 2 are shown some computations of $P_0^{(2)}$ for the bandpass spectrum

$$E(\sigma) = \begin{pmatrix} 1, & \sigma_1 < \sigma < 1 \\ 0, & \text{otherwise} \end{pmatrix}. \quad (23)$$

The abscissa and ordinate of the peak, as well as the width of the distribution at half the peak height, are shown in Figure 3 (solid curves) compared with experimental data of Blötekjaer [7]. The broken curves represent characteristics of a narrow-band approximation due to Rice [1]. It appears that this approximation is very good for $\sigma_1 > \frac{1}{2}$ (less than one octave bandwidth), tolerable for $\frac{1}{4} < \sigma_1 < \frac{1}{2}$ (one to two octaves), and poor at bandwidths greater

ZEROS OF PROCESSES AND RELATED QUESTIONS

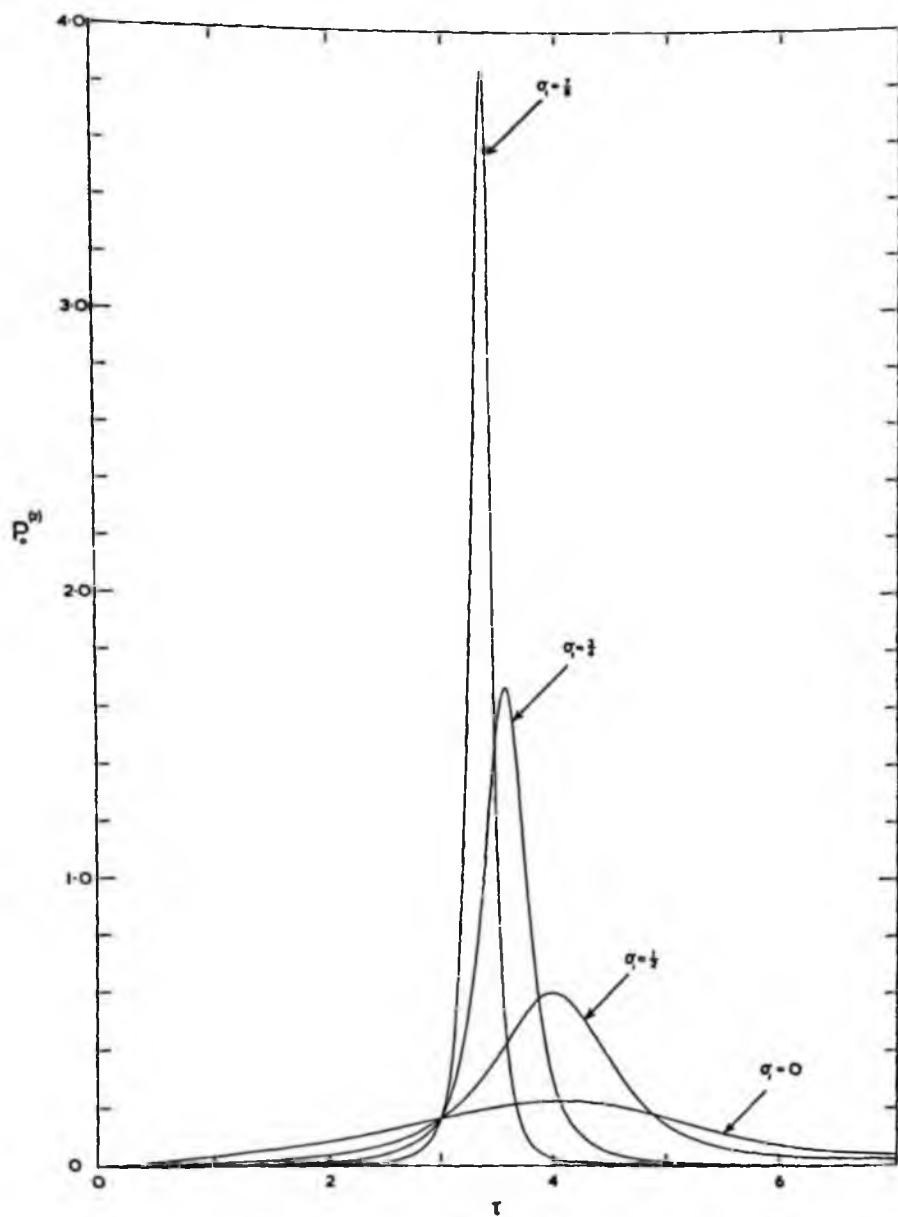


Figure 2. Computed curves of $P_0^{(2)}(\tau)$ for bandpass spectra (23).

INTERVALS BETWEEN ZEROS OF A STATIONARY GAUSSIAN PROCESS 71

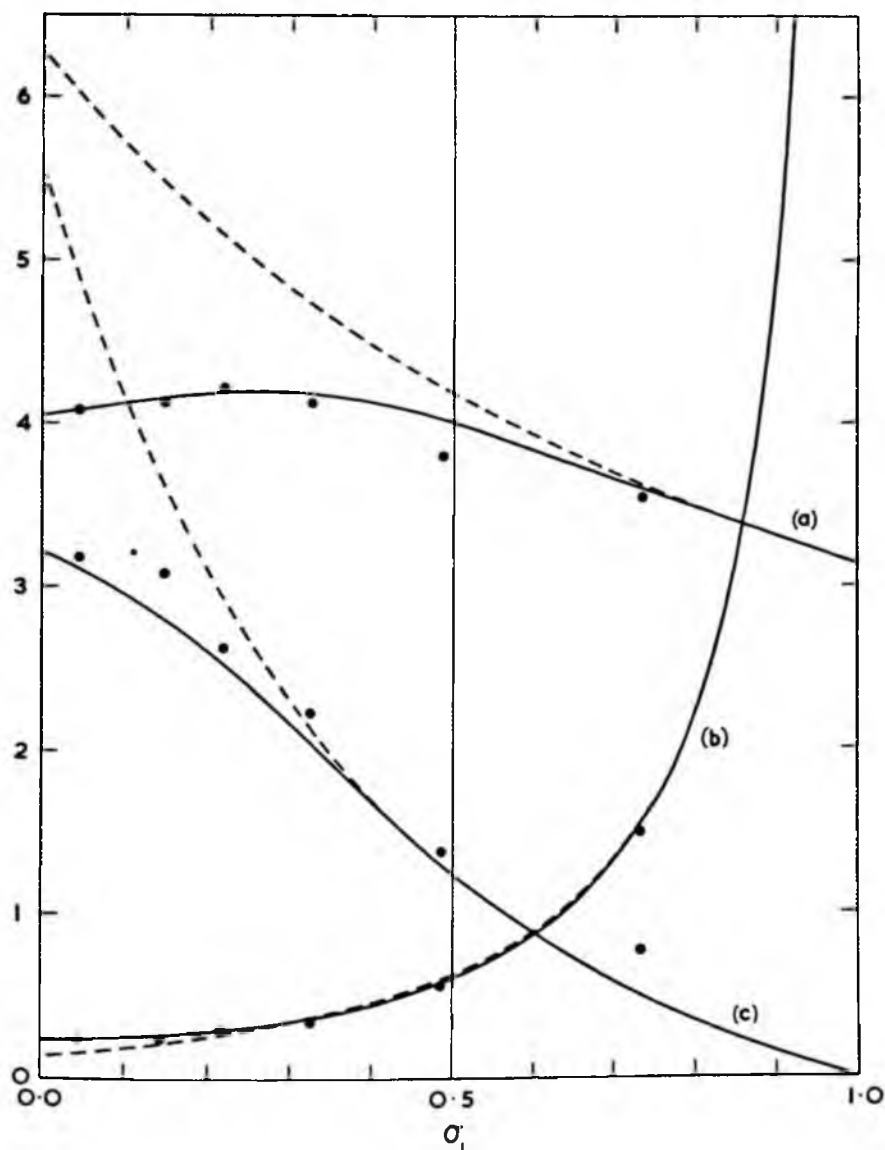


Figure 3. Characteristics of the curves of Figure 2, compared with observation: (a) abscissa of peak, (b) ordinate of peak, (c) width of distribution at half the peak height. Plotted points correspond to the observations of Blötekjaer [7]. Broken curves correspond to the narrow-band approximation of Rice [1].

than two octaves. Computation of $P_0^{(2)}$ for several other spectra are shown in [6].

4. BEHAVIOR NEAR THE ORIGIN

It is interesting to examine the behavior of $P_0(\tau)$ and $P_0^{(N)}(\tau)$ for small values of the interval τ . Here the behavior depends on the character of the covariance function $\psi(t)$ at the origin. Suppose first that $\psi(t)$ is a regular function at $t = 0$:

$$\psi(t) = \psi_0 + \frac{1}{2!} \psi_0'' t^2 + \frac{1}{4!} \psi_0^{(4)} t^4 + \dots ; \tag{24}$$

it can be shown [6] that as $(t_n - t_1) \rightarrow 0$

$$W(+, -, \dots (-)^{n-1}) \sim C_n \prod_{i < j} (t_j - t_i), \tag{25}$$

where C_n is a constant (independent of the t_i):

$$C_n = \frac{1!2! \dots (n-1)!}{2\pi^{(n+1)/2} (n!)^n} \left(\frac{n-1}{2}\right)! \left(\frac{D_{n+1}^n}{D_n^{n+1}}\right)^{1/2}$$

with

$$D_m = (-1)^{(1/2)m(m-1)} \begin{vmatrix} \psi_0 & \psi_0' & \dots & \psi_0^{(m-1)} \\ \psi_0' & \psi_0'' & \dots & \psi_0^{(m)} \\ \vdots & \vdots & \ddots & \vdots \\ \psi_0^{(m-1)} & \psi_0^{(m)} & \dots & \psi_0^{(2m-2)} \end{vmatrix}$$

By substituting in (4) and performing the integration, we find

$$X_{n,n-1} = \frac{[1!2!3! \dots (n-1)!]^2 C_n d^2}{1!3!5! \dots (2n-1)! C_1 d\tau^2} \tau^{n(n+1)/2}$$

which is of order $\tau^{(1/2)n(n+1)-2}$. Now by setting $s = n - 1$ in (5) we have

$$X_{n,n-1} = \sum_{r=0}^{\infty} \binom{n-2+r}{r} P_{n-2+2r}, \tag{26}$$

of which the solution is

$$P_m = \sum_{i=0}^{\infty} (-1)^i \frac{(m+1)(m+2i)!}{i!(m+i+1)!} X_{m+2+2i, m+1+2i}. \tag{27}$$

The first term in this series is $X_{m+2, m+1}$. Hence

$$P_m \sim X_{m+2, m+1} = O(\tau^{(1/2)(m+2)(m+3)-2}), \tag{28}$$

INTERVALS BETWEEN ZEROS OF A STATIONARY GAUSSIAN PROCESS 73

a power that increases rapidly with m . So, for example,

$$\begin{aligned} P_0 &= 0(\tau) \\ P_2 &= 0(\tau^8) \\ P_4 &= 0(\tau^{18}). \end{aligned} \quad (29)$$

Since $P_0(\tau) \rightarrow 0$ as $\tau \rightarrow 0$, neighboring zeros of $f(t)$ are strongly repelled. Further, the error in the approximation $P_0^{(1)}$, which is of order $-P_2(\tau)$, is $0(\tau^8)$. Thus $P_0^{(1)}$ is correct to order τ^7 at the origin. Similarly $P_0^{(2)}$ is correct to order τ^{18} .

A quite different behavior is seen in the case in which $\psi(t)$, instead of being regular at $t = 0$, has the expansion

$$\psi(t) = \psi_0 + \frac{1}{2}\psi_0''t^2 + \frac{1}{6}\psi_0'''|t|^3 + \dots \quad (30)$$

In other words $\psi'''(t)$ has a finite discontinuity at the origin. Such a singularity arises wherever the spectral density $E(\sigma)$ is of order σ^{-4} at high frequencies, for example, in the case

$$\begin{aligned} E(\sigma) &= \frac{1}{(1 + \sigma^2)^2} \\ \psi(t) &\propto (1 - |t|)e^{-|t|}. \end{aligned} \quad (31)$$

It is shown then in [6] that for all $n \geq 2$ as $\tau \rightarrow 0$

$$W(S) \sim \frac{F_n}{(t_3 - t_1)(t_4 - t_2) \cdots (t_n - t_{n-2})} \cdot \frac{\psi_0'''}{(-\psi_0''')^n} \quad (32)$$

where F_n is a function only of the ratios $(t_2 - t_1):(t_3 - t_2): \cdots : (t_n - t_{n-1})$ and of n and lies moreover between two positive bounds that depend *only* on n . When $n = 1$, $W(+)$ is given by (19) as before. By substitution in (4) it follows that

$$X_{n,s} = X(S) \sim K_{n,s}\alpha, \quad (33)$$

where $K_{n,s}$ is a constant depending only on n, s , and where we write for convenience

$$\alpha = \frac{\psi_0'''}{-6\psi_0''} \quad (34)$$

So from the series (8)

$$P_m(\tau) \sim K_m\alpha,$$

where K_m is a pure constant depending only on m . Since K_m is positive in general, $P_m(\tau)$ tends to a positive value $P_m(0)$. Thus, in contrast to the preceding case, the zeros of $f(t)$ are no longer so strongly repelled.

A heuristic explanation of the behavior of $P(\tau)$ in the two cases may be given as follows:

Let $p(n, \tau)$ denote the probability of exactly n zeros occurring in an arbitrary interval $(t_0, t_0 + \tau)$ of fixed length τ . The following general relations between

ZEROS OF PROCESSES AND RELATED QUESTIONS

74

$p(n, \tau)$ and $P_m(\tau)$ have been proved by McFadden [4]:

$$\begin{aligned} p''(0, \tau) &= 2W(+)P_0 \\ p''(1, \tau) &= 2W(+)(P_1 - 2P_0) \\ p''(n, \tau) &= 2W(+)(P_n - 2P_{n-1} + P_{n-2}), \quad (n \geq 2), \end{aligned} \quad (35)$$

where primes denote differentiation with respect to τ . In the first case, in which (24) is valid, $f(t)$ is a regular function; that is, it has derivatives of all orders, except in a set of measure zero. So, if $f(t)$ is to vanish n times in $(t_0, t_0 + \tau)$, $f'(t)$ must vanish at least $(n - 1)$ times in the same interval, $f''(t)$ must vanish at least $(n - 2)$ times, and so on; finally $f^{(n-1)}$ must vanish at least once in the interval. Now $f^{(n)}$ exists, and so $f^{(n-1)}(t_0)$ must be of order τ , $f^{(n-2)}$ must be of order τ^2 , etc., until finally $f(t_0)$ must be of order τ^n , that is, $f(t_0), f'(t_0), \dots, f^{(n-1)}(t_0)$ must lie in ranges $\delta f, \delta f', \dots, \delta f^{(n-1)}$ of order $\tau^n, \tau^{n-1}, \dots, \tau$, respectively. But the joint p.d. of $f(t_0), \dots, f^{(n-1)}(t_0)$ exists, so that the probability of such an event is

$$p(n, \tau) = 0(\delta f \cdot \delta f' \cdot \dots \cdot \delta f^{(n-1)}) = 0(\tau^{(3/2)n(n+1)}).$$

Differentiating twice and using (35), we see that

$$P_n - 2P_{n-1} + P_{n-2} = 0(\tau^{(3/2)n(n+1)-2}), \quad (n \geq 2).$$

Since the term of lowest order is P_{n-2} , we have, writing $n - 2 = m$,

$$P_m = 0(\tau^{(3/2)(m+2)(m+3)-2}) \quad (36)$$

in agreement with (29).

On the other hand, when the expansion (30) applies, the second derivative of f is, in this case, nonexistent almost everywhere, and the first derivative can be expected to behave like the Gaussian Markov process [8] in which $|f'(t_1) - f'(t_2)|$ increases like $|t_1 - t_2|^{1/2}$ for small time differences. Now if $f(t)$ has two or more zeros in $(t_0, t_0 + \tau)$, $f'(t)$ has at least one, and so $f'(t_0)$ is of order $\tau^{3/2}$. Hence $f(t_0)$ is of order $\tau^{3/2}$. So

$$p(n, \tau) = 0(\delta f \cdot \delta f') = 0(\tau^{3/2+1/2}) = 0(\tau^2)$$

for all $n \geq 2$. Substitution in (35) now gives

$$P_n - 2P_{n-1} + P_{n-2} = 0(1).$$

Therefore, assuming P_n, P_{n-1} to be of no lower order than P_{n-2} , we have

$$P_m = 0(1), \quad m = 0, 1, 2, \dots \quad (37)$$

in contrast to (36).

The argument can be extended to other types of spectrum. For example, when $E(\sigma)$ is $0(\sigma^{-6})$ as $\sigma \rightarrow \infty$, then $\psi(t)$ has no term in $|t|^3$ but a term in $|t|^6$, and $f''(t)$ behaves like a Gaussian Markov process. Thus, when $n \geq 3$, $\delta f'' = 0(\tau^{3/2})$, $\delta f' = 0(\tau^{3/2})$, and $\delta f = 0(\tau^{3/2})$. Hence

$$p(n, \tau) = 0(\tau^{3/2}), \quad n \geq 3$$

INTERVALS BETWEEN ZEROS OF A STATIONARY GAUSSIAN PROCESS 75

but $p(2, \tau) = 0(\tau^3)$, as it does when ψ is regular. Therefore, from (35),

$$\begin{aligned}
P_m(\tau) &= 0(\tau^{5/2}), \quad m \geq 1 \\
P_0(\tau) &= 0(\tau).
\end{aligned}
\tag{38}$$

Similar results can be deduced when $E(\sigma)$ is $0(\sigma^{-2r})$ at infinity and $r = 4, 5$, etc.

5. BOUNDS FOR $P_m(0)$ IN THE SINGULAR CASE

It is interesting to obtain bounds for the value of $P_0(0)$ in the singular case (30) since this enables us to test the validity of conjectures on the form of $P(\tau)$.

On returning to (16) and making expansions in powers of $(t_i - t_j)$, we find that for $n \geq 2$

$$\Delta \sim \frac{1}{3^{n-1}} (-\psi_0 \psi_0''') (\psi_0''')^{2(n-1)} (u_1 u_2 \dots u_{n-1})^{-4}
\tag{39}$$

and

$$(L_{n+i, n+j}) = \frac{1}{\psi_0'''} \begin{pmatrix} 2u_1 & u_1 & 0 & \dots & 0 \\ u_1 & 2(u_1 + u_2) & u_2 & \dots & 0 \\ 0 & u_2 & 2(u_2 + u_3) & \dots & 0 \\ \vdots & \vdots & \vdots & \ddots & \vdots \\ \vdots & \vdots & \vdots & \dots & \vdots \\ 0 & 0 & 0 & \dots & 2(u_{n-2} + u_{n-1}) \end{pmatrix}
\tag{40}$$

respectively, where

$$u_i = (t_{i+1} - t_i)^{-1}, \quad i = 1, 2, \dots, n - 1$$

[see [6], equations (4.1.5) and (4.1.6)]. By substituting in (16) and writing $\eta_i = (\psi_0'''/2)y_i$ and $\alpha = (-\psi_0'''/6\psi_0''')$, we find

$$\begin{aligned}
\frac{W(+, +, \dots +)}{W(+)} &= (3\alpha) \left(\frac{\sqrt{3}}{4\pi}\right)^{n-1} (u_1 u_2 \dots u_{n-1})^2 \\
&\int_0^\infty \dots \int_0^\infty \exp \left[-\frac{1}{2} \sum_{i=1}^n u_i (y_i^2 + y_i y_{i+1} + y_{i+1}^2) \right] y_1 \dots y_n dy_1 \dots dy_n.
\end{aligned}$$

Thus from (4)

$$\begin{aligned}
X_{n,0} &= (3\alpha) \left(\frac{\sqrt{3}}{4\pi}\right)^{n-1} \int_{t_1 < t_2 < \dots < t_n} dt_2 \dots dt_{n-1} \int_0^\infty \dots \int_0^\infty dy_1 \dots dy_n \\
&(u_1 \dots u_{n-1})^2 y_1 \dots y_n \exp \left[-\frac{1}{2} \sum_{i=1}^{n-1} u_i (y_i^2 + y_i y_{i+1} + y_{i+1}^2) \right].
\end{aligned}
\tag{41}$$

$X_{n,1}$ is given by an exactly similar expression, except that in the summation the first term is $u_1(y_1^2 - y_1y_2 + y_2^2)$ instead of $u_1(y_1^2 + y_1y_2 + y_2^2)$.

When $n = 2$ or 3 , the integration may be performed first with respect to the y_i and then with respect to the t_i , giving [6]

$$X_{2,1} = \left(\frac{\sqrt{3}}{\pi} + \frac{2}{3} \right) \alpha = 1.217,996\alpha \quad (42)$$

$$X_{2,0} = \left(\frac{\sqrt{3}}{\pi} - \frac{1}{3} \right) \alpha = 0.217,996\alpha$$

and

$$X_{3,1} = \left(\frac{\sqrt{3}}{8\pi^2} + \frac{1}{2\sqrt{3}\pi} - \frac{17}{288} \right) \alpha = 0.070,856\alpha \quad (43)$$

$$X_{3,0} = \left(\frac{\sqrt{3}}{8\pi^2} - \frac{1}{\sqrt{3}\pi} + \frac{49}{288} \right) \alpha = 0.024,358\alpha.$$

Using $X_{2,1}$ and $(X_{2,1} - X_{3,1})$ as upper and lower bounds for P_0 , we have immediately

$$1.147\alpha < P_0(0) < 1.218\alpha, \quad (44)$$

which is sufficient to disprove the conjecture of Favreau, Low, and Pfeffer [9] that for the process (31) $P(\tau)$ has the exponential form

$$P_0(\tau) = \frac{1}{\pi} e^{-\tau/\pi},$$

since for that special case $\alpha = \frac{1}{3}$ the conjecture would imply

$$P_0(0) = \frac{3}{\pi} \alpha = 0.955\alpha,$$

which is outside the bounds (44).

In order to examine the behavior of $P_m(0)$ as m increases, closer bounds are desirable. These bounds can be obtained by calculating two further terms in each of the series (7) and (8). When $n \geq 4$, exact integration of (41) does not appear possible. However (41) may be transformed to a form more amenable to numerical evaluation:

Since the integrand involves the t_i only through the differences $(t_{i+1} - t_i)$, we may set $t_1 = 0$ and so $t_n = \tau$. Now let us make the substitution

$$t_1 = \tau - \lambda_1$$

$$t_2 = \tau - \lambda_1\lambda_2$$

...

$$t_n = \tau - \lambda_1\lambda_2 \cdots \lambda_n,$$

where

$$\lambda_1 = \tau; \quad 0 < \lambda_i < 1, \quad (i = 2, 3, \dots, n-1); \quad \lambda_n = 0.$$

INTERVALS BETWEEN ZEROS OF A STATIONARY GAUSSIAN PROCESS 77

Thus

$$u_i = \frac{1}{t_{i+1} - t_i} = \frac{1}{\lambda_1 \cdots \lambda_i (1 - \lambda_{i+1})}$$

and

$$\frac{\partial(t_2, \dots, t_{n-1})}{\partial(\lambda_2, \dots, \lambda_{n-1})} = \lambda_1^{n-2} \lambda_2^{n-3} \cdots \lambda_{n-2}.$$

Also substitute

$$\frac{1}{2} y_1^2 = \mu_1 (1 - \mu_2)$$

$$\frac{1}{2} y_2^2 = \mu_1 \mu_2 (1 - \mu_3)$$

...

$$\frac{1}{2} y_n^2 = \mu_1 \cdots \mu_n (1 - \mu_{n+1}),$$

where

$$0 < \mu_1 < \infty; \quad 0 < \mu_i < 1 \quad (i = 2, \dots, n); \quad \mu_{n+1} = 0,$$

so that

$$y_1 \cdots y_n \frac{\partial(y_1 \cdots y_n)}{\partial(\mu_1 \cdots \mu_n)} = \mu_1^{n-1} \mu_2^{n-2} \cdots \mu_{n-1};$$

(41) then becomes

$$X_{n,0} = (3\alpha) \left(\frac{\sqrt{3}}{4\pi}\right)^{n-1} \int_0^1 d\lambda_2 \cdots \int_0^1 d\lambda_{n-1} \int_0^\infty d\mu_1 \int_0^1 d\mu_2 \cdots \int_0^1 d\mu_n \frac{\mu_1^{n-1} \mu_2^{n-2} \cdots \mu_{n-1}}{\lambda_1^n \lambda_2^{n-1} \cdots \lambda_{n-1}^2 (1 - \lambda_2)^2 \cdots (1 - \lambda_n)^2} \exp\left(-\frac{\mu_1}{\lambda_1} F_n\right),$$

where

$$F_n = \frac{(1 - \mu_2 \mu_3) + [\mu_2(1 - \mu_2)(1 - \mu_3)]^{1/2}}{(1 - \lambda_2)} + \frac{\mu_2(1 - \mu_3 \mu_4) + [\mu_3(1 - \mu_3)(1 - \mu_4)]^{1/2}}{\lambda_2(1 - \lambda_3)} + \cdots + \frac{\mu_2 \cdots \mu_{n-1} (1 - \mu_n \mu_{n+1}) + [\mu_n(1 - \mu_n)(1 - \mu_{n+1})]^{1/2}}{\lambda_2 \cdots \lambda_{n-1} (1 - \lambda_n)}.$$

Since

$$\int_0^\infty \mu_1^{n-1} \exp\left(-\frac{\mu_1}{\lambda_1} F_n\right) d\mu_1 = (n-1)! \left(\frac{\lambda_1}{F_n}\right)^n,$$

the integration with respect to μ_1 may be carried out immediately, giving

$$X_{n,0} = (3\alpha) \left(\frac{\sqrt{3}}{4\pi}\right)^{n-1} (n-1)! \int_0^1 \cdots \int_0^1 d\lambda_2 \cdots d\lambda_{n-1} d\mu_2 \cdots d\mu_n \frac{\mu_2^{n-2} \mu_3^{n-3} \cdots \mu_{n-1}}{\lambda_2^{n-1} \lambda_3^{n-2} \cdots \lambda_{n-1}^2 (1 - \lambda_2)^2 \cdots (1 - \lambda_{n-1})^2 F_n^n} \quad (45)$$

The expression for $X_{n,1}$ is identical with that for $X_{n,0}$ except that in F_n the sign of the first square root is reversed.

The foregoing expressions were evaluated for $n = 4, 5$ by quadratures, as described in Appendix I. The results are

$$X_{4,1} = 0.010,90\alpha$$

$$X_{4,0} = 0.004,34\alpha$$

with a possible error of one unit in the fifth decimal place; and

$$X_{5,1} = 0.002,18\alpha$$

$$X_{5,0} = 0.000,91\alpha$$

with a possible error of one unit in the fourth decimal place. Together with (42) and (43), these lead to the following inequalities on the P_m :

$$1.155,6\alpha < P_0(0) < 1.158,0\alpha$$

$$0.197,1\alpha < P_1(0) < 0.198,0\alpha$$

$$0.049,1\alpha < P_2(0) < 0.055,6\alpha$$

$$0.015,7\alpha < P_3(0) < 0.018,4\alpha$$

$$0.004,4\alpha < P_4(0) < 0.010,9\alpha$$

$$0.001,6\alpha < P_5(0) < 0.004,3\alpha$$

$$0 < P_6(0) < 0.002,2\alpha$$

$$0 < P_7(0) < 0.000,9\alpha,$$

with a maximum error of 0.000,2.

By inserting these inequalities in the relations (35), we deduce the following bounds for $p(n, \tau)$:

$$0.808,7\beta\tau^2 < p(2, \tau) < 0.819,5\beta\tau^2$$

$$0.101,5\beta\tau^2 < p(3, \tau) < 0.118,3\beta\tau^2$$

$$0.016,6\beta\tau^2 < p(4, \tau) < 0.035,1\beta\tau^2$$

$$0 < p(5, \tau) < 0.014,0\beta\tau^2$$

$$0 < p(6, \tau) < 0.009,7\beta\tau^2$$

$$0 < p(7, \tau) < 0.005,2\beta\tau^2$$

where

$$\beta = W(+)\alpha = \frac{1}{12\pi} \frac{\psi_0'''}{(-\psi_0\psi_0'')^{3/2}}$$

6. FURTHER ESTIMATES OF $P_m(0)$

The computed values of $X_{n,s}$ for $n = 2, 3, 4, 5$ are shown graphically in Figure 4, plotted on a logarithmic scale. It will be seen that the $X_{n,s}$ tend to lie on two parallel but not quite coincident curves. For higher values of n

INTERVALS BETWEEN ZEROS OF A STATIONARY GAUSSIAN PROCESS 79

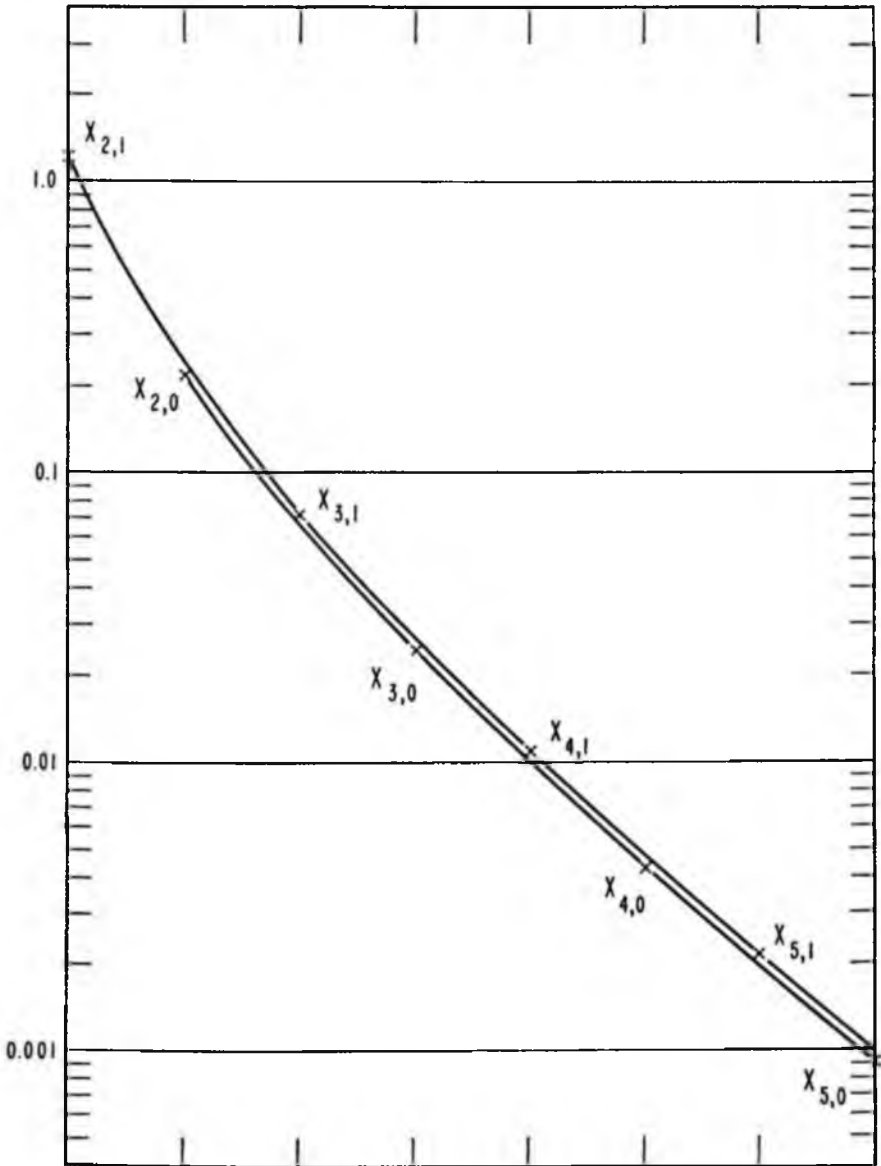


Figure 4. Numerical values of $X_{n,1}$ and $X_{n,0}$.

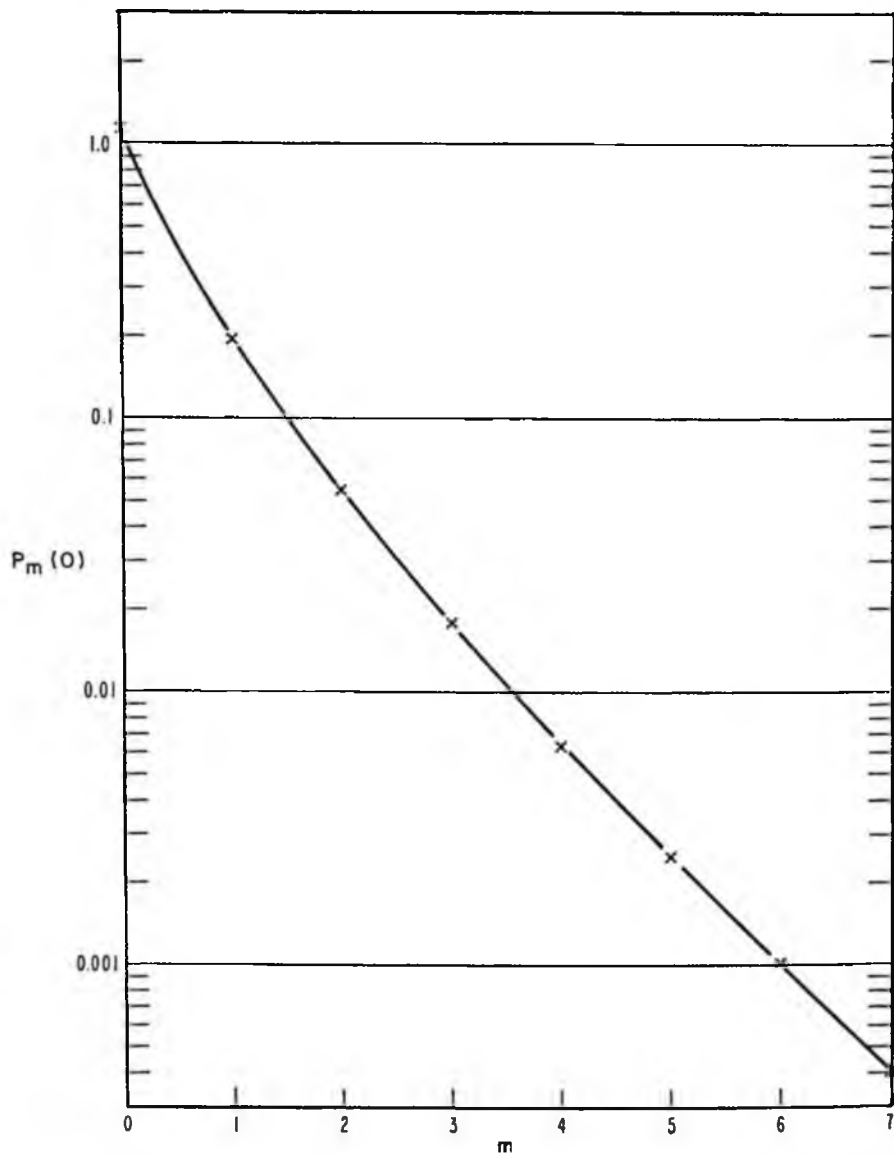


Figure 5. Estimated numerical values of $P_m(0)$.

INTERVALS BETWEEN ZEROS OF A STATIONARY GAUSSIAN PROCESS 81

the calculated values are quite closely fitted by

$$\begin{aligned} X_{n,1} &= \frac{Ax^{2n-3}}{2n-3} \alpha \\ Y_{n,0} &= \frac{Bx^{2n-2}}{2n-2} \alpha \end{aligned} \quad (46)$$

where $A = 13.2$, $B = 11.8$, and $x^2 = 0.28$. Using these formulas to estimate higher terms in the series (9), we find

$$\begin{aligned} P_0 &\doteq 1.155,97\alpha & P_1 &\doteq 0.197,23\alpha \\ P_2 &\doteq 0.054,12\alpha & P_3 &\doteq 0.017,77\alpha \\ P_4 &\doteq 0.006,40\alpha & P_5 &\doteq 0.002,49\alpha \\ P_6 &\doteq 0.001,01\alpha & P_7 &\doteq 0.000,41\alpha \end{aligned} \quad (47)$$

These are plotted in Figure 5, and it will be seen that they lie all on the same smooth curve.

From (47) and (35) we find

$$\begin{aligned} p(2, \tau) &\doteq 0.815,63\beta\tau^2 & p(3, \tau) &\doteq 0.106,76\beta\tau^2 \\ p(4, \tau) &\doteq 0.024,98\beta\tau^2 & p(5, \tau) &\doteq 0.007,46\beta\tau^2 \\ p(6, \tau) &\doteq 0.002,43\beta\tau^2 & p(7, \tau) &\doteq 0.000,88\beta\tau^2 \end{aligned} \quad (48)$$

7. BEHAVIOR AT INFINITY

If the covariance $\psi(t)$ tends to zero as $t \rightarrow \infty$, we expect that as $|t_i - t_j| \rightarrow \infty$ the probability density of a zero at t_i will become independent of the probability density of a zero at t_j , hence

$$W(S) \sim [W(+)]^n.$$

Therefore from (4)

$$W(S) \sim [W(+)]^{n-1} \frac{\tau^{n-2}}{(n-2)!}$$

and from (12)

$$P_0^{(N)} \sim (-)^{N+1} [W(+)]^N \frac{\tau^{N-1}}{(N-1)!}.$$

Since $P_0(\tau)$ must tend to zero at infinity, the approximations $P_0^{(N)}$ clearly fail there. Like the power series for $e^{-\tau}$, the series (7) is nonuniformly convergent over the infinite interval $0 < \tau < \infty$.

Thus for large values of τ an altogether different type of approximation is required. One promising method seems to be that of Kuznetsov, Stratonovich, and Tikhonov [10]. A rough method of approximation, based on the idea that $P_0(\tau)$ behaves exponentially for large τ , has been suggested by Rice [11]. Some rigorous, but not necessarily close, bounds on probabilities related to $P_0(\tau)$ have been proved by Slepian [2] and by Newell and Rosenblatt [12].

APPENDIX 1. NUMERICAL EVALUATION OF $X_{n,s}$, WHEN $n = 4, 5$

The multiple integral (45) was approximated by the k -point Gaussian quadrature formula

$$\int \cdots \int f(x_1, \cdots, x_r) dx_1 \cdots dx_r \doteq \sum_{i_1, i_2, \dots, i_r=1}^k w_{i_1} \cdots w_{i_r} f(x_{i_1}, \cdots, x_{i_r}),$$

the weights w_i and abscissas x_i (which depend on k) being quoted, to 10 decimal places, from [13]. Let $X(k)$ denote the right-hand side of the foregoing equation. It is clear that this formula involves the evaluation of $f(x_1, \cdots, x_r)$ at k^r points. This places a practical limit on k , and so the final result was obtained from $X(2), X(3), \cdots, X(k_{\max})$ by extrapolation. The approximants $X(k)$ may be expected to behave similarly to the approximants to $\int_0^1 \log x dx$, whose errors are $O(1/k^2)$; but, if $X(k)$ has an error $(C/k^p + D/k^{p+1} + \cdots)$, then $X(k) + (k/p)[X(k) - X(k-1)]$ has an error of order $1/k^{p+1}$. Hence a closer sequence of approximations should be given by

$$X'(k) = X(k) + \frac{k}{2}[X(k) - X(k-1)]$$

and then

$$X''(k) = X'(k) + \frac{k}{3}[X'(k) - X'(k-1)]$$

and so on.

TABLE 1a
SUCCESSIVE APPROXIMATIONS TO $X_{3,1}$

K	(1)	(2)	(3)	(4)	(5)
2	0.072 354 108 3				
3	0.071 863 612 9	0.071 127 870			
4	0.071 710 196 3	0.071 403 363	0.071 770 69		
5	0.071 565 901 8	0.071 205 166	0.070 874 84	0.069 755 0	
6	0.071 445 127 6	0.071 082 805	0.070 838 08	0.070 783 0	0.072 016
7	0.071 348 926 2	0.070 012 221	0.070 847 53	0.070 864 0	0.070 978
8	0.071 272 693 2	0.070 967 761	0.070 849 20	0.070 852 6	0.070 834
9	0.071 211 938 9	0.070 938 545	0.070 850 89	0.070 854 7	0.070 859
10	0.071 163 055 8	0.070 918 640	0.070 852 29	0.070 855 8	0.070 858
11	0.071 123 300 3	0.070 904 645	0.070 853 33	0.070 856 2	0.070 857
12	0.071 090 619 4	0.070 894 534	0.070 854 09	0.070 856 4	0.070 857
13	0.071 063 477 1	0.070 887 052	0.070 854 63	0.070 856 4	0.070 856
14	0.071 040 717 2	0.070 881 398	0.070 855 01	0.070 856 3	0.070 856
15	0.071 021 461 8	0.070 877 046	0.070 855 29	0.070 856 3	0.070 856

$$\left(\frac{3}{8\pi^2} + \frac{1}{2\sqrt{2}\pi} - \frac{17}{288} \right) = 0.070,856$$

INTERVALS BETWEEN ZEROS OF A STATIONARY GAUSSIAN PROCESS 83

TABLE 1b
SUCCESSIVE APPROXIMATIONS TO $X_{3,0}$

K	(1)	(2)	(3)	(4)	(5)
2	0.020 625 884 4				
3	0.022 038 333 6	0.024 157 007			
4	0.022 807 980 3	0.024 347 274	0.024 600 96		
5	0.023 256 744 2	0.024 378 654	0.024 430 95	0.024 218 4	
6	0.023 537 634 8	0.024 380 307	0.024 383 61	0.024 312 6	0.024 426
7	0.023 724 142 9	0.024 376 921	0.024 369 02	0.024 343 5	0.024 387
8	0.023 853 964 8	0.024 373 252	0.024 363 47	0.024 352 4	0.024 367
9	0.023 947 824 0	0.024 370 190	0.024 361 00	0.024 355 5	0.024 361
10	0.024 017 818 3	0.024 367 790	0.024 359 79	0.024 356 7	0.024 359
11	0.024 071 374 9	0.024 365 936	0.024 359 14	0.024 357 4	0.024 359
12	0.024 113 250 3	0.024 364 503	0.024 358 77	0.024 357 7	0.024 358
13	0.024 146 601 8	0.024 363 387	0.024 358 55	0.024 357 8	0.024 358
14	0.024 173 590 1	0.024 362 508	0.024 358 41	0.024 357 9	0.024 358
15	0.024 195 733 6	0.024 361 810	0.024 358 32	0.024 358 0	0.024 358

$$\left(\frac{3}{8\pi^2} - \frac{1}{\sqrt{3}\pi} + \frac{49}{288}\right) = 0.024,358$$

The method was first tested on the three-fold integrals $X_{3,1}$ and $X_{3,0}$, whose exact values are known (43). The approximants $X(k)$ for $X_{3,1}$ are shown in the first column of Table 1a, $X'(k)$ is shown in the second column, X'' in the third, etc. It will be noted that $X'''(k)$ is already correct to the sixth decimal place when $k \geq 10$. The convergence of $X_{3,0}$, shown in Table 1b, is equally rapid. However, the convergence of $X''''(k)$ is not more rapid than $X'''(k)$, possibly because of rounding errors.

Similar calculations for $X_{4,1}$ and $X_{4,0}$ are shown in Tables 2a and 2b, in

TABLE 2a
SUCCESSIVE APPROXIMATIONS TO $X_{4,1}$

K	(1)	(2)	(3)	(4)	(5)
2	0.007 592 467 3				
3	0.008 930 321 0	0.010 937 102			
4	0.009 531 476 3	0.010 733 787	0.010 462 70		
5	0.009 883 793 6	0.010 764 587	0.010 815 92	0.011 257 4	
6	0.010 113 668 5	0.010 803 293	0.010 880 71	0.010 977 9	0.010 642
7	0.010 272 773 8	0.010 829 642	0.010 891 12	0.010 909 4	0.010 813
8	0.010 387 646 8	0.010 847 139	0.010 893 80	0.010 899 1	0.010 883
9	0.010 473 378 7	0.010 859 172	0.010 895 27	0.010 898 6	0.010 898
10	0.010 539 109 3	0.010 867 762	0.010 896 40	0.010 899 2	0.010 900
11	0.010 590 642 3	0.010 874 074	0.010 897 22	0.010 899 5	0.010 900
12	0.010 631 810 8	0.010 878 822	0.010 897 81	0.010 899 6	0.010 900

84 ZEROS OF PROCESSES AND RELATED QUESTIONS

TABLE 2b
SUCCESSIVE APPROXIMATIONS TO $X_{4,0}$

K	(1)	(2)	(3)	(4)	(5)
2	0.002 761 049 9				
3	0.003 178 844 7	0.003 805 537			
4	0.003 442 463 6	0.003 969 701	0.004 188 59		
5	0.003 621 953 6	0.004 070 679	0.004 238 97	0.004 302 0	
6	0.003 750 374 7	0.004 135 638	0.004 265 56	0.004 305 4	0.004 310
7	0.003 845 865 1	0.004 180 082	0.004 283 78	0.004 315 7	0.004 330
8	0.003 919 046 4	0.004 211 772	0.004 296 28	0.004 321 3	0.004 330
9	0.003 976 519 0	0.004 235 146	0.004 305 27	0.004 325 5	0.004 333
10	0.004 022 577 7	0.004 252 871	0.004 311 96	0.004 328 7	0.004 335
11	0.004 060 124 3	0.004 266 631	0.004 317 08	0.004 331 2	0.004 337
12	0.004 091 181 3	0.004 277 523	0.004 321 09	0.004 333 1	0.004 338

which $k_{\max} = 12$. It appears that

$$X_{4,1} = 0.010,90$$

$$X_{4,0} = 0.004,34,$$

with a possible error of 1 unit in the fifth decimal place of $X_{4,0}$.

TABLE 3a
SUCCESSIVE APPROXIMATIONS TO $X_{5,1}$

K	(1)	(2)	(3)	(4)	(5)
2	0.001 055 668 0				
3	0.001 368 765 4	0.001 838 412			
4	0.001 537 181 2	0.001 874 013	0.001 921 48		
5	0.001 653 178 3	0.001 943 171	0.002 058 43	0.002 229 6	
6	0.001 738 354 2	0.001 993 882	0.002 095 31	0.002 150 6	0.002 056
7	0.001 803 133 6	0.002 029 861	0.002 113 81	0.002 146 2	0.002 140
8	0.001 853 876 9	0.002 056 850	0.002 128 82	0.002 158 8	0.002 179

TABLE 3b
SUCCESSIVE APPROXIMATIONS TO $X_{5,0}$

K	(1)	(2)	(3)	(4)	(5)
2	0.000 412 953 6				
3	0.000 518 728 3	0.000 677 390			
4	0.000 589 878 3	0.000 732 178	0.000 805 23		
5	0.000 641 435 0	0.000 770 327	0.000 833 91	0.000 869 8	
6	0.000 680 662 2	0.000 798 344	0.000 854 38	0.000 885 1	0.000 903
7	0.000 711 480 1	0.000 819 343	0.000 868 34	0.000 892 8	0.000 904
8	0.000 736 294 7	0.000 835 553	0.000 878 78	0.000 899 7	0.000 911

INTERVALS BETWEEN ZEROS OF A STATIONARY GAUSSIAN PROCESS 85

The calculations for $X_{5,1}$ and $X_{5,0}$ are shown in Tables 3a and 3b, with $k_{\max} = 8$. The convergence is not much less rapid than that of $X_{4,1}$ and $X_{4,0}$ at the same values of k . We take

$$X_{5,1} = 0.002,18$$

$$X_{5,0} = 0.000,91,$$

allowing a possible error of one unit in the *fourth* decimal place.

It may be mentioned that other methods of extrapolation, assuming, for example, initial errors of order $O(1/k)$ or using the nonlinear transformations $e_1^{(m)}$ (see [14]), lead to estimates consistent with those just stated, though the convergence is less rapid.

The computations were carried out on the IBM 1604 of the University of California, San Diego.

APPENDIX 2. AN ALTERNATIVE APPROACH TO THE EVALUATION OF $P_m(\tau)$ IN A SINGULAR CASE

F. J. Dyson

Consider the random process $f(t)$ which satisfies

$$\left(1 + \frac{d}{dt}\right)^2 f(t) = q(t), \quad (49)$$

where $\overline{q(t)q(t')} = \delta(t - t')$. This is identical with the example (31); in fact

$$\psi(t) = \frac{1}{2}(1 + |t|)e^{-|t|}. \quad (50)$$

Let $P(x, y, t)$ denote the p.d. of finding

$$f, \frac{df}{dt} = \frac{1}{2}x, \frac{1}{2}y$$

at time t . From the equation of motion (49) it is easy to derive the Boltzmann equation

$$\frac{\partial P}{\partial t} + y \frac{\partial P}{\partial x} - (x + 2y) \frac{\partial P}{\partial y} - 2 \frac{\partial^2 P}{\partial y^2} - 2P = 0. \quad (51)$$

The stationary solution of (51) is

$$\Pi(x, y) = \frac{1}{2\pi} e^{-(1/2)(x^2 + y^2)}. \quad (52)$$

We want a solution $P(x, y, t)$ to describe the probability of arriving at (x, y, t) without crossing $x = 0$ at any time $t' > 0$. So $P(x, y, t)$ must satisfy (51) with the boundary conditions

$$\begin{aligned} P(x, y, t) &= \Pi(x, y) & \text{when } t = 0 \\ P(x, y, t) &= 0 & \text{when } x = 0, t > 0 \end{aligned} \quad (53)$$

We can convert the differential equation for $P(x, y, t)$ into an integral equation if we know Green's function $Q(x, y, t; \xi, \eta, t_0)$, which gives the probability for arriving at (x, y) at time t if we start from (ξ, η) at time $t_0 < t$, crossings of $x = 0$ being allowed. This function can be calculated explicitly for any gaussian process. We find in fact

$$Q = \frac{1}{2\pi M^{1/2}} \exp \left(-\frac{1}{2M} \{ [1 - (1 - 2s + s^2)e^{-2s}] \hat{x}^2 - 4s^2 e^{-2s} \hat{x} \hat{y} + [1 - (1 + 2s + 2s^2)e^{-2s}] \hat{y}^2 \} \right), \quad (54)$$

where

$$\begin{aligned} M &= (1 - e^{-2s})^2 - 4s^2 e^{-2s} \\ s &= t - t_0 \\ \hat{x} &= x - [\xi + s(\xi + \eta)]e^{-s} \\ \hat{y} &= y - [\eta - s(\xi + \eta)]e^{-s}. \end{aligned} \quad (55)$$

The integral equation for $P(x, y, t)$ is then

$$P(x, y, t) = \Pi(x, y) - \int_0^t dt_0 \int_{-\infty}^{\infty} Q(x, y, t; 0, \eta, t_0) P(0, \eta, t_0) |\eta| d\eta. \quad (56)$$

The rate of crossing the barrier at $x = 0$ per unit time t is

$$C(t) = \int_{-\infty}^{\infty} P(0, y, t) |y| dy. \quad (57)$$

This is related to the quantity $P_0(0)$ in the earlier part of the chapter by

$$P_0(0) = -\pi \left[\frac{dC(t)}{dt} \right]_{t=0} \quad (58)$$

provided we take $\alpha = \frac{1}{3}$. All that is necessary is to solve (56) for an infinitesimal range of time $0 < t < \epsilon$.

Since we are interested only in short times, we may approximate (54). We find for small s

$$Q(0, y, t; 0, \eta, t_0) \sim G(y, \eta, t - t_0) \quad (59)$$

where

$$G(y, \eta, s) = \frac{\sqrt{3}}{4\pi s^2} \exp \left[-\frac{1}{2s} (y^2 + y\eta + \eta^2) \right].$$

One may expect (59) to be valid for *any* gaussian process with $\alpha = \frac{1}{3}$, although, of course, (54) holds only for the special example (49).

Let $R_k(y, s)$ be the p.d. for arriving at the position $(0, y, s)$ along a trajectory that crosses $x = 0$ precisely k times between time zero and time s . In particular,

$$R_0(y, s) = P(0, y, s). \quad (60)$$

INTERVALS BETWEEN ZEROS OF A STATIONARY GAUSSIAN PROCESS 87

We also introduce the generating function

$$R^*(y, s) = \sum \nu^k R_k(y, s). \quad (61)$$

The integral equation (56) becomes

$$R_0(y, s) = \pi(0, y) - \int_0^s dt \int_0^\infty [G(y, \eta, t) + G(y, -\eta, t)] R_0(\eta, t) \eta d\eta, \quad (62)$$

which for short we write

$$R_0 = \Pi - (G_+ + G_-) R_0. \quad (63)$$

A complete set of integral equations for all the R_k is given by

$$R^* = \Pi - (1 - \nu)(G_+ + G_-) R^*. \quad (64)$$

The quantity $P_m(0)$ is given by

$$P_m(0) = -2\pi \frac{d}{ds} \left[\int_0^\infty R_m(y, s) y dy \right]_{s=0}. \quad (65)$$

If we iterate (63), we find a series expansion equivalent to equation (13). For more rapid convergence, we should use a set of equations equivalent to (7). These equations are

$$R^* = \Pi - (1 - \nu)H - (1 - \nu^2)G_+ R^*, \quad (66)$$

where H denotes the known function

$$H = \sum_k R^{2k+1} = (G_- - G_+) \Pi. \quad (67)$$

Note that in (66) only G_+ and not G_- appears. If $\nu = 0$, (66) gives

$$R_0 = \Pi - H - G_+ R_0 \quad (68)$$

which when iterated gives (7). The first power of ν in (66) gives

$$R_1 = H - G_+ R_1, \quad (69)$$

which when iterated gives (8).

Let us look in detail at (68). The solution for small s will look like

$$R_0(y, s) = \frac{1}{2\pi} \left[1 - F \left(\frac{y}{\sqrt{s}} \right) \right]. \quad (70)$$

When this is put into (68), the dependence on s disappears, and we have an integral equation for the function $F(x)$ of one variable:

$$F(x) = \frac{\sqrt{3}}{4\pi} \int_1^\infty d\lambda \int_0^\infty u du \left\{ e^{-(\frac{1}{2})\lambda(x^2 - xu + u^2)} - e^{-(\frac{1}{2})\lambda(x^2 + xu + u^2)} F \left[u \left(\frac{\lambda}{\lambda - 1} \right)^{\frac{1}{2}} \right] \right\}. \quad (71)$$

When this is solved, we have immediately

$$P_0(0) = \int_0^{\infty} xF(x) dx. \quad (72)$$

As a check, we may note that neglecting the term in F on the right of (71) gives

$$P_0(0) = \frac{\sqrt{3}}{4\pi} \int_1^{\infty} d\lambda \int_0^{\infty} x dx \int_0^{\infty} u du e^{-(\frac{1}{2})\lambda(x^2-xu+u^2)}, \quad (73)$$

which is identical with $X_{2,1}$ (see Section 5). ($N - 1$) successive substitutions for F on the right-hand side will produce the series (12).

A solution of (73) in closed form would be of interest.

REFERENCES

1. Rice, S. O. The mathematical analysis of random noise. *Bell System Tech. J.*, **23**, 282-332 (1944), and **24**, 46-156 (1945).
2. Slepian, D. The one-sided barrier problem for Gaussian noise. *Bell System Tech. J.*, **41**, 463-501 (1962).
3. Ehrenfeld, S., et al. Theoretical and observed results for the zero and ordinate crossing problems of stationary Gaussian noise with application to pressure records of ocean waves. Tech. Rep. No. 1., Research Division, College of Engineering, New York University (1958).
4. McFadden, J. A. The axis-crossing intervals of random functions II. *IRE Trans. Inform. Theory*, **4**, 14-24 (1958).
5. Longuet-Higgins, M. S. On the intervals between successive zeros of a random function. *Proc. Roy. Soc. (London)*, **A. 263**, 99-118 (1958).
6. Longuet-Higgins, M. S. The distribution of intervals between zeros of a stationary random function. *Phil. Trans. Roy. Soc. (London)*, **A. 264**, 557-599 (1962).
7. Blotekjaer, K. An experimental investigation of some properties of band-pass limited gaussian noise. *IRE Trans. Inform. Theory*, **4**, 100-102 (1958).
8. Wang, M. C., and G. E. Uhlenbeck. On the theory of Brownian motion. *Rev. Mod. Phys.*, **17**, 323-342 (1945).
9. Favreau, R. R., H. Low, and I. Pfeffer. Evaluation of complex statistical functions by an analog computer. *IRE Natl. Conv. Record*, Pt. 4, 31-37 (1956).
10. Kuznetsov, P. I., P. L. Stratonovich, and V. I. Tikhonov. On the duration of exceedences of a random function. *Zh. Tekhn. Fiz.*, **24**, 103-112 (1954). English translation by N. R. Goodman, Sci. Paper No. 5, Eng. Stat. Group, College of Engineering, New York University (1956).
11. Rice, S. O. Distribution of the duration of fades in radio transmission: Gaussian noise model. *Bell System Tech. J.*, **37**, 581-635 (1938).
12. Newell, G. F., and M. Rosenblatt. Zero crossing probabilities for gaussian stationary processes. *Ann. Math. Statist.* (1962).
13. Lowan, A. N., N. Davids, and A. Levenson. Tables of the Legendre polynomials of order 1-16 and the weight coefficients for Gauss' mechanical quadrature formula. *Bull. Amer. Math. Soc.*, **48**, 739-743 (1942).
14. Shanks, D. Non-linear transformations of divergent and slowly convergent sequences. *J. Math. Phys.*, **34**, 1-42 (1955).

*Reprinted without change of pagination from the
Journal of Fluid Mechanics, volume 17, part 3, pp. 459-480, 1963*

The effect of non-linearities on statistical distributions in the theory of sea waves

By M. S. LONGUET-HIGGINS

National Institute of Oceanography, Wormley

(Received 15 March 1963)

The statistical density function is derived for a variable (such as the surface elevation in a random sea) that is 'weakly non-linear'. In the first approximation the distribution is Gaussian, as is well known. In higher approximations it is shown that the distribution is given by successive sums of a Gram-Charlier series; not quite in the form that has sometimes been used as an empirical fit for observed distributions, but in a modified form due to Edgeworth.

It is shown that the cumulants of the distribution are much simpler to calculate than the corresponding moments; and the approximate distributions are in fact derived by inversion of the cumulant-generating function.

The theory is applied to random surface waves on water. The third cumulant and hence the skewness of the distribution of surface elevation is evaluated explicitly in terms of the directional energy spectrum. It is shown that the skewness λ_3 is generally positive, and positive upper and lower bounds for λ_3 are derived. The theoretical results are compared with some measurements made by Kinsman (1960).

It is found that for free, undamped surface waves the skewness of the distribution of surface slopes is of a higher order than the skewness of the surface elevation. Hence the observed skewness of the slopes may be a sensitive indicator of energy transfer and dissipation within the water.

1. Introduction

It is well known that in the linear theory of wind-generated water waves, in which squares and higher powers of the surface displacement are neglected, the statistical distribution of the surface elevation and its derivatives is Gaussian, under quite general conditions. Moreover, the Gaussian distribution of the surface elevation and bottom pressure has been fairly well verified in some circumstances (see, for example, Rudnick 1950; Barber 1950; Pierson 1955; MacKay 1959). Quite early, however, Birkhoff & Kotik (1952) pointed out significant departures from the Gaussian distribution for waves in shallow water. Similar, though less pronounced, effects for waves in deep water were found by Burling (1955) and Kinsman (1960).

The distribution of surface slopes was shown by Cox & Munk (1956) to have an appreciable skewness in the direction of the wind; and surface curvatures in wind-generated waves may be even more radically non-Gaussian (Schooley 1955).

Several theoretical investigations have lately been made into the dynamical effects which non-linearities produce in the quadratic spectrum of the sea surface (Tick 1959, 1961; Phillips 1960, 1961; Hasselmann 1960, 1961, 1962). However, the effect of such non-linearities on the statistical distributions has received less attention. Phillips (1961) has pointed out that the surface elevation must in fact have a coefficient of skewness of the same order of magnitude as the surface slope; but the higher moments of the distribution have not been calculated, nor has the complete distribution been derived.

Some authors (Cox & Munk 1956; Kinsman 1960) have fitted the observed distributions of surface slope or elevation by means of a Gram-Charlier series, with apparently no justification beyond the fact that any function that is sufficiently well-behaved can be expanded in such a series. The coefficients of successive terms are related to the moments of the function itself.

In the present paper we derive the theoretical distribution of quantities (such as the surface elevation or surface slope) which can be described as 'weakly non-linear', that is to say the ordinary representation as the sum of independent random components is valid to a first approximation, but quadratic and higher-order interactions between the components cannot be entirely neglected. At each stage the calculation is carried uniformly to a certain power of the component amplitudes.

As one would expect, the first approximation corresponds to the ordinary Gaussian distribution. It is found that higher approximations are described by the Gaussian law multiplied by certain polynomials. These expressions correspond in fact to successive terms in a Gram-Charlier series; not, however, in the form that has been commonly used for fitting the distributions, but in a modified form due to Edgeworth (1906 *a, b, c*). For example, in the second approximation a cubic polynomial occurs, but in the third approximation one must include a quartic polynomial plus another of degree six.

Roughly the method is as follows: from the dynamical equations it is possible to calculate successively higher *moments* of the statistical variable. It turns out that certain combinations of the moments, namely, the *cumulants*, are simpler to calculate, and just as convenient to handle, as the moments themselves. By calculating the cumulant-generating function to a certain order and taking the Fourier transform one obtains the desired approximation to the distribution function.

The analysis is essentially similar to Edgeworth's (1906) generalization of the Gaussian 'law of error' for a single variable, but is presented here in a rather different form and is moreover extended to two or more dependent variables.

The device of truncating the cumulant-generating function has been used in the analytical theory of turbulence (see, for example, O'Brien & Francis 1962) but not, so far as the author is aware, for the specific purpose of calculating probability densities. Hence some of the results of the present study may be applicable also to turbulent fluctuations.

The basic analysis for a single non-linear variable is given in § 2. This is then applied, in § 3, to the distribution of surface elevation in a random sea. In § 4 the results are compared with recent observations made by Kinsman (1960).

The next three sections follow a similar scheme: the joint distribution of two related non-linear variables is derived in § 5; this is applied to the joint distribution of surface slopes in § 6, and in § 7 the well-known observations of Cox & Munk (1956) are discussed. The conclusions are restated in § 8.

2. A single non-linear variable

As will be shown in § 3, the linear spectral representation of the sea surface elevation ζ can be expressed in the form

$$\zeta = \sum_{i=1}^N \alpha_i \xi_i,$$

where the α_i are constants and the ξ_i are independent random variables symmetrically distributed about 0 with variance V_i , say. The convergence of $p(\zeta)$ to a Gaussian distribution, with variance $\sum V_i$, is a case of the so-called 'law of large numbers'.

In the more exact non-linear theory, in order to satisfy the dynamical equations for ζ , quadratic and higher-order terms must be added to ζ . Let us then consider, in a general way, the distribution of the variable

$$\zeta = \alpha_i \xi_i + \alpha_{ij} \xi_i \xi_j + \alpha_{ijk} \xi_i \xi_j \xi_k + \dots, \quad (2.1)$$

where α_i , α_{ij} , α_{ijk} , etc., are constants, and the summation convention is used. Thus in (2.1) each product is summed over all repeated suffices, from 1 to N . With each value of i is associated a vector \mathbf{u}_i (the wavenumber). Later, we shall make $N \rightarrow \infty$ and each $V_i \rightarrow 0$ in such a way that over any small but fixed region $d\mathbf{u}$

$$\sum_{\mathbf{u} \in d\mathbf{u}} V_i \rightarrow F(\mathbf{u}) d\mathbf{u} + O(d\mathbf{u})^2. \quad (2.2)$$

The first few moments of ζ can be written down by inspection. Thus taking mean values in (2.1) one has

$$\bar{\zeta} = \alpha_i \bar{\xi}_i + \alpha_{ij} \bar{\xi}_i \bar{\xi}_j + \alpha_{ijk} \bar{\xi}_i \bar{\xi}_j \bar{\xi}_k + \dots$$

All mean values of odd-order terms vanish, while among the terms of even order only those remain in which each ξ_i is paired with a similar ξ_i . Thus*

$$\bar{\zeta} = \alpha_{ii} V_i + 3\alpha_{iij} V_i V_j + \dots \quad (2.3)$$

(It is assumed that the α are symmetric in their suffices so that, for example, $\alpha_{ijij} = \alpha_{ijji} = \alpha_{iijj}$.) There are, in general, terms involving $\bar{\xi}_i^4$, $\bar{\xi}_i^6$, etc.; these become negligible on passing to the limit as $N \rightarrow \infty$, and so will be ignored.

In a similar way, by squaring both sides of (2.1) one has

$$\zeta^2 = (\alpha_i \xi_i + \alpha_{ij} \xi_i \xi_j + \dots) (\alpha_k \xi_k + \alpha_{kl} \xi_k \xi_l + \dots)$$

and on taking mean values

$$\bar{\zeta}^2 = \alpha_i \alpha_i V_i + (2\alpha_{ij} \alpha_{ji} + \alpha_{ii} \alpha_{jj}) V_i V_j + 6\alpha_{iij} \alpha_{iij} V_i V_j + \dots \quad (2.4)$$

The higher moments may be calculated similarly, but a direct approach leads to complications. We shall show how these can be circumvented.

* The usual summation convention is extended to three repeated indices.

It will be noticed that some of the terms in (2.4) and in higher moments can be factorized*

$$\alpha_{ii}\alpha_{jj}V_iV_j = (\alpha_{ii}V_i)(\alpha_{jj}V_j),$$

but other terms, e.g. $\alpha_{ij}\alpha_{ji}V_iV_j$ cannot. The latter terms may be called 'irreducible', and it will be convenient to introduce an abbreviated notation for them. Thus let $\alpha_{i,j,\dots,l}$ be denoted shortly by A_r , where r is the number of suffices i, j, \dots, l ; and let the sum of all the irreducible terms in the mean product

$$\overline{(A_p \xi_{i_1} \dots \xi_{i_p})(A_q \xi_{j_1} \dots \xi_{j_q}) \dots (A_s \xi_{l_1} \dots \xi_{l_s})}$$

be denoted simply by

$$(A_p A_q \dots A_s).$$

Clearly when $(p+q+\dots+s)$ is odd, the above expression vanishes. Also

$$(A_1^2) = \alpha_i \alpha_i V_i, \quad (A_2) = \alpha_{ii} V_i, \quad (2.5)$$

$$(A_1^n) = 0 \quad (n \geq 4),$$

$$(A_1^2 A_2) = 2\alpha_i \alpha_j \alpha_{ij} V_i V_j, \quad (A_1 A_3) = 3\alpha_i \alpha_{ijj} V_i V_j, \quad (2.6)$$

$$(A_2^2) = 2\alpha_{ij} \alpha_{ji} V_i V_j, \quad (A_4) = 3\alpha_{iiij} V_i V_j,$$

$$(A_1^2 A_2^2) = 8\alpha_i \alpha_j \alpha_{ik} \alpha_{jk} V_i V_j V_k, \quad (A_1^3 A_3) = 6\alpha_i \alpha_j \alpha_k \alpha_{ijk} V_i V_j V_k,$$

$$(A_1^2 A_4) = 12\alpha_i \alpha_j \alpha_{ijk} V_i V_j V_k, \quad (A_1 A_5) = 15\alpha_{iiijjk} V_i V_j V_k,$$

$$(A_1 A_2 A_3) = (6\alpha_i \alpha_{ij} \alpha_{jkk} + 6\alpha_i \alpha_{jk} \alpha_{ijk}) V_i V_j V_k, \quad (A_2^3) = 8\alpha_{ij} \alpha_{jk} \alpha_{kii} V_i V_j V_k, \quad (2.7)$$

$$(A_3^2) = (9\alpha_{ijj} \alpha_{ikk} + 6\alpha_{ijk} \alpha_{ijk}) V_i V_j V_k, \quad (A_2 A_4) = 12\alpha_{ij} \alpha_{ijk} V_i V_j V_k,$$

$$(A_6) = 15\alpha_{iiijjk} V_i V_j V_k.$$

The first few moments can now be written shortly as

$$\left. \begin{aligned} \bar{\xi} &= \sum_p (A_p), & \bar{\xi}^2 &= \sum_{p,q} [(A_p A_q) + (A_p)(A_q)], \\ \bar{\xi}^3 &= \sum_{p,q,r} [(A_p A_q A_r) + 3(A_p A_q)(A_r) + (A_p)(A_q)(A_r)], \end{aligned} \right\} \quad (2.8)$$

etc., where the summations are over all positive integral values of p, q, r (including equal values). Generally,

$$\bar{\xi}^n = \sum_{p,q,\dots,s} [C(n) \varpi(n) + C(n-1,1) \varpi(n-1,1) + \dots], \quad (2.9)$$

where $\varpi(i, j, \dots, l)$ denotes some grouping of A_p, A_q, \dots, A_s into unordered† sets containing i, j, \dots, l members, and $C(i, j, \dots, l)$ denotes the number of ways of choosing such sets. If r denotes the number of sets in ϖ we have

$$C(i, j, \dots, l) = \frac{1}{r!} \frac{n!}{i! j! \dots l!}. \quad (2.10)$$

* The factorization of any given product can be shown to be unique.

† Both the sets and the members of each set are unordered. Each ϖ is considered as distinct from the rest.

We have thus calculated $\bar{\xi}^n = \mu_n$, the n th moment of the distribution. It turns out, however, that the *cumulants* of the distribution are much simpler. Whereas the moments correspond to the coefficients of $(it)^n$ in the function

$$\begin{aligned}\phi(it) &= \int_{-\infty}^{\infty} p(\xi) e^{i\mu\xi} d\xi \\ &= 1 + \frac{\mu_1}{1!}(it) + \frac{\mu_2}{2!}(it)^2 + \dots,\end{aligned}\quad (2.11)$$

the cumulants, by definition, correspond to the coefficients of $(it)^n$ in

$$\begin{aligned}K(it) &= \log \phi(it) \\ &= \frac{\kappa_1}{1!}(it) + \frac{\kappa_2}{2!}(it)^2 + \dots\end{aligned}\quad (2.12)$$

On equating coefficients of $(it)^n$ in (2.12) one has

$$\kappa_1 = \mu_1, \quad \kappa_2 = \mu_2 - \mu_1^2, \quad \kappa_3 = \mu_3 - 3\mu_1\mu_2 + 2\mu_1^3,$$

etc., and so on substitution from (2.8) we have

$$\kappa_1 = \sum_p (A_p), \quad \kappa_2 = \sum_{p,q} (A_p A_q), \quad \kappa_3 = \sum_{p,q,r} (A_p A_q A_r),$$

etc. This suggests the relation

$$\kappa_n = \sum_{p,q,\dots,s} (A_p A_q \dots A_s). \quad (2.13)$$

To prove this, we note that since

$$\phi(it) = e^{K(it)} = \exp \left[1 + \frac{\kappa_1}{1!}(it) + \frac{\kappa_2}{2!}(it)^2 + \dots \right] \quad (2.14)$$

one has, on equating coefficients of $(it)^n$ in this expression,

$$\begin{aligned}\mu_n &= \sum_{r=1}^{\infty} \frac{n!}{r!} \sum_{i+j+\dots+l=n} \frac{\kappa_i \kappa_j \dots \kappa_l}{i! j! \dots l!} \\ &= \sum_{r=1}^{\infty} \sum_{i+j+\dots+l=n} C(i, j, \dots, l) \kappa_i \kappa_j \dots \kappa_l,\end{aligned}\quad (2.15)$$

where $C(i, j, \dots, l)$ is given by (2.10). Therefore the equations for μ_n in terms of the κ_n are formally identical with the equations for μ_n in terms of $\Sigma(A_p A_q \dots A_s)$. Since $\mu_1 = \Sigma(A_p)$ the general result (2.13) follows by induction.

Retaining all terms up to the sixth order in the ξ_i (i.e. third order in V_i) we have from (2.13)

$$\left. \begin{aligned}\kappa_1 &= (A_2) + (A_4) + (A_6), \\ \kappa_2 &= (A_1^2) + (A_3^2) + (A_5^2) + 2(A_1 A_3) + 2(A_1 A_5) + 2(A_2 A_4), \\ \kappa_3 &= (A_2^3) + 3(A_1^2 A_2) + 3(A_1^2 A_4) + 6(A_1 A_2 A_3), \\ \kappa_4 &= (A_1^4) + 4(A_1^2 A_3) + 6(A_1^2 A_5).\end{aligned}\right\} \quad (2.16)$$

From (2.16) it is seen that κ_1 and κ_2 are both of order V , in general. However, when $n \geq 2$ the lowest non-vanishing term in κ_n is $n(A_1^{n-1} A_{n-1})$, which is $O(V^{n-1})$.

The coefficients of skewness and of kurtosis will be defined by

$$\lambda_3 = \kappa_3/\kappa_2^{\frac{3}{2}}, \quad \lambda_4 = \kappa_4/\kappa_2^2, \tag{2.17}$$

which are of order $V^{\frac{1}{2}}$ and V , respectively. More generally,

$$\lambda_n = \kappa_n/\kappa_2^{\frac{1}{2}n} = O(V^{\frac{1}{2}n-1}). \tag{2.18}$$

The density of ζ

Now provided that the probability density $p(\zeta)$ is uniquely determined by its moments, $p(\zeta)$ can be obtained directly from (2.8) by inverting the Fourier transform:

$$\begin{aligned} p(\zeta) &= \frac{1}{2\pi} \int_{-\infty}^{\infty} \phi(it) e^{-it\zeta} dt = \frac{1}{2\pi} \int_{-\infty}^{\infty} \exp [K(it) - it\zeta] dt \\ &= \frac{1}{2\pi} \int_{-\infty}^{\infty} \exp [(\kappa_1 - \zeta) it + \frac{1}{2}\kappa_2(it)^2 + \frac{1}{6}\kappa_3(it)^3 + \dots] dt. \end{aligned}$$

Substituting $t = s/\kappa_2^{\frac{1}{2}}, (\zeta - \kappa_1) = f\kappa_2^{\frac{1}{2}}$, we have

$$p(\zeta) = \frac{1}{2\pi\kappa_2^{\frac{1}{2}}} \int_{-\infty}^{\infty} \exp [-\frac{1}{2}(s^2 + 2if s) + \frac{1}{6}\lambda_3(is)^3 + \frac{1}{24}\lambda_4(is)^4 + \dots] ds,$$

where λ_n , as we have seen, is $O(V^{\frac{1}{2}n-1})$. The second group of terms under the exponential can now be expanded in powers of $V^{\frac{1}{2}}$, giving

$$p(\zeta) = \frac{1}{2\pi\kappa_2^{\frac{1}{2}}} \int_{-\infty}^{\infty} \exp [-\frac{1}{2}(s^2 + 2if s)] [1 + \frac{1}{6}\lambda_3(is)^3 + \{\frac{1}{24}\lambda_4(is)^4 + \frac{1}{72}\lambda_3^2(is)^6\} + \dots] ds.$$

But we have identically

$$\begin{aligned} \frac{1}{(2\pi)^{\frac{1}{2}}} \int_{-\infty}^{\infty} \exp [-\frac{1}{2}(s^2 + 2if s)] (is)^n ds &= \frac{(-1)^n}{(2\pi)^{\frac{1}{2}}} \frac{d^n}{df^n} \int_{-\infty}^{\infty} \exp [-\frac{1}{2}(s^2 + 2if s)] ds \\ &= (-1)^n \frac{d^n}{df^n} e^{-\frac{1}{2}f^2} = e^{-\frac{1}{2}f^2} H_n(f), \end{aligned}$$

where H_n denotes the Hermite polynomial of degree n :

$$H_n = f^n - \frac{n(n-1)}{1!} \frac{f^{n-2}}{2} + \frac{n(n-1)(n-2)(n-3)}{2!} \frac{f^{n-4}}{2^2} - \dots \tag{2.19}$$

Hence we have

$$p(\zeta) = (2\pi\kappa_2)^{-\frac{1}{2}} e^{-\frac{1}{2}f^2} [1 + \frac{1}{6}\lambda_3 H_3 + (\frac{1}{24}\lambda_4 H_4 + \frac{1}{72}\lambda_3^2 H_6) + \dots] \tag{2.20}$$

From (2.19)

$$\left. \begin{aligned} H_3 &= f^3 - 3f, & H_4 &= f^4 - 6f^2 + 3, \\ H_5 &= f^5 - 10f^3 + 15f, & H_6 &= f^6 - 15f^4 + 45f^2 - 15. \end{aligned} \right\} \tag{2.21}$$

Equation (2.20) is the distribution sought. It corresponds quite closely to Edgeworth's form of the type A Gram-Charlier series (Kendall & Stuart 1958, § 6.18).

In a first approximation, λ_3 and λ_4 can be neglected and we take

$$\kappa_2 = (A_2^2) = \alpha_4 \alpha_1 V_1.$$

Thus
$$p(\zeta) \doteq e^{-\frac{1}{2}f^2}/(2\pi\kappa_2)^{\frac{1}{2}}, \quad f = \zeta/\kappa_2^{\frac{1}{2}}. \quad (2.22)$$

This is the well-known Gaussian law.

In the next approximation λ_3 is taken into account, but λ_3^2 and λ_4 are neglected. To the same approximation

$$\left. \begin{aligned} \kappa_1 &= (A_2) = \alpha_{ii}V_i, & \kappa_2 &= (A_1^2) = \alpha_i\alpha_iV_i, \\ \kappa_3 &= 3(A_1^2A_2) = 6\alpha_i\alpha_j\alpha_kV_iV_j, & \kappa_n &= 0, \quad (n \geq 4), \end{aligned} \right\} \quad (2.23)$$

and so
$$p(\zeta) \doteq (2\pi\kappa_2)^{-\frac{1}{2}} e^{-\frac{1}{2}f^2} [1 + \frac{1}{6}\lambda_3(f^3 - 3f)], \quad (2.24)$$

where
$$f = \zeta/\kappa_2^{\frac{1}{2}} - \kappa_1/\kappa_2^{\frac{1}{2}} \quad (2.25)$$

and
$$\lambda_3 = 6\alpha_i\alpha_j\alpha_{ij}V_iV_j/(\alpha_i\alpha_iV_i)^{\frac{3}{2}}. \quad (2.26)$$

Thus the mean value of ζ is shifted by an amount $\alpha_{ii}V_i$ and the density is multiplied by the factor

$$[1 + \frac{1}{6}\lambda_3(f^3 - 3f)] \quad (2.27)$$

which introduces a skewness λ_3 . The kurtosis is zero, as are all the higher cumulants.

In the next approximation, the distribution is given by the full equation (2.20). The mean κ_1 , variance κ_2 and skewness λ_3 are all slightly modified, and a non-zero kurtosis λ_4 appears, given by κ_4/κ_2^2 , where

$$\begin{aligned} \kappa_4 &\doteq 4(A_1^3A_3) + 6(A_1^2A_2^2) \\ &= 24\alpha_i\alpha_j\alpha_k\alpha_{ijk}V_iV_jV_k + 48\alpha_i\alpha_j\alpha_{ikjk}V_iV_jV_k. \end{aligned} \quad (2.28)$$

3. Application to gravity waves

Consider a random, homogeneous surface displacement on water of infinite depth. To a first approximation such a surface may be represented in the form $z = \zeta^{(1)}$ where

$$\zeta^{(1)} = \sum_{n=1}^{N'} a_n \cos \psi_n, \quad \psi_n = (\mathbf{k}_n \cdot \mathbf{x} - \sigma_n t + \theta_n), \quad (3.1)$$

where \mathbf{x} is the horizontal Cartesian co-ordinate, t the time, \mathbf{k}_n a horizontal vector wave-number, σ_n the frequency, related to \mathbf{k}_n by

$$\sigma_n^2 = g |\mathbf{k}_n| = gk_n$$

(where g is the acceleration of gravity). a_n and θ_n are amplitude and phase constants, chosen randomly so that $a_n \cos \theta_n$ and $a_n \sin \theta_n$ are jointly normal, with θ_n uniformly distributed and

$$\sum_{\mathbf{k}_n \geq d\mathbf{k}} \frac{1}{2} \overline{a_n^2} \doteq E(\mathbf{k}) d\mathbf{k}.$$

Let
$$a_n \cos \theta_n = \xi_n, \quad a_n \sin \theta_n = \xi'_n; \quad (3.2)$$

then we have
$$\zeta^{(1)} = \sum_{n=1}^{N'} [\xi_n \cos(\mathbf{k} \cdot \mathbf{x} - \sigma t) + \xi'_n \sin(\mathbf{k} \cdot \mathbf{x} - \sigma t)],$$

which, if we write $\xi_{N'+n} = \xi'_n$, is of the form

$$\zeta^{(1)} = \sum_{i=1}^{2N'} \alpha_i \xi_i,$$

the α being constants for a fixed position and time. Also

$$\bar{\xi}_i^2 = \frac{1}{2} \alpha_i^2 \quad (i = 1, \dots, 2N').$$

By the assumption of homogeneity we may consider the distribution of $\zeta^{(1)}$ at the special point $\mathbf{x} = 0$ and time $t = 0$; hence we may take

$$\alpha_i = \begin{cases} 1 & (i = 1, \dots, N'), \\ 0 & (i = N' + 1, \dots, 2N'). \end{cases} \quad (3.3)$$

We can now make (3.3) correspond to the linear part of (2.1) by setting $N = 2N'$ and $\mathbf{u}_i = \mathbf{k}_i, \mathbf{u}_{N'+i} = \mathbf{k}_i$ ($i = 1, \dots, N'$). Moreover

$$\sum_{\mathbf{a}_i} \bar{\xi}_i^2 = \sum_{\mathbf{a}_i} \frac{1}{2} \alpha_i^2 = E(\mathbf{k}) d\mathbf{u} \quad (3.4)$$

in each range $i = 1, \dots, N', i = N' + 1, \dots, 2N'$. So compared with (2.2) we have

$$F(\mathbf{u}) = E(\mathbf{k})$$

in each range also.

Corresponding to the free surface elevation $\zeta^{(1)}$ is a velocity potential

$$\phi^{(1)} = \sum_i b_i e^{k_i z} \sin \psi_i \quad (b_i = a_1 \sigma_i / k_i).$$

However, $\zeta^{(1)}$ and $\phi^{(1)}$ are only first approximations. To satisfy the boundary conditions at the free surface to higher order one must add further terms in the series

$$\left. \begin{aligned} \zeta &= \zeta^{(1)} + \zeta^{(2)} + \dots, \\ \phi &= \phi^{(1)} + \phi^{(2)} + \dots, \end{aligned} \right\}$$

in which $\zeta^{(2)}, \phi^{(2)}$ contain terms proportional to the squares of the amplitudes; $\zeta^{(3)}, \phi^{(3)}$ contain terms proportional to the cubes of the amplitudes, and so on. The equations for $\phi^{(2)}$ and $\zeta^{(2)}$ are

$$\left. \begin{aligned} \nabla^2 \phi^{(2)} &= 0; \\ \nabla \phi^{(2)} &\rightarrow 0, \text{ when } z \rightarrow -\infty; \\ \left(\frac{\partial^2}{\partial t^2} + g \frac{\partial}{\partial z} \right) \phi^{(2)} &= -\frac{\partial}{\partial t} (\nabla \phi^{(1)})^2 - \zeta^{(1)} \frac{\partial}{\partial z} \left(\frac{\partial^2}{\partial t^2} + g \frac{\partial}{\partial z} \right) \phi^{(1)} \text{ when } z = 0, \end{aligned} \right\} \quad (3.5)$$

and
$$\zeta^{(2)} = -\frac{1}{g} \left[\frac{\partial \phi^{(2)}}{\partial t} + \frac{1}{2} (\nabla \phi^{(1)})^2 + \zeta^{(1)} \frac{\partial^2 \phi^{(1)}}{\partial z \partial t} \right]_{z=0}. \quad (3.6)$$

It is assumed that the mean level $\bar{\zeta}^{(2)}$ is zero. Substituting for $\phi^{(1)}$ in the third of equations (3.5) we have

$$\begin{aligned} \left(\frac{\partial^2}{\partial t^2} + g \frac{\partial}{\partial z} \right) \phi_{z=0}^{(2)} &= -\sum_{i,j} b_i b_j [(\sigma_i - \sigma_j) (\mathbf{k}_i \cdot \mathbf{k}_j + k_i k_j) \sin(\psi_i - \psi_j) \\ &\quad + (\sigma_i + \sigma_j) (\mathbf{k}_i \cdot \mathbf{k}_j - k_i k_j) \sin(\psi_i + \psi_j)] \end{aligned}$$

and so
$$\phi^{(2)} = \sum_{i,j} b_i b_j \left[\frac{(\sigma_i - \sigma_j) (\mathbf{k}_i \cdot \mathbf{k}_j + k_i k_j)}{(\sigma_i - \sigma_j)^2 - g |\mathbf{k}_i - \mathbf{k}_j|} e^{i\mathbf{k}_i \cdot \mathbf{x}_j} \sin(\psi_i - \psi_j) + \frac{(\sigma_i + \sigma_j) (\mathbf{k}_i \cdot \mathbf{k}_j - k_i k_j)}{(\sigma_i + \sigma_j)^2 - g |\mathbf{k}_i + \mathbf{k}_j|} e^{i\mathbf{k}_i \cdot \mathbf{x}_j} \sin(\psi_i + \psi_j) \right].$$

Inserting this in (3.6) and substituting for b_i , b_j and σ_i , σ_j we find

$$\zeta^{(2)} = \sum_{i,j} \frac{a_i a_j}{(k_i k_j)^{\frac{1}{2}}} \left[(B_{i,j}^- + B_{i,j}^+ - \mathbf{k}_i \cdot \mathbf{k}_j + (k_i + k_j)(k_i k_j)^{\frac{1}{2}}) \cos \psi_i \cos \psi_j \right. \\ \left. + (B_{i,j}^- - B_{i,j}^+ - k_i k_j) \sin \psi_i \sin \psi_j \right], \quad (3.7)$$

where

$$B_{i,j}^- = \frac{(\sqrt{k_i} - \sqrt{k_j})^2 (\mathbf{k}_i \cdot \mathbf{k}_j + k_i k_j)}{(\sqrt{k_i} - \sqrt{k_j})^2 - |\mathbf{k}_i \cdot \mathbf{k}_j|}, \quad B_{i,j}^+ = \frac{(\sqrt{k_i} + \sqrt{k_j})^2 (\mathbf{k}_i \cdot \mathbf{k}_j - k_i k_j)}{(\sqrt{k_i} + \sqrt{k_j})^2 - |\mathbf{k}_i + \mathbf{k}_j|}. \quad (3.8)$$

Now at the point $\mathbf{x} = \mathbf{0}$, $t = 0$, the phase ψ_i reduces to θ_i and so

$$(a_i \cos \psi_i, a_i \sin \psi_i) = (\xi_i, \xi_{N+i}).$$

Hence to a second approximation we have

$$\zeta = \sum_i \alpha_i \xi_i + \sum_{i,j} \alpha_{ij} \xi_i \xi_j,$$

where α_{ij} is given by (3.3) and

$$\alpha_{ij} = \begin{cases} (k_i k_j)^{-\frac{1}{2}} \{B_{i,j}^- + B_{i,j}^+ + \mathbf{k}_i \cdot \mathbf{k}_j + (k_i + k_j)(k_i k_j)^{\frac{1}{2}}\} & \text{when } i, j = 1, \dots, N', \\ (k_i k_j)^{-\frac{1}{2}} (B_{i,j}^- - B_{i,j}^+ - k_i k_j) & \text{when } i, j = N' + 1, \dots, 2N', \\ 0 & \text{otherwise.} \end{cases} \quad (3.9)$$

The diagonal terms α_{ii} are given as the limit of the above expressions as $\mathbf{k}_j \rightarrow \mathbf{k}_i$. Then B_{ij}^- and B_{ij}^+ both vanish and

$$\alpha_{ii} = \begin{cases} k_i & (i = 1, \dots, N'), \\ -k_i & (i = N' + 1, \dots, 2N'). \end{cases}$$

Taking account of (3.3) we have then

$$\left. \begin{aligned} \kappa_1 &\doteq \alpha_{ii} V_i = \sum_{i=1}^{N'} k_i V_i - \sum_{i=1}^{N'} k_i V_i = 0, \\ \kappa_2 &\doteq \alpha_i \alpha_j V_i = \sum_{i=1}^{N'} V_i, \\ \kappa_3 &\doteq 6\alpha_i \alpha_j \alpha_{ij} V_i V_j = 6 \sum_{i,j=1}^{N'} \alpha_{ij} V_i V_j. \end{aligned} \right\} \quad (3.10)$$

The first equation simply states that the mean surface level is zero, to second order, as was specified. The next two equations, in integral form, can be written

$$\kappa_2 \doteq \iint E(\mathbf{k}) d\mathbf{k}, \quad \kappa_3 \doteq 6 \iiint K(\mathbf{k}, \mathbf{k}') E(\mathbf{k}) E(\mathbf{k}') d\mathbf{k} d\mathbf{k}', \quad (3.11)$$

where

$$K(\mathbf{k}, \mathbf{k}') = \frac{1}{(kk')^{\frac{1}{2}}} \left[\frac{(\sqrt{k} - \sqrt{k'})^2 (\mathbf{k} \cdot \mathbf{k}' + kk')}{(\sqrt{k} - \sqrt{k'})^2 - |\mathbf{k} - \mathbf{k}'|} + \frac{(\sqrt{k} + \sqrt{k'})^2 (\mathbf{k} \cdot \mathbf{k}' - kk')}{(\sqrt{k} + \sqrt{k'})^2 - |\mathbf{k} + \mathbf{k}'|} \right. \\ \left. - \mathbf{k} \cdot \mathbf{k}' + (k + k')(kk')^{\frac{1}{2}} \right]. \quad (3.12)$$

If we take polar co-ordinates (k, θ) in the \mathbf{k} -plane and introduce the directional spectrum $F(\sigma, \theta)$ by

$$F(\sigma, \theta) d\sigma d\theta = E(\mathbf{k}) d\mathbf{k} = E(\mathbf{k}) k dk d\theta$$

so that

$$F(\sigma, \theta) = k \frac{dk}{d\sigma} E(\mathbf{k}) = \frac{k^2}{2\sigma} E(\mathbf{k}),$$

then we have

$$\kappa_2 = \iint F(\sigma, \theta) d\sigma d\theta, \quad \kappa_3 = 6 \iiint \iiint K(\mathbf{k}, \mathbf{k}') F(\sigma, \theta) F(\sigma', \theta') d\sigma d\sigma' d\theta d\theta'. \quad (3.13)$$

In the one-dimensional case when $F(\sigma, \theta)$ vanishes everywhere except when $\theta = 0$ the above expressions simplify very considerably. For when \mathbf{k}' is parallel (or anti-parallel) to \mathbf{k} we find

$$K(\mathbf{k}, \mathbf{k}') = \min(k, k')$$

and hence

$$\kappa_2 = \int F(\sigma) d\sigma, \quad \kappa_3 = 6 \iint \min(k, k') F(\sigma) F(\sigma') d\sigma d\sigma', \quad (3.14)$$

where $F(\sigma) = \int F(\sigma, \theta) d\theta$ denotes the spectral density with regard to frequency. The above expression for κ_3 may be written

$$\kappa_3 = 12 \iint_{k < k'} k F(\sigma) F(\sigma') d\sigma d\sigma' \quad (3.15)$$

$$= 12 \int_0^\infty \left[\int_0^{\sigma'} k F(\sigma) d\sigma \right] F(\sigma') d\sigma', \quad (3.16)$$

where $k = \sigma^2/g$.

Let us examine the form of $K(\mathbf{k}, \mathbf{k}')$ in the general case, when the angle between \mathbf{k} and \mathbf{k}' is equal to γ , say. Writing

$$(k + k')/2(kk')^{\frac{1}{2}} = \eta \geq 1$$

(by Schwarz's inequality) we find from (3.12) that

$$K(\mathbf{k}, \mathbf{k}') = (kk')^{\frac{1}{2}} f(\eta, \gamma), \quad (3.17)$$

$$\text{where } f(\eta, \gamma) = \frac{(\eta - 1)(1 + c)}{(\eta - 1) - (\eta^2 - \frac{1}{2} - \frac{1}{2}c)^{\frac{1}{2}}} - \frac{(\eta + 1)(1 - c)}{(\eta + 1) - (\eta^2 - \frac{1}{2} + \frac{1}{2}c)^{\frac{1}{2}}} + (2\eta - c) \quad (3.18)$$

and $c = \cos \gamma$. It can be shown that $f(\eta, \gamma)$ is non-negative. For from (3.18)

$$f(\eta, \gamma) = \frac{2(\eta - 1)(1 + c)[(\eta - 1) + (\eta^2 - \frac{1}{2} - \frac{1}{2}c)^{\frac{1}{2}}]}{- (4\eta - c - 3)} - \frac{2(\eta + 1)(1 - c)[(\eta + 1) + (\eta^2 - \frac{1}{2} + \frac{1}{2}c)^{\frac{1}{2}}]}{(4\eta - c + 3)} + (2\eta - c).$$

Since all the factors in each expression are non-negative, the two radicals may be replaced by $(\eta^2)^{\frac{1}{2}} = \eta$ without diminishing the right-hand side. After some reduction we then find

$$f(\eta, \gamma) \geq \frac{(2\eta + c)(1 - c^2)}{(4\eta - c)^2 - 9} \geq 0. \quad (3.19)$$

It follows that $K(\mathbf{k}, \mathbf{k}')$ is non-negative, and that so also is κ_3 , in the general case.

The form of $f(\eta, \gamma)$ can be seen from the curves in figure 1. The two extreme values are equal:

$$f(\eta, 0) = f(\eta, \pi) = \eta - (\eta^2 - 1)^{\frac{1}{2}}, \quad (3.20)$$

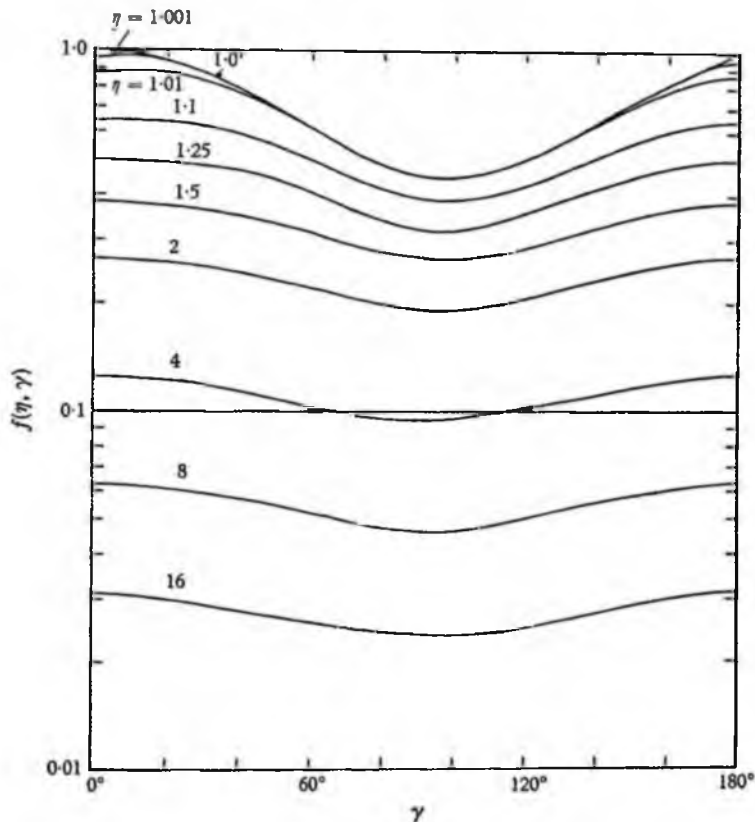


FIGURE 1. Graphs of $f(\eta, \gamma)$, defined by (3.17), for various values of η .

and for fixed values of η there is a minimum, at about $\eta = 90^\circ$. However, the curves are not symmetrical about the mid-point of the range of η . For example, $f(1, \gamma)$ has a stationary point at $\gamma = 0$ but not at $\gamma = \pi$. Further, though it appears at first sight that $f(\eta, \gamma)$ never exceeds $f(\eta, 0)$, in fact $f(\eta, \gamma)$ is an increasing function of γ when γ is small and η is very close to 1. A numerical investigation shows that

$$0.44f(\eta, 0) \leq f(\eta, \gamma) \leq 1.01f(\eta, 0) \quad (3.21)$$

over all values of γ . From (3.13) and (3.17) it then follows that in general

$$0.44I \leq \kappa_3 \leq 0.01I, \quad (3.22)$$

where I denotes the integral on the right-hand side of (3.15) or (3.16). Further, writing

$$L = I/\kappa_2^{\frac{1}{2}}, \quad (3.23)$$

we deduce the following theoretical bounds for the skewness:

$$0.44L \leq \lambda_3 \leq 1.01L. \quad (3.24)$$

In the two-dimensional case we have always

$$\lambda_3 = L. \quad (3.25)$$

It will be seen from (2.28) that the next cumulant κ_4 generally involves the third- and fourth-order terms α_{ijk} and α_{ikjk} . These can be calculated in a similar way. In general, however, they will be weakly dependent on the time t , owing to resonant interactions between the wave components ξ_i (cf. Phillips 1960; Hasselmann 1960). Moreover α_{ijk} , for example, will generally be of the same order as $\min(k_i^2, k_j^2, k_k^2)$. Hence the convergence of the corresponding integrals will depend rather critically on the behaviour of the spectral density $E(k)$ at high wave-numbers. We shall not calculate the higher-order moments here, beyond remarking that according to the present analysis κ_4 and λ_4 are proportional to $\{E(k)\}^2$ and $\{E(k)\}$, respectively. Hence if the integrals substantially converged over the region in which viscous damping was negligible then λ_4 would be of the same order as λ_3^2 .

4. Comparison with observation

An extensive study of the power spectra of water waves over short fetches, and of the corresponding statistical distribution of surface elevation, has been made by Kinsman (1960). In the second column of table 1 are shown Kinsman's observed values of κ_2 , and in the third column the value calculated from the power spectra* using equation (3.11). The first group of calculations, from records 009 to 067, are based on estimates of spectral density at frequencies of 0(0.1)2.5 c/s; the second group are based on estimates at more closely spaced intervals from 0(0.05)2.5 c/s (not available for records 009 to 028). It will be seen that the agreement between the observed and calculated values of κ_2 is within 5% except in the case of two records, 028 and 087 (for which there seems no obvious explanation). There is only a slight difference, of the order of 1%, in record 067, between the values of calculated from the less closely spaced, and from the more closely spaced, spectral estimates.

In the fourth column of table 1 are listed the values of the skewness coefficient λ_3 , as observed by Kinsman.† It will be seen at once that all except three of the observations are positive, as predicted, and of the three negative values, two are very small.

In the next column of table 1 are shown the values of L calculated from equation (3.20), that is to say the theoretical values of λ_3 if the spectrum were uni-directional. (The two theoretical estimates for record 067, which differ by about 12%, suggest that the estimates derived from the more closely spaced spectral estimates are significantly more accurate.) The ratio λ_3/L is shown in the sixth column of table 1. According to equation (3.24) this ratio should lie between 0.44 and 1.01. Out of the total of 24 records it will be seen that 18 satisfy the inequality $\lambda_3/L \leq 1.01$ and that 15 satisfy $\lambda_3/L \geq 0.44$.

In the last column of table 1 are shown the observed values of λ_4 as found by

* Kinsman tabulates $P(f)$ where f = frequency in c/s. He uses a slightly different definition of the power spectrum, so that $Pdf = \frac{1}{2}F(\sigma)d\sigma$.

† In table 5.10 of Kinsman (1960) it is $\frac{1}{2}\lambda_3$, that is tabulated.

Kinsman (who tabulates $\frac{1}{2}\lambda_4$). Although some of these values are of order λ_3^2 , as might be expected, there are several values of nearly 0.4, which is unexpectedly high. Part of the variability in λ_4 may no doubt be attributed to the finite size of the sample; but probably it reflects also the sensitivity of the integrals to the high-frequency end of the spectrum, which is not included in the measured values.

Record	κ_2 (cm ²)		λ_3 obs.	L	λ_3/L	λ_4 obs.
	obs.	th.				
009	8.45	8.30	0.344	0.284	1.21	0.092
010	8.94	8.94	0.286	0.293	0.98	-0.030
011	10.82	10.77	0.192	0.234	0.82	-0.250
012	8.45	8.46	0.364	0.273	1.33	0.202
017	3.30	3.24	0.350	0.274	1.28	0.100
018	4.12	4.09	0.438	0.257	1.70	0.366
027	3.87	3.83	0.316	0.264	1.20	-0.392
028	3.13	3.77	0.356	0.204	1.75	0.118
067	4.99	4.95	0.164	0.282	0.58	-0.014
067	4.99	5.02	0.164	0.258	0.64	-0.014
068	5.57	5.60	0.174	0.260	0.67	0.050
069	7.71	7.71	0.138	0.248	0.56	0.414
070	7.23	7.23	0.054	0.243	0.22	0.090
075	9.65	9.62	0.202	0.249	0.81	0.086
076	7.37	7.37	0.184	0.240	0.77	-0.062
081	3.46	3.40	0.058	0.169	0.34	-0.130
082	3.64	3.59	0.068	0.196	0.35	-0.232
083	7.57	7.37	-0.004	0.192	-0.02	-0.202
084	6.64	6.59	0.088	0.217	0.41	0.048
085	7.91	7.77	-0.010	0.203	-0.05	-0.448
086	7.72	7.71	0.022	0.223	0.10	-0.156
087	3.45	7.45	0.010	0.068	0.15	0.330
088	4.06	4.05	-0.092	0.177	-0.52	0.300
093	9.34	9.33	0.288	0.336	0.86	0.432
094	11.30	11.29	0.272	0.363	0.75	0.046

TABLE 1. Comparison of observed and theoretical coefficients of distributions of surface elevation.

The observed distributions $p(\xi)$ themselves have been compared by Kinsman (1960) with the expressions

$$[\exp(-\frac{1}{2}\xi^2/\kappa_2)](2\pi\kappa_2)^{-\frac{1}{2}}[1 + \frac{1}{8}\lambda_3 H_3 + \frac{1}{24}\lambda_4 H_4] \quad (4.1)$$

(see figures A III 2.01-2.24 of Kinsman 1960) and it is found that the observations are an appreciably better fit to (4.1) than to the corresponding Gaussian distributions, from which (4.1) differs by terms of order λ_3 . Equation (4.1) differs from the theoretical distribution (2.20) by the term

$$[\exp(-\frac{1}{2}\xi^2/\kappa_2)](2\pi\kappa_2)^{-\frac{1}{2}}\frac{1}{72}\lambda_3^2 H_6 \quad (4.2)$$

which is of order λ_3^2 . Since the maximum value of

$$|(2\pi)^{-\frac{1}{2}} \exp(-\frac{1}{2}\xi^2/\kappa_2) \frac{1}{72} H_6|$$

is equal to 0.083 at $\zeta = 0$, and since the maximum value of λ_3 , from table 1, is 0.438 ($\lambda_3^2 = 0.192$) it will be seen that the terms (4.2) are in fact rather small. It is found that they make no appreciable difference to the theoretical distributions (for the values of λ_3 observed) and that the agreement with observation is not significantly improved. Equation (2.20) is indeed a significant improvement over the Gaussian distribution, but this is brought about mainly by the term in λ_3 which is already included in (4.1).

5. Joint distribution of two non-linear variables

The joint distribution of two or more variables of type similar to (2.1) may be investigated in an exactly similar way. In the present section we shall evaluate the distribution for two such variables. This will enable us, in the following section, to evaluate the joint distribution of the two components of surface slope in a random sea.

Consider two variables ζ, η defined by

$$\left. \begin{aligned} \zeta &= \alpha_i \xi_i + \alpha_{ij} \xi_i \xi_j + \alpha_{ijk} \xi_i \xi_j \xi_k + \dots, \\ \eta &= \beta_i \xi_i + \beta_{ij} \xi_i \xi_j + \beta_{ijk} \xi_i \xi_j \xi_k + \dots, \end{aligned} \right\} \quad (5.1)$$

where $\alpha_i, \alpha_{ij}, \dots$ and $\beta_i, \beta_{ij}, \dots$ are constants and the ξ_i are defined as before. We denote by A_p and B_q the terms $\alpha_{ij\dots i}$ and $\beta_{ij\dots j}$ which contain respectively p and q suffices, and by $(A_p B_q \dots)$ the irreducible part of the mean product

$$\overline{(A_p \xi_i \xi_j \dots \xi_i)} \overline{(B_q \xi_i \xi_j \dots \xi_m)} \dots$$

For example

$$\left. \begin{aligned} (A_1 B_1) &= \alpha_i \beta_i V_i, & (A_1^2 B_1^2) &= 0 \quad (n+m > 2); \\ (A_1 B_1 B_2) &= 2\alpha_i \beta_j \beta_{ij} V_i V_j, & (A_1 B_3) &= 3\alpha_i \beta_{ijj} V_i V_j, \\ (A_1^2 B_2) &= 2\alpha_i \alpha_j \beta_{ij} V_i V_j. \end{aligned} \right\} \quad (5.2)$$

The the joint moments of ζ and η may be written down by inspection. Thus

$$\mu_{11} = \overline{\zeta \eta} = \sum_{p,q} [(A_p B_q) + (A_p)(B_q)],$$

$$\mu_{21} = \overline{\zeta^2 \eta} = \sum_{p,q} [(A_p A_q B_r) + (A_p A_q)(B_r) + 2(A_p)(A_q B_r) + (A_p)(A_q)(B_r)],$$

and in general

$$\mu_{n,m} = \overline{\zeta^n \eta^m} = \sum_{p,q,\dots,s} C(\omega) \omega(i_1, j_1; i_2, j_2; \dots), \quad (5.3)$$

where ω denotes a grouping of A_p, \dots, B_q, \dots into unordered sets containing i_1 of A_p and j_1 of B_q ; i_2 of A_p and j_2 of B_q ; etc., with $(i_1 + i_2 + \dots) = n$ and $(j_1 + j_2 + \dots) = m$; and ω is the number of distinct ways of choosing such a grouping.

If $p(\zeta, \eta)$ denotes the joint density of ζ and η the moment-generating function for the joint distribution is defined by

$$\phi(it, is) = \iint p(\zeta, \eta) \exp(it\zeta + is\eta) d\zeta d\eta = \sum_{i,j} \frac{\mu_{ij}}{i! j!} (it)^i (is)^j$$

and the cumulant-generating function is defined by

$$K(it, is) = \log \phi(it, is) = \sum_{(i,j) \neq (0,0)} \frac{\kappa_{ij}}{i!j!} (it)^i (is)^j,$$

where in the summation i and j take all pairs of non-negative integral values except $(i, j) = (0, 0)$. Thus we have

$$\phi(it, is) = \exp [K(it, is)] = \sum_{r=0}^{\infty} \frac{1}{r!} \left[\sum_{(i,j) \neq (0,0)} \frac{\kappa_{ij}}{i!j!} (it)^i (is)^j \right]^r$$

and by equating coefficients of $t^m s^n$ in this expression we have

$$\mu_{mn} = \sum C(i_1, j_1; i_2, j_2; \dots) \kappa_{i_1, j_1} \kappa_{i_2, j_2} \dots$$

where $C(i_1, j_1; i_2, j_2; \dots)$ is the same constant as in (5.3). Hence we have simply

$$\kappa_{ij} = \sum_{p_1, \dots, p_q, q_1, \dots, q_j} (A_{p_1} \dots A_{p_i} B_{q_1} \dots B_{q_j}). \quad (5.4)$$

In particular, $\kappa_{i0} = \kappa_i$, which is given as far as the terms in V^3 by equation (2.13). Similarly

$$\left. \begin{aligned} \kappa_{11} &= (A_1 B_1) + [(A_1 B_3) + (A_2 B_2) + (A_3 B_1)] \\ &\quad + [(A_1 B_5) + (A_2 B_4) + \dots + (A_5 B_1)], \\ \kappa_{21} &= [(A_1^2 B_2) + 2(A_1 A_2 B_1)] + [(A_1^2 B_4) + 2(A_1 A_2 B_3) \\ &\quad + 2(A_1 A_3 B_2) + (A_2^2 B_2) + 2(A_1 A_4 B_1) + 2(A_2 A_3 B_1)], \\ \kappa_{22} &= [2(A_1^2 B_1 B_3) + (A_1^2 B_2^2) + 4(A_1 A_2 B_1 B_2) + (A_2^2 B_1^2) + 2(A_1 A_3 B_1^2)], \\ \kappa_{31} &= [(A_1^3 B_3) + 3(A_1^2 A_2 B_2) + 3(A_1 A_2^2 B_1)], \end{aligned} \right\} (5.5)$$

etc. It is evident that in general κ_{ij} is of order $V^{(i+j-1)}$.

The joint density $p(\zeta, \eta)$ can now be found from

$$\begin{aligned} p(\zeta, \eta) &= \frac{1}{(2\pi)^2} \iint \phi(it, it') \exp[-i(\zeta t + \eta t')] dt dt' \\ &= \frac{1}{(2\pi)^2} \iint \exp\left[-i\zeta t - i\eta t' + \sum_{(i,j) \neq (0,0)} \frac{\kappa_{ij}}{i!j!} t^i t'^j\right] dt dt' \\ &= \frac{1}{(2\pi)^2} \iint \exp\left[\{(\kappa_{10} - \zeta) it + (\kappa_{01} - \eta) it'\} - \frac{1}{2}\{\kappa_{20} t^2 + 2\kappa_{11} tt' + \kappa_{02} t'^2\} \right. \\ &\quad \left. + \frac{1}{6}\{\kappa_{30}(it)^3 + 3\kappa_{21}(it)^2(it') + 3\kappa_{12}(it)(it')^2 + \kappa_{03}(it')^3\} + \dots\right] dt dt'. \end{aligned} \quad (5.6)$$

Writing

$$\begin{aligned} t &= u/\kappa_{20}^{\frac{1}{2}}, & (\zeta - \kappa_{10}) &= f\kappa_{20}^{\frac{1}{2}}, \\ t' &= u'/\kappa_{02}^{\frac{1}{2}}, & (\eta - \kappa_{01}) &= f'\kappa_{02}^{\frac{1}{2}}, \\ & & \lambda_{ij} &= \kappa_{ij}/(\kappa_{20}^{\frac{i}{2}} \kappa_{02}^{\frac{j}{2}})^{\frac{1}{2}}, \end{aligned}$$

and we have

$$\begin{aligned} p(\zeta, \eta) &= \frac{1}{(2\pi)^2 (\kappa_{20} \kappa_{02})^{\frac{1}{2}}} \int_{-\infty}^{\infty} \int_{-\infty}^{\infty} \exp\left[-i(fu + f'u') - \frac{1}{2}(u^2 + 2\lambda_{11} uu' + u'^2)\right] \\ &\quad \times \exp\left[\frac{1}{6}f^3\{\lambda_{30} u^3 + 3\lambda_{21} u^2 u' + \dots\} + \dots\right] du du'. \end{aligned} \quad (5.7)$$

Now

$$\begin{aligned} & \frac{1}{2\pi} \int_{-\infty}^{\infty} \int_{-\infty}^{\infty} \exp[-i(fu + f'u') - \frac{1}{2}(u^2 + 2\rho uu' + u'^2)] (iu)^m (iu')^n du du' \\ &= \frac{(-1)^{m+n}}{2\pi} \frac{\partial^m}{\partial f^m} \frac{\partial^n}{\partial f'^n} \int_{-\infty}^{\infty} \int_{-\infty}^{\infty} \exp[-i(fu + f'u') - \frac{1}{2}(u^2 + 2\rho uu' + u'^2)] du du' \\ &= \frac{(-1)^{m+n}}{(1-\rho^2)^{\frac{1}{2}}} \frac{\partial^m}{\partial f^m} \frac{\partial^n}{\partial f'^n} \exp[-\frac{1}{2}(f^2 + 2\rho ff' + f'^2)/(1-\rho^2)] \\ &= (1-\rho^2)^{-\frac{1}{2}} H_{mn}(f, f'; \rho) \exp[-\frac{1}{2}(f^2 + 2\rho ff' + f'^2)/(1-\rho^2)] \end{aligned}$$

say, where H_{mn} is a two-dimensional analogue of the Hermite polynomial. Thus

$$\left. \begin{aligned} H_{00} &= 1, \\ H_{10} &= (f - \rho f')/(1 - \rho^2)^{\frac{1}{2}}, \\ H_{01} &= (f' - \rho f)/(1 - \rho^2)^{\frac{1}{2}}, \\ H_{20} &= (f - \rho f')^2/(1 - \rho^2) - 1, \\ H_{11} &= (f - \rho f')(f' - \rho f)/(1 - \rho^2) + \rho, \\ H_{02} &= (f' - \rho f)^2/(1 - \rho^2) - 1, \end{aligned} \right\} \quad (5.8)$$

etc., and when $\rho = 0$

$$H_{nm}(f, f'; 0) \equiv H_n(f) H_m(f').$$

So writing $\lambda_{11} = \rho$ in (5.7) we have

$$p(\zeta, \eta) = \{2\pi(\kappa_{20}\kappa_{02} - \kappa_n^2)^{\frac{1}{2}}\}^{-1} \exp[-\frac{1}{2}(f^2 + 2\rho ff' + f'^2)/(1-\rho^2)] \times [1 + \frac{1}{2}(\lambda_{30}H_{30} + 3\lambda_{21}H_{21} + \dots) + \dots]. \quad (5.9)$$

In the first approximation, when terms of order $V^{\frac{1}{2}}$ are neglected,

$$p(\zeta, \eta) = \{2\pi(\kappa_{20}\kappa_{02} - \kappa_{11}^2)^{\frac{1}{2}}\}^{-1} \exp[-\frac{1}{2}(f^2 + 2\rho ff' + f'^2)/(1-\rho^2)],$$

where $f = \zeta/\kappa_{20}^{\frac{1}{2}}$, $f' = \eta/\kappa_{02}^{\frac{1}{2}}$ and

$$\kappa_{20} = \alpha_i \alpha_i, \quad \kappa_{02} = \beta_i \beta_i, \quad \kappa_{11} = \alpha_i \beta_i.$$

This is the familiar Gaussian bivariate distribution.

In the second approximation, taking into account $V^{\frac{1}{2}}$ but neglecting V , the mean of the distribution is shifted to

$$(\bar{\zeta}, \bar{\eta}) = (\kappa_{10}, \kappa_{01})$$

and the abscissa is multiplied by the factor

$$[1 + \frac{1}{2}(\lambda_{30}H_{30} + 3\lambda_{21}H_{21} + \dots)]$$

introducing various kinds of skewness, specified by the parameters λ_{30} , λ_{21} , λ_{12} and λ_{03} .

6. Application to the distribution of surface slopes

We shall now apply the results of the last section to evaluate the joint distribution of the two components of slope of a random sea surface.

Suppose that the surface elevation is given by equation (2.1). Then on partial differentiation with respect to x and y respectively we have

$$\left. \begin{aligned} \partial \zeta / \partial x &= \beta_i \xi_i + \beta_{ij} \xi_i \xi_j + \dots, \\ \partial \zeta / \partial y &= \gamma_i \xi_i + \gamma_{ij} \xi_i \xi_j + \dots, \end{aligned} \right\} \quad (6.1)$$

where, if (u_i, v_i) denote the components of the wave-number \mathbf{k}_i , we have

$$\beta_i = \alpha_i u_i, \quad \gamma_i = \alpha_i v_i.$$

Using the form of α_i as given by equation (3.3) we see that β_i and γ_i , when expressed as vectors, have the form

$$\left. \begin{aligned} (\beta_i) &= (0, 0, \dots, 0; -u_1, -u_2, \dots, -u_N), \\ (\gamma_i) &= (0, 0, \dots, 0; -v_1, -v_2, \dots, -v_N). \end{aligned} \right\} \quad (6.2)$$

Similarly from (3.9) we see that β_{ij} , when expressed as a matrix, has the form

$$(\beta_{ij}) = \begin{pmatrix} \mathbf{0} & \mathbf{M} \\ \mathbf{M}' & \mathbf{0} \end{pmatrix}, \quad (6.3)$$

where

$$\mathbf{M} = \begin{pmatrix} (u_1 \alpha_{N+1, N+1} - u_1 \alpha_{11}) & \dots & (u_1 \alpha_{N+1, 2N} - u_N \alpha_{1, N}) \\ \vdots & & \vdots \\ (u_N \alpha_{2N, N+1} - u_1 \alpha_{N, 1}) & \dots & (u_N \alpha_{2N, 2N} - u_N \alpha_{N, N}) \end{pmatrix}; \quad (6.4)$$

(γ_{ij}) has an exactly similar form, except that v_i replaces u_i .

Let C_r denote the term $\gamma_{ij\dots n}$ which contains just r suffices. We see now that the results of §6 are applicable to the two non-linear variables $\partial\zeta/\partial x$, $\partial\zeta/\partial y$ provided that we replace A_p, B_q by B_p, C_q , respectively. In particular we have for the first few cumulants of the joint distribution (retaining only the lowest-order terms) the following: for the second-order cumulants

$$\left. \begin{aligned} \kappa_{20} &= (B_1^2) = u_i^2 V_i = \iint u^2 E(\mathbf{k}) d\mathbf{k}, \\ \kappa_{11} &= (B_1 C_1) = u_i v_i V_i = \iint uv E(\mathbf{k}) d\mathbf{k}, \\ \kappa_{02} &= (C_1^2) = v_i^2 V_i = \iint v^2 E(\mathbf{k}) d\mathbf{k}. \end{aligned} \right\} \quad (6.5)$$

Each of these is proportional to $E(\mathbf{k})$ (or V). In the expressions for the *third-order* cumulants $\kappa_{30}, \kappa_{21}, \kappa_{12}, \kappa_{03}$ it will be seen from (6.2) and (6.3) that all the leading terms vanish identically,

$$(B_1^2 B_2) = (B_1^2 C_2) = (C_1^2 B_2) = (C_1^2 C_2) = 0.$$

Hence in the joint distribution of the surface slopes, the *third-order cumulants are of order V^3 at least*. The terms of next lowest order are

$$\left. \begin{aligned} \kappa_{30} &= 3(B_1^2 B_4) + 6(B_1 B_2 B_3), \\ \kappa_{21} &= (B_1^2 C_4) + 2(B_1 B_2 C_3) + 2(B_1 B_3 C_2) + 2(B_1 B_4 C_1) + 2(B_2 B_3 C_1), \end{aligned} \right\} \quad (6.6)$$

with similar expressions for κ_{12} and κ_{03} .

If the distribution of slopes were symmetrical about the mean, then clearly all cumulants of odd order, such as the third-order cumulants, would necessarily vanish identically. This would certainly follow if, for example, it were possible to reverse the direction of time (so that forward slopes became rear slopes, and vice versa) without altering the statistics of the surface. However, we know in

fact that the time cannot be reversed, even for free, undamped waves, for it has been shown that there exists a slow transfer of energy from one part of the spectrum to another (Phillips 1960; Hasselmann 1960). This transfer is represented by certain terms of the third-order which occur in A_3 and hence in B_3 and C_3 .* Since either B_3 or C_3 occur in (6.6) we expect that the third-order cumulants are indeed of order V^3 .

Similarly from (5.5) we have for the leading terms in the cumulants of fourth order

$$\left. \begin{aligned} \kappa_{40} &= 4(B_1^3 B_3) + 6(B_1^2 B_2^2), \\ \kappa_{31} &= (B_1^3 C_3) + 3(B_1 B_2^2 C_1), \\ \kappa_{22} &= (B_1^2 C_2^2) + 2(B_1^2 C_2 C_3) + 4(B_1 B_2 C_1 C_2) + 2(B_1 B_3 C_1^2) + (B_2^2 C_1^2), \end{aligned} \right\} \quad (6.7)$$

etc. These also are of order V^3 .

It follows that the coefficients of skewness

$$\lambda_{30} = \kappa_{30}/(\kappa_{20})^{\frac{3}{2}}, \quad \lambda_{21} = \kappa_{21}/\kappa_{20}\kappa_{02}, \quad \text{etc.},$$

are each of order $V^{\frac{3}{2}}$ in general, and that the coefficients of kurtosis

$$\lambda_{40} = \kappa_{40}/\kappa_{20}^2, \quad \lambda_{31} = \kappa_{31}/\kappa_{20}^{\frac{3}{2}}\kappa_{02}, \quad \text{etc.},$$

are each of order V .

It should be emphasized that the present model of the sea surface is a model of 'free' waves, in which not only is the viscous damping neglected but it is also assumed that the stresses at the free surface are identically zero. On the other hand, both the viscosity, and also the stresses due to the action of the atmosphere on the surface, may be expected to produce some asymmetry in the wave profile. Since for free waves the skewness is theoretically of such a high order, $\sim (\kappa_{20} + \kappa_{02})^{\frac{3}{2}}$, the actual skewness of sea waves may be a rather sensitive indicator of energy transfer to the water, or dissipation of energy in the medium.

7. Comparison with observation

It follows that in any comparison of the theoretical results with observation, some consideration must be given to whether the conditions of the theory (i.e. free, undamped surface waves) are actually satisfied. If there is any appreciable transfer of energy from the atmosphere to the sea surface, or if there is a considerable contribution to the slope distribution from the very short waves, which are the most highly damped, then the free-wave model cannot be expected to apply.

In model experiments, Cox (1958) has shown that in winds of between 3 and 12 m/sec a large part of the contribution to the mean square slope (observed optically) is associated with frequencies above 10 c/s, and hence with waves that are influenced predominantly by surface tension.† If the analysis of the preceding section were modified so as to include the effect of surface tension, it would still be found that the third-order cumulants were of fourth order in the wave amplitudes. On the other hand it is unlikely that, even with surface tension

* If the spectrum is one-dimensional, these terms vanish.

† The frequency of waves having the minimum phase-velocity is about 11 c/s.

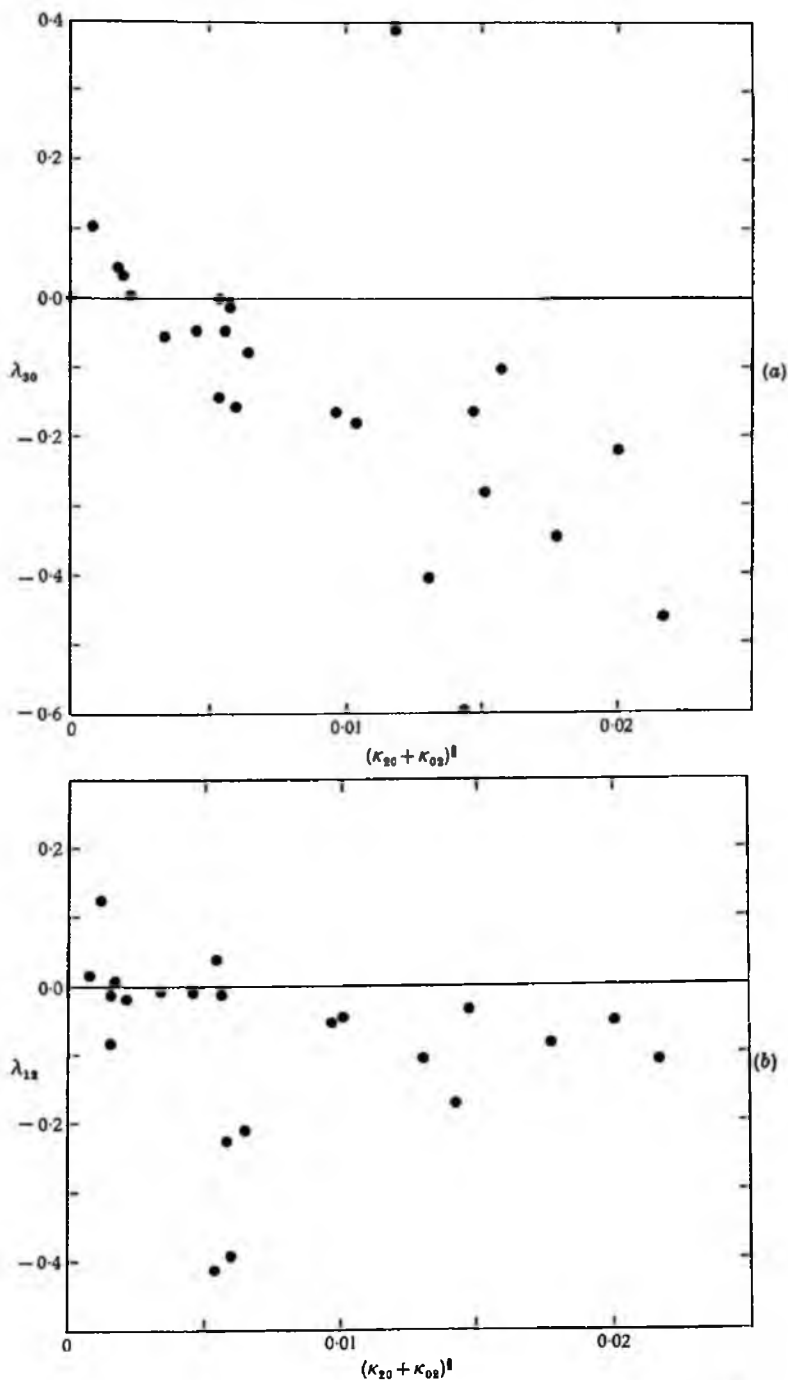


FIGURE 2. Observed values of the coefficients of skewness, plotted against (mean-square slope)^{1/2}, from the data of Cox & Munk (1956).

included, the perturbation analysis of § 5 would apply in such a situation, for the following reasons.

First, as the wavelength decreases, the short waves become increasingly influenced by viscosity, the time-constant being equal to $(2\nu k^2)^{-1}$ or about $0.71\lambda^2$ where λ is the wavelength in cm (see Lamb 1932, § 348). In § 5 this damping was entirely neglected.

Secondly, it is unlikely that a linear first approximation is appropriate when the wavelengths and time-constants of the short waves are small compared with the orbital displacements and the periods of the longer waves. It is known also that there is a direct transfer of energy to capillary waves from the steep crests of the gravity waves (Longuet-Higgins 1963), which can hardly be described in terms of the linear perturbation scheme.

Thirdly, the direct action of the airflow over the water surface, which is perhaps most important at high frequencies, has been neglected.

Hence the conclusions of § 5 cannot be expected to apply to the observed slope distribution, certainly if the wind exceeds 3.18 m/sec and probably if it exceeds the minimum phase-velocity of 19 cm/sec. An exception may occur in the presence of oil slicks, which are known to remove the energy in the highest wave-numbers.

In the measurements of surface slope made by Cox & Munk (1956), the local wind-speed ranged from 72 to 1380 cm/sec. Nevertheless, using the data given in table 1 of Cox & Munk's paper we have calculated the coefficients of skewness in terms of the quantities defined in their paper, that is (if the x -axis is taken in the direction of the wind):

$$\left. \begin{aligned} \lambda_{30} &= c_{03} = -6\sigma_u^3(a'_1 + a_3), \\ \lambda_{12} &= c_{21} = -2\sigma_w\sigma_c^2(a'_1 - 3a_3). \end{aligned} \right\} \quad (7.1)$$

Also

$$\kappa_{20} = \sigma_w^2, \quad \kappa_{02} = \sigma_c^2. \quad (7.2)$$

A plot of λ_{30} and λ_{12} against $(\kappa_{20} + \kappa_{02})^{\frac{3}{2}}$ is shown in figure 2(a) and (b), for those cases when the sea surface was free of slicks.

From figure 2(a) it does appear that λ_{30} is approximately proportional to $(\kappa_{20} + \kappa_{02})^{\frac{3}{2}}$, as predicted. However, since the order of magnitude of λ_{30} is about twenty times that of $(\kappa_{20} + \kappa_{02})^{\frac{3}{2}}$ it appears more likely that the theory does not really apply to these observations.

On the other hand, Cox & Munk observed that in the presence of oil slicks the coefficients of skewness were very greatly reduced, and were in fact so small as not to be measurable by their technique. Though not conclusive, this observation is certainly consistent with the theoretical result.

8. Conclusions

We have rederived the statistical distribution of weakly non-linear variables of the type given by equation (2.1) or equations (5.1). The distribution of such quantities is shown to be Gaussian in the first approximation, and in successively higher approximations to be given by Edgeworth's form of a Gram-Charlier series, as in equations (2.20) and (5.9), respectively. These series differ from the

series used, for example, by Kinsman and by Cox & Munk as empirical fits to observed data, but the differences occur only in the third and higher approximations; they are practically negligible in the cases considered.

The coefficients in the distribution depend essentially on the cumulants of the original variables, which can be calculated simply in terms of the constants in (2.1) or (5.1). If one assumes that the sea surface consists of free, undamped waves then it can be shown that the skewness of the surface elevation is always positive and lies between the two bounds (3.24). This agrees, for the most part, with Kinsman's observations. The skewness increases proportionally to the r.m.s. surface slope s . On the other hand the skewness of the *slope* distribution is of a higher order and increases proportionally to s^3 . While this prediction is consistent with the observations of Cox & Munk, nevertheless, if the local wind is appreciable the skewness may be largely affected by energy transfer from air to water, and by viscous dissipation.

I am indebted to Dr K. Hasselmann and Dr C. S. Cox for valuable comments on a first draft of this paper, and to Mr C. L. Gulliver and Mrs W. Wilson for assistance with the calculations for table 1 and the diagrams.

REFERENCES

- BARBER, N. F. 1950 Ocean waves and swell. Lecture, *Inst. Elec. Eng., London*.
- BIREHOFF, G. & KOTIK, J. 1952 Fourier analysis of wave trains. *Proc. Symp. Gravity Waves, Nat. Bur. Stand., Circular 521*, 221-34.
- BURLING, R. W. 1955 Wind generation of waves on water. Ph.D. Thesis, London University.
- COX, C. S. 1958 Measurements of slopes of high-frequency wind waves. *J. Mar. Res.* 16, 199-225.
- COX, C. & MUNK, W. 1956 Slopes of the sea surface deduced from photographs of sun glitter. *Bull. Scripps Instn Oceanogr.* 6, 401-88.
- EDGEWORTH, F. Y. 1906a The law of error. *Trans. Camb. Phil. Soc.* 20, 36-65.
- EDGEWORTH, F. Y. 1906b The law of error. Part II. *Trans. Camb. Phil. Soc.* 20, 113-41.
- EDGEWORTH, F. Y. 1906c The generalised law of error, or law of great numbers. *J.R. Statist. Soc.* 69, 497-530.
- HASSELMANN, K. 1960 Grundgleichungen der Seegangsvoraussage. *Schiffstechnik*, 7, 191-5.
- HASSELMANN, K. 1961 On the non-linear energy transfer in a wave spectrum. *Proc. Conf. Ocean Wave Spectra*, Easton, Md.
- HASSELMANN, K. 1962 On the non-linear energy transfer in a gravity-wave spectrum. Part I. General theory. *J. Fluid Mech.* 12, 481-500.
- KENDALL, M. G. & STUART, A. 1958 *The Advanced Theory of Statistics*, Vol. 1. London: Griffin & Co.
- KINSMAN, B. 1960 Surface waves at short fetches and low wind speed—a field study. *Chesapeake Bay. Inst., Tech. Rep.* no. 19.
- LAMB, H. 1932 *Hydrodynamics*, 6th ed. Cambridge University Press.
- LONGUET-HIGGINS, M. S. 1963 The generation of capillary waves by steep gravity waves. *J. Fluid Mech.* 16, 138-59.
- MACKAY, J. H. 1959 On the gaussian nature of ocean waves. *Tech. Note*, no. 8, Engng Exp. Sta., Georgia Inst. Tech.
- O'BRIEN, E. & FRANCIS, G. E. 1962 A consequence of the zero fourth cumulant approximation. *J. Fluid Mech.* 13, 369-382.

M. S. Longuet-Higgins

- PHILLIPS, O. M. 1960 On the dynamics of unsteady gravity waves of finite amplitude. Part 1. The elementary interactions. *J. Fluid Mech.* **9**, 193-217.
- PHILLIPS, O. M. 1961 On the dynamics of unsteady gravity waves of finite amplitude. Part 2. Local properties of a random wave field. *J. Fluid Mech.* **11**, 143-55.
- PIERSON, W. J. 1955 Wind-generated gravity waves. *Advanc. Geophys.* **2**, 93-178.
- RUDNICK, P. 1950 Correlograms for Pacific Ocean waves. *Proc. 2nd Berkeley Symp. Math. Stat. Prob.*, pp. 627-38. University of California Press.
- SCHOOLEY, A. H. 1955 Curvature distributions of wind-created water waves. *Trans. Amer. Geophys. Un.* **36**, 273-8.
- TIOK, L. J. 1959 A non-linear random model of gravity waves, I. *J. Math. Mech.* **8**, 643-52.
- TIOK, L. J. 1961 Non-linear probability models of ocean waves. *Proc. Conf. Ocean Wave Spectra*, Easton, Md.

Modified Gaussian Distributions for Slightly Nonlinear Variables

M. S. Longuet-Higgins

National Institute of Oceanography, Wormley, Surrey, England

(Received December 27, 1963)

Many random variables are almost linear, in the sense that they can be represented approximately as the sum of independent components in random phase. Such variables (for example, the surface elevation in a random sea) may have a gaussian distribution in the first approximation. However in higher approximations the phases of the different components become correlated, due to nonlinear interactions. The purpose of this paper is to show theoretically what is the effect of such nonlinearities on the basic gaussian distribution.

The modified distribution is derived both for a single variable and for two or more related variables (such as the components of slope of a random surface). The results are applied in the first place to sea waves, and are compared with observations. However the analysis is applicable quite generally to any such nonlinear variables.

Two further problems are solved for weakly nonlinear variables: the mean number of zeros per unit time of a stationary random function $\zeta(t)$ and the distribution of the maximum values of $\zeta(t)$. These solutions are essentially generalizations of the well-known results of Rice for gaussian variables.

1. Introduction

Many random variables occurring in physical problems may be considered as the sum of a large number of independent components; thus we write

$$\zeta = \sum_{i=1}^N \alpha_i \xi_i \quad (1)$$

where the α_i are constants and the ξ_i are independent random variables symmetrically distributed about 0 with variance V_i , say. Under certain conditions as $N \rightarrow \infty$ and each $V_i \rightarrow 0$, the distribution of ζ tends to a gaussian distribution with variance $\sum V_i$.

In particular it is possible to consider some stationary stochastic processes as the limit of a sum such as (1), the ξ_i being components corresponding to particular frequencies σ_i or wave numbers k_i ; there may exist a continuous function $E(\sigma)$, the spectral density of ζ , such that in any small interval $(\sigma, \sigma + d\sigma)$ the sum of the variances V_i is given by

$$\lim_{N \rightarrow \infty} \left(\sum_{\sigma < \sigma_i < \sigma + d\sigma} V_i \right) = E(\sigma) d\sigma + o(d\sigma)^2.$$

Such a representation (equivalent to a stochastic integral) has been widely used in the theory of noise in electrical circuits [Rice, 1944 and 1945], in the theory of random sea surfaces, microseisms, turbulence, and other physical phenomena [Longuet-Higgins, 1960]. The representation gives most satisfactory results when the variable ζ satisfies a linear differential equation and can be shown physically to be the resultant of large number of independent contributions.

In some instances, however, the assumption of linearity is only approximately justified, and the variable in question may actually satisfy a nonlinear differential equation whose nonlinear terms are small but not completely negligible. Such is the case with variables ζ associated with sea waves. The distribution $p(\zeta)$ is then nearly gaussian, but not exactly so. The question we wish to discuss is: what is the effect of the nonlinearities on $p(\zeta)$, and how can they be calculated in terms of the differential equation satisfied by ζ ?

In a recent paper [Longuet-Higgins, 1963], the representation (1) was generalized in the following way. Consider the variable

$$\zeta = \alpha_i \xi_i + \alpha_{ij} \xi_i \xi_j + \alpha_{ijk} \xi_i \xi_j \xi_k + \dots \quad (2)$$

where the α_i , α_{ij} , α_{ijk} , etc., are constants and the ξ_i as before are independent random variables with variance V_i . (The repetition of any subscript will be taken to imply summation.) If the α_i are given, then by substitution in the differential equation for ζ it may be possible to determine by successive approximation the values of α_{ij} , α_{ijk} , etc. Assuming that these are bounded, then as $N \rightarrow \infty$ the contributions to ζ from successive terms in the series can be expected to be of decreasing order of magnitude.

To calculate $p(\zeta)$ from (2) it is assumed that $p(\zeta)$ is uniquely determined by the sequence of its cumulants, which can be found from (2) to any order required.

This generalization¹ of the representation (1) leads to a distribution $p(\zeta)$ which is a generalization of the gaussian distribution; in fact it is the gaussian distribution multiplied by a sequence of Hermite polynomials, of increasing degree but decreasing order of magnitude. The series may be only valid asymptotically, and nonuniformly with ζ . Nevertheless when applied to sea waves the second approximation has been shown in [Longuet-Higgins, 1963] to give reasonably good agreement with observation.

In the present paper what we propose to do is to state without detailed proof the general results of Longuet-Higgins [1963], and then to apply the results to the solution of two related problems: to determine (a) the mean number of zero-crossings of ζ per unit time and (b) the distribution of the values of ζ at a maximum.

2. Distribution of a Single Variable

We may start by writing down the moments of $p(\zeta)$. Thus taking mean values in (2) one has

$$\bar{\zeta} = \alpha_i \bar{\xi}_i + \alpha_{ij} \bar{\xi}_i \bar{\xi}_j + \alpha_{ijk} \bar{\xi}_i \bar{\xi}_j \bar{\xi}_k + \dots$$

The mean values of all odd-order terms vanish, while in the terms of even order only those remain in which each ξ_i is paired with a similar ξ_i . Thus

$$\bar{\zeta} = \alpha_i V_i + 3\alpha_{ijj} V_i V_j + \dots$$

it being assumed that the α 's are symmetric in their suffices. Terms involving $\bar{\xi}^4$, $\bar{\xi}^6$, etc. are assumed to become negligible in the limit as $N \rightarrow \infty$. Similarly since

$$\zeta^2 = (\alpha_i \xi_i + \alpha_{ij} \xi_i \xi_j + \dots)(\alpha_k \xi_k + \alpha_{kl} \xi_k \xi_l + \dots)$$

we have on taking mean values

$$\bar{\zeta}^2 = \alpha_i \alpha_i V_i + (2\alpha_{ij} \alpha_{ji} + \alpha_{ijj} \alpha_{jii}) V_i V_j + 6\alpha_{ijj} \alpha_{jii} V_i V_j + \dots$$

and so on for higher moments. Now some of the terms in the last expression can be factorized, e.g.,

$$\alpha_{ij} \alpha_{jj} V_i V_j = (\alpha_{ii} V_i) (\alpha_{jj} V_j)$$

while others, e.g., $\alpha_{ij} \alpha_{jii} V_i V_j$, cannot. We call terms which cannot be factorized "irreducible". For simplicity the following notation is introduced. $\alpha_{ij \dots i}$ is denoted simply by A_i , where i is the number of suffices i, j, \dots, l ; and the sum of all irreducible terms in the product

¹ A less direct approach is suggested by Wiener [1958]. It should be noted that in the present paper the individual ξ_i are not assumed necessarily to be gaussian.

$$\overline{(A_p \xi_{i_1} \dots \xi_{i_p})(A_q \xi_{j_1} \dots \xi_{j_q}) \dots (A_s \xi_{i_1} \dots \xi_{i_s})}$$

is denoted by $(A_p A_q \dots A_s)$. Then we have

$$\bar{\xi} = \sum_p (A_p)$$

$$\bar{\xi}^2 = \sum_{p,q} [(A_p A_q) + (A_p)(A_q)]$$

etc. However, much simpler than the moments of $p(t)$ are the cumulants κ_n , defined by

$$\int_{-\infty}^{\infty} p(t) e^{it} dt = \exp \left[\frac{K_1}{1!} (it) + \frac{K_2}{2!} (it)^2 + \dots \right]. \quad (3)$$

We have

$$K_1 = \bar{\xi} = \sum_p (A_p)$$

$$K_2 = \bar{\xi}^2 - (\bar{\xi})^2 = \sum_{p,q} (A_p A_q)$$

and in general it can be shown that [Lougnet-Higgins, 1963]

$$\kappa_n = \sum_{p,q,\dots,s} (A_p A_q \dots A_s) \quad (4)$$

where p, q, \dots, s run through all values from 1 to ∞ independently. Thus if we retain terms up to the third order in the V , we have

$$\left. \begin{aligned} K_1 &= (A_2) + (A_4) + (A_6) \\ K_2 &= (A_1^2) + (A_2^2) + (A_3^2) + 2(A_1 A_3) + 2(A_1 A_5) + 2(A_2 A_4) \\ K_3 &= (A_3^3) + 3(A_1^2 A_2) + 3(A_1^2 A_4) + 6(A_1 A_2 A_3) \\ K_4 &= (A_4^4) + 4(A_1^3 A_3) + 6(A_1^2 A_2^2) \end{aligned} \right\} \quad (5)$$

We see that K_1 and K_2 are both of order V in general, but when $n \geq 2$ the lowest nonvanishing term in κ_n is $O(V^{n-1})$. If we define the coefficients

$$\begin{aligned} \lambda_3 &= K_3/K_2^{3/2} \\ \lambda_4 &= K_4/K_2^2 \end{aligned} \quad (6)$$

and generally

$$\lambda_n = K_n/K_2^{n/2} \quad (7)$$

we see that λ_n is of order V^{n-1} in general.

The density $p(t)$ is now found by inverting the expression (3):

$$p(t) = \frac{1}{2\pi} \int_{-\infty}^{\infty} \exp \left[\frac{K_1}{1!} (it) + \frac{K_2}{2!} (it)^2 + \dots \right] e^{-it} dt:$$

Writing

$$\frac{\xi - K_1}{K_2^{1/2}} = f \quad (8)$$

we find [Longuet-Higgins, 1963] that

$$p(\zeta) = \frac{e^{-\zeta^2}}{(2\pi K_2)^{1/2}} \left[1 + \frac{1}{6} \lambda_3 H_3 + \left(\frac{1}{24} \lambda_4 H_4 + \frac{1}{72} \lambda_3^2 H_2 \right) + \dots \right] \tag{9}$$

where $H_n(\zeta)$ denotes the Hermite polynomial of degree n :

$$H_n = f^n - \frac{n(n-1)}{1!} \frac{f^{n-2}}{2} + \frac{n(n-1)(n-2)(n-3)}{2!} \frac{f^{n-4}}{2^2} - \dots \tag{10}$$

This is the required distribution. In the first approximation $\lambda_3, \lambda_4, \dots$ are neglected and the distribution is gaussian with mean K_1 and variance K_2 . In the next approximation a term $\lambda_3 H_3$ is included, where H_3 is the cubic polynomial $(f^3 - 3f)$. In the third approximation the quartic polynomial H_4 and the sextic polynomial H_2 are both involved. Higher approximations can be written down at will.

Equation (9) will be recognized as essentially similar to Edgeworth's form of the Gram-Charlier distribution [Edgeworth, 1906].

3. Application to a Stochastic Variable

Suppose now that the variable ζ is a stationary random function of the space coordinate \mathbf{x} and the time t , satisfying a nonlinear partial differential equation (or boundary condition) in \mathbf{x} and t . How is the distribution $p(\zeta)$ related to the spectral density of ζ ?

Let the equation satisfied by ζ be represented symbolically by

$$L(\zeta) + Q(\zeta) + C(\zeta) + \dots = 0 \tag{11}$$

where L, Q, C , etc., represent operators that are linear, quadratic, cubic, etc., in ζ . To solve (11) for small perturbations we naturally substitute

$$\zeta = \epsilon \zeta^{(1)} + \epsilon^2 \zeta^{(2)} + \epsilon^3 \zeta^{(3)} + \dots, \tag{12}$$

where ϵ is a small parameter. Writing (11) in the form

$$L(\zeta) = -Q(\zeta) - C(\zeta) - \dots \tag{13}$$

and equating coefficients of $\epsilon, \epsilon^2, \epsilon^3, \dots$ on the two sides of the equation we have successively

$$L(\zeta^{(1)}) = 0 \tag{14}$$

$$L(\zeta^{(2)}) = -Q(\zeta^{(1)}) \tag{15}$$

$$L(\zeta^{(3)}) = -Q(\zeta^{(1)}, \zeta^{(2)}) - C(\zeta^{(1)}) \tag{16}$$

etc., where $Q(\zeta^{(1)}, \zeta^{(2)})$ denotes an expression that is bilinear in $\zeta^{(1)}$ and $\zeta^{(2)}$. If there are wave-like solutions to (14) then we can write

$$\zeta^{(1)} = \sum_{n=1}^{N'} a_n \cos(\mathbf{k}_n \cdot \mathbf{x} - \sigma_n t + \theta_n) \tag{17}$$

where a_n and θ_n are amplitude and phase constants and \mathbf{k}_n and σ_n are wave numbers and frequencies respectively. Generally (14) implies a relation between \mathbf{k}_n and σ_n . Thus in the case of gravity waves on water we have

$$\sigma_n^2 = g|k_n|.$$

Now (17) can be written

$$\zeta^{(1)} = \sum_{n=1}^{N'} \{ a_n \cos \theta_n \cos(\mathbf{k}_n \cdot \mathbf{x} - \sigma_n t) + a_n \sin \theta_n \sin(\mathbf{k}_n \cdot \mathbf{x} - \sigma_n t) \}.$$

If now we suppose that $a_n \cos \theta_n$, $a_n \sin \theta_n$ are normally and independently distributed then we have

$$\zeta^{(1)} = \sum_{n=1}^{2N'} \alpha_n \xi_n$$

where

$$\left. \begin{aligned} \xi_n &= a_n \cos \theta_n, & \alpha_n &= \cos(\mathbf{k}_n \cdot \mathbf{x} - \sigma_n t) \\ \xi_{N+n} &= a_n \sin \theta_n, & \alpha_{N+n} &= \sin(\mathbf{k}_n \cdot \mathbf{x} - \sigma_n t) \end{aligned} \right\} n=1, N'.$$

Thus $\zeta^{(1)}$ is expressed in the same form as in (1).

To find $\zeta^{(2)}$ we now substitute for $\zeta^{(1)}$ in (15). Since the terms on the right are quadratic they can in general be expressed as a series of sum or difference wave numbers, i.e., harmonic terms in $\{(\mathbf{k}_n \pm \mathbf{k}_m)x - (\sigma_n \pm \sigma_m)t\}$. Hence we can in general find expressions for $\zeta^{(2)}$. On writing the solutions again as products of the original harmonics constituents we find

$$\zeta^{(2)} = \sum_{n, m} \alpha_{n, m} \xi_n \xi_m.$$

Thus $\zeta^{(1)} + \zeta^{(2)}$ has the form of (2), as far as the second-order terms. The evaluation of $\zeta^{(2)}$, etc., proceeds similarly.

The application to gravity waves on water is given in Longuet-Higgins [1963]. It is convenient to use the assumption of homogeneity so that we can consider the waves at the special point $x=0$ and time $t=0$. That is, we may take

$$\alpha_i = \begin{cases} 1, & i=1, 2, \dots, N' \\ 0, & i=N'+1, \dots, 2N' \end{cases}.$$

Then for gravity waves it is found that

$$\alpha_{ij} = \begin{cases} \frac{1}{\sqrt{k_i k_j}} (B_{ij}^- + B_{ij}^+ - \mathbf{k}_i \cdot \mathbf{k}_j + (k_i + k_j)\sqrt{k_i k_j}), & i, j=1, \dots, N' \\ \frac{1}{\sqrt{k_i k_j}} (B_{ij}^- - B_{ij}^+ - k_i k_j), & i, j=N'+1, \dots, N \\ 0 \end{cases}$$

where

$$B_{ij}^- = \frac{(\sqrt{k_i} - \sqrt{k_j})^2 (\mathbf{k}_i \cdot \mathbf{k}_j + k_i k_j)}{(\sqrt{k_i} - \sqrt{k_j})^2 - |\mathbf{k}_i - \mathbf{k}_j|},$$

$$B_{ij}^+ = \frac{(\sqrt{k_i} + \sqrt{k_j})^2 (\mathbf{k}_i \cdot \mathbf{k}_j - k_i k_j)}{(\sqrt{k_i} + \sqrt{k_j})^2 - |\mathbf{k}_i + \mathbf{k}_j|}.$$

The diagonal terms α_{ii} are simply given by

$$\alpha_{ii} = \begin{cases} k_i, & i=1, \dots, N', \\ -k_i, & i=N'+1, \dots, N. \end{cases}$$

So we find, for example, that, to the second order of approximation

$$K_1 = \alpha_{ii} V_i = \sum_{i=1}^{N'} k_i V_i + \sum_{i=N'+1}^N (-k_i) V_i = 0 \quad (18)$$

as was to be expected; while

$$K_2 = \alpha_{ii} \alpha_{ij} V_i = \sum_{i=1}^{N'} V_i = \iint E(\mathbf{k}) d\mathbf{k} \quad (19)$$

and

$$\begin{aligned}
 K_3 &= 6 \alpha_i \alpha_j \alpha_k V_i V_j V_k \\
 &= 6 \sum_{i,j=1}^{N'} \alpha_{ij} V_i V_j \\
 &= 6 \iiint K(\mathbf{k}, \mathbf{k}') E(\mathbf{k}) E(\mathbf{k}') d\mathbf{k} d\mathbf{k}'
 \end{aligned} \tag{20}$$

where K is a function of \mathbf{k} and \mathbf{k}' .

In the special case when the waves travel all in the same direction the above expressions become very simple, and it turns out that

$$K(k, k') = \min(k, k').$$

Hence introducing the frequency spectrum $F(\sigma)$ of ζ we have

$$K_2 = \int F(\sigma) d\sigma \tag{21}$$

$$\begin{aligned}
 K_3 &= 6 \iint \min(k, k') F(\sigma) F(\sigma') d\sigma d\sigma' \\
 &= 12 \int_0^\infty \left\{ \int_0^{\sigma'} \frac{\sigma^2}{g} F(\sigma) d\sigma \right\} F(\sigma') d\sigma'
 \end{aligned} \tag{22}$$

since $k = \sigma^2/g$.

Returning to the general case, when the waves are not unidirectional, it can be shown that the expression on the right of (22), which we denote by I , is related to K_3 by the inequalities

$$0.44 I \leq K_3 \leq 1.01 I.$$

Combined with (21) this gives us bounds for the skewness coefficient $\lambda_3 = K_3/K_2^3$, in terms of the frequency spectrum $F(\sigma)$ and irrespective of the directional properties of the spectrum.

These results have been compared with the observations of Kinsman [1960; Longuet-Higgins, 1963]. It is found that the inequality on the skewness is satisfied in most cases of observed wave spectra.

Some observed distributions of wave height have been compared by Kinsman with a Gram-Charlier distribution based on the measured coefficients of skewness and kurtosis. As shown in figure 1, these are a better fit to the observations than the simple uncorrected gaussian distribution. Kinsman's suggested distribution differs from the form of the Gram-Charlier distribution found in section 2 of this paper, since it does not include a term in H_6 . Nevertheless the difference resulting from the terms in H_4 and H_6 is so small in his measurements that the correction is essentially given by the second term $\lambda_3 H_3$. Hence his figure can be used effectively as an assessment of the present theory.

If one attempts to carry the formal calculation of the moments to third and higher approximations in the application to water waves, the calculation breaks down. This is because of the occurrence of resonant interactions at the third approximation [Phillips, 1960; Hasselmann, 1962; and Benney, 1962], which render some of the third-order terms α_{ijk} in the series (2) slowly dependent on the time t . Thus the present method of calculation is consistent only as far as the second approximation in water waves.

In general, however, there seems no reason why the process should not be carried further and the higher-order terms in (2) be evaluated.

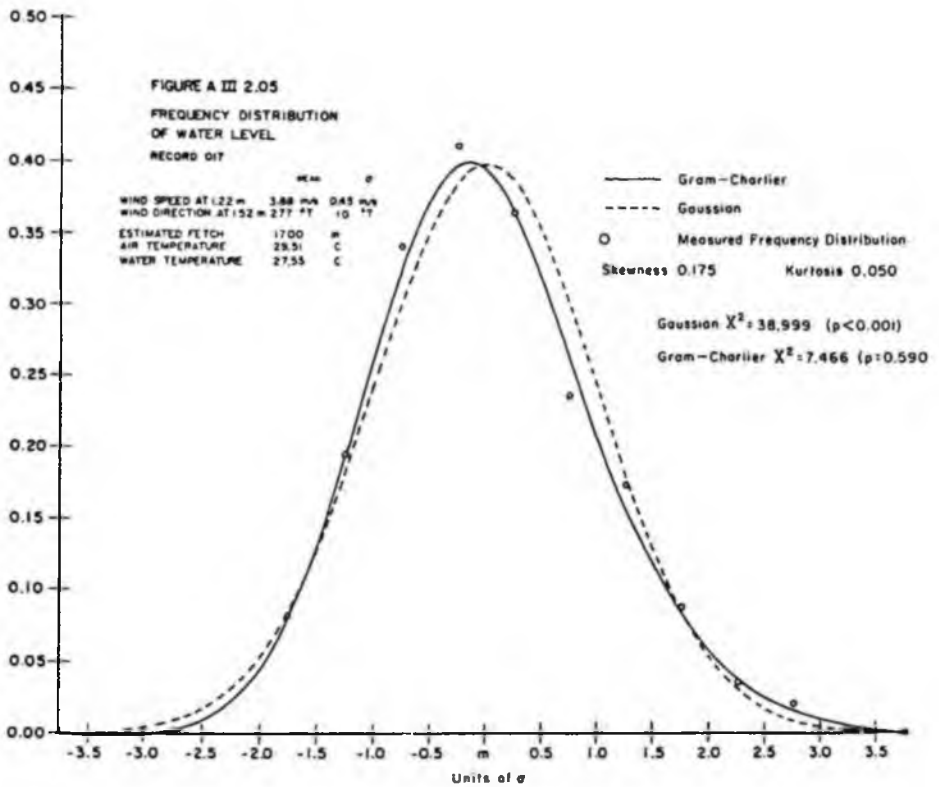


FIGURE 1. From Kinsman 1960. Comparison of an observed distribution of wave height in sea waves with the normal distribution (broken line) and with a Gram-Charlier distribution (solid line).

4. The Joint Distribution of Two Variables

The method of section 2 can be extended to the determination of the joint distribution of any number of variables of the type

$$\zeta = \alpha_1 \xi_1 + \alpha_{12} \xi_1 \xi_2 + \alpha_{123} \xi_1 \xi_2 \xi_3 + \dots \quad \eta = \beta_1 \xi_1 + \beta_{12} \xi_1 \xi_2 + \beta_{123} \xi_1 \xi_2 \xi_3 + \dots \quad (23)$$

where the α 's and β 's are known constants and the ξ_i are random variables defined as before. For simplicity we state the results for two variables ζ, η .

Let us denote by A_p and B_q the terms $\alpha_{i_1 \dots i_p}$ and $\beta_{i_1 \dots i_q}$ where p and q are the numbers of suffices i, j, \dots, l and i, j, \dots, m ; and let $(A_p B_q \dots)$ denote the irreducible part of the mean product

$$(A_p \xi_{i_1} \xi_{i_2} \dots \xi_{i_p}) (B_q \xi_{j_1} \xi_{j_2} \dots \xi_{j_q}) \dots$$

Then it can be shown [Longuet-Higgins, 1963] that the cumulants K_{mn} in the joint distribution of ζ and η are given by

$$K_{mn} = \sum_{p_1 \dots p_m \dots q_1 \dots q_n} (A_{p_1} \dots A_{p_m} B_{q_1} \dots B_{q_n}) \quad (24)$$

the summation extending over all positive integral values of the p_i and q_j . In particular we have $K_{m_0} = K_m$, the cumulant of $p(\zeta)$, as found in section 2, and as far as the terms in V^3 we have

$$K_{11} = (A_1 B_1) + [(A_1 B_2) + (A_2 B_2) + (A_3 B_1)] + [(A_1 B_3) + (A_2 B_3) + \dots + (A_3 B_1)],$$

$$K_{21} = [(A_1^2 B_2) + 2(A_1 A_2 B_1)] + [(A_1^2 B_3) + 2(A_1 A_2 B_2) + 2(A_1 A_3 B_1) + (A_2^2 B_2) + 2(A_1 A_4 B_1) + 2(A_2 A_3 B_1^2)],$$

$$K_{22} = [2(A_1^2 B_1 B_2) + (A_1^2 B_2^2) + 4(A_1 A_2 B_1 B_2) + (A_2^2 B_1^2) + 2(A_1 A_3 B_1^2)],$$

$$K_{31} = [(A_1^3 B_2) + 3(A_1^2 A_2 B_2) + 3(A_1 A_2^2 B_1)].$$

The joint distribution of ζ , η is now given by

$$p(\zeta, \eta) = \frac{\exp[-\frac{1}{2}(f^2 - 2\rho ff' + f'^2)/(1-\rho^2)]}{2\pi(K_{20}K_{02} - K_{11}^2)^{1/2}} \left[1 + \frac{1}{6} (\lambda_{30}H_{30} + 3\lambda_{21}H_{21} + 3\lambda_{12}H_{12} + \lambda_{03}H_{03}) + \dots \right] \quad (25)$$

where

$$\left. \begin{aligned} f &= \frac{\zeta - K_{10}}{K_{20}^{1/2}}, & f' &= \frac{\eta - K_{01}}{K_{02}^{1/2}} \\ \lambda_{mn} &= \frac{K_{mn}}{(K_{20}K_{02})^{m+n/2}}, & \rho &= \lambda_{11} \end{aligned} \right\} \quad (26)$$

and $H_{mn}(f, f'; \rho)$ is a two-dimensional analog of the Hermite polynomial, viz.

$$H_{mn} \exp[-\frac{1}{2}(f^2 - 2\rho ff' + f'^2)/(1-\rho^2)] = (-1)^{m+n} \frac{\partial^{m+n}}{\partial f^m \partial f'^n} \exp[-\frac{1}{2}(f^2 - 2\rho ff' + f'^2)/(1-\rho^2)] \quad (27)$$

In particular

$$\left. \begin{aligned} H_{00} &= 1 \\ H_{10} &= (f - \rho f')/(1-\rho^2) \\ H_{01} &= (f' - \rho f)/(1-\rho^2) \\ H_{20} &= (f - \rho f')^2/(1-\rho^2) - 1 \\ H_{11} &= (f - \rho f')(f' - \rho f)/(1-\rho^2) + \rho \\ H_{02} &= (f' - \rho f)^2/(1-\rho^2) - 1. \end{aligned} \right\} \quad (28)$$

The first approximation, in which λ_{mn} ($m+n > 2$) are neglected, is the familiar bivariate gaussian distribution, as we would expect. In the second approximation cubic polynomials in f, f' must be included, which introduce various types of skewness depending on the coefficients λ_{30} , λ_{21} , λ_{12} , and λ_{03} . In higher approximations we encounter further terms in a bivariate Gram-Charlier series.

In the paper [Longuet-Higgins, 1963] this distribution was applied to the joint distribution of the two components of slope of a random surface. In the present paper we shall apply it to two different problems: the mean number of zeros per unit time of a nonlinear random function $\zeta(t)$; and the distribution of the maximum values of $\zeta(t)$.

5. Mean Number Of Zeros Per Unit Time

We now consider the problem of determining the average number of zero-crossings (or of maxima and minima, which are zeros of the derivative) per unit time in a wave record. We assume that the process is stationary to all orders.

A general formula for the number of crossings of a level ζ per unit time t is due to Kac [1943].

$$N(\zeta) = \int_{-\infty}^{\infty} p(\zeta, \zeta_t) |\zeta_t| d\zeta_t, \quad (29)$$

where $p(\zeta, \zeta_t)$ denotes the joint distribution of ζ and its time-derivative ζ_t . Now for this distribution we have

$$K_{10} = \bar{\zeta} = 0$$

$$K_{01} = \bar{\zeta}_t = 0$$

and

$$K_{11} = \overline{\zeta \zeta_t} - \bar{\zeta} \bar{\zeta}_t = \frac{\partial}{\partial t} \frac{1}{2} (\zeta^2) = 0$$

for any stationary process ζ , so that $\rho = \lambda_{11} = 0$ and from (25)

$$p(\zeta, \zeta_t) = \frac{e^{-\frac{1}{2}(\zeta^2 + \zeta_t^2)}}{2\pi(K_{20}K_{02})^{\frac{1}{2}}} \left[1 + \frac{1}{6} \{ \lambda_{30} H_3(f) H_0(f') + \dots \} + \dots \right] \quad (30)$$

where

$$f = \frac{\zeta}{(K_{20})^{\frac{1}{2}}}, \quad f' = \frac{\zeta_t}{(K_{02})^{\frac{1}{2}}}$$

Now since $e^{-\frac{1}{2}(\zeta^2 + \zeta_t^2)}$ is an even function of f' , the integral of this function multiplied by $H_n(f')$ will vanish whenever n is odd. Moreover, when n is even and greater than 0

$$\begin{aligned} \int_{-\infty}^{\infty} e^{-\frac{1}{2}(\zeta^2 + \zeta_t^2)} |f'| H_n(f') df' &= 2 \int_{-\infty}^{\infty} f' (-1)^n \frac{d^n}{df'^n} (e^{-\frac{1}{2}(\zeta^2 + \zeta_t^2)}) df' \\ &= 2H_{n-2}(0) \end{aligned}$$

on integration by parts. So on substitution in (29) we find

$$N(\zeta) = \frac{e^{-\frac{1}{2}\zeta^2}}{\pi(K_{20}K_{02})^{\frac{1}{2}}} \left[1 + \frac{1}{6} \{ \lambda_{30}(\zeta^3 - 3f) + 3\lambda_{12}f \} + \dots \right] \quad (31)$$

Thus the number of zeros per unit time, considered as a function of ζ , has a skewness λ_{30} similar to that of $p(\zeta)$, but a mean value

$$\frac{1}{2} \lambda_{12} K_{20}^{-\frac{1}{2}} = \frac{1}{2} K_{12}/K_{02}$$

different from the mean of ζ .

If we take $f=0$ in (31) then the third-order terms vanish and we have, to fourth order

$$\begin{aligned} N(0) &= \frac{1}{\pi(K_{20}K_{02})^{\frac{1}{2}}} \left[1 + \frac{1}{24} \{ \lambda_{40} H_4(0) + 6\lambda_{22} H_2(0) - \lambda_{04} H_0(0) \} \right] \\ &= \frac{1}{\pi(K_{20}K_{02})^{\frac{1}{2}}} \left[1 + \frac{1}{8} \lambda_{40} - \frac{1}{4} \lambda_{22} - \frac{1}{24} \lambda_{04} \right]. \end{aligned} \quad (32)$$

6. Distribution of Heights of Maxima

The distribution $p(\zeta_{\max})$ of the heights of the maxima of ζ is given quite generally by

$$p(\zeta_{\max}) = \int_{-\infty}^{\infty} p(\zeta, 0, \zeta_{tt}) |\zeta_{tt}| d\zeta_{tt} \quad (33)$$

where $p(\zeta, \zeta_t, \zeta_{tt})$ denotes the joint distribution of ζ and its first two derivatives with respect to t [Rice, 1944-1945; Cartwright and Longuet-Higgins, 1956]. Now if K_{ijkl} denotes the (i, j, k) th joint cumulant of $\zeta, \zeta_t, \zeta_{tt}$, it is clear that $K_{100}, K_{010}, K_{001}$ all vanish, as do K_{110} and K_{011} . Hence we have (as in sec. 3)

$$p(\xi, \xi_{11}, \xi_{12}) = \frac{1}{(2\pi)^3} \iiint \exp \left[-i(\xi t + \xi_{11} t' + \xi_{12} t'') - \frac{1}{2} (K_{200} t^2 + K_{020} t'^2 + K_{002} t''^2 + 2K_{101} t t' + \dots) + \dots \right] dt dt' dt''.$$

Writing now

$$\left. \begin{aligned} t &= s/K_{200}, & \xi &= K_{200}^{\frac{1}{2}} f, \\ t' &= s'/K_{020}, & \xi_{11} &= K_{020}^{\frac{1}{2}} f', \\ t'' &= s''/K_{002}, & \xi_{12} &= K_{002}^{\frac{1}{2}} f'', \end{aligned} \right\}$$

we have

$$p(\xi, \xi_{11}, \xi_{12}) = \frac{1}{(2\pi)^3 (K_{200} K_{020} K_{002})^{\frac{3}{2}}} \iiint e^{-i(s + s' + s'')} \times \exp \left[-\frac{1}{2} (s^2 + s'^2 + s''^2 + 2\rho s s') + \frac{1}{6} \{ \lambda_{300} (is)^3 + 3\lambda_{210} (is)^2 (is') + \dots \} + \dots \right] ds ds' ds''$$

where $\rho = K_{101} / (K_{200} K_{002})^{1/2}$. Now in

$$\frac{1}{(2\pi)^3} \iiint e^{-i(s + s' + s'')} \times \exp \left[-\frac{1}{2} (s^2 + s'^2 + s''^2 + 2\rho s s') + \dots \right] ds ds' ds''$$

the terms in s' are separable from the terms in s and s'' and hence as in sections 2 and 5 the above expression equals

$$\frac{1}{(1-\rho^2)^{\frac{3}{2}}} H_{r,r''}(f, f''; \rho) H_{r'}(f') e^{-i(f^2 + (1-2\rho f f'' + f''^2)/(1-\rho^2))}.$$

Hence we find

$$p(\xi, \xi_{11}, \xi_{12}) = \frac{e^{-i(f^2 + (1-2\rho f f'' + f''^2)/(1-\rho^2))}}{(2\pi)^{\frac{3}{2}} (K_{200} K_{020} K_{002})^{\frac{3}{2}} (1-\rho^2)^{\frac{3}{2}}} \times \left[1 + \frac{1}{6} \{ \lambda_{300} H_{30}(f, f''; \rho) H_0(f') + 3\lambda_{210} H_{20}(f, f''; \rho) H_1(f) + \dots \} + \dots \right]. \quad (34)$$

To find $p(\xi_{\max})$ from (33) we set $\xi_{11} = 0 = f'$, multiply by $|\xi_{11}|$ and integrate with respect to ξ_{11} from $-\infty$ to 0. Writing

$$\left. \begin{aligned} f &= (1-\rho^2)^{\frac{1}{2}} x \\ f'' &= -(1-\rho^2)^{\frac{1}{2}} y \end{aligned} \right\}$$

in the resulting integral we have

$$p(\xi_{\max}) = \frac{K_{020}^{\frac{1}{2}} (1-\rho^2)^{\frac{1}{2}}}{(2\pi)^{\frac{3}{2}} (K_{200} K_{002})^{\frac{3}{2}}} \int_0^{\infty} y e^{-i(x + 2\rho xy + y^2)} \times \left[1 + \frac{1}{6} \{ (\lambda_{300} H_{30} + 3\lambda_{210} H_{21} + 3\lambda_{102} H_{12} + \lambda_{003} H_{03}) - 3\lambda_{120} H_{10} - 3\lambda_{021} H_{01} \} + \dots \right] dy \quad (35)$$

where

$$\left. \begin{aligned} H_{10} &= x + \rho y \\ H_{01} &= \rho x + y \\ H_{20} &= (x + \rho y)^2 - 1 \\ H_{11} &= (x + \rho y)(\rho x + y) - \rho \\ H_{02} &= (\rho x + y)^2 - 1 \end{aligned} \right\}$$

and generally

$$H_{m,n} e^{-1(x^2+2axy+y^2)} = (-1)^{m+n} \frac{\partial^{m+n}}{\partial x^m \partial y^n} e^{-1(x^2+2axy+y^2)} \quad (36)$$

To evaluate the integrals we use the following results. Straightforward integration by parts gives

$$\int_0^\infty y H_{m,n} e^{-1(x^2+2axy+y^2)} dy = (H_{m,n-2})_{y=0} e^{-1x^2} \quad (37)$$

whenever $n \geq 2$. To deal with the cases $n=1, 0$, we note that

$$-\left(\frac{\partial}{\partial x} - \rho \frac{\partial}{\partial y}\right) e^{-1(x^2+2axy+y^2)} = x(1-\rho^2) e^{-1(x^2+2axy+y^2)}.$$

So by repeated application of the operator $-\left(\frac{\partial}{\partial x} - \rho \frac{\partial}{\partial y}\right)$:

$$H_{10} - \rho H_{01} = x(1-\rho^2) = G_1$$

$$H_{20} - 2\rho H_{11} + \rho^2 H_{02} = x^2(1-\rho^2)^2 - (1-\rho^2) = G_2$$

$$H_{30} - 3\rho H_{21} + 3\rho^2 H_{12} - \rho^3 H_{03} = x^3(1-\rho^2)^3 - 3x(1-\rho^2)^2 = G_3$$

and in general

$$H_{n,0} - \binom{n}{1} \rho H_{n-1,1} + \dots = (1-\rho^2)^{1n} H_n \{x(1-\rho^2)^{\dagger}\} = G_n,$$

say. Thus in general,

$$\begin{aligned} \int_0^\infty y H_{n,1} e^{-1(x^2+2axy+y^2)} dy &= \int_0^\infty H_{n,0} e^{-1(x^2+2axy+y^2)} dy \\ &= \int_0^\infty \left[\binom{n}{1} \rho H_{n-1,1} - \binom{n}{2} \rho^2 H_{n-2,2} + \dots + (-1)^{n-1} \rho^n H_{0,n} + G_n \right] \\ &\quad \times e^{-1(x^2+2axy+y^2)} dy \\ &= \left[\binom{n}{1} \rho H_{n-1,0} - \binom{n}{2} \rho^2 H_{n-2,1} + \dots + (-1)^{n-1} \rho^n H_{0,n-1} \right]_{y=0} \\ &\quad + G_n F(x; \rho) \end{aligned} \quad (38)$$

where

$$F(x; \rho) = \int_0^\infty e^{-1(x^2+2axy+y^2)} dy = e^{-1x^2(1-\rho^2)} \int_{ax}^\infty e^{-1z^2} dz. \quad (39)$$

Similarly, when $m=0$,

$$\begin{aligned} \int_0^\infty y H_{n,0} e^{-1(x^2+2axy+y^2)} dy &= \int_0^\infty y \left[\binom{n}{1} \rho H_{n-1,1} - \binom{n}{2} \rho^2 H_{n-2,2} + \dots + G_n \right] e^{-1(x^2+2axy+y^2)} dy \\ &= n\rho \left[\left\{ \binom{n-1}{1} \rho H_{n-2,0} - \binom{n-1}{2} \rho^2 H_{n-3,1} + \dots \right\}_{y=0} e^{-1x^2} + G_{n-1} F(x; \rho) \right] \\ &\quad + \left[-\binom{n}{2} \rho^2 H_{n-2,0} + \binom{n}{3} \rho^3 H_{n-3,1} - \dots \right]_{y=0} e^{-1x^2} + G_n [e^{-1x^2} - \rho x F(x; \rho)] \\ &= \left[1 \binom{n}{2} \rho^2 H_{n-2,0} - 2 \binom{n}{3} \rho^3 H_{n-3,1} + \dots + G_n \right] e^{-1x^2} \\ &\quad + \rho (n G_{n-1} - x G_n) F(x; \rho). \end{aligned} \quad (40)$$

Using formulas (7.5) to (7.8) we find altogether

$$\begin{aligned}
 p(\zeta_{m_{12}}) &= \frac{[K_{020}(K_{200}K_{002} - K_{101}^2)^{1/2}]}{(2x)^{3/2}K_{200}K_{002}} \times \left[e^{-x^2} - \rho x F(x; \rho) \right. \\
 &+ \frac{1}{6} \lambda_{300} \{ ((1-\rho^2)^3 x^3 - (3-9\rho^2+5\rho^4)x) e^{-x^2} - (\rho(1-\rho^2)^2 x^4 - 6(1-\rho^2)^2 x^2 + 3\rho(1-\rho^2)) F(x; \rho) \} \\
 &+ \frac{1}{2} \lambda_{201} \{ \rho(2-\rho^2)x e^{-x^2} + ((1-\rho^2)^2 x^2 - (1-\rho^2)) F(x; \rho) \} \\
 &+ \left. \frac{1}{2} \lambda_{102} x e^{-x^2} + \frac{1}{6} \lambda_{003} \rho x e^{-x^2} - \frac{1}{2} \lambda_{120} \{ (1-\rho^2)x e^{-x^2} + (\rho - \rho x + \rho^3 x) F(x; \rho) \} - \frac{1}{2} \lambda_{021} F(x; \rho) \right] \quad (41)
 \end{aligned}$$

where

$$\left. \begin{aligned}
 x &= \frac{f}{(1-\rho^2)^{1/2}} = \frac{\zeta_{m_{12}}}{[K_{200}(1-\rho^2)]^{1/2}} \\
 \rho &= \frac{K_{101}}{(K_{200}K_{002})^{1/2}}
 \end{aligned} \right\}$$

The cumulants can be expressed in terms of the spectrum in the following way. If

$$\left. \begin{aligned}
 \zeta &= \alpha_i \xi_i + \alpha_{ij} \xi_i \xi_j + \alpha_{ijk} \xi_i \xi_j \xi_k + \dots \\
 \zeta_i &= \beta_i \xi_i + \beta_{ij} \xi_i \xi_j + \alpha_{ijk} \xi_i \xi_j \xi_k + \dots \\
 \zeta_{ii} &= \gamma_i \xi_i + \gamma_{ij} \xi_i \xi_j + \gamma_{ijk} \xi_i \xi_j \xi_k + \dots
 \end{aligned} \right\}$$

then we may take

$$\left. \begin{aligned}
 \alpha_i &= (1, 1, \dots, 1; 0, 0, \dots, 0) \\
 \beta_i &= (0, 0, \dots, 0; -\sigma_1, -\sigma_2, \dots, -\sigma_N) \\
 \gamma_i &= (\sigma_1^2, \sigma_2^2, \dots, \sigma_{N1}^2, 0, 0, \dots, 0)
 \end{aligned} \right\}$$

Also if

$$(\alpha_{ij}) = \begin{bmatrix}
 \alpha_{11} & \dots & \dots & \alpha_{1,N} & 0 & \dots & \dots & 0 \\
 \cdot & \cdot & \cdot & \cdot & \cdot & \cdot & \cdot & \cdot \\
 \cdot & \cdot & \cdot & \cdot & \cdot & \cdot & \cdot & \cdot \\
 \cdot & \cdot & \cdot & \cdot & \cdot & \cdot & \cdot & \cdot \\
 \alpha_{N,1} & \dots & \dots & \alpha_{N,N} & 0 & \dots & \dots & 0 \\
 0 & \dots & \dots & 0 & \alpha_{N+1,N+1} & \dots & \dots & \alpha_{N+1,2N} \\
 \cdot & \cdot & \cdot & \cdot & \cdot & \cdot & \cdot & \cdot \\
 \cdot & \cdot & \cdot & \cdot & \cdot & \cdot & \cdot & \cdot \\
 \cdot & \cdot & \cdot & \cdot & \cdot & \cdot & \cdot & \cdot \\
 0 & \dots & \dots & 0 & \alpha_{2N} & \dots & \dots & \alpha_{2N,2N}
 \end{bmatrix}$$

then

$$(\beta_{ij}) = \begin{bmatrix} 0 & \dots & 0 & (-\sigma_1 \alpha_{N+1, N+1} + \sigma_1 \alpha_{11}) & \dots & (-\sigma_1 \alpha_{N+1, 2N} + \sigma_N \alpha_{1, N}) \\ \vdots & & \vdots & \vdots & & \vdots \\ \vdots & & \vdots & \vdots & & \vdots \\ \vdots & & \vdots & \vdots & & \vdots \\ 0 & \dots & 0 & (-\sigma_N \alpha_{2N, N+1} + \sigma_1 \alpha_{N, 1}) & \dots & (-\sigma_N \alpha_{2N, 2N} + \sigma_N \alpha_{NN}) \\ (\sigma_1 \alpha_{11} - \sigma_1 \alpha_{N+1, N+1}) & \dots & (\sigma_1 \alpha_{1N} - \sigma_N \alpha_{N+1, 2N}) & 0 & \dots & 0 \\ \vdots & & \vdots & \vdots & & \vdots \\ \vdots & & \vdots & \vdots & & \vdots \\ \vdots & & \vdots & \vdots & & \vdots \\ (\sigma_N \alpha_{N, 1} - \sigma_1 \alpha_{2N, N+1}) & \dots & (\sigma_N \alpha_{NN} - \sigma_N \alpha_{2N, 2N}) & 0 & \dots & 0 \end{bmatrix}$$

and

$$(\gamma_{ij}) = \begin{pmatrix} C & 0 \\ 0 & D \end{pmatrix}$$

where

$$C = \begin{bmatrix} (-2\sigma_1^2 \alpha_{11} + 2\sigma_1^2 \alpha_{N+1, N+1}) & \dots & \dots & [-(\sigma_1^2 + \sigma_N^2) \alpha_{1, N} + 2\sigma_1 \sigma_N \alpha_{N+1, 2N}] \\ \vdots & & & \vdots \\ \vdots & & & \vdots \\ \vdots & & & \vdots \end{bmatrix}$$

and in D the suffices of α_{ij} are each increased or decreased by N . The nonvanishing cumulants can now be expressed as follows:

$$\left. \begin{aligned} K_{200} &\doteq (A_1^2) = \alpha_i \alpha_i V_i = \int E d\sigma = m_0 \\ K_{020} &\doteq (B_1^2) = \beta_i \beta_i V_i = \int \sigma^2 E d\sigma = m_2 \\ K_{002} &\doteq (C_1^2) = \gamma_i \gamma_i V_i = \int \sigma^4 E d\sigma = m_4 \\ K_{101} &\doteq (A_1 C_1) = \alpha_i \gamma_i V_i = - \int \sigma^2 E d\sigma = -m_2 \end{aligned} \right\}$$

Also

$$K_{100} \doteq 3(A_1^2 A_2) = 6\alpha_i \alpha_j \alpha_{ij} V_i V_j = 6 \iint \alpha(\sigma, \sigma') EE' d\sigma d\sigma'$$

$$K_{020} \doteq 3(B_1^2 B_2) = 6\beta_i \beta_j \beta_{ij} V_i V_j = 0$$

$$K_{002} \doteq 3(C_1^2 C_2) = 6\gamma_i \gamma_j \gamma_{ij} V_i V_j = 6 \iint \sigma^2 \sigma'^2 \{ -(\sigma^2 + \sigma'^2) \alpha(\sigma, \sigma') + 2\sigma \sigma' \alpha^*(\sigma, \sigma') \} EE' d\sigma d\sigma'$$

and

$$K_{201} \doteq (A_1^2 C_2) = 2\alpha_i \alpha_j \gamma_{ij} V_i V_j = 2 \iint [-(\sigma^2 + \sigma'^2) \alpha(\sigma, \sigma') - 2\sigma \sigma' \alpha^*(\sigma, \sigma')] EE' d\sigma d\sigma'$$

$$K_{102} \doteq (C_1^2 A_2) = 2\gamma_i \gamma_j \alpha_{ij} V_i V_j = 2 \iint \sigma^2 \sigma'^2 \alpha(\sigma, \sigma') EE' d\sigma d\sigma'$$

$$K_{120} \doteq (B_1^2 A_2) = 2\beta_i \beta_j \alpha_i \alpha_j V_i V_j = 2 \iint \sigma^2 \alpha'^2 \alpha^*(\sigma, \sigma') EE' d\sigma d\sigma'$$

$$K_{021} \doteq (B_1^2 C_2) = 2\beta_i \beta_j \gamma_i \gamma_j V_i V_j = 2 \iint \sigma \sigma' \{-(\sigma^2 + \sigma'^2) \alpha^*(\sigma, \sigma') + 2\sigma \sigma' \alpha(\sigma, \sigma')\} EE' d\sigma d\sigma'$$

One can if necessary retain the next term in K_{200} , K_{020} , K_{002} , and K_{101} ; thus

$$K_{200} \doteq (A_2^2) + (A_3^2) = \alpha_i \alpha_i V_i + 2\alpha_i \alpha_j \alpha_i \alpha_j V_i V_j = \int E d\sigma + 2 \iint [\alpha(\sigma, \sigma')]^2 EE' d\sigma d\sigma',$$

with similar expressions for K_{020} and K_{002} . (Note that $K_{101} = -K_{020}$ to all orders).

In the first approximation (7.9) gives

$$P(\xi_{\max}) = \frac{m_2(m_0 m_4 - m_2^2)^{\frac{1}{2}}}{(2\pi)^{3/2} m_0 m_4} [e^{-\xi^2} - \rho x F(x; \rho)]$$

where

$$x = \xi / (1 - \rho^2)^{\frac{1}{2}}, \quad \rho = -m_2 / (m_0 m_4)^{\frac{1}{2}}$$

This is the distribution obtained by Rice [1944-1945] and studied by Cartwright and Longuet-Higgins [1956].

The remaining terms in (7.9) represent the corrections to this distribution, which are order $V^{1/2}$.

7. References

- Benney, D. J. (1962), Nonlinear gravity wave interactions, *J. Fluid Mech.* **14**, 577-584.
- Cartwright, D. E., and M. S. Longuet-Higgins (1956), The statistical distribution of the maxima of a random function, *Proc. Roy. Soc. A*, **237**, 212-232.
- Edgeworth, F. Y. (1906), The generalized law of error, or law of great numbers, *J. Roy. Statist. Soc.* **68**, 497-530.
- Hasselmann, K. (1960), Grundgleichungen der Seegangsvoraussage, *Schiffstechnik* **7**, 191-195.
- Hasselmann, K. (1961), On the nonlinear energy transfer in a wave spectrum, *Proc. Conference on Ocean Wave Spectra*, Easton, Md.
- Hasselmann, K. (1962), On the nonlinear energy transfer in a gravity-wave spectrum. Part I. General theory, *J. Fluid Mech.* **12**, 481-500.
- Kac, M. (1943), On the average number of real roots of a random algebraic equation, *Bull. Am. Math. Soc.* **49**, 314-320.
- Kinsman, B. (1960), Surface waves at short fetches and low wind speed—a field study. *Chesapeake Bay Inst. Tech. Report* 19.
- Longuet-Higgins, M. S. (1960), The statistical geometry of random surfaces, *Proc. Symposium Applied Math., Am. Math. Soc.* **13**, 105-143.
- Longuet-Higgins, M. S. (1963), The effect of nonlinearities on statistical distributions in the theory of sea waves, *J. Fluid Mech.* **17**, 459-480.
- Phillips, O. M. (1960), On the dynamics of unsteady gravity waves of finite amplitude. Part 1. The elementary interactions. *J. Fluid Mech.* **9**, 193-217.
- Phillips, O. M. (1961), On the dynamics of unsteady gravity waves of finite amplitude. Part 2. Local properties of a random wave field, *J. Fluid Mech.* **11**, 143-155.
- Rice, S. O. (1944), The mathematical analysis of random noise, *Bell System Tech. J.* **23**, 282-332.
- Rice, S. O. (1945), The mathematical analysis of random noise, *Bell System Tech. J.* **24**, 46-155.
- Wiener, N. (1958), *Nonlinear problems in random theory*, p. 131 (Chapman and Hall, London).

(Paper 68D9-406)

On the Joint Distribution of the Periods and Amplitudes of Sea Waves

M. S. LONGUET-HIGGINS

*Department of Applied Mathematics and Theoretical Physics, Cambridge, England
Institute of Oceanographic Sciences, Godalming, Surrey, England*

A theoretical expression for the joint distribution of wave period and amplitude, which was previously derived for a Gaussian record with a narrow spectrum, is restated in simple form. According to this distribution the variability of wave periods, for waves of a given height, is inversely proportional to the wave height, so that the higher waves tend to be more regular. The distribution is found to agree well with some observations of wave periods and amplitudes from the Gulf of Mexico, as given by Bretschneider (1959).

INTRODUCTION

A problem of some interest in ocean engineering is to find the joint distribution of the heights and periods of sea waves. By this we mean the wave heights and periods observed visually, or from an instrumental record, over an interval of time during which the sea conditions may be regarded as statistically stationary. One would hope to relate this distribution to the underlying energy spectrum of the sea surface.

A useful collection of such wave observations was made by Bretschneider [1959]. Unfortunately, many of the analytical expressions that he used to describe his observations were complicated and had little physical basis. On the other hand, the statistical theory of random functions first developed by Rice [1944, 1945] for noise in electrical circuits is naturally suited to describe wind-generated waves. For some time it has been known that this model is remarkably successful in predicting both the crest-to-trough heights of sea waves [Longuet-Higgins, 1952] and also the distribution of the heights of wave crests above the mean surface level [Cartwright and Longuet-Higgins, 1956]. This is in spite of the essentially linear character of the model.

To determine the distribution of wave 'periods,' defined as the intervals between successive up-crossings of the mean level, is a more difficult problem. Various approximations have been discussed, for example, by Rice [1944, 1945] and by Longuet-Higgins [1958, 1962, 1963].

The joint distribution of wave heights and periods is still more difficult, in the most general case. Nevertheless, in the special case when the frequency spectrum of the waves is narrow, some progress toward a theory can be made. The overall distribution of the intervals between two successive zeros for a narrow spectrum was first given by Rice [1944, 1945, section 3.4]. Then from the density of the wave envelope and its time derivative, Wooding [1955] derived the joint density of the wave frequency and amplitude for a narrow spectrum. A similar analysis for the joint density of wave period and amplitude was given independently by Longuet-Higgins [1957] for a cross section of a random surface.

The purpose of this note is to draw attention to the theoretical joint distribution mentioned above and to show how it can be applied to ocean waves. Particularly, we shall compare the distribution of period and amplitude with the data given by Bretschneider [1959]. It is concluded that the agreement, as in previous experience with this theoretical model, is remarkably good.

Copyright © 1975 by the American Geophysical Union.

STATEMENT OF THEORETICAL RESULTS

We first state briefly those theoretical results of the random noise model which we shall apply. These results are derived concisely in the appendix on the hypothesis that the sea surface is Gaussian and that the energy spectrum is sufficiently narrow.

The probability density of the wave amplitude a (defined as half the crest-to-trough wave height) by itself is given by the well-known Rayleigh distribution

$$p(\xi) = \xi \exp(-\xi^2/2) \quad \xi = a/\mu_0^{1/2} \quad (1)$$

where μ_0 is the zeroth moment of the energy spectrum. (In fact, μ_0 is the mean square wave amplitude.)

The probability density of the wave period τ (defined as the time interval between successive up-crossings of the mean level) by itself is given by

$$p(\eta) = \frac{1}{2(1 + \eta^2)^{3/2}} \quad \eta = (\tau - \langle \tau \rangle)/\nu(\tau) \quad (2)$$

where $\langle \tau \rangle$ is the mean wave period and ν is proportional to the width of the energy spectrum. In fact

$$\nu = (\mu_2/\mu_0)^{1/2}(\tau/2\pi) \quad (3)$$

where μ_2 denotes the second moment of the energy spectrum about the mean. The distribution (2) is illustrated by the bell-shaped curve (which is not Gaussian) in Figure 1. The dotted lines show the two quartiles at a distance $1/(3)^{1/2}$ from the mean. It follows from (2) that the interquartile range (IQR) of the wave period is given by

$$\text{IQR}(\tau) = 2\nu(\tau)/(3)^{1/2} \quad (4)$$

Thirdly, the joint probability density of wave period and amplitude is given theoretically by

$$p(\xi, \eta) = \frac{\xi^2}{(2\pi)^{1/2}} \exp[-\xi^2(1 + \eta^2)/2] \quad (5)$$

where ξ and η have the same meanings as before. Here $p(\xi, \eta) d\xi d\eta$ denotes the probability that ξ and η shall simultaneously take values in small intervals $(\xi, \xi + d\xi)$, $(\eta, \eta + d\eta)$, respectively. Contours of the density (3) are indicated by the 'cocked hat' curves of Figure 2. Evidently at the smaller wave amplitudes (nearer the horizontal axis) the distribution of wave periods becomes broader.

From (5) and (2) the density of wave periods at a specified

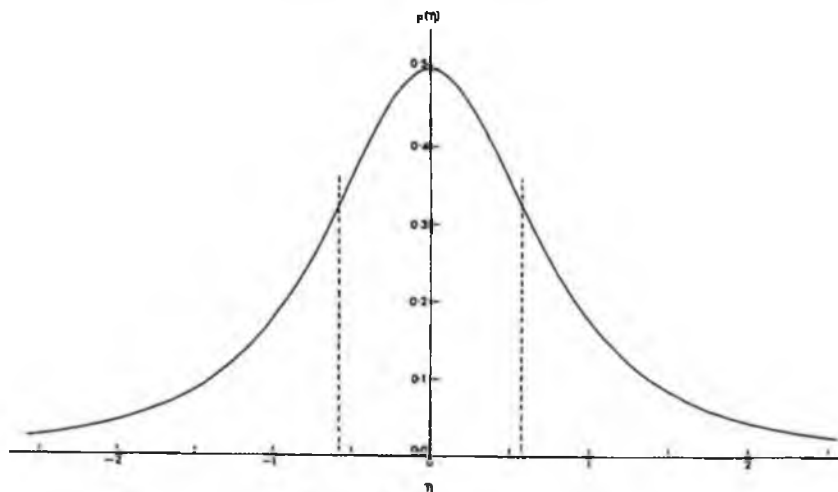


Fig. 1. Graph of the function $p(\eta) = \frac{1}{2}(1 + \eta^2)^{-3/2}$, giving the probability density of the wave period τ , where $\eta = (\tau/\tau) - 1/\nu$. The broken vertical lines mark the quartiles.

wave amplitude (the 'marginal' density) is given by

$$p_1(\eta) = \frac{\xi}{(2\pi)^{1/2}} \exp(-\xi^2 \eta^2 / 2) \quad (6)$$

Since ξ is fixed, the density of η is exactly Gaussian, with variance ξ^{-2} . The quartiles of the distribution correspond to the broken lines in Figure 2. The interquartile range is $1.35\xi^{-1}$. Hence the interquartile range of the wave periods (for a particular wave amplitude) is

$$1.35\nu(\tau)/\xi \quad (7)$$

which is inversely proportional to the wave amplitude. Thus the higher the waves, the less variable are their apparent periods.

COMPARISON WITH OBSERVATION

Bretschneider [1959] has published extensive observations of visual wave properties, in particular a set of data including the apparent wave heights and wavelengths of 399 waves from a continuous record taken in the Gulf of Mexico. Figure 3 is a reproduction of *Bretschneider's* Figure 5.1, on which we have superposed certain grid lines to help in the analysis. The vertical scale indicates the 'relative wave height,' that is, the wave height normalized by the average of all the observations. The horizontal scale indicates the 'relative wavelength,' that is, the square of the wave period τ divided by the mean square τ .

First, to test the Rayleigh distribution (1), we divided the range of relative wave heights into equal intervals and counted the numbers of waves in each interval, regardless of wave period. The resulting histogram is shown in Figure 4, compared to the corresponding Gaussian distribution (equation (1)). The appropriate horizontal scale has been obtained by using the property that for the Rayleigh distribution the mean value ξ is just $\frac{1}{2}\pi^{1/2} = 0.862$ times the rms value. There appears to be a reasonable fit, though with a slight excess of waves with heights near the middle of the range and a deficiency at the two extremes.

To compare the wave periods with the theoretical distribution (2), the value of the parameter ν was chosen to satisfy (4), that is, we took

$$\nu = \frac{(3)^{1/2}}{2} \times \text{IQR}(\tau) \quad (8)$$

The area of the curve in Figure 1 was divided into 10 equal parts by ordinates η_1, \dots, η_{10} , using the fact that

$$\int_0^{\eta} p(\eta) d\eta = \frac{\eta}{2(1 + \eta^2)^{1/2}} = \frac{1}{2} \sin \alpha$$

where $\alpha = \arctan \eta$. Thus taking $\sin \alpha = -0.8, -0.6, \dots, 0.8$, the corresponding ordinates are given by

$$\eta = \tan \alpha$$

$$\tau/\langle\tau\rangle = (1 + \nu\eta)$$

$$\lambda = (\tau/\langle\tau\rangle)^2$$

Then counting the number of waves in each range of λ , we obtain a histogram which is compared with the theoretical distribution in Figure 5. Again there is a reasonable fit.

Lastly, to test (7), we calculated the quartiles of the distribution of wave periods in each subrange of wave amplitudes. These are shown in Table 1. According to (7) the central quartile, or median, of each distribution should be independent of the wave amplitude. On inspection of Table 1 we see that if we exclude the range of smallest amplitudes, which contains only six waves, there is indeed no marked trend in the medians.

Consider now the interquartile ranges. According to (7) the interquartile range should be approximately $1.35\nu/\xi$, where ξ corresponds to the midpoint of the subrange. A comparison between the observed and the theoretical values (with $\nu = 0.234$) is shown in Figure 6. Again there is good agreement, with the exception of the point corresponding to the lowest wave amplitude.

DISCUSSION

Consider first the applicability of the theory. From Tables 4.1 and 4.3 of *Bretschneider* [1959] the mean height and period of the waves in records e-11 to e-15, from which the data were taken, are $H = 4.88$ feet and $T = 4.8$ s, respectively. The waves being in fairly deep water, their height-to-length ratio, on average, was given by

$$\frac{H}{L} = \frac{2\pi H}{T^2} = 0.041$$

This steepness would correspond approximately to the point $\xi = \eta = 1$ in Figure 3. The limiting steepness of progressive waves, on the other hand, is about 0.142, or 3.5 times this value. Hence not more than a small fraction, perhaps 0.3%, of the waves would be of limiting steepness. Hence it is not unreasonable to expect that the linear theory would apply. The detailed effects of nonlinearity can be calculated [*Longuet-Higgins*, 1963] but only if the energy spectrum is well specified.

As regards the second assumption, that the spectrum is narrow, we note that the value of ν , the dimensionless width of the energy spectrum, as calculated from (8), was 0.234. Relative errors in the probability densities may be expected to be of the same order of magnitude. Hence such discrepancies between the theoretical and the observed quantities in Figures 4, 5, and 6 are certainly not unduly large. Indeed the agreement is surprisingly good. The expected disagreement is such that it is hardly worthwhile to perform any elaborate test for goodness-of-fit.

It is worth remarking that the parameter ν , used in this paper to define the width of the spectrum, is, for a narrow spectrum, quite closely related to the more general parameter ϵ defined by *Carrwright and Longuet-Higgins* [1956]. In fact for a

narrow spectrum we have approximately

$$\nu \doteq \frac{1}{2}\epsilon \quad (9)$$

(see Appendix B). In the case of the wave record studied in the previous section this would indicate a value of ϵ of about 0.47, comparable with the values for the wave records analyzed by *Carrwright and Longuet-Higgins* [1956, Table 1].

As is well known, pressure recordings in general tend to filter out the high frequencies and so reduce the width of the spectrum. For records of surface elevation, larger values of ν are probably more typical.

The three parameters μ_0 , $\langle r \rangle$, and ν , which occur in the theoretical distributions of the section on statement of theoretical results are defined in the first place in relation to the basic energy spectrum of the record (see Appendix A). Since the energy spectrum for the record we analyzed was not presented by *Bretschneider* [1959], we were compelled to estimate these parameters from the data themselves. Nevertheless, to judge from the examples given by *Carrwright and Longuet-Higgins* [1956], we would expect that the values of statistical parameters derived from the energy spectrum will usually be close to those estimated from the statistical data.

CONCLUSIONS

We have compared the theoretical distribution of wave heights and periods, applicable to a narrow Gaussian wave spectrum, with ocean wave data from the Gulf of Mexico and found good agreement. It has to be remembered, however, that in pressure records, much of the high-frequency tail of the spectrum is reduced, and in unfiltered records of surface elevation the narrow band approximation is probably less applicable.

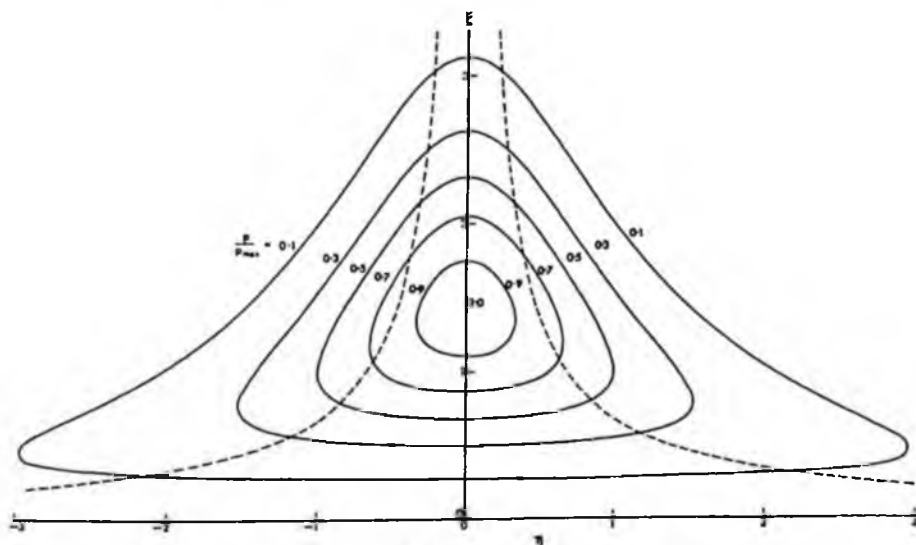


Fig. 2. Contours of the function $\mu(\xi, \eta) = (2\pi)^{-1/2} \exp[-\xi^2(1 + \eta^2)/2]$ giving the joint probability density of the wave amplitude $a = \mu_0^{1/2}\xi$ and $\tau = \langle r \rangle(1 + \eta^2)$.

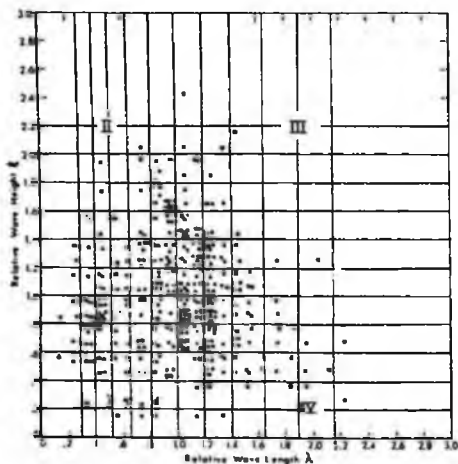


Fig. 3. Scatter diagram of the relative wave height ξ and the relative wavelength λ from 399 consecutive waves from the Gulf of Mexico (data from Breitschneider [1959]).

The data were also taken in moderately deep water. In shallow water, especially for steep waves, the distribution can again be expected to be less applicable because of the enhanced nonlinearity.

Nevertheless, it appears that under the appropriate conditions the theoretical distribution may be of some use.

APPENDIX A: PROOFS OF EQUATIONS (1)-(7)

For convenience we give here a direct and simple derivation of the results stated in the section on statement of theoretical results.

Let $\zeta(t)$ be any function of the time (representing for example the elevation of the sea surface at a given point), which is given by

$$\zeta(t) = \sum c_n \cos(\sigma_n t + \epsilon_n) \quad (\text{A1})$$

where the frequencies σ_n are distributed densely in the interval $(0, \infty)$, the phases ϵ_n are random variables distributed uniformly over the interval $(0, 2\pi)$, and the amplitudes c_n are such that over any frequency interval $(\sigma_n, \sigma_n + d\sigma_n)$ we have, to order $d\sigma$,

$$\sum \frac{1}{2} c_n^2 = E(\sigma) d\sigma \quad (\text{A2})$$

Here $E(\sigma)$ denotes the energy spectrum of $\zeta(t)$.

Now let $\langle \sigma \rangle$ denote the mean frequency of the spectrum, defined by the property that if

$$\mu_r = \int_0^\infty (\sigma - \langle \sigma \rangle)^r E(\sigma) d\sigma \quad (\text{A3})$$

denotes the r th moment of the frequency spectrum about the mean, then

$$\mu_1 = 0 \quad (\text{A4})$$

We define the wave envelope as follows. Let (A1) be written

$$\zeta(t) = \Re \sum c_n \exp [i(\sigma_n t + \epsilon_n)] \quad (\text{A5})$$

$$\zeta(t) = \Re \rho e^{i\phi} \exp [i\langle \sigma \rangle t]$$

where ρ and ϕ are real functions of t defined by

$$\rho e^{i\phi} = \sum c_n \exp [i(\sigma_n - \langle \sigma \rangle)t + \epsilon_n] \quad (\text{A6})$$

In (A5) we may think of $\exp [i\langle \sigma \rangle t]$ as representing a carrier wave and $\rho e^{i\phi}$ as representing a complex wave envelope. The functions ρ and ϕ may be called the amplitude and phase functions, respectively. If most of the energy in the spectrum is concentrated near the mean frequency $\langle \sigma \rangle$, then from (A6) we see that ρ and ϕ are slowly varying functions of t compared to the carrier wave. It will be shown that a sufficient condition for this to occur is that

$$\nu^2 = (\mu_2/\mu_0(\sigma^2)) \ll 1 \quad (\text{A7})$$

If (A7) is satisfied, we shall say that the frequency spectrum is narrow.

We shall need to know the joint probability density of ρ and ϕ ($\rho = \partial/\partial t$). Following Rice [1944, 1945], we write

$$\xi_1 = \rho \cos \phi = \sum c_n \cos [(\sigma_n - \langle \sigma \rangle)t + \epsilon_n] \quad (\text{A8})$$

$$\xi_2 = \rho \sin \phi = \sum c_n \sin [(\sigma_n - \langle \sigma \rangle)t + \epsilon_n]$$

and also

$$\xi_3 = \xi_1 = -\sum (\sigma_n - \langle \sigma \rangle) c_n \sin [(\sigma_n - \langle \sigma \rangle)t + \epsilon_n] \quad (\text{A9})$$

$$\xi_4 = \xi_2 = \sum (\sigma_n - \langle \sigma \rangle) c_n \cos [(\sigma_n - \langle \sigma \rangle)t + \epsilon_n]$$

Using angle brackets to denote mean values with respect to the ensemble (or with respect to the time t) we have

$$\langle \xi_i \rangle = \langle \xi_j \rangle = \langle \xi_k \rangle = \langle \xi_l \rangle = 0 \quad (\text{A10})$$

and for the second-order correlation matrix

$$\langle \xi_i \xi_j \rangle = \begin{pmatrix} \mu_0 & 0 & 0 & \mu_1 \\ 0 & \mu_0 & -\mu_1 & 0 \\ 0 & -\mu_1 & \mu_2 & 0 \\ \mu_1 & 0 & 0 & \mu_2 \end{pmatrix} \quad (\text{A11})$$

Since μ_1 vanishes (equation (A4)) this reduces to a diagonal matrix. Hence assuming that the conditions necessary for the central limit theorem are satisfied, we have for the joint density of ξ_1, ξ_2, ξ_3 , and ξ_4

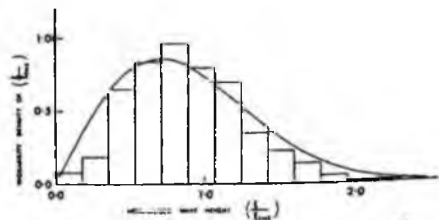


Fig. 4. Histogram of the normalized wave amplitude $\xi/\rho_0^{1/2}$ compared with the Rayleigh distribution (1).

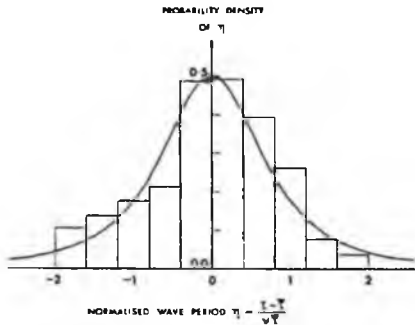


Fig. 5. Histogram of the normalized wave period η compared with the narrow normal distribution (2).

$$p(\xi_1, \xi_2, \xi_3, \xi_4) = \frac{1}{(2\pi)^2 \mu_0 \mu_2} \exp [-(\xi_1^2 + \xi_2^2)/2\mu_0] \cdot \exp [-(\xi_3^2 + \xi_4^2)/2\mu_2] \quad (A12)$$

Now since

$$\xi_3 = \bar{\rho} \cos \phi - \rho \phi \sin \phi \quad (A13)$$

$$\xi_4 = \bar{\rho} \sin \phi + \rho \phi \cos \phi$$

it follows that

$$\frac{\partial(\xi_1, \xi_2, \xi_3, \xi_4)}{(\rho, \phi, \bar{\rho}, \phi)} = \rho^2 \quad (A14)$$

and hence the joint density of $\rho, \phi, \bar{\rho}$, and ϕ is

$$p(\rho, \phi, \bar{\rho}, \phi) = \frac{\rho^2}{(2\pi)^2 \mu_0 \mu_2} \exp(-\rho^2/2\mu_0) \cdot \exp[-(\bar{\rho}^2 + \rho^2 \phi^2)/2\mu_2] \quad (A15)$$

The joint density of ρ and ϕ can now be found by integrating with respect to $\bar{\rho}$ from 0 to 2π and with respect to ϕ from $-\infty$ to ∞ , giving

$$p(\rho, \phi) = \frac{\rho^2}{(2\pi)^{1/2} \mu_0 \mu_2^{1/2}} \exp(-\rho^2/2\mu_0) \exp(-\rho^2 \phi^2/2\mu_2) \quad (A16)$$

The density of ρ alone is then the Rayleigh distribution

$$p(\rho) = \frac{\rho}{\mu_0} \exp(-\rho^2/2\mu_0) \quad (A17)$$

and the density of ϕ alone is

$$p(\phi) = \frac{(\mu_0/\mu_2)^{1/2}}{2[1 + (\mu_0/\mu_2)\phi^2]^{3/2}} \quad (A18)$$

Equation (A18) shows that the range of ϕ is of the same order as $(\mu_2/\mu_0)^{1/2}$. Hence if the condition (A7) is satisfied, it is unlikely that ϕ will exceed (σ) in absolute magnitude. This implies that the total phase

$$\chi = (\sigma)t + \phi \quad (A19)$$

is almost certainly an increasing function of the time t , as shown in Figure 7.

We now assume that the spectrum is narrow, so that the

total phase χ will nearly always increase with t . Zeros of $f(t)$ will occur whenever χ takes the value $n\pi$ (n being an integer). (Other zeros of $f(t)$ will of course occur when ρ vanishes, but statistically this will be a rare event.) A wave period may then be defined as the time interval between successive up-crossings of the phase χ through the value $2n\pi$.

Assuming $\bar{\chi}$ small compared to $(\sigma)\chi$ we shall have

$$\tau \doteq \frac{2\pi}{\dot{\chi}} \doteq (\tau)(1 - \phi/(\sigma)) \quad (A20)$$

where

$$(\tau) = 2\pi(\sigma) \quad (A21)$$

We therefore need the probability density of ϕ at the instants when $\chi = 2n\pi$. This is given by

$$p(\phi|\chi) = C|\dot{\chi}|p(\chi, \phi) \quad (A22)$$

where C is a normalizing constant such that

$$\int_{-\infty}^{\infty} p(\phi|\chi) d\phi = 1 \quad (A23)$$

Since $p(\chi, \phi)$ is independent of χ , and since

$$\dot{\chi} = (\sigma)(1 + 0(\sigma)) \quad (A24)$$

we have, to lowest order in σ ,

$$p(\phi|\chi) = C p(\phi) \quad (A25)$$

where evidently C must be unity.

The probability density of τ is given by

$$p(\tau) = \left| \frac{d\phi}{d\tau} \right| p(\phi) = \langle (\tau)/(\sigma) \rangle p(\phi) \quad (A26)$$

So from (A18) we find

$$p(\tau) \doteq \frac{\sigma^2 \langle \tau \rangle^2}{2[\sigma^2 \langle \tau \rangle^2 + (\tau - \langle \tau \rangle)^2]^{3/2}} \quad (A27)$$

where ν is given by (A7).

If we now make the substitution

$$\xi = \rho/\mu_0^{1/2} \quad \eta = -(\sigma)\phi/\nu \quad (A28)$$

and since the amplitude a is nearly equal to ρ , we have

$$a = \mu_0^{1/2} \xi \quad \tau = (\tau)(1 + \eta\nu) \quad (A29)$$

From (A17) there follows (1), from (A18) follows (2), and from

TABLE 1. Quartiles of the Distribution of Wave Periods in Figure 3

Range of η	Number of Waves	Quartiles ($\tau/\langle \tau \rangle = (\lambda/\lambda_0)^{3/2}$)		
0.0-0.2	6	---	0.88	---
0.2-0.4	15	0.81	0.93	1.28
0.4-0.6	52	0.78	0.98	1.17
0.6-0.8	67	0.88	1.05	1.19
0.8-1.0	77	0.73	1.01	1.11
1.0-1.2	64	0.88	0.98	1.11
1.2-1.4	56	0.86	0.99	1.11
1.4-1.6	28	0.91	1.02	1.06
1.6-1.8	18	0.93	0.97	1.03
1.8-2.0	11	0.92	0.94	1.06
2.0-2.2	4	---	1.10	---
2.2-2.6	1	---	1.03	---
Total	399			

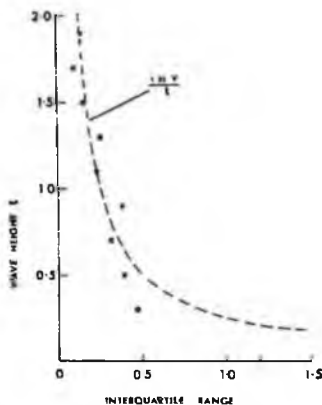


Fig. 6. The observed interquartile range of the relative wave period $\tau/\bar{\tau}$ (plotted points) as a function of the relative wave height $\xi = a/\lambda$. The broken curve represents the narrow band approximation.

(A16) follows the joint distribution (5). To obtain the marginal distribution (6), we simply divide (5) by (1).

Because of the assumption that the phases in (A1) are statistically independent, the Gaussian model that we have used is essentially a linear one. We may therefore expect that it will be somewhat more accurate for low surface waves in deep water than for steep waves or for waves in shallow water.

The effect of nonlinearities may also be somewhat diminished by our definition of the wave period τ as the time interval between alternate crossings of the mean level, rather than as twice the interval τ' between two adjacent crossings. For the period measured over a complete wavelength will probably be less affected by the presence of harmonics.

The distribution of the half-period τ' could indeed be determined theoretically by precisely the same argument, according to which we should have, in place of (A20), the relation $\tau' \approx \pi/\bar{\omega}$. But the corresponding wave periods $2\tau'$ would then be more subject to errors from the third and higher harmonics, of odd order.

A different kind of error may be expected to arise from the finite width of the spectrum, that is, from terms of higher order in ν . It should be possible in theory to obtain higher approximations on replacing (A20) by partial sums of the Taylor expansion

$$2\pi = \tau\bar{\omega} + \frac{1}{2}\tau^3\bar{\omega}^3 + \dots \quad (A30)$$

and then making use of the theoretical densities $p(\rho, \phi, \dot{\phi})$, etc., which may be derived in the same way as $p(\rho, \phi)$. However, since $p(\rho, \phi, \dot{\phi})$, for example, depends on the higher moments μ_3 and μ_4 , with two further moments being added for each new derivative of ϕ , the analytical details rapidly become complicated. Perhaps the approximation derived in the present paper is all that is really useful.

It should be noted that for a broad spectrum but relatively low waves the corresponding series for τ' , namely,

$$\pi = \tau'\bar{\omega} + \frac{1}{2}\tau'^3\bar{\omega}^3 + \dots \quad (A31)$$

may converge more rapidly than the series (A30) for τ . In such

circumstances, $p(\tau')$ may be determined more accurately than $p(\tau)$.

APPENDIX B: PROOF OF EQUATION (9)

Let m_n denote the n th moment of the energy spectrum:

$$m_n = \int \sigma^n E(\sigma) d\sigma$$

so that

$$\mu_0 = m_0 \quad (\sigma) = m_1/m_0$$

and

$$\mu_2 = (m_2 m_0 - m_1^2)/m_0$$

From the definition (A7) we have then

$$\begin{aligned} \nu^2 m_1^2 &= \mu_2 m_0 = (m_2 m_0 - m_1^2) \\ &= \iint (\sigma^2 - \sigma\sigma') E(\sigma) E(\sigma') d\sigma d\sigma' \end{aligned}$$

Reversing σ and σ' and adding, we get

$$2\nu^2 m_1^2 = \iint (\sigma - \sigma')^2 E(\sigma) E(\sigma') d\sigma d\sigma' \quad (B1)$$

Similarly from the definition of ϵ in Cartwright and Longuet-Higgins [1956] we have

$$\begin{aligned} \epsilon^2 m_4 m_0 &= (m_4 m_0 - m_2^2) \\ &= \iint (\sigma^4 - \sigma^2\sigma'^2) E(\sigma) E(\sigma') d\sigma d\sigma' \end{aligned}$$

hence

$$2\epsilon^2 m_4 m_0 = \iint (\sigma^2 - \sigma'^2)^2 E(\sigma) E(\sigma') d\sigma d\sigma' \quad (B2)$$

Now when the spectrum is narrow, we have $m_4 = (\sigma^4)m_0$. Also $(\sigma + \sigma')^2$, which is a factor of the integrand in (B2), is nearly constant over the important part of the region of integration, where $\sigma \approx \sigma' = (\sigma)$. So from (B2) we have

$$2\epsilon^2 (\sigma^4) m_0 \approx \iint (2(\sigma))^2 (\sigma - \sigma')^2 E(\sigma) E(\sigma') d\sigma d\sigma'$$

So from (B1),

$$\epsilon^2 (\sigma^4) m_0 \approx 4\nu^2 m_1^2$$

which is equivalent to (9).

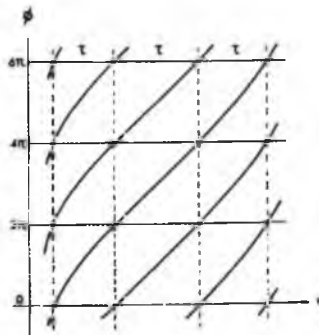


Fig. 7. Sketch of the total phase $\chi = (\sigma)t + \phi$ as a function of the time t .

REFERENCES

- Bretschneider, C. L., Wave variability and wave spectra for wind-generated gravity waves, *Tech. Memo. 118*, U.S. Beach Erosion Board, Washington, D. C., 1959.
- Curtwright, D. E., and M. S. Longuet-Higgins, The statistical distribution of the maxima of a random function, *Proc. Roy. Soc., Ser. A*, **237**, 212-232, 1956.
- Longuet-Higgins, M. S., On the statistical distribution of the heights of sea waves, *J. Mar. Res.* **9**, 245-266, 1952.
- Longuet-Higgins, M. S., The statistical analysis of a random, moving surface, *Phil. Trans. Roy. Soc. London, Ser. A*, **249**, 321-387, 1957.
- Longuet-Higgins, M. S., On the intervals between successive zeros of a random function, *Proc. Roy. Soc., Ser. A*, **246**, 99-118, 1958.
- Longuet-Higgins, M. S., The distribution of intervals between zeros of a stationary random function, *Phil. Trans. Roy. Soc. London, Ser. A*, **254**, 557-599, 1962.
- Longuet-Higgins, M. S., The effect of non-linearities on statistical distributions in the theory of sea waves, *J. Fluid Mech.*, **17**, 459-480, 1963.
- Rice, S. O., The mathematical analysis of random noise, *Bell Syst. Tech. J.*, **23**, 282-332, 1944.
- Rice, S. O., The mathematical analysis of random noise, *Bell Syst. Tech. J.*, **24**, 46-156, 1945.
- Wooding, R. A., An approximate joint probability distribution for amplitude and frequency in random noise, *N. Z. J. Sci. Tech., Sect. B*, **36**, 537-544, 1955.

(Received September 25, 1974;
accepted October 10, 1974.)

On the Distribution of the Heights of Sea Waves: Some Effects of Nonlinearity and Finite Band Width

MICHAEL S. LONGUET-HIGGINS

*Department of Applied Mathematics and Theoretical Physics, University of Cambridge, England
Institute of Oceanographic Sciences, Wormley, Surrey, England*

It is shown that some recent data on the crest-to-trough heights of sea waves are fitted just as well as by the one-parameter Rayleigh distribution as by the two-parameter Weibull distribution, provided that the rms amplitude \bar{a} is taken as $0.925(2m_0)^{1/2}$, where m_0 is the lowest moment of the frequency spectrum. Reasons why the ratio $\bar{a}/(2m_0)^{1/2}$ should differ from unity are discussed. It is shown that the effect of finite wave steepness would be to increase the ratio by a factor $\{1 + \frac{1}{2}(ak)^2\}$ approximately, contrary to observation. The effect of finite band width is estimated from a model assuming low background noise superposed linearly on a delta function spectrum. For narrow band widths one obtains the formula $\bar{a}^2/2m_0 = 1 - 0.734v^2$, where v is the rms spread of the noise about the mean frequency. Values of v^2 corresponding to Pierson-Moskowitz spectra give results in close agreement with observation.

1. INTRODUCTION

The distribution of the heights of wind waves is a question of some practical and theoretical interest. Some years ago the present author [Longuet-Higgins, 1952] showed that if the sea surface is assumed to be the sum of many sine waves in random phase, and if the frequency spectrum is sufficiently narrow, then the wave amplitudes (a wave amplitude is here defined as one half of the height of a wave crest above the preceding trough) are distributed according to a Rayleigh distribution. That is, the probability P that the amplitude a of any given wave exceeds the value a_0 is given by

$$P = \exp(-a_0^2/\bar{a}^2) \quad (1)$$

where \bar{a} denotes the rms amplitude. In the derivation of this law it was implied that the sea surface slopes were sufficiently small that the component waves could be linearly superposed and hence that there was no correlation between the phases of the different Fourier components.

Surprisingly, the distribution (1) has been found to agree well with many field observations, for example, the recent high-quality data of Earle [1975], even though the rms surface slope may exceed 0.1 in magnitude and the frequency spectrum may not necessarily be narrow.

Following Cartwright and Longuet-Higgins [1956] some authors [e.g., Haring *et al.*, 1976; Forristall, 1978] have used an alternative expression,

$$P = \exp(-a_0^2/2m_0) \quad (2)$$

where m_0 denotes the lowest moment of the frequency spectrum:

$$m_0 = \int_0^\infty E(\sigma) d\sigma \quad (3)$$

Since by the Khintchine theorem

$$m_0 = \bar{\eta}^2 \quad (4)$$

where η is the instantaneous surface elevation, it follows that for linear motions, when the individual wave crests are approximately sinusoidal,

$$m_0 = \frac{1}{2}\bar{a}^2 \quad (5)$$

Copyright © 1980 by the American Geophysical Union.

Paper number 9C1462.
0148-0221/80/009C-1462\$01.00

When and only when this relation is satisfied, then (2) is equivalent to (1).

However, Haring *et al.* [1976] and Forristall [1978], using data which include those analyzed by Earle [1975] have come to the conclusion that the distribution (2) does not fit their data so well. In place of (2), Forristall has proposed more complicated expressions (see section 5 and equation (6)). The purpose of the present note is, first, to show that the data presented by Forristall do nevertheless fit the distribution (1) rather well and second, to discuss theoretical reasons for the difference between distributions (1) and (2).

2. FIELD OBSERVATIONS

Figure 1 shows the same data as presented by Forristall [1978, Figure 2] and also by Haring *et al.* [1976]. These are essentially wave height distributions from storms in the Gulf of Mexico, each data set being normalized by the value $m_0^{1/2}$.

The broken curve in Figure 1 corresponds to the distribution

$$P = \exp(-\xi^2/\beta) \quad \xi = a_0/2m_0^{1/2} \quad (6)$$

which is called by Forristall 'the empirical distribution.' The values $\alpha = 2.126$ and $\beta = 1.052$ were fitted to the data points.

It appeared to me that the data in Figure 1 might equally well be fitted by a simple Rayleigh distribution of the form of (1) but with a suitably chosen value of a . By inspection, I tried the value

$$\bar{a} = 0.925 (2m_0)^{1/2} \quad (7)$$

The corresponding distribution is shown by the solid curve in Figure 1. It will be seen that the solid curve fits the data about as well as the broken curve.

3. DISCUSSION

From a practical point of view, when pondering whether to use the Rayleigh distribution (1) or the Weibull distribution (6), one may well give preference to an expression in which only one parameter, a , has to be estimated and not two parameters, α and β . Moreover, the simpler distribution appears to fit the data somewhat better at the higher wave amplitudes, which may be critical for certain applications.

Some confusion has been introduced by Forristall [1978] in referring to (2) as 'the Rayleigh distribution,' when in fact there is more than one possible such distribution, and when

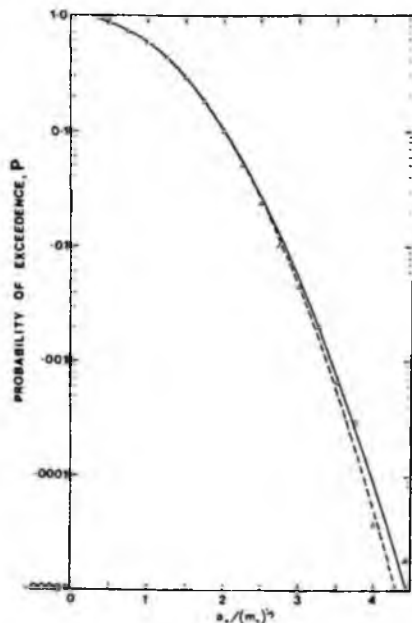


Fig. 1. Probability of the wave heights exceeding a given value $H_0 = 2a_0$. Plotted points are Forristall's (1978) data. Full curve represents (1) with $a = 0.925(2m_0)^{1/2}$. Broken curve represents (6).

(1), and not (2), was the form originally proposed by Longuet-Higgins [1952]. Forristall also refers to (6) as the empirical distribution, whereas (1) is also fitted to the data and is about as good a fit. Somewhat inconsistently, he suggests that (1) is defective, since it requires the fitting of a parameter \bar{a} from the data. Two similar 'defects' seem to apply to (6).

It is interesting to consider possible reasons for the discrepancy between (1) and (2). We shall consider two possible reasons: the finite steepness of the dominant waves and the finite width of the spectrum.

4. FINITE-AMPLITUDE EFFECTS: BOUND HARMONICS

One feature of a nonlinear wave of finite amplitude is a correlation between the phases of the fundamental Fourier component with wave number k and the second harmonic, wave number $2k$. This gives rise to the well-known narrowing of the wave crests and flattening of the wave troughs. Another correlation is between the fundamental and its third harmonic $3k$, which gives rise to an increase in the measured crest-to-trough height $2a$, relative to a simple sine wave of the same rms amplitude.

Consider now the potential energy of a uniform, deep-water wave train of finite amplitude. The mean potential energy V per unit horizontal area is

$$V = \frac{1}{2} \bar{\eta}^2 \quad (8)$$

where $\eta(x, t)$ is the surface elevation and we take for convenience $\rho = g = k = 1$. According to Stokes's theory of irrotational waves, however, if $2a$ denotes the crest-to-trough wave height, we have

$$V = \frac{1}{4} a^2 f(ak) \quad (9)$$

where f tends to 1 only in the limit as $ak \rightarrow 0$. The function f , and hence V , has been calculated by Longuet-Higgins [1975a, b, Figure 1 and Table 2]. In Figure 2 we show V as a function of $(ak)^2$ (solid curve). The broken line corresponds to linear theory, or sinusoidal waves. For small values of ak it is found that

$$V = \frac{1}{4} a^2 \left(1 - \frac{1}{2} (ak)^2 - \frac{19}{12} (ak)^4 - \frac{3077}{720} (ak)^6 - \dots \right) \quad (10)$$

(see Longuet-Higgins [1975a, b]; not all subsequent terms are negative). Note that V has a maximum at around $ak = 0.41$, $(ak)^2 = 0.19$, compared with the steepest uniform wave which has $ak = 0.443$, $(ak)^2 = 0.196$. The maximum V has been confirmed by Longuet-Higgins and Fox [1978] by a quite independent method of calculation. Such a maximum occurs also in solitary waves [Longuet-Higgins and Fenton, 1974] and is in fact characteristic of all steady gravity waves in water of uniform depth [see Cokelet, 1977].

From Figure 2 it follows that we would, in general, expect the potential energy of finite-amplitude waves to be somewhat less than that of a purely sinusoidal wave of the same crest-to-trough height.

Suppose now we have a random sea with a continuous spectrum. Note first that (4), connecting the lowest moment m_0 of the Fourier spectrum and the mean-square elevation $\bar{\eta}^2$, remains valid even if the phases of Fourier components are correlated. It follows that for nonlinear waves also we have, in general,

$$m_0 = \bar{\eta}^2 - 2V \quad (11)$$

where V denotes the mean potential energy of the sea surface, per unit horizontal area. The mean kinetic energy will, however, differ from V , so that the total energy is not equal to m_0 .

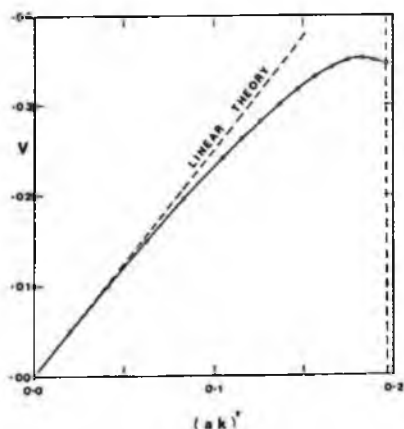


Fig. 2. Plot of the potential energy density V for a uniform train of deep-water waves of amplitude a .

Now suppose that the sea surface can be modelled as a succession (in space, or in time) of waves of nearly constant wave number k but of varying crest-to-trough height $2a$. We shall then have

$$m_0 = 2 \int V(a) dP \quad (12)$$

where $V(a)$ denotes the potential energy of a wave of amplitude a and P is the probability distribution of a .

But we already have seen both from Earle [1975] and from Figure 1 of the present paper that the distribution of a is given approximately by (1) even for waves of finite steepness and for spectra that are not very narrow. Suppose that for each individual wave the potential energy is given by (9) as for a steady Stokes wave of finite amplitude. Some of the waves may of course be breaking and some that are not quite breaking may be unsteady and asymmetric. Let us assume nevertheless that the curve for V in Figure 2 is valid as far as $(ak)^2 = 0.196$, and that beyond this value, V takes the same value as when $(ak)^2 = 0.196$. The approximation will be adequate so long as only a small proportion of the waves are actually breaking. From (1) and (12) we shall have

$$m_0 = \int_0^{a_{\max}} 2V(a) d \exp(-a^2/a^2) + \delta \quad (13)$$

where

$$\delta = 2V(a_{\max}) \exp(-a_{\max}^2/a^2) \quad (14)$$

For large values of a_{\max}^2/a^2 the 'remainder' δ will be exponentially small. Using the result

$$\int_0^{\infty} b^x d \exp(-b/\delta) = n! \delta^n \quad (15)$$

we have from (10) that

$$m_0 = \frac{1}{2} a^2 \left\{ 1 - (\delta k)^2 - \frac{19}{2} (\delta k)^4 - \frac{3077}{30} (\delta k)^6 - \dots \right\} \quad (16)$$

for sufficiently small ak .

Figure 3 shows a plot of the ratio

$$R = 2m_0/a^2 \quad (17)$$

by which the potential energy is reduced, relative to a uniform sine wave of amplitude equal to a . So long as δ/m_0 is small, any errors in R arising from the assumption that V is independent of a when $a > a_{\max}$, will be negligible. It appears that this is the case so long as a/a_{\max} is less than about 0.25, which is easily sufficient for our purposes.

Now from the data of Grden and Dorrestein [1958] quoted by Lake and Yuen [1978] it appears that over a wide range of conditions the mean steepness $a^{1/3}k$ of wind waves lies between about 0.14 and 0.18. Since from (1),

$$\delta/a^{11} = 2\pi^{-1/2} = 1.128 \quad (18)$$

[see Longuet-Higgins, 1952], it follows that generally

$$0.158 < \delta k < 0.203 \quad (19)$$

From Figure 3 we have then

$$0.968 < R < 0.935 \quad (20)$$

In other words, for the same rms amplitude a the effect of nonlinearity is to reduce the potential energy $\frac{1}{2}m_0$ by between

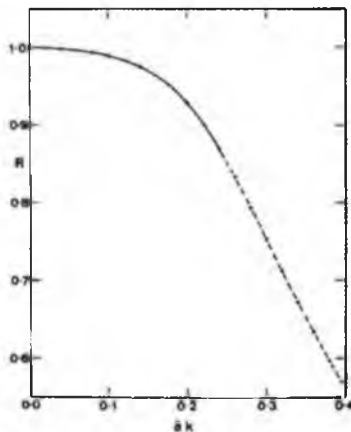


Fig. 3. The reduction of the mean potential energy $\frac{1}{2}m_0$ of a non-uniform train of waves with rms amplitude a , relative to a uniform sine wave of amplitude a .

3.2 and 6.5%. Hence the ratio $a/m_0^{1/2}$ is increased by between 1.6 and 3.3%.

Clearly, the effect works in the opposite direction to the observed effect (equation (7)).

5. FINITE BAND WIDTH: FREE HARMONICS

We shall now consider the effect of superposing on a narrow-band spectrum a small perturbation consisting of free waves, propagated independently of the unperturbed signal. Throughout this section we shall operate within the framework of the linear theory in which different components in the spectrum may be simply added without any dynamical interaction.

To begin, suppose we have some function of the time t of the form

$$y(t) = (A + \frac{1}{2}Ct^2) + (a + \beta t + \frac{1}{2}\gamma t^2) \quad (21)$$

where $A, C, \alpha, \beta, \gamma$ are constants. The first two terms represent a basic function having a maximum or a minimum at $t = 0$, $\gamma = A$, according as $C \leq 0$. The remaining terms represent a perturbation, in which we suppose that α, β, γ are of order $\epsilon \ll 1$ compared to $|C|$. It is easy to check that the derivative of the complete expression $y(t)$ vanishes not at $t = 0$ but at

$$t = -\frac{\beta}{C + \gamma} \quad (22)$$

when we have

$$y = (A + \alpha) - \frac{\beta^2}{2(C + \gamma)} \quad (23)$$

Since, further, $\gamma \ll C$, we may write, to order ϵ^2 ,

$$y = (A + \alpha) - \frac{\beta^2}{2C} \quad (24)$$

Consider, for example, the perturbed sine wave

$$y = b \cos \omega t + a_n \cos(\omega_n t + \theta) \quad (25)$$

where θ is a fixed phase and

$$a_n \ll b \quad a_n^2 a_n \ll \sigma^2 b \quad (26)$$

Considering the maximum near $t = 0$ we have in (23) to set $A = b$, $C = -A\sigma^2$, etc., and hence

$$y_{\max} = (b + a_n \cos \theta) + \frac{a_n^2 a_n^2}{b\sigma^2} \sin^2 \theta \quad (27)$$

To first order the correction to y_{\max} is just $a_n \cos \theta$. But the phase θ is random. If we now take average values (in angle brackets) with respect to the variable phase θ , we obtain simply

$$\langle y_{\max} \rangle = b + \frac{1}{4} \frac{a_n^2 a_n^2}{b\sigma^2} \quad (28)$$

In other words the height of the maximum is on average increased by an amount proportional to the mean-square slope of the perturbation.

Similarly, for the minimum near $t = \pi/\sigma$ we have in (23) to set $A = -b$, $C = b\sigma^2$, etc. Hence

$$y_{\min} = -b + a_n \cos(\theta + \pi\sigma_n/\sigma) - \frac{1}{4} \frac{a_n^2 a_n^2}{b\sigma^2} \sin^2(\theta + \pi\sigma_n/\sigma) \quad (29)$$

and taking phase averages

$$\langle y_{\min} \rangle = -b - \frac{1}{4} \frac{a_n^2 a_n^2}{b\sigma^2} \quad (30)$$

Now when we write for the wave amplitude

$$a = \frac{1}{2}(y_{\max} - y_{\min}) \quad (31)$$

we find

$$\langle a \rangle = b + \frac{1}{4} \frac{a_n^2 a_n^2}{b\sigma^2} \quad (32)$$

The proportional increment in wave height, namely, $a_n^2 a_n^2 / (4b^2 \sigma^2)$, is clearly dependent on the wave amplitude b . It follows that the distribution of a will not necessarily be a Rayleigh distribution.

Consider now the mean-square value of a . Returning to (31), we have

$$a = b + a_n \sin(\theta + \frac{1}{2}\pi\sigma_n/\sigma) \sin(\frac{1}{2}\pi\sigma_n/\sigma) + \frac{1}{4} \frac{a_n^2 a_n^2}{b\sigma^2} (\sin^2 \theta + \sin^2(\theta + \pi\sigma_n/\sigma)) \quad (33)$$

so that on squaring and taking mean values with respect to θ , we find, to second order,

$$\langle a^2 \rangle = b^2 + \frac{1}{2} a_n^2 \sin^2(\frac{1}{2}\pi\sigma_n/\sigma) + \frac{1}{2} a_n^2 a_n^2 / \sigma^2 \quad (34)$$

The additional terms on the right are now indeed independent of b .

Next let us suppose that y is a random process, given by

$$y = b \cos(\theta t + \phi) + \sum_n a_n \cos(\sigma_n t + \theta_n) \quad (35)$$

where all the phases θ_n are random. The summation on the right is the usual representation of a stochastic sum. Thus we write

$$\sum_n \frac{1}{2} a_n^2 \sim E(\sigma) d\sigma \quad (36)$$

where $E(\sigma)$ represents the spectrum of the perturbation. The appropriate generalization of (34) is that

$$\langle a^2 \rangle = b^2 + \int_0^\infty \{\sin^2(\frac{1}{2}\pi\sigma/\bar{\sigma}) + (\sigma/\bar{\sigma})^2\} E(\sigma) d\sigma \quad (37)$$

the amplitude b being fixed. Now let us further suppose that in (35) the amplitude b and phase ϕ are slowly varying in such a way that the first term has a narrow-band spectrum. Thus the spectrum of the unperturbed wave will be

$$E(\sigma) = \frac{1}{2} \delta(\sigma - \bar{\sigma}) \quad (38)$$

where δ is the Dirac delta function. The distribution of b will be Rayleigh:

$$P(b) = \exp(-b^2/\delta^2) \quad (39)$$

Equation (37) will be valid except for the very low values of the amplitude b when the contribution of b^2 to the expectancy $\langle a^2 \rangle$ will be relatively small. Therefore on multiplying dP and integrating over $0 < b < \infty$, we shall have, to the present order,

$$\bar{a}^2 = \langle a^2 \rangle = \delta^2 + \int_0^\infty \{\sin^2(\frac{1}{2}\pi\sigma/\bar{\sigma}) + (\sigma/\bar{\sigma})^2\} E(\sigma) d\sigma \quad (40)$$

Now the lowest moment of the spectrum is

$$m_0 = \int_0^\infty (E + E') d\sigma = \frac{1}{2} \delta^2 + \int_0^\infty E(\sigma) d\sigma \quad (41)$$

It follows that, to first order in E'/m_0 ,

$$\bar{a}^2 - 2m_0 + \int_0^\infty \{(\sigma^2/\bar{\sigma}^2 - 1) - \cos^2(\frac{1}{2}\pi\sigma/\bar{\sigma})\} E(\sigma) d\sigma \quad (42)$$

In other words, the mean-square amplitude \bar{a}^2 is changed relative to $2m_0$ by the value of the integral on the right.

The first term in the integral may be positive or negative according to the form of the perturbation spectrum E' ; energy at frequencies higher than $\bar{\sigma}$ will tend to increase the integrand, while energy at lower frequencies will tend to reduce it. The second term in the integral (42) is, however, always negative.

One special case can be discussed very simply, namely, when the energy of the perturbation is concentrated near σ itself. Then, since

$$(\sigma^2/\bar{\sigma}^2 - 1) = 2(\sigma/\bar{\sigma} - 1) + (\sigma/\bar{\sigma} - 1)^2 \quad (43)$$

and

$$\cos^2(\frac{1}{2}\pi\sigma/\bar{\sigma}) = \frac{1}{2}(1 - \cos\pi(\sigma/\bar{\sigma} - 1)) = \frac{\pi^2}{4} (\sigma/\bar{\sigma} - 1)^2 + \dots \quad (44)$$

we can express (42) in terms of the moments

$$\mu_r = \int_0^\infty (\sigma - \bar{\sigma})^r E'(\sigma) d\sigma \quad (45)$$

where $r = 1, 2, \dots$. Thus we obtain

$$\bar{a}^2 = 2m_0 + 2\mu_1/\bar{\sigma} - \left(\frac{\pi^2}{4} - 1\right) \mu_2/\bar{\sigma}^2 \quad (46)$$

correct to second order, and hence

$$\bar{a}^2/2m_0 = 1 + \frac{\mu_1}{\bar{\sigma}m_0} - \left(\frac{\pi^2}{8} - \frac{1}{2}\right) \frac{\mu_2}{\bar{\sigma}^2 m_0} \quad (47)$$

To lowest order in the band width, the sign of $(\bar{a}^2/2m_0 - 1)$ depends upon μ_1 , but if $\mu_1 = 0$, that is, the perturbation spectrum is weighted evenly about $\bar{\sigma}$, then to second order,

$$\bar{a}^2/2m_0 = 1 - \left(\frac{\sigma^2}{8} - \frac{1}{2}\right) \nu^2 = 1 - 0.734\nu^2 \quad (48)$$

where

$$\nu^2 = \mu_2/\sigma^2 m_0 \quad (49)$$

6. COMPARISON WITH OBSERVATION

The parameter ν in (48) represents a dimensionless band width of the spectrum. In the example from the Gulf of Mexico discussed by Longuet-Higgins [1975b] it was found that ν was equal to about 0.23, so $\nu^2 = 0.055$, but this spectrum was unusually narrow. For the more typical Pierson-Moskowitz spectrum

$$E(a) = \alpha a^{-5} \exp\{-(\beta/a)^4\} \quad (50)$$

where α and β are constants, it is easily shown that

$$m_0 = \frac{\alpha}{4\beta^{1/4}} \Gamma(1 - r/4) \quad (51)$$

where Γ denotes the usual gamma function, and hence

$$\nu^2 = \frac{m_0 m_2 - m_1^2}{m_1^2} = \frac{\Gamma(1)\Gamma(4)}{(\Gamma(3/4))^2} - 1 = 0.1803 \quad (52)$$

independently of α and β . Then (48) gives

$$\bar{a}/(2m_0)^{1/2} = 0.931 \quad (53)$$

which is quite close to the empirically determined value 0.925.

For the more general spectrum

$$E(a) = \alpha a^{-5} \exp\{-(\beta/a)^\gamma\} \quad (54)$$

we find similarly,

$$\nu^2 = \frac{\Gamma(4/\gamma)\Gamma(2/\gamma)}{(\Gamma(3/\gamma))^2} - 1 \quad (55)$$

so that in the cases $\gamma = 3$ and 5, for example, we have $\nu^2 = 0.2092$ and 0.1645, hence $\bar{a}/(2m_0)^{1/2} = 0.889$ and 0.938, respectively. Allowing for the finite-amplitude effects discussed in section 4, it appears that the observed value of $\bar{a}/(2m_0)^{1/2}$ can be accounted for.

It should be emphasized that we have used the Pierson-Moskowitz spectrum for illustration only. Any other spectrum with a narrow peak and with the same total moments, m_0 , m_1 , and m_2 , would yield the same result. Moreover, there appears no need to identify precisely which parts of the spectrum belong to the peak and which to the background noise.

7. CONCLUSIONS

We have shown that the data of Forristall [1978] support the conclusion that the distribution of wave heights in a storm is well described by the Rayleigh distribution (1), provided the rms amplitude a is estimated from the original record and not from the frequency spectrum. The introduction of the two-parameter Weibull distribution offers no obvious advantage, either empirical or theoretical.

Forristall's storm wave data fit a distribution in which a is about $0.925(2m_0)^{1/2}$. Our discussion has shown that the observation that $\bar{a}/(2m_0)^{1/2}$ is slightly less than unity cannot be accounted for as a finite-amplitude effect but may on the other hand be due to the presence of free background 'noise' in the spectrum, outside the dominant peak.

Acknowledgments This paper was prepared partly during a visit by the author to the Department of Engineering Sciences at the University of Florida, Gainesville. He is grateful to K. Millsaps and to other members of the Department for their hospitality and assistance.

REFERENCES

- Catwright, D. E., and M. S. Longuet-Higgins, The statistical distribution of the maxima of a random process, *Proc. Roy. Soc. London, Ser. A*, 237, 212-232, 1956.
- Cokelet, E. D., Steep gravity waves in water of arbitrary uniform depth, *Phil. Trans. Roy. Soc. London, Ser. A*, 286, 183-230, 1977.
- Earle, M. D., Extreme wave conditions during Hurricane Camille, *J. Geophys. Res.*, 80, 377-379, 1975.
- Forristall, G. Z., On the statistical distribution of wave heights in a storm, *J. Geophys. Res.*, 83, 2353-2358, 1978.
- Gr en, P., and R. Dorrestein, Zeegolven, *Rep. 11*, Kon. Ned. Meteorol. Inst., De Bilt, 1958.
- Haring, R. E., A. R. Osborne, and L. P. Spencer, Extreme wave parameters based on continental shelf storm wave records, *Proceedings of the 15th Conference on Coastal Engineering*, Amer. Soc. Civil Eng., New York, July 1976.
- Lake, B. M., and H. C. Yuen, A new model for nonlinear wind waves. I. Physical model and experimental evidence, *J. Fluid Mech.*, 88, 33-62, 1978.
- Longuet-Higgins, M. S., On the statistical distribution of the heights of sea waves, *J. Mar. Res.*, 11, 245-266, 1952.
- Longuet-Higgins, M. S., Integral properties of periodic gravity waves of finite amplitude, *Proc. Roy. Soc. London, Ser. A*, 342, 157-174, 1975a.
- Longuet-Higgins, M. S., On the joint distribution of the periods and amplitudes of sea waves, *J. Geophys. Res.*, 80, 2688-2694, 1975b.
- Longuet-Higgins, M. S., and J. D. Fenton, On the mass, momentum, energy and circulation of a solitary wave II, *Proc. Roy. Soc. London, Ser. A*, 340, 471-493, 1974.
- Longuet-Higgins, M. S., and M. J. H. Fox, Theory of the almost-highest wave II: Matching and analytic extension, *J. Fluid Mech.*, 85, 769-782, 1978.

(Received April 17, 1979;
revised October 9, 1979;
accepted October 15, 1979.)

On the Skewness of Sea-Surface Slopes

M. S. LONGUET-HIGGINS

*Department of Applied Mathematics and Theoretical Physics, Cambridge, England
 and Institute of Oceanographic Sciences, Wormley, Surrey*

(Manuscript received 1 December 1981, in final form 6 July 1982)

ABSTRACT

Sunlight reflected from a wind-roughened sea surface produces a glitter pattern in which the region of maximum intensity tends to be shifted horizontally by an apparent angle Δ , depending on the wind speed. It is shown that Δ is related directly to the skewness of the distribution of surface slopes. From the observed data of Cox and Munk (1956) it is possible to deduce a simple correlation between Δ and the wind stress τ .

The physical mechanism underlying slope skewness is investigated. The skewness which results from damping of individual waves is shown to be negligible. A two-scale model is proposed, in which damped ripples or short gravity waves ride on the surface of longer gravity waves. The model is found to give skewness of the observed magnitude. The sign of the skewness depends on the angle between the wind maintaining the ripples and the direction of the longer waves, in agreement with observation.

Certain theoretical relations between Δ and the phase γ of the short-wave modulation may be of interest in interpreting observations of the sea surface by other types of remote sensing.

1. Introduction

The glitter-pattern of reflected sunlight has been used by Cox and Munk (1956) to study the distribution of sea-surface slopes, in relation to the local wind speed. Among the effects that they observed was that the location of the most intense reflection tended to be shifted horizontally, relative to its position in the absence of wind or waves. The angular displacement was evidently associated with a skewness in the measured distribution of the surface slope. Since an angle is easier to measure, in general, than an intensity, the question arises: can we use such a measurement to obtain information on the slope distribution, and hence the wind stress?

Some encouragement for this view can be derived from a theoretical demonstration (Longuet-Higgins, 1963) that in the absence of applied surface forces or viscous stresses, the distribution of surface slopes is highly symmetric; the coefficient of skewness is at most of order σ^3 where σ is the rms slope. Hence any actual surface skewness may be a sensitive indicator of wind stress.

The questions to be addressed in this paper are the following:

1) How precisely is the observed angular displacement Δ of the maximum optical intensity related to the slope distribution? This is answered by Eqs. (2.13) and (2.14).

2) Is there an empirical relation between Δ and the horizontal wind stress? This is answered in the

affirmative by Eq. (3.12), for wind speeds up to 15 m s^{-1} .

3) What is the physical explanation for the observed skewness? We show first in Section 4 that although a simple phase shift in the first harmonic of a travelling wave causes no slope skewness, any shift in the bound *second* harmonic does tend to cause such a skewness [see Fig. 4 and Eq. (4.6)]. In free but undamped waves, such a phase-shifted harmonic occurs only in a transient state, which can lead to breaking.

Section 5 treats damped waves, where it is shown by a simple argument that viscous dissipation also gives rise to a phase-shifted second harmonic and hence to a skewness in the slopes. However, the magnitude of this effect is too small to account for the observations.

Accordingly in Section 6 we propose a different, two-scale model in which short ripples, or capillary-gravity waves, are assumed to ride on the surface of much longer gravity waves, the shorter waves being modulated by the presence of the longer waves. It is shown that this gives rise to a slope skewness [Eqs. (6.10) and (6.13)] of the same magnitude and sign as is actually observed.

These results enable us to discuss in Section 7 a fourth underlying question, namely whether there is any necessary, fundamental relation between slope skewness and wind stress, and to answer it in the negative.

On the other hand, some of the simple relations

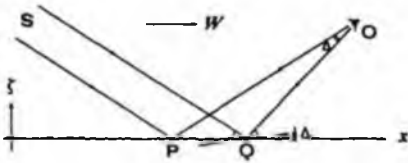


FIG. 1. The reflection of rays from the sun S towards an observer O, when wind and waves are in the same direction.

derived in the course of the paper may well be of use in the interpretation of radar backscatter at centimeter wavelengths. In particular, we may mention Eq. (6.10), which relates Δ to the steepness s of the longer waves, the phase angle γ of short-wave modulation, and the depth of modulation δ . These relations follow from the geometry of the model, and are independent of any particular dynamical assumptions.

2. Geometry

Throughout this paper we shall restrict the discussion to the two-dimensional situation when the direction of the sun, wind and swell are all in line. This suffices to elucidate the main principles, and the reader will readily supply the appropriate generalizations to the case of arbitrary relative directions.

Suppose then that the direction of the wind is in the vertical plane containing the sun S and the observer O, and is towards the observer, as in Fig. 1. If the sea surface were calm, the rays would be reflected from near a specular point P, say, where SP and PO make equal angles with the horizontal. When the wind blows, the region of most intense reflection (after allowing for reflectance and background radiation) is from the neighborhood of a point Q, say, shifted downwind from P by an apparent angle Δ . Accordingly, the mode of the slope distribution must be shifted by a positive angle $1/2\Delta$.

If we take axes as in Fig. 1 with the x -axis horizontal in the plane OPQS, and if the surface elevation

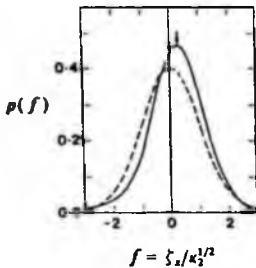


FIG. 2. Schematic diagram of the distribution of upwind slope. Compare with Fig. 15 of Cox and Munk (1956).

is $\zeta(x, t)$ with downwind slope ζ_x , then the probability density $p(\zeta_x)$ has a maximum when

$$\zeta_x = 1/2\Delta. \tag{2.1}$$

This is shown experimentally in Fig. 2, which is a downwind section through a typical joint distribution $p(\zeta_x, \zeta_y)$ as observed by Cox and Munk (1956). The distribution is normalized by dividing ζ_x by the rms downwind slope $\mu_2^{1/2}$.

We now derive a simple expression for Δ in terms of the moments of $p(\zeta_x)$.

Suppose that the distribution of ζ_x is approximately Gaussian, and may be represented by the Gram-Charlier series¹

$$p(\zeta_x) = \frac{1}{(2\pi\kappa_2)^{1/2}} \exp(-1/2f^2) [1 + 1/6H_3 + (1/24\lambda_4H_4 + 1/72\lambda_3^2H_6) + \dots], \tag{2.2}$$

in which κ_n is the n th cumulant of $p(\zeta_x)$, i.e., if

$$\mu_n = \int \zeta_x^n p(\zeta_x) d\zeta_x, \tag{2.3}$$

then

$$\left. \begin{aligned} \kappa_1 &= \mu_1 \\ \kappa_2 &= \mu_2 - \mu_1^2 \\ \kappa_3 &= \mu_3 - 3\mu_1\mu_2 + 2\mu_1^3 \\ &\dots \end{aligned} \right\} \tag{2.4}$$

Also

$$\lambda_n = \kappa_n / \kappa_2^{n/2}, \tag{2.5}$$

$$f = (\zeta_x - \kappa_1) / \kappa_2^{1/2}, \tag{2.6}$$

and H_n is the n th Hermite polynomial:

$$\left. \begin{aligned} H_3 &= f^3 - 3f \\ H_4 &= f^4 - 6f^2 + 3 \\ &\dots \end{aligned} \right\} \tag{2.7}$$

In deep water we can assume that the sea surface has a negligible mean tilt, so $\mu_1 = 0$ and hence

$$\kappa_1 = 0, \quad \kappa_2 = \mu_2, \quad \kappa_3 = \mu_3. \tag{2.8}$$

Also

$$f = \zeta_x / \kappa_2^{1/2}. \tag{2.9}$$

Then to order f^2 , and if we neglect λ_4 and λ_3^2 compared to 1,

$$p(\zeta_x) = (2\pi\kappa_2)^{-1/2} (1 - 1/2f^2)(1 - 1/2\lambda_3f). \tag{2.10}$$

Hence $p(\zeta_x)$ has a maximum when

$$f = -1/2\lambda_3 = -1/2\lambda_3 / \kappa_2^{1/2}, \tag{2.11}$$

this is when

¹ A theoretical justification for this form, which differs slightly from Cox and Munk (1956), was given by Longuet-Higgins (1963).

$$\zeta_x = -1/2\kappa_3/\kappa_2. \quad (2.12)$$

From (2.1) and (2.12) it follows that

$$\Delta = -\kappa_3/\kappa_2, \quad (2.13)$$

where κ_2 and κ_3 are equal to the second and third moments, respectively, of the distribution of $p(\zeta_x)$. This can also be written

$$\Delta = -\overline{\zeta_x^3}/\overline{\zeta_x^2} \quad (2.14)$$

in which a bar denotes the ensemble average.

Three comments are in order. First, it does not appear from Fig. 2 that the mean slope μ_1 is zero. However, this is because only the central part of the distribution is shown, the tails not being measured accurately. In Fig. 2, the rightward shift of the distribution over the central range, say $-2 < f < 2$, is actually compensated by a leftward shift in the "tails" of the distribution, when $|f| > 2$.

Likewise it would appear from Fig. 2 that the third moment μ_3 is positive. But the compensation from the tails of the distribution is relatively greater for μ_3 than for μ_1 , so that in fact μ_3 turns out to be *negative*.

In the actual evaluation of the coefficients in the series (2), Cox and Munk (1956) found it convenient not to calculate the moments of $p(\zeta_x)$ directly, but to use a method of curve-fitting to the central, accurately determined, range of slopes.

3. The wind stress: an empirical result

Regardless of the cause of the skewness, we may use the results of Section 2, combined with the field observations of Cox and Munk (1956), to derive an empirical relation between the angle Δ and the horizontal wind stress, at moderate wind speeds.

Fig. 3 shows a plot of the coefficient of skewness

$$\lambda_3 = \kappa_3/\kappa_2^{3/2} \quad (3.1)$$

as a function of $\kappa_2^{3/2}$, calculated from their data (see Table 1) (cf. also Longuet-Higgins, 1963, Fig. 2). In their notation

$$\left. \begin{aligned} \kappa_2 &= \sigma_w^2 \\ \lambda_3 &= -6\sigma_w^3(a_1' + a_3) \end{aligned} \right\} \quad (3.2)$$

in other words, we take a one-dimensional section through their two-dimensional slope distribution. From Fig. 3 it would appear that

$$\lambda_3 = -45\kappa_2^{3/2} \quad (3.3)$$

approximately. Hence

$$\kappa_3 = -45\kappa_2^3, \quad (3.4)$$

and so from (2.13)

$$\Delta = 45\kappa_2. \quad (3.5)$$

But Cox and Munk also found (see their Fig. 13)

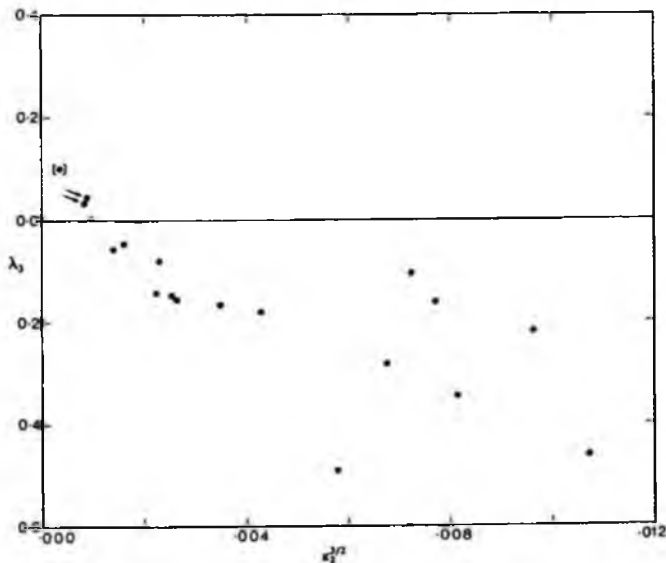


FIG. 3. The observed coefficient of skewness λ_3 plotted against (rms slope)³ from the data of Cox and Munk.

TABLE 1. Calculated values of Δ and $s \cos \psi$, from the data of Cox and Munk (1956).^a

W ($m \text{ s}^{-1}$)	H_s (ft)	T_s (s)	ψ (deg)	κ_1	λ_1	Δ	$s \cos \psi$
11.6	3.5	4	—	0.0390	-0.163	0.072	—
13.3	6	5	6	0.0484	-0.463	0.217	0.10
13.8	6	5	6	0.0452	-0.220	0.101	0.10
13.7	6	5	6	0.0404	-0.345	0.155	0.10
0.72	1.5	3	9	0.0005	+0.100	-0.015	0.07
8.58	2	3	19	0.0230	-0.165	0.064	0.09
0.89	—	—	—	0.0153	-0.004	0.001	—
3.93	1	2	0	0.0098	+0.003	-0.001	0.11
8.00	2	3	6	0.0191	-0.156	0.213	0.10
6.30	4	3	5	0.0170	-0.143	0.052	0.19
6.44	4	3	5	0.0186	-0.148	0.055	0.19
4.92	4	3	10	0.0174	-0.080	0.029	0.18
1.83	3	4	120	0.0090	+0.043	-0.013	-0.04
1.39	3	4	176	0.0087	+0.033	-0.010	-0.08
3.35	5	4	85	0.0125	-0.053	0.018	0.01
10.2	4	4	0	0.0357	-0.283	0.123	-0.11
11.7	5	4	0	0.0374	-0.105	0.046	0.14
5.45	2	3	90	0.0137	-0.046	0.016	0.00
9.79	4	3	6	0.0264	-0.180	0.075	0.19
9.74	4	3	8	0.0322	-0.491	0.208	0.19
10.5	5	3	12	0.0365	-0.598	0.261	0.24

^a Notes: W was measured at 41 ft, H_s denotes significant wave height, T_s denotes period of significant waves.

$$\kappa_2 \approx 0.0032W, \tag{3.6}$$

where W denotes the wind speed ($m \text{ s}^{-1}$). Combining (3.5) and (3.6) yields

$$\Delta \approx 4.6 \times 10^{-4} W^2, \tag{3.7}$$

This relates the angle of deflection Δ directly to the wind speed W , when $W \leq 15 \text{ m s}^{-1}$.

On the other hand, the shear stress τ exerted by the wind is given approximately by

$$\tau = C_D \rho_a (100W)^2, \tag{3.8}$$

where $C_D = 1.5 \times 10^{-3}$ is a drag coefficient, and $\rho_a \approx 1.2 \times 10^{-3} \text{ g/cm}^{-3}$ is the density of air. Comparing (3.7) and (3.8) we see that

$$\tau \approx 39 \Delta \text{ dyn cm}^{-2}, \tag{3.9}$$

In other words, the wind stress is directly proportional to the angular displacement of the glitter maximum.

To express Eq. (3.9) in dimensionless form it is convenient to introduce the basic shear stress

$$\tau_0 = \rho_a c_{\min}^2, \tag{3.10}$$

where c_{\min} denotes the minimum phase speed of capillary-gravity waves, i.e.,

$$c_{\min} = (2gT)^{1/4} \approx 23 \text{ cm s}^{-1} \tag{3.11}$$

(see Lamb 1932, Section 267); thus $\tau_0 = 0.53 \text{ dyn cm}^{-2}$. As a result Eq. (3.10) may be written

$$\tau/\tau_0 \approx 74\Delta. \tag{3.12}$$

4. Skewness of individual waves

We consider first the skewness of the slope distribution that may arise from the individual waves, as illustrated in Fig. 4. Let

$$\zeta = a \cos \theta + O(a^2 k) \cos 2\theta + b \sin 2\theta, \tag{4.1}$$

where

$$\theta = k(x - ct), \quad b \ll a. \tag{4.2}$$

In other words suppose there is a second harmonic $b \sin 2\theta$ phase locked to the fundamental wave, but in quadrature with the ordinary second harmonic in a steady surface wave. If $b > 0$, the effect will be to steepen slightly the forward face of the wave and to correspondingly flatten the rear slope, as in Fig. 4. In fact, the slope ζ_x is given by

$$\zeta_x = -ak \sin \theta + O(ak)^2 \sin 2\theta - 2bk \cos 2\theta, \tag{4.3}$$

so that to lowest order

$$\left. \begin{aligned} \kappa_1 &= \overline{\zeta_x} = 0 \\ \kappa_2 &= \overline{\zeta_x^2} a^2 k^2 \sin^2 \theta = \frac{1}{2} a^2 k^2 \\ \kappa_3 &= \overline{\zeta_x^3} = 6a^2 b k^3 \sin^2 \theta \cos 2\theta = -\frac{3}{2} a^2 b k^3 \end{aligned} \right\}, \tag{4.4}$$

where a bar denotes the average with respect to x . Therefore

$$\lambda_3 = \kappa_3 / \kappa_2^{3/2} = -3\sqrt{2}b/a \tag{4.5}$$

and from (2.13)

$$\Delta = -\kappa_3 \kappa_2^{-1} = \frac{3}{2} b k. \tag{4.6}$$

It is then possible for the asymmetric second harmonic to exist? If linear theory is applicable, the free speed of a gravity wave with wavenumber $2k$ is not c but $c/\sqrt{2}$. To maintain the harmonic as a forced wave with speed c requires the application of a surface pressure p' given by

$$p'/\rho = -\phi'_i - g\zeta', \tag{4.7}$$

where

$$\left. \begin{aligned} \phi'_i &= -cbe^{2ky} \cos 2\theta \\ \zeta' &= b \sin 2\theta \end{aligned} \right\} \tag{4.8}$$

and $c^2 = g/k$. This yields

$$p' = \rho g b \sin 2\theta = O(\lambda_3 \rho g a), \tag{4.9}$$

from (4.5). However, the surface pressures due to the wind are probably of order $10^{-3} \rho g a$, considerably smaller.



FIG. 4. Schematic diagram showing how skewness of individual waves can arise from a second harmonic.

However, if the steepness ak of the fundamental is sufficiently great, the contribution of its orbital velocity to the dynamics of the harmonic ζ' becomes appreciable. Since the orbital velocity is forward at the crest, where the energy of the harmonic tends to be greatest, the effective relative speed between the free harmonic and the fundamental will be reduced. Hence p' is also reduced. Finally, as shown by precise calculation (Longuet-Higgins, 1978, Figs. 1 and 4), the speeds of the free second harmonic and of its fundamental become equal at $ak = 0.436$ (less than the maximum steepness $ak = 0.443$). At this point the second harmonic exists as a neutrally stable perturbation of the fundamental Stokes wave, and $p' = 0$. When $ak > 0.436$ the perturbation becomes *unstable*, that is to say it grows exponentially in time. This presumably leads very rapidly to an overturning of the free surface, as was found in a similar case studied numerically by Longuet-Higgins and Cokelet (1978).

We conclude that skewness of individual, undamped waves can exist, but only in a transient state, just before breaking.² It might be possible to base a theory of skewness on the assumption of a supply of energy from the wind, sufficient to maintain the wave field in face of losses due to overturning of the free surface. But since the rates of growth of the instabilities depend strongly on the difference between the actual steepness ak and the critical value $ak = 0.436$, the rate of growth of the skewness is difficult to estimate precisely.

This type of skewness may be most important for records of the sea surface in which the high-frequency part of the spectrum has been eliminated by a low-pass instrument or filter.

5. Skewness in damped waves

In the previous section it was assumed that individual waves were undamped. We show now that the action of viscous damping on the otherwise free gravity wave is to induce a slight asymmetry in the wave profile.

As pointed out by Lamb (1932, Section 348), surface waves in a viscous fluid can be maintained in a steady state by the application of the appropriate normal and tangential stresses at the free surface. Let these be denoted by τ_{ns} and τ'_{ns} respectively. In the absence of these applied stresses, there develops a thin boundary layer, as if fictitious stresses $-\tau_{ns}$ and $-\tau'_{ns}$ were applied to an otherwise inviscid fluid.

Now in a steady wave, with symmetric profile, the normal stresses $-\tau_{ns}$ are symmetric also, and so produce no asymmetry. However, the tangential stress $-\tau'_{ns}$ is asymmetric, and so produces some asymmetry. By a very simple argument it may be shown

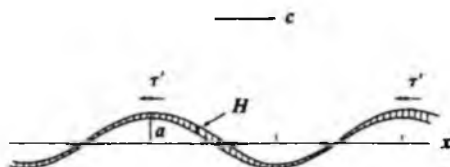


FIG. 5. Thickening of the boundary layer due to variable tangential stresses on a surface wave.

(see Longuet-Higgins, 1969) that any tangential stress τ' acting at the surface of the wave produces a local thickening of the boundary layers given by

$$\frac{\partial H}{\partial t} = \frac{\tau'}{\rho c}, \quad (5.1)$$

where H is the boundary-layer thickness (see Fig. 5). This produces an excess pressure $\rho g H$ at the surface which generally is in quadrature with τ' , and does work on the fluid in a way entirely equivalent to an applied normal stress.

To prove (5.1) we note that if M is the excess mass flux or momentum within the boundary layer then

$$\frac{\partial M}{\partial t} = \tau', \quad (5.2)$$

and if (u', v') denote the components of the excess velocity in the directions (s, n) tangential and normal to the surface, then

$$\begin{aligned} \frac{\partial H}{\partial t} = [v'] &= \int \frac{\partial v'}{\partial n} dn \\ &\approx - \int \frac{\partial u'}{\partial s} du = - \frac{\partial M}{\partial s \rho}, \end{aligned} \quad (5.3)$$

since $M = \int \rho u' dn$. But if the motion is (approximately) progressive with phase speed c , then correct to second order in ak

$$\frac{\partial}{\partial s} = - \frac{1}{c} \frac{\partial}{\partial t}. \quad (5.4)$$

Hence

$$\frac{\partial H}{\partial t} = \frac{1}{\rho c} \frac{\partial M}{\partial t}, \quad (5.5)$$

from which (5.1) follows.

In fact by applying (5.4) again, Eq. (5.1) can be put in still more convenient form

$$\frac{\partial H}{\partial s} = - \frac{\tau'}{\rho c}. \quad (5.6)$$

In the present case we have

$$\tau' = -\tau_{ns} = -2\mu\phi_{ns}, \quad (5.7)$$

where μ is the coefficient of viscosity and ϕ denotes the velocity potential of the irrotational flow just beyond the boundary layer. To first order in the wave

² For capillary-gravity waves this conclusion must be modified.

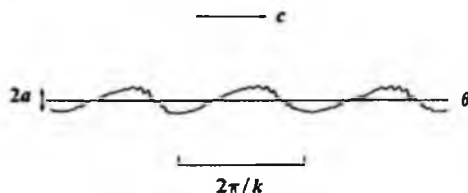


FIG. 6. A modulated train of short waves riding on the surface of longer waves ($C > 0$).

steepness ak , this stress produces a thickening of the boundary layer on the forward slopes of the wave as indicated in Fig. 5, but no change in the slope distribution, because the surface is still sinusoidal, though shifted slightly in phase.

To second order, it is easy to show (see Appendix B) that

$$\phi_{ns} = ak^2c \cos\theta + a^2k^3c(\cos^2\theta - 2 \sin^2\theta). \quad (5.8)$$

The nonlinear terms now give rise to a term in $\cos 2\theta$:

$$\phi'_{ns} = \frac{3}{2}a^2k^3c \cos 2\theta, \quad (5.9)$$

and so from (5.7) the relevant contribution to the stress is

$$\tau' = -3\mu a^2k^3c \cos 2\theta, \quad (5.10)$$

which is greatest at the wave crests. By (5.6) this produces a small change $\zeta' = H$ to the surface elevation, the change in the surface slope ζ'_x being

$$\zeta'_x \approx \frac{\partial H}{\partial s} = 3(ak)^2\nu\sigma/c^2 \cos 2\theta, \quad (5.11)$$

where

$$\sigma = ck \quad (5.12)$$

and $\nu = \mu/\rho$ is the kinematic viscosity.

The formula (4.6) for the angle Δ now applies, so that we have

$$\Delta = \frac{9}{4}(ak)^2\nu\sigma/c^2. \quad (5.13)$$

Also

$$\lambda_3 = -\frac{9}{2\sqrt{2}}(ak)^2\nu\sigma/c^2 \quad (5.14)$$

from (4.5).

However, it will be seen that for gravity waves the effect is quite small. For if we take

$$\left. \begin{aligned} \nu &= 0.013 \text{ cm s}^{-1} \\ \sigma &= 10 \text{ rad s}^{-1} \\ c &\geq c_{min} = 23 \text{ cm s}^{-1} \end{aligned} \right\}$$

then

$$\nu\sigma/c^2 \leq 2.5 \times 10^{-5}$$

and so Δ is $O(10^{-4})$ at most, while λ_3 is $O(10^{-3})$, generally much smaller than in the observations of Fig. 3.

For capillary or capillary-gravity waves similar conclusions will apply.

6. Skewness due to ripples: a two-scale model

It was shown experimentally by Cox (1958) that a significant proportion of the variance of surface slope may be contributed by short gravity-capillary waves and ripples, rather than by longer gravity waves. Moreover, the ripples are found preferentially on the forward faces of the steep gravity waves, even in the absence of wind.

Theoretically, the spontaneous generation of capillary waves at the crests of steep gravity waves was analyzed by Longuet-Higgins (1962). Furthermore, Phillips (1981) has shown that capillary waves of whatever origin can be trapped on the forward face of a gravity wave, by convergence of the orbital motion.

Even if the shorter waves are not trapped, however, viscous damping of the short waves, combined with the action of the radiation stresses, may tend to produce a greater steepening of the short waves on the forward slopes of the longer waves than on the rear slopes. A theoretical example is given below in Appendix A.

Accordingly we consider a simple two-scale model of the sea surface in which short (capillary or gravity-capillary) waves ride on a random sea of much longer waves, as in Fig. 6. The steepness of the shorter waves is assumed to be modulated by the longer waves, and in such a way that the short waves are steeper, on the average, when riding on the forward faces of the longer waves. Thus we let

$$\zeta = a \cos\theta + a' \cos\theta', \quad (6.1)$$

where a and θ denote the amplitude and phase function for the longer waves, with wavenumber

$$k = \partial\theta/\partial x. \quad (6.2)$$

Here a and k are assumed to be slowly varying functions of x and t . Primed symbols a' , θ' , etc., will denote corresponding quantities for the short waves, and we assume

$$a'k' = \alpha + \beta ak \cos(\theta - \gamma), \quad (6.3)$$

where α , β and γ are constants. We expect $0 < \gamma < 90^\circ$.

Since by hypothesis $k' \gg k$, the surface slope ζ'_x is found from (6.1) to be

$$\zeta'_x = -ak \sin\theta - [\alpha + \beta ak \cos(\theta - \gamma)] \sin\theta'. \quad (6.4)$$

From this we may calculate the moments of $\rho(\zeta'_x)$ by averaging ζ'^n , first with respect to the fast phase θ' and then with respect to the slower phase θ . In this way we obtain

$$\kappa_1 = \overline{\zeta'_x} = 0 \quad (6.5)$$

as required. Next

$$\kappa_2 = \overline{\xi_x^2} = \frac{1}{2}s^2 + \frac{1}{2}(\alpha^2 + \frac{1}{2}\beta^2 s^2), \quad (6.6)$$

where $s^2 = \overline{(\alpha k)^2}$, twice the mean-square slope of the longer waves. Finally,

$$\begin{aligned} \kappa_3 = \overline{\xi_x^3} &= -3(\alpha k \sin\theta) \cdot 2\alpha\beta ak \cos(\theta - \gamma) \cdot \frac{1}{2} \\ &= -\frac{3}{2}\alpha\beta s^2 \sin\gamma. \end{aligned} \quad (6.7)$$

If the maximum ripple slopes occur on the forward faces of the longer waves, then $\alpha\beta \sin\gamma > 0$, and so κ_3 is negative. To interpret this, we note that on the rear slopes of the waves, where the ripple slopes are smallest in magnitude, the effect of the longer waves is to shift the slopes in the positive sense. Hence the central part of the distribution tends to be shifted to the right, as in Fig. 2. On the other hand, where the magnitude of the ripple slopes is greatest, i.e., on the forward face of the longer waves, the slopes are shifted negatively. Hence the tails of the distribution are shifted to the left. Because of the predominant effect of the tails, the third cumulant κ_3 becomes negative.

Further, if the ripples make a preponderant contribution to the slope variance, so that $\alpha^2 \gg s^2$, we have from (6.6)

$$\kappa_2 = \frac{1}{2}\alpha^2(1 + \frac{1}{2}\delta^2), \quad (6.8)$$

where

$$\delta = \beta s/\alpha \quad (6.9)$$

represents a "depth of modulation" of the shorter waves. Finally from Eq. (2.13) we have

$$\Delta = \frac{3\delta}{1 + \frac{1}{2}\delta^2} s \sin\gamma. \quad (6.10)$$

In other words, the apparent angular displacement Δ of the mode is independent of the mean-square ripple steepness, and depends only on the rms steepness of the longer waves, together with the relative depth of ripple modulation δ and the phase shift γ . Since $\delta/(1 + \frac{1}{2}\delta^2)$ is monotonic in the range $0 < \delta < 1$, the first factor in (6.10) has as its upper bound the value taken when $\delta = 1$, so we have always

$$\Delta \leq 2s \sin\gamma. \quad (6.11)$$

Hence it follows immediately that

$$\Delta \leq 2s. \quad (6.12)$$

We have supposed the direction of the ripples to be the same as that of the longer waves. If, on the other hand, the direction of the longer waves is opposite to that assumed, i.e., it is away from the observer, the sign of the right-hand side in (6.10) would be reversed (regardless of the ripple direction).

Are these results consistent with the observations shown in Fig. 3? In those observations, which are summarized in Table 1, the wind direction, which presumably determines the direction of the ripples, generally differed from that of the significant waves

by an angle $\psi < 90^\circ$. There were two exceptions, marked by arrows, which happen both to correspond to positive values of λ_3 . The only other positive values are the plot very close to the horizontal axis at $\kappa_3^{3/2} = 0.0010$, for which $|\lambda_3|$ was only 0.003, and the plot at $\kappa_3^{3/2} = 0.00034$, which was in a wind speed $< 1 \text{ m s}^{-1}$, and for which the determination of λ_3 was probably less accurate. This has been marked with square brackets.

The simplest generalization of (6.10) to a situation in which the longer waves travel at an arbitrary angle ψ to the wind is

$$\Delta = F(\delta) \sin\gamma \cdot s \cos\psi, \quad (6.13)$$

where $F(\delta)$ denotes the first factor on the right of (6.10). The counterparts of the inequalities (6.12) are

$$|\Delta| \leq 2|\sin\gamma \cdot s \cos\psi| \quad (6.14)$$

and

$$|\Delta| \leq 2s|\cos\psi|. \quad (6.15)$$

To test whether (6.14) is satisfied, we have plotted in Fig. 7 the values of

$$\Delta = -\kappa_3/\kappa_2 = -\kappa_3^{3/2}\lambda_3 \quad (6.16)$$

against the corresponding values of $s \cos\psi$, where $s = \alpha k$ is estimated from the relation

$$\delta = H_s/2.83, \quad (6.17)$$

and H_s is the significant wave height. Also $k = \sigma^2/g$ where σ is the radian frequency of the longer waves, taken equal to $2\pi/T_s$.

The inequality (6.15) corresponds to the sectors bounded by the diagonal line in Fig. 7 and the horizontal axis. It will be seen that the plots do in fact lie more or less in this region, apparently confirming our simple model. (It should be borne in mind, however, that some of the measured parameters, particularly for the swell, are not given very accurately.)

We note that for points lying close to the diagonal line in Fig. 7 both δ and $|\sin\gamma|$ must approach 1. Hence the ripple modulation must be a maximum, and it must be nearly in quadrature with the elevation of the longer waves.

7. Discussion

We have suggested three possible mechanisms for producing skewness of the surface slopes, and have shown that one of them—modulation of short waves riding on longer waves—predicts a skewness agreeing with observation in both magnitude and sign. One other mechanism—viscous damping of individual waves—gives an effect that is too small, and does not conform with the observed change of sign when wind and swell are in opposite directions.

We have also demonstrated an empirical relation between the skewness and the mean horizontal wind

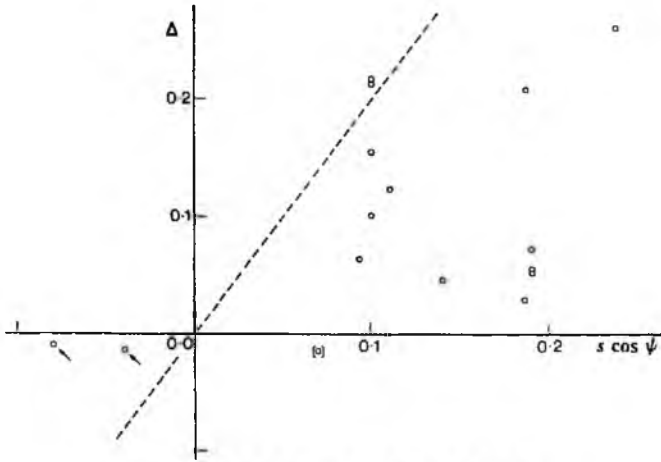


FIG. 7. A plot of Δ vs $s \cos \psi$, from the data of Table 1.

stress, which however is valid only when wind and swell are in the same direction. Thus there seems to be no necessary connexion between skewness and windstress. This conclusion is confirmed by the illustrative model discussed in Appendix A.

It appears that, if we are to gain information on wind stress from the observed skewness, we must rely on the empirical correlation of Fig. 3. Moreover, the direction of the underlying swell relative to the wind is a factor to be taken into account.

Acknowledgment. I am indebted to Walter Munk for suggesting to me some of the questions in this paper, and for encouragement in finding the answers.

APPENDIX A

On Ripple Dynamics

We show by an example that the phase γ of capillary waves riding on the surface of longer gravity waves may well be positive.

Within the approximations of Section 3, an equation for the short waves can be written as

$$\frac{\partial E}{\partial t} + \frac{\partial}{\partial x} [E(c_g + U)] + S \frac{\partial U}{\partial x} + D = G, \quad (A1)$$

where

$$E = \frac{1}{2} T (a' k')^2 \quad (A2)$$

denotes the energy density for capillary waves (T is surface tension), and

$$c_g = \frac{3}{2} \left(\frac{T k'}{\rho} \right)^{1/2} \quad (A3)$$

is the corresponding group velocity. Also

$$U = a \alpha \cos \theta \quad (A4)$$

is the horizontal orbital velocity in the long waves,

$$S = \frac{3}{2} E \quad (A5)$$

is the radiation stress for the short waves (see Longuet-Higgins and Stewart, 1964, Section 3);

$$D = NE, \quad N = 4\nu k'^2, \quad (A6)$$

is the energy dissipation due to the kinematic viscosity ν (see Lamb, 1932), and G is the direct input of energy from the wind. We assume that

$$G = KE, \quad (A7)$$

that is, the input of energy to the short waves is directly proportional to the local short-wave energy itself.

Owing to the horizontal convergence of the long-wave orbital motion, the wavenumber k' of the short waves is greatest at the long-wave crests; in fact to order ak

$$k' = k'_0(1 + ak \cos \theta). \quad (A8)$$

The group-velocity c_g given by (A3) varies accordingly, that is

$$c_g = c_{g0}(1 + \frac{1}{2}ak \cos \theta). \quad (A9)$$

Similarly

$$N = N_0(1 + 2ak \cos \theta). \quad (A10)$$

Now writing

$$E = E_0 + E_1 ak \cos \theta + E_2 a^2 k^2 \sin^2 \theta \quad (A11)$$

and substituting in Eq. (A1) we find, from the terms

independent of θ , that

$$\frac{\partial E_0}{\partial t} = (K - N_0)E_0. \quad (\text{A12})$$

Likewise from the terms in $\cos\theta$ and $\sin\theta$ we find

$$\begin{aligned} (K - N_0)E_1 + (\sigma - kc_g)E_1^* &= 2N_0E_0 \\ (\sigma - kc_g)E_1 - (K - N_0)E_1^* &= (\frac{1}{2}\sigma + \frac{1}{2}kc_g + K)E_0. \end{aligned} \quad (\text{A13})$$

If K and N_0 were both zero we should have the solution: $E_0 = \text{constant}$, $E_1^* = 0$ and

$$E_1 = \frac{(5c + c_g)}{2(c - c_g)} E_0. \quad (\text{A14})$$

In this situation the steepness of the ripples fluctuates in-phase with the elevation of the long waves and $\gamma = 0$. (Note the "resonance" when $c_g = c$.)

Suppose on the other hand K and N_0 do not both vanish, but that we have a quasi-steady state in which the short-wave energy is saturated. (Since the dissipation may be due partly to breaking or turbulence, the kinematic viscosity ν must be replaced by an effective coefficient $N_0/4k_0^2$.) Then in (A12) we have $\partial E_0/\partial t = 0$, hence

$$N_0 = K \quad (\text{A15})$$

and from (A13)

$$E_1^* = \frac{2KE_0}{(c - c_g)k}, \quad (\text{A16})$$

with E_1 being given by (A14) as before. Hence the phase angle γ is given by

$$\tan\gamma = \frac{E_1^*}{E_1} = \frac{4K}{k(5c + c_g)}. \quad (\text{A17})$$

When $(5c + c_g) > 0$ the angle γ will lie between 0° and 90° , and when $c_g \ll c$ we have simply

$$\tan\gamma = \frac{4K}{5\sigma}. \quad (\text{A18})$$

Similar conclusions would apply if the short waves were assumed to be not pure ripples but short gravity-capillary waves.

If the underlying swell is in a direction opposite to that of the short waves, then the signs of c and σ are reversed. Eq. (A18) then indicates that the phase-angle γ lies between -90° and 0° .

In the limit when the rate of energy dissipation in

the ripples is large compared with the long-wave frequency σ , then (A18) implies that $\tan\gamma$ will be large and that γ will be near 90° .

APPENDIX B

Evaluation of ϕ_{ns}

Let ϵ denote the angle of inclination of the free surface, hence the angle between the coordinates (s, n) and (x, z) . We have then

$$\phi_{ns} = \phi_{xz}(\cos^2\epsilon - \sin^2\epsilon) + (\phi_{zx} - \phi_{xz})\cos\epsilon \sin\epsilon. \quad (\text{B1})$$

Since $\tan\epsilon = \zeta_x$ and $\phi_{xx} + \phi_{zz} = 0$ we have, to second order in ak ,

$$\phi_{ns} = \phi_{xz} - 2\zeta_x\phi_{xz}, \quad (\text{B2})$$

or if we expand the right-hand side in a Taylor series about $z = 0$,

$$\phi_{ns} = (\phi_{xz} + \zeta\phi_{xzz} - 2\zeta_x\phi_{xz}). \quad (\text{B3})$$

For gravity waves in deep water

$$\left. \begin{aligned} \phi &= ace^{kz} \sin\theta + O(a^3k^3c) \\ \zeta &= a \cos\theta + O(a^2k) \end{aligned} \right\}, \quad (\text{B4})$$

with $\theta = kx - \sigma t$. Substitution into (B3) gives Eq. (5.8).

REFERENCES

- Cox, C. S., 1958: Measurements of slopes of high-frequency wind waves. *J. Mar. Res.*, **16**, 199-225.
- , and W. Munk, 1956: Slopes of the sea surface deduced from photographs of sun glitter. *Bull. Scripps Inst. Oceanogr.*, **6**, 401-488.
- Lamb, H., 1932: *Hydrodynamics*, 6th ed. Cambridge University Press, 738 pp.
- Longuet-Higgins, M. S., 1962: The generation of capillary waves by steep gravity waves. *J. Fluid Mech.*, **16**, 138-159.
- , 1963: The effect of nonlinearities on statistical distributions in the theory of sea waves. *J. Fluid Mech.*, **17**, 459-480.
- , 1969: Action of a variable stress at the surface of water waves. *Phys. Fluids*, **12**, 737-740.
- , 1978: The instabilities of gravity waves of finite amplitude in deep water. I. Superharmonics. *Proc. Roy. Soc. London*, **A360**, 471-488.
- , and E. D. Cokelet, 1978: The deformation of steep surface waves on water II. Growth of normal-mode instabilities. *Proc. Roy. Soc. London*, **A364**, 1-28.
- , and R. W. Stewart, 1964: Radiation stresses in water waves; a physical discussion, with applications. *Deep-Sea Res.*, **11**, 529-562.
- Phillips, O. M., 1981: The dispersion of short wavelets in the presence of a dominant long wave. *J. Fluid Mech.*, **107**, 465-485.

On the joint distribution of wave periods and amplitudes in a random wave field

BY M. S. LONGUET-HIGGINS, F.R.S.

Department of Applied Mathematics and Theoretical Physics,

Silver Street, Cambridge CB3 9EW, U.K.

and Institute of Oceanographic Sciences, Wormley, Surrey GU8 5UB, U.K.

(Received 15 March 1983)

A theoretical probability density is derived for the joint distribution of wave periods and amplitudes which has the following properties: (1) the distribution is asymmetric, in accordance with observation; (2) it depends only on three lowest moments m_0 , m_1 , m_2 of the spectral density function. It is therefore independent of the fourth moment m_4 , which previously was used to define the spectral width (Cavanié *et al.* 1976). In the present model the width is defined by the lower-order parameter

$$\nu = (m_0 m_2 / m_1^2 - 1)^{\frac{1}{2}}.$$

The distribution agrees quite well with wave data taken in the North Atlantic (Chakrabarti & Cooley 1977) and with other data from the Sea of Japan (Goda 1978). Among the features predicted is that the total distribution of wave heights is slightly non-Rayleigh, and that the interquartile range of the conditional wave period distribution tends to zero as the wave amplitude diminishes.

The analytic expressions are simpler than those derived previously, and may be useful in handling real statistical data.

1. INTRODUCTION

In a previous contribution (Longuet-Higgins 1975; to be referred to as I) the author proposed a theoretical expression for the joint distribution of the periods and amplitudes of sea waves, which was based on a narrow-band approximation applied to the well known linear theory of gaussian noise. While giving a fairly good fit to wave data with a narrow spectrum such as those of Bretschneider (1959), the model did not account for the asymmetry in the distribution of wave period τ which is commonly observed in wave spectra with a broader bandwidth (see, for example, Goda 1978).

At about the same time, Cavanié *et al.* (1976) proposed a theoretical distribution, also based on a narrow-band, gaussian model, which accounted very successfully for the asymmetry in the distribution of τ . However it involved the use of the well known spectral width parameter ϵ where $\epsilon^2 = 1 - m_2^2 / m_0 m_4$, and m_n denotes the n th moment of the spectral density. For some practical purposes this parameter is

inconvenient, since the fourth moment, m_4 , may depend rather critically on the behaviour of the spectrum at high frequencies.

Some lengthy and perhaps accurate approximations to the distribution of wave-length and amplitude in gaussian noise have been given by Lindgren (1972) and by Lindgren & Rychlik (1982), but for their evaluation these require a great deal of computation. Moreover, these expressions also involve high moments of the spectrum.

The purpose of this note is to present an alternative theoretical distribution, also based on narrow-band theory, which has the same merit as the Cavanié distribution in being asymmetric in τ , but which depends only on the lower-order moments m_0 , m_1 , m_2 , as in paper I. A measure of the spectral width is provided by the parameter ν , where $\nu^2 = m_0 m_2 / m_1^2 - 1$. As we shall see, this also accounts well for the observations, and in addition the theoretical expressions are somewhat simpler to handle than those in Cananié's distribution.

2. THEORY

As in paper I we begin with the representation of the sea surface elevation ζ in the form

$$\zeta = \text{Re } A e^{i\bar{\sigma}t}, \quad (2.1)$$

where $A(t)$ is a complex-valued envelope function:

$$A = \rho e^{i\phi}, \quad (2.2)$$

with amplitude ρ and phase ϕ both real but slowly varying functions of the time t . It is convenient to choose the carrier frequency $\bar{\sigma}$ so that

$$\bar{\sigma} = m_1 / m_0, \quad (2.3)$$

where m_n denotes the n th moment of the spectral density $E(\sigma)$:

$$m_n = \int_0^\infty \sigma^n E(\sigma) d\sigma. \quad (2.4)$$

A spectral width parameter ν can then be defined in terms of the variance of $E(\sigma)$ about the mean:

$$\nu^2 = \mu_2 / \bar{\sigma}^2 m_0, \quad (2.5)$$

where

$$\mu_n = \int_0^\infty (\sigma - \bar{\sigma})^n E(\sigma) d\sigma. \quad (2.6)$$

Clearly,

$$\mu_0 = m_0, \quad \mu_1 = 0, \quad \mu_2 = m_2 - m_1^2 / m_0, \quad (2.7)$$

and so

$$\nu^2 = m_0 m_2 / m_1^2 - 1. \quad (2.8)$$

We shall adopt the narrow-band hypothesis, namely,

$$\nu^2 \ll 1. \quad (2.9)$$

In practice we assume that $\nu^2 \leq 0.36$. This ensures (as we shall see) that the envelope function varies slowly compared with the carrier wave $\exp(i\bar{\sigma}t)$ so that the wave crests lie almost on the envelope $\zeta = \rho$. Also, the rate of change of the total phase, $\dot{\chi} = \dot{\phi} + \dot{\bar{\sigma}}t$, that is,

$$\dot{\chi} = \dot{\phi} + \bar{\sigma} \quad (2.10)$$

(where a dot denotes differentiation with respect to t) is almost equal to $\bar{\sigma}$. In other words $\dot{\phi} \ll \bar{\sigma}$, in general. We shall assume further that $\dot{\phi} \ll \bar{\sigma}\phi$, so that ϕ varies little over a wave period (an assumption discussed below). Then the local wave period τ can be approximated by

$$\tau = 2\pi/\dot{\chi} = 2\pi/(\bar{\sigma} + \dot{\phi}). \quad (2.11)$$

The wave amplitude ρ and the wave period τ may be normalized by writing

$$R = \rho/(2m_0)^{1/2}, \quad T = \tau/\bar{\tau}, \quad (2.12)$$

where we define

$$\bar{\tau} = 2\pi/\bar{\sigma} = 2\pi m_0/m_1. \quad (2.13)$$

Now it can be shown rigorously (see paper I, and earlier papers referred to therein) that the joint probability density of ρ and ϕ is given by

$$p(\rho, \phi) = \{\rho^2/(2\pi\mu_0^2\mu_2)\} e^{-\frac{1}{2}\rho^2(\mu_0 + \phi^2/\mu_2)}. \quad (2.14)$$

We can now find the joint density of R and T from

$$p(R, T) = p(\rho, \phi) |\partial(\rho, \phi)/\partial(R, T)|. \quad (2.15)$$

Applying the above formulae we obtain immediately

$$p(R, T) = (2/\pi^{1/2}\nu) (R^2/T^2) e^{-R^2[1+(1-1/T^2)\nu^2]} L(\nu), \quad (2.16)$$

where $L(\nu)$ is a normalization factor introduced to take account of the fact that we consider only positive values of T :

$$\frac{1}{L} = \frac{2}{\pi^{1/2}} \int_0^\infty \int_0^\infty \frac{R^2}{T^2} e^{-R^2[1+(1-1/T^2)\nu^2]} dR dT. \quad (2.17)$$

On evaluating the integral (see the Appendix) we find,

$$1/L = \frac{1}{2}[1 + (1 + \nu^2)^{-1/2}]. \quad (2.18)$$

For small values of ν this is close to unity:

$$L \approx 1 + \frac{1}{4}\nu^2. \quad (2.19)$$

Some values of L are listed in table 1.

TABLE 1. PARAMETERS OF $p(R, T)$

ν	L	mode		
		R	T	\mathcal{P}_{\max}
0.1	1.0025	0.955	0.990	4.203
0.2	1.0098	.981	.962	2.180
0.3	1.0215	.958	.917	1.541
0.4	1.0371	.928	.862	1.248
0.5	1.0557	.894	.800	1.096
0.6	1.0767	.857	.735	1.013

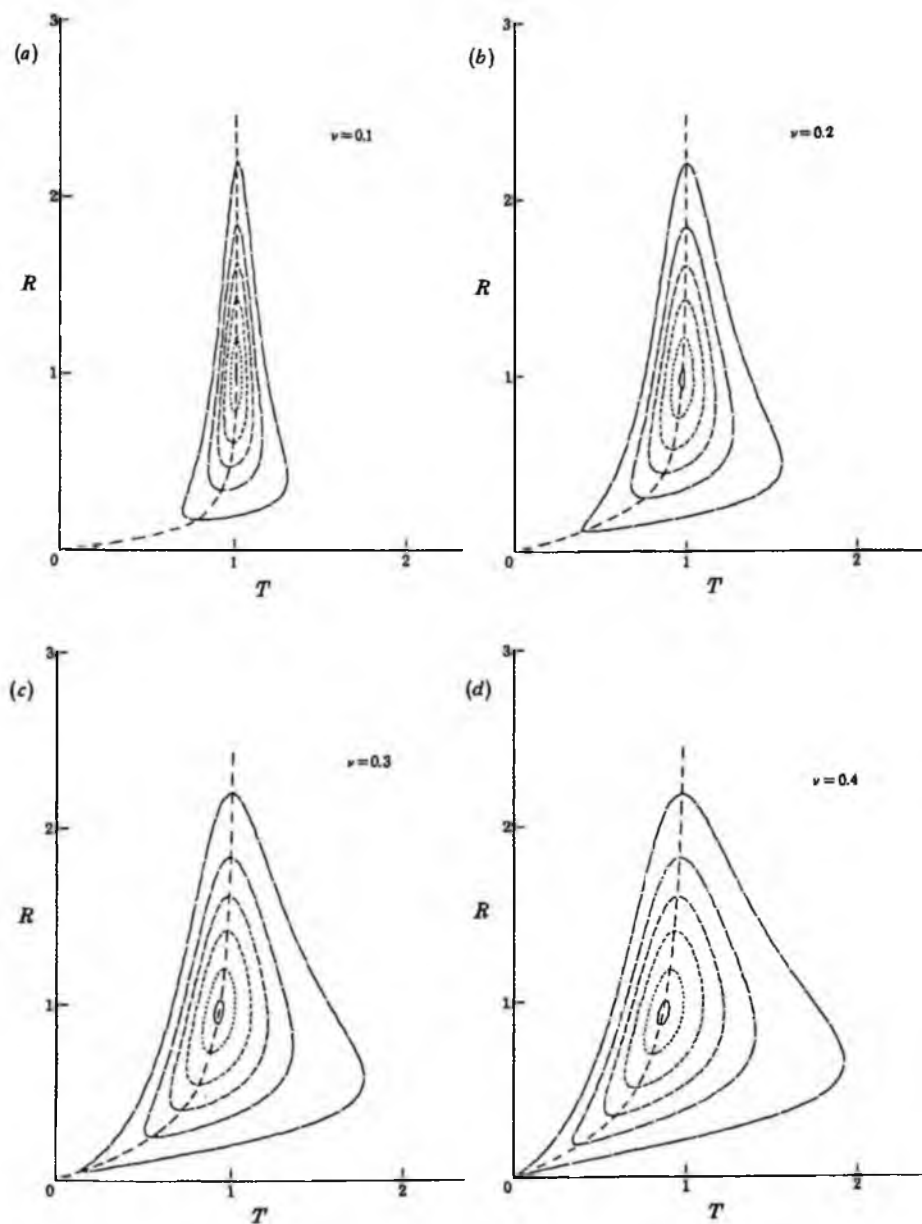


FIGURE 1a-f. Contours of $p(R, T)/p_{\max}$, where $p(R, T)$ is the joint density of the normalized wave amplitude R and normalized period T and p_{\max} is the density at the mode, see (4.2); p/p_{\max} takes the values 0.99, 0.90, 0.70, 0.50, 0.30 and 0.10 respectively from the centre contour outwards.

3. DISCUSSION

Strictly speaking, (2.16) gives the probability density of R and T (the dimensionless wave amplitude and period) at points uniformly distributed with regard to t . To find the density of R and T at particular points, say, the maxima of ζ , we would have to consider the joint density of ζ , $\dot{\zeta}$ and $\ddot{\zeta}$ at least, as is done by Arhan *et al.* (1976), or equivalently the joint distribution of ρ , $\dot{\rho}$, $\ddot{\rho}$ and ϕ , $\dot{\phi}$. But the variance of $\dot{\rho}$

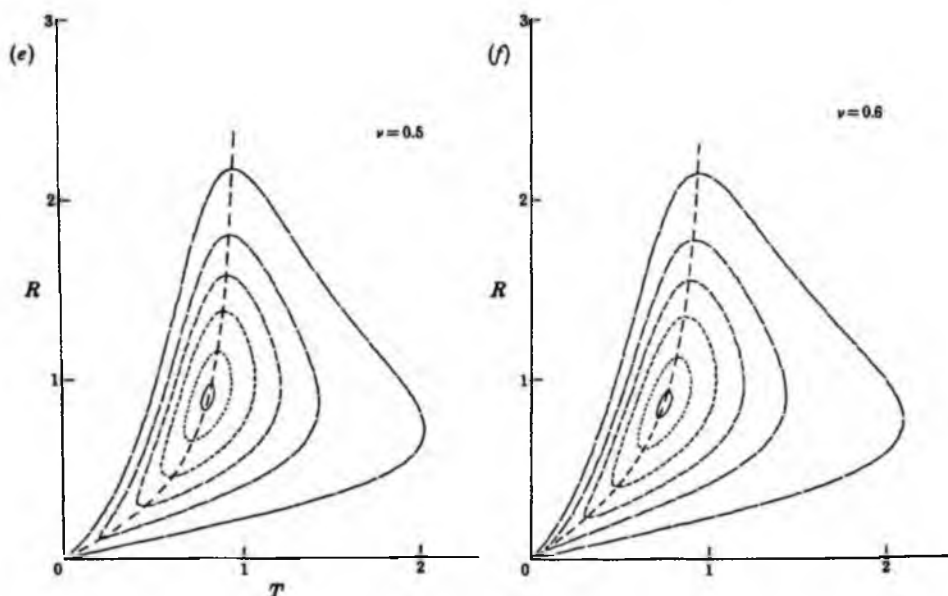


FIGURE 1 *e-f*. For legend see opposite.

is proportional to ν^2 or μ_2 (see Longuet-Higgins 1957) so that $\dot{\rho}$ is negligible, by our assumption (2.9). This implies that ρ varies slowly compared with $\bar{\sigma}$. Similarly, we have assumed $\dot{\phi} \ll \bar{\sigma}\phi$, that is, ϕ is also slowly varying. Hence the crests will occur at almost regularly spaced intervals in time, and it matters not, in this approximation, whether the density is for values at the crests of the waves, or values uniformly distributed with regard to t as in (2.16).

In figure 1 we show contours of $p(R, T)$ for a sequence of values of the parameter ν . The density clearly shows some asymmetry with regard to T , in general. However, in the limit as $\nu \rightarrow 0$ if we write, as in paper I,

$$\xi = \rho/m_0^{\frac{1}{2}} = 2^{\frac{1}{2}}R, \quad \eta = (T-1)/\nu, \quad (3.1)$$

and assume $|T-1|$ is of order ν , then (2.16) reduces to

$$p(\xi, \eta) = (2\pi)^{-\frac{1}{2}} \xi^2 e^{-\frac{1}{2}\xi^2(1+\eta^2)}, \quad (3.2)$$

as in I, equation (5). In other words, in the neighbourhood of $T=1$ the distribution becomes symmetric about the mean wave period, independently of R .

It is pertinent to enquire whether the general expression (2.16) is any more accurate, theoretically, than the expression (3.2) which is restricted to small values of ν and of $|T-1|$. One reason why this may be so is that in the derivation of (3.2) in paper I, the 'period', τ , as defined by (2.11) of the present paper, was approximated by $\bar{\tau}(1-\phi/\bar{\sigma})$ (see paper I, equation (A 20)). In the present paper this approximation, though formally legitimate, has not been made.

Another way of stating the situation is that though the distribution of the time derivative $\dot{\chi}$ is exactly symmetric about its mean value $\bar{\sigma}$, the distribution of the reciprocal $2\pi/\dot{\chi}$ is asymmetric. In other words, the distribution of apparent wave 'frequencies' is symmetric, but the distribution of wave periods is not.

In making the approximation (2.11) we assumed implicitly that $(\bar{\sigma} + \phi)$ was positive, for it is difficult to attach any meaning to a negative period. We therefore agree to ignore the part of the density (2.16) for which $\phi < -\sigma$, or $T < 0$.

4. PROPERTIES OF $p(R, T)$

The position of the mode, or maximum value of $p(R, T)$ is found from the condition that $\partial p/\partial R$ and $\partial p/\partial T$ both vanish. Hence we find

$$R = 1/(1+\nu^2)^{\frac{1}{2}}, \quad T = 1/(1+\nu^2). \quad (4.1)$$

The value of $p(R, T)$ at this point is therefore

$$p_{\max} = (2L/\pi^{\frac{1}{2}}e)(1+\nu^2)/\nu = 0.415(\nu+\nu^{-1})L(\nu). \quad (4.2)$$

The effect of broadening the spectrum is therefore to reduce the 'most probable' joint values of the wave period and amplitude, and also to reduce their probability density (when $\nu < 1$).

Consider now the behaviour of $p(R, T)$ near the origin. When R and T are both small, we have

$$p(R, T) \approx (2L/\pi^{\frac{1}{2}}\nu)(R^2/T^2)e^{-R^2\nu^2T^2}, \quad (4.3)$$

that is,

$$p(R, T) \approx (2\nu L/\pi^{\frac{1}{2}})\lambda^2 e^{-\lambda^2}, \quad (4.4)$$

where $\lambda = R/\nu T$. Hence the contours of p become tangent to the radii $R/T = \lambda\nu$, constant. The axes $R = 0$ and $T = 0$ both correspond to $p = 0$. The direction from 0 in which p is greatest is given by the maximum of (4.4), which corresponds to $\lambda^2 = 1$, hence

$$R/T = \nu, \quad p = p_0 = (2/\pi^{\frac{1}{2}}e)\nu L, \quad (4.5)$$

(compare (4.2)). The contour $p = p_0$ actually has a cusp at the origin. When $p < p_0$, the contours $p = \text{constant}$ all pass through the origin. On the other hand when $p_0 < p < p_{\max}$, the contours enclose the mode once, but do not pass through the origin.

From (4.2) and (4.5) it follows that

$$p_0/p_{\max} = \nu^2/(1+\nu^2), \quad (4.6)$$

so that in figures 1(a-c) no contours pass through the origin, and in figures 1(d-f) only the lowest contour: $p = 0.1$.

5. THE DENSITY OF R

The density of the wave amplitude R by itself is found on integrating $p(R, T)$ with respect to T over $0 < T < \infty$, that is,

$$p(R) = \frac{2L(\nu)}{\pi^{\frac{1}{2}}\nu} R^2 e^{-R^2} \int_0^\infty \frac{1}{T^2} e^{-R^2(1-1/T)^2 \nu^2} dT. \quad (5.1)$$

Setting

$$R(1-1/T) = \nu\beta, \quad (5.2)$$

we have

$$p(R) = \frac{2L}{\pi^{\frac{1}{2}}} R e^{-R^2} \int_{-\infty}^{R/\nu} e^{-\beta^2} d\beta \quad (5.3)$$

$$= 2R e^{-R^2} L(\nu) F(R/\nu), \quad (5.4)$$

where

$$F(R/\nu) = \frac{1}{\pi^{\frac{1}{2}}} \int_{-\infty}^{R/\nu} e^{-\beta^2} d\beta, \quad (5.5)$$

a well known error function. Equation (5.4) states that the density of R is almost Rayleigh, but must be corrected by the factor $LF(R/\nu)$. For values of R that are of order 1 or larger, the correction will be exponentially small. However when R is of order ν , that is, close to the origin, the correction becomes significant. Figure 2

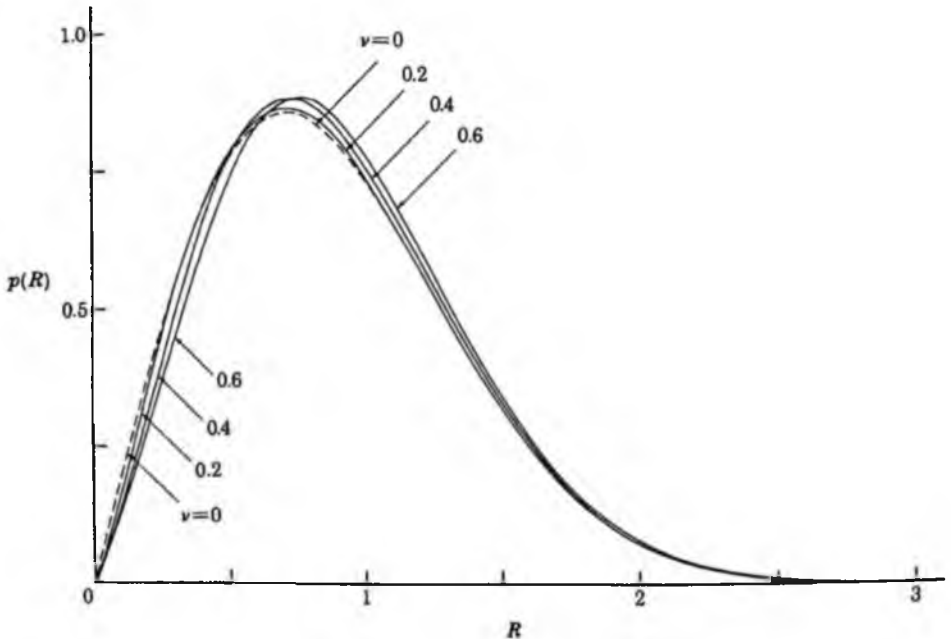


FIGURE 2. The density of R (see (5.4)) when $\nu = 0.2, 0.4$ and 0.6 (full curves) compared with the Rayleigh distribution (broken curve).

shows some examples. The effect of the correction factor is to reduce the number of very low waves, and to shift the mode of the distribution, which otherwise is at $R = 2^{-\frac{1}{2}}$, somewhat to the right of this point.

TABLE 2. PARAMETERS OF $p(R)$

ν	R_{av}	R_{rms}^2	$(R_{av} - \frac{1}{2}\pi^{\frac{1}{2}})$	$(R_{rms} - 1)$
0.1	0.8832	1.0025	0.0020	0.0012
0.2	.8935	1.0095	.0072	.0047
0.3	.9006	1.0202	.0144	.0100
0.4	.9087	1.0332	.0224	.0165
0.5	.9167	1.0472	.0304	.0233
0.6	.9241	1.0611	.0378	.0301

The lower order moments of $p(R)$, found by numerical integration, are shown in table 2. From this it will be seen that the r.m.s. value of R differs only slightly from unity. When $\nu = 0.3$, for example, the difference is only 1 %.

6. THE CONDITIONAL DISTRIBUTION OF WAVE PERIODS $p(T/R)$

The distribution of T at fixed values of the wave amplitude R is found on dividing $p(R, T)$ by $p(R)$; hence

$$p(T|R) = (\pi^{\frac{1}{2}} \nu F(R/\nu))^{-1} (R/T^2) e^{-R^2(1-1/T)^2/\nu^2}. \quad (6.1)$$

To find the mode, or peak, of this function we set $\partial p/\partial T = 0$ to obtain

$$(1/T)(1/T - 1) = \nu^2/R^2, \quad (6.2)$$

and so

$$T = 2/[1 + (1 + 4\nu^2/R^2)^{\frac{1}{2}}]. \quad (6.3)$$

This curve is shown by the dashed lines in figure 1. It must clearly pass through the mode (4.1) and where it intersects any contour $p = \text{constant}$, the tangent to that contour is parallel to the axis of T . For small R we have $T \approx R/\nu$, so that the curve touches the contour (4.5). On the other hand, for large R the curve is asymptotic to the vertical line $T = 1$. In general, the curve expresses very well the asymmetry in the distribution of T .

Now the quartiles of $p(T/R)$ are given by

$$\int_0^{Q_n} p(T|R) dT = \frac{1}{4}n, \quad n = 1, 2, 3, \quad (6.4)$$

that is

$$\frac{1}{\pi^{\frac{1}{2}}} \int_{\beta}^{\infty} e^{-\beta^2} d\beta = \frac{1}{4}n F(R/\nu), \quad (6.5)$$

where

$$\beta = R(1 - 1/T)/\nu. \quad (6.6)$$

So we have to solve numerically

$$F(\beta) = \frac{1}{4}n F(R/\nu) \quad (6.7)$$

for β , and then

$$Q_n = 1/(1 - \beta\nu/R). \quad (6.8)$$

These curves are illustrated in figure 3, in the case $\nu = 0.3$. Clearly all the quartiles

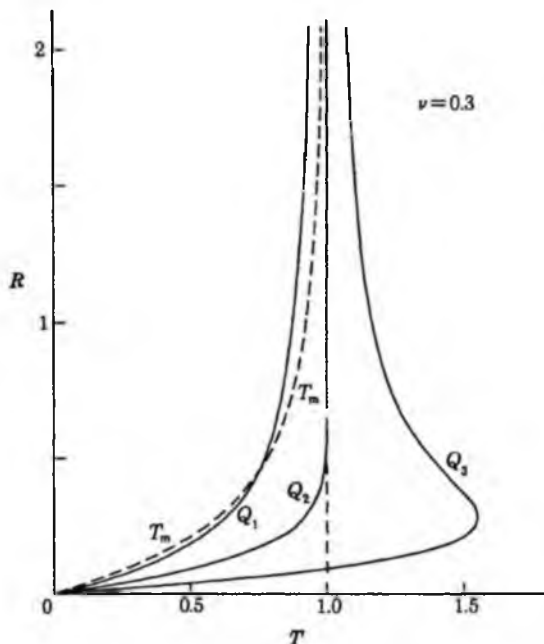


FIGURE 3. Curves showing the mode and quartiles of the conditional density of wave periods when $\nu = 0.3$.

are now asymmetric, and pass through the origin. Moreover, the interquartile range ($Q_3 - Q_1$), instead of being proportional to $1/R$ for all values of R , as in paper I, has a maximum at around $R = 0.22$ ($\xi = 0.31$) and tends to 0 both as $R \rightarrow \infty$ and as $R \rightarrow 0$.

7. THE TOTAL DENSITY $p(T)$

The density of T regardless of R is found by integrating $p(R, T)$ with respect to R over $0 < R < \infty$, to give

$$p(T) = (L/2\nu T^2)[1 + (1 - 1/T)^2/\nu^2]^{-\frac{1}{2}}. \quad (7.1)$$

This is shown in figure 4 for some representative values of ν . The median and quartiles are found by the substitution

$$\alpha = (1 - 1/T)/\nu, \quad (7.2)$$

leading to

$$\frac{1}{2}L \int_{-\infty}^{\alpha} \frac{d\alpha}{(1 + \alpha^2)^{\frac{3}{2}}} = \frac{1}{4}, \frac{1}{2} \text{ or } \frac{3}{4}, \quad (7.3)$$

hence

$$\alpha/(1 + \alpha^2)^{\frac{1}{2}} = n/2L - 1, \quad n = 1, 2, 3. \quad (7.4)$$

Solving for α we find,

$$\alpha = (n/2L - 1)/[1 - (n/2L - 1)^2]^{\frac{1}{2}}, \quad (7.5)$$

and then

$$Q_n = T = 1/(1 - \nu\alpha), \quad n = 1, 2, 3. \quad (7.6)$$

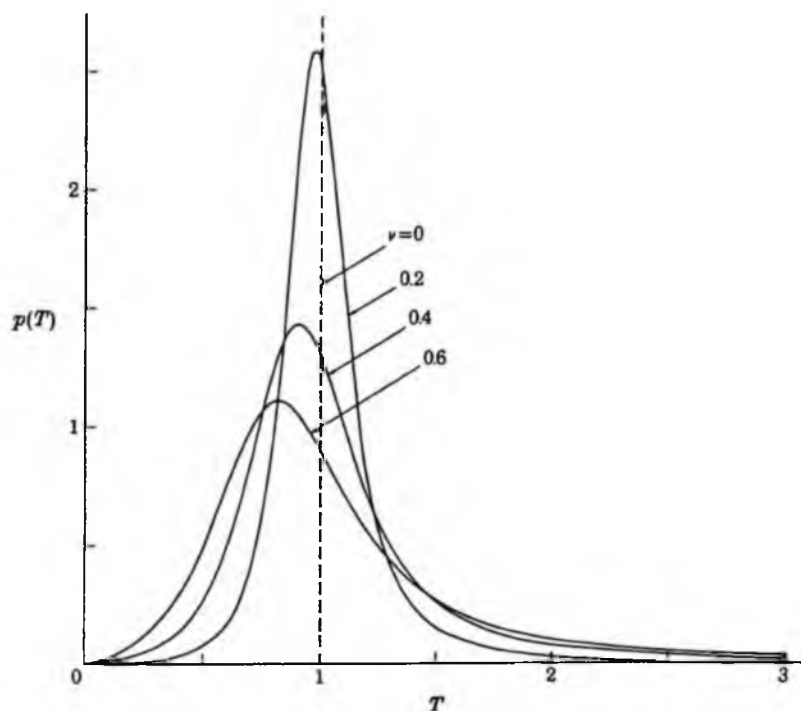


FIGURE 4. The density of the wave period T . (see (6.9)) when $\nu = 0.2, 0.4$ and 0.6 .

Some representative values of Q_n are given in table 3. Also shown is the interquartile range

$$\text{IQR} = Q_3 - Q_1. \quad (7.7)$$

The mode of the distribution is also easily found and is given by

$$T_m = 2/[(9 + 8\nu^2)^{1/2} - 1]. \quad (7.8)$$

Note that the mean of the distribution is theoretically infinite, since for large values of T the density $p(T)$ behaves like T^{-2} . This implies only that as $T \rightarrow \infty$ the

TABLE 3. PARAMETERS OF THE DISTRIBUTION OF PERIODS, $p(T)$

ν	T_m	Q_1	Q_2	Q_3	IQR	$T_{1\%}$
0.1	0.9934	0.9452	0.9998	1.0606	0.1154	0.9950
0.2	.9742	.8953	.9981	1.1249	.2296	.9806
0.3	.9444	.8488	.9937	1.1891	.3403	.9578
0.4	.9065	.8050	.9859	1.2492	.4442	.9285
0.5	.8633	.7636	.9743	1.3020	.5384	.8944
0.6	.8174	.7243	.9589	1.3450	.6207	.8574

integrated error becomes infinite. An alternative estimate of the mean does, however, exist. For we know the exact result that the average frequency of up-crossings of the mean level is

$$N = (2\pi)^{-1} (m_2/m_0)^{\frac{1}{2}}. \quad (7.9)$$

From the relations (2.3), (2.5) and (2.7), this can be written

$$N = (1 + \nu^2)^{\frac{1}{2}} \bar{\sigma} / 2\pi. \quad (7.10)$$

Hence

$$\tau_{av} = N^{-1} = \pi / (1 + \nu^2)^{\frac{1}{2}}, \quad (7.11)$$

and so

$$T_{av} = \tau_{av} / \bar{\tau} = (1 + \nu^2)^{-\frac{1}{2}}. \quad (7.12)$$

These parameters are all shown in table 3.

8. COMPARISON WITH OBSERVATION

The measurement of the local wave height and period from a wave record is liable to some ambiguities. For example, in figure 5, should the 'period' be taken as the crest-to-crest interval τ_1 or the up-crossing interval τ_2 ? Not all authors specify their choice precisely. It may be that for the Cavanié distribution, depending on the higher moment m_4 , the choice of τ_1 is more appropriate, whereas for the present distribution, depending only on m_2 , it is more appropriate to choose τ_2 .

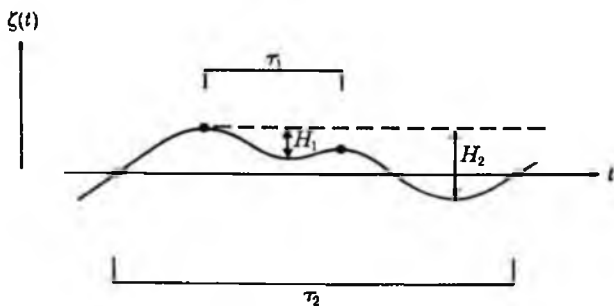


FIGURE 5. Alternative measures of the local wave height and period.

Without knowing precisely the authors' procedure we shall nevertheless compare the theoretical model described in §§ 2-6 with some previous observations.

Chakrabarti & Cooley (1977) measured 1624 waves from a North Atlantic storm, over an interval of 3.5 days. The scatter diagram of their observations is shown in figure 6, where the vertical scale is the wave height normalized by the 'r.m.s. wave height' H_{rms} ; the horizontal scale is the wave period normalized by the 'mean period' T_{av} . To judge by the spread of wave periods (see figure 7 of their paper) an appropriate value of ν for these data was 0.30.

To make a comparison with $p(R, T)$, we replot the contours to a new vertical scale $R' = R/R_{rms}$, and a new horizontal scale $T' = T/T_{av}$ where $T_{av} = (1 + \nu^2)^{-\frac{1}{2}}$. There will be a new value of p_{max} , namely $p'_{max} = R_{rms} T_{av} p_{max}$, but the relative values of p , namely $p'(R', T')/p'_{max}$, will be unchanged.

This is done in figure 7, and it will be seen that the resemblance between figures 6 and 7 is close, in particular as regards the shape of the distributions and the tendency for plotted points to be drawn down towards the origin. However, the absolute densities are not easy to determine from the scatter diagram.

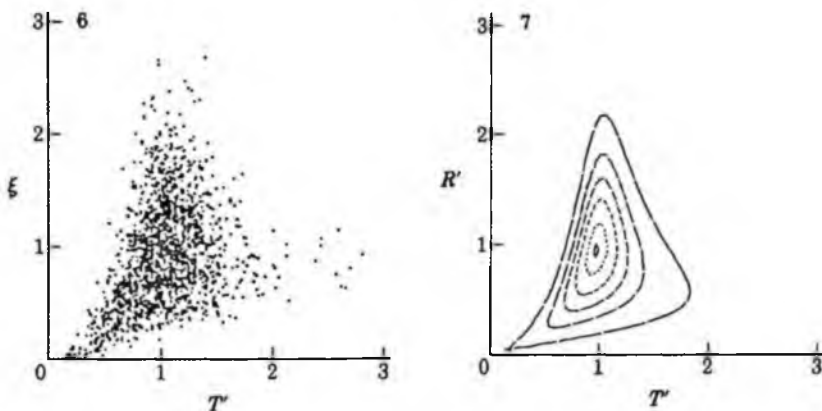


FIGURE 6. (From Chakrabarti & Cooley 1977.) A scatter diagram of normalized heights against normalized wave period, for a storm in the North Atlantic.

FIGURE 7. Contours of $p'(\xi, T')/p_{\max}$ when $\nu = 0.3$, for comparison with the data of figure 6. The contour values are as in figure 1.

Figure 8 shows a histogram of the wave heights measured by Chakrabarti & Cooley (1977). The horizontal scale has been normalized by the r.m.s. value of the observations. In the same diagram, the full curve indicates the theoretical density

$$p(R/R_{\text{rms}}) = R_{\text{rms}} p(R), \quad (8.1)$$

where $p(R)$ is given by (5.4) and $\nu = 0.30$. The broken curve shows the Rayleigh distribution corresponding to $\nu = 0$. It will be seen that the curve for $\nu = 0.30$ is a slightly better fit to the observations when R is small, and near the peak of the distribution.

In figure 9 we show a comparison of the interquartile range ($Q_3 - Q_1$), corresponding to the theory of figure 3, and the data plotted by Chakrabarti & Cooley (1977). At large values of ξ , the theoretical curve is asymptotic to the hyperbola given by the narrow-band theory: $Q_3 - Q_1 = 1.35 \nu/\xi$, but at lower values of ξ the curve reaches a maximum and then returns to the origin. The plotted observations follow the theory down to about $\xi = 1$, and then lie inside the curve. The discrepancy between theory and observation is less than previously, but is still appreciable.

Goda (1978) has presented diagrams of the relative wave height H/H_{av} against the relative wave period T/T_{av} , as in figure 10, the data being classified according to the value of a certain 'skewness parameter' τ . Goda has found a fairly good correlation

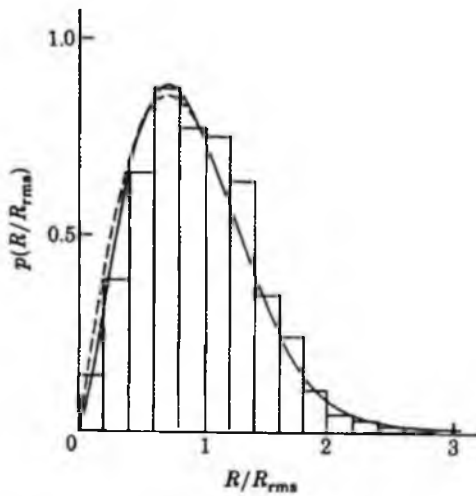


FIGURE 8. Histogram of wave heights from Chakrabarti & Cooley (1977) normalized by the r.m.s. value. The full curve represents $p = R_{rms} p(R)$ (equation (5.4)) when $\nu = 0.3$. The broken curve is the Rayleigh distribution: $p = 2R e^{-R^2}$.

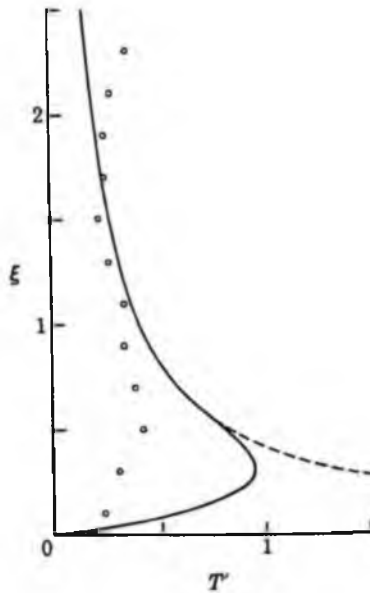


FIGURE 9. The interquartile range of the wave periods, as a function of the normalized wave height ξ . Data are from Chakrabarti & Cooley (1977). The full curve represents the difference $(Q_3 - Q_1)$ in figure 3. The dashed curve is the narrow-band asymptote.

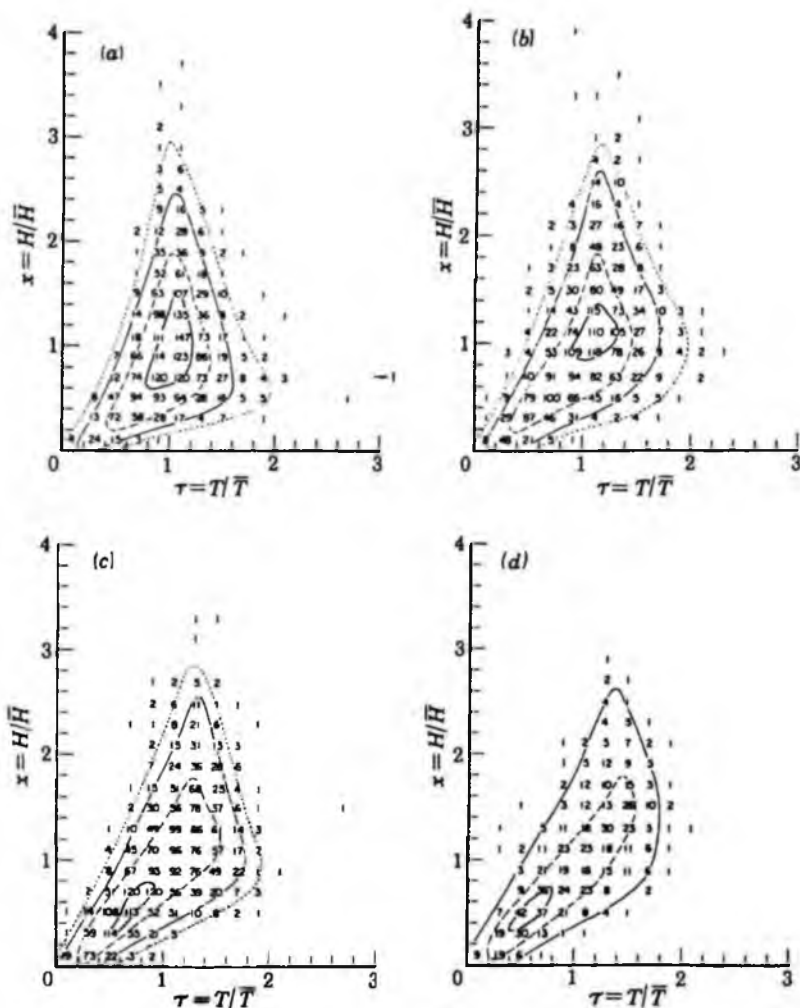


FIGURE 10. (From Goda 1978.) Scatter diagrams of H/H_{av} against T/T_{av} for different ranges of τ . The contours of $p(x, t)$ take the values 1.0, 0.5, 0.1, 0.03 respectively from the centre curve outwards. The parameter $r(H, T)$ lies in the range (a) 0.20–0.39; (b) 0.40–0.59; (c) 0.60–0.69; (d) 0.70–0.79.

between r and the parameter ν_T (derived from the distribution of wave periods) which corresponds roughly to ν . In table 4 we indicate the average values of ν chosen (from Goda's figure 10) to correspond to the stated ranges of τ .

We note also that since Goda plotted H/H_{av} rather than ξ , the vertical scale of his plots is different from that of Chakrabarti & Cooley (1977). Accordingly the scale must be modified by the factor $1/R_{av}$; see table 4. The horizontal scale has also to be modified by the factor $1/T_{av}$, which we assume is given by the formula $T_{av} = (1 + \nu^2)^{-1/2}$ derived from zero-crossings (see § 7). This factor also is shown in table 4. Finally the theoretical value

$$p_{max}^* = R_{av} T_{av} \bar{p}_{max}, \quad (9.2)$$

TABLE 4. PARAMETERS FOR THE DATA OF GODA (1978)

	τ	ν	R_{ν}	T_{ν}	P_{\max}	
					theor.	obs.
(a)	0.20-0.39	0.29	0.8999	0.9604	1.34	1.37
(b)	0.40-0.59	0.38	.9070	.9348	1.06	1.14
(c)	0.60-0.69	0.50	.9167	.8944	0.85	1.05
(d)	0.70-0.79	0.58	.9226	.8650	0.76	0.96

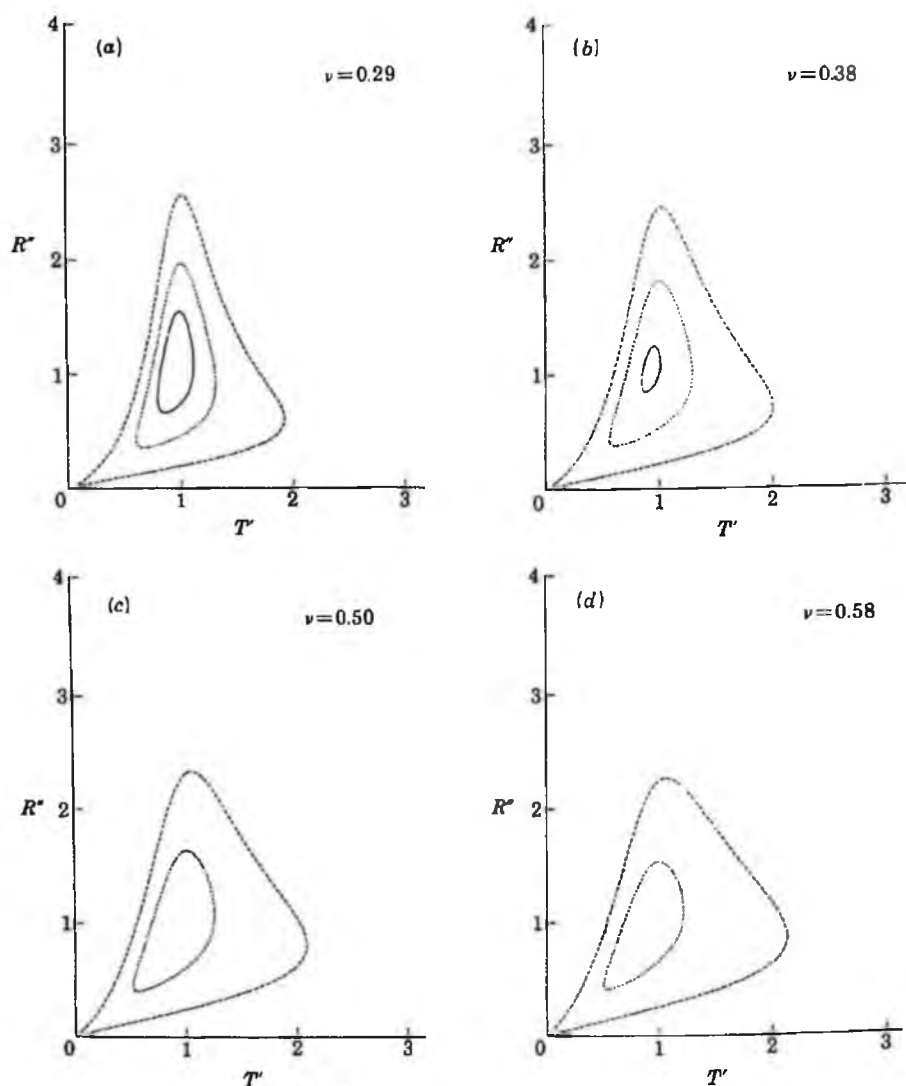


FIGURE 11. Contours of $R_{\nu} T_{\nu} p(R, T)$ for values of ν corresponding to figure 7. Contours take values 1.0, 0.5, 0.1 in (a) and (b) and 0.5, 0.1 in (c) and (d) from inner to outer.

where p_{\max} is given by (4.2) is shown in the next-to-last column of table 4, compared with the maximum observed value, from Goda's figure 10. The agreement is reasonable, except that the theory is consistently lower. Most of the discrepancy seems due to our choice of $T_{2\nu}$, and it is possible that a value nearer to unity would be more appropriate.

In figure 11 we show contours of $R_{2\nu} T_{2\nu} p(R, T)$, which may be compared with the corresponding contours in figure 10. We have not plotted any contours corresponding to $p^* = 0.03$, since Goda's data appear insufficient for him to trace the corresponding curves with any accuracy.

The agreement between figures 10 and 11 seems reasonable. In particular the position of the modes agrees fairly well, though in figure 10 there is an indication that for the larger values of ν the mode of the distribution splits into two, one further from and one nearer to the origin.

Other authors, for example, Cavanié *et al.* (1976), have combined data for many different spectra, which precludes any precise comparison with theory. However Cavanié's data, containing 28 240 waves with a mean value $\epsilon = 0.865$ do appear to resemble in a general way the contours of figures 1 (*d-f*).

9. CONCLUSION

We have derived an approximation to the joint distribution of wave periods and amplitudes that gives a reasonably good fit to some typical data, and that depends only on the low-order parameter ν . Technically the approximation is correct only to order ν , but by not making certain approximations, legitimate to this order, which were made in a previous paper I, the distribution is given an asymmetry with respect to T in agreement with the observations. Undoubtedly there are further corrections of order ν^2 to be made if the distribution is to be entirely correct to this order, but the observational evidence suggests that such corrections are small and not very significant for practical applications.

In comparison with the analysis of Cavanié *et al.* (1976) the present model has the advantage of comparative simplicity, and in depending only on ν rather than on the higher-order parameter ϵ . This seems desirable, since for many spectra that behave like σ^{-4} or σ^{-5} at infinity (such as the Pierson-Moskowitz spectrum) m_4 becomes infinite, making $\epsilon = 1$. Thus ϵ becomes insensitive to other parts of the spectrum. On the other hand, ν , which depends only on m_2 , is less subject to this difficulty. Rye & Svee (1976) have suggested that even ν is unduly influenced by the high-frequency cut-off but the examples given are for rather broad spectra. The most satisfactory procedure may be to estimate ν not from the spectrum $E(\sigma)$ but from the measured distribution of wave periods, as is done by Longuet-Higgins (1975) and Goda (1978). Indeed Goda finds that ν_T is highly correlated with certain other parameters which shows that it is reasonably stable. Apparently the reason for the success of this method of estimating ν is that it reflects whatever subjective choices are made by the observer when measuring τ from the wave record, choices which may amount to applying a subjective low-pass filter to the record.

Finally, the parameter ν has one clear advantage in being related theoretically to other statistical properties of the record and in particular to the lengths of the wave groups, (see, for example, Longuet-Higgins 1957, 1983).

This paper was written during a visit to the Department of Engineering Sciences at the University of Florida, Gainesville, Florida. The author is indebted to Dr K. Millsaps and his staff for their hospitality and assistance. Valuable comments on a first draft have been given by Professor M. K. Ochi, Dr M. Y. Su, Dr O. S. Madsen and Dr S. J. Hogan.

APPENDIX. EVALUATION OF $L(\nu)$

To carry out the integration in (2.17) set

$$(1 - 1/T)/\nu = \alpha, \quad (\text{A } 1)$$

so that
$$\frac{1}{L} = \frac{2}{\pi^{\frac{1}{2}}} \int_0^{\infty} \int_{-\infty}^{1/\nu} R^2 e^{-\pi^2(1+\alpha^2)R} dR d\alpha. \quad (\text{A } 2)$$

Then
$$\begin{aligned} \frac{1}{L} &= \frac{1}{2} \int_{-\infty}^{1/\nu} \frac{d\alpha}{(1+\alpha^2)^{\frac{3}{2}}} \\ &= \frac{1}{2} \left[\frac{\alpha}{(1+\alpha^2)^{\frac{1}{2}}} \right]_{-\infty}^{1/\nu} \\ &= \frac{1}{2} [1 + (1+\nu^2)^{-\frac{1}{2}}]. \end{aligned} \quad (\text{A } 3)$$

REFERENCES

- Arhan, M. K., Cavanié, A. & Ezraty, R. 1976 Etude théorique et expérimentale de la relation hauteur-période des vagues de tempête. *Centre National pour l'Exploitation des Océans, Centre Océanologique de Bretagne, Brest, France Rep. no. I.F.P. 24191.*
- Bretschneider, C. L. 1959 Wave variability and wave spectra for wind-generated gravity waves. *U.S. Beach Erosion Board tech. Memo. 118, Washington, D.C.*
- Cavanié, A., Arhan, M. & Ezraty, R. 1976 A statistical relationship between individual heights and periods of storm waves. In *Proc. Conf. on Behaviour of Offshore Structures, Trondheim*, pp. 354-360. Trondheim, Norway: Norwegian Inst. of Tech.
- Chakrabarti, S. K. & Cooley, R. P. 1977 Statistical distribution of periods and heights of ocean waves. *J. geophys. Res.* **82**, 1363-1368.
- Goda, Y. 1978 The observed joint distribution of periods and heights of sea waves. In *Proc. 16th Int. Conf. on Coastal Eng., Sydney, Australia*, pp. 227-246.
- Lindgren, G. 1972 Wavelength and amplitude in gaussian noise. *Adv. appl. Prob.* **4**, 81-108.
- Lindgren, G. & Rychlik, I. 1982 Wave characteristic distribution for gaussian waves—wavelength, amplitude and steepness. *Ocean Engng* **9**, 411-432.
- Longuet-Higgins, M. S. 1957 The statistical analysis of a random, moving surface. *Phil. Trans. R. Soc. Lond. A* **249**, 321-387.
- Longuet-Higgins, M. S. 1975 On the joint distribution of the periods and amplitudes of sea waves. *J. geophys. Res.* **80**, 2688-2694.
- Longuet-Higgins, M. S. 1980 On the distribution of the heights of sea waves: Some effects of nonlinearity and finite band width. *J. geophys. Res.* **85**, 1519-1523.

- Longuet-Higgins, M. S. 1983 On the definition of wave groups in random seas. (Submitted for publication.)
- Nolte, K. G. 1979 Joint probability of wave period and height. *Proc. Am. Soc. civ. Engrs* **105** (WW4), 470-474.
- Rye, H. & Svee, R. 1976 Parametric representation of a wind-wave field. In *Proc. 15th Conf. Coastal Eng. Honolulu, Hawaii*, pp. 183-201. New York: Am. Soc. civ. Engrs.

STATISTICAL PROPERTIES OF WAVE GROUPS IN A RANDOM SEA STATE

By M. S. LONGUET-HIGGINS, F.R.S.

*Department of Applied Mathematics and Theoretical Physics, Silver Street, Cambridge CB3 9EW, U.K.
and Institute of Oceanographic Sciences, Wormley, Godalming, Surrey GU8 5UB, U.K.*

(Received 22 November 1983)

CONTENTS

	PAGE
1. INTRODUCTION	220
2. DEFINITIONS: THE WAVE ENVELOPE	222
3. PRELIMINARY RESULTS	223
4. THE AVERAGE GROUP LENGTH	224
5. RUNS OF HIGH WAVES	225
6. PARAMETERS FOR OCEAN WAVES	226
7. CALCULATION OF THE WAVE ENVELOPE	227
8. EXAMPLES	228
9. THE DISTRIBUTION OF GROUP LENGTHS	234
10. CORRELATION BETWEEN SUCCESSIVE WAVE HEIGHTS	237
11. THE CORRELATION COEFFICIENT: EXAMPLES	239
12. DISTRIBUTION OF G_j AND H_j : MARKOV THEORY	242
13. DISCUSSION AND CONCLUSIONS	247
APPENDIX A. THE SWELL SPECTRUM (6.3)	247
APPENDIX B. ON THE RELATION BETWEEN DISCRETE AND CONTINUOUS VALUES OF THE GROUP LENGTH	248
REFERENCES	249

Two apparently distinct approaches to the analysis of wave groups in a random sea state are described. In the first, the probabilities of the group-length G and the length of a 'high run' H are defined in terms of a wave envelope function $\rho(t)$. These lead naturally to expressions in terms of a single parameter ν that defines the spectral width.

In the second approach, the sequence of wave heights is treated as a Markov chain, with a non-zero correlation only between successive waves. This leads to expressions for G and H in terms of transition probabilities p_+ and p_- .

In this paper we find approximate analytic expressions for p_+ and p_- that show that the two approaches are roughly equivalent, to order ν .

Throughout the paper it is emphasized that the concept of a wave group assumes implicitly the neglect of those harmonic components that are either very short or very long compared with the peak frequency σ_p . That is, some filtering of the original record is implied. For typical records of wind waves it is found that a band-pass filter with upper and lower cut-offs at $1.5\sigma_p$ and $0.5\sigma_p$ is the most suitable.

Calculations are done for typical records of sea waves, and for some numerically simulated data, and there is agreement between the data and the analysis.

1. INTRODUCTION

A casual observer of the sea surface will notice that the heights of wind-generated waves are not uniform; they occur in successive groups of higher or lower waves; this leads to the popular but mistaken notion that 'every n th wave is the highest' where $n = 3, 7$ or 10 , for example. In fact the wave groups are not all of equal length, as we shall see, but their group behaviour and other properties may be described with remarkable success by treating a typical record of the sea-surface elevation as a random Gaussian process, statistically steady in the short term, say over a duration of less than 30 min.

The Gaussian model, as applied to noise in electrical circuits, was first developed in well known papers by Rice (1944, 1958) and was applied to other aspects of sea waves by Longuet-Higgins (1952, 1957), Pierson (1962) and others. For a recent survey of the subject see Ochi (1982). The physical basis for the model is of course that the energy of surface waves at any point in the ocean arises from the action of wind in many different parts of the sea surface, in an essentially uncorrelated way. So long as linear superposition of the motions is valid, the surface displacements should therefore be Gaussian.

Particular attention to properties of *wave groups* in Gaussian noise was paid by Longuet-Higgins (1957, 1962) and Rice (1958). Recent interest in the subject (Goda 1970, 1983; Ewing 1973; Rye 1974; Kimura 1980 and others) has been stimulated by the suggestion that exceptional damage to ships, coastal defences or offshore structures may be caused by the occurrence of runs of successive high waves.

A further reason for interest in the subject is the relation of wave groups to the occurrence of wave breaking (see Donelan *et al.* 1972); also the probable effect of steep or breaking waves on the flow of air over the sea surface.

An essential preliminary to the analysis is to consider what we mean by a wave group, or indeed by a single wave, in a random sea. A typical observer counting high waves is not interested in the very short fluctuations, either ripples or short gravity waves, riding on the backs of the dominant waves. He does not include them in his count. Even if presented with an accurate instrumental record of the sea surface for analysis, he tends either to ignore the short waves or to smooth them out, for example by drawing a straight line between adjacent crests of the dominant waves, to represent the local wave height. Thus by paying attention at all to the group aspect of the wave record he is, consciously or otherwise, dealing with a filtered version of the wave record, from which the high frequencies have been eliminated or suppressed.

Similar considerations apply to the low frequency end of the spectrum. In analysing a record of a certain duration, say 20 min, we are not generally interested in the total mean surface level, but only in the crest-to-trough heights of the waves, or in the height of the crests relative to some local mean value, taken over a few waves only. Thus we subconsciously filter out those harmonic components of zero frequency or of frequency much lower than the dominant waves.

Part of our problem is then to arrive at a satisfactory method of filtering the record so as to retain only those aspects in which we are interested. This question is discussed in detail in §8.

The above point of view is implicit in the approach of Rice (1945, 1958), Longuet-Higgins (1957), and Nolte & Hsu (1972). These authors recognized that for a sufficiently narrow-band

record a remarkably apt description of the group properties of a wave record can be given in terms of the wave-envelope function. For a Gaussian noise process, the envelope function can always be defined, even if the spectrum is not narrow; see §2. The statistics of the wave-envelope function $\rho(t)$ can be explored in much the same way as the statistics of the instantaneous surface elevation $\zeta(t)$. For example, the length of a wave group can be defined in terms of the number of times that the envelope $\rho(t)$ crosses a given reference level, say the 'significant' height of the waves. These statistics are all given in terms of the r th moments m_r of the spectral density function of $\zeta(t)$.

This classical approach has encountered some objections (Rye 1974) on the grounds that for typical spectra of wind-waves, the higher moments m_r , and in particular m_4 , depend critically upon the high-frequency cut-off in the spectrum. But we have seen that the existence of such a cut-off, or filter, is really inherent in the phenomenon under discussion: the shorter the waves that we consider, then the shorter also must be the average group-length. Moreover, as we shall emphasize below, if the definitions of group-length suggested by Longuet-Higgins (1957) and by Nolte & Hsu (1972) are employed, then only the lower moment m_2 is involved, unlike Rice's (1945) definition, which depended on the maxima of ρ , hence the fourth moment m_4 .

An alternative approach has been suggested by Sawnhey (1962), Wilson & Baird (1972), Kimura (1980) and others, namely to consider the correlation between successive, or almost successive, waves, without consideration of the frequency spectrum. Besides separating the model further from the physics, it should be clear that this approach by no means avoids the question of what filter is in fact applied to the wave record by an observer who selects, by some unstated criterion, the local wave height. None the less, the relation of this theory to the previous theory is of some interest.

The present paper falls into two parts. In §§2-9 we state and develop essentially the Rice, or envelope, theory, based on the spectral moments. Formulae are given for the average number of waves \bar{G} in a group and for the mean number of waves \bar{H} in a high run (see §§4 and 5 respectively). These are seen to depend only on the critical level $\rho = \rho^*$ and on the dimensionless bandwidth parameter

$$\nu^2 = m_2 m_0 / m_1^2 - 1. \quad (1.1)$$

For swell, it appears that ν lies typically between 0.05 and 0.15. For wind waves, ν has a lower bound at about 0.35, before filtering. In §7 we discuss the calculation of the wave envelope (figures 1*c-e*) and in §8 we show by applying this to typical wave records that the theoretical expressions for \bar{G} and \bar{H} agree well with the data (see for example figures 3-5). The frequency filter which gives results best in accord with visual measurements is found to be one having lower and upper cut-offs at 0.5 and 1.5 times the peak frequency.

In §9 we give a very rough theory for the probability density of G and H . Simple arguments suggest that for large G and H the densities $p(G)$ and $p(H)$ are both exponential, and this is supported by the available data. However the reasoning is not really applicable to smaller values of G and H .

Accordingly in the remainder of the paper we consider the alternative approach mentioned above, in which the wave heights are treated as a Markov chain, with a positive correlation γ only between successive waves. We derive an approximate relation between γ and ν , namely

$$\gamma \doteq 1 - 4\pi^2\nu^2, \quad (1.2)$$

which, however, is valid only for sufficiently small values of ν . It is shown in §11 that the effect

of filtering can be to bring the spectral width to within the range of validity of (1.2). In §12 we give a simplified version of the Markov theory for $p(G)$ and $p(H)$ and show that filtering of the spectrum produces a perceptible improvement in the agreement between the theoretical distributions and Kimura's (1980) data (see figures 17–20).

Finally, by adopting further rough approximations to the Markov transition probabilities p_+ and p_- we show that the Rice (envelope) theory and the Markov chain theory are in remarkably good agreement, over a useful intermediate range of ν .

The main conclusions, together with further discussion, are restated in §13.

In an Appendix we derive the properties of an analytic expression for the spectral density function that may be of use in the description of ocean swell.

2. DEFINITIONS: THE WAVE ENVELOPE

We assume that the surface elevation ζ may be represented as a stationary random function of the time t , with correlation function

$$\psi(\tau) = \overline{f(t)f(t+\tau)} \quad (2.1)$$

(a bar denoting the mean value with respect to t). The energy spectrum $E(\sigma)$ is related to $\psi(\tau)$ by

$$E(\sigma) = \frac{1}{\pi} \int_0^\infty \psi(\tau) \cos \sigma\tau \, d\tau \quad (2.2)$$

and so

$$\psi(\tau) = \int_0^\infty E(\sigma) \cos \sigma\tau \, d\sigma, \quad (2.3)$$

We assume also that over some finite time interval $(-\frac{1}{2}T, \frac{1}{2}T)$ the function ζ may be represented as a Fourier sum:

$$\zeta = \sum_{n=0}^{\infty} c_n \cos(\sigma_n t + \epsilon_n), \quad (2.4)$$

where $\sigma_n = 2n\pi/T$, the phases ϵ_n are distributed uniformly over $(0, 2\pi)$ and the amplitudes c_n are such that

$$\lim_{T \rightarrow \infty} \sum_{\sigma} \frac{1}{2} c_n^2 = E(\sigma) \, d\sigma \quad (2.5)$$

to order $d\sigma$, the summation being over any small but fixed frequency range $(\sigma, \sigma + d\sigma)$.

The spectral moments m_r are defined by

$$m_r = \int_0^\infty \sigma^r E(\sigma) \, d\sigma, \quad (2.6)$$

so that by (2.1)

$$m_0 = \int_0^\infty E(\sigma) \, d\sigma = \psi(0) = \overline{\zeta^2} \quad (2.7)$$

represents the mean-square surface displacement and

$$\bar{\sigma} = m_1/m_0 \quad (2.8)$$

may be defined as the 'mean frequency'. If μ_r denotes the r th moment of $E(\sigma)$ about the mean, i.e.

$$\mu_r = \int_0^\infty (\sigma - \bar{\sigma})^r E(\sigma) \, d\sigma, \quad (2.9)$$

then clearly

$$\mu_0 = m_0, \quad \mu_1 = 0, \quad \mu_2 = m_2 - m_1^2/m_0 \quad (2.10)$$

and we may define the spectral width parameter ν by

$$\nu^2 = \mu_2/\mu_0 \bar{\sigma}^2 = m_2 m_0/m_1^2 - 1. \quad (2.11)$$

When $\nu^2 \ll 1$ we say that the spectrum is narrow.

Even when the spectrum is not necessarily narrow, it is possible to define the complex envelope function $A(t)$ by writing (2.4) in the form

$$\zeta = \text{Re } A(t) e^{i\sigma t}, \quad (2.12)$$

where

$$A = \sum_n c_n e^{i(\sigma_n - \sigma)t + i\epsilon_n} = \rho e^{i\phi} \quad (2.13)$$

say. Here $\rho(t)$ may be called the real envelope function, or wave-amplitude, and $\phi(t)$ the phase. The real and imaginary parts of A are given by

$$\left. \begin{aligned} \rho \cos \phi &= \sum_n c_n \cos [(\sigma_n - \sigma)t + \epsilon_n], \\ \rho \sin \phi &= \sum_n c_n \sin [(\sigma_n - \sigma)t + \epsilon_n]. \end{aligned} \right\} \quad (2.14)$$

and we shall see in §7 how these may always be computed, given only the initial function $\zeta(t)$.

From (2.13) it will be seen that the time derivative $\dot{A} = dA/dt$ contains, under the summation on the right, the factor $(\sigma_n - \sigma)$, so that

$$\overline{|\dot{A}|^2} = \mu_2 \quad (2.15)$$

and when the spectrum is narrow A varies slowly, on average, compared with the carrier wave $e^{i\sigma t}$. Thus the wave record is practically sinusoidal, and the local, crest-to-trough, wave height is given by 2ρ , very nearly. A closer inspection suggests that the assumption is correct at least to order ν . Some terms of order ν^2 will nevertheless be carried along in the analysis.

3. PRELIMINARY RESULTS

We begin by stating some known exact results of which proofs may be found, for example, in the papers by Rice (1944-1945, 1958) or Longuet-Higgins (1957).

The probability density (or simply 'density') of the function ζ is Gaussian:

$$p(\zeta) = (2\pi m_0)^{-1/2} e^{-\zeta^2/2m_0}; \quad (3.1)$$

and similarly for the derivative $\dot{\zeta}$ of ζ :

$$p(\dot{\zeta}) = (2\pi m_2)^{-1/2} e^{-\dot{\zeta}^2/2m_2}. \quad (3.2)$$

The joint density of ζ and $\dot{\zeta}$ satisfies

$$p(\zeta, \dot{\zeta}) = p(\zeta) p(\dot{\zeta}), \quad (3.3)$$

so that ζ and $\dot{\zeta}$ are statistically independent. The number of up-crossings by ζ of a given level ξ per unit time, is given by

$$N = \int_0^\infty p(\zeta, \dot{\zeta}) \dot{\zeta} d\zeta = (2\pi)^{-1/2} (m_2/m_0)^{1/2} e^{-\xi^2/2m_0}. \quad (3.4)$$

This number is a maximum at the mean level $\zeta = 0$, so

$$N_{\max} = (2\pi)^{-1} (m_2/m_0)^{\frac{1}{2}}. \quad (3.5)$$

Corresponding results for the wave envelope ρ are as follows:

$$p(\rho) = (\rho/\mu_0) e^{-\rho^2/2\mu_0}, \quad (3.6)$$

and

$$p(\rho) = (2\pi\mu_2)^{-\frac{1}{2}} e^{-\rho^2/2\mu_2}, \quad (3.7)$$

(i.e. the densities of ρ and ρ are Rayleigh and Gaussian respectively), and

$$p(\rho, \rho) = p(\rho) p(\rho) \quad (3.8)$$

as in (3.3). The number of up-crossings of a given level per unit time by the wave envelope is

$$N' = \int_0^{\infty} p(\rho, \rho) \rho d\rho = (\mu_2/2\pi)^{\frac{1}{2}} p(\rho). \quad (3.9)$$

This number is a maximum when $p(\rho)$ is a maximum, i.e. when $\rho = \mu_0^{\frac{1}{2}}$, hence

$$N'_{\max} = (2\pi e)^{-1} (\mu_2/\mu_0)^{\frac{1}{2}}. \quad (3.10)$$

4. THE AVERAGE GROUP LENGTH

In defining a group of high waves, we might consider the statistics of the *maxima* of the wave envelope. However, the mean number of maxima of $\rho(t)$, given by

$$\int_{-\infty}^{\infty} p(\rho, \rho)_{\rho=0} |\rho| d\rho, \quad (4.1)$$

involves the joint density $p(\rho, \rho)$, which depends on the fourth moment μ_4 , hence m_4 (see Rice 1945). In addition, we are not really interested in small fluctuations of the wave height, but only in broader features of the group.

We therefore adopt a lower-order definition of the length l of a wave group as the time interval between two successive upcrossings of some chosen level ρ ; see Longuet-Higgins 1957; Ewing 1973. The mean length of wave groups, so defined, is then

$$\bar{l} = 1/N', \quad (4.2)$$

where $N'(\rho)$ is given by (3.9). Clearly \bar{l} depends upon the arbitrary chosen level ρ . However there is one particular level for which N' is a maximum. At this level \bar{l} is stationary with respect to small variations in ρ . Such a level may be particularly useful for determining \bar{l} empirically, since the value of \bar{l} so determined will be insensitive to small errors in the chosen level. From (3.6) this level occurs precisely when $\rho/\mu_0^{\frac{1}{2}} = 1$, giving

$$\bar{l}_{\min} = (2\pi e)^{\frac{1}{2}} (\mu_0/\mu_2)^{\frac{1}{2}}. \quad (4.3)$$

Since for a narrow spectrum the wavelength is almost constant at $1/N_{\max}$, where N_{\max} is given by (3.5), the mean number of waves in a group, in general, is

$$\bar{G} = \bar{l} N_{\max} = (2\pi)^{-1} (m_2/\mu_0)^{\frac{1}{2}} (\mu_0^{\frac{1}{2}}/\rho) e^{\rho^2/2\mu_0}. \quad (4.4)$$

WAVE GROUP STATISTICS

TABLE 1. VALUES OF \bar{G} AND \bar{H} AS FUNCTIONS OF THE SPECTRAL WIDTH PARAMETER ν

ν	\bar{G}				\bar{H}	
	$\rho/\mu_0^{\frac{1}{2}}=1$	$(\frac{1}{2}\pi)^{\frac{1}{2}}$	2	1	$(\frac{1}{2}\pi)^{\frac{1}{2}}$	2
0.05	13.2	14.0	29.5	8.0	6.4	4.0
0.06	11.0	11.7	24.6	6.7	5.3	3.3
0.08	8.2	8.8	18.5	5.0	4.0	2.5
0.10	6.6	7.0	14.8	4.0	3.2	2.0
0.12	5.5	5.9	12.4	3.3	2.7	1.7
0.15	4.4	4.7	9.9	2.7	2.1	1.3
0.20	3.4	3.6	7.5	2.0	1.6	1.0
0.25	2.7	2.9	6.1	1.6	1.3	0.8
0.30	2.3	2.4	5.1	1.4	1.1	0.7
0.35	2.0	2.1	4.5	1.2	1.0	0.6

In terms of the parameter ν this is

$$\bar{G} = (2\pi)^{-\frac{1}{2}} [(1 + \nu^2)^{\frac{1}{2}}/\nu] (\mu_0^{\frac{1}{2}}/\rho) e^{\rho^2/2\mu_0}, \quad (4.5)$$

which is inversely proportional to ν , when ν is small. The minimum group length is when $\rho/\mu_0^{\frac{1}{2}} = 1$, so

$$\bar{G}_{\min} = (e/2\pi)^{\frac{1}{2}} (1 + \nu^2)^{\frac{1}{2}}/\nu = 0.6577 (1 + \nu^2)^{\frac{1}{2}}/\nu. \quad (4.6)$$

The values of \bar{G}_{\min} for some representative values of ν are shown in the second column of table 1. In the third column are shown the corresponding values of \bar{G} when the critical value of ρ is taken as the mean wave amplitude $\rho = (\frac{1}{2}\pi)^{\frac{1}{2}}\mu_0^{\frac{1}{2}}$. In the fourth column are the values when $\rho = 2\mu_0^{\frac{1}{2}}$, which is close to the significant wave amplitude $\rho = 2.003\mu_0^{\frac{1}{2}}$. For these two columns, the numerical constant in (4.6) is replaced by 0.6981 and 1.4739 respectively.

5. RUNS OF HIGH WAVES

Consider now a different quantity: the number of successive waves exceeding a specified level ρ . We denote this by $H(\rho)$.

To obtain an average value $\bar{H}(\rho)$, Rice (1958) reasoned that from the known density (3.6) the proportion of time during which ρ exceeded the given level would be

$$q(\rho) = \int_{\rho}^{\infty} p(\rho) d\rho = e^{-\rho^2/2\mu_0}. \quad (5.1)$$

Hence the average length of a 'high run' would be

$$\bar{l} = q\bar{l} = q/N'. \quad (5.2)$$

By (3.6) and (3.9) this is

$$\bar{l} = (2\pi/\mu_2)^{\frac{1}{2}}\mu_0/\rho. \quad (5.3)$$

To estimate the average number \bar{H} of waves in a high run we multiply \bar{l} by the mean up-crossing rate N_{\max} (see equation (3.5)) to give

$$\bar{H} = (2\pi)^{-\frac{1}{2}} (m_2/\mu_2)^{\frac{1}{2}}\mu_0^{\frac{1}{2}}/\rho, \quad (5.4)$$

or in terms of ν

$$\bar{H} = (2\pi)^{-\frac{1}{2}} [(1 + \nu^2)^{\frac{1}{2}}/\nu] \mu_0^{\frac{1}{2}}/\rho. \quad (5.5)$$

This varies very simply like ρ^{-1} . If we take the reference level as $\rho = \mu_0^{\frac{1}{2}}$, then

$$\bar{H} = 0.3989 (1 + \nu^2)^{\frac{1}{2}} / \nu. \quad (5.6)$$

On the other hand, at the mean level $\rho/\mu_0^{\frac{1}{2}} = (\frac{1}{2}\pi)^{\frac{1}{2}}$ or the significant wave amplitude $\rho/\mu_0^{\frac{1}{2}} \approx 2$ the numerical constant in (5.6) is replaced by 0.3183 or 0.1995 respectively.

Representative values for \bar{H} are given in table 1. It will be observed that since

$$\bar{H}/\bar{G} < q < 1, \quad (5.7)$$

\bar{H} is always less than \bar{G} .

6. PARAMETERS FOR OCEAN WAVES

For ocean swell, values of ν equal to 0.15 or less may be typical, as we shall see below. A spectrum of pure swell is band-limited, so that as a very simple model it is fair to assume

$$E(\sigma) = \begin{cases} \alpha, & |\sigma - \bar{\sigma}| < \delta\bar{\sigma}, \\ 0, & |\sigma - \bar{\sigma}| > \delta\bar{\sigma}, \end{cases} \quad (6.1)$$

where $\delta \leq 0.5$ say. For such a spectrum we have

$$\nu = \delta/\sqrt{3} \leq 0.289. \quad (6.2)$$

A convenient expression for an ocean swell spectrum having a smooth cut-off is

$$E(\sigma) = \alpha\sigma^{-\frac{1}{2}} e^{-\frac{1}{2}n|\delta\sigma + (\beta\sigma)^{-1}|}, \quad (6.3)$$

where α , β and n are constants. For such a spectrum it may be shown (see the Appendix) that

$$\left. \begin{aligned} m_0 &= 2\alpha(\pi/\beta)^{\frac{1}{2}}/ne^n, \\ \bar{\sigma} &= (1 + 1/n)/\beta, \\ \nu &= (n+2)^{\frac{1}{2}}/(n+1). \end{aligned} \right\} \quad (6.4)$$

When n is large we have $\nu \sim n^{-\frac{1}{2}}$. Hence useful values of n will lie in the range 50 to 500. We note that the spectrum (5.3) has a half-width $\beta\delta'$ given approximately by

$$\beta\sigma + (\beta\sigma)^{-1} = 2 \ln 2, \quad (6.5)$$

hence

$$\delta' \sim (\ln 4)^{\frac{1}{2}}/n + O(n^{-1}), \quad (6.6)$$

corresponding to

$$\nu \sim n^{\frac{1}{2}} \sim 0.849 \delta', \quad (6.7)$$

as compared with

$$\nu = \delta/\sqrt{3} = 0.577 \delta \quad (6.8)$$

for the simple band-pass spectrum. The rule (6.7) should be fairly easy to apply in practice.

On the other hand for wind-waves, a typical form is the Pierson-Moskowitz spectrum

$$E(\sigma) = \alpha\sigma^{-5} e^{-(\beta/\sigma)^\gamma} \quad (6.9)$$

where α , β and γ are constants depending on the wave field. It is easily shown that the r th moment m_r is given by

$$m_r = (\alpha\beta^{-r-4}/\gamma) \Gamma((4-r)/\gamma), \quad (6.10)$$

where $\Gamma(z)$ is the usual gamma function: $\Gamma(n) = (n-1)!$ Hence we have

$$\bar{\sigma} = \beta \Gamma(3/\gamma) / \Gamma(4/\gamma) \quad (6.11)$$

independently of α , and

$$\nu^2 = \frac{\Gamma(2/\gamma) \Gamma(4/\gamma)}{[\Gamma(3/\gamma)]^2} - 1, \quad (6.12)$$

independently of both α and β . Some values of m_0 , $\bar{\sigma}$ and ν are given in table 2. It can be seen that as γ decreases from ∞ to 1, so ν ranges from $8^{-1} = 0.3536$ to $2^{-1} = 0.7071$. The value $\gamma = \infty$ corresponds to the Phillips spectrum

$$E(\sigma) = \begin{cases} 0, & \sigma/\beta < 1, \\ \alpha\sigma^{-5}, & \sigma/\beta > 1. \end{cases} \quad (6.13)$$

A common value of γ is 4, when $\nu = 0.4247$.

TABLE 2. PARAMETERS FOR THE PIERSON-MOSKOWITZ SPECTRUM (6.9)

γ	$m_0\beta^4/\alpha$	$\bar{\sigma}/\beta$	ν	ν'
∞	0.2500	1.3333	0.3536	0.1132
10	.2218	1.3487	.3713	.1314
8	.2216	1.3374	.3790	.1405
6	.2257	1.3089	.3933	.1570
5	.2328	1.2791	.4056	.1711
4	.2500	1.2254	.4247	.1804
3	.2977	1.1198	.4574	.1939
2	.5000	0.8862	.5227	.2151
1	6.0000	0.3333	.7071	.2483

However, we shall see later (§8) that for broad spectra, such as the Pierson-Moskowitz spectrum, it is implicit in the definition of a wave group that we use a filtered version of the spectrum, the T.P.M. or 'Truncated Pierson-Moskowitz' spectrum. This in general reduces the value of ν to a value ν' depending on the cut-off frequencies. Some values of ν' are given in the last column of table 2.

7. CALCULATION OF THE WAVE ENVELOPE

Records of sea waves are commonly in digital form, the surface elevation $\zeta(t)$ being specified at discrete but uniformly spaced times t_1, t_2, \dots, t_M say. To calculate the wave envelope function

$$\rho = (\zeta^2 + \eta^2)^{1/2} \quad (7.1)$$

of §2, we need both the surface elevation $\zeta(t)$ itself and its Hilbert transform $\eta(t)$. For very long records it may be convenient to use a discrete form of the formula

$$\eta(t) = \frac{1}{\pi} \int_{-\infty}^{\infty} \frac{\zeta(s)}{t-s} ds, \quad (7.2)$$

where \int denotes the principal value of the integral. For example, if $\zeta = \cos \sigma t$ then $\eta = \sin \sigma t$. However, for short or moderately long records, say $M \leq 10^4$, a method based on Fourier analysis is practical and more feasible.

Let ζ_m denote $\zeta(t_m)$, and set

$$\left. \begin{aligned} a_n &= \frac{1}{M} \sum_{m=1}^M \zeta_m \cos m\sigma_n, \\ b_n &= \frac{1}{M} \sum_{m=1}^M \zeta_m \sin m\sigma_n, \end{aligned} \right\} \quad (7.3)$$

where

$$\sigma_n = 2n\pi/M. \quad (7.4)$$

In particular,

$$a_M = \frac{1}{M} \sum_m \zeta_m, \quad b_M = 0. \quad (7.5)$$

It is easy to show that

$$\zeta_m = \sum_{n=1}^M (a_n \cos m\sigma_n + b_n \sin m\sigma_n). \quad (7.6)$$

However, we shall dispense with the upper frequencies ($n > \frac{1}{2}M$) by using instead the identity

$$\zeta_m = 2 \sum_{n=1}^{\frac{1}{2}M} (a_n \cos m\sigma_n + b_n \sin m\sigma_n) - (-1)^M a_{\frac{1}{2}M} + a_M \quad (7.7)$$

(M is assumed even). We may then take

$$\eta_m = 2 \sum_{n=1}^{\frac{1}{2}M} (a_n \sin m\sigma_n - b_n \cos m\sigma_n). \quad (7.8)$$

In practice, the low-frequency component of the record is of no interest generally when considering crest-to-trough wave heights; for example, a non-zero mean value a_M is irrelevant. Hence in any examination of the properties of wave heights, or of the wave envelope, it is appropriate to work with a filtered version of the record and its transform:

$$\left. \begin{aligned} \zeta'_m &= 2 \sum_n^{n'} (a_n \cos m\sigma_n + b_n \sin m\sigma_n), \\ \eta'_m &= 2 \sum_n^{n''} (a_n \sin m\sigma_n - b_n \cos m\sigma_n), \end{aligned} \right\} \quad (7.9)$$

where n' and n'' are suitably chosen numbers such that $1 \leq n' < n'' < \frac{1}{2}M$. A reduction in the upper limit may be desirable to avoid the aliasing of energy from frequencies higher than the Nyquist frequency $\sigma_{\frac{1}{2}M}$.

We may then calculate the envelope function $\rho'(t)$ for the filtered record $\zeta'(t)$ from

$$\rho' = \pm (\zeta'^2 + \eta'^2)^{\frac{1}{2}}. \quad (7.10)$$

8. EXAMPLES

Figure 1*a* shows a typical section of a record of surface elevation taken in the southern North Sea by a ship-borne wave recorder. The record is digitized at time intervals of 1 s.

The spectrum of a stretch of the record lasting $19\frac{1}{2}$ min ($M = 1170$) is shown in figure 2. Each ordinate represents $\sum_n^{\frac{1}{2}c_n^2}$ summed over 10 successive harmonics. The vertical scale has been normalized so that

$$\bar{\zeta} = a_M = 0 \quad (8.1)$$

and

$$\bar{\zeta}^2 = \sum_{n=1}^M \frac{1}{2} c_n^2 = 1, \quad (8.2)$$

where $c_n^2 = a_n^2 + b_n^2$. It can be seen that, apart from the slight rise in energy at very low frequencies (which may be partly due to the method of measurement) there is a single dominant

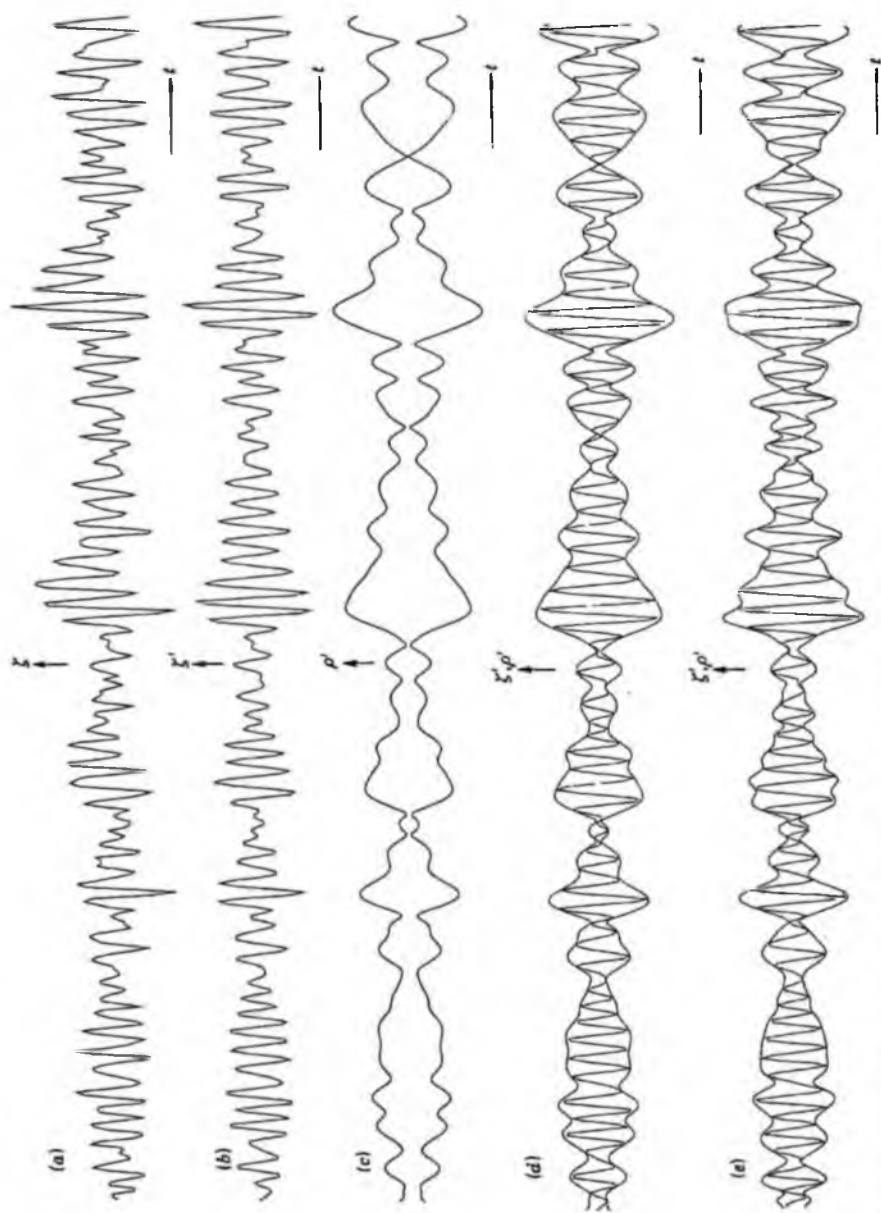


FIGURE 1. Part of a record of sea-surface elevation made with a shipborne wave recorder in the North Sea, at $55^{\circ} 04' N$, $7^{\circ} 32' E$, on 22 Sep. 1973. Digitization: 1 Hz. (a) original record; (b) filtered record: $\pi/\pi_p = 0.6$, $\pi/\pi_p = 1.5$; (c) envelope function (7.10) of (b); (d) superposition of (b) and (c); (e) As (d), but with $\pi/\pi_p = 0.25$, $\pi/\pi_p = 1.75$.

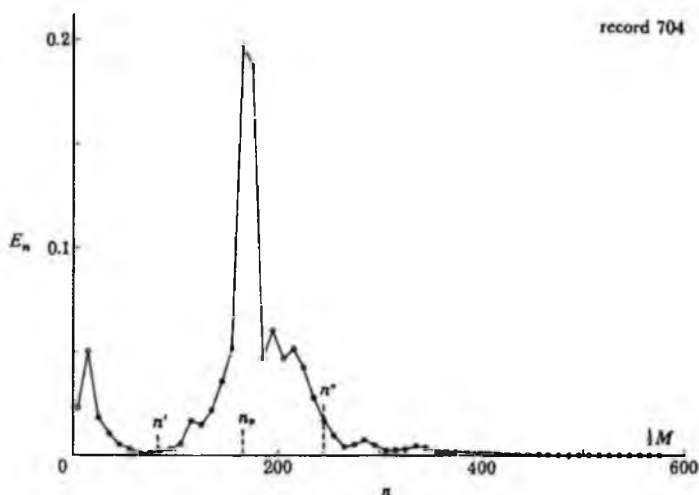


FIGURE 2. Frequency spectrum of the complete record shown partly in figure 1a.

peak in the spectrum at about $n = n_p = 165$ (corresponding to a frequency $n/M = 0.141$ Hz). On the high-frequency side, the energy falls away rapidly. For reasons mentioned in §1, the energy at $n > 2n_p$ is irrelevant to a study of dominant-wave grouping, if we neglect nonlinear effects.

Suppose we take the lower and upper cut-off frequencies at $n' = 0.5n_p$ and $n = 1.5n_p$, for example. Figure 1*b* shows the resulting filtered record ζ' . Corresponding crests and troughs of the dominant waves between figures 1*a* and *b* can easily be identified. The envelope function $\pm\rho'$ is shown by itself in figure 1*c*, and it will be noticed at once that there are a surprising number of points where ρ' seems to approach zero, so that the positive and negative branches cross over. The function $\zeta'(t)$ and its envelope are shown superimposed in figure 1*d*.

Figure 3*a* shows the total number of up-crossings of a given level ρ by the envelope function throughout the record (with the same choice of n', n''). The solid curve represents equation (3.9). The fit appears reasonable; statistical fluctuations might be expected to produce differences of order $(TN)^{1/2}$. It will be noticed that the maximum theoretical value $TN = 43$ is quite close to the value $TN = 45$ which is obtained if one constructs a visual envelope of the original record ζ by drawing straight lines between successive crests.

Figure 1*e* shows the effect of taking different cut-off frequencies, so that now $n = 0.25n_p$ and $n'' = 1.75n_p$. The envelope has many more fluctuations (maxima and minima) which seem to be irrelevant to the fluctuations in the height of the dominant waves. The corresponding number of level-crossings TN is shown in figure 3*b*. Again, the empirical points agree reasonably with the theoretical curve, but the maximum value of TN is now 56, or somewhat greater than the visual value.

Table 3 summarizes the results for various values of n'/n_p and n''/n_p . It will be seen that a change in n'/n_p from 0.5 to 0.25 has relatively little effect, but as n''/n_p is varied from 1.5 to 2.5, so TN departs more and more from the visual value.

Figure 4 shows the average number \bar{G} of waves in a group, corresponding to figure 3*a*, that

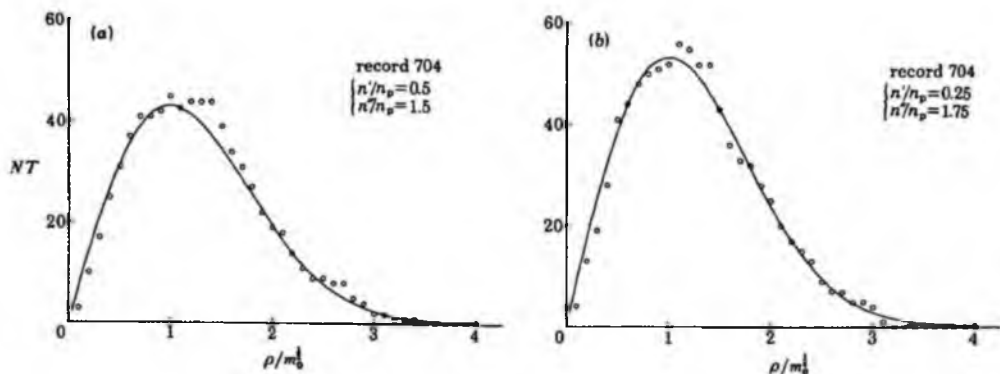


FIGURE 3. Number of level crossings of the wave envelope in the complete length of record shown partly in figure 1, as a function of the critical level (a) when $n'/n_p = 0.5$, $n''/n_p = 1.5$; (b) when $n'/n_p = 0.25$, $n''/n_p = 1.75$.

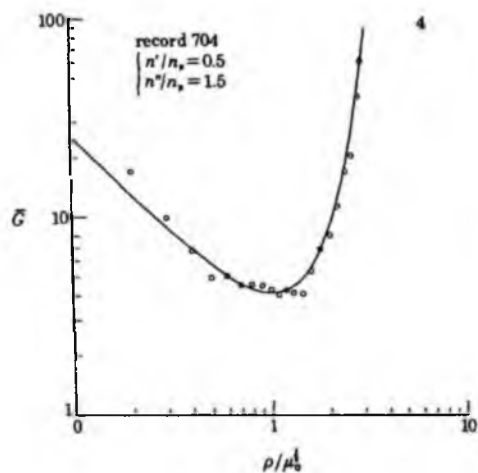


FIGURE 4. Plot of the mean group length \bar{G} corresponding to figure 1d, as a function of the critical level. The theoretical curve represents (4.5).

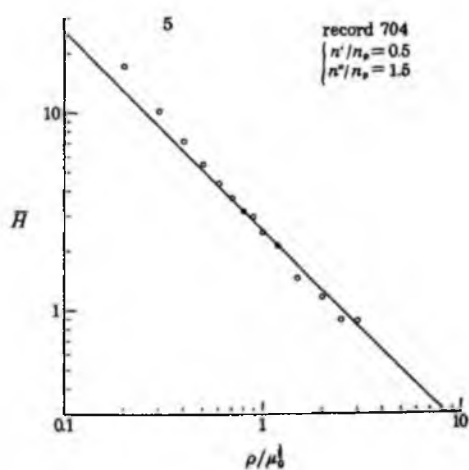


FIGURE 5. Plot of the mean length of high runs \bar{H} corresponding to the record of figure 1d. The line represents (5.5).

TABLE 3. SUMMARY OF THE EFFECT OF VARYING THE CUT-OFF FREQUENCIES n' AND n'' ON THE ANALYSIS OF THE RECORD IN FIGURE 1

n'/n_p	n''/n_p	ν	$m_0^{\frac{1}{2}}$	$\rho_0 = m_0^{\frac{1}{2}}$		$\rho_0 = 2m_0^{\frac{1}{2}}$		
				theor.	obs.	theor.	obs.	
0.50	1.50	0.160	15.5	43.2	45	19.3	19	
0.50	1.75	.172	15.8	48.9	52	21.8	24	
0.25	1.75	.196	15.9	53.4	56	23.8	25	
0.25	2.00	.213	16.1	58.8	59	26.2	25	
0.25	2.25	.237	16.2	66.1	69	29.5	26	
0.25	2.50	.250	16.2	70.5	72	31.5	30	
visual						45		18.5

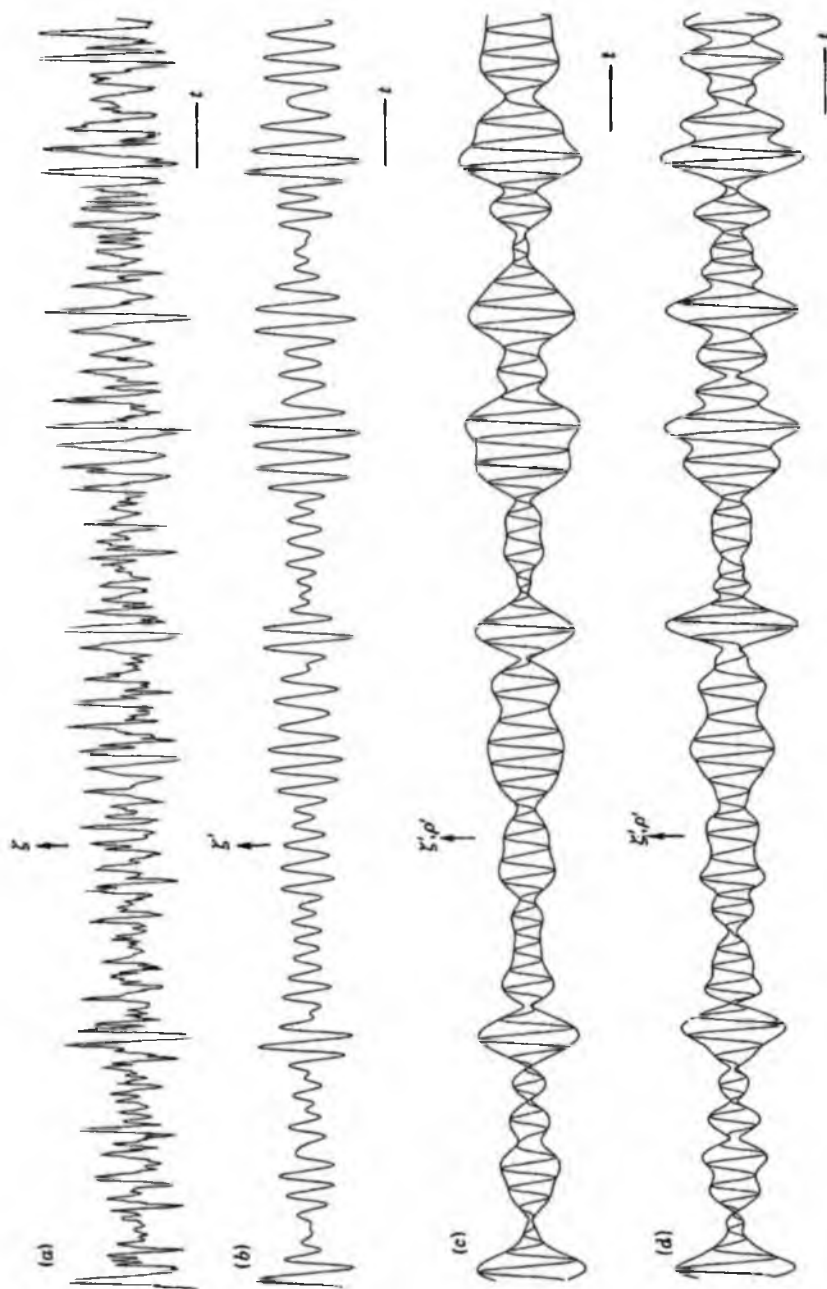


FIGURE 6. Part of a record of sea-surface elevation made with a surface wave follower at the Noordwijk Platform, $52^{\circ} 16' N$, $4^{\circ} 8' E$, on 18 Oct. 1979. Digitization: 1 Hz. (a) original record; (b) filtered record: $\pi/n_p = 0.6$, $\pi'/n_p = 1.5$; (c) superposition of (b) and its envelope function; (d) as (c), but with $\pi'/n_p = 0.25$, $\pi''/n_p = 1.75$.

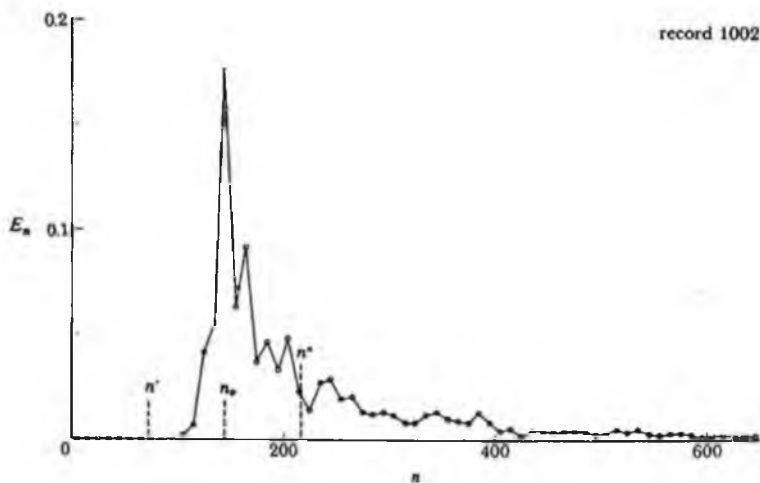


FIGURE 7. Frequency spectrum of the complete record shown partly in figure 6a.

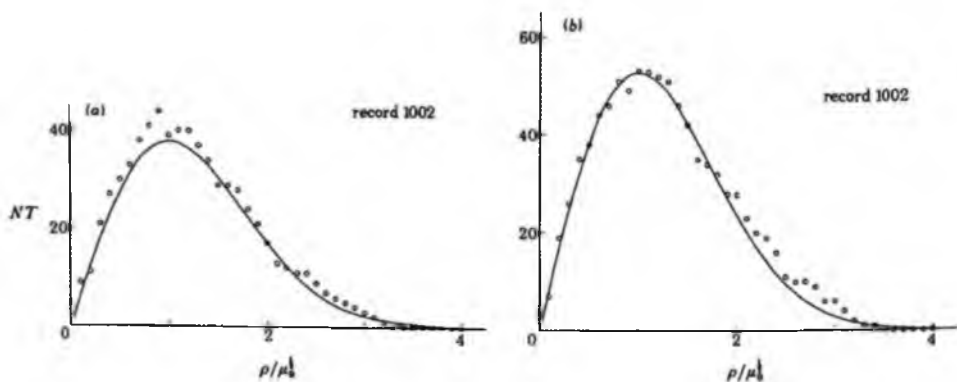


FIGURE 8. Number of level crossings of the wave envelope in the complete length of record shown partly in figure 6, as a function of the critical level (a) when $n^*/n_p = 0.5$, $n^{**}/n_p = 1.5$; (b) when $n^*/n_p = 0.25$, $n^{**}/n_p = 1.75$.

is to say when $n^*/n_p = 0.5$ and $n^{**}/n_p = 1.5$. The full curve represents the theory, equation (4.5). Except for very low levels ρ there is fair agreement. The minimum value \bar{G}_{\min} at $\rho/\mu_0^{1/2} = 1$ is about 4.1, and at the significant wave amplitude ($\rho/\mu_0^{1/2} = 2$) \bar{G} is about 9.2.

Figure 5 shows corresponding results for the mean number of waves \bar{H} in a high run, given by equation (6.5). Though the two curves for \bar{G} and \bar{H} are quite different, the agreement between theory and observation is of course similar in figures 4 and 5.

As a second example, we show in figure 6a a typical wave record taken from the Nordwijk tower in the North Sea during MARSEN. The instrument used was the 'wave follower' described by Hsiao & Shemdin (1983). Figure 7 shows the spectral density function. This has a slightly longer high-frequency tail than the previous example, figure 2. However, if we take the cutoffs $n^*/n_p = 0.5$ and $n^{**}/n_p = 1.5$ we obtain the reasonably smooth envelope function

shown in figure 6*c*. The wider cut-offs $n'/n_p = 0.25$, $n''/n_p = 1.75$ give the record in figure 6*d*, in which the envelope has a greater number of 'wiggles'. The corresponding numbers of level-crossings are shown in figures 8*a* and *b*. Again, there is fair agreement, but the scale value TN_{\max} (at $\rho/\mu_0^{\frac{1}{2}} = 1$) agrees better with the visually determined value ($TN = 35$) when the cut-off limits are narrower ($n'/n_p = 0.5$, $n''/n_p = 1.5$). Graphs of \bar{G} and \bar{H} are shown in figures 9 and 10.

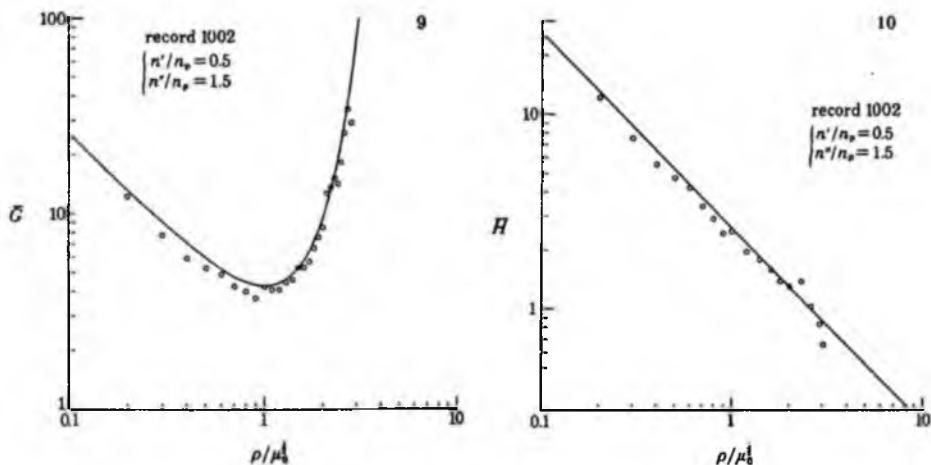


FIGURE 9. Plot of the mean group-length \bar{G} corresponding to figure 6*c* as a function of the critical level. The theoretical curve represents (4.5).

FIGURE 10. Plot of the mean length of high runs \bar{H} corresponding to figure 6*c*. The line represents (5.5).

From these examples we may conclude that typical wind-wave spectra are effectively filtered by a 'group analysis', and that the cut-off frequencies $n' = 0.5 n_p$, $n'' = 1.5 n_p$ are appropriate. As seen from table 3, this filtering of the record reduces slightly the total energy m_0 in the record. For a satisfactory analysis we may specify that m_0 shall not be changed significantly by the filtering. Such a limitation appears to be inherent in the idea of a wave-group analysis. For, any energy outside the dominant wave band is irrelevant to the quantities of interest. Thus, any spectrum that is not of the unimodal type, say one that has energy distributed in two or more widely separated frequency bands, is essentially unsuitable for simple group analysis. More complicated definitions may of course be sought.

9. THE DISTRIBUTION OF GROUP LENGTHS

The length l of a group was defined in §4 as the interval between two successive up-crossings of $\rho(t)$. The statistical distribution of l , apart from its mean \bar{l} , is difficult to determine in general (see Rice 1958). However, for narrow spectra an approximation may be derived from the notion that since the spectrum of ρ is predominantly low-pass, we expect successive up-crossings to be uncorrelated, at least when l is sufficiently large. Hence the distribution of l will be

asymptotically the same as in a 'shot-effect', where the time-axis is peppered randomly with points at a mean rate

$$\lambda = 1/\bar{l} \quad (9.1)$$

per unit time. The density $p(l)$ for this process is known to be simply

$$p(l) = \lambda e^{-\lambda l}, \quad (9.2)$$

that is a negative exponential (see Rice 1954, section 3.4). Rice gives a proof involving an infinite series of terms. A more direct proof is as follows. Divide a given interval $(l, l+l)$ into a large number m of equal parts. The probability that ρ has no level crossing in any of these sub-intervals is $(1 - \lambda l/m)^m$, and in the limit as $m \rightarrow \infty$ this tends to

$$P(l) = e^{-\lambda l}. \quad (9.3)$$

The density (9.2) then follows on applying the general formula

$$p(l) = (1/\lambda) d^2 P/dl^2, \quad (9.4)$$

where λ is the mean number of up-crossings per unit time (see Longuet-Higgins 1958, section 2).

Incidentally it may be noted that for the low-pass spectrum $E(\sigma) = (1 + \sigma^2)^{-2}$, the distribution of zero-crossing intervals of ζ is almost (but not quite) negative exponential; see Favreau *et al.* (1956); Longuet-Higgins (1962).

Assuming (9.2) to be valid, we have simply

$$p(l) = \bar{l} e^{-l/\bar{l}} \quad (9.5)$$

and so for the number of waves G in a complete group

$$p(G) = \bar{G} e^{-G/\bar{G}}, \quad (9.6)$$

where \bar{G} is given by (4.8). Some comparisons with observation will be given below.

The question arises as to what meaning we should attach to a fractional number of waves in a group. This can occur because the wave envelope ρ may exceed the reference level for only a short interval of time. In any given case a wave crest may or may not be present during the interval. However, the fractional number of waves is still a measure of the *probability* of a wave crest exceeding the given level in that interval. As a matter of fact, owing to the dispersive properties of gravity waves, the phase velocity is greater than the group velocity. Hence any particular wave tends to advance through the group, and any section of the envelope contains a wave crest at least some of the time.

To estimate the statistical density $p(H)$ of high runs, we may assume as an approximation that each high run H is, on the whole, in proportion to the corresponding group length G , so $H = qG$, where q is given by (5.1). It follows that the distribution of H , like that of G , is also a negative exponential:

$$p(H) \doteq \bar{H} e^{-H/\bar{H}}. \quad (9.7)$$

Does this fit existing observations? Most data are given for integer values of the group length G or run length H . We may reasonably assume that the probability H_j of H for an integer value $j > 0$ is related to the continuous probability density $p(H)$ by

$$H_j \propto \int_{j-1}^{j+1} p(H) dH, \quad (9.8)$$

that is to say, the probability density of a run of length H contributes to the probability of the discrete run having the nearest integer value. The densities for runs H less than $\frac{1}{2}$ contribute only to runs of zero length, that is they are ignored.

If $p(H)$ is a negative exponential, then the assumption (9.8) has two simple consequences: (1) the probability H_j is also negative exponential, that is

$$H_j \propto e^{-jH}, \quad (9.9)$$

and (2) because of the effective truncation of the distribution at $H = \frac{1}{2}$, the mean value \bar{H}_j is increased by approximately the same amount, i.e.

$$\bar{H}_j = \bar{H} + 0.5. \quad (9.10)$$

Sufficiently long wave records are quite rare, but the numerically simulated data of Kimura (1980), reproduced in part in figures 17 and 18 below, show conclusively that the distribution of H_j is indeed negative exponential, over practically the whole range of j . Figures 19 and 20 show that the distribution of G_j is almost exponential, particularly when j is large, as expected, but for small values of j there are systematic differences.

For H_j it is therefore worth testing the second conclusion (9.8) just mentioned. The 'target spectra' used by Kimura (1980) and shown in his figure 8 appear to be of the form

$$S(f) = f^{-n} e^{-(n/\gamma)(1-f^{-\gamma})} \quad (f = \sigma/2\pi), \quad (9.11)$$

where $\gamma = 4$ and n runs from 4 to 8 in Kimura's cases 1 to 5, respectively. It will be seen that the analytic form (9.11) has a peak at $f = f_p = 1$, where $S = S_{\max} = 1$, as required.

TABLE 4. COMPARISON OF THEORETICAL AND OBSERVED VALUES OF THE MEAN PROBABILITY \bar{H}_j OF HIGH RUNS, IN THE DATA OF KIMURA (1980)

case	n	ν	$\rho = \rho_{\text{mean}}$			$\rho = \rho_1$		
			\bar{H}	\bar{H}_j	data	\bar{H}	\bar{H}_j	data
1	4	0.1879	1.72	2.22	2.20	1.08	1.58	1.28
2	5	.1805	1.82	2.32	2.29	1.12	1.62	1.29
3	6	.1742	1.85	2.35	2.34	1.16	1.66	1.29
4	7	.1686	1.92	2.42	2.42	1.20	1.70	1.37
5	8	.1635	1.96	2.46	2.45	1.23	1.73	1.53

With cut-off frequencies at $f = 0.5$ and 1.5, we calculate the values of ν , \bar{H} and \bar{H}_j seen in table 4, both for $\rho = \rho_{\text{mean}}$ ($\rho/\mu_0^{\frac{1}{2}} = \sqrt{2/\pi}$) and for $\rho = \rho_1$ ($\rho/\mu_0^{\frac{1}{2}} = 2$). Comparison with the data, taken from table 1 of Kimura (1980) shows good agreement when $\rho = \rho_{\text{mean}}$, though less so when $\rho = \rho_1$.

In the following three sections (§§ 10–12) we shall outline a different approach for finding the distributions of H_j and G_p based partly on the work of Kimura (1980), but with some significant modifications.

10. CORRELATION BETWEEN SUCCESSIVE WAVE HEIGHTS

Consider the joint density of $\rho_1 = \rho(t_1)$ and $\rho_2 = \rho(t_2)$ at two points separated by a constant time interval $\tau = t_2 - t_1$. This is known exactly from the work of Uhlenbeck (1943) and Rice (1944, 1958). The general result may be written

$$p(\rho_1, \rho_2) = \frac{\rho_1 \rho_2}{\mu_0^2 (1 - \kappa^2)} e^{-(\rho_1 + \rho_2)/2\mu_0(1 - \kappa^2)} I_0\left(\frac{\kappa}{1 - \kappa^2} \frac{\rho_1 \rho_2}{\mu_0}\right), \quad (10.1)$$

where

$$\left. \begin{aligned} X &= \int_0^\infty E(\sigma) \cos(\sigma - \bar{\sigma}) \tau d\sigma, \\ Y &= \int_0^\infty E(\sigma) \sin(\sigma - \bar{\sigma}) \tau d\sigma, \end{aligned} \right\} \quad (10.2)$$

$$\kappa = (X^2 + Y^2)^{1/2} / \mu_0, \quad (10.3)$$

and I_0 denotes the modified Bessel function of order zero:

$$I_0(z) = \frac{1}{2\pi} \int_0^{2\pi} e^{z \cos \theta} d\theta. \quad (10.4)$$

When $\kappa = 0$ then $p(\rho_1, \rho_2)$ reduces to the product of two Rayleigh distributions: $p(\rho_1) p(\rho_2)$.

We shall assume that when the separation τ equals $2\pi/\bar{\sigma}$, then ρ_1 and ρ_2 approximate the amplitudes of two successive waves.

The correlation coefficient γ , defined as $M_{11}/(M_{20}M_{02})^{1/2}$ where

$$M_{pq} = \int_0^\infty \int_0^\infty (\rho_1 - \bar{\rho})^p (\rho_2 - \bar{\rho})^q p(\rho_1, \rho_2) d\rho_1 d\rho_2, \quad (10.5)$$

has been evaluated by Uhlenbeck (1943); see also Middleton (1960), as

$$\gamma = [E - \frac{1}{2}(1 - \kappa^2)K - \frac{1}{4}\pi]/(1 - \frac{1}{4}\pi), \quad (10.6)$$

where E and K are complete elliptic integrals:

$$E(\kappa) = \int_0^{\frac{1}{2}\pi} (1 - \kappa^2 \sin^2 \theta)^{1/2} d\theta, \quad (10.7)$$

and

$$K(\kappa) = \int_0^{\frac{1}{2}\pi} (1 - \kappa^2 \sin^2 \theta)^{-1/2} d\theta. \quad (10.8)$$

γ is shown as a function of κ^2 in figure 11 (cf. Kimura 1980, figure 1, where γ is shown as a function of κ).

For values of κ very close to 1 it may be shown that

$$\gamma \sim 1 - (1 - \kappa^2)/(4 - \pi), \quad (10.9)$$

and this is represented by the tangent at $\kappa = 1$ to the curve in figure 11. However, it can be seen immediately that for values of κ^2 less than 0.6 a closer approximation to γ is given by the simple expression

$$\gamma \doteq \kappa^2 \quad (10.10)$$

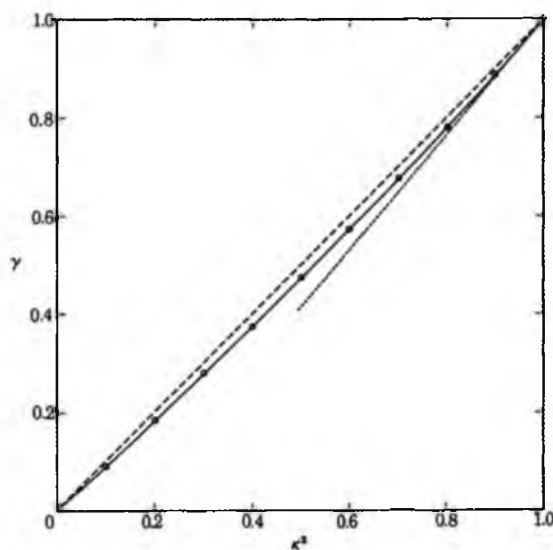


FIGURE 11. The correlation coefficient γ between ρ_1 and ρ_2 shown as a function of the parameter κ^2 .

represented by the straight diagonal in figure 11. This holds good to within a small percentage over the whole range of κ .

Consider the interpretation of these results for a narrow spectrum. From (2.10) and (2.7) we have

$$\mu_0^2 = \int_0^\infty \int_0^\infty E(\sigma) E(\sigma') d\sigma d\sigma' \quad (10.11)$$

and similarly from (10.2)

$$X^2 + Y^2 = \int_0^\infty \int_0^\infty E(\sigma) E(\sigma') \cos(\sigma - \sigma') \tau d\sigma d\sigma'. \quad (10.12)$$

So by (10.3)

$$\mu_0^2(1 - \kappa^2) = 2 \int_0^\infty \int_0^\infty E(\sigma) E(\sigma') \sin^2 \frac{1}{2}(\sigma - \sigma') \tau d\sigma d\sigma'. \quad (10.13)$$

For a narrow spectrum let us formally replace the trigonometric term in (10.12) by the first term in its power series, that is set

$$\sin^2 \frac{1}{2}(\sigma - \sigma') \tau \doteq \frac{1}{4}(\sigma - \sigma')^2 \tau^2 \quad (10.14)$$

$$= \frac{1}{4}[(\sigma - \bar{\sigma})^2 - (\sigma' - \bar{\sigma})^2] \tau^2. \quad (10.15)$$

Then we obtain

$$\mu_0^2(1 - \kappa^2) \doteq \frac{1}{2}(\mu_2 \mu_0 - 2\mu_1^2 + \mu_0 \mu_2) = \mu_0 \mu_2 \tau^2, \quad (10.16)$$

since $\mu_1 = 0$. Hence writing

$$\tau = 2\pi/\bar{\sigma} \quad (10.17)$$

we see from (10.13) that, to lowest order,

$$1 - \kappa^2 = (\mu_2/\mu_0) \tau^2 = 4\pi^2 \nu^2. \quad (10.18)$$

So from (10.9)

$$\gamma \doteq 1 - 45.99 \nu^2, \quad (10.19)$$

Because of the coefficient $4\pi^2$ in (10.19) this formula for γ can be expected to be adequate only when $\nu < 0.1$, say. A similar limitation on the value of ν arises from the representation of the sinusoidal term in (10.13) by a single term $\frac{1}{2}(\sigma - \sigma')^2 \tau^2$. This can be valid at best only so long as $|\sigma - \sigma'| \tau < \frac{1}{2}\pi$. But for substitution in the double integral (10.15), we should require $|\sigma - \sigma'|$ to be at least as great as twice the spectral width $(\mu_2/\mu_0)^{\frac{1}{2}}$. Hence

$$2(\mu_2/\mu_0)^{\frac{1}{2}} \tau < \frac{1}{2}\pi, \quad (10.20)$$

which with τ given by (10.19) is equivalent to

$$(\mu_2/\mu_0)^{\frac{1}{2}} < \frac{1}{2}\bar{\sigma}, \quad (10.21)$$

that is

$$\nu < 0.125. \quad (10.22)$$

If we wished to calculate the correlation γ_2 between *alternate* wave heights, we would have to substitute $\tau = 4\pi/\bar{\sigma}$ in (10.16), thus doubling τ and restricting the range of validity of the linear theory to $\nu < 0.025$, at most. None the less the linearized theory does suggest qualitatively the very drastic reduction in γ to be expected as ν and τ are increased beyond the limits estimated above.

For larger values of ν or τ we may use the accurate expressions for κ^2 provided by (10.2) and (10.3), together with the relation between γ and κ indicated by the solid curve in figure 11, or its approximation, equation (10.10). Alternatively, κ^2 may be determined directly from observation since it is equal to coefficient of correlation between ρ_1^2 and ρ_2^2 .

11. THE CORRELATION COEFFICIENT: EXAMPLES

To illustrate the dependence of κ on ν for typical spectra, consider the band-pass spectrum (6.1), for which $\nu = 3^{-1}\delta$. From (10.1) we have immediately

$$X = m_0(\sin \delta \bar{\sigma} \tau) / \delta \bar{\sigma} \tau, \quad Y = 0. \quad (11.1)$$

Hence

$$\kappa^2 = [(\sin \delta \bar{\sigma} \tau) / \delta \bar{\sigma} \tau]^2. \quad (11.2)$$

To find $\gamma = \gamma_2$, write $\tau = 2\pi/\bar{\sigma}$, so

$$\kappa^2 = [(\sin 2\pi\delta) / 2\pi\delta]^2. \quad (11.3)$$

As $\delta \rightarrow 0$ we have $\kappa^2 = 1 - \frac{1}{3}\pi^2\delta^2$, in agreement with (10.20). As δ increases from 0, at first κ^2 decreases monotonically to 0 at $\delta = 0.5$ ($\nu = 0.289$). However, as δ increases further, κ^2 rises again to a maximum value 0.047 before falling finally to zero at $\delta = 1$ ($\nu = 0.577$).

In figure 12 we also show κ_m , the correlation coefficient corresponding to $\tau = 2m\pi/\bar{\sigma}$. This shows that $\gamma_2 < \gamma_1$ always, but as m increases, it is not always true that $\gamma_{m+1} < \gamma_m$. For instance when $\nu = 1.4$, γ_3 may exceed γ_2 .

This non-monotonic behaviour may be associated with the sharp cut off in a band-pass spectrum. An example when the cut-off is smooth, but still decisive, is provided by the 'ocean-swell' spectrum (6.3). For this spectrum it may be shown that

$$\kappa^2 = (1 + r^2)^{-1} e^{-2n[(\frac{1}{2}(1+r^2)^{\frac{1}{2}} + \frac{1}{2})^2 - 1]} \quad (11.4)$$

where

$$r = 4m\pi / (n+1). \quad (11.5)$$

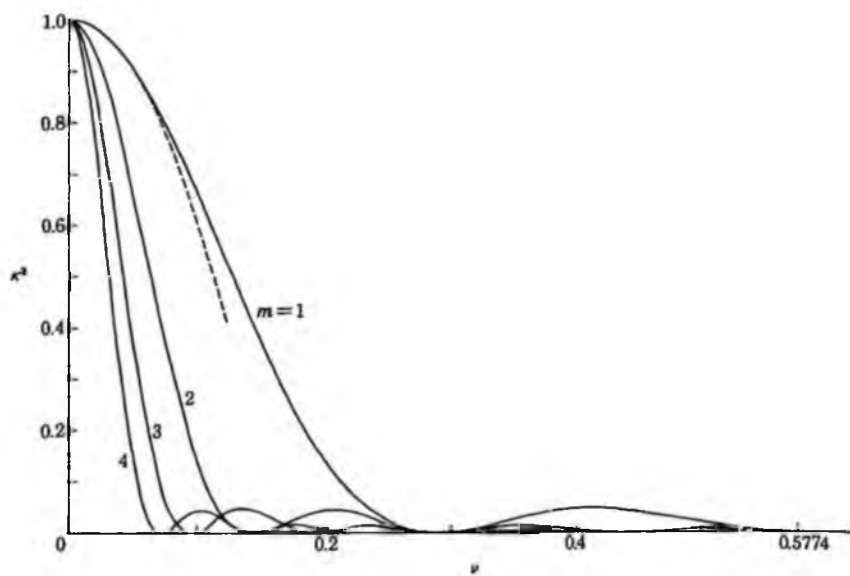


FIGURE 12. κ^2 as a function of ν for the band-pass spectrum (6.1). The broken curve represents the asymptote (10.18) when $m = 1$.

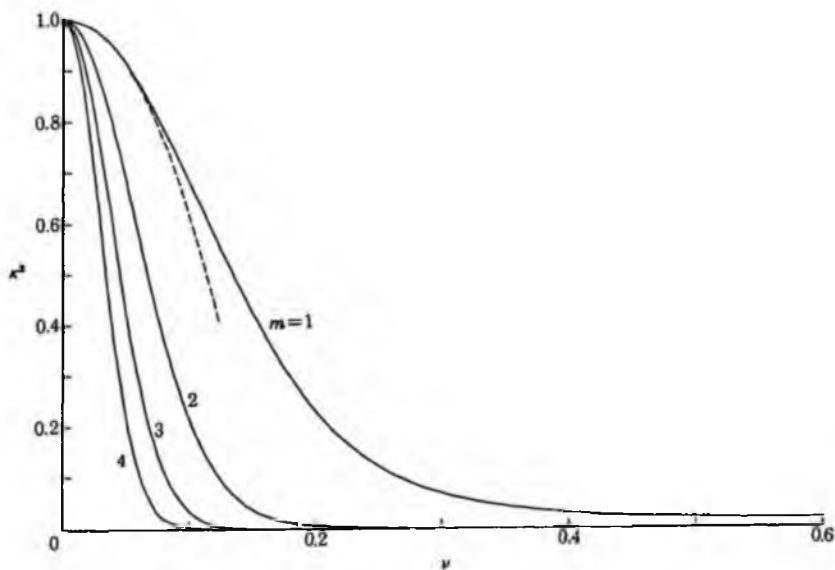
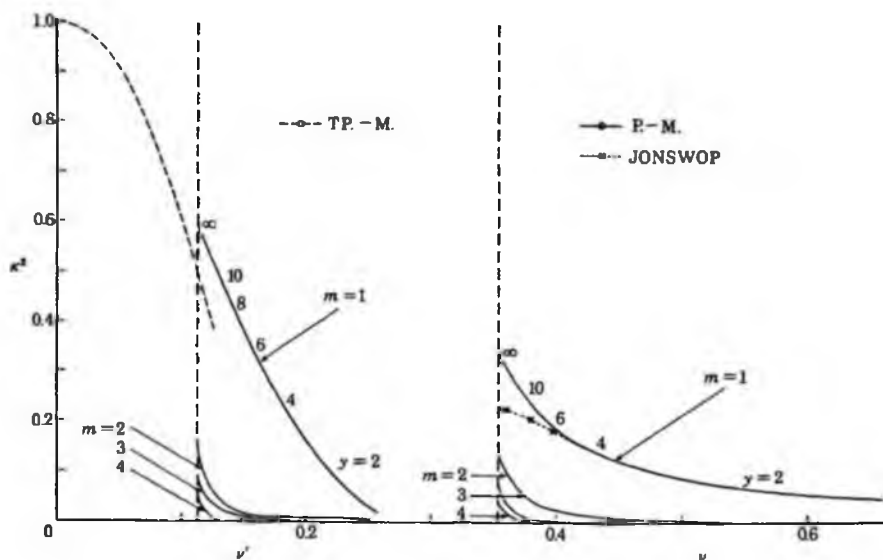


FIGURE 13. κ^2 as a function of ν for the 'ocean swell spectrum' (6.3). The broken curve represents the asymptote (10.18) when $m = 1$.



The expression (11.4) is plotted against ν in figure 13. Each curve is now monotonic in both ν and m , over the ranges shown, and when $\nu > 0.15$, γ_2 , γ_3 and γ_4 are all very small.

When $\nu = 0.082$, for example, the sequence of values of κ^2 for $m = 1, 2, 3$ and 4 is $0.76, 0.34, 0.10$ and 0.02 , giving $\gamma_m = 0.74, 0.32, 0.10$ and 0.02 . This compares with Goda's (1983) values for swell of $\gamma_m = 0.65, 0.35, 0.18$ and 0.07 .

For wind-waves, however, very different results are to be expected. Figure 14 shows κ^2 plotted against ν for the Pierson-Moskowitz spectrum, equation (6.9). In general, the integrals X and Y of (10.2) were found by quadratures, through in two cases the numerical values could be checked against explicit expressions. For in the case $\gamma = \infty$ (the Phillips spectrum), integration of (10.2) by parts gives

$$X + iY = \frac{1}{24} \left[(6 + 2i\tau - \tau^2 - i\tau^3) e^{i\tau} + \tau^4 \int_{\tau}^{\infty} \frac{e^{iu}}{u} du \right], \quad (11.6)$$

the last function being tabulated in Abramowitz & Stegun (1965), table 5.3. Also when $\gamma = 1$, we find from Erdelyi (1954) (1.4.21) and (2.4.31) that

$$X + iY = 2\alpha(\tau/\beta)^2 K_4(z), \quad (11.7)$$

where $z = 2(i\beta\tau)^{1/2}$ and K_4 denotes the modified Bessel function of order four (see Erdelyi 1953, ch. 8).

The behaviour of κ^2 shown in figure 14 differs from that in figure 13. For one thing, the value of ν for the Pierson-Moskowitz spectrum is never less than 0.3536 . Also the maximum value of κ^2 is always less than 0.34 . It is clear that for this spectrum the narrow-band expression (10.18) never applies.

However, for the truncated Pierson-Moskowitz spectrum, as shown on the left of figure 14, the situation is again different. The lower bound for ν' is now reduced to 0.113 (see table 2) and κ^2 can be as great as 0.595 compared with the narrow-band approximation 0.500. The sequence of values for $\gamma_1, \gamma_2, \gamma_3, \gamma_4$ is then 0.595, 0.139, 0.080 and 0.052. However, only a slight shift to the right, to say $\nu' = 0.16$ reduces γ_1 to about 0.33, which is typical of wind-waves. Further, γ_2, γ_3 and γ_4 are each reduced to less than 0.01, which can be considered insignificant.

12. DISTRIBUTION OF G_j AND H_j : MARKOV THEORY

Kimura (1980) has given a rough but simple theory for the distribution of group lengths and of high runs, treating the sequence of wave-heights as a Markov chain, as first suggested by Sawney (1962). Kimura's theory can be presented in an even simpler way, without the use of matrices, as follows.

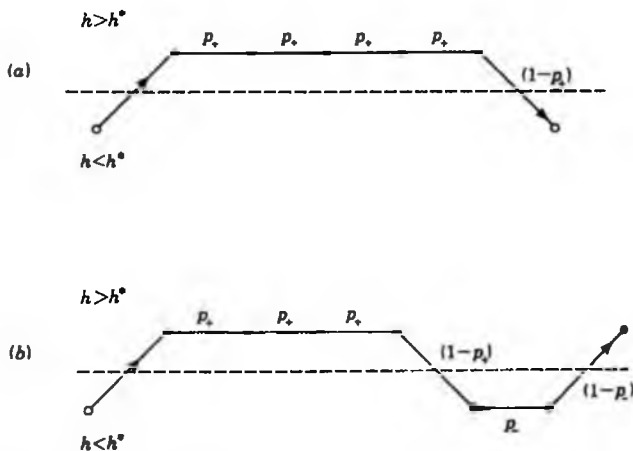


FIGURE 15. Diagram showing the basis for (a) the probability of a high run of j waves (12.1) when $j = 5$, and (b) the probability of a wave group of j waves, (12.3) and (12.4) when $i = 4, j = 6$.

Choose a critical wave-height h^* as in figure 15. Given that a certain wave-height h_1 exceeds h^* , let p_+ denote the probability that the next wave-height h_2 also exceeds h^* . To determine the probability of a high run of length j we know already that the first wave-height exceeds h^* ; the next $(j-1)$ wave-heights must then exceed h^* and the one after must *not* exceed h^* (see figure 15a). The probabilities being assumed independent, the combined probability is

$$p(H_j) = p_+^{j-1} (1-p_+). \quad (12.1)$$

The mean length of high runs is then given by

$$H = \sum_1^{\infty} j p(H_j) = 1/(1-p_+). \quad (12.2)$$

To find the distribution of total runs we may reason as follows. In a total run of length j the first i waves, say, will be a high run of length i and the remaining $(j-i)$ waves will be a low run of length $(j-i)$ (see figure 15b). The probability of such an event is clearly

$$p_+^{i-1}(1-p_+)p_-^{j-i-1}(1-p_-), \tag{12.3}$$

where p_- denotes the probability that $h_2 < h^*$ given that $h_1 < h^*$. Summing the above expression from $i = 1$ to $i = j - 1$ we obtain

$$p(G_j) = (1-p_+)(1-p_-)(p_+^{j-1}-p_-^{j-1})/(p_+-p_-) \tag{12.4}$$

when $n \geq 2$. The mean length of a total run is then

$$\bar{G} = \sum_j j p(G_j) = 1/(1-p_+) + 1/(1-p_-). \tag{12.5}$$

The only question then is to determine p_+ and p_- for a given wave record.

Kimura (1980) proposed that $p(h_1, h_2)$ be approximated by a two-dimensional Rayleigh distribution of the form (10.1), which is reasonable if we assume that h_1 and h_2 can be approximated by $2\rho_1$ and $2\rho_2$ respectively (though Kimura does not make this assumption explicitly). Then the conditional probabilities p_+ and p_- can be calculated directly from

$$\left. \begin{aligned} p_+ &= \int_{\rho^*}^{\infty} \int_{\rho^*}^{\infty} p(\rho_1, \rho_2) d\rho_1 d\rho_2 / \int_0^{\infty} \int_{\rho^*}^{\infty} p(\rho_1, \rho_2) d\rho_1 d\rho_2, \\ p_- &= \int_0^{\rho^*} \int_0^{\rho^*} p(\rho_1, \rho_2) d\rho_1 d\rho_2 / \int_0^{\infty} \int_0^{\rho^*} p(\rho_1, \rho_2) d\rho_1 d\rho_2, \end{aligned} \right\} \tag{12.6}$$

where $\rho^* = \frac{1}{2}h^*$. Such probabilities are then a function only of κ^2 , as shown in figure 16. Here we plot p_+ and p_- against κ^2 , and not against γ as was done by Kimura (1980).

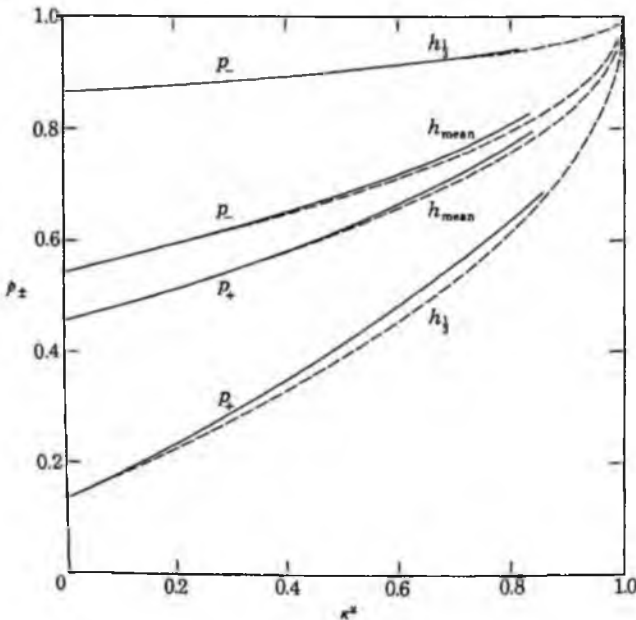


FIGURE 16. Graphs of p_+ and p_- as functions of κ^2 according to (12.6) and §10. The dashed curves represent the parabolic approximations (12.8).

TABLE 5a. PARAMETERS OF THE KIMURA SPECTRUM (9.12)

case	π	ν	κ^2	γ	h_{mean}		h_j	
					ρ_+	ρ_-	ρ_+	ρ_-
1	4	0.8319	0.1253	0.116	0.490	0.574	0.194	0.874
2	5	.6980	.1513	.140	.498	.581	.207	.876
3	6	.6118	.1820	.169	.507	.589	.225	.879
4	7	.5507	.2152	.200	.517	.598	.242	.881
5	8	.5047	.2493	.232	.528	.606	.260	.883

TABLE 5b. PARAMETERS OF THE TRUNCATED KIMURA SPECTRUM

case	π	ν	κ^2	γ	h_{mean}		h_j	
					ρ_+	ρ_-	ρ_+	ρ_-
1	4	0.5857	0.2071	0.192	0.516	0.595	0.237	0.880
2	5	.5453	.2412	.224	.526	.604	.256	.883
3	6	.5113	.2723	.254	.535	.613	.275	.885
4	7	.4820	.3011	.281	.545	.620	.292	.888
5	8	.4565	.3284	.307	.555	.628	.303	.890

TABLE 5c. MEAN VALUES OF H_j FOR THE TRUNCATED KIMURA SPECTRUM

case	h_{mean}		h_j	
	(12.2)	obs.	(12.5)	obs.
1	1.96	2.20	1.16	1.28
2	1.99	2.29	1.26	1.29
3	2.03	2.34	1.29	1.29
4	2.07	2.42	1.32	1.37
5	2.12	2.45	1.35	1.53

TABLE 5d. MEAN VALUES OF G_j FOR THE TRUNCATED KIMURA SPECTRUM

case	h_{mean}		h_j	
	(12.2)	obs.	(12.2)	obs.
1	4.31	4.66	9.18	9.33
2	4.38	4.67	9.33	9.47
3	4.46	4.94	9.55	10.00
4	4.56	5.17	9.72	9.95
5	4.66	5.32	9.90	10.71

Assuming that Kimura's five 'target spectra' are given by (9.12), we have calculated (see table 5a) the corresponding values of κ^2 and hence of ρ_+ and ρ_- from figure 16. The corresponding values for the truncated spectra are given in table 5b. It will be seen that while the truncation changes the values of ν , κ^2 and γ very considerably, the values of ρ_+ and ρ_- are much less affected†.

The distributions of G_j and H_j corresponding to the two extreme spectra (cases 1 and 5) are seen in figures 17-20. Also shown are Kimura's observations. From these results we may conclude

(1) that truncation of the spectra has a small but appreciable effect upon the theoretical distributions,

† The values of γ used by Kimura (1980) to calculate ρ_+ and ρ_- were determined empirically, and not calculated from the frequency spectra as here.

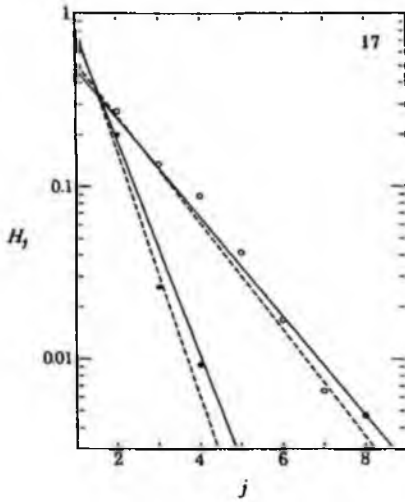


FIGURE 17. The probability H_j of a high run, as a function of j for the Kimura spectrum (9.12) when $n = 4$. The curves represent (12.1): ---, original spectrum; —, truncated spectrum. Plotted points are data from Kimura (1980), figure 9a.

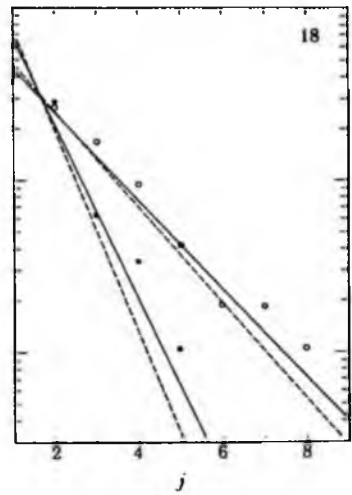


FIGURE 18. As figure 17, but with $n = 8$. The plotted points are from Kimura (1980), figure 9c.

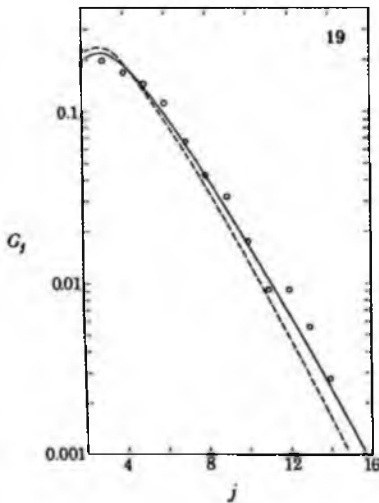


FIGURE 19. The probability G_j of a group of total length j for the Kimura spectrum (9.12) when $n = 4$. The curves represent (12.4): ---, original spectrum; —, truncated spectrum. Plotted points are data from Kimura (1980), figure 10a.

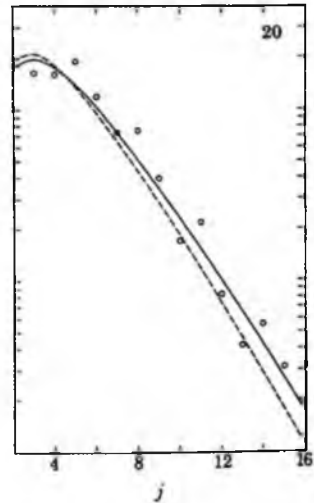


FIGURE 20. As in figure 19, but with $n = 8$. The plotted points are from Kimura (1980), figure 10c.

(2) that the observations agree fairly well with either set of curves, but distinctly better with those for the truncated spectra (solid lines).

Based on figure 16, we may also give some rough analytic expressions for \bar{H} and \bar{G} . For the values of ρ_+ and ρ_- on the left axis ($\gamma = 0$) are known:

$$\rho_+ = e^{-\frac{1}{2}\xi^2}, \quad \rho_- = 1 - e^{-\frac{1}{2}\xi^2}, \quad (12.7)$$

where $\xi = \rho/\mu_0^{\frac{1}{2}}$. If we approximate the curves in figure 16 by parabolas through the point (1, 1) with horizontal axes we must have in general

$$\left. \begin{aligned} 1 - \rho_+ &= (1 - e^{-\frac{1}{2}\xi^2})(1 - \kappa^2)^{\frac{1}{2}} \\ 1 - \rho_- &= e^{-\frac{1}{2}\xi^2}(1 - \kappa^2)^{\frac{1}{2}} \end{aligned} \right\} \quad (12.8)$$

Now by (10.18) we have $(1 - \kappa^2)^{\frac{1}{2}} \doteq 2\pi\nu$ and so

$$\left. \begin{aligned} 1 - \rho_+ &= 2\pi\nu(1 - e^{-\frac{1}{2}\xi^2}) \\ 1 - \rho_- &= 2\pi\nu e^{-\frac{1}{2}\xi^2} \end{aligned} \right\} \quad (12.9)$$

Now substituting in (12.2) we get

$$\bar{H}_j = (2\pi\nu)^{-1} e^{\frac{1}{2}\xi^2} / (e^{\frac{1}{2}\xi^2} - 1), \quad (12.10)$$

and similarly from (12.5)

$$\bar{G}_j = (2\pi\nu)^{-1} e^{\xi^2} / (e^{\xi^2} - 1). \quad (12.11)$$

These equations indicate that \bar{H} and \bar{G} are both inversely proportional to ν , as was also found in §§4 and 5. In fact if ν^2 is negligible, (4.5) and (5.5) can be written

$$\bar{G} = (2\pi)^{-\frac{1}{2}} e^{\frac{1}{2}\xi^2} / \nu\xi, \quad (12.12)$$

and
respectively.

$$\bar{H} = (2\pi)^{-\frac{1}{2}} / \nu\xi \quad (12.13)$$

TABLE 6. A COMPARISON OF THEORETICAL VALUES OF $\nu\bar{H}$ AND $\nu\bar{G}$

h^*	ξ	$\nu\bar{H}_j$ (12.10)	$\nu\bar{H}$ (12.13)	$\nu\bar{G}_j$ (12.11)	$\nu\bar{G}$ (12.12)
h_{mode}	1	0.404	0.399	0.687	0.658
h_{mean}	$(\frac{1}{2}\pi)^{\frac{1}{2}}$	0.293	0.318	0.642	0.698
h_1	2	0.184	0.199	1.360	1.474

The functional dependence on ξ in (12.10) and (12.11) is quite different from that in the two last equations. However, a numerical comparison is interesting. Table 6 shows the functions of ξ evaluated at three different levels: $h^* = h_{\text{mode}}$, h_{mean} and h_1 ($\xi = 1, \sqrt{\frac{1}{2}\pi}$ and 2). In every case the pairs of formulae, though analytically different, agree to within 10%. Hence over a certain range of ν and of ξ the two theories give quite similar results†.

† In fact, according to (9.10) we would expect the corresponding values of $\nu\bar{H}_j$ and $\nu\bar{H}$ to differ by a small amount of order 0.5ν . For further discussion see Appendix B

13. DISCUSSION AND CONCLUSIONS

We have seen how two different approaches to the analysis of wave grouping can lead to almost identical results. Of these approaches, the first or Gaussian noise theory is more closely related to the wave spectrum, and is valid asymptotically as $\nu \rightarrow 0$. The second, or Markov, theory has been related roughly to the wave spectrum over an intermediate range of ν , which includes typical spectra of sea swell, and also suitably filtered spectra of wind waves.

As against this, the Gaussian theory is applicable strictly only to linear surface waves. When the waves become steep the harmonic components in a wave record are not independent, and the surface must become non-Gaussian. Markov theory, however, can still be applied, though its physical basis is not yet secure.

Whatever the relative merits of the two approaches, it appears that neither can be applied in a sensible way except to sufficiently narrow-band processes, or to data that have been filtered so as to eliminate both high and low frequencies. The same conclusion was also reached by Nolte & Hsu (1972, 1979) though the arguments for the tapered filter suggested in their 1979 paper do not appear to be conclusive. We have recommended a surface 'square-topped' filter with limits $0.5 f_p$ and $1.5 f_p$ which has two advantages:

- (1) it leaves the peak frequency f_p unchanged;
- (2) two successive applications of the filter have the same effect as only one.

Moreover, the chosen limits have been shown to give answers in agreement with a visual assessment of the group properties of the record.

This paper has confined attention to the essentially linear properties of wave groups. Some nonlinear statistical properties of wave groups deserve further attention, and studies directed towards this aspect are under way.

APPENDIX A. THE SWELL SPECTRUM (6.3)

To evaluate the moments of the spectrum $E(\sigma)$ of (6.3) we have from Erdelyi *et al.* (1954), equations (1.4.22) and (2.4.32), that when

$$f(x) = x^{-1} e^{-(\alpha x + \beta x^{-1})}, \quad (\text{A } 1)$$

then

$$\left. \begin{aligned} \int_0^{\infty} f(x) \cos xy \, dx &= \frac{\pi^{\frac{1}{2}}}{(\alpha^2 + y^2)^{\frac{1}{2}}} e^{-2\beta^{\frac{1}{2}}u} (u \cos w - v \sin w), \\ \int_0^{\infty} f(x) \sin xy \, dx &= \frac{\pi^{\frac{1}{2}}}{(\alpha^2 + y^2)^{\frac{1}{2}}} e^{-2\beta^{\frac{1}{2}}u} (u \sin w + v \cos w), \end{aligned} \right\} \quad (\text{A } 2)$$

where

$$\left. \begin{aligned} u &= \left\{ \frac{1}{2} [(\alpha^2 + y^2)^{\frac{1}{2}} + \alpha] \right\}^{\frac{1}{2}}, \\ v &= \left\{ \frac{1}{2} [(\alpha^2 + y^2)^{\frac{1}{2}} - \alpha] \right\}^{\frac{1}{2}}, \end{aligned} \right\} \quad (\text{A } 3)$$

and

$$w = 2\beta^{\frac{1}{2}}v. \quad (\text{A } 4)$$

Now letting $y \rightarrow 0$ in (A 3) we have

$$\left. \begin{aligned} u &= \alpha^{\frac{1}{2}}(1 + y^2/8\alpha^2), \\ v &= y/2\alpha^{\frac{1}{2}}, \end{aligned} \right\} \quad (\text{A } 5)$$

to order y^2 and then from (A 2), on equating coefficients of 1, y and y^2 ,

$$\left. \begin{aligned} m_0^* &= (\pi^{\frac{1}{2}}/\alpha^{\frac{1}{2}}) e^{-2(\alpha\beta)^{\frac{1}{2}}}, \\ m_1^* &= (\pi^{\frac{1}{2}}/\alpha^{\frac{1}{2}}) e^{-2(\alpha\beta)^{\frac{1}{2}}} [\frac{1}{2} + (\alpha\beta)^{\frac{1}{2}}], \\ m_2^* &= (\pi^{\frac{1}{2}}/\alpha^{\frac{1}{2}}) e^{-2(\alpha\beta)^{\frac{1}{2}}} [\frac{3}{4} + \frac{3}{2}(\alpha\beta)^{\frac{1}{2}} + \alpha\beta]. \end{aligned} \right\} \quad (\text{A } 6)$$

Now writing

$$(\alpha\beta)^{\frac{1}{2}} = \frac{1}{2}n, \quad (\alpha/\beta)^{\frac{1}{2}}x = \sigma, \quad (\text{A } 7)$$

we have

$$\left. \begin{aligned} m_0 &= (\alpha/\beta)^{\frac{1}{2}} m_0^*, \\ \bar{\sigma} &= (\alpha/\beta)^{\frac{1}{2}} m_1^*/m_0^*, \\ \nu &= (\alpha/\beta)^{\frac{1}{2}} (m_2^* - m_1^{*2}/m_0^*). \end{aligned} \right\} \quad (\text{A } 8)$$

Substitution from (A 6) and (A 7) leads immediately to equations (6.4).

From (A 2) we have also, in the notation of §10

$$\begin{aligned} X^2 + Y^2 &= [\pi/(\alpha^2 + y^2)] e^{-4\beta^{\frac{1}{2}}y} (u^2 + v^2) \\ &= [\pi/(\alpha^2 + y^2)^{\frac{1}{2}}] e^{-4(\alpha\beta)^{\frac{1}{2}}[\frac{1}{4}(1 + y^2/\alpha^2)^{\frac{1}{2}} + \frac{1}{2}]} \end{aligned} \quad (\text{A } 9)$$

and

$$\mu_0^2 = (\pi/\alpha) e^{-4(\alpha\beta)^{\frac{1}{2}}}, \quad (\text{A } 10)$$

whence

$$\kappa^2 = (\alpha^2 + y^2)^{-\frac{1}{2}} e^{-4(\alpha\beta)^{\frac{1}{2}}[\frac{1}{4}(1 + y^2/\alpha^2)^{\frac{1}{2}} + \frac{1}{2}]} - 1. \quad (\text{A } 11)$$

On making the substitution (A 7) this becomes equation (11.4).

APPENDIX B. ON THE RELATION BETWEEN DISCRETE AND CONTINUOUS VALUES OF THE GROUP LENGTH

Suppose that discrete waves are identified by their crests, and that these are nearly equally spaced in regard to the time t . Take the wave period as unit of time.

In a continuous time interval of magnitude τ such that

$$i < \tau < i + 1, \quad (\text{B } 1)$$

where i is a positive integer, there must be either i or $(i + 1)$ wave crests. Assuming the crests are distributed uniformly in time, the probability of there being $(i + 1)$ crests in the interval is $(\tau - i)$, and the probability of i crests is $(i + 1 - \tau)$. Hence we have

$$p(H_j) = \int_{j-1}^j (\tau - j + 1) p(\tau) d\tau + \int_j^{j+1} (j + 1 - \tau) p(\tau) d\tau, \quad (\text{B } 2)$$

where $p(\tau)$ is the density of τ . Identifying τ with H , we see that H_j is the weighted mean of $p(H)$ by the triangular weighting function with base $(j - 1, j + 1)$ and height 1 (see figure 21).

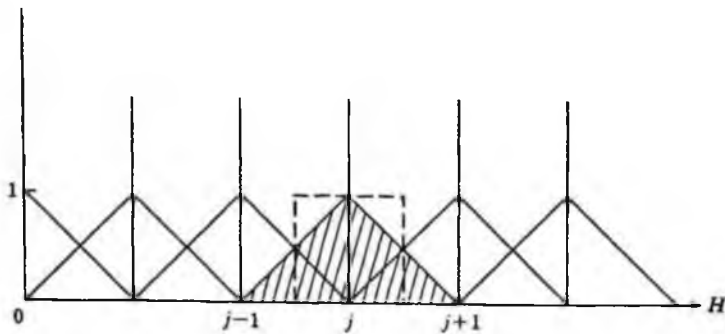


FIGURE 21. Form of the weighting function for $p(H)$ in the integral for H_j . Full-line: equation (B 2); broken line: equation (9.8).

Exceptionally when $j = 0$, only the right-hand half of the triangle is used. If $p(H_0)$ is set equal to zero, then $p(H_j)$, $j > 0$ must be renormalized.

Now the rough approximation (9.8) amounts to replacing the triangular weighting function by the square with base $(j - \frac{1}{2}, j + \frac{1}{2})$ and height 1. Again, when $j = 0$ only the right-hand half of the square is used, and setting $p(H_0) = 0$ necessitates a renormalization.

This paper was begun while the author was visiting the California Technology Jet Propulsion Laboratory, Pasadena, in July 1983. He is indebted to Dr O. H. Shemdin, Dr V. Hsaio and Mr J. A. Ewing for kindly supplying the wave data discussed in §8. Useful discussions have been held with Mr D. J. T. Carter and Mr P. G. Challenor at I.O.S., Wormley. A first version of this paper was presented at the Whitecap Workshop held at University College, Galway, in September 1983.

REFERENCES

- Abramowitz, M. & Stegun, I. A. (eds) 1965 *Handbook of mathematical functions*. New York: Dover.
- Ahram, M. & Ezratty, R. 1978 Statistical relations between successive wave heights. *Oceanologia Acta* **1**, 151-158.
- Burcharth, H. F. 1980 A comparison of nature waves and model waves, with special reference to wave grouping. *Proc. 17th Int. Conf. on Coastal Engng, Sydney*, pp. 2992-3009.
- Donelan, M., Longuet-Higgins, M. S. & Turner, J. S. 1972 Periodicity in whitecaps. *Nature, Lond.* **239**, 449-451.
- Erdelyi, A. (ed.) 1953 *Higher transcendental functions*. London: McGraw-Hill.
- Erdelyi, A. (ed.) 1954 *Tables of integral transforms*. London: McGraw-Hill.
- Erdelyi, A., Magnus, W., Oberhettinger, F. & Tricomi, F. G. 1954 *Tables of integral transforms*, vol. 1. New York: McGraw Hill. (391 pages.)
- Ewing, J. A. 1973 Mean length of runs of high waves. *J. geophys. Res.* **78**, 1933-1936.
- Favreau, R. R., Low, H. & Pfeffer, I. 1956 Evaluation of complex statistical functions by an analog computer. *Inst. Rad. Eng. Nat. Convention Record*, part 4, pp. 31-37.
- Goda, Y. 1970 Numerical experiments on wave statistics with spectral simulation. *Rep. Port Harbour Res. Inst.* **9**, 3-75.
- Goda, Y. 1976 On wave groups. *Proc. Conf. on Behaviour of Offshore Structures, Trondheim, Norway*, vol. 1, pp. 1-14. Trondheim: Norwegian Inst. of Tech.
- Goda, Y. 1983 Analysis of wave grouping and spectra of long-travelled swell. *Rep. Port Harbour Res. Inst.* **22**, 3-41.
- Hsaio, V. & Shemdin, O. H. 1983 Measurement of wind velocity and pressure with a wave follower during MARSEN. *J. geophys. Res.* **88**, 9841-9849.
- Kimura, A. 1980 Statistical properties of random wave groups. *Proc. 17th Int. Conf. on Coastal Engng, Sydney*, pp. 2955-2973. New York: Am. Soc. Civ. Engngs.

- Longuet-Higgins, M. S. 1952 The statistical distribution of the heights of sea waves. *J. mar. Res.* **11**, 245-266.
- Longuet-Higgins, M. S. 1957 The statistical analysis of a random moving surface. *Phil. Trans. R. Soc. Lond. A* **249**, 321-387.
- Longuet-Higgins, M. S. 1958 On the intervals between zeros of a random function. *Proc. R. Soc. Lond. A* **246**, 99-118.
- Longuet-Higgins, M. S. 1962 The distribution of intervals between a stationary random function. *Phil. Trans. R. Soc. Lond. A* **254**, 557-599.
- Longuet-Higgins, M. S. 1983 On the joint distribution of wave periods and amplitudes in a random wave field. *Proc. R. Soc. Lond. A* **389**, 241-258.
- Middleton, D. 1960 *Statistical communication theory*. New York: McGraw-Hill.
- Nolte, K. G. & Hsu, F. H. 1972 Statistics of ocean wave groups. *Proc. 4th Offshore Tech. Conf., Dallas, Texas*. Preprint no. 1688, pp. 139-146.
- Nolte, K. G. & Hsu, F. H. 1979 Statistics of larger waves in a sea state. *Am. Soc. Civ. Engrs, J. Waterway, Port, Coastal Ocean Div.* **105**, 389-404.
- Ochi, M. K. 1982 Stochastic analysis and probabilistic prediction of random seas. *Adv. Hydrosci.* **13**, 217-375.
- Pierson, W. J. (ed.) 1962 The directional spectrum of a wind generated sea as determined from data obtained by the Stereo Wave Observation Project. *N.Y. University Coll. Engrs, Met. Pap.* **2**, no. 6.
- Rice, S. O. 1944-1945 The mathematical analysis of random noise. *Bell Syst. Tech. J.* **23**, 282-332; **24**, 46-156.
- Rice, S. O. 1958 Distribution of the duration of fades in radio transmission-gaussian noise model. *Bell Syst. Tech. J.* **37**, 581-635.
- Rye, H. 1974 Wave group formation among storm waves. *Proc. 14th Int. Conf. on Coastal Engng*, pp. 164-183. New York: Am. Soc. Civ. Engrs.
- Rye, H. & Lervik, E. 1981 Wave grouping studies by means of correlation techniques. *Norw. mar. Res.* **4**, 12-21.
- Sawnhcy, M. D. 1962 A study of ocean wave amplitudes in terms of the theory of runs and a Markov chain process.
- Siefert, W. 1974 Wave investigation in shallow water. *Proc. 14th Int. Conf. on Coastal Engng*, pp. 151-178. New York: Am. Soc. Civ. Engrs.
- Uhlenbeck, G. E. 1943 Theory of random process. M.I.T. Radiation Lab. Rep. 454, October 1943.
- Watson, G. N. 1958 *Theory of Bessel functions*. 2nd edn. Cambridge University Press. (804 pages.)
- Wilson, J. R. & Baird, W. F. 1972 A discussion of some measured wave data. *Proc. 13th Int. Conf. on Coastal Engng*, pp. 113-130. New York: Am. Soc. Civ. Engrs.

On the skewness of sea-surface elevation

By M. A. SROKOSZ AND M. S. LONGUET-HIGGINS

Institute of Oceanographic Sciences, Wormley, Godalming, Surrey, England,
and Department of Applied Mathematics and Theoretical Physics, Silver Street, Cambridge

(Received 23 April 1985 and in revised form 25 November 1985)

Surface skewness is a statistical measure of the vertical asymmetry of the air-sea interface – exemplified by the sharp crests and rounded troughs of surface gravity waves. Some authors have proposed a constant ratio between surface skewness and the ‘significant slope’ of the waves. Here it is shown theoretically that no such simple relation is to be expected.

Wave records are of at least two different types; Eulerian (as made with a fixed probe) or Lagrangian (as with a free-floating buoy). The corresponding statistical properties are examined. At first sight it might appear that the degree of skewness in corresponding records would be different. However it is shown that to lowest order the skewness is invariant; only the apparent mean level is different, at second order.

1. Introduction

With the advent of radar altimetry from orbiting satellites, and its application to the measurement of ocean waves, currents and surface winds, certain questions concerning the statistical properties of surface waves have come increasingly to the fore. Among these is the magnitude of the surface ‘skewness’, defined as follows. If we suppose the vertical displacement ζ of the ocean surface to be recorded as a function of the time t at some fixed location, then, in a given sea state, the elevation ζ will have a probability density $p(\zeta)$, say. For waves of small slopes, $p(\zeta)$ is known to be nearly Gaussian (see for example Longuet-Higgins 1957). However, in steep waves, including sometimes very short gravity or capillary waves, $p(\zeta)$ becomes asymmetric about its mean level $\zeta = 0$ and may have an appreciable skewness λ_3 , as defined in terms of the second and third cumulants of $p(\zeta)$. One familiar manifestation of surface skewness is the up-down asymmetry of a steep gravity wave, in which the crests are more peaked, the troughs flatter or more rounded.†

The value of λ_3 can be related to the nonlinear dynamics of free surface waves. Phillips (1961) first showed theoretically that λ_3 was of the same order of magnitude as the r.m.s. surface slope. Longuet-Higgins (1963) gave a detailed theory, deriving the skewness and kurtosis of $p(\zeta)$ in terms of the underlying frequency spectrum of ζ . However, in some more recent papers (Walsh 1979; Huang & Long 1980; Huang *et al.* 1981) there have been suggestions, made on empirical grounds, that there exists a simple linear relationship between λ_3 and a quantity s , the ‘significant slope’, defined in terms of the frequency spectrum of ζ . Thus Huang & Long (1980) proposed that

$$\lambda_3 = 8\pi s. \quad (1.1)$$

† This type of asymmetry is to be distinguished from the horizontal asymmetry in some wind waves, which is related to the distribution of the surface slopes (see Longuet-Higgins 1982).

Such a relation would indeed be convenient. However, one of the conclusions of the present paper is that no such simple relation exists.

In the first part of the paper, which is theoretical, we introduce a simple model of the wavefield, appropriate to long-crested waves with a narrow frequency spectrum. In this case it is easy to derive a simple relation between the skewness and the significant slope. The result (2.16) is shown in §3 to be consistent with the more general theory of Longuet-Higgins (1963) after correction of an elusive factor. The more general theory is then used to investigate the effects of finite spectral bandwidth and varying shape of the frequency spectrum, on the ratio between λ_3 and s . The relation is found not to be unique. In §4 we review recent observations of λ_3 in the light of our theoretical results.

In situ measurements of waves are often made with different types of instrument, giving rise to wave records of either Eulerian or Lagrangian type. The latter, for example, would include measurements with a free-floating buoy. Are there any differences in the skewness as evidenced by different types of measurement? This question is investigated in §§5 and 6. In §5 we obtain a general relation, correct to second order, between the two types of measurement ((5.9)) and apply it to the narrow-band spectral model. In §6 we consider a more general case. The conclusions are summarized in §7.

2. Model for a narrow spectrum

Suppose first that the waves are long-crested and have a narrow frequency spectrum, in the sense of Longuet-Higgins (1957). Choosing the horizontal x -axis in the direction of propagation we may write

$$\zeta(x, t) = a \cos \theta + \frac{1}{2} a^2 k \cos 2\theta + O(a^3 k^2), \quad (2.1)$$

where a represents the local wave amplitude, k is a fixed wavenumber and θ is the phase function

$$\theta = kx - \sigma t + \epsilon. \quad (2.2)$$

Here σ is the (fixed) radian frequency and a and ϵ vary slowly with x and t . The first term on the right of (2.1) represents a linear, sinusoidal wave, of slowly varying amplitude and phase. The second term represents the nonlinear correction appropriate to a deep-water gravity wave of uniform amplitude (see for example Lamb 1932, p. 417).

By linear theory, and for a narrow spectrum, the distribution of wave heights $2a$ is Rayleigh:

$$p(a) = \frac{2a}{\bar{a}^2} e^{-a^2/\bar{a}^2}, \quad (2.3)$$

where \bar{a} is the r.m.s. value of a . We note that, even after the addition of the second, nonlinear term on the right of (2.1), the crest-to-trough wave height is still equal to $2a$, if we neglect quantities of order $a^3 k^2$. We shall assume that a is distributed according to (2.3) in the nonlinear case also, and that the phase θ is distributed uniformly in $(0, 2\pi)$, as in narrowband linear theory (see Longuet-Higgins 1963). Thus the joint density of a and θ is

$$p(a, \theta) = \frac{a}{\pi \bar{a}^2} e^{-a^2/\bar{a}^2}. \quad (2.4)$$

From (2.1) and (2.4) we may at once calculate the surface skewness. The r th moments μ_r being defined by

$$\mu_r = \int_0^\infty \int_0^{2\pi} \zeta^r p(a, \theta) da d\theta, \quad (2.5)$$

we easily find $\mu_1 = 0$ and

$$\mu_2 = \frac{1}{2}\bar{a}^2, \quad \mu_3 = \frac{3}{4}\bar{a}^4 k, \quad \mu_4 = \frac{3}{4}\bar{a}^4 k^2. \quad (2.6)$$

Hence the cumulants κ_r are given by $\kappa_1 = 0$ and

$$\kappa_2 = \frac{1}{2}\bar{a}^2, \quad \kappa_3 = \frac{3}{4}\bar{a}^4 k, \quad \kappa_4 = 0, \quad (2.7)$$

to the present approximation. The coefficient of skewness is then

$$\lambda_3 \equiv \frac{\kappa_3}{\kappa_2^{3/2}} = \frac{3}{\sqrt{2}}\bar{a}k \quad (2.8)$$

and the coefficient of kurtosis is

$$\lambda_4 \equiv \frac{\kappa_4}{\kappa_2^2} = 0, \quad (2.9)$$

to this order.

These results should agree with the expressions for the cumulants given by Longuet-Higgins (1963) for a general long-crested frequency spectrum $F(\sigma)$. These are (after correction† of a factor $\frac{1}{2}$ in his equation (3.7))

$$\kappa_1 = 0, \quad (2.10)$$

$$\kappa_2 = \int_0^\infty F(\sigma) d\sigma, \quad (2.11)$$

$$\kappa_3 = 3 \int_0^\infty \int_0^\infty \min(k, k') F(\sigma) F(\sigma') d\sigma d\sigma'. \quad (2.12)$$

κ_4 was of higher order, as noted. If in (2.11) and (2.12) we introduce the narrow spectrum

$$F(\sigma) = \frac{1}{2}\bar{a}^2 \delta(\sigma - \sigma_0), \quad (2.13)$$

where δ denotes the Dirac delta function, we retrieve precisely (2.8).

Consider now the relation of the skewness to the 'significant slope' s . This was defined by Huang & Long (1980) as

$$s = \bar{\zeta}/L_p \quad (2.14)$$

where a bar denotes the r.m.s. value and L_p is the wavelength corresponding to the peak in the spectrum. So in our model

$$s = \frac{\kappa_2^{1/2} k}{2\pi} = \frac{\bar{a}k}{2^{1/2}\pi} \quad (2.15)$$

and from (2.8) we have the relation

$$\lambda_3 = 6\pi s. \quad (2.16)$$

† See Bitner (1976) and Bitner-Gregersen (1980). There should be a factor $\frac{1}{2}$ multiplying the right-hand sides of equations (3.7), (3.9), (3.12) and (3.17). Hence the numerical factors in (3.14), (3.15) and (3.16) should be 3, 6 and 6 respectively. The ratio λ_3/L in (3.24), (3.25) and table 1 is unaffected.

Lastly, in this section, we note that by (2.1) the r.m.s. surface slope $\bar{\zeta}_x$ is given by

$$\bar{\zeta}_x^2 = \frac{1}{2}(\bar{\alpha}k)^2, \quad (2.17)$$

so that from (2.7)

$$\lambda_3 = 3\bar{\zeta}_x. \quad (2.18)$$

This can also be written

$$\langle \zeta^3 \rangle = 3\langle \zeta_x^2 \rangle^{\frac{1}{2}} \langle \zeta^2 \rangle^{\frac{1}{2}}. \quad (2.19)$$

This is the correct form† of a relation first given by Phillips (1961, p. 154) in which the factor on the right was given as $\frac{3}{8}$.

3. Effects of finite bandwidth

We now generalize some of the results of §2 to seas that are still long-crested, that is to say unidirectional, but have a non-zero bandwidth. For such waves, (2.10)–(2.12) will apply, and from the definitions of λ_3 and s given above we have

$$\lambda_3 = 12\pi s \frac{I_2}{I_1^2}, \quad (3.1)$$

where

$$I_1 = \sigma_p \int_0^\infty F(\sigma) d\sigma \quad (3.2)$$

and

$$I_2 = \int_0^\infty \left\{ \int_0^\sigma \sigma^2 F(\sigma) d\sigma \right\} F(\sigma') d\sigma'. \quad (3.3)$$

In (3.3) we used the dispersion relation $\sigma^2 = gk$, and in (3.2) the relation $\sigma_p^2 = 2\pi g/L_p$ for the radian frequency σ_p at the spectral peak.

We shall now evaluate the factor I_2/I_1^2 on the right of (3.1) for some typical wave spectra.

Consider first spectra of the special form

$$F(\sigma) = \begin{cases} \alpha\sigma^{-n}, & \sigma > \sigma_p \\ 0, & \sigma < \sigma_p \end{cases}, \quad (3.4)$$

n being a constant greater than 3. (The case $n = 5$ corresponds to the Phillips spectrum, Mark I). Substituting into (3.1) we find

$$\lambda_3 = \frac{6(n-1)}{n-2} \pi s. \quad (3.5)$$

This is the correct version of equation (5.9) of Huang *et al.* (1983) and the result, for $n = 5$, given previously by Jackson (1979). When $n \rightarrow \infty$, (3.5) reduces to (2.16), as would be expected. When $n = 5$ (and only in this case) (3.5) agrees with the empirical relation (1.1) given by Huang & Long (1980).

To assess roughly the dependence of λ_3/s upon the spectral width we may introduce the spectral-width parameter ν defined by

$$\nu^2 = \frac{m_0 m_2}{m_1^2} - 1 \quad (3.6)$$

(cf. Longuet-Higgins 1980), where m_r denotes the r th spectral moment

$$m_r = \int_0^\infty \sigma^r F(\sigma) d\sigma. \quad (3.7)$$

† We are indebted to Professor Phillips for verifying this statement.

n	ν	$\lambda_3/\pi s$
4	0.5774	9
5	0.3536	8
6	0.2582	7.5
10	0.1260	6.75
100	0.0102	6.06
∞	0	6

TABLE 1. Dimensionless parameters ν and $\lambda_3/\pi s$ for the ideal spectrum (3.4)

(Note that $m_0 = \mu_2$). From (3.4), (3.6) and (3.7) we find

$$\nu^2 = \frac{1}{(n-1)(n-3)}. \quad (3.8)$$

Table 1 gives the results for some integer values of n . It suggests that, as the spectral width decreases, so also does the ratio λ_3/s .

Next consider a generalized form of the Pierson-Moskowitz (P-M) spectrum used successfully by Liu (1983, 1985):

$$F(\sigma) = \alpha \sigma^{-n} e^{-(\beta/\sigma)^m}, \quad (3.9)$$

which has a peak at $\sigma = \sigma_p = \beta(m/n)^{1/m}$. When $m = 4$ and $n = 5$ (3.9) gives the well-known P-M spectrum, while for $m = 4$ and n arbitrary we obtain the Wallops spectrum (Huang *et al.* 1981). Lastly when $n = 5$ and m is arbitrary we obtain the spectrum used by Longuet-Higgins (1980).

From (3.7) we find, when $r < (n-1)$,

$$m_r = \frac{\alpha}{m\beta^{n-r-1}} \Gamma\left(\frac{n-r-1}{m}\right) \quad (3.10)$$

and so from (3.8)
$$\nu^2 = \Gamma\left(\frac{n-3}{m}\right) \Gamma\left(\frac{n-1}{m}\right) / \Gamma\left(\frac{n-2}{m}\right)^2 - 1. \quad (3.11)$$

Furthermore from (3.1) we find (see Appendix) that

$$\lambda_3 = 3\pi s \left(\frac{\pi}{2}\right)^{\frac{1}{2}} \left(\frac{n}{m}\right)^{2/m} {}_2F_1\left(1, \frac{2(n-2)}{m}; \frac{n-1}{m} + 1; \frac{1}{2}\right) / \Gamma\left(\frac{n-1}{m}\right)^2 \quad (3.12)$$

where ${}_2F_1$ is a generalized hypergeometric function, from which numerical values may readily be computed.

Results for various values of n and m are given in table 2. It can be clearly seen that the ratio of skewness to significant slope varies widely, is crucially dependent on the form of the wave spectrum and is not simply a function of the bandwidth parameter ν .

We note that (3.1) and (3.3) apply only to long-crested waves. However, for a more general three-dimensional spectrum it has been shown that the coefficient of skewness λ_3 satisfies

$$0.44L_3 \leq \lambda_3 \leq 1.01L_3, \quad (3.13)$$

where L_3 denotes the corresponding skewness for a long-crested sea (Longuet-Higgins 1963, pp. 469-470). The proof of this result is unaffected by the presence of a factor $\frac{1}{2}$ in equation (3.7)*.†

† We use a star * to denote equation numbers in Longuet-Higgins (1963).

$\frac{m}{n}$	ν				$\lambda_3/\pi s$			
	4	5	6	7	4	5	6	7
4	0.64	0.62	0.61	0.60	3.66	2.16	1.41	0.98
4	0.42	0.41	0.39	0.39	6.96	4.33	2.88	2.03
6	0.33	0.31	0.30	0.29	10.26	6.95	4.81	3.46
7	0.28	0.26	0.25	0.24	12.66	9.51	6.97	5.17

TABLE 2. Values of ν and $\lambda_3/\pi s$ for the generalized P-M spectrum (3.9)

4. Discussion

Consider first the observations reported by Huang & Long (1980). In their figure 6 (where λ_3 is plotted against s) the data fall mainly into two groups: the field observations, for which $0 < s < 0.02$, and the laboratory data, for which $0.02 < s < 0.04$. The former show considerably more scatter. Thus their empirical result (1.1) is probably weighted in favour of the laboratory measurements. The field data alone would not suggest such a definite relationship.

We note that a similar scatter in field data is reported by McClain, Chen & Hart (1982, figure 3). This certainly supports our conclusion that the relation (1.1) is not unique.

There may also be systematic differences between field and laboratory data arising from different ranges of the parameter u^*/c (where u^* is the wind friction velocity and c the phase speed of the dominant waves). For waves in the open ocean u^*/c is typically of order 0.1, compared with values of order 1 for wind waves in the laboratory (Phillips 1977, p. 129). The laboratory data of Huang & Long (1980) include results with $u^*/c > 0.6$; below this value their measurements of skewness are considerably more scattered.

A non-Gaussian model of the sea surface somewhat similar to that in §2 above was proposed by Huang *et al.* (1983), except that they include a term $\frac{1}{2}a^2k$ in (2.1), as well as higher-order terms. Such a term, however, does not arise dynamically in deep water; it would correspond to a local change in the mean surface level, i.e. a 'wave set-up'. Although such terms are significant in shallow water (Longuet-Higgins & Stewart 1962, 1964), nevertheless in deep water they become negligible when $\Delta k \ll k$, where Δk is the spectral bandwidth, that is when the spectrum is narrow and there are many waves in a group – the situation considered in §2.

5. Lagrangian measurements: narrow spectrum

In determining the skewness of the surface elevation from instrumental records, some attention must be paid to the method of measurement, since different methods may give apparently different answers.

The definition of surface skewness given in §2 applies directly to measurements made with a fixed probe or wave staff. However an alternative method of observation is often used, in which the vertical displacement is derived by twice integrating the vertical acceleration in a free, or almost free, floating buoy. To first order in ak the two wave records are equivalent, but to second order, which is required for an assessment of the skewness, the records are different, as we shall show.

Note first that an irrotational deep-water Stokes wave can be considered as the

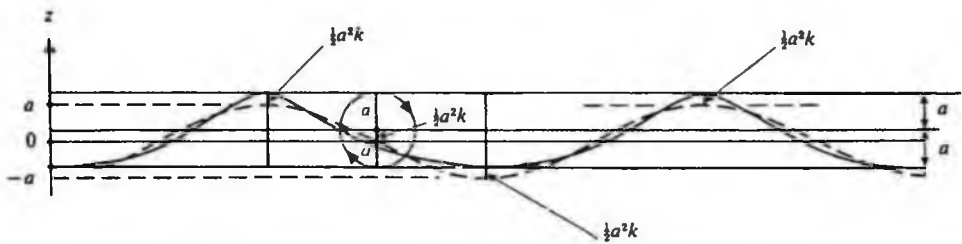


FIGURE 1. Sketch of orbital motion in a steep, irrotational wave, when the frame of reference moves with the Stokes drift velocity for surface particles. The broken curve corresponds to linear theory.

sum of a rotational Gerstner wave (Lamb 1932, section 251) in which the particles describe perfectly circular orbits, plus a steady, second-order Stokes drift. The superposition of the two motions is accurate to third order in the wave steepness (see Dubreil-Jacotin 1934). Hence in a Stokes wave each particle at the surface describes a circular path, if seen in a frame of reference moving with the steady drift; see figure 1. Moreover, its orbital velocity in this circular path is constant (see Lamb 1932). So apparently there is no asymmetry in its vertical displacement, to third order, and one might expect the corresponding skewness in the wave record to be small.

To analyse the situation further, let z be the vertical coordinate and u, w the horizontal and vertical components of the velocity. We shall suppose that

$$\zeta = \gamma \zeta^{(1)} + \gamma^2 \zeta^{(2)} + \dots, \quad (5.1)$$

where γ is a small parameter proportional to the maximum surface slope, and we shall use suffices L and E to denote quantities following a particle or with fixed spatial coordinates, respectively. Then the horizontal displacement of a particle is given by

$$\Delta x = \int u_L dt = \int u_E(x + \Delta x) dt \quad (5.2)$$

and on expanding in a Taylor series about x , we find

$$\Delta x = \int u_E(x) dt + \Delta x \cdot \int \nabla u_E(x) dt + \dots \quad (5.3)$$

Thus to first order in γ we have simply

$$\Delta x = \int u dt. \quad (5.4)$$

In a similar way the kinematic surface condition leads to

$$\frac{\partial \zeta}{\partial t} = w \quad (5.5)$$

correct to first order, and

$$\zeta_L = \zeta_E(x + \Delta x) = \zeta_E + \Delta x \frac{\partial \zeta}{\partial x} \quad (5.6)$$

correct to order γ^2 . But, to first order,

$$\frac{\partial \zeta}{\partial x} = \frac{\partial}{\partial x} \int \frac{\partial \zeta}{\partial t} dt = \frac{\partial}{\partial x} \int w dt = \int \frac{\partial w}{\partial x} dt. \quad (5.7)$$

Since the motion is irrotational to first order at least, $\partial w/\partial x$ may be replaced by $\partial u/\partial z$. Hence

$$\frac{\partial \zeta}{\partial x} = \int \frac{\partial u}{\partial z} dt = \frac{\partial}{\partial z} \int u dt = \frac{\partial}{\partial z} \Delta x. \quad (5.8)$$

Combining this result with (5.5) we find, correct to second order, that

$$\zeta_L = \zeta_E + \frac{\partial}{\partial z} \frac{1}{2} (\Delta x)^2, \quad (5.9)$$

where Δx is given by (5.4). This relates the vertical displacement ζ_L as measured by a free-floating buoy to that measured by a fixed probe.

The relation (5.9) can be applied in the first place to the narrowband model of §2. For, associated with the first-order terms $a \cos \theta$ there is a horizontal velocity

$$u = a\sigma e^{kz} \cos \theta. \quad (5.10)$$

So on evaluating the second term in (5.9) at $z = 0$ we obtain

$$\zeta_L = \zeta_E + a^2 k \sin^2 \theta + O(a^3 k^2). \quad (5.11)$$

From (2.1) this is

$$\zeta_L = a \cos \theta + \frac{1}{2} a^2 k, \quad (5.12)$$

correct to second order. In other words the motion is purely sinusoidal, apart from a term which varies only on the longer timescale of the wave groups. The latter represents a displaced mean level, midway between the level of crest and trough. The Eulerian mean level being taken as zero, it follows that this local mean level must be equal to the amplitude of the second harmonic in ζ_E , that is $\frac{1}{2} a^2 k$; see figure 1.

Physically, the reason for this displaced mean is that a particle in the free surface lingers for longer near the wave crests, where it is moving forwards with the wave, than it does in the wave troughs, where its motion is opposite to the phase speed. Hence, Lagrangian averages will tend to overweight crest values and underweight trough values, relative to Eulerian averages. A first consequence is that the Lagrangian mean surface level is higher than the Eulerian.†

To calculate the moments μ_r of ζ_L from (5.12) we have, to lowest order,

$$\mu_1 = \frac{1}{2} \bar{a}^2 k, \quad \mu_2 = \frac{1}{2} \bar{a}^2, \quad \mu_3 = \frac{3}{2} \bar{a}^4 k. \quad (5.13)$$

Hence the cumulants are given by

$$\kappa_1 = \frac{1}{2} \bar{a}^2 k, \quad \kappa_2 = \frac{1}{2} \bar{a}^2, \quad \kappa_3 = \frac{3}{4} \bar{a}^4 k. \quad (5.14)$$

Remarkably, although the first cumulant κ_1 is now positive, the second and third cumulants are the same as for ζ_E (see (2.7)). Hence the coefficient of skewness $\lambda_3 = \kappa_3/\kappa_2^3$ is the same!

A qualitative explanation is as follows. In a wavetrain of *uniform* height the vertical displacement is indeed symmetric about its mean value; but that mean value is displaced from zero by a second-order amount depending on the wave steepness. Now even in a narrowband spectrum, the waves are not of uniform height. So the 'tails' of the distribution, which are due mainly to the larger waves, are shifted *more* in a positive sense, relative to the average, than is the region in the centre, which

† For uniform waves, this effect was noticed independently by I. D. James (personal communication).

depends partly on the lower waves. But the third moment of the distribution is influenced by the 'tails' more than is the mean value. The net effect is to produce a positive coefficient of skewness.

6. Lagrangian measurements in random wavefields

Equation (5.9) can easily be generalized to three dimensions to give

$$\zeta_L = \zeta_E + \frac{\partial}{\partial z} \frac{1}{2} \left\{ \left(\int u dt \right)^2 + \left(\int v dt \right)^2 \right\}, \quad (6.1)$$

where v is the y -component of the particle velocity, and this may be used to evaluate the skewness in a random wavefield.

Adopting the approach of Longuet-Higgins (1963), in which the first-order motion is represented by

$$\zeta = \sum_{i=1}^N a_i \cos \theta_i, \quad \theta_i = \mathbf{k}_i \cdot \mathbf{x} - \sigma_i t + \epsilon_i, \quad (6.2)$$

the phases ϵ_i being random, we find

$$\frac{\partial}{\partial z} \frac{1}{2} \left\{ \left(\int u dt \right)^2 + \left(\int v dt \right)^2 \right\} = \frac{1}{2} \sum_{i,j} a_i a_j \frac{\mathbf{k}_i \cdot \mathbf{k}_j}{k_i k_j} (k_i + k_j) \sin \theta_i \sin \theta_j, \quad (6.3)$$

where $k_i = |\mathbf{k}_i|$. To obtain ζ_L we have only to add the above terms to the right-hand side of the (corrected) equation (3.7)* for $\zeta_E^{(2)}$. Following through the argument of that section we find that, to a second approximation,

$$\zeta_L = \sum_i \alpha_i \xi_i + \sum_{i,j} \alpha_{ij} \xi_i \xi_j, \quad (6.4)$$

where

$$\alpha_i = \begin{cases} 1 & (i = 1, 2, \dots, N) \\ 0 & (i = (N+1), \dots, 2N), \end{cases} \quad (6.5)$$

as before, but now

$$\alpha_{ij} = \begin{cases} \frac{1}{2}(k_i k_j)^{\frac{1}{2}} \{B_{i,j}^- + B_{i,j}^+ - \mathbf{k}_i \cdot \mathbf{k}_j + (k_i + k_j)(k_i k_j)^{-\frac{1}{2}}\}, & \text{when } i, j = 1, 2, \dots, N, \\ \frac{1}{2}(k_i k_j)^{-\frac{1}{2}} \{B_{i,j}^- - B_{i,j}^+ - \mathbf{k}_i \cdot \mathbf{k}_j + (k_i + k_j)(k_i k_j)^{-\frac{1}{2}} k_i k_j\} & \text{when } i, j = (N+1), \dots, 2N, \\ 0 & \text{otherwise.} \end{cases} \quad (6.6)$$

In (6.4) the ξ_i denote independent random variables, $a_i \cos \theta_i$ or $-a_i \sin \theta_i$. The constants $B_{i,j}^+$ and $B_{i,j}^-$ are functions of \mathbf{k}_i and \mathbf{k}_j given by equations (3.8)*. When $i = j$, then $B_{i,j}^+$ and $B_{i,j}^-$ both vanish and we have

$$\alpha_{ii} = \frac{1}{2} k_i \quad (i = 1, 2, \dots, 2N). \quad (6.7)$$

The expressions for the cumulants then become, in integral form,

$$\left. \begin{aligned} \kappa_1 &= \iint k E(k) dk, \\ \kappa_2 &= \iint E(k) dk, \\ \kappa_3 &= 6 \iint K(k, k') E(k) E(k') dk dk', \end{aligned} \right\} \quad (6.8)$$

where $E(k)$ denotes the two-dimensional spectral density and $K(k, k')$ is the same function as given in (3.12)*.

In the one-dimensional case these equations reduce to

$$\left. \begin{aligned} \kappa_1 &= \int_0^\infty k F(\sigma) d\sigma \quad (k = \sigma^2/g), \\ \kappa_2 &= \int_0^\infty F(\sigma) d\sigma, \\ \kappa_3 &= 3 \int_0^\infty \int_0^\infty \min(k, k') F(\sigma) F(\sigma') d\sigma d\sigma'. \end{aligned} \right\} \quad (6.9)$$

The only difference between these expressions and those for the Eulerian cumulants, (2.9)–(2.11), lies in the value of κ_1 . Whereas for the Eulerian cumulants $\kappa_1 = 0$ (which is a consequence of the choice of origin for z), in the Lagrangian case κ_1 is positive, on account of the second harmonic in ζ_E , which raises both crests and troughs by an equal, second-order quantity.

However, the non-zero value of κ_1 has no effect upon the values of κ_2 and κ_3 . Hence the measured skewness is unaltered, just as in the narrowband case (§5).

7. Conclusions

We have shown by a simple model that in a narrowband, unidirectional sea the skewness λ_3 and the 'significant slope' s are related by (2.16), not (1.1), and that in a broader spectrum the ratio $\lambda_3/\pi s$ may have a rather wide range of values, as shown in table 3. This conclusion is consonant with the available field data (§4) and there may be reasons why laboratory measurements are not truly representative of ocean wave conditions.

We have derived a general relation (5.9) between the surface elevation ζ_E as measured in an Eulerian sense, say by a fixed probe, and the corresponding Lagrangian elevation ζ_L as recorded by an ideal small float. This relation is generalized in (6.1). When the statistical properties of ζ_E and ζ_L are compared, it is found, contrary to expectation, that the skewness and the variance in the two records are equal, although the apparent mean level in the Lagrangian record is slightly raised. Thus the relation between λ_3 and s is the same. The change in mean level, which would of course not be noticed by an accelerometer, is due to the fact that particles in the surface remain somewhat longer near the crests of the waves than in the troughs.

In practice, Lagrangian wave observations are often made by means of accelerometer buoys which have a response falling off at low frequencies. For our theoretical conclusions to apply to such measurements, it appears necessary that the frequency range should include at least the group frequencies. The possible effect of mooring forces on the buoy motions is left for a separate study.

Appendix. Derivation of equation (3.12)

On substituting $(\beta/\sigma)^m = \xi$, $(\beta/\sigma')^m = \eta$ in (2.12) and (3.9) we have

$$\kappa_3 = \frac{6\alpha^2}{m^2 g \beta^{2(n-2)}} \int_0^\infty \left\{ \int_\eta^\infty \xi^{(n-3)/m-1} e^{-\xi} d\xi \right\} \eta^{(n-1)/m-1} e^{-\eta} d\eta. \quad (A 1)$$

This may be written

$$\kappa_3 = \frac{6\alpha^2}{m^2 g \beta^{2(n-2)}} \int_0^\infty \Gamma\left(\frac{n-3}{m}, \eta\right) \eta^{(n-1)/m-1} e^{-\eta} d\eta, \quad (\text{A } 2)$$

where $\Gamma(z, \eta)$ is the incomplete gamma function:

$$\Gamma(z, \eta) = \int_\eta^\infty e^{-t} t^{z-1} dt. \quad (\text{A } 3)$$

Equation (A 2) may be further simplified by using a result from Erdélyi *et al.* (1953, vol. II, p. 138), to obtain

$$\kappa_3 = \frac{6\alpha^2}{m^2 g \beta^{2(n-2)}} 2^{-\frac{1}{2}} \Gamma\left(\frac{3}{2}\right) {}_2F_1\left(1, \frac{2(n-2)}{m}; \frac{n-1}{m} + 1, \frac{1}{2}\right), \quad (\text{A } 4)$$

where ${}_2F_1$ is a generalized hypergeometric function. On using the definitions of λ_3 in (2.8), κ_3 in (2.11) and s in (2.14), together with $\sigma_p = \beta(m/n)^{1/m}$ and $\kappa_2 = \mu_2 = 0$, given by (3.10), we obtain equation (3.12).

In the special case $m = n - 1$ (which for $n = 5$ gives the P-M spectrum) it is possible to reduce (3.12) by use of the relations

$${}_2F_1(p, 1-q; p+1; \eta) = p\eta^{-p} B_\eta(p, q), \quad (\text{A } 5)$$

where

$$B_\eta(p, q) = \int_0^\eta t^{p-1} (1-t)^{q-1} dt \quad (\text{A } 6)$$

(Erdélyi *et al.* 1953, vol. I, p. 87). This leads to

$$\lambda_3 = 6\pi s \frac{n-1}{n-3} \left(\frac{n}{n-1}\right)^{2/(n-1)} \left(\frac{\pi}{2}\right)^{\frac{1}{2}} (2^{(n-3)/(n-1)} - 1). \quad (\text{A } 7)$$

However, as $n \rightarrow \infty$ (A 7) does not reduce to (3.12) owing to non-uniform convergence in the narrowband case. In the special case considered here, we have also from (3.11) that

$$\nu^2 = \Gamma\left(\frac{n-3}{n-1}\right) / \Gamma\left(\frac{n-2}{n-1}\right) - 1. \quad (\text{A } 8)$$

Some numerical values derived from (A 7) and (A 8) are shown in table 3. In this case the ratio $\lambda_3/\pi s$ does not differ greatly from 7. But in the more general case (table 2) the variation is considerably greater.

We thank David Carter for suggesting the topic of this paper, and Peter Challenor, David Evans, Trevor Guymer and David Webb for useful discussions. Financial

n	ν	$\lambda_3/\pi s$
4	0.679	7.103
5	0.425	6.965
6	0.314	6.952
10	0.157	7.072
100	0.013	7.463
∞	0	7.520

TABLE 3. Parameters ν and $\lambda_3/\pi s$ for the spectrum (3.9), when $m = n - 1$

support came from the Department of Trade and Industry through the Marine Technology Committee, as part of their Support for Innovation scheme. We are indebted to Witold Cieslikiewicz, of the Institute of Hydroengineering at Gdansk, for constructive criticism of an earlier draft.

REFERENCES

- BITNER, E. 1976 Nieliniowe osabliwosci probabilistycznego modelu far lowania wiatrowego na ograniczonej glebokosci. Doctoral thesis, Inst. of Hydroeng., Gdansk, Poland.
- BITNER-GREGERSEN, E. M. 1980 Non-linear shallow-water wind waves and their statistics. *Rozpr. Hydrotech.* **42**, 3-12.
- DUBREIL-JACOTIN, M.-L. 1934 Sur la détermination rigoureuse des ondes permanentes périodiques d'ampleur finie. *J. Math. Pures et Appl.* (9) **13**, 217-291.
- ERDÉLYI, A., MAGNUS, W., OBERHETTINGER, F. & TRICOMI, F. 1953 *Higher Transcendental Functions*, vols. 1 and 2. McGraw-Hill.
- HUANG, N. E. & LONG, S. R. 1980 An experimental study of the surface elevation probability distribution and statistics of wind-generated waves. *J. Fluid Mech.* **101**, 179-200.
- HUANG, N. E., LONG, S. R., TUNG, C.-C., YUEN, Y. & BLIVEN, L. F. 1981 A unified two-parameter wave spectral model for a general sea state. *J. Fluid Mech.* **112**, 203-224.
- HUANG, N. E., LONG, S. R., TUNG, C.-C., YUEN, Y. & BLIVEN, L. F. 1983 A non-gaussian statistical model for surface elevation of nonlinear wave fields. *J. Geophys. Res.* **88**, 7597-7606.
- JACKSON, F. C. 1979 The reflection of impulses from a nonlinear random sea. *J. Geophys. Res.* **84**, 4929-4943.
- LAMB, H. 1932 *Hydrodynamics*, 6th edn. Cambridge University Press, 738 pp.
- LIPA, B. J. & BARRICK, D. E. 1981 Ocean surface height-slope probability density function from SEASAT altimeter echo. *J. Geophys. Res.* **86**, 10, 921-10,930.
- LIU, P. C. 1983 A representation for the frequency spectrum of wind-generated waves. *Ocean Engng* **10**, 429-441.
- LIU, P. C. 1985 Representing frequency spectra for shallow water waves. *Ocean Engng* **12**, 151-160.
- LONGUET-HIGGINS, M. S. 1957 The statistical analysis of a random moving surface. *Phil. Trans. R. Soc. Lond.* **A 249**, 321-387.
- LONGUET-HIGGINS, M. S. 1963 The effect of nonlinearities on statistical distributions in the theory of sea waves. *J. Fluid Mech.* **17**, 459-480.
- LONGUET-HIGGINS, M. S. 1980 On the distribution of the heights of sea waves: some effects of nonlinearity and finite band width. *J. Geophys. Res.* **85**, 1519-1523.
- LONGUET-HIGGINS, M. S. 1982 On the skewness of sea surface slopes. *J. Phys. Oceanogr.* **12**, 1283-1291.
- LONGUET-HIGGINS, M. S. & STEWART, R. W. 1962 Radiation stress and mass transport in gravity waves, with applications to 'surf beats'. *J. Fluid Mech.* **13**, 481-504.
- LONGUET-HIGGINS, M. S. & STEWART, R. W. 1964 Radiation stress in water waves; a physical discussion with applications. *Deep-Sea Res.* **11**, 529-562.
- MCCLAINE, R. C., CHEN, D. T. & HART, W. D. 1982 On the use of laser profilometry for ocean wave studies. *J. Geophys. Res.* **87**, 9509-9515.
- PHILLIPS, O. M. 1961 On the dynamics of unsteady gravity waves of finite amplitude. Part 2. *J. Fluid Mech.* **11**, 143-155.
- PHILLIPS, O. M. 1977 *The Dynamics of the Upper Ocean*, 2nd edn. Cambridge University Press.
- WALSH, E. J. 1979 Extraction of ocean wave height and dominant wavelength from GEOS-3 altimeter data. *J. Geophys. Res.* **84**, 4003-4009.

An Effect of Sidewalls on Waves in a Wind Wave Channel

MICHAEL LONGUET-HIGGINS

Center for Studies of Nonlinear Dynamics, La Jolla Institute, La Jolla, California
 Department of Applied Mathematics and Theoretical Physics, Cambridge, England

Many experiments on the generation of surface waves by wind have been carried out in laboratory wind wave channels with vertical sidewalls. In this note it is shown that surprisingly, the waves near the wall may be considerably steeper than those along the center line of the tank, by a factor of about $2^{1/2}$.

Many valuable experiments on the generation of surface waves by wind have been carried out in laboratory wind wave channels. Such channels usually have vertical sidewalls, and the effect of such walls on the damping of the waves by viscosity or surface tension effects has sometimes been considered. However, a possibly much stronger effect has apparently been overlooked. This applies particularly to three-dimensional, random waves. In the following note it is shown that surprisingly, the waves near the wall may be considerably steeper than those along the center line of the tank, by a factor of about $2^{1/2}$.

According to linear theory, the surface elevation η in an unbounded wave field may be represented approximately by

$$\eta = \sum_{n=1}^N a_n \cos(\phi_n + \epsilon_n) \quad (1)$$

where $\phi_n = \mathbf{k}_n \cdot \mathbf{x} - \sigma_n t$, and as $N \rightarrow \infty$ the wave numbers \mathbf{k}_n are assumed to become distributed densely over the wave number plane. The phases ϵ_n are distributed uniformly over the interval $(0, 2\pi)$. The mean square amplitude $\bar{\eta}^2$ is then given simply by

$$\bar{\eta}^2 = \sum a_n^2 = A \quad (2)$$

The above representation might well apply in a wind wave channel at points far from the walls compared with the correlation distance L across the channel (the y direction).

Near to a wall, however, we can no longer assume that the phases ϵ_n are uncorrelated. For according to inviscid theory the boundary condition at the wall is that the normal component of velocity must vanish; hence

$$\frac{\partial \eta}{\partial y} = 0 \quad (3)$$

for all values of x and t . Hence each complex wave amplitude $a_n e^{i\phi_n}$ must be paired with an opposite or reflected amplitude $a_m e^{i\phi_m}$ having the same phase ϵ_n at the wall. The absolute amplitudes a_n are the same as in (1). To find the mean square surface elevation, we have now to consider the mean square amplitude of half the number of independent vectors:

Copyright © 1990 by the American Geophysical Union.

Paper number 89JC03532.
 0148-0227/90/89JC-01532\$02.00

$$b_n e^{i\phi_n} = a_n e^{i\phi_n} + a_m e^{i\phi_m} = 2a_n e^{i\phi_n} \quad (4)$$

Thus if Σ^* denotes the sum over all pairs of such wave numbers,

$$\bar{\eta}^2 = \Sigma^* |b_n|^2 = \frac{1}{2} \Sigma \{2a_n\}^2 = 2A \quad (5)$$

Hence at the wall the rms wave elevation is multiplied by $2^{1/2}$.

Since the component of any wave number parallel to the wall is unaffected by reflection at the sides, the rms steepness of waves near the sidewall also is increased. This may lead to breaking of the waves near the sidewall, even though near the center of the tank the waves may not be breaking. (For use of this fact to study breaking waves in deep water, in a nonrandom case, see *Longuet-Higgins* [1974]). Loss of energy near the sidewalls will lead to a reduction in the amplitude of the reflected wave components. Hence if the cross-wind correlation distance L is much less than the width of the tank, and if the waves are regenerated in a horizontal distance which is larger than $L \tan \alpha$, where α is the mean square directional spread of the wave energy, then breaking at the wall could lead to a minimum of $\bar{\eta}^2$ on either side of the center line. In other words, the distribution of energy as a function of cross-wave distance would have the form of a "W."

Finally, we note that if L is comparable to the width of the channel the waves will (by definition) be mainly two dimensional. This certainly will be true if the dominant wavelength exceeds the critical wavelength for trapping of waves between the sidewalls. Then the most important three-dimensional effects may arise from viscosity and surface tension at the sidewalls.

Acknowledgment. This work was supported by the La Jolla Institute's Independent Research and Development Fund.

REFERENCE

Longuet-Higgins, M. S., Breaking waves—in deep or shallow water, in *Proceedings of the 10th Symposium on Naval Hydrodynamics*, pp. 597–605. Office of Naval Research, Washington, D. C., 1974.

M. Longuet-Higgins, Center for Studies of Nonlinear Dynamics, La Jolla Institute, 7855 Fay Avenue, Suite 320, La Jolla, CA 92037.

(Received August 9, 1989;
 accepted September 18, 1989.)

Introductory Notes for Part F

F. Wave Analysis and Wave Generation

Papers F1 to F7

Papers F1 to F3 concern the distribution of the energy of wind-generated waves with respect to their direction of propagation (θ). Paper F1 is preliminary; it discusses how to extract information about a function $f(\theta)$ when the observations yield only a finite number n of the Fourier coefficients of f . The most important case is when $n=2$. The second paper (F2) is an account of wave measurements made with the pitch-and-roll buoy, designed by NF Barber. The observations and analysis yielded important results regarding the frequency-spectrum of the waves, their rate of growth under the action of the wind, and the spread in direction of the wave energy. (An attempt to measure the local air pressure on the sea surface was less successful). Paper F3 is largely a summary and review of the findings of Paper F2.

Papers F4 and F5 are about various mechanisms for the generation of waves by wind. Note that the "maser mechanism" described in paper C4 was later shown by K Hasselmann to be incomplete; the effect of mass flux by the short waves riding on the longer waves is actually cancelled by the effect of their momentum flux when viscosity is ignored. But OM Phillips then showed that when viscous damping of the short waves is taken into account there is indeed a (smaller) net transfer of energy to the longer waves. Paper F5 discusses the effect of an uneven tangential wind-stress at the surface, greater at the wave crests than in the wave troughs, and shows that it is equivalent to a normal pressure 90° out of phase with the applied tangential stress. In Paper F6, the theory is extended so as to include surface tension, and it is shown to provide a physical explanation for the system of equations proposed by Ruvinsky and Freedman (1985, 1987).

Paper F7 discusses the possibility that in very steep waves both the normal and tangential stresses at the surface become localized near the crests of the waves. This localization will produce waves traveling at a certain angle either side of the direction of the wind, depending on the wave number. The calculations are extended so as to include capillarity.

F. Wave Analysis and Wave Generation

Reprinted from the *Proceedings of the Cambridge Philosophical Society*,
Volume 51, Part 4, pp. 590-603, 1955.

[590]

BOUNDS FOR THE INTEGRAL OF A NON-NEGATIVE FUNCTION IN TERMS OF ITS FOURIER COEFFICIENTS

BY M. S. LONGUET-HIGGINS

Received 28 October 1954

ABSTRACT. The first $2N + 1$ Fourier coefficients of an unknown, non-negative function $f(\theta)$ are given, and it is required to find bounds for $\int_E f(\theta) d\theta$, where E is some given region of integration. We also wish to find the interval E for which the bounds are most strict, when the width of E is specified. $f(\theta)$ may represent a distribution of energy in the interval $0 \leq \theta \leq 2\pi$; the object is to determine where the energy is chiefly located.

In the present paper we show that if the energy is located mainly in the neighbourhood of not more than M distinct points, significant lower bounds for $\int_E f(\theta) d\theta$ can be found in terms of the first $2M + 1$ Fourier coefficients. The effectiveness of the method is illustrated by applying the inequalities to some known functions.

The results have application in determining the direction of propagation of ocean waves and other forms of energy.

1. *Introduction.* The following problem arises in connexion with the analysis of ocean waves (Barber (1)). Let $f(\theta)$ be an unknown, non-negative function of θ , integrable and periodic with period 2π . We are given the first $2N + 1$ Fourier coefficients of $f(\theta)$:

$$\left. \begin{aligned} a_n &= \frac{1}{\pi} \int_0^{2\pi} f(\theta) \cos n\theta d\theta \quad (n = 0, 1, \dots, N), \\ b_n &= \frac{1}{\pi} \int_0^{2\pi} f(\theta) \sin n\theta d\theta \quad (n = 1, 2, \dots, N). \end{aligned} \right\} \quad (1.1)$$

Can we find upper and lower bounds for the function

$$F(E) = \int_E f(\theta) d\theta, \quad (1.2)$$

where E is some given region of integration?

In practice $f(\theta)$, or a related function, may represent the energy density of ocean waves approaching a recording station from a direction specified by θ . Barber (1) has shown that, if the waves are recorded at m different points, then $a_0, a_1, b_1, \dots, a_N, b_N$, where $N \leq \frac{1}{2}m(m-1)$, can be determined from the correlation coefficients of the components of wave motion at the m points; from this information it is required to find, so far as possible, the angular distribution of the wave energy.

For convenience we shall refer to θ as the 'direction' and to (1.2) as the 'energy' contained in the interval E .

An approximation $f_N(\theta)$ to the required function $f(\theta)$ might be given by summing the first $2N + 1$ terms of its Fourier series

$$f_N(\theta) = \frac{1}{2}a_0 + \sum_{k=1}^N (a_k \cos k\theta + b_k \sin k\theta), \quad (1.3)$$

for, under certain conditions, $f_N(\theta)$ tends to $f(\theta)$ as $N \rightarrow \infty$. But this approximation may be inadequate, for it often happens that most of the energy comes from a very restricted range of directions; $f(\theta)$ will then have one or more pronounced maxima which can be only poorly approximated by the smooth function $f_N(\theta)$. In addition, $f_N(\theta)$ may take negative values, while $f(\theta)$ is non-negative. (The Cesaro sums $C1$, however, are non-negative; see, for example, Zygmund (12), p. 46.)

In the present paper we make use of the fact that $f(\theta)$ is non-negative, and it is when the energy is concentrated in one or more narrow ranges of direction that our method yields the most information.

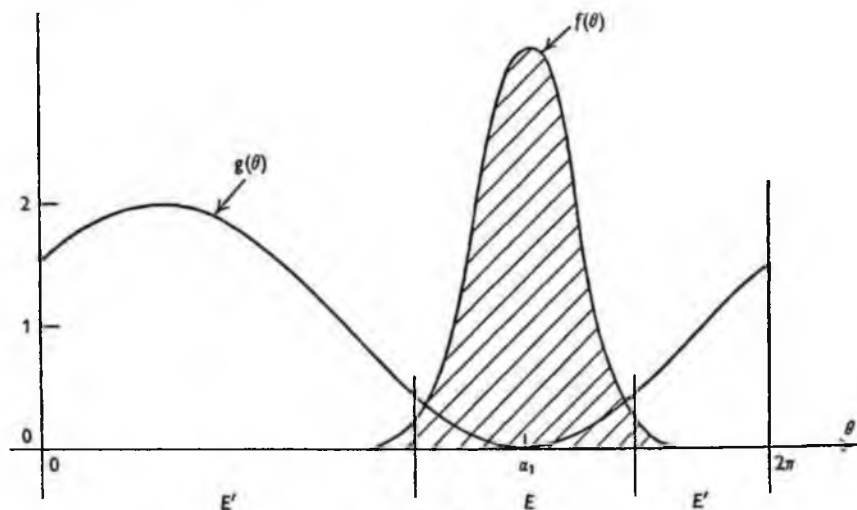


Fig. 1.

The argument is as follows. Let $g(\theta; \alpha_1, \alpha_2, \dots, \alpha_N)$ be a polynomial in $\cos \theta$ and $\sin \theta$ of degree N at most, with coefficients involving $\alpha_1, \dots, \alpha_N$. Then the integral

$$I(\alpha_1, \dots, \alpha_N) = \frac{1}{\pi} \int_0^{2\pi} f(\theta) g(\theta; \alpha_1, \alpha_2, \dots, \alpha_N) d\theta \quad (1.4)$$

is expressible in terms of $\alpha_1, \dots, \alpha_N$ and the first $2N+1$ Fourier coefficients of $f(\theta)$. Suppose that g is always positive, except at $\theta = \alpha_1, \dots, \alpha_N$, where it vanishes (see Fig. 1 for the case $N = 1$). Then I is never negative, and is small if and only if the energy is nearly all concentrated in the neighbourhood of the points $\alpha_1, \dots, \alpha_N$. For if E denotes a set of N narrow intervals surrounding $\alpha_1, \dots, \alpha_N$, the contribution to the integral from within E is small, since g is small there, and the contribution from the remaining regions E' is also small, since the proportion of energy in E' is small. Conversely, if I is small, then the proportion of energy lying outside E is small, for otherwise there would be an appreciable positive contribution to I from the regions E' .

More precisely, let p denote the proportion of energy lying outside E (that is, in E'). Then since the total energy equals πa_0 , we have

$$F(E') = p\pi a_0, \quad F(E) = (1-p)\pi a_0. \quad (1.5)$$

In E we shall have $0 \leq g \leq G$, say, and in E' , $G' < g \leq G''$. Thus from (1.4)

$$\frac{I}{a_0} = \frac{1}{\pi a_0} \left[\int_E fg d\theta + \int_{E'} fg d\theta \right] \quad (1.6)$$

$$\leq \frac{1}{\pi a_0} [GF(E) + G''F(E')] \quad (1.7)$$

$$= G(1-p) + G''p. \quad (1.8)$$

When the intervals E are so narrow that $G \ll 1$, and if at the same time $p \ll 1$, then it follows that $I/a_0 \ll 1$. Conversely, since

$$\frac{I}{a_0} \geq \frac{1}{\pi a_0} \int_{E'} fg d\theta \geq \frac{1}{\pi a_0} G'F(E') = G'p, \quad (1.9)$$

we have

$$p \leq \frac{I}{G'a_0}. \quad (1.10)$$

Thus if $I/G'a_0$ is small then p is also small, and so nearly all the energy lies within E . In general, a knowledge of $I/G'a_0$ provides an upper bound for p and so a lower bound for $F(E)$ (by (1.5)).

The smaller the value of $I/G'a_0$, the greater the amount of energy known to be contained in E . We therefore seek the values of $\alpha_1, \dots, \alpha_N$ which make $I(\alpha_1, \dots, \alpha_N)$ a minimum. (G' depends also on the subsequent choice of E .) The directions $\alpha_1, \dots, \alpha_N$ which make $I(\alpha_1, \dots, \alpha_N)$ a minimum will correspond to the predominant directions of the energy, so far as these can be defined. The chief mathematical problem is then to find the minimum of the integral (1.4) and to determine the corresponding directions $\theta = \alpha_1, \dots, \alpha_N$.

The cases $N = 1$ and $N > 1$ will be considered in §§ 2 and 3 respectively. In § 4 we give some practical examples, where the inequalities are applied to the Fourier coefficients of known functions $f(\theta)$. The tests are found to be reasonably effective.

2. $N = 1$. Let

$$g(\theta; \alpha_1) = 2 \sin^2 \frac{\theta - \alpha_1}{2} \quad (2.1)$$

$$= 1 - \cos \theta \cos \alpha_1 - \sin \theta \sin \alpha_1. \quad (2.2)$$

$g(\theta; \alpha_1)$ is positive everywhere except at $\theta = \alpha_1$, where it vanishes (see Fig. 1), and hence it satisfies the conditions stated in § 1. Consider then the function

$$I(\alpha_1) = \frac{2}{\pi} \int_0^{2\pi} f(\theta) \sin^2 \frac{\theta - \alpha_1}{2} d\theta \quad (2.3)$$

$$= a_0 - a_1 \cos \alpha_1 - b_1 \sin \alpha_1, \quad (2.4)$$

which is a function of α_1 with known coefficients a_0, a_1, b_1 . For E we may take the interval of width 2δ having α_1 as mid-point. Everywhere outside E we have

$$g > 2 \sin^2 \frac{1}{2} \delta = G', \quad (2.5)$$

and so the inequality (1.10) becomes

$$p \leq \frac{I(\alpha_1)}{2a_0 \sin^2 \frac{1}{2} \delta}. \quad (2.6)$$

Now from (2.4) the minimum value of $I(\alpha_1)$ is

$$I = a_0 - \sqrt{(a_1^2 + b_1^2)}, \quad (2.7)$$

and occurs when $\cos \alpha_1 : \sin \alpha_1 : 1 = -a_1 : -b_1 : \sqrt{(a_1^2 + b_1^2)}$. (2.8)

The best possible inequality (2.6) is therefore

$$p \leq \frac{a_0 - \sqrt{(a_1^2 + b_1^2)}}{2a_0 \sin^2 \frac{1}{2}\delta}. \quad (2.9)$$

The corresponding direction α_1 , given by (2.8), defines the 'predominant' direction of the energy.

We may remark that the maximum and minimum values of $I(\alpha_1)$ are the roots of

$$I^2 - 2a_0 I + (a_0^2 - a_1^2 - b_1^2) = 0; \quad (2.10)$$

also that a necessary and sufficient condition for the energy to be concentrated within a single interval of infinitesimal width is

$$a_0^2 - a_1^2 - b_1^2 = 0. \quad (2.11)$$

3. $N > 1$. Generalizing equation (2.1) we take

$$g(\theta; \alpha_1, \alpha_2, \dots, \alpha_N) = 2^{2N-1} \sin^2 \frac{\theta - \alpha_1}{2} \sin^2 \frac{\theta - \alpha_2}{2} \dots \sin^2 \frac{\theta - \alpha_N}{2}, \quad (3.1)$$

which is positive everywhere except at the points $\theta = \alpha_1, \alpha_2, \dots, \alpha_N$, where it vanishes. The integral

$$I(\alpha_1, \dots, \alpha_N) = \frac{2^{2N-1}}{\pi} \int_0^{2\pi} f(\theta) \sin^2 \frac{\theta - \alpha_1}{2} \dots \sin^2 \frac{\theta - \alpha_N}{2} d\theta \quad (3.2)$$

is expressible in terms of $\alpha_1, \dots, \alpha_N$ and the first $2N + 1$ Fourier coefficients

$$a_0, a_1, b_1, \dots, a_N, b_N;$$

we have to investigate the minimum values of $I(\alpha_1, \dots, \alpha_N)$. We shall now show that under certain conditions the maximum and minimum values of $I(\alpha_1, \dots, \alpha_N)$ are the roots of the quadratic

$$\Delta_{N-2} I^2 - 2\Delta_{N-1} I + \Delta_N = 0, \quad (3.3)$$

where

$$\Delta_N = \begin{vmatrix} A_0 & A_1 & \dots & A_N \\ A_1^* & A_0 & \dots & A_{N-1} \\ \vdots & \vdots & \ddots & \vdots \\ A_N^* & A_{N-1}^* & \dots & A_0 \end{vmatrix}, \quad (3.4)$$

and we have written $A_n = a_n - ib_n = \frac{1}{\pi} \int_0^{2\pi} f(\theta) e^{-in\theta} d\theta$. (3.5)

(A_n^* denotes the complex conjugate of A_n .) When $N = 1$ equation (3.3) reduces to (2.10) provided we take conventionally $\Delta_{-1} = 1$.

Since

$$\sin^2 \frac{\theta - \alpha_n}{2} = \frac{1}{2}(e^{i\theta} - e^{i\alpha_n})(e^{-i\theta} - e^{-i\alpha_n}), \quad (3.6)$$

we have

$$I(\alpha_1, \dots, \alpha_N) = \frac{1}{2\pi} \int_0^{2\pi} f(\theta) (e^{i\theta} - e^{i\alpha_1}) \dots (e^{i\theta} - e^{i\alpha_N}) (e^{-i\theta} - e^{-i\alpha_1}) \dots (e^{-i\theta} - e^{-i\alpha_N}) d\theta \quad (3.7)$$

$$= \frac{1}{2\pi} \int_0^{2\pi} f(\theta) (t - x_1) \dots (t - x_N) (t^{-1} - x_1^{-1}) \dots (t^{-1} - x_N^{-1}) d\theta, \quad (3.8)$$

where $t = e^{i\theta}$ and $x_n = e^{i\alpha_n}$. Thus

$$x_1 \dots x_N I = \frac{(-1)^N}{2\pi} \int_0^{2\pi} f(\theta) t^{-N} (t - x_1)^2 \dots (t - x_N)^2 d\theta. \quad (3.9)$$

$$\text{At a stationary value of } I, \quad \frac{\partial I}{\partial x_n} = -ie^{-i\alpha_n} \frac{\partial I}{\partial \alpha_n} = 0, \quad (3.10)$$

and so on differentiating both sides of (3.9) with respect to x_n ,

$$\frac{x_1 \dots x_N I}{x_n} = \frac{(-1)^{N+1}}{\pi} \int_0^{2\pi} f(\theta) t^{-N} \frac{(t - x_1)^2 \dots (t - x_N)^2}{t - x_n} d\theta. \quad (3.11)$$

We shall make use of two lemmas:

LEMMA 1.

$$\begin{vmatrix} x_1^m x_2 \dots x_N & x_1 x_2^m \dots x_N & \dots & x_1 x_2 \dots x_N^m \\ x_1^{N-2} & x_2^{N-2} & \dots & x_N^{N-2} \\ x_1^{N-3} & x_2^{N-3} & \dots & x_N^{N-3} \\ \vdots & \vdots & \dots & \vdots \\ 1 & 1 & \dots & 1 \end{vmatrix} = \begin{cases} (-1)^{N+1} D_N & (m = 0), \\ 0 & (m = 1, 2, \dots, N-1), \end{cases} \quad (3.12)$$

where

$$D_N = \begin{vmatrix} x_1^{N-1} & x_2^{N-1} & \dots & x_N^{N-1} \\ x_1^{N-2} & x_2^{N-2} & \dots & x_N^{N-2} \\ \vdots & \vdots & \dots & \vdots \\ 1 & 1 & \dots & 1 \end{vmatrix} = \prod_{n>m} (x_n - x_m). \quad (3.13)$$

For the value of the left-hand determinant is unaltered by dividing the first row by $x_1 x_2 \dots x_N$ and multiplying the first column by x_1 , the second by x_2 and so on. If $m = 0$, the determinant is then identical with D_N except for an interchange of rows. If $m = 1, 2, \dots, N-1$, two rows of the determinant are identical.

LEMMA 2. When $m = 0, 1, \dots, N-1$,

$$\begin{vmatrix} \frac{x_1^m}{t-x_1} & \frac{x_2^m}{t-x_2} & \dots & \frac{x_N^m}{t-x_N} \\ x_1^{N-2} & x_2^{N-2} & \dots & x_N^{N-2} \\ x_1^{N-3} & x_2^{N-3} & \dots & x_N^{N-3} \\ \vdots & \vdots & \dots & \vdots \\ 1 & 1 & \dots & 1 \end{vmatrix} = \frac{t^m D_N}{(t-x_1)(t-x_2)\dots(t-x_N)}. \quad (3.14)$$

For on multiplying the top row of the left-hand determinant by

$$(t-x_1)(t-x_2)\dots(t-x_N),$$

the first term, for example, becomes

$$x_1^m(t-x_2) \dots (t-x_N) = x_1^m[S_0^{(1)}t^{N-1} - S_1^{(1)}t^{N-2} + \dots + (-1)^{N-1}S_N^{(1)}], \tag{3.15}$$

where $S_n^{(1)}$ denotes the symmetric sum, of degree n , of the roots x_2, \dots, x_N , and $S_0^{(1)}$, by convention, equals 1. $S_n^{(1)}$ may be expressed in terms of the symmetric sums S_n of all the roots x_1, x_2, \dots, x_N by successive substitution as follows:

$$\left. \begin{aligned} S_1^{(1)} &= S_1 - x_1 S_0^{(1)} = S_1 - x_1 S_0, \\ S_2^{(1)} &= S_2 - x_1 S_1^{(1)} = S_2 - x_1 S_1 + x_1^2 S_0, \\ S_3^{(1)} &= S_3 - x_1 S_2^{(1)} = S_3 - x_1 S_2 + x_1^2 S_1 - x_1^3 S_0, \\ &\dots \dots \dots \\ S_{N-m-1}^{(1)} &= S_{N-m-1} - x_1 S_{N-m-2} + \dots + (-1)^{N-m-1} x_1^{N-m-1} S_0, \end{aligned} \right\} \tag{3.16}$$

all the powers of x_1 on the right-hand side being of degree less than or equal to $(N-m-1)$. For the remaining coefficients we start from the other end:

$$\left. \begin{aligned} S_{N-1}^{(1)} &= x_1^{-1} S_N, \\ S_{N-2}^{(1)} &= x_1^{-1} (S_{N-1} - S_{N-1}^{(1)}) = x_1^{-1} S_{N-1} - x_1^{-2} S_N, \\ S_{N-3}^{(1)} &= x_1^{-1} (S_{N-2} - S_{N-2}^{(1)}) = x_1^{-1} S_{N-2} - x_1^{-2} S_{N-1} + x_1^{-3} S_{N-2}, \\ &\dots \dots \dots \\ S_{N-m}^{(1)} &= x_1^{-1} S_{N-m+1} - x_1^{-2} S_{N-m+2} + \dots + (-1)^{m-1} x_1^{-m} S_N. \end{aligned} \right\} \tag{3.17}$$

On substitution in (3.15) we see that the first term of the top row of the determinant is of the form

$$P_1 x_1^{N-1} + P_2 x_1^{N-2} + \dots + P_N, \tag{3.18}$$

where the P_n are symmetrical expressions in x_1, x_2, \dots, x_N and

$$P_1 = t^m. \tag{3.19}$$

Each of the terms $P_n x_1^{N-m}$ ($m = 2, 3, \dots, N-1$) can be eliminated by subtracting P_n times the n th row from the first row of the determinant. Only the first term $P_1 x_1^{N-1}$ remains. By (3.19) this proves the lemma.

Now let the n th of equations (3.11) be multiplied by x_n^m times the cofactor of the n th term of the first row of D_N , and let the equations be added. For $m = 0$ this gives

$$(-1)^{N+1} D_N I = \frac{(-1)^{N+1}}{\pi} \int_0^{2\pi} f(\theta) t^{-N} (t-x_1) \dots (t-x_N) D_N d\theta, \tag{3.20}$$

and therefore, if $D_N \neq 0$,

$$\begin{aligned} I &= \frac{1}{\pi} \int_0^{2\pi} f(\theta) [1 - S_1 t^{-1} + S_2 t^{-2} - \dots + (-1)^N S_N t^{-N}] d\theta \\ &= A_0 S_0 - A_1 S_1 + A_2 S_2 - \dots + (-1)^N A_N S_N. \end{aligned} \tag{3.21}$$

Similarly, for $m = 1, 2, \dots, N-1$, we have

$$0 = A_m^* S_0 - A_{m-1}^* S_1 + \dots + (-1)^N A_{N-m} S_N. \tag{3.22}$$

Finally, we add the equation for $m = N$, which is most conveniently obtained by taking the conjugate of equation (3.21) and using $S_n^* = S_{N-n}/S_N$:

$$I S_N = A_N^* S_0 - A_{N-1}^* S_1 + \dots + (-1)^N A_0 S_N. \tag{3.23}$$

These equations may be written in matrix form:

$$\begin{pmatrix} A_0 - I & A_1 & A_2 & \dots & A_N \\ A_1^* & A_0 & A_1 & \dots & A_{N-1} \\ A_2^* & A_1^* & A_0 & \dots & A_{N-2} \\ \vdots & \vdots & \vdots & \ddots & \vdots \\ A_N^* & A_{N-1}^* & A_{N-2}^* & \dots & A_0 - I \end{pmatrix} \begin{pmatrix} S_0 \\ -S_1 \\ S_2 \\ \vdots \\ (-1)^N S_N \end{pmatrix} = \begin{pmatrix} 0 \\ 0 \\ 0 \\ \vdots \\ 0 \end{pmatrix}. \quad (3.24)$$

The diagonal terms of the square matrix are all A_0 except the first and last, which are $A_0 - I$. Since the symmetric sums S_n are not all zero ($S_0 = 1$), it follows that

$$\begin{vmatrix} A_0 - I & A_1 & A_2 & \dots & A_N \\ A_1^* & A_0 & A_1 & \dots & A_{N-1} \\ A_2^* & A_1^* & A_0 & \dots & A_{N-2} \\ \vdots & \vdots & \vdots & \ddots & \vdots \\ A_N^* & A_{N-1}^* & A_{N-2}^* & \dots & A_0 - I \end{vmatrix} = 0, \quad (3.25)$$

which on expansion is seen to be identical with (3.3), the result to be proved.

To find the corresponding angles α_n , we first choose the smaller root I of equation (3.25) and then solve any N of equations (3.24) to obtain the N ratios $S_0 : S_1 : \dots : S_N$. The roots x_1, x_2, \dots, x_N of

$$S_0 t^N - S_1 t^{N-1} + \dots + (-1)^N S_N = 0 \quad (3.26)$$

then give the required angles, through the relations $x_n = e^{i\alpha_n}$.

It was assumed in the proof that $D_N \neq 0$, i.e. that all the roots x_n are distinct. Since $I(\alpha_1, \dots, \alpha_N)$ is a bounded function of $\alpha_1, \dots, \alpha_N$, it must always possess at least one maximum and one minimum; but only if these correspond to unequal values of $\alpha_1, \dots, \alpha_N$ does the present theorem necessarily hold.

In one important case, however, the above analysis is certainly valid, namely when the energy is concentrated in N infinitesimal intervals surrounding N distinct directions $\theta_1, \theta_2, \dots, \theta_N$, say. For, when $(\alpha_1, \dots, \alpha_N) = (\theta_1, \dots, \theta_N)$, I vanishes, from (3.2), and further

$$\frac{\partial I}{\partial \alpha_n} = -\frac{2^{2N-1}}{\pi} \int_0^{2\pi} f(\theta) \sin^2 \frac{\theta - \alpha_1}{2} \dots \sin(\theta - \alpha_n) \dots \sin^2 \frac{\theta - \alpha_N}{2} d\theta = 0. \quad (3.27)$$

Therefore $(\alpha_1, \dots, \alpha_N) = (\theta_1, \dots, \theta_N)$ is a solution of equation (3.11) and hence also of equations (3.25) and (3.5), with $I = 0$. The determinant (3.25) is of rank N , as will be shown in the appendix, and so the ratios $S_0 : S_1 : \dots : S_N$ are uniquely determined. Therefore $t = e^{i\theta_n}$ satisfies (3.26). But (3.26) has not more than N roots, which must therefore be identical with the N distinct quantities $e^{i\theta_1}, e^{i\theta_2}, \dots, e^{i\theta_N}$.

When the minimum value of I is small, equation (3.3) shows that it is given by

$$I = \frac{\Delta_N}{2\Delta_{N-1}} \quad (3.28)$$

very nearly. Therefore by (1.10) all except a proportion p of the energy is contained in E where

$$p \leq \frac{\Delta_N}{2G'\Delta_0\Delta_{N-1}}. \quad (3.29)$$

If

$$\frac{\Delta_N}{2\Delta_0\Delta_{N-1}} \ll G', \quad (3.30)$$

then nearly all the energy is contained in E .

Suppose that we take as E the set of N intervals of width 2δ with mid-points $\alpha_1, \dots, \alpha_N$. If δ is small compared with the distances between successive α 's we have, in the n th interval,

$$g(\theta; \alpha_1, \alpha_2, \dots, \alpha_N) = 2^{2N-1} \sin^2 \frac{\theta - \alpha_n}{2} \prod' \sin^2 \frac{\alpha_m - \alpha_n}{2} \quad (3.31)$$

very nearly, where in the product m runs from 1 to N excluding n . Thus, outside E ,

$$g \geq 2^{2N-1} \sin^2 \frac{1}{2}\delta \min \left(\prod' \sin^2 \frac{\alpha_m - \alpha_n}{2} \right) = G'. \quad (3.32)$$

A rough estimate of G' may be obtained by replacing $\sin \frac{1}{2}\delta$ by $\frac{1}{2}\delta$ and each of the terms $\sin^2 \frac{1}{2}(\alpha_m - \alpha_n)$ by a mean value $\frac{1}{2}$. Thus

$$G' \doteq 2^{N-2}\delta^2, \quad (3.33)$$

and (3.30) becomes

$$\frac{\Delta_N}{2^{N-1}\Delta_0\Delta_{N-1}} \ll \delta^2. \quad (3.34)$$

If one of the distances $|\alpha_m - \alpha_n|$ is only of order δ or less, then G' will be an order of magnitude less than (3.33). But in that case we may expect that a smaller number of directions α_n would give a significant inequality, for the same value of δ . Therefore a criterion for the energy to be grouped mainly in N separate intervals of width δ is that N shall be the *least* integer for which (3.34) is true.

4. *Applications.* To illustrate the method we shall discuss some examples when the energy distribution $f(\theta)$ has certain simple forms; we shall find how much information about $\int_E f(\theta) d\theta$ can be obtained from a knowledge of the first five Fourier coefficients.

Example 1. Suppose that

$$f(\theta) = \begin{cases} \frac{\pi}{2\epsilon} & \text{if } \theta_1 - \epsilon < \theta < \theta_1 + \epsilon, \\ 0 & \text{elsewhere,} \end{cases} \quad (4.1)$$

that is, the energy is evenly distributed in a narrow interval of width 2ϵ and mid-point θ_1 (see Fig. 2a). Then we have

$$A_0 = 1, \quad A_n = e^{in\theta_1} \frac{\sin n\epsilon}{n\epsilon} \quad (n = 1, 2, \dots, N), \quad (4.2)$$

and so

$$\left. \begin{aligned} \Delta_0 &= 1, \\ \Delta_1 &= 1 - \left(\frac{\sin \epsilon}{\epsilon} \right)^2 \doteq \frac{1}{3}\epsilon^2, \\ \Delta_2 &= \left(1 - \frac{\sin 2\epsilon}{2\epsilon} \right) \left(1 - 2 \left(\frac{\sin \epsilon}{\epsilon} \right)^2 + \frac{\sin 2\epsilon}{2\epsilon} \right) \doteq \frac{4}{135}\epsilon^6. \end{aligned} \right\} \quad (4.3)$$

Since Δ_1/Δ_0^2 is of order ϵ^2 , we know at once that the energy is mainly grouped in a single interval whose width is of order ϵ .

Let us apply the test when $N = 1$. From (2.8) we find that the 'predominant' direction is given by $\alpha_1 = \theta_1$, and further from (2.9) that

$$p \leq \frac{\epsilon^2}{3\delta^2} \quad (4.4)$$

($\sin \frac{1}{2}\delta$ has been replaced by $\frac{1}{2}\delta$). Thus, taking $\delta = \epsilon$, we could tell that not more than one-third of the energy lies outside the original interval, or taking $\delta = 2\epsilon$, that not more than one-twelfth lies outside an interval of twice this width.

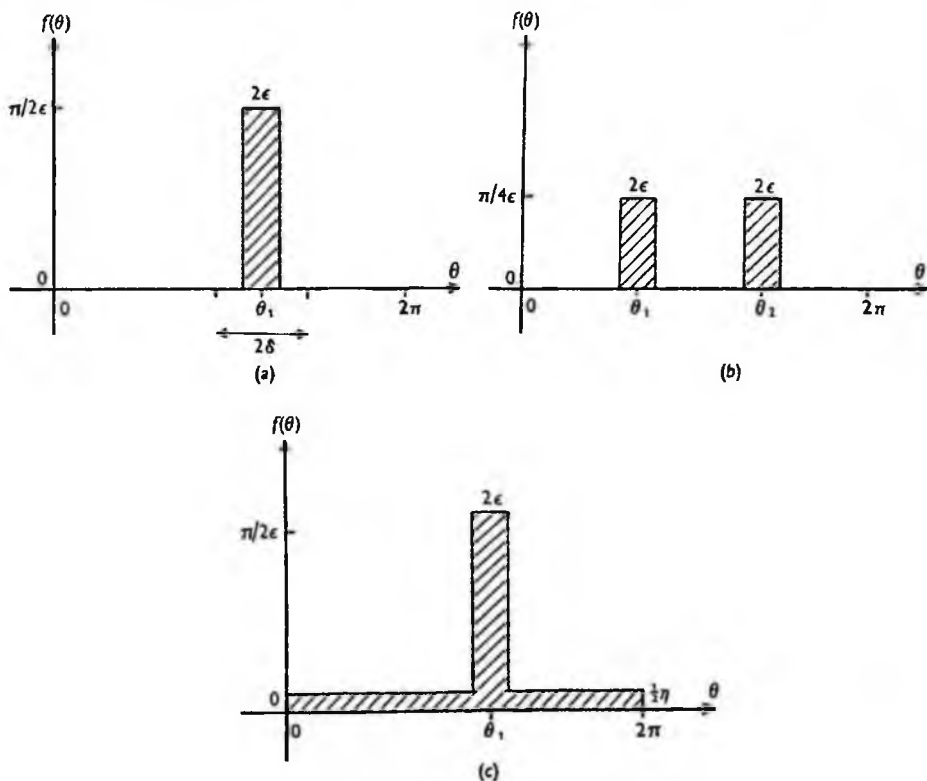


Fig. 2.

To apply the test when $N = 2$ we have to solve

$$\left. \begin{aligned} (1-I)S_0 - e^{-i\theta_1} \frac{\sin \epsilon}{\epsilon} S_1 + e^{-2i\theta_1} \frac{\sin 2\epsilon}{2\epsilon} S_2 &= 0, \\ e^{i\theta_1} \frac{\sin \epsilon}{\epsilon} S_0 - S_1 + e^{-i\theta_1} \frac{\sin \epsilon}{\epsilon} S_2 &= 0, \\ e^{2i\theta_1} \frac{\sin 2\epsilon}{2\epsilon} S_0 - e^{i\theta_1} \frac{\sin \epsilon}{\epsilon} S_1 + (1-I)S_2 &= 0. \end{aligned} \right\} \quad (4.5)$$

On subtracting the first equation from the third we find

$$S_2 = e^{2i\theta_1} S_0, \quad (4.6)$$

and so from the second

$$S_1 = 2 \frac{\sin \epsilon}{\epsilon} e^{i\theta_1} S_0. \quad (4.7)$$

Equation (3.26) then becomes

$$t^2 - 2 \frac{\sin \epsilon}{\epsilon} e^{i\theta_1} t + 2e^{2i\theta_1} = 0, \quad (4.8)$$

of which the solution, to order ϵ , is

$$t = e^{i(\theta_1 \pm \epsilon/\sqrt{3})}. \quad (4.9)$$

The predominant directions α_1, α_2 are therefore given by

$$\alpha_1, \alpha_2 = \theta_1 \pm \epsilon/\sqrt{3}. \quad (4.10)$$

The separation of α_1 and α_2 is $2\epsilon/\sqrt{3}$. If we take as E two separate intervals of width 2δ surrounding α_1 and α_2 , δ being less than $\epsilon/\sqrt{3}$, we shall obtain a bound G' of order $\delta^2\epsilon^2$. Thus (3.29) will be of order ϵ^2/δ^2 , and no advantage is obtained by taking δ much smaller than ϵ (as, indeed, we should expect from the actual form of $f(\theta)$). If, on the other hand, we take for E a single interval $(\theta_1 - \delta, \theta_1 + \delta)$, where $\delta \geq \epsilon/\sqrt{3}$, we have

$$G' = 2^3 \sin^2 \frac{\delta - \epsilon/\sqrt{3}}{2} \sin^2 \frac{\delta + \epsilon/\sqrt{3}}{2} = \frac{(\delta^2 - \frac{1}{3}\epsilon^2)^2}{3} \quad (4.11)$$

approximately, and so from (3.29)

$$p \leq \frac{4}{5} \frac{\epsilon^4}{(3\delta^2 - \epsilon^2)^2}. \quad (4.12)$$

If $\delta = \epsilon$, we have $p \leq 1/5$, showing that not more than one-fifth of the energy lies outside the interval (compared with one-third in the previous test). If $\delta = 2\epsilon$, we have $p \leq 1/180$, showing that only about 0.5% of the energy lies outside the interval (compared with one-twelfth previously).

Thus the test for $N = 2$ provides a stricter inequality than the test for $N = 1$, but not by an order of magnitude.

Example 2. Let

$$f(\theta) = \begin{cases} \frac{\pi}{4\epsilon} & \text{if } \theta_1 - \epsilon < \theta < \theta_1 + \epsilon, \\ \frac{\pi}{4\epsilon} & \text{if } \theta_2 - \epsilon < \theta < \theta_2 + \epsilon, \\ 0 & \text{elsewhere,} \end{cases} \quad (4.13)$$

where $2\epsilon < \theta_2 - \theta_1 < 2\pi - 2\epsilon$, so that the energy is evenly distributed in two non-overlapping intervals of width 2ϵ (see Fig. 2*b*). For simplicity we shall suppose also that $\theta_2 - \theta_1 = \frac{1}{2}\pi$, i.e. the average directions for the two intervals are at right angles. Then we have

$$A_0 = 1, \quad A_n = e^{-in\theta_0} \cos \frac{n\pi \sin n\epsilon}{4n\epsilon} \quad (n = 1, 2, \dots, N), \quad (4.14)$$

where $\theta_0 = \frac{1}{2}(\theta_1 + \theta_2)$, and

$$\left. \begin{aligned} \Delta_0 &= 1, \\ \Delta_1 &= 1 - \frac{1 \sin \epsilon}{2 \epsilon} \div \frac{1}{2}, \\ \Delta_2 &= 1 - \left(\frac{\sin \epsilon}{\epsilon} \right)^2 \div \frac{1}{3} \epsilon^2, \end{aligned} \right\} \quad (4.15)$$

600

M. S. LONGUET-HIGGINS

approximately. Since $\Delta_2/2\Delta_0\Delta_1$ is of order ϵ^2 , $\ll 1$, whereas Δ_1/Δ_0^2 is of order unity, we can tell at once that the energy lies mainly within *two* separate intervals whose width is of order ϵ .

In the test for $N = 1$, $I(\alpha_1)$ is a minimum when $\alpha_1 = \theta_0 = \frac{1}{2}(\theta_1 + \theta_2)$. But since Δ_1/Δ_0^2 is of order unity the test gives a barely significant result. If we take, for example, $\delta = \frac{1}{2}\pi$, so that E is the interval of width π and mid-point θ_0 , we have from (2.9)

$$p \leq 1 - \sqrt{\frac{1}{2}} = 0.293, \quad (4.16)$$

so that only about seven-tenths of the energy certainly lies in this semicircle.

Now let us apply the test for $N = 2$. We have

$$\left. \begin{aligned} (1-I)S_0 - \frac{e^{-i\theta_0} \sin \epsilon}{\sqrt{2}} \frac{S_1}{\epsilon} &= 0, \\ \frac{e^{i\theta_0} \sin \epsilon}{\sqrt{2}} S_0 - S_1 + \frac{e^{-i\theta_0} \sin \epsilon}{\sqrt{2}} \frac{S_2}{\epsilon} &= 0, \\ -\frac{e^{i\theta_0} \sin \epsilon}{\sqrt{2}} \frac{S_1}{\epsilon} + (1-I)S_2 &= 0. \end{aligned} \right\} \quad (4.17)$$

Proceeding as before, we find

$$\alpha_1 = \theta_1 + \frac{1}{3}\epsilon^2, \quad \alpha_2 = \theta_2 - \frac{1}{3}\epsilon^2. \quad (4.18)$$

Thus the two 'predominant' directions differ from the directions θ_1 and θ_2 by quantities of order ϵ^2 only. If E is taken to be two small intervals of width 2δ surrounding α_1 and α_2 we may take

$$G' = 2^3 \sin^2 \frac{1}{2}\delta \sin^2 \frac{\alpha_2 - \alpha_1}{2} = \delta^2 \quad (4.19)$$

approximately, and so from (3.29) $p \leq \frac{\epsilon^2}{3\delta^2}$. (4.20)

Thus we could tell that at least two-thirds of the energy comes from within two intervals of width 2ϵ almost coinciding with the original intervals, or that eleven-twelfths of the energy comes from within two intervals of twice this width.

As expected, there is a marked improvement in the inequalities obtained from the test for $N = 2$ compared with those obtained from the test for $N = 1$, in this example. However, from the experience of Example 1 we should expect that tests of higher order would give only a smaller improvement.

Example 3. In the two previous examples we assumed that the energy was entirely confined to one or two narrow intervals, that is to say there was no 'background' of energy outside those intervals. To investigate the effect of such a background we may add to the energy distribution of Example 1 a small constant term. Thus

$$f(\theta) = \begin{cases} \frac{1}{2}\eta + \frac{\pi}{2\epsilon} & \text{if } \theta_1 - \epsilon < \theta < \theta_1 + \epsilon, \\ \frac{1}{2}\eta & \text{elsewhere,} \end{cases} \quad (4.21)$$

where η is a small quantity (see Fig. 2c). The effect of this is to increase A_0 by η but to leave the other Fourier coefficients unaltered:

$$A_0 = 1 + \eta, \quad A_n = e^{-in\delta_1} \frac{\sin n\epsilon}{n\epsilon} \quad (n = 1, 2, \dots, N). \quad (4.22)$$

Equation (2.9) then gives

$$p \leq \frac{2\eta + \frac{1}{3}\epsilon^2}{\delta} \tag{4.23}$$

(higher powers of δ, ϵ, η being neglected).

In order that the background shall be negligible, therefore, we must have $\eta \ll \epsilon^2$, or in other words the background must be an order of magnitude smaller than the square of the width of the interval. It appears, therefore, that the effectiveness of the present tests depends rather critically on the absence of such a background.

APPENDIX

Properties of Δ_N

We now prove the result used in §3. This is part of a more general theorem (Theorem A 9) which was first proved algebraically by Toeplitz (11); other proofs have been given by Fischer (6), Schur (10) and Frobenius (7)†. The proof we now give is more direct than any of those mentioned, and brings to light more clearly the significance of Δ_N .

First we establish the identity

$$\Delta_N \equiv \frac{2^{2N(N+1)}}{(N+1)! \pi^{N+1}} \int_0^{2\pi} \dots \int_0^{2\pi} f(\theta_1) \dots f(\theta_{N+1}) \prod_{m>n} \sin^2 \frac{\theta_m - \theta_n}{2} d\theta_1 \dots d\theta_{N+1}, \tag{A 1}$$

where, in the double product, n runs from 1 to $N+1$ and m from $n+1$ to $N+1$. From (3.4) and (3.5) we have

$$\begin{aligned} \Delta_N &= \frac{1}{\pi^{N+1}} \left| \begin{array}{ccc} \int_0^{2\pi} f(\theta_1) d\theta_1 & \int_0^{2\pi} f(\theta_2) e^{-i\theta_2} d\theta_2 & \dots \int_0^{2\pi} f(\theta_{N+1}) e^{-iN\theta_{N+1}} d\theta_{N+1} \\ \int_0^{2\pi} f(\theta_1) e^{i\theta_1} d\theta_1 & \int_0^{2\pi} f(\theta_2) d\theta_2 & \dots \int_0^{2\pi} f(\theta_{N+1}) e^{-i(N-1)\theta_{N+1}} d\theta_{N+1} \\ \vdots & \vdots & \vdots \\ \int_0^{2\pi} f(\theta_1) e^{iN\theta_1} d\theta_1 & \int_0^{2\pi} f(\theta_2) e^{i(N-1)\theta_2} d\theta_2 \dots & \int_0^{2\pi} f(\theta_{N+1}) d\theta_{N+1} \end{array} \right| \\ &= \frac{1}{\pi^{N+1}} \int_0^{2\pi} \dots \int_0^{2\pi} f(\theta_1) \dots f(\theta_{N+1}) \\ &\quad \times \left| \begin{array}{cccc} 1 & e^{-i\theta_2} & \dots & e^{-iN\theta_{N+1}} \\ e^{i\theta_1} & 1 & \dots & e^{-i(N-1)\theta_{N+1}} \\ \vdots & \vdots & \vdots & \vdots \\ e^{iN\theta_1} & e^{i(N-1)\theta_2} & \dots & 1 \end{array} \right| d\theta_1 \dots d\theta_{N+1} \\ &= \frac{1}{\pi^{N+1}} \int_0^{2\pi} \dots \int_0^{2\pi} f(\theta_1) \dots f(\theta_{N+1}) e^{-i\theta_2} e^{-2i\theta_3} \dots e^{-iN\theta_{N+1}} \\ &\quad \times \left| \begin{array}{cccc} 1 & 1 & \dots & 1 \\ e^{i\theta_1} & e^{i\theta_2} & \dots & e^{i\theta_{N+1}} \\ \vdots & \vdots & \vdots & \vdots \\ e^{iN\theta_1} & e^{iN\theta_2} & \dots & e^{iN\theta_{N+1}} \end{array} \right| d\theta_1 \dots d\theta_{N+1}. \tag{A 2} \end{aligned}$$

† Some equivalent geometrical conditions on the Fourier coefficients were given by Carathéodory (2, 3). The equivalence of the algebraic and geometrical conditions was established by Carathéodory and Fejér (4). See also Riesz (8, 9) for related results.

602

M. S. LONGUET-HIGGINS

Interchanging any two of the θ_n does not affect the value of the left-hand side, but interchanges two rows of the determinant on the right-hand side. The two rows can be changed back if at the same time the sign of the right-hand side is changed. Hence, adding all the $(N+1)!$ possible permutations we have

$$\begin{aligned}
 (N+1)! \Delta_N &= \frac{1}{\pi^{N+1}} \int_0^{2\pi} \dots \int_0^{2\pi} f(\theta_1) \dots f(\theta_{N+1}) \\
 &\quad \times \begin{vmatrix} 1 & 1 & \dots & 1 \\ e^{i\theta_1} & e^{i\theta_2} & \dots & e^{i\theta_{N+1}} \\ \vdots & \vdots & \dots & \vdots \\ e^{iN\theta_1} & e^{iN\theta_2} & \dots & e^{iN\theta_{N+1}} \end{vmatrix} \begin{vmatrix} 1 & 1 & \dots & 1 \\ e^{-i\theta_1} & e^{-i\theta_2} & \dots & e^{-i\theta_{N+1}} \\ \vdots & \vdots & \dots & \vdots \\ e^{-iN\theta_1} & e^{-iN\theta_2} & \dots & e^{-iN\theta_{N+1}} \end{vmatrix} d\theta_1 \dots d\theta_{N+1} \\
 &= \frac{1}{\pi^{N+1}} \int_0^{2\pi} \dots \int_0^{2\pi} f(\theta_1) \dots f(\theta_{N+1}) \prod_{m>n} (e^{i\theta_m} - e^{i\theta_n})(e^{-i\theta_m} - e^{-i\theta_n}) d\theta_1 \dots d\theta_{N+1}.
 \end{aligned} \tag{A 3}$$

If equation (3.6) is now used, the identity (A 1) follows immediately.

Since $f(\theta)$ is non-negative, the whole integrand on the right-hand side of equation (A 1) is non-negative, from which it follows that

$$\Delta_N \geq 0. \tag{A 4}$$

Suppose now that $f(\theta)$ consists of N 'pulses' of energy, that is, $f(\theta)$ is zero everywhere except near N points $\theta = \theta^{(m)}$, where it becomes infinite in such a way that $\int f(\theta) d\theta$ has a finite discontinuity C_m at this point. In Dirac's notation (5) we may write

$$f(\theta) = \sum_{m=1}^N C_m \delta(\theta - \theta_m). \tag{A 5}$$

The function $f(\theta_1) \dots f(\theta_{N+1})$ is zero everywhere except where each θ_n equals some $\theta^{(m)}$. But since there are only N $\theta^{(m)}$, this implies that at least two of the θ_n must be equal. The part of the integrand *under the product sign* then vanishes, and the contribution from the neighbourhood of this point is zero. Hence

$$\text{If } f(\theta) \text{ is the sum of } N \text{ pulses, then } \Delta_N = 0. \tag{A 6}$$

Conversely, if it is assumed that $f(\theta)$ is continuous except possibly for a finite number of pulses, we may show that

$$\text{If } \Delta_N = 0 \text{ and if } f(\theta) \geq 0, \text{ then } f(\theta) \text{ is the sum of at most } N \text{ pulses.} \tag{A 7}$$

For, suppose that $f(\theta)$ is continuous and positive, or has a positive pulse, at more than N points, say $\theta = \theta^{(1)}, \dots, \theta^{(N+1)}$. When $\theta_1, \dots, \theta_{N+1}$ are in the neighbourhood of these points there will be a positive contribution to the integral (A 1), and since the integrand is never negative Δ_N must be greater than zero, contrary to hypothesis. Therefore $f(\theta)$ cannot be different from zero at more than N distinct points.

The first part (A 6) of the theorem can also be quite simply proved algebraically. For if $f(\theta)$ is given by (A 5) then from (3.5)

$$A_n = \frac{1}{\pi} \sum_{m=1}^N C_m e^{-in\theta_m}. \tag{A 8}$$

If these expressions for A_n are substituted in (3.4) it will be found that Δ_N vanishes identically. However, the converse (A 7) is necessarily more difficult to prove, since it depends upon $f(\theta)$ being non-negative.

From (A 7) we deduce that if f is the sum of just N pulses, then $\Delta_{N-1} > 0$; for if Δ_{N-1} vanished $f(\theta)$ would consist of no more than $(N-1)$ pulses. Now Δ_{N-1} is a minor of Δ_N , so that Δ_N must be of rank N (which is the result used in §3). Conversely, if $\Delta_N = 0$ but $\Delta_{N-1} > 0$, then $f(\theta)$ consists of just N pulses. Hence

A necessary and sufficient set of conditions for a non-negative function $f(\theta)$ to consist of just N pulses is that

$$\Delta_0 > 0, \quad \Delta_1 > 0, \quad \dots, \quad \Delta_{N-1} > 0, \quad \Delta_N = 0. \quad (\text{A } 9)$$

REFERENCES

- (1) BARBER, N. F. Finding the direction of travel of sea waves. *Nature, Lond.*, 174 (1954), 1048-50.
- (2) CARATHÉODORY, C. Über den Variabilitätsbereich der Koeffizienten von Potenzreihen die gegebene Werte nicht annehmen. *Math. Ann.* 64 (1907), 95-116.
- (3) CARATHÉODORY, C. Über den Variabilitätsbereich der Fourierschen Konstanten von positiven harmonischen Funktionen. *R.C. Circ. mat. Palermo*, 32 (1911), 193-217.
- (4) CARATHÉODORY, C. and FEJÉR. Über den Zusammenhang der Extremen von harmonischen Funktionen mit ihren Koeffizienten und über den Picard-Landau'schen Satz. *R.C. Circ. mat. Palermo*, 32 (1911), 218-39.
- (5) DIRAC, P. A. M. *The principles of quantum mechanics* (Oxford, 1930).
- (6) FISCHER, E. Über das Carathéodory'sche Problem, Potenzreihen mit positivem reellen Teil betreffend. *R.C. Circ. mat. Palermo*, 32 (1911), 240-56.
- (7) FROBENIUS, G. Ableitung eines Satzes von Carathéodory aus einer Formel von Kronecker. *S.B. preuss. Akad. Wiss.* (1912), pp. 16-31.
- (8) RIESZ, F. Sur certains systèmes singuliers d'équations intégrales. *Ann. sci. Éc. norm. sup., Paris*, (3), 28 (1911), 33-61.
- (9) RIESZ, F. *Les systèmes d'équations linéaires à une infinité d'inconnues* (Paris, 1913, reprinted 1952).
- (10) SCHUR, I. Über einen Satz von C. Carathéodory. *S.B. preuss. Akad. Wiss.* (1912), pp. 4-15.
- (11) TOEPLITZ, O. Über die Fourier'sche Entwicklung positiver Funktionen. *R.C. Circ. mat. Palermo*, 32 (1911), 191-2.
- (12) ZYGMUND, A. *Trigonometrical series*, 2nd ed. (New York, 1952).

Reprint of: pp. 111-136 of *Ocean Wave Spectra*.
New Jersey: Prentice Hall Inc. 1963

M. S. LONGUET-HIGGINS
D. E. CARTWRIGHT
N. D. SMITH

O N E

**OBSERVATIONS OF THE DIRECTIONAL SPECTRUM OF SEA WAVES
USING THE MOTIONS OF A FLOATING BUOY**

ABSTRACT

The vertical acceleration of a floating buoy, and the two angles of pitching and rolling, can be used to determine the first five Fourier coefficients (a_0, a_1, b_1, a_2, b_2) of the angular distribution of energy in each band of frequency.

From these coefficients can be found a weighted average of the directional spectrum with respect to the horizontal azimuth ϕ , and also certain useful parameters: the total spectral density ($C_{11}(\sigma)$), the mean direction of the energy ($\bar{\phi}$), the angular spread of the energy (ψ), and a parameter indicating the shape of the distribution (I_{mis}/a_0).

Five complete records were analysed, corresponding to local wind speeds that ranged from 8 to 23 knots. The record with the highest wind speed (Record No. 5) fortunately corresponded to a very simple weather situation, with a well-defined fetch and constant wind direction. In this record it was found that at the higher frequencies the total spectral density tended to Phillips's limiting law, proportional to (frequency)⁻⁵. The angular spread of the spectrum increased with the frequency. At low frequencies it approximated the "resonance" angle $\sec^{-1}(U/c)$, where U and c

denote wind speed and wave speed respectively. At intermediate frequencies the angular spread was somewhat less than the resonance angle, owing probably to the growth of the waves by shear-flow instability. At the highest frequencies the angular width was again increased, owing probably to nonlinear effects.

The parameters of the spectrum were consistent with an angular distribution proportional to $\cos^2(s\phi)$, where the parameter s varies markedly with frequency. Thus s decreases from about 4 at low frequencies to less than 1 at high frequencies. The parameters of the spectrum did not fit a "square-topped" distribution of energy so well, much less a distribution with two narrow directional bands of energy. However, the possibility of a mildly "bimodal" spectrum cannot be entirely ruled out.

The atmospheric pressure fluctuations at the sea surface were also recorded. These were generally of an order of magnitude smaller than those assumed by Phillips (1957) to exist in a turbulent air stream. Moreover, the recorded pressure fluctuations can be attributed mostly to the aerodynamic pressure changes produced by the flow of the air over the waves, together with the hydro-

static pressure changes due to the vertical displacement of the buoy. The pressure fluctuations were consistent with the cosine-power law for the angular distribution, stated above.

INTRODUCTION

The question of how the energy in sea waves is distributed with regard to direction of propagation is not only essential from the point of view of the wave forecaster, but is also of great interest because it throws light on the processes of wave generation. Very few determinations of the complete two-dimensional spectrum have been attempted. Among those hitherto published we may mention Barber's (1954) technique using an array of wave height recorders, and also the analysis of aerial stereophotographs described in the SWOP report (Chase *et al.*, 1957; Cote *et al.*, 1960). In the present paper we propose to describe some results obtained by a different method, which makes use of the recorded motions of a free-floating buoy. The method was first suggested by Barber (1946) and was developed by Longuet-Higgins (1946, 1955); the observations have been made at the National Institute of Oceanography since 1955. Simultaneously with the motions of the buoy, we have recorded the atmospheric pressure fluctuations close to the sea surface. Our present object is to describe the method and the results and to discuss them in the light of recent theories of the generation of water waves by wind.

THEORY OF THE METHOD

To a first approximation, a floating object may be regarded as performing small oscillations about a fixed point, with horizontal co-ordinates x, y and vertical co-ordinate z (measured upwards). Further, for waves sufficiently long compared with its diameter, a floating buoy will tend to have the same vertical and horizontal displacements as a particle in a free wave, and to take up the same orientation as the free surface.¹ Hence, if the motions of the buoy (i.e., vertical displacement and angles of pitching and rolling) can be recorded we shall have available the quantities

$$\xi, \frac{\partial \xi}{\partial x}, \frac{\partial \xi}{\partial y} \quad (1)$$

as functions of time, where $\xi(x, y, t)$ denotes the elevation of the free surface.

As a representation of the sea surface we may take the stochastic integral

$$\xi = \mathcal{R} \iint e^{i(kx - \sigma t)} dA(k), \quad (2)$$

where $\mathbf{x} = (x, y)$ and $\mathbf{k} = (k \cos \phi, k \sin \phi)$ represents a vector wave-number. To a first approximation the frequency σ satisfies the well-known relation for waves on deep water:

$$\sigma^2 = gk. \quad (3)$$

The directional spectrum $F(\sigma, \phi)$ of the waves is defined by

$$F(\sigma, \phi) = \frac{\overline{\frac{1}{2} dA dA^*}}{d\sigma d\phi} \quad (4)$$

(where a star denotes the complex conjugate, and a bar denotes the mean value). In other words, $F(\sigma, \phi) d\sigma d\phi$ is the contribution to the mean-square value of ξ arising from wave elements which lie in the infinitesimal ranges of frequency and direction $(\sigma, \sigma + d\sigma)$ and $(\phi, \phi + d\phi)$.²

Suppose then that the three quantities of (1) are denoted by ξ_1, ξ_2, ξ_3 . We have

$$\left. \begin{aligned} \xi_1 &= \mathcal{R} \iint e^{i(kx - \sigma t)} dA \\ \xi_2 &= \mathcal{R} \iint ik \cos \phi e^{i(kx - \sigma t)} dA \\ \xi_3 &= \mathcal{R} \iint ik \sin \phi e^{i(kx - \sigma t)} dA \end{aligned} \right\} \quad (5)$$

By numerical methods or otherwise we may form the co-spectra C_{ij} and the quadrature-spectra Q_{ij} of any pair of quantities ξ_i and ξ_j . From the definitions we have

$$\left. \begin{aligned} C_{11} &= \int_0^{2\pi} F(\sigma, \phi) d\phi \\ C_{22} &= \int_0^{2\pi} k^2 \cos^2 \phi F(\sigma, \phi) d\phi \\ C_{33} &= \int_0^{2\pi} k^2 \sin^2 \phi F(\sigma, \phi) d\phi \end{aligned} \right\} \quad (6)$$

² In terms of the two-dimensional spectrum $E(\mathbf{k})$ used in Longuet-Higgins (1957) we have $F = \frac{1}{2} \frac{dk}{d\sigma} E = \frac{2k^3}{\sigma} E$.

¹ Later on, calibrated response factors, appropriate to each wave length and frequency, are used.

OBSERVATIONS OF DIRECTIONAL SPECTRUM OF SEAWAVES USING FLOATING BUOY MOTIONS

and

$$\left. \begin{aligned} C_{23} &= \int_0^{2\pi} k^2 \cos \phi \sin \phi F(\sigma, \phi) d\phi \\ Q_{12} &= \int_0^{2\pi} k \cos \phi F(\sigma, \phi) d\phi \\ Q_{13} &= \int_0^{2\pi} k \sin \phi F(\sigma, \phi) d\phi \end{aligned} \right\} (7)$$

each of the above six quantities being a function of σ . The right-hand sides are clearly related to the Fourier coefficients

$$a_n + ib_n = \frac{1}{\pi} \int_0^{2\pi} e^{in\phi} F(\sigma, \phi) d\phi \quad (8)$$

of the spectrum $F(\sigma, \phi)$, and in fact

$$\left. \begin{aligned} a_0 &= \frac{1}{\pi} C_n \\ a_1 &= \frac{1}{\pi k} Q_{12}, \quad b_1 = \frac{1}{\pi k} Q_{13} \\ a_2 &= \frac{1}{\pi k^2} (C_{23} - C_{32}), \quad b_2 = \frac{2}{\pi k^2} C_{23} \end{aligned} \right\} (9)$$

We can therefore obtain from the motions of the buoy, the first five Fourier coefficients of the angular distribution of energy and thus the first five terms of the series

$$\begin{aligned} F_1(\sigma, \phi) &= \frac{1}{2} a_0 + (a_1 \cos \phi + b_1 \sin \phi) \\ &\quad + (a_2 \cos 2\phi + b_2 \sin 2\phi) \\ &\quad + \dots \end{aligned} \quad (10)$$

From ζ , $\partial\zeta/\partial x$, and $\partial\zeta/\partial y$ it is not possible to get higher coefficients, but more terms could be obtained if quantities such as $\partial^2\zeta/\partial x^2$, $\partial^2\zeta/\partial x \partial y$, etc., could be measured.³

What then can be done with this amount of information? In the first place we can form the partial Fourier sum

$$F_1(\sigma, \phi) = \frac{1}{2} a_0 + (a_1 \cos \phi + b_1 \sin \phi) + (a_2 \cos 2\phi + b_2 \sin 2\phi). \quad (11)$$

This may be a fair approximation to the infinite series (Equation 10) provided that terms of higher order are relatively small. On the other hand, substitution for a_0 , a_1 , b_1 , a_2 , b_2 in Equation 11 shows that

$$F_1(\sigma, \phi) = \frac{1}{2\pi} \int_0^{2\pi} F(\sigma, \phi') W_1(\phi' - \phi) d\phi' \quad (12)$$

where

$$\begin{aligned} W_1 &= 1 + 2 \cos(\phi' - \phi) + 2 \cos 2(\phi' - \phi) \\ &= \frac{\sin \frac{5}{2}(\phi' - \phi)}{\sin \frac{1}{2}(\phi' - \phi)} \end{aligned} \quad (13)$$

In other words, the partial sum $F_1(\sigma, \phi)$ is the smoothed average of the actual distribution $F(\sigma, \phi)$ by the weighting function $W_1(\phi' - \phi)$. Since W_1 can be negative, it is possible that F_1 may be negative too, whereas $F(\sigma, \phi)$ itself is essentially positive. One may therefore prefer, as in the present paper, to take an alternative approximation to $F(\sigma, \phi)$, namely

$$\begin{aligned} F_2(\sigma, \phi) &= \frac{1}{2} a_0 + \frac{2}{3} (a_1 \cos \phi + b_1 \sin \phi) \\ &\quad + \frac{1}{3} (a_2 \cos 2\phi + b_2 \sin 2\phi) \end{aligned} \quad (14)$$

which corresponds to the weighted average of $F(\sigma, \phi)$ by the weighting function

$$\begin{aligned} W_2 &= 1 + \frac{4}{3} \cos(\phi' - \phi) + \frac{1}{3} \cos 2(\phi' - \phi) \\ &= \frac{2}{3} \cos^2 \frac{1}{2}(\phi' - \phi) \end{aligned} \quad (15)$$

W_2 is not only non-negative but is also a decreasing function of $|\phi' - \phi|$. Other weighting functions are of course possible; which particular function one chooses is to some extent a matter of taste, since each of the averages $F_i(\sigma, \phi)$ is a weighted average of each of the others.

Apart from the weighted averages just mentioned, the first five coefficients a_0 , a_1 , b_1 , a_2 , b_2 can be used to provide some useful and significant parameters of the spectrum $F(\sigma, \phi)$. The simplest of these is a_0 itself, which measures the total energy per unit of frequency, summed over all possible directions.

Second, as a measure of the directional properties at each frequency we may define the two angles ϕ_1 and ϕ_2 which "best" fit the distribution, in the following sense. Consider the integral

$$I = \frac{1}{2\pi} \int_0^{2\pi} 16 \sin^2 \frac{\phi - \phi_1}{2} \sin^2 \frac{\phi - \phi_2}{2} F(\sigma, \phi) d\phi \quad (16)$$

where ϕ_1 and ϕ_2 are any angles. I may easily be expressed in terms of ϕ_1 , ϕ_2 and the five known coefficients a_0 , a_1 , b_1 , a_2 , b_2 . We now choose ϕ_1 and ϕ_2 so as to make I a minimum.

This definition is clearly appropriate in the extreme case when swell is coming from two direc-

³ An experimental program to measure the second derivatives of ζ is in progress.

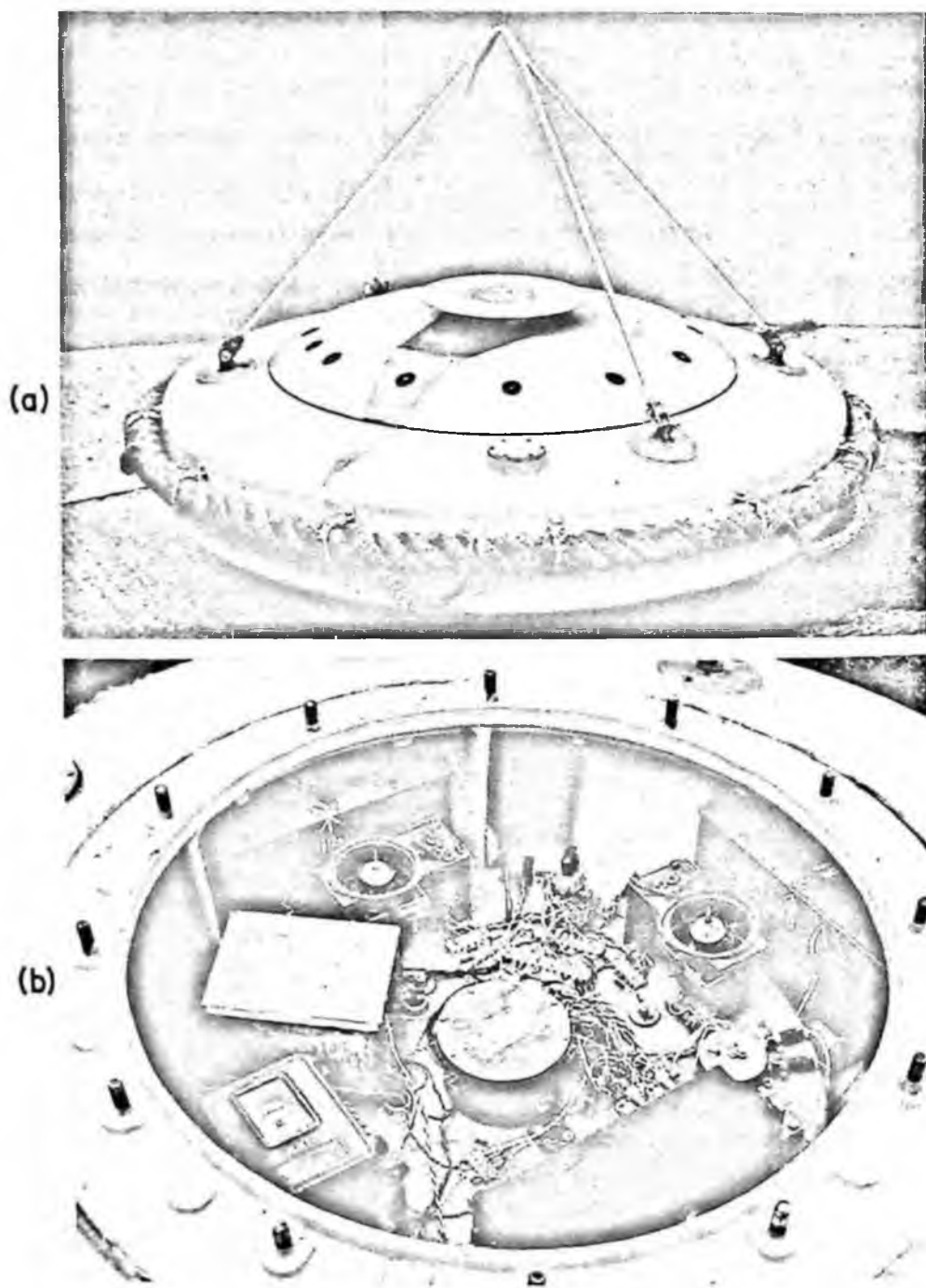


Figure 3-1-1. (a) Exterior view of the wave recording buoy;
(b) The instrument panel.

OBSERVATIONS OF DIRECTIONAL SPECTRUM OF SEAWAVES USING FLOATING BUOY MOTIONS

tions only, say α_1 and α_2 . For then $I/a_0 = 0$ only if ϕ_1, ϕ_2 coincide with α_1, α_2 ; if ϕ_1, ϕ_2 do not coincide with α_1, α_2 , then I/a_0 is positive, since there is a positive contribution to the integral at $\phi = \alpha_1, \alpha_2$, and the integrand is never negative.

In a more general case, when $F(\sigma, \phi)$ has a continuous distribution, the two "best" angles ϕ_1, ϕ_2 still have a useful significance. For if the spectrum is not too broad, the mean value

$$\bar{\phi} = \frac{1}{2}(\phi_1 + \phi_2) \quad (17)$$

approximates the mean direction of energy in the spectrum, and the half-difference

$$\psi = \frac{1}{2}|\phi_1 - \phi_2| \quad (18)$$

is a measure of the angular width of the spectrum. It is shown in the Appendix that ψ is approximately equal to the r.m.s. angular deviation of the energy from the mean direction.

Last, if I_{\min} is the minimum value of I (corresponding to the two "best" angles ϕ_1 and ϕ_2), then I_{\min}/a_0 is an indicator of the *shape* of the distribution $F(\sigma, \phi)$. For example, very small values of I_{\min}/a_0 would indicate that the energy was concentrated near two directions α_1, α_2 at most. In the Appendix it is shown that in general I_{\min}/a_0 is related to the fourth moment of the angular distribution of energy about the mean.

Formulae for calculating ϕ_1, ϕ_2 , and I_{\min}/a_0 in terms of the known coefficients a_0, a_1, b_1, a_2, b_2 are given in the Appendix.

APPARATUS

A general view of the buoy is shown in Figure 3-1-1. The frame is an aluminium alloy casting, of horizontal diameter 5'6", which when loaded floats in water up to the top of the vertical rim. It is surrounded by a stout hemp fender. The four-legged hoisting gear is secured at the base by four steel pins, which can quickly be removed. Inside the buoy (Figure 3-1-1(b)) can be seen the instrument panel. In the center is an accelerometer of a design similar to that used in the shipborne wave recorder (Tucker, 1952, 1956). The working part of the accelerometer is mounted on gimbals so that it tends to take up an orientation in line with the vector acceleration plus gravity. Since the water surface also tends to do just this, the accelerometer remains practically fixed relative to the buoy.

The electrical output from the accelerometer is integrated twice electronically before being re-

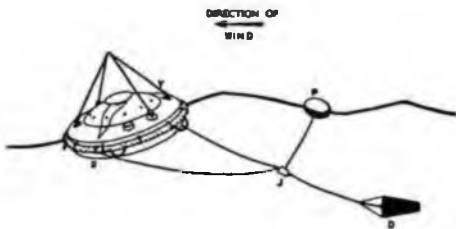
corded. (The integrating circuits are contained in the metal box nearest the accelerometer.) All recording was done by the 12-channel galvanometer-recording camera seen in the foreground.

Two gyroscopes for measuring angles of pitch and roll can be seen on the far side of the instrument board. Each is center-seeking with a time constant of about 6 minutes. The other instruments on the panel are time switches for making time marks on the record and for automatic operation of the equipment over predetermined intervals. The batteries are seen surrounding the instrument panel.

To record atmospheric pressure a very sensitive condenser-type microbarograph was built very similar to that described, for example, by Baird and Banwell (1948). For modifications to the interior design and to the accompanying electronic circuits we are indebted to Mr. R. Dobson and Mr. M. J. Tucker. The microbarograph and its electronics were situated in the lid of the buoy (see Figure 3-1-1(a)) and access to the atmosphere was through 12 small orifices (diameter 0.04 inch). To prevent sea water from blocking the instrument, a series of precautions was taken: the openings were raised 2.4 inches above the surface of the buoy (Figure 3-1-1(a)); the orifices themselves were surrounded by small heating elements (dissipating 5 watts per coil) so as to evaporate any spray blocking the passages (the time taken to clear any hole was a fraction of a second); the passages to the microbarograph were designed so that liquid penetrating the orifices was drained off into a drip-can beneath the instrument; and last, the passages were surrounded by dessicators. Together these arrangements proved effective.

To keep the buoy in a constant alignment relative to the wind, a drogue and pellet were attached, as in Figure 3-1-2. So far as could be judged from visual observation, the orientation of the buoy remained quite constant during any period of observation.

Figure 3-1-2. Arrangement for aligning the buoy with the wind.



OCEAN WAVE SPECTRA

Both the microbarograph and the integrated acceleration possessed phase and amplitude characteristics dependent upon frequency, which were measured in the laboratory. The buoy itself, because of its finite dimensions, had a varying response at the higher frequencies. Calibration of the heaving and pitching motions of the buoy relative to the elevation and slope of the waves in the absence of the buoy was carried out for us in the 1200-ft. wave tank at the Ship Hydrodynamics Laboratory (National Physical Laboratory). The calibrations covered the range $2.1 < \sigma < 4.5$ radians/sec. and indicated a "resonance" at around $\sigma = 4.0$ radians/sec. in both heave and pitch. However, because of the high damping, the amplitude response factors did not differ much from unity whenever $\sigma \geq 3.5$ radians/sec. All the response factors have been allowed for in the subsequent determination of the frequency spectra.

TREATMENT OF THE DATA

Out of 16 records obtained during 1955 and 1956, 5 were selected as being apparently free of faults over continuous stretches of time lasting 12 minutes or more. The corresponding positions, dates, and times, together with local wind speeds and directions as measured by the ship's anemometer, are given below in Table 1. It will be seen that conditions ranged from light winds (8 knots) to a fairly constant wind of force 6 (23 knots); this was near the limit for safe launching and recovery of the buoy. Charts showing the synoptic weather situations at about the times of recording are shown in Figure 3-1-3.

A typical record of the outputs from the two gyroscopes, the accelerometer (after integration), and the microbarograph is reproduced in Figure 3-1-4. Each of the four traces was digitized (manually) at intervals of approximately 0.5 sec., so that the records, 12-17 minutes long, contained about 2,000 sets of readings each. These were

stored on punched cards. The computation of the co-spectra and quadrature-spectra, which was carried out on the *Deuce* at the Royal Aircraft Establishment at Farnborough, was similar to that described by Blackman and Tukey (1958). A standard program computed the mean variance and auto- and cross-correlations of two given series of observations, with a total number of "lags" between 57 and 66. Another program was then used to compute the Fourier sine- and cosine-transforms, and the result was smoothed by consecutive weighting factors $\frac{1}{2}, \frac{1}{2}, \frac{1}{2}$.

The numerical results showed that the spectral density dropped to negligible values beyond $\sigma = 5$ radians/sec. confirming that the sampling interval was small enough not to introduce "aliasing" difficulties. Full calculations, however, were made only up to $\sigma = 4$ radians/sec., owing to the response characteristics of the buoy.

Finally, to allow for "noise" introduced by errors in reading the traces, a small constant was subtracted from each auto-spectrum. The errors were easily estimated by repeating a few digital conversions and corresponded to a standard error of about $1\frac{1}{2}$ units in 1,000 (about 0.2 mm. of the original film record).

Consideration was given to possible correction of the spectra for nonlinear effects. Tick (1958) has estimated the second-order correction to a uni-directional spectrum to allow for nonlinear terms in the boundary conditions at the free surface. The correction consists mainly of a superposed spectrum, largest in the region of frequencies double those of the largest waves. A rough calculation of the correction to $C_{11}(\sigma)$ for Record No. 5 (corresponding to the steepest waves) showed it to be small—about 10 per cent of C_{11} at $\sigma = 2$ to 3 radians/sec. Such corrections were therefore ignored. The corrections for non-verticallity of the accelerometer (Tucker, 1959) were appreciable only at low frequencies, for $\sigma < 0.4$ radians/sec., and similarly for the second-order corrections to slope. Since these corrections are

TABLE 1
DATA CONCERNING WAVE RECORDS

	Number of record	Date	Time (G.M.T.)	Position		Wind speed and direction (ship's anemometer)
Cruise I	1	31.5.55	0915-0935	41°08'N	14°37'W	19 kts. from 340°
	2	31.5.55	1435-1455	41°08'N	14°37'W	14 kts. from 350°
	3	3.6.55	0910-0930	39°16'N	11°53'W	17 kts. from 320°
Cruise II	4	30.10.56	1450-1510	50°58'N	12°15'W	8 kts. from 080°
	5	1.11.56	1525-1545	50°19'N	11°54'W	23 kts. from 065°

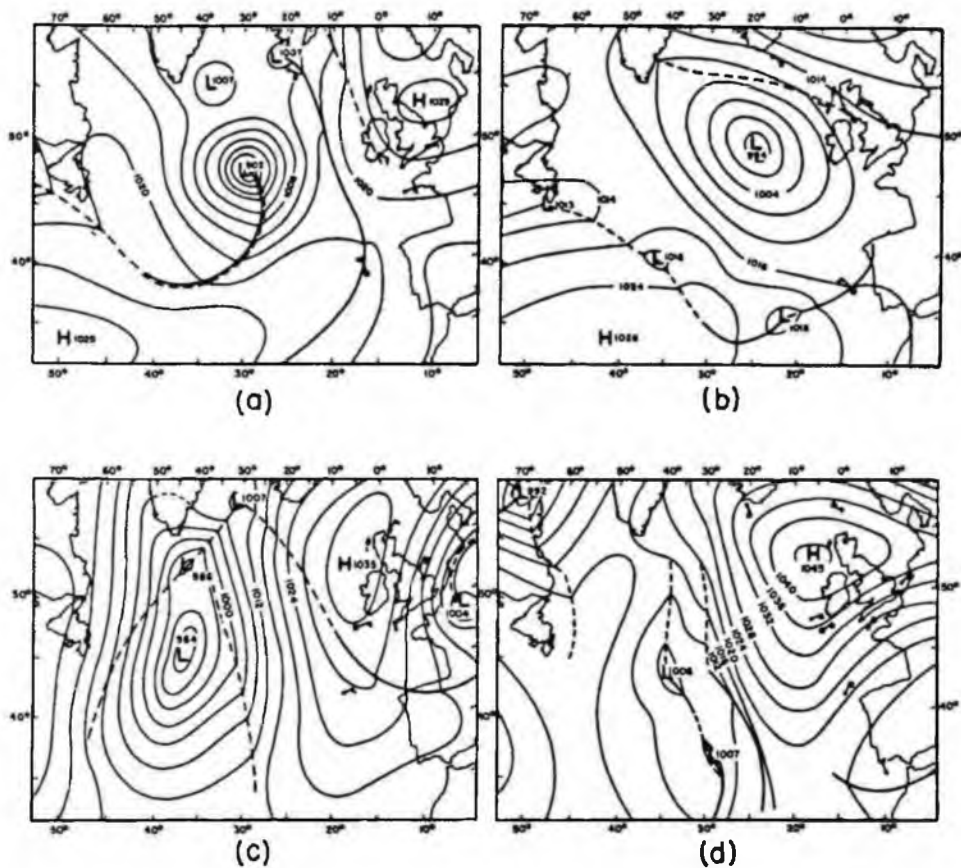


Figure 3-1-3. Synoptic charts of the weather situation a few hours before the times of recording. The position of the ship is marked by a full circle ●.

- (a) 0001 G.M.T., 31.5.55;
- (b) 0001 G.M.T., 3.6.55;
- (c) 0001 G.M.T., 30.10.56;
- (d) 0001 G.M.T., 1.11.56;

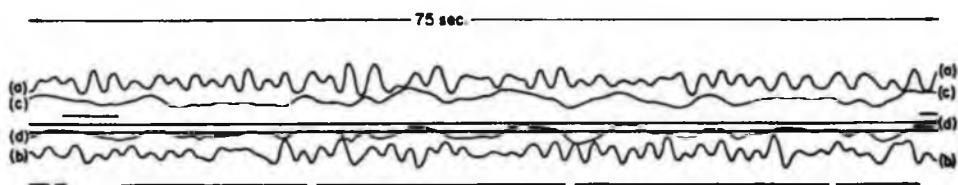


Figure 3-1-4. A typical length of film record, showing the traces of the four measured quantities:

- (a) angle of pitch;
- (b) angle of roll;
- (c) twice-integrated vertical acceleration;
- (d) atmospheric pressure.

OCEAN WAVE SPECTRA

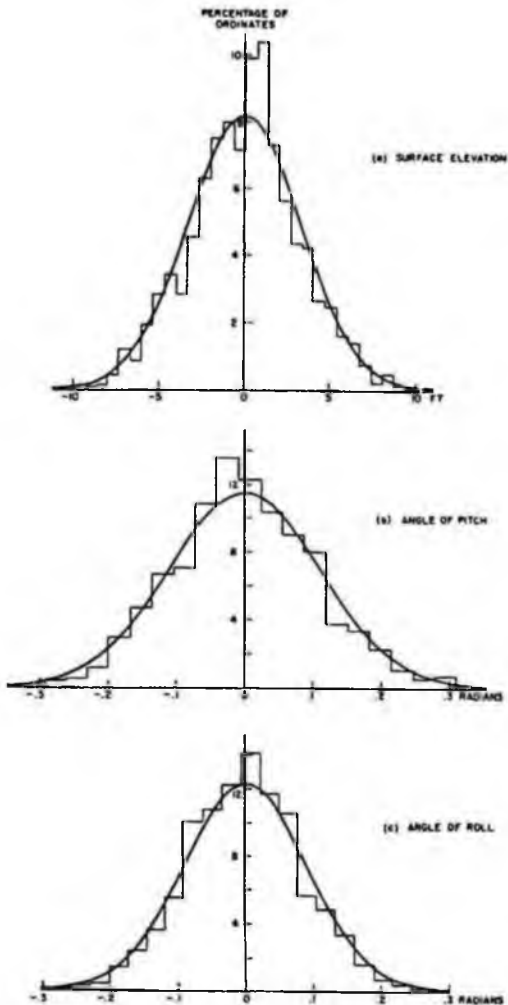


Figure 3-1-5. Histograms of the film traces, for record No. 5 (wind speed 23 knots).

(a) Heave; (b) Pitch; (c) Roll.

proportional to the square of the first-order spectra, they must be even smaller for records other than No. 5. They were not investigated further.

A further indication of the linearity of the waves was afforded by a comparison of the observed distributions of height and slope with the theoretical Gaussian distributions. The histograms for Record 5 (the highest wind speed) are shown in Figure 3-1-5. Visually the data fit the Gaussian curves fairly well, though a χ^2 -test based on the total number of observations (2,000) in each record does in fact give probabilities well below the 1 per cent significance level in each case.

RESULTS

The total variances of the wave elevation ζ and of the two components of slope $\partial\zeta/\partial x$, $\partial\zeta/\partial y$, in the frequency range $0.4 \leq \sigma \leq 4.0$ radians/sec., are listed in Table 2.

In only one case, Record No. 5, were the waves sufficiently free from external swell for the wave height to be directly related to the local wind speed. In that case the wind speed was $V = 23$ knots over a well-defined fetch of 300 miles. The observed r.m.s. elevation of 2.6 ft. may be compared with the value 2.8 ft. given by the empirical formula $\sqrt{0.121(V/10)^2}$ of Pierson, Neumann and James (1955) and 2.2 ft. given by the formula $0.00405V^2$ of Darbyshire (1959).

The variances of the surface slopes, which depend chiefly upon the shorter waves, have been plotted against local wind speed in Figure 3-1-6. As was found by Cox and Munk (1954, 1956), the variances increase about proportionally to the wind speed. However, the actual values for the total variance are only about 20 per cent of those suggested by Cox and Munk's optical method (0.053 radians² at 10 m/sec.). This presumably is because most of the slope variance is contributed by waves of frequency σ greater than 4.0 radians/sec.

TABLE 2
VARIANCES OF WAVE HEIGHTS AND SLOPES

Number of record	Wave height (ft)	Angle of roll (deg ² x 10 ³)	Angle of pitch (deg ² x 10 ³)	Total angle (deg ² x 10 ³)	Ratio of angular variances
1	1.92	2.80	3.25	6.1	1.16
2	2.09	2.34	3.65	6.0	1.56
3	2.33	1.95	3.83	5.8	1.97
4	2.03	1.82	2.24	4.1	1.23
5	6.58	4.19	7.81	12.0	1.86

OBSERVATIONS OF DIRECTIONAL SPECTRUM OF SEAWAVES USING FLOATING BUOY MOTIONS

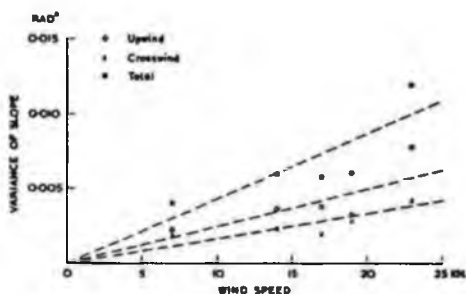


Figure 3-1-6. Variances of surface slope:
(a) up-wind; (b) cross-wind; (c) total.

The frequency spectra of the surface elevation (regardless of direction) are shown in Figure 3-1-7 (i) to (v). Both the scales are logarithmic. In each of the figures a straight line has been inserted corresponding to Phillips' (1958a) limiting spectrum¹

$$C_{11}(\sigma) = Cg^2\sigma^{-5}, \quad (19)$$

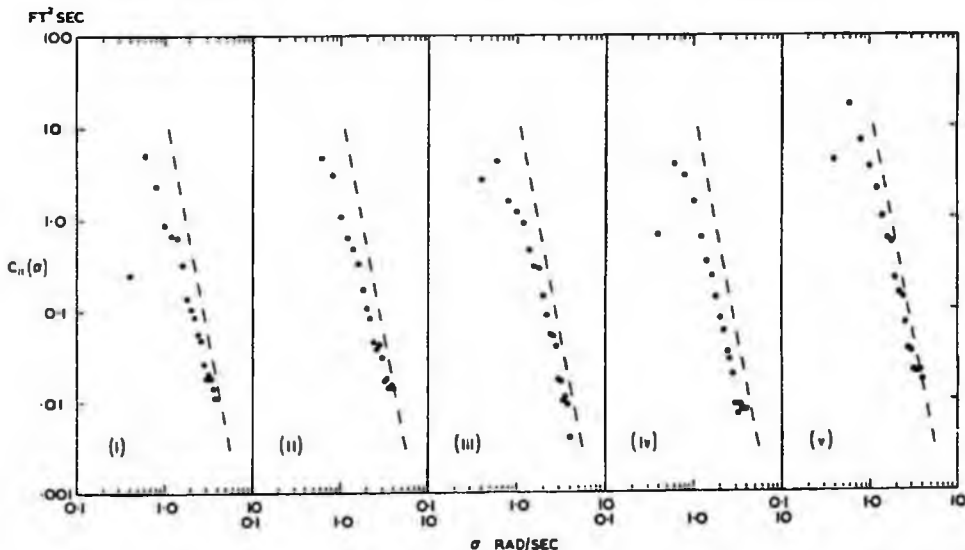
¹ Phillips' (1958a) uses $\Phi(\sigma)$, equivalent to $\frac{1}{2} C_{11}(\sigma)$.

with the constant $C = 14.8 \times 10^{-1}$ chosen to fit Burling's (1955) data. It will be seen that the nearest approach to this spectrum is in Record 5, corresponding to the highest wind speed.

We come now to the directional properties of the spectra. For each of the five records, the "smoothed" spectra $F_3(\sigma, \phi)$, defined by equation (15), have been computed, and these are shown in Figure 3-1-8.

The weather charts in Figure 3-1-3 show that the mean directions in each frequency band do in fact correspond fairly closely to the directions of the winds expected to generate the waves ($\phi = 0$ corresponds to the local wind. In Records 1, 2, and 4, and to a lesser extent in Record 3 there is some change in the mean direction with frequency. In Record 5 the mean direction is practically constant between $\sigma = 0.6$ and 3.6, and this corresponded to a situation in which the wind was in a steady direction from the ENE with little possibility of interfering swell. On the other hand, in Records 1 and 2 there is evidence of secondary maxima in the spectrum (necessarily smoothed out by the weighting function W_3), which can be shown to correspond to swell from different wind systems.

Figure 3-1-7. Frequency spectra of surface elevation.



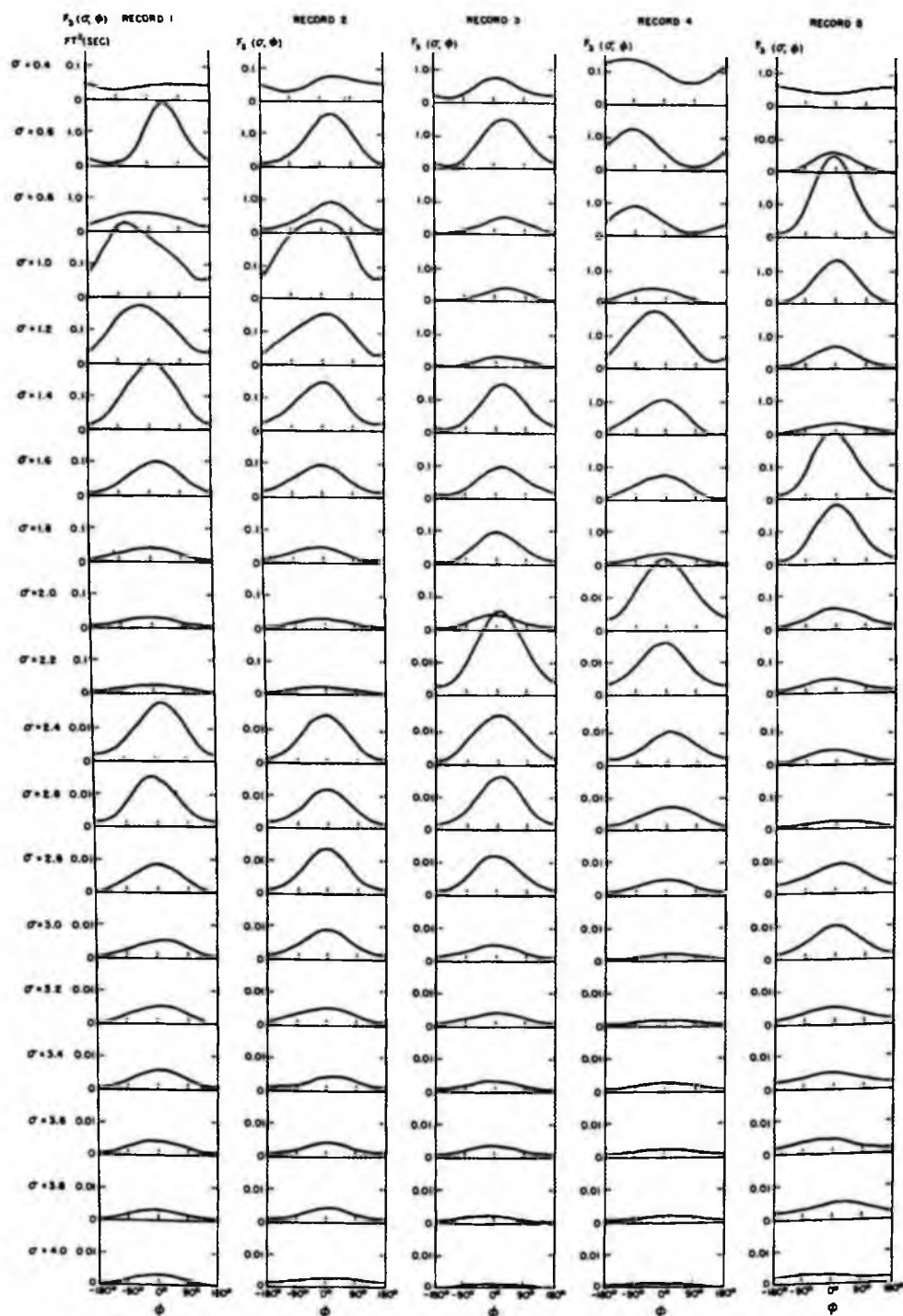


Figure 3-1-8. Smoothed estimates of the directional spectrum.
 [Note added in proof: In Record 4, $\sigma = 1.2$ to 1.8 , the vertical scale should be 0.1]

OBSERVATIONS OF DIRECTIONAL SPECTRUM OF SEAWAVES USING FLOATING BUOY MOTIONS

ANGULAR WIDTH OF THE SPECTRUM

The angle ψ defined in Section 2 has been plotted in Figure 3-1-9 as a function of the ratio U_1/c , where U_1 is the reference wind velocity, defined on page 123, and $c = g/\sigma$ is the speed of the waves of frequency σ . Only those data from Records 3 and 5 have been used in which the wind direction was practically constant over the region of wave generation.

If we neglect the two observations at $\sigma = 0.4$, which may be influenced by external swell, it appears that the angle ψ increases as the ratio U_1/c increases; in other words, that the angular width of the spectrum increases with the ratio of wind speed to wave speed.

The curves inserted in Figure 3-1-9 are discussed below (page 124).

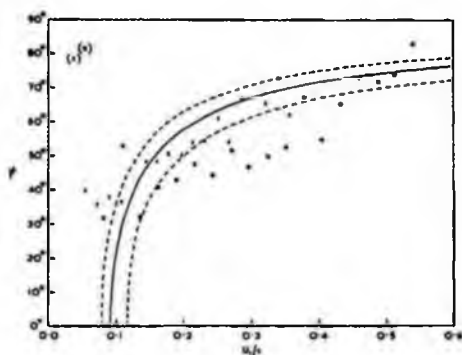


Figure 3-1-9. Observations of the angular width ψ . \times = Record 3; \bullet = Record 5.

COMPARISON WITH THE SWOP RESULTS

An exact comparison with the results obtained by the stereographic method of Chase *et al.* (1957) is not possible, since an instantaneous stereophotograph does not in principle distinguish opposite directions in the spectrum. Hence, the stereographic method is unable, without some further assumption, to yield the coefficients a_n , b_n corresponding to *odd* harmonics of the angular distribution of energy. In face of this situation, Chase *et al.* have assumed $F(\sigma, \phi)$ to be zero when ϕ differs by more than 90 degrees from the wind direction — an assumption which we prefer not to make. It follows that any comparison of our data

with the SWOP data must be carried out through the harmonics a_n , b_n of *even* order.

One suitable parameter for this purpose can be defined as follows. Let

$$m_2(\sigma, \phi') = \int_0^{2\pi} \sin^2(\phi - \phi') F(\sigma, \phi) d\phi \quad (20)$$

denote the second moment of the distribution of energy about the direction ϕ' . In terms of the Fourier coefficients,

$$m_2(\sigma, \phi') \propto a_0 - (a_2 \cos 2\phi' + b_2 \sin 2\phi') \quad (21)$$

The maximum and minimum values of this function are $a_0 \pm \sqrt{a_2^2 + b_2^2}$, and they occur in two pairs of directions, mutually at right angles. A measure of the angular spread of the spectrum in the frequency band $(\sigma, \sigma + d\sigma)$ is, therefore,

$$\gamma(\sigma) = \left[\frac{(m_2)_{\min}}{(m_2)_{\max}} \right]^{1/2} = \left[\frac{a_0 - \sqrt{a_2^2 + b_2^2}}{a_0 + \sqrt{a_2^2 + b_2^2}} \right]^{1/2} \quad (22)$$

When the spectrum is narrow, it can be shown that $\gamma(\sigma)$ is almost equal to the r.m.s. angular deviation of energy in the spectrum.

To fit the SWOP data, Chase *et al.* have suggested the empirical formula

$$F(\sigma, \phi) = P(\sigma) \times \begin{cases} 1 + [0.50 + 0.82Q(\sigma)] \cos 2\phi \\ \quad + 0.32Q(\sigma) \cos 4\phi, & |\phi| < \frac{\pi}{2}, \\ 0, & |\phi| > \frac{\pi}{2}, \end{cases} \quad (23)$$

where

$$Q(\sigma) = e^{-1/2(\sigma V/\sigma)^4} \quad (24)$$

and $P(\sigma)$ is another function of σ and V only. According to this formula we should have

$$a_2 = 0.25 + 0.41Q(\sigma), \quad b_2 = 0, \quad (25)$$

and so

$$\gamma(\sigma) = \left[\frac{0.75 - 0.41Q(\sigma)}{1.25 + 0.41Q(\sigma)} \right]^{1/2} \quad (26)$$

The theoretical curve is shown in Figure 3-1-10 together with our observed results. It will be seen that our results are not inconsistent with the SWOP curve.

SHAPE OF THE SPECTRUM

It was seen in Section 2 above that an indicator of the shape of the spectrum is the ratio I_{\min}/a_0 .

OCEAN WAVE SPECTRA

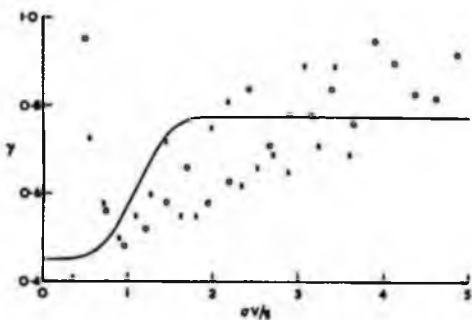
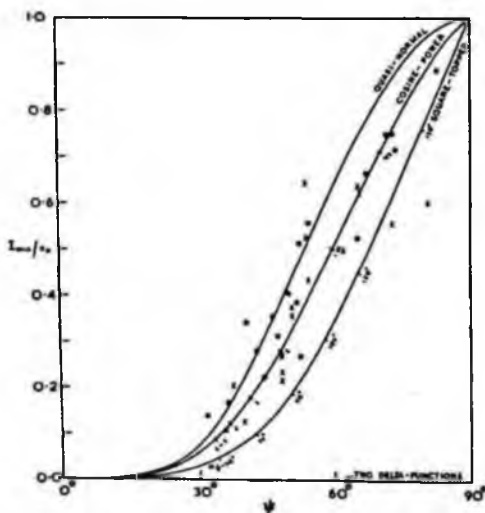


Figure 3-1-10. Observations of ψ (σ), compared with the SWOP curve. \times = Record 3; \circ = Record 5.

In Figure 3-1-11 this ratio has been plotted against the corresponding angular half-width ψ for the two Records 3 and 5 for which the wind system was simplest (from this point of view greater weight should be given to Record 5, the data for which are indicated by circles).

For comparison, we have plotted in the same figure the values of I_{\min}/a_0 and ψ corresponding to some very simple distributions.

Figure 3-1-11. I_{\min}/a_0 plotted against ψ . \times = Record 3; \circ = Record 5.



(1) The line drawn along the ψ -axis corresponds to an idealised distribution consisting of (at most) two narrow bands of long-crested waves:

$$F(\sigma, \phi) \propto \delta(\phi - \alpha_1) + \delta(\phi - \alpha_2). \quad (27)$$

For such a distribution we have seen that I_{\min}/a_0 vanishes.

(2) The lowest of the three curves corresponds to a "square-topped" angular distribution of given width $2\phi_0$:

$$F(\sigma, \phi) \propto \begin{cases} 1, & |\phi| < \phi_0 \\ 0, & |\phi| > \phi_0 \end{cases} \quad (28)$$

(The given values of ϕ_0 are indicated along the curve.)

(3) The middle continuous curve corresponds to the cosine-power distribution

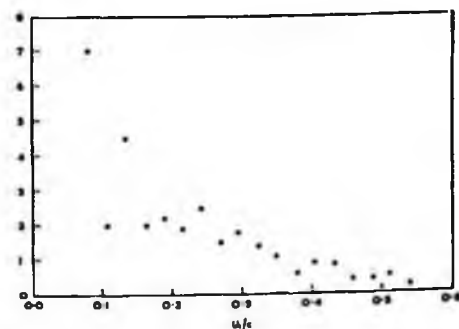
$$F(\sigma, \phi) \propto (1 + \cos \phi)^s \propto \cos^{2s}(\frac{1}{2}\phi) \quad (29)$$

for which

$$\frac{a_n}{a_0} = \frac{s(s-1) \dots (s-n+1)}{(s+1)(s+2) \dots (s+n)} \quad (30)$$

(The value of the parameter s is indicated along the curve.) When $s = 0$, then the distribution is independent of ϕ , and as s increases, the distributions become more and more concentrated about the mean direction $\phi = 0$. When s is large, the distributions are approximately normal, with angular variance equal to $(2/s)$ radians².

Figure 3-1-12. Closest values of the parameter s corresponding to the plotted points of Fig. 3-1-11 (data from Record 5).



OBSERVATIONS OF DIRECTIONAL SPECTRUM OF SEAWAVES USING FLOATING BUOY MOTIONS

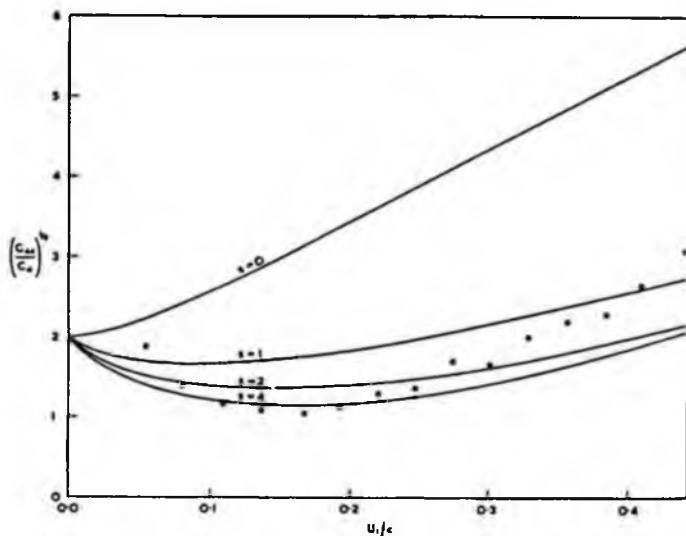


Figure 3-1-13. Values of $(C_u/C_{11})^{1/2}$, giving ratio of spectral densities of pressure (in ft. of air) and surface elevation.

(4) The upper continuous curve corresponds to the "quasi-normal" distribution

$$F(\sigma, \phi) \propto e^{-2\Delta^{-2} \sin^2 \phi/2} \quad (31)$$

which when Δ is small also approximates a normal distribution. For this distribution it is found that

$$\frac{\alpha_n}{\alpha_0} = \frac{I_n(\Delta^{-2})}{I_0(\Delta^{-2})} \quad (32)$$

where $I_n(z)$ is the Bessel function of imaginary argument.

Of the four laws considered, it appears that the cosine-power (28) is the best fit to the observations. For each observation, a corresponding value of s may be allotted by taking the point on the "cosine-power" curve nearest to the observation. The values of s so obtained have been plotted in Figure 3-1-12 against the value of U_1/c for each observation. It will be seen that in general s is a decreasing function of U_1/c .

THE PRESSURE FLUCTUATIONS

From the typical length of record shown in Figure 3-1-4 it will be seen that the trace of atmospheric pressure has a general tendency to follow the trace of surface elevation; and when the spectra of the pressure fluctuations were computed

they were found to be very similar in general to the spectra of surface elevation. Figure 3-1-13 gives the ratio of the spectral density of pressure (units are feet of air) to the spectral density of surface elevation in the typical case of Record 5. The theoretical curves drawn in the same figure are based on the discussion given below.

DISCUSSION OF RESULTS

We propose now to discuss our results relating to the angular distribution of energy in the light of what is known or conjectured about the processes of wave generation by wind.

In the first place, we need some estimate of the wind profile. Observations at sea (Roll, 1948; Hay, 1955) appear to support a logarithmic form for the mean wind velocity U , in conditions of neutral stability:

$$U = U_1 \log_e \left(\frac{z}{z_0} \right) \quad (33)$$

where U_1 and z_0 are constants. We have

$$U_1 = \frac{U_*}{K} \quad (34)$$

where U_* is the friction velocity ($= \sqrt{\tau_0/\rho_a}$) and K is von Karman's constant ($=0.41$). U_* may,

in turn, be expressed in terms of the "anemometer wind speed" U_0 by

$$U_*^2 = c_D U_0^2, \quad (35)$$

where c_D is a drag coefficient. Sheppard (1958) quotes the empirical formula

$$c_D = (0.08 + 0.00114 U_0) \times 10^{-3}, \quad (36)$$

U_0 in cm/sec.

U_0 will be identified with the measured wind speed V , so that

$$U_1 = \frac{c_D^{1/2}}{K} U_0, \quad (37)$$

is of order $V/10$.

On dimensional grounds, Charnock (1955) has suggested that

$$z_0 = \frac{U_*^2}{g\alpha} \quad (38)$$

where α is a constant. Not all observations give a consistent value of α , but Hay's (1955) data support a value of around 13 (see Ellison, 1956). Miles (1957) has introduced the parameter

$$\Omega = \frac{gz_0}{U_1^2} = \frac{gz_0 K^2}{U_*^2} = \frac{K^2}{\alpha}, \quad (39)$$

whose value is thus about 1.3×10^{-2} ; but it may well vary by a factor of 2. Since surface waves of length $2\pi/k$ must travel with almost the free-wave velocity $c = (g/k)^{1/2}$, it follows that (33) can be written

$$\frac{U}{c} = \frac{U_1}{c} \log_* \left(\frac{kz}{\Omega(U_1/c)^2} \right), \quad (40)$$

the right-hand side being a function only of kz , U_1/c , and Ω .

THE RESONANCE ANGLE

At the present time, two kinds of mechanism for the transfer of energy to water waves from the atmosphere are under active discussion. On the one hand, the effect of pressure fluctuations (associated with atmospheric turbulence) acting on the surface of the water has been considered by Phillips (1957, 1958b). According to Phillips' original hypothesis, the spectrum of the water surface in the principal stage of development would be given by¹

$$F(\sigma, \phi) = \frac{k^3 \sigma t}{2(g\rho_0)^2} \int_0^\infty \Pi(\mathbf{k}, \tau) \cos \left[\left(\frac{U \cos \phi}{c} - 1 \right) \sigma \tau \right] d\tau, \quad (41)$$

where t denotes the time since the wind started to blow, $\Pi(\mathbf{k}, \tau)$ is the pressure spectrum, defined by Phillips, and U is the "convection velocity" of the eddies of wavenumber \mathbf{k} . This velocity is probably not very different from the mean wind speed at a height above the surface of order $2\pi/k$. Phillips pointed out that if the pressure spectrum is reasonably isotropic, the integral on the right-hand side of (41) is likely to be greatest when

$$U \cos \phi = c \quad (42)$$

in other words, when the component of the wind velocity in the direction of propagation is just equal to the wave speed. This may be called the resonance condition, and the corresponding angle

$$\phi = \sec^{-1} \frac{U}{c} \quad (43)$$

may be called the resonance angle.

Let us assume that the convection velocity, as defined by Phillips (1957), can be identified with the mean velocity U at a height $z = 2\pi/k$. Writing $kz = 2\pi$ in Equation (9.40), we have

$$\phi = \sec^{-1} \left[\frac{U_1}{c} \left(\log \frac{2\pi}{\Omega} - 2 \log \frac{U_1}{c} \right) \right] \quad (44)$$

If we were to take the velocity at a different height, say π/k , this would be equivalent to a change in the assumed value of Ω by a factor 2.

We have calculated the angle ϕ corresponding to (43) taking, for definiteness, $\Omega = 1.3 \times 10^{-2}$; the result is indicated by the full curve in Figure 3-1-9. The lower broken curve shows the effect of taking a value of Ω five times greater than this, and the upper curve the effect of taking Ω five times less.

Two conclusions are obvious. In the first place, the value of the resonance angle ϕ depends only slightly on the parameters of the logarithmic profile, and second, the angle ψ does indeed show a trend similar to the resonance angle.

On the other hand, Miles (1957, 1959) has considered the growth of an air-water interfacial disturbance as an instability in the shearing flow of the air, or rather, of the combined air-water system. An input of energy into the waves is brought about (according to this model) by a coupling of the surface pressure fluctuations to the already existing waves. Assuming that the air-

¹ Phillips' $\phi(k, t)$ is equivalent to $2F(\sigma, \phi) \frac{d\sigma}{k} \frac{d\phi}{d\sigma}$, that is to say, to $(g/\sigma k)F$. Our $\Pi(k, t)$ is the same as his.

OBSERVATIONS OF DIRECTIONAL SPECTRUM OF SEAWAVES USING FLOATING BUOY MOTIONS

flow may be treated as a small perturbation of the mean wind profile (so that the perturbed potential satisfies the Orr-Sommerfeld equation) and that the mean profile is logarithmic, Miles has computed values for the rate of growth of the waves which are in substantial agreement with observation.

More recently (1960) Miles has combined his mechanism with that of Phillips, in such a way that the turbulent pressure fluctuations in the air-stream appear as the means of initiating the waves, which are then augmented by the instability of the shear flow. Thus, in place of (41) Miles proposes a more general equation (4.5a)¹ which we rewrite as follows:

$$F(\sigma, \phi) = \frac{k^2 \sigma t}{2(g\rho_w)^2} \mathcal{F}(MT) \int_0^\infty \Pi(k, t) \cos \left[\left(\frac{U \cos \phi}{c} - 1 \right) \sigma t \right] dt, \quad (45)$$

where

$$M = \frac{\rho_a}{\rho_w} \left(\frac{U_1 \cos \phi}{c} \right)^2 \frac{U_1}{c} \beta, \quad (46)$$

$$T = \frac{gt}{U_1}$$

and

$$\mathcal{F}(MT) = \frac{e^{MT} - 1}{MT} \quad (47)$$

Here β is a dimensionless coefficient which has been computed by Miles (1959). For small values of T , and so for small values of MT , the function $\mathcal{F}(MT)$ tends to 1, and equation (45) tends to (41). Initially, therefore, the Phillips spectrum is applicable. However, as t increases, MT may become large, and $\mathcal{F}(MT)$ exponentially large. In that case, if (45) is still valid, the function $\mathcal{F}(MT)$ represents a factor by which the original spectrum F is distorted. Since M depends upon the direction of propagation ϕ , so also does $\mathcal{F}(MT)$.

Using Miles' values of β , and taking as before $\Omega = 1.3 \times 10^{-2}$, we have computed M as a function of ϕ for various values of U_1/c (see Figure 3-1-14). From this graph it is fairly simple to compute $\mathcal{F}(MT)$ for any given record, if T is known. For Record 5, for example, we have taken

$$U_a = 23 \text{ kn} = 1,180 \text{ cm/sec}$$

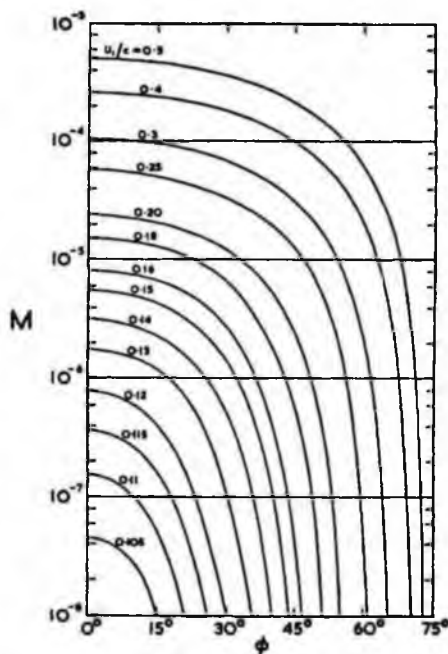


Figure 3-1-14. M as a function of the angle ϕ , (taking $\Omega = 1.3 \times 10^{-2}$).

$$c_D = (0.08 + 0.00114U_a) \times 10^{-2}$$

$$= 2.15 \times 10^{-3}$$

$$U_1 = \frac{c_D^2}{K} U_a = 134 \text{ cm/sec}$$

$$\frac{U_1}{c} = \frac{\sigma U_1}{g} = 0.136\sigma \quad (\sigma \text{ in radians/sec})$$

According to the weather charts, the length of time since the wind began to blow was about 45 hours. However, the fetch L being limited to 300 miles, the spectrum at the lower frequencies is limited by fetch. We have taken $t \leq L \div$ group velocity $= 2\sigma L/g$, and so

$$T = \frac{gt}{U_1} = \min \left\{ \begin{array}{l} 0.72 \times 10^6 \sigma \\ 1.28 \times 10^6 \end{array} \right\}$$

With these values, the factor $\mathcal{F}(MT)$ is as shown in Figure 3-1-15.

The most striking feature of the figure is the very large amplification factors involved, especially at the higher frequencies. These, however, need not be taken literally, for we saw in Section 5

¹ Compare Phillips (1960).

OCEAN WAVE SPECTRA

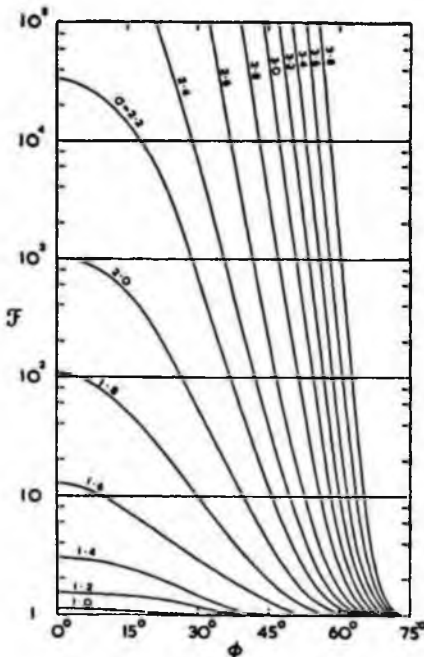


Figure 3-1-15. Curves of the distortion factor \mathcal{F} as a function of angle ϕ , for Record No. 5.

that at the higher frequencies ($\sigma > 2.0$ radians/sec) the total spectrum approaches Phillips' equilibrium law; this indicates that nonlinear effects associated with breaking of the waves are predominant, and a linear theory would no longer apply. Nevertheless, at some of the lower frequencies ($1.3 < \sigma < 2.0$) it would appear that the effect of Miles' coupled mechanism would be to narrow somewhat the angular distribution of energy. Referring again to Figure 3-1-9, we have apparent confirmation of this, since in the range $0.15 < U_1/c < 0.4$ (i.e., $1.1 < \sigma < 3.0$) the angular width of the spectrum for Record 5 is somewhat less than the resonance angle.

On this interpretation then, the sequence of events would be as follows: in the first stage of development of the waves, exemplified by the range $\sigma < 1.1$ in Record 5, the waves are due mainly to uncoupled turbulent pressure fluctuations in the air. At a later stage, exemplified by the range $1.3 < \sigma < 2.0$, the shear-flow instability mechanism takes over, and this has the effect of reducing the r.m.s. angular width of the spectrum in any given frequency band from the value indi-

cated by the resonance angle. Finally the spectrum is limited by breaking of the waves, and it would appear from Figure 3-1-9 that there is some associated broadening of the directional spectrum. This also can be understood from Figure 3-1-15, for if \mathcal{F} is limited by nonlinear effects to a certain value, say 10^4 , it will be seen that the higher the frequency the broader is the angular spread of \mathcal{F} . This is quite apart from any broadening of the spectrum that may be due to breaking and other nonlinear effects.

INTERPRETATION OF THE PRESSURE FLUCTUATIONS

In his original paper (1957) Phillips assumed a value for the m.s. turbulent pressure fluctuations in the air equal to

$$\overline{p^2} = 9 \times 10^{-2} \rho_a^2 U_a^4 \quad (48)$$

where U_a denotes anemometer wind speed. This is equivalent to

$$\left(\frac{p}{\rho_a c}\right)^2 = \frac{0.09 U_a^4}{g^2} \quad (49)$$

In Table 3 the above value is compared with the mean-square values actually observed in Records 1-5. The comparison confirms what had been suspected by both Phillips (1958b) and Miles (1960), namely that the pressure fluctuations are generally smaller than those originally assumed in Phillips (1957).

TABLE 3
VARIANCES OF THE ATMOSPHERIC PRESSURE FLUCTUATIONS

Record No.	U_a (ft./sec.)	$\frac{0.09 U_a^4}{g^2}$ (ft. ²)	$\left(\frac{p}{\rho_a c}\right)^2$ (ft. ²)
1	32	91	7.3
2	24	29	8.2
3	29	62	5.2
4	14	3	9.8
5	39	203	13.1

Moreover, we shall now show that a substantial part of the observed pressure fluctuations can be attributed simply to the flow of air over the undulating surface of the sea.

In Miles' (1957, 1959) model the aerodynamical pressure exerted on a sinusoidal boundary

$$\zeta = \Re a e^{i(kx - \omega t)} \quad (50)$$

OBSERVATIONS OF DIRECTIONAL SPECTRUM OF SEAWAVES USING FLOATING BUOY MOTIONS

by an airstream in the direction of wave propagation has the form

$$p = \Re(\alpha + i\beta)\rho_a U_1^2 k\xi, \quad (51)$$

where α and β are real, non-dimensional quantities depending on the wind profile. To (51) we must add the static pressure term $-\rho_a g\xi$. Thus, the total pressure measured by an apparatus floating in the surface is

$$p = \Re \left\{ -\rho_a g\xi \left[1 - (\alpha + i\beta) \left(\frac{U_1}{c} \right)^2 \right] \right\} \quad (52)$$

The phase lag χ of the pressure relative to the surface depression $-\xi$ is given by

$$\chi = \tan^{-1} \frac{\beta(U_1/c)^2}{1 - \alpha(U_1/c)^2} \quad (53)$$

From the numerical values given by Miles (1959) for the logarithmic profile we have computed χ (see Figure 3-1-16)¹. It appears that over the

range $0 < U_1/c < 0.5$ the phase-angle does not exceed 0.35 , $= \cos^{-1}(0.94)$. Hence, the amplitude of the pressure fluctuation is due almost entirely to the in-phase component of the pressure:

$$\left| \frac{p}{\rho_a g\xi} \right| \approx 1 - \alpha \left(\frac{U_1}{c} \right)^2, \quad (54)$$

with an error of at most 6 per cent.

¹ Miles' Figure 6 gives the angle $\tan^{-1}(-\beta/\alpha)$.

Figure 3-1-16. The theoretical phase-angle χ between the surface depression, on Miles's shear-flow model.

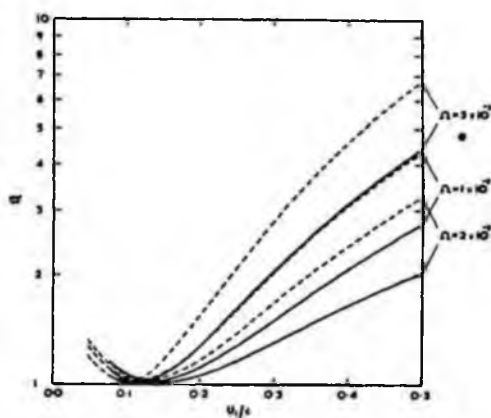
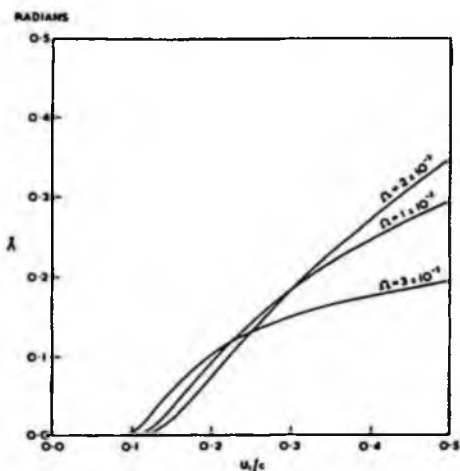


Figure 3-1-17. The theoretical in-phase component of the pressure: ——— according to Miles (1959); ——— approximation from Brooke Benjamin (1959).

We have computed the right-hand side of (54) (denoted by ω) from the numerical values given by Miles (1959), and the results are shown in Figure 3-1-17 for representative values of β . It will be seen that ω has a minimum at around $U_1/c = 0.11$, that is, at around $U_a/c = 1$.

The behaviour of ω can be understood if we consider the well-known Kelvin-Helmholtz model in which the wind profile is assumed to be vertical: the velocity U is constant. In that case (see Lamb, 1932, p. 370) it is easily found that

$$\omega = 1 + [(U/c) - 1]^2 \quad (55)$$

which is clearly a minimum when $U = c$, that is to say, when the wind speed just equals the phase velocity of the waves.

More generally, Brooke-Benjamin (1959) has shown that an approximation to the in-phase component of the pressure is given by

$$\omega_1 = 1 + \int_0^{\infty} \{[(U/c) - 1]^2 e^{-\eta d(k\eta)} \quad (56)$$

(we have added the static term), where η is a co-ordinate orthogonal to the free surface. On substituting for U from Equation (40) and replacing z by η , we find on evaluating the integral

$$\omega_1 = 1 + \frac{\pi^2}{6} \left(\frac{U_1}{c} \right)^2 + \left[\frac{U_1}{c} \log_e \frac{\gamma \Omega U_1^2}{c^2} + 1 \right]^2 \quad (57)$$

where $\gamma = \exp(0.5772 \dots)$. The curves for ω_1 have been plotted in Figure 3-1-17 for comparison with Miles' numerical results. It will be seen that ω_1 somewhat exceeds ω but that the general behaviour of ω and ω_1 is very similar.

Consider now the more general case of a sine-wave travelling at an arbitrary angle ϕ relative to the wind. By Squire's theorem (cf. Lin, 1955, C. 3), the component of the wind parallel to the crests has no effect on the pressure perturbations, which may thus be calculated as though the mean wind-field were equal to $U \cos \phi$ in the direction of wave propagation. Returning to (40), we see that the effective wind profile $U \cos \phi$ remains logarithmic; but to maintain the form of the results the parameter Ω must be multiplied by $\sec^2 \phi$. Since the dependence of ω upon ϕ cannot be readily expressed analytically,¹ we use as an approximation Equation (57), generalised to arbitrary directions of propagation; that is to say

$$\omega \doteq 1 + \frac{\pi^2}{6} \left(\frac{U_1 \cos \phi}{c} \right)^2 + \left[\frac{U_1 \cos \phi}{c} \log_e \frac{\gamma \Omega U_1^2}{c^2} + 1 \right]^2 \quad (58)$$

Let the right-hand side of (58) be denoted by $\omega(\sigma, \phi)$. We see that the spectrum of the pressure (in square feet of air) is then

$$C_{44}(\sigma) = \int_0^{2\pi} \omega^2 F(\sigma, \phi) d\phi; \quad (59)$$

and since ω^2 involves only the fourth power of $\cos \phi$, $C_{44}(\sigma)$ may be expressed in terms of the coefficients a_n, b_n up to $n = 4$. On division by

$$C_{11}(\sigma) = \int_0^{2\pi} F(\sigma, \phi) d\phi = \pi a_0, \quad (60)$$

we have the ratio C_{44}/C_{11} in terms of a_n/a_0 and b_n/a_0 up to $n = 4$. In particular for a symmetrical spectrum ($b_n = 0$) we find

$$\frac{C_{44}}{C_{11}} = 4 + 8P \frac{a_1}{a_0} + (4P^2 + 2Q^2) \left(1 + \frac{a_2}{a_0} \right)$$

$$+ P(P^2 + Q^2) \left(3 \frac{a_1}{a_0} + \frac{a_2}{a_0} \right) + \frac{1}{6} (P^2 + Q^2)^2 \left(3 + 4 \frac{a_2}{a_0} + \frac{a_4}{a_0} \right) \quad (61)$$

where

$$P = \frac{U_1}{c} \log_e \frac{\gamma \Omega U_1^2}{c^2}, \quad Q = \frac{\pi^2}{6} \left(\frac{U_1}{c} \right)^2 \quad (62)$$

The curves drawn in Figure 3-1-14 illustrate the ratio $(C_{44}/C_{11})^{1/2}$ computed for the cosine-law spectrum (29). The (constant) values of U_1 and Ω are those appropriate to the data of Record 5. It appears that the behaviour of the observations (a minimum at around $U_1/c = 0.11$), corresponds quite well with the behaviour of the theoretical curves. It should be borne in mind that at larger values of U_1/c the theoretical curves may be somewhat high, since ω_1 generally exceeds ω . Nevertheless, there is qualitative agreement even in this part of the range of U_1/c . Moreover, there is a tendency for the equivalent value of s to diminish with U_1/c , as shown independently in Figure 3-1-13.

From this comparison it appears that the greater part of the pressure fluctuations at the surface are simply the aerodynamical pressure changes due to the flow of air over the undulating surface, together with the statical pressure changes arising from the buoy's vertical displacement.

Confirmation is provided by considering the phase differences between the pressure and the surface elevation. If the pressure fluctuations were due only to uncoupled turbulence, there would be no definite phase relation between p and ζ . If, however, the pressure fluctuations are due mainly to the local shear flow and not to the turbulence, then from Figure 3-1-16 we expect the phase-differences between p and $-\zeta$ to be small.

Owing to uncertainties in the phase calibrations of the microbarograph, the accelerometer and its integrating circuit, and of the heaving motion of the buoy, the phases could be determined only to within about 10 degrees for $\sigma < 3.0$, and within wider limits at higher frequencies. The estimated phase differences are shown in Table 4.

It will be seen that over the most energetic part of the spectrum, p and ζ are about 180 degrees out of phase. (However, for $\sigma > 3.0$ the angles cannot be relied upon.) From this evidence it would seem that more than 90 per cent of pressure spectrum is coupled to the waves, and less than 10 per cent is associated directly with turbulence.

¹ And in any case the numerical values of α and β may be sensitive to actual departures from the logarithmic wind profile.

OBSERVATIONS OF DIRECTIONAL SPECTRUM OF SEAWAVES USING FLOATING BUOY MOTIONS

TABLE 4
PHASE LAG OF PRESSURE BEHIND WAVE HEIGHT
(RECORD 5)

σ (radians/sec.)	Phase lag on film	Instrumental corrections	Corrected phase lag
0.4	214°	-50°	164°
0.6	220	-36	184
0.8	210	-30	180
1.0	209	-26	183
1.2	207	-24	183
1.4	207	-23	184
1.6	210	-22	188
1.8	202	-22	180
2.0	205	-22	183
2.2	206	-22	184
2.4	213	-22	191
2.6	211	-22	189
2.8	197	-23	174
3.0	230	-23	207
3.2	224	-22	202
3.4	221	-13	208
3.6	222	+14	236
3.8	221	38	259
4.0	225	86	311

It appears then that the mean-square pressure fluctuations originally assumed by Phillips may be in error by a factor of the order of 10^2 . This would invalidate Phillips' formulae (1957, p. 442) for the mean-square surface displacement after time t . On the other hand, we have seen that over much of the spectrum Miles' instability mechanism is probably responsible for much of the wave growth. If Miles' more general expression for the wave spectrum (Equation 45) is used, a reduction in the estimated turbulent pressure fluctuations by the amount indicated is not inconsistent with the observed wave spectrum.

APPENDIX: Calculation of the "Best" Angles

It is shown in Longuet-Higgins (1955) that to minimise the integral of Equation (16) in this paper, the angles ϕ_1 and ϕ_2 must be roots of the quadratic

$$S_0 e^{2i\theta} - S_1 e^{i\theta} + S_2 = 0 \quad (63)$$

whose coefficients S_0, S_1, S_2 satisfy

$$\left. \begin{aligned} (a_0 - I)S_0 - (a_1 + ib_1)S_1 + (a_2 + ib_2)S_2 &= 0 \\ (a_1 - ib_1)S_0 - a_0 S_1 + (a_1 + ib_1)S_2 &= 0 \\ (a_2 - ib_2)S_0 - (a_1 + ib_1)S_1 + (a_0 - I)S_2 &= 0 \end{aligned} \right\} (64)$$

The value of I is found from the condition that the simultaneous equations (64) shall be consistent, that is, that the determinant of the coefficients shall vanish. Thus,

$$\Delta_0 I^2 - 2\Delta_1 I + \Delta_2 = 0 \quad (65)$$

where Δ_N denotes the determinant

$$\Delta_N = \begin{vmatrix} a_0 & a_1 + ib_1 & \dots & a_N + ib_N \\ a_1 - ib_1 & a_0 & & a_{N-1} + ib_{N-1} \\ \vdots & \vdots & \ddots & \vdots \\ a_N - ib_N & a_{N-1} - ib_{N-1} & \dots & a_0 \end{vmatrix} \quad (66)$$

The lower root of (65) gives the minimum value of I .

In terms of real quantities we have

$$I = \frac{1}{a_0} [(a_0^2 - a_1^2 - b_1^2) - \sqrt{(\mathcal{P}^2 + \mathcal{Q}^2)}], \quad (67)$$

where

$$\begin{aligned} \mathcal{P} &= a_0 a_2 - a_1^2 + b_1^2 \\ \mathcal{Q} &= a_0 a_2 - 2a_1 b_1 \end{aligned} \quad (68)$$

and so

$$a_0 - I = \frac{1}{a_0} [(a_1^2 + b_1^2) + \sqrt{(\mathcal{P}^2 + \mathcal{Q}^2)}]. \quad (69)$$

To find ϕ_1 and ϕ_2 we note that in Equations (63) and (64) only the ratios $S_0 : S_1 : S_2$ are relevant. So we may take S_1 to be real, and then the first and third of Equations (64) show that S_0 and S_2 are conjugate complex quantities. So writing

$$S_0 : S_1 : S_2 = e^{-i\theta} : r : e^{i\theta}, \quad (70)$$

we have

$$(a_0 - I + a_2) \cos \theta - b_2 \sin \theta - a_1 r = 0 \quad (71)$$

$$b_2 \cos \theta - (a_0 - I - a_1) \sin \theta - b_1 r = 0$$

and so

$$\frac{\cos \theta}{X} = \frac{\sin \theta}{Y} = \frac{r}{Z}, \quad (72)$$

where

$$\left. \begin{aligned} X &= (a_0 - I)a_1 - (a_1 a_2 + b_1 b_2) \\ Y &= (a_0 - I)b_1 - (a_1 b_2 - a_2 b_1) \\ Z &= (a_0 - I)^2 - (a_2^2 + b_2^2) \end{aligned} \right\} (73)$$

or

OCEAN WAVE SPECTRA

$$\cos \vartheta = \frac{X}{\sqrt{(X^2 + Y^2)}}, \quad \sin \vartheta = \frac{Y}{\sqrt{(X^2 + Y^2)}},$$

$$r = \frac{Z}{\sqrt{(X^2 + Y^2)}} \quad (74)$$

From (63) and (70), the product of the roots is given by

$$e^{i(\phi_1 + \phi_2)} = \frac{S_2}{S_0} = e^{-2i\vartheta} \quad (75)$$

Thus,

$$\bar{\phi} = \frac{1}{2}(\phi_1 + \phi_2) = \vartheta, \quad (76)$$

where ϑ is given by (74). Further,

$$\phi_1, \phi_2 = \vartheta \pm \chi, \quad (77)$$

where from (63)

$$e^{i\chi} - r + e^{i\chi} = 0 \quad (78)$$

or

$$\cos \chi = \frac{1}{2} r = \frac{\frac{1}{2} Z}{\sqrt{(X^2 + Y^2)}}. \quad (79)$$

This is the required general expression.

A Symmetrical Spectrum

The most interesting special case is when the spectrum is symmetrical about one particular direction, say $\phi = 0$. Then b_1 and b_2 are both zero, and Equation (67) reduces to

$$I = \frac{1}{a_0} [(a_0^2 - a_1^2) - |a_0 a_2 - a_1^2|]. \quad (80)$$

Two cases now arise, corresponding to whether $(a_0 a_2 - a_1^2)$ is positive or negative. Examples may be given of both. Thus, if $F(\sigma, \phi)$ consists of two equal delta functions at $\phi = 0$ and π (corresponding to "standing" waves), then

$$a_0 : a_1 : a_2 = 1 : 0 : 1 \quad (81)$$

and so

$$(a_0 a_2 - a_1^2) > 0 \quad (82)$$

If, on the other hand, $F(\sigma, \phi)$ consists of two delta functions at arbitrary angles $\phi = \pm \alpha$ on either side of the mean direction, we have

$$a_0 : a_1 : a_2 = 1 : \cos \alpha : \cos 2\alpha \quad (83)$$

and so

$$(a_0 a_2 - a_1^2) \propto -\sin^2 \alpha < 0. \quad (84)$$

In all the practical cases met in this paper we have $(a_0 a_2 - a_1^2) < 0$, and so from (80)

$$I = \frac{1}{a_0} (a_0^2 - 2a_1^2 + a_0 a_2). \quad (85)$$

The formulae for $\bar{\phi}$ and χ then reduce simply to

$$\bar{\phi} = 0, \quad \chi = \cos^{-1} \frac{a_1}{a_0}. \quad (86)$$

Interpretation of χ and I_{min}/a_0

From (86),

$$\sin^2 \frac{1}{2} \psi = \frac{1}{2} (1 - \cos \psi) = \frac{a_0 - a_1}{2a_0}. \quad (87)$$

But on expressing a_0 and a_1 as Fourier coefficients, we have

$$a_0 - a_1 = \frac{1}{\pi} \int_0^{2\pi} (1 - \cos \phi) F(\sigma, \phi) d\phi$$

$$= \frac{1}{\pi} \int_0^{2\pi} 2 \sin^2 \frac{1}{2} \phi F(\sigma, \phi) d\phi \quad (88)$$

Suppose now that the distribution $F(\sigma, \phi)$ is fairly narrow, that is to say that the direction of most of the energy is not widely different from the mean direction. Then in (88) $\sin \frac{1}{2} \phi$ may be replaced by $\frac{1}{2} \phi$; and if we define the r th angular moment of the distribution by

$$m_r = \int_0^{2\pi} \phi^r F(\sigma, \phi) d\phi \quad (89)$$

it is apparent that

$$a_0 - a_1 \doteq \frac{1}{2\pi} m_2. \quad (90)$$

But also

$$a_0 = \frac{1}{\pi} m_0 \quad (91)$$

so from (87)

$$\sin^2 \frac{1}{2} \psi = \frac{m_2}{4m_0}. \quad (92)$$

But this is small by hypothesis so the l.h.s. can be replaced by $\frac{1}{4} \psi^2$. Hence,

$$\psi^2 \doteq \frac{m_2}{m_0} \quad (93)$$

In other words ψ equals the r.m.s. angular deviation of energy from the mean direction.

In a similar way we have from (85)

$$I a_0 = a_0^2 - 2a_1^2 + a_0 a_2$$

OBSERVATIONS OF DIRECTIONAL SPECTRUM OF SEAWAVES USING FLOATING BUOY MOTIONS

$$\begin{aligned}
 &= \frac{1}{\pi^2} \iint \left[1 - 2 \cos \phi \cos \phi' \right. \\
 &\quad \left. + \frac{1}{2} (\cos 2\phi + \cos 2\phi') \right] \\
 &\quad \times F(\sigma, \phi) F(\sigma, \phi') d\phi d\phi' \\
 &= \frac{4}{\pi^2} \iint \left(\sin^2 \frac{1}{2} \phi - \sin^2 \frac{1}{2} \phi' \right)^2 \\
 &\quad F(\sigma, \phi) F(\sigma, \phi') d\phi d\phi' \quad (94)
 \end{aligned}$$

an exact formula. Again, if the energy is not too broadly distributed in direction, then

$$\begin{aligned}
 I\alpha_0 &\doteq \frac{1}{4\pi^2} \iint (\phi^2 - \phi'^2)^2 F(\sigma, \phi) F(\sigma, \phi') d\phi d\phi' \\
 &= \frac{1}{2\pi^2} (m_0 m_4 - m_2^2) \quad (95)
 \end{aligned}$$

Hence,

$$\frac{I}{\alpha_0} \doteq \frac{m_0 m_4 - m_2^2}{m_0^2} \quad (96)$$

However, since (96) involves the fourth moment m_4 , this approximation will generally be less accurate than (92), which involves only m_0 and m_2 .

For very narrow spectra the ratio

$$\frac{2I}{\alpha_0 \psi^4} \doteq \frac{m_0 m_4 - m_2^2}{m_2^2} \quad (97)$$

is an indicator of the "peakedness" of the energy distribution with regard to direction. Thus, for a normal distribution of energy with regard to ϕ this ratio takes the value 2; for a "square-topped" distribution it is $\frac{4}{3}$; and for two isolated delta-functions it is theoretically zero. However, for most forms of $F(\sigma, \phi)$ the approximation (97) will be accurate to within 10 per cent only if ψ is less than about 30 degrees.

* * *

ACKNOWLEDGMENTS

We would like to acknowledge our debt to the Ship Hydrodynamics Laboratory, Feltham, for calibrating the motions of the buoy; to the Royal Aircraft Establishment, Farnborough, for allowing us generous use of their *Duce* computer; and to many members of the National Institute of Oceanography. In particular, the design and construction of the buoy itself, apart from the instruments, were carried out by Mr. F. E. Pierce. We are indebted to the Captain and crew of R.R.S.

Discovery II for expert handling of both the ship and the buoy in rough weather. Finally we are grateful to Dr. O. M. Phillips, Professor J. W. Miles and Professor L. N. Howard for useful discussions based on a preliminary report.

REFERENCES

- Baird, H. F., and C. J. Banwell (1940): "Recording of Air Pressure Oscillations Associated with Microseisms at Christchurch." *N.Z.J.Sci. Tech.*, 21 B: 314-329.
- Barber, N. F. (1946). *Measurements of Sea Conditions by the Motion of a Floating Buoy*. Admiralty Res. Lab. Report 103.40/N.2/W, Teddington (bound as one of *Four Theoretical Notes on the Estimation of Sea Conditions*, by M. S. Longuet-Higgins and N. F. Barber, 1946).
- Barber, N. F. (1954): "Finding the Direction of Travel of Sea Waves." *Nature*, 174: 1048-1050.
- Barber, N. F., and D. Doyle (1956): "A Method of Recording the Direction of Travel of Ocean Swell." *Deep-Sea Res.*, 3: 206-213.
- Blackman, R. B., and J. W. Tukey (1958): *The Measurement of Power Spectra*. Dover Publ., New York, 190 pp.
- Brooke-Benjamin, T. (1959): "Shearing Flow Over a Wavy Boundary." *J. Fl. Mech.*, 6: 161-205.
- Burling, R. W. (1955): "Wind Generation of Waves on Water." Ph.D. Thesis, University of London.
- Charnock, H. (1955): "Wind Stress on a Water Surface." *Quart. J. Roy. Met. Soc.*, 81: 639-642.
- Chase, J., et al. (1957): *The Directional Spectrum of a Wind-Generated Sea as Determined from Data Obtained by the Stereo Wave Observation Project*. New York U., Coll. Eng. Report, July, 1957.
- Cote, L. J., et al. (1960): (title as in preceding reference). *Met. Pap.*, New York U., Coll. Eng. 2: No. 6.
- Cox, C., and W. Munk (1954): "Statistics of the Sea Surface Derived from Sun Glitter." *J. Mar. Res.*, 13: 198-227.
- Cox, C., and W. Munk (1956): "Slopes of the Sea Surface Deduced from Photographs of Sun Glitter." *Bull. Scripps Inst. Oceanogr.*, 6: 401-488.
- Darbyshire, J. (1959): "A Further Investigation of Wind-Generated Gravity Waves." *Deut. Hydr. Zeitschr.*, 12: 1-13.
- Ellison, T. H. (1956): "Atmospheric Turbulence." *Surveys in Mechanics*, Cambridge U. P., pp. 400-430.

- Hay, J. S. (1955): "Some Observations of Air Flow Over the Sea." *Quart. J. Roy. Met. Soc.*, **81**: 307-319.
- Lamb, H. (1932): *Hydrodynamics* (6th ed.), Dover Publ., New York.
- Longuet-Higgins, M. S. (1946): *Measurement of Sea Conditions by the Motion of a Floating Buoy. Detection of Predominant Groups of Swell*. Admiralty Res. Lab. Report 103.40/N5.
- Longuet-Higgins, M. S. (1955): "Bounds for the Integral of a Non-Negative Function in Terms of its Fourier Coefficients." *Proc. Camb. Phil. Soc.*, **51**: 590-603.
- Longuet-Higgins, M. S. (1957): "The Statistical Analysis of a Random, Moving Surface." *Phil. Trans. Roy. Soc., A*, **249**: 321-387.
- Miles, J. W. (1957): "On the Generation of Surface Waves by Shear Flows." *J. Fl. Mech.*, **3**: 185-204.
- Miles, J. W. (1959): "On the Generation of Surface Waves by Shear Flows," (Part 2). *J. Fl. Mech.*, **6**: 568-582.
- Miles, J. W. (1960): "On the Generation of Surface Waves by Turbulent Shear Flows." *J. Fl. Mech.*, **7**: 469-478.
- Phillips, O. M. (1957): "On the Generation of Waves by Turbulent Wind." *J. Fl. Mech.*, **2**: 417-445.
- Phillips, O. M. (1958a): "The Equilibrium Range in the Spectrum of Wind-Generated Waves." *J. Fl. Mech.*, **4**: 426-434.
- Phillips, O. M. (1958b): "On Some Properties of the Spectrum of Wind-Generated Ocean Waves." *J. Mar. Res.*, **16**: 231-245.
- Phillips, O. M. (1960): "Resonance Phenomena in Gravity Waves." *Proc. Am. Math. Soc. Symposium on Hydrodynamic Instability and Related Problems*, New York, April, 1960. pp. 91-103.
- Lin, C. C. (1955): *The Theory of Hydrodynamic Stability*. Cambridge U. P., 155 pp.
- Pierson, W. J., G. Neumann and R. W. James (1955): *Practical Methods for Observing and Forecasting Ocean Waves by Means of Wave Spectra and Statistics*. U. S. Navy Hydrogr. Off. Pub. 603, 284 + xx pp.
- Roll, H. U. (1948): "Wassernahes Windprofil und Wellen auf dem Wattenmeer." *Ann. Met.*, **1**: 139-151.
- Sheppard, P. A. (1958): "Transfer Across the Earth's Surface and Through the Air Above." *Quart. J. Roy. Met. Soc.*, **84**: 205-224.
- Tick, L. J. (1958): *A Non-Linear Model of Gravity Waves I*. New York U., Coll. of Eng. Tech. Report 10.
- Tucker, M. J. (1952): "A Wave-Recorder for Use in Ships." *Nature*, **170**: 657-659.
- Tucker, M. J. (1956): "A Shipborne Wave Recorder." *Trans. Instn. Naval Architects*, **98**: 236-250.
- Tucker, M. J. (1959): "The Accuracy of Wave Measurements Made with Vertical Accelerometers." *Deep-Sea Res.*, **5**: 185-192.

DISCUSSION

Dr. Hasselmann: I should like to congratulate the authors for their most interesting and original measurements. On one point, however, I feel there may be some danger of a misunderstanding.

The high correlation observed between the pressure p and the surface elevation ζ implies a small correlation between p and the normal surface velocity $\dot{\zeta}$, as ζ and $\dot{\zeta}$ are orthogonal random variables. Unfortunately, it is the small mean product $\overline{p\dot{\zeta}}$, i.e., the work done by the pressure forces, which determines the rate of wave growth, and only the spectral analysis of this term can yield direct insight into the mechanism of wave generation by pressure forces. The authors, however, restricted their analysis to the mean prod-

uct $\overline{p\dot{\zeta}}$, apparently because the instrumental error was too great to determine $\overline{p\dot{\zeta}}$ with sufficient accuracy. As a result the information gained from the pressure measurements, though interesting in itself, is irrelevant to the question of wave generation.

Nor do the pressure measurements alone yield indirect evidence as to whether an internal instability mechanism or external turbulent pressure fluctuations are responsible for wave growth.

The fact that Miles' instability theory predicts $\overline{p\dot{\zeta}}$ correctly does not imply that $\overline{p\dot{\zeta}}$ is also predicted correctly, since all models, if worth considering at all (e.g., the Kelvin-Helmholtz model, Jeffries sheltering theory, etc.), give reasonably

OBSERVATIONS OF DIRECTIONAL SPECTRUM OF SEAWAVES USING FLOATING BUOY MOTIONS

correct results for the first order term $\overline{p_1^2}$ but can differ considerably in the crucial second order term $\overline{p_2^2}$.

Furthermore, the fact that the observed mean square turbulent pressure fluctuations $\overline{p_1^2}$ are considerably smaller than originally assumed by Phillips does not imply that the resulting wave growth is also correspondingly smaller than Phillips' original estimate, as Phillips' derivation of the rate of wave growth from $\overline{p_1^2}$ was based on an incorrect assumption. This can best be seen by writing Phillips' formula for the wave growth in a different form.

If the three-dimensional spectrum of the turbulent pressure fluctuations $\ddot{p}(\mathbf{k}, \omega)$ in $\mathbf{k} \times \omega$ -space is introduced, Phillips' formula becomes simply

$$E(\mathbf{k}) = \frac{\pi k t}{\rho^2 g} \ddot{p}(\mathbf{k}, -\sigma), \quad (98)$$

where $E(\mathbf{k})$ is Longuet-Higgins (1957) spectrum and $\sigma = \sqrt{gk}$. According to Equation (98), the growth of $E(\mathbf{k})$ is determined by the spectral density of the pressure fluctuations on the "resonance surface" $\omega + \sqrt{gk} = 0$ in $\mathbf{k} \times \omega$ -space, corresponding to pressure fluctuations $dP(\mathbf{k}, -\sigma) \exp[i(\mathbf{k}\mathbf{x}) - i\sigma t]$ in resonance with free gravity waves. Now the pressure fluctuations $dP(\mathbf{k}, \omega) \exp[i(\mathbf{k}\mathbf{x}) + i\omega t]$ will generally have phase velocities in wind direction approximately equal to the "local convection velocity" $U(k)$. In other words, the spectral density $\ddot{p}(\mathbf{k}, \omega)$ will be concentrated mainly around the "local convection surface" $\omega + kU \cos \phi = 0$, where ϕ is the angle between \mathbf{k} and the wind direction. We shall, therefore, expect the spectral density $\ddot{p}(\mathbf{k}, -\sigma)$ in Equation (1) to have a maximum on the curve of intersection of the "resonance" and "local convection" surfaces, i.e., for wave-numbers corresponding to free gravity waves with phase velocities equal to the wind velocity (see Figure 3-D-1). Phillips, however, assumed that the pressure fluctuations corresponding to these very low wave-numbers would be negligible (except for very light winds) and that $\ddot{p}(\mathbf{k}, -\sigma)$ is appreciable only in the region of small wave-numbers well away from the "local convection" surface, corresponding to phase velocities considerably smaller than the wind velocity. In the derivation following, Phillips then equated a differential time scale with an integral time scale, arguing that both would be of the same order of magnitude. Although the assumption appeared reasonable in Phillips' formulation,

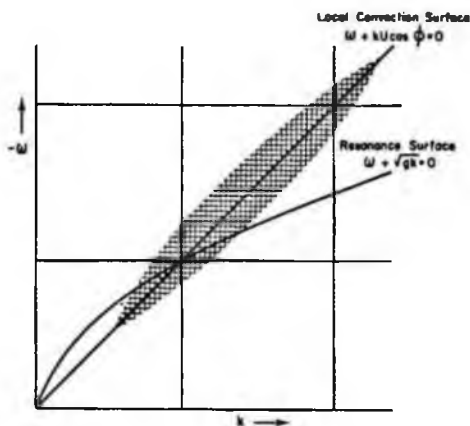


Figure 3-D-1. Local convection and resonance curves for fixed ϕ , $U(k)$ constant (Kelvin-Helmholtz model).

it can now immediately be seen that it is in fact incorrect, the two time scales describing completely independent properties of the pressure spectrum. The integral time scale determines in effect the pressure density $\ddot{p}(\mathbf{k}, -\sigma)$ away from the "local convection" surface and is thus a measure of the spread of $\ddot{p}(\mathbf{k}, \omega)$ on both sides of the maximal surface, i.e., of the degree to which Taylor's hypothesis (that fluctuating components can be considered as "frozen waves" being convected by the local mean velocity) does *not* hold. The differential time scale, on the other hand, is simply the fluctuation period of a point on the "local convection" surface as seen from a system moving with the phase velocity of the corresponding point with the same wave number on the "resonance" surface. As a characteristic time scale it is thus based on Taylor's hypothesis and is independent of the degree of accuracy of the hypothesis.

The order of magnitude of wave generation by turbulent pressure fluctuations is thus still an open question. It appears probable that the mechanism will be effectively mainly, if at all, for longer waves moving with phase velocities approximately equal to the wind velocity. This view is supported by the fact that despite the small instability of these waves (for waves with phase velocities greater than the wind velocity most instability theories predict damping rather than instability), the observed fully-developed spectra always show a pronounced peak for wave-numbers correspond-

ing to these waves. However, the energy loss of long waves is small, so that only relatively small generating forces need be involved and further observations will be necessary in order to determine the relative importance of the two proposed generating mechanisms in this wave-number region. For shorter waves, the expected increase in instability and decrease in turbulent-pressure excitation, together with the observed strongly exponential growth of shorter waves as discussed by Phillips in the session on one-dimensional spectra all point to the predominance of an instability mechanism.

It should be emphasized, however, that our concepts of wave generation by pressure forces are still based entirely on indirect arguments and that it has not yet been possible to obtain further hints as to which generating mechanism is most effective for which wave-number region by direct pressure measurements. This, of course, does not imply that the pressure measurements described by the authors are not valuable and will not perhaps later yield a useful estimate of the order of magnitude of Phillips' pressure term, for example, when more is known about the distribution of the three-dimensional pressure spectrum.

Dr. Longuet-Higgins (in reply to Dr. Hasselmann's comments): We are grateful to Dr. Hasselmann for clarifying certain points in our paper. We agree that the approximations involved in the later part of Phillips' 1957 paper cannot be relied upon and hence that the observed low value for the turbulent pressure fluctuations are not themselves conclusive evidence against the turbulence theory. However, our reasons for thinking that shear-flow instability is responsible for the greater part of the wave energy are based not so much on the pressure fluctuations but on the observed angular distribution of energy, as discussed in Section IX of our paper (on pp. 124-126). The pressure measurements in Section X are quoted only as being consistent with this hypothesis.

We would like to emphasize that Phillips' expression for the spectrum (our Equation 41) and Miles' corresponding expression (our Equation 45) do not depend for their validity upon the approximations discussed by Dr. Hasselmann; in (41) there is no approximation involving the equality of integral and differential time-scales. Nevertheless, it is still probable that the integral in (41) is a maximum with regard to ϕ , when $\cos \phi = c/U$. Hence, the discussion in Section IX of our paper is not affected.

Certainly we would like to have measured $\overline{p_1^2}$; but the accuracy of our observations did not allow us to do this except to verify that it was reasonably small.

A claim to have measured $\overline{p_1^2}$ directly was made by A. G. Kolesnikov at the Helsinki meeting of the U.G.G.I. last August. We have not seen the details of Kolesnikov's work.

Dr. Phillips: The stability analysis should, I think, provide us with estimates of these two quantities. Certainly $\overline{p_1^2}$ is the one you would really like to know from the point of view of wave generation. However, if the other quantities given by the stability analysis and the experiments indicate that this is about the right order of magnitude, isn't it reasonable to say that this fact alone, although not a direct confirmation, gives us reason to believe that this is on the right track?

Dr. Barber: I only have to say how much I admire the way in which this is being put into practice and brought to a working state. My own experiments lead me to appreciate the great difference between thinking of ways in which an experiment might be done and actually doing it.

In the discussion it does strike me — and this was an outcome of some comments by Dr. Cartwright on my own paper — that the buoy can determine the number of waves of a particular frequency. Of course, we know what the wave number is, or at least we think we do; but it would be nice if the buoy actually did measure the wave number and I rather think it does.

Dr. Longuet-Higgins: Yes. One of the things that we did was to see whether the frequency wave number relationship, as measured by the buoy's motion, was in agreement with the theoretical relation

$$\sigma^2 = gk$$

In the case of a continuous spectrum the relation analogous to this is

$$C_{22} + C_{33} = k^2 C_{11}$$

So the ratio

$$k = \frac{g}{\sigma^2} \left(\frac{C_{22} + C_{33}}{C_{11}} \right)^{1/2}$$

equals unity. We calculated this ratio and I would have shown it, if the paper had not been rather long already. I have left it until the dis-

OBSERVATIONS OF DIRECTIONAL SPECTRUM OF SEAWAVES USING FLOATING BUOY MOTIONS

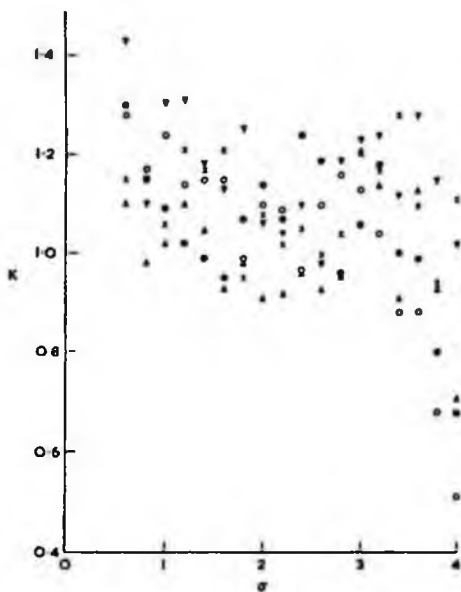


Figure 3-D-2. A plot of $k = [(C_{21} + C_{22})/C/11]^{1/2} g/\sigma$ as a function of σ .

cussion (Figure 3-D-2). We found the usual expected statistical scatter, but it is the scatter about a mean value which is a little greater than one — perhaps 1.1 — and there is some odd behavior at very high frequencies which makes us rather skeptical of our calibrations in that region. I think it is probably the calibration that is in error because the buoy has a natural response curve, which was measured as I mentioned. It varies very rapidly in the neighborhood of its natural resonance, which is just about at σ equals 4.0.

Dr. Pierson: I think we all recognize that this is a very interesting and valuable contribution to the study of the actual sea surface. May I compliment Dr. Longuet-Higgins and his fine group of co-workers in this area?

I cannot resist the temptation to compare some of these results with those of SWOP in a little more detail. I think the first principle we have to recognize is that of the invariance of the difficulty. It turns out to be about as difficult to obtain meaningful results by these procedures as it was by a stereophotogrammetric technique. We both encountered a high attenuation in the amount of data that was taken and the amount of data that was finally reduced and analyzed.

In the end we had one good set of data. Dr.

Longuet-Higgins ended up with two good sets of data. So we now have three directional spectra, one by stereo and two by his methods. There is the problem of calibration. We could not get a wave pole record to agree with the stereo results. The ship-borne recorder was properly calibrated against a directional spectrum for a ship underway in such a sea, which is a major accomplishment that Mr. Cartwright told us about yesterday.

This is quite important to the naval architect. We find that the pressure sensor of the shipboard recorder behaves as if it were $2\frac{1}{2}$ times deeper than it actually is in the water.

There is another interesting problem. The question of the possibility of the double peak, as a function of θ for high frequencies has not been resolved by this analysis nor was it resolved in our data. We might ask ourselves how it could be resolved. What kind of experiment or set of observations would have to be carried out? Here we would have to pay a great deal more attention to sampling variability. In Dr. Longuet-Higgins' report to us I missed the confidence interval, or something akin to it, in the charts. I think they would be quite important.

Scatter may or may not be comparable to the confidence interval that you would compute from theoretical grounds if possible. I don't know how it would be done from these data. If possible, it would be helpful to see whether the scatter exceeded or fell within the estimates that you might expect due to sampling variability.

The question of the double peaked function of θ as opposed to the single peak, is a very interesting and very important one for many applications and in particular for forecasting swell correctly.

My feeling is that it will be necessary to go to much higher resolution; but a complicated buoy system is required to get the desired resolution. I submit to you that in this particular case stereo has advantages, and we can go to an increased amount of resolution for the even harmonics. Of course, the disadvantages of stereo are that the nonlinear features of the surface as a function of X and Y observed at a fixed instant of time may be far more severe than the nonlinear effects that are encountered in the integrated response of a buoy. This makes the analysis much more complicated.

Is the actual wave length shorter or longer than the theoretical?

Dr. Longuet-Higgins: The ratios were greater than one, so the waves appeared a little shorter than suggested by linear theory.

Dr. Pierson: The last point is that it is quite likely that we would learn a great deal more by combining the two methods than we would by using either one alone.

The described method of analysis, even for the low frequencies in the spectrum, yields the result that some portion of the spectrum as a function of direction is travelling opposite to the wind, or at an angle greater than 90 degrees to the wind. I would ask, does Dr. Longuet-Higgins really believe that this is the case?

Dr. Longuet-Higgins: We have estimated confidence limits for the one-dimensional spectrum. The plotted points have a 95 per cent probability of lying within 20 per cent of their actual values.

As for the question of energy travelling at angles of more than 90 degrees to the wind, our observations, of course, cannot really determine this question rigorously because we have only two harmonics.

I myself have an open mind on this question, and I certainly would not like to assert dogmatically that there is no energy going at angles of more than 90 degrees from the wind. My reasons

for this are that I think that nonlinear mechanisms, such as the breaking of the waves and the tertiary wave interactions, may contribute something.

Dr. Pierson: Do you think that we made a serious mistake in assuming that the major part of the spectrum was contained within 90 degrees of the wind direction?

Dr. Longuet-Higgins: I am not saying that you made a serious mistake. All I am saying is that I have an open mind on the question.

Dr. Cox: I would like to say that I consider this work a monumental undertaking, which is giving people who are working in the field of waves a profound sense of admiration for the work at N.I.O. Has anyone measured the coherency between the pressure fluctuations and the wave amplitudes? This will give some information on the turbulent characteristics of the pressure fluctuations.

Dr. Cartwright: I did measure the coherency on one set of data. It was certainly high — about 0.8, but it should be less than 1 theoretically.

Proc. Roy. Soc. A. **311**, 371-389 (1969)

Printed in Great Britain

A nonlinear mechanism for the generation of sea waves

BY M. S. LONGUET-HIGGINS, F.R.S.

Oregon State University, Corvallis, Oregon

(Received 3 September 1968)

Recent observations of the growth of sea waves under the action of wind have established that the rate of growth is several times greater than has yet been accounted for. In this paper a new mechanism of wave generation is proposed, based on the idea of a maser-like action of the short waves on the longer waves.

It is shown that when surface waves decay they impart their momentum to the surrounding fluid. Short waves are readily regenerated by shear instability. But a longer wave passing through shorter waves causes the short waves to steepen on the long-wave crests. Hence the short waves impart more of their momentum to the crests of the long waves, where the orbital motion of the long waves is in the direction of wave propagation. If the short waves are decaying only weakly (under the action of viscosity), the effect on the long waves is slight. But when the short waves are forced to decay strongly by breaking on the forward slopes of the long waves the gain of energy by the latter is greatly increased.

Calculations suggest that the mechanism is capable of imparting energy to sea waves at the rate observed.

1. INTRODUCTION

After a decade of intense study, which has seen the development of wave generation theories by Phillips (1957 to 1966), Miles (1957 to 1962), Hasselmann (1967) and others, it is now evident that the mechanism mainly responsible for the most rapid stage of growth of sea waves under the action of the wind still remains to be found.

The 'resonance' mechanism suggested by Phillips predicts a small but constant rate of growth of the energy in the initial stages of development, and gives correctly the initial angular distribution of the waves. The 'shear instability' mechanism proposed by Miles predicts an exponential rate of growth, which should eventually overtake the linear rate. Yet recent observations of the growth rates by Snyder & Cox (1966) and by Barnett & Wilkerson (1967) have shown, first, that the observed initial growth rate, though similar in form to that predicted by Phillips, is some 50 times greater than would be expected on the basis of the measured intensities of turbulence in air flow over rough surfaces; and secondly that the rate of growth in the main stage of development is roughly an order of magnitude larger than predicted by Miles's mechanism. Since the turbulent parameters of an airstream over a moving water surface are not yet well known the discrepancy in magnitude between the initial rate of growth and that predicted by Phillips's theory may still be soluble. The discrepancy between the later stages of growth and that predicted by Miles seems at present to be more serious.

In addition, neither of the above theories accounts for two well-marked features

of wave generation: the existence of some wave energy in a frequency range corresponding to waves which travel *faster* than the wind-speed; and secondly the rapid damping of a swell by an adverse wind.

There has been some revival of interest in a previous theory proposed by Jeffreys (1924, 1925) that there is a separation of the airflow at the crests of the waves, leading to a sheltering of the lee slopes of the waves, and hence a net rate of working on the waves by normal pressure fluctuations. But it is difficult to see how long, low waves could be associated with this effect. Nor does it explain the generation of waves travelling faster than the wind.

Hasselmann (1967) has recently proposed that the waves react in a nonlinear way with turbulent components in the airstream. But so little being known about the atmospheric turbulence, and the difficulty of observation being so great, it seems unlikely that this mechanism can ever be satisfactorily tested.†

The purpose of the present paper is to point out another nonlinear mechanism, which is demonstrably operating in a normal sea state and which appears to be capable of supplying enough energy to the waves to account for the observed rates of growth.

The essence of the mechanism may be stated quite briefly. With any train of surface waves there is associated both an energy density E , say, and a horizontal momentum density M , related to E by the simple equation

$$E = Mc \quad (1.1)$$

where c denotes the phase velocity. If the wave decays under the action of viscosity, or even more drastically by breaking, it gives up a proportion of its energy. Consequently, it must impart an identical proportion of its momentum to the surrounding fluid.

Consider now a train of short waves riding on the crests of longer waves. It can be shown that the short waves tend to be both shorter and steeper at the crests of the longer waves than they are in the long-wave troughs, being compressed by the horizontal orbital motion of the long waves. Hence the short waves have a pronounced tendency to break on the crests of the longer waves, rather than in the troughs. In breaking they give up a significant proportion γ of their momentum to the longer waves. But since the orbital velocity u_2 of the longer waves is positive at the wave crests, the energy so imparted to the longer waves is also positive, and at most equal to $\gamma M u_2$.

So we have the following picture: the wind continually supplies energy to the shorter waves, imparting to them a momentum at a rate comparable to the wind stress τ . The short waves cover the whole surface of the longer waves. The longer waves, however, travel with a greater velocity and so move through the short

† Stewart (1967) has pointed out a more serious objection to this mechanism, namely that the total energy in the atmospheric turbulence appears insufficient to generate ocean waves of the observed magnitude. In the same paper Stewart (1967) suggests that appreciable energy may be imparted by variations in the tangential stress of the wind on the sea surface. A correction to his calculation is given in another paper (Longuet-Higgins 1969b).

Nonlinear mechanism for the generation of sea waves 373

waves, causing the latter to break on the forward face of the long wave crests. In this way the long waves gain energy at a rate comparable to τu_2 .

This sweeping up of short-wave momentum by long waves, in a way favourable to growth of the long waves, is similar to the action of a maser and is conveniently called the 'maser mechanism' of wave generation. It is shown in § 8 that the maser mechanism may indeed be of an order of magnitude sufficient to account for the main stage of growth of the sea waves, and accounts quite well for the observations of Barnett & Wilkerson.

First, however, in §§ 2 to 4, we give an account of the emergence of momentum from a slowly decaying wave train, and show how it may contribute to the momentum of its surroundings by a 'virtual wave stress' exerted by the boundary layer at the free surface. The presence of this virtual stress corresponds to a small but significant part of the total stress τ . Even if the short waves were not forced to break, they would still do some work on the lower waves since the virtual stress is greater at the long wave crests than it is in the troughs. Then in §§ 6 and 7 we discuss the much more drastic 'maser mechanism' which results from breaking of the short waves. Lastly in § 8 the consequences for generation of energy of the long waves are discussed.

It will be seen that the maser mechanism can account for both the generation of waves travelling faster than the wind, and the observed damping of waves by an adverse wind.

2. THE MASS-TRANSPORT VELOCITY

We first recall some known results from the theory of surface waves on deep water.

The surface elevation ζ in a progressive wave of small amplitude a may be described by the expression

$$\zeta = a \cos(kx - \sigma t) \tag{2.1}$$

where x is a horizontal coordinate, t is the time and k and σ denote the wavenumber and the radian frequency. The latter are connected by the relation

$$\sigma^2 = gk + (T/\rho)k^3 \tag{2.2}$$

in which g , ρ and T denote gravity, density and surface tension (Lamb 1932). Equation (2.1) is correct to order (ak) , the maximum surface slope. To the same order, the components u , w of the particle velocity in the interior are given by

$$\left. \begin{aligned} u &= a\sigma \cos(kx - \sigma t) e^{kz} \\ w &= a\sigma \sin(kx - \sigma t) e^{kz} \end{aligned} \right\} \tag{2.3}$$

the vertical coordinate z being measured upwards from the free surface. Close to the surface, however, there is a thin boundary layer, with thickness of order

$$\delta = (\nu/\sigma)^{\frac{1}{2}} \tag{2.4}$$

where ν denotes the kinematic viscosity. This will be discussed in detail in § 3.

In the interior of the fluid the particle trajectories are circles, to a first approximation in powers of (ak) . But in the second approximation, as was pointed out by Stokes (1847), a marked particle possesses a small second-order mean velocity U given by

$$U = \bar{u} + \int \overline{u dt \frac{\partial u}{\partial x}} + \int \overline{w dt \frac{\partial u}{\partial z}} \quad (2.5)$$

where \bar{u} denotes the mean value of u at a fixed point (the Eulerian mean) and the remaining terms arise from the orbital displacement of the particle combined with the gradients of the velocity field. The second term on the right of (2.5), when evaluated by (2.3), gives a positive contribution $\frac{1}{2}a^2\sigma k e^{2kz}$. This arises because when the orbital displacement of a particle is positive, as it is on the rear slope of the wave, the horizontal gradient of the velocity field is also positive. Similarly, the third term on the right of (2.5) also gives a positive contribution $\frac{1}{2}a^2\sigma k e^{2kz}$. This is because when a particle is at the top of its orbit its forwards velocity is greater than the velocity at the centre of the orbit and when the particle is at the bottom of its orbit the backwards velocity is less. Together the second and third terms on the right of (2.5) may be called the Stokes velocity; thus

$$U = \bar{u} + U_{\text{Stokes}} \quad (2.6)$$

where

$$U_{\text{Stokes}} = \int \overline{u dt \frac{\partial u}{\partial x}} + \int \overline{w dt \frac{\partial u}{\partial z}} \quad (2.7)$$

and for the interior of a progressive wave

$$U_{\text{Stokes}} = a^2\sigma k e^{2kz} \quad (2.8)$$

If the motion is started from rest it is initially irrotational, and by a well-known theorem must remain irrotational in the interior until vorticity is diffused or convected inwards from the boundary. Under these conditions, if one chooses axes at rest relative to the deep water, we find that in the interior

$$\bar{u} = 0 \quad (2.9)$$

everywhere except near the upper boundary. Hence

$$U_{\text{Irrrot}} = U_{\text{Stokes}} \quad (2.10)$$

This is greatest near the surface and diminishes rapidly with depth (see figure 1). The gradient of U near the surface is given by

$$\left(\frac{\partial U}{\partial z}\right)_{\text{Irrrot}} = 2(ak)^2 \sigma \quad (2.11)$$

The total forwards momentum within the wave is given by

$$M = \int_{-\infty}^0 \rho U dz = \frac{1}{2}\rho a^2 \sigma \quad (2.12)$$

This forwards momentum is somewhat paradoxical. If one takes any volume within the fluid, wholly below the level of the wave troughs then since $\bar{u} = 0$ everywhere within this fixed space it appears that the total momentum contained within this volume is zero. Thus from the Eulerian viewpoint (Phillips 1966, §3.2) the whole momentum appears to be above the wave troughs: under the crests, where

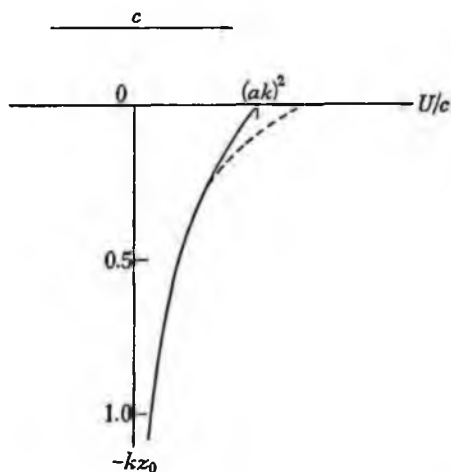


FIGURE 1. Profile of the mass-transport velocity in a progressive wave. —, irrotational motion; ---, profile modified by viscosity.

there is an excess of fluid, the motion is forwards, and under the troughs, where there is a deficiency, the motion is backwards. Analytically this viewpoint is represented by the formula

$$M = \int_{-h}^{\zeta} \rho u \, dz = \overline{\rho u \zeta} \quad (2.13)$$

which on substitution from (2.1) and (2.2) gives the same result as equation (2.12).

The two viewpoints may be reconciled by noting that at any mean level z_0 within the fluid a surface $z = \zeta(x, z_0, t)$ may be drawn consisting of the same particles, and that by the same argument the total momentum contained below this surface is given by

$$M(z_0) = \overline{u \zeta(x, z_0, t)} \quad (2.14)$$

Since $\zeta \doteq \int w \, dt$ it follows that

$$M(z_0) = \rho u \int w \, dt = \frac{1}{2} \rho a^2 \sigma e^{2kz_0} \quad (2.15)$$

Hence the *distribution* of momentum within the fluid is given by

$$\rho U = \frac{dM}{dz_0} = \rho a^2 \sigma k e^{2kz_0} \quad (2.16)$$

in agreement with (2.8).

There are good reasons, in the present context, for adopting the Lagrangian rather than the Eulerian viewpoint, that is to say for regarding the momentum as being attached to marked particles rather than to particular regions of space. This is because of the important role played by the viscous boundary layer at the surface (which will be described in the next section), combined with the fact that the thickness of the boundary layer is generally small compared to the vertical displacement of the surface itself. Hence we require coordinates and dynamical quantities related to the moving particles; in other words a Lagrangian description of the motion.

3. THE GENERATION OF VORTICITY IN THE BOUNDARY LAYER

Let us take coordinates n and s normal and tangential to the free surface, as in figure 2. The boundary conditions at a free surface are that both the normal and the tangential stress shall vanish:

$$p_{nn} = p_{ns} = 0 \tag{3.1}$$

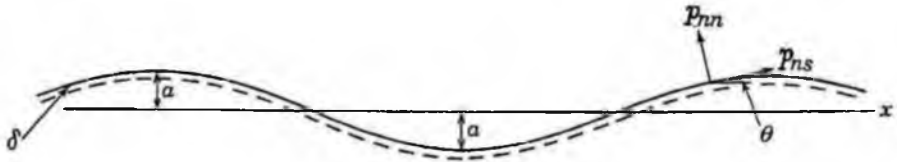


FIGURE 2. The boundary layer at the free surface. p_{nn} and p_{ns} denote the normal and tangential components of stress across the surface.

Now the vanishing of p_{ns} implies that the vorticity *cannot vanish* at the free surface. For, if θ denotes the inclination of the surface to the horizontal, we have

$$\begin{aligned} p_{ns} &= (\cos^2 \theta - \sin^2 \theta) p_{zx} - \cos \theta \sin \theta (p_{xx} - p_{zz}) \\ &= p_{zx} (1 + O(ak)^2) \\ &\doteq \mu \left(\frac{\partial u}{\partial z} + \frac{\partial w}{\partial x} \right) \end{aligned} \tag{3.2}$$

Therefore the vanishing of p_{ns} implies that

$$\frac{\partial u}{\partial z} = - \frac{\partial w}{\partial x} \tag{3.3}$$

and so

$$\omega \equiv \left(\frac{\partial w}{\partial x} - \frac{\partial u}{\partial z} \right) = 2 \frac{\partial w}{\partial z} \neq 0 \tag{3.4}$$

in general. Since in the interior of the fluid the vorticity vanishes identically (to start with, at least) it follows that ω has a sharp gradient near the surface. A closer inspection (Longuet-Higgins 1953) shows that to the first order in ak we have

$$\omega = \omega_0 e^{\alpha n} \tag{3.5}$$

where

$$\omega_0 \doteq 2(\partial w / \partial z)_{z=0} \quad \alpha = (-i\sigma/\nu)^{\frac{1}{2}} \tag{3.6}$$

377

Nonlinear mechanism for the generation of sea waves

and n is the outwards normal. This represents an oscillating distribution of vorticity which does not penetrate beyond a distance of order δ , $= (\nu/\sigma)^{\frac{1}{2}}$, from the surface. However, to the second order in ak there is found, just beyond the boundary layer, a mean (second-order) vorticity

$$\bar{\omega} = 4 \left(\frac{\partial w}{\partial x} \int \frac{\partial w}{\partial z} dt \right)_{z=0} = -2(\alpha k)^2 \sigma \quad (3.7)$$

which is independent of ν and of the boundary-layer thickness δ (see Longuet-Higgins 1953, 1960). This vorticity adds to the mass-transport gradient a term $2(\alpha k)^2 \sigma$ which is exactly equal to the irrotational gradient given by equation (2.11). Thus the total gradient of the mass-transport just outside the boundary layer is

$$(\partial U / \partial z)_{\text{viscous}} = 4(\alpha k)^2 \sigma \quad (3.8)$$

or just twice the Stokes gradient (see figure 1). The velocity gradient in gravity waves has been carefully checked by measurements in the laboratory (Longuet-Higgins 1960) and found to agree well with equation (3.8) and not with the irrotational formula (2.11).

We expect that the vorticity given by equation (2.7), being of constant sign, will gradually diffuse downwards from the boundary layer into the fluid. At a time t , after initiating the wave motion, the depth of the fluid affected by the diffusion of vorticity will be of order $(\nu t)^{\frac{1}{2}}$.

The wave-induced vorticity (3.7) is in fact entirely equivalent to a virtual tangential stress.

$$\tau_{\text{wave}} = 2\rho\nu(\alpha k)^2 \sigma \quad (3.9)$$

applied to the surface of the fluid. We shall now interpret this stress in terms of the loss of momentum in a decaying wave.

4. THE WEAK DECAY OF A UNIFORM WAVE TRAIN

If left to itself, a uniform train of free surface waves will decay under the action of viscosity. Thus we have, in the linear theory

$$a = a_0 e^{-t/t_0} \quad (4.1)$$

where the decay time t_0 is given by

$$t_0 = (2\nu k^2)^{-1} \quad (4.2)$$

(see Lamb 1932, §348). Now the original momentum M of the wave cannot be destroyed. How then is it redistributed?

One might expect it to be distributed with depth as in the original motion, that is to say proportionally to e^{2kz} . But the existence of the virtual tangential stress τ_{wave} shows that the decaying waves are in fact transferring all their momentum to

the boundary layer at the free surface. For, if we calculate the total momentum M' transferred by the virtual stress (3.9) during the decay of the wave we find it to be given by

$$M' = \int_0^\infty \tau_{\text{wave}} dt = \int_0^\infty 2\rho\nu(a_0 e^{-4t/t_0} k)^2 \sigma dt \quad (4.3)$$

that is

$$M' = \rho\nu a_0^2 k^2 \sigma t_0 \quad (4.4)$$

On substituting for t_0 from equation (4.2) we find that

$$M' = \frac{1}{2} \rho a_0^2 \sigma = M \quad (4.5)$$

Hence all the momentum is transferred to the mean flow by the surface wave stress.

Hence the final distribution of momentum will be very different from the initial distribution ρU . It will be the result of downwards diffusion from the free surface. We shall have

$$\rho U' = \int_0^t f(t-t_1) \tau_{\text{wave}}(t_1) dt_1 \quad (4.6)$$

where

$$f(t) = \frac{\exp(-z^2/4\nu t)}{\sqrt{(\pi\nu t)}}$$

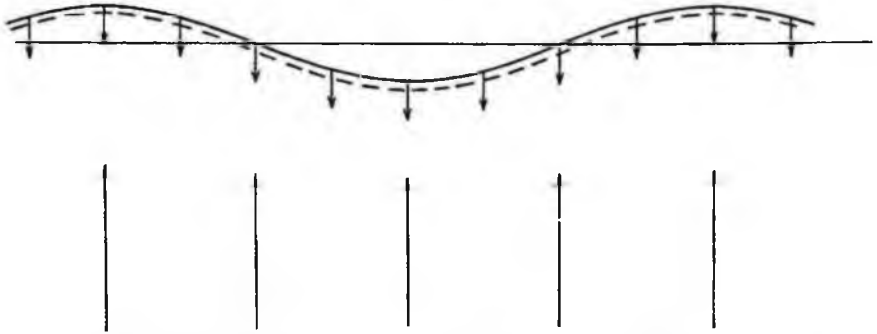


FIGURE 3. The flux of (Lagrangian) momentum in a damped water wave. The momentum is first driven upwards the surface and then diffused downwards from the boundary layer by viscosity.

After a time t of order t_0 , the depth of the layer so affected will be of order k^{-1} which is of the same order as the depth to which the motion originally extended. But for much larger values of t the depth affected will increase like $(t/t_0)^{\frac{1}{2}}$.

This interpretation is illustrated in figure 3. The horizontal momentum ρU of the waves per unit depth (which initially may have been imported solely by normal stresses at the surface) is, during the process of decay, expelled upwards towards the free surface and then diffused downwards again by viscosity.

Thus the waves act somewhat as a reservoir of horizontal momentum for the sea surface. The momentum is drawn upon more or less gradually during the process of decay.†

† The upwards-pointing arrows in figure 3 represent the Lagrangian momentum flux. The Eulerian momentum flux vanishes.

Nonlinear mechanism for the generation of sea waves 379

In this process the boundary layer acts as an essential link. However, for long and steep waves it may, under the influence of intense shear, become unstable and break up spasmodically, shedding vorticity into the interior far more rapidly than by viscous diffusion.

5. MAGNITUDE OF THE VIRTUAL WAVE STRESS

It is interesting to estimate the magnitude of the virtual stress

$$\tau_{\text{wave}} = 2\rho\nu(ak)^2\sigma \quad (5.1)$$

in a typical sea state.

The formula (5.1) holds for a discrete wave of amplitude a and maximum slope (ak) . With a continuous slope spectrum $S(\sigma)$ defined by

$$d(\frac{1}{2}a^2k^2) = S(\sigma) d\sigma \quad (5.2)$$

equation (5.1) is replaced by

$$\tau_{\text{wave}} = 4\rho\nu \int_0^\infty \sigma S(\sigma) d\sigma \quad (5.3)$$

Consider now the contribution to this integral from different parts of the frequency spectrum.

For the equilibrium range of gravity waves, in which the spectrum of the elevation ζ is given by

$$F(\sigma) = \alpha g^2 \sigma^{-5} \quad (\sigma_1 < \sigma < \sigma_2) \quad (5.4)$$

we have simply

$$\sigma S(\sigma) = \alpha \quad (5.5)$$

where α is a constant determined experimentally (Phillips 1966) and theoretically (Longuet-Higgins 1969a) to be about 1.2×10^{-2} .

TABLE 1. VALUES OF σ_3 AND σ_4 AS DERIVED FROM THE OBSERVATIONS OF COX (1958), AND A COMPARISON OF THE VIRTUAL WAVE STRESS τ_{wave} WITH THE TOTAL WIND STRESS τ_{wind} .

U (cm/s)	σ_3 (rad/s)	σ_4 (rad/s)	τ_{wave} (dyn/cm ²)	τ_{wind} (dyn/cm ²)	$\frac{\tau_{\text{wave}}}{\tau_{\text{wind}}}$
318	35	300	0.15	1.2	0.13
608	25	900	0.45	4.3	0.11
920	15	1000	0.5	9.6	0.05
1202	12	1000	0.5	17	0.03

In the capillary range, the slope spectrum as measured by Cox (1958) in a wind-tunnel, is closely approximated by

$$\sigma S(\sigma) = \beta \quad (\sigma_3 < \sigma < \sigma_4) \quad (5.6)$$

where σ_3 and σ_4 depend to some extent on wind-speed and fetch and β is about 1.0×10^{-2} . Some typical values of σ_3 and σ_4 are given in table 1. It appears that at higher wind-speeds the two ranges (5.4) and (5.6) merge, and that over the combined range $\sigma_1 < \sigma < \sigma_4$ we have

$$\sigma S(\sigma) \doteq 10^{-2} \quad (5.7)$$

as pointed out by Phillips (1966). From (5.3) it then follows that

$$\tau_{\text{wave}} \doteq 0.04\rho\nu(\sigma_4 - \sigma_1) \quad (5.8)$$

Since $\sigma_4 \gg \sigma_1$ the lower frequency σ_1 can be omitted. Indeed, by far the largest part of the stress comes from the high-frequency end of the range. We can therefore take

$$\tau_{\text{wave}} = 0.04\sigma\rho\nu\sigma_4 \quad (5.9)$$

where σ_4 is the high-frequency cut-off.

The values of τ_{wave} , as determined by equation (5.9) and the observed values of σ_4 are shown in the fourth column of table 1; in the fifth column are shown the corresponding values of the total horizontal stress as determined by the empirical formula

$$\tau_{\text{wind}} = C\rho_{\text{air}}U^2 \quad (5.10)$$

where U is the wind-speed at a height of 4 cm above the free surface (as measured by Cox 1958) and C is the corresponding drag coefficient. We take $C = 6 \times 10^{-3}$. It can be seen that at the lower wind-speeds the capillary wave stress appears to account for a small but significant part of the total stress exerted by the wind. At higher wind-speeds the proportion appears to diminish.

However, it may be pointed out that if the laminar motion breaks down, as it probably will, the damping of the short waves may be greatly increased, leading to a corresponding increase in the virtual wave stress.

The part of the total wind stress in table 1 which is not accounted for by direct viscous decay of the wave field may be attributed to wave breaking and to the supply of momentum to increasingly long waves. We shall see in §7 that these two effects are closely related.

6. THE WEAK DECAY OF SHORT WAVES RIDING ON LONG WAVES

It is commonly observed that short gravity waves riding on the backs of longer waves are steeper on the crests of the longer waves than they are in the troughs (see figure 4). A quantitative analysis was carried out by Longuet-Higgins & Stewart (1960). The steepening is due to a combination of effects: the primary effect is a shortening of the wavelength due to the horizontal contraction of the surface near the crests of the long waves; next, the same horizontal contraction does work on the short waves, causing their amplitude to increase; thirdly, owing to the vertical acceleration in the long waves the ratio of the potential to the kinetic energy of the short waves is increased.

Let a_1 , k_1 and σ_1 denote the amplitude, wave number and frequency of the short waves and a_2 , k_2 and σ_2 the corresponding quantities for the longer waves, so that $k_1 \gg k_2$, $\sigma_1 \gg \sigma_2$. Then in the paper just quoted it was shown that if viscous dissipation is altogether neglected

$$\left. \begin{aligned} a_1 &= \bar{a}_1(1 + a_2 k_2 \cos(k_2 x - \sigma_2 t)) \\ k_1 &= \bar{k}_1(1 + a_2 k_2 \cos(k_2 x - \sigma_2 t)) \\ \sigma_1 &= \bar{\sigma}_1 \end{aligned} \right\} \quad (6.1)$$

Nonlinear mechanism for the generation of sea waves 381

to first order in $(a_1 k_1)$ and $(a_2 k_2)$. The ratio of $(a_1 k_1)^2 \sigma_1$ at the crests to the corresponding value in the troughs, is thus

$$r = \left(\frac{1 + a_2 k_2}{1 - a_2 k_2} \right)^4 \quad (6.2)$$

For small values of $(a_2 k_2)$ (to which the theory strictly applies) this ratio is equal to

$$r = 1 + 8a_2 k_2 \quad (6.3)$$

If for example $a_2 k_2 = 0.1$, then $r = 1.8$. Thus the virtual stress of the short waves will be considerably greater at the crests of the long waves, where the long wave orbital velocity is forwards, than in the troughs, where it is backwards.

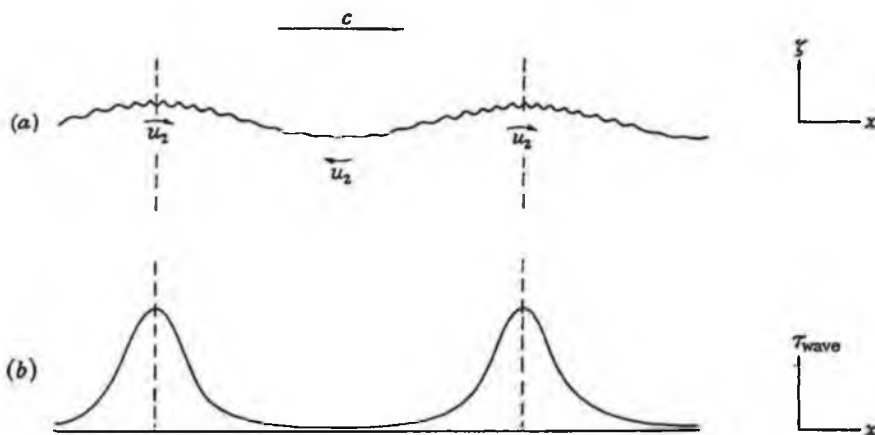


FIGURE 4. (a) A long wave of amplitude a_2 passing through a train of short waves of amplitude a_1 , when the short waves do not break. (b) The virtual stress $2\rho\nu(a_1 k_1)^2 \sigma_1$ of the short waves.

Suppose now that the short waves are subject to viscous damping, but that the rate of working by the wind is such as to keep the wave amplitude a_1 steady and given by equation (6.1). The net work done by the long wave against the radiation stresses in the short waves is then zero.

From equations (5.1) and (6.1), the virtual stress τ_1 of the short waves is given by

$$\tau_1 = 2\rho\nu(\bar{a}_1 k_1)^2 \bar{\sigma}_1 (1 + 4a_2 k_2 \cos(k_2 x - \sigma_2 t)) \quad (6.4)$$

to order $(a_2 k_2)$. Now the work W done by a small tangential stress τ_1 on the energy of a wave motion in which the orbital velocity is u_2 is given by

$$W = \overline{\tau_1 u_2} \quad (6.5)$$

the bar denoting the mean value with respect to time†. But near the surface,

$$u_2 \doteq a_2 \sigma_2 \cos(k_2 x - \sigma_2 t).$$

† This can be justified by a simple boundary-layer argument (see Longuet-Higgins 1969b).

So on substituting from (6.4) and taking mean values we find

$$W = 8\rho\nu(\bar{a}_1\bar{k}_1)^2\bar{\sigma}_1 a_2^2 k_2 \sigma_2 \quad (6.6)$$

and denoting the energy density $\frac{1}{2}\rho g a_2^2$ of the long waves by E_2 we have

$$\frac{\dot{E}_2}{E_2} \sim \frac{8\nu}{g^2} (\bar{a}_1\bar{k}_1)^2 \sigma_1 \sigma_2^3 \quad (6.7)$$

If we take, say $(\bar{a}_1\bar{k}_1)^2 \sigma_1 \sim 10^{-2}\sigma_4$ where σ_4 is the cut-off frequency for the short waves, ca. 10^3 rad/s, then we have, in c.g.s. units,

$$\dot{E}_2/E \sim 10^{-6}\sigma_2^3 \quad (6.8)$$

This rate of growth depends rather critically on the frequency of the longer waves. For waves of period 6 s ($\sigma_2 \doteq 1$) it is negligible, but for waves of period 0.5 s we have

$$\dot{E}_2/E \sim 2 \times 10^{-3} \quad (6.9)$$

which corresponds to a time constant of 250 s.

7. THE BREAKING OF SHORT WAVES ON LONG WAVES

We have so far assumed a small steepness for the longer waves ($a_2 k_2 \ll 1$). If $a_2 k_2$ is no longer small, it can be seen qualitatively from equation (6.2) that the steepening of the shorter waves becomes much more drastic. For example, on putting $a_2 k_2 = 0.5$ in (6.2) we find $r = 81$.

Hence the short waves must frequently be forced to break on the forward slopes of the longer waves, and to give up a large part of their momentum to the latter. In fact, when the long waves are on the point of breaking they are incapable of supporting any further gravity waves near the crest. The short waves then lose presumably all their energy in breaking on the forward face of the long waves.

This is confirmed by the visual observation that long steep waves are often very smooth on their rear faces, while their forwards faces are quite rough.

One might say that a long, steep wave passing through a field of short waves tend to 'clean up' the short waves by causing them to break in the forwards face of the long waves (see figure 5).

Now when the short waves give up their momentum to the longer waves they contribute to the energy of the latter at a rate proportional to the orbital velocity in the long waves. Since this is forwards on the upper part of the wave, the short waves supply a positive amount of energy to the long waves.

Meanwhile between the crests of the long waves the momentum of the short waves is replenished, mainly by the wind, and to a less extent by the radiation stresses.

Let us attempt a quantitative estimate of this effect. Suppose that on passing through each crest of the long waves the short waves lose on the average a proportion γ of their energy (or momentum) where γ is of order 1. We suppose that the proportion of momentum lost over the remainder of the wave is small compared

Nonlinear mechanism for the generation of sea waves 383

to γ . It follows that *nearly all* of the momentum supplied by the wind to the short waves is ultimately imparted to the long waves on the forwards faces of the long-wave crests.

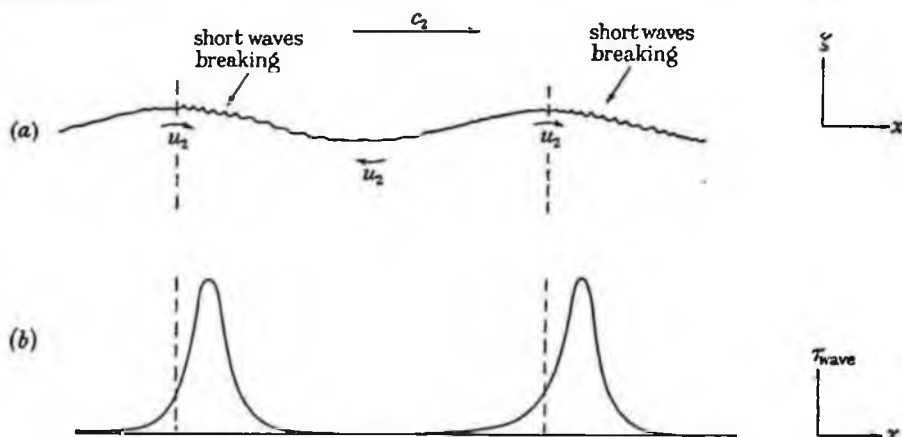


FIGURE 5. (a) The breaking of short waves on the forward face of a longer wave. (b) The distribution of the virtual stress.

If the wind-stress τ is assumed to supply momentum solely to the shorter waves it follows that the rate of energy supply to the longer waves is given by

$$W \sim \tau |u_2| \quad (7.1)$$

where $|u_2| = a_2 \sigma_2$ denotes the orbital velocity of the longer waves.

It is important to show that the energy supplied to the longer waves in this way is not appreciably reduced by the work done by the long waves against the radiation stress.† Now if E_1 denotes the energy density of the short waves per unit distance, the momentum density per unit distance is E_1/c_1 . Hence the momentum lost to the short waves, per unit time in one wavelength of the long waves, is

$$\gamma (E_1/c_1) c_2 \quad (7.2)$$

The energy supplied to the long waves per unit time, per wavelength, is thus

$$\gamma (E_1/c_1) c_2 |u_2| \quad (7.3)$$

On the other hand the rate of working by the long waves on the short waves through the radiation stress, per wavelength, is of order

$$S \frac{\partial u_2}{\partial x} / k_2 \sim S |u_2| \quad (7.4)$$

where $S = \frac{1}{2} E$, denotes the radiation stress in the shorter waves. Comparing this with (7.3) we see that the latter is negligible provided that

$$c_1/c_2 \ll \gamma \quad (7.5)$$

which is true by hypothesis, since $\gamma = O(1)$.

† Phillips (1963) has taken into account only the work done by the radiation stresses and so concludes that the long waves are damped.

It may be noted that equation (7.1) is the same relation that would have been obtained had we assumed that all the wind stress were applied tangentially at the crests of the longer waves. But we emphasize that this is not the present assumption. Rather, the longer waves sweep up the momentum that was imparted to the short waves (possibly by normal stresses) over the whole extent of the longer waves.

In practice the amplitude of the long waves is variable (having a Rayleigh distribution; see Longuet-Higgins 1952) and in equation (7.1) \bar{u}_2 must be replaced by some mean value

$$W \sim \tau |\bar{u}_2| \sim \overline{\tau a_2 k_2} c_2 \quad (7.6)$$

to first order. However, the greater the value of $a_2 k_2$, the higher the proportion of energy swept up by the long wave, so that (7.6) may be an underestimate.

The mean value of the wave steepness ($a_2 k_2$) may be determined either from observation or from theoretical considerations (see below) to be of order 10^{-1} , if the highest waves are breaking. Hence we have

$$W \sim 0.1 \tau c_2 \quad (7.7)$$

where c_2 denotes the velocity of the longer waves.

This last estimate of the energy input may be compared with the estimate

$$W \sim \tau u_* \quad (7.8)$$

where u_* denotes the friction velocity, defined by $u_*^2 = \tau / \rho_{\text{air}}$. The two estimates (7.7) and (7.8) are equal if

$$u_* \sim 0.1 c_2 \quad (7.9)$$

If we denote by C the drag coefficient, defined as u_*^2 / U^2 , where U denotes the wind velocity at some standard height, then the condition (7.9) is equivalent to

$$C \sim 10^{-2} (c_2 / U)^2 \quad (7.10)$$

which is consistent with observation (see Phillips 1966, p. 144).

To show theoretically that $(a_2 k_2)$ is of order 10^{-1} we may note that in the equilibrium spectrum

$$F(\sigma) = \alpha g^2 \sigma^{-5} \quad (7.11)$$

the ratio of the breaking wave amplitude a_0 to the r.m.s. amplitude \bar{a} is given by

$$\frac{a_0^2}{\bar{a}^2} \sim \frac{1}{8\alpha} \sim 10 \quad (7.12)$$

(see Longuet-Higgins 1969*a*). Assuming that the value of $(a_2 k_2)$ appropriate to a breaking wave is 0.5, this gives

$$(a_2 k_2)_{\text{r.m.s.}} \sim 0.5 \times 10^{-\frac{1}{2}} = 0.16 \quad (7.13)$$

Then assuming that the slope $(a_2 k_2)$ has a Rayleigh distribution it follows that

$$\overline{a_2 k_2} = \frac{1}{2} \pi^{\frac{1}{2}} (a_2 k_2)_{\text{r.m.s.}} \sim 0.13 \quad (7.14)$$

which is of order 10^{-1} as stated.

8. DISCUSSION

Let us explore some of the consequences of equation (7.1) for wave generation. We shall deal only with orders of magnitude.

Assuming that the long waves are steep enough for equation (7.1) to apply, but not so steep as to be limited by breaking, then their rate of growth, in a spacially homogeneous ocean unlimited by the fetch, will be given by

$$\frac{d}{dt} (\frac{1}{2} \rho g a^2) \sim \tau a \sigma \quad (8.1)$$

that is to say

$$\frac{da}{dt} \sim \frac{\tau}{\rho g} \sigma \quad (8.2)$$

This represents a linear rate of growth† for the wave amplitude:

$$a \sim \frac{\tau}{\rho g} \sigma t \quad (8.3)$$

and for the wave steepness

$$ak \sim \left(\frac{\tau k}{\rho g} \right) \sigma t = \frac{\tau}{\rho c^2} \sigma t \quad (8.4)$$

at least before dissipation of the long waves by breaking becomes important.

Let us consider the order of magnitude of this growth rate. Since $\tau = C \rho_{\text{air}} U^2$, equation (8.4) can be written

$$ak \sim 2\pi C \left(\frac{\rho_{\text{air}}}{\rho_{\text{water}}} \right) \left(\frac{U}{c} \right)^2 \left(\frac{t}{T} \right) \quad (8.5)$$

where $T = 2\pi/\sigma$ denotes the wave period. Thus (t/T) denotes the number N of wave cycles. On substituting the numerical values

$$C = 1.5 \times 10^{-3} \quad \text{and} \quad (\rho_{\text{air}}/\rho_{\text{water}}) = 1.3 \times 10^{-3}$$

we obtain

$$ak \sim 1.2 \times 10^{-5} (U/c)^2 N \quad (8.6)$$

Now the maximum value of \overline{ak} corresponding to breaking waves is, as we saw earlier, of order 10^{-1} . Hence if we consider the growth of those waves whose phase speed c is equal to the wind-speed U the number N of wave cycles required for them to achieve their maximum steepness would be, according to equation (8.6), of order 10^4 . This is in agreement with wave observations at sea (see, for example, Sverdrup & Munk 1947).

In a situation where the wave field is limited by the fetch x rather than by the duration t we may substitute for t in equation (8.3) using the relation $x/t =$ group velocity $= \frac{1}{2}c$, that is to say $t = 2x/c$. This gives

$$a \sim \frac{2\tau}{\rho c^2} x \sim 2C \frac{\rho_{\text{air}}}{\rho_{\text{water}}} \left(\frac{U}{c} \right)^2 x \quad (8.7)$$

† If σ is assumed constant. If, on the other hand, σ is allowed to decrease gradually with the time t then (8.3) represents a lower bound for the wave amplitude.

or with the same numerical values as before,

$$a \sim 0.4 \times 10^{-5} (U/c)^2 x \quad (8.8)$$

This formula may be compared with the recent observations of Barnett & Wilkerson (1967) who contoured spectral density (in m^2/Hz) against fetch x and frequency f (Hz) for a wind-speed U of about 15 m/s (see figure 6). Consider, for example, the situation when $x = 200 \text{ km} = 2 \times 10^5 \text{ m}$. Formula (8.8) then gives

$$a \sim 0.8 (U/c)^2 \text{ metres} \quad (8.9)$$

The peak frequency for this distance in figure 6 is about 0.105 Hz, corresponding to a wave period of 9.5 s and hence a phase velocity $c = 15 \text{ m/s}$. Hence $(U/c) \sim 1$, and (8.9) gives $a \sim 0.8 \text{ m}$. On the other hand, the total mean-squared surface elevation,

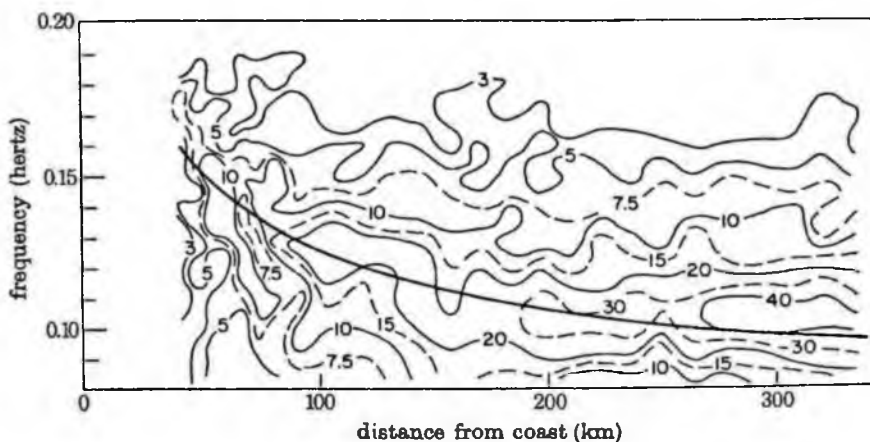


FIGURE 6. (From Barnett & Wilkerson, 1967.) Contours of spectral density as a function of fetch (distance from shore) and frequency.

from the section of the contour map at $x = 200 \text{ km}$, is about 0.5 m^2 . Equating this to $\frac{1}{2}a^2$ we should have $a = 1.0 \text{ m}$. Hence the order of magnitude of the total energy transfer predicted by (8.8) appears to be correct.

Since the wave-number k is equal to g/c^2 , equation (8.8) also predicts that before the waves are limited by breaking

$$ak \propto (U/c)^2 (gx/c^2) \quad (8.10)$$

Hence the distance x at which the wave steepness ak achieves a given value is proportional to c^4 . Since $c = g/\sigma$, we might expect the frequency $f = 2\pi\sigma$ corresponding to the peak spectral density in figure 6 to be proportional to $x^{-\frac{1}{4}}$. Such a curve has been drawn in figure 6. The constant of proportionality has been adjusted so as to give the best fit to the spectral peaks. One sees that the fit is fairly good, though the curve is evidently rather too high for the shorter fetches and too low for the longer fetches.

On the high-frequency side of the spectral peak, the spectral density is presumably limited by wave breaking. But on the low-frequency side, before the waves are

Nonlinear mechanism for the generation of sea waves 387

limited by breaking, it may be justifiable to assume that the spectral density is given by a formula analogous to equation (8.8), namely

$$F(\sigma) = \frac{d}{d\sigma} \left(\frac{1}{2} a^2 \right) = K \left(\frac{U}{c} \right)^4 \frac{x^2}{\sigma} \quad (8.11)$$

where K is a constant. For fixed values of U and x this gives

$$F(\sigma) \propto \sigma^{-3} \quad (8.12)$$

Although such a conclusion is not inconsistent with the spectral densities at the shorter fetches in figure 6, nevertheless the very steep lower face of the spectrum in the lower right-hand corner of figure 6 suggests that the rapid rate of growth on the low-frequency side of the peak is probably due to the operation of another mechanism.

We suggest that this mechanism may be as follows. The phase velocity of a wave of finite amplitude is somewhat greater than that of a small-amplitude wave of the same length, by an amount of order $(ak)^2 c$. It is thus plausible that such a wave should interact with a lower wave of slightly greater length (and lower frequency) but travelling with the same phase velocity—particularly if the wave groups are of finite length. In other words here may be a transfer of energy to a lower frequency.

A manifestation of this same mechanism is the instability of surface waves discovered by Benjamin & Feir (1967) in which the main wave gives up energy to each of two side-bands. For steep waves, the side-band of higher frequency would be limited by breaking, more than the side-band of lower frequency. Hence the energy would appear to be shifted continually towards slightly lower frequencies. This effect will be further investigated in a subsequent paper.

An interesting consequence of the maser mechanism described earlier is that the phase velocity of the longer waves is not limited to be less than the wind velocity, as it would be if only the resonance or shear instability mechanisms were operating. For, in order that energy be imparted to the longer waves by maser action it is necessary only that the wind generate short waves at some point on the long-wave profile, and this it can theoretically do no matter how great the phase speed of the long waves.

We see also that some damping of long waves by an adverse wind is also to be expected by the maser action of the short waves. For, the momentum of the short waves will be in the same direction as the wind and therefore opposite to the orbital velocity u_2 at the crests of the longer waves. So in breaking, the short waves will take energy away from the longer waves.

The damping action of an adverse wind may in fact be more pronounced than the generating action of a following wind. For by considering the waves in a frame of reference moving with the velocity of the longer waves, the longer waves are reduced to a steady stream in the same direction as the wind. The shorter waves are propagated on the stream in the same direction as the stream. However, because of the orbital velocity of the long waves the speed of the stream varies with distance

M. S. Longuet-Higgins

(according to Bernoulli's law). Now if the adverse velocity in the stream exceeds the group velocity $\frac{1}{2}c_1$ of the shorter waves the latter cannot be propagated against the stream, and must be reflected or break (see, for example, Longuet-Higgins & Stewart 1961). In either case they give up their momentum to the stream, so that the maser action is clearly very effective.

It will be seen that some explanation is still required for the generation of the short gravity waves. These can be attributed to the maser action of even shorter gravity waves, and so on down to capillary wavelengths. The latter may be due to shear instability, essentially as described by Miles (1962).

It would be interesting to record instrumentally the form of the surface elevation ζ in ocean waves under the action of wind. If it can be established that the short waves on the forward faces of long wave crests are significantly steeper than those on the rear faces, so that the proportion γ of the energy difference is of order unity, one of the critical assumptions of the present theory would be verified.

Some indications of this effect, though on a small scale are already given by the observations of Cox (1958) in a laboratory flume. These need to extend to oceanic scales. Cox indeed observed steeper capillary wave action on the forward faces of longer, gravity waves than on the rear slopes. Some capillary waves were found even in the absence of the wind—a phenomenon attributable to the action of surface tension at the sharp gravity wave crests (Longuet-Higgins 1963). However, in the presence of the wind the shorter waves were of far greater amplitude.

This paper is partly based on a contribution to the Symposium on Turbulence in the Ocean, held at the University of British Columbia, Vancouver, B.C. from 11 to 14 June 1968. It was completed at the Woods Hole Oceanographic Institution during August 1968. The research has been supported under NSF Grant GA-1452 and ONR Contract 241-11. The author is indebted to Dr N. P. Fofonoff and to other colleagues at the Woods Hole Summer School for stimulating discussions.

REFERENCES

- Barnett, T. P. & Wilkerson, J. C. 1967 On the generation of ocean wind waves as inferred from airborne radar measurements of fetch-limited spectra. *J. Mar. Res.* **25**, 292–321.
- Benjamin, T. B. & Feir, J. E. 1967 The disintegration of wave trains on deep water. Part I, Theory. *J. Fluid Mech.* **27**, 417–430.
- Cox, C. S. 1958 Measurements of slopes of high-frequency wind waves. *J. Mar. Res.* **16**, 199–225.
- Hasselmann, K. 1967 Nonlinear interactions located by the methods of theoretical physics (with application to the generation of waves by wind). *Proc. Roy. Soc. A* **299**, 77–100.
- Jeffreys, H. 1924 On the formation of waves by wind. *Proc. Roy. Soc. A* **107**, 189–206.
- Jeffreys, H. 1925 On the formation of waves by wind. II. *Proc. Roy. Soc. A* **110**, 341–347.
- Lamb, H. 1932 *Hydrodynamics*, 6th ed. Cambridge University Press.
- Longuet-Higgins, M. S. 1953 Mass transport in water waves. *Phil. Trans. A* **245**, 535–581.
- Longuet-Higgins, M. S. 1960 Mass transport in the boundary layer at a free oscillating surface. *J. Fluid Mech.* **8**, 293–306.
- Longuet-Higgins, M. S. 1963 The generation of capillary waves by steep gravity waves. *J. Fluid Mech.* **16**, 138–159.

Nonlinear mechanism for the generation of sea waves 389

- Longuet-Higgins, M. S. 1969*a* On wave breaking and the equilibrium spectrum of wind-generated waves. *Proc. Roy. Soc. A* **310**, 151.
- Longuet-Higgins, M. S. 1969*b*. On the action of a variable stress at the surface of water waves. *Phys. Fluids* (in the Press).
- Longuet-Higgins, M. S. & Stewart, R. W. 1960 Changes in the form of short gravity waves on long waves and tidal currents. *J. Fluid Mech.* **8**, 565-583.
- Longuet-Higgins, M. S. & Stewart, R. W. 1961 The changes in amplitude of short gravity waves on steady non-uniform currents. *J. Fluid Mech.* **10**, 529-549.
- Miles, J. W. 1957 On the generation of surface waves by shear flows. *J. Fluid Mech.* **3**, 185-204.
- Miles, J. W. 1959*a* On the generation of surface waves by shear flows. Part 2. *J. Fluid Mech.* **6**, 568-582.
- Miles, J. W. 1959*b* On the generation of surface waves by shear flows. Part 3. *J. Fluid Mech.* **6**, 583-598.
- Miles, J. W. 1960 On the generation of surface waves by turbulent shear flows. *J. Fluid Mech.* **7**, 469-478.
- Miles, J. W. 1962 On the generation of surface waves by shear flows. Part 4. *J. Fluid Mech.* **13**, 433-448.
- Phillips, O. M. 1957 On the generation of waves by turbulent wind. *J. Fluid Mech.* **2**, 417-445.
- Phillips, O. M. 1958 On some properties of the spectrum of wind-generated ocean waves. *J. Mar. Res.* **16**, 231-245.
- Phillips, O. M. 1963 On the attenuation of long gravity waves by short breaking waves. *J. Fluid Mech.* **16**, 321-332.
- Phillips, O. M. 1966 *The dynamics of the upper ocean*. Cambridge University Press.
- Snyder, R. L. & Cox, C. S. 1966 A field study of the wind generation of ocean waves. *J. Mar. Res.* **24**, 141-178.
- Stewart, R. W. 1967 Mechanics of the air-sea interface. *Phys Fluids* **10**. Supplement on boundary layers and turbulence, pp. S 47-S 55.
- Stokes, G. G. 1847 On the theory of oscillatory waves. *Trans. Camb. Phil. Soc.* **8**, 441-55.
- Sverdrup, H. U. & Munk, W. H. 1947 Wind, sea and swell. Theory of relations for forecasting. *U.S. Hydrogr. Office, Washington*, Publ. 601.

Reprinted from
 THE PHYSICS OF FLUIDS
 Volume 12, Number 4, April 1969

Action of a Variable Stress at the Surface of Water Waves

M. S. LONGUET-HIGGINS
Oregon State University, Corvallis, Oregon
 (Received 15 November 1968)

A boundary-layer argument shows that, paradoxically, a variable tangential stress which is greatest at the wave crests and least in the wave troughs produces a thickening of the boundary layer on the rear slopes of the waves and a thinning on the forward slopes. In deep water, a variable tangential stress τ is precisely equivalent to a normal stress $\bar{\tau}$ in quadrature with the tangential stress. The corresponding rate of growth of the waves is calculated.

A problem which is of interest in the theory of wave generation by wind is the following: A tangential stress is supposed to act on the surface of already existing waves in water of constant depth. The stress is applied unequally over the surface of the waves, being greatest at the wave crests and least in the wave troughs. What is its effect on the rate of growth of the waves?

If the flow is purely laminar, the problem may be treated by the methods of classical hydrodynamics¹; the rate of growth is given simply by the imaginary part of the complex frequency. However, this solution does not provide a satisfactory physical explanation of the wavegrowth, nor does it cover the case when the flow is turbulent.

Clearly the tangential stress must create, in the first place, a shearing motion in a thin boundary-layer close to the surface. How then is it possible for this shear to increase the energy of the potential flow in the interior of the fluid?

In a recent review² Stewart has intuitively seen that the explanation lies in the convergence of the tangential motion in the surface boundary layer producing a small additional component of velocity normal to the free surface. Unfortunately, however, he has given an analytical solution which is certainly incorrect since it does not satisfy the requirement

of energy conservation (see below). In the following we give a boundary-layer discussion differing significantly from Stewart's. We then show that this boundary-layer solution is consistent with the classical solution, and so satisfies the conservation of energy. Thirdly, we indicate how Stewart's analysis may be modified so as to bring it into agreement with the other two approaches.

Consider a progressive wave in which the surface elevation is approximately given by

$$\zeta = a \exp [i(kx - \sigma t)], \quad \sigma/k = c, \quad (1)$$

where a denotes the amplitude, and the wave-number k and frequency σ are related by the dispersion relation for free waves in water of finite depth h :

$$\sigma^2 = gk \tanh kh. \quad (2)$$

A small tangential stress of the form

$$\tau = \bar{\tau} + \tau_1 \exp [i(kx - \sigma t)], \quad (3)$$

having a maximum at the wave crests and minimum in the troughs, is now applied to the upper surface of the water; the normal stress remaining constant. In time, the mean stress $\bar{\tau}$ will produce a mean current in the direction of wave propagation. We are not concerned with this here. On the other hand, the fluctuating part of the wind stress $\tau_1 \exp [i(kx - \sigma t)]$ which we denote by τ' , can be expected to produce a thin boundary layer whose

¹ H. Lamb, *Hydrodynamics* (Cambridge University Press, Cambridge, England, 1932), 6th ed. See especially Sec. 349.

² R. W. Stewart, *Phys. Fluids Suppl.*, 10, S54 (1967).



FIG. 1. The boundary layer at the free surface induced by a tangential stress in phase with the surface elevation. The boundary layer is thickest on the rear slope of the wave.

thickness is of order $(\nu/\sigma)^{1/2}$, as described, for example by Lamb.¹

We need not enter into the details of the boundary-layer solution but deal only with the integrated properties of the motion. Let u' denote the additional velocity in the boundary layer produced by the tangential stress and define the mass flux M in the boundary layer by³

$$M = \int \rho u' dz, \quad (4)$$

the integral being taken across the layer. If at first we neglect the tangential stress beneath the layer, then by the conservation of momentum parallel to the boundary we have simply

$$\frac{\partial M}{\partial t} = \tau'. \quad (5)$$

Now, if D denotes the local thickness of the boundary layer, conceived as always consisting of the same marked particles, and if w' denotes the additional component of velocity normal to the boundary, we have

$$\frac{\partial D}{\partial t} = [w'] = \int \frac{\partial w'}{\partial z} dz = - \int \frac{\partial u'}{\partial z} dz \quad (6)$$

by continuity. But since the motion is progressive, $\partial/\partial x \sim -(1/c) \partial/\partial t$. Hence,

$$\frac{\partial D}{\partial t} = \frac{1}{c} \frac{\partial}{\partial t} \int u' dz = \frac{1}{\rho c} \frac{\partial M}{\partial t} = \frac{\tau'}{\rho c} \quad (7)$$

by Eqs. (4) and (5). Since τ' is proportional to $\exp[i(kx - \sigma t)]$ it follows on integrating with respect to time that

$$D = \frac{\tau'}{-i\sigma\rho c} + \text{const.} \quad (8)$$

Thus, the boundary layer is thinnest on the forward slopes of the waves, and thickest on the rear slopes.

We may interpret this result physically (see

³ Here x and z denote horizontal and vertical coordinates; more exactly they may be taken as tangential and normal to the surface. See M. S. Longuet-Higgins, Phil. Trans. Roy. Soc. (London) A245, 535 (1953).

Fig. 1) by remarking that the greatest acceleration in the boundary layer is where the stress is greatest, that is, on the crests of the waves. Hence, the forward velocity is greatest just *after* the crests have passed, that is, on the rear slope of the waves, and is least on the forward face. Hence, the rate of convergence of the horizontal velocity u' , which coincides with the rate of thickening of the layer, is greatest between these two positions, that is to say, at the wave crests. Lastly, the layer is thickest just after the crest has passed, that is, on the rear slopes, in accordance with the analysis.

Now, the pressure at the free surface, or more strictly the normal component of the stress, is assumed to be constant. The thickening of the layer is equivalent, in its effect on the waves, to an additional pressure δp on the upper surface of the wave, given by

$$\delta p = \rho g D = \frac{\partial \tau'}{-i\sigma c} + \text{const.} \quad (9)$$

Neglecting the constant, whose significance is irrelevant here, and using Eq. (2) we find

$$\delta p = i\tau' \coth kh \quad (10)$$

or in deep water ($e^{2k} \gg 1$) simply

$$\delta p = i\tau'. \quad (11)$$

In other words a fluctuating tangential stress τ applied at the free surface is dynamically equivalent to a normal pressure fluctuation $i\tau'$ lagging in space 90° behind the tangential stress.

Now that the mean rate of working by the tangential stress on the waves is given by

$$W = \overline{\tau'(u + u')}, \quad (12)$$

where u and w denote the components of the orbital velocity in the wave at the surface. If the waves are already well developed, we may assume that $u' \ll u$. Using the relation that $u = a\sigma \coth kh \exp[i(kx - \sigma t)]$ we find

$$W = \frac{1}{2} \tau_1 a \sigma \coth kh. \quad (13)$$

Likewise, the work done on the waves by the additional normal pressure δp is given by

$$W' = \overline{\delta p \frac{\partial \tau}{\partial t}} = \frac{1}{2} \tau_1 a \sigma \coth kh, \quad (14)$$

from (1) and (10). Clearly, $W' \neq W$, implying that the loss of energy in the boundary layer is negligible. This conclusion depends directly on our assumption that $u' \ll u$.

Now consider the rate of growth of the wave

amplitude. We fix our attention on the deep-water case when the boundary layer at the bottom can be neglected. The mean density of energy per unit horizontal area being given by

$$E = \frac{1}{2} \rho g a^2; \quad (15)$$

clearly we must have

$$\frac{dE}{dt} \leq W, \quad (16)$$

that is,

$$\rho g a \frac{da}{dt} \leq \frac{1}{2} \tau_1 a \sigma \quad (17)$$

or

$$\frac{da}{dt} \leq \frac{\tau_1}{2\rho c} \quad (18)$$

If the work done by the surface stress is much larger than the internal dissipation due to viscosity, then in (16)–(18) equality signs are appropriate.

It will be noted that we have neglected the stress on the boundary layer due to the shear associated with the wave motion in the interior of the fluid. This stress is given by

$$\tau'' = -\rho\nu \left(\frac{\partial u}{\partial z} + \frac{\partial w}{\partial x} \right), \quad (19)$$

where u and w are the components of the orbital velocity in the interior. Since the motion in the interior is irrotational, we have $\partial u/\partial z = \partial w/\partial x$ and so

$$-\frac{\tau''}{\rho\nu} = 2 \frac{\partial w}{\partial x} = 2 \frac{\partial^2 \zeta}{\partial x \partial t} = 2\sigma k \zeta \quad (20)$$

from Eq. (1). To include this effect in the previous analysis we simply have to replace τ' by $(\tau' + \tau'')$ giving, instead of Eq. (11),

$$\delta p = i(\tau' - 2\rho\nu\sigma k \zeta). \quad (21)$$

To the same order, we must include the viscous part of the normal stress component $p_{..}$ at the surface. This is given by

$$2\rho\nu \frac{\partial w}{\partial z} = 2\rho\nu k w = -2i\rho\nu\sigma k \zeta \quad (22)$$

[see Ref. (2) Sec. 348]. Altogether then the applied stress τ' and the action of viscosity are equivalent to an additional pressure

$$\delta p = i(\tau' - 4\rho\nu\sigma k \zeta) \quad (23)$$

applied at the free surface. Instead of (18) we now have

$$\frac{da}{dt} = \frac{\tau_1}{2\rho c} - 2\nu k^2 a. \quad (24)$$

When the applied stress τ' vanishes, we have $\tau_1 = 0$ and so Eq. (24) reduces to

$$\frac{da}{dt} = -2\nu k^2 a \quad (25)$$

giving the classical law of viscous decay

$$a \propto \exp(-2\nu k^2 t) \quad (26)$$

[see Ref. 1, p. 624]. In this case the tangential stress beneath the boundary layer acts to produce a thickening on the forward slopes of the waves, which combines with the normal stress to produce the wave damping.

By adopting a boundary-layer approximation we have implied that the thickness $(\nu/\sigma)^{1/2}$ of the layer is small compared with the wavelength $2\pi/k$, and hence that $(\nu k^2/\sigma) \ll 1$. However, detailed solutions of the full (linearized) equations of motion and boundary conditions including an applied tangential stress at the upper surface, can readily be obtained by the techniques implicit in Lamb's treatment of the problem,¹ not only for small values of $(\nu k^2/\sigma)$ but for all nonzero values. Thus, if ψ denotes the stream function, satisfying the vorticity equation

$$\left(\nabla^2 - \nu \frac{\partial}{\partial t} \right) \nabla^2 \psi = 0, \quad (27)$$

a solution satisfying the condition that $\psi \rightarrow 0$ as $z \rightarrow -\infty$ is of the form

$$\psi = \{ A \exp(kz) + B \exp[(i\sigma/\nu)^{1/2} z] \} \exp[i(kx - \sigma t)], \quad (28)$$

where A and B are complex constants, which can be chosen so as to satisfy the conditions

$$p_{..} = 0, \quad p_{..} = \tau \quad (29)$$

when $z = \zeta = -\int (\partial\psi/\partial x) dt$. For a given k the solution to this problem yields a value of the frequency σ which is, in general, complex giving a rate of wave growth (or decay) in agreement with (24) when $(\nu k^2/\sigma) \ll 1$.

On the other hand, Stewart, in the paper referred to previously,² found, instead of (18), the result

$$\frac{da}{dt} = \frac{\tau_1}{\rho c} \quad (30)$$

This is clearly impossible, for by Eq. (18) it would imply a rate of growth of the wave energy in excess of that supplied by the wind. The explanation appears to lie in the fact that Stewart's solution does not

satisfy the requirement of constant pressure at the free surface. To his expression for the potential ϕ in the interior must be added another term, in quadrature with the first, which can be determined by applying Bernoulli's theorem. This gives an additional term to his second expression for the vertical velocity W_1 (his notation), so that on equating it to his first expression and comparing coefficients of $\cos kx$ and $\sin kx$ one obtains

$$\frac{da}{dt} - \frac{\tau_1}{\rho c} = -\frac{da}{dt} \quad (31)$$

in place of (30). Equation (31) now agrees substantially with (18) above.

Because of the integrated boundary-layer argument used here and by Stewart² it can be seen that the simple results (11) and (18) are quite insensitive to the actual value of the viscosity or of the eddy viscosity, if the flow is turbulent. Therefore, they should be very useful in discussing certain aspects of wave generation.⁴

One may easily generalize the conclusions so as to include surface tension by noting that the

⁴M. S. Longuet-Higgins, Proc. Roy. Soc. (London) (to be published).

boundary layer produces an additional normal stress $-T \partial^2 D / \partial x^2$ in quadrature with the surface elevation, where T is the surface tension constant.

In addition, one can consider the effect of an applied stress τ which is not necessarily sinusoidal in space, acting on a wave field that contains more than one wave component. To find the work W_1 done by the stress τ on a particular wave component having wavenumber k it will be seen by Fourier decomposition that, provided the wave motions are linear and superposable, the rule

$$W_1 = \overline{\tau u_1} \quad (32)$$

is always valid, where u_1 denotes the tangential velocity corresponding to that particular wave component. Thus, even if τ were independent of u_1 , the work done by the stress on a particular Fourier component would depend on the energy already present in that component.

ACKNOWLEDGMENT

I am indebted to Professor Stewart for pointing out his paper to me.

This work has been supported under National Science Foundation Grant GA-1452.

Reprinted from *A voyage of discovery: George Deacon 70th anniversary volume* edited by Martin Angel. © by Pergamon Press Ltd., Oxford 1977.

Some effects of finite steepness on the generation of waves by wind*

MICHAEL S. LONGUET-HIGGINS

University of Cambridge. Dept. of Applied Mathematics and Theoretical Physics, and Institute of Oceanographic Sciences, Wormley, Surrey

Abstract—General reasons are given for expecting the localization of the stresses exerted by the wind on the surface of steep gravity-waves. Some recent observations of the phase velocities of wind-generated waves can be very simply interpreted by supposing that the energy of waves at frequencies higher than that of the dominant waves is propagated at an angle θ to the wind, given by $\cos \theta = c/c_0$, where c denotes the phase speed and c_0 the speed of the dominant waves. This in turn is explained by the hypothesis that the stresses are localized on the dominant waves, probably near the wave crests. The hypothesis is similar to the resonance theory of wave generation by a turbulent wind, except that the angle θ is related to the phase speed c_0 of the steep waves, and not to the convection velocity U of the turbulent eddies.

Rough estimates of the energy imparted by the tangential stresses confirm that they could play a significant part in the growth of the waves.

1. INTRODUCTION

THE inadequacy of linear theories of wave generation to explain the observed rates of growth of sea waves under the action of wind has led to the suggestion by STEWART (1967), HASSELMANN (1967) and others of various non-linear mechanisms for wind-wave generation. In this paper we wish to emphasize one likely mechanism that has received little attention, namely the localization of the surface stresses, brought about by the very non-sinusoidal profile of steep gravity waves.

General reasons for expecting the localization of both the normal and the tangential stresses in the neighbourhood of the wave crests are given in Sections 2 and 3. At the same time, in a recent paper (1976) RAMAMONJARISSOA and COANTIC have described some unexpected measurements of the phase-velocities of wind-generated waves which it appears can best be interpreted by assuming that the energy has a bimodal distribution with regard to direction, and hence that the surface stresses are localized at certain phases of the dominant waves (see Section 4).

The normal stress at the air-water interface has usually been regarded as the probable agent for wave generation. But of the two kinds of stress, it is the tangential wind stress which is more likely to become localized. In Section 5 we make estimates which suggest that it may indeed be possible for the tangential wind-stress to account for a significant part of the observed growth of the dominant waves.

Attention is also drawn to the probable existence of strong non-linear interactions in the wave field, associated with instabilities and even breaking at the crests of the dominant

* Submitted to *Deep-Sea Research* on 24.6.76.

waves. These will tend to give a similar angular distribution of energy. Such a process may be called 'speed-locking'.

2. THE TANGENTIAL WIND STRESS

There are at least two factors affecting the distribution of tangential wind stress over the profile of gravity-waves, namely variations in the relative wind speed and variations in the small-scale roughness of the surface.

Variations in the relative wind speed

By continuity of mass flux we expect the air speed to be generally greater over the wave crests than over the troughs. For low waves, a qualitative estimate is provided by considering the perturbation of a uniform, frictionless air stream, of speed U , flowing over a sinusoidal boundary $z = a \cos(kx - \sigma t)$ propagated with phase speed $c = \sigma/k$. The tangential velocity of the air is given, to first order, by

$$u_1 = U + (U - c)ak \cos(kx - \sigma t). \quad (2.1)$$

When $U > c$, the velocity is greatest at the wave crests. The tangential velocity of the water, however, is given by

$$u_2 = c \cdot ak \cos(kx - \sigma t) \quad (2.2)$$

so that the relative velocity is

$$(u - u_2) = U + (U - 2c)ak \cos(kx - \sigma t). \quad (2.3)$$

This is greater or less at the crests than in the troughs according as $U \geq 2c$. In reality, the critical ratio of U/c will be affected by the presence of shear in the mean flow, which also introduces phase differences between u_1 and u_2 (see, for example, Miles, 1957).

At larger wave steepnesses, the sharper curvature of the surface near the crests tends initially to accentuate the difference between u_1 and u_2 . This effect will be somewhat modified by shearing of the air stream and by the tendency of the airflow to separate in the lee of sharp corners. Nevertheless, qualitatively we may expect an increase in $(u_1 - u_2)$ at the wave crests, at least for waves of moderate steepness ak and for larger values of U/c . If $U/c \approx 1$ then it is possible for $(u_1 - u_2)$ to be less at the wave crests than in the troughs, just as for waves of low amplitude.

Variations in surface roughness

Among the factors contributing to a variation in the small-scale roughness of the surface are the following.

(a) The horizontal scale of the roughnesses is reduced by the lateral contraction of the surface near the wave crests. For low waves, this has been discussed quantitatively by LONGUET-HIGGINS and STEWART (1960, 1963). For steep waves, we note that the tangential separation Δs of two neighbouring particles at the surface is simply proportional to the surface velocity q , in the frame of reference travelling with the wave:

$$\Delta s \propto q. \quad (2.4)$$

Hence the relative contraction between trough and crest is given by

$$(\Delta s)_{\text{crest}}/(\Delta s)_{\text{trough}} = q_{\text{crest}}/q_{\text{trough}} \quad (2.5)$$

If the roughnesses consist of short waves, whose speed of propagation c' is small compared to q , then the ratio (2.5) gives the relative change in wavelength of the short waves, assuming that they persist throughout the passage of the long wave.

As the crests become sharp, q_{crest} tends to zero, and the scale of the roughnesses becomes so compressed that, if the waves do not break, their speed is increased due to capillarity. The condition $c' \gg q$ is then not met. If the group-velocity c_g of the capillaries exceeds q , then the short waves will tend to accumulate on the forward face of the long waves, in the neighbourhood of the point where $c_g = q$. A general discussion, taking account of the shearing current near the interface, has been given by PHILLIPS and BANNER (1974).

(b) Closely associated with the kinematical effect (a) is the dynamical effect of the surface contraction in doing work against the radiation stress of the short waves, and so increasing the short wave amplitude. For low gravity waves this effect was calculated by LONGUET-HIGGINS and STEWART (1960), but for steep gravity waves the effect is far more pronounced. A detailed calculation would have to take into account the effects of viscous dissipation and possible breaking of the shorter waves, as well as possible replenishment of short-wave energy by the wind.

(c) Because of the variation in wind speed over the longer waves the wind will have a greater capacity to generate short waves at the long wave crests (at sufficiently large values of U/c). If short-wave generation takes place preferentially at the wave crests, and if $q_{\text{crest}} > c'_g$, the short-wave energy will tend to be left behind, and increased roughness will be observed on the rear slopes of the waves. If on the other hand short-wave generation takes place preferentially in the troughs of the long waves, increased roughness will be found on the forward face of the longer waves, possibly at some critical position not far from the crest.

(d) There is probably a tendency, even in the absence of wind, for steep gravity waves to develop instabilities near the wave crest. One such instability, resulting in the formation of capillary waves ahead of a sharply curved wave crest, was analysed by LONGUET-HIGGINS (1963); see also VANDEN-BROEK (1974). A more extreme instability is apparent in the breaking of steep gravity waves and the formation of white caps on the forward face. When, owing to the advance of a steep wave through a group, a steep wave ceases to break, the whitecap is left behind, and the surface roughness which it represents is distributed over other phases of the wave and possibly reduced by horizontal extension of the elements at the free surface.

Significant variations in the surface roughness have been found experimentally by LAI and SHEMDIN (1971) and by KITAIGORODSKII (1976). The latter reports variations in short-wave energy in plunger-generated waves under the action of wind. The mean-square of the high-frequency roughness $\langle \zeta^2 \rangle$ was found to vary by a factor of order 10 over the phase of the longer waves, with the highest roughness generally occurring near the crests of the longer waves. Further observations of this nature would seem to be very desirable.* Some distinction may be necessary between conditions when the longer waves are essentially passive swell, as in the case just mentioned, and when they are being actively generated by the wind.

The above discussion strongly suggests that the combined effect of the variation in the

* Measurements at lower values of U/c_0 have been made by KELLER and WRIGHT (1975).

surface roughness and of the variation in wind speed will be to produce a tangential stress that is strongly localized near the crests of the dominant waves, particularly for the steeper waves and for larger values of U/c_0 .

3. THE NORMAL WIND STRESS

Most calculations of the normal stress have assumed that the dominant waves are of sufficiently low amplitude that the perturbations in normal pressure are small and sinusoidal.* In fact, as the waves become steeper and the crests more sharply curved, a separation of the airflow near the crest becomes increasingly likely. This implies a marked difference in pressure between the rear and the forward face of the wave, with the strongest pressure gradient occurring near the crest itself.

The work done by the normal stress, is however, limited by the fact that in a progressive surface wave the surface slope never significantly exceeds 30° . Thus the normal velocity does not exceed $\frac{1}{2}c_0$. The horizontal component of velocity, on the other hand, may be equal to c_0 if the crest is sharp-angled. This suggests that the steepness of the waves may increase the work done by the tangential stresses in a greater proportion than the work done by the normal stresses.

4. EVIDENCE FROM MEASUREMENT OF PHASE SPEED

Some interesting observations of the phase speeds of waves under the direct action of wind have been published by RAMAMONJIARISOA and COANTIC (1976). In a laboratory wind-wave channel of length 40 m and width 1.6 m and with wind-speeds of 0.5 to 14 m/s, they recorded the surface elevation at two points simultaneously in line with the mean wind, separated by a distance Δx of several centimetres. Using two independent methods, they deduced the apparent speed of each frequency component, in the direction parallel to the wind. Typical results, reproduced in Fig. 1, show that while the speed of the dominant waves agrees fairly closely with the theoretical speed at the frequency corresponding to the energy peak, the speeds of the higher-frequency components are almost constant, and equal to the speed of the dominant waves.

Various explanations may be considered and rejected. The first is that the higher frequencies represent harmonics bound to the dominant waves. If this were so, the effect would appear only in the neighbourhood of certain frequencies, namely integral multiples of the peak frequency. In fact, the speed is remarkably constant at all frequencies to the right of the peak.

Secondly, the effect is not due to a smooth spread of directions among the higher frequencies, the effect of which, for spectral densities varying as $\cos \theta$ or $\cos^2 \theta$, is shown in Fig. 1. The constancy of the observed speed is also an argument against this interpretation.

Thirdly, the effect could not be produced entirely by a surface current, unless this were comparable in magnitude to the phase speed. Since surface currents are generally only about

* In a recent paper, GENT (1976) has introduced a second harmonic into the wave profile, which does not, however, correspond precisely with water waves.

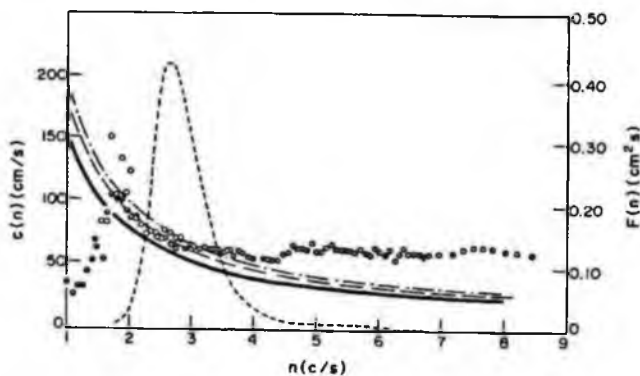


Fig. 1. Phase velocities parallel to the wind, as a function of frequency, measured in a laboratory wave channel. $U = 5 \text{ m/s}$, $c_0 = 0.6 \text{ m/s}$ (from RAMAMONJARISSOA, 1974).

3% of the wind speed, while the observed discrepancies are much larger, this explanation also is ruled out.

However, we can interpret the observations on the assumption that the waves of frequency greater than the peak frequency are propagated at an angle θ to the wind such that their *apparent* phase speed in the wind direction is just equal to c_0 , the speed of the dominant waves. This implies the relation

$$\cos \theta = c/c_0 \quad (4.1)$$

where c is the phase velocity of the waves.

Among the possible physical reasons for this effect are, first, a localized effect at the wave crests, such as wave breaking, which, by non-linearity in the fluid motion, would tend to transfer energy to other wave components. This would not be a *weak* non-linearity, such as that suggested by Phillips and Hasselmann, but rather a *strong* non-linearity, scattering energy from one steep, short-crested wave into an infinity of free wave components. We may call this a phase-locked wave interaction; and the resulting effect 'speed-locking'.

A second possibility is that such a local instability might arise from the boundary layer at the side walls of the tank, where the wave amplitude is likely to be enhanced by reflection. This possibility cannot yet be ruled out, except by experiments in a broader channel or in the open sea. We note, however, that a similar though less pronounced effect has also been reported by YEFIMOV, SOLOV'YEV and KRISTOFOROV (1972) in wave measurements over open water.

A third hypothesis, in the light of the previous discussion, is that the wind stresses themselves are localized on the wave crests. For the crests of the dominant waves are not generally uniform along their length.* Where they are particularly steep we expect a concentration of surface stress, either normal or tangential to the long-wave profile. Moreover, these spots of high stress will travel forward with the local phase velocity of the dominant waves. Hence they will tend to generate waves travelling at an angle with the

*The view of the wave surface in fig. 12b of RAMAMONJARISSOA (1974) shows clearly that the waves in this instance are quite short-crested. Hence localization occurs both in the down-wind and cross-wind directions.

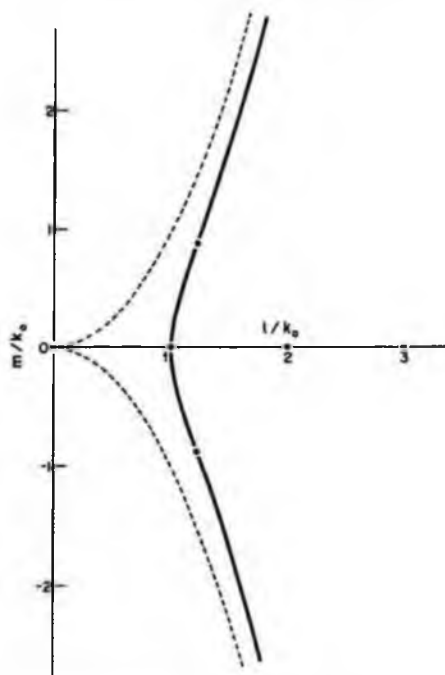


Fig. 2. Wavenumber locus for gravity waves generated by a localized surface stress, or by strong non-linear wave interactions. k_0 is the wavenumber of the dominant waves.

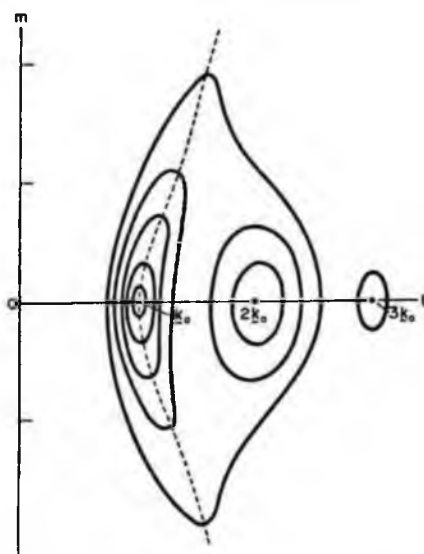


Fig. 3. Sketch of the contours of spectral density at an early stage of wave generation, when $U/c_0 \gg 1$. On the left is the free-wave energy clustered round the resonance curve. Also shown are subsidiary peaks near $2k_0$ and $3k_0$, representing energy bound to the lowest harmonic.

wind direction, but with the same speed in the κ -direction as the speed of the dominant waves.

The effect is very similar to that proposed in PHILLIPS'S theory (1957) of the production of waves by spots of pressure in a turbulent wind stream, except that the patches of stress arise not from the free turbulence but from the existing waves; and hence the angle θ is related not to the wind velocity but to the phase speed of the dominant waves.

Whichever interpretation is chosen, equation (4.1) implies a relation between the wave-number and the direction of the shorter waves. Let \mathbf{k} be the vector wavenumber with components (l, m) in the (x, y) directions, and let $k = |\mathbf{k}| = (l^2 + m^2)^{\frac{1}{2}}$. Assuming the linear dispersion relation $c = (g/k)^{\frac{1}{2}}$, we have from (4.1)

$$(k_0/k)^{\frac{1}{2}} = \cos \theta = l/k$$

so

$$l^2 = k k_0$$

and hence

$$l^4 = k_0^2(l^2 + m^2). \quad (4.2)$$

This curve is shown in Fig. 2. It passes through the point $(l, m) = (k_0, 0)$ where it has radius of curvature k_0 . At large wavenumbers, it is asymptotic to the parabolas

$$m = \pm l^2/k_0.$$

There are two points of inflexion, where

$$(l, m) = \left\{ \left(\frac{3}{2} \right)^{\frac{1}{2}}, \pm \frac{3}{2} \right\}^{\frac{1}{2}} k_0, \quad k = \frac{3}{2} k_0,$$

and where

$$\frac{dm}{dl} = \pm 2\sqrt{2}.$$

In a continuous spectrum, we may expect the wave energy to lie generally in the neighbourhood of this curve, with some dispersion about it, as in Fig. 3. This portion of the spectrum represents the free-wave energy. Waves bound to frequencies in the spectral peak may be found in the neighbourhood of the wavenumbers $2k_0, 3k_0, \dots$

As a function of direction, the spectrum is bimodal rather than unimodal. This type of spectrum is to be expected only under conditions of strong wave generation, and possibly only in the earlier stages. At later stages, the spectrum will be slowly modified by dissipation and by weak non-linear interactions, the energy being dispersed from the peak in the characteristic directions $dm/dl = \pm 1/\sqrt{2}$; see LONGUET-HIGGINS (1976) and FOX (1976).

In the observations of RAMAMONLIARISA and COANTIC (1976) the waves were being strongly generated, with $U/c_0 \approx 8$ or more. In the field observations of YEFIMOV, SOLOV'YEV and KHRISTOPOROV (1972), where a comparable effect was observed, the ratio U/c was generally less.

It is not difficult to take into account the effect of capillarity on the form of the resonance curve (4.2). Adopting the dispersion relation

$$c = (g/K + T/\rho \cdot k)^{\frac{1}{2}}$$

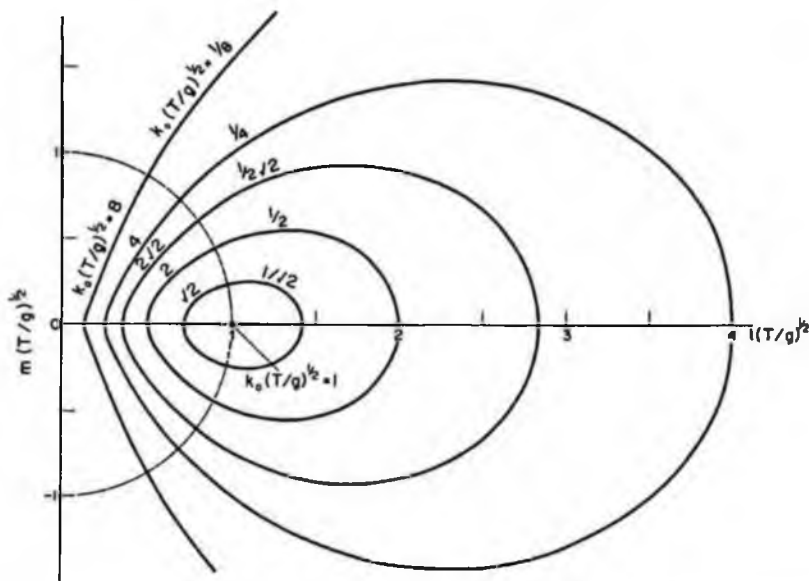


Fig. 4. Wavenumber loci for gravity-capillary waves, showing the effect of capillarity on the resonance curve of Fig. 2.

and choosing units with $\rho = T = g = 1$ we have

$$\cos \theta = \left(\frac{k + k^{-1}}{k_0 + k_0^{-1}} \right)^{\frac{1}{2}}. \quad (4.3)$$

The family of resonance curves is shown in Fig. 4, with k_0 as parameter. The resonance curves corresponding to the longer, gravity-type waves lie inside the circle $k = 1$. The effect of capillarity on these is to bend them round towards the l -axis, so that ultimately they form closed ovals. The parts of the curve lying outside the circle $k = 1$ corresponds to capillary-type waves. Evidently these bend backwards towards the origin, meeting the circle $k = 1$ in points increasingly close to the m -axis. In the special case $k_0 = (1, 0)$, corresponding to gravity-capillary waves of minimum phase-velocity, the resonance curve shrinks to zero, as would be expected; there are no other waves with phase-velocities less than c_0 .

5. DISCUSSION; RATES OF WAVE GROWTH

In wind-generated waves it is universally observed that the dominant waves occur in groups, the wave amplitude varying both in time and space. This is a well-known property of any stationary stochastic process having a non-zero spectral bandwidth. An important consequence, however, is that the effects of non-linearities in the generating process may be accentuated. For even when most of the individual waves are linear and sinusoidal, there can still be a few which are steep and sharp crested. Hence the bulk of the energy transfer from the wind may be imparted to the steepest waves.

Table 1. Observed phase angles ϕ between air pressure variations and the dominant surface waves; and the estimated values of τ_n^*/τ^*

Author	ϕ	τ_n^*/τ^*
DOBSON (1971)	40°	0.80
ELLIOTT (1972)	20°	0.20
SNYDER (1974)	45°	0.02

Despite many attempts, the distribution of the normal stress on the surface of a steep water wave in conditions of active wave generation has still not been well determined experimentally. The distribution of the tangential stress is even less well known. We can, however, use the comparatively well-determined value of the total mean wind stress τ^* to estimate the rates of growth due to the wind, according to various hypotheses.

Let us divide the total horizontal wind stress τ^* into two parts: a part τ_n^* corresponding to normal pressures on the dominant waves, and a part τ_s^* corresponding to the 'tangent stress', which may also include normal stresses on the small-scale elements.

The direct observations of surface pressure by DOBSON (1971), ELLIOTT (1972) and SNYDER (1974) have led to widely differing estimates of the ratio of τ_n^*/τ^* (see Table 1). Nevertheless it does appear that the mean tangential stress τ_s^* is generally of the same order as τ^* .

Let us write τ_s for the local tangential stress, so that $\tau_s = \tau_s^* + \tau'$ and

$$\tau_s = \tau_s^* + \tau'$$

where τ' is a variable stress with mean zero. We may estimate the work done on the waves by the tangential stress under two different hypotheses. First, assume the waves are sinusoidal and τ' varies in-phase with the surface elevation. Then it was shown by LONGUET-HIGGINS (1969a) that the work done on the waves, per unit time and unit surface area, is

$$W = \overline{\tau' u_s}$$

where u_s is the tangential velocity of the particles at the free surface.* in sinusoidal waves, the amplitude $|u_s|$ is equal to $ak \cdot c$, and if we take

$$|\tau'| = K\tau_s^*$$

where K is a constant we have

$$W = \frac{1}{2} |\tau'| |u_s| = \frac{1}{2} K \overline{ak} \cdot c_0 \tau_s^*.$$

For waves under the action of wind it is reasonable to take $\overline{ak} \approx 0.14$ (LONGUET-HIGGINS, 1969a), and since the maximum value of K is not likely to exceed 1 we have

$$W \leq 0.07 c_0 \tau_s^* \leq 0.07 c_0 \tau^*. \quad (5.1)$$

If, on the other hand, we adopt the extreme hypothesis that all of the tangential stress is concentrated at the sharpest wave crests, where the particle velocity is of order c_0 ,

* In a recent contribution GARRETT and SMITH (1976) have shown that this formula effectively applies also when τ' includes the transfer of momentum from the wind to the short waves.

it follows that

$$W \sim c_0 \tau_*^* \quad (5.2)$$

A large part of this work can be expected to go into the dominant waves. Comparing (5.1) and (5.2) we see that the work done on waves by the tangential stress is increased by an order of magnitude.

Working now with orders of magnitude, if we take

$$\tau_*^* \sim \tau^* \sim C \rho' U^2 \quad (5.3)$$

where ρ' is the density of air and C a drag coefficient of order 2×10^{-3} , and if we take the mean energy density of the waves to be

$$E = \frac{1}{2} \rho g a^2 \quad (5.4)$$

where $g = kc_0^2 = \sigma c_0$ and $ak = 0.14$, then from the last three equations, the proportional growth of the energy in one wave cycle T_p is given by

$$\frac{T_p dE}{E dt} = \frac{2\pi W}{\sigma E} \gg C \frac{\rho' 4\pi U^2}{\rho g a^2 \sigma} \sim 10^{-3} (U/c_0)^2.$$

If $U/c_0 \approx 4$, say, this leads to a proportional rate of growth exceeding 10^{-2} , which in turn is greater than the observed rates by at least one order of magnitude (see PHILLIPS, 1967).

We have not, of course, allowed for the weak non-linear interactions, or for the probably more important dissipation of energy by wave breaking and viscosity. Nevertheless the above estimate suggests that the action of the tangential stress in generating the dominant waves may well be significant.

As against this it should be pointed out that if the wind speed should fall so that $U/c_0 \approx 1$, say, then relative velocity of air and water will be greater in the troughs, where the orbital velocity is negative, than at the crests. Though the surface roughness of the troughs may be less, it is nevertheless possible that in such a case the tangential wind stress might act so as to damp the energy of the dominant waves.

REFERENCES

- DOBSON F. W. (1971) Measurements of atmospheric pressure on wind-generated sea waves. *Journal of Fluid Mechanics*, **48**, 91-127.
- ELLIOTT J. A. (1972) Microscale pressure fluctuations near waves being generated by wind. *Journal of Fluid Mechanics*, **54**, 427-448.
- FOX M. J. H. (1976) On the nonlinear transfer of energy in the peak of a gravity-wave spectrum, II. *Proceedings of the Royal Society, London, A*, **348**, 467-483.
- GARRETT C. and J. SMITH (1976) On the interaction between long and short surface waves (Preprint, submitted to the *Journal of Physics and Oceanography*)
- GENT P. R. and P. A. TAYLOR (1976) A numerical model of the air flow above water waves. *Journal of Fluid Mechanics* (in press).
- HASSELMANN K. (1967) Nonlinear interactions treated by the methods of theoretical physics (with application to the generation of waves by wind). *Proceedings of the Royal Society, London, A*, **299**, 77-100.
- HASSELMANN K. (1971) On the mass and momentum transfer between short gravity waves and larger-scale motions. *Journal of Fluid Mechanics*, **50**, 189-205.

* In a recent contribution GARRETT and SMITH (1976) have shown that this formula effectively applies also when τ' includes the transfer of momentum from the wind to the *short* waves.

- KELLER W. C. and J. W. WRIGHT (1975) Microwave scattering and the straining of wind-generated waves. *Radio Science*, **10**, 139–147.
- KITAIGORODSKII S. A. (1976) Personal communication.
- LAI R. J. and O. H. SHEMDIN (1971) Laboratory investigation of air turbulence above simple water waves. *Journal Geophysical Research*, **76**, 7334–7350.
- LONGUET-HIGGINS M. S. (1963) The generation of capillary waves by steep gravity waves. *Journal of Fluid Mechanics*, **16**, 138–159.
- LONGUET-HIGGINS M. S. (1969a) A nonlinear mechanism for the generation of sea waves. *Proceedings of the Royal Society, London, A*, **311**, 371–389.
- LONGUET-HIGGINS M. S. (1969b) Action of a variable stress at the surface of water waves. *Physics of Fluids*, **12**, 737–740.
- LONGUET-HIGGINS M. S. (1976) On the nonlinear transfer of energy in the peak of a gravity-wave spectrum: a simplified model. *Proceedings of the Royal Society, London A*, **347**, 311–328.
- LONGUET-HIGGINS M. S. and R. W. STEWART (1960) Changes in the form of short gravity-waves on long waves and tidal currents. *Journal of Fluid Mechanics*, **8**, 565–583.
- LONGUET-HIGGINS M. S. and R. W. STEWART (1964) Radiation stresses in water waves; a physical discussion, with applications. *Deep-Sea Research*, **11**, 529–562.
- MILES J. W. (1957) On the generation of surface waves by shear flows. *Journal of Fluid Mechanics*, **3**, 185–204; see also **6**, 568–598 (1959), **7**, 469–478 (1960) and **13**, 433–448 (1962).
- PHILLIPS O. M. (1957) On the generation of waves by turbulent wind. *Journal of Fluid Mechanics*, **2**, 417–445.
- PHILLIPS O. M. (1963) On the attenuation of long gravity waves by short breaking waves. *Journal of Fluid Mechanics*, **16**, 321–332.
- PHILLIPS O. M. (1966) *The dynamics of the upper ocean*, Cambridge University Press.
- PHILLIPS O. M. and M. L. BANNER (1974) Wave breaking in the presence of wind drift and swell. *Journal of Fluid Mechanics*, **66**, 625–640.
- RAMAMONJARISSOA A. (1974) *Contribution à l'étude de la structure statistique et des mécanismes de génération des vagues de vent*. Thèse, D. es Sc., Université de Provence.
- RAMAMONJARISSOA A. and M. COANTIC (1976) Loi expérimentale de dispersion des vagues produites par le vent sur une faible longueur d'action. *Comptes Rendus de l'Académie des Sciences, Paris*, **282 B**, 111–114.
- REECE A. M. and O. H. SHEMDIN Modulation of capillary waves by long waves. *Report*. Coastal and Oceanography Engineering Laboratory, University of Florida, Gainesville, pp. 1–12.
- SNYDER R. L. (1974) A field study of wave-induced pressure fluctuations above surface gravity-waves. *Journal of Marine Research*, **32**, 497–531.
- STEWART R. W. (1967) Mechanics of the air–sea interface. *Physics of Fluids*, **10**, (Supplement on Boundary layers and Turbulence), pp. S47–S55.
- VANDEN-BROECK J.-M. (1974) *Mécanique des vagues de grande amplitude*. Thesis for Ingen. Phys., Université de Liège.
- YEFIMOV V. V., YU. P. SOLOV'YEV and G. N. KHRISTOFOROV (1972) Observational determination of the phase velocities of spectral components of wind waves. *Izvestiya Akademii Nauk SSSR*, **8**, 435–446.

Theory of weakly damped Stokes waves: a new formulation and its physical interpretation

By MICHAEL S. LONGUET-HIGGINS

Institute for Nonlinear Science, University of California, San Diego, La Jolla,
 CA 92093-0402, USA

(Received 8 November 1990 and in revised form 29 July 1991)

A tractable theory for weakly damped, nonlinear Stokes waves on deep water was recently formulated by Ruvinsky & Friedman (1985*a, b*; 1987). In this paper we show how the theory can be simplified, and that it is equivalent to a boundary-layer model for surface waves proposed by Longuet-Higgins (1969), when the latter is generalized to include surface tension and nonlinearity. The potential part of the flow is determined by boundary conditions applied at the base of the vortical boundary layer. The theory may be of use in discussing the generation of waves by wind.

1. Introduction

Since Stokes's original paper (1847) the irrotational theory of surface waves on water of infinite or uniform finite depth has been outstandingly successful in predicting many observed wave phenomena. For certain applications, however, viscous damping of the waves is important, and it would be highly convenient to have equations and boundary conditions of comparable simplicity as for undamped waves. A first step in this direction was made by Lamb (1932) who showed that for most wavelengths of interest the effects of viscosity on linear, deep-water waves are confined to a thin vortex layer near the free surface, of thickness $D_0 = (2\nu/\sigma)^{\frac{1}{2}}$ (where ν denotes the kinematic viscosity and σ the radian frequency). When $kD_0 \ll 1$ (k the wavenumber) we may say that the waves are weakly damped. Lamb (1932) calculated the tangential stress at the surface that would be required in a perfectly periodic state; hence the energy loss and consequent wave damping in the absence of such applied stresses.

Longuet-Higgins (1960) considered the action of a general, tangential stress at the free surface, varying sinusoidally in the horizontal direction.† He showed that the stress would tend to produce a vortical boundary layer that was thicker at points 90° out of phase with the stress. For example, a stress greatest at the wave crest would produce a thickening of the layer on the rear wave slopes, tending to pump energy into the potential flow in the interior. Similarly, in the absence of any wind the viscous stresses at the base of the vortical layer would tend to thicken the layer on the *forward* slopes of the wave and to produce the calculated wave damping (see figure 1.)

In several papers Ruvinsky & Friedman (1985*a, b*; 1987) have independently formulated a system of equations for weakly damped surface waves in deep water,

† At second order in the wave steepness it is known that vorticity may diffuse into the interior of the fluid (see Longuet-Higgins 1953, 1960). Here we confine attention mainly to the linear theory, or at least to times after the start of the motion that are short enough for the diffusion or convection of vorticity to be still negligible.

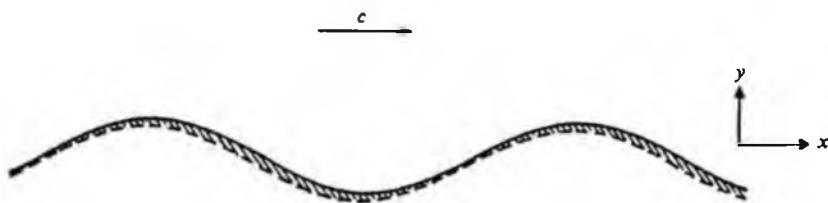


FIGURE 1. Sketch of the vortical boundary-layer induced by viscous stresses in a deep-water wave.

and have successfully applied it to the calculation of capillary-gravity ripples riding on the forward face of steep gravity waves. They formally separated the velocity field into its irrotational and vortical components and hence were led to the coupled system: (3.1) to (3.5) below. This they then solved for periodic waves by numerical integration. Their analysis is summarized in the Appendix to a recent paper (Ruvinsky, Feldstein & Freidman, 1991). As a final remark they state that it is possible to use a certain 'simpler set of equations', but they give no derivation or physical explanation. They justify the simpler system solely on the grounds that it yields the correct expression for the decay of weakly damped surface waves.

The purpose of the present note is, first, to give an analytical derivation of this simpler set of equations and, secondly, to provide a physical explanation for them. Indeed we show that the simpler equations express precisely the physical argument given by Longuet-Higgins (1969).

In a further discussion (§4 below) we point out that the simplified system of equations may be generalized so as to include applied surface stresses. Thus it may be of use in the theory of wave generation by wind.

2. Dynamics of the vortical layer

In this section we summarize the physical argument given by Longuet-Higgins (1969) for gravity waves and extend it to include capillarity.

Consider a surface wave travelling to the right with speed c as in figure 1. Let n and s denote coordinates normal and tangential to the free surface, and v', u' the vortical components of the orbital velocities v, u in the corresponding directions. If D denotes the thickness of the vortical layer and $M = \int \rho u' dn$, the integrated mass flux across the layer, we have by continuity

$$\rho \frac{\partial D}{\partial t} = -\frac{\partial M}{\partial s} = \frac{1}{c} \frac{\partial M}{\partial t} = \frac{\tau}{c}, \quad (2.1)$$

where τ is the tangential stress acting on the layer. If τ is proportional to $\exp i(k s - \sigma t)$ where k is the wavenumber, then integration of (2.1) with respect to the time t gives

$$D = \frac{i\tau}{\rho\sigma c} + \text{constant}. \quad (2.2)$$

Thus D leads τ by 90° . Now in the case when the tangential stress at the surface vanishes, the only other tangential force acting on the boundary layer is the viscous force at the base of the boundary layer, which is given by

$$-\tau = 2\mu \frac{\partial v}{\partial s} = 2\mu \frac{\partial^2 \eta}{\partial s \partial t} = 2\mu \sigma k \eta, \quad (2.3)$$

where μ is the coefficient of viscosity and η is the surface elevation. From (2.2) and (2.3) we see that the tangential stress produces an additional surface elevation

$$\eta' = -\frac{2i\mu k}{\rho c} \eta. \quad (2.4)$$

This produces an added normal stress

$$\delta_1 p = \left(\rho g - T \frac{\partial^2}{\partial s^2} \right) \eta', \quad (2.5)$$

where g and T denote gravity and surface tension. But from the dispersion relation

$$\sigma^2 = gk + (T/\rho) k^3 \quad (2.6)$$

for capillary-gravity waves, equation (2.5) can be written

$$\delta_1 p = \frac{\rho \sigma}{k} \eta' = -2i\mu \sigma k \eta. \quad (2.7)$$

In addition we must take into account the viscous component of the normal stress p_{nn} at the surface, which may be written

$$2\mu \frac{\partial v}{\partial n} = 2\mu k v = -2i\mu \sigma k \eta. \quad (2.8)$$

Adding this to (2.5) we find that it doubles the total pressure, giving altogether

$$\delta p = -4i\mu \sigma k \eta. \quad (2.9)$$

Clearly δp is greatest on the forward face of the wave where the orbital velocity is upwards. Hence δp does work against the orbital motion and so damps the waves. In fact (2.9) leads to the classical law for viscous decay of waves of amplitude a , namely

$$a \propto \exp(-2\nu k^2 t). \quad (2.10)$$

3. The theory of Ruvinsky & Freidman

We shall now reconcile the analysis of Ruvinsky & Freidman (1985*a*, *b*; 1987) with the above physical argument. These authors formally separate the potential and vortical components of the flow by writing

$$\mathbf{u} = \nabla \phi + \mathbf{u}', \quad \mathbf{u}' = \nabla \wedge \hat{\psi} \quad (3.1)$$

where $\hat{\psi}$ is a vector stream function. They apply to \mathbf{u}' a boundary-layer approximation similar to that used in Longuet-Higgins (1953, 1960) and arrive at the following system of coupled equations:

$$\nabla^2 \phi = 0, \quad (3.2)$$

$$\frac{\partial \phi}{\partial t} + \frac{1}{2} (\nabla \phi)^2 + g\eta - \frac{T}{\rho} \kappa(\eta) + 2\nu \frac{\partial^2 \phi}{\partial z^2} = 0 \quad \text{on } z = \eta, \quad (3.3)$$

$$\frac{\partial \eta}{\partial t} + \frac{\partial \eta}{\partial x} \frac{\partial \phi}{\partial x} = \frac{\partial \phi}{\partial z} + v' \quad \text{on } z = \eta, \quad (3.4)$$

$$\frac{\partial \phi}{\partial z} \rightarrow 0 \quad \text{as } z \rightarrow -\infty, \quad (3.5)$$

together with

$$\frac{\partial v'}{\partial t} = 2\nu \frac{\partial^2 \phi}{\partial x^2 \partial z} \Big|_{z=\eta}. \quad (3.6)$$

In equation (3.3) $\kappa(\eta)$ denotes the curvature operator: $\partial^2 \eta / \partial x^2 / (1 + \partial \eta / \partial x^2)^{1/2}$.

In the above equations the outstanding coupling term is v' on the right of the kinematic condition (3.4). To remove this we may write

$$\eta = \eta^* + \eta', \quad \eta' = \int v' dt \quad (3.7)$$

and evaluate the boundary conditions on the new surface $\eta = \eta^*$. For simplicity we consider first only the linear terms. Treating η' as of the same order or smaller than η , we see that (3.4) becomes simply

$$\frac{\partial \eta^*}{\partial t} = \frac{\partial \phi}{\partial z} \Big|_{z=\eta^*} \quad (3.8)$$

without the additional term on the right-hand side. Similarly (3.3) becomes

$$\frac{\partial \phi}{\partial t} + \left(g - \frac{T}{\rho} \kappa \right) (\eta^* + \eta') + 2\nu \frac{\partial^2 \phi}{\partial z^2} = 0 \quad (3.9)$$

to be satisfied on $z = \eta^*$. But by (3.6)

$$\eta' = \int v' dt = \int \int \frac{\partial v'}{\partial t} (dt)^2 = -\frac{2\nu}{\sigma^2} \frac{\partial^2 \phi}{\partial x^2 \partial z} \quad (3.10)$$

to within a constant. Now operating on both sides of (3.10) by $(g - T/\rho \partial^2 / \partial x^2)$ and using the dispersion relation (2.6) we see

$$\left(g - \frac{T}{\rho} \kappa \right) \eta' = \frac{\sigma^2}{\kappa} \eta' = -2\nu \frac{\partial^2 \phi}{\partial x^2}. \quad (3.11)$$

So by virtue of Laplace's equation (3.2), equation (3.9) becomes simply

$$\frac{\partial \phi}{\partial t} + \left(g - \frac{T}{\rho} \kappa \right) \eta^* + 4\nu \frac{\partial^2 \phi}{\partial z^2} = 0 \quad (3.12)$$

on $z = \eta^*$. Lastly we note that the term $-4\nu \partial^2 \phi / \partial z^2$ represents precisely the additional pressure term given by (2.9). For since $i\sigma = -\partial / \partial t$ and $k = \partial / \partial z$ we have, apart from the constant term,

$$-\delta p = 4\mu k \frac{\partial \eta}{\partial t} = 4\mu k v = 4\mu \frac{\partial^2 \phi}{\partial z^2}. \quad (3.13)$$

We see then that the last term in equation (3.12) represents an additional pressure, half of which comes from the viscous component in the normal stress p_{nn} . The other half comes from the thickening of the vortical boundary layer due to the piling up of mass induced by the tangential stress at the base of the boundary layer.

It is important to recognize that the boundary conditions (3.8) and (3.12) for the potential ϕ are to be evaluated not at the free surface $z = \eta$ but at the modified free surface $z = \eta^*$. After the solution for ϕ is determined, together with η^* , the free surface $z = \eta$ may be recovered by means of (3.7).

4. Discussion

In §3 we simplified the analysis by linearizing the two boundary conditions (3.3) and (3.4). Some linearization is already inherent in any case in the last two terms on the right of these equations. It is not difficult to show that if we retain nonlinear terms on the surface slope ϵ , but not in the ratio kD_0 of the boundary-layer thickness to the wavelength, then (3.8) and (3.12) above are generalized to

$$\frac{\partial\phi}{\partial t} + \frac{1}{2}(\nabla\phi)^2 + g\eta^* - \frac{T}{\rho}\kappa(\eta) + 4\nu\frac{\partial^2\phi}{\partial n^2} = 0 \quad (4.1)$$

and

$$\frac{\partial\eta^*}{\partial t} + \frac{\partial\eta^*}{\partial x}\frac{\partial\phi}{\partial x} = \frac{\partial\phi}{\partial z} \quad (4.2)$$

on $z = \eta^*$, at least to order ϵ^2 . At order ϵ^2 , we find a contribution to the mass transport and its normal gradient just beneath the vortical boundary layer, which, to this order, may simply be added to the solutions of (4.1) and (4.2). The centrifugal forces associated with the mass transport velocity must however be incorporated into (4.2) at order ϵ^3 .

However, the second-order vorticity generated by parasitic capillary waves and released from beneath the boundary layers (Longuet-Higgins 1955, 1960) is much greater than that from the original gravity wave. This vorticity may accumulate very rapidly (in one gravity-wave period) near the crest of the gravity wave and produce a crest vortex. This in turn may significantly affect the dynamics of the parasitic capillaries (see Longuet-Higgins 1991).

We note that all of the above analysis applies to non-breaking and non-turbulent motions in which the kinematic viscosity ν represents the molecular viscosity. It is highly interesting to consider whether an analogous theory might be formulated for breaking waves, in which ν would be replaced by a turbulent eddy coefficient. A full discussion of this question is beyond the scope of the present note, except to remark that generally it will be necessary to include an exchange of mass between the vortical and non-vortical parts of the flow across the lower boundary of the vortical layer. For plunging breakers, a flux of mass and momentum across the upper boundary will also be required. A further requirement is that the vorticity in the surface layer should decay in a time interval of the order of a wave period at most. A residual mean vorticity may however be added in the form of a surface shear current.

REFERENCES

- LAMB, H. 1932 *Hydrodynamics*, 6th edn. Cambridge University Press.
- LONGUET-HIGGINS, M. S. 1953 Mass transport in water waves. *Phil. Trans. R. Soc. Lond.* A 245, 535-581.
- LONGUET-HIGGINS, M. S. 1960 Mass transport in the boundary-layer at a free oscillating surface. *J. Fluid Mech.* 8, 293-306.
- LONGUET-HIGGINS, M. S. 1969 Action of a variable stress at the surface of water waves. *Phys. Fluids* 12, 737-740.
- LONGUET-HIGGINS, M. S. 1991 Capillary rollers and bores. *Proc. IUTAM Symp. on Breaking Waves*. Sydney, Australia, 15-19 July 1991.
- RUVINSKY, K. D. & FREIDMAN, G. I. 1985a Improvement of the first Stokes method for the investigation of finite-amplitude potential gravity-capillary waves. In *9th All Union Symp. on Diffraction and Propagation Waves*, Tbilisi, Theses of Reports vol. 2, pp. 22-25.

together with

$$\frac{\partial v'}{\partial t} = 2\nu \frac{\partial^3 \phi}{\partial x^2 \partial z} \Big|_{z=\eta} \quad (3.6)$$

In equation (3.3) $\kappa(\eta)$ denotes the curvature operator: $\partial^2 \eta / \partial x^2 / (1 + \partial \eta / \partial x^2)^{\frac{1}{2}}$.

In the above equations the outstanding coupling term is v' on the right of the kinematic condition (3.4). To remove this we may write

$$\eta = \eta^* + \eta', \quad \eta' = \int v' dt \quad (3.7)$$

and evaluate the boundary conditions on the new surface $\eta = \eta^*$. For simplicity we consider first only the linear terms. Treating η' as of the same order or smaller than η , we see that (3.4) becomes simply

$$\frac{\partial \eta^*}{\partial t} = \frac{\partial \phi}{\partial z} \Big|_{z=\eta^*} \quad (3.8)$$

without the additional term on the right-hand side. Similarly (3.3) becomes

$$\frac{\partial \phi}{\partial t} + \left(g - \frac{T}{\rho} \kappa \right) (\eta^* + \eta') + 2\nu \frac{\partial^2 \phi}{\partial z^2} = 0 \quad (3.9)$$

to be satisfied on $z = \eta^*$. But by (3.6)

$$\eta' = \int v' dt = \int \int \frac{\partial v'}{\partial t} (dt)^2 = -\frac{2\nu}{\sigma^2} \frac{\partial^2 \phi}{\partial x^2 \partial z} \quad (3.10)$$

to within a constant. Now operating on both sides of (3.10) by $(g - T/\rho \partial^2/\partial x^2)$ and using the dispersion relation (2.6) we see

$$\left(g - \frac{T}{\rho} \kappa \right) \eta' = \frac{\sigma^2}{\kappa} \eta' = -2\nu \frac{\partial^2 \phi}{\partial x^2} \quad (3.11)$$

So by virtue of Laplace's equation (3.2), equation (3.9) becomes simply

$$\frac{\partial \phi}{\partial t} + \left(g - \frac{T}{\rho} \kappa \right) \eta^* + 4\nu \frac{\partial^2 \phi}{\partial z^2} = 0 \quad (3.12)$$

on $z = \eta^*$. Lastly we note that the term $-4\nu \partial^2 \phi / \partial z^2$ represents precisely the additional pressure term given by (2.9). For since $i\sigma = -\partial/\partial t$ and $k = \partial/\partial z$ we have, apart from the constant term,

$$-\delta p = 4\mu k \frac{\partial \eta}{\partial t} = 4\mu k v = 4\mu \frac{\partial^2 \phi}{\partial z^2} \quad (3.13)$$

We see then that the last term in equation (3.12) represents an additional pressure, half of which comes from the viscous component in the normal stress p_{nn} . The other half comes from the thickening of the vortical boundary layer due to the piling up of mass induced by the tangential stress at the base of the boundary layer.

It is important to recognize that the boundary conditions (3.8) and (3.12) for the potential ϕ are to be evaluated not at the free surface $z = \eta$ but at the modified free surface $z = \eta^*$. After the solution for ϕ is determined, together with η^* , the free surface $z = \eta$ may be recovered by means of (3.7).

4. Discussion

In §3 we simplified the analysis by linearizing the two boundary conditions (3.3) and (3.4). Some linearization is already inherent in any case in the last two terms on the right of these equations. It is not difficult to show that if we retain nonlinear terms on the surface slope ϵ , but not in the ratio kD_0 of the boundary-layer thickness to the wavelength, then (3.8) and (3.12) above are generalized to

$$\frac{\partial\phi}{\partial t} + \frac{1}{2}(\nabla\phi)^2 + g\eta^* - \frac{T}{\rho}\kappa(\eta) + 4\nu\frac{\partial^2\phi}{\partial n^2} = 0 \quad (4.1)$$

and

$$\frac{\partial\eta^*}{\partial t} + \frac{\partial\eta^*}{\partial x}\frac{\partial\phi}{\partial x} = \frac{\partial\phi}{\partial z} \quad (4.2)$$

on $z = \eta^*$, at least to order ϵ^2 . At order ϵ^2 , we find a contribution to the mass transport and its normal gradient just beneath the vortical boundary layer, which, to this order, may simply be added to the solutions of (4.1) and (4.2). The centrifugal forces associated with the mass transport velocity must however be incorporated into (4.2) at order ϵ^3 .

However, the second-order vorticity generated by parasitic capillary waves and released from beneath the boundary layers (Longuet-Higgins 1955, 1960) is much greater than that from the original gravity wave. This vorticity may accumulate very rapidly (in one gravity-wave period) near the crest of the gravity wave and produce a crest vortex. This in turn may significantly affect the dynamics of the parasitic capillaries (see Longuet-Higgins 1991).

We note that all of the above analysis applies to non-breaking and non-turbulent motions in which the kinematic viscosity ν represents the molecular viscosity. It is highly interesting to consider whether an analogous theory might be formulated for breaking waves, in which ν would be replaced by a turbulent eddy coefficient. A full discussion of this question is beyond the scope of the present note, except to remark that generally it will be necessary to include an exchange of mass between the vortical and non-vortical parts of the flow across the lower boundary of the vortical layer. For plunging breakers, a flux of mass and momentum across the upper boundary will also be required. A further requirement is that the vorticity in the surface layer should decay in a time interval of the order of a wave period at most. A residual mean vorticity may however be added in the form of a surface shear current.

REFERENCES

- LAMB, H. 1932 *Hydrodynamics*, 6th edn. Cambridge University Press.
- LONGUET-HIGGINS, M. S. 1953 Mass transport in water waves. *Phil. Trans. R. Soc. Lond.* A 245, 535-581.
- LONGUET-HIGGINS, M. S. 1960 Mass transport in the boundary-layer at a free oscillating surface. *J. Fluid Mech.* 8, 293-306.
- LONGUET-HIGGINS, M. S. 1969 Action of a variable stress at the surface of water waves. *Phys. Fluids* 12, 737-740.
- LONGUET-HIGGINS, M. S. 1991 Capillary rollers and bores. *Proc. IUTAM Symp. on Breaking Waves*. Sydney, Australia, 15-19 July 1991.
- RUVINSKY, K. D. & FREIDMAN, G. I. 1985a Improvement of the first Stokes method for the investigation of finite-amplitude potential gravity-capillary waves. In *9th All Union Symp. on Diffraction and Propagation Waves*, Tbilisi, Theses of Reports vol. 2, pp. 22-25.

M. S. Longuet-Higgins

324

- RUVINSKY, K. D. & FREIDMAN, G. I. 1985*b* Ripple generation on capillary-gravity wave crests and its influence on wave propagation. *Inst. Appl. Phys., Acad. Sci. USSR Gorky, Preprint N132*, 46 pp.
- RUVINSKY, K. D. & FREIDMAN, G. I. 1987 The fine structure of strong gravity-capillary waves. In *Nonlinear Waves: Structures and Bifurcations* (ed. A. V. Gaponov-Grekhov, M. I. Rabinovich, pp. 304–326. Moscow: Nauka.
- RUVINSKY, K. D., FELDSTEIN, F. I. & FREIDMAN, G. I. 1991 Numerical simulations of the quasi-stationary stage of ripple excitation by steep gravity-capillary waves. *J. Fluid Mech.* **230**, 339–353.
- STOKES, G. G. 1847 On the theory of oscillatory waves. *Trans. Camb. Phil. Soc.* **8**, 441–455; reprinted in *Mathematica and Physical Papers*, Vol. 1, pp. 314–326, Cambridge University Press.

Introductory Notes for Part G

G. Radiation Stresses

Papers G1 to G13

The flux of energy associated with progressive water is well recognized; see for example Lamb's classic work (Lamb 1932). The flux of *momentum*, on the other hand, has been little, if ever, discussed. The *radiation stress*, as defined in paper G1, is the *additional flux of momentum* associated with a train of waves, and it has many practical consequences. In Paper G1, it is used to explain the coupling between a short surface wave and the orbital motion of a longer wave on which it rides. Paper G2 extends the analysis to waves riding on an arbitrary surface current. Some specific examples are worked out. The radiation stress is in general a tensor S_{ij} , defining the additional transfer of i -momentum in the j -direction. In G3, it is shown that the concept explains the phenomenon of "surf-beats" and in G4 how it explains the wave "set-up", which is especially important during hurricanes near a shoreline. Paper G5, which could well be read first, is a simplified account of the theory, with a number of applications. It also extends the theory so as to include surface-tension.

Note that a subsequent paper by Bretherton and Garrett (1986) derived many of the foregoing results from the general principle of the *conservation of wave action*. While this supplies deep insight, the radiation stress remains a useful and easily visualized concept.

Papers G7 and G8 apply the theory to gravity waves approaching a shoreline obliquely, and show that it is the diagonal term in the radiation stress tensor that drives the observed "longshore currents" parallel to the shoreline.

Papers G9 and G10 were motivated by various proposals for extracting energy from sea waves. They point out that if some energy is extracted, by whatever means, then a corresponding quantity of wave momentum must be extracted at the same time. This will produce a mean horizontal force on the device, which must be taken into practical consideration. The principle is demonstrated by some simple experiments. It is shown also that radiation stresses may be used to propel a boat forwards.

Paper G12 is included in this section because of its involvement with the principle of action conservation. G13 is an experimental paper on short, wind-generated waves riding on longer waves. The theoretical results of Paper G1 are used in interpreting the observations.

G. Radiation Stresses

*Reprinted without change of pagination from the
Journal of Fluid Mechanics, volume 8, part 4, pp. 585-583, 1960*

Changes in the form of short gravity waves on long waves and tidal currents

By M. S. LONGUET-HIGGINS

National Institute of Oceanography, Surrey

AND R. W. STEWART

University of British Columbia

(Received 2 January 1960)

Short gravity waves, when superposed on much longer waves of the same type, have a tendency to become both shorter and steeper at the crests of the longer waves, and correspondingly longer and lower in the troughs. In the present paper, by taking into account the non-linear interactions between the two wave trains, the changes in wavelength and amplitude of the shorter wave train are rigorously calculated. The results differ in some essentials from previous estimates by Unna. The variation in energy of the short waves is shown to correspond to work done by the longer waves against the *radiation stress* of the short waves, which has previously been overlooked. The concept of the radiation stress is likely to be valuable in other problems.

1. Introduction

It is well known that when gravity waves of fairly short wavelength ride upon the surface of much longer waves such as ocean swell or tidal currents then the wavelength of the short waves is diminished at the crests of the long waves and increased in the troughs. The phenomenon was pointed out by Unna in a series of papers (1941, 1942, 1947). The relative shrinking of the short wavelength L' compared to its mean value L was expressed by Unna (1947) as

$$\frac{L'}{L} = 1 - a_2 k_2 \coth k_2 h \quad (1.1)$$

at the crests of the long waves, where a_2 denotes the amplitude and $2\pi/k_2$ the wavelength of the long waves; h denotes the total mean depth.

Besides this contraction of the wavelength on the long-wave crests, the amplitude of the short waves can be expected to be correspondingly increased. On intuitive grounds Unna (1947) suggested the formula

$$\frac{a'}{a_1} = 1 + a_2 k_2 \coth k_2 h, \quad (1.2)$$

where a_1 is the mean value of a' .

Being unconvinced by Unna's reasoning, we carried out a systematic evaluation of the wave motion by Stokes's method of approximation, as far as the second order. This method allows one to calculate rigorously the change in

wavelength and amplitude arising from non-linear interactions between the two wave trains. The results are given in § 2 of the present paper. Equation (1.1) is verified, but in place of (1.2) we find

$$\frac{a'}{a_1} = 1 + a_2 k_2 \left(\frac{3}{4} \coth k_2 h + \frac{1}{4} \tanh k_2 h \right). \quad (1.3)$$

In deep water (when $k_2 h \rightarrow \infty$) both (1.2) and (1.3) tend to the same result

$$\frac{a'}{a_1} = 1 + a_2 k_2. \quad (1.4)$$

An interesting physical interpretation of (1.3) can be given. In § 3 of this paper it is shown that when a train of gravity waves of amplitude a ride upon a steady current U , the transfer of energy across any vertical plane normal to the motion is the sum of four terms

$$E c_g + E U + S_x U + \frac{1}{2} \rho h U'^3, \quad (1.5)$$

where E denotes the mean energy density, c_g denotes the group velocity and U' is a modified stream velocity. S_x is defined below. The first two terms of (1.5) represent simply the bodily transport of energy by the group velocity c_g and by the stream velocity U . The last term in (1.5) represents the transport by the stream U' of its own kinetic energy. All these terms are to be expected. However, the third term $S_x U$ represents the work done by the current U against the radiation stress of the waves. S_x is given by

$$S_x = E \left(\frac{2c_g}{c} - \frac{1}{2} \right), \quad (1.6)$$

which for short waves reduces to $\frac{1}{2} E$. The quantity S_x is one component of a two-dimensional stress tensor defined in § 3. The presence of this term does not seem to have been pointed out previously.

If the short waves are riding not upon a uniform current but upon much longer waves, then the alternate contraction and expansion at the surface of the longer waves results in work being done against the radiation stress of the short waves. In § 5 it is shown that if this work is assumed to appear as additional energy in the short waves, then there must be a change in the amplitude of the short waves precisely by (1.3). This confirms the conclusions of § 2.

By the same method we are also able to calculate the change in the form of short waves riding on very long waves such as tidal currents. Setting $k_2 h \ll 1$ in equation (1.3) gives

$$\frac{a'}{a} \doteq 1 + \frac{3a_2}{4h}. \quad (1.7)$$

This, however, is valid only when the ratio of the wave frequencies σ_2/σ_1 is still small compared with $k_2 h$. If both σ_2/σ_1 and $k_2 h$ are small but of the same order of magnitude we find, on the crests of the long waves,

$$\frac{a'}{a} = 1 + a_2 k_2 \frac{3k_2 h - 2\sigma_2/\sigma_1}{(2k_2 h - \sigma_2/\sigma_1)^2}. \quad (1.8)$$

This reduces to (1.7) when $\sigma_2/\sigma_1 \ll k_2 h$.

The results of the present paper may be extended without difficulty to systems of waves crossing at an arbitrary angle, and to wavelengths short enough to be influenced by capillarity. In the latter case, however, viscosity probably plays a predominant role.

2. Determination of the wave profile

In this section we shall give a rigorous evaluation of the wave motion by the method of Stokes (1847) as far as the second approximation.

It is well known that in a real fluid the motion does not remain irrotational for long after it is generated from rest, and that a second-order vorticity ultimately penetrates the interior (Longuet-Higgins 1953). However, except in the boundary layers, which are very thin, the vorticity is quasi-steady and produces only second-order currents which, to the second approximation, are simply superposed upon the oscillatory motion. Since we shall be concerned only with the oscillatory part of the motion, it is therefore sufficient to assume the existence of a velocity potential ϕ ; any steady second-order currents may be added afterwards.

Infinite depth

Take rectangular axes with the x -axis horizontal in the mean surface and the z -axis vortically upwards. Let \mathbf{u} , p , ρ , ζ denote the velocity, pressure, density and surface elevation respectively. Within the fluid we have the following relations

$$\left. \begin{aligned} \mathbf{u} &= \nabla\phi, \\ \nabla^2\phi &= 0, \\ \frac{p}{\rho} + gz + \frac{1}{2}\mathbf{u}^2 + \frac{\partial\phi}{\partial t} &= 0, \end{aligned} \right\} \quad (2.1)$$

the second equation being the equation of continuity and the third being Bernoulli's integral with the arbitrary function of t absorbed into ϕ . The boundary conditions are

$$\left. \begin{aligned} \left(\frac{p_0}{\rho} + gz + \frac{1}{2}\mathbf{u}^2 + \frac{\partial\phi}{\partial t} \right)_{z=\zeta} &= 0, \\ \left(\frac{\partial\zeta}{\partial t} + \frac{\partial\phi}{\partial x} \frac{\partial\zeta}{\partial x} - \frac{\partial\phi}{\partial z} \right)_{z=\zeta} &= 0, \end{aligned} \right\} \quad (2.2)$$

and

$$\lim_{z \rightarrow -\infty} \nabla\phi = 0, \quad (2.3)$$

where p_0 denotes the pressure at the free surface (hereafter assumed to be zero). The surface conditions (2.2) may be replaced by conditions to be satisfied at $z = 0$ by assuming the left-hand sides to be expansible in a power series in z

$$\left. \begin{aligned} g\zeta + \left(\frac{1}{2}\mathbf{u}^2 + \frac{\partial\phi}{\partial t} \right)_{z=0} + \zeta \left[\frac{\partial}{\partial z} \left(\frac{1}{2}\mathbf{u}^2 + \frac{\partial\phi}{\partial t} \right) \right]_{z=0} + \dots &= 0, \\ \frac{\partial\zeta}{\partial t} + \left(\frac{\partial\phi}{\partial x} \frac{\partial\zeta}{\partial x} - \frac{\partial\phi}{\partial z} \right)_{z=0} + \zeta \left[\frac{\partial}{\partial z} \left(\frac{\partial\phi}{\partial x} \frac{\partial\zeta}{\partial x} - \frac{\partial\phi}{\partial z} \right) \right]_{z=0} + \dots &= 0. \end{aligned} \right\} \quad (2.4)$$

Now let us assume expansions of the form

$$\left. \begin{aligned} \mathbf{u} &= \epsilon \mathbf{u}^{(1)} + \epsilon^2 \mathbf{u}^{(2)} + \dots, \\ \phi &= \epsilon \phi^{(1)} + \epsilon^2 \phi^{(2)} + \dots, \\ \zeta &= \epsilon \zeta^{(1)} + \epsilon^2 \zeta^{(2)} + \dots, \\ \frac{p}{\rho} + gz &= \epsilon p^{(1)} + \epsilon^2 p^{(2)} + \dots, \end{aligned} \right\} \quad (2.5)$$

where ϵ is a small quantity.* On substituting in equations (2.1), (2.3), (2.4), we have

$$\left. \begin{aligned} \mathbf{u}^{(1)} &= \nabla \phi^{(1)}, \\ \frac{x^{(1)}}{\rho} + \frac{\partial \phi^{(1)}}{\partial t} &= 0, \end{aligned} \right\} \quad (2.6)$$

$$\left. \begin{aligned} \nabla^2 \phi^{(1)} &= 0, \\ \lim_{\epsilon \rightarrow 0} \nabla \phi^{(1)} &= 0, \end{aligned} \right\} \quad (2.7)$$

and

$$\left. \begin{aligned} g \zeta^{(1)} + \left(\frac{\partial \phi^{(1)}}{\partial t} \right)_{z=0} &= 0, \\ \frac{\partial \zeta^{(1)}}{\partial t} - \left(\frac{\partial \phi^{(1)}}{\partial z} \right)_{z=0} &= 0, \end{aligned} \right\} \quad (2.8)$$

Elimination of $\zeta^{(1)}$ from the last two equations gives

$$\left(\frac{\partial^2 \phi^{(1)}}{\partial t^2} + g \frac{\partial \phi^{(1)}}{\partial z} \right)_{z=0} = 0. \quad (2.9)$$

Equations (2.7) and (2.9) are equations for $\phi^{(1)}$ alone, while the remaining equations give $\mathbf{u}^{(1)}$, $p^{(1)}$ and $\zeta^{(1)}$ in terms of $\phi^{(1)}$.

As a solution of these equations we select the first-order motion corresponding to two progressive surface waves of wave-numbers k_1 and k_2 ; that is

$$\phi^{(1)} = A_1 e^{k_1 z} \cos(k_1 x - \sigma_1 t + \theta_1) + A_2 e^{k_2 z} \cos(k_2 x - \sigma_2 t + \theta_2), \quad (2.10)$$

where $A_1, A_2, \sigma_1, \sigma_2, k_1, k_2$ are constants and

$$\sigma_1^2 = g k_1, \quad \sigma_2^2 = g k_2. \quad (2.11)$$

The corresponding free surface is given by

$$\zeta^{(1)} = a_1 \sin(k_1 x - \sigma_1 t + \theta_1) + a_2 \sin(k_2 x + \sigma_2 t + \theta_2), \quad (2.12)$$

where

$$a_1 = -\frac{A_1 k_1}{\sigma_1}, \quad a_2 = -\frac{A_2 k_2}{\sigma_2}. \quad (2.13)$$

* ϵ is proportional roughly to the surface slope; here, however, ϵ will be used only as an ordering parameter.

Proceeding now to the second approximation, we have to satisfy

$$\left. \begin{aligned} \mathbf{u}^{(2)} &= \nabla \phi^{(2)}, \\ \frac{p^{(2)}}{\rho} + \frac{1}{2} \mathbf{u}^{(1)2} + \frac{\partial \phi^{(2)}}{\partial t} &= 0, \\ \nabla^2 \phi^{(2)} &= 0, \\ \lim_{z \rightarrow -\infty} \nabla \phi^{(2)} &= 0, \\ g \zeta^{(2)} + \left(\frac{1}{2} \mathbf{u}^{(1)2} + \frac{\partial \phi^{(2)}}{\partial t} + \zeta^{(1)} \frac{\partial^2 \phi^{(1)}}{\partial z \partial t} \right)_{z=0} &= 0, \\ \frac{\partial \zeta^{(2)}}{\partial t} + \left(\frac{\partial \phi^{(1)}}{\partial x} \frac{\partial \zeta^{(1)}}{\partial x} - \frac{\partial \phi^{(2)}}{\partial z} + \zeta^{(1)} \frac{\partial^2 \phi^{(1)}}{\partial z^2} \right)_{z=0} &= 0. \end{aligned} \right\} \quad (2.14)$$

Elimination of $\zeta^{(2)}$ from the last two equations gives

$$\left(\frac{\partial^2 \phi^{(2)}}{\partial t^2} + g \frac{\partial \phi^{(2)}}{\partial z} \right)_{z=0} = - \left[\frac{\partial}{\partial t} (\mathbf{u}^{(1)2}) + \zeta^{(1)} \frac{\partial}{\partial z} \left(\frac{\partial^2 \phi^{(1)}}{\partial t^2} + g \frac{\partial \phi^{(1)}}{\partial z} \right) \right]_{z=0}. \quad (2.15)$$

On substituting the special solution (2.10) in the right-hand side, we see that the last group of terms vanishes identically, and we have

$$\begin{aligned} \frac{\partial^2 \phi^{(2)}}{\partial t^2} + g \frac{\partial \phi^{(2)}}{\partial z} &= - \frac{\partial}{\partial t} (\mathbf{u}^{(1)2}) \\ &= 2A_1 A_2 k_1 k_2 (\sigma_1 - \sigma_2) \cos \{ (k_1 - k_2)x - (\sigma_1 - \sigma_2)t + (\theta_1 - \theta_2) + \frac{1}{2}\pi \}. \end{aligned} \quad (2.16)$$

This and the above equations for $\phi^{(2)}$ are satisfied by

$$\phi^{(2)} = (A_1 A_2 k_1 k_2 / \sigma_2) e^{i(k_1 - k_2)x} \cos \{ (k_1 - k_2)x - (\sigma_1 - \sigma_2)t + (\theta_1 - \theta_2 - \frac{1}{2}\pi) \} + Ct, \quad (2.17)$$

where C is an arbitrary constant to be determined by the condition that the origin is in the mean surface level. In fact $\zeta^{(2)}$ may be found from (2.14):

$$g \zeta^{(2)} = - \left(\frac{\partial \phi^{(2)}}{\partial t} + \frac{1}{2} \mathbf{u}^{(1)2} + \zeta^{(1)} \frac{\partial^2 \phi^{(1)}}{\partial z \partial t} \right)_{z=0}. \quad (2.18)$$

On making the substitutions and writing for short

$$k_1 x - \sigma_1 t + \theta_1 = \psi_1, \quad k_2 x - \sigma_2 t + \theta_2 = \psi_2, \quad (2.19)$$

we find

$$\zeta^{(2)} = - \frac{1}{2} a_1^2 k_1 \sin 2\psi_1 - \frac{1}{2} a_2^2 k_2 \sin 2\psi_2, \quad - a_1 a_2 (k_1 \cos \psi_1 \cos \psi_2 - k_2 \sin \psi_1 \sin \psi_2). \quad (2.20)$$

Thus if the small parameter ϵ is absorbed into a_1, a_2 by writing $\epsilon = 1$, we have

$$\begin{aligned} \zeta &= (a_1 \sin \psi_1 - \frac{1}{2} a_1^2 k_1 \sin 2\psi_1) + (a_2 \sin \psi_2 - \frac{1}{2} a_2^2 k_2 \sin 2\psi_2) \\ &\quad - a_1 a_2 (k_1 \cos \psi_2 \cos \psi_2 - k_2 \sin \psi_1 \sin \psi_2) + \dots \end{aligned} \quad (2.21)$$

It is supposed that one of the waves is short compared with the other, say $k_1 \gg k_2$, and we wish to examine the influence of the second wave upon the first. For this purpose the terms in a_1^2, a_2, a_2^2 are irrelevant, and the remaining terms in (2.21) may be written

$$a_1 \sin \psi_1 (1 + a_2 k_2 \sin \psi_2) - a_1 \cos \psi_1 (a_2 k_1 \cos \psi_2). \quad (2.22)$$

Now if P , Q are any small quantities (varying slowly compared to ψ_1), the expression

$$\zeta = a_1(1 + P) \sin \psi_1 + a_1 Q \cos \psi_1 \quad (2.23)$$

represents a wave of slightly modified amplitude

$$a' = a_1(1 + P), \quad (2.24)$$

and of slightly modified wave-number

$$k' = k_1 \left(1 + \frac{1}{k_1} \frac{\partial Q}{\partial x} \right). \quad (2.25)$$

Writing

$$P = a_2 k_2 \sin \psi_2, \quad Q = -a_2 k_1 \cos \psi_2, \quad (2.26)$$

we see that the amplitude of the small waves is increased by a factor

$$\frac{a'}{a_1} = 1 + P = 1 + a_2 k_2 \sin \psi_2, \quad (2.27)$$

and the wave-number is increased by the same factor; the wavelength is therefore correspondingly reduced. This factor varies between $(1 + a_2 k_2)$ on the crests of the long wave and $(1 - a_2 k_2)$ in the troughs.

Finite depth

We now suppose that the water is of uniform finite depth h and that $k_1 h$, $k_2 h$ are not necessarily large. The boundary condition at the bottom ($z = -h$) is that the vertical velocity vanishes

$$\left(\frac{\partial \phi}{\partial z} \right)_{z=-h} = 0, \quad (2.28)$$

and so

$$\left(\frac{\partial \phi^{(1)}}{\partial z} \right)_{z=-h} = \left(\frac{\partial \phi^{(2)}}{\partial z} \right)_{z=-h} = 0. \quad (2.29)$$

In order that the elevation of the free surface may be given by

$$\zeta^{(1)} = a_1 \sin \psi_1 + a_2 \sin \psi_2 \quad (2.30)$$

in the first approximation, we must have

$$\phi^{(1)} = -\frac{a_1 \sigma_1}{k_1 \sinh k_1 h} \cosh k_1(z+h) \cos \psi_1 - \frac{a_2 \sigma_2}{k_2 \sinh k_2 h} \cosh k_2(z+h) \cos \psi_2, \quad (2.31)$$

where

$$\sigma_1^2 = g k_1 \tanh k_1 h, \quad \sigma_2^2 = g k_2 \tanh k_2 h. \quad (2.32)$$

The evaluation of the second approximation now proceeds exactly as before. The algebra is somewhat longer, but may be simplified by omitting all terms except those involving the product $a_1 a_2$ in which alone we are interested. This being understood we have for the surface condition

$$\left(\frac{\partial^2 \phi^{(2)}}{\partial t^2} + g \frac{\partial \phi^{(2)}}{\partial z} \right)_{z=0} = A \sin(\psi_1 - \psi_2) + B \sin(\psi_1 + \psi_2), \quad (2.33)$$

where

$$\begin{aligned} A &= -\frac{1}{2} a_1 a_2 [2\sigma_1 \sigma_2 (\sigma_1 - \sigma_2) (1 + \alpha_1 \alpha_2) + \sigma_1^3 (\alpha_1^2 - 1) - \sigma_2^3 (\alpha_2^2 - 1)], \\ B &= -\frac{1}{2} a_1 a_2 [2\sigma_1 \sigma_2 (\sigma_1 + \sigma_2) (1 - \alpha_1 \alpha_2) - \sigma_1^3 (\alpha_1^2 - 1) - \sigma_2^3 (\alpha_2^2 - 1)], \end{aligned} \quad (2.34)$$

and where we have written

$$\alpha_1 = \coth k_1 h, \quad \alpha_2 = \coth k_2 h \quad (2.35)$$

for brevity. The solution of this equation satisfying Laplace's equation and equation (2.29) is

$$\begin{aligned} \phi^{(2)} = & \frac{A \cosh(k_1 - k_2)(z + h) \sin(\psi_1 - \psi_2)}{-(\sigma_1 - \sigma_2)^2 \cosh(k_1 - k_2)h + g(k_1 - k_2) \sinh(k_1 - k_2)h} \\ & + \frac{B \cosh(k_1 + k_2)(z + h) \sin(\psi_1 + \psi_2)}{-(\sigma_1 + \sigma_2)^2 \cosh(k_1 + k_2)h + g(k_1 + k_2) \sinh(k_1 + k_2)h}. \end{aligned} \quad (2.36)$$

On substituting this expression in (2.18) and using the period equations (2.32), we find

$$g\zeta^{(2)} = \frac{1}{2}a_1 a_2 [C \cos(\psi_1 - \psi_2) - D \cos(\psi_1 + \psi_2)], \quad (2.37)$$

where

$$\begin{aligned} C = & \frac{[2\sigma_1 \sigma_2 (\sigma_1 - \sigma_2) (1 + \alpha_1 \alpha_2) + \sigma_1^2 (\alpha_1^2 - 1) - \sigma_2^2 (\alpha_2^2 - 1)] (\sigma_1 - \sigma_2) (\alpha_1 \alpha_2 - 1)}{\sigma_1^2 (\alpha_1^2 - 1) - 2\sigma_1 \sigma_2 (\alpha_1 \alpha_2 - 1) + \sigma_2^2 (\alpha_2^2 - 1)} \\ & + (\sigma_1^2 + \sigma_2^2) - \sigma_1 \sigma_2 (\alpha_1 \alpha_2 + 1), \end{aligned} \quad (2.38)$$

and D is given by a similar expression with the signs of α_2 , σ_2 reversed. A more convenient form for $\zeta^{(2)}$, equivalent to the above, is

$$\zeta^{(2)} = a_1 a_2 k_1 / \alpha_1 [E \cos \psi_1 \cos \psi_2 + F \sin \psi_1 \sin \psi_2], \quad (2.39)$$

where

$$E = \frac{\alpha_1 \alpha_2 [(\alpha_1^2 - 1)^2 - \lambda^2 (3\alpha_1^2 + 1) (\alpha_2^2 - 1) - \lambda^4 (3\alpha_2^2 + 1) (\alpha_1^2 - 1) + \lambda^6 (\alpha_2^2 - 1)^2] + 2\lambda^3 (\alpha_1^2 \alpha_2^2 - 1) (\alpha_1^2 + \alpha_2^2)}{[(\alpha_1^2 - 1) - 2\lambda \alpha_1 \alpha_2 + \lambda^2 (\alpha_2^2 - 1)]^2 - 4\lambda^2}, \quad (2.40)$$

$$F = \frac{-2\alpha_1 \alpha_2 [\lambda (\alpha_1^4 - 1) + \lambda^5 (\alpha_2^4 - 1)] + (\alpha_1^2 + \alpha_2^2 + 2\alpha_1^2 \alpha_2^2) [\lambda^2 (\alpha_1^2 - 1) + \lambda^4 (\alpha_2^2 - 1)]}{[(\alpha_1^2 - 1) - 2\lambda \alpha_1 \alpha_2 + \lambda^2 (\alpha_2^2 - 1)]^2 - 4\lambda^2}, \quad (2.41)$$

and where we have written

$$\sigma_2 / \sigma_1 = \lambda. \quad (2.42)$$

The quantities P , Q of equation (2.23) are now given by

$$\begin{cases} P = (a_2 k_1 / \alpha_1) F \sin \psi_2, \\ Q = (a_2 k_1 / \alpha_1) E \cos \psi_2. \end{cases} \quad (2.43)$$

The case of deep water is easily retrieved from the above expressions by letting

$$\alpha_1 \rightarrow 1, \quad \alpha_2 \rightarrow 1 \quad (2.44)$$

(in that order, since $\sigma_1 > \sigma_2$). We then find

$$E \rightarrow -1, \quad F \rightarrow \lambda^2 = k_2 / k_1, \quad (2.45)$$

and the equations (2.43) for P and Q reduce to (2.26).

Let us now suppose that the shorter waves are effectively in deep water ($e^{-k_1 h}$ is negligible) but that the depth h is not necessarily great compared with

the wavelength of the long waves. Under these conditions α_1 tends to 1 and $\lambda^2(\alpha_2^2 - 1)$ becomes a factor in both numerator and denominator of E and F . Hence

$$\left. \begin{aligned} E &= \frac{-2\alpha_2(2 - \lambda\alpha_2) + 2\lambda - \lambda^4\alpha_2(\alpha_2^2 - 1)}{(2 - \lambda\alpha_2)^2 - \lambda^2} \\ F &= \frac{-2\alpha_2\lambda^3(1 + \alpha_2^2) + \lambda^2(1 + 3\alpha_2^2)}{(2 - \lambda\alpha_2)^2 - \lambda^2} \end{aligned} \right\} \quad (2.46)$$

Of particular interest to us is the case when λ is very small. Then

$$E = -\alpha_2, \quad F = \lambda^2 \frac{1 + 3\alpha_2^2}{4}, \quad (2.47)$$

and so

$$\left. \begin{aligned} P &= a_2 k_2 \frac{1 + 3\alpha_2^2}{4\alpha_2} \sin \psi_2, \\ Q &= -a_2 k_2 \alpha_2 \cos \psi_2. \end{aligned} \right\} \quad (2.48)$$

Hence the wave amplitude is increased by a factor

$$\frac{a'}{a_1} = 1 + a_2 k_2 \left(\frac{1}{4} \tanh k_2 h + \frac{3}{4} \coth k_2 h \right) \sin \psi_2 \quad (2.49)$$

and the wave-number is increased by a factor

$$\frac{k'}{k_1} = 1 + a_2 k_2 \coth k_2 h \sin \psi_2. \quad (2.50)$$

This is always assuming that $k_2 h$ is not very small also.

The case when the longer waves are effectively in shallow water, that is

$$\tanh k_2 h = \frac{1}{\alpha_1} \equiv \mu \ll 1 \quad (2.51)$$

may also be studied. Such a situation may occur, for example, with waves riding on a tidal current. But the small quantities λ, μ may be of the same order of magnitude. In a typical situation we might have waves of period $T_1 = 10$ seconds riding on a tidal stream of period $T_2 = 12.4$ hours, in 50 fathoms of water. Then

$$\lambda = \frac{\sigma_2}{\sigma_1} = \frac{T_1}{T_2} = 2.2 \times 10^{-4} \quad (2.52)$$

$$\text{and} \quad \mu \doteq k_2 h = \frac{2\pi h}{T_2 \sqrt{gh}} = 4.4 \times 10^{-4}. \quad (2.53)$$

Retaining the terms of lowest order in both λ and μ , we find from (2.46)

$$\left. \begin{aligned} E &= -\frac{2}{2\mu - \lambda} + \frac{\lambda^4}{\mu(2\mu - \lambda)^2}, \\ F &= \frac{\lambda^2(3\mu - 2\lambda)}{\mu(2\mu - \lambda)^2}, \end{aligned} \right\} \quad (2.54)$$

and so from (2.43)

$$\left. \begin{aligned} P &= a_2 k_2 \frac{3\mu - 2\lambda}{(2\mu - \lambda)^2} \sin \psi_2, \\ Q &= -a_2 k_1 \left(\frac{2}{2\mu - \lambda} - \frac{\lambda^4}{\mu(2\mu - \lambda)^2} \right) \cos \psi_2. \end{aligned} \right\} \quad (2.55)$$

Changes in the form of short gravity waves

573

The changes in wave amplitude and wave-number are therefore given by

$$\frac{a'}{a_1} = 1 + a_2 k_2 \frac{3\mu - 2\lambda}{(2\mu - \lambda)^2} \sin \psi_2, \quad (2.56)$$

and

$$\frac{k'}{k_1} = 1 + a_2 k_2 \left(\frac{2}{2\mu - \lambda} - \frac{\lambda^4}{\mu(2\mu - \lambda)^2} \right) \sin \psi_2. \quad (2.57)$$

When λ/μ is small these equations reduce to

$$\frac{a'}{a_1} = 1 + \frac{3a_2}{4h} \sin \psi_2, \quad (2.58)$$

and

$$\frac{k'}{k} = 1 + \frac{a_2}{h} \sin \psi_2, \quad (2.59)$$

respectively.

The above results for shallow water may also be deduced directly starting from a velocity potential

$$\phi^{(1)} = -\frac{a_1 \sigma_1}{k_1} e^{k_1 z} \cos \psi_1 - \frac{a_2 \sigma_2}{k_2^2 h} \left[1 + \frac{1}{2} k_2^2 (z+h)^2 \right] \cos \psi_2. \quad (2.60)$$

The only other special cases of interest are when the longer waves are shallow-water waves and the shorter waves are either shallow-water or deep-water waves. However, the results are all contained in equation (2.41), and the appropriate simplifications may be left to the reader.

Standing waves

So far we have considered only waves of progressive type riding on longer waves, also of progressive type, travelling in the same direction.

It is evident, however, that when λ is very small ($\lambda \ll \mu$) the expressions for the shortening or the steepening of the waves are unaffected if λ is reversed in sign, that is if the direction of one of the waves is reversed. Hence the shortening and steepening of the waves are the same whether the second system of waves is travelling in the same or opposite direction to the first.

Further, the interaction terms, on which these effects depend, are evidently linear in the two wave amplitudes a_1, a_2 separately. It follows that, if two of the longer waves are superposed to give a standing wave, and if the short progressive waves ride on top of these, the relative shortening and steepening will be similar. More precisely if

$$\begin{aligned} \zeta^{(2)} &= a_1 \sin(k_1 x - \sigma_1 t + \theta_1) + a_2 \sin(k_2 x - \sigma_2 t + \theta_2) + a_2 \sin(k_2 x + \sigma_2 t + \theta_2) \\ &= a_1 \sin(k_1 x - \sigma_1 t + \theta_1) + 2a_2 \sin k_2 x \cos(\sigma_2 t + \theta_2), \end{aligned} \quad (2.61)$$

then on the crests of the longer waves the amplitude of the shorter waves is found to increase by a factor

$$1 + a_2 k_2 \left(\frac{1}{2} \tanh k_2 h + \frac{3}{2} \coth kh \right), \quad (2.62)$$

and the wavelength is diminished by a factor

$$1 + 2a_2 k_2 \coth k_2 h. \quad (2.63)$$

If a_2 is written for $2a_2$ these formulae are similar to (2.49) and (2.50).

Similarly, if two short waves are added to produce a short standing wave, then by the linearity of the interaction terms it follows that the changes in amplitude and wavelength of the combined wave are given by identical expressions, both when the longer waves are progressive and when they are standing waves.

On the other hand, in shallow water when λ is not much less than μ , the change of form of short progressive waves depends upon their direction relative to the longer waves. Hence different formulae for standing waves result, which may be deduced without difficulty from equations (2.56) and (2.57).

3. The radiation stresses

In order to interpret physically the conclusions of § 2, we first consider from a general point of view the transfer of energy by surface waves on a steady, uniform current.

In a non-viscous fluid, the rate of transfer of energy across a surface fixed in space is given by

$$R = \iint_S (p + \frac{1}{2}\rho u^2 + \rho gz) \mathbf{u} \cdot \mathbf{n} dS, \quad (3.1)$$

where \mathbf{n} denotes the unit normal to the surface, and z is measured vertically upwards. Hence the mean rate of transfer across a vertical plane $x = \text{const.}$, per unit distance in the y -direction, is

$$R_x = \overline{\int_{-h}^{\zeta} (p + \frac{1}{2}\rho u^2 + \rho gz) u dz}, \quad (3.2)$$

where $z = \zeta(t)$ denotes the free surface, and the mean value with respect to time, indicated by a bar, is taken after performing the integration. We now express the velocity as the sum of two parts

$$\mathbf{u} = \mathbf{U} + \mathbf{u}', \quad (3.3)$$

where $\mathbf{U} = (U, 0, 0)$ denotes the mean stream velocity and \mathbf{u}' is the additional velocity due to the wave motion. It may be assumed that the mean value of \mathbf{u}' at any point in the interior is zero $\overline{\mathbf{u}'} = 0$

and further that U is independent of z .* On substituting (3.3) into (3.2) and taking mean values, we have identically

$$R_x = R_0 + R_1 + R_2 + R_3, \quad (3.5)$$

where

$$\left. \begin{aligned} R_0 &= \overline{\int_{-h}^{\zeta} (p + \frac{1}{2}\rho u'^2 + \rho gz) u' dz}, \\ R_1 &= \overline{\int_{-h}^{\zeta} (p + \frac{1}{2}\rho u'^2 + \rho gz + \rho u'^2) dz} U, \\ R_2 &= \overline{\int_{-h}^{\zeta} \frac{3}{2}\rho u' dz} U^2, \\ R_3 &= \overline{\int_{-h}^{\zeta} \frac{1}{2}\rho dz} U^3. \end{aligned} \right\} \quad (3.6)$$

* These assumptions taken together are valid only for irrotational flow; vorticity may be taken into account by supposing U to depend upon z .

Let us consider these terms separately. The first term R_0 is simply equal to the energy transfer by the waves in the absence of a steady stream. Adapting the notation of § 2, we have

$$\left. \begin{aligned} \zeta &= a \cos(kx - \sigma t + \theta) + O(a^2 k), \\ \phi &= \frac{a\sigma}{k \sinh kh} \cosh k(z+h) \sin(kx - \sigma t + \theta) + O(a^2 \sigma), \end{aligned} \right\} \quad (3.7)$$

where $\sigma^2 = gk \tanh kh, \quad \sigma/k = c. \quad (3.8)$

Hence it is easily found that, to second order,

$$R_0 = \frac{1}{4} \rho g a^2 c \left(1 + \frac{2kh}{\sinh 2kh} \right) = E c_\sigma, \quad (3.9)$$

where $E = \frac{1}{2} \rho g a^2 \quad (3.10)$

denotes the mean energy density per unit horizontal area and

$$c_\sigma = \frac{d\sigma}{dk} = \frac{1}{2} c \left(1 + \frac{2kh}{\sinh 2kh} \right) \quad (3.11)$$

denotes the group velocity (cf. Lamb 1932, § 237).

The second term in (3.6) may be separated into two parts

$$R_1 = R_{11} + R_{12}, \quad (3.12)$$

where
$$\left. \begin{aligned} R_{11} &= \int_{-h}^{\zeta} (\frac{1}{2} \rho u'^2 + \rho g z) dz \quad U + \frac{1}{2} \rho g h^2 U = E U, \\ R_{12} &= \int_{-h}^{\zeta} (p + \rho u'^2) dz \quad U - \frac{1}{2} \rho g h^2 U = S_x U. \end{aligned} \right\} \quad (3.13)$$

The term R_{11} is self-explanatory; it is the bodily transport of kinetic and gravitational energy by the mean velocity U . The term R_{12} is more interesting and its presence does not seem to have been previously noticed. It represents the work done by the mean velocity U against the radiation stress defined by

$$S_x = \int_{-h}^{\zeta} (p + \rho u'^2) dz - \frac{1}{2} \rho g h^2. \quad (3.14)$$

To interpret this expression we divide it again into two parts: first take the integral with respect to z up to a fixed point, say the mean level $z = 0$. (If $\zeta < 0$ then p and u may be extended analytically.) Thus we have

$$T_x = \int_{-h}^0 (p + \rho u'^2) dz - \frac{1}{2} \rho g h^2, \quad (3.15)$$

say. In this expression the quantity $\overline{\rho u'^2}$ represents the well-known Reynolds stress, which arises because the excess velocity u' transfers horizontal momentum $\rho u'$ at a rate $\rho u'^2$; even when u' is negative the contribution to the Reynolds stress is positive.

To obtain S_x we have only to add to T_x the quantity

$$Z_x = \int_0^{\zeta} (p + \rho u'^2) dz \quad (3.16)$$

(the integral being interpreted in the usual way when $\zeta < 0$). In this expression the term $\rho u'^2$ contributes only a small quantity of the third order. The remaining term p gives a positive contribution to Z_x since when ζ is positive (the surface is above the mean level) so also is the pressure, and when ζ is negative so also is p ; in fact near the mean level p is given almost by the hydrostatic pressure term $\rho g(\zeta - z)$; hence

$$Z_x \doteq \int_0^{\zeta} \rho g(\zeta - z) dz = \frac{1}{2} \rho g \zeta^2. \quad (3.17)$$

It will be seen that this term arises essentially from the deformation of the free surface.

On the other hand, to evaluate T_x we must express \bar{p} to the second order in the wave amplitude a : assuming $\bar{\zeta} = 0$, we find

$$\bar{p} = -\rho g z - \frac{\rho g a^2 k}{\sinh 2kh} \cosh^2 k(z+h). \quad (3.18)$$

It will be seen that the second term on the right is negative, so that the mean pressure at a point is actually reduced by the presence of the waves. On substituting in (3.15) and (3.17) we have, to order a^2 ,

$$\left. \begin{aligned} T_x &= \frac{1}{2} \rho g a^2 \frac{2kh}{\sinh 2kh}, \\ Z_x &= \frac{1}{4} \rho g a^2. \end{aligned} \right\} \quad (3.19)$$

Combining these, we have

$$S_x = \frac{1}{2} \rho g a^2 \left(\frac{2kh}{\sinh 2kh} + \frac{1}{2} \right) = E \left(\frac{2c_g}{c} - \frac{1}{2} \right). \quad (3.20)$$

Thus S_x is an additional stress, due to the wave motion, per unit length across a plane normal to the direction of wave propagation. It is composed of the integrated Reynolds stress, plus the stress due to the correlation between surface elevation and pressure, less the effect of the reduction in the average pressure in the body of the fluid due to the presence of the waves. Altogether

$$R_1 = (E + S_x) U = E \left(\frac{2c_g}{c} + \frac{1}{2} \right) U. \quad (3.21)$$

The last two terms in (3.6) are easily evaluated. Since \bar{u}' vanishes everywhere in the interior of the fluid, and $\bar{\zeta} = 0$, we have

$$R_2 = \frac{3}{2} E U^2 / c, \quad R_3 = \frac{1}{2} \rho h U^3. \quad (3.22)$$

But since the motion is irrotational there is, owing to the mass-transport velocity, a net momentum E/c in the direction of wave propagation (Stokes 1847), that is, a mean velocity $E/c\rho h$. Writing

$$U + E/c\rho h = U' \quad (3.23)$$

and substituting in (3.22) we have, to the present order of approximation,

$$R_2 + R_3 = \frac{1}{2} \rho h U'^3 \quad (3.24)$$

which represents the transport of the kinetic energy of the current by itself.

Collecting together the various terms, we find

$$R_x = E c_g + E U + S_x U + \frac{1}{2} \rho h U'^2, \quad (3.25)$$

where S_x and U' are given by (3.20) and (3.23).

In an exactly similar way we may calculate the flow of energy in the y -direction in the presence of a steady transverse current $\mathbf{U} = (0, V, 0)$. This is given by the integral

$$R_y = \int_{-h}^{\xi} \overline{(p + \frac{1}{2} \rho u'^2 + \rho g z + V^2) V} dz, \quad (3.26)$$

which is easily found to be

$$R_y = E V + S_y V + \frac{1}{2} \rho h V^3, \quad (3.27)$$

where

$$S_y = \frac{1}{4} \rho g a^2 \frac{2kh}{\sinh 2kh} = E \left(\frac{c_g}{c} - \frac{1}{2} \right). \quad (3.28)$$

In the general case of a mean stream velocity $\mathbf{U} = (U, V, 0)$ the transfer of energy across a vertical plane in direction $\mathbf{n} = (l, m, 0)$ is

$$\bar{R} = \int_{-h}^{\xi} \overline{(p + \frac{1}{2} \rho \mathbf{u}'^2 + \rho g z + \rho \mathbf{u}' \cdot \mathbf{U} + \frac{1}{2} \rho U^2) (\mathbf{u}' + \mathbf{U}) \cdot \mathbf{n}} dz, \quad (3.29)$$

which by exactly similar analysis is found to be

$$\bar{R} = E c_g \cdot \mathbf{n} + E \mathbf{U} \cdot \mathbf{n} + \mathbf{U} \cdot \mathbf{S} \cdot \mathbf{n} + \frac{1}{2} \rho h U'^2 (\mathbf{U}' \cdot \mathbf{n}), \quad (3.30)$$

where

$$\mathbf{c}_g = (c_g, 0, 0) \quad (3.31)$$

denotes the vector group velocity,

$$\mathbf{U}' = (U + E/\rho c h, V, 0) \quad (3.32)$$

denotes the modified stream velocity, and where \mathbf{S} denotes the tensor

$$\mathbf{S} = \begin{pmatrix} S_x & 0 \\ 0 & S_y \end{pmatrix}. \quad (3.33)$$

\mathbf{S} may be called the *stress tensor* of the wave motion. In full it is

$$\mathbf{S} = \begin{pmatrix} E \left(\frac{2c_g}{c} - \frac{1}{2} \right) & 0 \\ 0 & E \left(\frac{c_g}{c} - \frac{1}{2} \right) \end{pmatrix}. \quad (3.34)$$

In very deep water ($c_g = \frac{1}{2}c$) it becomes

$$\mathbf{S} = \begin{pmatrix} \frac{1}{2}E & 0 \\ 0 & 0 \end{pmatrix}, \quad (3.35)$$

and in shallow water ($c_g = c$) it becomes

$$\mathbf{S} = \begin{pmatrix} \frac{3}{2}E & 0 \\ 0 & \frac{1}{2}E \end{pmatrix}. \quad (3.36)$$

It is interesting to note that there is also a transport of energy corresponding to a vertical component of velocity W across the horizontal plane $z = \text{constant}$. In fact the mean energy transport per unit horizontal area is

$$\overline{(p + \frac{1}{2} \rho \mathbf{u}'^2 + \rho g z + \rho w' W + \frac{1}{2} \rho W^2) (w' + W)}. \quad (3.37)$$

The terms independent of W together vanish identically (there is no upwards transport of energy in an ordinary surface wave). The terms proportional to W are

$$(p + \frac{1}{2}\rho u'^2 + \rho gz + \rho w'^2) W = \frac{\rho g a^2 k}{2 \sinh 2kh} \cosh 2k(z+h) W. \quad (3.38)$$

In deep water ($kh \gg 1$) this becomes

$$\frac{1}{2} W \rho g a^2 k e^{-2kz}, \quad (3.39)$$

which is negligible below about half a wavelength.

4. The relation between wave amplitude and energy in an accelerated wave

In the preceding section we have calculated the transfer of energy horizontally when surface waves are superposed upon a steady, uniform current. We propose in the following to investigate the case when the surface waves ride not upon a steady current but upon a much longer wave, as in § 2, that is to say in place of the steady current U of § 3 we have instead the orbital velocity of the long waves. (This latter velocity is however supposed small compared with the phase velocity of the short waves.)

If the wavelength of the longer waves is sufficiently great compared with that of the shorter waves, then it is permissible to regard the orbital velocity U as being approximately constant and uniform over a period and wavelength, respectively, of the shorter waves. To a certain extent therefore we may make use of the formulae of § 3. However, a significant factor is introduced by the presence of a vertical acceleration in the longer waves; this alters the relation between the amplitude and the energy of the short waves, as will now be shown.

We shall consider from a general point of view the relation between the potential and the kinetic energy of a system undergoing vertical movements.

The discussion of energy relations in frames of reference not moving with constant acceleration leads generally to complications. Therefore we shall agree from the start to refer all energies to a stationary frame of reference.

In the stationary frame of reference, a progressive wave train of amplitude a' will have a gravitational potential energy

$$\text{P.E.} = \frac{1}{2} \rho g a'^2 \quad (4.1)$$

per unit horizontal distance (apart from terms independent of the wave amplitude a' and terms of higher order than the second).

Consider on the other hand the kinetic energy, measured in the same frame of reference. A very general theorem in dynamics states that the kinetic energy of a system of particles of mass m_i and velocity v_i is given by

$$\text{K.E.} = \frac{1}{2} M V^2 + \sum_i \frac{1}{2} m_i (v_i - V)^2, \quad (4.2)$$

where M is the total mass and V the velocity of the centre of mass. Now the vertical co-ordinate Z of the centre of mass of a wave train differs from the vertical co-ordinate Z_S of the mean free surface by an amount

$$Z - Z_S = \frac{1}{2} \rho a'^2 / M + \text{constant} \quad (4.3)$$

(neglecting terms of higher order). Hence the vertical velocity of the centre of mass differs from that of the free surface by an amount

$$\mathbf{V} - \mathbf{V}_S = \left[0, 0, \frac{\partial}{\partial t} \left(\frac{1}{2} \rho \alpha'^2 / M \right) \right]. \quad (4.4)$$

The first term on the right of (4.2) can therefore be written

$$\frac{1}{2} M \mathbf{V}_S^2 + W_S \frac{\partial}{\partial t} \left(\frac{1}{2} \rho \alpha'^2 \right). \quad (4.5)$$

The last term in (4.2) represents simply the kinetic energy calculated with reference to a frame moving (nearly) with the free surface and is therefore given by

$$\frac{1}{4} \rho \alpha'^2 \sigma'^2 / k', \quad (4.6)$$

where $2\pi/\sigma'$ and $2\pi/k'$ are the period and wavelength of the waves in the moving frame. But since this frame is accelerated these are related by the equations

$$\sigma'^2 = g' k', \quad (4.7)$$

where g' is the apparent value* of gravity

$$g' = g + \frac{\partial W_S}{\partial t}. \quad (4.8)$$

Altogether then we have

$$\text{K.E.} = \frac{1}{2} M \mathbf{V}_S^2 + \frac{1}{4} \rho g \alpha'^2 + \frac{\partial}{\partial t} \left(\frac{1}{2} \rho \alpha'^2 W_S \right). \quad (4.9)$$

The total wave energy E' may be defined as those parts of the kinetic-plus-potential energy which depend on the wave amplitude only, i.e.

$$E' = \frac{1}{2} \rho g \alpha'^2 + \frac{\partial}{\partial t} \left(\frac{1}{2} \rho \alpha'^2 W_S \right). \quad (4.10)$$

When $\partial \alpha'^2 / \partial t$ and W_S are both small quantities this expression becomes

$$E' = \frac{1}{2} \rho g \alpha'^2 \left(1 + \frac{1}{2g} \frac{\partial W_S}{\partial t} \right). \quad (4.11)$$

5. A physical interpretation of the results of §2

In the situation described in §2 we may regard the shorter waves as being superposed upon the longer waves, whose orbital velocity near the free surface has the components

$$\left. \begin{aligned} U &= a_2 \sigma_2 \coth k_2 h \sin \psi_2, \\ W &= -a_2 \sigma_2 \cos \psi_2. \end{aligned} \right\} \quad (5.1)$$

Consider first the changes in wavelength of the shorter waves. We make the physical assumption that *the wavelength of the short waves expands in proportion to the stretching of the surface by the long waves.*

* It is assumed that $(1/g') \partial g' / \partial t$ is small compared with σ' .

Now two particles in the surface which initially are separated by a distance dx have a small relative velocity $(\partial U/\partial x) dx$. The separation of these particles after time t is therefore given by

$$dx + \int_0^t \frac{\partial U}{\partial x} dx dt = dx \left[1 + \int_0^t \frac{\partial U}{\partial x} dt \right], \quad (5.2)$$

where to a first approximation $\partial U/\partial x$ may be evaluated at the original position x . The relative stretching of the surface is therefore given by

$$1 + \int_0^t \frac{\partial U}{\partial x} dt = 1 - a_2 k_2 \coth k_2 h \sin \psi_2. \quad (5.3)$$

The relative increase in wave-number of the short waves is the reciprocal of this expression, or

$$1 + a_2 k_2 \coth k_2 h \sin \psi_2, \quad (5.4)$$

in agreement with (2.50).

Now to account for the change in the wave amplitude we shall make the following assumptions.

(a) *The energy density of the short waves is given by (4.11) (despite the distortion caused by stretching of the surface).*

(b) *The rate of transfer of short-wave energy is given by*

$$E'(c_g + U) + S_x U \quad (5.5)$$

as in § 3.

(c) *The short-wave energy is conserved (and in particular that work done against the radiation stress appears as short-wave energy).*

With these assumptions the equation for the budget of short-wave energy becomes

$$\frac{\partial E'}{\partial t} = - \frac{\partial}{\partial x} [E'(c_g + U) + S_x U]. \quad (5.6)$$

To the order of approximation with which we are concerned we may take on the right-hand side of (5.6)

$$E' = \text{const.} = \frac{1}{2} \rho g a_1^2 = E_1, \quad (5.7)$$

and similarly $S_x = \text{const.}$, so that (5.6) reduces to

$$\frac{\partial E'}{\partial t} = - E_1 \frac{\partial}{\partial x} (c_g + U) - S_x \frac{\partial U}{\partial x}. \quad (5.8)$$

The physical interpretation of this last equation is that the rate of change of the short-wave content between x and $x + dx$ is determined by the divergence of the energy transport due to the group velocity c_g and the ambient flow U , plus the rate at which the convergence of the ambient flow, $(\partial U/\partial x)$, does work against the radiation stress S_x . Our assumption is that in this case the work done against the radiation stress appears as additional wave energy (although it is not possible to assert that such would be the case in other circumstances).

The term $S_x \partial U/\partial x$ appearing in (5.8) is closely analogous to the term $u_i u_j \partial U_i/\partial x_j$ which appears in the equations for turbulent energy and the term $p \nabla \cdot \mathbf{V}$ which occurs in the energy expression for turbulent flows.

Changes in the form of short gravity waves

581

Now, on relating S_x by (3.19) and E by E_1 , we have

$$\frac{\partial E'}{\partial t} = -E_1 \frac{\partial}{\partial x} \left[(c_g + U) + \left(\frac{2c_g}{c_1} - \frac{1}{2} \right) U \right], \quad (5.9)$$

or, since $\partial c_g / \partial x \ll \partial U / \partial x$,

$$\frac{\partial E'}{\partial t} = -E_1 \left(\frac{2c_g}{c_1} + \frac{1}{2} \right) \frac{\partial U}{\partial x}. \quad (5.10)$$

Since U represents a progressive wave motion, the operation $\partial / \partial x$ may be replaced by $-(1/c_2) \partial / \partial t$, giving

$$\frac{\partial E'}{\partial t} = E_1 \left(\frac{2c_g}{c_1} + \frac{1}{2} \right) \frac{1}{c_2} \frac{\partial U}{\partial t}. \quad (5.11)$$

Integration with respect to t (from an instant when the surface crosses the mean level and $U = 0$, $E = E_1$) gives

$$E' - E_1 = E_1 \left(\frac{2c_g}{c_1} + \frac{1}{2} \right) \frac{U}{c_2}, \quad (5.12)$$

or

$$\frac{E'}{E_1} = 1 + \left(\frac{2c_g}{c_1} + \frac{1}{2} \right) \frac{U}{c_2}. \quad (5.13)$$

Substituting for E' from (4.11), we obtain

$$\frac{a'^2}{a_1^2} = 1 + \left(\frac{2c_g}{c_1} + \frac{1}{2} \right) \frac{U}{c_2} - \frac{1}{2g} \frac{\partial W}{\partial t}, \quad (5.14)$$

and so, since U and W are both of order $a_2 \sigma_2$,

$$\frac{a'}{a_1} = 1 + \left(\frac{c_g}{c_1} + \frac{1}{4} \right) \frac{U}{c_2} - \frac{1}{4g} \frac{\partial W}{\partial t}. \quad (5.15)$$

In the case when the shorter waves are in deep water, $c_g/c_1 = \frac{1}{2}$ and hence

$$\frac{a'}{a_1} = 1 + \frac{3U}{4c_2} - \frac{1}{4g} \frac{\partial W}{\partial t}. \quad (5.16)$$

Since, from (5.1) and (2.32),

$$\left. \begin{aligned} \frac{U}{c_2} &= a_2 k_2 \coth k_2 h \sin \psi_2, \\ -\frac{1}{g} \frac{\partial W}{\partial t} &= \frac{a_2 \sigma_2^2}{g} \sin \psi_2 = a_2 k_2 \tanh k_2 h \sin \psi_2, \end{aligned} \right\} \quad (5.17)$$

equation (5.16) is equivalent to (2.49). Thus we have verified both equations (2.49) and (2.50) by alternative reasoning.

It will be seen that in shallow water, when the term $(1/g) \partial W / \partial t$ proportional to the vertical acceleration, is negligible, we have from (5.15) and (5.16)

$$\frac{a'}{a_1} = 1 + \left(\frac{c_g}{c_1} + \frac{1}{4} \right) \frac{U}{c_2} \quad (5.18)$$

and

$$\frac{a'}{a_1} = 1 + \frac{3U}{4c_2}, \quad (5.19)$$

respectively, the last equation being equivalent to (2.58).

The derivation of (5.16), (5.18) and (5.19) does not depend upon the sinusoidal character of the longer waves but only upon their being progressive. These formulae can therefore be expected to remain valid for short waves riding on cnoidal or solitary waves, or any other kind of progressive disturbance, provided it is sufficiently long.

Equation (5.16) can be further generalized to any disturbance consisting of the sum of a number of wave motions in which the velocities $c_2^{(i)}$ may be positive or negative. Thus we have

$$\frac{a'}{a_1} = 1 + (\Sigma^{(+)} - \Sigma^{(-)}) \left(\frac{3}{4} \frac{U^{(i)}}{c_2^{(i)}} - \frac{1}{4g} \frac{\partial W^{(i)}}{\partial t} \right), \quad (5.20)$$

where $\Sigma^{(+)}$ denotes the sum over all values of i for which $c_2^{(i)}$ is positive, and $\Sigma^{(-)}$ the corresponding sum for $c_2^{(i)}$ negative. In shallow water, when $c_2^{(i)} = \pm \sqrt{gh}$ we have

$$\frac{a'}{a_1} = 1 + \frac{3}{4\sqrt{gh}} (\Sigma^{(+)} U^{(i)} - \Sigma^{(-)} U^{(i)}). \quad (5.21)$$

It should be noted that the present method is not capable of yielding in a simple way the more refined formulae (2.56) and (2.57) which are applicable when the ratio of the wave frequencies is no longer small compared with $k_2 h$. For deriving these, the longer but more rigorous method of § 2 is to be preferred.

6. On a result of Unna

As mentioned in § 1, a formula for the change in amplitude essentially different from that which we have found was suggested by Unna (1941, 1947); his result is stated in equation (1.2).

Unna apparently did not work out the wave interactions exactly but relied on a physical argument. His reasoning differs from ours in two respects. First, he neglects entirely the work done by the longer waves against the radiation stress S_x , which we have taken into account. Secondly, he calculates the potential energy of the waves in the accelerated frame of reference, replacing g by $g + \partial W_S / \partial t$ in equation (4.1). He then assumes that kinetic and potential energy are conserved in the *accelerated* system.

It is not difficult to show that the kinetic-plus-potential energy is not generally conserved in an accelerated frame of reference, even when the acceleration is slow compared to the natural period of oscillation of the system. As examples we may quote a simple pendulum hinged at a point which is accelerated vertically, or the oscillations of water in a U-tube likewise accelerated.

The argument from conservation of energy therefore fails unless it is applied in a fixed or inertial frame of reference, as in §§ 4 and 5. If an accelerated frame of reference is used it must be supposed that there is some kind of interaction between the dynamical system and the accelerating forces.

In the case of deep water ($k_2 h \gg 1$) it happens that Unna's two mistakes—neglect of the radiation stress and assumption of energy conservation in the accelerated system—exactly cancel. But that they do not generally cancel is shown by the difference between equations (1.2) and (1.3).

7. Conclusions

The change in wavelength of short waves on the crests of longer waves can be interpreted as being due simply to the contraction of the particles in the longer wave.

However, to account for the increase in the amplitude of the short waves it is necessary to allow for the work done by the longer waves against the *radiation stress* of the short waves. This work is converted into short-wave energy, and produces a steepening of the short waves beyond what was previously expected.

The radiation stress is likely to play an important part in other situations, for example in waves riding on steady but non-uniform currents. Without close examination it cannot be assumed that work done against the radiation stress must necessarily appear as additional wave energy. But we have shown that in the present situation at least this assumption proves correct.

REFERENCES

- LAMB, H. 1932 *Hydrodynamics*, 6th ed. Cambridge University Press.
- LONGUET-HIGGINS, M. S. 1953 Mass-transport in water waves. *Phil. Trans. A*, **245**, 535-81.
- STOKES, G. G. 1847 On the theory of oscillatory waves. *Trans. Camb. Phil. Soc.* **8**, 441-55. (Reprinted in *Math. and Phys. Papers*, **1**, 314-26.)
- UNNA, P. J. 1941 White horses. *Nature, Lond.*, **148**, 226-7.
- UNNA, P. J. 1942 Waves and tidal streams. *Nature, Lond.*, **149**, 219-20.
- UNNA, P. J. 1947 Sea waves. *Nature, Lond.*, **159**, 239-42.

*Reprinted without change of pagination from the
Journal of Fluid Mechanics, volume 10, part 4, pp. 529-549, 1961*

The changes in amplitude of short gravity waves on steady non-uniform currents

By M. S. LONGUET-HIGGINS

National Institute of Oceanography, Wormley, Surrey

AND R. W. STEWART

University of British Columbia, Vancouver

(Received 9 November 1960)

The common assumption that the energy of waves on a non-uniform current U is propagated with a velocity $(U + c_g)$ where c_g is the group-velocity, and that no further interaction takes place, is shown in this paper to be incorrect. In fact the current does additional work on the waves at a rate $\gamma_{ij} S_{ij}$ where γ_{ij} is the symmetric rate-of-strain tensor associated with the current, and S_{ij} is the radiation stress tensor introduced earlier (Longuet-Higgins & Stewart 1960).

In the present paper we first obtain an asymptotic solution for the combined velocity potential in the simple case (1) when the non-uniform current U is in the direction of wave propagation and the horizontal variation of U is compensated by a vertical upwelling from below. The change in wave amplitude is shown to be such as would be found by inclusion of the radiation stress term.

In a second example (2) the current on the x -axis is assumed to be as in (1), but the horizontal variation in U is compensated by a small horizontal inflow from the sides. It is found that in that case the wave amplitude is also affected by the horizontal advection of wave energy from the sides.

From cases (1) and (2) the general law of interaction between short waves and non-uniform currents is inferred. This is then applied to a third example (3) when waves encounter a current with vertical axis of shear, at an oblique angle. The change in wave amplitude is shown to differ somewhat from the previously accepted value.

The conclusion that non-linear interactions affect the amplification of the waves has some bearing on the theoretical efficiency of hydraulic and pneumatic breakwaters.

1. Introduction

When short surface waves of any kind are propagated over the surface of a medium in steady but non-uniform motion, they tend to undergo refractive changes in length, direction and amplitude. The changes in length and direction depend on kinematical considerations only; a quite general treatment applicable to water waves has been given, for example, by Ursell (1960). But changes in the wave amplitude are less straightforward. Commonly (see Unna 1942; Suthons 1945; Johnson 1947; Evans 1955; Groen & Dorrestein 1958) it has been

assumed without justification that no coupling between the waves and current takes place, and that the wave energy is simply propagated with a velocity equal to $(U + c_g)$, where c_g is the vector group-velocity and U the local stream velocity. On the contrary, in a recent paper (Longuet-Higgins & Stewart 1960; this paper will be referred to as I), it was found that short gravity waves, riding on the backs of longer waves, are modified to a much greater extent than would be predicted if there were no interchange of energy between the short and the long waves. The discrepancy may be attributed to a term in the equation of energy transfer, called by us the *radiation stress*, and previously overlooked. The stress term occurs quite generally, and must give rise to changes in the wave amplitude in other situations besides the particular one that was considered.

The purpose of the present paper is to study the changes in amplitude of gravity waves riding on steady but non-uniform currents. The subject is of special interest owing to its possible application to bubble-breakwaters, whose action is probably to be ascribed largely to the stopping power of a horizontal current opposing the waves (Taylor 1955; Evans 1955; Straub, Bowers & Tarrapore 1959). Ocean waves entering tidal streams or crossing river flows are known to be subject to a similar effect (Unna 1942; Johnson 1947). The following discussion will be limited to the case of deep currents, that is to say, those for which the change in current velocity in a vertical distance equal to the wavelength is small compared with the wave velocity itself. But quite similar results would apply to waves on shearing currents which penetrated to a depth of only a fraction of a wavelength.

In our first example we consider a system of waves superposed on a current which varies gradually in the x -direction (the direction of wave propagation), and in which the variation in surface current is made up by a vertical upwelling (or downwelling). The modification which the currents produce in the wave form is calculated rigorously by a perturbation method. It is found that, while the variation in the wave-number k is given by the expected formula

$$\frac{1}{k} \frac{\partial k}{\partial x} = - \frac{1}{c + 2U} \frac{\partial U}{\partial x}, \quad (1.1)$$

the variation in the wave amplitude, on the other hand, is given by

$$\frac{1}{a} \frac{\partial a}{\partial x} = - \frac{2c + 3U}{(c + 2U)^2} \frac{\partial U}{\partial x}, \quad (1.2)$$

which is a higher rate of change than if there were no interaction between waves and currents. It is shown that this last result is consistent with the assumption that the equation governing the growth of wave energy E is

$$\frac{\partial}{\partial x} [E(c_g + U)] + S_x \frac{\partial U}{\partial x} = 0, \quad (1.3)$$

where S_x is the radiation stress mentioned earlier. (In deep water, $S_x = \frac{1}{2}E$.) This is to say that in addition to the transport of energy by the group-velocity and stream velocity, the current does work on the waves at a rate $S_x \partial U / \partial x$ per unit distance. In §4, this conclusion is shown also to be consistent with our earlier

results in I concerning the steepening of surface waves on long waves or tidal streams. Integration of (1.3) leads to the result

$$a \propto [c(c + 2U)]^{-\frac{1}{2}}. \quad (1.4)$$

In our second example we consider a situation very similar to the first, but in which the increase in surface current U is made up, not by a vertical upwelling from below, but by a horizontal inflow from the sides. The results are strikingly different. Although the variation in wave-number is the same as in (1.1), the variation in amplitude is now given by

$$\frac{1}{a} \frac{\partial a}{\partial x} = -\frac{c + U}{(c + 2U)^2} \frac{\partial U}{\partial x}. \quad (1.5)$$

This is accounted for by including in the energy balance the advection of wave energy by the transverse current V , as well as the work done against the corresponding stress component (equation (6.4)). The amplitude a is now found to be

$$a \propto [(c + 2U)/c]^{-\frac{1}{2}}, \quad (1.6)$$

which is a weaker variation than in the previous case.

The appropriate generalization of the equation of energy balance is shown to be

$$\nabla \cdot [E(\mathbf{c}_p + \mathbf{U})] + \frac{1}{2} S_{ij} \left(\frac{\partial U_i}{\partial x_j} + \frac{\partial U_j}{\partial x_i} \right) = 0, \quad (1.7)$$

where S_{ij} denotes the radiation stress tensor. In § 8 this is applied to a third example, that of waves crossing a shearing current obliquely. The changes in wavelength and direction of propagation θ are as found by Johnson (1947), but the law governing the wave amplitude is shown to be

$$a \propto (\sin 2\theta)^{-\frac{1}{2}}, \quad (1.8)$$

which differs from Johnson's result.

2. Two-dimensional current: an asymptotic solution

In this section we shall obtain a formal solution for surface waves on a non-uniform current $U(x)$ which has no transverse component. The solution is to be valid when

$$\sigma^{-1} \frac{\partial U}{\partial x} \ll 1, \quad (2.1)$$

where σ is the wave frequency; in other words, the change in stream velocity U over one wavelength L (that is, $L \partial U / \partial x$) is assumed small compared with the wave velocity $L\sigma/2\pi$.

General equations

It will be supposed that the velocity field \mathbf{u} is irrotational:

$$\mathbf{u} = \nabla \phi; \quad (2.2)$$

that the fluid is incompressible:

$$\nabla \cdot \mathbf{u} = \nabla^2 \phi = 0; \quad (2.3)$$

and that viscous effects are negligible. Then we have Bernoulli's integral

$$\frac{p}{\rho} + gz + \frac{1}{2} \mathbf{u}^2 + \frac{\partial \phi}{\partial t} = C, \quad (2.4)$$

where p , ρ , g denote the pressure, density and acceleration of gravity, and z is the vertical co-ordinate, directed upwards. C is a constant. If $z = \zeta$ is the equation of the free surface, then for the two boundary conditions there are the kinematical condition

$$\frac{\partial \zeta}{\partial t} + \left(\frac{\partial \phi}{\partial x} \frac{\partial \zeta}{\partial x} + \frac{\partial \phi}{\partial y} \frac{\partial \zeta}{\partial y} - \frac{\partial \phi}{\partial z} \right)_{z=\zeta} = 0, \quad (2.5)$$

and the condition of constant pressure, which by (2.4) may be written

$$g\zeta + \left(\frac{1}{2} \mathbf{u}^2 + \frac{\partial \phi}{\partial t} \right)_{z=\zeta} = C. \quad (2.6)$$

It is convenient to replace these last two equations by conditions to be satisfied at the mean surface level $z = 0$; this may be done by assuming the potential ϕ to be analytic and by expanding in a Taylor series in z :

$$\left. \begin{aligned} \frac{\partial \zeta}{\partial t} + \left(\frac{\partial \phi}{\partial x} \frac{\partial \zeta}{\partial x} + \frac{\partial \phi}{\partial y} \frac{\partial \zeta}{\partial y} - \frac{\partial \phi}{\partial z} \right)_{z=0} + \zeta \left[\frac{\partial}{\partial z} \left(\frac{\partial \phi}{\partial x} \frac{\partial \zeta}{\partial x} + \frac{\partial \phi}{\partial y} \frac{\partial \zeta}{\partial y} - \frac{\partial \phi}{\partial z} \right) \right]_{z=0} + \dots = 0, \\ g\zeta + \left(\frac{1}{2} \mathbf{u}^2 + \frac{\partial \phi}{\partial t} \right)_{z=0} + \zeta \left[\frac{\partial}{\partial z} \left(\frac{1}{2} \mathbf{u}^2 + \frac{\partial \phi}{\partial t} \right) \right]_{z=0} + \dots = C. \end{aligned} \right\} \quad (2.7)$$

Lastly, we assume that the waves are effectively in deep water, so that as $z \rightarrow -\infty$ the periodic part of the motion tends to zero.

Form of the solution

We seek a solution having the character of a time-periodic wave-motion superimposed upon a non-uniform steady flow. Let us then substitute

$$\left. \begin{aligned} \phi &= U_0 x + (\alpha \phi_{10} + \beta \phi_{01}) + (\alpha^2 \phi_{20} + \alpha \beta \phi_{11} + \beta^2 \phi_{02}) + \dots, \\ \zeta &= (\alpha \zeta_{10} + \beta \zeta_{01}) + (\alpha^2 \zeta_{20} + \alpha \beta \zeta_{11} + \beta^2 \zeta_{02}) + \dots, \end{aligned} \right\} \quad (2.8)$$

where U_0 is a steady uniform velocity, the velocity of the stream at $x = 0$; ϕ_{01} represents a steady non-uniform current, zero at $x = 0$; and ϕ_{10} represents an undisturbed surface wave; α and β are arbitrary small parameters proportional to wave steepness and to the velocity gradient of the current respectively. The terms $\alpha^2 \phi_{20}$, etc., are correction terms of higher order, necessary in order to satisfy the boundary conditions at the free surface. We are particularly interested in evaluating the second-order term $\alpha \beta \phi_{11}$, which is the lowest-order interaction potential between the waves and the current.

It may be worth remarking that to eliminate the uniform current U_0 by taking axes moving with velocity U_0 would not be convenient, since in the new frame of reference the motion would no longer be perfectly periodic in time. This is because the modified wavelength is generally a function of x , as will be seen below. Clearly the choice of axes must be made so as to correspond with the physical problem; if the source of the wave-motion is periodic this determines the appropriate frame of reference uniquely.

Retaining terms as far only as $\alpha\beta$, we have from (2.8)

$$\left. \begin{aligned} \nabla\phi &= (U_0, 0, 0) + \alpha\nabla\phi_{10} + \beta\nabla\phi_{01} + \alpha\beta\nabla\phi_{11}, \\ \frac{\partial\phi}{\partial t} &= \alpha\frac{\partial\phi_{10}}{\partial t} + \alpha\beta\frac{\partial\phi_{11}}{\partial t}, \\ \zeta &= \alpha\zeta_{10} + \beta\zeta_{01} + \alpha\beta\zeta_{11}, \end{aligned} \right\} \quad (2.9)$$

and so

$$\left. \begin{aligned} \frac{1}{2}\mathbf{u}^2 &= \frac{1}{2}U_0^2 + U_0\left(\alpha\frac{\partial\phi_{10}}{\partial x} + \beta\frac{\partial\phi_{01}}{\partial x}\right) \\ &\quad + \alpha\beta\left(U_0\frac{\partial\phi_{11}}{\partial x} + \frac{\partial\phi_{10}}{\partial x}\frac{\partial\phi_{01}}{\partial x} + \frac{\partial\phi_{10}}{\partial y}\frac{\partial\phi_{01}}{\partial y} + \frac{\partial\phi_{10}}{\partial z}\frac{\partial\phi_{01}}{\partial z}\right) + \dots, \\ \frac{\partial}{\partial z}\left(\frac{1}{2}\mathbf{u}^2\right) &= U_0\left(\alpha\frac{\partial^2\phi_{10}}{\partial x\partial z} + \beta\frac{\partial^2\phi_{01}}{\partial x\partial z}\right) + \dots \end{aligned} \right\} \quad (2.10)$$

Substitution in (2.7) shows at once that

$$C = \frac{1}{2}U_0^2. \quad (2.11)$$

The terms in α now give

$$\left. \begin{aligned} \left(\frac{\partial}{\partial t} + U_0\frac{\partial}{\partial x}\right)\zeta_{10} - \frac{\partial\phi_{10}}{\partial z} &= 0, \\ g\zeta_{10} + \left(\frac{\partial}{\partial t} + U_0\frac{\partial}{\partial x}\right)\phi_{10} &= 0, \end{aligned} \right\} \quad (2.12)$$

to be satisfied at $z = 0$. On eliminating ζ_{10} , we have

$$\left(\frac{\partial}{\partial t} + U_0\frac{\partial}{\partial x}\right)^2\phi_{10} + g\frac{\partial\phi_{10}}{\partial z} = 0 \quad (z = 0). \quad (2.13)$$

If we choose for ϕ_{10} the wave potential

$$\phi_{10} = A e^{k_0 q - i\sigma t}, \quad (2.14)$$

where A and k_0 are constants and

$$q = z + ix, \quad (2.15)$$

then ϕ_{10} satisfies Laplace's equation (2.3), and from (2.13)

$$(\sigma - U_0 k_0)^2 = g k_0. \quad (2.16)$$

Introducing the reference velocity

$$c_0 = \sqrt{(g/k_0)} \quad (2.17)$$

and the non-dimensional parameter

$$\gamma = U_0/c_0 \quad (2.18)$$

we have from (2.16)

$$\sigma = c_0 k_0 (1 + \gamma). \quad (2.19)$$

(To ensure continuity as γ (or U_0) tends to zero, we have adopted the positive sign in the square root.) From (2.12) and (2.10), we have also

$$\zeta_{10} = -\frac{1}{g} \left[\left(\frac{\partial}{\partial t} + \gamma c_0 \frac{\partial}{\partial x} \right) \phi_{10} \right]_{z=0} = \frac{i}{c_0} (\phi_{10})_{z=0}. \quad (2.20)$$

534

M. S. Longuet-Higgins and R. W. Stewart

Returning to equation (2.7), we see that the terms in β give equations for ϕ_{01} formally identical with (2.12) except that the time derivatives are now zero:

$$\left. \begin{aligned} U_0 = \frac{\partial \zeta_{01}}{\partial x} - \frac{\partial \phi_{01}}{\partial z} = 0 \\ g \zeta_{01} + U_0 \frac{\partial \phi_{01}}{\partial x} = 0 \end{aligned} \right\} (z = 0), \quad (2.21)$$

whence
$$U_0^2 \frac{\partial^2 \phi_{01}}{\partial x^2} + g \frac{\partial \phi_{01}}{\partial z} = 0 \quad (z = 0). \quad (2.22)$$

We require a potential ϕ_{01} to represent a steady flow having no transverse component $\partial \phi_{01} / \partial y$, which satisfies Laplace's equation, and also the condition $(\partial \phi_{01} / \partial x)_{x=0} = 0$. Such a potential is

$$\phi_{01} = c_0 k_0 (x^2 - z^2) + D c_0 z, \quad (2.23)$$

where D is a constant to be determined. From (2.22),

$$D = -2\gamma^2. \quad (2.24)$$

Therefore

$$\left. \begin{aligned} \phi_{01} = c_0 k_0 (x^2 - z^2) - 2\gamma^2 c_0 z, \\ \zeta_{01} = -2\gamma x; \end{aligned} \right\} \quad (2.25)$$

also
$$\frac{\partial U}{\partial x} = \beta \frac{\partial^2 \phi_{01}}{\partial x^2} = 2\beta c_0 k_0 = 2\beta \sigma (1 + \gamma)^{-1} \quad (2.26)$$

in accordance with (2.1), since β is assumed small.

The interaction potential

In equations (2.7) the terms in $\alpha\beta$ yield

$$\left. \begin{aligned} \left(\frac{\partial}{\partial t} + U_0 \frac{\partial}{\partial x} \right) \zeta_{11} - \frac{\partial \phi_{11}}{\partial z} + \left(\frac{\partial \phi_{10}}{\partial x} \frac{\partial \zeta_{01}}{\partial x} + \frac{\partial \phi_{01}}{\partial x} \frac{\partial \zeta_{10}}{\partial x} \right) - \left(\zeta_{10} \frac{\partial^2 \phi_{01}}{\partial z^2} + \zeta_{01} \frac{\partial^2 \phi_{10}}{\partial z^2} \right) = 0, \\ g \zeta_{11} + \left(\frac{\partial}{\partial t} + U_0 \frac{\partial}{\partial x} \right) \phi_{11} + \left(\frac{\partial \phi_{10}}{\partial x} \frac{\partial \phi_{01}}{\partial x} + \frac{\partial \phi_{10}}{\partial z} \frac{\partial \phi_{01}}{\partial z} \right) + \zeta_{01} \left(\frac{\partial}{\partial t} + U_0 \frac{\partial}{\partial x} \right) \frac{\partial \phi_{10}}{\partial z} = 0, \end{aligned} \right\} \quad (2.27)$$

to be satisfied when $z = 0$. (Note that $\partial^2 \phi_{01} / \partial t \partial z = \partial^2 \phi_{01} / \partial x \partial z = 0$.) From these equations ζ_{11} may be eliminated by applying the operator $g^{-1}(\partial/\partial t + U_0 \partial/\partial x)$ to the second equation and then subtracting the first. Without substituting explicit expressions for ϕ_{10} , ϕ_{01} , ζ_{10} and ζ_{01} but using (2.12) and (2.21) and the fact that $\partial \phi_{10} / \partial z = k_0 \phi_{10}$, we obtain*

$$\begin{aligned} \frac{1}{g} \left(\frac{\partial}{\partial t} + U_0 \frac{\partial}{\partial x} \right)^2 \phi_{11} + \frac{\partial \phi_{11}}{\partial z} \\ = 2 \left(\frac{\partial \phi_{10}}{\partial x} \frac{\partial \zeta_{01}}{\partial x} + \frac{\partial \phi_{01}}{\partial x} \frac{\partial \zeta_{10}}{\partial x} + k_0 \zeta_{10} \frac{\partial \phi_{01}}{\partial z} \right) - \zeta_{10} \frac{\partial^2 \phi_{01}}{\partial z^2} \quad (z = 0). \end{aligned} \quad (2.28)$$

Now, after substitution from (2.20) and (2.25), the right-hand side of this equation becomes

$$[2ik_0(1 - 2\gamma - 2\gamma^2) - 4k_0^2 x] \phi_{10}. \quad (2.29)$$

* In the calculation of ϕ_{11} the complex form of ϕ_{10} can be used, since on the right of (2.28) only products involving ϕ_{10} and ϕ_{01} occur, and ϕ_{01} is real.

As a trial solution let us write

$$\phi_{11} = i(k_1 q + l_1^2 q^2) \phi_{10}, \quad (2.30)$$

where $q = z + ix$ and k_1, l_1 are constants to be determined. Then the left-hand side of (2.28), when $z = 0$, reduces to

$$[(1 + 2\gamma) i(k_1 + 2il_1^2 x) - 2i\gamma^2 l_1^2 / k_0] \phi_{10}. \quad (2.31)$$

On equating coefficients of ϕ_{10} and $x\phi_{10}$ in (2.29) and (2.31) we obtain

$$\left. \begin{aligned} k_1 &= 2k_0 \frac{1 - 4\gamma^2 - 4\gamma^3}{(1 + 2\gamma)^2}, \\ l_1^2 &= 2k_0^2 \frac{1}{(1 + 2\gamma)}. \end{aligned} \right\} \quad (2.32)$$

The second of equations (2.27) also gives

$$g\zeta_{11} = [(\gamma k_1 + 2\gamma^2 k_0) - ix(2k_0^2 + 2\gamma k_0^2 - 2\gamma l_1^2 + k_0 k_1) + k_0 l_1^2 x^2] c_0 \phi_{10}. \quad (2.33)$$

This then is a formal solution of our problem.

Interpretation

Combining (2.33) with (2.20), we have

$$\alpha\zeta_{10} + \alpha\beta\zeta_{11} = \alpha\zeta_{10} \left[1 - i\beta \left(\frac{\gamma k_1}{k_0} + 2\gamma + l_1^2 x^2 \right) - 2\beta k_0 x \left(1 + \gamma - \frac{\gamma l_1^2}{k_0^2} + \frac{k_1}{2k_0} \right) \right]. \quad (2.34)$$

Correct to order β , this expression may be written

$$\begin{aligned} \alpha\zeta_{10} + \alpha\beta\zeta_{11} &= \alpha i \left(\frac{A}{c_0} \right) \exp \left\{ i \left[k_0 x - \beta \left(\frac{\gamma k_1}{k_0} + 2\gamma + l_1^2 x^2 \right) \right] \right\} \\ &\quad \times \left[1 - 2\beta k_0 x \left(1 + \gamma - \frac{\gamma l_1^2}{k_0^2} + \frac{k_1}{2k_0} \right) \right]. \end{aligned} \quad (2.35)$$

Now this represents a wave of slowly varying amplitude and wavelength. The local wave-number k is given by the x -derivative of the exponent:

$$k = k_0 - 2\beta l_1^2 x. \quad (2.36)$$

The proportional rate of change of the wave-number at $x = 0$ is therefore

$$\left(\frac{1}{k} \frac{\partial k}{\partial x} \right)_{x=0} = -\frac{2\beta l_1^2}{k_0} = -\frac{4\beta k_0}{1 + 2\gamma} \quad (2.37)$$

by (2.32). From (2.19) this may be written

$$\left(\frac{1}{k} \frac{\partial k}{\partial x} \right)_{x=0} = -\frac{2}{1 + 2\gamma} \frac{1}{c_0} \frac{\partial U}{\partial x}. \quad (2.38)$$

The amplitude a of the wave is given by

$$a = \alpha \left(\frac{A}{c_0} \right) \left[1 - 2\beta k_0 x \left(1 + \gamma - \frac{\gamma l_1^2}{k_0^2} + \frac{k_1}{2k_0} \right) \right], \quad (2.39)$$

so that the proportional rate of increase is

$$\left(\frac{1}{a} \frac{\partial a}{\partial x}\right)_{x=0} = -2\beta k_0 \left(1 + \gamma - \frac{\gamma l_1^2}{k_0^2} + \frac{k_1}{2k_0}\right) = -2\beta k_0 \frac{2+3\gamma}{(1+2\gamma)^2} \quad (2.40)$$

by equation (2.32), or, from (2.26),

$$\left(\frac{1}{a} \frac{\partial a}{\partial x}\right)_{x=0} = -\frac{2+3\gamma}{(1+2\gamma)^2} \frac{1}{c_0} \frac{\partial U}{\partial x}. \quad (2.41)$$

The mean surface level

Equation (2.25) shows that there is a small change in the mean surface level given by

$$\beta \zeta_{01} = -2\beta \gamma x, \quad (2.42)$$

corresponding to a mean gradient $-2\beta\gamma$, as we should expect in a non-uniform flow. The additional terms $\alpha\zeta_{10} + \alpha\beta\zeta_{11}$ give no change in the mean level. Therefore to order $\alpha\beta$ the mean surface level is unaffected; only at higher approximations is any change apparent.

3. A physical discussion

We have seen that the interaction between the waves and the current can be interpreted as a distortion of the waves, resulting in a change of wavelength and amplitude. In this section we shall try to interpret these changes on the basis of rough physical reasoning.

As before, we denote by σ the angular frequency of the waves (constant over the whole field of motion) and by a , k , U , c the local wave amplitude, wave-number, stream velocity, and wave velocity relative to the stream. Our object is to obtain a , k and c as functions of U and of their values a_0 , k_0 , U_0 , c_0 in some fixed plane $x = 0$.

The change in wavelength

Consider first the variation in wavelength. Now, the apparent velocity of the waves relative to a fixed plane $x = \text{constant}$ is equal to $(c + U)$. The apparent angular frequency of the waves is therefore $k(c + U)$. But by hypothesis this quantity is equal to σ at all points, so that

$$k(c + U) = \sigma = k_0(c_0 + U_0). \quad (3.1)$$

Thus
$$\frac{k}{k_0} = \frac{c_0 + U_0}{c + U}. \quad (3.2)$$

But the waves being in deep water we expect that their velocities c , c_0 relative to the current will be given by the classical formulae

$$c^2 = g/k, \quad c_0^2 = g/k_0. \quad (3.3)$$

Combining (3.2) and (3.3), we have

$$\frac{c^2}{c_0^2} = \frac{k_0}{k} = \frac{c + U}{c_0 + U_0} = \frac{1}{1 + \gamma} \left(\frac{c}{c_0} + \frac{U}{c_0}\right), \quad (3.4)$$

where $\gamma = U_0/c_0$ as before. On differentiation with respect to x , we have

$$\frac{2c}{c_0^2} \frac{\partial c}{\partial x} = \frac{1}{1+\gamma} \frac{1}{c_0} \left(\frac{\partial c}{\partial x} + \frac{\partial U}{\partial x} \right), \quad (3.5)$$

and hence at $x = 0$, where $c = c_0$,

$$\frac{\partial c}{\partial x} = \frac{1}{1+2\gamma} \frac{\partial U}{\partial x}. \quad (3.6)$$

Since by (3.4) k varies as c^{-2} , we have (by logarithmic differentiation)

$$\frac{1}{k} \frac{\partial k}{\partial x} = -\frac{2}{c} \frac{\partial c}{\partial x} = -\frac{2}{1+2\gamma} \frac{1}{c} \frac{\partial U}{\partial x} \quad (3.7)$$

in agreement with (2.38).

It will be seen that equation (3.4) is a quadratic in c/c_0 , and has the solution

$$\frac{c}{c_0} = \frac{1}{2(1+\gamma)} \left\{ 1 + \sqrt{1 + \frac{4(1+\gamma)U}{c_0}} \right\} \quad (3.8)$$

(see Unna (1942), for the case $\gamma = 0$). In the square root, the positive sign has been taken to ensure continuity as $x \rightarrow 0$. It is interesting to note that no solution can exist when

$$1 + \frac{4(1+\gamma)U}{c_0} < 0, \quad (3.9)$$

$$\text{or} \quad -U > \frac{c_0}{4(1+\gamma)}, \quad (3.10)$$

that is to say, when the stream velocity is in the opposite direction and exceeds in magnitude about one-quarter of the initial phase velocity of the waves. At the critical point, when the radical vanishes, equation (3.8) shows that

$$\frac{c}{c_0} = \frac{1}{2(1+\gamma)}, \quad (3.11)$$

and so

$$\frac{U}{c} = \frac{U c_0}{c_0 c} = -\frac{1}{2}. \quad (3.12)$$

In other words the stream velocity becomes equal and opposite to the local group-velocity $\frac{1}{2}c$; the wave energy can no longer be propagated against the stream. We shall see below that the waves tend to break before this point is reached. From (3.8) we have also

$$\frac{k}{k_0} = \left(\frac{c}{c_0} \right)^{-2} = \left\{ \frac{2(1+\gamma)}{1 + \sqrt{1 + 4(1+\gamma)U/c_0}} \right\}^2. \quad (3.13)$$

The changes in wave amplitude

The change in wave amplitude is interesting, for it enables us to decide between various conflicting hypotheses.

It was shown in I that if waves of amplitude a are propagated over a stream of uniform velocity U , the mean rate of energy transfer across a plane $x = \text{const.}$ is given (to order a^2) by

$$\bar{R}_x = E(c_g + U) + S_x U + \frac{3}{2} E U^2 / c + \frac{1}{2} \rho h U^3, \quad (3.14)$$

where E denotes the wave energy per unit horizontal area:

$$E = \frac{1}{2} \rho g a^2; \quad (3.15)$$

c_g denotes the group-velocity of the waves; in 'deep' water,

$$c_g = \frac{1}{2} c = \frac{1}{2} \sigma / k; \quad (3.16)$$

h is the mean depth of the stream, and S_x is defined by

$$S_x = E \left(\frac{2c_g}{c} - \frac{1}{2} \right). \quad (3.17)$$

The first term $E(c_g + U)$ on the right-hand side of (3.14) represents simply the transfer of wave energy by the group-velocity plus the stream velocity, and is to be expected. The last two terms may be written together as $\frac{1}{2} \rho h U'^2$, where

$$U' = U + E / \rho c h \quad (3.18)$$

represents the mean stream velocity modified by the presence of the mass transport. The intermediate term $S_x U$ has been discussed in I. It represents a kind of coupling between the waves and the current. By analogy with the Reynolds stress, S_x has been called the 'radiation stress'.

Now, in the present problem of waves on a non-uniform stream, let us suppose that the transfer of total energy is given with sufficient accuracy by equation (3.14) and further that between the planes $x = 0$ and $x = \text{const.}$ there is no reflexion of wave energy. It follows then that

$$\bar{R}_x = \bar{R}_0 = \text{const.} \quad (3.19)$$

and so

$$\frac{\partial}{\partial x} \bar{R}_x = 0. \quad (3.20)$$

Equation (3.20) is merely an expression of the conservation of the energy, when dissipative mechanisms are ignored. However, it is possible to regard it as the sum of two equations, one representing the balance of wave energy and the other the balance of mean flow energy.

For the exact form of this division, no unique answer is given by physical intuition. (At least *our* initial intuition, as well as that of Unna (1942), Evans (1955), Suthons (1945), Groen & Dorrestein (1958) and Drent (1959) yielded results which sometimes differed from one another but which were all, it as appears, incorrect.) Now, however, we have an arbiter for conflicts of intuition, for the correct division of (3.20) must yield results consistent with § 2.

The first five of the authors just named made the assumption that there was no interchange of energy between waves and current and thus obtained

$$\frac{\partial}{\partial x} [E(c_g + U)] = 0. \quad (3.21)$$

It is clear both from the results of I and from § 2 of the present paper that this assumption cannot be correct.

One might then argue that all the terms dependent on E belong properly to the wave-energy equation, and write

$$\frac{\partial}{\partial x} \left[E(c_g + U) + S_x U + \frac{3}{2} \frac{E U^2}{c} \right] = 0, \quad (3.22)$$

or, since the last term may be included with the mean flow,

$$\frac{\partial}{\partial x} [E(c_g + U) + S_x U] = 0. \quad (3.23)$$

Each of these equations (3.21), (3.22) and (3.23) yields results in conflict with § 2.

If, on the other hand, it is argued that the effect of the current variation on the wave energy is through the work done by the rate of strain against the radiation stress, then we have

$$\frac{\partial}{\partial x} [E(c_g + U)] + S_x \frac{\partial U}{\partial x} = 0. \quad (3.24)$$

Thus, in deep water,

$$\frac{\partial}{\partial x} [E(\frac{1}{2}c + U)] + \frac{1}{2}E \frac{\partial U}{\partial x} = 0. \quad (3.25)$$

Carrying out the differentiation at $x = 0$, where $U = \gamma c$, and using equation (3.6), we have

$$\frac{\partial E}{\partial x} [\frac{1}{2}c(1 + 2\gamma)] + E \left[\frac{1}{2(1 + 2\gamma)} + \frac{3}{2} \right] \frac{\partial U}{\partial x} = 0, \quad (3.26)$$

whence
$$\left(\frac{1}{E} \frac{\partial E}{\partial x} \right)_{x=0} = - \frac{4 + 6\gamma}{(1 + 2\gamma)^2} \frac{1}{c} \frac{\partial U}{\partial x}, \quad (3.27)$$

or, since E is proportional to a^2 ,

$$\left(\frac{1}{a} \frac{\partial a}{\partial x} \right)_{x=0} = - \frac{2 + 3\gamma}{(1 + 2\gamma)^2} \frac{1}{c} \frac{\partial U}{\partial x} \quad (3.28)$$

in exact agreement with equation (2.41).

It appears then that the correct assumption to make is equation (3.24), rather than the alternatives (3.21) to (3.23). We interpret this as follows:

In a non-uniform current the energy of the waves may be regarded as being transported with the group-velocity plus stream velocity, provided in addition we suppose that the mean stream does work on the waves at a rate $S_x \partial U / \partial x$ per unit distance, where S_x is the radiation stress. Equation (3.24) is then the expression of the energy balance for the waves.

An integral for the wave amplitude

An exact integral of equation (3.25) is

$$E(\frac{1}{2}c + U)c = \text{const.}, \quad (3.29)$$

for on differentiating the above and dividing by c , we have

$$\frac{\partial}{\partial x} [E(\frac{1}{2}c + U)] + E(\frac{1}{2}c + U) \frac{1}{c} \frac{\partial c}{\partial x} = 0, \quad (3.30)$$

which by (3.6) is equivalent to (3.25). From equation (3.29) we deduce

$$\frac{E}{E_0} = \frac{c_0(c_0 + 2U_0)}{c(c + 2U)}, \quad (3.31)$$

and thence

$$\frac{a}{a_0} = \left[\frac{c_0(c_0 + 2U_0)}{c(c + 2U)} \right]^{\frac{1}{2}}. \quad (3.32)$$

This law of amplification is illustrated by curve (1) of figure 1. At the critical point, where $U = -\frac{1}{2}c$, the amplification of the waves becomes theoretically infinite. In practice the waves may be expected to break, but the present small-amplitude theory becomes inapplicable before this point is reached.

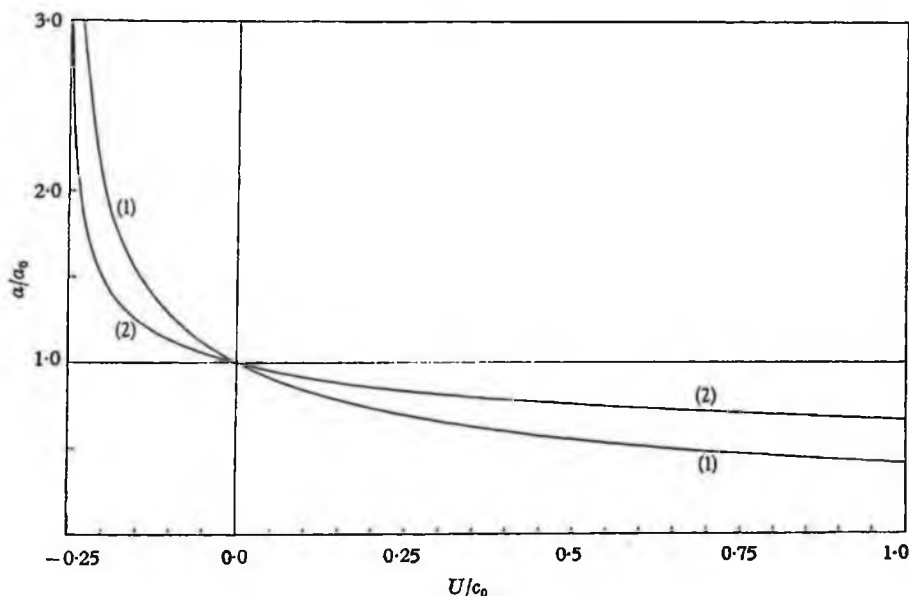


FIGURE 1. The amplification factor a/a_0 for waves on a current U in the direction of wave propagation: (1) with vertical upwelling from below; (2) with horizontal inflow from the sides. [a_0 and c_0 denote the values of a and c when $U = 0$.]

We are indebted to a referee for pointing out that a result similar to (3.29) was derived in an unpublished report by Kreisel (c. 1944, pp. 23-24). Kreisel started from the energy integral

$$\int_{-\infty}^{\zeta} \frac{\partial \phi}{\partial t} \frac{\partial \phi}{\partial x} dz = \text{const.},$$

and assumed that (in our notation)

$$\phi = Ux - ac e^{kz} \cos(kx - \sigma t),$$

$$\zeta = a \sin(kx - \sigma t),$$

where

$$c^2 = gk = (\sigma - kU)^2.$$

Substituting in the integral and treating U , c , a and k as constants during differentiation, one finds eventually

$$\frac{1}{2} \sigma a^2 c (c + 2U) = \text{const.}$$

(higher powers of a being neglected). Since σ is constant this agrees with (3.29), and indeed provides a physical explanation of that equation. The crux of Kreisel's argument is the assumption that $\partial\phi/\partial t$ contains no constant terms proportional to a^2 . This is true for deep water, but not in water of finite depth.

The rules for the variation of wave-number and wave amplitude expressed by (3.13) and (3.32) may be regarded as generalizations of the results found in § 2, the only additional assumptions being that $k^{-1}\partial k/\partial x$ and $a^{-1}\partial a/\partial x$ depend on the local values of U , c and $\partial U/\partial x$ and are linearly proportional to $\partial U/\partial x$.

The analysis of § 2 is correct as far as the first power of $\beta k_0 x$ only. In order to verify that (3.13) and (3.32) are correct to this order we write

$$\frac{U - U_0}{U_0} = \epsilon, \quad (3.33)$$

so that
$$\frac{U}{U_0} = 1 + \epsilon, \quad \frac{U}{c_0} = \gamma(1 + \epsilon). \quad (3.34)$$

Substituting in equations (3.13) and (3.32) and neglecting ϵ^2 we find, after some reduction,

$$\left. \begin{aligned} \frac{k}{k_0} &= 1 - \frac{2\gamma}{1 + 2\gamma} \epsilon, \\ \frac{a}{a_0} &= 1 - \frac{\gamma(2 + 3\gamma)}{(1 + 2\gamma)^2} \epsilon, \end{aligned} \right\} \quad (3.35)$$

of which (2.36) and (2.39) will be seen to be special cases.

4. An application to tidal currents

As an example of the application of the general formulae, and as an independent check, we apply the formulae to the case of surface waves on a tidal current, for which a solution was obtained independently in I.

A short wave of mean amplitude a_1 , mean wave-number k_1 and frequency σ is assumed to be superposed upon a long (shallow-water) wave of amplitude a_2 , wave-number k_2 and frequency σ_2 , travelling in the same direction as the first. The conditions of the problem are that

$$\left. \begin{aligned} \sigma_2/\sigma_1 &= \lambda \ll 1, \\ k_2 h &= \mu \ll 1, \end{aligned} \right\} \quad (4.1)$$

where h is the mean depth of water; also

$$e^{-k_1 h} \ll 1. \quad (4.2)$$

This last assumption ensures that the short waves are effectively in deep water, so that

$$\sigma_1 = (gk_1)^{\frac{1}{2}}, \quad \sigma_2 = (gh)^{\frac{1}{2}} k_2; \quad k_1 h = (\mu/\lambda)^2. \quad (4.3)$$

In the case of tidal currents both λ and μ may be of order 10^{-4} in a typical case, but the ratio μ/λ , $= (k_1 h)^{\frac{1}{2}}$, need not be greater than about 2 in order for the condition (4.2) to be satisfied.

Now let us reduce the long wave to a steady current U by superposing on the whole system a uniform stream $-(gh)^{\frac{1}{2}}$. Choosing the origin of x at a node of the longer wave, we have

$$U = -(gh)^{\frac{1}{2}} \left(1 - \frac{a_2}{h} \sin k_2 x \right) + O(a^2). \quad (4.4)$$

At $x = 0$ the stream velocity and the velocity of the short waves are given by

$$U_0 = -(gh)^{\frac{1}{2}}; \quad c_0 = (g/k_1)^{\frac{1}{2}}. \quad (4.5)$$

Thus,
$$\gamma = \frac{U_0}{c_0} = -(k_1 h)^{\frac{1}{2}} = -\frac{\mu}{\lambda}. \quad (4.6)$$

Also
$$\epsilon = \frac{U - U_0}{U_0} = -\frac{a_2}{h} \sin k_2 x. \quad (4.7)$$

On substitution in (3.35), we find

$$\left. \begin{aligned} \frac{k}{k_0} &= 1 - \frac{2\mu}{\lambda - 2\mu} \frac{a_2}{h} \sin k_2 x, \\ \frac{a}{a_0} &= 1 - \frac{(2\lambda - 3\mu)\mu}{(\lambda - 2\mu)^2} \frac{a_2}{h} \sin k_2 x, \end{aligned} \right\} \quad (4.8)$$

in agreement with equations (2.56) and (2.57) of I.* When μ/λ is sufficiently large, then

$$\left. \begin{aligned} \frac{k}{k_0} &= 1 + \frac{a_2}{h} \sin k_2 x, \\ \frac{a}{a_0} &= 1 + \frac{3}{4} \frac{a_2}{h} \sin k_2 x. \end{aligned} \right\} \quad (4.9)$$

5. Waves on a converging current: no upwelling

In the last three sections we have been concerned with an entirely two-dimensional motion in which the transverse component of the mean current was zero; the increase in the stream velocity with horizontal distance was made up by a compensating current upwelling from below. We now study a somewhat different situation in which the *vertical* component of current vanishes and the increase in the horizontal x -component U is compensated entirely by a horizontal in-flow V from the sides:

$$\frac{\partial U}{\partial x} + \frac{\partial V}{\partial y} = 0. \quad (5.1)$$

The analysis for the asymptotic solution is identical with that in the previous case, § 2, as far as equation (2.22). Now, however, instead of the potential (2.23) we must choose a potential ϕ_{01} to represent a flow having zero vertical component, and satisfying the equation of continuity (5.1). We take

$$\phi_{01} = c_0 k_0 (x^2 - y^2) + D c_0 z, \quad (5.2)$$

and from (2.22) we see that the constant D has to be $-2\gamma^2$ as before. Thus,

$$\left. \begin{aligned} \phi_{01} &= c_0 k_0 (x^2 - y^2) - 2\gamma^2 c_0 z, \\ \zeta_{01} &= -2\gamma x, \end{aligned} \right\} \quad (5.3)$$

and (2.26) still applies.

In the equations (2.27) for the interaction potential, the additional terms all vanish identically, so that (2.28) is still valid; the only difference is that the last term $\zeta_{10} \partial^2 \phi_{01} / \partial x^2$ vanishes, and so in place of (2.29) we have

$$[2ik_0(-2\gamma - 2\gamma^2) + 4k_0^2 x] \phi_{10}. \quad (5.4)$$

* In equation (2.57) of I, the second term in the curly bracket can be neglected, since $\lambda < \mu \ll 1$.

Now, on equating coefficients between (2.31) and (5.4), we find

$$\left. \begin{aligned} k_1 &= -4k_0 \frac{\gamma + 2\gamma^2 + 2\gamma^3}{(1 + 2\gamma)^2}, \\ l_1^2 &= 2k_0^2 \frac{1}{1 + 2\gamma}. \end{aligned} \right\} \quad (5.5)$$

Since the value of l_1^2 is still the same, equations (2.34) to (2.38) are still applicable and in particular (2.38) shows that we have the same rate of change of the wave-number k as in the previous case.

But, since k_1 has a different value, equation (2.41) must now be replaced by

$$\left(\frac{1}{a} \frac{\partial a}{\partial x} \right)_{x=0} = - \frac{1 + \gamma}{(1 + 2\gamma)^2} \frac{1}{c_0} \frac{\partial U}{\partial x}, \quad (5.6)$$

showing that the change in *amplitude* of the waves is different from the previous case.

6. Physical interpretation

The current U along the x -axis being as in § 3, the changes in wave velocity and wave-number which were derived in that section (by arguments depending only on kinematical considerations) are still given by (3.6) and (3.7). This confirms what was found in § 5 concerning the change in wave-number.

The change in wave amplitude, however, must be related to the equation of energy transfer. Now it was found in I that in the presence of a horizontal stream $\mathbf{U} = (U, V, 0)$ not necessarily in the x -direction, the mean transfer of energy across a vertical plane whose normal is $\mathbf{n} = (l, m, 0)$ is given by

$$\bar{R} = E(\mathbf{c}_g + \mathbf{U}) \cdot \mathbf{n} + \mathbf{U} \cdot \mathbf{S} \cdot \mathbf{n} + \frac{1}{2} \rho h U^2 (\mathbf{U}' \cdot \mathbf{n}), \quad (6.1)$$

where \mathbf{c}_g denotes the vector group-velocity, \mathbf{U}' denotes the stream velocity as modified by the mass-transport and \mathbf{S} is a stress tensor. If the x -direction is the direction of wave propagation, then $\mathbf{c}_g = (c_g, 0, 0)$, $\mathbf{U}' = \mathbf{U} + (E/\rho ch, 0, 0)$, and

$$\mathbf{S} = \begin{pmatrix} S_x & 0 & 0 \\ 0 & S_y & 0 \\ 0 & 0 & 0 \end{pmatrix}, \quad (6.2)$$

where S_x is given by (3.17) and

$$S_y = E \left(\frac{c_g}{c} - \frac{1}{2} \right). \quad (6.3)$$

Therefore a natural generalization of equation (3.14) is to assume

$$\nabla \cdot [E(\mathbf{c}_g + \mathbf{U})] + \left[S_x \frac{\partial U}{\partial x} + S_y \frac{\partial V}{\partial y} \right] = 0. \quad (6.4)$$

In other words, the divergence of the energy flux is exactly compensated by work done by the mean current against the radiation stress. In deep water this becomes

$$\frac{\partial}{\partial x} [E(\frac{1}{2}c + U)] + \frac{\partial}{\partial y} [EV] + \frac{1}{2}E \frac{\partial U}{\partial x} = 0. \quad (6.5)$$

By the symmetry of the flow about the plane $y = 0$, we see that, on the x -axis, $\partial E/\partial y$ vanishes identically, and so making use of (5.1) we have

$$\frac{\partial E}{\partial x} \left(\frac{1}{2}c + U \right) + \frac{1}{2}E \left(\frac{\partial c}{\partial x} + \frac{\partial U}{\partial x} \right) = 0. \quad (6.6)$$

On substituting for $\partial c/\partial x$ from (3.6), we find

$$\left(\frac{1}{E} \frac{\partial E}{\partial x} \right)_{x=0} = - \frac{2(1+\gamma)}{(1+2\gamma)^2} \frac{1}{c} \frac{\partial U}{\partial x}, \quad (6.7)$$

from which follows
$$\left(\frac{1}{a} \frac{\partial x}{\partial x} \right)_{x=0} = - \frac{1+\gamma}{(1+2\gamma)^2} \frac{1}{c} \frac{\partial U}{\partial x}, \quad (6.8)$$

in exact agreement with (5.7).

Equation (6.5) may also be written as

$$\frac{\partial}{\partial x} [E(\frac{1}{2}c + U)] - \frac{1}{2}E \frac{\partial U}{\partial x} = 0, \quad (6.9)$$

which has the integral

$$E(\frac{1}{2}c + U)/c = \text{const.}, \quad (6.10)$$

as may be verified in the same way as (3.28). Hence, in the present situation,

$$\frac{E}{E_0} = \frac{c(c_0 + 2U_0)}{c_0(c + 2U)}, \quad (6.11)$$

and

$$\frac{a}{a_0} = \left[\frac{c(c_0 + 2U_0)}{c_0(c + 2U)} \right]^{\frac{1}{2}}. \quad (6.12)$$

It will be seen that as the critical point is approached, $a/a_0 \rightarrow \infty$ as before.

The amplitude variation corresponding to equation (6.12) is shown in figure 1, curve (2), compared with the corresponding variation in the case of no lateral flow.

7. Waves on currents of arbitrary form

To generalize our previous results, we note that \mathbf{S} is a Cartesian tensor of rank 2, which we may write S_{ij} ; equation (6.2) gives S_{ij} in diagonal form, when referred to axes perpendicular and parallel to the local wave front.

The velocity gradients $\partial U/\partial x$ and $\partial V/\partial y$ are also components of the symmetric rate-of-strain tensor

$$\gamma_{ij} = \frac{1}{2} \left(\frac{\partial U_i}{\partial x_j} + \frac{\partial U_j}{\partial x_i} \right), \quad (7.1)$$

and the generalization of the interaction term in the wave-energy equation is $S_{ij}\gamma_{ij}$, which is, of course, an invariant.

Hence the correct generalization of equation (6.4) for steady currents of arbitrary form is

$$\nabla \cdot [E(\mathbf{c}_0 + \mathbf{U})] + \frac{1}{2} S_{ij} \left(\frac{\partial U_i}{\partial x_j} + \frac{\partial U_j}{\partial x_i} \right) = 0. \quad (7.2)$$

For time-varying currents we assume

$$\frac{\partial E}{\partial t} + \nabla \cdot [E(\mathbf{c}_0 + \mathbf{U})] + \frac{1}{2} S_{ij} \left(\frac{\partial U_i}{\partial x_j} + \frac{\partial U_j}{\partial x_i} \right) = 0. \quad (7.3)$$

In the case of purely two-dimensional motion ($\partial/\partial y = 0$), this reduces to

$$\frac{\partial E}{\partial t} + \frac{\partial}{\partial x} [E(\mathbf{c}_v + \mathbf{U})] + S_x \frac{\partial U}{\partial x} = 0, \quad (7.4)$$

an equation that was verified approximately in § 5 of I. In that paper it was not possible to distinguish between equation (7.4) and the same equation with $\partial(S_x U)/\partial x$ replacing $S_x \partial U/\partial x$, since the difference, $(\partial S_x/\partial x) U$, was negligibly small. However, the technique adopted in § 4 of the present paper, whereby the long wave was reduced to rest by superposing a finite negative velocity, removes the ambiguity in the final term.

Given the appropriate boundary conditions, equation (7.3) is generally sufficient to determine the variation in the wave-energy density E . From this the variation in wave amplitude may be deduced on the assumption that the relation between amplitude and energy-density is

$$E = \frac{1}{2} \rho g a^2 (1 + \bar{W}/2g), \quad (7.5)$$

where \bar{W} denotes the vertical acceleration of a particle carried by the mean current.* (See § 4 of I.) For steady currents we have

$$\bar{W} = \kappa(U^2 + V^2), \quad (7.6)$$

where κ is the curvature of the path of the particle. If \bar{W} is small compared with g then we may take

$$E = \frac{1}{2} \rho g a^2, \quad (7.7)$$

as has been assumed throughout this paper.

It may be mentioned that some experiments have recently been performed by Hughes (1960) on the interaction of waves and shear flows. These he has analysed using an assumption equivalent to (7.2), and his results tend to confirm the theory.

8. Waves on a shearing current

As a final example we shall apply the general equation (7.2) to the interesting case of waves traversing a simple horizontal current with vertical axis of shear. This was previously considered by Johnson (1947) without taking into account the transfer of energy between the waves and the current.†

The stream velocity $(0, V, 0)$ is supposed to be everywhere parallel to the y -axis, and also

$$\frac{\partial V}{\partial y} = \frac{\partial V}{\partial z} = 0. \quad (8.1)$$

The wavelength and amplitude of the waves are supposed also to be independent of y . The angle which the waves make locally with the x -axis is denoted by θ (see figure 2).

Purely kinematical considerations yield the following: since the wave-number in the y -direction ($k \sin \theta$) must be independent of x , we have

$$k \sin \theta = m, \quad (8.2)$$

* It is assumed that the current is nearly horizontal.

† Some of the results of this section were obtained by Drent (1959) who, adopting a different approach, was led to make an assumption equivalent to (7.2) in this case.

a constant. Since the apparent velocity of the waves at right-angles normal to their crests is $(c + V \sin \theta)$ and their wave-number is k , the apparent angular frequency of the waves relative to a fixed point is

$$k(c + V \sin \theta) = \sigma, \quad (8.3)$$

also a constant. Thirdly, we have the relation connecting local wave-number and velocity:

$$kc^2 = g. \quad (8.4)$$

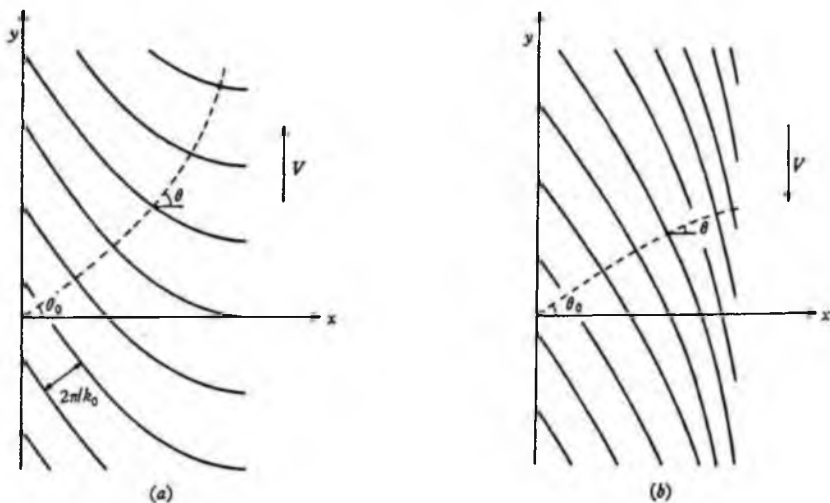


FIGURE 2. Definition diagram for waves on a shearing current, showing the qualitative effect of the current (a) when $V > 0$, (b) when $V < 0$.

From equation (8.3), by use of (8.4) and (8.2), it follows that

$$\frac{g}{c} + mV = \sigma, \quad (8.5)$$

or

$$c = \frac{g}{\sigma - mV}. \quad (8.6)$$

Then, from (7.4),

$$k = \frac{(\sigma - mV)^2}{g}, \quad (8.7)$$

and, from (7.2),

$$\sin \theta = \frac{m\sigma}{(\sigma - mV)^2}. \quad (8.8)$$

If c_0 , k_0 , θ_0 denote the values of c , k , θ when the transverse velocity V vanishes, then we have

$$\left. \begin{aligned} \frac{c}{c_0} &= \frac{1}{1 - (V/c_0) \sin \theta_0}, \\ \frac{k}{k_0} &= [1 - (V/c_0) \sin \theta_0]^2, \\ \sin \theta &= \frac{\sin \theta_0}{[1 - (V/c_0) \sin \theta_0]^2}. \end{aligned} \right\} \quad (8.9)$$

Since $\sin \theta$ cannot exceed unity, there is clearly an upper limit to V for which a solution exists:

$$V/c_0 \leq \frac{1 - (\sin \theta_0)^{\frac{1}{2}}}{\sin \theta_0}. \quad (8.10)$$

At this upper limit θ becomes equal to $\frac{1}{2}\pi$, and the waves are totally reflected by the current.

On the other hand, for negative currents $V < 0$, there is no kinematic limit to V . However, as $V \rightarrow -\infty$, k becomes very large, that is to say the wavelength becomes very small (figure 2(b)). The angle θ approaches zero, that is, the direction of propagation becomes nearly normal to the current.

Now the vector group-velocity is given by

$$\mathbf{c}_g = \frac{1}{2}\mathbf{c} = (\frac{1}{2}c \cos \theta, \frac{1}{2}c \sin \theta). \quad (8.11)$$

Hence equation (7.2) becomes in this case

$$\frac{\partial}{\partial x} [E \cdot \frac{1}{2}c \cos \theta] + \frac{\partial}{\partial y} [E(\frac{1}{2}c \sin \theta + V)] + \frac{1}{2}E \frac{\partial V}{\partial x} \cos \theta \sin \theta = 0. \quad (8.12)$$

Since all derivatives with respect to y vanish identically, we find, on substitution from (8.6) and (8.8),

$$\frac{\partial}{\partial x} \left(\frac{E \cos \theta}{\sigma - mV} \right) + \frac{Em \cos \theta}{(\sigma - mV)^2} \frac{\partial V}{\partial x} = 0, \quad (8.13)$$

of which the integral is

$$\frac{E \cos \theta}{(\sigma - mV)^2} = \text{const.}, \quad (8.14)$$

or, from (8.8),

$$E \cos \theta \sin \theta = \text{const.} \quad (8.15)$$

The relative amplification of the waves is therefore given by

$$\frac{a}{a_0} = \left(\frac{E}{E_0} \right)^{\frac{1}{2}} = \left(\frac{\sin 2\theta_0}{\sin 2\theta} \right)^{\frac{1}{2}}. \quad (8.16)$$

This ratio is shown graphically in figure 3 as a function of V/c_0 , for various values of the initial angle θ_0 .

Evidently the amplification of the waves becomes infinite both when $\theta \rightarrow 90^\circ$ and when $\theta \rightarrow 0$. In the first case the infinity is not significant: it is due to the fact that the ray-paths intersect, and the corresponding line $x = \text{const.}$ is a caustic. To the left of this line there are essentially two systems of waves, the incident and transmitted systems, while to the right of it there is a 'shadow zone'. In the neighbourhood of such a line the ordinary approximations of ray optics do not apply; a higher-order theory, generally involving Airy functions, must be used. One may expect that the wave amplitude in fact remains finite even in the neighbourhood of the critical line.

The second case, when $\theta \rightarrow 0$, corresponds to the limit $V \rightarrow -\infty$. In that case the infinity is genuine and is due mainly to the fact that the wavelength and wave velocity are so much reduced that, in order to maintain the energy flux in the x -direction, the amplitude must increase. In practice the waves may break; but for no finite velocity $V < 0$ is the ratio a/a_0 theoretically infinite.

We may note that it is possible for the component of stream velocity opposite to the waves to exceed the group-velocity:

$$\frac{1}{2}c + V \sin \theta < 0. \quad (8.17)$$

The waves are not thereby stopped, for the wave amplitude tends to be diminished by a lateral stretching of the wave crests.

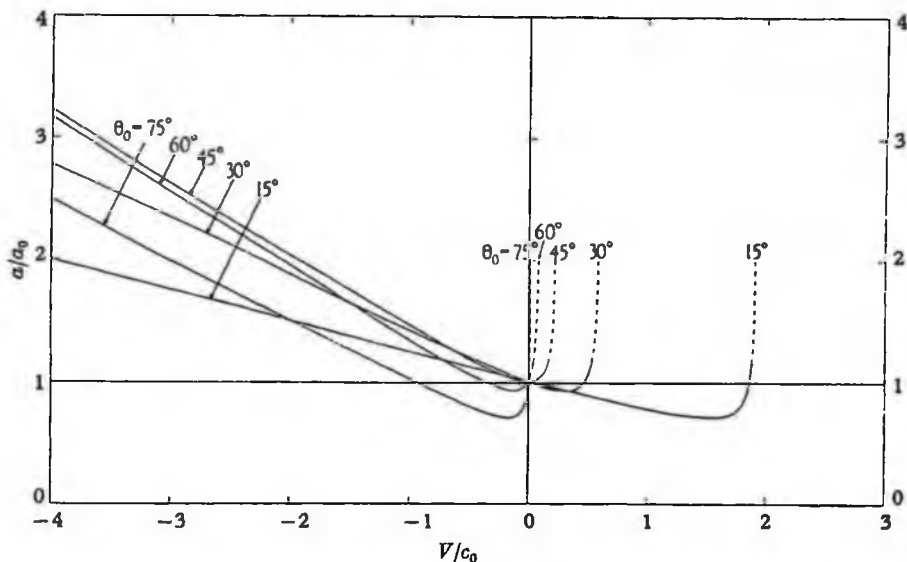


FIGURE 3. The amplification factor for waves crossing a shearing current V at an oblique angle θ , for various angles of entry θ_0 .

9. Conclusions

The amplitude of surface waves on non-uniform currents is affected by a non-linear interaction between the waves and the components of the currents; the coupling terms are proportional to the radiation stresses, and the general equation governing the transfer of wave energy is equation (7.3).

Waves travelling on a non-uniform current U that varies in the direction of wave propagation undergo an amplification that is greater than previously supposed, and is dependent on whether the variation in current is made up by a small vertical upwelling from below or by a small horizontal inflow from the sides; this difference is illustrated by the two curves in figure 1.

The amplification of waves on a transverse shearing current has also been calculated. Here the interaction between waves and current also produces an amplification different from that obtained by neglecting the interaction terms.

The results show that the efficiency of a hydraulic or pneumatic breakwater should be affected not only by the surface currents directly opposing the waves but also by the transverse or vertical components of the secondary circulating flow, for these produce different effects on the wave steepening. The absolute limits to the wavelenghts that can be transmitted are still set by Taylor's kinematical theory (1955). But for waves longer than the critical wavelength,

whether breaking occurs must depend on the amplification factor. We suggest that differences in the secondary circulation may account for some of the anomalies in past experimental work, both on models and on prototypes.

Since the currents have been seen to do work on the waves, then we would expect the waves also to react on the currents. From (6.1), by conservation of the total energy, one would expect for steady currents

$$\nabla \cdot [E(\mathbf{c}_g + \mathbf{U}) + \mathbf{S} \cdot \mathbf{U} + (\frac{1}{2}\rho h U'^2) \mathbf{U}'] = 0. \quad (9.1)$$

Hence, on subtracting (7.2) and using the fact that S_{ij} is symmetric, we have

$$\nabla \cdot [(\frac{1}{2}\rho h U'^2) \mathbf{U}'] + U_i \frac{\partial S_{ij}}{\partial x_j} = 0. \quad (9.2)$$

A fuller account of equation (9.2) will be given subsequently.

REFERENCES

- DEENT, J. 1959 A study of waves in the open ocean and of waves on shear currents. Ph.D. Thesis, University of British Columbia, Vancouver.
- EVANS, J. T. 1955 Pneumatic and similar breakwaters. *Proc. Roy. Soc. A*, **231**, 457-86.
- GROEN, P. & DOBBESTEIN, R. 1958 Zeegolven. *Kon. Ned. Met. Inst. Publ.* 111-11.
- HUGHES, B. A. 1960 Interaction of waves and a shear flow. M.A. Thesis, University of British Columbia, Vancouver.
- JOHNSON, J. W. 1947 The refraction of surface waves by currents. *Trans. Amer. Geophys. Un.* **28**, 867-74.
- KREISEL, G. c. 1944 Surface waves. *Admiralty Report SRE/Wave/1*.
- LONGUET-HIGGINS, M. S. & STEWART, R. W. 1960 Changes in the form of short gravity waves on long waves and tidal currents. *J. Fluid Mech.* **8**, 565-83.
- STRAUB, L. G., BOWERS, C. E. & TARRAPORE, Z. S. 1959 Experimental studies of pneumatic and hydraulic breakwaters. *Univ. Minnesota, St Anthony Falls Lab., Tech. Papers*, no. 25, Ser. B.
- SUTHERS, C. T. 1945 (revised 1950) Forecasting of sea and swell waves. *Admiralty, Naval Weather Service Dep.*, Memo. no. 135/45. Also *N.W.S. Memos.* nos. 180/52 and 135B/58.
- TAYLOR, G. I. 1955 The action of a surface current used as a breakwater. *Proc. Roy. Soc. A*, **231**, 466-78.
- UNNA, P. J. H. 1942 Waves and tidal streams. *Nature, Lond.*, **149**, 219-20.
- UESELL, F. 1960 Steady wave patterns on a non-uniform steady fluid flow. *J. Fluid Mech.* **9**, 333-46.

*Reprinted without change of pagination from the
Journal of Fluid Mechanics, volume 13, part 4, pp. 481-504, 1962*

Radiation stress and mass transport in gravity waves, with application to 'surf beats'

By M. S. LONGUET-HIGGINS

National Institute of Oceanography, Surrey

AND R. W. STEWART

University of British Columbia

(Received 1 September 1961 and in revised form 10 April 1962)

This paper studies the second-order currents and changes in mean surface level which are caused by gravity waves of non-uniform amplitude. The effects are interpreted in terms of the radiation stresses in the waves.

The first example is of wave groups propagated in water of uniform mean depth. The problem is solved first by a perturbation analysis. In two special cases the second-order currents are found to be proportional simply to the square of the local wave amplitude: (*a*) when the lengths of the groups are large compared to the mean depth, and (*b*) when the groups are all of equal length. Then the surface is found to be depressed under a high group of waves and the mass-transport is relatively negative there. In case (*a*) the result can be simply related to the radiation stresses, which tend to expel fluid from beneath the higher waves.

The second example considered is the propagation of waves of steady amplitude in water of gradually varying depth. Assuming no loss of energy by friction or reflexion, the wave amplitude must vary horizontally, to maintain the flux of energy constant; it is shown that this produces a negative tilt in the mean surface level as the depth diminishes. However, if the wave height is limited by breaking, the tilt is positive. The results are in agreement with some observations by Fairchild.

Lastly, the propagation of groups of waves from deep to shallow water is studied. As the mean depth decreases, so the response of the fluid to the radiation stresses tends to increase. The long waves thus generated may be reflected as free waves, and so account for the 'surf beats' observed by Munk and Tucker.

Generally speaking, the changes in mean sea level produced by ocean waves are comparable with those due to horizontal wind stress. It may be necessary to allow for the wave stresses in calculating wind stress coefficients.

1. Introduction

In two previous papers in this series (Longuet-Higgins & Stewart 1960, 1961) we have studied the non-linear action between water waves and steady or fluctuating currents, when the latter are non-uniform in space. It was shown that the currents generally do work on the waves, and that the coupling between them depends on a stress tensor associated with the waves, called the radiation stress

tensor. (The component corresponding to two-dimensional waves propagated in the x -direction is denoted by S_x .)

Correspondingly, one may expect that the waves will do work on the surrounding medium. The change in current velocity should be proportional, like the radiation stresses, to the square of the wave amplitude. The purpose of the present paper is to investigate some examples where the effects may be appreciable.

It is known that the currents produced by a steady train of waves of uniform amplitude are largely affected by the viscosity (Longuet-Higgins 1953, 1960). In the first part of this paper, however, we deal with waves of non-uniform amplitude (the variations of amplitude being due to the presence of more than one frequency) in water of uniform depth. In this situation, the groups of high and low waves are found to cause fluctuations in the mass-transport currents more rapid than the slow effects of viscosity, and the two effects may be treated independently.

Our initial approach to the problem is to solve systematically the field equations and boundary conditions by the method of Stokes as far as the second order in the wave amplitude. For the first approximation we assume a linear sum of waves of nearly equal wavelength and frequency; these of course form 'beats' or wave groups in the usual way. In the second approximation the 'difference frequencies' give rise to currents and changes in surface level having wavelengths comparable to the length of the groups. These are the currents in which we are interested.

In two special cases, the currents are very simply related to the local amplitude of the wave groups: (*a*) when the groups are long compared to the mean depth, and (*b*) when there are only two first-order waves present, so that the wave groups are all of equal length. Associated with the currents are fluctuations in the mean level of the sea surface. Contrary to expectation, it is found that in a group of high waves the mass-transport tends to be *negative* (i.e. opposite to the direction of wave propagation) and the mean level tends to be depressed.

In the special cases (*a*) and (*b*) a simplified method of solution can be given, which confirms these results.

A third approach, in some ways the most interesting, applies only in case (*a*), when the length of the wave groups is long compared to the depth. Then it is shown that changes in the mean level and in the mass-transport are such as would be produced by a horizontal force $-\partial S_x/\partial x$ applied to the fluid.† In terms of this force, a simple physical explanation can be given as to why the surface tends to be depressed below a group of high waves: the radiation stress, being greater in a group of high waves, tends to expel fluid from that region. However, in general, when the groups are not long compared to the depth, the situation is complicated by the existence of a mean vertical acceleration which is no longer negligible.

In §§ 4–6 the results are extended to waves in water of non-uniform depth. It is well known that even a steady train of waves undergoes changes in amplitude in water of gradually varying depth, in order to maintain a constant flux of energy. But the variations in depth and wave amplitude also cause a variation in the

† This result has been given independently Whitham (1962), but without stating the restriction on the length of the wave groups.

transfer of momentum, and it is shown that this causes a tilt in the mean level $\bar{\zeta}$ such as would be produced by a constant horizontal force $-\partial S_x/\partial x$ applied to the fluid.

Moreover, it appears that the equation for $\partial \bar{\zeta}/\partial x$ may be integrated, so that the mean level $\bar{\zeta}$ can be found as a function only of the local depth and of conditions at infinity. If there is no loss of energy then as the depth becomes shallower the mean level is depressed. If, on the other hand, the wave amplitude is limited by breaking, it appears that the mean level must rise.

These results account qualitatively for some observations of Fairchild (1958) in wave-tank experiments, and for the observed rise in level shorewards sometimes produced by ocean waves.

Consideration of wave groups in water of non-uniform depth suggests that these may account for the 'surf beats' observed by Tucker (1950). For many years it remained a puzzle why a high group of incoming swell was associated with a *negative* pulse of pressure reflected from the shore. But this now appears as a natural consequence.

2. The Stokes approximation

In the usual notation, let (x, y, z) be rectangular co-ordinates with the x -axis horizontal and in the direction of wave propagation and with the z -axis vertically upwards. Let $\mathbf{u} = (u, v, w)$ denote the velocity vector; p, ρ and g the pressure, density and gravitational acceleration; $z = \zeta(x, y, t)$ the equation of the free surface and $z = -h$ the equation of the rigid bottom.

Now the fluid motion in a periodic train of waves, outside boundary layers at the bottom and free surface, contains generally a second-order vorticity (see Longuet-Higgins 1953, 1960) which, on the time-scale that we are considering, can be considered as independent of the time t . This vorticity is associated with a steady second-order current. However, to the second approximation this current does not affect the distribution of pressure, and may be simply added to the field of motion. Hence, to the second approximation we may regard the fluid motion outside the boundary-layers as irrotational, afterwards adding the second-order current so as to satisfy the special conditions just inside the boundary-layers.

The equations to be satisfied by \mathbf{u}, p and ζ are then the field equations

$$\left. \begin{aligned} \mathbf{u} &= \nabla\phi, \\ \nabla^2\phi &= 0, \\ p/\rho + gz + \frac{1}{2}\mathbf{u}^2 + \partial\phi/\partial t &= 0, \end{aligned} \right\} \quad (2.1)$$

with the boundary conditions

$$\left. \begin{aligned} (\mathbf{n} \cdot \nabla\phi)_{\text{fixed boundary}} &= 0, \\ (p)_{z=\zeta} &= 0, \\ \left[\left(\frac{\partial}{\partial t} + \mathbf{u} \cdot \nabla \right) (z - \zeta) \right]_{z=\zeta} &= 0. \end{aligned} \right\} \quad (2.2)$$

In Stokes's method of approximation an expansion of \mathbf{u} , ϕ , ζ and p is made in the form

$$\left. \begin{aligned} \mathbf{u} &= \mathbf{u}^{(1)} + \mathbf{u}^{(2)} + \dots, \\ \phi &= \phi^{(1)} + \phi^{(2)} + \dots, \\ \zeta &= \zeta^{(1)} + \zeta^{(2)} + \dots, \\ p + \rho g z &= p^{(1)} + p^{(2)} + \dots, \end{aligned} \right\} \quad (2.3)$$

where $\mathbf{u}^{(1)}$, $\phi^{(1)}$, etc. satisfy the linearized equations and boundary conditions; $\mathbf{u}^{(1)} + \mathbf{u}^{(2)}$, $\phi^{(1)} + \phi^{(2)}$, etc. satisfy the equations as far as the quadratic terms, and so on. The equations for $\phi^{(1)}$ are:

$$\left. \begin{aligned} \nabla^2 \phi^{(1)} &= 0, \\ (\partial \phi^{(1)} / \partial z)_{z=-h} &= 0, \\ \left(\frac{\partial^2 \phi^{(1)}}{\partial z^2} + g \frac{\partial \phi^{(1)}}{\partial z} \right)_{z=0} &= 0, \end{aligned} \right\} \quad (2.4)$$

and then $\mathbf{u}^{(1)}$, $p^{(1)}$ and $\zeta^{(1)}$ may be found from the further relations

$$\left. \begin{aligned} \mathbf{u}^{(1)} &= \nabla \phi^{(1)}, \\ p^{(1)} / \rho &= -\partial \phi^{(1)} / \partial t, \\ g \zeta^{(1)} &= -(\partial \phi^{(1)} / \partial t)_{z=0}. \end{aligned} \right\} \quad (2.5)$$

For the present it is assumed that the mean values of $\mathbf{u}^{(1)}$ and $\zeta^{(1)}$ are zero, that is to say in the first approximation there is no mean current, and the origin of z is in the mean surface level.

The equations for the second approximation $\phi^{(2)}$ are

$$\left. \begin{aligned} \nabla^2 \phi^{(2)} &= 0, \\ (\partial \phi^{(2)} / \partial z)_{z=-h} &= 0, \\ \left(\frac{\partial^2 \phi^{(2)}}{\partial z^2} + g \frac{\partial \phi^{(2)}}{\partial z} \right)_{z=0} &= - \left[\frac{\partial}{\partial t} (\mathbf{u}^{(1)2}) + \zeta^{(1)} \frac{\partial}{\partial z} \left(\frac{\partial^2 \phi^{(1)}}{\partial t^2} + g \frac{\partial \phi^{(1)}}{\partial z} \right) \right]_{z=0} \end{aligned} \right\} \quad (2.6)$$

(see for example Longuet-Higgins & Stewart 1960). The remaining quantities $\mathbf{u}^{(2)}$, $p^{(2)}$ and $\zeta^{(2)}$ may then be found from

$$\left. \begin{aligned} \mathbf{u}^{(2)} &= \nabla \phi^{(2)}, \\ p^{(2)} / \rho &= -(\partial \phi^{(2)} / \partial t + \frac{1}{2} \mathbf{u}^{(1)2}), \\ g \zeta^{(2)} &= -(\partial \phi^{(2)} / \partial t + \frac{1}{2} \mathbf{u}^{(1)2} + \zeta^{(1)} \partial^2 \phi^{(1)} / \partial z \partial t)_{z=0}. \end{aligned} \right\} \quad (2.7)$$

The classical first-order solution for a wave of constant amplitude a , frequency σ and wave-number k is

$$\left. \begin{aligned} \phi^{(1)} &= \frac{a\sigma \cosh k(z+h)}{k \sinh kh} \sin(kx - \sigma t), \\ \zeta^{(1)} &= a \cos(kx - \sigma t), \end{aligned} \right\} \quad (2.8)$$

provided that†

$$\sigma^2 = gk \tanh kh. \quad (2.9)$$

† If approximations higher than the second are considered, σ must also be expanded in powers of (ak) . Thus strictly we should write $\sigma^{(1)}$ for σ .

This determines the phase velocity

$$c = \frac{\sigma}{k} = (gh)^{\frac{1}{2}} \left(\frac{\tanh kh}{\tanh h} \right)^{\frac{1}{2}} \quad (2.10)$$

and the group velocity

$$c_g = \frac{d\sigma}{dk} = \frac{1}{2}c \left(1 + \frac{2kh}{\sinh 2kh} \right). \quad (2.11)$$

Also
$$\omega = \frac{1}{2}(\overline{u^{(2)2}} - \overline{w^{(2)2}}) = \frac{a^2 g k}{2 \sinh 2kh} = \frac{a^2 g}{2h} \left(\frac{c_g}{c} - \frac{1}{2} \right), \quad (2.12)$$

which is independent of z .

The next approximation, found by solving equations (2.6), is

$$\phi^{(2)} = \frac{3a^2\sigma}{8 \sinh^4 kh} \cosh 2k(z+h) \sin 2(kx - \sigma t) + Cx + Dt, \quad (2.13)$$

where C and D are arbitrary constants, of the second order. From (2.7) it can be seen that these constants are related to the average values of $u^{(2)}$ and $\zeta^{(2)}$; in fact

$$\left. \begin{aligned} \overline{u^{(2)}} &= C, \\ g\overline{\zeta^{(2)}} &= -(D + \omega). \end{aligned} \right\} \quad (2.14)$$

The last equation follows from (2.7) on replacing $\partial\phi^{(2)}/\partial z$ by $\partial\zeta^{(2)}/\partial t$ and noting that

$$\overline{\zeta^{(2)} \frac{\partial^2 \zeta^{(2)}}{\partial t^2}} + \overline{\left(\frac{\partial \zeta^{(2)}}{\partial t} \right)^2} = \frac{\partial}{\partial t} \left(\overline{\zeta^{(2)} \frac{\partial \zeta^{(2)}}{\partial t}} \right) = 0,$$

so that

$$\overline{\zeta^{(2)} \frac{\partial^2 \phi^{(2)}}{\partial z \partial t}} = - \overline{\left(\frac{\partial \zeta^{(2)}}{\partial t} \right)^2} = - \overline{u^{(2)2}}.$$

Hence a change in C corresponds to the superposition of a small, uniform horizontal current, i.e. to a different choice of the frame of reference. A change in D corresponds to a small addition to the vertical co-ordinate, in other words a different choice of origin for z . It can easily be verified that the mean pressure on the bottom always equals the hydrostatic pressure:

$$\overline{p_{z=-h}} = \rho g(h + \zeta). \quad (2.15)$$

As in Lamb (1932) it is found that the mean energy density of the waves is given by

$$E = \frac{1}{2} \rho g a^2$$

correct to second order, and the horizontal flux of energy, also to second order, is given by

$$F = E c_g.$$

3. Propagation of a wave group

In this section we shall treat the problem of a group of waves propagated freely in water of uniform depth, using three different methods. The first method is a systematic application of the perturbation procedure outlined above; this is valid irrespective of the length of the wave groups relative to the depth h . The second method is a simplified version of the first, valid only when the wave

groups are long compared to \hbar , or when the groups are of uniform length. The third method is an application of the conservation of momentum, similar to that of Whitham (1962), but is valid only for long wave groups.

Method 1

Consider a wave disturbance containing a narrow range of frequencies, for example a disturbance represented, to first order, by the expression

$$\zeta^{(1)} = \sum_n a_n \cos(k_n x - \sigma_n t + \chi_n), \quad (3.1)$$

where a_n and χ_n are amplitude and phase constants, and all the wave-numbers k_n lie close to a fixed wave-number k . The frequency and wave-number of each component are related by

$$\sigma_n^2 = g k_n \tanh k_n \hbar. \quad (3.2)$$

Equation (3.1) may also be written

$$\zeta^{(1)} = a \cos(kx - \sigma t + \chi), \quad (3.3)$$

where a and χ are slowly varying functions of x and t , representing the envelope of the waves; in fact

$$a e^{i\chi} = \sum_n a_n \exp i\{(k_n - k)x - (\sigma_n - \sigma)t + \chi_n\}. \quad (3.4)$$

The square of the amplitude a is given by

$$a^2 = \sum_{n,m} a_n a_m \exp i\{(k_n - k_m)x - (\sigma_n - \sigma_m)t + (\chi_n - \chi_m)\}. \quad (3.5)$$

Since

$$\frac{\sigma_n - \sigma_m}{k_n - k_m} \doteq \frac{d\sigma}{dk} = c_g \quad (3.6)$$

the whole envelope (3.4) progresses with the group velocity c_g .

The first-order potential corresponding to (3.1) is

$$\phi^{(1)} = \sum_n \frac{a_n \sigma_n \cosh k_n(z + \hbar)}{k_n \sinh k_n \hbar} \sin(k_n x - \sigma_n t + \chi_n). \quad (3.7)$$

The equations for the second approximation are equations (2.6). Now the right-hand side is a quadratic expression in $\zeta^{(1)}$ and $\phi^{(1)}$, and so may be expressed as the sum of terms with wave-numbers $(k_n + k_m)$ and $(k_n - k_m)$ respectively. Hence $\phi^{(2)}$, and $\zeta^{(2)}$ will contain terms with sum and difference wave-numbers also. Since we are interested only in *average* values taken over several wavelengths, only the terms which depend on the *difference* wave-numbers will be retained. Thus we have

$$\mathbf{u}^{(1)2} = \sum_{n,m} \frac{a_n a_m \sigma_n \sigma_m \cosh(k_n + k_m)\hbar}{2 \sinh k_n \hbar \sinh k_m \hbar} \cos\{(k_n - k_m)x - (\sigma_n - \sigma_m)t + (\chi_n - \chi_m)\}.$$

Writing $(k_n - k_m)$, $(\sigma_n - \sigma_m)$, $(\chi_n - \chi_m) = \Delta k$, $\Delta \sigma$, $\Delta \chi$,

and neglecting squares of Δk and $\Delta \sigma$ we have

$$\frac{\partial}{\partial t} \mathbf{u}^{(1)2} = \sum_{n,m} \frac{a_n a_m \sigma^2 \cosh 2k\hbar}{2 \sinh^2 k\hbar} \sin(\Delta kx - \Delta \sigma t + \Delta \chi).$$

Similarly, using (3.2) we find

$$\frac{\partial}{\partial z} \left(\frac{\partial^2}{\partial t^2} + g \frac{\partial}{\partial z} \right) \phi_{z=0}^{(1)} = \sum_n \frac{a_n \sigma_n^3}{\sinh k_n h} \sin(k_n x - \sigma_n t + \chi_n),$$

and hence

$$\zeta^{(1)} \frac{\partial}{\partial z} \left(\frac{\partial^2}{\partial t^2} + g \frac{\partial}{\partial z} \right) \phi_{z=0}^{(1)} = \sum_{n,m} \frac{a_n a_m \sigma_n^3}{2 \sinh^2 k_n h} \sin(\Delta k x - \Delta \sigma t + \Delta \chi)$$

(only the difference terms being retained). By reversing m and n in the summation and taking one half of the sum, the right-hand side becomes

$$\sum_{n,m} \frac{a_n a_m}{4} \left(\frac{\sigma_n^3}{\sinh^2 k_n h} - \frac{\sigma_m^3}{\sinh^2 k_m h} \right) \sin(\Delta k x - \Delta \sigma t + \Delta \chi).$$

which, to the first order in $\Delta \sigma$, can be written

$$\sum_{n,m} \frac{a_n a_m}{4} \Delta \sigma \frac{d}{d\sigma} \left(\frac{\sigma^3}{\sinh^2 kh} \right) \sin(\Delta k x - \Delta \sigma t + \Delta \chi).$$

Altogether, then, the last of equations (2.6) becomes

$$\left(\frac{\partial^2 \phi^{(2)}}{\partial t^2} + g \frac{\partial \phi^{(2)}}{\partial z} \right)_{z=0} = - \sum_{m,n} (K a_m a_n \Delta \sigma) \sin(\Delta k x - \Delta \sigma t + \Delta \chi),$$

where

$$K = \frac{\sigma^2 \cosh 2kh}{2 \sinh^2 kh} + \frac{1}{4} \frac{d}{d\sigma} \left(\frac{\sigma^3}{\sinh^2 kh} \right). \quad (3.8)$$

It will be noted that K is independent of Δk and $\Delta \sigma$. The solution of equations (2.6) is

$$\phi^{(2)} = - \sum_{m+n} \frac{K a_m a_n \Delta \sigma \cosh \Delta k(z+h)}{g \Delta k \sinh \Delta kh - (\Delta \sigma)^2 \cosh \Delta kh} \sin(\Delta k x - \Delta \sigma t + \Delta \chi) + Cx + Dt, \quad (3.9)$$

where C and D are arbitrary constants. To the same order in Δk , $\Delta \sigma$ this may be written

$$\phi^{(2)} = - \frac{K}{\sum_{m,n}} \frac{a_m a_n c_g}{gh\theta - c_g^2} \frac{\cosh \Delta k(z+h)}{\cosh \Delta kh} \frac{\sin(\Delta k x - \Delta \sigma t + \Delta \chi)}{\Delta k}, \quad (3.10)$$

where

$$\theta = \frac{\tanh \Delta kh}{\Delta k \bar{n}}. \quad (3.11)$$

In the summation in (3.10) we have included terms corresponding to $m = n$. These are taken to be the limits of the terms under the summation as $\Delta k \rightarrow 0$; in other words we have chosen

$$Cx + Dt = - K \sum_n \frac{a_n^2 c_g}{gh - c_g^2} (x - c_g t). \quad (3.12)$$

Further terms of the type $(C'x + D't)$ may of course be added. From (3.10) we have immediately

$$u^{(2)} = - K \sum_{m,n} \frac{a_m a_n c_g}{gh\theta - c_g^2} \frac{\cosh \Delta k(z+h)}{\cosh \Delta kh} \cos(\Delta k x - \Delta \sigma t + \Delta \chi), \quad (3.13)$$

and for the mean velocity with respect to z ,

$$|u^{(2)} = - K \sum_{m,n} \frac{a_m a_n c_g}{gh\theta - c_g^2} \theta \cos(\Delta k x - \Delta \sigma t + \Delta \chi). \quad (3.14)$$

The mean surface elevation $\zeta^{(2)}$ is found from equations (2.7):

$$g\zeta^{(2)} = -K \sum_{m,n} \frac{a_m a_n c_g^2}{gh\theta - c_g^2} \cos(\Delta kx - \Delta\sigma t + \Delta\chi) - \sum_{m,n} \frac{a_m a_n \sigma^2}{4 \sinh^2 kh} \cos(\Delta kx - \Delta\sigma t + \Delta\chi). \quad (3.15)$$

The constant K may be evaluated from (3.8) and (2.9); we find

$$K = \frac{\sigma^2}{4 \sinh^2 kh} \frac{\sinh 4kh + 3 \sinh 2kh + 2kh}{\sinh 2kh + 2kh}. \quad (3.16)$$

We may distinguish two principal cases:

(a) *The wave groups are long compared to the depth h .* Then

$$\Delta kh \ll 1, \quad \cosh \Delta k(z+h) \doteq 1, \quad \theta \doteq 1.$$

The factor $(gh\theta - c_g^2)^{-1}$ may be taken outside the summations and we have simply

$$\left. \begin{aligned} |u^{(2)}| &= - \left(\frac{Kcg}{gh - c_g^2} \right) a^2, \\ g\zeta^{(2)} &= - \left(\frac{Kc_g^2}{gh - c_g^2} + \frac{\sigma^2}{4 \sinh^2 kh} \right) a^2, \end{aligned} \right\} \quad (3.17)$$

where

$$a^2 = \sum_{m,n} a_m a_n \cos(\Delta kx - \Delta\sigma t + \Delta\chi),$$

as in (3.5).

(b) *The wave groups are not long compared with the depth.* There is no such convenient simplification as in (a), since the factor $(gh\theta - c_g^2)^{-1}$ is generally different for each sinusoidal component in the summations. However, since $k \gg \Delta k$ and Δkh is at least of order 1, one may assume that $e^{-kh} \ll 1$, i.e. the individual waves are effectively deep-water waves. From (3.14) $K = \sigma^2 = gk$, and equations (3.14) and (3.15) reduce to

$$\left. \begin{aligned} |u^{(2)}| &= -2\sigma k \sum_{m,n} \frac{a_m a_n}{4\theta kh - 1} \theta \cos(\Delta kx - \Delta\sigma t + \Delta\chi), \\ g\zeta^{(2)} &= -\sigma^2 \sum_{m,n} \frac{a_m a_n}{4\theta kh - 1} \cos(\Delta kx - \Delta\sigma t + \Delta\chi), \end{aligned} \right\} \quad (3.18)$$

θ being given by (3.11). These solutions are not generally expressible in terms of the local wave amplitude a . However, in the special case when only one pair of waves is present, with amplitudes a_1 and a_2 , then we have

$$\left. \begin{aligned} |\bar{u}| &= 2\sigma k \left[\frac{a_1^2 + a_2^2}{4kh - 1} + \frac{2a_1 a_2}{4\theta kh - 1} \theta \cos(\Delta kx - \Delta\sigma t + \Delta\chi) \right], \\ g\zeta^{(2)} &= \sigma^2 \left[\frac{a_1^2 + a_2^2}{4kh - 1} + \frac{2a_1 a_2}{4\theta kh - 1} \cos(\Delta kx - \Delta\sigma t + \Delta\chi) \right]. \end{aligned} \right\}$$

Since

$$a^2 = (a_1^2 + a_2^2) + 2a_1 a_2 \cos(\Delta kx - \Delta\sigma t + \Delta\chi)$$

this can be written

$$\left. \begin{aligned} u^{(2)} &= \frac{2\theta\sigma k a^2}{4\theta k h - 1} + \text{const.}, \\ g_S^{(2)} &= \frac{\sigma^2 a^2}{4\theta k h - 1} + \text{const.} \end{aligned} \right\} \quad (3.19)$$

Moreover, since an expression of the form $(C'x + D')$ may still be added to the potential, the constants of integration can be taken as vanishing.

Method 2

This method is more indirect than method 1, but avoids the lengthy calculations. It also leads to an interpretation of some of the algebraic expressions which occur in the solution.

From the form of equations (2.11) it will be seen that the potential $\phi^{(2)}$ corresponds to the motion that would be generated by a 'virtual pressure'

$$p_s = \rho \left[u^{(1)2} + \int dt \left\{ \zeta^{(1)} \frac{\partial}{\partial z} \left(\frac{\partial^2}{\partial t^2} + g \frac{\partial}{\partial z} \right) \phi^{(1)} \right\} \right]$$

applied at the upper surface of the fluid. Without evaluating this complex expression, we note that it can be expressed as the sum of terms containing both sum and difference frequencies, the latter travelling with the group velocity c_g . Thus $\phi^{(2)}$ will contain a part ϕ_a such that

$$\frac{\partial \phi_a}{\partial x} = -\frac{1}{c_g} \frac{\partial \phi_a}{\partial t}.$$

Added to this there will in general be a potential of the form $(Cx + Dt)$ where C and D are arbitrary constants. Since $\partial\phi/\partial t$ occurs only in the Bernoulli integral, we may, by a suitable choice of origin for z , make $D = -c_g C$. The constant C is still arbitrary. So if $\bar{\phi}$ denotes the average of ϕ over one wave cycle we have

$$\bar{\phi} = \phi_a + C(x - c_g t),$$

and clearly

$$\frac{\partial \bar{\phi}}{\partial x} = -\frac{1}{c_g} \frac{\partial \bar{\phi}}{\partial t}.$$

If \bar{u} , $\bar{\zeta}$ and \bar{w} denote similar averages of u , ζ and w we have analogously to (2.14)

$$\bar{u} = \partial \bar{\phi} / \partial x, \quad g \bar{\zeta} = -(\partial \bar{\phi} / \partial t)_{z=0} - \bar{w}.$$

Hence

$$c_g(\bar{u})_{z=0} - g \bar{\zeta} = \bar{w}. \quad (3.20)$$

Since the wave amplitude is a gradually varying function of x we may assume that locally the waves are given by (2.8) and so

$$\bar{w} = \frac{1}{2}(\overline{u^{(1)2}} - \overline{w^{(1)2}}) = \frac{E}{\rho h} \left(\frac{c_g}{c} - \frac{1}{2} \right). \quad (3.21)$$

The mean horizontal momentum M is defined by

$$M = \int_{-h}^{\zeta} \rho u \, dz.$$

Correct to the second order we have

$$M = m + \rho h |\bar{u}| \quad (m = E/c) \quad (3.22)$$

(Stokes 1847; for an alternative proof see the Appendix). The equation of continuity of mass is then

$$\frac{\partial}{\partial t}(\rho \bar{\zeta}) + \frac{\partial M}{\partial x} = 0,$$

or, since $\bar{\zeta}$ and M are both functions of $(x - c_g t)$,

$$\frac{\partial}{\partial x}(M - c_g \rho \bar{\zeta}) = 0.$$

Substituting for M and integrating we have

$$m + \rho h |\bar{u}| - \rho c_g \bar{\zeta} = \text{const.}$$

By a suitable choice of axes (or of the constant C) we may ensure that the constant of integration vanishes, and then

$$h |\bar{u}| - c_g \bar{\zeta} = -m/\rho. \quad (3.23)$$

Equations (3.20) and (3.23) can now be solved for $\bar{\zeta}$, provided we have some relation between $|\bar{u}|$ and $\bar{u}_{z=0}$, i.e. between the mean horizontal velocity and the velocity at the surface.

(a) *The wave groups are long compared to the depth.* Then the potential $\bar{\phi}$ represents a shallow water wave, so that \bar{u} is independent of depth. Equations (3.20) and (3.23) become simply

$$\left. \begin{aligned} c_g \bar{u} - g \bar{\zeta} &= \bar{w}, \\ h \bar{u} - c_g \bar{\zeta} &= -m/\rho, \end{aligned} \right\} \quad (3.24)$$

of which the solution is

$$\left. \begin{aligned} \bar{u} &= -\frac{c_g \bar{w} + gm/\rho}{gh - c_g^2}, \\ \bar{\zeta} &= -\frac{h\bar{w} + c_g m/\rho}{gh - c_g^2}. \end{aligned} \right\} \quad (3.25)$$

Substitution for \bar{w} and m gives

$$\left. \begin{aligned} \bar{u} &= -\frac{1}{2} \frac{a^2 g}{hc(gh - c_g^2)} (gh + c_g^2 - \frac{1}{2}cc_g), \\ \bar{\zeta} &= -\frac{1}{2} \frac{ga^2}{gh - c_g^2} \left(\frac{2c_g}{c} - \frac{1}{2} \right). \end{aligned} \right\} \quad (3.26)$$

These solutions will be seen to be identical with (3.17) in view of the identity

$$K \equiv \frac{g}{2hc c_g} (gh + c_g^2 - \frac{1}{2}cc_g)$$

which can be verified at some length.

From equations (3.25) one can also derive a simple expression for the virtual pressure \bar{p}_s . Since $\partial \bar{\phi} / \partial z$ vanishes at $z = -h$ we have

$$\left(\frac{\partial \bar{\phi}}{\partial z} \right)_{z=0} = - \int_{-h}^0 \frac{\partial^2 \bar{\phi}}{\partial z^2} dz = \int_{-h}^0 \frac{\partial^2 \bar{\phi}}{\partial x^2} dz = -h \frac{\partial^2 \bar{\phi}}{\partial x^2},$$

for $\partial^2 \bar{\phi} / \partial x^2 = \partial \bar{u} / \partial x$, which is independent of z . Hence

$$\left(\frac{\partial^2 \bar{\phi}}{\partial t^2} + g \frac{\partial \bar{\phi}}{\partial z} \right)_{z=0} = (c_g^2 - gh) \frac{\partial^2 \bar{\phi}}{\partial x^2} = \frac{gh - c_g^2}{c_g} \frac{\partial \bar{u}}{\partial t}.$$

The right-hand side equals $-(1/\rho) \partial p_s / \partial t$ and so

$$\bar{p}_s = -\frac{gh - c_g^2}{c_g} \rho \bar{u} + \text{const.}$$

Substituting from the first of (3.25) gives

$$\bar{p}_s = \rho \bar{w} + gm/c_g + \text{const.} \quad (3.27)$$

In the case when $e^{-kh} \ll 1$ then \bar{w} vanishes and we have

$$p_s = gm/c_g + \text{const.} \quad (3.28)$$

This has a simple physical interpretation. m represents the additional mass transport due to the waves which, because it is non-uniform in x , tends to produce a piling-up of mass near the free surface:

$$-\int \frac{\partial m}{\partial x} dt = \int \frac{1}{c_g} \frac{\partial m}{\partial t} dt = \frac{m}{c_g} + \text{const.}$$

The virtual pressure \bar{p}_s is simply this quantity multiplied by g .

(b) *The wave groups are not long compared to the depth.* The problem can still be solved by the simple method provided only two wave components are present. For then $\bar{\phi}$ has a single wave-number Δk , and from Laplace's equation, together with the condition at the bottom, it follows that \bar{u} depends on z through the factor $\cosh \Delta k(z+h)$. Therefore

$$\frac{|\bar{u}}{(\bar{u})_{z=0}} = \frac{\tanh \Delta kh}{\Delta kh} = \theta.$$

In equation (3.20) we may therefore substitute $(\bar{u})_{z=0} = \theta^{-1} |\bar{u}$ and also $\bar{w} = 0$, since $e^{-kh} \ll 1$. Together with (3.23) we have

$$\left. \begin{aligned} c_g |\bar{u} - \theta_g \bar{\xi} &= 0, \\ h |\bar{u} - c_g \bar{\xi} &= -m/\rho, \end{aligned} \right\}$$

where $c_g = g/2\sigma$. Solving these equations we find

$$\left. \begin{aligned} |\bar{u} &= -\frac{\theta g m / \rho}{gh - \theta c_g^2} = -\frac{2\theta \alpha^2 \sigma k}{4\theta kh - 1}, \\ \bar{\xi} &= -\frac{c_g m / \rho}{\theta gh - c_g^2} = -\frac{\alpha^2 k}{4\theta kh - 1}, \end{aligned} \right\} \quad (3.29)$$

which are equivalent to (3.19).

When more than two sine-waves are present it is obvious that $|\bar{u}$ and $\bar{\xi}$ cannot be simply related to the local wave amplitude, for then the fluid has a different response to each of the harmonic components of the virtual pressure \bar{p}_s .

Method 3

This is essentially the method given by Whitham (1962); as will be seen, it is valid only when the groups are long compared to the depth.

Let S denote the flux of momentum across a vertical plane $x = \text{constant}$:

$$S = \int_{-h}^{\xi} (p + \rho u^2) dz, \quad (3.30)$$

and let S_x denote the difference between this and the part due to the hydrostatic pressure:

$$\begin{aligned} S_x &= \int_{-h}^{\xi} (p + \rho u^2) dz - \int_{-h}^{\xi} \rho g(\xi - z) dz \\ &= S - \frac{1}{2} \rho g(h + \xi)^2 \\ &\doteq S - \rho g\left(\frac{1}{2}h^2 + h\bar{\xi}\right). \end{aligned} \quad (3.31)$$

S_x is the radiation stress introduced by Longuet-Higgins & Stewart (1960), and may be thought of as the excess transfer of momentum due to the waves (Whitham 1962). When the vertical acceleration is negligible we find, correct to the second order of approximation,

$$S_x = E\left(\frac{2c_g}{c} - \frac{1}{2}\right) \quad (3.32)$$

(Longuet-Higgins & Stewart 1960, §3).

Now from the continuity of mass and momentum

$$\partial(\rho\bar{\xi})/\partial t + \partial M/\partial x = 0, \quad (3.33)$$

and

$$\partial M/\partial t + \partial S/\partial x = 0. \quad (3.34)$$

But the last equation may be written

$$\frac{\partial M}{\partial t} + gh \frac{\partial}{\partial x} (\rho\bar{\xi}) = -\frac{\partial S_x}{\partial x}. \quad (3.35)$$

Equations (3.33) and (3.35) together show that $\bar{\xi}$ and M are equivalent to the surface elevation and horizontal momentum in a long (shallow-water) wave when a horizontal force $-\partial S_x/\partial x$ per unit distance is applied to the fluid. Since S_x is proportional to a^2 , the applied force travels with the group velocity, so that $\partial/\partial t$ may be replaced by $-c_g \partial/\partial x$. Then we have

$$\begin{aligned} -\rho c_g \partial \bar{\xi} / \partial x + \partial M / \partial x &= 0, \\ \rho gh \partial \bar{\xi} / \partial x - c_g \partial M / \partial x &= -\partial S_x / \partial x, \end{aligned}$$

of which the solution is

$$\begin{aligned} \rho \frac{\partial \bar{\xi}}{\partial x} &= -\frac{1}{gh - c_g^2} \frac{\partial S_x}{\partial x}, \\ \frac{\partial M}{\partial x} &= -\frac{c_g}{gh - c_g^2} \frac{\partial S_x}{\partial x}. \end{aligned}$$

Thus on integration

$$\left. \begin{aligned} \rho \bar{\zeta} &= -\frac{S_x}{gh - c_g^2}, \\ M &= -\frac{c_g S_x}{gh - c_g^2}, \end{aligned} \right\} \quad (3.36)$$

the constants of integration being at our disposal. The mean velocity \bar{u} may be found from the relation (3.22) between M and $\bar{\zeta}$. Hence

$$\bar{u} = \frac{1}{\rho h} (M - E/c) = -\frac{c_g}{h(gh - c_g^2)} S_x \frac{E}{\rho h c}.$$

This will be seen to be equivalent to (3.26).

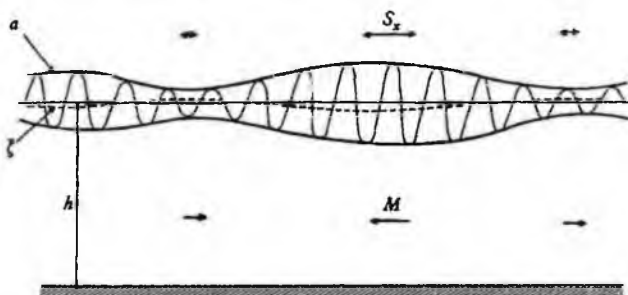


FIGURE 1. The effect of the radiation stress in depressing the mean level in a group of high waves.

It will be noticed that beneath a group of high waves, where S_x and E are both large, $\bar{\zeta}$ and \bar{u} are more negative, that is to say there is a relative depression in the mean surface level, coupled with a mean flow opposite to the direction of wave propagation. Beneath a group of low waves, on the other hand, the mean surface level is raised and the flow is positive.

The sign of the response may be accounted for in the following way (see figure 1). In a group of high waves S_x is large, so that the applied force $-\partial S_x/\partial x$ is positive in advance of the group and negative behind it. Now the wave groups are travelling with a velocity c_g which is generally less than the free-wave velocity $(gh)^{\frac{1}{2}}$, and so the response of the system to the applied force is in the same direction as if the groups were stationary; in other words, the applied force acts in opposition to the restoring force arising from the deformation of the surface. So the restoring force is negative in advance of the high wave group, implying an upwards mean tilt, and positive behind the group. Directly beneath the group, therefore, there is a depression.

More graphically, we may say that the greater stress in the high waves tends to force the water apart there, and so to produce a depression in the surface level.

In the more general case, when the groups are not long compared to the depth, the above argument breaks down, on account of vertical accelerations in the mean motion. For to retain the form (3.32) of S_x one would have to add to the right-hand side of (3.31) a term depending on the vertical acceleration $D\bar{w}/Dt$:

$$S_x = \int_{-h}^{\zeta} (p + \rho u^2) dz - \int_{-h}^{\zeta} dz \left[\rho g(\bar{\zeta} - z) + \int_h^{\zeta} \rho \frac{D\bar{w}}{Dt} dz \right].$$

Thus, to the second order,

$$S_x = S - \frac{1}{2} \rho g (h + \zeta)^2 - \int_{-h}^{\zeta} dz \left[\rho \frac{\partial \bar{v}}{\partial t} \right]_z.$$

The effect of this is to add a further term to the left-hand side of (3.35). Hence the simple argument no longer suffices.

Waves advancing into still water

This problem may be treated by the same methods as we have outlined, except that the representation of $\zeta^{(1)}$ as a sum of sine-waves must be replaced by the Fourier integral representation:

$$\zeta^{(1)} = \int_0^{\infty} A(k) \cos \{kx - \sigma t + \chi(k)\} dk,$$

σ being the function of k defined by (2.9). The analysis proceeds along exactly similar lines, Fourier integrals replacing the Fourier sums. The choice of the arbitrary constants C' and D' , however, is naturally determined by the consideration that the mean level $\zeta^{(2)}$ and the mean velocity $|u^{(2)}$ each be zero in the undisturbed part of the fluid.

If the transition from the undisturbed to the disturbed zone is sufficiently gradual, and if the breadth of the transition zone is large compared with h , then we may suppose that the conclusions previously found for long wave groups will apply. In particular, $|u^{(2)}$ and $\zeta^{(2)}$ will be related to the local wave amplitude as in equation (3.17). Moreover, the constants of integration are as chosen, namely zero, for both $|u^{(2)}$ and $\zeta^{(2)}$ vanish in the undisturbed region, where the wave amplitude is also zero. In this special instance then, the solution (3.17) is applicable. However, if the transition is more abrupt, compared to the depth, then the solution is more complicated.

In very deep water, where the length of a group is small compared to the depth, the effect of the radiation stress can be seen very simply. Consider a group of waves, of energy density E , advancing through still water. Letting $\Delta kh \rightarrow \infty$ in (3.13) we see that the mean velocity $u^{(2)}$ tends to zero. So if M' denotes the mean horizontal momentum in the uppermost layer (say within a wavelength of the free surface) we have

$$M' = m = E/c.$$

Hence

$$\frac{\partial M'}{\partial t} = \frac{1}{c} \frac{\partial E}{\partial t} = \frac{1}{2c_g} \frac{\partial E}{\partial t} = -\frac{1}{2} \frac{\partial E}{\partial x},$$

i.e.

$$\frac{\partial M'}{\partial t} = -\frac{\partial S_x}{\partial x},$$

since $S_x = \frac{1}{2}E$. In such deep water, then, we see that the radiation stress gradient provides just the acceleration required to give the uppermost layer of water its known momentum.

The total momentum M , on the other hand, tends to vanish in deep water. For on letting $\Delta kh \rightarrow \infty$ in (3.18) we find

$$\rho h |u^{(2)}| \sim -\frac{1}{2} \rho \sigma a^2 = -E/c, \quad g\zeta^{(2)} = O(\sigma^2 a^2 \Delta k/k),$$

and so $M \rightarrow 0$ by (3.22). Thus the fluid responds so as to keep the mean surface level almost constant and the total momentum zero. With shallower depths the water is unable to do this. There is a resulting change in the value of M and an additional stress gradient due to the mean surface slope.

4. Water of variable depth. (1) Steady wave trains

So far the mean depth h has been assumed to be independent of x . In this and the following section we shall extend the previous results to include the case when h varies rather gradually with horizontal distance, so that dh/dx and higher derivatives of h are small. In this section it is assumed that the wave amplitude is steady, i.e. independent of the time. In §5 we discuss the effect of a wave amplitude which fluctuates in time.

Again, use is made of the small-amplitude wave theory. It turns out that considerations of energy are sufficient to determine the local wave amplitude; then the momentum equation will determine the mean surface elevation or depression, if the mean pressure on the bottom can be evaluated. One of the crucial steps is to show that the mean pressure on the bottom is in fact equal to the mean hydrostatic pressure, correct to the second order of approximation.

To fix the ideas, suppose that a regular train of waves advances into water of gradually diminishing depth $h(x)$. If there is no loss of energy by breaking of the waves and internal friction, and if the reflexion of energy is negligible, then the wave amplitude $a(x)$ may be determined by the consideration that the flux of energy F towards the shore is a constant (see Burnside 1915). So to the second order

$$E c_g = F = \text{const.}, \quad (4.1)$$

where $E = \frac{1}{2} \rho g a^2$. As is well known,† c_g at first increases slightly above the deep-water value $g/2\sigma$ and then diminishes asymptotically to $(gh)^{\frac{1}{2}}$. So the wave amplitude a at first decreases slightly, and then increases asymptotically like $h^{-\frac{1}{2}}$. The wavelength, on the other hand, steadily decreases with h , and also the ratio c/c_g .

Consider now the balance of momentum between two fixed vertical planes $x = x_0$, $x = x_0 + dx$. The fluxes of momentum across these planes are S and $(S + \partial S/\partial x dx)$ respectively. Across the bottom there is no normal component of velocity, but the pressure \bar{p}_h contributes a normal force $-p_h dl$ where dl is the distance between the two planes, measured along the bottom. The horizontal component of this force is $-p_h dl(dh/dl)$ or $-p_h dh$. In the quasi-steady state this must equal $-\partial S/\partial x dx$ and hence

$$\frac{\partial S}{\partial x} = \bar{p}_h \frac{dh}{dx}. \quad (4.2)$$

Our next task is to evaluate \bar{p}_h . Since both ∇u and $\nabla(\partial u/\partial t)$ vanish by continuity, the equation of vertical motion

$$-\frac{1}{\rho} \frac{\partial p}{\partial z} = g + \frac{\partial w}{\partial t} + \left(u \frac{\partial w}{\partial x} + w \frac{\partial w}{\partial z} \right)$$

† For graphs of a , k and c/c_g , relative to their deep-water values see, for example, figure 5 of Longuet-Higgins (1956).

may also be written

$$-\frac{1}{\rho} \frac{\partial p}{\partial z} = g + \frac{\partial}{\partial z} \left(z \frac{\partial w}{\partial t} + w^2 \right) + \frac{\partial}{\partial x} \left(z \frac{\partial u}{\partial t} + uw \right).$$

On integrating over the range $-h < z < \zeta$ we have

$$\frac{1}{\rho} (p_h - p_s) = g(\zeta + h) + \left[z \frac{\partial w}{\partial t} + w^2 \right]_{-h}^{\zeta} + \int_{-h}^{\zeta} \frac{\partial}{\partial x} \left(z \frac{\partial u}{\partial t} + uw \right) dz,$$

where p_s is the surface pressure, assumed zero. Now

$$\left(z \frac{\partial w}{\partial t} + w \right)_{z=\zeta} = \zeta \frac{\partial^2 \zeta}{\partial t^2} + \left(\frac{\partial \zeta}{\partial t} \right)^2 + O(a^3),$$

and hence, neglecting terms of order a^3 , we have

$$\frac{p_h}{\rho} = g(\zeta + h) + \frac{\partial^2}{\partial t^2} \left(\frac{1}{2} \zeta^2 \right) - \left(z \frac{\partial w}{\partial t} + w^2 \right)_{z=-h} + \int_{-h}^0 \frac{\partial}{\partial x} \left(z \frac{\partial u}{\partial t} + uw \right) dz. \quad (4.3)$$

On taking mean values with respect to t , the time-derivatives vanish, by periodicity, and we have

$$\frac{1}{\rho} \bar{p}_h = g(\bar{\zeta} + h) - (\bar{w}^2)_{z=-h} + \int_{-h}^0 \frac{\partial}{\partial x} (\bar{uw}) dz.$$

Now on the bottom w is of order udh/dx , and so \bar{w}^2 is proportional to $a^2(dh/dx)^2$, which we neglect, since it involves the square of dh/dx . Further, since in uniform depth \bar{uw} vanishes, in general it is of order $a^2 dh/dx$ at most, and $\partial(\bar{uw})/\partial x$ is of order $a^2(dh/dx)^2$ or $a^2 d^2h/dx^2$, which again we neglect. To this order of approximation, then, the previous equation gives simply

$$\bar{p}_h = \rho g(h + \bar{\zeta}), \quad (4.4)$$

i.e. the mean pressure on the bottom equals the mean hydrostatic pressure, as in the case of uniform depth (equation (2.15)).

So from (4.2) we have

$$\partial S/\partial x = \rho g(h + \bar{\zeta}) dh/dx. \quad (4.5)$$

But by the definition of S_x in (3.31) we have

$$\frac{\partial S_x}{\partial x} = \frac{\partial S}{\partial x} - \rho g(h + \bar{\zeta}) \frac{dh}{dx} - \rho g h \frac{\partial \bar{\zeta}}{\partial x},$$

and therefore altogether

$$\partial S_x/\partial x = -\rho g h \partial \bar{\zeta}/\partial x, \quad (4.6)$$

or

$$\frac{\partial \bar{\zeta}}{\partial x} = -\frac{1}{\rho g h} \frac{\partial S_x}{\partial x}. \quad (4.7)$$

This is just the equation for the gradient of the surface level $\bar{\zeta}$ when a constant, small horizontal force $-\partial S_x/\partial x$ is applied.

Integration of equation (4.7)

Let us assume at first that no energy is lost by wave breaking, bottom friction, etc. Then equation (4.7) admits an exact integral. For from (3.31) and (4.1) we have

$$S_x = F \left(\frac{2}{c} - \frac{1}{2c_g} \right) = \sigma F \left[\frac{2k}{\sigma^2} - \left(\frac{\partial k}{\partial \sigma^2} \right)_h \right], \quad (4.8)$$

where F is a constant and the subscript indicates that h is to be held constant in the differentiation. Now if we introduce the non-dimensional quantities $kh = \xi$, $\sigma^2 h/g = \eta$ then the period equation (2.9) may be written

$$\xi \tanh \xi = \eta, \quad (4.9)$$

and we have

$$\left(\frac{\partial k}{\partial \sigma^2} \right)_h = \left(\frac{\partial(\xi/h)}{\partial(\eta g/h)} \right)_h = \frac{1}{g} \frac{d\xi}{d\eta}.$$

Substituting in (4.8) we have

$$S_x = \frac{\sigma F}{g} \left(\frac{2\xi}{\eta} - \frac{d\xi}{d\eta} \right). \quad (4.10)$$

In equation (4.7), h and hence ξ and η may be regarded as functions of x only, and we have

$$d\bar{\xi} = -\frac{1}{\rho g h} dS_x = \frac{\sigma^3 F}{\rho g^3} \frac{1}{\eta} d \left(\frac{d\xi}{d\eta} - \frac{2\xi}{\eta} \right).$$

Integration by parts yields

$$\bar{\xi} = \frac{\sigma^3 F}{\rho g^3} \frac{d}{d\eta} \left(\frac{\xi}{\eta} \right) + \text{const.}$$

But $\xi/\eta = \coth \xi$, which tends to unity in deep water ($\xi \gg 1$). So if $\bar{\xi}$ is measured relative to the deep-water level the constant of integration vanishes:

$$\bar{\xi} = \frac{\sigma^3 F}{\rho g^3} \frac{d}{d\eta} (\coth \xi). \quad (4.11)$$

Now

$$F = E c_g = E \left(\frac{\partial \sigma}{\partial k} \right)_h = \frac{E}{2\sigma} \left(\frac{\partial \sigma^2}{\partial k} \right)_h = \frac{E g d\eta}{2\sigma d\xi}.$$

Thus

$$\bar{\xi} = \frac{\sigma^2 E}{2\rho g^2} \frac{d}{d\xi} (\coth \xi)$$

or, on substituting $E = \frac{1}{2} \rho g a^2$ and performing the differentiation,

$$\bar{\xi} = -\frac{1}{2} \frac{a^2 k}{\sinh 2kh}. \quad (4.12)$$

As the water becomes shallow ($kh \gg 1$) we have the asymptotic expression

$$\bar{\xi} \sim -\frac{a^2}{4h}. \quad (4.13)$$

Equation (4.12) shows that when there is no loss of energy the surface is depressed relative to the deep-water level. The values of a in that equation, however, depend on the local depth. To obtain the actual profile of $\bar{\xi}$ we return to equation (4.11) in which F is assumed constant and equal to $\frac{1}{2} \rho g^2 a_0^2 / \sigma$, where a_0 is the wave amplitude in deep water. Substituting for F in that equation we find

$$\left. \begin{aligned} \bar{\xi} &= -a_0^2 k_0 f(\eta), \\ \text{where } f(\eta) &= -\frac{1}{4} \frac{d}{d\eta} (\coth \xi) = \frac{\coth^2 \xi}{4(\xi + \sinh \xi \cosh \xi)}, \end{aligned} \right\} \quad (4.14)$$

and ξ is related to η by (4.11). $f(\eta)$ is plotted in figure 2. The very sharp down-turn in level at around $\eta = 0.5$ will be noted. In shallow water ($\eta \ll 1$) we have

$$f(\eta) \sim \frac{1}{8}\xi^{-3} \sim \frac{1}{8}\eta^{-\frac{3}{2}}. \quad (4.15)$$

This asymptote is indicated by the broken line in figure 2: it lies remarkably close to $f(\eta)$ when $\eta < 0.5$. From equation (4.15) we have

$$\xi \sim -\frac{a_0^2 k_0}{8(\sigma^2 h/g)^{\frac{3}{2}}} = -\frac{a_0^2 g^{\frac{1}{2}}}{8\sigma h^{\frac{3}{2}}}. \quad (4.16)$$

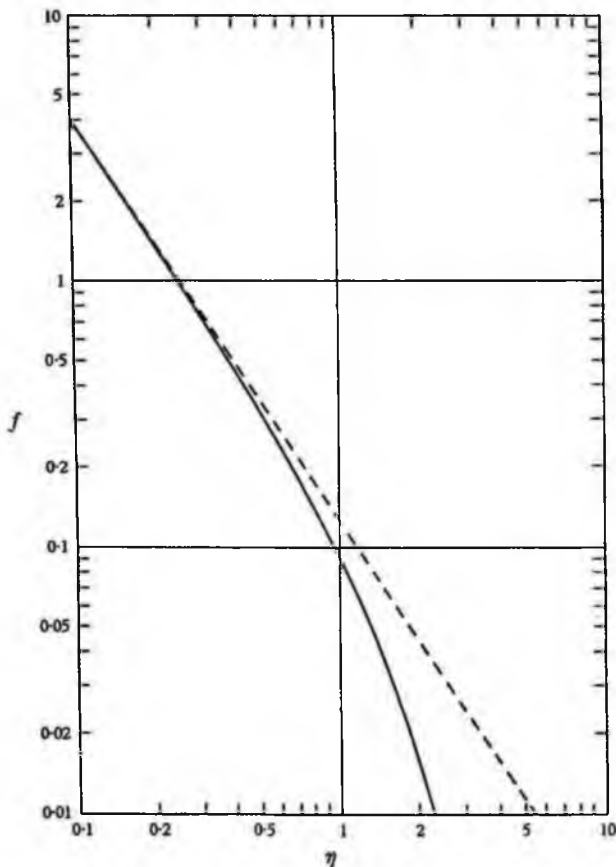


FIGURE 2. Graph of $f(\eta)$, giving the depression of the mean surface level in water of finite depth, relative to the level in deep water. The broken curve represents the asymptote $1/(8\eta^{\frac{3}{2}})$.

Thus the surface depression is inversely proportional to the three-halves power of the depth.

The above formulae apply only so long as there is no appreciable loss of energy and so long as the small-amplitude theory is valid. A necessary condition for the latter is that

$$ak \ll (kh)^3 \quad (4.17)$$

(see Stokes 1847). The theory is certainly not precisely valid when the waves are so steep as to be breaking.

However, one may perhaps expect a qualitative result from the observation that swell in shallow water tends to break when the depth is about 1.3 times the crest-to-trough height (Munk 1949*b*). In shallow water $c_0/c = 1$ so that from (3.32)

$$S_x = \frac{3}{2}E = \frac{3}{4}\rho g a^2.$$

If we now write $2a = h/1.3$ equation (4.5) gives

$$\partial \bar{\zeta} / \partial x = -0.22 \partial h / \partial x. \quad (4.18)$$

Since for shoaling water $\partial h / \partial x$ is negative, the mean level tends now to *rise* towards the shore. In fact, (4.18) suggests that the mean gradient of $\bar{\zeta}$ may be practically independent of the initial wave amplitude and period under these conditions.

Some confirmation of these conclusions is to be found in the experiments of Fairchild (1958). These were made on a 1:75 model of the beach profile off Narragansett pier, with wave amplitudes $a = \frac{1}{2}H$, ranging from 15 ft. down to $2\frac{1}{2}$ ft., and periods of 15 and 9 sec. With the larger wave amplitudes, where breaking might be expected, there was a positive 'set-up' (rise in level) towards the shoreline. The difference in $\bar{\zeta}$ between say 200 and 400 ft. from the shoreline is remarkably independent of wave amplitude and period. The mean value is $\Delta \bar{\zeta} = -0.75$ ft., corresponding to a difference in depth $\Delta h = 6$ ft. Thus

$$\frac{\Delta \bar{\zeta}}{\Delta x} = -0.12 \frac{\Delta h}{\Delta x},$$

which is in order-of-magnitude agreement with (4.18).

Significantly also, at the smaller wave amplitudes, where breaking is delayed, the observations show that $\bar{\zeta}$ can be negative. The author states: "Other tests in the Beach Erosion Board laboratory have shown that for considerably steeper beach slopes (1 on 3 and 1 on 6) and wave of somewhat lesser height (2-4 ft.), there is no wave set-up but rather there is wave set-down". This is to be expected, for under the conditions described the breaking of the waves would be delayed. If there is little loss of energy apart from wave breaking, then our analysis suggests that the greatest depression of the mean level will be at about the point where breaking first occurs.

The magnitude of the change in level is of the same order as that caused by wind stress over the water surface. At first glance this appears anomalous since the momentum of the waves is only a small proportion of the total momentum transferred from the wind into the water. However, the increase in surface level caused by the wind stress produces an increased pressure effective through the full depth of the basin. On the other hand, the momentum associated with the waves produces a change in level only when the water becomes shallow, and so the force is exerted over only a small depth. As has been shown by Taylor (1962) the wave momentum may be transferred directly to the boundaries by the radiation stress, with only a depression of mean level resulting. This occurs when the bottom slope is sufficiently abrupt.

5. Water of variable depth. (2) Groups of waves

We now generalize to the case of a train of waves of fluctuating amplitude.

It can be assumed that at each point the wavelength and velocity of the waves correspond to the local depth of water, and that the wave groups advance towards the shore with a velocity equal to the local group-velocity. To determine the amplitude, suppose first that there is no loss of energy due to breaking or friction. Then we may assume that the flux of energy F across any (fixed) vertical plane with co-ordinate x , at time t , is constant for an observer advancing with the group-velocity c_g .

On the other hand, if breaking occurs then the amplitude of the higher waves may be limited by the local depth h .

To find the effect on the mean surface level $\bar{\xi}$ we generalize the analysis of the preceding section so as to include the effect of a time-varying mass-transport M . In place of equation (4.2) we obtain

$$\partial M / \partial t + \partial S / \partial x = \bar{p}_h dh / dx. \quad (5.1)$$

Equation (4.2) is the special case of this equation when $\partial M / \partial t = 0$, and (3.34) is the special case when $dh / dx = 0$. On the other hand, by taking local averages in (4.3) we have,

$$\frac{\bar{p}_h}{\rho} = g(h + \bar{\xi}) - \left(z \frac{\partial \bar{w}}{\partial t} \right)_{z=-h} + \int_{-h}^0 \left(z \frac{\partial^2 \bar{u}}{\partial z \partial t} \right) dz$$

(compared with equation (4.4)). Substituting $-\partial^2 \bar{w} / \partial z \partial t$ for $\partial^2 \bar{u} / \partial z \partial t$ in the integral and integrating by parts we find

$$\frac{\bar{p}_h}{\rho} = g(h + \bar{\xi}) + \int_{-h}^0 \frac{\partial \bar{w}}{\partial t} dz. \quad (5.2)$$

Suppose now that the wave groups are long, so that $\partial \bar{w} / \partial t$ is negligible. Then \bar{p}_h is given simply by $\bar{p}_h = \rho g(h + \bar{\xi})$. Combining this with (5.1) we obtain equation (3.35) as before. Moreover, the equation of continuity of mass is still valid also. So we have shown that for long wave groups, even when the depth is variable, the mean surface $\bar{\xi}$ responds as though a horizontal stress $-\partial S_x / \partial x$ were applied at the surface.

The explicit calculation of $\bar{\xi}$ must depend upon the entire form of bottom profile $h(x)$ and not merely on the local depth if, as is generally true, there is an appreciable change of depth h within a horizontal distance equal to the length of a wave group. A detailed calculation will not be attempted here. However, it may be noted that as the depth diminishes, and the group-velocity c_g approaches $(gh)^{1/2}$, so the response of the surface to the applied stress will increase. For example, the surface elevation $\bar{\xi}$, which in the case of uniform depth h is given by

$$\bar{\xi} = -\frac{S_x / \rho}{gh - c_g^2} + \text{const.}, \quad (5.3)$$

will become large on account of the vanishing of the denominator. From (2.10) and (2.11) we have

$$c_g^2 = \frac{1}{2} gh \frac{\tanh kh}{kh} \left(1 + \frac{2kh}{\sinh 2kh} \right)^2 = gh [1 - (kh)^2 + O(kh)^4], \quad (5.4)$$

so that, if the resonant response had time to develop fully,

$$\xi \sim -\frac{S_x}{\rho gh(kh)^2} \sim -\frac{S_x}{\rho \sigma^2 h^2}. \quad (5.5)$$

When there is no loss of energy, we should have from (4.6)

$$\bar{\xi} \sim -\frac{3}{2} \frac{f}{\rho \sigma^2 h^2 (gh)^{\frac{1}{2}}}, \quad (5.6)$$

which is increasingly negative as h diminishes. However, the validity of these formulae is limited by the condition (4.10) and by the fact that the resonant response needs time to build up. In practice, the waves are often limited by breaking, so that ξ may not increase towards the shore to the extent indicated by (5.6).

6. Surf beats

Off-shore records of wave pressure on the sea-bed when there is an incoming swell often show the existence of longer waves, of 2–3 min period, very similar to the envelope of the visual swell (Munk 1949*a*; Tucker 1950); but the long waves

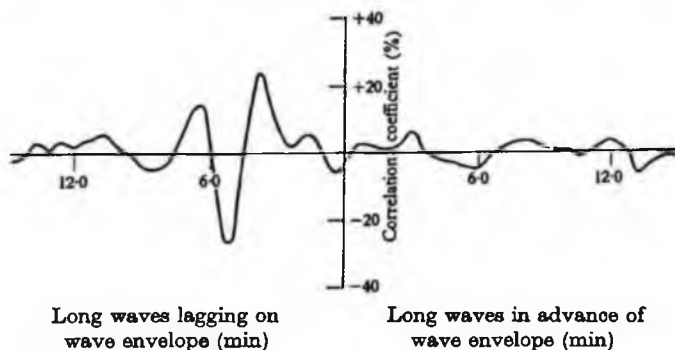


FIGURE 3. Correlation of long waves with the envelope of incoming swell, as a function of the time difference between them: mean of the five best correlograms. (From Tucker 1950.)

are delayed relative to the envelope of the swell by several minutes. Munk and Tucker have both suggested that the long waves may be caused by an excess of mass carried forward by the groups of high swell; the swell waves, it is assumed, are destroyed on the beach, but the mass-transport associated with them is reflected back and is measured as a long wave by the pressure recorder after an appreciable time delay.

To demonstrate this, Tucker correlated the long waves with the envelope of the swell, at varying time shifts (see figure 3) and found a maximum (negative) correlation at a time shift of about 5 min—about the time required for the groups of waves to reach shore with velocity c_g and for the long waves to travel back with velocity $(gh)^{\frac{1}{2}}$. Tucker also compared the height of the long waves with the height of the corresponding groups of swell (see figure 4).

Tucker made the following remark: "Such a simple explanation disagrees with the observations in two major respects: according to theory, the mass-transport

within a wave (in a given depth) is proportional to the square of the height, whereas the observations show that the long wave height is approximately linearly proportional to the ordinary wave height. The simple explanation also requires that the long wave should be an elevation, whereas figure 2 shows that the outstanding feature of the observed wave is a depression in water level."

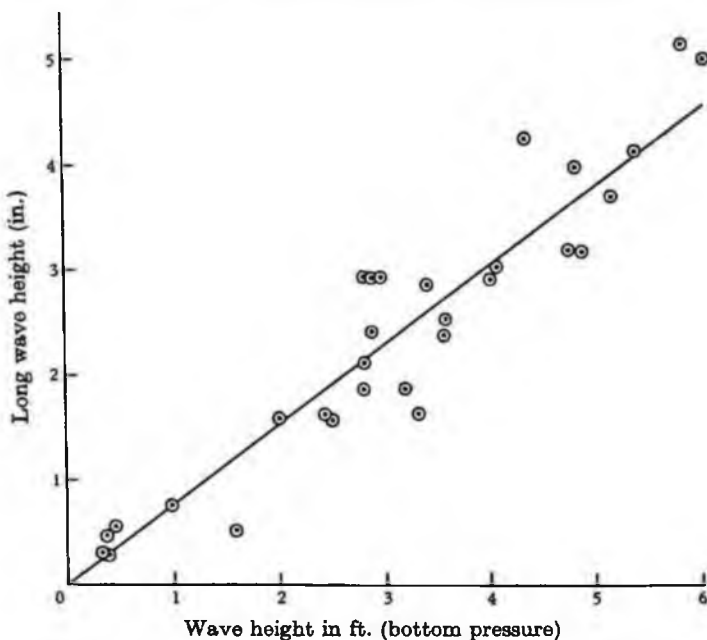


FIGURE 4. Relation between the height of the long waves and the height of the corresponding swell. (From Tucker 1950.)

The reader will at once perceive that the second objection is immediately answered, for we have shown that in fact, contrary to expectation, a group of high waves is associated with a *depression* of the mean surface level and a consequent reduction of pressure on the bottom.

To account for Tucker's first point, however, we shall now try to construct a very crude theory of surf beats, on the lines previously suggested.

Since long waves are more readily reflected by non-uniformities in the transmitting medium than are shorter waves, it is reasonable to suppose that at some depth h_0 the long wave associated with the mass-transport undergoes partial reflexion while the shorter waves are allowed to pass on and be destroyed in shallower water. If C_R denotes the coefficient of reflexion of the long wave, then its amplitude at the point of reflexion would, according to (5.6) be given by

$$\bar{\zeta}_R = -\frac{3}{2} \frac{C_R F}{\rho \sigma^2 h_0^2 (g h_0)^{\frac{1}{2}}}.$$

On propagation outwards the height of the reflected wave will be diminished like $(h_0/h)^{\frac{1}{2}}$, so that at any other depth h , and after the appropriate lapse of time,

$$\bar{\zeta}_R = -\frac{3}{2} \frac{C_R F}{\rho \sigma^2 h_0^2 (g h_0)^{\frac{1}{2}}} \left(\frac{h_0}{h} \right)^{\frac{1}{2}},$$

which represents also the long-wave pressure, in feet of water, recorded on the bottom.

Since ξ_{SR} is proportional to F and hence to a^2 , it would seem that the amplitude of the long waves is proportional to the square of the envelope of the incoming swell. On the other hand, if breaking has taken place before the point of reflexion, the higher waves at least will have been reduced in amplitude, and so one expects in fact a law of variation rather weaker than a^2 . This is not inconsistent with Tucker's observations.

It should be said that the choice of one particular depth h_0 for reflexion of the long wave is probably not realistic, and that reflexion may take place at more than one place, depending also on the length of the wave groups. Further reflexion by deep water (Isaacs, Williams & Eckart 1951) is also not out of the question. All such possibilities would tend to lower the correlation between the wave envelope and the subsequent surf beat.

Finally it may be worth mentioning that Munk (1949*a*) has attempted a comparison of the observed long waves with the time-integral of (breaker height)², using a fixed time lag. However, from our point of view this time-integral would be 90° out of phase with the appropriate quantity for a periodic wave envelope. The fact that Munk obtains reasonable coincidence over four cycles of the envelope is not evidence against our hypothesis, for with a slightly different time lag, the evidence could equally well be used in support of our hypothesis. The appropriate time-lag was not certain "in view of the 1000 ft. distance separating the swell and tsunami records and of other uncertainties" (see p. 853). The procedure adopted by Tucker, namely to plot the correlation coefficient between the surf envelope and the long waves as a function of the time lag, appears to be the most convincing.

Appendix: the momentum integral

The relation

$$M = \rho h |\bar{u} + E/c \tag{A 1}$$

used in § 3 is due essentially to Stokes (1847), and in the case $|\bar{u} = 0$ was rediscovered by Starr (1959) as a hydrodynamical analogy to Einstein's law $M = E/c^2$. The method of derivation given by Whitham (1962) is similar to Stokes's. Here we give a simple way of deriving the relation, which avoids the explicit evaluation of integrals.

The mean horizontal momentum M may be expressed as

$$M = \int_{-h}^{\xi} \rho U dz, \tag{A 2}$$

where U denotes the mean velocity of a particle, in the Lagrangian sense: in other words the mass-transport velocity. Now the displacement of a particle due to its orbital motion is, to the first order,

$$\Delta \mathbf{x} = \int \mathbf{u}^{(1)} dt$$

and so the horizontal velocity of the particle in the neighbourhood of a fixed point \mathbf{x} is

$$u + \Delta \mathbf{x} \cdot \nabla u.$$

The mass-transport velocity, to second order, is the mean value of this expression:

$$U = \bar{u} + \overline{\int \mathbf{u}^{(1)} dt \cdot \nabla u^{(1)}}.$$

Now $\mathbf{u}^{(1)}$ is periodic in time and so

$$\overline{\int \mathbf{u}^{(1)} dt \cdot \nabla u^{(1)} + \mathbf{u}^{(1)} \cdot \nabla \int u^{(1)} dt} = \frac{\partial}{\partial t} \overline{\int \mathbf{u}^{(1)} dt \cdot \nabla \int u^{(1)} dt}$$

which vanishes by periodicity. So we have

$$\begin{aligned} U &= \bar{u} - \overline{\mathbf{u}^{(1)} \cdot \nabla \int u^{(1)} dt} \\ &= \bar{u} - \overline{\mathbf{u}^{(1)} \int \frac{\partial u^{(1)}}{\partial x} dt + u^{(1)} \int \frac{\partial u^{(1)}}{\partial z} dt}. \end{aligned}$$

Since the motion is progressive, $\partial u^{(1)}/\partial x$ may be replaced by $-(1/c)\partial u^{(1)}/\partial t$; and $\partial u^{(1)}/\partial z$, which equals $\partial w^{(1)}/\partial x$, may be replaced by $-(1/c)\partial w^{(1)}/\partial t$. Hence

$$U = \bar{u} + \frac{1}{c} \overline{(u^{(1)2} + w^{(1)2})} = \bar{u} + \overline{\mathbf{u}^{(1)2}}/c.$$

Substituting in (A 2) gives $M = \rho h \{ \bar{u} + 2 \text{K.E.}/c$

where K.E. denotes the density of kinetic energy. Since K.E. equals half the total energy E , the result (A 1) follows.

REFERENCES

- BURNSIDE, W. 1915 On the modification of a train of waves as it advances into shallow water. *Proc. Lond. Math. Soc.* (2), 14, 131.
- FAIRCHILD, J. C. 1958 Model study of wave set-up induced by hurricane waves at Narragansett pier, Rhode Island. *Bull. Beach Erosion Board*, 12, 9-20.
- ISAACS, J. D., WILLIAMS, A. E. & ECKART, C. 1951 Total reflection of surface waves by deep water. *Trans. Amer. Geophys. Un.* 32, 37-40.
- LAMB, H. 1932 *Hydrodynamics*, 6th ed. Cambridge University Press.
- LONGUET-HIGGINS, M. S. 1953 Mass-transport in water waves. *Phil. Trans. A*, 245, 535-81.
- LONGUET-HIGGINS, M. S. 1956 The refraction of sea waves in shallow water. *J. Fluid Mech.* 1, 163-76.
- LONGUET-HIGGINS, M. S. 1960 Mass transport in the boundary layer at a free oscillating surface. *J. Fluid Mech.* 8, 293-306.
- LONGUET-HIGGINS, M. S. & STEWART, R. W. 1960 Changes in the form of short gravity waves on long waves and tidal streams. *J. Fluid Mech.* 8, 565-83.
- LONGUET-HIGGINS, M. S. & STEWART, R. W. 1961 The changes in amplitude of short gravity waves on steady non-uniform currents. *J. Fluid Mech.* 10, 529-49.
- MUNK, W. H. 1949a Surf beats. *Trans. Amer. Geophys. Un.* 30, 849-54.
- MUNK, W. H. 1949b The solitary wave theory and its application to surf problems. *Ann. New York Acad. Sci.* 51, 376-424.
- STARR, V. P. 1959 Hydrodynamical analogy to $E = mc^2$. *Tellus*, 11, 135-8.
- STOKES, G. G. 1847 On the theory of oscillatory waves. *Trans. Camb. Phil. Soc.* 8, 441-55. (Reprinted in *Math. and Phys. Papers*, 1, 314-26.)
- TAYLOR, G. I. 1962 *J. Fluid Mech.* 13, 182.
- TUCKER, M. J. 1950 Surf beats: sea waves of 1 to 5 minutes' period. *Proc. Roy. Soc. A*, 202, 565-73.
- WHITHAM, G. B. 1962 Mass, momentum and energy flux in water waves. *J. Fluid Mech.* 12, 135-47.

REPRINT FROM

SEARS FOUNDATION: JOURNAL OF MARINE RESEARCH

Volume 21, Number 1, January 15, 1963, Pp. 4-10

A Note on Wave Set-up

M. S. Longuet-Higgins¹

*National Institute of Oceanography,
Wormley, England*

R. W. Stewart

*Institute of Oceanography,
Vancouver, B. C., Canada*

ABSTRACT

Seaward of the breaker zone, the observations of Saville are in good qualitative agreement with the prediction that the mean surface level is increasingly depressed towards the shoreline, proportionally to $F(\eta)$, *i. e.*, to $(\sigma^2 h/g)^{-3/2}$, very nearly. The observed depressions are on the average greater than the theoretical by a factor of about 1.7. Between the breaker zone and the still-water level the surface tends to rise again in the way described by $d\xi/dx = Q(dh/dx)$, with the factor Q equal to 0.15.

1. *Introduction.* It was found experimentally by Fairchild (1958), and confirmed more recently by Saville (1961), that when a steady train of waves is propagated in water of non-uniform depth, the mean level of the water surface may differ appreciably from the still-water level. An effect of this kind was also recently suggested on theoretical grounds (Longuet-Higgins and Stewart, 1962)². This note compares the theory with the experimental results.

2. *Definitions.* Regular, two-dimensional waves, of constant period and amplitude, are supposed advancing into a region of non-uniform depth. Let σ = radian frequency = 2π /wave period; k = wavenumber = 2π /wave length; a = wave amplitude, = $1/2$ wave height; h = local still-water depth; x = horizontal co-ordinate in direction of wave propagation.

It is assumed that the depth varies only gradually, so that $(dh/dx)^2$ is negligible. When the waves originate in deep water ($kh \gg 1$) their amplitude and wavenumber there are denoted by a_∞ and k_∞ respectively. We have simply $k_\infty = \sigma^2/g$.

¹ At present visiting the Institute of Geophysics, UCSD, La Jolla, California.

² A similar prediction, in less explicit form, is made by Dorrestein (1962). See also a report by Forstak (1962).

3. *Theoretical Predictions.* In the paper by Longuet-Higgins and Stewart (1962; henceforward referred to as [I]), two types of prediction were made:

(1) Assuming that there is no loss of energy in the waves, either by friction, breaking or reflection, then the mean surface level at any point is lowered by an amount

$$-\bar{\zeta} = a_{\infty}^2 k_{\infty} F(\eta), \quad (1)$$

where

$$\eta = \sigma^2 h/g, \quad (2)$$

and $F(\eta)$ is a dimensionless function defined as follows:

$$\left. \begin{aligned} F(\eta) &= -\frac{1}{4} \frac{d}{d\eta} \coth \xi, \\ \xi \tanh \xi &= \eta. \end{aligned} \right\} \quad (3)$$

The function $F(\eta)$ is plotted in [I]: fig. 1. For values of η less than 1 (*i. e.*, in moderately deep water), $F(\eta)$ lies close to the asymptote

$$F(\eta) \sim \frac{1}{8 \eta^{3/2}}, \quad \eta \ll 1. \quad (4)$$

For the validity of this result it is necessary that the conditions

$$ak \ll 1, \quad ak \ll (kh)^3 \quad (5)$$

for the small-amplitude theory of water waves be satisfied.

If the waves do not originate in deep water, but in a long channel of depth h_0 , then the generalization of eq. (1) is

$$-\bar{\zeta} = a_{\infty}^2 k_{\infty} [F(\eta) - F(\eta_0)], \quad (6)$$

where

$$\eta_0 = \sigma^2 h_0/g, \quad (7)$$

and a_{∞} is a virtual amplitude at infinity, which may be calculated by the condition that the energy flux ($1/2 \rho g a^2 \times$ group velocity) is a constant. A graph giving the ratio of a_0 , the amplitude in water of depth h_0 , to a_{∞} , is given, for example, in Longuet-Higgins (1956).

(2) The second result of [I] applies to the altogether different situation in which the waves are in shallow water ($kh \ll 1$) and are limited in height by breaking. A rough argument suggested that

$$\frac{d\bar{\zeta}}{dx} = Q \frac{dh}{dx}, \quad (8)$$

where Q is a quantity of the order of 0.2.

Finally, we note that, according to the theory of solitary waves (Munk, 1949), the depth h_b at the initial breaking point is related to the wave amplitude in deep water by

$$\frac{h_b}{a_\infty} = 1.14 (a_\infty k_\infty)^{-1/3}. \quad (9)$$

4. *Experimental Data.* For comparison with eq. (6), the most suitable and extensive data are those given by Saville (1961: table 4). These are the observed differences in level $\bar{\zeta}$ when waves approached a ramp of slope 1:10, topped by another ramp of slope 1:6 or 1:3. The wave amplitude a_0 was measured in a depth of water equal to 10 feet (on the model scale), and the mean levels at four different distances from the shoreline. By reconstructing the beach graphically, one finds for the mean depth h at these positions the following:

	Upper slope 1:6				Upper slope 1:3			
Position:	1	2	3	4	1	2	3	4
Distance from shoreline:	18.5	23.6	30.8	51.0	6.5	11.6	18.8	39.0 feet
Depth h :	3.1	3.9	4.6	6.6	2.2	3.9	4.6	6.7

In order to plot all of the experimental points on the same diagram we have calculated a_∞ , k_∞ and η_0 as defined in §§ 2 and 3, and plotted

$$\frac{-\bar{\zeta}}{a_\infty^2 k_\infty} + F(\eta_0) \quad (10)$$

against $F(\eta)$, the above expression being the value of $F(\eta)$ given by eq. (6). The result is shown in Fig. 1. The circles refer to the 1:6 slope (scale model 1:10); the triangles refer to the 1:3 slope (prototype tank data), and the squares to the 1:3 slope (scale model 1:10).

In Fig. 1 a distinction has been made between whether the breaking point had or not had been reached, according to eq. (9). If $h > h_b$, *i. e.*, the waves had not yet broken, the plotted symbols have been filled in solidly. At the largest value of h for which $h \leq h_b$ (at any fixed value of a_∞ and σ), a line has been drawn through the center of the symbol; these presumably correspond to waves on the point of breaking. All other plotted symbols in Fig. 1 are left empty; these represent waves which had almost certainly broken.

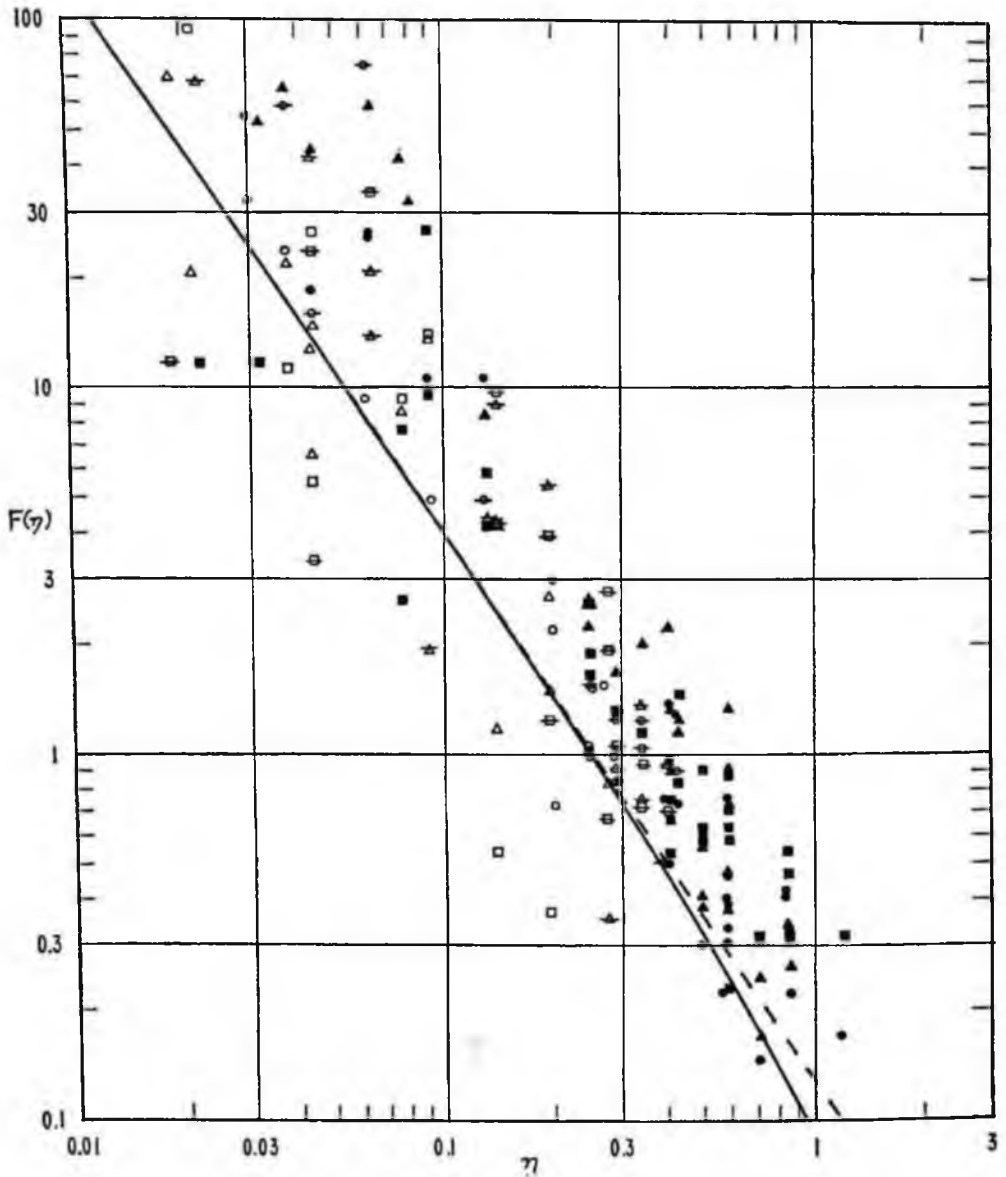


Figure 1. Observations of the surface depression [in the form of eq. (10)] compared with the theoretical function $F(\eta)$ (solid line). The horizontal co-ordinate is proportional to the local mean depth. Data are from Saville (1961): table 4.

The full curve in Fig. 1 represents the theoretical value of $F(\eta)$, and the broken curve is the asymptote, eq. (4).

It is seen that generally the trend of the observations is very similar to that of the theoretical curve, over a range of 1:1000. The plotted points corresponding to waves which had not broken lie generally above the theoretical

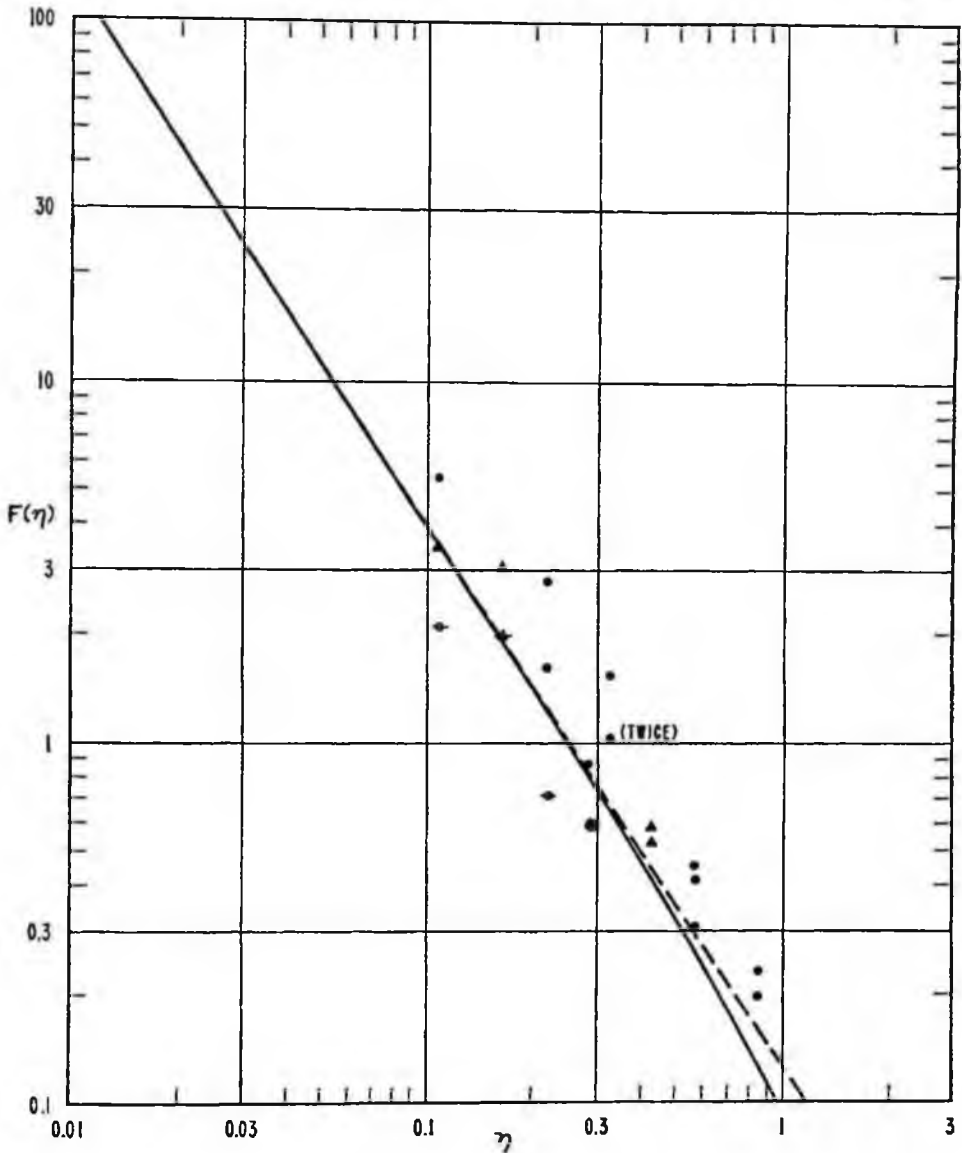


Figure 2. As in Fig. 1. Data also from Saville (1961): table 1.

curve, *i. e.*, the *depression* of the mean level is greater than predicted, by an average factor of about 1.7.

A second set of data, derived from Saville (1961: table 1), is shown in Fig. 2. These measurements were made on uniform slopes of 1:30 and 1:15 (indicated by circles and triangles respectively). Only those data are shown for which the waves had not yet broken (full plots) or had only just broken (plots with horizontal lines). Also the plots have been confined to those cases

when the waves did not over-top the slope. The agreement with the theoretical curve is comparable to that in Fig. 1, if anything somewhat better. This may be because the waves had lost more energy on the less inclined slope.

Saville's observations were, in the latter case, continued well beyond the breaking point of the waves, so that the gradient of the set-up in the region of breaking can be compared with the theoretical prediction of eq. (8) above. The observations, which are shown graphically by Saville (1961: figs. 4, 5), do indeed suggest that the gradient of the set-up is practically constant in this region. The magnitude of the set-up is shown in Table I. Here $\Delta\zeta$ denotes the difference in set-up between the still-water line and the first break-point (as computed by Saville³), and Δx is the horizontal distance between them. Δh is the consequent difference in height, *i. e.*, Δx times the bottom gradient.

TABLE I. OBSERVATIONS OF SET-UP IN THE BREAKER ZONE.

Wave period (sec)	Wave height (ft)	Bottom gradient	$\Delta\zeta$ (ft)	Δx (ft)	Δh (ft)	$\frac{\Delta\zeta}{\Delta h}$
9.25	10	1:30	1.7	390	13	0.13
9.25	20	1:30	4.2	780	26	0.16
9.25	30	1:30	4.1	1180	39	0.11
15.0	10	1:30	1.8	390	13	0.14
15.0	20	1:30	4.7	780	26	0.18
15.0	30	1:30	4.0*	900	30	0.13
9.25	10	1:15	2.0	200	13	0.15
9.25	20	1:15	5.7	390	26	0.22
9.25	30	1:15	5.9	580	39	0.15

* Measured from the lowest available observation.

In the last column of Table I the ratio $\Delta\zeta/\Delta h$ is shown. It is seen that this ratio is virtually independent of wave period and bottom slope, and also of wave amplitude. The observed values differ little from the mean value 0.15. This indicates that the quantity Q in eq. (8) is in fact about 0.15.

Saville's observations include other interesting features, such as the effect of a breakwater and of overtopping at a berm. These are not covered by the presently available theory.

5. *Conclusions.* Seaward of the breaker zone, the observations of Saville are in good qualitative agreement with the prediction of eq. (6); that is to say, the mean surface level is increasingly depressed towards the shoreline, proportionally to $F(\eta)$, *i. e.*, to $(\sigma^2 h/g)^{-3/2}$ very nearly. The observed depressions are on the average greater than the theoretical by a factor of about 1.7. Between the breaker zone and the still-water level the surface tends to rise again in the way described by eq. (8), with the factor Q equal to 0.15.

³ Saville's predicted break-points do not differ significantly from those given by eq. (9) above.

REFERENCES

- DORRESTEIN, R.
1962. Wave set-up on a beach. Proc. Second Tech. Conf. on Hurricanes, U.S. Dept. of Commerce, Nat. Hurricane Res. Proj., Rep. 50. pp. 230-241.
- FAIRCHILD, J. S.
1958. Model study of wave set-up induced by hurricane waves at Narragansett pier, Rhode Island. Bull. Beach Eros. Bd., 12: 9-20.
- FORTAK, H. G.
1962. Concerning the general vertically averaged hydrodynamic equations with respect to basic storm surge equations. Nat. Hurricane Res. Proj., Rep. 51: 25 pp.
- LONGUET-HIGGINS, M. S.
1956. The refraction of sea waves in shallow water. J. Fluid Mech., 8: 293-306.
- LONGUET-HIGGINS, M. S. and R. W. STEWART
1962. Radiation stress and mass transport in gravity waves, with application to "surf beats." J. Fluid. Mech., 13: 481-504.
- MUNK, W. H.
1949. The solitary wave theory and its application to surf problems. Ann.N.Y. Acad. Sci., 51: 376-424.
- SAVILLE, T.
1961. Experimental determination of wave set-up. Proc., Second Tech. Conf. on Hurricanes, U.S. Dept. of Commerce, Nat. Hurricane Res. Proj., Rep. 50. pp. 242-252.

Radiation stresses in water waves ; a physical discussion, with applications

M. S. LONGUET-HIGGINS* and R. W. STEWART†

(Received 17 June 1964)

Abstract—The radiation stresses in water waves play an important role in a variety of oceanographic phenomena, for example in the change in mean sea level due to storm waves (wave “set-up”); the generation of “surf-beats”; the interaction of waves with steady currents; and the steepening of short gravity waves on the crests of longer waves. In previous papers these effects have been discussed rigorously by detailed perturbation analysis. In the present paper a simplified exposition is given of the radiation stresses and some of their consequences. Physical reasoning, though less rigorous, is used wherever possible. The influence of capillarity on the radiation stresses is fully described for the first time.

INTRODUCTION

In a series of recent papers (1960, 1961, 1962, see also TAYLOR 1962, WHITHAM 1962) we have attempted to elucidate some of the non-linear properties of surface gravity waves in terms of what we have called the “radiation stress.” Some of these non-linear properties have turned out to be unexpected (or at least to differ from properties widely assumed previously in the literature). For this reason a major part of the above mentioned papers has been used for a careful check of the results obtained by using the radiation stress concept, by means of detailed perturbation analysis to the required order of approximation.

One effect of this approach (which we believe to have been necessary) has been that the papers are somewhat analytical, and the straightforward simplicity of the concept may have been partly obscured for some readers. It is the purpose of the present paper to attempt a simple exposition, setting forth the nature and uses of the radiation stress. In many cases results will be stated without proof; readers dissatisfied with any of these are referred to the previous papers. (We shall refer to LONGUET-HIGGINS and STEWART, 1960, 1961, and 1962 as I, II and III). At the same time we shall extend some of our previous results for pure gravity waves so as to include effects of capillarity.

In the first sections of the paper we describe a simple derivation of the radiation stress, both for gravity waves and for capillary waves. In the second part we shall describe the application of these results to a number of interesting phenomena observed in the oceans; in particular to wave “set-up,” “surf beats,” the steepening of short waves on adverse currents or tidal streams, and the generation of capillary waves by steep gravity waves.

*National Institute of Oceanography Wormley, Godalming, Surrey.

†Institute of Oceanography, University of British Columbia, Vancouver, British Columbia, Canada.

PART I—THE RADIATION STRESSES; A PHYSICAL DISCUSSION

It is well known that electromagnetic radiation impinging on a surface, or originating on a surface, produces a force which is referred to as the "radiation pressure." It is perhaps less well known that a similar phenomenon occurs in the case of acoustic waves and of waves on the surface of fluids (or indeed of internal waves in a stratified fluid). In each case the force is principally in the direction of wave propagation. It is therefore not an isotropic one unless the waves themselves are isotropically distributed (as is the case for electromagnetic waves in an isothermal enclosure). In fluid mechanics it has become customary to use the term "pressure" for the isotropic stress which figures in the equation of state. We have therefore considered it wise to coin the term radiation *stress* as a more general one which does not carry any implication of isotropy‡.

Qualitatively§, the following argument may serve to introduce the concept :

It is well known (LAMB, 1932, Section 250) that surface waves possess momentum which is directed parallel to the direction of propagation and is proportional to

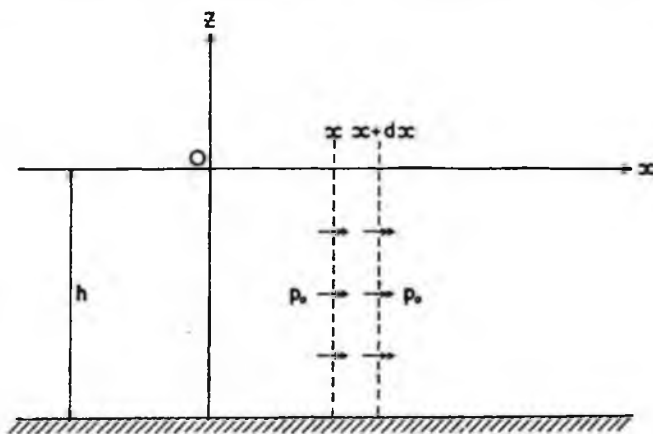


Fig. 1. The momentum flux in a stationary fluid.

the square of the wave amplitude. Now if a wave train is reflected from an obstacle, its momentum must be reversed. Conservation of momentum then requires that there be a force exerted on the obstacle, equal to the rate of change of a wave momentum. This force is a manifestation of the radiation stress.

A stress is by definition equivalent to a flow of momentum. The radiation stress may thus be defined as *the excess flow of momentum due to the presence of the waves*. Let us consider in detail how this stress arises in gravity waves.

1. Progressive waves in water of uniform depth

Consider first an undisturbed body of water of uniform depth h (Fig. 1). The pressure p at any point is equal to the hydrostatic pressure :

‡It might be argued that "radiative stress" would be grammatically more correct, but we wish to retain the implied analogy to the well established term "radiation pressure"—and in any case the use of nouns as adjectives is widespread in English.

§Quantitatively, in some special cases, it leads to difficulties and to errors, because some phenomena are incompletely described by the discussion in this paragraph.

$$p = -\rho g z, \quad (1)$$

where ρ , g and z denote density, gravity, and distance measured upwards from the mean surface. If we denote the above expression by p_0 then the flux of horizontal momentum across any vertical plane $x = \text{constant}$ is simply p_0 per unit vertical distance. Thus the total flux of horizontal momentum between surface and bottom ($z = -h$) is

$$\int_{-h}^0 p_0 dz \quad (2)$$

Since this quantity is independent of x , the flux of momentum across an adjacent plane ($x + dx$) just balances the flux across the first plane, and there is no net change of momentum between the two planes (Fig. 1).

Now consider the momentum flux in the presence of a simple progressive wave motion (Fig. 2). The surface elevation $z = \zeta$ is given approximately by

$$\zeta = a \cos(kx - \sigma t) \quad (3)$$

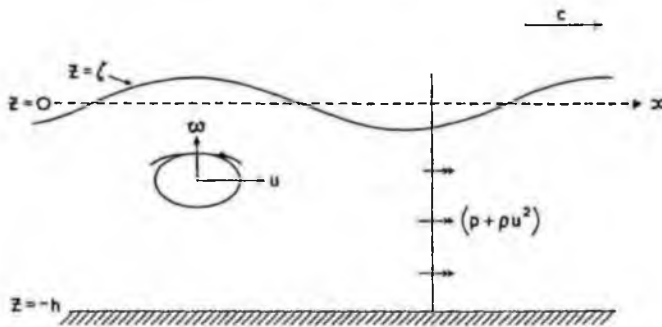


Fig. 2. The momentum flux in a progressive wave.

where a is the amplitude, $k = 2\pi/\text{wavelength}$ and $\sigma = 2\pi/\text{wave period}$. The particle orbits are roughly ellipses, with the major axes horizontal in general. (In deep water the orbits are circular). The corresponding components of velocity are given by

$$\left. \begin{aligned} u &= \frac{a\sigma}{\sinh kh} \cosh k(z+h) \cos(kx - \sigma t) \\ w &= \frac{a\sigma}{\sinh kh} \sinh k(z+h) \sin(kx - \sigma t). \end{aligned} \right\} \quad (4)$$

A quite general expression for the instantaneous flux of horizontal momentum across unit area of a vertical plane in the fluid is

$$p + \rho u^2. \quad (5)$$

In this expression the second term ρu^2 represents a bodily transfer of momentum ρu (per unit volume) at a rate u per unit time (Fig. 3). The term ρu^2 is evidently analogous to a pressure. Even if the mean value of u itself is zero, the mean value $\overline{u^2}$ is of course generally positive.

(Similarly, fluid crossing the plane $x = \text{constant}$ possesses z -momentum associated with the velocity component w . A mean product such as $\rho \bar{uw}$, which represents the mean transport of z -momentum across a plane $x = \text{constant}$ —or vice versa—is equivalent to a shear stress. In turbulence theory, such mean values are known collectively as Reynolds stresses, and it will be appreciated that the above

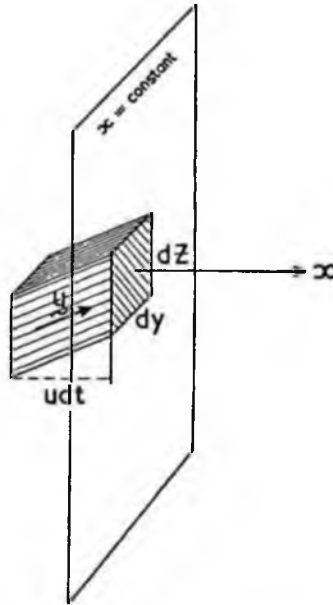


Fig. 3. Bodily transport of momentum across a plane $x = \text{constant}$. In time t a volume udt per unit area has been transported across the plane. The momentum transported is thus $\rho u udt$.

concepts are also similar physically to those used to explain the origin of pressure and viscosity in the kinetic theory of gasses. If due to turbulent fluctuations, the Reynolds shear stress is frequently parameterised by the concept of “eddy viscosity.” Reynolds stresses also occur in waves, but in this case we must seek a different kind of description. For a discussion of the Reynolds stresses particularly appropriate in the present context, see STEWART, (1956)).

To find the total flux of horizontal momentum across a plane $x = \text{constant}$ we have to integrate (5) between the bottom $z = -h$ and the free surface $z = \zeta$:

$$\int_{-h}^{\zeta} (p + \rho u^2) dz. \quad (6)$$

We now define the principal component S_{xx} of the radiation stress as the mean value of the function (6) with respect to time, minus the mean flux in the absence of the waves, that is to say

$$S_{xx} = \int_{-h}^{\zeta} (p + \rho u^2) dz - \int_{-h}^0 p_0 dz. \quad (7)$$

Special care must be taken to take the mean value *after* integration, since the fluctuation of the free surface itself contributes to the momentum flux. We can see this best by separating the right-hand side of (7) into three parts, that is by writing

$$S_{xx} = S_{xx}^{(1)} + S_{xx}^{(2)} + S_{xx}^{(3)} \tag{8}$$

where

$$\left. \begin{aligned} S_{xx}^{(1)} &= \int_{-h}^{\zeta} \rho u^2 dz \\ S_{xx}^{(2)} &= \int_{-h}^0 (p - p_0) dz \\ S_{xx}^{(3)} &= \int_0^{\zeta} p dz. \end{aligned} \right\} \tag{9}$$

Consider the first contribution $S_{xx}^{(1)}$. Since the integrand is of second order, the upper limit $z = \zeta$ may be replaced effectively by the mean level $z = 0$, since the additional range $0 < z < \zeta$ contributes only a third-order term. Now, both the limits of integration $0, h$, being constant, we can transfer the mean value to the integrand. Thus

$$S_{xx}^{(1)} = \int_{-h}^0 \overline{\rho u^2} dz = \int_{-h}^0 \rho \overline{u^2} dz. \tag{10}$$

The contribution $S_{xx}^{(1)}$, then, is effectively *the Reynolds stress $\overline{\rho u^2}$ integrated from the bottom up to the free surface*. It is obviously positive in general.

Consider now the contribution $S_{xx}^{(2)}$. As in equation (10), we may take the mean value inside the limits of integration :

$$S_{xx}^{(2)} = \int_{-h}^0 (\overline{p} - p_0) dz. \tag{11}$$

In other words $S_{xx}^{(2)}$ arises from *the change in mean pressure within the fluid*. Now the pressure \overline{p} generally contains terms proportional to a^2 , which can be found by a second order analysis. However, we do not need to calculate all the second-order terms explicitly since \overline{p} may be found directly from a consideration of the *vertical* flux of vertical momentum as follows.

We know that the mean flux of vertical momentum across any horizontal plane, which is $\overline{p + \rho w^2}$, must be just sufficient to support the weight of the water above it. Since the mean level of the water is at $z = 0$, we have then

$$\overline{p + \rho w^2} = -\rho g z = p_0 \tag{12}$$

or

$$\overline{p} - p_0 = -\rho \overline{w^2} \tag{13}$$

Thus \overline{p} is generally less than the hydrostatic pressure p_0 . Substitution in equation (11) gives

$$S_{xx}^{(2)} = \int_{-h}^0 (-\rho \overline{w^2}) dz. \quad (14)$$

This contribution is then negative in general.

Combining equations (10) and (14) we have

$$S_{xx}^{(1)} + S_{xx}^{(2)} = \int_{-h}^0 \rho (\overline{u^2} - \overline{w^2}) dz \geq 0. \quad (15)$$

For, since the major axes of the particle orbits are horizontal we have $\overline{u^2} \geq \overline{w^2}$. After substituting for the velocities from equations (4) and carrying out the integration we find in fact*

$$S_{xx}^{(1)} + S_{xx}^{(2)} = \frac{1}{2} \frac{\rho a^2 \sigma^2 h}{\sinh^3 kh} = \frac{\rho g a^2 kh}{\sinh 2kh} \quad (16)$$

having used in the last step the frequency relation

$$\sigma^2 = gk \tanh ph \quad (17)$$

for waves of small amplitude.

In deep water the particle orbits are circles, and $\overline{u^2}$ equals $\overline{w^2}$; the Reynolds stresses are isotropic in x and z . The positive contribution $\rho \overline{u^2}$ from the horizontal Reynolds stress is then exactly cancelled by the pressure defect $-\rho \overline{w^2}$ arising from the vertical Reynolds stress. On the other hand in shallow water the particle orbits are elongated horizontally, and $\overline{w^2}$ becomes small compared with $\overline{u^2}$. Then $\rho (\overline{u^2} - \overline{w^2})$ becomes simply $\rho \overline{u^2}$. Since, for the same reason, the kinetic energy is then just $\frac{1}{2} \rho u^2$ per unit volume, we see that $S_{xx}^{(1)} + S_{xx}^{(2)}$ is then twice the kinetic energy density, that is, the total energy density of the waves.

There remains the important contribution $S_{xx}^{(3)}$. This is equal to the pressure p integrated† between 0 and ζ and then averaged with respect to time. It is easily evaluated, for near to the free surface p is nearly equal to the hydrostatic pressure below the free surface :

$$p = \rho g (\zeta - z). \quad (18)$$

Thus the pressure at any point near the surface fluctuates in phase with the surface elevation ζ . Substitution in the integral gives

$$S_{xx}^{(3)} = \frac{1}{2} \rho g \overline{\zeta^2}. \quad (19)$$

So $S_{xx}^{(3)}$ is generally positive and is in fact equal to the density of potential energy, that is to say half the total energy density E :

$$S_{xx}^{(3)} = \frac{1}{2} \rho g a^2 = \frac{1}{2} E \quad (20)$$

*It may be noted that $(\overline{u^2} - \overline{w^2})$ is independent of z , for using the incompressible, irrotational and progressive character of the motion we have :

$$\frac{\partial}{\partial z} (\overline{u^2} - \overline{w^2}) = 2 \left(u \frac{\partial u}{\partial z} - w \frac{\partial w}{\partial z} \right) = 2 \left(u \frac{\partial w}{\partial x} + w \frac{\partial u}{\partial x} \right) = 2 \frac{\partial}{\partial x} (uw) = 0.$$

†When the free surface is below the mean level, the velocity field is assumed to be extended analytically up to the mean level. This device leads to the simplest algebra. If preferred, however, the upper limit of integration may be taken at any arbitrary fixed level in the fluid, within a distance of order a from the mean level; the final result is the same.

where

$$E = \frac{1}{2} \rho g a^2. \quad (21)$$

Altogether we have from equations (15) and (19)

$$S_{xx} = S_{xx}^{(1)} + S_{xx}^{(2)} + S_{xx}^{(3)} \geq 0, \quad (22)$$

or on inserting the values found in equations (16) and (20)

$$S_{xx} = E \left(\frac{2kh}{\sinh 2kh} + \frac{1}{2} \right). \quad (23)$$

The ratio $2kh/\sinh 2kh$ lies always between 0 and 1. In deep water ($kh \geq 1$) the ratio tends to 0 and so

$$S_{xx} = \frac{1}{2} E, \quad (24)$$

while the shallow water ($kh < 1$) it tends to 1 and so

$$S_{xx} = \frac{3}{2} E. \quad (25)$$

The transverse components of the radiation stress. Now let us consider in a similar way the flow of y -momentum (momentum parallel to the wave crests) across a plane $y = \text{constant}$. Denoting this by S_{yy} we have corresponding to equation (7) the relation

$$S_{yy} = \int_{-h}^{\zeta} (\overline{p + \rho v^2}) dz - \int_{-h}^0 p_0 dz \quad (26)$$

where v is the transverse component of velocity. Just as for S_{xx} we can consider S_{yy} as the sum of three parts :

$$S_{yy} = S_{yy}^{(1)} + S_{yy}^{(2)} + S_{yy}^{(3)} \quad (27)$$

where

$$\left. \begin{aligned} S_{yy}^{(1)} &= \int_{-h}^{\zeta} \overline{\rho v^2} dz \\ S_{yy}^{(2)} &= \int_{-h}^0 \overline{(p - p_0)} dz \\ S_{yy}^{(3)} &= \int_0^{\zeta} \overline{p} dz \end{aligned} \right\} \quad (28)$$

In gravity waves the transverse velocity vanishes everywhere and so

$$S_{yy}^{(1)} = 0, \quad (29)$$

while $S_{yy}^{(2)}$ and $S_{yy}^{(3)}$ are equal to $S_{xx}^{(2)}$ and $S_{xx}^{(3)}$ respectively.

Thus

$$S_{yy}^{(2)} = \int_{-h}^0 \overline{(-\rho w^2)} dz \leq 0, \quad (30)$$

$$S_{yy}^{(3)} = \frac{1}{2} \rho g \overline{\zeta^2} \geq 0. \quad (31)$$

Substitution for w from equations (4) and use of the frequency relation equation (17) leads to

$$S_{yy} = E \times \frac{kh}{\sinh 2kh}. \quad (32)$$

In deep water, $\overline{w^2} = \overline{u^2} = \frac{1}{2}(\overline{u^2} + \overline{v^2} + \overline{w^2})$; then $S_{yy}^{(2)}$ is equal to minus the density of kinetic energy, which is $-\frac{1}{2}E$. Thus $S_{yy}^{(2)}$ just cancels $S_{yy}^{(3)}$ and S_{yy} vanishes:

$$S_{yy} = 0 \quad (kh \gg 1) \quad (33)$$

In other words, the deficiency in the mean pressure \bar{p} arising from the Reynolds stress $\rho\overline{w^2}$ is exactly cancelled, in deep water, by the surface deformation effect. In shallow water, on the other hand, the mean square vertical velocity $\overline{w^2}$ is small. Hence $S_{yy}^{(2)}$ is negligible and

$$S_{yy} = S_{yy}^{(3)} = \frac{1}{2}E. \quad (34)$$

Lastly the flow of x -momentum across the plane $y = \text{constant}$ is given by

$$S_{xy} = \int_{-h}^{\zeta} \rho uv \, dz;$$

there is no contribution from the mean pressure. Since \overline{uv} vanishes identically we have always

$$S_{xy} = 0 \quad (35)$$

provided, of course, that the x -direction is the direction of wave propagation. If for some reason we choose a co-ordinate system at an angle (other than a right angle), then there *will* be a non-zero shear stress S_{xy} . Its magnitude may be calculated by the ordinary tensor transformation rules from the two-dimensional tensor S , which in diagonal form is given by

$$S = E \begin{pmatrix} \frac{2kh}{\sinh 2kh} + \frac{1}{2} & 0 \\ 0 & \frac{kh}{\sinh 2kh} \end{pmatrix}. \quad (36)$$

2. Standing gravity waves

Let us combine two progressive waves of equal amplitude a and wavelength $2\pi/k$ so as to produce a standing wave. The free surface is then described by

$$\zeta = 2a \cos kx \cos \sigma t \quad (1)$$

and the components of velocity by

$$\left. \begin{aligned} u &= \frac{2a\sigma}{\sinh 2kh} \cosh k(z+h) \sin kx \sin \sigma t \\ w &= \frac{2a\sigma}{\sinh 2kh} \sinh k(z+h) \cos kx \sin \sigma t. \end{aligned} \right\} \quad (2)$$

The surface elevation has antinodes at $kx = n\pi$ (where n is an integer) and nodes at $kx = (n + \frac{1}{2})\pi$, as in Fig. 4. The two components of velocity fluctuate in-phase,

proportionally to $\sin \sigma t$, so that the particle orbits are straight lines. Beneath the antinodes the orbits are vertical, beneath the nodes they are horizontal, and at intermediate positions the orbits are inclined generally to the horizontal. The mean product \overline{uw} and also the shearing stress $\overline{\rho uw}$ do not vanish in general, and are functions of the horizontal co-ordinate x . The horizontal variation of $\overline{\rho uw}$ supports a difference in mean surface level between node and antinode. We can use the radiation stress to calculate this difference.

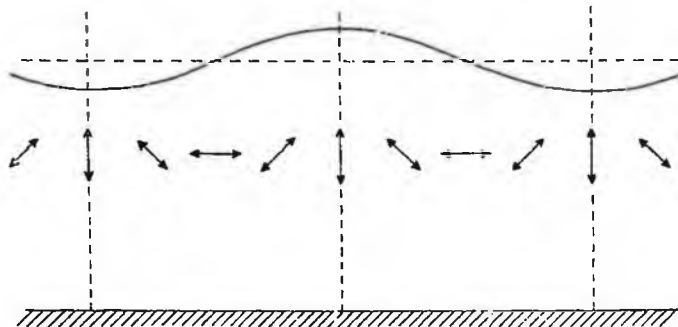


Fig. 4. Particle velocities in a standing wave. The components u and w fluctuate in-phase, and the mean product \overline{uw} is non-zero in general.

Consider the stress S_{xx} , representing the flux of horizontal momentum parallel to the x -axis. This is given by the general relation in equation (7), Section 1, (in which an overbar denotes the average with respect to time). As before we may consider the right-hand side as the sum of three parts $S_{xx}^{(1)}$, $S_{xx}^{(2)}$, $S_{xx}^{(3)}$ given approximately by

$$\left. \begin{aligned} S_{xx}^{(1)} &= \int_{-h}^0 \overline{\rho u^2} dz. \\ S_{xx}^{(2)} &= \int_{-h}^0 (\overline{p} - p_0) dz \\ S_{xx}^{(3)} &= \int_0^{\xi} p dz. \end{aligned} \right\} \quad (3)$$

where $p_0 = -\rho g z$. The third component $S_{xx}^{(3)}$ is found to be

$$S_{xx}^{(3)} = \frac{1}{2} \rho g \overline{\xi^2} \quad (4)$$

as before. In the second component $S_{xx}^{(2)}$, the time-mean pressure \overline{p} cannot be deduced quite so simply as in the progressive wave, being no longer independent of x . However, it can be found from the more general relation for the vertical flux of vertical momentum :

$$\overline{p} + \overline{\rho w^2} - \frac{\partial}{\partial x} \int_z^0 \overline{\rho u w} dz = p_0 + \rho g \xi, \quad (5)$$

in which the terms on the right represent the total weight (per unit cross-section) of a vertical column of water from z to ζ (Fig. 5); the terms on the left show how this weight is supported: the first two terms represent the mean flux of vertical momentum through the base of the column, while the third term is the resultant of the fluxes of vertical momentum through the vertical sides of the column. Taking

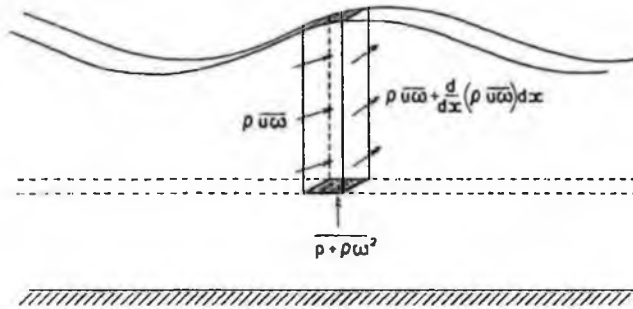


Fig. 5. The balance of momentum in a vertical column of unit cross-section.

$\bar{p} - \rho_0$ to the left-hand side and the other terms to the right, we have after integration with respect to z :

$$S_{xx}^{(2)} = \rho g h \bar{\zeta} - \int_{-h}^0 \rho \bar{w}^2 + \frac{\partial}{\partial x} \int_{-h}^0 \int_{z'}^0 \rho \bar{u} \bar{w} dz dz'. \quad (6)$$

Adding this to $S_{xx}^{(1)}$ and $S_{xx}^{(2)}$ we deduce

$$S_{xx} = \rho g h \bar{\zeta} + \int_{-h}^0 \rho (\bar{u}^2 - \bar{w}^2) dz + \frac{\partial}{\partial x} \int_{-h}^0 \int_{z'}^0 \rho \bar{u} \bar{w} dz dz' + \frac{1}{2} \rho g \bar{\zeta}^2. \quad (7)$$

Now clearly S_{xx} must be a constant, independent of x , for otherwise horizontal momentum would accumulate at some parts of the wave*. Therefore S_{xx} is equal to its horizontal average, that is to say its average with respect to x over a wavelength. Among the terms on the right of equation (7), the horizontal average of $\bar{\zeta}$ is identically zero, while the horizontal average of the third term also vanishes by the periodicity (the momentum fluxes across two vertical walls a wavelength apart just cancel). So we have simply

$$S_{xx} = \int_{-h}^0 \rho (\overline{u^2 - w^2}) dz + \frac{1}{2} \rho g \overline{\zeta^2} \quad (8)$$

where an underbar denotes the horizontal mean value. Substituting from equations (1) and (2) we find

$$S_{xx} = \rho g a^2 \left(\frac{2kh}{\sinh 2kh} + \frac{1}{2} \right). \quad (9)$$

Comparison with equation (23) Section 1 shows that the radiation stress in a

*This follows from the conservation equation for x -momentum: $\partial S_{xx} / \partial x + \partial S_{xy} / \partial y = 0$, and the fact that $S_{xy} = 0$ in these co-ordinates.

standing wave is exactly twice the value in each progressive wave; it represents the sum of the stresses in the incident and reflected waves, as we should expect.

The *local* mean level $\bar{\xi}$ can now be found from equation (7) since all other terms in the equation are known to the required approximation. In this way we find†

$$\bar{\xi} = a^2 k \coth 2kh \cos 2kx. \quad (10)$$

This shows that the mean surface level is slightly raised at the antinodes and correspondingly lowered at the nodes.

The various terms on the right of equation (7) do not all give contributions in the same sense; some tend to raise the level at the antinodes and others to lower it. A simpler way to estimate $\bar{\xi}$ is to return to the momentum flux equation (5) and set $z = 0$. This gives us

$$\overline{(p + \rho w^2)}_{z=0} = \rho g \bar{\xi} \quad (11)$$

(the flux of vertical momentum across the vertical sides of the column is of third order only). But on taking time averages in the Bernoulli equation

$$\left[p + \frac{1}{2} \rho (u^2 + w^2) + \frac{\partial \phi}{\partial t} \right]_{z=0} = f(t)$$

we have also

$$\overline{\left[p + \frac{1}{2} \rho (u^2 + w^2) \right]}_{z=0} = C, \quad (12)$$

where C is a constant, not necessarily zero. From equations (11) and (12) we deduce

$$g \bar{\xi} = -\frac{1}{2} \overline{(u^2 - w^2)}_{z=0} - C. \quad (13)$$

The constant C is determined by the condition that $\bar{\xi} = 0$. Substitution for u and w now gives us equation (10) as before. We note in particular that in deep water ($kh \gg 1$) equation (10) becomes

$$\bar{\xi} = a^2 k \cos 2kx \quad (14)$$

and in shallow water ($kh \ll 1$)

$$\bar{\xi} = \frac{a^2}{2h} \cos 2kx. \quad (15)$$

As the depth h diminishes, a and k being fixed, the changes in mean level which are represented by $\bar{\xi}$ become accentuated.

The evaluation of the transverse stress S_{yy} follows exactly similar lines; it is necessary only to replace \bar{u}^2 by \bar{v}^2 , = 0 throughout. Hence

$$\begin{aligned} S_{yy} &= S_{xx} - \int_{-h}^0 \rho \bar{u}^2 dz \\ &= S_{xx} - \rho g a^2 \left(\frac{2kh}{\sinh 2kh} + 1 \right) \sin^2 kx \\ &= \frac{1}{2} \rho g a^2 \left[\frac{2kh}{\sinh 2kh} + \left(\frac{2kh}{\sinh 2kh} + 1 \right) \cos 2kx \right]. \end{aligned} \quad (16)$$

Hence S_{yy} , unlike S_{xx} , is a function of x in a standing wave. Perhaps surprisingly,

†This result is in agreement with TADJBAKSH and KELLER (1960) provided that account is taken of a misprinted sign in their equation (30).

it will be noted that the maximum values of S_{yy} occur at the *nodes* of the surface elevation. The mean value of S_{yy} is given by

$$\overline{S_{yy}} = \rho g a^2 \frac{kh}{\sinh 2kh} \quad (17)$$

which is just twice the value for the progressive wave (equation (32) Section 1) as we should expect.

The radiation shear stress is given by

$$S_{xy} = S_{yx} = 0 \quad (18)$$

as in the progressive wave.

3. Capillary-gravity waves

The effect of capillarity is equivalent to the stretching of a thin membrane over the surface with constant tension T per unit length. This modifies the previous calculations in the following ways.

First, the tension produces a flux of x -momentum across the plane $x = \text{constant}$ given by $-T \cos \theta$, where θ is the inclination of the surface to the horizontal. The difference between this flux and the equivalent flux in the absence of waves is therefore

$$-T \cos \theta + T = T(1 - \cos \theta) = \frac{1}{2} T \theta^2 \quad (1)$$

when θ is small. Hence the mean additional flux of momentum due to the presence of the wave is equal to $\frac{1}{2} T \overline{\theta^2}$, which must be added to equation (7) Section 1. Since $\theta = \partial \zeta / \partial x$ we have

$$S_{xx} = \int_{-h}^{\zeta} (p + \rho u^2) dz - \int_{-h}^0 p_0 dz + \frac{1}{2} T \overline{\left(\frac{\partial \zeta}{\partial x}\right)^2}. \quad (2)$$

For a progressive wave, the evaluation of $S_{xx}^{(1)}$ and $S_{xx}^{(2)}$ can be carried out as before, up to equation (15). However in calculating $S_{xx}^{(3)}$ the pressure p near the surface is to be decreased by an amount KT , where K is the curvature of the free surface, that is by an amount $T \partial^2 \zeta / \partial x^2$. This adds to $S_{xx}^{(3)}$ the amount

$$-T \zeta \overline{\frac{\partial^2 \zeta}{\partial x^2}} \quad (3)$$

which, because the wave is progressive, is equal to

$$T \overline{\left(\frac{\partial \zeta}{\partial x}\right)^2}. \quad (4)$$

For a progressive wave,

$$\overline{\left(\frac{\partial \zeta}{\partial x}\right)^2} = \frac{1}{2} a^2 k^2. \quad (5)$$

Therefore altogether we have

$$S_{xx} = \frac{1}{2} \rho g a^2 \left(\frac{\sigma^3 h}{g \sinh^2 kh} + \frac{1}{2} + \frac{3}{2} \frac{T k^3}{\rho g} \right). \quad (6)$$

Secondly, the stretching of the surface by the waves stores additional energy T per unit extension of the surface, that is to say

$$T \sec \theta - T, = \frac{1}{2} T \theta^2 \quad (7)$$

per unit horizontal area. The mean density of potential energy is therefore increased by an amount.

$$\frac{1}{2} T \overline{\theta^2} = \frac{1}{2} T \overline{\left(\frac{\partial \xi}{\partial x} \right)^2} = \frac{1}{4} T a^2 k^2. \quad (8)$$

Hence the total energy density E , being twice the potential energy density, becomes

$$E = \frac{1}{2} \rho g a^2 \left(1 + \frac{T k^2}{\rho g} \right). \quad (9)$$

Thirdly, surface tension modifies the relation between σ and k , so that

$$\sigma^2 = g k \tanh kh \cdot \left(1 + \frac{T k^2}{\rho g} \right). \quad (10)$$

On combining the last two equations with equation (6) we find

$$S_{xx} = E \left(\frac{2kh}{\sinh 2kh} + \frac{1 + 3\epsilon}{2(1 + \epsilon)} \right) \quad (11)$$

where

$$\epsilon = \frac{T k^2}{\rho g}. \quad (12)$$

This of course reduces to equation (23) Section 1 when $\epsilon = 0$. In the opposite limit when $\epsilon \gg 1$, that is to say for pure capillary waves, we have

$$S_{xx} = E \left(\frac{2kh}{\sinh 2kh} + \frac{3}{2} \right) \quad (13)$$

where

$$E = \frac{1}{2} T a^2 k^2, \quad (14)$$

and in particular in deep water ($kh \gg 1$)

$$S_{xx} = \frac{3}{2} E; \quad (15)$$

in the shallow-water case ($kh \ll 1$)

$$S_{xx} = \frac{5}{2} E. \quad (16)$$

To find the transverse stress S_{yy} we note that although the surface has no inclination in the y -direction nevertheless the corrugations of the wave system produce a greater surface area per unit distance in the y -direction and therefore more tensile stress. Hence equation (26) Section 1 is replaced by

$$S_{yy} = \int_{-h}^{\xi} (p + \rho v^2) dz - \int_0^h p_0 dz - \frac{1}{2} T \overline{\left(\frac{\partial \xi}{\partial x} \right)^2} \quad (17)$$

This may be split up as before. Since v vanishes, $S_{yy}^{(1)} = 0$. Further since $\overline{w^2}$ is related to the kinetic energy we have

$$S_{yy}^{(2)} = \int_{-h}^0 (-\rho \overline{w^2}) dz = \frac{1}{2} E \left(\frac{2kh}{\sinh 2kh} - 1 \right) \quad (18)$$

as for pure gravity waves. The third component $S_{yy}^{(3)}$ is equal to $S_{xx}^{(3)}$:

$$S_{yy}^{(3)} = \frac{1}{2} \rho g a^2 \left(1 + \frac{2Tk^2}{\rho g} \right). \quad (19)$$

However

$$-\frac{1}{2} T \overline{\left(\frac{\partial \xi}{\partial x} \right)^2} = -\frac{1}{2} T a^2 k^2 \quad (20)$$

so that the sum of the last two terms is

$$S_{yy}^{(3)} - \frac{1}{2} T \overline{\left(\frac{\partial \xi}{\partial x} \right)^2} = \frac{1}{2} \rho g a^2 \left(1 + \frac{Tk^2}{\rho g} \right) = \frac{1}{2} E. \quad (21)$$

Altogether then

$$S_{yy} = E \frac{kh}{\sinh 2kh}, \quad (22)$$

the form of which is independent of the surface tension. In deep water

$$S_{yy} = 0 \quad (23)$$

as for pure gravity waves, and in shallow water

$$S_{yy} = \frac{1}{2} E. \quad (24)$$

The radiation shear stress is unaffected by surface tension :

$$S_{xy} = S_{yz} = 0. \quad (25)$$

PART II APPLICATIONS

We propose now to describe some of the effects of the radiation stresses upon phenomena observable in the oceans.

First we shall consider instances where the radiation stresses either generate or modify motions on a scale larger than the waves themselves. As will be seen, such effects are liable to occur where there are horizontal gradients of the radiation stresses. Such gradients may arise in a variety of ways.

4. Wave "set-up"

One of the most important of these wave-driven effects occurs when deep water waves encounter a sloping beach. The waves shorten, steepen, and eventually break—but continue to advance with decreasing amplitude after breaking. The resulting changes in radiation stress lead to changes in the level of the mean surface.

In the steady state, the shoreward flux of momentum must be independent of x , which we take perpendicular to the shore. Let us now consider the momentum balance in a slice of water bounded by the (sloping) surface $z = \xi$, the sloping bottom $z = -h$ and two vertical planes $x = x_0$ and $x = x_0 + dx$ (see Fig. 6). If the bottom slope is sufficiently small that \overline{uw} and $\overline{w^2}$ at the bottom* are negligible, then the flux of momentum into the slice, crossing the plane $x = x_0$ is

*By bottom, of course, we refer to the bottom of the irrotational flow. The boundary layer between this and the true bottom we assume to be thin and inconsequential.

$$S_{xx} + \int_{-h}^{\bar{\zeta}} \rho g (\bar{\zeta} - z) dz = S_{xx} + \frac{1}{2} \rho g (\bar{\zeta} + h)^2. \quad (1)$$

Across the plane $x = x_0 + dz$ the flow out of the slice will be greater than this by

$$\frac{d}{dx} [S_{xx} + \frac{1}{2} \rho g (\bar{\zeta} + h)^2] dx. \quad (2)$$

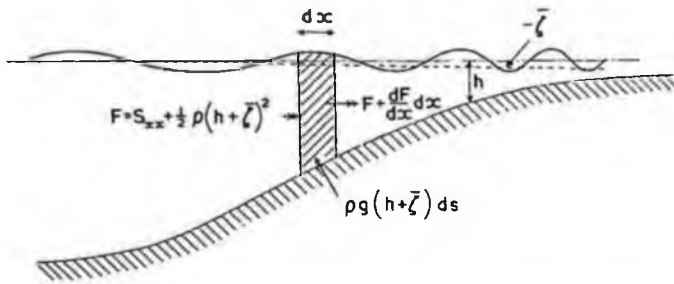


Fig. 6. The balance of horizontal momentum for waves entering shallow water.

There is an additional flux of horizontal momentum due to the bottom pressure, since the bottom is not horizontal, amounting to

$$\rho g (\bar{\zeta} + h) \frac{dh}{dx} dx. \quad (3)$$

(The validity of the approximations used here is discussed in III). Momentum balance then gives

$$\frac{dS_{xx}}{dx} + \rho g (\bar{\zeta} + h) \frac{d\bar{\zeta}}{dx} = 0 \quad (4)$$

and so, since $\bar{\zeta} \ll h$,

$$\frac{d\bar{\zeta}}{dx} = -\frac{1}{\rho g h} \frac{dS_{xx}}{dx}. \quad (5)$$

Wave energy approaching a shore may either be reflected or dissipated to heat. If the beach slope is very abrupt, for example like a sea wall, almost all of the energy will be reflected. Alternatively, the slope may be very gradual, so that almost no reflection takes place.

Here we shall consider in detail only the case of slopes sufficiently gentle that reflection is of negligible importance. Two distinct regions can be identified: seawards and shorewards of the line of breakers.

Seawards of the breaker line, in the absence of reflection, we can obtain an expression for the wave energy density as a function of water depth from the requirement that the shoreward flux of energy be independent of the distance from shore, e.g. if we take the simple but important case of wave crests normal to the direction of beach slope:

$$Ec_g = \text{constant}. \quad (6)$$

As the depth h changes, c_g changes and so E also changes. The radiation stress

S_{xx} thus varies because both kh and E vary. It is shown in III that with these conditions equation (5) may be integrated† to yield

$$\xi = -\frac{1}{2} \frac{a^2 k}{\sinh 2kh}. \quad (7)$$

In deep water, ξ vanishes, while in shallow water ($kh \ll 1$) we have

$$\xi = -\frac{a^2}{4h}. \quad (8)$$

Formula (7) and (8) express the wave set-up in terms of the *local* wave amplitude, wavenumber and depth. However by using equation (6) it is also possible to express ξ as a function of the (constant) wavenumber k_0 and amplitude a_0 in deep water, together with the local depth h , so that we gain an idea of the dependence of ξ on the depth h for a given wave train. Thus if we substitute in equation (6) the known value of the group-velocity :

$$c_g = \frac{\sigma}{2k} \left(\frac{2kh}{\sinh 2kh} + 1 \right) \quad (9)$$

we obtain

$$\frac{a^2 \sigma}{2k} \left(\frac{2kh}{\sinh 2kh} + 1 \right) = \text{constant} = \frac{a_0^2 \sigma}{2k_0} \quad (10)$$

and so

$$a^2 k = a_0^2 k_0 \left(\frac{k}{k_0} \right)^2 \left(\frac{2kh}{\sinh 2kh} + 1 \right)^{-1}. \quad (11)$$

But from the frequency relation equation (17) Section 1,

$$k/k_0 = \coth kh. \quad (12)$$

So we have from equation (7)

$$\xi = -\frac{1}{2} a_0^2 k_0 \frac{\coth^2 kh}{2kh + \sinh 2kh}. \quad (13)$$

Since from equation (17) Section 1

$$kh \tanh kh = \frac{\sigma^2 h}{g} = k_0 h \quad (14)$$

it follows that we may write

$$\xi = -a_0^2 k_0 f(k_0 h)$$

where f is a function solely of the non-dimensional depth $k_0 h$. The form of f is shown in Fig. 7. It will be seen that as the depth diminishes, the *depression* of the mean surface level increases very sharply. In shallow water, we have from equations (13) and (14) that

$$f \sim \frac{1}{8} (kh)^{-3} \sim \frac{1}{8} (k_0 h)^{-3/2}$$

in agreement with equation (8), since in shallow water $a^2 \propto h^{-1}$ by energy conservation. It will be noted that as h decreases the mean water level is actually *lowered* by the presence of unbreaking waves, i.e. there is a "set-down." This is because, with no loss of energy, the radiation stress steadily increases.

†Alternatively equation (7) can be derived from equation (13) Section 2, by substituting for u and w from equations (4) Section 1.

On the other hand, inside the line of breakers the wave energy decreases shorewards leading to a decrease in radiation stress. No adequate theory exists for this situation, but we are nevertheless able to draw some approximate conclusions using a semi-empirical argument.

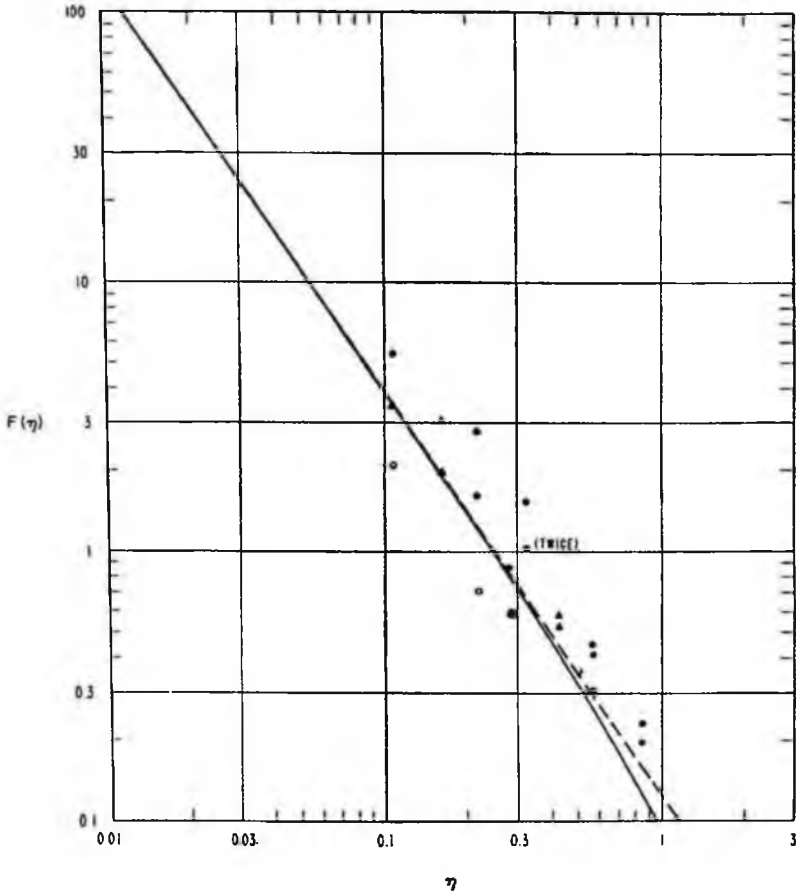


Fig. 7. (from LONGUET-HIGGINS and STEWART, 1963). The non-dimensional form of the wave set-up outside the breaker zone, compared with the observations of SAVILLE (1961).

The theory of similarity suggests that the amplitude of a breaking wave remains an approximately fixed proportion of the mean water depth, i.e.

$$a = \alpha h \quad (15)$$

where α is a constant of proportionality. Although the waves are now far too steep for our second-order treatment to remain valid, it is probably a not unreasonable inaccurate assumption to continue to assume that $S_{xx} = \frac{3}{2} E$. This gives

$$S_{xx} = \frac{3}{4} \rho g a^2 = \frac{3}{4} \rho g \alpha^2 h^2. \quad (16)$$

If we insert this expression in equation (5) we get

$$\frac{d\zeta}{dx} = -\frac{3}{2}\alpha^2 \frac{dh}{dx}. \quad (17)$$

The observations of SAVILLE (1961) confirm that a rise in level starts to occur at about the point where the waves first break (Fig. 8). Moreover in the breaker zone it has been shown that $d\zeta/dx$ was roughly proportional to dh/dx , with a constant of proportionality equal to about -0.15 : (LONGUET-HIGGINS and STEWART, (1963)). We therefore estimate α to be about 0.32 .

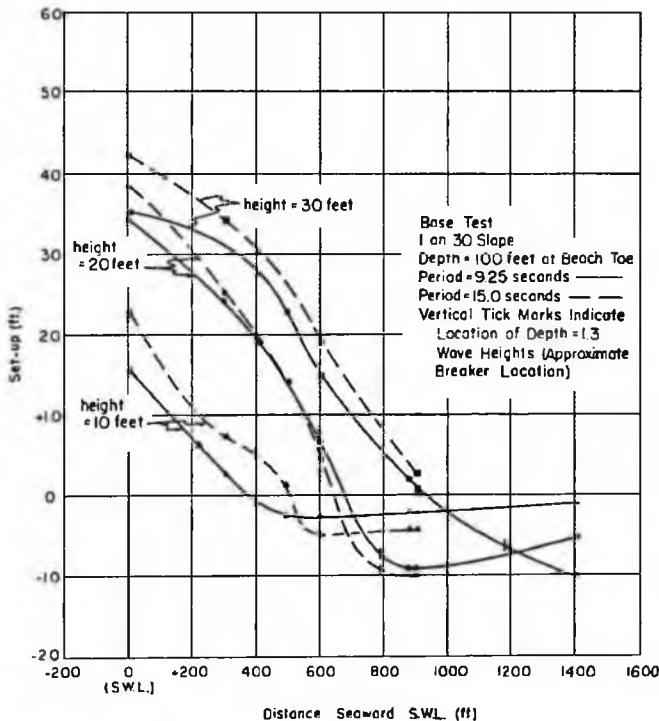


Fig. 8. (from SAVILLE, 1961). Observed wave set-up on beaches of different slope. The vertical tick marks the breaker point.

MUNK (1949) observed that swell tends to break when the depth is about 1.3 times the crest to trough height, i.e.

$$h = 1.3 \times 2a. \quad (18)$$

This corresponds to $\alpha = 0.39$, so the two sets of observations are entirely consistent.

The importance of waves in producing set-up seems only recently to have been realized. Contemporary with our work, contributions to the topic have been made by DORRESTEIN (1962), FORTAK (1962) and LUNDGREN (1963). HARRIS (1963) points out that since waves are subject to modification by refraction and diffraction, variations in wave set-up are to be expected even over short distances. He describes the observed variations in the height of storm surges to this effect. Since these variations may amount to "two to four feet in the peak water level within a distance

of half a mile" it can be seen that wave set-up produces very far from negligible contributions to storm surges.

Another practically important effect of wave set-up is its influence on the apparent "tilt" due to wind stress on the surface of an enclosed body of water. Measurement of such tilts is one of the standard techniques for determining the magnitude of the wind stress. In his well-known critical article on "*Wave Generation by Wind*," URSELL (1956) speculated upon the possible importance of "radiation pressure" effects upon measured water levels.

As we have seen, such effects do occur, and are important. They may well account for much of the variability and unreliability which have beset efforts to determine the laws governing wind stress upon water.

5. Groups of waves advancing in deep water

Horizontal gradients of radiation stress can also arise when the waves have amplitudes which vary in time, and therefore in space. The simplest illustrative example is one where we have sinusoidal wave trains of nearly the same frequency and wavelength propagated in the same direction, resulting in the formation of "groups" of waves.

We shall assume that the groups are such that the energy density, rather than the envelope of the amplitude, varies sinusoidally. By this artifice we avoid some problems with non-linearities which are irrelevant to our present purpose. The energy density is then given by

$$E = E_0 \{1 + b \cos \Delta k (x - c_g t)\} \quad (1)$$

where Δk is a measure of the "band width" of wavenumbers making up the groups, which propagate with speed c_g .

Let us assume also that the depth h is large relative to the lengths of the individual waves, but not necessarily large relative to the length of the groups themselves, i.e. $kh \gg 1$, but not necessarily $\Delta kh \gg 1$. Accordingly, the radiation stress will be

$$S_{xx} = \frac{1}{2} E_0 \{1 + b \cos \Delta k (x - c_g t)\}. \quad (2)$$

We may now divide the depth into two regions: an upper one with thickness $D \sim k^{-1}$, in which virtually all of the radiation stress is concentrated, and a lower one which responds only to any variations in mean surface level produced by the radiation stresses. The problem is now analogous to that which arises in the study of flow induced by horizontal variations of surface tension.

Within the upper region, the horizontal momentum equation is:

$$\frac{\partial \bar{u}}{\partial t} = -\frac{1}{D\rho} \frac{\partial S_{xx}}{\partial x} - g \frac{\partial \bar{\xi}}{\partial x}, \quad (3)$$

where \bar{u} and $\bar{\xi}$ are associated with the groups, i.e. the average is over one wavelength of the individual waves. Since D is small, it is not unreasonable to assume that the first term on the right of equation (3) is much larger than the second. We shall be able to check the validity of this assumption *post hoc*. We therefore put

$$D \frac{\partial \bar{u}}{\partial t} = -\frac{1}{\rho} \frac{\partial S_{xx}}{\partial x}. \quad (4)$$

Now if we integrate the equation of continuity over our upper region, we find

$$w_D = -D \frac{\partial \bar{\eta}}{\partial x} + \frac{\partial \bar{\xi}}{\partial t} \quad (5)$$

where w_D is the mean vertical velocity at the depth D , the mean being taken over the individual waves as with $\bar{\eta}$ and $\bar{\xi}$. These last two equations may be combined to give

$$\frac{\partial w_D}{\partial t} - \frac{\partial^2 \bar{\xi}}{\partial t^2} = \frac{1}{\rho} \frac{\partial^2 S_{xx}}{\partial x^2}. \quad (6)$$

Equation (6) may be interpreted as follows: variations in the radiation stress produce convergences in the upper layer. Continuity is preserved by pushing water up, thus producing variations in the surface elevation, and by pushing water down, resulting in an induced flow in the deeper region. Our equations are closed by the fact that these deep induced flows must be dynamically driven by pressure gradients produced by the variations in surface elevation.

The flow in the deep region is a periodic irrotational flow and so must be of the form of equation (4) Section 1, and derivable from a velocity potential:

$$\phi = \frac{Ac_g}{\sinh kh} \cosh \Delta k(z+h) \sin \Delta k(x - c_g t). \quad (7)$$

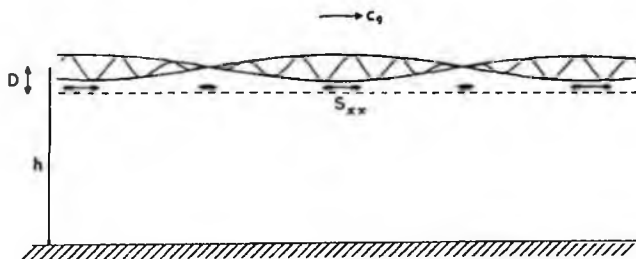


Fig. 9. Groups of waves in deep water. The radiation stress acts in a shallow layer near the surface.

For this flow we have, at $z = -D \neq 0$, two requirements on the pressure \bar{p}_D : First, it must be given by the hydrostatic equation,

$$\frac{1}{\rho} \bar{p}_D = g(\bar{\xi} + D). \quad (8)$$

Second it must satisfy the linearized Bernoulli equation.

$$\frac{\partial \bar{\phi}_D}{\partial t} + \frac{1}{\rho} \bar{p}_D - gD = 0. \quad (9)$$

Together, these conditions give us

$$\bar{\xi} = -\frac{1}{g} \frac{\partial \bar{\phi}_D}{\partial t}. \quad (10)$$

We may now substitute for w_D , $\bar{\xi}$ and S_{xx} in equation (6), remembering that $D\Delta k \ll 1$:

$$-Ac_g^2 + \frac{A}{g} \Delta k c_g^4 \coth h\Delta k = -\frac{E_0 b}{2\rho}. \quad (11)$$

Since $kh \gg 1$, $c_g^2 = g/4k$, so we can write equation (11) as

$$A = \frac{E_0 bk}{2\rho g \{1 - (\Delta k/k) \coth h\Delta k\}} \quad (12)$$

We are now able to find ξ ; from equation (10)

$$\xi = \frac{-E_0 b \Delta k \sin \Delta k(x - c_g t)}{2\rho g \{\tanh h\Delta k - \Delta k/k\}} = -\frac{(E - E_0) \Delta k}{2\rho g \{\tanh h\Delta k - \Delta k/k\}} \quad (13)$$

Since $E = \frac{1}{2}\rho g a^2$, where a is the individual wave amplitude,

$$\xi = -\frac{(a^2 - a_0^2) \Delta k}{4 \{\tanh h\Delta k - \Delta k/k\}}. \quad (14)$$

This expression is in agreement with the result (3.19) of III, which was obtained by perturbation analysis. We note that ξ is always out of phase with a^2 , that is, the mean level is depressed under the largest waves.

Equation (14) simplifies to some extent at the two extreme cases $h\Delta k \ll 1$ and $h\Delta k \gg 1$. For $h\Delta k \ll 1$, when the group length is great compared with the depth, we find

$$\xi = -\frac{(a^2 - a_0^2) k}{4kh - 1} \quad (15)$$

or, since we have already assumed $kh \gg 1$,

$$\xi = -\frac{(a^2 - a_0^2)}{4h}. \quad (16)$$

For $h\Delta k \gg 1$, if we assume $\Delta k/k \ll 1$, equation (14) becomes

$$\xi = -\frac{1}{4} (a^2 - a_0^2) \Delta k. \quad (17)$$

To get a numerical order of magnitude, we might take $(a^2 - a_0^2)$ to be about 10 m^2 . If the individual waves are about 100 m long, and the groups about 1 km long, we have $k \doteq 0.06 \text{ m}^{-1}$, $\Delta k \doteq 0.006 \text{ m}^{-1}$. In deep water ($h \geq 500 \text{ m}$) this results in a surface depression of about 1.5 cm, while the water 100 m deep the depression would be 2.5 cm. These figures, of course, increase rapidly as the individual wave amplitude increases*.

*We are now in a position to make the *post hoc* check of our assumption that

$$g \frac{\partial \xi}{\partial x} \ll \frac{1}{\rho D} \frac{\partial S_{xx}}{\partial x}.$$

Since $\Delta k \ll k$ and $kh \gg 1$,

$$\frac{\partial \xi}{\partial x} \doteq \frac{(a^2 - a_0^2) (\Delta k)^2}{4 \tanh h\Delta k}.$$

Also

$$\frac{\partial S_{xx}}{\partial x} \sim \frac{1}{2} (E - E_0) \Delta k = \frac{1}{2} \rho g (a^2 - a_0^2) \Delta k.$$

Then

$$g \frac{\partial \xi}{\partial x} / \frac{1}{\rho D} \frac{\partial S_{xx}}{\partial x} \doteq \frac{D \Delta k}{\tanh h\Delta k}.$$

Since

$$\tanh h\Delta k = \begin{cases} 0(1), & h\Delta k > \frac{1}{2} \\ 0(h\Delta k), & h\Delta k < \frac{1}{2} \end{cases}$$

our assumption is seen to be justified.

It is worth noting that the frequency of the induced motions is the group frequency—in practice periods are of the order of one minute. This may be important since often it is assumed that there is little motion in the ocean with such periods, and buoys are sometimes designed with a natural period of this order, in the hope that their free oscillations will not be excited.

6. Wave groups in shallow water; surf beat

Let us now consider the situation when waves enter water which is shallow enough so that kh is no longer large compared with unity. In this case we can no longer assume that the radiation stress acts in a thin layer near the surface. On the other hand since the length of the wave groups is certainly large compared to k^{-1} we may certainly assume that the groups are long compared to the depth, i.e. that $h\Delta k < 1$.

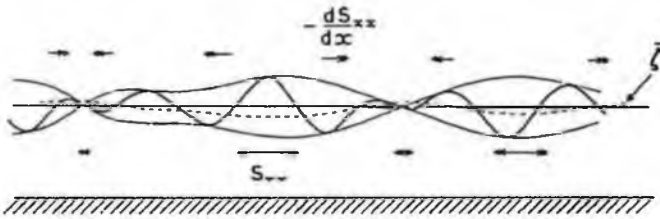


Fig. 10. Groups of waves entering shallow water, when the wavelength is no longer small compared to the depth.

Figure 10 illustrates the situation. Groups of waves (whose energy need not vary exactly sinusoidally) are propagated to the right with the group-velocity c_g . The depth h is at first assumed uniform. In regions of high energy the radiation stress S_{xx} is greater than in regions of low energy. Hence there is a tendency for fluid to be expelled from under regions of high energy density. The medium responds to the stress as to a horizontal force $-\partial S_{xx}/\partial x$ per unit distance, progressing with the group-velocity c_g .

The response of the system can be calculated as follows. The additional mean pressure due to a displacement ζ of the free surface is $\rho g\zeta$. Hence if M is the mean horizontal momentum we have for the rate of change of momentum

$$\frac{\partial M}{\partial t} = -\frac{\partial}{\partial x} (S_{xx} + \rho g h \zeta). \quad (1)$$

On the other hand by continuity we have

$$\frac{\partial}{\partial t} (\rho \zeta) = -\frac{\partial M}{\partial x}. \quad (2)$$

Since the pattern progresses with velocity c_g , we may replace $\partial/\partial t$ by $-c_g \partial/\partial x$ in each equation, giving

$$\left. \begin{aligned} c_g \frac{\partial M}{\partial x} + \rho gh \frac{\partial \xi}{\partial x} &= - \frac{\partial S_{xx}}{\partial x} \\ \frac{\partial M}{\partial x} + c_g \rho \frac{\partial \xi}{\partial x} &= 0. \end{aligned} \right\} \quad (3)$$

Solving these simultaneous equations for $\partial M/\partial x$ and $\partial \xi/\partial x$ and integrating with respect to x we find

$$\left. \begin{aligned} M &= - \frac{c_g S_{xx}}{gh - c_g^2} + \text{constant} \\ \rho \xi &= - \frac{S_{xx}}{gh - c_g^2} + \text{constant}. \end{aligned} \right\} \quad (4)$$

Now the group-velocity c_g cannot exceed the free-wave velocity \sqrt{gh} of the long waves, so that $(gh - c_g^2) > 0$, i.e. the response of the free surface is in the same sense as if the group pattern were stationary ($c_g = 0$); below a group of high waves ξ tends to be negative, and below a group of lower waves it is relatively positive. Since the groups are long, the mean pressure \bar{p} on the bottom fluctuates in the same way as $\rho g \xi$, i.e. it tends to be negative under the higher waves. This is in agreement with some recent observations in swell off the Californian coast (see HASSELMAN, MUNK and MACDONALD 1962).

In very shallow water, c_g approaches \sqrt{gh} and hence the denominator in equation (4) becomes small. Since in that case

$$c_g^2 \doteq gh [1 - (kh)^2] \quad (5)$$

we have

$$\xi \doteq - \frac{S_{xx}}{\rho \sigma^2 h^2} = - \frac{3ga^2}{2\sigma^2 h^2}. \quad (6)$$

If we now suppose that the depth is not quite uniform, but changes with x so slowly that dynamical equilibrium has time to be established, then, with no loss of energy, $a^2 \propto h^{-1}$ and so $\xi \propto h^{-1/2}$. Thus there will be a tendency for the displacement ξ to be amplified as the waves enter shallower water.

It is possible that such an effect accounts for the occurrence of "surf-beats," as observed by MUNK (1949a) and TUCKER (1950). These are waves of long period associated with groups of high waves entering shallow water. TUCKER (1950) showed that in his observations there was a correlation between the surf beats at a point some way off-shore and the envelope of the incoming swell; but with a time-lag of a few minutes. The time-lag just corresponded with the time required for the swell to be propagated into the breaker zone and for the associated long wave to be reflected back as a free wave. If we suppose that, at some point shorewards of the wave recorder, the swell is destroyed by breaking but that the longer waves associated with the groups are reflected back as free waves (with relatively little attenuation in amplitude) then it seems possible to account for Tucker's observations. Tucker found that a group of high waves tended to be associated (after a time-lag) with a *negative* pressure pulse, which would accord with the present hypothesis.

7. Interaction of waves and currents

In the theory of elasticity and rheology, where stress is measured in force per

unit area, it is well known that the product stress times rate of strain yields power per unit volume. Similarly, in our case of radiation stress (which is a force per unit length) stress times rate of strain is power per unit area. We expect that if a fluid, upon which are surface waves, is strained due to some other flow, the radiation stress due to the waves will interact with the rate of strain due to the other flow. In general, we argue that the straining flow must do work against the radiation stress. Energy must then be lost by the straining flow. In many cases we have been able to show that this energy is transferred to the waves. Indeed, if the sign of the interaction is changed, so that the stress does work against the rate of strain there seems to be no source for the energy added to the straining motion other than that residing in the waves. It thus seems legitimate to argue that the energy transfer will always be to or from the waves.

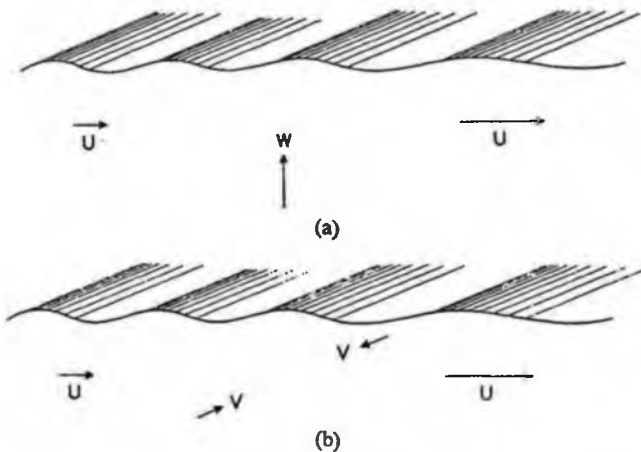


Fig. 11. Waves on a non-uniform current (a) with upwelling from below and (b) with horizontal inflow from the sides.

Interaction with irrotational plane strains. The simplest motions to deal with analytically are irrotational plane strains. They also serve as valuable examples of the nature of the interaction phenomenon.

Let us consider first a situation in which a contraction of the surface along the x -axis is combined with a vertical extension, i.e.

$$\frac{\partial U}{\partial x} = -\frac{\partial W}{\partial z} \quad (1)$$

where U and W are the mean straining velocities in the x and z directions (Fig. 11). For the moment we shall assume that the mean motion is not time-dependent. The situation we envisage is approximately that which occurs when a stream flows along a bed of fixed width but varying depth. The only component of radiation stress which is of consequence in this flow is S_{xx} . It interacts with the rate of strain $\partial U/\partial x$, which describes an extension of the surface, in such a way that work is done by the stress at the rate

$$S_{xx} \frac{\partial U}{\partial x} \quad (2)$$

per unit surface area. It seems that the only source of energy for this work is the energy residing in the waves. Since wave energy is propagated with celerity c_g and transported with velocity U , we postulate a "continuity" equation for wave energy in the form*

$$\frac{\partial}{\partial x} [E(U + c_g)] + S_{xx} \frac{\partial U}{\partial x} = 0. \quad (3)$$

We also have another general expression which might be called an expression for "conservation of phase." It states that in the steady state the rate at which wave crests enter a region must be equal to the rate at which they leave. Another way of stating it is that the apparent frequency observed is independent of the position of the observer. This general expression is

$$(U + c)k = \text{constant} = c_0 k_0 \quad (4)$$

where the subscript 0 refers to some position, perhaps hypothetical, where $U = 0$.

Since when the depth is known, c and c_g are determined by k and S_{xx} by E , evidently equations (3) and (4) are sufficient for the determination of E as a function of U . In the general case this relation is analytically rather complex, but all the important features may be demonstrated by the example of the deep water case, which is simple. In deep water, we may assume

$$c = (g/k)^{1/2}, \quad c_g = \frac{1}{2}c, \quad S_{xx} = \frac{1}{2}E. \quad (5)$$

Thus equation (3) becomes

$$\frac{\partial}{\partial x} [E(U + \frac{1}{2}c)] + \frac{1}{2}E \frac{\partial U}{\partial x} = 0. \quad (6)$$

Equation (4), in view of (5), can be expressed as

$$\frac{\partial}{\partial x} \left[\frac{U + c}{c^2} \right] = 0 \quad (7)$$

or

$$\frac{\partial c}{\partial x} = \frac{\frac{1}{2}c}{U + \frac{1}{2}c} \frac{\partial U}{\partial x}. \quad (8)$$

Equation (6) has the exact integral

$$E(U + \frac{1}{2}c)c = \text{constant} = E_0 \cdot \frac{1}{2}c_0^2, \quad (9)$$

as may be demonstrated by differentiating :

$$c \frac{\partial}{\partial x} [E(U + \frac{1}{2}c)] + E(U + \frac{1}{2}c) \frac{\partial c}{\partial x} = 0. \quad (10)$$

If equation (8) is substituted into (10), we obtain the differential equation (6). The corresponding variation in amplitude a , $\propto E^{1/2}$, is shown as a function of U by curve (1) in Fig. 12. The result (9) was also obtained by perturbation methods in II.

Laterally converging current. Another illustrative example of waves superimposed on a plane strain occurs when the mean motion is two-dimensional and horizontal (Fig. 11b). Such a situation may arise, for example, at a river mouth. For simplicity,

*For a further justification of this equation see Whitham (1962).

let us take the waves moving in one of the directions of principal rate of strain, so that if they are propagating in the x -direction

$$\frac{\partial U}{\partial x} + \frac{\partial V}{\partial y} = 0 \quad (11)$$

V being the mean motion in the y -direction, which is parallel to the wave crests.

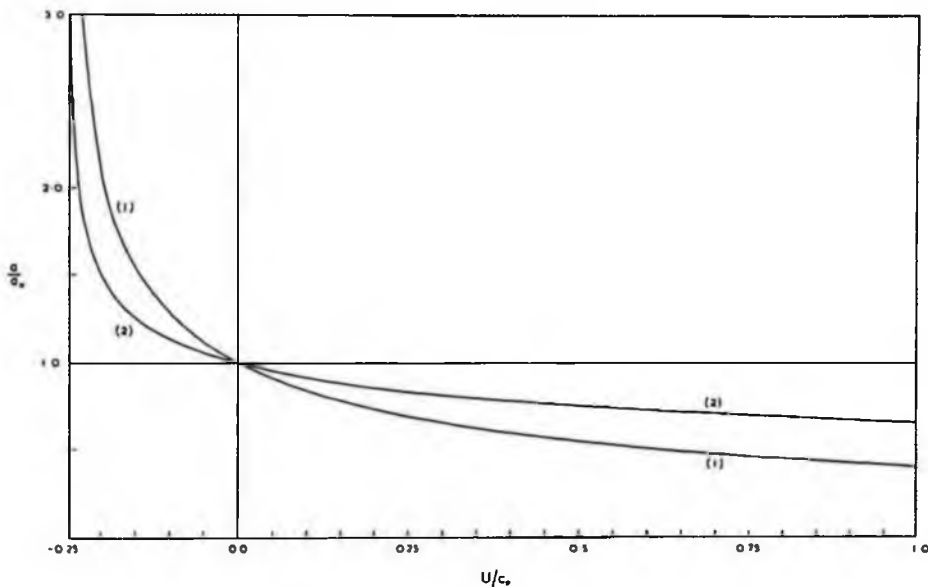


Fig. 12. (from LONGUET-HIGGINS and STEWART, 1961). The relative amplitude of waves propagated on a steady, non-uniform current U , (1) with upwelling from below (2) with horizontal inflow from the sides.

Equation (3) must now be modified to take account of the lateral divergence of wave energy and the work done by the lateral radiation stress S_{yy} , and so becomes

$$\frac{\partial}{\partial x} [E(U + c_g)] + \frac{\partial}{\partial y} (EV) + S_{xx} \frac{\partial U}{\partial x} + S_{yy} \frac{\partial V}{\partial y} = 0. \quad (12)$$

If we assume $\partial E/\partial y = 0$ and employ equation (11) this simplifies to

$$\frac{\partial E}{\partial x} U + E \frac{\partial c_g}{\partial x} + (S_{xx} - S_{yy}) \frac{\partial U}{\partial x} = 0. \quad (13)$$

If we once more consider the simple deep water case, then $S_{yy} = 0$ and equation (8) is valid. Equation (13) can then be integrated, as demonstrated in II, to obtain

$$E(U + \frac{1}{2}c)/c = \text{constant} = E_0. \quad (14)$$

The corresponding change in amplitude ($\propto E^{\frac{1}{2}}$) is shown as a function of U by curve (2) in Fig. 12.

At the other extreme of very shallow water we have :

$$c_g = c = \text{constant}, \quad S_{xx} - S_{yy} = E. \quad (15)$$

It is then readily seen that (13) can be integrated to

$$E(U + c) = \text{constant} = E_0 c_0. \quad (16)$$

It will be noted that in every case so far considered, E must diverge when $U = -c_g$. In practice, of course, the waves break. This result is to be expected since it is merely a statement of the fact that no energy can be propagated upstream against a current faster than c_g . Apart from this common property, it can be seen that the behaviour of wave energy differs from case to case.

TAYLOR (1962) has discussed a slightly different case, where a standing wave is compressed longitudinally, thus both reducing the wave length and increasing the frequency. There also work is done against the radiation stress. Taylor shows that in this situation, too, the energy used in the compression appears as increased wave energy.

Waves on a shear flow. We may use the same kind of arguments to discuss the interaction of a wave train with a shear flow. In this case, however, the waves will generally be refracted, so that it is not possible to use the direction of wave propagation as a fixed Cartesian co-ordinate direction. It is therefore necessary to put our radiation stress tensor into general, non-diagonalized form.

To keep the discussion as simple as possible we shall again confine ourselves to the case of waves on deep water. The diagonalized form of the radiation stress tensor is then

$$S = \frac{1}{2}E \begin{pmatrix} 1 & 0 \\ 0 & 0 \end{pmatrix}. \quad (17)$$

For a co-ordinate system orientated at an angle θ from the direction of propagation, the tensor transformation formula gives us

$$S = \frac{1}{2}E \begin{pmatrix} \cos^2 \theta & \cos \theta \sin \theta \\ \cos \theta \sin \theta & \sin^2 \theta \end{pmatrix}. \quad (18)$$

The rate-of-strain tensor for the mean flow is

$$\boldsymbol{\gamma} = \begin{pmatrix} \frac{\partial U}{\partial x} & \frac{1}{2} \left(\frac{\partial U}{\partial y} + \frac{\partial V}{\partial x} \right) \\ \frac{1}{2} \left(\frac{\partial U}{\partial y} + \frac{\partial V}{\partial x} \right) & \frac{\partial V}{\partial y} \end{pmatrix}. \quad (19)$$

Equations of the form (3) and (12) may thus be generalized to

$$\frac{\partial E}{\partial t} + \nabla \cdot [E(U + c_g)] + S : \boldsymbol{\gamma} = 0. \quad (20)$$

As a simple illustrative example we choose the case of a mean flow with velocity in the y -direction only. If we assume steady state (except for the periodic motion) we have

$$U = 0, \quad V = V(x). \quad (21)$$

Putting in the appropriate value for the radiation stress, we get from (20) :

$$\frac{\partial}{\partial x} [E \cdot \frac{1}{2} c \cos \theta] + \frac{1}{2} E \frac{\partial V}{\partial x} \cos \theta \sin \theta = 0, \quad (22)$$

since the component of c_y in the x -direction is $\frac{1}{2} c \cos \theta$.

In order to solve (22) we require some relation between V and c . One is available from the "wave kinematics," because the wavenumber in the y -direction must be independent of x . Otherwise θ would be a function of y . Thus

$$k \sin \theta = \text{constant} = k_0 \sin \theta_0. \quad (23)$$

As is shown in II, we are then able to integrate (22), getting

$$E \cos \theta \sin \theta = \text{constant} = E_0 \cos \theta_0 \sin \theta_0. \quad (24)$$

In less special cases, (20) can be integrated numerically. This was the procedure adopted by HUGHES and STEWART (1961), who studied the interaction of a wave train with a stable Couette shear flow. They found that their experimental observations were in quite good agreement with numerical calculations made from (20). However, HUGHES and STEWART were unaware of the full effect of capillarity on the radiation stress. (The influence of capillarity is given for the first time in the present paper). Since their waves were short enough to be influenced by surface tension, the actual effect of the radiation stress is greater than that which they assumed. It is noteworthy that the observations of HUGHES and STEWART indicated a somewhat greater influence of the radiation stress than was obtained from their calculations.

It should be emphasized that the changes in wave energy which are due to the non-linear interaction of waves with shear flow are of the same order of magnitude as those which occur due to the geometrical focussing effects produced by the currents. At first glance this may seem surprising, since the radiation stresses are a second order phenomenon, while the focussing effects appear to be first order. The fact is, however, that the focussing effects are first order in the *energy*, i.e. of second order in the amplitude and comparable with the radiation stresses.

8. *Non-linear interaction between waves*

In recent years there has been a considerable amount of interest shown in the problem of the non-linear interaction of surface waves. For some aspects of the problem, in particular in the study of the irreversible redistribution of energy over the wave spectrum (PHILLIPS, 1960; HASSELMANN, 1962, 1963), the interaction must be taken to the third or higher order. For such purposes the radiation stress concept is not particularly useful.

On the other hand there are cases where the radiation stress idea is valuable conceptually and, in some limiting situations, sufficient for calculations. These cases are ones in which one wave is much shorter than the other with which it interacts. Then it becomes reasonable to treat the long wave as a straining motion interacting with the radiation stress due to the short waves.

As a concrete example, we consider here the case of the long waves upon which are superimposed waves short enough that they are uninfluenced by the bottom. Most of the important features are illustrated by this example.

In any non-linear interaction between one Fourier component of wavenumber and frequency k_1, σ_1 , and another specified by k_2, σ_2 , the second-order terms describe

the generation of components $k_1 \pm k_2$, $\sigma_1 \pm \sigma_2$. However, if one of the wave numbers, say k_1 , is very much greater than the other, then the generated wave numbers will all be in the neighbourhood of k_1 . The second-order interaction can thus be considered to describe the influence of the long waves on the shorter ones. For the reverse interaction of the shorter waves on the longer ones, higher order terms are needed.

If both short and long waves are progressing in the same direction, the problem is two-dimensional. Equation (20) Section 8 then becomes

$$\frac{\partial E}{\partial t} + \frac{\partial}{\partial x} [E(U + c_g)] + S_{xx} \frac{\partial U}{\partial x} = 0 \quad (1)$$

where we interpret E and c_g as pertaining to the short waves and U as the horizontal component of the orbital (particle) velocity of the long wave.

The motion due to the long wave will be described by (4) Section 1. We are concerned only with motion near the surface, so that the horizontal and vertical velocities are given by

$$\left. \begin{aligned} U &= A \sigma_2 \coth k_2 h \cos(k_2 x - \sigma_2 t) \\ W &= A \sigma_2 \sin(k_2 x - \sigma_2 t) \end{aligned} \right\} \quad (2)$$

The horizontal variation of E and c_g arises only because of the interaction, and so is irrelevant to (1) if the equation is taken only to the lowest order. Since the short waves are uninfluenced by the bottom, $S_{xx} = \frac{1}{2}E$. Hence (1) becomes

$$\frac{\partial E}{\partial t} + \frac{3}{2} E \frac{\partial U}{\partial x} = 0 \quad (3)$$

or, since U is due to a wave motion and so $\partial/\partial x = -(1/c_2) \partial/\partial t$,

$$\frac{\partial E}{\partial t} - \frac{3}{2} \frac{E}{c_2} \frac{\partial U}{\partial t} = 0 \quad (4)$$

where c_2 is the phase speed of the long wave. This may be integrated to give

$$E \left(1 - \frac{3}{2} \frac{U}{c_2} \right) = \text{constant} = E_0 \quad (5)$$

or, considering that $U \ll c_2$,

$$E = E_0 \left[1 + \frac{3}{2} A k_2 \coth k_2 h \cos(k_2 x - \sigma_2 t) \right]. \quad (6)$$

Although (6) describes the energy variation, the noticeable feature will be the amplitude variation. As shown in I, here the relation between amplitude and energy is not quite so straight-forward as it is in most cases. The water surface upon which the short waves are running is subject to vertical acceleration due to the presence of the long wave. This results in a distribution of E between potential energy and kinetic energy which differs from that which obtains in the absence of the vertical acceleration.

The question is discussed in some detail in I. In the present paper we shall be content with an outline. To an observer moving in an (accelerated) frame of reference tied to one point on the surface of the *long* wave, the apparent value of

g is $g' = g + \partial W/\partial t$. To this observer, the short wave energy is equally distributed between kinetic and potential, i.e.

$$K.E.' = P.E.' = \frac{1}{2} \rho g' a^2 \quad (7)$$

where a is the short wave amplitude. An observer in an inertial frame of reference finds himself in agreement with the accelerated observer as to the kinetic energy, but calculates a different potential energy. Thus

$$\left. \begin{aligned} K.E. &= \frac{1}{2} \rho g' a^2 = K.E.' \\ P.E. &= \frac{1}{2} \rho g a^2 \neq P.E.' \end{aligned} \right\} \quad (8)$$

so

$$E = K.E. + P.E. = \frac{1}{2} \rho g a^2 \left(1 + \frac{1}{2g} \frac{\partial W}{\partial t} \right). \quad (9)$$

Since $\partial W/\partial t \ll g$, we can write this as

$$a = \left(\frac{2E}{\rho g} \right)^{\frac{1}{2}} \left(1 - \frac{1}{4g} \frac{\partial W}{\partial t} \right). \quad (10)$$

After using (2) and (6) this becomes

$$a = a_0 \left[1 + A \left(\frac{3}{4} k_2 \coth k_2 h + \frac{\sigma_2^2}{4g} \right) \cos(k_2 x - \sigma_2 t) \right]. \quad (11)$$

if the long waves are also effectively in deep water, the expression simplifies to

$$a = a_0 [1 + A k_2 \cos(k_2 x - \sigma_2 t)]. \quad (12)$$

It will be noted that the maximum small-wave amplitude occurs on the crests of the long waves. Such amplification of short waves on the crests of the long wave is a matter of common observation.

These effects may be of some consequence in the spectrum of wind-raised waves. It is generally considered (PHILLIPS, 1957) that on a wind swept sea all waves shorter than a certain length are "saturated." That is, they possess as much energy as they are statistically able to. If they gain more energy, wave breaking becomes so widespread in both time and space that the energy rapidly reverts to the "saturated" level.

We see from the above discussion, however, that for waves riding on the backs of longer waves peak amplitudes occur at the crests of the longer waves. It is there that the shorter waves break, and there that the overall energy of these shorter waves is controlled. Since the average short wave energy will be less than that at the crests of the long waves, it seems entirely possible that the average energy of short waves may be somewhat less when they are superimposed upon longer waves than when the long waves are absent.

Long waves develop only after high winds have blown for long times over long fetches. If we envisage a situation where the wind speed increases to a high level and then remains constant for some time, it seems possible that the spectral energy density corresponding to the short waves will first rise to the saturation level and then actually decrease as the long waves grow to significant amplitude. Similarly it seems possible that the short wave energy may be less at longer fetches than at shorter fetches.

Another point is worthy of consideration: The excess energy in the short waves at the crests of the long ones must have been gained at the expense of the long waves. If these short waves then lose their energy due to breaking at the crest, it is no longer available to be fed back into the long waves during their next half cycle. The net result is a mechanism for the dissipation of *long wave* energy. This has been discussed in detail by PHILLIPS (1963). A similar, and equally important, mechanism involving capillary waves is described in the next section.

9. Damping of gravity waves by capillary waves

Capillary waves on the surface of the sea can be generated by at least two mechanisms. One is instability of the shearing flow of wind over water, as described by MILES (1962). Capillaries generated in this way can occur, in theory, on any part of the sea surface which is exposed to a sufficiently strong wind. A second cause of capillaries is the sharp *curvature* near the crests of steep gravity waves which produces a local accentuation of the surface tension forces. If the waves are progressive, these forces act like any other travelling disturbance to produce capillary waves ahead of the disturbance. Capillaries generated this second way are observed only on the forward face of steep gravity waves; they may occur in the absence of wind. Their steepness has been shown theoretically to be given approximately by

$$\frac{2\pi}{3} \exp\left(-\frac{\rho g}{6TK^2}\right) \quad (1)$$

where K is the maximum curvature at the crest of the gravity wave (LONGUET-HIGGINS, 1963*), a result in agreement with observations made by COX (1958).

Whatever their origin, however, capillary waves will subsequently undergo rapid modification from two causes: damping by viscosity and non-linear interaction with the surrounding velocity field. The interactions with gravity waves may be especially strong owing to the relatively short wavelength of the capillaries.

Consider pure capillary waves, of energy density E and wavelength $2\pi/k$, riding on the surface of a two-dimensional flow $U = (U, V, W)$ where $V = 0$ and U, W are independent of y . We suppose that x is measured along the surface of the free gravity flow, and z normal to it, and we assume that the curvature of the mean surface is always small compared to k . Now the rate of dissipation of energy by viscosity in a capillary wave is $4\nu k^2 E$ (LAMB 1932, Section 347). Hence, as in Section 7, we have the following equation for the capillary wave energy:

$$\frac{\partial E}{\partial t} + \frac{\partial}{\partial x} [E(U + c_g)] + S_{xx} \frac{\partial U}{\partial x} + 4\nu k^2 E = 0. \quad (2)$$

Since for capillary waves

$$c_g = \frac{3}{2} c, \quad S_{xx} = \frac{3}{2} E, \quad c^2 = Tk, \quad (3)$$

this can also be written

$$\frac{\partial E}{\partial t} + \frac{\partial}{\partial x} [E(U + \frac{3}{2}c)] + \frac{3}{2} E \frac{\partial U}{\partial x} + 4(\nu/T^2) Ec^4 = 0. \quad (4)$$

To apply this equation in any particular case we need a further relation between U and c . As an example let us take the case of capillary waves propagated on the

*This paper will be referred to as (IV).

forward face of a gravity wave (as described above) and sufficiently far from the wave crest that the curvature of the gravity wave profile is small compared to k . The gravity wave being progressive, we may take axes moving with the wave and so reduce the motion to a steady state. The velocity U will have one component due to the orbital velocity in the gravity wave and another due to the negative velocity associated with the forwards motion of the frame of reference. Since the capillary waves originate at the (stationary) crest of the gravity wave, they will appear stationary in the new frame of reference. Hence their phase velocity c must be equal to $-U$. In the steady state $\partial E/\partial t$ vanishes and (4) becomes now

$$\frac{\partial}{\partial x} \left(-\frac{1}{2} EU \right) + \frac{3}{2} E \frac{\partial U}{\partial x} + 4(\nu/T^2) EU^3 = 0. \quad (5)$$

Ignoring for one moment the viscous term in (5) we have

$$\frac{1}{E} \frac{\partial E}{\partial x} = \frac{2}{U} \frac{\partial U}{\partial x} \quad (6)$$

and so

$$E \propto U^2. \quad (7)$$

In other words the energy of the capillaries increases proportionally to the square of the opposing current. This increase is due not only to the shortening of the wavelength by the contracting current but also to the work done by the current against the radiation stress. The same result (7) was derived also by a perturbation analysis in (IV).

If we take full account of the viscous damping in (5) we have now

$$\frac{1}{E} \frac{\partial E}{\partial x} = \frac{2}{U} \frac{\partial U}{\partial x} + \frac{8\nu}{T^2} U^3 \quad (8)$$

which has the integral

$$E \propto U^2 \exp \left[\frac{8\nu}{T^2} \int_0^x U^3 dx \right], \quad (U < 0). \quad (9)$$

We see that E may at first increase, owing to the radiation stresses, but ultimately the waves are damped out by viscosity. From (8) it follows that the maximum amplitude is attained where

$$\frac{1}{U^4} \frac{\partial U}{\partial x} = -\frac{4\nu}{T^2}. \quad (10)$$

the law of energy variation (9) was shown in (IV) to be in good agreement with observation.

All the energy in the capillary waves is ultimately dissipated by viscosity, including any work done against the radiation stresses by contraction of the current U . Even without the radiation stresses, the energy lost in the capillary waves could be several times that in the basic gravity wave (see IV, Section 10), so that the capillaries must be important in damping the gravity waves when they are near to their maximum steepness. The effect is enhanced by the action of the radiation stresses.

Moreover, capillary waves of any origin, whether due to sharp crests or direct wind action, may dissipate energy derived from the gravity waves through the radiation stresses.

CONCLUSION

As has been shown in the series of examples outlined above, the radiation stress concept permits straightforward calculation of a range of important phenomena. In every case the same results could have been obtained by a detailed perturbation analysis, but comparison with the original papers (I, II, III & IV) in which such analyses were carried out will reveal the considerable reduction of effort required and gain in clarity achieved.

It is our belief that the radiation stress should be regarded not as a "virtual" effect but as real, at least in the same sense as the radiation pressure in electromagnetic theory and the Reynolds stress in turbulence theory are real. Viewed thus, such phenomena as wave set-up (and set-down), where the stress must be balanced by hydrostatic pressure, become entirely natural and expected. Also the non-linear energy exchanges between waves and currents and among waves can, with this concept, be regarded as strictly analogous to corresponding cases in the theory of elasticity and the theory of turbulence, where the rate of energy exchange is given by the product stress times rate of strain.

Radiation stresses will arise not only due to surface waves, but due to internal waves. In the oceans the interaction of internal waves and currents may be considerably more important than interaction involving surface waves, because of the much lower propagation speeds. Small propagation speeds tend to increase the strength of the interaction, as can be seen from two points of view: First, in any wave current interaction, the energy exchange can be written so as to be seen to be proportional to U/c or U/c_0 , so small values of c lead to large interactions. From the other point of view, we note that for almost all species of wave the ratio of energy density: momentum density equals the phase speed. Surface and internal waves are no exception, so internal waves, with their low propagation speed, are particularly efficient at transferring momentum.

REFERENCES

- COX C. S. (1958) Measurements of slopes of high-frequency wind waves. *J. Mar. Res.* **16**, 199-225.
- DORRESTEIN R. (1962) Wave set-up on a beach. *Proc. 2nd. Tech. Conf. on Hurricanes*, Miami Beach, Fla. pp. 230-241. U.S. Dept. of Commerce, Nat. Hurricane Res. Proj. Rep. No. 50.
- FORTAK H. (1962) On the mathematical formulation of the storm surge. *Proc. 2nd Tech. Conf. on Hurricanes*, Miami Beach, Fla. pp. 196-210. U.S. Dept. of Commerce, Nat. Hurricane Res. Proj. Rep. No. 50.
- HARRIS D. L. (1963) Characteristics of the hurricane storm surge. *U.S. Weather Bur. Tech. Pap. No. 48*. 139 pp.
- HASSELMANN K. (1962) On the non-linear energy transfer in a gravity-wave spectrum. Part 1. General theory. *J. Fl. Mech.* **12**, 481-500.
- HASSELMANN K. (1963) On the non-linear energy transfer in a gravity-wave spectrum. Part 2. Conservation theorems; wave-particle analogy; irreversibility. *J. Fl. Mech.* **15**, 273-281.
- HASSELMANN K. (1963) On the non-linear energy transfer in a gravity-wave spectrum. Part 3. Evaluation of the energy flux and sea-swell interaction for a Neumann spectrum. *J. Fl. Mech.* **15**, 385-398.
- HUGHES B. A. and STEWART R. W. (1961) Interaction between gravity waves and a shear flow. *J. Fl. Mech.* **10**, 385-400.
- LAMB H. (1932) *Hydrodynamics*, 6th ed. Cambridge U. Press.

- LONGUET-HIGGINS M. S. and STEWART R. W. (1960) Changes in the form of short gravity waves on long waves and tidal currents. *J. Fl. Mech.* **8**, 565-583.
- LONGUET-HIGGINS M. S. and STEWART R. W. (1961) The changes in amplitude of short gravity waves on steady non-uniform currents. *J. Fl. Mech.* **10**, 529-549.
- LONGUET-HIGGINS M. S. and STEWART R. W. (1962) Radiation stress and mass transport in gravity waves, with application to "surf-beats." *J. Fl. Mech.* **13**, 481-504.
- LONGUET-HIGGINS M. S. and STEWART R. W. (1963) A note on wave set-up. *J. Mar. Res.* **21**, 4-10.
- LONGUET-HIGGINS M. S. (1963) The generation of capillary waves by steep gravity waves. *J. Fl. Mech.* **16**, 138-159.
- LUNDGREN H. (1963) Wave thrust and energy level. *Proc. Int. Ass. Hydr. Res. Congr.* London, pp. 147-151.
- MILES J. W. (1962) On the generation of waves by shear flows. Part 4. *J. Fl. Mech.* **13**, 433-448.
- MUNK W. H. (1949a) The solitary wave and its application to surf problems. *Ann. N. Y. Acad. Sci.* **51**, 376-424.
- MUNK W. H. (1949b) Surf beats. *Trans. Amer. geophys. Un.* **30**, 849-854.
- PHILLIPS O. M. (1958) The equilibrium range in the spectrum of wind-generated waves. *J. Fl. Mech.* **4**, 426-434.
- PHILLIPS O. M. (1960) On the dynamics of unsteady gravity waves of finite amplitude. Part I. The elementary interactions. *J. Fl. Mech.* **9**, 193-217.
- PHILLIPS O. M. (1963) On the attenuation of long gravity waves by short breaking waves. *J. Fl. Mech.* **16**, 321-332.
- SAVILLE T. (1961) Experimental determination of wave set-up. *Proc. 2nd Tech. Conf. on Hurricanes*, Miami Beach, Fla. pp. 242-252. U.S. Dept of Commerce, Nat. Hurricane Res. Proj. Rep. No. 50.
- STEWART R. W. (1956) A new look at the Reynolds stresses. *Canad. J. Phys.* **34**, 722-725.
- TADJBAKHSH I. and KELLER J. B. (1960) Standing surface waves of finite amplitude. *J. Fl. Mech.* **8**, 442-451.
- TAYLOR, SIR GEOFFREY (1962) Standing waves on a contracting or expanding current. *J. Fl. Mech.* **13**, 182-192.
- TUCKER M. J. (1950) Surf beats : sea waves of 1 to 5 minutes' period. *Proc. Roy. Soc. A* **207**, 565-73.
- URSELL F. (1956) Wave generation by wind. *Surveys in Mechanics*. G. I. Taylor. 70th Anniversary Vol. Cambridge Monog. on Mech. and Appl. Math. ed. G. K. Batchelor and R. M. Davies. Cambridge U. Press pp. 216-249.
- WHITHAM G. B. (1962) Mass, momentum and energy flux in water waves. *J. Fl. Mech.* **12**, 135-147.

REPRINT FROM
SEARS FOUNDATION: JOURNAL OF MARINE RESEARCH
Volume 25, Number 2, May 15, 1967, Pp. 148-153

*On the Wave-induced Difference
in Mean Sea Level Between the Two Sides
of a Submerged Breakwater¹*

M. S. Longuet-Higgins

*National Institute of Oceanography, England
and*

Scripps Institution of Oceanography, La Jolla, California

ABSTRACT

Very simple formulae are derived for the difference in mean level between the two sides of a submerged breakwater when waves are incident on it at an arbitrary angle. The formulae apply also to waves undergoing refraction due to changes in depth and to waves in open channel transitions.

When sea waves approach a submerged breakwater or an offshore sand bar, the mean level of the water on the far side of the bar or breakwater is commonly observed to be higher than on the side from which the waves are incident. The purpose of this note is to show that the difference in mean water level can be calculated very simply in certain circumstances, once the height of the incident waves and the coefficient of reflection are both known.

The situation is as shown in Fig. 1. A submerged "breakwater" separates two uniform regions in which the undisturbed depths are h_1 and h_2 , say. Waves of amplitude a_1 are propagated from the left and are incident (not necessarily normally) on the "breakwater." There is a transmitted wave of amplitude a_2 and a reflected wave of amplitude a'_1 .

If the steepness of the waves is sufficiently small everywhere, then the coefficients of transmission and reflection, namely

$$T = a_2/a_1 \text{ and } R = a'_1/a_1,$$

are nearly independent of a_1 . The coefficients R and T may be determined by experiment or, in some ideal cases, by the linear theory of water waves. (For some examples, see the REFERENCES.) In the neighborhood of the breakwater

1. Accepted for publication and submitted to press 17 February 1967.
Contribution from the Scripps Institution of Oceanography.

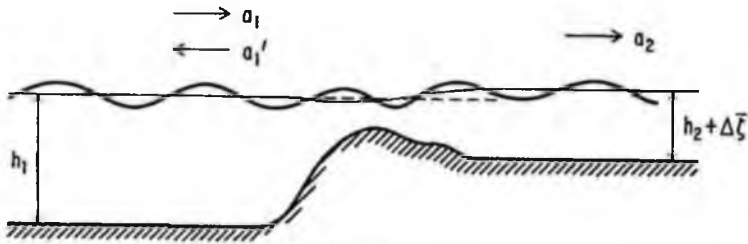


Figure 1.

itself the waves are not generally sinusoidal; nevertheless, the motion everywhere fluctuates harmonically with time, say with period $2\pi/\sigma$. The wavelength, $2\pi/k_1$, of the waves on the near side of the breakwater is related to the frequency σ and to the local depth by the usual relationship

$$\sigma^2 = gk_1 \tanh k_1 h_1,$$

and similarly for the waves on the far side.

These results can be derived from the well-known small-amplitude theory of water waves. However, on the two sides of the barrier there will be a difference, $\Delta \bar{\zeta}$, in mean surface level that is of second order in the wave amplitude. We shall see that $\Delta \bar{\zeta}$, though of second order, can be determined directly from the first approximation in the following way.

Let x and y be horizontal coordinates and z be measured vertically upward from the still-water level. Let u , v , and w denote the corresponding components of velocity and p the pressure. Let ρ and g denote the density and the acceleration of gravity, both assumed constant. The free surface is denoted by $z = \zeta(x, y, t)$. Neglecting viscous forces, we then have two simple relationships (cf Longuet-Higgins and Stewart 1964).

First, consider the flux of *vertical momentum* into a vertical column of water of unit cross section contained between $z = 0$ and $z = \zeta$. The flux upward through the base of the column equals $(p + \rho w^2)$ evaluated at $z = 0$. The flux through the upper surface of the column is zero. The flux of vertical momentum through the *sides* of the column, which is $\rho u w$ per unit area, is of third order when integrated over the height ζ of the column. Hence this can be neglected. The total flux of vertical momentum into the column is therefore

$$(p + \rho w^2)_{z=0}.$$

This is opposed by gravity, which produces a downward force, $\rho g \zeta$. But since the motion is periodic, the vertical momentum within the column remains, on average, unchanged. Thus, on taking mean values we have

$$\overline{(p + \rho w^2)_{z=0}} - \rho g \bar{\zeta} = 0, \quad (\text{A})$$

150

where a bar denotes the average with respect to time. This is our first equation.

Second, if the motion everywhere is assumed irrotational (which excludes wave breaking, for example), then we have the Bernoulli integral

$$p + \frac{1}{2} \rho (u^2 + v^2 + w^2) + \rho g z + \rho \frac{\partial \varphi}{\partial t} = 0 .$$

Here φ denotes the velocity potential, which includes an arbitrary function of the time, t . If we take time-averages in this equation and set $z = 0$, we have

$$\bar{p}_{z=0} + \frac{1}{2} \rho \overline{(u^2 + v^2 + w^2)}_{z=0} + C = 0 , \quad (B)$$

C being at most a constant.

From the two equations (A) and (B) we may eliminate the pressure to obtain the basic relationship

$$g \bar{\zeta} = - \frac{1}{2} \rho \overline{(u^2 + v^2 - w^2)}_{z=0} + C . \quad (C)$$

From this relationship it is very easy to determine the difference in mean surface level, $\bar{\zeta}$, at two different points $(x_1, y_1, 0)$ and $(x_2, y_2, 0)$, say. Clearly the constant C is immaterial, so we have

$$\rho g (\bar{\zeta}_1 - \bar{\zeta}_2) = - \frac{1}{2} \rho \overline{[(u^2 + v^2 - w^2)_{z=0}]_2^1} .$$

Thus, in the present problem, $\Delta \bar{\zeta}$ is given by

$$\Delta \bar{\zeta} = \frac{1}{2g} \overline{[(u^2 + v^2 - w^2)_{z=0}]_2^1} . \quad (D)$$

This is the simple relationship promised earlier.

Now, in a wave of amplitude a traveling in some direction that makes an angle θ with the x -axis, the components of orbital velocity are given by

$$\left. \begin{aligned} u &= \frac{a\sigma \cos \theta}{\sinh kh} \cosh k(z-h) \cos(kx' - \sigma t + \varepsilon) \\ v &= \frac{a\sigma \sin \theta}{\sinh kh} \cosh k(z-h) \cos(kx' - \sigma t + \varepsilon) \\ w &= \frac{a\sigma}{\sinh kh} \sinh k(z-h) \sin(kx' - \sigma t + \varepsilon) , \end{aligned} \right\}$$

1967]

Longuet-Higgins: Difference in Mean Sea Level

151

where $x' = x \cos \theta + y \sin \theta$ and ε denotes a constant phase. On squaring the velocities and taking averages with respect to time, we find

$$\left. \begin{aligned} \overline{u^2} &= \frac{1}{2} \frac{a^2 \sigma^2 \cos^2 \theta}{\sinh^2 kh} \cosh^2 k(z-k) \\ \overline{v^2} &= \frac{1}{2} \frac{a^2 \sigma^2 \sin^2 \theta}{\sinh^2 kh} \cosh^2 k(z-h) \\ \overline{w^2} &= \frac{1}{2} \frac{a^2 \sigma^2}{\sinh^2 kh} \sinh^2 k(z-h), \end{aligned} \right\}$$

so

$$\overline{u^2 + v^2 - w^2} = \frac{1}{2} \frac{a^2 \sigma^2}{\sinh^2 kh}. \quad (\text{E } 1)$$

Using the relationship that $\sigma^2 = gk \tanh kh$ locally, we then have

$$\frac{1}{2g} (\overline{u^2 + v^2 - w^2}) = \frac{a^2 k}{2 \sinh 2kh}. \quad (\text{E } 2)$$

If two systems of waves are present (as on the seaward side of the breakwater), then in place of a^2 we shall have $(a_1^2 + a_2^2)$. There will also be a contribution from the *product* terms, proportional to $a_1 a_2$. However, on averaging with respect to the horizontal coordinates, x, y , as well as with respect to t , we find that these product terms vanish.

From equations (D) and (E 1), (E 2) we deduce that in the present situation

$$\Delta \bar{\zeta} = \frac{\sigma^2}{4g} \left(\frac{a_1^2 + a_2^2}{\sinh^2 k_1 h_1} - \frac{a_3^2}{\sinh^2 k_2 h_2} \right), \quad (\text{F } 1)$$

or alternatively,

$$\Delta \bar{\zeta} = \frac{(a_1^2 + a_2^2) k_1}{2 \sinh 2k_1 h_1} - \frac{a_3^2 k_2}{2 \sinh 2k_2 h_2}. \quad (\text{F } 2)$$

When the depths h_1 and h_2 on the two sides of the breakwater are equal, then we have simply

$$\Delta \bar{\zeta} = \frac{(a_1^2 + a_2^2 - a_3^2) k}{2 \sinh 2kh}, \quad (\text{G})$$

where $k = k_1 = k_2$; $h = h_1 = h_2$. Since $a_2^2 \leq a_1^2$, the right-hand side is non-negative, showing that the difference in level is then positive in general.

The outstanding feature of this result is that in deep water, if both $k_1 h_1$ and $k_2 h_2$ are large,

$$\Delta \bar{\zeta} = 0.$$

In other words, the difference in level is essentially a finite-depth effect.

In shallow water, where both $k_1 h_1$ and $k_2 h_2$ are small, equation (F 2) becomes

$$\Delta \bar{\zeta} = \frac{a_1^2 + a_1'^2}{4h_1} - \frac{a_2^2}{4h_2}, \quad (\text{H})$$

and, if $h_1 = h_2 = h$, then

$$\Delta \bar{\zeta} = \frac{a_1^2 + a_1'^2 - a_2^2}{4h}. \quad (\text{I})$$

Of course these results are subject to the usual limitations of the small-amplitude theory of surface waves, in particular that

$$ak \ll 1 \quad \text{and} \quad ak \ll (kh)^3$$

in each particular region. In addition, the loss of energy by friction or other means (such as breaking) must not be so great as to affect the results.

Nevertheless, the formulae are so simple and their application so straightforward that it would seem worthwhile to check their range of validity by experiments in the laboratory.

REFERENCES AND BIBLIOGRAPHY

BARTHOLOMEUSZ, E. F.

1958. The reflexion of long waves at a step. *Proc. Cambridge philos. Soc.*, 54: 106-118.

BIESEL, F., and B. LE MÉHAUTÉ

1955. Étude theorique de la reflexion de la houle sur certains obstacles. *La Houille Blanche*, 10: 130-138.

BOURODIMOS, E. L., and A. T. IPPEN

1966. Wave reflection and transmission in open channel transitions. *Hydrodynamics Lab. Rep., Mass. Inst. Techn.*, No. 98 (August); 201 pp.

COOPER, R. I. B., and M. S. LONGUET-HIGGINS

1950. An experimental study of the pressure variations in standing water waves. *Proc. Roy. Soc., (A)* 206: 424-435.

DEAN, R. G.

1964. Long wave modification by linear transitions. *Proc. Amer. Soc. civ. Engrs.*, 90 (WW1): 1-29.

DEAN, R. G., and F. URSELL

1959. Interaction of a fixed, semi-immersed circular cylinder with a train of surface waves. *Hydrodynamics Lab. Rep., Mass. Inst. Techn.*, No. 37; unpublished.

DEAN, W. R.

1945. On the reflexion of surface waves by a submerged plane barrier. *Proc. Cambridge philos. Soc.*, 41: 231-238.

1947. On the reflexion of surface waves by a submerged circular cylinder. *Proc. Cambridge philos. Soc.*, 44: 483-491.

- 1967] *Longuet-Higgins: Difference in Mean Sea Level* 153
- HASKIND, M. D.
1948. The pressure of waves on a barrier. *Inzhen. Sb.*, 4: 147-160.
- JEFFREYS, H.
1944. Motion of waves in shallow water. *Wave Rep.*, U. K. Ministry of Supply; unpublished.
- JOHN, F.
1948. Waves in the presence of an inclined barrier. *Comm. appl. Math.*, 1: 149-200.
- JOLAS, P.
1960. Passage de la houle sur un seuil. *La Houille Blanche*, 15: 148-152.
- KREISEL, G.
1949. Surface waves. *Quart. appl. Math.*, 7: 21-44.
- LAMB, SIR HORACE
1932. *Hydrodynamics*. 6th ed. Cambridge Univ. Press. 738 pp.
- LEVINE, H.
1957. Scattering of surface waves on an infinitely deep fluid, pp. 712-716. *Proc. Symposium on Behaviour of Ships in a Waterway*. Wageningen, 1957. 1045 pp.
- LEVINE, H., and E. RODEMICH
1958. Scattering of surface waves on an ideal fluid. *Tech. Rep. Appl. Math. Stat.*, Stanford Univ., No. 78; 64 pp.
- LONGUET-HIGGINS, M. S., and R. W. STEWART
1964. Radiation stresses in water waves: a physical discussion, with applications. *Deep-sea Res.*, 11: 529-562.
- MACAGNO, E. O.
1954. Houle dans un canal présentant un passage en charge. *La Houille Blanche*, 9: 10-37.
- NEWMAN, J. N.
1965. Propagation of water waves over an infinite step. *J. fluid Mech.*, 23: 399-415.
- TAKANO, K.
1959a. Effet de passage d'une houle linéaire plane sur un seuil. *C. R. Acad. Sci. Paris*, 248: 1768-1771.
1959b. Effects de second order d'un seuil semi-indefini sur une houle irrotationnelle. *C. R. Acad. Sci. Paris*, 249: 622-624.
1960. Effets d'un obstacle parallélépipédique sur la propagation de la houle. *La Houille Blanche*, 15: 247-267.
1963. Effet du second order d'un obstacle parallélépipédique sur la propagation de la houle dans un canal. *Rec. oceanogr. Wks. Jap.*, 7: 9-17.
- URSELL, F.
1947a. The effect of a fixed vertical barrier on surface waves in deep water. *Proc. Cambridge philos. Soc.*, 43: 374-382.
1947b. The reflection of waves from a submerged low reef. *Admiralty Res. Lab.*, Teddington, Rep. R5/103.41/W (unpublished).
1950a. Surface waves on deep water in the presence of a submerged circular cylinder, I. *Proc. Cambridge philos. Soc.*, 46: 141-152.
1950b. Surface waves on deep water in the presence of a submerged circular cylinder, II. *Proc. Cambridge philos. Soc.*, 46: 153-158.

Longshore Currents Generated by Obliquely Incident Sea Waves, 1

M. S. LONGUET-HIGGINS¹

Oregon State University, Corvallis 97331

By using known results on the radiation stress associated with gravity waves, the total lateral thrust exerted by incoming waves on the beach and in the nearshore zone is rigorously shown to equal $(E_0/4) \sin 2\theta_0$ per unit distance parallel to the coastline, where E_0 denotes the energy density of the waves in deep water and θ_0 denotes the waves' angle of incidence. The local stress exerted on the surf zone in steady conditions is shown to be given by $(D/c) \sin \theta$ per unit area, where D is the local rate of energy dissipation and c is the phase velocity. These relations are independent of the manner of the energy dissipation, but, because breaker height is related to local depth in shallow water, it is argued that ordinarily most of the dissipation is due to wave breaking, not to bottom friction. Under these conditions the local mean longshore stress in the surf zone will be given by $(5/4)\rho u_{\max}^2 s \sin \theta$, where ρ is the density, u_{\max} is the maximum orbital velocity in the waves, s is the local beach slope, and θ is the angle of incidence. It is further shown that, if the friction coefficient C on the bottom is assumed constant and if horizontal mixing is neglected, the mean longshore component of velocity is given by $(5\pi/8)(s/C) u_{\max} \sin \theta$. This value is proportional to the longshore component of the orbital velocity. When the horizontal mixing is taken into account, the longshore currents observed in field observations and laboratory experiments are consistent with a friction coefficient of about 0.010.

1. INTRODUCTION

It is well known [Wiegand, 1963; Inman and Bagnold, 1963] that when sea waves or swell approach a straight coastline at an oblique angle (Figure 1) a mean current tends to be set up parallel to the coastline. Such longshore currents and the associated longshore transport of sand or other sedimentary material are of prime importance for both the coastal engineer and the submarine geologist.

Many hypotheses, of a very rough kind, have been advanced to account for this phenomenon. However, a recent review of the subject by Galvin [1967] arrives at the justifiable conclusion that, 'A proven prediction of longshore current velocity is not available, and reliable data on longshore currents are lacking over a significant range of possible flows.'

It has often been suggested [e.g., Putnam et al., [1949] that the magnitude of the longshore current is related in some way to the

energy or the momentum of the incoming waves. Of these two approaches, that employing momentum is the more promising since momentum is conserved, whereas energy can be dissipated by breaking and other processes not immediately associated with sediment transport.

It goes without saying that any momentum theory must be correctly formulated. The estimate of the momentum made by Putnam et al. [1949] has been already criticized on theoretical grounds by Galvin [1967]. Moreover, Inman and Quinn [1952] showed that, in order to make the theory fit the observations, the friction coefficient C would have to be assumed to vary over a wide range of $3\frac{1}{2}$ orders of magnitude. A version of the theory of Putnam et al. modified by Galvin and Eagleson [1965] also requires a large variation in C .

The aim of this paper is to introduce a more satisfactory estimate of the momentum of the incoming waves, which is based on the concept of the radiation stress as developed by Longuet-Higgins and Stewart [1960, 1961, 1962, 1963, 1964]. This estimate of the excess transfer of momentum due to the waves has already proved remarkably successful in the prediction of several wave phenomena, particularly the setup, or change in mean level of the sea sur-

¹ Now at National Institute of Oceanography, Wormley, Godalming, England, and Department of Applied Mathematics and Theoretical Physics, Silver Street, Cambridge, England.

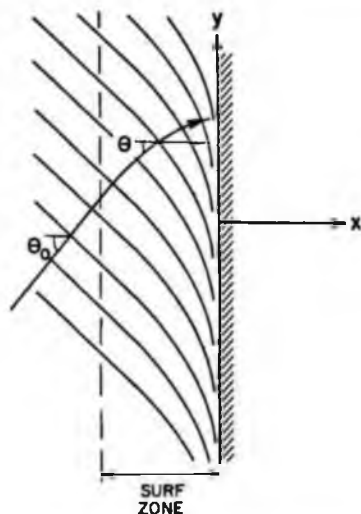


Fig. 1. Definition diagram for waves approaching a straight shoreline at an oblique angle.

face in the breaker zone [Longuet-Higgins and Stewart, 1963, 1964; Bowen, 1967].

In the present paper it is pointed out, first, that there exists a simple and precise relationship between the total longshore thrust exerted by the incoming waves on the one hand and their direction and amplitude in deep water on the other (see equation 10). This result can be derived either from the concept of the radiation stress mentioned earlier, or by a direct evaluation of the momentum flux due to the waves.

Next it is shown that the local longshore stress due to the waves is very simply related to the local rate of dissipation of wave energy, regardless of whether the dissipation is due to wave breaking or to bottom friction. Hence, using the known relation of breaker height to local depth in the surf zone, one can estimate accurately the local longshore stress due to the waves (section 4).

When the local longshore wave stress is known, it is possible to write an equation of motion for the longshore current that involves in general both the bottom friction and the horizontal mixing by turbulent eddies. If the horizontal mixing is negligible, the momentum balance gives an exceedingly simple expression for the longshore current $\langle v \rangle$. The addition of

horizontal mixing generally reduces the current, although not drastically.

A comparison with the available data (section 7) shows that even without the assumption of mixing there is already an order-of-magnitude agreement between the observed and the theoretical current if one takes an a priori estimate of the friction coefficient (about 0.010) based on experiments with flow in rough pipes [Prandtl, 1952]. The comparison indicates also that horizontal mixing is significant, though not dominant, in most circumstances.

Note added in processing. Since this paper was prepared, a somewhat similar approach to the theory of longshore currents has been published by Bowen [1969]. Besides containing new results, the present treatment differs both in the derivation of equation 34 (since Bowen takes θ to be constant during differentiation) and in the assumed form of the bottom friction. For further comparisons see the companion paper.

2. WAVES APPROACHING COASTLINE

Imagine a straight coastline, as in Figure 1, in which the local still water depth h is some function of the coordinate x normal to the shoreline and is independent of the distance y along the shore. The shoreline itself is at $x = 0$. A train of two-dimensional waves of amplitude a is advancing from deep water toward the coast, the local direction of propagation being inclined at an angle of incidence θ to the normal, as shown.

Both θ and a will vary with the distance $|x|$ from the shoreline. If σ denotes the frequency of the waves and k denotes the local wave number, Snell's law, which expresses the constancy of the wave number in the direction parallel to the shoreline, can be written as

$$k \sin \theta = \text{constant} \quad (1)$$

or equivalently

$$(\sin \theta)/c = \text{constant} \quad (2)$$

where $c = \sigma/k$ denotes the local phase velocity. If the bottom slope is gradual, so that the proportional change in depth over one wavelength is small, it is reasonable to assume that σ and k are related to the local depth $h(x)$ by the Stokes relation for waves of small ampli-

tude:

$$\sigma^2 = gk \tanh kh \tag{3}$$

The phase velocity c is then given by

$$c = \sigma/k = [(g/k) \tanh kh]^{1/2} \tag{4}$$

and the group velocity, or velocity of energy propagation, is given by

$$c_g = \frac{d\sigma}{dk} = \frac{\sigma}{2k} \left(1 + \frac{2kh}{\sinh 2kh} \right) \tag{5}$$

With the local energy density per unit horizontal area being given by

$$E = \frac{1}{2} \rho g a^2 \tag{6}$$

correct to second order, the flux of energy toward the coast, per unit distance parallel to the shoreline, is given by

$$F_x = E c_g \cos \theta \tag{7}$$

If the waves are losing no energy by breaking, bottom friction, or otherwise, we have

$$F_x = \text{constant} \tag{8}$$

independently of x , from which one can deduce the law of variation of the wave amplitude a with distance offshore [Burnside, 1915; Longuet-Higgins, 1956]. Inside the breaker zone, however, some energy will be lost, and hence a will diminish toward the shoreline and become zero at or near $x = 0$. If D denotes the rate of dissipation of wave energy, either by breaking or friction, we have identically

$$\partial F_x / \partial x = -D \tag{9}$$

3. RADIATION STRESSES

So much is well accepted. We propose now to calculate the force exerted on the nearshore region by the incoming waves, by using the notion of the radiation stress, as introduced by Longuet-Higgins and Stewart [1960, 1961, 1962, 1963, 1964].

It can be shown [Longuet-Higgins and Stewart, 1960] that the presence of a wave train of amplitude a in water of depth h increases the flux of momentum parallel to the direction of propagation across any plane normal to that direction by an amount

$$S_{11} = E \left(\frac{1}{2} + \frac{2kh}{\sinh 2kh} \right) \tag{10}$$

Similarly the flux of momentum normal to the direction of wave propagation across a plane parallel to the direction of propagation is increased by an amount

$$S_{22} = E(kh/\sinh 2kh) \tag{11}$$

where $E = \frac{1}{2} \rho g a^2$. In general the momentum flux tensor, referred to coordinates (ξ_1, ξ_2) parallel and perpendicular to the direction of wave propagation, is given by

$$S_{ii} = \begin{bmatrix} E \left(\frac{1}{2} + \frac{2kh}{\sinh 2kh} \right) & 0 \\ 0 & E \frac{kh}{\sinh 2kh} \end{bmatrix} \tag{12}$$

the off-diagonal elements being zero.

Now let us calculate the flux of y momentum parallel to the shoreline across a plane $x = \text{constant}$, parallel to the shoreline. Since the axes (x, y) are inclined at an angle θ to the principal axes (ξ_1, ξ_2) of the waves, we have

$$\begin{aligned} S_{xy} &= \sum_{i,j} S_{ij} \frac{\partial x}{\partial \xi_i} \frac{\partial y}{\partial \xi_j} \\ &= S_{11} \sin \theta \cos \theta + S_{22} \cos \theta (-\sin \theta) \\ &= E \left(\frac{1}{2} + \frac{kh}{\sinh 2kh} \right) \cos \theta \sin \theta \\ &= E(c_g/c) \cos \theta \sin \theta \end{aligned} \tag{13}$$

By (7) this relation can be written as

$$S_{xy} = F_x(\sin \theta)/c \tag{14}$$

or, if we make use of Snell's law in the form of (2), we then have

$$S_{xy} = F_x(\sin \theta_0)/c_0 \tag{15}$$

where θ_0 and c_0 refer to the (constant) values of θ and c in deep water.

This very simple and exact relation states that the flux of y momentum across the plane $x = \text{constant}$ is proportional, by a fixed, known constant, to the energy flux across the same plane.

Because of the simplicity and fundamental importance of relation 15 we give here an alternative proof.

The flux of y momentum across any vertical plane $x = \text{constant}$ is simply equal to $\rho u v$,

LONGSHORE CURRENTS, I

6781

where u and v are the components of velocity in the x and y directions. On integrating this with respect to the vertical coordinate z we find

$$S_{xy} = \left\langle \int_{-h}^{\xi} \rho uv \, dz \right\rangle \quad (16)$$

The angle brackets denote the mean value with respect to time. Now for waves traveling at an angle θ to the x axis we have

$$u = u_x \cos \theta \quad v = u_x \sin \theta \quad (17)$$

where u_x denotes the horizontal component of the orbital velocity in the direction of wave propagation. Also in (16) the upper limit of integration can be replaced by the mean value $z = 0$, since the difference $\int_0^{\xi} \rho uv \, dz$ is only of the third order at most in the wave amplitude. (The mean value is actually of fourth order.) We have then, correct to second order,

$$S_{xy} = \int_{-h}^0 \rho \langle u_x^2 \rangle \, dz \cos \theta \sin \theta \quad (18)$$

Now the flux of energy in the direction of wave propagation is given by

$$F = \left\langle \int_{-h}^{\xi} [p + \frac{1}{2} \rho (u_x^2 + v_x^2)] u_x \, dz \right\rangle \quad (19)$$

So to the same order of approximation

$$F = \int_{-h}^0 \langle p u_x \rangle \, dz \quad (20)$$

From the linearized equation of horizontal momentum, however, we have

$$\frac{\partial u_x}{\partial t} = -\frac{1}{\rho} \frac{\partial p}{\partial \xi_1} = \frac{1}{\rho c} \frac{\partial p}{\partial t} \quad (21)$$

since in progressive wave motion $\partial/\partial t \sim c \partial/\partial \xi_1$. Then on integration with respect to time we have

$$u_x = (p/\rho c) + \text{constant} \quad (22)$$

On substituting in (18) and noting that for irrotational waves $\langle u_x \rangle = 0$ correct to second order we obtain from (18) and (20)

$$S_{xy} = (1/c) F \cos \theta \sin \theta \quad (23)$$

The energy flux F_x being equal to $F \cos \theta$, we obtain (14) and hence (15) as before.

From (15) we can at once calculate the total longshore thrust of the waves, as follows.

Outside the breaker line (or the line at which energy losses become significant) we have

$$F_x = \text{constant} = E_0 (\frac{1}{2} c_0) \cos \theta_0 \quad (24)$$

c_0 being the phase velocity in deep water, where the group velocity $c_g = \frac{1}{2} c_0$, and E_0 being the energy density in deep water. Therefore from (15)

$$(S_{xy})_{\infty} = \frac{1}{2} E_0 \cos \theta_0 \sin \theta_0 \quad (25)$$

On the other hand, at the shoreline $x = \delta > 0$ (just beyond the reach of the waves) we have

$$F_x = 0 \quad S_{xy} = 0 \quad x = \delta \quad (26)$$

Therefore, by considering the balance of momentum of the water between the breaker line and the shoreline, we see that the total external force G_x parallel to the shoreline acting on the water and sediment inside the breaker zone is given by

$$(S_{xy})_{\infty} + G_x = 0 \quad (27)$$

In the absence of wind or other surface stresses the only external force must come from bottom friction. Hence the total lateral littoral force exerted by the waves on the bottom is given by $H_x = -G_x$, that is to say

$$H_x = \frac{1}{2} E_0 \sin 2\theta_0 \quad (28)$$

It is interesting that the force is a maximum, for a given wave amplitude at infinity, when $\sin 2\theta_0 = 1$ or $\theta_0 = 45^\circ$.

4. LOCAL WAVE STRESS

Inside the breaker zone F_x gradually diminishes toward the shoreline. A consideration of the momentum balance between two planes $x = x_1$ and $x_1 + dx$ parallel to the shoreline and separated by a distance dx shows at once that the net stress τ_x per unit area exerted by the waves on the water in the surf zone is given by

$$\tau_x = -\partial S_{xy} / \partial x \quad (29)$$

and by (15) this equation becomes

$$\tau_x = -\frac{\partial F_x}{\partial x} \left(\frac{\sin \theta_0}{c_0} \right) = D \left(\frac{\sin \theta_0}{c_0} \right) \quad (30)$$

where D denotes the local rate of energy dissipation. In other words, the local stress exerted by the waves is directly proportional to the local rate of dissipation of wave energy. Outside the

breaker zone the mean bottom stress vanishes.

In some situations the loss of wave energy can be attributed to bottom friction (due mainly to the orbital velocity of the waves). However, the observation by *Munk* [1949] that in the surf zone the breaker height is proportional to the mean depth suggests that under normal circumstances most of the loss of wave energy is due to wave breaking, not to bottom friction.

It is found that the rule

$$a = \alpha h \quad (31)$$

where α is a constant between 0.3 and 0.6 is in agreement both with direct observations (see Table 1 below) and with laboratory measurements of wave setup [*Longuet-Higgins and Stewart*, 1963, 1964; *Bowen*, 1967] the approximate linear shallow-water theory is used. On the basis of this theory we have from section 2, when $kh \ll 1$,

$$c = (gh)^{1/2} = c_0 \quad (32)$$

If it is assumed that in the breaker zone θ is small enough that $\cos \theta$ can be approximated

by unity, we have from (7), (31), and (32)

$$F_x = \frac{1}{2} \rho g a^2 c_0 = \frac{1}{2} \alpha^2 \rho g^{3/2} h^{5/2} \quad (33)$$

and so from (30)

$$\begin{aligned} \tau_v &= -\frac{1}{4} \alpha^2 \rho (gh)^{3/2} \frac{dh \sin \theta}{dx c} \\ &= \frac{5}{4} \alpha^2 \rho g h (s \sin \theta) \end{aligned} \quad (34)$$

where $s = -dh/dx$ denotes the local bottom slope.

Some values of α as determined by various authors are shown in Table 1. Though the later determinations of α tend to be higher than the earlier ones, no determination departs by more than 50% from the theoretical value of 0.41 calculated by *Davies and Long* for the solitary wave.

Using (31) and the linear shallow-water theory, we can also express (34) in terms of the maximum horizontal orbital velocity given by

$$u_{\max} = (a\sigma)/(kh) = \alpha(\sigma/k) = \alpha(gh)^{1/2} \quad (35)$$

Then we have simply

$$\tau_v = \frac{5}{4} \rho u_{\max}^2 (s \sin \theta) \quad (36)$$

where s denotes the bottom slope and θ denotes the local angle of incidence.

We note that in this simple relation there are no adjustable parameters.

Beyond the breaker line, i.e. where the energy dissipation is negligibly small, D vanishes, and so by (31)

$$\tau_v = 0 \quad (37)$$

5. BOTTOM FRICTION

The tangential stress B excited by the water on the bottom will be assumed to be given adequately by a relation of the form

$$B = C \rho |u| u \quad (38)$$

where u is the instantaneous velocity vector near the bottom and C is a constant coefficient.

If there were no longshore velocity, and if the amplitude of the motion were small and the bottom impermeable, the horizontal orbital velocity would be expected to be to-and-fro in the same straight line, making an angle θ with the normal to the shoreline (see Figure 2a).

TABLE 1. Observed and Theoretical Values of α

Investigator	s	α	$\langle \alpha \rangle$
Observed Values			
<i>Putnam et al.</i> [1949]	0.066	0.37	0.35
	0.098	0.36	
	0.100	0.33	
	0.139	0.32	
	0.143	0.37	
	0.144	0.32	
	0.241	0.35	
	0.260	0.36	
<i>Iverson</i> [1952]	0.020	0.41	0.44
	0.033	0.38	
	0.050	0.42	
	0.100	0.52	
<i>Larras</i> [1952]	0.010	0.34	0.39
	0.020	0.37	
	0.091	0.43	
<i>Ippen and Kulin</i> [1955]	0.023	0.60	0.60
<i>Eagleson</i> [1956]	0.067	0.56	0.56
<i>Galvin and Eagleson</i> [1965]	0.104	0.59	0.59
<i>Bowen</i> [1968]	0.082	0.45-0.62	0.56
Values Determined from Solitary Wave Theory			
<i>McCowan</i> [1894]	0.000	0.39	
<i>Davies</i> [1952]	0.000	0.41	
<i>Long</i> [1956]	0.000	0.406	

LONGSHORE CURRENTS, I

6783

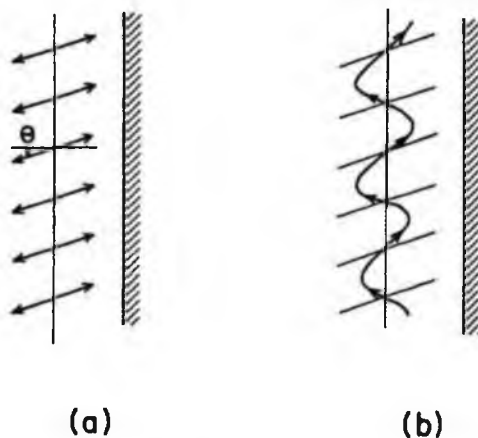


Fig. 2. Schematic representation of particle orbits (a) with zero mean littoral velocity and (b) with positive littoral velocity $\langle v \rangle$.

The frictional stress \mathbf{B} given by

$$\mathbf{B} = C\rho |\mathbf{u}_{orb}| \mathbf{u}_{orb} \quad (39)$$

would then vanish in the mean (according to linear theory).

Now suppose that a small component of velocity $\langle v \rangle$ in the longshore direction is added to the orbital velocity (Figure 2b). When θ is small, this component of velocity is almost perpendicular to the orbital velocity. Therefore the magnitude of the velocity $\mathbf{u} = \mathbf{u}_{orb} + (0, \langle v \rangle)$ is unchanged, to first order, but the direction of

the bottom stress is changed by a small angle $\langle v \rangle / |\mathbf{u}_{orb}|$ approximately. Hence there is an additional stress in the y direction given by

$$B_y = C\rho |\mathbf{u}_{orb}|^2 \langle v \rangle / |\mathbf{u}_{orb}| = C\rho |\mathbf{u}_{orb}| \langle v \rangle \quad (40)$$

Physically, when the orbital velocity is onshore, the direction of the bottom stress is inclined more toward the positive y direction (if $\langle v \rangle$ is positive); when the orbital velocity is offshore, the bottom stress, now almost in the opposite direction, is again more toward the positive y direction. Taking mean values in (40), we have the relation

$$\langle B_y \rangle = C\rho \langle |\mathbf{u}_{orb}| \rangle \langle v \rangle \quad (41)$$

Assuming \mathbf{u}_{orb} to be sinusoidal, we have

$$\langle |\mathbf{u}_{orb}| \rangle = (2/\pi)u_{max} \quad (42)$$

and hence

$$\langle B_y \rangle = (2/\pi)C\rho u_{max} \langle v \rangle \quad (43)$$

As a guide to the appropriate value of the friction coefficient we consider first the values for a rough horizontal plate in uniform flow, as given for example by Prandtl [1952] and based on Nikuradse's experiments with roughened pipes. For convenience we reproduce Prandtl's [1952, p. 195] diagram as Figure 3 below. The friction coefficient appears to depend on just two parameters. The first is the Reynolds number

$$Re = Ul/\nu \quad (44)$$

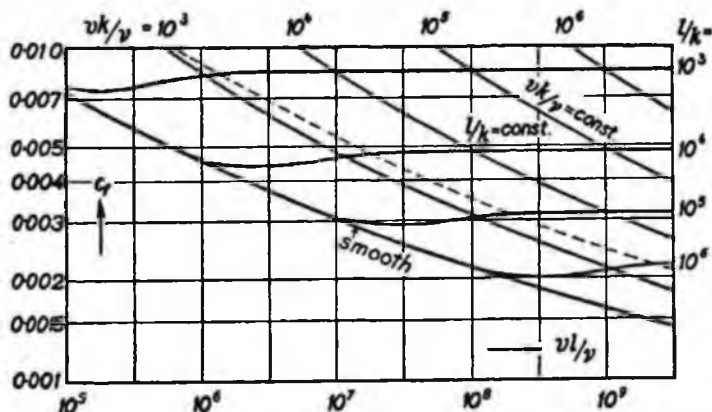


Fig. 3. Values of the friction coefficient C for flow over rough plates, as deduced from the experiments of Nikuradse [from Prandtl, 1952]. (Figure reprinted by permission of Haffner Co.)

where U denotes the horizontal velocity, l denotes the length of the plate, and ν is the kinematic viscosity. The second parameter is the ratio (l/K) , where K denotes a typical scale for a roughness element. Here we can take as an appropriate value of U the horizontal component of the orbital velocity, u_{\max} , and for l the horizontal excursion of a water particle from its mean position, that is $l = u_{\max}/\sigma$. Thus we have

$$Re = u_{\max}^2/\nu\sigma = \alpha^2 gh/\nu\sigma \quad (45)$$

As typical values for field data we can take

$$\begin{aligned} \alpha &= 0.4 & g &= 10\text{m/sec}^2 \\ h &= 1\text{ meter} & \sigma &= 1\text{ rad/sec} \end{aligned} \quad (46)$$

corresponding to 6-sec waves 0.8 meter high. With the approximate value $\nu = 1.3 \times 10^{-6}$ m²/sec and with a sand grain diameter of 1 mm we obtain

$$Re = 1.3 \times 10^6 \quad l/K = 1.3 \times 10^3 \quad (47)$$

and so from Figure 3 $C_r \div 0.007$. On the other hand, for laboratory data more typical values are

$$h = 0.1\text{ meter} \quad \sigma = 5\text{ rad/sec} \quad (48)$$

With the same values of α , g , and ν , this leads to

$$Re = 2.5 \times 10^4 \quad l/K = 20 \quad (49)$$

if the roughness scale K is the same. In that case Figure 3 suggests that C_r is somewhat larger, about 0.010.

Bretschneider [1954] has found that the observed damping of swell which is propagated over a smooth, level, impermeable sea bed is consistent with a friction coefficient lying between 0.034 and 0.097. These values appear to agree well with Prandtl's values. On the other hand, *Bretschneider* also found that the spectral limitation of wave growth under the action of wind suggested higher values of C , between 0.01 and 0.02. These coefficients may include other significant effects such as bottom percolation. R. E. Mayer (personal communication) has found, however, that the theory of run-up of surf on beaches [*Shen and Meyer*, 1963; *Freeman and Le Méhauté*, 1964] can be made to agree fairly well with the model experiments of *Miller* [1968] over a hard sloping concrete bot-

tom by assuming that C lies between 0.01 and 0.02. These values cannot be the result of bottom percolation, but might be attributable in part to turbulence arising from the breaking of the waves as they run up the slope.

Taken together, the above data suggest that it is not unreasonable to expect a friction coefficient C of the order of 0.01.

6. EQUATIONS FOR LONGSHORE CURRENT

To estimate the longshore current $\langle v \rangle$, let us assume first that the mean current is steady and two-dimensional, being independent of the time t and of the longshore coordinate y . Then the equation of motion in the longshore direction can be written as

$$0 = \tau_y + \frac{\partial}{\partial x} \left(N \frac{\partial \langle v \rangle}{\partial x} \right) - \langle B_y \rangle \quad (50)$$

where in the surf zone τ_y and $\langle B_y \rangle$ are given by (37) and (43), respectively. The second term represents the exchange of momentum due to horizontal turbulent eddies, with eddy coefficient N .

In this equation the magnitude of N is unknown. Suppose first that the exchange of momentum by turbulence is negligible in comparison with that due to the waves; then in general the second term on the right of (50) can be neglected in comparison with the first. There remains a balance between the first and third terms:

$$\langle B_y \rangle = \tau_y \quad (51)$$

Substituting from equations (36) and (43), we have in the breaker zone

$$\frac{2}{\pi} C \rho u_{\max} \langle v \rangle = \frac{5}{4} \rho u_{\max}^2 (s \sin \theta) \quad (52)$$

and hence

$$\langle v \rangle = (5\pi/8C) u_{\max} (s \sin \theta) \quad (53)$$

This very simple relation implies that for constant values of C and s the longshore current is simply proportional to $u_{\max} \sin \theta$, or to the longshore component of the orbital velocity.

The proportionality of $\langle v \rangle$ and u_{\max} has been inferred on quite different grounds by P. Komar (personal communication, 1969).

Using (36) the relation between u_{\max} and the local phase velocity c , we can also write (52) in

the form

$$\langle v \rangle = \frac{5\pi}{8} \frac{\alpha}{C} g h s \left(\frac{\sin \theta}{c} \right) \quad (53')$$

where $c = (gh)^{1/2}$. Now by Snell's law the last factor is a constant. Equation (53') then states that in a given wave situation, if both C and s are constant, the longshore velocity (v) is simply proportional to the local depth h .

If we assume that the shallow-water theory is valid as far out as the breaker line where the depth h is equal to h_B , the mean longshore current, in the absence of horizontal mixing, can be written as

$$\langle v \rangle = \left(\frac{h}{h_B} \right) \times \begin{cases} v_0 & h < h_B \\ 0 & h > h_B \end{cases} \quad (54)$$

where

$$v_0 = \frac{5\pi}{8} \frac{\alpha}{C} (gh_B)^{1/2} (s \sin \theta_B) \quad (55)$$

This relation is shown in Figure 4 by the dashed line (corresponding to $\gamma = 0$). The total longshore flux in the surf zone is given by

$$\begin{aligned} Q &= \int_{h-h_B}^{h=0} h(v) dx \\ &= \int_0^{h_B} h(h/h_B) v_0 dh/s \\ &= \frac{1}{2} h_B^2 v_0/s = \frac{1}{2} h_B |x_B| v_0 \end{aligned} \quad (56)$$

We have so far neglected the horizontal mixing entirely. In this idealized model there is a sharp discontinuity in the velocity profile at the breaker line. The presence of any horizontal

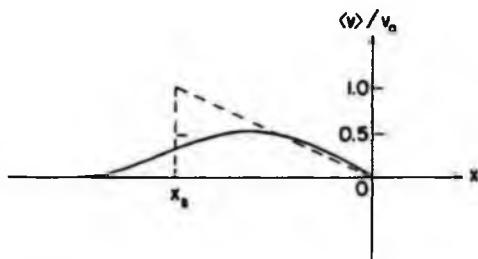


Fig. 4. Schematic representation of the longshore velocity profile as a function of distance offshore. Broken line denotes values without horizontal mixing; full line, with horizontal mixing.

TABLE 2. Theoretical Values of β

$\gamma = L/ x_B $	β
0.00	0.500
0.25	0.386
0.50	0.290
0.75	0.218
1.00	0.167

mixing, as well as any variability in wave height and position of breaker line, will tend to smooth out the discontinuity at the breaker line and produce a smoother velocity profile; this shifts the maximum velocity closer to shore, as in Figure 4.

A very rough estimate of the effect of mixing on the velocity v_B at the breaker line can be obtained by taking the average of the momentum $h(v)$ over a distance L on either side of the breaker line, where L represents a mixing length. When L is small in comparison with the width $|x_B|$ of the surf zone, the velocity v_B is equal to the mean value of the velocities on the two sides of the discontinuity in Figure 4. Hence $v_B = \frac{1}{2} v_0$. More generally if we take

$$L = \gamma |x_B| \quad 0 < \gamma < 1 \quad (57)$$

we obtain for constant bottom gradient

$$v_B = \beta v_0 \quad (58)$$

where

$$\beta = \frac{1 - \gamma}{2} + \frac{\gamma^2}{6} \quad (59)$$

As γ increases from 0 to 1, β decreases from $\frac{1}{2}$ to $\frac{1}{6}$. Then we can write

$$v_B = \frac{5\pi}{8} \frac{\alpha \beta}{C} (gh_B)^{1/2} (s \sin \theta_B) \quad (60)$$

where θ_B denotes the angle of incidence at the breaker line and β is a constant between 0.5 and about 0.167. The dependence of β on γ is shown in Table 2.

7. COMPARISON WITH OBSERVATION

Because of the dependence of the longshore velocity on the distance from the shoreline it is particularly important to define precisely the position of the point of observation relative to the shoreline and breaker line.

6786

M. S. LONGUET-HIGGINS

TABLE 3. Laboratory Data by Brebner and Kamphuis from *Galvin and Nelson* [1965, p. 12]

H_B , feet	θ_B , deg	s	v_B , ft/sec	$(gH_B)^{1/2}/v_B$	$s \sin \theta_B$	r
0.092	7.0	0.10	0.44	3.92	0.012	0.048
0.097	7.5	0.10	0.47	3.77	0.013	0.049
0.110	9.0	0.10	0.67	2.81	0.016	0.045
0.118	10.0	0.10	0.82	2.38	0.017	0.041
0.118	7.5	0.10	0.49	3.97	0.013	0.052
0.138	8.0	0.10	0.67	3.15	0.014	0.044
0.153	10.0	0.10	0.83	2.68	0.017	0.047
0.159	12.0	0.10	0.99	2.29	0.021	0.047
0.157	9.0	0.10	0.63	3.57	0.016	0.056
0.159	9.5	0.10	0.80	2.83	0.016	0.047
0.200	12.0	0.10	0.96	2.65	0.021	0.055
0.203	13.0	0.10	1.07	2.39	0.022	0.054
0.177	9.0	0.10	0.63	3.79	0.016	0.059
0.220	11.0	0.10	0.88	3.02	0.019	0.058
0.228	12.5	0.10	1.04	2.60	0.022	0.056
0.231	14.0	0.10	1.16	2.35	0.024	0.057
0.092	10.0	0.10	0.60	2.87	0.017	0.050
0.112	11.0	0.10	0.81	2.35	0.019	0.045
0.110	13.0	0.10	0.84	2.24	0.022	0.050
0.118	15.0	0.10	0.91	2.14	0.026	0.055
0.118	11.0	0.10	0.83	2.35	0.019	0.145
0.133	12.5	0.10	0.97	2.14	0.022	0.046
0.153	15.0	0.10	1.04	2.14	0.026	0.055
0.159	17.0	0.10	1.14	1.99	0.029	0.058
0.170	13.0	0.10	0.94	2.49	0.022	0.056
0.158	14.0	0.10	1.12	2.01	0.024	0.049
0.200	17.0	0.10	1.25	2.03	0.029	0.059
0.194	18.0	0.10	1.32	1.89	0.031	0.058
0.184	13.0	0.10	1.07	2.28	0.022	0.051
0.204	16.0	0.10	1.25	2.05	0.027	0.056
0.231	18.0	0.10	1.29	2.12	0.031	0.065
0.234	21.0	0.10	1.32	2.08	0.036	0.074
0.085	12.0	0.10	0.70	2.36	0.021	0.049
0.097	14.0	0.10	0.83	2.13	0.024	0.052
0.110	17.0	0.10	0.88	2.14	0.029	0.062
0.112	18.0	0.10	1.05	1.81	0.031	0.056
0.118	14.0	0.10	0.91	2.14	0.024	0.052
0.133	16.0	0.10	0.96	2.16	0.027	0.059
0.141	18.0	0.10	1.10	1.94	0.031	0.060
0.147	21.0	0.10	1.22	1.79	0.036	0.064
0.151	17.0	0.10	1.08	2.04	0.029	0.060
0.153	18.0	0.10	1.18	1.88	0.031	0.059
0.176	22.0	0.10	1.36	2.75	0.037	0.066
0.187	24.0	0.10	1.53	1.60	0.041	0.065
0.177	17.0	0.10	1.21	1.97	0.029	0.057

The profiles of velocity versus offshore distance measured by *Galvin and Eagleson* [1965] show a maximum velocity about halfway between the mean shoreline (not the still water level) and the breaker line, as one would expect from section 6 if horizontal mixing were important. In the above instance, however, the flow was being accelerated downstream from a side wall, so that the compensating inflow would also contribute to the redistribution of longshore

momentum and could have an effect similar to the presence of a large horizontal eddy viscosity.

A useful summary of the available field and laboratory data has been compiled by *Galvin and Nelson* [1967]; these data have been critically discussed by *Galvin* [1967]. It seems that the most commonly observed parameters of the wave field are the breaker height

$$H_B = 2\alpha h_B \quad (61)$$

LONGSHORE CURRENTS, I

6787

and the angle of incidence θ_B at the breaker line, though in some instances these quantities must be deduced from the wave height and angle of incidence as measured in deep water. *Galvin and Eagleson* [1965] have shown that there is considerable uncertainty in the measurement of H_B and θ_B (especially θ_B) even under laboratory conditions.

Now substituting for h_B in (60) we have for the longshore velocity v_B at the breaker line

$$v_B = \frac{5r}{8\sqrt{2}} \frac{\sqrt{\alpha\beta}}{C} (gH_B)^{1/2} (s \sin \theta_B) \quad (62)$$

In other words, if we write

$$\frac{(gH_B)^{1/2}}{v_B} (s \sin \theta_B) = r \quad (63)$$

a dimensionless ratio, we have

$$C = 1.39 \sqrt{\alpha\beta} r \quad (64)$$

With little uncertainty we can take α to be the mean value of the entries in the last column of Table 1, namely $\alpha = 0.42$; then (64) further simplifies to

$$C = 0.90\beta r \quad (65)$$

For each entry in the data compiled by *Galvin and Nelson* [1967] we have computed the quantity r as given by (63). The results of these computations for a typical page of laboratory data [*Brebner and Kamphuis*, 1963] are shown in Table 3 and for the field data of *Inman and Quinn* [1952] in Table 4. Despite the great range in the values of the breaker height H_B it will be seen that the computed value of r remains remarkably consistent. There is somewhat more scatter in the field data than

TABLE 4. Field Data by Inman and Quinn from *Galvin and Nelson* [1965, p. 17]

H_B , feet	θ_B , deg	s	v_B , ft/sec	$(gH_B)^{1/2}/v_B$	$s \sin \theta_B$	r
2.8	6.5	0.027	0.38	25.0	0.0030	0.076
3.1*	1.5*	0.027	0.04	25.0	0.0007	0.018*
3.7	4.0	0.027	0.22	49.6	0.0019	0.093
3.6*	0. *	0.027	0.04	269.0	0.0000	0.000*
4.9	5.0	0.027	0.84	14.9	0.0024	0.035
3.8	5.0	0.027	0.21	52.6	0.0024	0.124
3.4*	0. *	0.027	0.55	19.0	0.0000	0.000*
2.6*	0. *	0.035	0.04	22.9	0.0000	0.000*
3.0*	1.0*	0.035	0.01	98.2	0.0006	0.600*
2.7*	0. *	0.035	0.15	62.1	0.0000	0.000*
3.5*	0. *	0.035	0.09	117.9	0.0000	0.000*
4.9*	0. *	0.035	0.21	59.8	0.0000	0.000*
2.9*	0. *	0.035	0.50	19.3	0.0000	0.000*
4.6*	0. *	0.035	0.88	13.8	0.0000	0.000*
3.7*	0. *	0.028	0.20	54.5	0.0000	0.000*
5.1	6.0	0.027	0.29	44.1	0.0028	0.124
4.7	7.0	0.027	0.53	23.2	0.0033	0.076
4.5	4.0	0.027	0.70	17.2	0.0019	0.032
4.8	4.0	0.027	1.19	10.4	0.0019	0.020
4.2	4.5	0.027	0.40	29.1	0.0021	0.062
2.0	4.0	0.027	0.36	22.3	0.0019	0.042
1.7	7.0	0.027	0.23	31.2	0.0033	0.103
2.9	5.0	0.027	0.56	17.2	0.0023	0.041
1.6	5.0	0.027	0.11	65.2	0.0023	0.153
6.2	5.0	0.014	0.54	26.1	0.0012	0.032
3.1	7.0	0.014	0.62	16.1	0.0017	0.028
4.5	3.0	0.014	0.49	24.6	0.0007	0.018
3.5	4.0	0.014	0.17	62.4	0.0010	0.061
2.7	3.5	0.014	0.13	71.7	0.0009	0.061
4.7	7.0	0.014	1.37	9.0	0.0017	0.015
2.6*	2.0*	0.014	0.04	228.6	0.0005	0.116*
2.0	4.0	0.014	0.11	72.9	0.0010	0.071
1.8	2.5	0.014	0.06	126.8	0.0006	0.077

* Values for which θ_B is reckoned to be 2° or less.

TABLE 5. Summary of Observations: Mean Values

Investigators	Type of Beach	(s)	(H_B)	(θ_B)	N	(r)
<i>Putnam et al.</i> [1949]*	Bonded sand	0.133	0.28	14.4	14	0.121
	Metal or smooth cement	0.172	0.23	36.8	14	0.134
	Gravel, 1/4 inch in diam.	0.123	0.22	22.0	9	0.322
	Concrete or 0.3 mm sand	0.100	0.14	6.5	7	0.087
<i>Saville</i> [1950]*		0.100	0.15	13.9	45	0.054
	<i>Brebner and Kamphuis</i> [1963]	Roughened concrete	0.100	0.14	21.2	48
		0.100	0.16	14.6	48	0.035
<i>Galvin and Eagleson</i> [1965]	Smooth concrete	0.109	0.16	11.8	18	0.044
<i>Putnam et al.</i> [1949]	Oceanside	0.021	6.42	11.1	18	0.020
<i>Inman and Quinn</i> [1951]	Torrey Pines and Pacific Beach	0.022	3.58	4.9	21	0.064
<i>Galvin and Savage</i> [1966]	Nags Head	0.027	3.75	15.4	4	0.035

* Data rejected by *Galvin* [1967].

in the laboratory data, as is to be expected, especially considering the difficulty in measuring the angle of incidence θ_B . If we omit from consideration all observations (marked with an asterisk) for which θ_B is reckoned to be 2° or less, the mean value of the entries in the last column is $\langle r \rangle = 0.054$ for the laboratory measurements and $\langle r \rangle = 0.064$ for the field data.

A summary of such mean values is given in Table 5, for all the data compiled by *Galvin and Nelson* [1967] with the exception of the field observations of *Moore and Scholl* [1961], which contained a large proportion of zero or negative values of v_s and were thought to be influenced by disturbances other than wave action. In the laboratory measurements of *Saville* [1950] and of *Galvin and Eagleson* [1965] the entries corresponding to angles θ_B less than 6° have also been discarded on the grounds of unreliability.

On quite different grounds *Galvin* [1967] has rejected all the early laboratory measurements of *Putnam et al.* [1949] since they were found not to be reproducible under almost the same conditions either by *Brebner and Kamphuis* [1963] or by *Galvin and Eagleson* [1965]. It is possible that *Putnam et al.* employed a different definition of breaker height than *Brebner and Kamphuis* or *Galvin and Eagleson*. *Galvin* also suggests that less weight should be attached to the observations of *Saville* [1950], since he did not actually measure H_B and θ_B ; these entries in the table are estimated from H_o and θ_o .

Retaining then only the most reliable meas-

urements in Table 5 (namely those not rejected by *Galvin* [1967]), we find for the field observations $\langle r \rangle = 0.040$ and for the laboratory data $\langle r \rangle = 0.050$.

According to (65), these values of r correspond to mean values of the friction coefficient C given by

$$C = 0.036\beta \quad C = 0.045\beta \quad (66)$$

where β , as we have seen, is between 0.50 and 0.167, depending on the horizontal mixing.

Assuming a friction coefficient C of about 0.010, we see that both field observations and laboratory data are consistent with a mean value of β equal to about 0.2. This suggests that horizontal mixing played some part, though not a dominant one, in the distribution of the longshore current.

A more precise estimate of the effects of horizontal mixing are given in the accompanying paper.

8. CONCLUSIONS

By the use of the concept of radiation stress and the small-amplitude theory of water waves, we have shown that the total longshore thrust exerted by the waves on the water and sea bed inside the surf zone is very simply related to the energy density and direction of propagation of the waves in deep water (equation 28). This relation is quite different from that given by previous authors, and it would be interesting to test it directly by experiment.

The local wave stress τ_r is also simply related to the local rate of energy dissipation, and, it

would be interesting to test this relation also.

The comparisons so far made between theory and observation suggest that the rational prediction of longshore currents may be practically possible. There is no need, as some authors have suggested, to fall back on empirical correlations.

Acknowledgments. My interest in this topic was stimulated by a seminar given in Corvallis by Mr. Paul Komar. I am indebted to him and to my colleague, Dr. Victor Neal for references to recent literature. Professor Inman, Dr. Elliott, and Dr. Quinn kindly commented on a first draft of this paper.

The present research was supported under NSF grant GA-1452.

REFERENCES

- Bowen, A. J., Rip currents, Ph.D., thesis, Scripps Institution of Oceanography, University of California, San Diego, 115 pp., 1967.
- Bowen, A. J., The generation of longshore currents on a plane beach, *J. Mar. Res.*, **27**, 206-215, 1969.
- Brebner, A., and J. W. Kamphuis, Model tests on relationship between deep-water wave characteristics and longshore currents, *Queens Univ. Civil Eng. Res. Rep.*, **31**, 1-25, 1963.
- Bretschneider, C. L., Field investigation of wave energy loss of shallow water ocean waves, *U.S. Army, Beach Erosion Board, Tech. Mem.* **46**, 1954.
- Burnside, W., On the modification of a train of waves as it advances into shallow water, *Proc. London Math. Soc.*, **14**, 131-133, 1915.
- Davies, T. V., Symmetrical, finite amplitude gravity waves, in *Gravity Waves*, chap. 9, *NBS Circ.* **621**, 55-60, 1952.
- Eagleson, P. S., Properties of shoaling waves by theory and experiment, *Trans. AGU*, **37**, 565-572, 1956.
- Freeman, J. C., and B. Le Méhauté, Wave breakers on a beach and surges on a dry bed, *J. Hydr. Div. Amer. Soc. Civil Eng.*, **90**, 187-216, 1964.
- Galvin, C. J., Longshore current velocity: A review of theory and data, *Rev. Geophys.*, **6**, 287-304, 1967.
- Galvin, C. J., and P. S. Eagleson, Experimental study of longshore currents on a plane beach, *U.S. Army Coast. Eng. Res. Center, Tech. Mem.* **10**, 1-80, 1965.
- Galvin, C. J., and R. A. Nelson, Compilation of longshore current data, *U.S. Army Coast. Eng. Res. Center, Misc. Pap.* **2-67**, 1-19, 1967.
- Inman, D. L., and R. A. Bagnold, Beach and nearshore processes, 2, Littoral processes, in *The Sea*, edited by M. N. Hill, pp. 529-553, Interscience, New York, 1963.
- Inman, D. L., and W. H. Quinn, Currents in the surf zone, *Proc. 2nd Conf. on Coastal Eng., Council on Wave Research, University of California Berkeley*, 24-36, 1952.
- Ippen, A. T., and G. Kulin, Shoaling and breaking characteristics of the solitary wave, *MIT Hydrodynamics Lab. Rep.* **15**, 1955.
- Iverson, H. W., Laboratory study of breakers, in *Gravity Waves*, chap. 3, *NBS Circ.* **621**, 9-32, 1952.
- Larras, J., Experimental research on the breaking of waves, *Ann. Ponts Chaussees*, **122**, 525-542, 1952.
- Long, R. R., Solitary waves in one- and two-fluid systems, *Tellus*, **8**, 460-471, 1956.
- Longuet-Higgins, M. S., The refraction of sea waves in shallow water, *J. Fluid Mech.*, **1**, 163-176, 1956.
- Longuet-Higgins, M. S., and R. W. Stewart, Changes in the form of short gravity waves on long waves and tidal currents, *J. Fluid Mech.*, **8**, 565-583, 1960.
- Longuet-Higgins, M. S., and R. W. Stewart, The changes in amplitude of short gravity waves on steady non-uniform currents, *J. Fluid Mech.*, **10**, 529-549, 1961.
- Longuet-Higgins, M. S., and R. W. Stewart, Radiation stress and mass transport in gravity waves, *J. Fluid Mech.*, **13**, 481-504, 1962.
- Longuet-Higgins, M. S., and R. W. Stewart, A note on wave set-up, *J. Mar. Res.*, **21**, 4-10, 1963.
- Longuet-Higgins, M. S., and R. W. Stewart, Radiation stresses in water waves; a physical discussion, with applications, *Deep-Sea Res.*, **11**, 529-562, 1964.
- McCowan, J., On the highest wave of permanent type, *Phil. Mag.*, **39**, 351-359, 1894.
- Miller, R. L., Experimental determination of run-up of undular and fully developed bores, *J. Geophys. Res.*, **73**, 4497-4510, 1968.
- Moore, G. W., and D. W. Scholl, Coastal sedimentation in northwestern Alaska, *U.S. Geol. Surv. Rep. TE 1-779*, 43-65, 1961.
- Munk, W. H., The solitary wave and its application to surf problems, *Ann. N.Y. Acad. Sci.*, **61**, 376-424, 1949.
- Prandtl, L., *Essentials of Fluid Dynamics*, 452 pp., Haffner, New York, 1952.
- Putnam, J. A., W. H. Munk, and M. A. Traylor, The prediction of longshore currents, *Trans. AGU*, **30**, 337-345, 1949.
- Saville, T., Model study of sand transport along an infinitely long straight beach, *Trans. AGU*, **31**, 555-565, 1950.
- Shen, M. C., and R. E. Meyer, Climb of a bore on a beach, 3, Run-up, *J. Fluid Mech.*, **16**, 113-125, 1963.
- Wiegell, R. L., *Oceanographical Engineering*, Prentice-Hall, 532 pp. Englewood Cliffs, N. J., 1963.

(Received January 29, 1970;
revised June 30, 1970.)

Longshore Currents Generated by Obliquely Incident Sea Waves, 2

M. S. LONGUET-HIGGINS¹

Oregon State University, Corvallis, Oregon 97331

The profile of the longshore current, as a function of distance from the swash line, is calculated by using the concept of radiation stress (introduced in an earlier paper) together with a horizontal eddy viscosity μ_s of the form $\mu_s = \rho N \alpha (gh)^{1/2}$, where ρ is the density, α is the distance offshore, g is gravity, h is the local mean depth, and N is a numerical constant. This assumption gives rise to a family of current profiles whose form depends only on the nondimensional parameter $P = (\pi/2)(sN/\alpha C)$, where s denotes the bottom slope, α is a constant characteristic of breaking waves ($\alpha \doteq 0.41$), and C is the drag coefficient on the bottom. The current profiles are of simple analytic form, having a maximum in the surf zone and tending to zero at the swash line. Comparison with the laboratory experiments of Galvin and Eagleson (1965) shows remarkably good agreement if the drag coefficient C is taken as 0.010. The theoretical profiles are insensitive to the exact value of P , but the experimental results suggest that P never exceeds a critical value of 2/5.

1. INTRODUCTION

In the companion paper (hereafter referred to as paper 1) a new theory for the generation of longshore currents by sea waves was developed; it is based on the concept of the radiation stresses associated with the incoming waves. The theory was found to be consistent with observed currents at the breaker line, in both model experiments and field observations, provided that the friction coefficient on the bottom was of order 0.010 and that the horizontal mixing length was of the same order, but less than, the distance between breaker line and shoreline.

To make further progress in predicting the longshore current, one must make some further detailed assumption about the horizontal mixing in the surf zone. This we propose to do by adopting a certain form for the coefficient μ_s of the horizontal eddy viscosity, as a function of distance from the shoreline.

It is fairly clear that μ_s must tend to zero as the shoreline is approached, since the dimensions of the turbulent eddies responsible for horizontal mixing can hardly be greater than the distance to the shoreline. For comparison, one can consider the analogous situation of turbulent flow over a rough plate, in which μ_s is proportional

to height above the plate [e.g., Prandtl, 1952]. However, the present flow differs from flow over a plate in that horizontal driving forces (in the form of the gradient of the radiation stresses) are also present throughout the surf zone. Thus, although μ_s should tend to zero, it does not necessarily do so linearly.

In fact, we assume in the following that μ_s is proportional to the offshore distance α multiplied by a typical velocity $(gh)^{1/2}$, where h denotes the local depth. When the bottom slope s is uniform, this particular form for the eddy viscosity μ_s yields a very simple analytical form for the longshore current profile, which is found to be in remarkably good quantitative agreement with the detailed laboratory measurements by Galvin and Eagleson [1957]. In particular, the position and magnitude of the maximum current appear to be correctly predicted.

While this paper was in preparation, the author's attention was drawn to a then unpublished paper by Bowen [1969] in which the concept of radiation stress was also applied to the same problem. Bowen also takes into account both bottom friction and horizontal mixing, though in a somewhat different way. Although in general agreement with Bowen's approach we should like to point out two primary differences. The first is that he has assumed a bottom friction proportional to the longshore current v , whereas it was shown in section 5 of paper 1 that the bottom friction is proportional to uv , where u is the amplitude of the local orbital

¹ Now at National Institute of Oceanography, Wormley, Godalming, England, and Department of Applied Mathematics and Theoretical Physics, Cambridge, England.

LONGSHORE CURRENTS. 2

6791

velocity (normal to the coastline). This is the form adopted in the present paper. Second, in Bowen's model the coefficient of horizontal eddy viscosity μ_e is taken to be a constant, not tending to zero at the shoreline. This apparently simpler assumption leads in fact to a more complicated analytical form for the velocity profile, which is at variance in some respects with the velocity profiles as measured by *Galvin and Eagleson* [1957]. It appears then that the present formulation of the theory is both more plausible on physical grounds and better in agreement with the observations now available.

2. EQUATIONS OF MOTION

We take axes Ox , Oy normal and parallel to the coastline, with the origin O at the coastline (which may differ from the still-water line because of wave setup). The local mean depth $h(x)$ will be taken as including the change in level due to wave setup, or 'set down,' so that $h(0) = 0$ exactly.

If the longshore current v is steady and independent of y , then, as was shown in section 6 of paper 1, the momentum balance in the y direction can be expressed by the equation

$$0 = \tau_v + \frac{\partial}{\partial x} \left(\mu_e h \frac{\partial v}{\partial x} \right) - \langle B_v \rangle \quad (1)$$

in which τ_v denotes the driving force due to the radiation stresses, which is given in shallow water by

$$\tau_v = \frac{5}{4} \alpha^2 \rho (gh)^{3/2} s \left(\frac{\sin \theta}{c} \right) \quad \text{or} \quad 0 \quad (2)$$

as $x \leq x_B$, the breaker distance (see section 4 of paper 1). In (2) α is a constant, about 0.41, ρ denotes the density, g is the acceleration of gravity, $s = dh/dx$ is the local depth gradient, θ is the local angle of incidence ($\theta^2 \ll 1$), and c is the local velocity of shallow-water waves where $c = (gh)^{1/2}$. By Snell's law $(\sin \theta)/c$ is a constant independent of x . Also in (1) the mean stress $\langle B_v \rangle$ on the bottom is given by

$$\langle B_v \rangle = \frac{2}{\pi} \alpha C \rho (gh)^{1/2} v \quad (3)$$

where C is the drag coefficient on the bottom. The middle term on the right of (1) represents the effect of horizontal mixing. Now μ_e has the dimensions of $\rho L U$, where L is a typical length

scale and U is a typical velocity. Following the reasoning outlined in the introduction we take $L \propto x$ and $U \propto (gh)^{1/n}$, where h is the local depth. As the simplest possible assumption, we take

$$\mu_e = N \rho x (gh)^{1/2} \quad (4)$$

where N is a dimensionless constant. Since L is not likely to exceed Kx , where K is von Kármán's constant, 0.40, and since the turbulent velocities are not likely to exceed $0.1u_{max}$ at most, where $u_{max} = \alpha(gh)^{1/2}$, the probable limits of N can be set as

$$0 < N < 0.016 \quad (5)$$

(for $N \rho x (gh)^{1/2} = \mu_e = \rho L U \leq \rho(Kx) 0.1 \alpha(gh)^{1/2}$).

We are particularly interested in a constant (or almost constant) beach gradient. We shall therefore suppose that

$$h = sx \quad (6)$$

where $s = dh/dx$ is a constant that is nearly but not exactly equal to the bottom gradient m . Then (1) can be written in the form

$$p \frac{\partial}{\partial x} \left(x^{s/2} \frac{\partial v}{\partial x} \right) - qx^{1/2} v = \begin{cases} -rx^{3/2} & 0 < x < x_B \\ 0 & x_B < x < \infty \end{cases} \quad (7)$$

where p , q , and r are constants, independent of x , given by

$$\begin{aligned} p &= N \rho g^{1/2} s^{3/2} \\ q &= \frac{2}{\pi} \alpha C \rho g^{1/2} s^{1/2} \\ r &= \frac{5}{4} \alpha^2 \rho g^{3/2} s^{5/2} \frac{\sin \theta_B}{(gh_B)^{1/2}} \end{aligned} \quad (8)$$

In the expression for r the quantities θ_B and h_B signify the values of θ and h at the breaker line, but the values at any other particular location might also be chosen.

Now let us introduce the nondimensional variables

$$X = x/x_B \quad V = v/v_0 \quad (9)$$

where v_0 is the velocity defined by equation 55 of paper 1:

$$v_0 = \frac{5\pi}{8} \frac{\alpha}{C} (g h_s)^{1/2} s \sin \theta_s \quad (10)$$

Then, noting that $h_s = s x_s$, we find that (7) reduces to the simple form

$$P \frac{\partial}{\partial X} \left(X^{5/2} \frac{\partial V}{\partial X} \right) - X^{1/2} V = \begin{cases} -X^{3/2} & 0 < X < 1 \\ 0 & 1 < X < \infty \end{cases} \quad (11)$$

where

$$P = (\pi/2)(sN/\alpha C) \quad (12)$$

Thus P is a nondimensional parameter representing the relative importance of the horizontal mixing.

If there is no horizontal mixing, $P = 0$ and we obtain the simple solution

$$V = \begin{cases} X & 0 < X < 1 \\ 0 & 1 < X < \infty \end{cases} \quad (13)$$

noted in section 6 of paper 1. That is to say, the current increases linearly from the shoreline to the breaker line. Beyond the breaker line it is zero. At the breaker line itself the current velocity is discontinuous.

For general values of P equations 11 are to be solved subject to the boundary conditions that V is bounded when $0 < X < \infty$ and that at the breaker line $X = 1$ both V and $\partial V/\partial X$ are to be continuous. (It is not necessary for V to vanish at $X = 0$, but we shall see that in fact it does.)

A particular integral of equations (11) in the region $0 < X < 1$ is given by

$$V = AX \quad 0 < X < 1 \quad (14)$$

where

$$A = 1/(1 - \frac{5}{2}P) \quad P \neq \frac{2}{5} \quad (15)$$

To this we must add a complementary function satisfying, in both regions, the homogeneous equation

$$P \frac{\partial}{\partial X} \left(X^{5/2} \frac{\partial V}{\partial X} \right) - X^{1/2} V = 0 \quad (16)$$

The above equation has a solution of the form

$$V = BX^p \quad (17)$$

where B is a constant, provided that

$$P(p + 3/2)p - 1 = 0 \quad (18)$$

In other words p must be a root of the quadratic equation

$$p^2 + 3/2p - 1/P = 0 \quad (19)$$

Denoting these roots by p_1 and p_2 , we have

$$p_1 = -\frac{3}{4} + \left(\frac{9}{16} + \frac{1}{P} \right)^{1/2} \quad (20)$$

$$p_2 = -\frac{3}{4} - \left(\frac{9}{16} + \frac{1}{P} \right)^{1/2}$$

Clearly $p_1 > 0$ and $p_2 < 0$. Hence the complete solution to (11) is of the form

$$V = \begin{cases} B_1 X^{p_1} + AX & 0 < X < 1 \\ B_2 X^{p_2} & 1 < X < \infty \end{cases} \quad (21)$$

The boundary conditions at $X = 1$ are then satisfied by taking

$$B_1 = \frac{p_2 - 1}{p_1 - p_2} A \quad B_2 = \frac{p_1 - 1}{p_1 - p_2} A \quad (22)$$

It is useful to note that from (19)

$$p_1 + p_2 = -3/2 \quad p_1 p_2 = -1/P \quad (23)$$

and so

$$\begin{aligned} (p_1 - 1)(p_2 - 1) &= p_1 p_2 - (p_1 + p_2) + 1 \\ &= \frac{5}{2} - \frac{1}{P} = \frac{-1}{AP} \end{aligned} \quad (24)$$

Then we have also

$$B_1 = [P(1 - p_1)(p_1 - p_2)]^{-1} \quad (25)$$

$$B_2 = [P(1 - p_2)(p_1 - p_2)]^{-1}$$

Equation 21, together with (22) or (25), represents the solution to the problem, for general values of P .

For $P = 2/5$ the particular integral (14) no longer applies. Instead we have a different particular integral

$$V = -\frac{5}{2} X \ln X \quad 0 < X < 1 \quad (26)$$

Since $p_1 = 1$ and $p_2 = -5/2$ for $P = 2/5$, we obtain, as before,

$$V = \begin{cases} \frac{1}{2} X - \frac{5}{2} X \ln X & 0 < X < 1 \\ \frac{1}{2} X^{-5/2} & 1 < X < \infty \end{cases} \quad (27)$$

The constants multiplying X and $X^{-5/2}$ are chosen to satisfy the continuity of V and $\partial V/\partial X$ at $X = 1$. Equation 27 also represents the limit of the solution (21) when $P \rightarrow 2/5$.

3. DISCUSSION

The current profiles given by equation 20 have been calculated and plotted in Figure 1 for various values of the horizontal mixing parameter P . These current profiles have the following properties.

1. *Velocity near the breaker line.* As $P \rightarrow 0$, the profile tends to the triangular form (13) appropriate to zero mixing. There is a single maximum velocity $V_{max} \rightarrow 1$ just to the left of the breaker line. To the right of the breaker line we have $V \rightarrow 0$.

2. *Velocity at the breaker line.* When $X = 1$ we have from (21) and (25)

$$V_B = [P(1 - p_2)(p_1 - p_2)]^{-1} \quad (28)$$

On using the values of p_1 and p_2 given by (20) we find that in the limit, as $P \rightarrow 0$, $V_B \rightarrow 0.5$. In other words, the velocity at the breaker line is the mean of the limiting velocities on either side. This was foreshadowed in paper 1, section 6. Now as P increases from zero to infinity, V_B decreases monotonically from 0.5 to 0. At large

values of P we find that asymptotically

$$V_B \sim 4/15P \quad \text{as } P \rightarrow \infty \quad (29)$$

Values of V_B for some representative values of P are given in Table 1. Also, when $P = 2/5$, we have

$$V_B = 10/49 = 0.2041 \quad (30)$$

3. *Maximum velocity.* The velocity profile generally has a single maximum value V_{max} lying within the surf zone ($0 < X < 1$). To find the position X_m of this maximum, we differentiate (21) and obtain

$$0 = B_1 p_1 X_m^{p_1-1} + A \quad (31)$$

Therefore from (22)

$$X_m = \left[\frac{p_1 - p_2}{p_1(1 - p_2)} \right]^{1/(p_1-1)} \quad (32)$$

From (21) and (31) the corresponding velocity is given by

$$V_{max} = \left(1 - \frac{1}{p_1} \right) A X_m \quad (33)$$

Using the values of p_1 and p_2 given by (20), we can show that, as $P \rightarrow 0$, $X_m \rightarrow 1$ and $V_{max} \rightarrow 1$, and, as $P \rightarrow \infty$, both X_m and V_{max} tend to

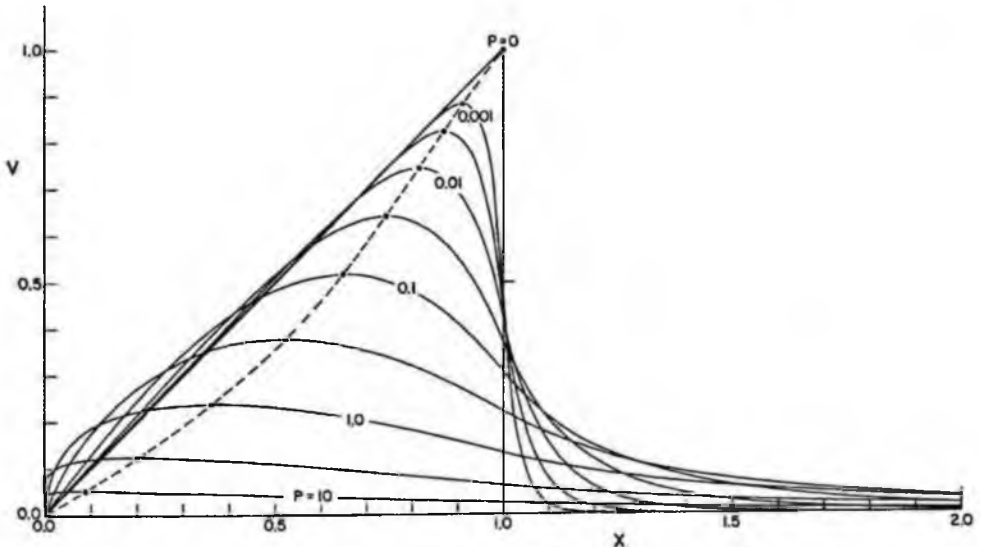


Fig. 1. The form of the current profiles as given by (21) for a sequence of values of the mixing parameter P .

TABLE 1. Parameters of the Velocity Profile (21) for Various Values of P

$\log_{10} P$	V_B	$\langle V \rangle$	V_{max}	X_m	Q_1	Q_2	Q
$-\infty$	0.5000	0.5000	1.0000	1.0000	1.0000	0.0000	1.0000
-3.0	0.4735	0.4847	0.8835	0.9108	0.9542	0.0467	1.0000
-2.5	0.4544	0.4733	0.8254	0.8699	0.9208	0.0824	1.0032
-2.0	0.4233	0.4542	0.7456	0.8148	0.8654	0.1447	1.0101
-1.5	0.3754	0.4230	0.6422	0.7422	0.7780	0.2546	1.0327
-1.0	0.3077	0.3736	0.5173	0.6466	0.6496	0.4615	1.1111
-0.5	0.2226	0.2992	0.3786	0.5198	0.4803	0.9822	1.4625
0.0	0.1333	0.2000	0.2400	0.3600	0.2933	∞	∞
0.5	0.0628	0.1024	0.1246	0.1984	0.1399	∞	∞
1.0	0.0240	0.0408	0.0524	0.0861	0.0537	∞	∞
1.5	0.0081	0.0141	0.0191	0.0316	0.0183	∞	∞
2.0	0.0026	0.0046	0.0064	0.0107	0.0059	∞	∞

0 in such a way that

$$V_{max} \sim \frac{2}{3} X_m \tag{34}$$

Thus X_m covers the entire range of X values between 0 and 1. For $P = 2/5$ we find from (27)

$$X_m = e^{-5/7} = 0.4895 \tag{35}$$

$$V_{max} = \frac{16}{15} X_m = 0.3496$$

The values of V_{max} and X_m corresponding to some representative values of P are shown in Table 1. It appears that, as P increases from 0 to ∞ , both V_{max} and X_m decrease steadily from 1 to 0.

Interpreting this result physically, we can say that the effect of increasing the horizontal mixing is to redistribute the momentum so that the fluid near the shoreline is dragged along at a faster speed by the fluid farther offshore, but farther offshore the fluid is slowed down by the mass beyond the breaker line.

4. *Gradient of velocity profile at the shoreline.* As $X \rightarrow 0$, we see from (21) that

$$\partial V / \partial X \sim B_1 p_1 X^{p_1 - 1} + A \tag{36}$$

$$P \neq 2/5$$

So long as $p_1 > 1$, the horizontal velocity gradient remains finite and equal to A . However, when $p_1 < 1$ the gradient at $X = 0$ becomes infinite. The critical case $p_1 = 1$ corresponds to $P = 2/5 = 0.4$. Thus we have

$$\lim_{X \rightarrow 0} \frac{\partial V}{\partial X} = \begin{cases} 1/(1 - \frac{2}{3}P) & 0 \leq P < 2/5 \\ \infty & 2/5 \leq P < \infty \end{cases} \tag{37}$$

5. *Total transport.* In the longshore direction the total transport can easily be found by integration of vh with respect to the offshore distance x . Without horizontal mixing the total transport Q_0 was shown in paper 1, section 6 to be given by

$$Q_0 = \frac{1}{3} v_0 h_B x_B \tag{38}$$

where v_0 is given by (10). This follows from the fact that vh is proportional to x^2 . When $P > 0$, the transport within the surf zone is given by

$$Q_1 = v_1 h_B x_B \int_0^1 V X \, dX \tag{39}$$

$$= \left(\frac{3B_1}{2 + p_1} + A \right) Q_0$$

On the other hand, the transport beyond the surf zone is given by

$$Q_2 = v_0 h_B x_B \int_1^\infty V X \, dX = \begin{cases} \frac{-3B_2}{2 + p_2} Q_0 & p_2 < -2 \\ \infty & p_2 \geq -2 \end{cases} \tag{40}$$

For $p_2 < -2$, which corresponds to $P < 1$, the total transport Q , which equals $(Q_1 + Q_2)$, is given by

$$Q = \left(\frac{3B_1}{2 + p_1} - \frac{3B_2}{2 - p_2} + A \right) Q_0 \tag{41}$$

which after some reduction becomes simply

$$Q = Q_0 / (1 - P) \tag{42}$$

When $P \geq 1$, the transport outside the surf zone (and hence the total transport) becomes infinite. This must mean that a steady state cannot be established in a finite time, over the whole field. However, the flow within any finite distance of the shoreline can still be established effectively within a finite time.

6. *Mean current* ($\langle V \rangle$). The mean current in the surf zone, given by

$$\langle V \rangle = \int_0^1 V dX$$

$$= \begin{cases} \frac{B_1}{p_1 + 1} + \frac{A}{2} & P \neq \frac{2}{3} \\ 55/196 & P = \frac{2}{3} \end{cases} \quad (43)$$

is plotted in Figure 2 with V_B and V_{max} as functions of the mixing parameter P . Each is a monotonically decreasing function of P . The corresponding ratios $V_B/\langle V \rangle$, V_B/V_{max} , and $\langle V \rangle/V_{max}$ (Figure 3) can be seen to vary between somewhat narrower limits. In particular, V_B/V_{max} lies always between 0.4 and 0.6.

The most remarkable feature of Figure 1 is that, even when the mixing parameter P varies by a factor of three orders of magnitude (from 0.001 to 1.0), the corresponding value of the velocity V_{max} changes by a factor of less than 4. This is in striking contrast to the dependence

of the velocity on the drag coefficient C on the bottom. Since v_0 is inversely proportional to C (but P depends also on C), we see that v itself is nearly inversely proportional to C .

4. COMPARISON WITH OBSERVATION

The most careful laboratory studies of longshore currents along a plane beach appear to be those of *Galvin and Eagleson* [1965]. Their model beach was 22 feet wide and had a gradient of about 0.11. Some care must be taken, even with these experiments, in comparing theory and observation since, as the authors themselves emphasize, the measured currents were not uniform along the beach but were being accelerated downstream from one end of the beach. This effect is probably present, but unrecognized, in many other laboratory measurements. One result of the acceleration must be to entrain fluid from beyond the surf zone into the surf zone itself, which may have an effect similar to a horizontal exchange of momentum by eddy viscosity.

The parameters for Galvin and Eagleson's experiments are summarized in Table 2. Their measurements for which the angle of incidence differed from zero were in series II, III, and IV, the deep-water angles of incidence for these series being 10°, 20°, and 51°, respectively. In

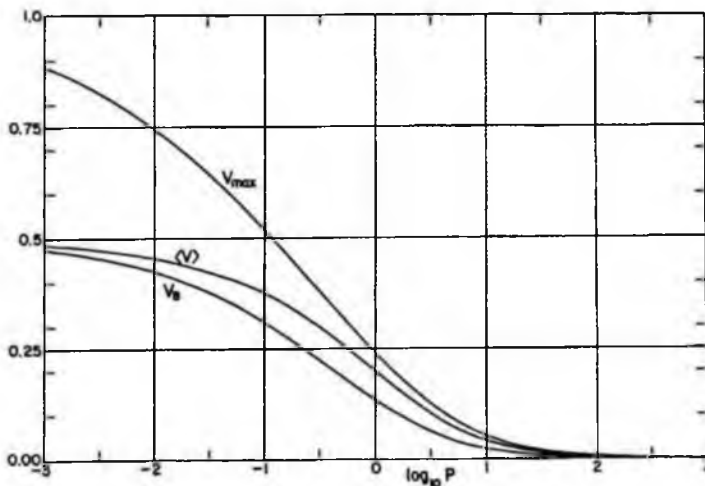


Fig. 2. The theoretical values of V_B (the velocity at the breaker line), V_{max} (the maximum velocity) and $\langle V \rangle$ (the mean velocity in the surf zone $0 < X < 1$) as functions of the mixing parameter P .

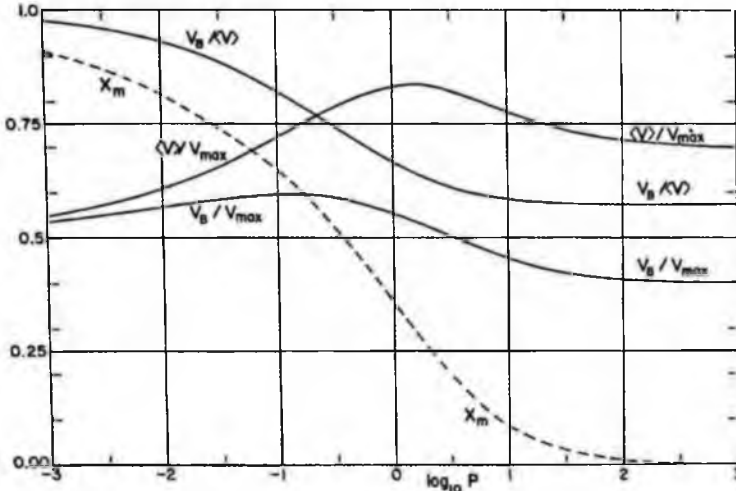


Fig. 3. The ratios V_s/V , V_s/V_{max} , and $(V)/V_{max}$ as functions of the mixing parameter P (full lines). The dashed line gives the coordinate X_m of the position of maximum velocity.

runs 2 to 6 of each series the wave period was varied, and in runs 7 to 11 the period was kept constant and the amplitude was varied.

The measurements thought most likely to represent steady unaccelerated conditions were those at a distance of 15 feet, or about $\frac{2}{3}$ the width of the beach, from the upstream end. For each velocity profile we have assumed as origin of X (in our notation) the mean position of the swash zone, taken at a distance $(r - W/2)$ from the still water line. Here r , as in Galvin and Eagleson [1965], denotes the runup distance and W denotes the width of the swash zone. No measurements being available, we have assumed W to be given closely enough by $\frac{1}{2}sgT^2$, which is the distance through which a particle would slide down the beach under gravity in a time equal to half the wave period T . The distance b of the breaker line offshore is tabulated by Galvin and Eagleson, so that altogether we have

$$X = \frac{\xi + r - W/2}{b + r - W/2} \quad (44)$$

where ξ is the horizontal distance offshore from the still water line ($\xi = Y$, in the notation of Galvin and Eagleson).

To normalize the measured velocity v , we define v_0 by (10), in which h_s is assumed to be very nearly equal to sb (if allowance is made

for wave setup, the appropriate value of s is reduced by about 10%; see appendix 1); θ_s is the measured angle of incidence at the breaker line (see Table 2). In series IV, however, the present approximate theory in which θ_s^* is negligible cannot very well be justified. Accordingly a rough correction has been made in Figure 4 by replacing the value of v_0 in Table 2 by $v_0 \cos \theta_s$, where θ_s is the angle of incidence in deep water. Though not rigorous, this correction factor can be justified on the grounds that the total longshore force exerted by the waves is equal to $\frac{1}{2} E_0 \cos \theta_s \sin \theta_s$, where E_0 is the wave energy density in deep water (see section 3 of paper 1). Since the total longshore thrust is proportional to $\cos \theta_s$, we expect the longshore current v will, on average, be reduced by approximately this amount.

In the experiments, the parameters r , b , and θ_s were found to fluctuate to some extent both with time and with distance along the shore. However, rather than use the local values of these quantities at the position of the current profile, we have adopted the longshore averages r_{av} , b_{av} , and $(\theta_s)_{av}$ given in Table A3 of Galvin and Eagleson [1965]. The purpose of doing so is to help reduce the statistical variability. In addition, we note that the longshore currents are, in fact, affected not only by the local values of h_s and θ_s but also by conditions along the

LONGSHORE CURRENTS, 2

6797

TABLE 2. Parameters for the Model Experiments of Galvin and Eagleson [1965]

Run	θ_B , deg	H_B , feet	T , sec	r_{av} , feet	b_{av} , feet	$W/2$, feet	v_0 , ft/sec	V_{max}	$\log_{10}P$
Series II									
2	5.4	0.191	1.000	1.01	1.62	0.22	2.08	0.25	-0.04
3	5.1	0.167	1.125	1.06	1.53	0.28	1.84	0.35	-0.40
4	3.3	0.143	1.250	1.07	1.33	0.34	1.12	0.48	-0.86
5	2.3	0.121	1.375	1.15	1.24	0.42	0.74	0.69	-1.72
6	3.7	0.105	1.500	1.04	1.17	0.50	1.18	0.35	-0.40
7	2.6	0.050	1.250	0.62	0.62	0.34	0.59	0.40	-0.58
8	3.1	0.098	1.250	0.77	0.87	0.34	0.83	0.35	-0.40
9	3.8	0.124	1.250	1.03	1.21	0.34	1.21	0.41	-0.62
10	3.7	0.130	1.250	1.03	1.07	0.34	1.12	0.46	-0.80
11	4.0	0.156	1.250	1.08	1.44	0.34	1.40	0.46	-0.80
Series III									
2	14.1	0.191	1.000	0.95	1.52	0.22	5.01	0.39	-0.55
3	12.1	0.167	1.125	1.05	1.51	0.28	4.30	0.42	-0.65
4	10.1	0.143	1.250	1.05	1.44	0.34	3.48	0.56	-1.17
5	9.2	0.121	1.375	1.05	1.13	0.42	2.80	0.61	-1.37
6	6.9	0.105	1.500	1.06	1.04	0.50	2.04	0.70	-1.77
8	6.6	0.098	1.250	0.75	0.85	0.34	1.76	0.66	-1.58
9	8.7	0.124	1.250	0.89	1.11	0.34	2.64	0.60	-1.33
11	11.2	0.156	1.250	1.10	1.55	0.34	4.01	0.49	-0.90
Series IV									
2	28.0	0.191	1.000	0.84	1.40	0.22	9.29	0.37	-0.47
3	21.9	0.167	1.125	0.88	1.15	0.28	6.74	0.44	-0.72
4	18.6	0.143	1.250	1.02	1.22	0.34	5.87	0.53	-1.05
5	15.8	0.121	1.375	1.17	1.32	0.42	5.04	0.55	-1.13
6	8.6	0.105	1.500	0.90	0.91	0.50	2.37	0.55	-1.13
7	13.4	0.050	1.250	0.59	0.69	0.34	3.18	0.39	-0.55
8	14.3	0.098	1.250	0.79	0.83	0.34	3.71	0.48	-0.86
9	19.7	0.124	1.250	0.86	1.19	0.34	6.13	0.39	-0.55
10	19.7	0.130	1.250	0.97	1.27	0.34	6.34	0.47	-0.83
11	22.6	0.156	1.250	1.12	1.29	0.34	7.26	0.46	-0.80
12	6.0	0.062	1.500	0.54	0.57	0.50	1.31	0.57	-1.21
13	20.2	0.110	1.000	0.72	0.88	0.22	5.37	0.46	-0.80

whole length of the beach. (There was some uncertainty in the measurement of θ_B [see Galvin and Eagleson, 1965] and hence in the appropriate values of v_0 and V_{max} .)

The results of the comparison are shown in Figure 4. Each plot in the diagram is identified by the number of the corresponding run in Table 2. It will be seen that most of the points lie between two of the theoretical curves derived in section 2, namely the curves corresponding to $P = 0.4$ and $P = 0.1$. Individual profiles (such as that numbered 11 in Figure 4a) tend to follow quite closely the predicted profile for some particular value of P ; the maximum velocity always lies not far from the dotted curve, which represents the locus of maximums in Figure 1.

The values of V_{max} corresponding to each of

the profiles in Figure 4 are shown in Table 2. Also shown are the corresponding values of P derived from Figure 2. It can be seen that P varies from 0.40 to about 0.01.

How does P vary with other parameters: the wave height and period, the angle of incidence, and the beach slope? Before a definite answer can be given, further experiments covering a wider range of conditions are necessary. There is some evidence from Table 2 that P is an increasing function of the wave frequency ($2\pi/T$) and also of the breaker height in deep water (H_D). The value of P can also increase with the angle of incidence θ_B .

It is striking that few profiles correspond to values of P greater than the critical value of 0.4 (see section 3). At this value of P the gra-

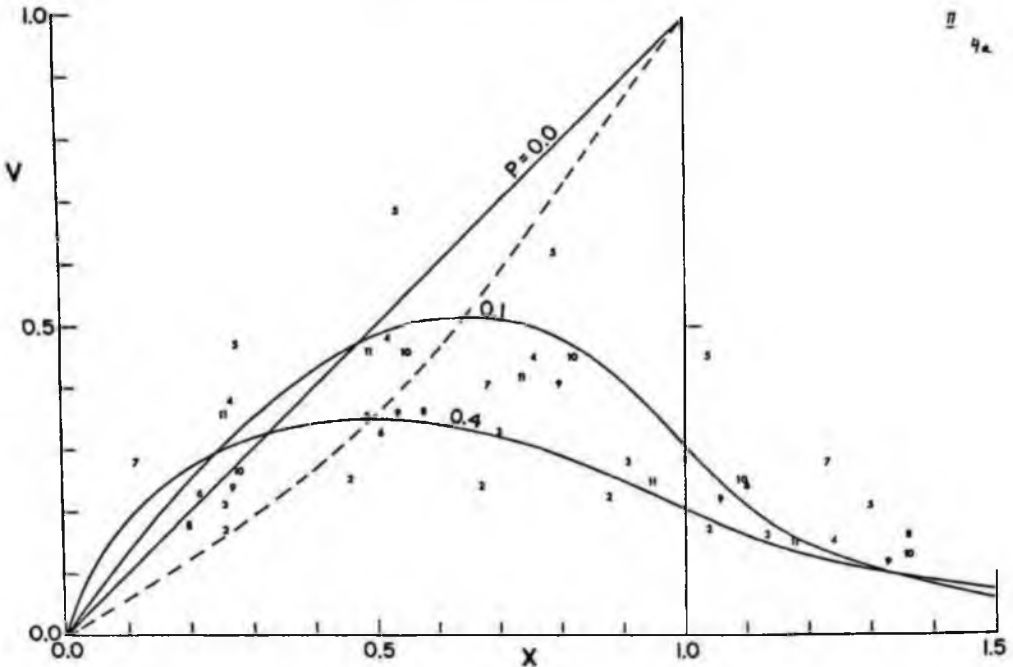


Fig. 4a. Comparison of the longshore velocities measured by Galvin and Eagleson [1965; series III] with the theoretical profiles derived in section 2 of the present paper. The plotted numbers correspond to the number of each run (Table 2).

dent of the current at $X = 0$ becomes infinite. One is tempted to conjecture that this is in fact the greatest possible value of P , and that the presence of the shoreline controls the horizontal mixing so that the value of 0.40 is not exceeded.

In support of this conjecture we can note that the corresponding value of V_s is about 0.20, or one-fifth, whereas a rough argument in section 6 of paper 1 showed that V_s should never be less than about one-sixth. As shown in paper 1, both laboratory measurements and field observations seem to point to 0.2 as being a common value for V_s .

APPENDIX 1. AN ALLOWANCE FOR WAVE SETUP

It is well known [Saville, 1961] that waves approaching a beach cause a change in the mean water level, or wave setup, in the shelving zone. The effect is caused by the onshore component of radiation stress [Longuet-Higgins and Stewart, 1962, 1963]. Outside the breaker zone, the wave setup η is slightly negative, but inside the surf zone, the region with which we are con-

cerned here, $d\eta/dx$ and hence η become appreciably positive. Thus the local depth $h(x)$ should, in practice, be replaced by the effective depth $(h + \eta)$, and the bottom slope s should be replaced by

$$s^* = -\frac{d}{dx}(h + \eta) \tag{A1}$$

Now it has been shown both theoretically and experimentally by Bowen *et al.* [1968] that within the surf zone

$$\frac{d\eta}{dx} = -\frac{1}{1 + (2/3\alpha^2)} \frac{dh}{dx} \tag{A2}$$

(see equation 12 and Figure 5 of their paper, with $y = 2\alpha$). Thus, if α is constant, the gradient of the mean surface level is simply proportional to the gradient of the beach. From (A2) it follows that

$$\frac{dh}{dx} + \frac{d\eta}{dx} = \frac{1}{1 + 3\alpha^2/2} \frac{dh}{dx} \tag{A3}$$

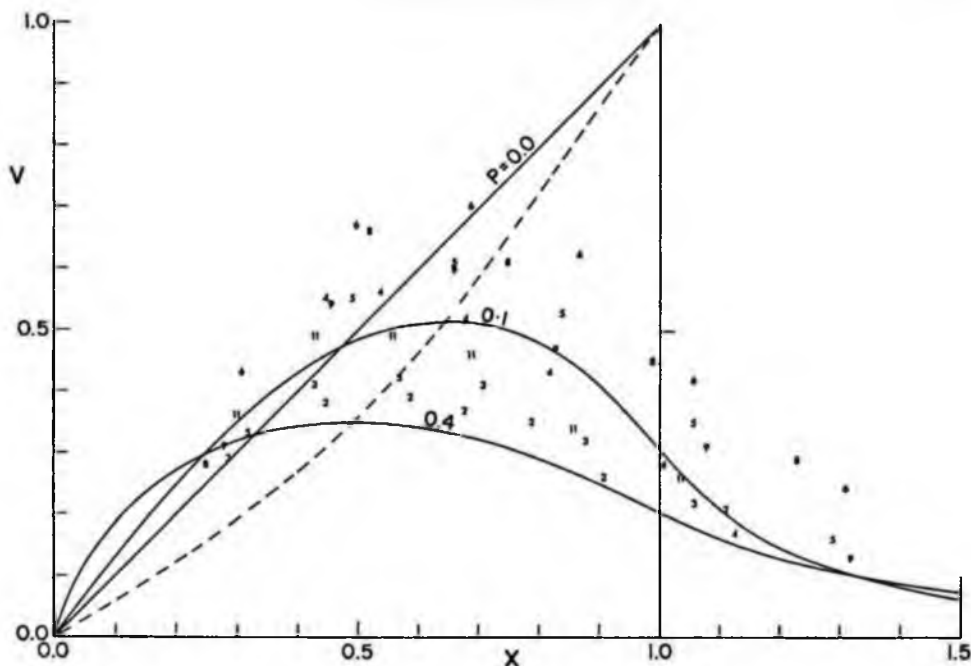


Fig. 4b. Comparison of the longshore velocities measured by Galvin and Eagleson [1965; series III] with the theoretical profiles derived in section 2 of the present paper. The plotted numbers correspond to the number of each run (Table 2).

and hence

$$s^* = \frac{s}{1 + 3\alpha^2/2} \quad (\text{A4})$$

Equation 10 can therefore be modified to read

$$v_0 = \frac{5\pi}{8} \frac{\alpha^* s}{C} (gh_B)^{1/2} \sin \theta_B \quad (\text{A5})$$

where

$$\alpha^* = \frac{\alpha s^*}{s} = \frac{\alpha}{1 + 3\alpha^2/2} \quad (\text{A6})$$

A graph of α^* as a function of α is shown in Figure 5. It should be noted that over much of the range of α the value of α^* differs little from its minimum value:

$$\alpha_{\text{max}}^* = (6)^{-1/2} = 0.4082 \quad (\text{A7})$$

In fact there is little error if we take $\alpha = 0.5$, about in the middle of the observed range. Correspondingly we have $\alpha^* = 0.36$. Hence the appropriate value of v_0 might be some 12% less than the value given by (10) with $\alpha = 0.41$.

APPENDIX 2. THE STOKES VELOCITY

In any fluctuating field of motion there is a systematic difference between the mean velocity measured by a freely floating object (the Lagrangian mean velocity) and the mean velocity recorded by a current meter at a fixed point (the Eulerian mean velocity). The difference between the Lagrangian and the Eulerian mean velocities has been called the Stokes velocity [Longuet-Higgins, 1969] after G. G. Stokes [1847], who discovered it for surface waves on water of uniform depth. A general expression for the Stokes velocity \bar{U}_s is given by

$$\bar{U}_s = \left\langle \int \mathbf{u}_1 dt \cdot \nabla \mathbf{u}_1 \right\rangle \quad (\text{B1})$$

where \mathbf{u}_1 denotes the first-order particle motion, assumed periodic with mean zero, and the angle brackets denote the mean value with respect to time. Thus \bar{U}_s depends on the space gradient of the orbital velocity \mathbf{u}_1 .

In shallow-water wave theory, the orbital velocity is independent of the vertical coordinate,

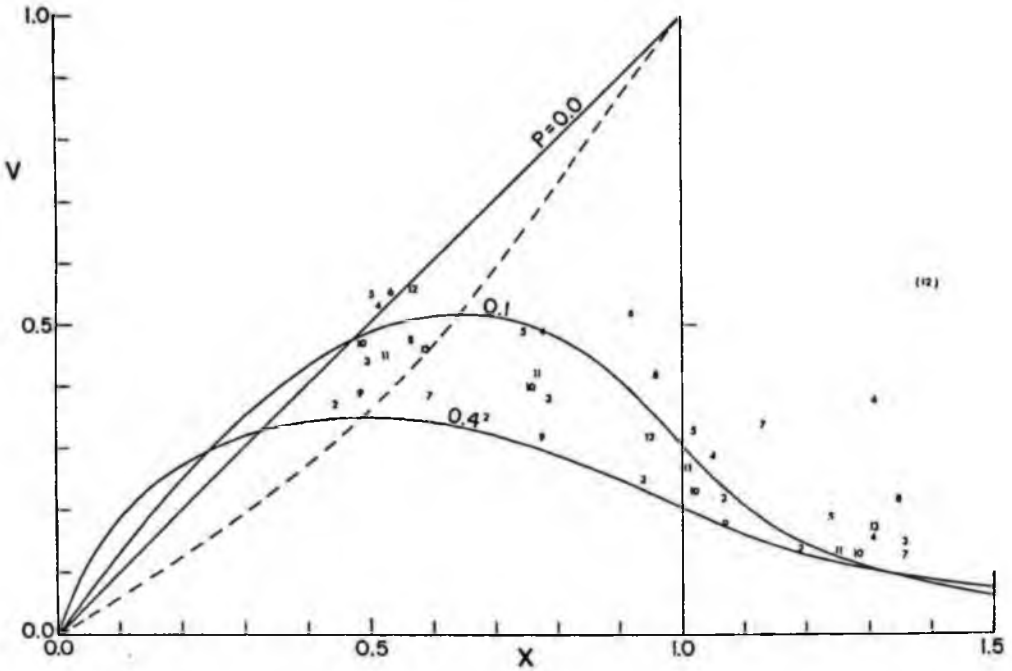


Fig. 4c. Comparison of the longshore velocities measured by Galvin and Eagleson [1965; series IV] with the theoretical profiles derived in section 2 of the present paper. The plotted numbers correspond to the number of each run (Table 2).

and so likewise is U_s . Nevertheless, the horizontal gradients of u_1 still give rise to a non-zero Stokes velocity. If u_1 and v_1 denote the x and y components of u_1 , the longshore component of U_s is given by

$$V_s = \left\langle \int u_1 dt \frac{\partial v_1}{\partial x} \right\rangle + \left\langle \int v_1 dt \frac{\partial v_1}{\partial y} \right\rangle \quad (B2)$$

Consistent with our previous use of the linearized shallow-water theory, we have

$$u_1 = \alpha(gh)^{1/2} \cos \theta \cos (lx + my - \sigma t) \quad (B3)$$

$$v_1 = \alpha(gh)^{1/2} \sin \theta \cos (lx + my - \sigma t)$$

where

$$l = k \cos \theta \quad m = k \sin \theta \quad (B4)$$

k being the absolute wave number. By Snell's law, the longshore wave number m is a constant, but the onshore wave number l is related to the frequency σ and the local depth h by the rela-

tion

$$\sigma^2 = k^2 gh = (l^2 + m^2)gh \quad (B5)$$

On substituting from (B3) into (B2) and noting that $\partial m/\partial x$, $\partial m/\partial y$, $\partial l/\partial y$, $\partial h/\partial y$, and $\partial \theta/\partial y$ all vanish we obtain

$$V_s = \frac{1}{2} \alpha^2 (gh/\sigma) [(l + x \partial l/\partial x) + m] \cdot \cos \theta \sin \theta \quad (B6)$$

If we ignore $\partial l/\partial x$ in comparison with l/x , the above expression reduces to

$$V_s = \frac{1}{2} \alpha^2 (gh/c) [\cos \theta + \sin \theta] \cos \theta \sin \theta \quad (B7)$$

where $c = \sigma/k$ denotes the phase velocity. When θ^2 is negligible, (B7) becomes simply

$$V_s = \frac{1}{2} \alpha^2 gh (\sin \theta/c) \quad (B8)$$

The last factor is constant, by Snell's law. Hence the Stokes velocity increases linearly with the

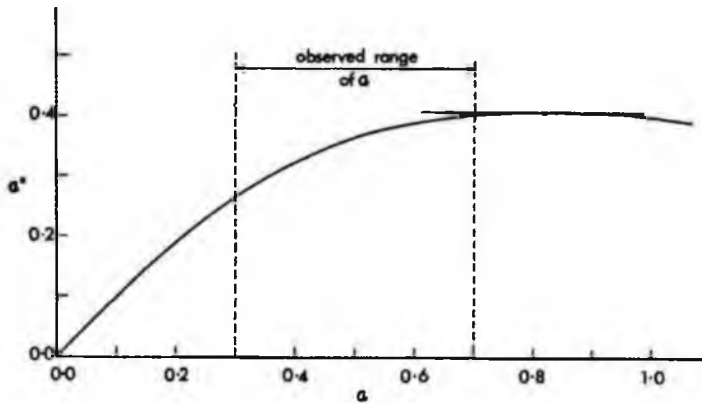


Fig. 5. The virtual coefficient α^* as a function of α .

depth h and hence linearly with distance from the shoreline.

To show that $\partial l/\partial x$ is negligible in comparison with l/x , we have from (B5)

$$l^2 = (\sigma^2/gh) - m^2 \quad (\text{B9})$$

$$2l \partial l/\partial x = -(\sigma^2/gh^2) \partial h/\partial x$$

Therefore, if $h = sx$

$$2l \partial l/\partial x = (l^2 + m^2)/x \quad (\text{B10})$$

Thus $\partial l/\partial x \ll l/x$, provided that

$$l^2 + m^2 \ll 2l^2 \quad (\text{B11})$$

that is to say $m^2 \ll l^2$ or $\tan^2 \theta \ll 1$. Since θ^2 has been neglected, this condition is already satisfied by our previous assumptions.

Let us now compare the magnitude of the Stokes velocity, as given by (B8), with the scale velocity v_0 defined by (10). At the breaker line the ratio of the two is given by

$$\frac{V_s}{v_0} = \frac{4}{5\pi} \frac{\alpha C}{s} \quad (\text{B12})$$

With the values $s = 0.11$, $C = 0.010$, and $\alpha = 0.41$ we have simply $V_s/v_0 = 0.01$, which is negligible.

On the other hand, with very gently sloping beaches, where s is much smaller than the value in Galvin and Eagleson's experiments, the Stokes velocity may very well have to be taken into account.

Acknowledgments. I am grateful to Dr. A. J. Bowen and Dr. C. J. Galvin for comments on the

first draft of this paper, which was prepared at Corvallis under NSF grant GA-1452. The two appendices were added after my return to England in June 1969.

REFERENCES

- Bowen, A. J., The generation of longshore currents on a plane beach, *J. Mar. Res.*, **27**, 206-215, 1969.
- Bowen, A. J., D. L. Inman, and V. P. Simmons, Wave 'set-down' and set-up, *J. Geophys. Res.*, **73**, 2569-2577, 1968.
- Galvin, C. J., and P. E. Eagleson, Experimental study of longshore currents on a plane beach, *U.S. Army Coast. Eng. Res. Cent., Tech. Mem.* **10**, 1-80, 1965.
- Longuet-Higgins, M. S., On the transport of mass by time-varying ocean currents, *Deep-Sea Res.*, **16**, 431-477, 1969.
- Longuet-Higgins, M. S., On the longshore currents generated by obliquely incident sea waves, **1**, *J. Geophys. Res.*, **75**, this issue, 1970.
- Longuet-Higgins, M. S., and R. W. Stewart, Radiation stress and mass transport in gravity waves, *J. Fluid Mech.*, **10**, 481-504, 1962.
- Longuet-Higgins, M. S., and R. W. Stewart, A note on wave set-up, *J. Mar. Res.*, **21**, 4-10, 1963.
- Prandtl, L., *Essentials of Fluid Dynamics*, 452 pp., Haffner, New York.
- Saville, T., Model study of sand transport along an infinitely long straight beach, *Trans. AGU*, **31**, 555-565, 1950.
- Saville, T., Experimental determination of wave set-up, *Proc. 2nd Tech. Conf. on Hurricanes*, U. S. Dep. Commerce, Rep. **50**, 242-252, 1961.
- Stokes, G. G., On the theory of oscillatory waves, *Trans. Cambridge Phil. Soc.*, **8**, 441-455, 1847.

(Received January 29, 1970.)

The mean forces exerted by waves on floating or submerged bodies with applications to sand bars and wave power machines

BY M. S. LONGUET-HIGGINS, F.R.S.

*Department of Applied Mathematics and Theoretical Physics,
Silver Street, Cambridge and Institute of Oceanographic Sciences,
Wormley, Surrey*

(Received 2 June 1976)

[Plates 1-4]

Water waves transport both energy and momentum, and any solid body which absorbs or reflects wave energy must absorb or reflect horizontal momentum also. Hence the body is subject to a mean horizontal force. In low waves, the force may be calculated immediately when the incident, reflected and transmitted wave amplitudes are known. For wave power devices the mean force can be large, so that anchoring presents practical problems.

Experiments with models of the Cockerell wave-raft and the Salter 'duck' accurately confirm the predicted magnitude of the force at low wave amplitudes. For steeper waves, however, the magnitude of the force can be less than that given by linear theory. By experiments with submerged cylinders, it is shown that this is due partly to the presence of a free second harmonic on the down-wave side.

In breaking waves, it is confirmed that the mean force on submerged bodies is sometimes reduced, and even reversed. An explanation is suggested in terms of the 'wave set-up' produced by breaking waves. Submerged cylinders act as a kind of double beach. A negative mean force arises from an asymmetry in the breaking waves, associated with a time-delay in the response to the change in depth.

Similar arguments apply to submerged reefs and sand bars. Experiments with a model bar show that long low waves propel the bar towards the shore, whereas steep, breaking waves propel it seawards. This is similar to the observed behaviour of off-shore sand bars.

The existence of a horizontal momentum flux (or radiation stress) in water waves is demonstrated by using it to propel a small craft.

1. INTRODUCTION

Economically interesting methods of extracting power from sea waves have recently been proposed by Masuda (1972), Salter (1974), Woolley & Platts (1975) and others. Remarkably high efficiencies have been obtained in the laboratory. The present investigation was prompted by the realization that any device which extracts energy must on general grounds be subject to a mean horizontal force. Not only can

this force be large, but it has a special practical significance in that its effect on an anchor cannot be reduced by any flexibility in the mooring cable.

Consider a two-dimensional irrotational wave train of amplitude a travelling with velocity c , in deep water. Owing to the mass transport velocity (see Lamb 1932, ch. 9) the waves have an average horizontal momentum I , which for low waves is simply proportional to the square of the wave amplitude:

$$I = \frac{1}{2}\rho g a^2/c, \quad (1.1)$$

where ρ is the density and g is gravity. Hence we expect a horizontal flux of momentum given by Ic_g , where c_g denotes the group-velocity. In deep water $c_g = \frac{1}{2}c$. So we expect a momentum flux

$$Ic_g = \frac{1}{4}\rho g a^2 \quad (1.2)$$

per unit distance across the waves. This flux is closely associated with the radiation stress (see Longuet-Higgins & Stewart 1964).

Suppose we have any wave power device acted on by the waves as in figure 1. If it absorbs all the wave energy then it must absorb the momentum also. Hence we expect that it will be subject to a mean horizontal force

$$F = \frac{1}{4}\rho g a^2 \quad (1.3)$$

per unit distance across the waves. If all the wave energy is reflected, then the momentum is all reversed, and the resulting force is just doubled. In general, we expect that the body will be subject to a force

$$F = (Ic_g)_{in} + (Ic_g)_{ref} - (Ic_g)_{trans} \quad (1.4)$$

where the terms on the right represent the momentum fluxes in the incident, reflected and transmitted waves respectively. In deep water this becomes

$$F = \frac{1}{4}\rho g(a^2 + a'^2 - b^2), \quad (1.5)$$

where a , a' and b are the respective wave amplitudes.

The maximum value of this expression $\frac{1}{4}\rho g a^2$ is equal to the horizontal stress acting on a dam, erected across a reservoir of depth a equal to the wave amplitude. If a is measured in metres, this force is $\frac{1}{2}a^2$ t/m (tonnes force per metre) measured along the dam. Thus waves of amplitude $a = 10$ m correspond to a maximum force of 50 t/m.

In water of finite depth h , the ratio c_g/c is more generally equal to $(\frac{1}{2} + kh/\sinh 2kh)$ where k is the wavenumber. This leads one to expect that in general

$$F = \frac{1}{4}\rho g(a^2 + a'^2 - b^2)(1 + 2kh/\sinh 2kh) \quad (1.6)$$

the last factor tending to unity as the depth tends to infinity.

In §2 of this paper we shall first establish equation (1.6) theoretically, under certain conditions. Thus the wave amplitude must be sufficiently small for the bilinear theory to apply, which excludes breaking waves, for example. Nevertheless under appropriate conditions equation (1.6) can be generalized so as to evaluate

the total force on any number of floating or submerged bodies, and to the situation where the undisturbed depths of water on the up-wave and down-wave sides are unequal. Hence we can consider applying the result to submerged bodies and submarine reefs.

In §3 we shall describe experiments which verify equation (1.6) experimentally for a Cockerell wave raft, and for a Salter 'duck' in waves of moderate amplitude.

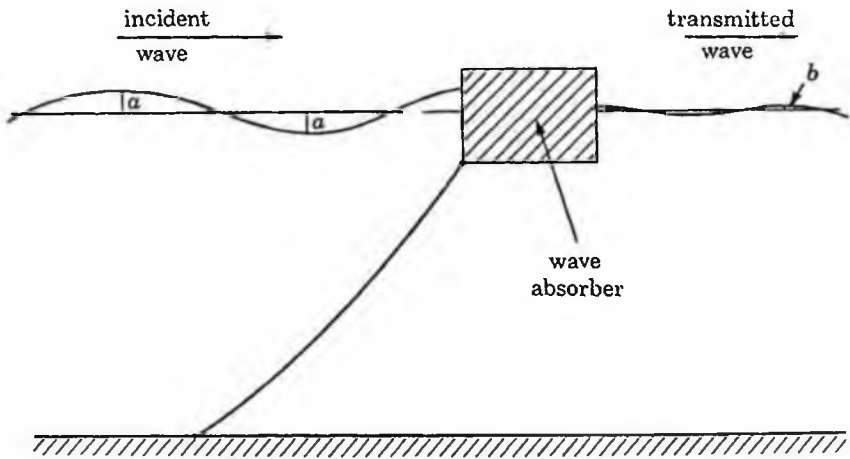


FIGURE 1. Schematic representation of a wave absorber situated in a train of waves.

For totally submerged bodies, however, it is found experimentally that the mean force can be less than expected, and in §5 we show theoretically and experimentally that this is due partly to the presence of a second harmonic in the transmitted wave.

In breaking waves, Salter has found an even more drastic reduction, and even a reversal, of the mean force. This is discussed in §6, and a qualitative explanation is put forward in terms of the wave set-up. In §7 it is verified experimentally that a similar reversal can occur on submerged sand bars, long low waves driving the bars shorewards, but shorter, breaking waves driving them seawards.

Finally we discuss briefly the possibility of using wave momentum to propel a small craft. This is demonstrated by means of a model.

2. THE BILINEAR THEORY

We shall first establish theoretically the results stated in the Introduction. The arguments, which are simple, depend solely on the conservation of the mean momentum.

Suppose that waves of low amplitude a approach from the left in water of undisturbed depth h . They are incident upon any number of floating or submerged bodies (which may be absorbing or generating wave energy at the same frequency) confined to a finite horizontal range. For simplicity, the mean depth on the right is assumed

to be the same as that on the left, in the first place. The amplitudes of the reflected and transmitted waves are denoted by a' and b respectively, and we allow for a small, second-order displacement $\bar{\zeta}$ of the mean surface level on the left, and $(\bar{\zeta} + \Delta\bar{\zeta})$ on the right, due to the waves.

Horizontal and vertical coordinates are denoted by x and z , with x in the direction of the incident wave and z measured vertically upwards from the undisturbed mean water level. The horizontal and vertical components of the particle velocity are denoted by u and w .

A general expression for the flux of horizontal momentum across a vertical plane $x = \text{constant}$ is

$$\int_{-h}^{\zeta} (p + \rho u^2) dz,$$

where p is the pressure, ρ the density and $\zeta(x, t)$ the local elevation of the free surface. Subtracting the corresponding flux in the *absence* of the waves (which arises solely from the hydrostatic pressure $p_0 = -\rho gz$, and taking averages with respect to the time, we obtain the excess flux of momentum due to the waves as

$$S = \overline{\int_{-h}^{\zeta} (p + \rho u^2) dz} - \int_{-h}^0 p_0 dz. \quad (2.1)$$

In the case $a' = 0$, $\bar{\zeta} = 0$, this is just the radiation stress, which for waves of small amplitude has been evaluated by Longuet-Higgins & Stewart (1960, 1964). Generalizing their argument we note first that (2.1) may be written

$$S = \overline{\int_0^{\zeta} p dz} + \int_{-h}^0 \overline{(p - p_0 + \rho u^2)} dz \quad (2.2)$$

correct to second order. Now by conservation of *vertical* momentum of the fluid contained between (1) the free surface $z = \zeta$, (2) the horizontal plane $z = \text{constant}$ and (3) any two vertical planes one wavelength apart, we have

$$\overline{p + \rho w^2} - \rho g(\bar{\zeta} - z) = \overline{p_0 + \rho gz},$$

where an overbar now denotes the double average over both a period and a wavelength. Therefore

$$\bar{p} - p_0 = \rho g \bar{\zeta} - \rho \bar{w}^2 \quad (2.3)$$

and on substituting in (2.2) and taking averages over a wavelength we obtain

$$\bar{S} = \overline{\int_0^{\zeta} p dz} + \int_{-h}^0 \overline{\rho(u^2 - w^2)} dz + \rho g h \bar{\zeta}. \quad (2.4)$$

In the above integrals we may substitute the well-known first-order expressions for the pressure p and the orbital velocities u , w in Stokes waves of arbitrary depth $h \doteq h + \bar{\zeta}$, namely

$$u = \phi_x, \quad w = \phi_z, \quad p/\rho = \phi_t - gz, \quad \zeta = g^{-1}(\phi_t)_{z=0}.$$

where
$$\phi = [a \cos(kx - \sigma t) + a' \cos(kx + \sigma t)] \frac{\sigma \cosh k(z+h)}{k \sinh kh}$$

and
$$\sigma^2 = gk \tanh kh$$

(see, for example, Lamb 1932, ch. 9). On taking averages with respect to x and t , all terms proportional to the product aa' vanish, and we obtain

$$\bar{S} = \frac{1}{2} \rho g (a^2 + a'^2) (1 + 4kh/\sinh 2kh) + \rho gh \bar{\zeta} \quad (2.5)$$

correct to second order. So the momentum fluxes in the incident and reflected waves are simply added. The last term $\rho gh \bar{\zeta}$ can be considered as the effect of an additional hydrostatic pressure $\rho g \bar{\zeta}$ exerted throughout the whole depth h .

Consider now the horizontal momentum of the fluid contained between two fixed vertical planes $x = x_1, x_2$, one far to the left and the other far to the right. If F denotes the sum of the mean horizontal forces exerted by the fluid on all the solid bodies contained between these two planes, then the flux of horizontal momentum from the bodies to the water is just $-F$. Assuming the mean horizontal momentum of the water to be conserved, we must therefore have

$$F = S_1 - S_2,$$

where S_1 and S_2 denote the fluxes of momentum across the two planes. In this equation we can take averages with respect to x_1 and x_2 , each over one wavelength, with the result

$$F = \frac{1}{4} \rho g (a^2 + a'^2 - b^2) (1 + 4kh/\sinh 2kh) - \rho gh \Delta \bar{\zeta} \quad (2.6)$$

from (2.4).

To complete the calculation we must now evaluate the difference $\Delta \bar{\zeta}$ in the mean level on the two sides. To do this we introduce the further assumption (see Longuet-Higgins 1967) that the motion is irrotational to second order. Then we may use the Bernoulli integral

$$p/\rho + \frac{1}{2}(u^2 + w^2) + gz + \partial\phi/\partial t = f(t)$$

and on taking both time and space averages we obtain

$$\bar{p}/\rho + \frac{1}{2}(\overline{u^2 + w^2}) + gz = C(t),$$

where C is independent of both x and z . Combining this with equation (2.3) and writing $z = 0$, $p_0 = 0$ we have

$$g \bar{\zeta} = -\frac{1}{2}(\overline{u^2 - w^2})_{z=0} + C/\rho$$

and so

$$g \Delta \bar{\zeta} = -\frac{1}{2}(\overline{u^2 - w^2})_{z=0} \Big|_{x=-\infty}^{x=\infty}. \quad (2.7)$$

Now substituting the first-order expression for the orbital velocities u and w we find

$$g \Delta \bar{\zeta} = \frac{1}{4} g (a^2 + a'^2 - b^2) \frac{2k}{\sinh 2kh}. \quad (2.8)$$

This combined with equation (2.5) gives us

$$F = \frac{1}{4}\rho g(a^2 + a'^2 - b^2)(1 + 2kh/\sinh 2kh), \quad (2.9)$$

the result to be proved.

When the depths of water on the two sides are unequal it is easily seen that the same arguments lead to

$$F = \frac{1}{4}\rho g(a^2 + a'^2)(1 + 2kh_1/\sinh 2kh_1) - \frac{1}{4}\rho gb^2(1 + 2kh_2/\sinh 2kh_2),$$

where h_1 and h_2 denote the mean depths on the two sides. That is to say

$$F = (Ic_g)_{in} + (Ic_g)_{ref} - (Ic_g)_{trans} \quad (2.10)$$

as expected.

We note that the assumption of a steady mean surface level ($\bar{\zeta} + \Delta\bar{\zeta}$) on the down-wave side may be appropriate only when there is a beach or other barrier to restrict the mean flow on the down-wave or the up-wave side. Otherwise, if the waves were started from rest, it would be difficult to achieve a steady state in a limited time.

The assumption that the flow is irrotational to second order also implies that the waves are not breaking.

3. EXPERIMENTAL VERIFICATION

A Cockerell wave raft, consisting of six hinged floats each 12 in long \times 23.5 in wide (see figures 8 and 9, plate 1) was placed in a wave tank of length 40 ft and width $W = 2$ ft. Periodic waves were generated by a plunger at one end of the tank, and absorbed by a sloping beach at the other. Power was extracted by a simple arrangement of pumps, generally two at each hinge, raising water to a height 1.6 m above the mean water level. The mean force on the float was measured with a spring balance.

Figure 2 shows a typical set of results for waves of period 1.0 s in water of depth $h = 0.36$ m. The measured force is plotted against the expression

$$WF = \frac{1}{4}\rho gW(a^2 + a'^2 - b^2)$$

at various wave amplitudes a . The broken line in figure 2 represents the force that would be exerted in deep water. The full line represents the theoretical force (1.6) after adjustment by the factor for finite depth, and it can be seen that the agreement is close. At higher values of the wave amplitude the accuracy of the measurements was reduced by a long-period seiche (about 10 s) which was set up in the tank and affected both the wave amplitude and the forces on the raft.

Further details of the experiments are given in table 1.

Salter, Jeffrey & Taylor (1976) have measured the mean forces on a nodding 'duck', which absorbs a high proportion of the incident wave energy. In figure 4 we have plotted their measured values against the theoretical value $\frac{1}{4}\rho gWa^2$ for low waves in deep water. Although there is greater scatter than in our measurements the

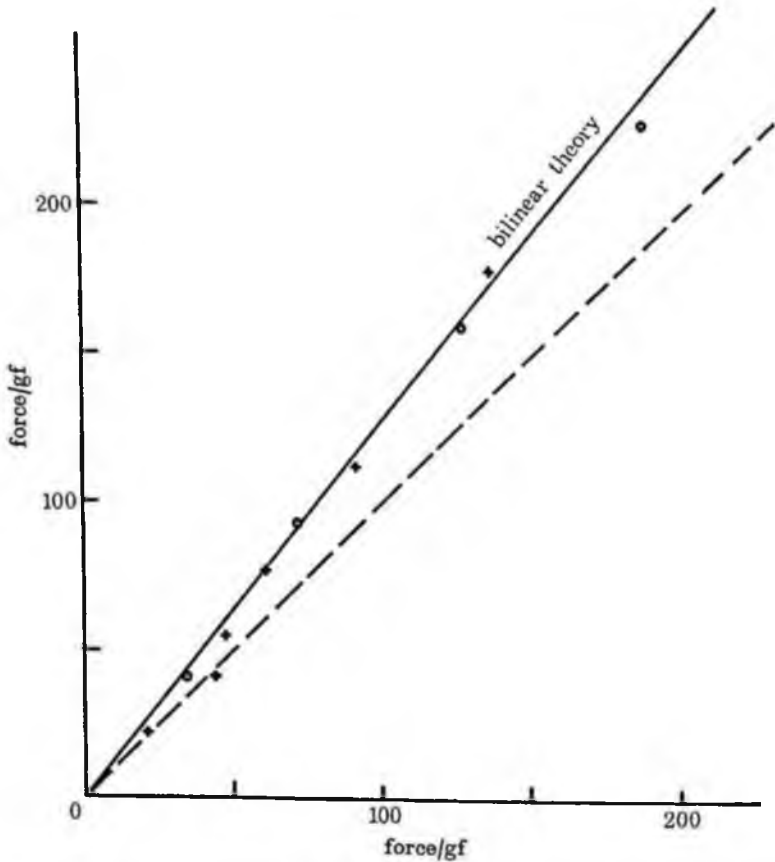


FIGURE 2. Mean horizontal forces on wave raft. Wave period $T = 1.0$ s; mean depth $h = 0.36$ m.

TABLE 1. PARAMETERS FOR THE DATA OF FIGURE 2

run	period/s	a/cm	$(a'/a)^2$	$(b/a)^2$	efficiency	loss
A1	1.00	1.71	.11	.34	.10	.44
A2	1.02	2.36	.07	.24	.14	.55
A3	1.04	3.03	.07	.17	.12	.64
A4	1.05	3.65	.07	.16	.15	.62
B1	1.01	1.31	.11	.32	.13	.44
B2	1.01	1.88	.11	.28	.16	.45
B3	1.02	1.88	.13	.25	.20	.42
B4	1.03	2.18	.05	.21	.19	.55
B5	1.04	2.68	.06	.22	.18	.54
B6	1.05	3.15	.08	.18	.17	.57

observed values in figure 4 are in fair agreement at low wave amplitudes. The points on the right of the figure are for breaking waves. It is not surprising that the agreement is less good. Nevertheless the reduction in force is interesting, and reasons for it will be discussed below.

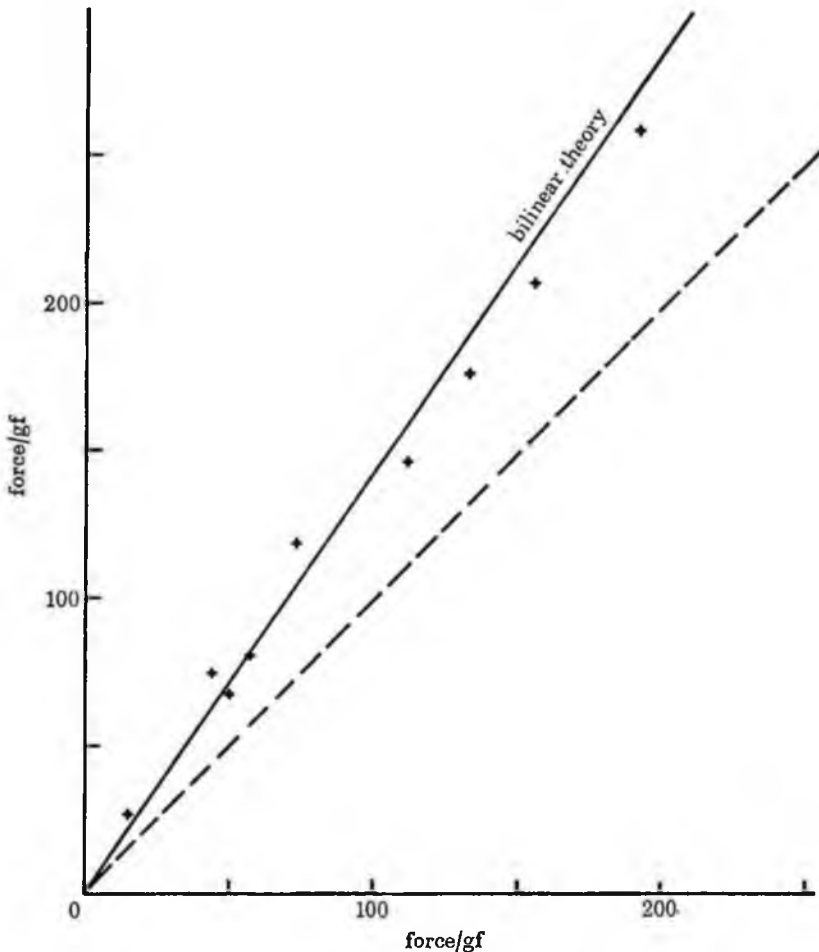


FIGURE 3. Mean horizontal forces on wave raft. $T = 1.0$ s, $h = 0.25$ m.

4. EXPERIMENTS WITH A SUBMERGED CIRCULAR CYLINDER

Salter *et al.* (1976) also measured the forces on a circular cylinder, held with axis horizontal so as to be completely submerged in still water. For non-breaking waves the mean horizontal force was found to be quite small, as would be expected from equation (1.5) since a submerged circular cylinder has in fact the remarkable property that its transmission coefficient is unity and its reflexion coefficient is zero, according to linearized non-viscous theory (Dean 1948; Ursell 1950; Ogilvie 1963). Thus in equation (1.5) we should have $a' = 0$, $b = a$.

At higher wave amplitudes, however, the horizontal force was observed to change sign, i.e. the mean force was found to be *towards* the wavemaker. How is this to be explained?

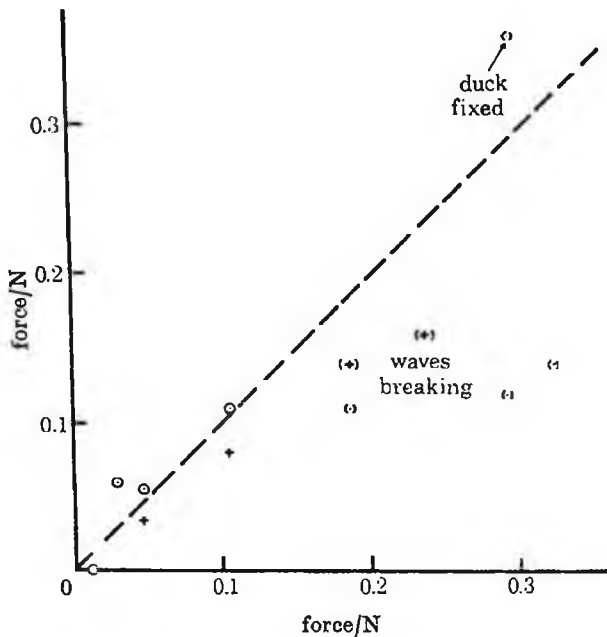


FIGURE 4. Mean horizontal forces acting on a Salter 'duck'.

The present author carried out a somewhat similar experiment in which a submerged cylinder of diameter 15 cm was suspended below the surface by a vertical arm, free to swing about a pivot above the surface (see figures 10 and 11, plate 2). In this way the cylinder was constrained vertically but was free to make small oscillations in a horizontal direction. Being flooded internally, the mean density only slightly exceeded that of the water, and the period of free oscillation (about 10 s) was long compared to the wave period.

Now the amplitude of the waves reflected from a submerged, neutrally buoyant cylinder, constrained vertically but free horizontally, may be shown (see the appendix) to be given by

$$a'/a = \sin(\psi_1 - \psi_2), \quad (4.1)$$

where ψ_1 is the phase-lag of the force on a *fixed* cylinder (relative to the force on a fluid particle on the axis in the absence of the cylinder), and ψ_2 is the phase-lag of the displacement of a *completely free* cylinder (relative to the displacement of a particle on the axis, in the absence of the cylinder). The amplitude of the transmitted wave is then

$$b'/a = \cos(\psi_1 - \psi_2). \quad (4.2)$$

The angles ψ_1 and ψ_2 have been computed by Ogilvie (1963), and with the parameters of the experiment it is found that a'/a is fairly small, lying between 0.25 and 0.35. For incident waves of moderate amplitude we therefore expect a small mean force on the cylinder, directed down-wave.

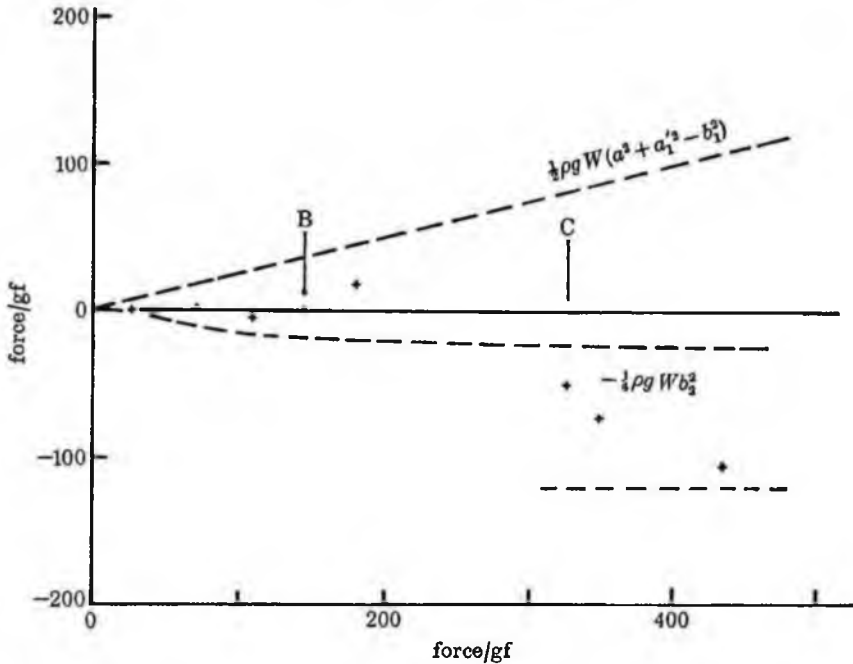


FIGURE 5. Mean horizontal forces on a submerged circular cylinder. Wave period 1.0 s, mean depth 0.52 m: depth of immersion 5.0 cm.

Figure 5 shows a typical set of measurements when the depth d of immersion (of the uppermost part of the cylinder below the still-water level) was 5.0 cm. The horizontal axis corresponds to the value of $\frac{1}{4}\rho g W a^2$, and is a measure of the incident momentum flux. The broken line represents the measured value of $\frac{1}{4}\rho g W (a^2 + a_1'^2 - b_1^2)$, where a , a_1' and b_1 are the measured amplitudes of the incident, reflected and transmitted fundamental frequencies. The ratios a_1'/a and b_1/a were found to be in fair agreement with equations (4.1) and (4.2). The measured mean forces are shown in figure 5 by crosses. Up to point *B*, where the waves were first observed to be breaking, the force was smaller than expected, though generally positive. After point *C* it had definitely reversed sign. Under these conditions the cylinder tended to be deflected strongly towards the wave-maker (see figure 11, plate 2). The effect was obviously similar to the one reported by Salter. We consider now some possible explanations.

5. THE EFFECT OF HIGHER HARMONICS

Waves in the presence of submerged bodies tend to behave quite non-linearly, and with a submerged cylinder it is easy to detect visually the presence of an appreciable second harmonic (twice the fundamental frequency) in the transmitted waves. The probable reason for this is that the wave amplitude above the cylinder quickly grows to a significant fraction of the local depth d . Also, the horizontal fluid velocity is of

order $(gd)^{\frac{1}{2}}$ or greater. Both these facts imply strong nonlinearity, and the production of higher harmonics. This is even without the occurrence of wave breaking.

Consider the effect of a second harmonic in the transmitted wave. Since the second harmonics have a frequency double that of the first harmonics, their group velocity in deep water is only $\frac{1}{2}c_g$. So their ratio of momentum flux to energy flux is doubled. Denoting the first and second harmonics in the reflected and transmitted waves by $a'_1, a'_2; b'_1, b'_2$ respectively, we have by conservation of energy

$$a^2 = (a'_1{}^2 + b'_1{}^2) + \frac{1}{2}(a'_2{}^2 + b'_2{}^2) + \epsilon, \quad (5.1)$$

where ϵ is a positive term representing the dissipation or extraction of energy. But by conservation of momentum

$$F = \frac{1}{4}\rho g[(a^2 + a'_1{}^2 - b'_1{}^2) + (a'_2{}^2 - b'_2{}^2)]. \quad (5.2)$$

If the reflected waves are small we may ignore $a'_1{}^2$ and $a'_2{}^2$ compared to the other terms, and on substituting for a^2 we have

$$F = \frac{1}{4}\rho g(\epsilon - \frac{1}{2}b'_2{}^2). \quad (5.3)$$

Thus the sign of the force depends on a balance between the dissipation term and the amplitude of the transmitted second harmonic. When the latter is larger, the radiation stress in the second harmonic reverses the sign of F .

To measure the second harmonic b_2 in the transmitted wave, the waves were abruptly shut off by lowering a gate into the water down-wave from the cylinder. The waves continued to be recorded at a fixed distance down-wave of the gate. The rear of the fundamental wave-train, of amplitude b_1 , passed first, with group velocity c_g ; then the rear of the second harmonic, travelling with velocity $\frac{1}{2}c_g$. Between the two times of arrival, the amplitude b_2 of the second harmonic could be measured.

The two upper curves in figure 5 show the measured values of $\frac{1}{4}\rho g W(a^2 + a'_1{}^2 - b'_1{}^2)$ and $-\frac{1}{4}\rho g W b'_2{}^2$. These represent the observed mean forces associated with the fundamental wave and with the transmitted second harmonic, respectively. The former, though not accurately measured, is necessarily positive. The latter is negative, and is of the same order as the measured force, but is limited in magnitude. (The lowest broken line corresponds to the force that would be exerted by a second harmonic of limiting steepness, in otherwise still water.)

We may conclude that the second harmonic contributes an appreciable part, but not all, of the observed negative force.

The explanation for the remainder of the force may lie partly in the existence of harmonics higher than the second, which are effectively damped before reaching the recording point (2.5 m from the cylinder). However, in breaking-wave conditions we must in all probability go beyond the range of small-amplitude, irrotational theory, as follows.

6. BREAKING WAVES

We suggest an explanation for the negative forces in breaking waves by analogy with the situation when waves approach a simple beach. The waves cause a change in the local mean water level ξ , called the wave 'set-up', which was studied experimentally by Saville (1961) and explained quantitatively by Longuet-Higgins & Stewart (1963, 1964). On entering shallow water the wave amplitude, after an initial decrease, begins to increase sharply. This produces an increase in the radiation stress (the momentum flux due to the waves) which has to be offset by a *decrease* in the hydrostatic pressure. The mean level therefore falls, and there is a wave 'set-down'. The set-down increases almost till the breaking point, when the waves begin to lose height and the radiation stress diminishes. The static pressure must now *increase*, and there is a dramatic rise in mean level, producing the much larger wave 'set-up'. Assuming that the breaker height is proportional to the local depth of water then it can be shown that the surface tilt is just proportional to the local slope s of the bottom ($\partial\xi/\partial s \doteq 0.2s$). This result has been rather accurately confirmed by Bowen, Inman & Simmons (1968).

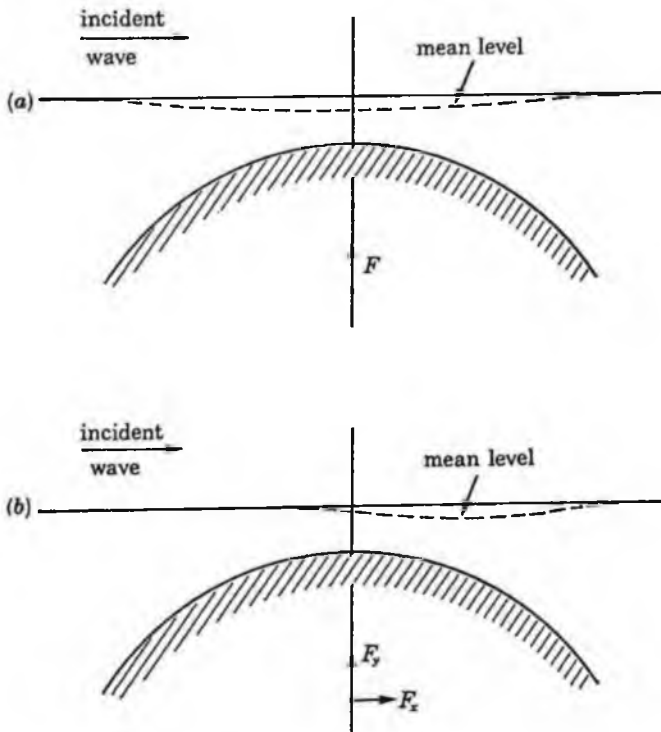


FIGURE 6. Schematic picture of the changes in mean sea level of waves in the presence of a submerged cylinder, if the waves are not breaking: (a) symmetrical; (b) unsymmetrical.

We may think of the set-up as being due to the waves shooting their horizontal momentum horizontally at the beach. The resulting pile-up is not statically maintained, but is balanced by the momentum flux term $(\rho u)u$, where u is the horizontal velocity of the particles.

Now we can think of a submerged circular cylinder as two beaches, back-to-back (see figures 6 and 7). Suppose first that there is no breaking (figure 6). Then there will be

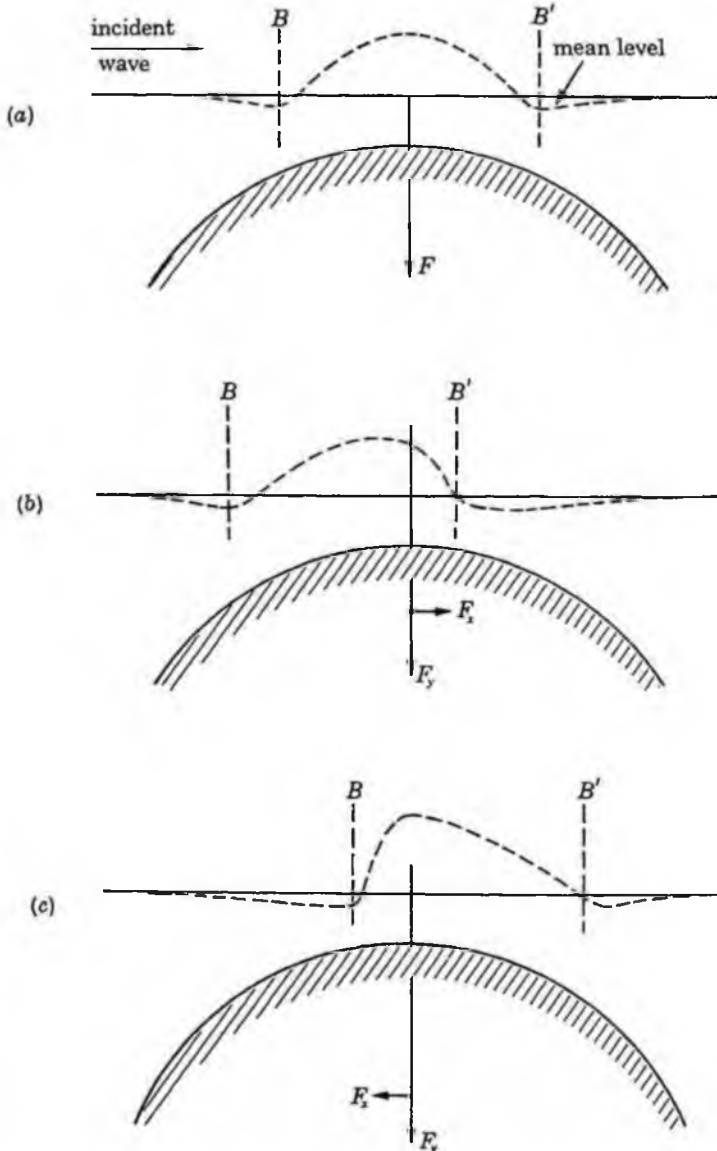


FIGURE 7. Schematic picture of the changes in mean level of waves in the presence of a submerged cylinder (a) symmetrical, (b) unsymmetrical, wavelength large compared to that of curvature (c) unsymmetrical, wavelength not large compared to radius of curvature.

a small wave set-down, but no set-up. If the set-down is symmetrical (figure 6*a*) there will be no mean horizontal force on the cylinder, but a small vertical force, directed upwards. This is in fact the situation for waves of *small* amplitude impinging on a submerged circular cylinder, either fixed or neutrally buoyant and free to move (see Ogilvie 1963). According to the linearized theory there is no reflexion. Hence the wave velocities may be all simply reversed in time, the incident and reflected waves having their rôles exchanged. The mean level must therefore be symmetric about the mid-point. For larger waves, however, both non-linearity and viscosity may make the mean level unsymmetrical, as in figure 6*b*. Then there can be a small horizontal force as well as a mean vertical force.

Suppose now that the waves are breaking as in figure 7. The points where the waves begin and end their breaking are shown by *B* and *B'* respectively. Outside these limits, approximately, there is a wave set-down. But inside, there is a much larger wave set-up, to balance the loss of horizontal momentum flux. If the set-up is symmetrical, as in figure 7*a*, there will be no mean horizontal force, but simply a large downwards force on the cylinder. If the set-up is unsymmetrical as in figure 7*b*, there will be a net horizontal force to the right. This is the situation we might expect if the wavelength is short compared to the diameter of the cylinder. For then the change in depth above the cylinder will be relatively slow and the breaker-height will have time to adjust to the local depth of water above the cylinder. To the right of the mid-point, when the depth begins to increase, breaking will soon cease, because the waves will no longer be forced to try to become steeper.

In the present experiments, however, the wavelength is not small compared to the diameter of the cylinder. The waves are forced to break, from their point of view, without much warning, and there is a delay in the onset of breaking until near the point of minimum depth. Moreover, breaking continues until some time after the depth begins to increase again. Hence the wave set-up is unsymmetrical as in figure 7*c*, with most of the set-up occurring on the right. This produces a net force to the left, as shown.

7. EXPERIMENTS WITH SUBMERGED BARS

If our reasoning is correct, a similar reversal of the mean force is to be expected when breaking waves impinge on a sand-bar or on any other submerged body resting on the bottom.

The author carried out exploratory tests with an artificial sand-bar mounted on wheels (see, figures 12 and 13, plate 3) which was free to move horizontally in either direction. When subjected to long, low waves (period $T = 1.15$ s, amplitude $a = 1.0$ cm) from the left (see plate 5) the mean force on the bar was positive. Thus the forces corresponding to the reflected wave predominated. If left entirely free, the bar tended to move towards the beach, with a mean speed of 0.95 cm/s.

When on the other hand the bar was subjected to short, steep waves ($T = 0.75$ s, $a = 4.0$ cm) the waves broke on the far side of the bar (see figure 13) and the mean

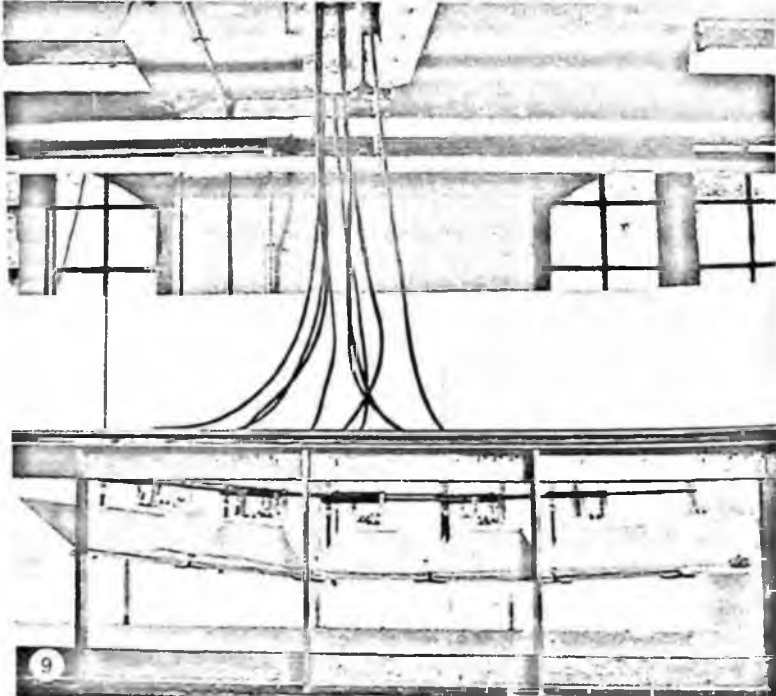
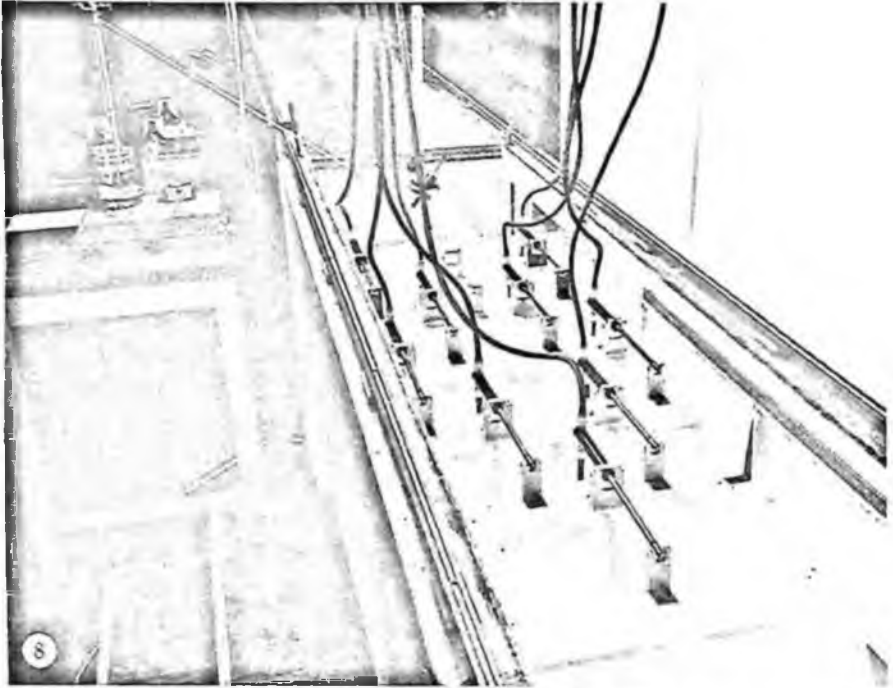


FIGURE 8. The wave raft in position, facing incident waves. On the left is the spring balance for measuring the mean horizontal force. Width of tank = 2 ft.

FIGURE 9. The raft under the action of waves: $T = 1.0$ s, $a = 2.0$ cm.

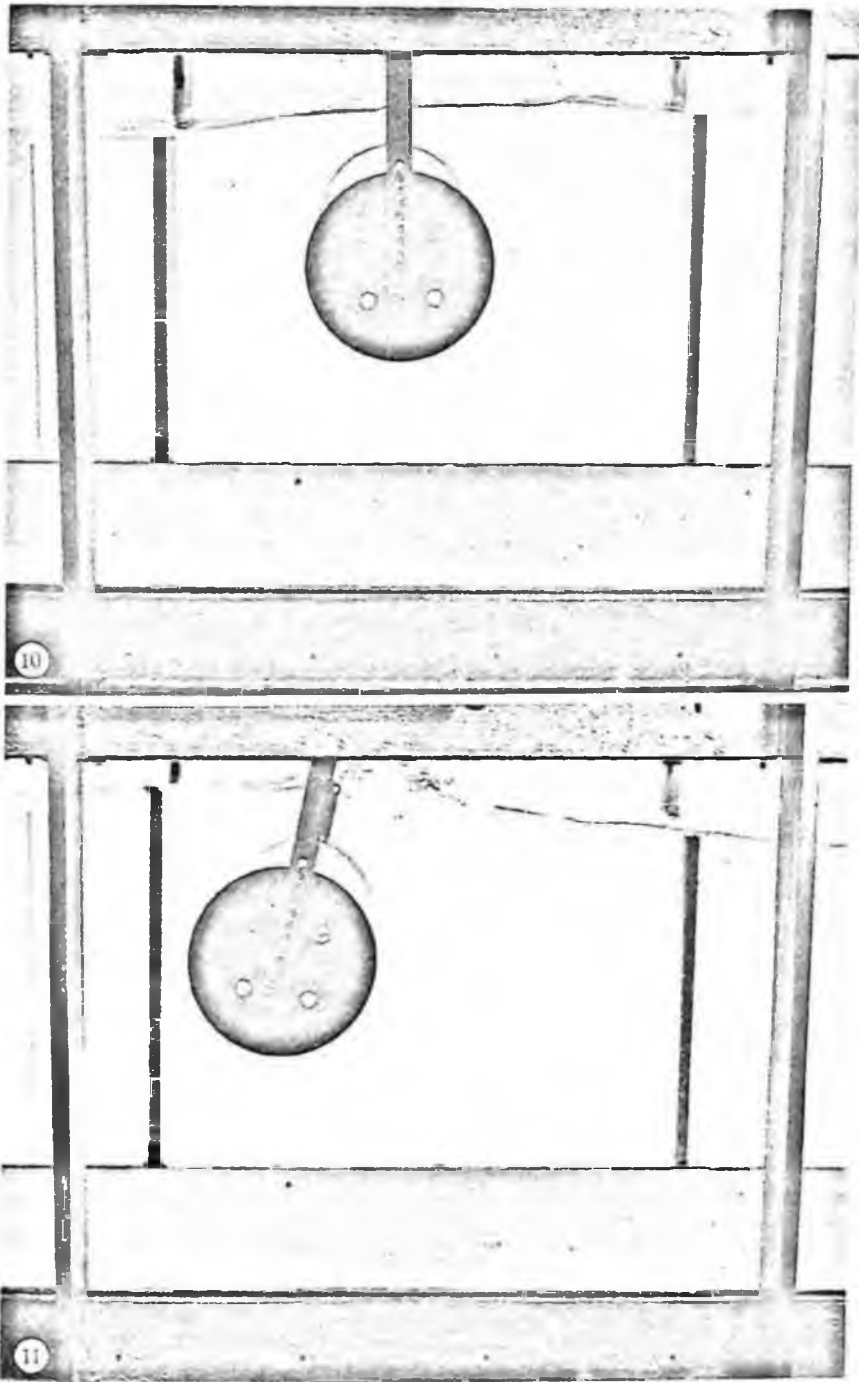


FIGURE 10. Submerged cylinder in low waves incident from the left: $d = 3.5$ cm, $T = 1.0$ s.
 $a = 1.5$ cm.

FIGURE 11. Submerged cylinder in breaking waves incident from the left: $d = 3.5$ cm,
 $T = 1.0$ s, $a = 4.0$ cm.

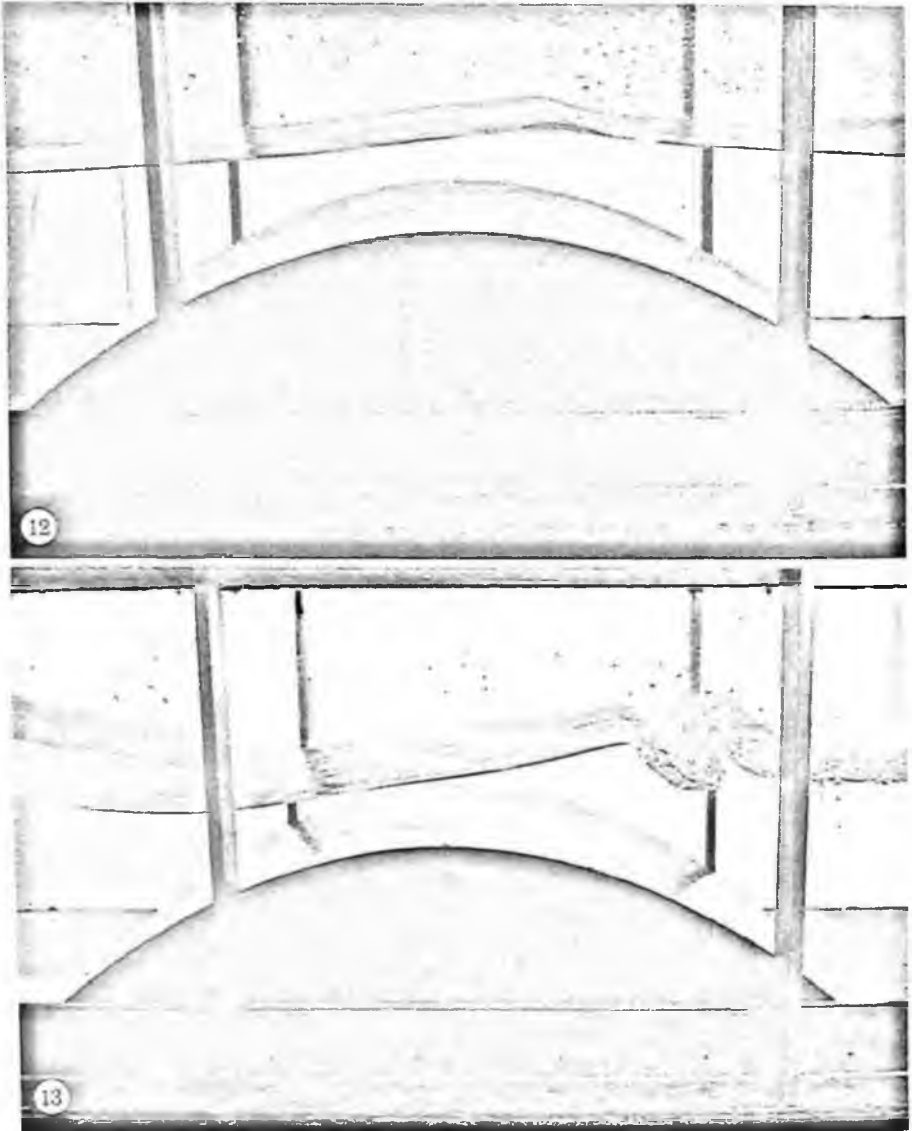
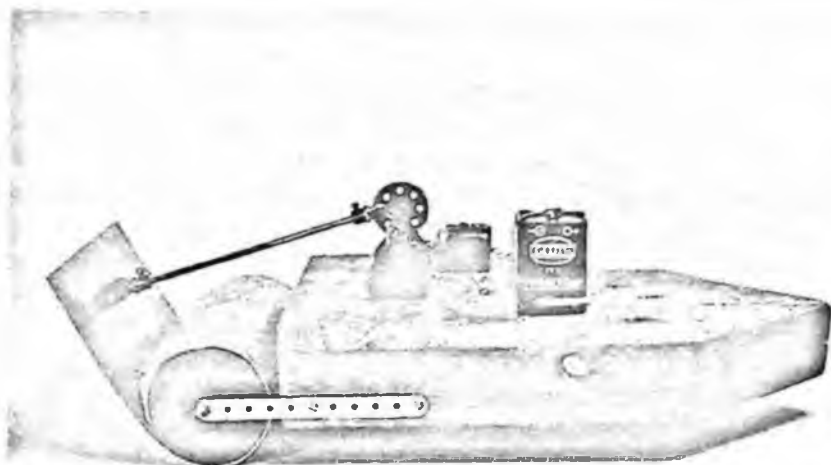
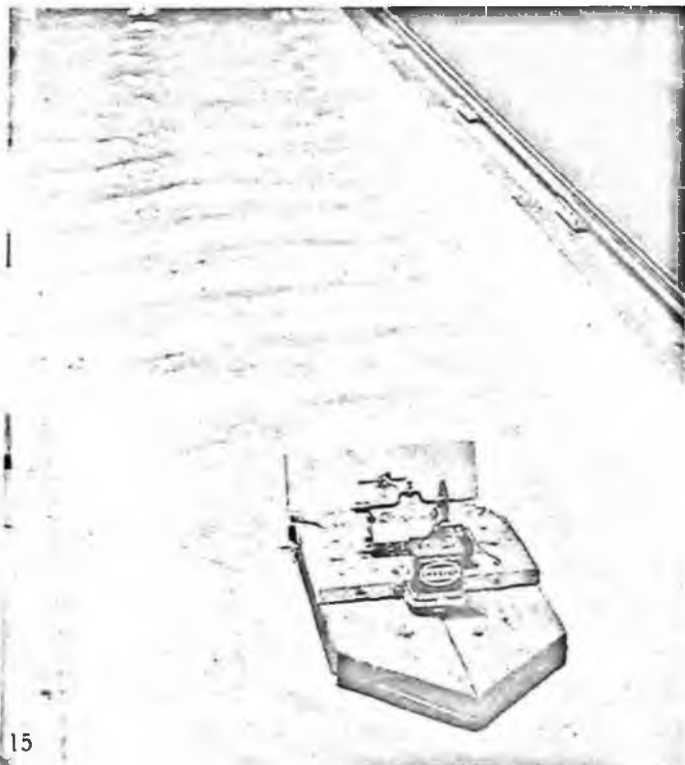


FIGURE 12. Artificial sand-bar in low waves incident from the left. $d = 7.0$ cm, $T = 1.15$ s, $a = 1.0$ cm. Mean motion of bar = 0.95 cm/s to the right.

FIGURE 13. Artificial sand-bar in steep waves incident from the left. $d = 7.0$ cm, $T = 0.75$ s, $a = 4.0$ cm. Mean motion of bar = 1.2 cm/s to the left.



14



15

FIGURE 14. Model boat (side view) with drive and Salter cam at stern.

FIGURE 15. Boat propelled by wave momentum flux. Forward speed 12 cm/s.

force was reversed. If left to itself the bar now tended to move in the reverse direction, with a mean speed -1.2 cm/s.

This behaviour is qualitatively similar to the well-known behaviour of offshore sand-bars; long, low waves tend to move them beachwards, but short, steep waves tend to move them seawards (Sheppard & LaFond 1940).

It is generally supposed that most of the sediment transport due to waves is either 'bed-load', taking place in a thin mobile layer close to the bottom, or else 'suspended load', i.e. carried at a higher level. However, preliminary observations by the author have suggested that it is also possible for the motion of the sand to penetrate much deeper, presumably in response to the horizontal pressure gradients in the waves above. In that case shear takes place at a lower level, and the mass above moves more nearly as a solid body.

It seems desirable to determine the importance of this effect by further experiments.

8. USE OF THE RADIATION STRESS FOR PROPULSION

The momentum flux in waves will necessarily produce a mean reaction on any wave-maker. Thus the radiation stress may be actually set up to use for propelling a small craft (see, figure 14, plate 4). In this model, a Salter cam is attached to the stern and is made to oscillate by attachment to a crank driven by a small electric motor. At wave-maker frequencies of 3 s^{-1} the boat is propelled along at speeds of 10–15 cm/s. The ratio of thrust to power expended on the waves is quite advantageous. For we have

$$I = E/c,$$

where E denotes the energy density $\frac{1}{2}\rho g a^2$ and c is the phase velocity. Hence the ratio of the thrust to the power expended is given by

$$F/Ec_g = Ic_g/Ec_g = 1/c.$$

This is larger than for some conventional propellers. The total thrust, at given frequency is however limited by the maximum steepness of the waves, and the need to avoid cross-waves, which only generate wave momentum in a transverse direction.

By designing a wave-power device in conjunction with a wave-maker on the down-wave side which generates waves at a higher frequency, it should be possible, on the basis of equation (5.3) to design a wave-powered craft which can advance against the waves. However, it is necessary for both the reflected wave amplitudes and the energy dissipated to be sufficiently small. In practice this requirement is quite stringent.

APPENDIX. PROOF OF EQUATIONS (4.1) AND (4.2)

Consider a submerged circular cylinder of radius R , either fixed or making small oscillations, with its axis horizontal and at a mean distance $(R+d)$ below the free surface. Let (x, y) be horizontal and vertical coordinates, with $x = 0$ as the plane of symmetry, and y vertically upwards, and let (ξ, η) denote the instantaneous displacements of the axis from its mean position. We consider two-dimensional motions, with waves approaching from, or diverging towards, $x = \infty$.

We know the following:

Theorem A. When the cylinder is fixed, then the coefficient of reflexion vanishes (Dean 1948; Ursell 1950).

Theorem B. When the cylinder is free and neutrally buoyant, then the coefficient of reflexion also vanishes (Ogilvie 1963).

Theorem C. When the centre describes a small circle, it generates or absorbs waves travelling only in the direction of the motion of the cylinder at the top of its orbit (Ogilvie 1963).

In general, let ζ_- and ζ_+ denote the free surface displacements as $x \rightarrow -\infty$ and $+\infty$ respectively. Consider the following situations.

(1) The cylinder generates waves by making small vertical oscillations:

$$\xi = 0, \quad \eta = ise^{-i\sigma t},$$

where s and σ are constants and t is the time. By symmetry about the plane $x = 0$ we have

$$\left. \begin{aligned} \zeta_+ &= ae^{i(kx - \sigma t + \alpha)}, \\ \zeta_- &= -ae^{i(-kx - \sigma t + \alpha)}, \end{aligned} \right\}$$

where a and α are amplitude and phase angles.

(2) The cylinder generates waves by making small horizontal oscillations:

$$\xi = se^{-i\sigma t}, \quad \eta = 0.$$

Because the motion is antisymmetric about $x = 0$,

$$\left. \begin{aligned} \zeta_+ &= \bar{a}e^{i(kx - \sigma t + \bar{\alpha})}, \\ \zeta_- &= -\bar{a}e^{i(-kx - \sigma t + \bar{\alpha})}, \end{aligned} \right\}$$

where \bar{a} and $\bar{\alpha}$ are new constants.

(3) The cylinder generates waves by making small circular motions in a clockwise sense:

$$\xi = se^{-i\sigma t}, \quad \eta = -ise^{-i\sigma t}.$$

We simply subtract (1) from (2). But by theorem C, ζ_- vanishes. Hence $\bar{a} = a$, $\bar{\alpha} = \alpha$ and we have

$$\left. \begin{aligned} \zeta_+ &= 2ae^{i(kx - \sigma t + \alpha)}, \\ \zeta_- &= 0. \end{aligned} \right\}$$

(4) The cylinder absorbs waves coming from $x = -\infty$. In (3), reverse the signs of x , t and ξ . Taking complex conjugate expressions, and adding a phase π we get

$$\xi = se^{-i\sigma t}, \quad \eta = -ise^{-i\sigma t}$$

and

$$\left. \begin{aligned} \zeta_+ &= 0, \\ \zeta_- &= -2ae^{i(kx - \sigma t - \alpha)}. \end{aligned} \right\}$$

(5) The cylinder is fixed and subject to waves incident from $x = -\infty$. Taking $\frac{1}{2}[(3) - (4)]$ we have

$$\xi = 0, \quad \eta = 0$$

and

$$\left. \begin{aligned} \zeta_+ &= ae^{i(kx - \sigma t + \alpha)}, \\ \zeta_- &= ae^{i(kx - \sigma t + \alpha)}. \end{aligned} \right\}$$

This incidentally proves theorem A.

Consider now the mean forces (X, Y) on the cylinder. In cases (1) and (2) these are, by symmetry,

$$X = 0, \quad Y = Qe^{i(-\sigma t + \delta)}$$

and

$$X = Pe^{i(-\sigma t + \gamma)}, \quad Y = 0,$$

where P, Q and γ, δ are real constants. Hence in case (5) we obtain

$$X = iP \sin \gamma e^{-i\sigma t}, \quad Y = -Q \sin \delta e^{-i\sigma t}.$$

The phase-lag ψ_1 of the force Y behind the vertical acceleration $\partial^2 \zeta / \partial t^2$ at $x = 0$ in the incident wave is therefore

$$\psi_1 = \pi + \alpha. \tag{A 1}$$

(6) The cylinder responds freely to waves incident from $x = -\infty$. By theorem B we know there is no reflected wave, so the motion has the form

$$(6) = \frac{1}{2} [(3) e^{i\epsilon} + (4) e^{-i\epsilon}],$$

where ϵ is a constant phase. Thus we have

$$\xi = s \cos \epsilon e^{-i\sigma t}, \quad \eta = -is \cos \epsilon e^{-i\sigma t}$$

and

$$\left. \begin{aligned} \zeta_+ &= ae^{i(kx - \sigma t + \alpha + \epsilon)}, \\ \zeta_- &= -ae^{i(-kx - \sigma t - \alpha - \epsilon)}. \end{aligned} \right\}$$

The phase-lag ψ_2 of the vertical displacement η behind the vertical displacement at $x = 0$ in the incident wave is therefore

$$\psi_2 = -\frac{1}{2}\pi - (-\alpha - \epsilon - \pi) = \frac{1}{2}\pi + \alpha - \epsilon. \tag{A 2}$$

It will not be necessary to determine ϵ , although this may easily be done from the condition that $X = M \partial^2 \xi / \partial t^2$ where M is the mass of the cylinder. Finally

(7) The cylinder is constrained vertically and free horizontally. We simply modify (6) by subtracting a fraction of the forced motion (1) to cancel the vertical displacement. Thus taking (7) = (6) - (1) $\cos \epsilon$, we have

$$\xi = s \cos \epsilon e^{-i\sigma t}, \quad \eta = 0.$$

The addition of the forced motion involved no extra displacement or force in the x -direction; hence the freedom of the motion in the horizontal is unaffected. Now the amplitudes of the incident and reflected waves are equal to a and $a \cos \epsilon$ respectively. Therefore the coefficient of reflexion is

$$\cos \epsilon = \cos (\psi_1 - \psi_2)$$

from equations (A 1) and (A 2). This proves equation (4.1). Since by conservation of energy $a'^2 + b^2 = a^2$, equation (4.2) follows immediately.

Equations (1.1)–(1.5) were pointed out by the present author in a memorandum to a meeting on wave power at the C.E.G.B. Headquarters on 17 March 1975, under the chairmanship of Dr D. T. Swift-Hook. A qualitative confirmation of the radiation stress was reported to the author on a subsequent visit to British Hovercraft Corporation, Isle of Wight at the invitation of Sir Christopher Cockerell and Mr Peter Crewe. The measurements by Salter *et al.*, made originally at the author's prompting, are here quoted by kind permission of Mr Salter. The author has had many interesting discussions with those mentioned and also with Mr J. Platts and Mr I. Glendenning. The contents of the present paper were outlined at a discussion meeting at the Society for Underwater Technology on 10 March 1976, and at the annual meeting of the British Theoretical Mechanics Colloquium in Edinburgh.

REFERENCES

- Bowen, A. T., Inman, D. L. & Simmons, V. P. 1968 Wave 'set-down' and wave set-up. *J. geophys. Res.* **73**, 2569–2577.
- Dean, W. R. 1948 On the reflection of surface waves by a submerged cylinder. *Proc. Camb. Phil. Soc.* **44**, 483–491.
- Lamb, H. 1932 *Hydrodynamics*, 6th ed., ch. 9. Cambridge University Press.
- Longuet-Higgins, M. S. 1967 On the wave-induced difference in mean sea level between the two sides of a submerged breakwater. *J. mar. Res.* **25**, 148–153.
- Longuet-Higgins, M. S. & Stewart, R. W. 1960 Changes in the form of short gravity waves on long waves and tidal currents. *J. Fluid Mech.* **8**, 565–583.
- Longuet-Higgins, M. S. & Stewart, R. W. 1963 A note on wave set-up. *J. mar. Res.* **21**, 4–10.
- Longuet-Higgins, M. S. & Stewart, R. W. 1964 Radiation stresses in water waves; a physical discussion, with applications. *Deep-Sea Res.* **11**, 529–562.
- Masuda, Y. 1972 Study of wave activated generator and future view as island power source. 2nd International Ocean Development Conference Preprints **2**, 2074.
- Ogilvie, T. F. 1963 First- and second-order forces on a cylinder submerged under a free surface. *J. Fluid Mech.* **16**, 451–472.
- Salter, S. H. 1974 Wave power. *Nature, Lond.* **249**, 720–724.
- Salter, S. H., Jeffrey, D. C. & Taylor, J. R. M. 1976 The architecture of nodding duck wave power generators. *The Naval Architect*, Jan. 1976, pp. 21–24.
- Saville, T. 1961 Experimental determination of wave set-up. *Proc. 2nd Tech. Conf. on Hurricanes*, Miami Beach, Florida, pp. 242–252. U.S. Dept. of Commerce.
- Sheppard, F. P. & LaFond, E. C. 1940 Sand movements along the Scripps Institution Pier, California. *Am. J. Sci.* **238**, 272–285.
- Ursell, F. 1950 Surface waves on deep water in the presence of a submerged circular cylinder. I. *Proc. Camb. Phil. Soc.* **49**, 141–152.
- Woolley, M. & Platts, J. 1975 Energy on the crest of a wave. *New Scientist*, 1 May 1975, pp. 241–243.

The propagation of short surface waves on longer gravity waves

By M. S. LONGUET-HIGGINS

Department of Applied Mathematics and Theoretical Physics, University of Cambridge, Silver Street, Cambridge CB3 9EW, UK, and Institute of Oceanographic Sciences, Wormley, Surrey, UK

(Received 18 June 1986)

To understand the imaging of the sea surface by radar, it is useful to know the theoretical variations in the wavelength and steepness of short gravity waves propagated over the surface of a train of longer gravity waves of finite amplitude. Such variations may be calculated once the orbital accelerations and surface velocities in the longer waves have been accurately determined – a non-trivial computational task.

The results show that the linearized theory used previously for the longer waves is generally inadequate. The fully nonlinear theory used here indicates that for longer waves having a steepness parameter $AK = 0.4$, for example, the short-wave steepness can be increased at the crests of the longer waves by a factor of order 8, compared with its value at the mean level. (Linear theory gives a factor less than 2.)

The calculations so far reported are for free, irrotational gravity waves travelling in the same or directly opposite sense to the longer waves. However, the method of calculation could be extended without essential difficulty so as to include effects of surface tension, energy dissipation due to short-wave breaking, surface wind-drift currents, and to arbitrary angles of wave propagation.

1. Introduction

An important component of radar backscatter from the sea surface arises from the Bragg scattering. This involves surface wavelengths of the order of a few centimetres for X-band radars, or tens of centimetres for L-band. In both cases the wavelengths are usually small compared to the dominant wavelengths of ocean surface waves (10 to 10^3 m). So it becomes an important question to study how the short-wave energy is distributed with respect to the phase of the longer waves.

In the present study we shall consider the classical model of a short train of gravity waves, of small but variable steepness ak , propagated over the surface of a longer train of gravity waves of *finite* steepness AK , as in figure 1. Early workers (Longuet-Higgins & Stewart 1960) assumed that $AK \ll 1$, and in that case it was found that the variation in the wavenumber k and amplitude a of the short waves, in deep water, was given by

$$\left. \begin{aligned} \frac{k}{\bar{k}} &= 1 + AK \cos \psi + O(AK)^2, \\ \frac{a}{\bar{a}} &= 1 + AK \cos \psi + O(AK)^2, \end{aligned} \right\} \quad (1.1)$$

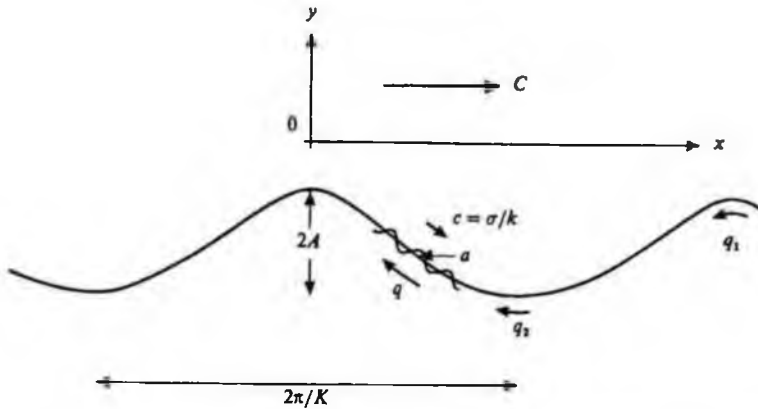


FIGURE 1. Definition sketch for short waves on long waves. The origin of y is chosen so that $q^2 + 2gy = 0$ on the free surface.

where \bar{k} and \bar{a} are the (constant) values of k and a at the mean surface level and $\psi = K(x - Ct)$ is the phase of the long waves. This gives

$$\frac{ak}{\bar{a}\bar{k}} = 1 + 2AK \cos \psi + O(AK)^2, \quad (1.2)$$

showing that the short waves are both shorter and steeper on the crests of the longer waves ($\psi = 2n\pi$). However, since $AK \leq (AK)_{\max} = 0.4432$ the maximum steepening predicted is less than 2.

Longuet-Higgins & Stewart (1960) interpreted equations (1.1) by assuming (i) that the phase of the short waves was conserved, i.e. that

$$kq - \sigma = \text{constant}, \quad (1.3)$$

where q is the particle speed in the long waves as seen by an observer travelling with the long-wave speed C , and σ is the intrinsic frequency of the short waves in a frame moving with speed q ; next, (ii) that the intrinsic frequency σ and local wavenumber k of the short waves were related by

$$\sigma^2 = g'k, \quad (1.4)$$

where g' was the effective value of gravity for the short waves, i.e.

$$g' = g + \frac{\partial W}{\partial t}, \quad (1.5)$$

W being the vertical component of orbital velocity in the long waves; and (iii) that the short-wave energy density E was given by

$$E = \frac{1}{2}ga^2 + \frac{\frac{1}{2}a^2\sigma^2}{k}, \quad (1.6)$$

representing the potential and kinetic energies respectively. The changes in short-wave energy E over the long wave could then be attributed to (a) advection by the long-wave orbital velocities, together with (b) work done by the straining of the long waves against the radiation stress of the short waves.

Garrett (1967) suggested that the same results (1.1) could be interpreted in terms of the conservation of *wave action*

$$N = E'/\sigma, \quad (1.7)$$

where

$$E' = \frac{1}{2}g'a^2 \quad (1.8)$$

is an alternative form of the short-wave energy density, and he introduced the equation

$$\frac{\partial N}{\partial t} - \frac{\partial}{\partial x} [(q - c_g) N] = 0, \quad (1.9)$$

where c_g is the group-velocity of the short waves ($c_g = \frac{1}{2}c$).

Finally, Bretherton & Garrett (1968) proved the validity of (1.9) for a general class of situations where a group of linearized short waves of wavenumber k is propagated through a *slowly varying medium* with local velocity q , under the general assumption that

$$|\nabla q| \ll kq, \quad \frac{\partial q}{\partial t} \ll \sigma q, \quad (1.10)$$

the energy density E' being defined as if the medium were locally uniform.

The great advantage of this formulation is its relative simplicity, and that there is no explicit restriction on the steepness AK of the long waves; it appears necessary to assume only that

$$ak \ll 1, \quad k \gg K. \quad (1.11)$$

In the case of AK finite, one would take as the effective (vector) gravity

$$g' = g - a \quad (1.12)$$

where a is the orbital acceleration in the long wave.

This principle has been partly applied (in principle) by Phillips (1981) to calculate the variation in amplitude of short capillary-gravity waves riding on longer gravity waves. The calculation could not be carried through in detail because the effective gravity g' was not at that time known with sufficient accuracy. However, the accurate calculation of accelerations in steep gravity waves has recently been carried out by Longuet-Higgins (1985c), and from this it is possible to infer g' by (1.12), hence both the shortening and steepening of the short waves. In this contribution we apply the results to short gravity waves, in the first place, with application particularly to backscattering in L-band. One significant result is that for finite values of AK the short-wave steepening can actually be much greater than that given by linear theory. Moreover, it will be seen that the basic calculation of g' opens the way to the solution of other important problems, including the case when the short waves are strongly affected by capillarity.

2. Formulation of the problem

Relatively short gravity waves, of local height $2a$ and wavelength $2\pi/k$, ride on longer, progressive gravity waves of finite height $2A$ and wavelength $2\pi/K$ in deep water, where $k \gg K$ (see figure 1). It is required to find k and ak as functions of the phase of the long wave.

The intrinsic frequency σ and the wavenumber k of the short waves are assumed to be related by (1.4), where g' is the magnitude of the *effective acceleration* g' given

by (1.12). Clearly, since the pressure gradient has no component tangential to the free surface, \mathbf{g}' is always normal to the surface of the longer waves. The frequency σ and the phase-speed

$$c = \sigma/k \quad (2.1)$$

are taken as positive or negative according as the short waves travel in the same or opposite direction to the long waves. q denotes the particle speed at the surface of the longer waves, as seen in a frame of reference moving with the long-wave phase speed C . In this reference frame the long waves appear steady and the free surface is a streamline. At the mean level $y = \bar{y}$, we have $q = C$; (see Lamb 1932, p. 420).

To determine the wavenumber k at points along the surface of the long waves we assume that *the phase of the short waves is conserved*, that is

$$k(q-c) = \text{constant} = \kappa, \quad (2.2)$$

say, Hence

$$c^2 = \frac{g'}{k} = \kappa^{-1}g'(q-c) \quad (2.3)$$

or

$$c^2 + \kappa^{-1}g'c - \kappa^{-1}g'q = 0. \quad (2.4)$$

This is a quadratic equation for c with solutions

$$c = -\beta \pm (\beta^2 + 2\beta q)^{\frac{1}{2}}, \quad \beta = \frac{g'}{2\kappa}. \quad (2.5)$$

Having found c we may calculate k from (2.3) in the form $k = g'/c^2$.

To determine the local wave amplitude a , we assume that action is conserved, that is equation (1.9). In the steady flow relative to the moving frame of reference this implies that the flux of wave action is a constant, i.e.

$$(q - c_g) \frac{E'}{\sigma} = \text{constant}, \quad (2.6)$$

where c_g the group velocity of the short waves ($= \frac{1}{2}c$) and E' is the intrinsic energy density of the short waves, given by (1.8). Since $\sigma = g'/c$, (2.6) can also be written

$$(q - \frac{1}{2}c)ca^2 = \text{constant} \quad (2.7)$$

or

$$a \propto [(q - \frac{1}{2}c)c]^{-\frac{1}{2}} \quad (2.8)$$

(cf. Longuet-Higgins & Stewart 1961).

Finally, the local wave steepening is defined as

$$r = ak/(\bar{a}\bar{k}) \quad (2.9)$$

where a bar denotes the values at the mean level $y = \bar{y}$.

Clearly the above approach depends upon the accurate evaluation of the velocity q and the orbital acceleration a in a (long) gravity wave of finite amplitude.

3. Method of calculation

The *real*, or orbital acceleration in a surface wave must be carefully distinguished from the *apparent* accelerations as measured by a fixed vertical wave gauge (see Longuet-Higgins 1985c). The real accelerations, both vertical and horizontal, vary

much more smoothly than the apparent accelerations, which can be very non-sinusoidal.

Numerical values of the real acceleration a were calculated by the method of Longuet-Higgins (1985*a*) which makes use of a set of quadratic relations between the Fourier coefficients a_n in Stokes's series for the Cartesian coordinates (x, y) in terms of the velocity potential. Thus if $K = g = 1$, and the free surface is given by

$$\left. \begin{aligned} y &= a_0 + \sum_1^{\infty} a_n \cos\left(\frac{n\phi}{c}\right), \\ x &= \frac{\phi}{c} + \sum_1^{\infty} a_n \sin\left(\frac{n\phi}{c}\right), \end{aligned} \right\} \quad (3.1)$$

where ϕ is the velocity potential, then the coefficients a_0, a_1, a_2, \dots satisfy the relations

$$\left. \begin{aligned} a_0 b_0 + a_1 b_1 + a_2 b_2 + a_3 b_3 + \dots &= -c^2, \\ a_1 b_0 + a_0 b_1 + a_1 b_2 + a_2 b_3 + \dots &= 0, \\ a_2 b_0 + a_1 b_1 + a_0 b_2 + a_1 b_3 + \dots &= 0, \end{aligned} \right\} \quad (3.2)$$

with $b_n = na_n$, $n > 0$ and $b_0 = 1$. These relations may be quickly and accurately solved for a given value of the phase-speed c (in general) or of the wave amplitude

$$A = a_1 + a_3 + a_5 + \dots \quad (3.3)$$

The speed g at the free surface is then found from the Bernoulli relation

$$q^2 = -2y, \quad (3.4)$$

and the vector acceleration a from the general relation

$$a = \chi_z \chi_{zz}^* = -q^6 z_{\chi}^2 z_{\chi\chi}^* \quad (3.5)$$

where $z = x + iy$ and $\chi = \phi + i\psi$, ψ the stream function. (An asterisk denotes the complex conjugate.) In real terms this is

$$a = -q^6 (x_{\phi} + iy_{\phi})^2 (x_{\phi\phi} - iy_{\phi\phi}). \quad (3.6)$$

The effective gravity g' is then found from (1.12).

Because of the slow initial rate of convergence of the series (3.1) at high values of AK , care must be taken to include enough terms in these series. A recent study (Longuet-Higgins 1985*b*) has shown that after an initial rate of convergence like n^{-1} , a_n ultimately converges exponentially, the transition to exponential behaviour occurs when $n = n_c = O(\epsilon^{-3})$, where

$$e^2 = 2.0 |AK - (AK)_{\max}|. \quad (3.7)$$

Since individual terms in the differentiated series for $x_{\phi\phi}$ and $y_{\phi\phi}$ at first increase like $n^{\frac{1}{2}}$, it is important, in order to ensure sufficient accuracy in the calculation, to include terms with n somewhat in excess of n_c .

Surface profile corresponding to $AK = 0.1, 0.2, 0.3, 0.4$ and the limiting value $AK = 0.4432$ are shown in figure 2. The corresponding values of the effective gravity g' are shown in figure 3. It will be seen that when $AK = 0.4$ these range from 0.65*g* at the crest of the wave ($x = 0$) to about 1.31*g* in the wave trough.

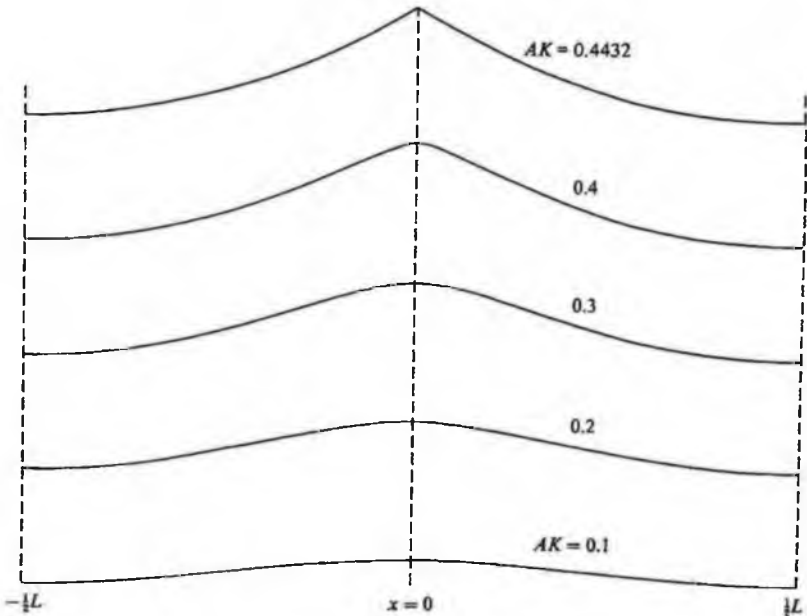


FIGURE 2. Surface profiles of gravity waves in deep water, when $AK = 0.1, 0.2, 0.3, 0.4$ and 0.4432 .

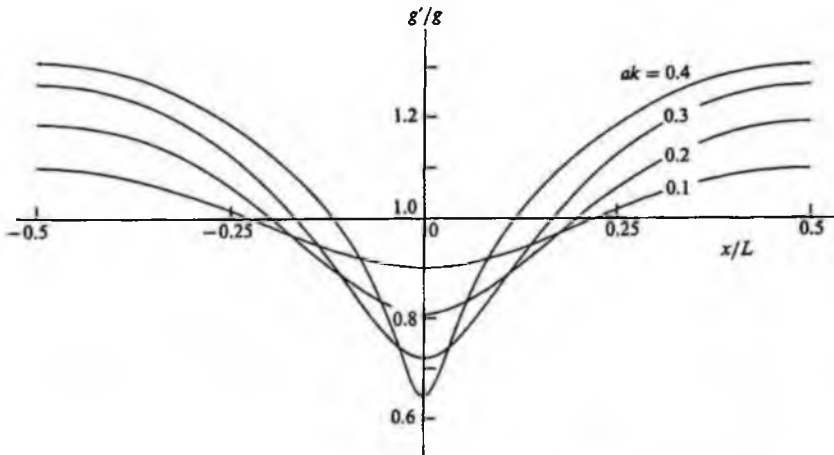


FIGURE 3. The effective value of gravity g' at the surface of steep waves, as a function of the horizontal coordinate x/L .

4. Results: variation in short-wave length

Using suffices 1 and 2 to denote values at the long-wave crest and trough respectively, figure 4 shows the relative shortening k_1/\bar{k} at the crests of the long waves as compared to the mean surface level, in the three cases when $\bar{k} = 2, 10$ and 100 . Similarly k_2/\bar{k} shows the lengthening in the long-wave troughs. For values of AK up to 0.2 the three curves corresponding to $\bar{k} = 2, 10$ and 100 are almost indistinguishable,

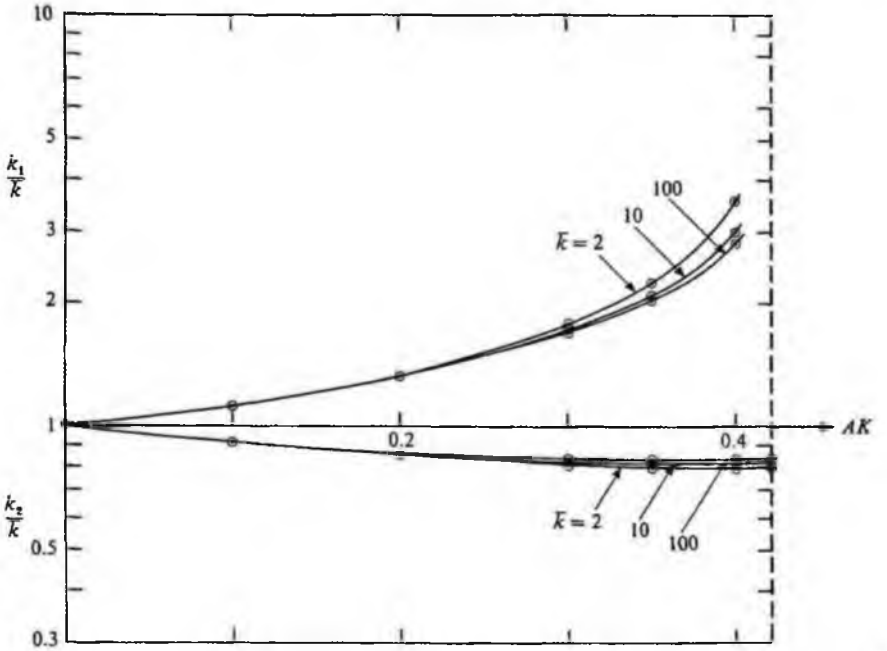


FIGURE 4. The relative shortening of short waves at the crests (k_1/\bar{k}) and in the troughs (k_2/\bar{k}) of long waves, as compared to the mean level, when $c > 0$. Note $K = 1$.

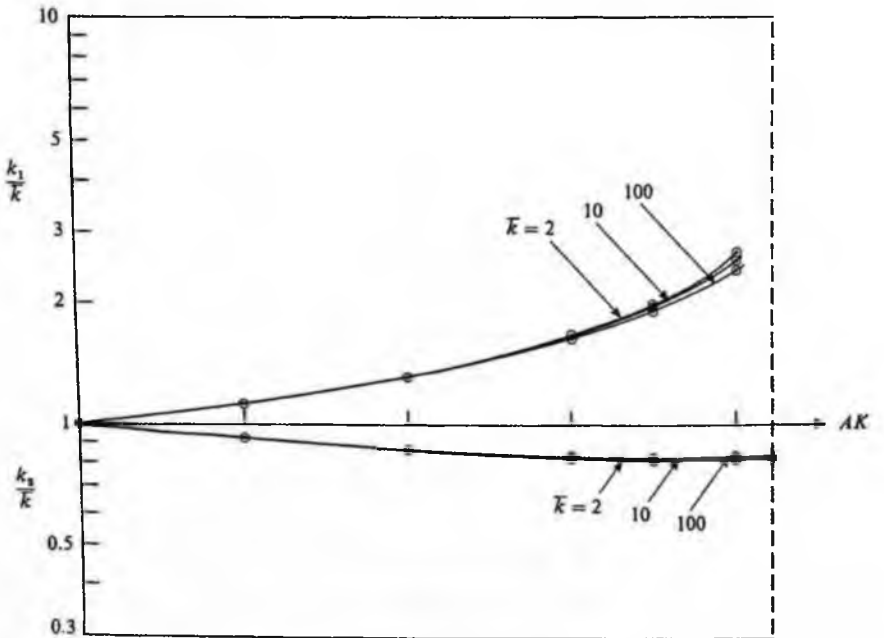


FIGURE 5. As figure 4, but for $c < 0$.

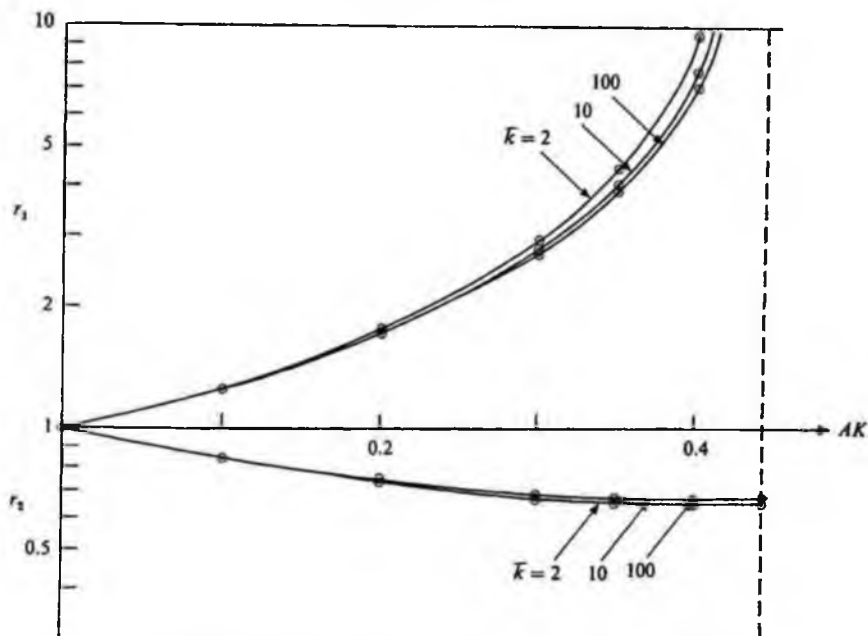


FIGURE 6. The relative steepening of short waves at the crests (r_1) and in the troughs (r_2) of long waves, as compared to the mean level, when $c > 0$.

and even when $AK = 0.4$ there is little departure from the representative curve $\bar{k} = 10$, when $k_1/\bar{k} = 3.0$ and $k_2/\bar{k} = 0.82$. Thus, the short-wave length varies over a range of about $3\frac{1}{2}$ to 1. This is for $c > 0$, when the short waves travel in the same sense as the longer waves. Figure 5 shows a similar plot when $c < 0$, and the short waves travel in the opposite sense. Here the variation in k is only slightly less. However, as $AK \rightarrow (AK)_{\max}$ it can be shown that $k_1/\bar{k} \rightarrow \infty$ when $c > 0$, but remains finite when $c < 0$.

5. Variation in the wave steepness

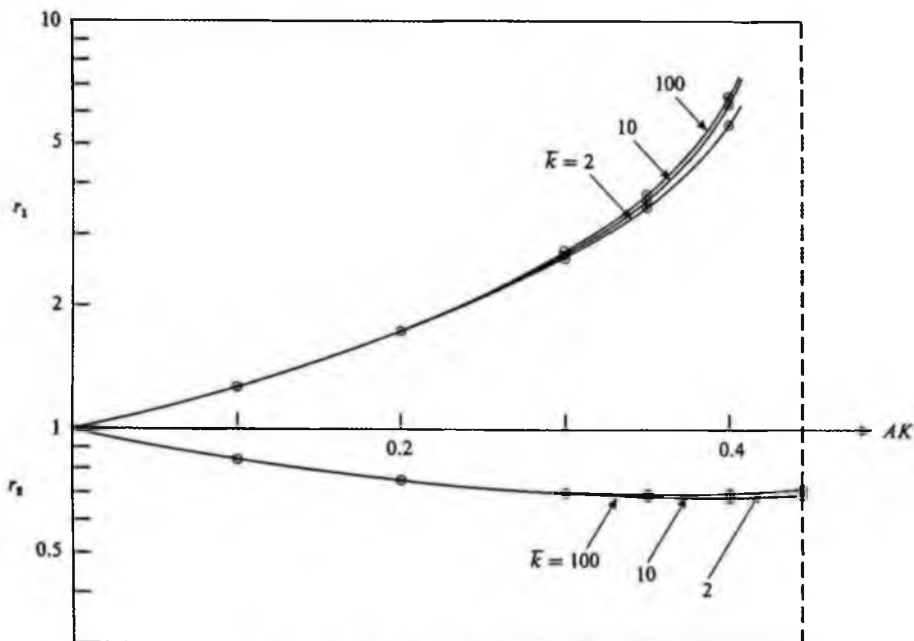
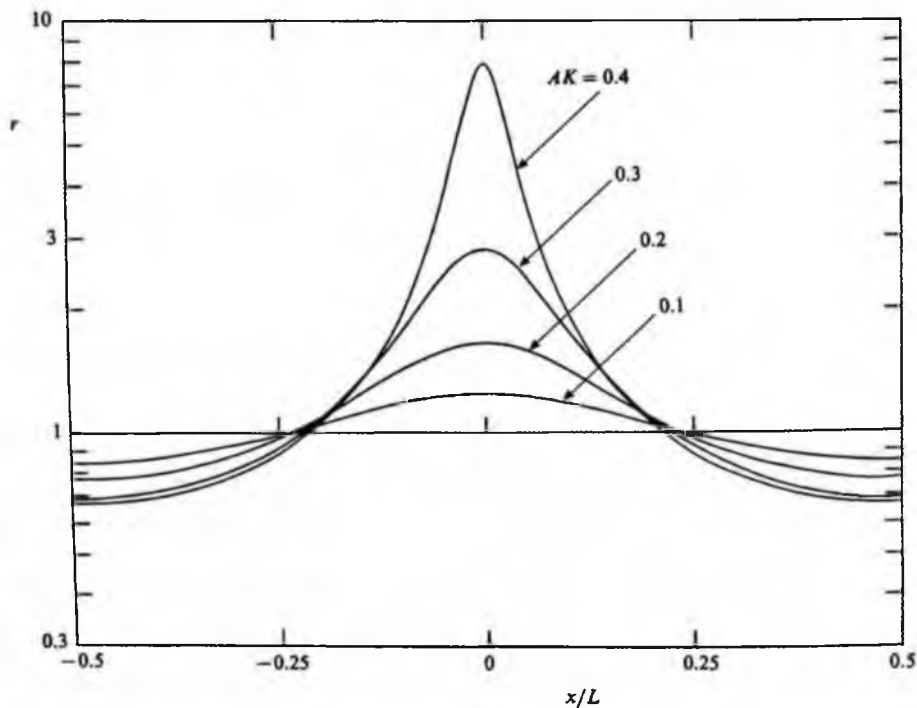
Figures 6 and 7 show the variation in steepening r of the shorter waves, in a similar manner to figures 4 and 5. Thus

$$r_1 = \frac{a_1 k_1}{\bar{a} k}, \quad r_2 = \frac{a_2 k_2}{\bar{a} k}. \quad (5.1)$$

Again the three curves corresponding to $\bar{k} = 2, 10$ and 100 lie very close together, showing that not only the wavelength variation but also the steepness variation is practically independent of short-wave length.

When $AK = 0.4$, however, the short-wave steepness may vary by a factor of as much as 8 between the long-wave crests and the mean level. This compares with a factor less than 2 given by linear theory.

The variation of steepness r over the profile of the long waves is shown in figure 8 as a function of x/L , and for different values of AK , using the representative short wavenumber $\bar{k} = 8$. Comparing $AK = 0.4$ with $AK = 0.1$, one sees the distorting effect of nonlinearity in the long waves.

FIGURE 7. As figure 6, but for $c < 0$.FIGURE 8. The relative steepening r as a function of the horizontal coordinate x/L , when $\bar{k} = 8$, $c > 0$.

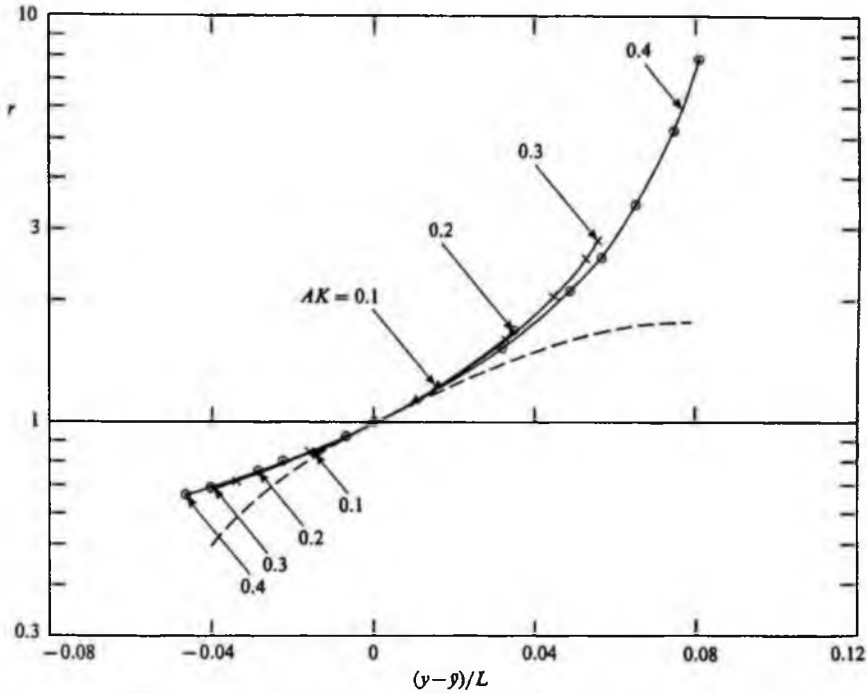


FIGURE 9. The relative steepening r as a function of the vertical coordinate $(y - \bar{y})/L$ when $k = 8$, $c > 0$.

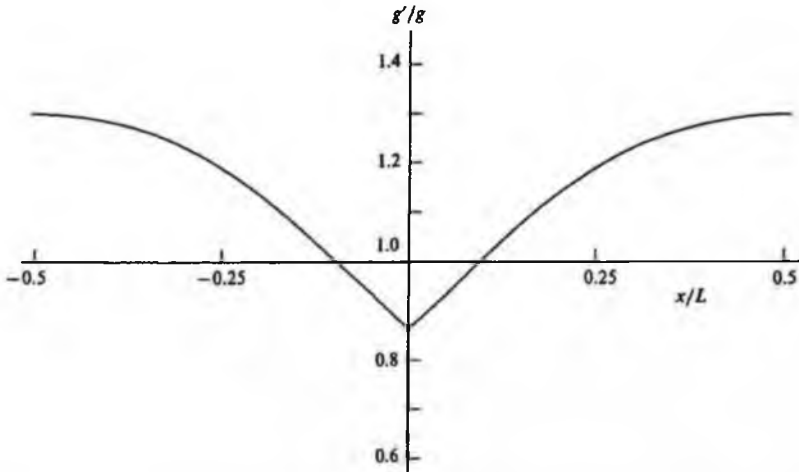


FIGURE 10. The effective value of gravity g' at the surface of deep-water waves of limiting steepness.

Finally, in figure 9 the three curves of figure 8 are plotted instead against $(y - \bar{y})/L$, that is the vertical height above the mean level \bar{y} . It now appears that all the curves collapse almost onto a single curve. This property may be useful in approximate analytical work. The appropriate nonlinear steepening is quite different from the linear theory, shown in figure 9 by the broken curve.

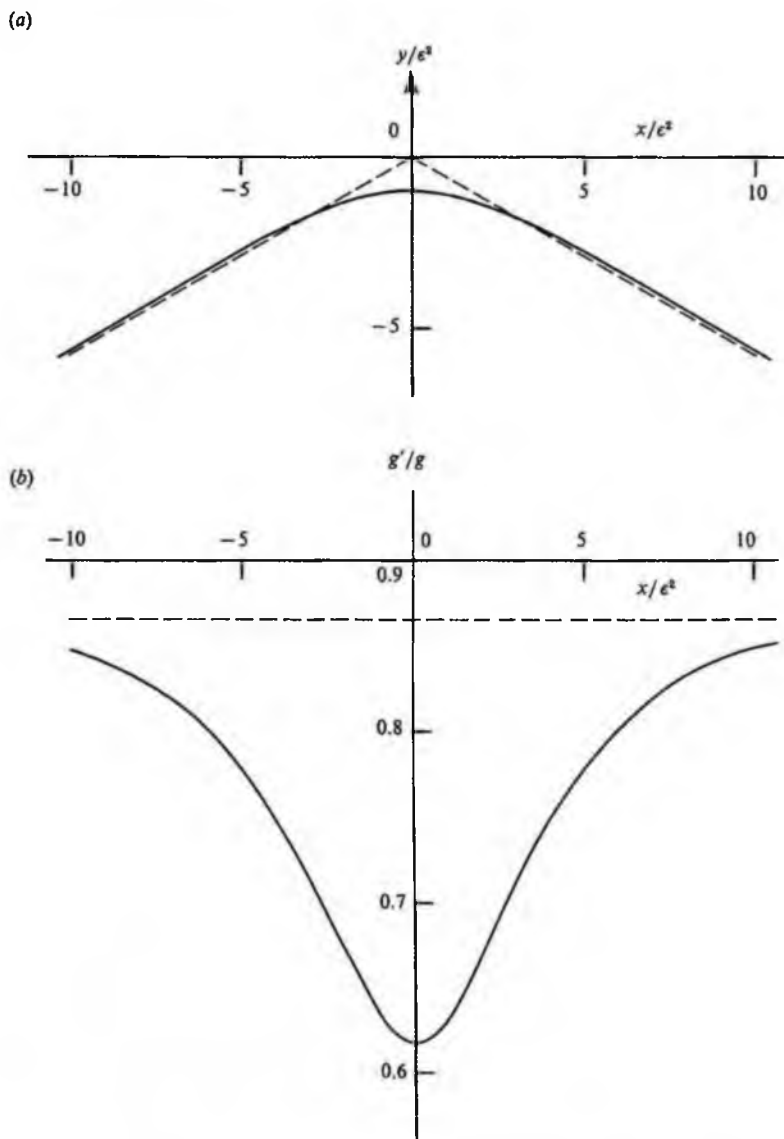


FIGURE 11. (a) The surface profile near the crest of a steep gravity wave, scaled according to $\epsilon^2 = q_1^2/2C$. (b) The effective value of gravity g' near the crest of a steep gravity wave.

6. Limiting waves

Our previous calculations have been carried only as far as $AK = 0.4$. In this Section we shall consider the limiting behaviour of the solutions as $AK \rightarrow (AK)_{\max}$, and the validity of the present approximations at large wave steepnesses.

Consider first the effective acceleration g' in a limiting wave. In figure 10 g'/g is plotted against the horizontal coordinate x/L , using the computations by Williams (1981, Table 12*d*). In the wave troughs, $g'/g = 1.301$ and near the crests, since the surface slope tends to 30° , we have $g'/g = 3^{1/2}/2 = 0.866$. At the crest itself, however, the downwards acceleration tends to $0.388g$ (Williams 1981), so that $g'/g = 0.612$.

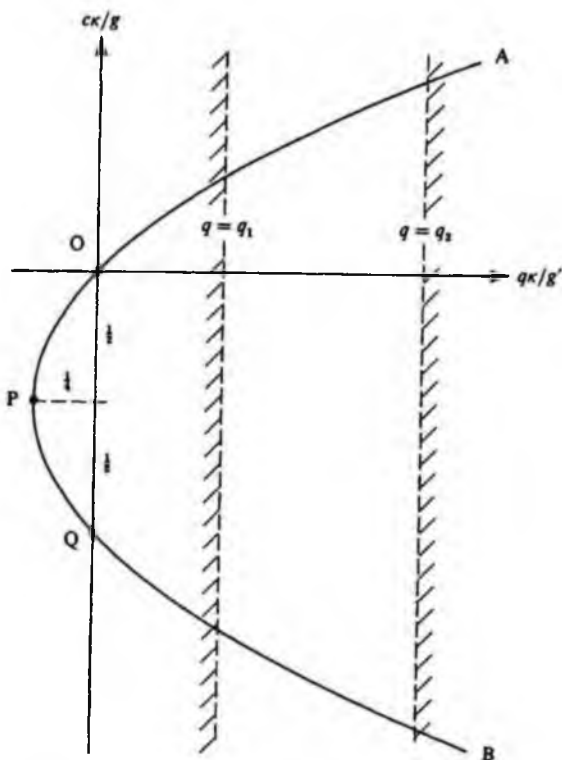


FIGURE 12. Graph to illustrate the behaviour of the phase-speed c , as given by (2.4).

For near-limiting waves, the behaviour near the crest is given by the theory of the almost-highest wave (Longuet-Higgins & Fox 1977, 1978), which is valid when

$$q^2/C^2 = 2\epsilon^2 \ll 1. \quad (6.1)$$

In this approach we introduce scaled coordinates $z_s = z/\epsilon^2$, where $z = x + iy$, and a scaled velocity potential $\chi_s = \chi/\epsilon^3$ where $\chi = \phi + i\psi$. Making use of the numerical coordinates of the free surface as given in table 3 of Longuet-Higgins & Fox (1977) we can easily calculate the radius of curvature R and hence the normal component of the particle acceleration

$$a_N = q^2/R = 2gy/R \quad (6.2)$$

at each point on the surface and hence the value of g' . This is shown in figure 11 (b), where g'/g is plotted against x/ϵ^2 . For comparison with the steepest wave in figure 2, (3.7) shows that when $AK = 0.40$, then $\epsilon^2 = 0.086$.

Now consider the propagation of short waves near the crest of a fairly steep longer wave. The values of the phase speed c for given values of q and κ/g' are shown in figure 12, $c\kappa/g'$ being plotted against $q\kappa/g'$ according to (2.4). Since q is always positive, the two roots (2.5) correspond to the branches OA and QB of the parabola respectively. In fact the relevant sectors of the parabola are those lying between $q = q_1$ and $q = q_2$. For moderate wave steepnesses, q_1 and q_2 are of order C while $\kappa = k(C - c)$ is of order kC when $k \gg 1$. Hence $q\kappa/g'$ is generally large.

However, when the longer waves become steep, we have $\epsilon \rightarrow 0$, hence $q/C \rightarrow 0$. For

any finite value of \bar{k} , suppose it were possible for the left-hand boundary in figure 12 to approach the axis $q\kappa/g' = 0$. Then the positive root of (2.4) would give $c \sim q$, and so from (2.3) $k \sim g'/q^2$, independently of \bar{k} . In other words the local wavelength $2\pi/k$ of the short waves would be of order ϵ^2 , comparable to the radius of curvature of the crest. Hence the short-wave approximation would not be applicable. Similar considerations apply even more strongly to the negative root of (2.4).

For the short-wave approximation to remain valid we must have $k\epsilon^2 \gg 1$. But since $k = g'/c^2$ and $\epsilon^2 = q^2/2C^2$ this implies $q^2 \gg c^2$. Hence q/c is at least moderately large, and the region of interest in figure 12 lies well to the right, where $q\kappa/g' \gg 1$. This in turn means that we must have $\epsilon^2\bar{k}^2 \gg 1$. For example, when $AK = 0.4$ then $\bar{k}^2 \gg 10$. Thus in figures 4–7 only the plots corresponding to $\bar{k} = 10$ and 100 are quantitatively valid, at this value of AK .

Nevertheless some qualitative conclusions may be drawn. From figure 12 it is clear that the phase speed c and hence the lengthscale k^{-1} is always greater for oppositely travelling short waves approaching the long-wave crest than it is for short waves travelling in the positive direction. This suggests that there may be a real distinction between 'spilling' and 'plunging' breakers, the former being caused by forwards-travelling short-wave energy, and the latter by perturbations travelling in the opposite sense.

7. Conclusions

We have shown that by taking full account of the nonlinearity of the longer waves and by using the principle of action conservation for the shorter waves one can calculate accurately the short-wave steepening. This can be several times greater than that predicted by linear theory. The short-wave approximation cannot, however, be extended to long waves of limiting, or near-limiting, steepness.

We note that according to our assumptions in (1.1), the principle of action conservation is expected to be only an approximation. To test this principle, we have studied in another paper (Dysthe *et al.* 1987) a simple model in which the governing equations are ordinary differential equations capable of exact integration by numerical methods. The model suggests that action for the shorter waves is indeed conserved closely, though not precisely.

All the results of the present paper depend upon a precise calculation of the local gravity g' . Hence we have considered only the case when the short waves are pure gravity waves. However, it must be realized that the basic calculation of g' for the long waves opens the way to a solution of other important problems, particularly the case when the short waves are capillary or capillary-gravity waves. A more general treatment is in progress which includes the dissipation of the short waves by breaking and the regeneration of the short waves by the wind.

Most of the calculations contained in this paper were first presented in a report to the TOWARD Hydrodynamics Committee at the Naval Research Laboratory, Washington D.C. in October 1985. The report was prepared at the Cal. Tech. Jet Propulsion Laboratory, Pasadena, with the kind cooperation of Dr C. Elachi and Dr O. H. Shemdin.

REFERENCES

- BRETHERTON, F. P. & GARRETT, C. J. R. 1968 Wavetrains in homogeneous moving media. *Proc. R. Soc. Lond. A* **302**, 529–554.
- DYSTHE, K., HENYEV, F. S., LONGUET-HIGGINS, M. S. & SCHULT, R. L. 1987 The double orbiting pendulum: an analogue to interacting gravity waves. *Proc. R. Soc. Lond. A* (submitted).
- GARRETT, C. J. F. 1967 The adiabatic invariant for wave propagation in a nonuniform moving medium. *Proc. R. Soc. Lond. A* **299**, 26–27.
- KENYON, K., SHERES, D. & BERNSTEIN, R. 1983 Short waves on long waves. *J. Geophys. Res.* **88**, 7589–7596.
- LAMB, H. 1932 *Hydrodynamics*, 6th edn. Cambridge University Press.
- LONGUET-HIGGINS, M. S. 1985*a* Bifurcation in gravity waves. *J. Fluid Mech.* **151**, 457–475.
- LONGUET-HIGGINS, M. S. 1985*b* Asymptotic behaviour of the coefficients in Stokes's series for surface gravity waves. *I.M.A. J. Appl. Maths* **34**, 267–277.
- LONGUET-HIGGINS, M. S. 1985*c* Accelerations in steep gravity waves. *J. Phys. Oceanogr.* **15**, 1570–1579.
- LONGUET-HIGGINS, M. S. & FOX, M. J. H. 1977 Theory of the almost-highest wave: the inner solution. *J. Fluid Mech.* **80**, 721–741.
- LONGUET-HIGGINS, M. S. & FOX, M. J. H. 1978 Theory of the almost-highest wave. Part 2. Matching and analytic extension. *J. Fluid Mech.* **85**, 769–786.
- LONGUET-HIGGINS, M. S. & STEWART, R. W. 1960 Changes in the form of short gravity waves on long waves and tidal currents. *J. Fluid Mech.* **8**, 565–583.
- LONGUET-HIGGINS, M. S. & STEWART, R. W. 1961 The changes in amplitude of short gravity waves on steady, non-uniform currents. *J. Fluid Mech.* **10**, 529–549.
- PHILLIPS, O. M. 1981 The dispersion of short wavelets in the presence of a dominant long wave. *J. Fluid Mech.* **107**, 465–485.
- WILLIAMS, J. M. 1981 Limiting gravity waves in water of finite depth. *Phil. Trans. R. Soc. Lond. A* **302**, 139–188.

The orbiting double pendulum: an analogue to interacting gravity waves

BY K. DYSTHE¹, F. S. HENYEV², M. S. LONGUET-HIGGINS³, F.R.S.,
AND R. L. SCHULT⁴

¹*Department of Physics, University of Tromsø, Tromsø, Norway*

²*Center for Studies of Nonlinear Dynamics, La Jolla Institute,
La Jolla, California 92037, U.S.A.*

³*Department of Applied Mathematics and Theoretical Physics,
University of Cambridge CB3 9EW, U.K.*

⁴*Department of Physics, University of Illinois, Urbana, Illinois 61801, U.S.A.*

(Received 2 February 1987 – Revised 26 February 1988)

The apparent gravity felt by a particle on the surface of water when a progressive train of gravity waves of finite amplitude passes is shown to be analogous to the apparent gravity on the bob of a rapidly rotating pendulum under weak gravity. A train of short gravity waves riding on longer waves will thus have some properties in common with those of a smaller, rapidly rotating pendulum attached to the first pendulum. The variation of the energy and action of the smaller pendulum are examined analytically and by numerical integration.

1. INTRODUCTION

The modulation of short surface waves riding on the surface of longer gravity waves is a phenomenon of some interest for the formation of whitecaps on the sea surface, and for the imaging of the ocean by radar backscatter. Accurate numerical calculations of the short-wave modulation have recently been presented by Longuet-Higgins (1987). The purpose of this paper is to describe a simple but useful analogue to the two-wave system, namely the motion of a short pendulum rotating around the bob of a similar and longer pendulum. The advantage of such a model is that it replaces the continuous fluid two-wave system by a discrete system having only two degrees of freedom, which is described by two ordinary differential equations. Because the latter can be integrated to any desired accuracy, it is then possible to test such approximations as the conservation of wave action of the shorter waves by reference to corresponding approximations made in the discrete model.

The plan of the paper is as follows. Section 2 introduces the pendulum analogue for a single water wave. Uniform fast rotation of the pendulum corresponds to a steady stream; the perturbation induced by gravity corresponds to a wave on the stream. There is a 'dispersion relation' connecting the frequency and amplitude of the perturbation, just as there is for a gravity wave of fixed wavelength.

In §4 we show that for a point on the bob of the pendulum, 'apparent gravity'

is always directed radially inwards, that is normally to the circular path. Similarly, in free-surface waves 'apparent gravity' is always directed normally to the free surface.

Section 5 introduces the double pendulum, in which a shorter pendulum, with a relatively small mass, is attached to the bob of the longer pendulum. Both describe complete orbits, the angular frequency of the shorter pendulum being relatively fast.

In §6 we discuss the energy and action of the small pendulum from an elementary point of view. It is shown analytically that by defining the energy E in terms of the local gravity g' induced by the large pendulum, the local fluctuations in E can be made relatively small. With certain definitions of the frequency σ the ratio E/σ can also be shown to be almost constant. However, some important ambiguities remain, which are removed by the hamiltonian treatment given in §7. Here it is shown that a more general formula for the action of the shorter pendulum yields unambiguous results. Some numerical examples are given in §8 which show that the action thus defined is indeed remarkably constant. The constancy is further improved by averaging over the initial phase of the small pendulum. Further discussion follows in §9.

This paper follows an earlier suggestion by one of us (Longuet-Higgins 1985), based on the elementary approach of §§2-6. A number of references to the early history of action conservation in discrete systems are given in the Appendix. This paper represents an alternative approach to the extension of action principles to waves in continuous media pioneered by Whitham (1965, 1974), Garrett (1967), Bretherton & Garrett (1968) and others.

2. THE SINGLE ORBITING PENDULUM

Consider a pendulum of length L and mass M under the action of gravity g , as in figure 1. If θ denotes the angle between the pendulum and the vertical, the kinetic and potential energies are given by

$$T = \frac{1}{2}ML^2\dot{\theta}^2, \quad V = MgL(\cos\theta + 1). \quad (2.1)$$

Thus Lagrange's equation of motion

$$\frac{d}{dt} \frac{\partial T}{\partial \dot{\theta}} - \frac{\partial T}{\partial \theta} = - \frac{\partial V}{\partial \theta} \quad (2.2)$$

yields

$$L\ddot{\theta} = g \sin\theta \quad (2.3)$$

with a first integral

$$\frac{1}{2}L^2\dot{\theta}^2 + gL(1 + \cos\theta) = \frac{1}{2}L^2R^2 = E/M, \quad (2.4)$$

R being the value of $\dot{\theta}$ when $\theta = \pi$. Writing

$$\alpha = \frac{1}{2}\theta, \quad \lambda^2 = 4g/LR^2 \quad (2.5)$$

we obtain

$$\dot{\alpha}^2 = \frac{1}{4}R^2(1 - \lambda^2 \cos^2\alpha), \quad (2.6)$$

whence

$$t = \frac{2}{R} \int \frac{d\alpha}{(1 - \lambda^2 \cos^2\alpha)^{1/2}}. \quad (2.7)$$

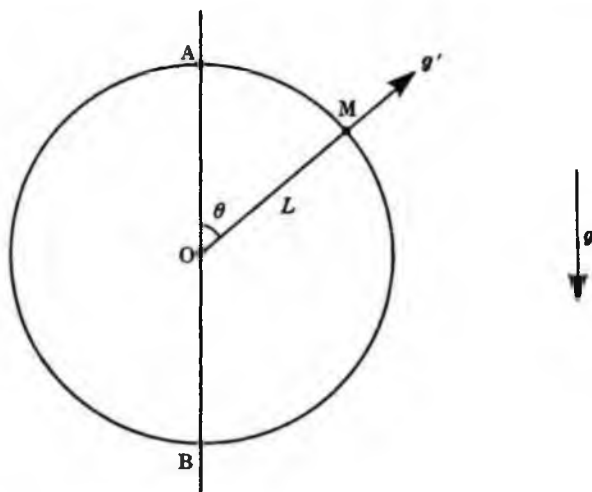


FIGURE 1. Notation for the single orbiting pendulum, showing the direction of the local gravity g' .

The angular velocity $\dot{\theta}$ at the highest point $\theta = 0$ is equal to $R(1 - \lambda^2)^{\frac{1}{2}}$. This is real provided that $\lambda^2 \leq 1$. The case $\lambda^2 = 1$ when the pendulum comes to rest at the top of its orbit (taking infinite time to do so) may be said to correspond to a wave of limiting height, which has a stagnation point at the crest.

Let us choose units in which $L = g = 1$. We are interested in relatively high speeds of rotation, when $\lambda^2 \ll 1$. Then the orbit is just a small perturbation of the state of uniform rotation

$$t = \lambda\alpha = \frac{1}{2}\lambda\theta, \quad \theta = 2t/\lambda. \quad (2.8)$$

Expansion of (2.7) in powers of λ gives as the next approximation

$$t = \left(\frac{1}{2}\lambda + \frac{1}{8}\lambda^3\right)\theta + \frac{1}{8}\lambda^3 \sin \theta, \quad (2.9)$$

the terms in λ^5 being neglected. Inversely we have

$$\theta = \sigma t - a \sin \sigma t, \quad (2.10)$$

where

$$\sigma = 2/\lambda(1 + \frac{1}{4}\lambda^2), \quad a = \frac{1}{4}\lambda^2. \quad (2.11)$$

This represents a rotation with the slightly modified radian frequency σ , and perturbation amplitude a . The motion is similar to a gravity wave of amplitude a , viewed by an observer moving with the horizontal phase speed $c = \sigma$. Conversely, if we view the pendulum in a reference frame rotating with the mean radian frequency σ , the angular displacement θ of the bob is sinusoidal, with frequency σ and amplitude a .

In higher approximations, θ will contain additional harmonics, proportional to $\cos n\sigma t$, where n takes all integer values. The mean frequency σ is found from

$$\frac{2\pi}{\sigma} = \lambda \int_0^\pi \frac{d\alpha}{(1 - \lambda^2 \cos^2 \alpha)^{\frac{1}{2}}} = 2\lambda K(\lambda^2), \quad (2.12)$$

where K is a complete elliptic integral. From the expansion

$$K(z) = \frac{\pi}{2} \left[1 + \left(\frac{1}{2}\right)^2 z + \left(\frac{1 \times 3}{2 \times 4}\right)^2 z^2 + \left(\frac{1 \times 3 \times 5}{2 \times 4 \times 6}\right)^2 z^3 + \dots \right] \quad (2.13)$$

we obtain

$$\frac{1}{\sigma} = \frac{1}{2} \lambda \left(1 + \frac{1}{4} \lambda^2 + \frac{9}{64} \lambda^4 + \frac{25}{256} \lambda^6 + \dots \right). \quad (2.14)$$

3. THE ACTION INTEGRAL

In dimensional units, the lagrangian \mathcal{L} is given by

$$\mathcal{L} = T - V = \frac{1}{2} M L^2 \dot{\theta}^2 - M g L (1 + \cos \theta) \quad (3.1)$$

so we may take as conjugate variables

$$q = \theta, \quad p = \partial \mathcal{L} / \partial \dot{\theta} = M L^2 \dot{\theta}. \quad (3.2)$$

Thus the action integral A is given by†

$$A = \oint p dq = M L^2 \oint \dot{\theta}^2 dt \quad (3.3)$$

or, from (2.4)–(2.6),

$$A = 4L(2EM)^{\frac{1}{2}} G(\lambda^2), \quad (3.4)$$

where

$$\lambda^2 = 2MgL/E \quad (3.5)$$

and $G(\lambda^2)$ is the elliptic integral of the second kind:

$$G(\lambda^2) = \int_0^{\pi} (1 - \lambda^2 \cos^2 \alpha)^{\frac{1}{2}} d\alpha \quad (3.6)$$

with expansion

$$G(\lambda^2) = \frac{\pi}{2} \left[1 - \left(\frac{1}{2}\right)^2 \frac{\lambda^2}{1} + \left(\frac{1 \times 3}{2 \times 4}\right)^2 \frac{\lambda^2}{3} - \left(\frac{1 \times 3 \times 5}{2 \times 4 \times 6}\right)^2 \frac{\lambda^2}{5} + \dots \right]. \quad (3.7)$$

Equation (3.4) is to be compared with the expression for E/σ which would be found from (2.12). In dimensional form this is

$$E/\sigma = \pi^{-1} L (2EM)^{\frac{1}{2}} K(\lambda^2) \quad (3.8)$$

For small perturbations of the rotation, that is when $\lambda \ll 1$, we have

$$A \sim 2\pi L (2EM)^{\frac{1}{2}} \quad (3.9)$$

and

$$E/\sigma \sim \frac{1}{2} L (2EM)^{\frac{1}{2}}, \quad (3.10)$$

so that the two expressions are equivalent. (For a rotor, the ratio of A to E/σ is 4π , compared with 2π for the harmonic oscillator and for linear surface waves.)

† Many authors define the action with an additional factor $1/(2\pi)$.

In general, however, A and E/σ are not equivalent. Note also that the action integral A , unlike E/σ , is independent of the origin chosen for the potential energy; a constant added to V will not affect the definitions of q and p in equations (3.2).

4. EFFECTIVE GRAVITY

Any small body attached to the bob of the pendulum will feel itself to be in a local gravitational field

$$\mathbf{g}' = \mathbf{g} - \mathbf{a}, \quad (4.1)$$

where \mathbf{g} is the vector acceleration of gravity and \mathbf{a} is the acceleration of the bob. By taking moments about the centre O it is easily seen that the tangential component \mathbf{a}_s of the acceleration is always balanced by the tangential component of gravity. Hence the tangential component of $(\mathbf{g} - \mathbf{a})$ vanishes, and so the direction of the virtual gravity \mathbf{g}' is always radial. This property has an analogue in surface gravity waves, namely that the local gravity vector \mathbf{g}' for a particle of fluid in the free surface is always directed normally to the surface.

The magnitude of \mathbf{g}' is thus the magnitude of the normal component g_n , that is to say

$$g' = g_n = L\theta^2 - g \cos \theta. \quad (4.2)$$

By (2.4) we have also

$$g' = g(4\lambda^{-2} - 2 - 3 \cos \theta). \quad (4.3)$$

Thus \mathbf{g}' is always directed away from the centre O provided that $\lambda^2 < \frac{4}{3}$. However, when $\frac{4}{3} < \lambda^2 < 2$ there are two positions θ in the orbit at which g_n changes sign. In the critical case $\lambda^2 = \frac{4}{3}$, g_n is positive everywhere except at the highest point $\theta = 0$, where the bob is in freefall. Then the centrifugal force $ML\theta^2$ at that point exactly balances the downwards gravity $Mg \cos \theta$.

5. THE DOUBLE PENDULUM

Suppose now that we have a second pendulum of mass m and length l attached to the bob of the first pendulum as in figure 2. It is convenient to choose units so that

$$L = 1, \quad M + m = 1, \quad g = 1. \quad (5.1)$$

The kinetic and potential energies now become

$$\left. \begin{aligned} T &= \frac{1}{2}\dot{\theta}^2 + lm\dot{\theta}\dot{\phi} \cos(\theta - \phi) + \frac{1}{2}l^2m\dot{\phi}^2, \\ V &= (\cos \theta + 1) + lm(\cos \phi + 1), \end{aligned} \right\} \quad (5.2)$$

where ϕ is the angle which the second pendulum makes with the vertical. Lagrange's equations

$$\left. \begin{aligned} \frac{d}{dt} \frac{\partial T}{\partial \dot{\theta}} - \frac{\partial T}{\partial \theta} &= - \frac{dV}{d\theta}, \\ \frac{d}{dt} \frac{\partial T}{\partial \dot{\phi}} - \frac{\partial T}{\partial \phi} &= - \frac{dV}{d\phi} \end{aligned} \right\} \quad (5.3)$$

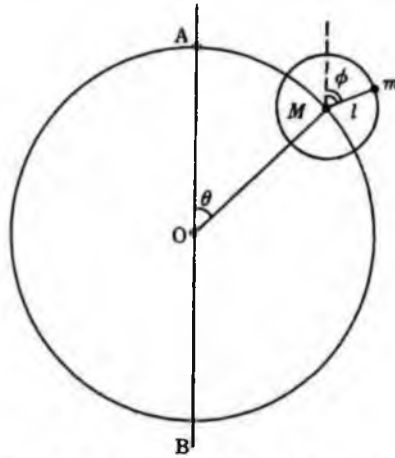


FIGURE 2. Notation for the double pendulum.

yield respectively

$$\ddot{\theta} + lm[\ddot{\phi} \cos(\theta - \phi) + \dot{\phi}^2 \sin(\theta - \phi)] = \sin \theta \quad (5.4)$$

and

$$l\ddot{\phi} + [\ddot{\theta} \cos(\theta - \phi) - \dot{\theta}^2 \sin(\theta - \phi)] = \sin \phi. \quad (5.5)$$

Equation (5.5) may also be written

$$l\ddot{\phi} = g_n \sin(\theta - \phi) - g_s \cos(\theta - \phi), \quad (5.6)$$

where

$$\left. \begin{aligned} g_n &= \dot{\theta}^2 - \cos \theta, \\ g_s &= \ddot{\theta} - \sin \theta. \end{aligned} \right\} \quad (5.7)$$

From (5.6) we see that if a local frame of reference be taken with the same orientation θ as the first pendulum, the angular acceleration of the second pendulum is the same as in a local gravitational field $\mathbf{g}' = (g_n, g_s)$, where g_n is (formally) the same local gravity as in equation (4.2), that is the local gravity due to the first mass alone.

We shall discuss the above equations on the assumption that

$$l \ll L, \quad m \ll M, \quad l\dot{\phi}^2 \gg L\dot{\theta}^2, \quad (5.8)$$

that is to say the second pendulum is relatively short, its mass is only a small fraction of the total mass, and the centrifugal acceleration of the first pendulum is small compared with that of the second.

Then, by (5.4) we have

$$g_s = -lm[\ddot{\phi} \cos(\theta - \phi) + \dot{\phi}^2 \sin(\theta - \phi)]. \quad (5.9)$$

If m is assumed small compared with unity, and compared with all other parameters, this acceleration is an order of magnitude smaller than g_n , so that

most of the local fluctuation in g' comes from the radial component g_n . Writing $\phi - \pi = \phi'$ we then have for $\dot{\phi}'$ the approximation relation

$$l\dot{\phi}' = g_n \sin(\phi' - \theta), \quad (5.10)$$

where g_n is given by (5.7). This is analogous to (2.3).

Because θ varies slowly compared with ϕ , we expect that the dynamical behaviour of the mass m will locally be similar to that of an orbiting pendulum in a constant gravitational field g_n .

6. DEFINITION OF THE ENERGY

How are we to define the energy E of the second pendulum? A straightforward approach might suggest, by analogy with (2.4),

$$E = m[\frac{1}{2}l^2\dot{\phi}^2 + lg(1 + \cos\phi)], \quad (6.1)$$

the first term representing the kinetic energy and the second the potential energy in the external gravity field. However, on differentiating with respect to the time we have

$$\begin{aligned} dE/dt &= lm\dot{\phi}(l\dot{\phi} - \sin\phi) \\ &= lm\dot{\phi}[\dot{\theta}^2 \sin(\theta - \phi) - \dot{\theta} \cos(\theta - \phi)] \end{aligned} \quad (6.2)$$

from (5.5). Because $\dot{\phi}$ is large, the oscillating terms $\sin(\theta - \phi)$ and $\cos(\theta - \phi)$ introduce fluctuations given by

$$\Delta E \approx lm[\dot{\theta}^2 \cos(\theta - \phi) + \dot{\theta} \sin(\theta - \phi)], \quad (6.3)$$

which are of the same order as E itself and so make the definition inappropriate.

Consider next the definition

$$E' = m[\frac{1}{2}l^2\dot{\phi}^2 + lg'\{1 + \cos(\phi - \theta + \pi)\}], \quad (6.4)$$

where g' is the virtual gravity given by equation (4.2). On differentiating with respect to t we now have

$$\begin{aligned} (1/lm) dE'/dt &= \dot{\phi}[l\dot{\phi} - (\dot{\theta}^2 - \cos\theta) \sin(\theta - \phi)] \\ &\quad + \dot{\theta}[(2\dot{\theta} + \sin\theta)\{1 - \cos(\theta - \phi)\} + (\dot{\theta}^2 - \cos\theta) \sin(\theta - \phi)]. \end{aligned} \quad (6.5)$$

Equations (5.4) and (5.5) show that, to lowest order in m , the coefficient of $\dot{\phi}$ in (6.5) now vanishes identically, and we have

$$\frac{1}{lm} \frac{dE'}{dt} = 3\dot{\theta} \sin\theta[1 - \cos(\phi - \theta)] - \dot{\theta}(\dot{\theta}^2 - \cos\theta) \sin(\phi - \theta). \quad (6.6)$$

The fluctuations in \dot{E}' are now of order $(\dot{\theta}/\dot{\phi})E'$, which is relatively small. The slow rate of change of E' is found by taking the average with respect to ϕ in (6.6):

$$\langle dE'/dt \rangle = 3lm\dot{\theta} \sin\theta \quad (6.7)$$

Now from (5.7) we have

$$dg'/dt = \dot{\theta}(2\dot{\theta} + \sin\theta) = 3\dot{\theta} \sin\theta. \quad (6.8)$$

Therefore, if we define alternatively

$$\bar{E} = E' - mlg' = m[\frac{1}{2}(l\dot{\phi})^2 - lg' \cos(\phi - \theta)], \quad (6.9)$$

which is just as natural a choice as (6.4), we shall have in this approximation

$$\langle d\bar{E}/dt \rangle = 0, \quad (6.10)$$

hence

$$\bar{E} = \text{const.} = \frac{1}{2}ml^2s^2, \quad (6.11)$$

where

$$s = (\dot{\phi})_{\phi = \theta + \frac{1}{2}\pi}. \quad (6.12)$$

This incidentally shows that the angular velocity of the smaller pendulum at the mean distance L from the origin is almost constant.

In the definition of \bar{E} in (6.9) we note that the potential energy has been defined relative to its level at the mean distance L from the centre O .

Corresponding to the parameter λ for the single pendulum (see equation (2.5)) we may define a dimensionless parameter ν by

$$\nu^2 = 4g'/lr^2 = 2mg'l/E', \quad (6.13)$$

where r is the angular velocity $\dot{\phi}$ at the outer point of the orbit, that is when $(\phi - \theta) = 2n\pi$; r is then related to s by

$$s^2 \approx r^2(1 - \frac{1}{2}\nu^2). \quad (6.14)$$

We note that under the third of the assumptions (5.8) the parameter ν , defined by (6.13), is small.

Corresponding to (2.12) we have for the estimated period of rotation of the shorter pendulum

$$2\pi/\sigma' = (4/r)K(\nu^2), \quad (6.15)$$

where ν is related to r by (6.13). By the expansion (2.13) for K we have then

$$\sigma' = r/(1 + \frac{1}{4}\nu^2 + \frac{9}{64}\nu^4 + \dots). \quad (6.16)$$

Because from (6.14) r is related to s by

$$r \approx s(1 - \frac{1}{2}\nu^2)^{-1} \quad (6.17)$$

we have also

$$\sigma' \approx s/[(1 - \frac{1}{2}\nu^2)^{-1}(1 + \frac{1}{4}\nu^2 + \frac{9}{64}\nu^4 + \dots)]. \quad (6.18)$$

For small values of ν this becomes

$$\sigma' \approx s(1 + O(\nu^4)). \quad (6.19)$$

So we expect σ' to be constant at least to order ν^2 . Hence \bar{E}/σ' is constant to this order also, as was expected.

However, in this elementary approach it is not clear why the particular definition (6.4) of the energy must be used. There is also a question whether it would be preferable to define both E' and σ' in a reference frame that is rotating with the angular velocity $\dot{\theta}$ of the longer pendulum. Both these questions are resolved in the following section.

7. A HAMILTONIAN DERIVATION

A more rigorous treatment can be given in terms of Hamiltonian mechanics as follows. If as generalized coordinates we take

$$q_1 = \theta, \quad q_2 = \phi \quad (7.1)$$

then the corresponding momenta are given by

$$\left. \begin{aligned} p_1 &= \partial T / \partial \dot{q}_1 = \dot{\theta} + lm \dot{\phi} \cos(\theta - \phi), \\ p_2 &= \partial T / \partial \dot{q}_2 = l^2 m \dot{\phi} + lm \dot{\theta} \cos(\theta - \phi) \end{aligned} \right\} \quad (7.2)$$

and, working to order m , we can write

$$T = \frac{1}{2} p_1^2 + \frac{1}{2l^2 m} [p_2 - lm p_1 \cos(\theta - \phi)]^2. \quad (7.3)$$

To diagonalize the kinetic energy, we make a canonical transformation of the coordinates p_i, q_i (see, for example, Landau & Lifshitz 1960, §45) to new coordinates p_i^*, q_i^* , by means of the generating function

$$\Phi(q_i, q_i^*, p_i^*) = \sum_i q_i p_i^* - lm p_i^* \sin(q_1 - q_2). \quad (7.4)$$

Thus we have

$$\left. \begin{aligned} p_1 &= \partial \Phi / \partial q^* = p_1^* - lm p_1^* \cos(q_1 - q_2), \\ p_2 &= \partial \Phi / \partial q_2 = p_2^* + lm p_1^* \cos(q_1 - q_2), \\ q_1^* &= \partial \Phi / \partial p_1^* = q_1 - lm \sin(q_1 - q_2), \\ q_2^* &= \partial \Phi / \partial p_2^* = q_2. \end{aligned} \right\} \quad (7.5)$$

On substituting in (7.3) and in the potential energy

$$\bar{V} = \cos q_1 + lm \cos q_2 \quad (7.6)$$

we find for the total energy $H = T + \bar{V}$ the expression

$$H = H_1^* + H_2^* + O(m^2), \quad (7.7)$$

where

$$H_1^* = \frac{1}{2} p_1^{*2} + \cos q_1^* \quad (7.8)$$

is the hamiltonian for a single pendulum of unit length L , unit mass M , coordinate q_1^* , and momentum p_1^* , and

$$H_2^* = (1/2l^2 m) p_2^{*2} - g^* lm \cos(q_2^* - q_1^*), \quad (7.9)$$

where

$$g^* = p_1^{*2} - \cos q_1^*. \quad (7.10)$$

We see that H_2^* represents the hamiltonian of a smaller pendulum of length l , mass m under a gravity field g^* directed at an angle $(q_1^* + \pi)$, i.e. parallel to the direction q_1^* . As seen from (7.5), q_1^* differs slightly from $q_1 (= \theta)$ by a term of order m , but the difference in H_2^* is of order m^2 at most. Thus H_2^* can be identified with the quantity \mathcal{E} of equation (6.9).

We have thus confirmed the physical reasoning of §§5 and 6. Moreover the action A^* of the small pendulum is given by

$$A^* = 4l(2E'm)^{\frac{1}{2}}G(\nu^2), \quad (7.11)$$

with E' given by (6.4) and not (6.9). We note that the angle q_1^* serves both as a coordinate and as a slowly varying parameter (through g^*). In the evaluation of an adiabatic invariant such as the action, the integral has to be calculated keeping the parameter fixed (see Landau & Lifschitz 1960, §43). Hence it makes no difference to the calculation of A^* whether the frame of reference is assumed to be rotating slowly or not.

8. NUMERICAL CALCULATIONS

Equations (5.4) and (5.5) may be considered as a pair of simultaneous equations which can be solved to give $\bar{\theta}$ and $\bar{\phi}$ in terms of $\theta, \phi, \dot{\theta}$ and $\dot{\phi}$. Given the initial conditions, these expressions can then be integrated numerically to give θ and ϕ accurately as functions of t .

To test the validity of the analysis in §7 we considered the case when $l = 0.1$ and $m = 10^{-4}$, with the initial conditions $\theta = 0, \phi = 0, \dot{\theta} = 1, \dot{\phi} = 20$, when $t = 0$. The trajectory of the mass m is shown in figure 3. One can see how the spacing of

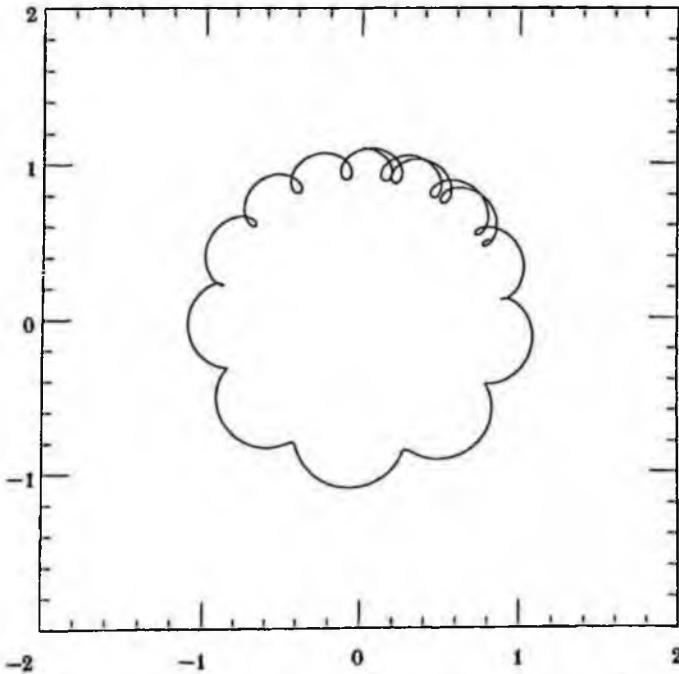


FIGURE 3. Calculated trajectory of the smaller mass when $l = 0.1, m = 10^{-4}$ and with initial conditions $\dot{\theta} = 1, \dot{\phi} = 20, \theta = \phi = 0$.

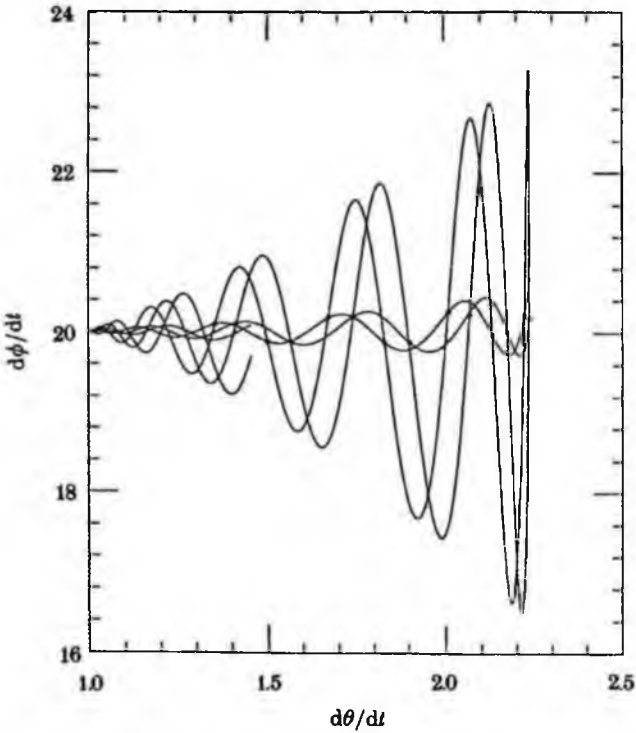


FIGURE 4. The outer curve shows $\dot{\phi}$ as a function of $\dot{\theta}$. The solid plots represent values of s . The inner curve represents $\dot{\phi} [1 - 2g' \cos(\theta - \phi)/l\dot{\phi}^2]$.

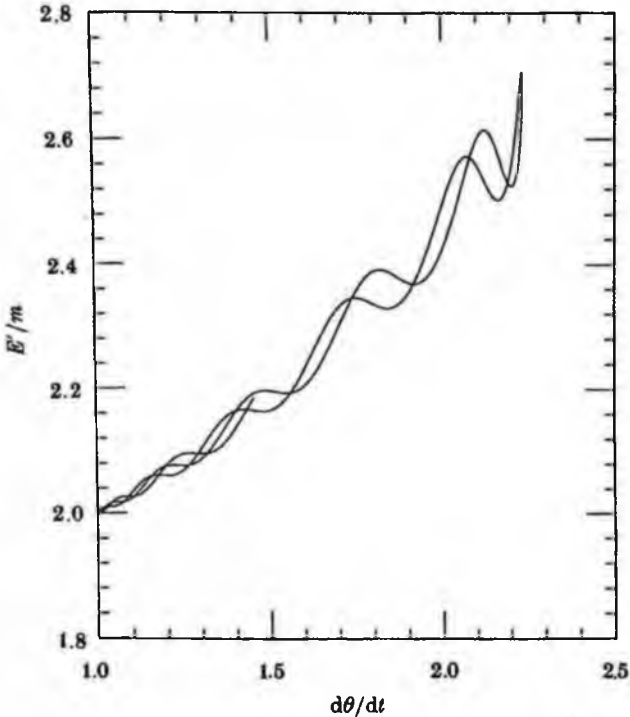
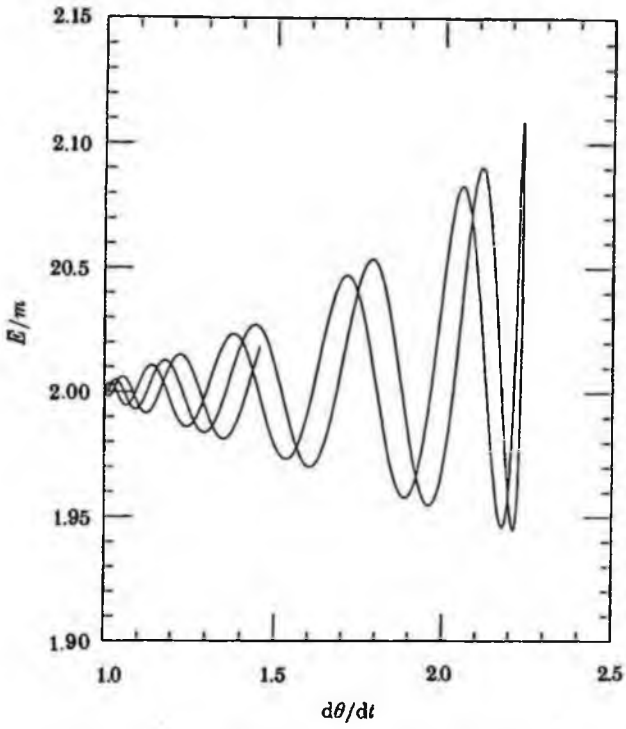
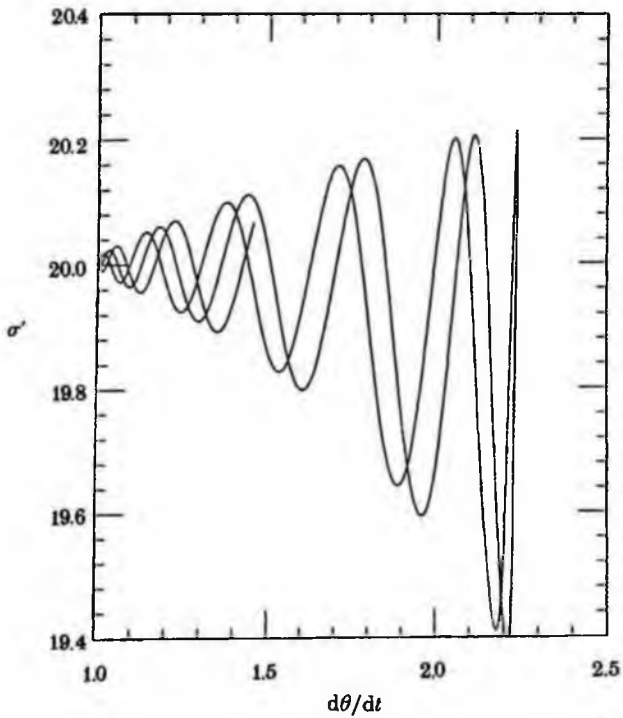


FIGURE 5. Graph of E'/m as a function of $\dot{\theta}$.

292

FIGURE 6. Graph of E/m as a function of θ .FIGURE 7. The intrinsic frequency σ' as a function of θ .

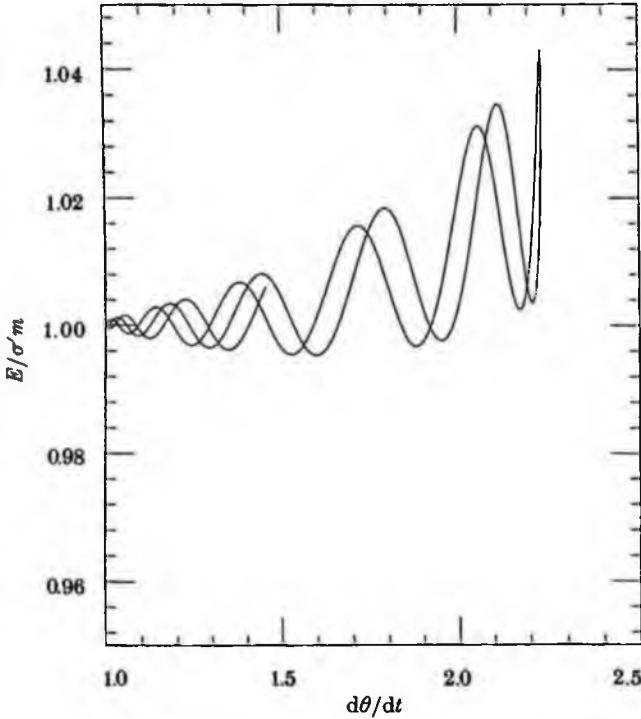


FIGURE 8. The ratio $E/m\sigma'$ for the short pendulum.

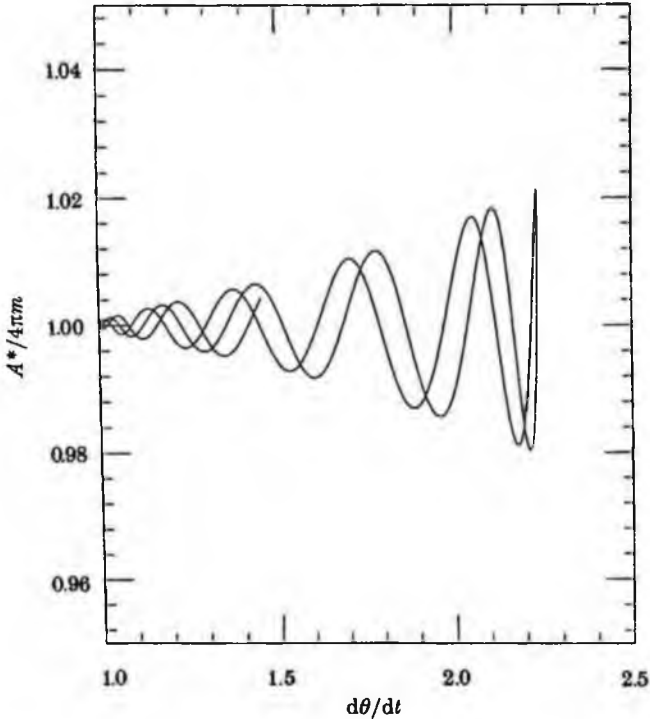


FIGURE 9. The action integral A^* for the short pendulum with initial phase $\phi = 0$.

294

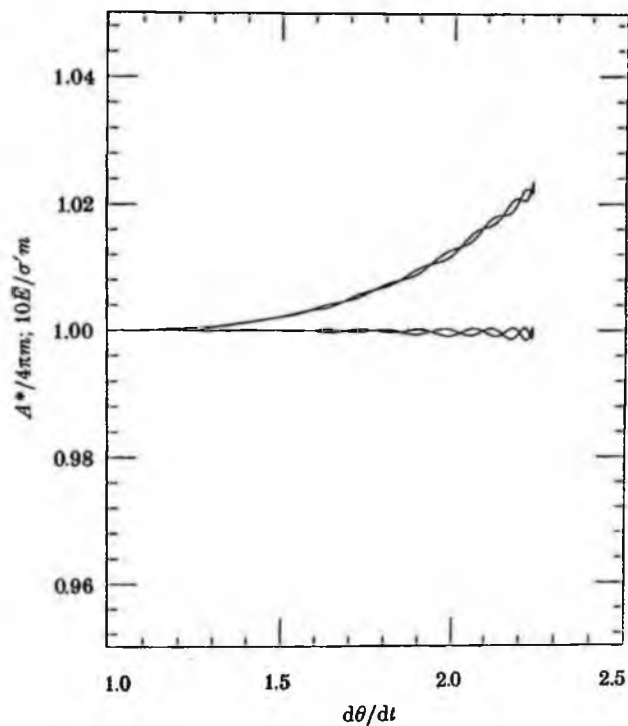


FIGURE 10. $\bar{E}/m\sigma'$ and $A^*/4\pi m$: average of two runs with initial phases $\phi = 0, \pi$.

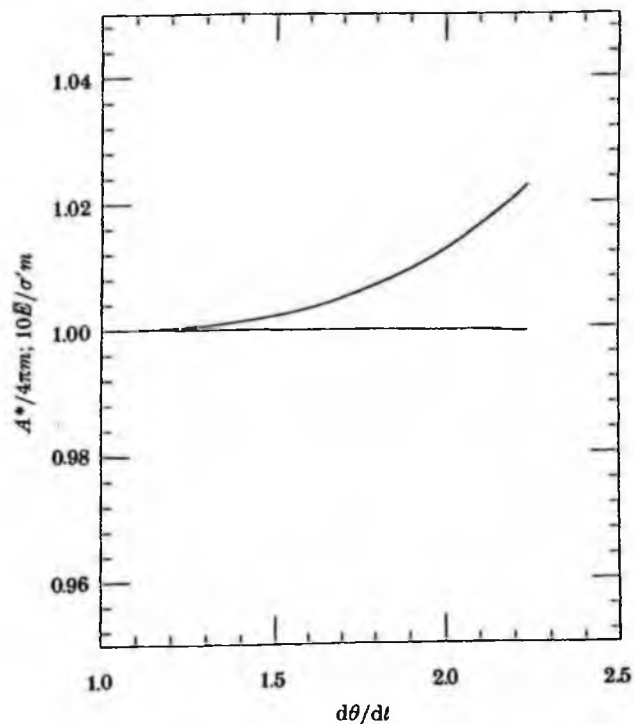


FIGURE 11. $\bar{E}/m\sigma'$ and $A^*/4\pi m$: average of four runs with initial phases $\phi = 0, \frac{1}{4}\pi, \pi, \frac{3}{4}\pi$.

the outermost points of the trajectory increases as θ increases from unity, when $\theta = 0$, to about 2.24 near the bottom of the orbit.

In figure 4, ϕ is plotted against θ . Near the highest point of the orbit ($\theta = 1$) the fluctuations are small, because g' happens to vanish there, but as θ increases, so also does g' and in consequence ϕ fluctuates by as much as 20% on either side of the mean. The values s of ϕ when $\phi - \theta = (n + \frac{1}{2})\pi$ are marked by circular plots. It can be seen that s is indeed nearly constant, to within about 1%.

Figure 5 shows the variation of E' as a function of θ . The short-period fluctuations in E' are much less than those in ϕ . Nevertheless, there is a considerable long-term variation, as was suggested by (6.7).

In figure 6 is shown the variation of \bar{E} . The short-period fluctuations are very similar to those in E' but the long-term fluctuation is almost eliminated, being now less than 1% of the mean.

In figure 7 we see the intrinsic frequency σ' calculated from (6.15). The mean variation in σ' over the complete cycle is again of order 1%.

In figure 8 the ratio $\bar{E}/m\sigma'$ is plotted against θ . The total variation here is about 4%. The variation of the mean is about 2%.

In figure 9 we show the corresponding variation of A^* , given by (7.11). The fluctuations about the mean are of similar magnitude to those in \bar{E}/σ' (figure 8). The fluctuations in the mean are much smaller.

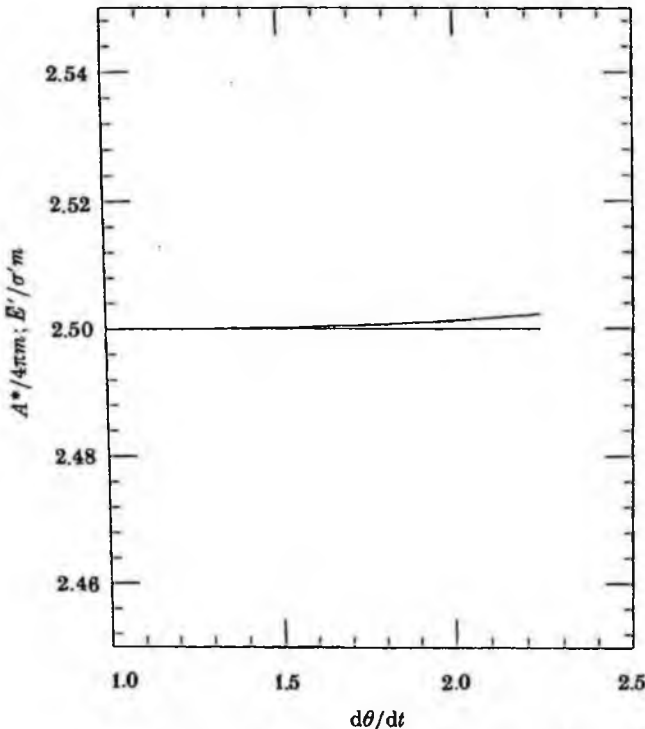


FIGURE 12. As figure 11, but with $l = 0.5$, $m = 10^{-4}$, $\phi_0 = 1$, $\theta_0 = 20$.

Till now we have used always the same initial value for the phase ϕ_0 of the smaller pendulum at time $t = 0$. In reality we are more interested in the behaviour of the average values over some ensemble. Let us consider the average over two or more initial values of the phase ϕ . Thus in figure 10 we show the mean values of $\bar{E}/m\sigma'$ and $A^*/4\pi m$ averaged over the two trajectories with initial phases $\phi = 0$ and $\phi = \pi$. Compared with figures 8 and 9 the fluctuations are much reduced. Now if we take the average over the four trajectories with initial phases $0, \frac{1}{2}\pi, \pi$ and $\frac{3}{2}\pi$ we obtain the results shown in figure 11. The relative constancy of the averaged action A^* is now very clear.

If instead of $m = 10^{-4}$ we integrate the equations in the limit $m = 0$ the curves obtained are found to lie just below the corresponding curves in figures 10 and 11 by amounts of order 10^{-4} only, as we might expect.

What are the corresponding results when either l or θ/ϕ is increased? Figure 12 shows the graph corresponding to figure 11 but with $l = 0.5$, $m = 10^{-4}$, $\theta_0 = 1$, $\phi_0 = 20$.

9. DISCUSSION AND CONCLUSIONS

We have shown both numerically and by a perturbation analysis that the action integral A^* for the small pendulum, as defined by (7.11), is indeed remarkably constant, especially when we consider the average values of A^* over two or more values of the initial phase. The nonlinear expression (7.11) for the action integral is to be preferred over the expressions E'/σ' or \bar{E}/σ' , which are in any case valid only for small values of ν .

By analogy, we would expect that for short surface waves riding on longer gravity waves, where the separation of scales is of order 10:1 or more, the principle of action conservation will be accurately valid. If the short waves are steep, Whitham's more general expression $\partial\mathcal{L}/\partial\omega$ is usually to be preferred to the linearized expression E'/σ' . (An exception is when the first-order variation of ω vanishes.)

In this paper we have assumed that m is very small, so that in the perturbation analysis (though not in the numerical calculations) quantities of order m^2 can be neglected. For water waves, the analogous assumption is that the short-wave energy is sufficiently small that any reaction on the longer waves is negligible, for this purpose.

It would be of some interest to explore other ranges of m , and of the other parameters, but this is beyond the scope of this paper. We note only the possibility of irregular and chaotic behaviour of the small pendulum when the scale separation is not large, or when higher harmonics of the longer pendulum induce

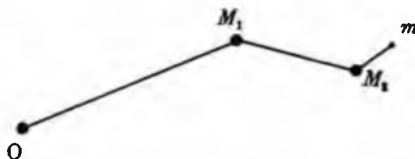


FIGURE 13. A coupled pendulum with masses M_1 , M_2 and m .

resonant oscillations of the small pendulum. Although the rates of growth of such oscillations may be small, nevertheless their effect may be felt over longer periods of time than we have investigated here.

The present two-scale model could be extended in another direction: by considering a short pendulum of small mass m attached to the last of N coupled pendulums of lengths L_i and masses M_i , say, as in figure 13. In this way, even with N as small as 2, one could model the behaviour of very short waves on long waves of non-uniform amplitude.

The earlier sections of this paper are based on work done for the TOWARD Hydrodynamics Committee (see Longuet-Higgins 1985) with the support of the U.S. Office of Naval Research. The joint work in this paper was supported in part by DARPA. K.D. and R.L.S. thank the La Jolla Institute for its hospitality during the academic year 1985-86.

APPENDIX. HISTORICAL NOTE

The principle of action conservation in mechanical systems with discrete degrees of freedom has an interesting and important history. In hamiltonian mechanics† the action was originally defined as the time integral of the kinetic energy T between two given instants, and was shown to be stationary. Applying this to periodic orbits, Boltzmann (1866; 1871; 1904, §§47-48) (see also Clausius 1871; Szily, 1872) pointed out that this implies that T/ω is stationary with respect to small perturbations, where T denotes the time-average of T and $2\pi/\omega$ is the period. Ehrenfest (1914) used this result to show that T/ω is an 'adiabatic invariant', that is to say an integral quantity that remains almost constant during the slow variation of some parameter of the system. Later (1916, pp. 591-595) Ehrenfest proved the adiabatic invariance of the action integral, defined as

$$A = \oint p dq, \quad (\text{A } 1)$$

where p and q are conjugate variables in the hamiltonian sense, and the integral is taken over a complete cycle.

The simple problem of a pendulum whose length is slowly varied was solved by Rayleigh (1902), as an analogue to electromagnetic radiation in a closed box. It was pointed out by Einstein (1912)‡ that in both cases the energy E of oscillation varies in such a way as always to be proportional to the frequency ω . The example of the slowly varying pendulum is often quoted in textbooks on classical and quantum mechanics (see, for example, Born 1960; Arnold 1978) as an analogue to the harmonic oscillator. (Note that in this paper we have been dealing with a different parameter range, where the pendulum describes complete orbits.) Proofs

† See, for example, Whittaker (1927). A clear and relevant account of hamiltonian theory is to be found in Landau & Lifschitz (1960). For an elegant geometrical treatment, see Arnold (1978).

‡ Rayleigh was unable to attend the first Solvay Conference, at which this result was discussed by Einstein and Lorentz.

of the adiabatic invariance of the action integrals under general conditions were given by Burgers (1917), Krutkow (1919), von Laue (1925) and Dirac (1925).

Another well-known instance of an adiabatic invariant is the magnetic moment of an electron spiralling in a non-uniform magnetic field (see Fermi 1949; Northrop 1963). This has important applications in plasma physics (Chandrasekhar 1960; Thompson 1962; Spitzer 1962; Clemmow & Dougherty 1969).

Lastly we mention that Whitham (1965, 1974) has shown the equivalence of the action integral and the expression $\partial\mathcal{L}/\partial\omega$ where \mathcal{L} is an averaged lagrangian. Thus his work is more general than that of Bretherton & Garrett (1968) and applies to nonlinear wave motions.

REFERENCES

- Arnold, V. I. 1978 *Mathematical methods of classical mechanics* (transl. K. Vogtmann & A. Weinstein). (462 pages.) New York: Springer.
- Boltzmann, L. 1866 Über die mechanische Bedeutung des zweiten Hauptsatzes der Wärmetheorie. *Abh. dt. Akad. Wiss. Berl.* **53**, 195.
- Boltzmann, L. 1871 Zur Priorität der Auffindung der Beziehung zwischen dem zweiten Hauptsatz der mechanischen Wärmetheorie und dem Prinzip der Kleinsten Wirkung. *Annln Phys.* **143**, 211–230.
- Boltzmann, L. 1904 *Vorlesungen über die Prinzipie der Mechanik, II.* (335 pages.) Leipzig: J. A. Barth.
- Born, M. 1960 *The mechanics of the atom* (German edn 1924; 1st English edn 1927) (transl. J. W. Fisher; rev. D. R. Hartree). (317 pages.) New York: Frederick Unger.
- Bretherton, F. P. & Garrett, C. J. R. 1986 Wavetrains in homogenous moving media. *Proc. R. Soc. Lond. A* **302**, 529–554.
- Burgers, J. M. 1917 Die adiabatischen Invarianten bedingt periodischer Systeme. *Annln Physik* **52**, 195–202.
- Chandrasekhar, S. 1960 *Plasma physics*. (217 pages.) University of Chicago Press.
- Clausius, R. 1871 Ueber die Zurückführung des zweiten Hauptsatzes der Mechanischen Wärmetheorie auf allgemeine mechanische Principien. *Annln Phys* **142**, 433–451.
- Clemmow, P. C. & Dougherty, J. P. 1969 *Electrodynamics of particles and plasmas*. (457 pages.) Reading, Massachusetts: Addison-Wesley.
- Dirac, P. A. M. 1925 The adiabatic invariance of the quantum integrals. *Proc. R. Soc. Lond. A* **107**, 725–734.
- Ehrenfest, P. 1914 A mechanical theorem of Boltzmann and its relation to the theory of energy quanta. *Proc. K. ned. Akad. Wet.* **16**, 591–597. (Collected papers pp. 340–346.)
- Ehrenfest, P. 1916 On adiabatic changes of system in connection with the quantum theory. *Annln Phys.* **51**, 327–352. (Collected Papers pp. 378–398.)
- Einstein, A. 1912 La Theorie du Rayonnement et des Quanta. In *Reports and Discussions of the 1st Solway Conf., 1911* (ed. P. Langevin & M. de Broglie), p. 450. Paris: Gauthier-Villars.
- Fermi, E. 1949 On the origin of the cosmic radiation. *Phys. Rev.* **75**, 1169–1174.
- Garrett, C. J. R. 1967 The adiabatic invariant for wave propagation in a non uniform moving medium. *Proc. R. Soc. Lond. A* **299**, 26–27.
- Krutkow, S. 1919 Contribution to the theory of adiabatic invariants. *Proc. K. ned. Akad. Wet.* **21**, 1112–1123.
- Landau, L. D. & Lifshitz, E. M. 1960 *Course of theoretical Physics, Vol. 1 (Mechanics)*, 3rd edn. (transl. J. B. Sykes & J. S. Bell). (165 pages.) Oxford: Pergamon Press.
- von Laue, M. 1925 Zum Prinzip der mechanischen Transformierbarkeit (Adiabatenhypothese). *Annln Physik* **76**, 619–628.
- Longuet-Higgins, M. S. 1985 The propagation of short surface waves. Report to TOWARD Hydrodynamics Committee, Washington, Office of Naval Res. October 1985.

- Longuet-Higgins, M. S. 1987 The propagation of short surface waves on longer gravity waves. *J. Fluid Mech.* **177**, 293-306.
- Northrop, T. G. 1963 *The adiabatic motion of charged particles*. (109 pages.) New York: Interscience.
- Rayleigh, Lord 1902 On the pressure of vibrations. *Phil. Mag.* (6) **3**, 338-346.
- Spitzer, L. 1962 *Physics of fully ionised gases*. (170 pages.) New York: Interscience. 170pp.
- Szily, C. 1872 Das Hamilton'sche Princip und der zweite Hauptsatz der mechanischen Wärmetheorie. *Annln Phys.* **145**, 295-302.
- Thompson, W. B. 1962 *An introduction to plasma physics*. (256 pages.) Reading, Massachusetts: Addison-Wesley.
- Whitham, G. B. 1965 A general approach to linear and nonlinear dispersive waves using a Lagrangian. *J. Fluid Mech.* **22**, 273-285.
- Whitham, G. B. 1974 *Linear and nonlinear waves*. (636 pages.) New York: John Wiley & Sons.
- Whittaker, E. T. 1927 *Analytical dynamics*, (3rd edn). (456 pages.) Cambridge University Press.

Laboratory measurements of modulation of short-wave slopes by long surface waves

By SARAH J. MILLER¹, OMAR H. SHEMDIN¹
AND MICHAEL S. LONGUET-HIGGINS²

¹Ocean Research and Engineering, 255 South Marengo Avenue, Pasadena, CA 91101, USA

²Institute for Nonlinear Science, University of California San Diego, La Jolla, CA 92093-0402, USA

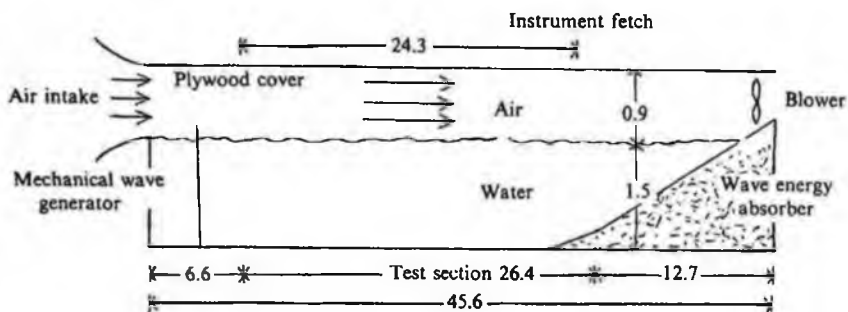
(Received 17 December 1990 and in revised form 28 May 1991)

Hydrodynamic modulation of wind waves by long surface waves in a wave tank is investigated, at wind speeds ranging from 1.5 to 10 m s⁻¹. The results are compared with the linear, non-dissipative, theory of Longuet-Higgins & Stewart (1960), which describes the modulation of a group of short gravity waves due to straining of the surface by currents produced by the orbital motions of the long wave, and work done against the radiation stresses of the short waves. In most cases the theory is in good agreement with the experimental results when the short waves are not too steep, and the rate of growth due to the wind is relatively small. At the higher wind speeds, the effects of wind-wave growth, dissipation and wave-wave interactions are dominant.

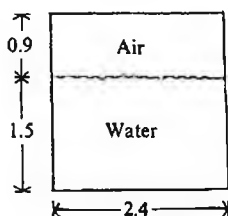
1. Introduction

The modulation of radar reflections from surface water waves depends, at least in part, on hydrodynamic modulation. A nonlinear theory for the propagation of short waves on longer gravity waves has been available for some time (Longuet-Higgins & Stewart 1960; Longuet-Higgins 1987). However, there have been relatively few *direct* measurements of hydrodynamic modulation of wind waves by longer surface waves. Reece (1978) studied the modulation of the frequency spectrum of short surface waves, as indicated by radar backscatter, in a wave tank and had to contend with the added complications of large, variable Doppler effects. Wright *et al.* (1980) used radar to investigate the variation of microwave power scattered by short ocean waves on long surface waves. Here, hydrodynamic effects represent just one contribution to the resultant backscatter modulation. Rather more experimental investigations have been focused on short-wave/internal-wave interactions (for example, Lewis, Lake & Ko 1974; Hughes & Grant 1978; Kwok, Lake & Rungaldier 1988), where the modulation tends to be large.

Direct measurements of modulation by surface waves are needed, made under the simplest possible conditions. In the laboratory, wave parameters can be controlled and stable environmental conditions can be reproduced. Also, long time series can be generated, and reliable statistics of short-wave quantities can be obtained by averaging over equal phases of the long wave, a technique which is only applicable in the laboratory. In the following we present the results of an experiment in which wind waves were generated in a wind-wave tank using a range of wind speeds from 1.5 to 10 m s⁻¹. These were modulated by a mechanically generated (6 m long) surface wave. One unexpected finding is that the higher harmonics in the



(a) Side view



(b) End view

FIGURE 1. Schematic diagram of SIO wind and wave facility (reproduced from Miller & Shemdin 1991). Dimensions in m.

mechanically generated wave, though invisible to the naked eye, play an important role in modulating the steepness of the wind-generated waves.

The same data set was the subject of a previous investigation by two of us (Miller & Shemdin 1991), but that work had a different emphasis from that presented here, being concerned with modulation in a *spectral* sense. The change in the level of the encountered frequency spectrum of short-wave slopes, due to hydrodynamic modulation and Doppler shifting caused by the long surface wave, was considered for spectral components in the frequency band 10 to 20 Hz. The observed modulation was compared with the predictions of a linearized solution of the radiative transfer equation.

The present paper considers modulation of the total mean-square slope of short waves. The details of the experimental configuration are described in §2. In §3 the variation of the mean-square slopes of the short waves over the long-wave profile is examined. The results are compared with the linear, non-dissipative theory of Longuet-Higgins & Stewart (1960) in §4. A discussion follows in §5.

2. Experimental set-up

The experimental conditions are described in Miller & Shemdin (1991) and are summarized here for completeness. The experiment was carried out using a wind-wave facility at the Scripps Institution of Oceanography. A diagram of the wind-wave tank is shown in figure 1. The facility test section is 26.4 m long and 2.4 m wide. The water depth was set at 1.5 m during the test. Wind waves were generated using a blower which was operated to obtain wind speeds in the range 1.5 to 10 m s⁻¹. Low-frequency mechanical waves could be generated using a paddle located at the upwind

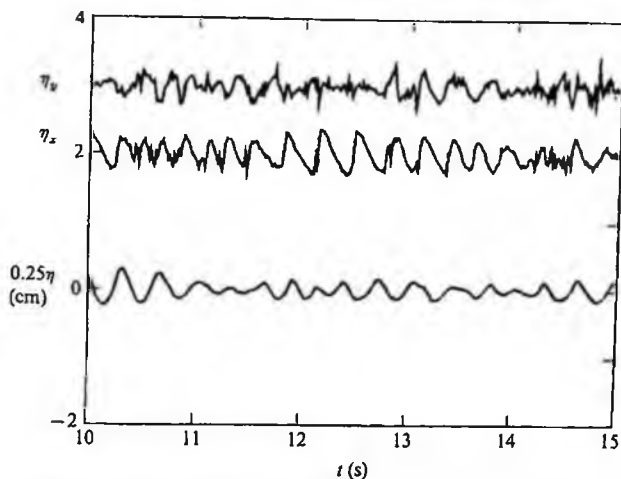


FIGURE 2. Time series of surface displacement (η), downwind slope (η_x) and crosswind slope (η_y). (η_x and η_y are offset by 2 and 3 units, respectively.) The wind speed is 4 m s^{-1} . No mechanical wave is present. (Reproduced from Miller & Shemdin 1991.)

end of the tank. The amplitude of the mechanical surface waves was kept constant at 4.1 cm and the fundamental period was 2 s. A wave absorber consisting of a transite asbestos cement surface with slope 1/12 for 3.5 m followed by a slope of 1/8 for 12.7 m was situated at the downwind end of the tank. The reflection coefficient of the fundamental 2 s wave was previously measured as about 0.1 and less than 0.05 for its harmonics. Time series of surface displacement were obtained using a capacitance wave gauge which responds to frequencies up to 8 Hz.

Crosswind and downwind components of the surface slope were measured at a fetch of 24.3 m using a laser slope sensor which measures the refraction of a light beam penetrating the air-water interface, as described by Tober, Anderson & Shemdin (1973) and Palm, Anderson & Reece (1977). Instruments of this type have been used by several authors (for example, Cox 1958; Long & Huang 1976; Hughes & Grant 1978; Tang & Shemdin 1983, Shemdin & Hwang 1988). Owing to the fast response of the optical system, rapid slope variations due to wave motion are easily detected. The shortest wave that can be detected is determined by the spot size of the laser beam, which is less than 3 mm in diameter. By positioning the laser slope sensor close to the capacitance wave gauge, and obtaining simultaneous measurements from the two instruments, changes in the short-wave slopes due to the passage of the long waves could be detected. However, the 'fish line' effect due to the passage of water past the wave gauge, was negligibly small.

3. Modulation of slope variance

Part of a time series of the surface displacement, η , of wind waves in the absence of a mechanical wave, as measured by the capacitance wave gauge, is plotted in figure 2. The dominant wave has a period of about 0.3 s at a wind speed of 4 m s^{-1} . The downwind and crosswind components of surface slope, η_x and η_y respectively, are also shown. Figure 3 shows the wind waves superimposed on the mechanically generated 2 s waves.

The variation of the statistics of wind waves at different phases of the current was found by averaging over equal phases of the mechanical wave. The period, T , and

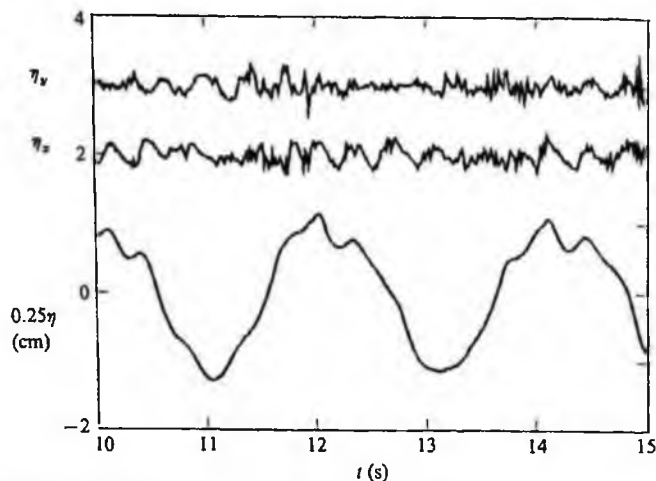


FIGURE 3. As for figure 2, but with 2 s mechanical wave present. (Reproduced from Miller & Shemdin 1991.)

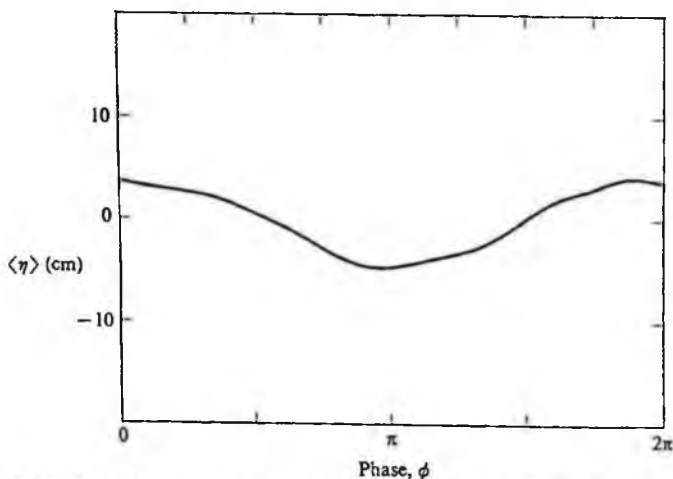


FIGURE 4. Surface displacement averaged over 75 periods, showing the 2 s mechanical wave. (Reproduced from Miller & Shemdin 1991.)

phase, ϕ , of the latter, were determined by maximizing the coherence of the surface displacement with a cosine of variable period, 2.0 ± 0.2 s, and variable phase. Figure 4 shows $\langle \eta \rangle$, the surface displacement, averaged over 75 periods. (Phase-averaged quantities are denoted using angle brackets.) The phase is defined by $\phi = 2\pi t/T$, with time, t , measured from the crest of $\langle \eta \rangle$. The wave paddle does not generate a purely sinusoidal disturbance, as is apparent in figure 5, which shows $\langle \eta_x \rangle$, the phase-averaged downwind component of the slope. Fourier analysis reveals components at the fundamental frequency,

$$\Omega_1 = 2\pi/T, \quad (1)$$

and at its harmonics,

$$\Omega_n = n\Omega_1. \quad (2)$$

The latter give only a small contribution to the surface displacement, but are significant in the downwind slope, which has contributions from up to the sixth harmonic (see table 1).

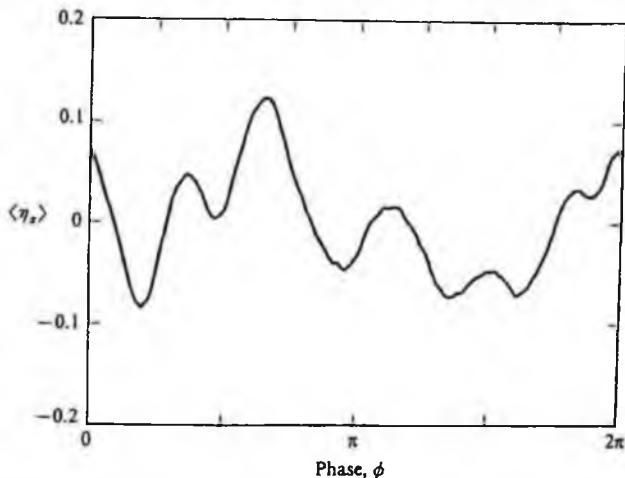


FIGURE 5. Downwind component of surface slope averaged over 75 periods. Significant amounts of the second and third harmonics of the fundamental oscillation are present. The wind speed is 1.5 m s^{-1} .

n	A_n (cm)	$K_n A_n$
1	4.11	0.043
2	0.40	0.015
3	0.46	0.038
4	0.08	0.013
5	0.01	0.008
6	0.02	0.003

TABLE 1. Fourier amplitudes of surface displacement, A_n , and downwind slope, $K_n A_n$, measured independently when no wind was blowing

$\langle \eta \rangle$ is modelled by

$$\langle \eta \rangle = \sum_{n=1}^N A_n \cos(\Omega_n t + \phi_n), \quad (3)$$

where the amplitudes A_n and phases ϕ_n were obtained numerically from Fourier decomposition of $\langle \eta \rangle$. Table 1 shows the Fourier amplitudes of surface displacement, A_n , measured with the capacitance wave gauge, together with the Fourier components of downwind slope, $K_n A_n$, measured independently with the laser slope gauge. Figure 6 shows K_n , the wavenumber of harmonic n , versus frequency Ω_n deduced from the ratio of $K_n A_n$ to A_n . The result is consistent with the dispersion relation for free surface waves,

$$\Omega_n^2 = g K_n \tanh(K_n d), \quad (4)$$

where g is acceleration due to gravity and d is the mean water depth. This result is expected for waves produced by a paddle wave generator of the type used here. It is noted that since the harmonics are coupled to the wave maker and have period T/n , the resultant disturbance at the instrument location due to the wave maker is periodic in time with period T .

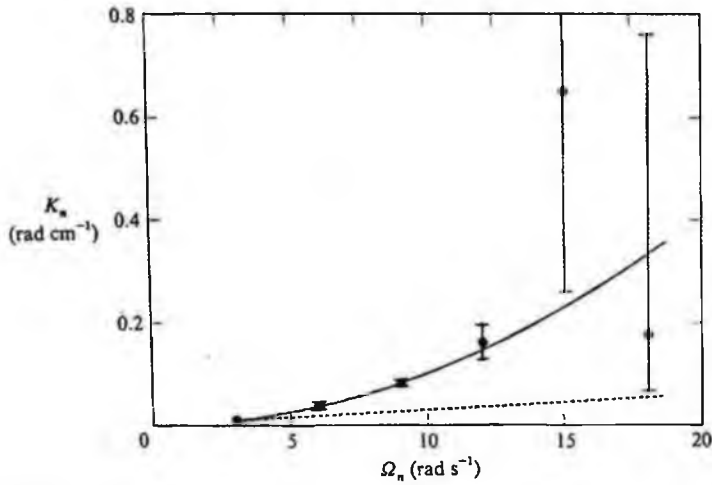


FIGURE 6. Dispersion relation of the waves produced by the paddle wave generator (solid circles), derived from the phase-averaged surface displacement and slope. The error bars show plus and minus one standard deviation of the estimate of K_n . Also shown are the dispersion relations of free gravity waves (solid line) and of waves bound to the fundamental oscillation (dashed line).

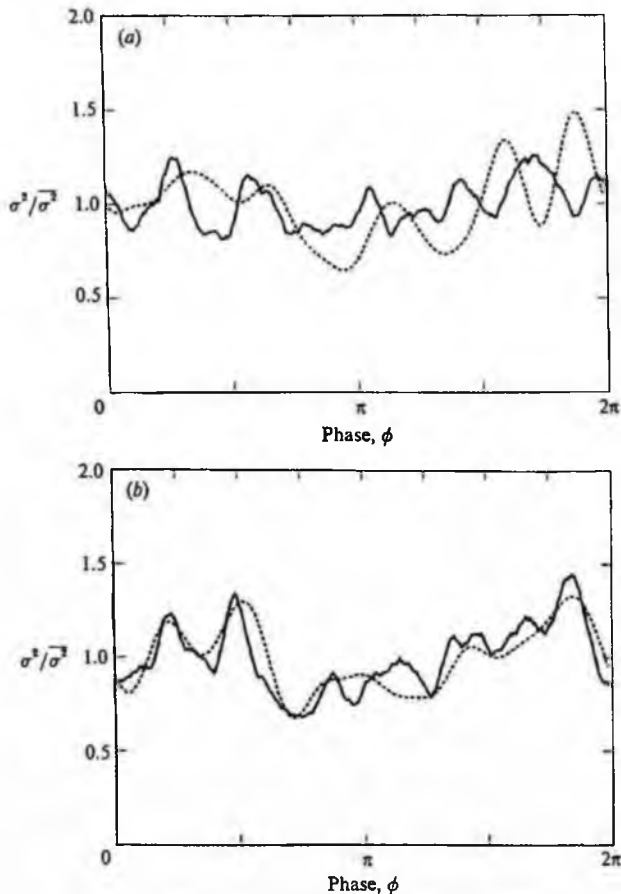


FIGURE 7 (a, b). For caption see facing page.

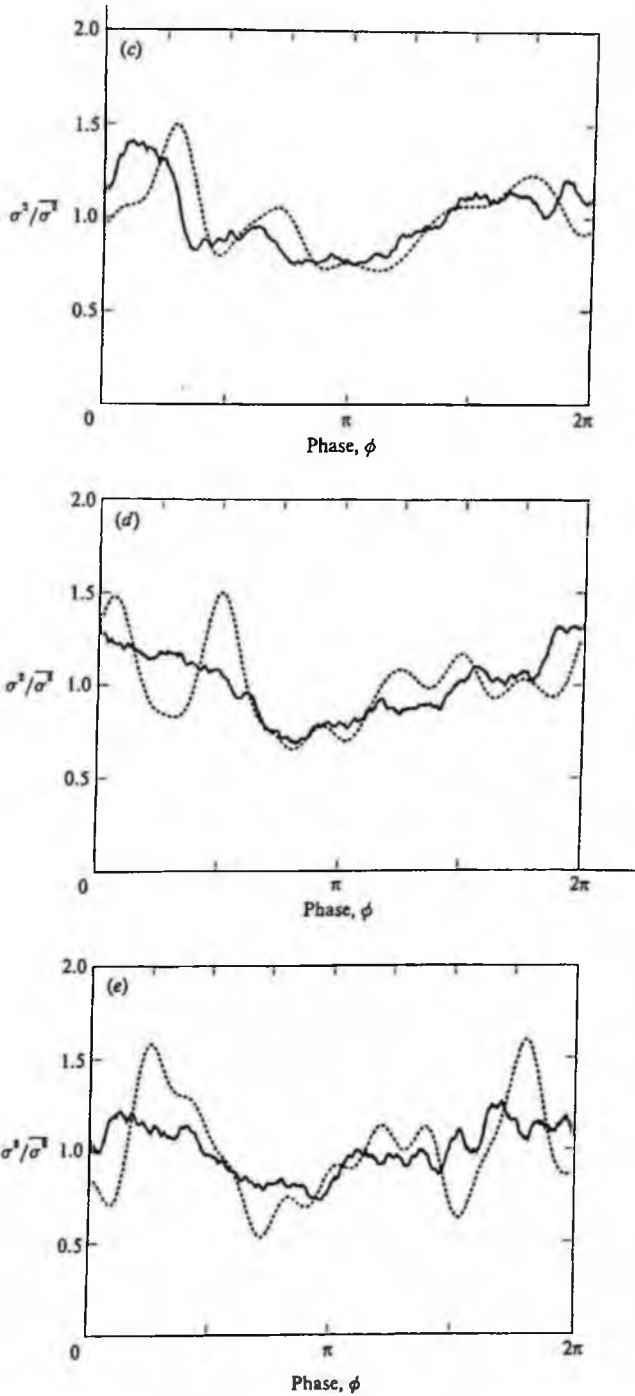


FIGURE 7. Variance of surface slope, normalized by its average value over a long-wave period. Data are shown by a solid line and the dashed line is the theoretical result of Longuet-Higgins & Stewart (1960), computed using 10 Fourier components. The wind speeds are (a) 1.5 m s⁻¹, (b) 4 m s⁻¹, (c) 6.5 m s⁻¹, (d) 9 m s⁻¹ and (e) 10 m s⁻¹.

Wind speed W (m s^{-1})	Short-wave age, c/W	Long-wave age, C_1/W	$\overline{\sigma^2}$ (without long wave)	$\overline{\sigma^2}$ (with long wave)
1.5	0.19	2.00	0.002	0.022
4.0	0.13	0.75	0.038	0.026
6.5	0.10	0.46	0.056	0.045
9.0	0.09	0.33	0.063	0.055
10.0	0.08	0.30	0.063	0.059

TABLE 2. Variance of short-wave slope averaged over the long-wave period. c and C_1 denote the phase speeds of the dominant short and long waves, respectively

The variance of the short surface slopes at different phases of the long wave, was examined by calculating

$$\sigma^2 = \langle (\eta_x - \langle \eta_x \rangle)^2 \rangle + \langle (\eta_y - \langle \eta_y \rangle)^2 \rangle. \quad (5)$$

In figure 7 $\sigma^2/\overline{\sigma^2}$ is plotted as a function of ϕ at the five wind speeds, W (full line). Here $\overline{\sigma^2}$ is the mean value of σ^2 over the wave period T , and is tabulated in table 2 as a function of wind speed. For comparison, the value of $\overline{\sigma^2}$ obtained when no modulating wave was present is also tabulated. We note that, for $W \geq 4.0 \text{ m s}^{-1}$, the presence of the long wave reduces $\overline{\sigma^2}$, the greatest reduction being at low wind speeds. The reduction of the wave amplitude of short waves on long waves has been reported by Mitsuyasu (1966), Phillips & Banner (1974), and Donelan (1987). Phillips & Banner (1974) showed that the orbital velocity of the long wave causes the surface drift velocity to vary with phase of the long wave. They proposed that this would result in enhanced breaking at the long-wave crests, leading to a reduction in the r.m.s. height of the short waves. Plant & Wright (1977), however, argued that the role of the wind drift current in limiting the short-wave amplitude was small.

The very low value of $\overline{\sigma^2}$ at 1.5 m s^{-1} is thought to be evidence of a surface slick. The minimum surface friction speed required for wave generation for a clean surface has been estimated by Miles (1962) and van Gastel, Janssen & Komen (1985) as about 5 cm s^{-1} . Assuming that in a wave tank the friction speed is given by $0.05W$ (Gottifredi & Jameson 1970; Plant & Wright 1977) this corresponds to a wind speed of $W \approx 1.0 \text{ m s}^{-1}$. When a film is present, Miles estimated that this minimum is increased to about 17.5 cm s^{-1} , whereas Gottifredi & Jameson found that it could increase up to 20 cm s^{-1} , corresponding to $W \approx 4.0 \text{ m s}^{-1}$. Evidently, the mean surface drift introduced by the deterministic wave disrupted the surface film, and wind waves could then be generated at the lowest wind speed.

4. Comparison with the theory of Longuet-Higgins & Stewart (1960)

Longuet-Higgins & Stewart (1960) considered the changes in a group of short gravity waves riding on a longer surface wave, $A_1 \cos(\Omega_1 t + \phi_1)$, of small slope, $K_1 A_1$. They showed that, in the absence of external sources and nonlinear effects such as wave breaking, the energy, E , of the short waves is governed by

$$\frac{\partial E}{\partial t} = \frac{\partial}{\partial x} [E(c_g + U) + S_x U], \quad (6)$$

where c_g and S_x are the group velocity and radiation stress of the short waves,

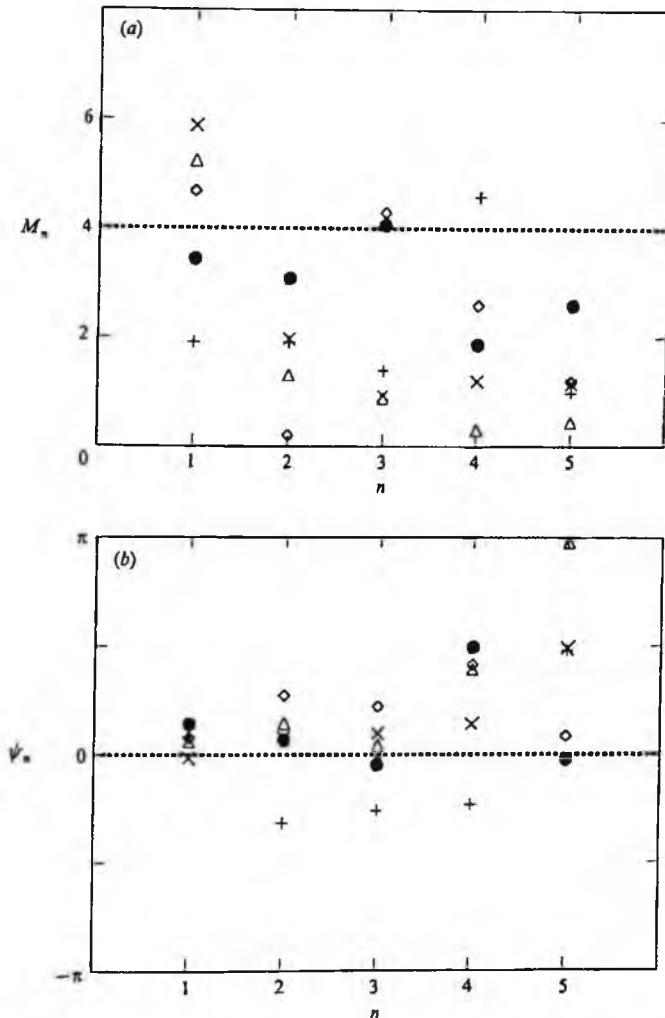


FIGURE 8. (a) Amplitude and (b) phase of the Fourier components of the modulation transfer function, defined by (9), at wind speeds 1.5 m s^{-1} (+), 4 m s^{-1} (●), 6.5 m s^{-1} (◇), 9 m s^{-1} (×) and 10 m s^{-1} (△).

respectively, and U is the current due to the orbital motions of the long wave. Generalizing their solution of (6) to a spectrum of non-interacting gravity waves travelling on a long wave with displacement given by (3), gives

$$\sigma^2(\phi) = \overline{\sigma^2} \left[1 + \sum_{n=1}^N \left(\frac{1}{2} \coth(K_n d) + \frac{1}{2} \tanh(K_n d) \right) K_n A_n \cos(\Omega_n t + \phi_n) \right]. \quad (7)$$

To compare this with the data, $\sigma^2(\phi)$, equation (7), was computed using K_n calculated from (4), and A_n obtained from the Fourier decomposition of $\langle \eta \rangle$ at each wind speed. The results are shown as dashed lines in figure 7.

A more detailed comparison is obtained by inspecting the complex Fourier

amplitudes of the linear modulation transfer function (MTF); if σ^2 is decomposed into

$$\sigma^2(\phi) = \overline{\sigma^2} \left[1 + \sum_{n=1}^N B_n \cos(\Omega_n t + \theta_n) \right], \quad (8)$$

the amplitude, M_n , and phase, ψ_n , of the n th component of the MTF are defined by

$$M_n = \frac{B_n}{K_n A_n}, \quad \psi_n = \theta_n - \phi_n. \quad (9)$$

A positive value of ψ_n indicates that modulation of σ^2 at frequency Ω_n lags that component of modulating current, that is, the modulation occurs at a later time. The first five components of the modulation are plotted in figure 8.

For the conditions of this experiment, the deep-water condition, $K_n d \geq 1.5$, is satisfied for all n . The MTF predicted by (7) therefore has $\psi_n = 0$ with $M_n \approx 4$ for all n , the levels being indicated by dashed lines in figure 8.

The goodness of fit of (7) to the data is clearly a function of wind speed, the best agreement being obtained at the intermediate values, 4 and 6.5 m s⁻¹, since in these cases M_n is close to 4. (The low value of M_2 at 6.5 m s⁻¹ is not significant since $\langle \eta \rangle$ and σ^2 have only small contributions from the first harmonic.) The phase agreement at 4 m s⁻¹ is also excellent, but at 6.5 m s⁻¹ harmonics $n = 2, 3$ and 4 in σ^2 lead those in $\langle \eta \rangle$ by about 45°, as is apparent in figure 7(c). At the lowest wind speed, 1.5 m s⁻¹, the agreement between data and theory is poor, the modulation in the data being too small at low frequencies. Also, in this case the harmonics in σ^2 lag those in $\langle \eta \rangle$ by 45°. At the highest speeds, 9 and 10 m s⁻¹, modulation at the fundamental frequency is somewhat amplified compared to the intermediate wind speed cases, while it is reduced in the harmonics. The phase agreement is, however, quite good.

5. Discussion

Equation (6) was formulated for short gravity waves isolated from external effects such as wind input, and for which nonlinear interactions and wave breaking are not important. Its applicability to the conditions of the present experiment are examined as follows.

The importance of energy input from wind to a wave group of dominant frequency, f_p , can be estimated by evaluating the ratio of the wind growth rate, β , to the long-wave frequency, Ω_1 . In this experiment $\Omega_1 \approx 3$ rad s⁻¹. When β is much less than Ω_1 the characteristic timescale of growth due to wind, β^{-1} , is long compared with the wave period, so that wind growth can be neglected. In this case (6) might be expected to describe the modulation of the variance of surface slopes. However, when β/Ω_1 is not small, the effect of wind input in the modulation process must be considered. Table 3 shows the growth rate, $\beta(f_p)$, evaluated using Plant's (1982) form with the friction speed evaluated as 0.05 W ,

$$\beta = 6.3 \times 10^{-4} (W/c)^2 f_p, \quad (10)$$

where c is the phase speed at frequency f_p .

As the wind speed increases, the wind wave spectrum becomes broader as the energy of the small waves increases. The slope frequency spectra of the short waves, $S(f)$, where

$$\overline{\sigma^2} = \int_0^\infty S(f) df, \quad (11)$$

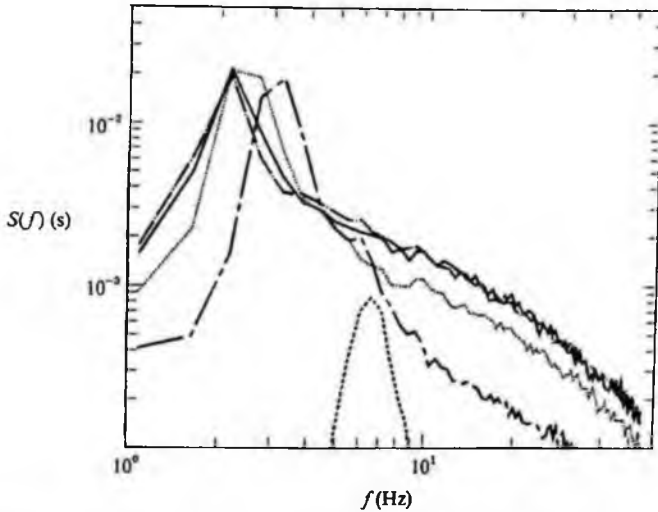


FIGURE 9. Slope frequency spectra at wind speeds 1.5 m s^{-1} (----), 4 m s^{-1} (-----), 6.5 m s^{-1} (.....), 9 m s^{-1} (—), and 10 m s^{-1} (-.-.-). No mechanical wave is present. (Reproduced from Miller & Shemdin 1991.)

W (m s^{-1})	f_p (Hz)	$\beta(f_p)$ (s^{-1})	f_{med} (Hz)	$\beta(f_{\text{med}})$ (s^{-1})	$\frac{\beta(f_{\text{med}})}{4\Omega_1 K_1 A_1}$
1.5	6.0	0.09	6.0	0.09	0.19
4.0	3.0	0.14	3.0	0.14	0.28
6.5	2.5	0.17	4.0	0.69	1.37
9.0	2.0	0.17	10.0	9.61	19.18
10.0	2.0	0.20	10.0	11.87	23.69

TABLE 3. Growth rate due to the wind

are plotted in figure 9. At 4 m s^{-1} 70% of the total area lies below 5 Hz, compared with only 40% at 9 m s^{-1} . A possibly more accurate estimation of the growth rate may be obtained, therefore, by evaluating β at, for example, the median frequency, f_{med} , of the slope spectrum, where

$$\int_0^{f_{\text{med}}} S(f) df = \frac{1}{2} \bar{\sigma}^2. \quad (12)$$

The results, which except for the lowest wind speed were obtained when no mechanical wave was present, are shown as $\beta(f_{\text{med}})$ in table 3. At 9 and 10 m s^{-1} , $\beta(f_{\text{med}})/\Omega_1 \geq 3$ suggesting that wind generation effects must be significant in those cases.

The relative importance of the energy input by the wind to the modulation of the short waves by the orbital straining of the long waves, can be estimated by considering the ratio of β/Ω_n to $4K_n A_n$. With β evaluated at f_{med} , this is shown in table 3 for the fundamental frequency of the long wave. Interestingly, $\beta/(4\Omega_1 K_1 A_1)$ is much greater than unity for the two highest wind speeds.

The steepness of the short waves increases with wind speed so that the nonlinear effects of wave breaking and wave-wave interactions are expected to become

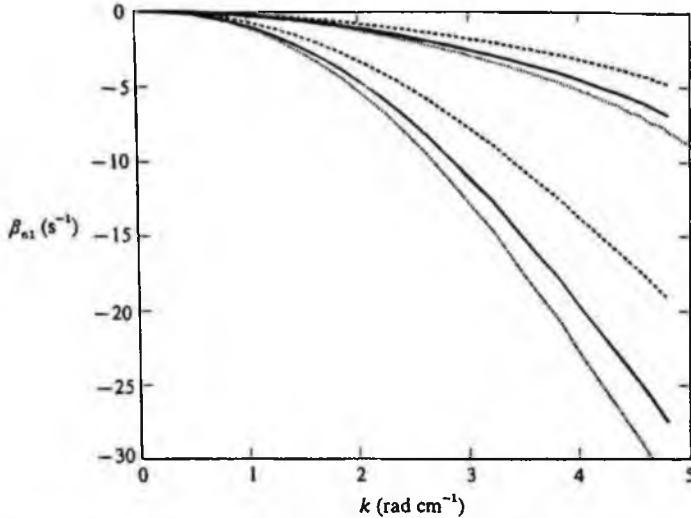


FIGURE 10. Nonlinear transfer for three-wave interactions for wind speeds 4 and 9 m s⁻¹ and $D(\theta, k) = a_p \cos^p(\frac{1}{2}\theta)$ with $p = 2$ (-----), 6 (——) and 10 (·····).

W (m s ⁻¹)	k_{med} (rad cm ⁻¹)	$\beta_{\text{nl}}(k_{\text{med}})$ (s ⁻¹)	$\frac{\beta_{\text{nl}}(k_{\text{med}})}{\Omega_1}$	$\frac{\beta_{\text{nl}}(k_{\text{med}})}{4\Omega_1 K_1 A_1}$
4.0	0.16	0.00	0.00	0.00
6.5	0.64	0.13	0.04	0.26
9.0	2.60	7.45	2.38	14.87
10.0	2.60	7.45	2.38	14.87

TABLE 4. Nonlinear transfer rate due to three-wave interactions

increasingly significant. The weakly nonlinear wave-wave interactions are of third order in the wave slope for short gravity waves, and second order for capillary-gravity waves. The rate of energy transfer due to the latter, β_{nl} , was computed using the expression derived by Valenzuela & Laing (1972). The results evaluated at $k = k_{\text{med}}$, where

$$2\pi f_{\text{med}} = \left(gk_{\text{med}} + \frac{\tau}{\rho} k_{\text{med}}^3 \right)^{\frac{1}{2}} \quad (13)$$

(τ and ρ are the surface tension and density of water), are given in table 4 for the four highest wind speeds (the lowest wind speed case was not computed). Details of the wavenumber spectrum used in the calculation are given in the Appendix.

Comparison of tables 3 and 4 shows that the estimates of β_{nl} are similar to those obtained for the growth rate due to the wind, with a sharp distinction between $W \leq 6.5$ m s⁻¹, where the transfer rate is small compared with the long-wave frequency and energy transfer is a minor effect in comparison with orbital straining, and $W \geq 9$ m s⁻¹, where the three-wave interactions play an important role.

The wind drift current, u_d , has not been considered in the above calculations. For short waves at high wind speeds the wind drift current can be of the same magnitude as the intrinsic phase speed of short gravity waves. For example, at a wind speed of 10 m s⁻¹, calculating the drift current as 3% of the wind speed, gives $u_d = 30$ cm s⁻¹,

which is equal to the phase speed of a 5 cm wave in still water. If β is evaluated using (10) with c in the denominator calculated as the advected phase speed, the value of β will be reduced by a factor of about 4 at $W = 9 \text{ m s}^{-1}$ and 10 m s^{-1} , and by a smaller factor at the lower wind speeds. Also, if (13) is modified to include the wind drift, k_{med} will be reduced by a factor of about 2 at the highest wind speeds so that, from figure 10, β_{nl} is reduced by factor of about 4 in these cases. The distinction between the low and high wind cases in the relative importance of orbital straining and energy input from the wind or energy transfer due to three wave interactions, would be less dramatic than estimated above, but the trend is unchanged.

We note that at the highest wind speeds, (7) should be modified to include capillary-gravity waves, which make a significant contribution to σ^2 . If this is done, the theoretical MTF due to the orbital motions of the long wave becomes somewhat smaller than the value 4 found above for a spectrum of pure gravity waves. However, the application of a simple two-scale model to these very short waves is probably not realistic.

6. Conclusions

The most striking conclusion to be drawn from these measurements is that the modulation of the short waves is determined not by the long-wave amplitude, A_n , but rather the long-wave steepness, $K_n A_n$. Hence, the apparent phase and amplitude of the modulation may be related to wave components that are invisible to the eye.

More generally, the modulation of the short waves will be determined not by the *elevation* spectrum of the long waves but by the *slope* spectrum, as is emphasized by Longuet-Higgins (1991).

We have found that the modulation transfer function of the short waves is in agreement with the linearized, non-dissipative theory of Longuet-Higgins & Stewart (1960) only where that would be expected, namely when the short waves are not too steep, and the rate of growth due to the wind is relatively small. (We found poor agreement at the lowest wind speed, however.) With steeper short waves, we may expect two additional effects: strong short-wave interactions due to breaking, and weak non-dissipative short-wave interactions. For short capillary-gravity waves they are of second order (Valenzuela & L aing 1972), and for short gravity waves they are of third order (Hasselmann 1962). Their relative importance will vary with short-wave steepness.

Finally we remark that since the tangential wind stress is in part mediated by the short wind waves, our findings will have implications for the effect of swell on the mean wind stress, and on the modulation of the wind stress by the longer waves.

Paul Hwang and Dave Hayt were responsible for the data collection and the initial data processing was done by Paul Hwang. The authors appreciate their cooperation during the period of the above work. The work reported here was supported by the Office of Naval Research under the SAR Accelerated Research Initiative Program.

Appendix. Calculation of β_{nl} , the capillary-gravity wave-wave interaction rate

The spectrum of wave heights,

$$\langle \eta^2 \rangle = \int_0^\infty \int_{-\pi}^\pi \Psi(k, \theta) k dk d\theta, \quad (\text{A } 1)$$

W (m s ⁻¹)	k_p (rad cm ⁻¹)	Γ
4.0	0.16	56
6.5	0.25	21
9.0	0.36	13
10.0	0.36	13

TABLE 5

was modelled using the separable form

$$\Psi(k, \theta) = F(k)D(\theta, k), \quad (\text{A } 2)$$

where

$$\int_{-\pi}^{\pi} D(\theta, k) d\theta = 1. \quad (\text{A } 3)$$

The directional spread function $D(\theta, k)$ was modelled by

$$D(\theta, k) = \alpha_p \cos^p(\frac{1}{2}\theta), \quad p = p(k), \quad (\text{A } 4)$$

where the downwind direction is taken as $\theta = 0$.

The model used here is derived from consideration of the two components of the frequency slope spectrum obtained before the long wave was generated. Taking the minimum wind speed required for wave generation, as $W_{\min} = 2.7 \text{ m s}^{-1}$, $F(k)$ is modelled, for $4 \text{ m s}^{-1} \leq W \leq 9 \text{ m s}^{-1}$, by (Shemdin & Miller 1991)

$$F(k) = 5 \times 10^{-4} (W - W_{\min}) \frac{k^{-3.5}}{(g + \tau k^2 / \rho)} \exp\left(-1.75 \left(\frac{k_p}{k}\right)^2\right) \Gamma^M \quad \text{for } k < k_p. \quad (\text{A } 5)$$

Here, g is gravitational acceleration, and ρ and τ are the density and surface tension of water. $k_p = 8 \text{ rad cm}^{-1}$ is the viscous cutoff, and

$$M = \exp\left(-\frac{(k^{\frac{1}{2}} - k_p^{\frac{1}{2}})^2}{0.32k_p}\right), \quad (\text{A } 6)$$

where $k_p = (2\pi f_p)^2/g$ is the peak wavenumber, and Γ and $M(k)$ define the height and shape of the spectral peak. Γ and k_p are wind-speed dependent as shown in table 5.

The part of the spectrum where viscosity is important is modelled by (Shemdin & Miller 1991)

$$F(k) = 4.8 \times 10^{-4} (W - W_{\min}) k^{-5.5} \quad \text{for } k > k_p. \quad (\text{A } 7)$$

Above $W = 9 \text{ m s}^{-1}$, the frequency spectrum was found to saturate, so at 10 m s^{-1} $F(k)$ was modelled by the same form as at 9 m s^{-1} .

The nonlinear transfer due to three-wave interactions between gravity and capillary-gravity waves, $\partial\Psi/\partial t$, was calculated numerically using the expression given by Valenzuela & Laing (1972). The transfer rate, $\beta_{nl} \equiv -(1/\Psi)(\partial\Psi/\partial t)$, was also calculated for spread functions, $D(\theta, k)$, with $p = 2, 6$ and 10 for all k . The results are shown in figure 10 for $k \leq 5 \text{ rad cm}^{-1}$ and for wind speeds 4 and 9 m s^{-1} . The plots show that, as expected, the energy transfer is small for small wavenumbers and increases with wind speed. The fact that the transfer is largest for wave triads that are inclined at small angles, is reflected in β_{nl} increasing with p .

At wavenumbers beyond the peak of the spectrum, the angular spread increases so that the ratio of the crosswind and downwind components of the slope spectrum

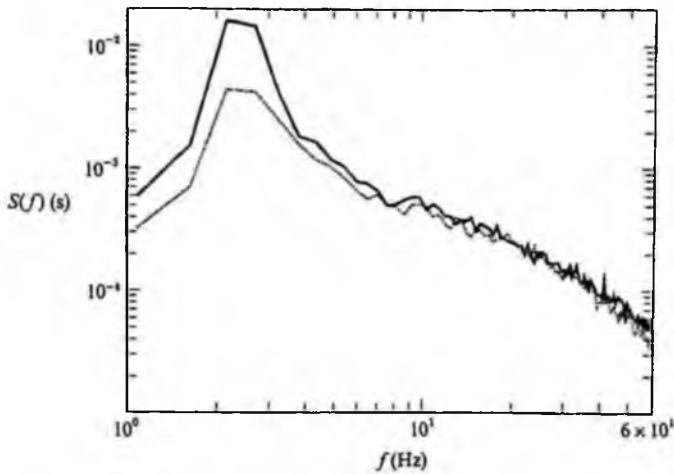


FIGURE 11. Downwind (—) and crosswind (.....) components of the slope frequency spectrum at wind speed 6.5 m s^{-1} , measured before the mechanical wave was generated. (Reproduced from Miller & Shemdin 1991.)

increases, as can be seen in figure 11. The model used here is $p = 10$ for $k \leq k_p$, $p = 2$ for $k > (g\tau/\rho)^{1/2}$ and decreasing linearly with k between the two limits. This model of the angular spreading function gives ratios of the crosswind to downwind slope spectrum which are in agreement with our observations. The resulting transfer rate is given in table 4.

REFERENCES

- COX, C. S. 1958 Measurements of slopes of high frequency wind waves. *J. Mar. Res.* **16**, 199–225.
- DONELAN, M. A. 1987 The effect of swell on the growth of wind waves. *Johns Hopkins Univ. APL Tech. Dig.* **8**, 18–23.
- GASTEL, K. VAN, JANSSEN, P. A. E. M. & KOMEN, G. J. 1985 On phase velocity and growth rate of wind induced gravity-capillary waves. *J. Fluid Mech.* **161**, 199–216.
- GOTTIFREDI, J. C. & JAMESON, G. J. 1970 The growth of short waves on liquid surfaces under the action of wind. *Proc. R. Soc. Lond. A* **319**, 373–397.
- HASSELMANN, K. 1962 On the non-linear energy transfer in a gravity wave spectrum. *J. Fluid Mech.* **12**, 481–500.
- HUGHES, B. A. & GRANT, H. L. 1978 The effect of internal waves on surface wind waves 1. Experimental measurements. *J. Geophys. Res.* **83**, 443–454.
- KWOH, D. S. W., LAKE, B. M. & RUNGALDIER, H. 1988 Microwave scattering from internal wave modulated surface waves: A shipboard real aperture coherent radar study in the Georgia Strait experiment. *J. Geophys. Res.* **93**, 12235–12248.
- LEWIS, J. E., LAKE, B. M. & KO, D. R. S. 1974 On the interaction of internal waves and surface gravity waves. *J. Fluid Mech.* **63**, 773–800.
- LONG, R. B. & HUANG, N. E. 1976 On the variation and growth of wave-slope spectra in the capillary-gravity range with increasing wind. *J. Fluid Mech.* **77**, 209–228.
- LONGUET-HIGGINS, M. S. 1987 The propagation of short surface waves on longer gravity waves. *J. Fluid Mech.* **177**, 293–306.
- LONGUET-HIGGINS, M. S. 1991 A stochastic model of sea-surface roughness II., *Proc. Roy. Soc. Lond. A*, in press.
- LONGUET-HIGGINS, M. S. & STEWART, R. W. 1960 Changes in form of short gravity waves on long waves and tidal currents, *J. Fluid Mech.* **8**, 565–583.
- MILES, J. W. 1962 On the generation of surface waves by shear flows. *J. Fluid Mech.* **13**, 433–448.

- 404 *S. J. Miller, O. H. Shemdin and M. S. Longuet-Higgins*
- MILLER, S. J. & SHEMDIN, O. H. 1991 Measurement of the hydrodynamic modulation of centimetre waves. *J. Geophys. Res.* **96**, 2749-2759.
- MITSUYASU, H. 1966 Interactions between water waves and wind, 1. *Rep. Res. Inst. Appl. Mech. Kyushu Univ.* **14**, 67-88.
- PALM, C. S., ANDERSON, R. C. & REECE, A. M. 1977 Laser probe for measuring 2D wave slope spectra of ocean capillary waves. *Appl. Opt.* **16**, 1074-1081.
- PHILLIPS, O. M. & BANNER, M. L. 1974 Wave breaking in the presence of wind drift and swell. *J. Fluid Mech.* **66**, 625-640.
- PLANT, W. J. 1982 A relationship between wind stress and wave slope. *J. Geophys. Res.* **87**, 1961-1967.
- PLANT, W. J. & WRIGHT, J. W. 1977 Growth and equilibrium of short gravity waves in a wind-wave tank. *J. Fluid Mech.* **82**, 767-793.
- REECE, A. M. 1978 Modulation of short waves by long waves. *Boundary-Layer Met.* **13**, 203-214.
- SHEMDIN, O. H. & HWANG, P. A. 1988 Comparison of measured and predicted sea surface spectra of short waves. *J. Geophys. Res.* **93**, 13883-13890.
- SHEMDIN, O. H. & MILLER, S. J. 1991 A model for the wave number spectrum of wind generated waves. (submitted).
- TANG, S. & SHEMDIN, O. H. 1983 Measurement of high frequency waves using a wave follower. *J. Geophys. Res.* **88**, 9832-9840.
- TOBER, G., ANDERSON, R. C. & SHEMDIN, O. H. 1973 Laser instruments for detecting water ripple slopes. *Appl. Opt.* **12**, 788-794.
- VALENZUELA, G. R. & LAING, M. B. 1972 Nonlinear energy transfer in a gravity-capillary wave spectra, with applications. *J. Fluid Mech.* **54**, 507-520.
- WRIGHT, J. A., PLANT, W. J., KELLER, W. C. & JONES, W. L. 1980 Ocean wave-radar modulation transfer functions from the west coast experiment. *J. Geophys. Res.* **85**, 4957-4966.

Advanced Series on Ocean Engineering — Volume 35

DYNAMICS OF WATER WAVES

Selected Papers of Michael Longuet-Higgins

This is a three-volume selection of classical papers by Michael Longuet-Higgins, who for many years has been a leading researcher in the fast-developing field of physical oceanography. Some of these papers were first published in scientific journals or in conference proceedings that are now difficult to access. All the papers are characterized by the novelty of their content, and the clarity of their style and exposition.

The papers are quite varied in their approach. They range from basic theory and new computational methods to laboratory experiments and field observations. An overall feature is the frequent comparison between theory and experiment and the constant attention to practical applications.

Among the many advances and achievements to be found in these three volumes are: the now generally accepted solution to the longstanding problem of how oceanic microseisms can be generated in deep water or near steep coastlines; a theoretical explanation of the strong drifting near the bottom in shallow water; the first introduction of a boundary-integral technique for calculating free surface flows; simple analytic expressions for the form and time-development of plunging breakers; and so on.

The book will be of particular interest to advanced students in ocean engineering; also more generally to fluid dynamicists and physical oceanographers concerned with the interaction of the ocean with the atmosphere and with sandy shorelines.

